

# POLYMER

*The Chemistry, Physics and Technology of  
High Polymers*

*Editorial Board*

C. H. BAMFORD, PH.D., SC.D.

*Campbell Brown Professor of Industrial Chemistry,  
University of Liverpool*

C. E. H. BAWN, C.B.E., F.R.S.

*Grant Brunner Professor of Inorganic and Physical Chemistry,  
University of Liverpool*

GEOFFREY GEE, C.B.E., F.R.S.

*Sir Samuel Hall Professor of Chemistry,  
University of Manchester*

ROWLAND HILL, PH.D.

*Director of Research,  
I.C.I. Fibres Division, Harrogate*

REPRINTED 1972 FOR

Wm. DAWSON & SONS Ltd., FOLKESTONE

WITH THE PERMISSION OF

IPC SCIENCE AND TECHNOLOGY PRESS, LTD.

# Dynamic Birefringence of Polymethylacrylate

B. E. READ

*In an attempt to investigate the molecular mechanism of relaxation processes in polymers, measurements have been made of the amplitudes and relative phases of the stress, strain and birefringence of polymethylacrylate samples subjected to a sinusoidal strain. The measurements were made in the frequency range 1 c/s to 20 c/s and temperature range 16.6°–61.5°C. A method of reduced variables is tentatively proposed whereby the effective frequency range is greatly extended. The data are presented in terms of the frequency dependence of the real and imaginary components of the complex strain-optical coefficient and complex stress-optical coefficient respectively. The results suggest that two types of segmental motion are involved in the relaxation processes associated with the glass-rubber transition in the polymer, namely (a), the motions of short chain segments due to the release of local distortions and (b), longer range diffusional motions of flexible chain segments.*

THE birefringence exhibited by an extended amorphous polymer arises from the orientation of optically anisotropic structural groups within the polymer chain molecules<sup>1</sup>. Birefringence measurements have occasionally been made during creep and stress-relaxation experiments in order to investigate the molecular orientational changes responsible for relaxation effects in polymers<sup>2</sup>. However, the birefringence technique has seldom been used to investigate relaxation under dynamic loading conditions. This method is capable of studying shorter time-scale ranges than the creep and stress-relaxation methods. Also it should yield more direct information since both the amplitude and phase of the birefringence relative to the stress and strain may be determined.

We have recently considered the problem of dynamic birefringence in rubberlike polymers by an extension of the molecular theory of viscoelasticity<sup>3</sup>. The dynamic birefringence equipment developed in this laboratory has been described and preliminary data presented for natural rubber and polymethylacrylate (PMA)<sup>4</sup>. During the course of this work Stein, Onogi and Keedy have described an alternative method used to determine the dynamic strain-optical coefficient of (crystalline) polyethylene films and have developed a phenomenological theory appropriate to crystallite orientation mechanisms<sup>5</sup>. In this paper the theory behind the method is surveyed, a brief account of our experimental technique is given and completed data on PMA are presented and discussed.

## PHENOMENOLOGICAL THEORIES

### *Mechanical*

The stress ( $f$ ) in a polymer specimen subjected to a periodic tensile strain



( $\epsilon$ ) generally leads the prescribed strain by some phase angle  $\delta$ . In complex notation we have:

$$\epsilon^* = \epsilon_0 \exp(i\omega t) \quad (1)$$

$$f^* = f_0 \exp[i(\omega t + \delta)] \quad (2)$$

where  $\epsilon_0$  is the strain amplitude,  $f_0$  the stress amplitude and  $\omega$  the experimental frequency in radians/sec. Equations (1) and (2) are plotted schematically in *Figure 1*. At small strains the dynamic mechanical

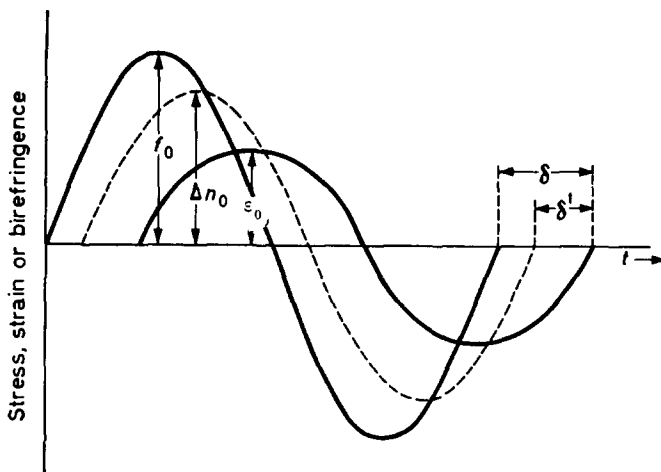


*Figure 1*—Schematic illustration of variation of stress, strain and birefringence during a single loading cycle

properties of the polymer may be expressed in terms of the absolute Young's modulus  $|E| = f_0/\epsilon_0$  and  $\delta$  (or  $\tan \delta$ ) both of which are functions of frequency. The properties may alternatively be specified by the frequency dependence of the real and imaginary components of a complex modulus  $E^* = f^*/\epsilon^* = E' + iE''$ . Both  $E'$  and  $E''$  are related to  $|E|$  and  $\delta$  by well-known equations<sup>6</sup>. Experimental plots of  $E'$  or  $E''$  against frequency may conveniently be analysed by the method of Williams and Ferry<sup>6</sup> to obtain the mechanical relaxation spectrum  $\phi_E(\ln \tau)$  to a second order approximation.

An alternative way of representing dynamic mechanical data is to plot, against frequency, the real and imaginary components of the complex tensile compliance  $D^* = \epsilon^*/f^* = D' - iD''$ . The mechanical *retardation* spectrum  $\phi_D(\ln \tau)$  may be calculated from these plots by the Williams-Ferry method<sup>6</sup>.

### Birefringence

The birefringence of an extended material is defined by

$$\Delta n = n_{\parallel} - n_{\perp} \quad (3)$$

where  $n_{\parallel}$  and  $n_{\perp}$  are the refractive indices along and perpendicular respectively to the stretching direction. Owing to relaxation processes  $\Delta n$  will

generally be out of phase with a prescribed sinusoidal strain by some phase angle  $\delta'$  as shown in *Figure 1*. Hence we may write

$$\Delta n^* = \Delta n_0 \exp [i(\omega t + \delta')] \quad (4)$$

where  $\Delta n_0$  is the amplitude of the birefringence. The relaxation of birefringence is given by the frequency dependence of the absolute strain-optical coefficient  $|K| = \Delta n_0 / \varepsilon_0$  and  $\delta'$  (or  $\tan \delta'$ ). We can also define a complex strain-optical coefficient  $K^* = \Delta n^* / \varepsilon^* = K' + iK''$ , where  $K'$  and  $K''$  are given by

$$K' = |K| \cos \delta', \quad K'' = |K| \sin \delta', \quad K''/K' = \tan \delta' \quad (5)$$

The dependence of  $K'$  and  $K''$  on frequency may generally be written as follows:

$$K' = \int_{-\infty}^{+\infty} \phi_K(\ln \tau) \frac{\omega^2 \tau^2}{1 + \omega^2 \tau^2} \cdot d \ln \tau \quad (6)$$

$$K'' = \int_{-\infty}^{+\infty} \phi_K(\ln \tau) \frac{\omega \tau}{1 + \omega^2 \tau^2} \cdot d \ln \tau \quad (7)$$

in which  $\phi_K(\ln \tau)$  may be termed the strain-optical relaxation spectrum, and represents the contribution to  $K'_\infty - K'_0$  from processes having strain-optical relaxation times between  $\ln \tau$  and  $\ln \tau + d \ln \tau$ .  $K'_\infty$  and  $K'_0$  are the values of  $K'$  at infinite frequency and zero frequency respectively. Equations (6) and (7) can be derived, for example, from a consideration of the dynamic behaviour of a distribution of Maxwell elements<sup>5</sup> in which the *spring only* of each element contributes (either positively or negatively) to the total strain-optical coefficient. In contrast to  $\phi_E(\ln \tau)$  and  $\phi_D(\ln \tau)$ , which are always positive,  $\phi_K(\ln \tau)$  may be either positive or negative in different regions of  $\tau$  depending on whether the molecular mechanism corresponding to the relaxation time  $\tau$  contributes a positive or negative amount to  $K'_\infty - K'_0$ . The evaluation of  $\phi_K(\ln \tau)$  from plots of either  $K'$  or  $K''$  against frequency is analogous to the methods used for obtaining the mechanical relaxation spectrum. The following first-order approximation equations, strictly valid only when  $\phi_K(\ln \tau)$  is independent of  $\tau$ , are obtained from equations (6) and (7) respectively:

$$[\phi_K(\ln \tau)]_{\tau=1/\omega} \approx \frac{1}{2.303} \frac{dK'}{d \log \omega} \quad (8)$$

and 
$$[\phi_K(\ln \tau)]_{\tau=1/\omega} \approx (2/\pi) K'' \quad (9)$$

Higher order approximations involving higher derivatives of experimental curves may be calculated, but the experimental precision so far obtained is insufficient to justify their use.

A further method of specifying dynamic birefringence data is by means of an absolute stress-optical coefficient,  $|C| = \Delta n_0 / f_0$  and the phase angle  $(\delta - \delta')$  by which the stress cycle leads the birefringence cycle. We may also define a complex stress-optical coefficient,  $C^* = \Delta n^* / f^* = C' - iC''$  where  $C'$  and  $C''$  are related to  $|C|$  and  $\delta - \delta'$  by equations analogous to (5)

above. The dependence of  $C'$  and  $C''$  on frequency may be described generally by the following equations:

$$C' = \int_{-\infty}^{+\infty} \phi_c(\ln \tau) \frac{1}{1 + \omega^2 \tau^2} d \ln \tau \quad (10)$$

and

$$C'' = \int_{-\infty}^{+\infty} \phi_c(\ln \tau) \frac{\omega \tau}{1 + \omega^2 \tau^2} d \ln \tau \quad (11)$$

where  $\phi_c(\ln \tau)$  is the stress-optical relaxation spectrum giving the contribution to  $C'_0 - C'_\infty$  from processes having stress-optical relaxation times between  $\ln \tau$  and  $\ln \tau + d \ln \tau$ . To a first approximation  $\phi_c(\ln \tau)$  may be calculated from the following relationship:

$$[\phi_c(\ln \tau)]_{\tau=1/\omega} \approx - \frac{1}{2 \cdot 303} \frac{dC'}{d \log \omega} \quad (12)$$

and

$$[\phi_c(\ln \tau)]_{\tau=1/\omega} \approx (2/\pi) C'' \quad (13)$$

#### MOLECULAR THEORIES

The basic idea underlying most so-called molecular theories of viscoelasticity in polymers<sup>6</sup> is that upon deforming a polymer a finite time is required for the chain molecules to diffuse to a new set of most probable configurations. The entropy increase resulting from these configurational changes is assumed to provide the driving force for the processes, all configurations being assumed to have the same internal energy. In the Rouse theory<sup>6,7</sup> each real molecular chain is replaced by an idealized chain comprising a large number,  $n$ , of freely jointed 'equivalent statistical links' each of length  $a$ . This chain is arbitrarily divided into  $\nu$  'submolecules' each of sufficient length that its end-to-end distance may be approximated by a Gaussian probability distribution. The configuration of the entire chain is described by a set of normal coordinates and relaxation is assumed to result from configurational changes along each normal coordinate. The relaxation time characterizing motions of the  $p$ th normal mode is given approximately (for  $p < \nu/5$ ) by

$$\tau_p \approx a^2 n^2 \xi / 6 \pi^2 p^2 kT \quad (14)$$

where  $\xi$  is a monomeric friction coefficient,  $k$  is Boltzmann's constant, and  $T$  the absolute temperature.  $E'$  and  $E''$  are given by the following summations:

$$E' = 3NkT \sum_{p=1}^{\nu} \frac{\omega^2 \tau_p^2}{1 + \omega^2 \tau_p^2} \quad \text{and} \quad E'' = 3NkT \sum_{p=1}^{\nu} \frac{\omega \tau_p}{1 + \omega^2 \tau_p^2} \quad (15)$$

in which  $N$  is the number of molecules per unit volume.

Except for the three longest relaxation times ( $\tau_1 \rightarrow \tau_3$ ), which are spaced too far apart, the discrete relaxation spectrum predicted by the theory

may be replaced to a good approximation by a continuous spectrum<sup>6</sup>,  $\phi_E(\ln \tau) d \ln \tau = -3NkT (dp/d\tau) d\tau$ . From equation (14) we have

$$\phi_E(\ln \tau) = \left( \frac{3anN}{2\pi} \right) \left( \frac{kT\xi}{6} \right)^{\frac{1}{2}} \tau^{-\frac{1}{2}} \quad (16)$$

Therefore a plot of  $\log \phi_E(\ln \tau)$  against  $\log \tau$  should be linear and of slope  $-\frac{1}{2}$ , and according to the limits of applicability of the theory this plot should extend over about three decades of time-scale<sup>6</sup>. This is observed approximately for many amorphous polymers in the long  $\tau$  region of the rubber to glass relaxation spectrum<sup>6</sup>.

The configurational (or orientational) changes responsible for mechanical relaxation in polymers will also lead to a relaxation of birefringence if the statistical links are optically anisotropic. The following equations for the frequency dependence of  $K'$  and  $K''$  were obtained by an extension of the above theory to the problem of dynamic birefringence<sup>3</sup>:

$$K' = K \sum_{p=1}^{\nu} \frac{\omega^2 \tau_p^2}{1 + \omega^2 \tau_p^2} \quad \text{and} \quad K'' = K \sum_{p=1}^{\nu} \frac{\omega \tau_p}{1 + \omega^2 \tau_p^2} \quad (17)$$

where 
$$K = \frac{(\bar{n}^2 + 2)^2}{\bar{n}} \cdot \frac{6\pi}{45} N (\alpha_{\parallel} - \alpha_{\perp}) \quad (18)$$

$\bar{n}$  is the mean refractive index of the polymer and  $\alpha_{\parallel} - \alpha_{\perp}$  is the polarizability anisotropy of a statistical link. According to equations (15) and (17) we have:

$$\tan \delta = E''/E' = K''/K' = \tan \delta' \quad (19)$$

so that the stress and birefringence are predicted to be in phase (i.e.  $\delta = \delta'$ ). It follows that:

$$\frac{(\bar{n}^2 + 2)^2}{\bar{n}} \cdot \frac{2\pi}{45kT} (\alpha_{\parallel} - \alpha_{\perp}) = K''/E'' = \frac{\Delta n_0 \sin \delta'}{f_0 \sin \delta} = |C| \quad (20)$$

Thus  $|C|$  is predicted to be independent of frequency and proportional to  $\alpha_{\parallel} - \alpha_{\perp}$ . Since the theory also predicts that  $\delta - \delta' = 0$  it follows that  $C'$  should equal  $|C|$  and should also be independent of frequency, and that  $C''$  and  $\phi_C(\ln \tau)$  should be zero at all frequencies or relaxation times.

It is to be emphasized that there is an upper frequency (or short  $\tau$ ) limit at which the mechanical and birefringence theories should be valid since configurational changes *within* the submolecules are ignored. Also at very high frequencies the polymer behaviour will approach that of a glass. The relaxation processes will then involve the release of local distortions within the polymer which will result in internal energy rather than entropy changes. Thus the predictions of equations (19) and (20) would only be expected to hold in the low frequency (or long  $\tau$ ) region of the rubber-glass relaxation where the corresponding  $\log \phi_B(\ln \tau)$  versus  $\log \tau$  plot should be linear and of slope  $-\frac{1}{2}$ .

## METHOD OF REDUCED VARIABLES

Since mechanical relaxation spectra for polymers are usually very broad it is very difficult to study an entire frequency dispersion at constant temperature with a single instrument. However, in the case of amorphous polymers the effective frequency range has often been successfully extended by the method of reduced variables<sup>6</sup>. Values of  $E'$  and  $E''$ , obtained at different temperatures and over a limited frequency range, are first reduced to a standard temperature  $T_0$  by multiplying by a factor  $T_0\rho_0/T\rho$ .  $\rho_0$  and  $\rho$  are the densities of the polymer at temperatures  $T_0$  and  $T$  respectively. The reduced experimental curves are then shifted horizontally along the log (frequency) axis until they superpose. Master curves of  $E'_{T_0}$  and  $E''_{T_0}$  (or  $D'_{T_0}$  and  $D''_{T_0}$ ) against  $\log a_T\omega$  are thus obtained where  $\log a_T$  is the amount by which the curve at temperature  $T$  is horizontally displaced on to the master curve at temperature  $T_0$ . Although the method of reduced variables is essentially an empirical procedure it finds support from the Rouse theory outlined above. The reduction factor  $T_0\rho_0/T\rho$  follows from the dependence of  $E'$  and  $E''$  on  $NkT$  in equations (15). The essential condition for the formation of a master curve from the horizontal shift procedure is that each relaxation time within the distribution shall have the same temperature dependence. This is predicted by equation (14) where all theoretical relaxation times are dependent on temperature largely through the temperature dependence of the same monomeric friction coefficient.

Since the relaxation times derived in the mechanical theory also apply to the birefringence theory, we would expect the superposition procedure to be valid also in extending the effective frequency range of optical data on amorphous polymers. It must be remembered, however, that the molecular theories to date are based on idealized models and, at best, are valid only in a limited time-scale region. The overall applicability of the method of reduced variables in the treatment of optical data is perhaps best judged by experiment. According to equations (17) and (18) the initial reduction of  $K'$  and  $K''$  (and thus  $|K|$ ) to temperature  $T_0$  should depend on the temperature dependence of  $K$  and therefore on the temperature dependence of  $\bar{n}$ ,  $N$  and  $\alpha_{\parallel} - \alpha_{\perp}$ . The variation of  $\bar{n}$  and  $N$  with temperature is determined largely by the thermal expansion coefficient of the polymer, and according to the flexible chain model  $\alpha_{\parallel} - \alpha_{\perp}$  should be independent of temperature. However, real molecular chains are not composed of freely jointed links and  $\alpha_{\parallel} - \alpha_{\perp}$  depends on the number of monomer units which are equivalent to the freely jointed link. This will generally vary with temperature owing to the energy barriers to rotation about main chain bonds. This is a complex theoretical problem. However, an experimental method for performing the reduction to temperature  $T_0$  is to measure the changes of birefringence of a sample held at constant length while it is slowly cooled after initially allowing it to relax to equilibrium at the highest temperature of interest:

$$\frac{K'_{T_0}}{K'_T} = \frac{K''_{T_0}}{K''_T} = \frac{|K|_{T_0}}{|K|_T} = \frac{\Delta n_{T_0}}{\Delta n_T} \quad (21)$$

Since the equilibrium values of both the modulus and the strain-optical

coefficient vary with temperature the reduction of  $C'$ ,  $C''$  and  $|C|$  may be effected by the following equations:

$$\frac{|C|_{T_0}}{|C|_T} = \frac{C'_{T_0}}{C'_T} = \frac{C''_{T_0}}{C''_T} = \frac{\Delta n_{T_0}}{\Delta n_T} \cdot \frac{T\rho}{T_0\rho_0} \quad (22)$$

## EXPERIMENTAL

*Apparatus and procedure*

The equipment used in this study has been described in detail elsewhere<sup>4</sup> and only a brief outline of the method will be given here. A variable speed motor drives an eccentric shaft which produces a sinusoidal vertical displacement of the lower end of a polymer strip. The frequency of oscillation is continuously variable between 50 c/s and  $10^{-3}$  c/s and the amplitude of the displacement can be varied by altering the throw of the eccentric, from zero to  $\pm 1$  mm. The prescribed strain is detected by a differential transformer displacement pick-up and is recorded on one  $Y$  channel of a two-channel oscilloscope. The stress is detected by a similar pick-up mounted inside a calibrated proof ring attached to the upper end of the sample and is recorded on the second  $Y$  channel of the oscilloscope. The ratio of the amplitudes of the force and deformation signals determines  $|E|$  or  $|D|$ .

The phase angle  $\delta$  between the force and deformation cycles is determined with the aid of a disc which rotates on the end of the drive shaft and which contains a slit in its periphery. Two lamp-photocell units are fixed  $180^\circ$  apart on a circular protractor which is graduated from  $0^\circ$  to  $360^\circ$  and which may be rotated manually relative to the rotating disc. The passage of the rotating slit between each lamp-photocell unit produces a pulse which is fed to the  $X$  plates of the oscilloscope, and two horizontal pulses are thus observed on each vertical oscilloscope trace. The difference between the two protractor readings corresponding to the coincidence of the pulses on the stress and strain signals respectively gives  $\delta$  directly. With the present arrangement phase angles can be determined to within  $\frac{1}{2}^\circ$ , but the technique is limited to frequencies above  $10^{-1}$  c/s.

In order to prevent the thin polymer strips from buckling they are maintained under tension during the dynamic measurements by superimposing a static extension upon the small dynamic strain. The temperature may be varied inside an insulated box surrounding the specimen and strain-free glass windows are located on two sides of the box to allow the passage of a light beam through the sample.

The optical components include, in order, a stroboscopic light source, interference filter (5461 Å), polarizer ( $P_1$ ), quarterwave ( $\lambda/4$ ) plate, and analyser ( $P_2$ ). The sample is placed between  $P_1$  and the  $\lambda/4$  plate both of which are oriented with their axes at  $45^\circ$  to the strain axes in the specimen. Under static conditions the birefringence of an extended sample would be determined from the angular rotation of  $P_2$  (away from its orientation crossed with  $P_1$ ) necessary to produce extinction. During the dynamic tests the pulses derived from either one or both lamp-photocell units are used to trigger the stroboscopic source so that the flashing of the source is locked to the vibration of the sample. Using one light pulse per cycle the

sample is viewed as under stationary conditions and birefringence measurements are made by rotating  $P_2$  to produce extinction. The birefringence at any point in the cycle is determined by rotation of the protractor carrying the lamp-photocell units, thus varying the position in the cycle at which the flashing occurs. It is generally unnecessary to explore the complete birefringence cycle, however, since only the amplitude and phase are required.

The procedure normally adopted for measuring the phase and amplitude of the birefringence is as follows. Using two light pulses per cycle and setting  $P_2$  slightly off extinction the pulses will generally be transmitted with unequal intensity giving rise to a flickering appearance. However, when the angular position of the photocell units corresponds to the zero point in the birefringence cycle, the pulses are transmitted with equal intensity and a 'steady' light intensity is observed. A comparison of this protractor reading with the readings corresponding to the zero points in the stress and strain cycles yields  $\delta'$  and  $\delta - \delta'$  directly. The photocell units are subsequently rotated through  $+90^\circ$  and  $-90^\circ$  and the birefringence amplitude determined at each angle using one light pulse per cycle as above. In conjunction with the stress and strain amplitudes,  $|K|$  and  $|C|$  are then evaluated. In its present form the stroboscopic technique is limited to frequencies between about 1 c/s and 20 c/s.

### Material

PMA was chosen for initial investigation because the relaxation region associated with its glass transition is conveniently situated close to room temperature at frequencies used in the present method. The polymer was an unfractionated sample prepared by the u.v. irradiation of a 50 per cent solution of methyl acrylate in ethyl acetate under nitrogen. The polymerization was effected in the absence of initiator. The polymer was isolated by precipitating twice from acetone solution with water. It was then dried by pumping under high vacuum for about three days. Strips of the polymer, approximately 2.5 in.  $\times$  0.5 in.  $\times$  0.05 in., were moulded under pressure at about 100°C for three hours. The weight average molecular weight, determined by light scattering in butanone solution, was  $2.04 \times 10^6$ . The glass transition temperature of the polymer, estimated from stress/temperature measurements of samples held at constant length, was  $10^\circ \pm 2^\circ\text{C}$ .

## RESULTS

### Mechanical

Figure 2 shows the original data for  $E'$  and  $E''$  against frequency at temperatures ranging from 16.6°C to 61.5°C. To avoid overcrowding, the data at some temperatures have been omitted from the diagram. All temperatures actually studied are shown in the key accompanying Figure 2 which applies also to the mechanical and optical results shown in the later diagrams.

Figure 2 includes results obtained on three different samples, each obtained from the same preparation. Further, in order to avoid buckling of the samples, and to maintain the stress and birefringence at measurable

## DYNAMIC BIREFRINGENCE OF POLYMETHYLACRYLATE

levels, it was necessary to use different combinations of static and dynamic extension in different temperature ranges, namely (a) 61.5°C to 39.4°C; 16 per cent static extension,  $\pm 2.3$  per cent dynamic extension, (b) 39.6°C to 32.0°C; 32.5 per cent static extension,  $\pm 0.57$  per cent dynamic extension and (c) 28.5°C to 16.6°C; 36.2 per cent static extension,  $\pm 0.14$  per cent

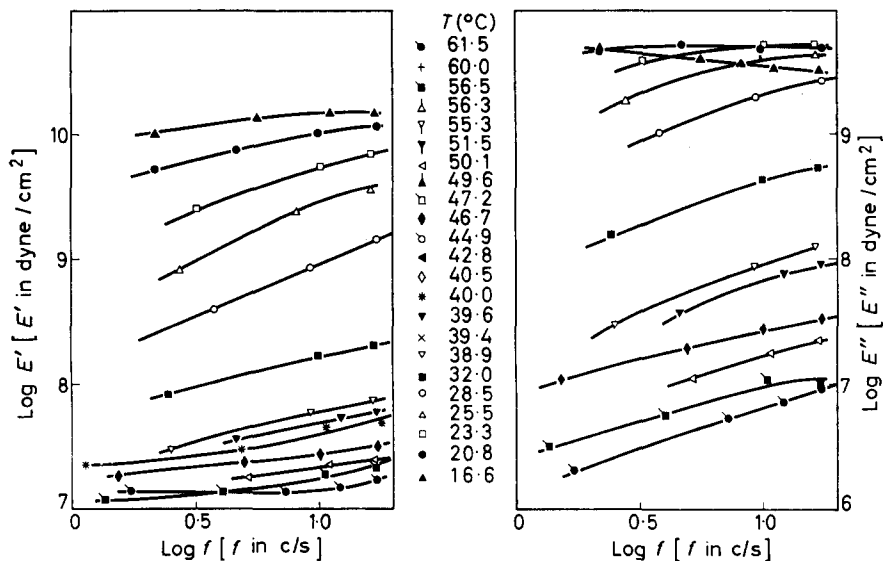


Figure 2—Plots of  $E'$  and  $E''$  against frequency at temperatures shown in the accompanying key

dynamic extension. The dynamic extensions are based on the lengths of samples *after* the application of the static extensions.  $E'$  is seen to increase with increasing frequency and decreasing temperature from a value of  $1.32 \times 10^7$  dyne/cm<sup>2</sup> at 61.5°C (1.7 c/s) to a value of  $1.54 \times 10^{10}$  dyne/cm<sup>2</sup> at 16.6°C (17 c/s) which are typical of values observed for rubberlike and glasslike polymers respectively.  $E''$  exhibits a maximum at 20.8°C and about 4.7 c/s corresponding to the region where  $E'$  is approaching its limiting 'glassy' value.

Reduced master curves of  $\log E'_{T_0}$ ,  $\tan \delta$  and  $\log E''_{T_0}$  versus  $\log a_T f$  are shown in Figure 3, where  $f$  is the frequency in c/s. The reference temperature  $T_0$  was conveniently selected as 61.5°C, the highest temperature of measurement. The successful formation of master curves from data obtained at different extensions indicates that within experimental error the results are unaffected by the variations made in both static and dynamic strain. The horizontal shift factors ( $\log a_T$ ) are given in Table 1.



Table 1

Temperature (°C)	log $a_T$	Temperature (°C)	log $a_T$
61.5	0	32.0	2.97
56.5	0.31	28.5	3.85
50.1	0.58	25.5	4.34
46.7	1.02	23.3	4.76
40.0	1.66	20.8	5.43
39.6	1.85	16.6	6.26
38.9	2.02		

The value of  $E'_{T_0}$  is observed to increase with reduced frequency and  $E''_{T_0}$  passes through a maximum at a reduced frequency of about  $10^6$  c/s. The maximum value of  $\tan \delta$  is about 2.8, in good agreement with the value of 2.85 obtained for PMA by Williams and Ferry<sup>8</sup>. The  $\tan \delta$  maximum is located at a reduced frequency of  $10^{4.2}$  c/s which is almost two decades lower than the frequency corresponding to the  $E''_{T_0}$  maximum.

The mechanical results have also been plotted in terms of  $D'$  and  $D''$  against frequency, and master curves of both  $D'_{T_0}$  and  $D''_{T_0}$  versus log  $a_T f$  have been constructed. The values of  $D'$  ranged from  $7.38 \times 10^{-8}$  cm<sup>2</sup>/dyne at 61.5°C (1.7 c/s) to  $6.20 \times 10^{-11}$  cm<sup>2</sup>/dyne at 16.6°C (17 c/s). A maximum was observed in  $D''$  at 56.5°C (4.1 c/s) and the corresponding maximum in  $D'_T$  occurs at a reduced frequency of 12 c/s.

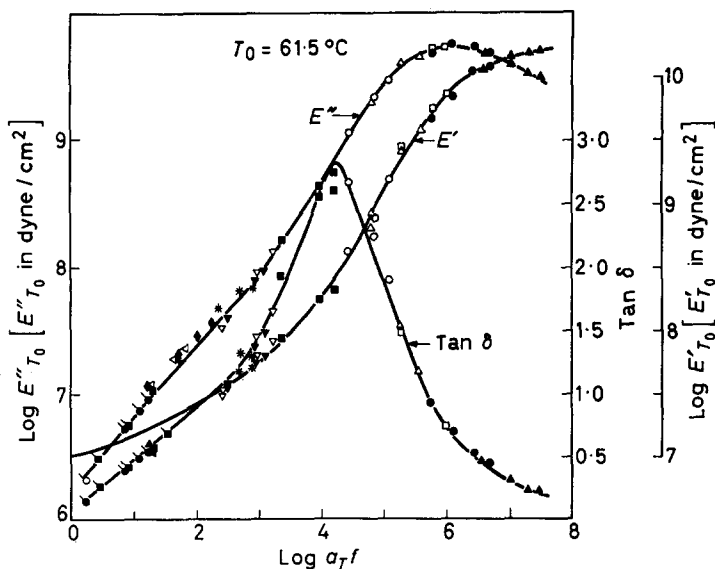


Figure 3—Reduced master curves of  $E'_{T_0}$ ,  $E''_{T_0}$  and  $\tan \delta$  against log  $a_T f$ . The reference temperature  $T_0 = 61.5^\circ\text{C}$ . The key to the points is shown with Figure 2

### Birefringence

The optical results obtained simultaneously with the above mechanical

data were originally plotted in terms of  $\delta'$  (and  $\tan \delta'$ ),  $\delta - \delta'$  (and  $\tan \delta - \delta'$ ),  $|K|$ ,  $|C|$ ,  $K'$ ,  $K''$ ,  $C'$  and  $C''$  against frequency at each temperature investigated. The precision of the optical data was generally insufficient for an accurate independent construction of the corresponding reduced master curves. Within experimental error, however, master curves were obtained by the horizontal shift method using the *mechanical*  $\log a_T$  values (Table I). Although the present optical data cannot therefore provide a very accurate test of the validity of the method of reduced variables these master curves (shown in Figures 5-7 below) give a clearer overall illustration of the optical data than the original plots.

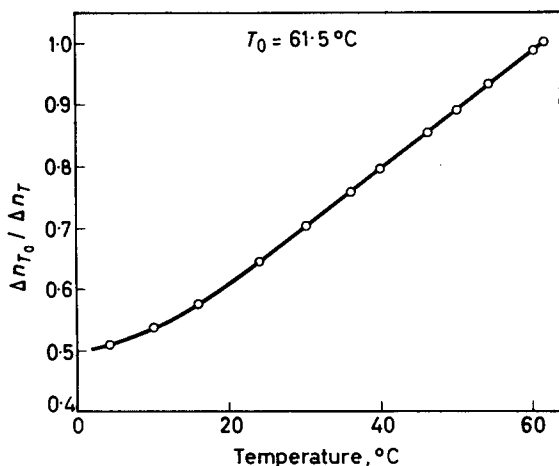


Figure 4—The factors  $\Delta n_{T_0} / \Delta n_T$ , used in the reduction of the optical data according to equations (21) and (22), plotted against temperature

The factors  $\Delta n_{T_0} / \Delta n_T$  necessary for the initial reduction of the birefringence data according to equations (21) and (22) were determined as follows. A strip of PMA was extended to a given length at about 65°C and the birefringence measured after it had relaxed to a steady value (about 15 min). While maintaining the sample at constant length, the temperature was then slowly reduced (0.3°C/min) and birefringence measurements made at about 5°C intervals. The original negative birefringence was found to increase in absolute value with decreasing temperature suggesting that the equilibrium optical anisotropy of the equivalent statistical link ( $\alpha_{\parallel} - \alpha_{\perp}$ ) decreases as the temperature decreases. The values of  $\Delta n_{T_0} / \Delta n_T$ , shown as a function of temperature in Figure 4, are averages determined from three separate runs.

Figure 5 shows curves of  $|K|_T$ ,  $\delta'$ ,  $|C|_{T_0}$  and  $\delta' - \delta$ , respectively, against  $\log a_{Tf}$ . In order to avoid confusion some of the experimental points have been omitted. The scatter of points shown on the  $\delta'$  and  $\delta' - \delta$  curves arises partly from direct experimental error ( $\pm 3^\circ$ ) and partly from errors involved in the horizontal shift procedure. Within the range of reduced frequency

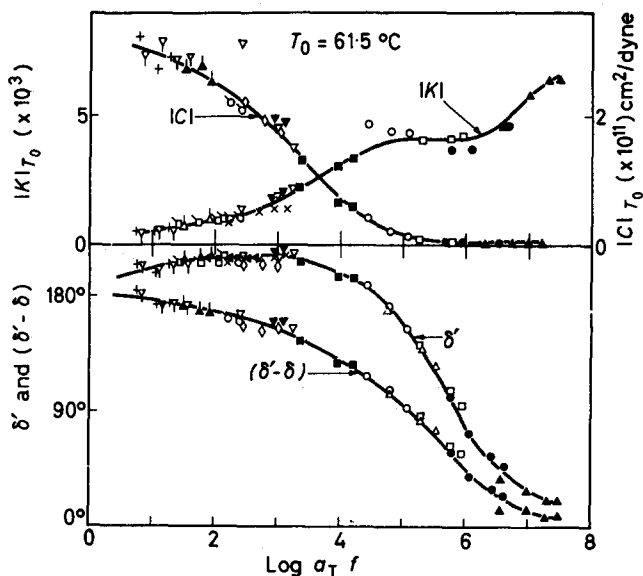


Figure 5—Master curves of the absolute strain-optical coefficient ( $|K|_{T_0}$ ), the absolute stress-optical coefficient ( $|C|_{T_0}$ ), the phase angle by which the birefringence leads the strain ( $\delta'$ ), and the phase angle by which the birefringence leads the stress ( $\delta' - \delta$ ).

The key to the points is shown with Figure 2

studied  $|K|_{T_0}$  increases from  $4.5 \times 10^{-4}$  to  $6.48 \times 10^{-3}$  and  $|C|_{T_0}$  decreases from  $3.2 \times 10^{-11}$  cm<sup>2</sup>/dyne to  $4.1 \times 10^{-13}$  cm<sup>2</sup>/dyne. At high frequencies, where the polymer behaviour is approaching that of a glass, both  $\delta'$  and  $\delta' - \delta$  are small and tending to zero so that the stress, strain and birefringence are all practically in phase and the birefringence amplitude is *positive*. As the reduced frequency decreases  $\delta'$  increases and after passing through a broad maximum (at a value of  $212^\circ$ ) subsequently decreases to  $180^\circ$  at the lowest frequency.  $\delta' - \delta$  increases asymptotically toward  $180^\circ$  with decreasing frequency. Phase angles of  $90^\circ + \theta$  may of course be regarded as angles of  $-(90^\circ - \theta)$  if the sign of the birefringence amplitude is reversed. In particular the approach of  $\delta'$  and  $\delta' - \delta$  to  $180^\circ$  at low reduced frequencies shows that as the rubbery region is approached the birefringence is again tending to be in phase with both the stress and strain if the birefringence amplitude is regarded as *negative*.

The  $K'_{T_0}$  and  $K''_{T_0}$  master curves are presented in Figure 6. At the highest reduced frequency, corresponding to the approach to the glassy state,  $K'_{T_0}$  has a positive value of  $6.06 \times 10^{-3}$ .  $K'_{T_0}$  then decreases with decreasing reduced frequency and at about  $10^{5.9}$  c/s (at which  $\delta' = 90^\circ$  or  $\cos \delta' = 0$ ) it passes through zero. Subsequently  $K'_{T_0}$  becomes negative and after passing through a minimum ( $10^{4.7}$  c/s) it increases with a further decrease in

DYNAMIC BIREFRINGENCE OF POLYMETHYLACRYLATE

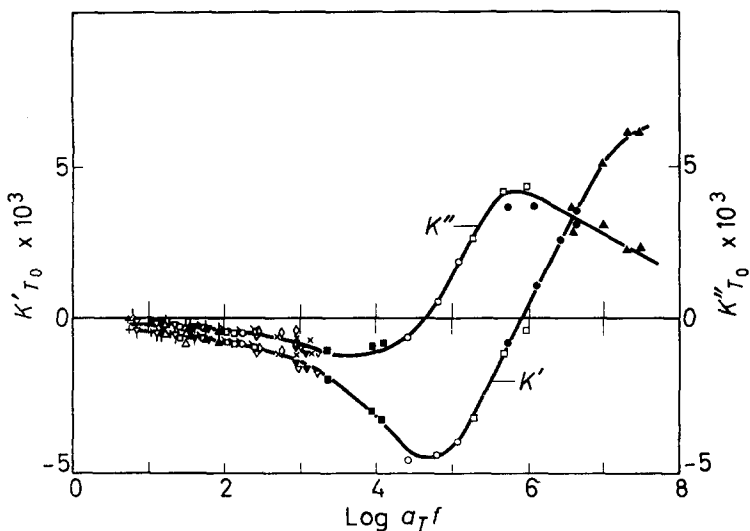


Figure 6—Master curves of the (reduced) real and imaginary components,  $K'T_0$  and  $K''T_0$  respectively, of the complex strain-optical coefficient.  $T_0=61.5^\circ\text{C}$ . The key to the points is shown with Figure 2

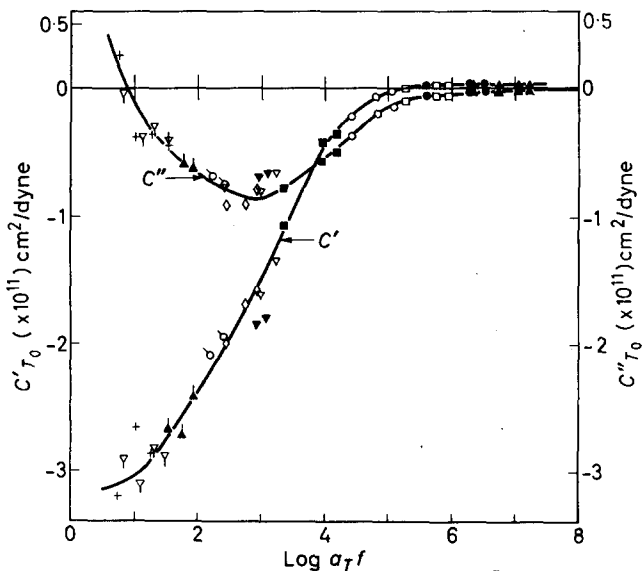


Figure 7—Reduced master curves of the real and imaginary components,  $C'T_0$  and  $C''T_0$  respectively, of the complex stress-optical coefficient. The key to the points is shown with Figure 2

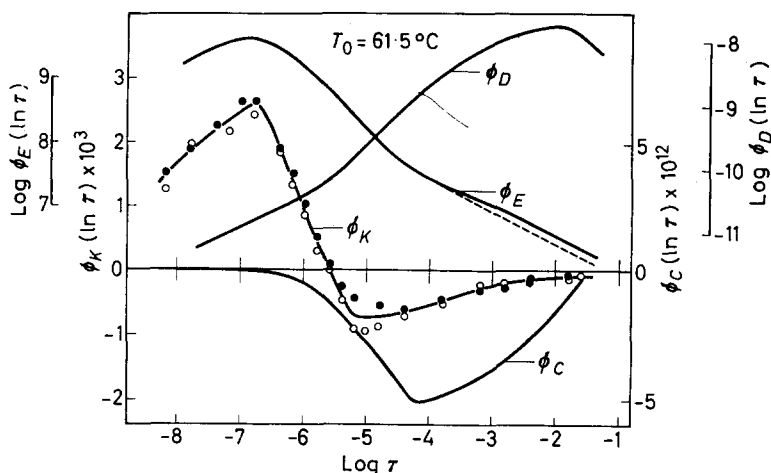


Figure 8—Plots of  $\log \phi_E(\ln \tau)$ ,  $\log \phi_D(\ln \tau)$ ,  $\phi_K(\ln \tau)$  and  $\phi_C(\ln \tau)$  versus  $\log \tau$  at  $61.5^\circ\text{C}$ . The open circles are values of  $\phi_K$  calculated from the  $K'_{T_0}$  master curve according to equation (8). The filled circles are values of  $\phi_K$  evaluated from the  $K''_{T_0}$  master curve according to equation (9). The dashed line indicates the slope of  $-\frac{1}{2}$  predicted theoretically for the  $\log \phi_E / \log \tau$  plot

reduced frequency toward a (rubberlike) value of  $-0.41 \times 10^{-3}$ . Above about  $10^{4.7}$  c/s  $K''_{T_0}$  is positive and shows a maximum in the region of zero  $K'_{T_0}$  and maximum  $E''_{T_0}$  (Figure 3). Below this frequency  $K''_{T_0}$  is negative and exhibits a minimum in the region of  $10^{3.7}$  c/s.

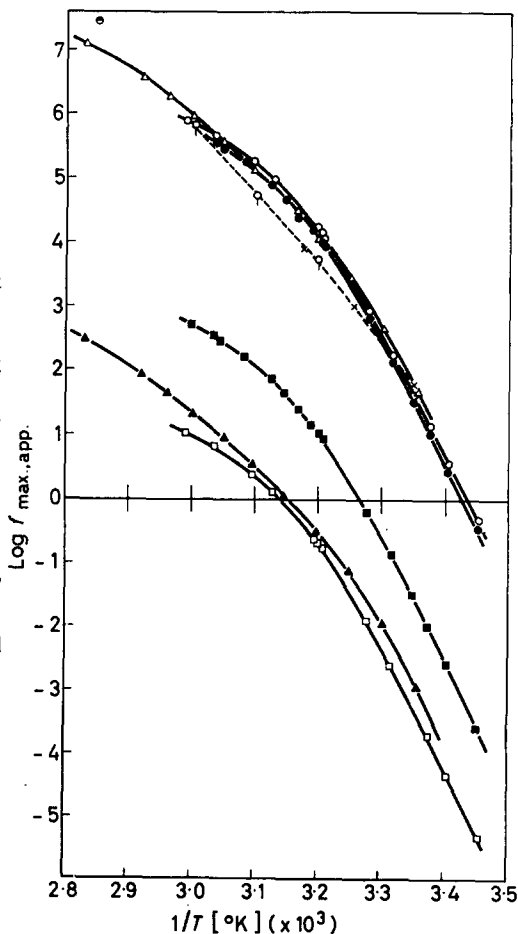
Figure 7 shows the  $C'_{T_0}$  and  $C''_{T_0}$  master curves.  $C'_{T_0}$  varies from  $4.1 \times 10^{-13}$  cm<sup>2</sup>/dyne to  $-3.2 \times 10^{-11}$  cm<sup>2</sup>/dyne with decreasing frequency and at about  $10^{5.2}$  c/s (at which  $\delta' - \delta = 90^\circ$ ) it passes through zero. A minimum in the  $C''_{T_0}$  plot is observed at about  $10^{2.9}$  c/s.

Plots of  $\log \phi_E(\ln \tau)$ ,  $\log \phi_D(\ln \tau)$ ,  $\phi_K(\ln \tau)$  and  $\phi_C(\ln \tau)$  against  $\log \tau$  at  $T_0 = 61.5^\circ\text{C}$  are shown in Figure 8. The mechanical relaxation spectrum ( $\phi_E$ ) was derived from the  $E'_{T_0}$  and  $E''_{T_0}$  master curves according to the method of Williams and Ferry<sup>6</sup>, and good agreement was observed between the spectra calculated independently from the real and imaginary components of the modulus. The spectrum on the double logarithmic plot has a slope of  $-\frac{1}{2}$  (indicated by the dotted line) in the long  $\tau$  region over about three decades of time-scale. At shorter relaxation times deviations from this slope are observed and the spectrum shows a maximum at  $\tau \approx 10^{-6.9}$  secs. The mechanical retardation spectrum ( $\phi_D$ ) was calculated by a similar approximation method from the  $D'_{T_0}$  and  $D''_{T_0}$  master curves and again good agreement was obtained between the  $\phi_D$  values calculated independently from the individual components of the compliance. The retardation spectrum exhibits a maximum (at  $61.5^\circ\text{C}$ ) at  $\tau \approx 10^{-2}$  secs. The strain-optical relaxation spectrum ( $\phi_K$ ) was evaluated from the  $K'_{T_0}$  and  $K''_{T_0}$  master curves according to equations (8) and (9) respectively. Apart from the region of the minimum

in the  $\phi_K$  curve, it can be seen that good agreement exists between the values of  $\phi_K$  calculated independently from the  $K'_{T_0}$  and  $K''_{T_0}$  curves, thus providing a check on the overall internal consistency of the results. The  $\phi_K$  spectrum naturally divides into two regions. Relaxation processes for which  $\tau < 10^{-5.6}$  sec contribute a net *positive* amount to  $K'_{\infty} - K'_0$ , and the spectrum has a maximum at  $\tau \approx 10^{-6.8}$  which coincides almost exactly with the mechanical  $\phi_E$  maximum. For  $\tau > 10^{-5.6}$  sec the relaxation processes contribute a net *negative* amount to  $K'_{\infty} - K'_0$ . The stress-optical relaxation spectrum was evaluated from the  $C'_{T_0}$  master curve by means of equation (13). Owing to the scatter of experimental points on the  $C'_{T_0}$  curve,  $\phi_C$  could not be determined accurately from its first derivative [equation (12)]. Qualitatively, however, this plot would yield a similar stress-optical spectrum. A single minimum is seen in the  $\phi_C$  curve at  $\tau \approx 10^{-4.2}$  sec.

The apparent frequencies of the  $E''$ ,  $D''$  and  $K''$  maxima and the  $C''$  minimum are plotted against  $1/T$  in Figure 9. These curves were constructed

**Figure 9**—Variation of apparent frequencies of  $E''$  (○),  $K''$  (●), and  $D''$  (□) maxima and the  $C''$  (■) minima with reciprocal temperature. The locations of the  $G''$  (△) and  $J''$  (▲) maxima, obtained from the data of Williams and Ferry, are shown for comparison. Also shown are the positions of the dielectric loss ( $\epsilon''$ ) maxima obtained from the data of Mead and Fuoss (×) and Williams (◇), and the temperature of the n.m.r. spin-lattice relaxation time ( $T_1$ ) minimum (⊙) observed by Kawai



by first plotting the points for which a maximum or minimum was directly observed in the limited frequency range studied (e.g.  $E''_{\max}$  at 20.8°C and 4.7 c/s). All other points were then determined by an effective extrapolation using the  $\log a_T$  values given in *Table I*. Shown for comparison are the apparent frequencies of maximum  $G''$  (shear loss modulus) and  $J''$  (shear loss compliance) obtained in a similar manner from the data on PMA by Williams and Ferry<sup>8</sup>. The agreement between the two sets of data is very good. Also shown for comparison are the temperatures of maximum dielectric loss factor  $\epsilon''_{\max}$  obtained at constant frequencies for the primary dielectric loss peak in PMA<sup>9,10</sup>. The point shown at a frequency of 25 Mc/s corresponds to the temperature at which a minimum was found in the n.m.r. spin-lattice relaxation time ( $T_1$ ) for PMA<sup>11</sup>. There is clearly a close correlation between the positions of the  $E''$ ,  $G''$ ,  $K''$  and  $\epsilon''$  maxima and the  $T_1$  minimum.

## DISCUSSION

The molecules of PMA have the chain structure  $(-\text{CH}_2-\text{CH}-)_n$



According to measurements of the n.m.r. line width<sup>12</sup> and the spin-lattice relaxation time<sup>11</sup> the onset of motion of the side chain methyl groups occurs below -196°C. A secondary dielectric loss peak observed at -80°C (10 c/s) has been attributed to the onset of rotation of the complete ester side group<sup>13</sup>. The relaxation behaviour observed in this work is related to the gradual transition from the rubberlike to glasslike state in PMA and probably results from the motions *within* the chain backbone.

The limiting glassy modulus observed on the high frequency side of the reduced modulus curve may be attributed to distortional effects such as the bending of valence angles and the separation of chains against their van der Waals forces of attraction. The birefringence resulting from this elastic mechanism, the so-called '*distortional* birefringence', is of positive sign and leads to *positive* values for both  $K'_{T_0}$  and  $C'_{T_0}$  in the limiting high frequency region. The initial decrease in  $E'_{T_0}$ ,  $K'_{T_0}$  and  $C'_{T_0}$  as the reduced frequency decreases probably reflects the rearrangement of very short chain segments arising from the release of local distortions. These local modes of chain motion would then give rise to the maximum in the  $E''_{T_0}$  curve and the positive peak in the  $K''_{T_0}$  master plot, and also the associated maxima in the mechanical ( $\phi_E$ ) and strain-optical ( $\phi_K$ ) relaxation spectra. The correlation observed in *Figure 9* between the locations of the  $E''$ ,  $K''$  and  $\epsilon''$  maxima and the  $T_1$  minimum suggests that similar average relaxation times characterize the mechanical, strain-optical, dielectric and n.m.r. relaxation processes. It further indicates that the dielectric and n.m.r. behaviour may be determined largely by the local distortional modes of chain motion. Since dielectric relaxation under prescribed voltage is formally analogous to mechanical *retardation* under prescribed stress we might have expected the positions of the  $\epsilon''$  maxima to correlate with the positions of the  $D''$  maxima or  $C''$  minima rather than the  $E''$  and  $K''$  maxima. The failure of

this correlation is perhaps due to the fact that the positions of the  $D''$  and  $C''$  peaks are largely determined by the longer-range chain rearrangements, discussed below, which may not make a very large contribution to the dielectric processes.

As the frequency decreases the local distortional processes are probably largely replaced by mechanisms involving the *orientation* of longer chain segments. Since chain orientation probably leads to an average orientation of anisotropic ester side groups perpendicular to the direction of extension, the sign of both  $K'_{\tau_0}$  and  $C'_{\tau_0}$  becomes negative. The subsequent increase in  $K'_{\tau_0}$  after passing through a minimum indicates that at constant extension the chains diffuse to less extended, more probable, configurations as the frequency decreases. At constant stress, however, the molecules become more extended with decreasing frequency, as reflected in the decrease in  $C'_{\tau_0}$ . The long range configurational changes also give rise to the negative peaks in the  $K''_{\tau_0}$  and  $C''_{\tau_0}$  curves and the corresponding negative peaks in the  $\phi_K$  and  $\phi_C$  spectra. The modulus in this region is determined largely by entropy elasticity rather than energy elasticity as in the distortional region. These orientational rearrangements form the basis of the molecular theories outlined earlier and, as predicted, in the appropriate long relaxation time region, the mechanical relaxation spectrum has a slope of about  $-\frac{1}{2}$ . However, the theories also suggest that  $\phi_C$  should be zero in the same region of  $\tau$ , which follows from the prediction that in the corresponding low frequency region  $C'$  should be independent of frequency and  $C''$  should be zero. The failure of these predictions may possibly be due to the fact that the distortional relaxation processes partially overlap the orientational processes which predominate in this region. In the absence of a molecular theory applicable to the high frequency or short  $\tau$  region, a method for resolving the optical relaxation behaviour into the two (possibly overlapping) proposed mechanisms has not been developed.

*The author acknowledges discussions with Dr D. H. Whiffen and thanks Mrs J. Hawkins for preparing the PMA and for general assistance. The work described above has been carried out as part of the research programme of the National Physical Laboratory and this paper is published by permission of the Director of the Laboratory.*

Basic Physics Division,  
D.S.I.R. National Physical Laboratory,  
Teddington, Middlesex

(Received September 1962)

#### REFERENCES

- <sup>1</sup> TRELOAR, L. R. G. *The Physics of Rubber Elasticity*. Oxford University Press: London, 1958
- <sup>2</sup> STEIN, R. S. in *Die Physik der Hochpolymeren* (Ed. H. A. Stuart), Vol. IV, Ch. 1, p 110. Springer: Berlin, 1956
- <sup>3</sup> READ, B. E. *Polymer*, Lond. 1962, **3**, 143
- <sup>4</sup> READ, B. E. *Techniques of Polymer Science*, S.C.I. Monograph No. 17, p 198. Society of Chemical Industry: London, 1963
- <sup>5</sup> STEIN, R. S., ONOGI, S. and KEEDY, D. A., *J. Polymer. Sci.* 1962, **57**, 801



B. E. READ

---

- <sup>6</sup> FERRY, J. D. *Viscoelastic Properties of Polymers*. Wiley: New York, 1961  
<sup>7</sup> ROUSE, P. E. *J. chem. Phys.* 1953, **21**, 1272  
<sup>8</sup> WILLIAMS, M. L. and FERRY, J. D. *J. Colloid Sci.* 1955, **10**, 474  
<sup>9</sup> MEAD, D. J. and FUOSS, R. M. *J. Amer. chem. Soc.* 1942, **64**, 2389  
<sup>10</sup> WILLIAMS, G. National Physical Laboratory. Unpublished data  
<sup>11</sup> KAWAI, T. *J. phys. Soc. Japan*, 1961, **16**, 1220  
<sup>12</sup> SINNOTT, K. M. *J. Polym. Sci.* 1960, **42**, 3  
<sup>13</sup> BROUCKÈRE, L. and OFFENGELD, G. *J. Polym. Sci.* 1958, **30**, 105

# *Solution and Bulk Properties of Branched Polyvinyl Acetates Part II—Synthesis of Some Branched Polyvinyl Acetates*

G. C. BERRY\* and R. G. CRAIG

*A series of comb-shaped branched polyvinyl acetates has been prepared by a graft polymerization technique. Branches of a specified average chain length have been grafted to a linear backbone polymer with a narrow molecular weight distribution. The branched polymers have a molecular weight distribution whose breadth is very close to the linear fraction used for the backbone chain. The number average molecular weight of the branches has been varied from 18 000 to 106 000. The molecular weight of the linear backbone polymers is of the order of one million.*

THE bulk and solution properties of branched macromolecules have been of considerable practical and theoretical interest for a number of years. The study of branched polymers is complicated by the increased complexity of the theoretical developments and the difficulty of obtaining a branched polymer with some *a priori* knowledge of its structure. The aim of this investigation has been to prepare a series of branched polyvinyl acetates with known structures, and to examine some of their solution and bulk properties. This paper will be concerned with the preparation of such a series of branched polymers. The solution and bulk properties of the polymer obtained will be presented elsewhere.

A previous study of some branched polyvinyl acetates by Long<sup>1</sup>, utilized samples of a polymer prepared at a high conversion. Even though these samples were fractionated according to their solubility characteristics, there remained some ambiguity in the assignment of a structure to each sample. In an attempt to avoid this difficulty, a graft polymerization has been used here to prepare branched polymers having a narrow molecular weight distribution, and a given number of branches of a certain average chain length. Vinyl acetate has been polymerized in the presence of narrow molecular weight fractions of a linear polyvinyl acetate (PVOAc), a chain transfer solvent, and an initiator. The average molecular weight of the new polymer formed in the graft polymer was kept considerably less than that of the linear backbone polymer by adjusting the molar ratio of the monomer to solvent to facilitate the later removal of the new unbound polymer. This condition placed an upper limit on the ratio of the branch to backbone chain length. The branches bound to the backbone have the same average length as the new unbound polymer formed concurrently in the polymerization<sup>2-4</sup>. Thus, the use of the chain transfer solvent allows the average length of the branches to be controlled, and one has an easy means of

---

\*Present address: Mellon Institute, Pittsburgh, Pennsylvania.

determining the length of the branches by examination of the unbound material. The number of branches per molecule resulting from the graft polymerization is dependent on the degree of conversion, allowing a series of branched polymers to be prepared with a relatively wide range of known structures.

There are several advantages to this method of preparation. The necessity of fractionating a branched polymer with a broad molecular weight distribution, as well as a wide distribution of molecular structures, is avoided<sup>5,6</sup>. Since no special active sites are required to either attach the branches to the backbone chemically<sup>7,8</sup>, or to initiate their growth from the backbone<sup>9-12</sup>, the problem of residual foreign groups in the branched polymer does not arise. The use of a chain transfer solvent provides better control over the chain length of the branches than is usually obtained in a graft polymerization<sup>2,13-18</sup>, and suppresses termination reactions which can lead to network formation. The choice of vinyl acetate as the monomer gives a system with the necessary high polymer chain transfer constant. Some ten to fifty branches have been placed on the backbone, approximately eighty to ninety per cent of these directly on the backbone with the remainder on other branches. This latter complication is undesirable since it broadens the chain length distribution of the branches, but it in no way limits the usefulness of the polymers. Some of the difficulties encountered will be discussed later in greater detail.

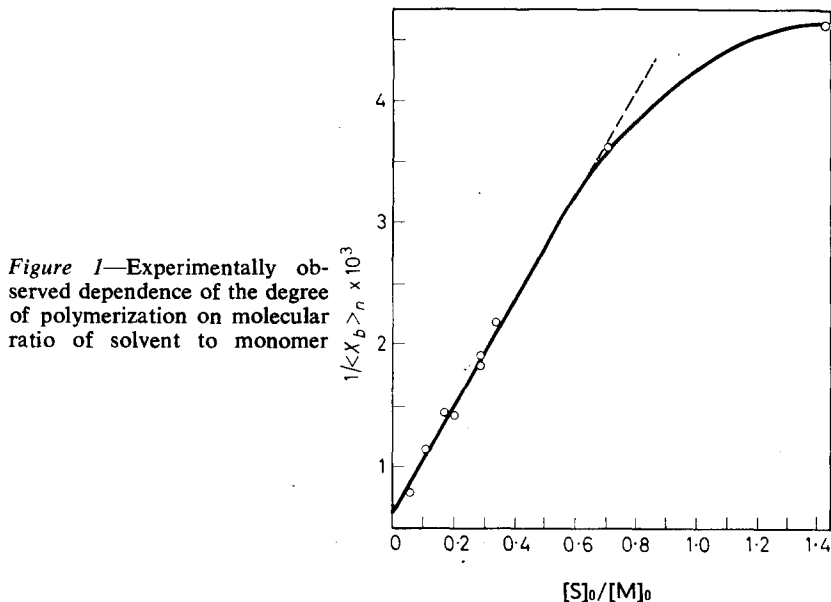
## EXPERIMENTAL

### *Polymerization procedure and materials*

The linear fractions of PVOAc used as the backbone polymer have been described fully by Long<sup>1</sup>. These linear polymers were prepared by the photo-sensitized polymerization of vinyl acetate at low temperatures to approximately ten per cent conversion. The linearity of narrow molecular weight fractions of the resultant polymer has been demonstrated by Long. Vinyl acetate (Niacet vinyl acetate, DPA, Carbide and Carbon Chemicals Co.) was the monomer, toluene the chain transfer solvent, and azo-bis-isobutyronitrile (Eastman Organic Chemicals) the catalyst. Monomer and chain transfer solvent were purified by distillation at about 300 mm of mercury under an atmosphere of dry oxygen-free nitrogen in a column packed with glass helices. A predetermined amount of polymer was evacuated at  $10^{-5}$  mm of mercury for 60 h after which middle fractions (boiling range of 0.1°C) of monomer and toluene and initiator were added to give an initial polymer concentration of 5 to 10 g/dl of liquid and initiator was added to give a concentration of about  $10^{-4}$  Molar. The total amount of liquid was adjusted so that the initial polymer concentration was about 5 to 10 g/100 ml of liquid.

The contents of the tube were then cooled to about  $-90^{\circ}\text{C}$ , and degassed at  $10^{-4}$  to  $10^{-5}$  mm of mercury to remove residual oxygen. None of the contents of the reaction vessel were lost in this degassing operation. After a degassing period of one hour, the reaction tubes were sealed and the contents agitated to cause solution of the polymer at room temperature. The tubes were then held at  $88^{\circ}\text{C}$ , the mixture being agitated with the

magnetic stirring bar. The polymerization was allowed to proceed to about 20 per cent conversion of the monomer.



The value of  $[S]_0/[M]_0$ , the initial solvent to monomer mole ratio, such that the new polymer formed would have the desired number-average molecular weight,  $\langle M_b \rangle_n$ , was determined from the correlation given in Figure 1 observed between these variables for the reaction conditions used. ( $\langle M_b \rangle_v$ , the viscosity average molecular weight is taken on twice  $\langle M_b \rangle_n$ ).

#### Isolation of the branched polymer

The contents of the tube were added dropwise to a large volume of petroleum ether after the polymerization. The isolated polymer was washed with petroleum ether and dissolved in 50 ml of methanol per gramme of polymer. A fractional precipitation was then performed to isolate as much of the graft polymer from the unbound polymer-graft polymer mixture as possible. The fractionation was carried out at 35°C in a litre screw-top bottle with the contents being agitated by a magnetic stirrer. Distilled water was added dropwise until the mixture became turbid, at which point a large excess of water was added. Some of the low molecular weight unbound polymer was inevitably carried down with the graft polymer in the process, but this was of no concern at this stage. The contents of the vessel were then heated to a temperature sufficient to dissolve the precipitate, and then allowed to cool slowly with stirring to reprecipitate the desired polymer. After a settling period of 12 hours, the precipitate was recovered by syphoning off the solution. The unbound polymer in the solution could be recovered by evaporation to dryness. In several instances, the solution was further treated with a large excess of water before further turbidity developed. There was never very much polymer in this second precipitate,

and it had an intrinsic viscosity very near that of the unbound polymer. Thus, the fractionation appeared to be removing almost all of the graft polymer from the graft polymerization mixture.

The polymer now could be subjected to either or both of two different operations. If the entire amount of the graft polymer was to be recycled in another grafting polymerization, the polymer was placed in a reaction vessel and dissolved in benzene. After freezing this solution along the sides of the tube, the benzene was sublimed off at 0°C, leaving the polymer in a porous form. The polymer was degassed at about 10<sup>-5</sup> mm of mercury in preparation for a new graft polymerization, repeating the cycle given above.

If the entire amount of a graft polymer was to be used as a fraction of the branched polymer with no further graft polymerization cycles, then the precipitate was dissolved in methanol to give a concentration of 1 g of polymer in 100 ml of methanol. The fractional precipitation described above was then repeated, but an effort was made to precipitate only about 1 to 2 g fractions of the graft polymer. Successive precipitations were performed until no polymer came down with further addition of water. The unbound polymer remaining in solution was then recovered by evaporation to dryness and added to that previously recovered. Usually, most of the graft polymer came down in the first fraction. The fractions of graft polymer were dissolved in acetone and then cast in a film for solvent removal. The film was freed from residual solvent by evacuation at 10<sup>-6</sup> mm of mercury for two to three days.

In some cases half of the graft polymer underwent further graft polymerization, the remainder being retained as a branched polymer for further study. In these instances, the polymer as recovered wet from the first precipitation fractionation was divided into equal parts by weight, and the two parts subjected to the two different operations as described above.

Some attention was given to the possibility of degradation of the backbone polymer under the graft polymerization conditions. A toluene solution of a linear polymer was held at 90°C for 12 h in the presence of the catalyst, which exceeded the usual reaction time of from one to six hours. No significant change was noted in the intrinsic viscosity of the polymer, indicating the absence of any serious degradation.

### *Polymer characterization*

Light scattering and intrinsic viscosity measurements were made on the first fractions. In some cases where the first fraction was less than one gram in weight, measurements were also made on a mixture comprised of the first two fractions (mixtures designated by *M* in *Table 2*). The intrinsic viscosity of the unbound polymer was measured and the molecular weight of the unbound polymer, and thus of the branches on the graft polymer, was calculated from the relationship<sup>1</sup>

$$\log \langle M \rangle_v = 5.426 + 1.48 \log [\eta] \quad (1)$$

All intrinsic viscosity measurements were performed in benzene at 35°C using a modified Ubbelohde viscometer. The data from these polymerizations are given in *Table 1*.

## PROPERTIES OF BRANCHED POLYVINYL ACETATES II

Table 1. Graft polymerization data

Polymer	Conversion $X$	Unbound polymer $[\eta]$	Unbound polymer $\langle M_b \rangle_v$	Backbone polymer $\langle M_i \rangle_w$	$\langle M_i \rangle_w \Sigma X$	$\langle M_b \rangle_v^*$
6-20	0.365	0.520	$\times 10^3$ 113.0	$\times 10^6$ 2.27	$\times 10^4$ 132	$\times 10^3$ 118
	0.218	0.563	127.0			
6-30	0.272	0.459	99.0			
	0.289	0.373	75.0			
	0.365	0.399	69.0	1.29	119	79.2
6-40	0.163	0.213	39.6			
	0.145	0.219	39.6			
	0.106	0.185	33.0			
	0.127	0.189	34.0	1.50	81	37.0
6-41	0.159	0.207	37.5			
	0.116	0.174	31.2			
	0.171	0.193	34.6	1.50	148	36.0
6-50	0.153	0.219	40.0			
	0.233	0.267	50.0			
	0.157	0.270	52.0			
	0.209	0.253	47.0	2.02	152	47.4
6-51	0.198	0.267	50.0			
	0.185	0.261	49.0			
	0.148	0.285	54.0	2.02	260	48.8
6-60	0.348	0.821	212	3.76	131	212
6-70	0.323	0.667	158			
	0.167	0.582	133	2.16	106	149.5
6-71	0.316	0.468	99			
	0.274	0.605	139	2.16	230	134
6-80	0.257	0.544	122			
	0.228	0.554	123	2.27	110	122
6-81	0.281	0.501	108			
	0.176	0.703	170	2.27	214	127
6-90	0.226	0.418	86			
	0.226	0.479	102	2.54	115	94.0
6-91	0.268	0.381	76.5			
	0.163	0.522	112	2.54	236	87.4

\*The average molecular weight of the branches after a series of graft polymerizations is calculated as  $\langle M_b \rangle_v = \Sigma X \langle M_b \rangle_v / \Sigma X$  where the sums are overall polymerizations in a grafting cycle.

Light scattering measurements were carried out in 1,2,4-trichlorobenzene by a method described in Part III of this series. The measured values of  $\langle M_g \rangle_w$ , the weight average molecular weight of the graft polymer, are given in Table 2.

## RESULTS AND DISCUSSION

The data given in *Table 2* are the primary evidence that the grafting polymerizations have provided the desired branched polymers. An increase in the molecular weight of the graft product relative to the backbone material is observed for every case. In order to better evaluate these results,

*Table 2.* Parameters of the branched polymer

Fraction	$\langle M_1 \rangle_w \Sigma X$	Backbone polymer $\langle M_1 \rangle_v$	Graft polymer $\langle M_g \rangle_w$	Branch polymer $\langle M_b \rangle_n$	No. branches molecule $\langle k \rangle$	Wt/frac. mat. in branches $\langle w \rangle$
	$\times 10^4$	$\times 10^6$	$\times 10^6$	$\times 10^3$		
6-20-1	—	2.27	3.81	59	26	0.38
6-20-M	132	2.27	2.80	59	9	0.18
6-30-1	—	1.29	2.33	40	26	0.44
6-30-M	119	1.29	1.68	40	10	0.24
6-30-M	119	1.29	1.61	40	8	0.20
6-40-1	81	1.50	2.00	18.5	27	0.25
6-41-1	—	1.50	2.24	18	41	0.33
6-41-M	148	1.50	2.09	18	33	0.29
6-50-1	152	2.02	2.71	23.7	29	0.26
6-51-1	—	2.02	3.67	24.4	67	0.48
6-51-M	260	2.02	3.21	24.4	45	0.36
6-60-1	131	3.76	5.60	106	17	0.33
6-60-1	131	3.76	5.43	106	16	0.31
6-70-1	106	2.16	2.65	74.8	7	0.18
6-70-1	106	2.16	2.92	74.8	10	0.26
6-71-1	230	2.16	3.43	67	19	0.37
6-80-1	110	2.27	3.29	61	17	0.31
6-80-1	110	2.27	3.55	61	21	0.36
6-81-1	214	2.27	4.11	63.5	29	0.45
6-90-1	115	2.54	3.45	47	19	0.26
6-91-1	236	2.54	3.96	43.7	33	0.36

however, some of the aspects of the kinetics of the polymerization will now be considered. Following this, a general evaluation of the structure parameters assigned to the comb-shaped branched polymers.

#### Kinetic analysis

A simplified steady-state analysis of the reaction kinetics for the polymerization of a monomer in the presence of its polymer and a chain transfer solvent has been given elsewhere<sup>19</sup>. It was shown that  $\langle k \rangle$ , the average number of branches per molecule grafted onto the backbone, is approximated at low conversion by

$$\langle k \rangle = C_p \langle x_i \rangle X \quad (2)$$

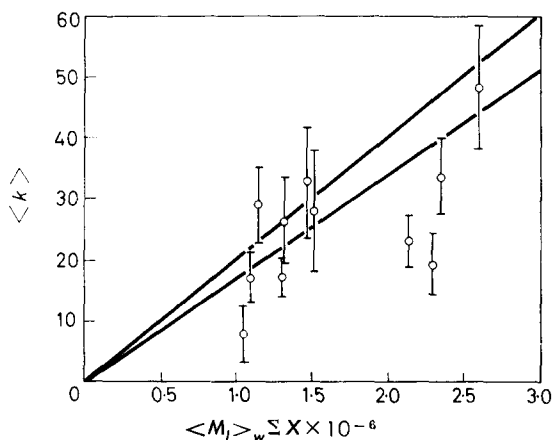
where  $C_p$  is the polymer chain transfer constant,  $\langle x_i \rangle$  is the average degree of polymerization of the backbone, and  $X$  is the degree of conversion in the the graft polymerization. The fraction  $F$  of the new polymer that is bound to the backbone is approximated at low conversion by

$$F = C_p (B/M)_0 \{C_m + C_s [s]_0 / [M]_0 + C_p (B/M)_0\}^{-1} \quad (3)$$

where  $(B/M)_0$  is the initial ratio of polymer to monomer on a weight basis

and  $C_s$  and  $C_m$  are the solvent and monomer transfer constants, respectively. (Certain terms in the denominator, small compared to those given, are omitted.) For a typical set of reaction conditions, these expressions give  $\langle k \rangle \sim .30X$  and  $F \sim 0.15$ .

Figure 2—Number of branches per molecule versus degree of conversion, equation (4)



Since the conversion must be kept below 25 per cent, it is evident that a single graft polymerization will only result in about six to eight branches per molecule for the conditions used here, and that the branched polymer will be contaminated by a considerable amount of new unbound polymer. This was, in fact, the observed behaviour. In order to obtain the desired number of branches and still prevent undesirable reactions such as monomer transfer leading to the formation of a crosslinked network at high conversion, it was necessary to subject the graft polymer to additional polymerization cycles. Thus, after a graft polymerization, the graft polymer was separated from most of the unbound new polymer by a fractional precipitation, redissolved in monomer and chain transfer solvent and used as the substrate in a new graft polymerization. This recycle procedure was continued as often as necessary to obtain the desired number of branches.

Equation (2) suggests a method of correlating the data obtained from these polymerizations. Calling  $\Sigma X$  the sum of the degrees of conversion  $X$  obtained for each of the graft polymerizations on a particular linear backbone polymer, then equation (2) becomes approximately

$$\langle k \rangle \simeq C_p \langle x_i \rangle \Sigma X \quad (4)$$

This expression ignores the change in the degree of polymerization of the graft polymer as it goes through a number of grafting cycles, but the approximation is not serious for the polymerizations considered here. The average number of branches per molecule may be computed by the expression

$$\langle k \rangle = (\langle M_g \rangle - \langle M_l \rangle) / \langle M_b \rangle_n \quad (5)$$

where  $\langle M_g \rangle$ ,  $\langle M_l \rangle$ , and  $\langle M_b \rangle$  are the average molecular weights of the graft, linear backbone and linear branch polymer, respectively. As previously



indicated, the molecular weight of the branch polymer is determined from measurements of the molecular weight of the unbound new polymer.

The values of  $\langle k \rangle$  estimated from equation (5) are shown in *Table 2* and *Figure 2* as a function of  $\langle M_i \rangle_w \Sigma X$ . The two straight lines drawn in that figure correspond to values of  $C_p$  at 90°C given in the literature<sup>21, 22</sup>. These data fit best with  $C_p$  equal to  $15 \times 10^{-4}$ . The vertical lines drawn for each point are indicative of the errors estimated for  $\langle k \rangle$  by assuming a seven per cent error in both  $\langle M_o \rangle_w$  and  $\langle M_i \rangle_w$  in equation (5). The weight fraction,  $\langle w \rangle$ , of the graft polymer to be found in the branches is also included in *Table 2*. An important point to note in *Table 2* is that the recycle operation always caused an increase in  $\langle k \rangle$ , as would be expected, and that this increase is within experimental error of that expected from equation (4).

#### *Molecular weight distribution*

The molecular weight distribution of a graft polymer resulting from the placement of  $\langle k \rangle$  branches of constant molecular weight  $M_b$  on a backbone polymer of molecular weight  $M_i$  has been calculated in the appendix. It is shown there that the ratio of  $\langle M \rangle_w / \langle M \rangle_n$  changes from the value for the linear backbone to approximately

$$\langle M_o \rangle_w / \langle M_o \rangle_n = (\langle M_i \rangle_w / \langle M_i \rangle_n) \{1 + \langle k \rangle / (\langle M_i \rangle / \langle M_b \rangle + \langle k \rangle)^2\} \quad (6)$$

for the branched polymer. Thus, if the backbone had a weight to number average molecular weight ratio of 1.1, then the corresponding ratio for the graft polymer would be calculated from equation (6) with  $\langle M_i \rangle_w / \langle M_i \rangle_n = 1.1$ . The change in the molecular weight ratio indicated by equation (6) is quite small for all of the samples of interest here, the term in brackets ranging from a value of 1.00<sub>3</sub> to 1.03. The effect of this change in the distribution is well within the experimental accuracy of the estimate of  $\langle k \rangle$ , and no attempt has been made to include this effect in the reported data. Thus, weight average values are used for  $\langle M_o \rangle$  and  $\langle M_i \rangle$  in equations (4) and (5). The correction to a number average would be about the same for both the graft and linear polymer, and would cause about a ten per cent decrease in the absolute value of  $\langle k \rangle$ .

#### *Chemical impurity*

Among other factors which could lead to some ambiguity in the specification of the structure of the branched polymer, is the presence of hydroxyl groups in the graft polymer. The polymerizations were performed in the absence of oxygen and water, using purified monomer, polymer and chain transfer solvent, conditions that should have prevented the formation of hydroxyl groups. An infra-red spectrum was obtained on one of the graft polymers and on one of the linear backbone polymers since it has been shown that even low percentages of hydroxyl can be detected in this manner<sup>23</sup>. No hydroxyl groups were indicated by the spectrum for either polymer.

#### *Fractionation*

The effect of the fractionation procedure on the measured and deduced chain lengths reported for the graft polymers is less easily determined. The fractionations of the graft polymer between recycle polymerizations were designed to recover as much of the graft polymer as possible. It must be

realized, however, that a certain amount of the high molecular weight material will remain in the soluble portion of the system in any given separation even if a large excess of non-solvent is present<sup>21</sup>. However, the fact that repeated additions of the non-solvent did not precipitate additional graft polymer after the first fraction was recovered is evidence that these fractionations were effective.

It was not desirable to add a large excess of non-solvent in the final fractionation since this step was designed to recover the graft polymer free from the unbound low molecular weight material. Thus, the amount of non-solvent added was adjusted to recover about three fourths of the graft polymer in the first fraction. The remainder was then recovered in the second fraction. In all cases, a considerable amount of non-solvent had to be added to recover the unbound low molecular weight polymer after the last of the graft polymer was recovered. The first and second fractions were combined in a few instances where less than three fourths of the polymer was recovered in the first fraction. The value of  $\langle k \rangle$  measured for this mixture was used in testing the data by equation (4), since this relationship requires a value of  $\langle k \rangle$  averaged over all of the graft polymer species. The exact value of  $\langle M_i \rangle$  to be used in equation (5) to compute  $\langle k \rangle$  becomes uncertain, however, when anything less than complete recovery of the graft polymer is achieved, since there may be some change in  $\langle M_i \rangle$  due to the selective loss of certain species of the graft polymer. There would, of course, be no ambiguity if the backbone polymer was monodisperse with respect to molecular weight. The assumption made here is that the value of  $\langle M_i \rangle$  is unchanged by the fractionation.

It is difficult to assess the validity of this assumption. It is made on the basis of the use of a backbone polymer which has a narrow molecular weight distribution. The effect of the fractionation of the graft polymer on  $\langle M_i \rangle$  is not necessarily the same as the direct fractionation of the linear polymer itself, since the branched polymer will tend to be more soluble than linear polymer of the same molecular weight<sup>10, 24</sup>. Thus, a trial fractionation of a mixture of a high molecular weight linear polymer, such as that used for the backbone material, and a low molecular weight polymer, such as that obtained in the graft polymerization, would not necessarily give a direct measure of the change to be expected in the average molecular weight of the backbone material in the graft polymer. It is seen from equation (5) that an error of  $x$  per cent in  $\langle M_i \rangle$  will cause an error of  $x \langle M_i \rangle / (\langle M_g \rangle - \langle M_i \rangle)$  per cent in  $\langle k \rangle$  or  $\langle w \rangle$ .

### *Chain configuration*

The above analysis has implicitly assumed that all of the branch material is bound directly to segments of the backbone polymer, although it is obvious that at least some must attach to other branches instead. This complication will not alter the figures given above, but may be important in a later discussion of the properties of the branched polymers. A simplified analysis of the branch placement shows that if the average ratio of the branch to backbone molecular weight is  $\langle r \rangle_n$ , then  $\langle k^* \rangle$  the average number of branches attached directly to the backbone when a total of  $\langle k \rangle$  branches have been placed is given by

$$\langle k^* \rangle = \sum_{j=0}^{k-1} (1 + j \langle r \rangle_n)^{-1} \quad (7)$$

For the range of  $k$  and  $r$  encountered here, this may be approximated by

$$\langle k^* \rangle \simeq (1/\langle r \rangle_n) \ln [1 + \langle k \rangle \langle r \rangle_n]$$

Inspection of the data in *Table 2* shows that for most of the samples, only *ca.* 15 per cent of the branch material will be attached to other branches, the figure being somewhat greater or smaller for some of the structures. The large percentage of the branches attached to the backbone is a consequence of the small branch to backbone length ratio, and was one reason for confining attention to such conditions. Similarly, the polymerizations were performed in the presence of a chain transfer solvent and limited to low conversions to preclude the possibility of network formation at high conversions.

#### CONCLUSION

A series of branched polymers has been synthesized to obtain a range of branching frequency and length of branches. Moreover, the molecular weight polydispersity of these branched polymers should not be appreciably different from good fractions of a linear polymer.

This method of synthesis offers several advantages. The average length of the branches can be controlled by the chain transfer solvent. Also, the presence of the chain transfer solvent in the quantities used precludes difficulties encountered from the termination of the branches on different substrate molecules by a coupling mechanism<sup>11,12</sup>. The recycle operation allowed a high number of branches to be placed without the formation of a network structure. Approximately eighty to ninety per cent of the branches were attached directly to the backbone, the remainder attaching to other branches. The latter is undesirable, but in no way limits the use of the branched polymer for the investigation to follow. Due to the control over the average length of the branches, the information about the kinetic scheme of the reaction, the use of a fractionated linear backbone polymer, and the estimate available for the average number of branches per molecule, this scheme gives a reasonably well characterized branched polymer.

*We wish to thank the Allied Chemical and Dye Corporation for financial assistance to one of us (G.C.B.) during the period when this work was being completed.*

*University of Michigan,  
Ann Arbor, Michigan*

*(Received December 1962)*

#### REFERENCES

- <sup>1</sup> LONG, V. C. *Ph. D. Thesis*. University of Michigan, 1958
- <sup>2</sup> GLEASON, E. H., MILLER, M. L. and SHEAT, G. F. *J. Polym. Sci.* 1959, **38**, 133
- <sup>3</sup> JONES, M. H. *Canad. J. Chem.* 1956, **34**, 948
- <sup>4</sup> MERRET, F. M. and WOOD, R. I. *Rubb. Chem. Technol.* 1956, **29**, 717
- <sup>5</sup> THURMOND, C. D. and ZIMM, B. H. *J. Polym. Sci.* 1952, **8**, 477
- <sup>6</sup> MANSON, J. A. and CRAGG, L. H. *Canad. J. Chem.* 1952, **30**, 482
- <sup>7</sup> MELVILLE, H. W., PEAKER, F. W. and VALE, R. L. *J. Polym. Sci.* 1958, **30**, 29

- <sup>8</sup> MELVILLE, H. W., PEAKER, F. W. and VALE, R. L. *Makromol. Chem.* 1958, **27**, 140
- <sup>9</sup> MANSON, J. A. and CRAGG, L. H. *Canad. J. Chem.* 1958, **36**, 858
- <sup>10</sup> MANSON, J. A. and CRAGG, L. H. *J. Polym. Sci.* 1950, **33**, 193
- <sup>11</sup> JONES, M. H. *et al. J. Colloid Sci.* 1956, **11**, 508
- <sup>12</sup> SOBOLEVA, J. G., MAKTLETSOVA, N. V. and MEDVEDEV, S. S. *Colloid J., U.S.S.R.*, 1957, **16**, 619
- <sup>13</sup> ALFREY, T. J. *Polym. Sci.* 1949, **4**, 767
- <sup>14</sup> CARLEN, R. B. and SHAKESPERE, M. E. *J. Amer. chem. Soc.* 1946, **68**, 876
- <sup>15</sup> SMETS, G. and CLASEN, M. *J. Polym. Sci.* 1952, **8**, 289
- <sup>16</sup> MELVILLE, H. W., BEVINGTON, J. C. and GUZMAN, G. M. *Proc. Roy. Soc. A*, 1954, **221**, 437; *Nature, Lond.* 1952, **170**, 1026
- <sup>17</sup> GUZMAN, G. W. *An. Soc. esp. Fis. Quim. B*, 1956, **50**, 701
- <sup>18</sup> OKAMURA, S. and MOTOYMA, T. *Chem. High Polymers, Tokyo*, 1958, **15**, 165, 170
- <sup>19</sup> BERRY, G. C. *Ph. D. Thesis*. University of Michigan, 1960
- <sup>20</sup> ZIMM, B. H. *J. chem. Phys.* 1948, **16**, 1093, 1099
- <sup>21</sup> FLORY, P. J. *Principles of Polymer Chemistry*. Cornell University Press: Ithaca. New York, 1953
- <sup>22</sup> HOWARD, R. O. *Ph. D. Thesis*. Massachusetts Institute of Technology, 1952
- <sup>23</sup> BOTELER, B. and FOX, T. G. *Mellon Institute Report*, February 1959
- <sup>24</sup> FLORY, P. J. *J. Amer. chem. Soc.* 1947, **69**, 2893

## APPENDIX

### EFFECT OF GRAFTING ON MOLECULAR WEIGHT DISTRIBUTION

This calculation is intended to show the effect on the molecular weight distribution of placing  $k$  branches of average molecular weight  $M_b$  on a monodisperse backbone polymer with  $n$  sites for branching and of molecular weight  $M_l$ .

If  $p$  is the probability that a site on the backbone contains a branch, then the number fraction of chains with  $i$  branches,  $f_i$ , is given by

$$f_i = \binom{n}{i} p^i (1-p)^{n-i}$$

where  $f_i$  is normalized by

$$\sum_{i=0}^n f_i = 1$$

Calling the average molecular weight of the branched polymer  $\langle M_g \rangle$ , the number average of  $M_g$  is calculated as

$$\langle M_g \rangle_n = \sum_{i=0}^n f_i (M_l + iM_b)$$

$$\langle M_g \rangle_n = M_l + npM_b$$

But  $p$  is simply  $k/n$  for  $n$  very large so that

$$\langle M_g \rangle_n = M_l + kM_b$$

The weight average value of  $M_g$  becomes

$$\langle M_g \rangle_w = \frac{\sum_{i=0}^n M_g^2 f_i}{\sum_{i=0}^n M_g f_i}$$

$$\langle M_g \rangle_n \langle M_g \rangle_w = (M_l + kM_b)^2 + kM_b^2 (1 - k/n)$$

Thus the new value for the ratio of the weight to number average molecular weight is seen to be (for  $k/n$  much less than unity)

$$\langle M_g \rangle_w / \langle M_g \rangle_n = 1 + k / (k + M_i / M_b)^2$$

This result is not strictly applicable here, however, since the backbone polymer used here is not monodisperse, but is instead a narrow molecular weight fraction with  $\langle M_i \rangle_w / \langle M_i \rangle_n$  less than about 1.1. It is assumed, however, that this expression does indicate to a good approximation the relative change to be expected in the weight to number molecular weight average. This final approximation is included in equation (6) given in the text.

# *Solution and Bulk Properties of Branched Polyvinyl Acetates Part III—Intrinsic Viscosity and Light Scattering Measurements*

G. C. BERRY\*, L. M. HOBBS† and V. C. LONG‡

*Light scattering and intrinsic viscosity measurements have been made on three different series of vinyl acetate polymers, one linear and two branched. One of the branched series was obtained by fractionation of a high conversion polymer, the other by a graft polymerization under conditions that allowed structural characterization of the resultant comb-shaped polymers. These data show that the ratio of the mean-square radii of gyration of branched and linear polymers of the same molecular weight is greater in good solvents than the ratio calculated theoretically for a theta solvent. The ratio of the second virial coefficients of the comb-shaped branched and linear polymers of the same molecular weight is equal within experimental error to the ratio of the intrinsic viscosities. The ratio of the intrinsic viscosities of branched and linear polymers is greater in a good solvent than in a theta solvent, in support of inferences from the behavior of the radius of gyration. A theoretical expression for the ratio of the intrinsic viscosities in a poor solvent is obeyed more nearly in a good solvent than in a theta solvent.*

THE preparation of a linear and two series of branched poly(vinyl acetate) polymers has been described elsewhere<sup>1,2</sup>. The linear polymer, series 5, was prepared by the careful fractionation of polymer that had been polymerized to low conversion at a low temperature using a photosensitive initiator<sup>1</sup>. One of the branched samples, series 4, was prepared in like manner from a polymer which had been polymerized to high conversion to give a randomly branched material<sup>1</sup>. The other, series 6, was prepared by a graft polymerization technique to place a specified number of branches of predetermined average chain length on fractions of series 5 which served as a linear backbone polymer with a narrow molecular weight distribution<sup>2</sup>. The purpose of this paper is to consider some of the dilute solution properties of these branched polymers. In particular, the second virial coefficients, the mean square radii of gyration, and the intrinsic viscosities of the branched polymers in thermodynamically good solvents will be compared to the corresponding parameters for linear polymers. The melt viscosities of these branched polymers will be considered elsewhere.

\*Present address: Mellon Institute, Pittsburgh, Pennsylvania.

†Present address: Bennettsville, South Carolina.

‡Present address: E. I. du Pont de Nemours and Co., Wilmington, Delaware.

## EXPERIMENTAL

*Intrinsic viscosity*

Intrinsic viscosities were determined with the viscometers and techniques described in Part I<sup>1</sup>.

The majority of the viscosity measurements were made on benzene solutions. The intrinsic viscosities for the linear polymers in benzene were fitted by the expression  $[\eta] = k_{\eta} \langle M \rangle_w^a$  with  $k_{\eta} = 2.16 \times 10^{-4}$  and  $a = 0.675$ . Sufficient measurements were made in 1,2,4-trichlorobenzene to establish the values of the constants to be  $k_{\eta} = 3.30 \times 10^{-4}$  and  $a = 0.623$ . Intrinsic viscosities  $[\eta]_1$ , measured in benzene can be related to those  $[\eta]_2$  in trichlorobenzene by the expression

$$[\eta]_2 = 0.788 [\eta]_1^{0.924} \quad (1)$$

Equation (1) is used further below. The intrinsic viscosity data for the comb-shaped polymers, series 6, are given in *Table 1*. The data for the linear fractions, series 5, and the randomly branched polymer, series 4, have been given previously<sup>1</sup>.

*Table 1.* Intrinsic viscosity data

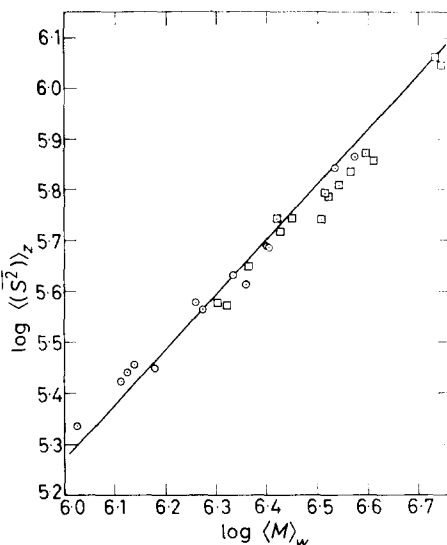
Fraction*	Solvent	$[\eta]$ (dl/g)	$k'$	$k' + \beta$
6-20-1	Benzene	5.20	0.401	0.501
6-20-M		4.18	0.347	0.498
6-30-1		2.96	0.366	0.502
6-30-M		2.77	0.367	0.502
6-40-1		3.18	0.368	0.498
6-41-1		3.64	0.344	0.498
6-41-M		3.34	0.347	0.498
6-50-1		4.52	0.338	0.502
6-51-1		4.48	0.338	0.500
6-51-M		4.15	0.366	0.501
6-60-1		5.76	0.356	0.500
6-70-1		4.00	0.366	0.500
6-71-1		4.32	0.355	0.500
6-80-1		4.27	0.369	0.502
6-81-1		4.04	0.359	0.501
6-90-1		5.01	0.383	0.502
6-91-1		4.19	0.381	0.502
5-2-2		2-Octanone	1.35	—
5-5-3	0.940		—	—
6-60-1	0.950		—	—
6-70-1	0.953		—	—
6-71-1	0.616		—	—
6-80-1	0.696	—	—	

\*Series 5 contains linear polymers.  
Series 6 contains comb-shaped branched polymers.

*Light scattering*

Light scattering measurements were made at the instrument temperature of 34° to 38°C in a Brice-Phoenix light scattering photometer with unpolarized 4358 Å light and a narrow slit system. The photometer was calibrated with solutions of colloidal silica ('Ludox') and a solution of the Cornell standard polymer in toluene (conc. 0.5 g/dl toluene). The cell was checked for symmetry with dilute fluorescein and the deviation from the

Figure 1—Mean square radius of gyration versus molecular weight in trichlorobenzene: □ comb-shaped, branched polymer, series 6; ○ linear polymer, series 5



expected angular dependence was less than one per cent. Both solvent and solution were filtered into centrifuge tubes and centrifuged for about five hours to remove foreign matter. A dust free pipette fitted with a syringe needle and stopcock, and a device to draw the liquid slowly into the pipette by suction was used to remove the clarified liquid in some cases. A syringe with a manually operated plunger was used otherwise. Solvent clarity was judged by visual observation and by the ratio of the intensities of scattered light at  $45^\circ$  and  $135^\circ$  from the exit beam. In no case did this ratio exceed 1.05. Solution clarity was judged visually and by the behaviour of the data. The same pipette was used to transfer the clarified solvent and the clarified solution. The relative intensity of the scattered light was measured at nine angles from  $28^\circ$  to  $135^\circ$ . Butanone, 1,2,4-trichlorobenzene, and methanol were used as solvents. The latter two were distilled over calcium sulphate prior to use.

The data were treated in the usual manner to obtain a double extrapolation to zero angle and infinite dilution<sup>8</sup>. Thus, the data were plotted as  $C/R_\theta$  versus  $\sin^2(\theta/2) + (\text{const.}) \times C$ , where  $R_\theta$  is the excess scattering ratio at  $\theta^\circ$ . The intercept gives  $\langle M \rangle_w^{-1} \times K^{-1}$  where

$$K = 32\pi^3 n^2 (dn/dc)^2 / 3N\lambda_0^4 \gamma_n \quad (2)$$

Here  $\gamma_n$  is a refraction correction for the solvent being used<sup>6</sup>,  $n$  is the solvent refractive index,  $\lambda_0$  is the wavelength of the light used,  $N$  is the Avagadro number and  $dn/dc$  is the refractive index gradient. The  $dn/dc$  values used for the three solvents were 0.080 for butanone<sup>7</sup>, 0.1030 for trichlorobenzene<sup>8</sup>, and 0.1319 for methanol<sup>9</sup>.

The reciprocal scattering curve,  $P^{-1}(\theta)$  normalized to unity at  $\theta=0$ , was computed as  $\lim_{c \rightarrow 0} (C/R_\theta)$  divided by the intercept. The initial slope of the curve multiplied by the factor  $3(\lambda_0/4\pi n_0)^2$  gives the mean square radius of gyration averaged over chain lengths, this average being a  $z$ -average,  $\langle (S^2) \rangle_z$ , in a theta solvent, and close to a  $z$ -average in a good solvent. The second



virial coefficient,  $A_2$ , is obtained from the slope of the curve for  $\lim (C/R_\theta)$ . Since the initial slope of the reciprocal scattering curve is sometimes difficult to establish empirically, the method of Zimm<sup>5</sup> was used to aid in its determination. The same procedure has arbitrarily been used to find the slopes of the  $P^{-1}(\theta)$  curve for both the linear and branched polymer, although

Table 2. Light scattering data for the linear polymer in trichlorobenzene (TCB), butanone (MEK), and methanol (ME)

Fraction	Solvent	$\langle M \rangle_w \times 10^{-6}$	$\langle (S^2) \rangle_z \times 10^4 A^2$	$A_2 \times 10^4$ $cm^3 \text{ mole}/g^2$	$\Phi_1^* \times 10^{-21}$	$A_2 \langle M \rangle_w / [\eta]$
5-2-1	TCB	3.76	73.2	1.75	1.86	155
5-2-1	MEK	3.58	93.4	2.74	—	175
5-2-2	TCB	3.43	69.5	1.94	1.87	176
5-2-2	MEK	3.54	66.0	1.33	—	—
5-2-3	TCB	2.53	49.3	1.90	1.78	157
5-2-3	TCB	2.54	48.5	—	1.84	—
5-3-2	MEK	2.66	68.4	2.30	—	123
5-4-2	TCB	2.27	40.8	2.09	2.20	156
5-4-2	MEK	2.28	61.5	2.64	—	140
5-4-1	TCB	2.16	42.5	2.05	2.00	134
5-5-2	TCB	1.87	36.4	1.99	1.79	142
5-5-2	MEK	1.84	44.0	2.62	—	130
5-5-2	ME	1.90	30.9	1.30	—	—
5-5-3	TCB	1.81	37.5	1.98	1.79	126
5-5-3	TCB	1.50	28.0	1.90	1.82	—
5-5-3	TCB	1.33	27.7	2.32	1.71	132
5-5-3	ME	1.62	24.4	1.14	—	—
5-6-1	TCB	1.29	26.3	2.39	1.62	145
5-6-1	TCB	1.38	28.5	2.29	1.54	150
5-6-2	MEK	1.14	27.2	3.42	—	130
5-6-3	MEK	1.05	17.2	2.35	2.16	134
5-6-3	MEK	0.99	21.5	3.38	—	134
5-7-2	MEK	0.65	14.6	3.26	—	120
5-7-4	MEK	0.44	10.9	3.39	—	109

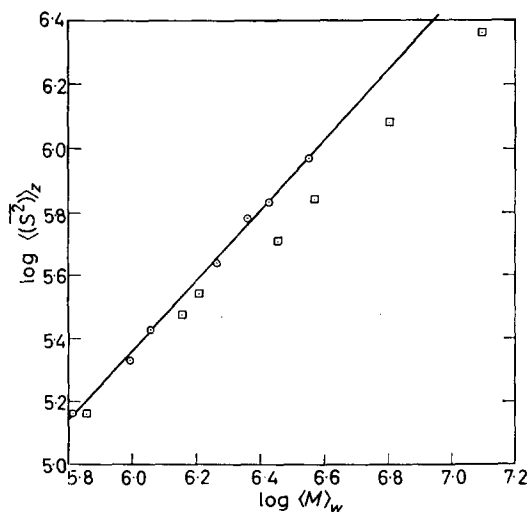


Figure 2—Mean square radius of gyration versus molecular weight in butanone:  $\square$  randomly branched polymers, series 4;  $\circ$  linear polymer, series 5

## PROPERTIES OF BRANCHED POLYVINYL ACETATES III

Table 3. Light scattering data for the randomly branched polymer (series 4) and the comb-shaped polymer (series 6) in butanone (MEK), methanol (ME) and trichlorobenzene (TCB)

Fraction	Solvent	$\langle M \rangle_w \times 10^{-6}$	$\langle (S^2) \rangle_z \times 10^4 \text{ \AA}^2$	$A_2 \times 10^4 \text{ cm}^3 \text{ mole/g}^2$	$\Phi_b \star \times 10^{-21}$	$S_i/S_a$
4-1-1	MEK	12.6	229	0.66	—	—
4-2-3	MEK	6.43	120	1.37	—	—
4-3-2	MEK	3.76	68.8	1.13	—	—
4-4-1	MEK	2.86	50.8	1.33	—	—
4-4-2	MEK	1.64	34.5	1.78	—	—
4-5-1	MEK	1.43	29.9	1.85	—	—
4-4-3	MEK	0.73	14.5	2.39	—	—
4-5-2	MEK	0.73	16.6	2.99	—	—
4-5-3	MEK	0.43	9.1	2.72	—	—
6-20-1	TCB	3.81	—	—	—	—
6-20-M	TCB	2.80	55.4	1.68	1.60	0.615
6-30-1	TCB	2.33	—	—	—	—
6-30-M	TCB	1.68	—	—	—	—
6-30-M	TCB	1.61	—	1.69	—	—
6-40-1	TCB	2.00	37.5	1.78	1.60	0.613
6-41-1	TCB	2.24	44.2	1.69	1.92	0.686
6-41-M	TCB	2.09	37.2	1.69	1.77	0.685
6-50-1	TCB	2.71	55.1	1.78	1.68	0.685
6-51-1	TCB	3.67	68.7	1.47	1.61	0.631
6-51-M	TCB	3.21	54.3	1.62	1.86	0.515
6-60-1	TCB	5.60	111.5	1.56	1.49	—
6-60-1	TCB	5.43	115.8	1.18	1.38	0.575
6-60-1	ME	6.10	99.6	0.99	—	—
6-70-1	TCB	2.65	52.0	1.75	1.24	0.623
6-70-1	ME	2.92	59.8	1.01	—	—
6-71-1	TCB	3.43	60.1	1.29	1.77	0.627
6-80-1	TCB	3.29	61.3	1.52	1.64	0.730
6-80-1	ME	3.58	59.7	1.06	—	—
6-81-1	TCB	4.11	71.8	1.18	1.54	0.615
6-91-1	TCB	3.45	64.1	1.48	1.88	0.715
6-91-1	TCB	3.96	74.1	1.29	1.46	0.624

the assumptions in the derivation of the procedure are most appropriate to a linear polymer. The sharpness of the fractions and the insensitiveness of the slopes to the exact choice of the adjusting parameters probably make any errors introduced here of secondary importance. The light scattering data are given in *Tables 2 and 3*. It is estimated that the experimental errors in  $\langle M \rangle_w$ , are approximately five per cent, and about ten per cent in both  $\langle (S^2) \rangle_z$  and  $A_2$ . Although these limits are estimates and not based on a statistical study, the several repeat runs shown give values which in general are within these limits.

## RESULTS

*Mean square radius of gyration*

The mean square radius of gyration in trichlorobenzene,  $\langle (S^2) \rangle_z$ , is shown as a function of  $\langle M \rangle_w$  for the comb-shaped branched and linear polymers (*Figure 1*). Similar data for the randomly branched and linear polymers in butanone are shown in *Figure 2*. No attempt has been made to correct the radii to the weight average value, which would be more appropriate since

a weight average molecular weight is used; the correction is neglected here since the shape of the curves and ratios to radii at constant  $\langle M \rangle_w$  would not be altered by such a correction if all of the samples studied have about the same degree of polydispersity. The linear polymers are judged to have a low degree of polydispersity on the basis of the fractionation procedure<sup>1</sup>, and it was shown previously that the comb-shaped branched polymers should have about the same degree of polydispersity as the linear material used as a backbone polymer<sup>2</sup>. The randomly branched polymers are liable to be more polydisperse than the linear polymers, even though considerable care was exercised in their fractionation. This is due to the dependence of the solubility on degree of branching as well as molecular weight. In the absence of a reliable estimate for the polydispersity of the randomly branched samples, we have assumed that they possess the same degree of polydispersity as the linear samples. The data for the linear polymers are fitted by the expression  $\langle S^2 \rangle = k_s \langle M \rangle_w^b$ , with  $b$  equal to 1.08 and 1.12 for trichlorobenzene and butanone, respectively, and  $k_s$  equal to 0.062 for trichlorobenzene. It is evident that other values of the exponent may be used to fit the data with the same accuracy as those given here. The values given were chosen to be consistent with the Flory-Fox expression for the intrinsic viscosity. Even if this expression is not strictly valid in good solvents, the weak dependence of the expansion factor on molecular weight allows the method to be used here to good advantage since the intrinsic viscosity data are considerably more precise than those for the radius of gyration. Thus, the exponent  $b$  is related to the exponent  $a$  in the expression  $[\eta] = k_\eta \langle M \rangle_w^a$  by  $b = \frac{2}{3}(a + 1)$ , where  $a$  is taken as 0.623 for polyvinylacetate in trichlorobenzene, and as 0.71 in butanone<sup>7</sup>.

The ratio of the radii for branched and linear polymers of the same molecular weight are given in *Table 4*. The ratio varies from about unity to values near 0.85 for the comb-shaped polymers, being generally somewhat lower for the randomly branched polymers. It is not easy to assess the errors in the ratio  $\langle \langle \overline{S}_b^2 \rangle \rangle_z / \langle \langle \overline{S}_l^2 \rangle \rangle_z$ . The ratios have been computed as  $\langle \langle \overline{S}_b^2 \rangle \rangle_z / k_s \langle M \rangle_w^b$  where  $k_s$  and  $b$  are the constants determined from the dependence of  $\langle \langle \overline{S}_l^2 \rangle \rangle_z$  on  $\langle M \rangle_w$ , and  $\langle \langle \overline{S}_b^2 \rangle \rangle_z$  and  $\langle M \rangle_w$  are the measured parameters for the branched polymer. Thus errors in the ratio may be caused by errors in the determination of  $\langle \langle \overline{S}_b^2 \rangle \rangle_z$  or  $\langle M \rangle_w$ , in the values chosen for  $k_s$  or  $b$ , or in the neglect of polydispersity corrections. The assumption that the branched and linear polymers have about the same degree of polydispersity is made with more confidence for the comb-shaped polymer than for the randomly branched polymer. We tentatively assign error limits of ten per cent to the ratio, recognizing that this may be a conservative estimate, and that this may influence conclusions to be drawn from the data.

#### *The intrinsic viscosity*

The effect of branching on the intrinsic viscosity of the polymers studied here may be seen in *Figure 3*. The intrinsic viscosity of the branched polymer is less than that of a linear polymer of the same molecular weight in all cases. The intrinsic viscosities have not been corrected for shear effects, since the data in Part I<sup>1</sup> indicated that comparisons of the intrinsic viscosities

of branched and linear polymers at a given molecular weight are only negligibly dependent on shear effects. The ratios  $[\eta_b]/[\eta_l]$  have been computed as  $[\eta_b]/k_\eta \langle M \rangle_w^a$  where  $k_\eta$  and  $a$  are the constants determined from the dependenc of  $[\eta_l]$  on  $\langle M \rangle_w$ , and  $[\eta_b]$  and  $\langle M \rangle_w$  are the parameters measured for the branched polymer. The primary source of error in this case is that in  $\langle M \rangle_w$ , so the ratio  $[\eta_b]/[\eta_l]$  should be good to within five to seven per cent. The ratios  $[\eta_b]/[\eta_l]$  are given in *Table 4*.

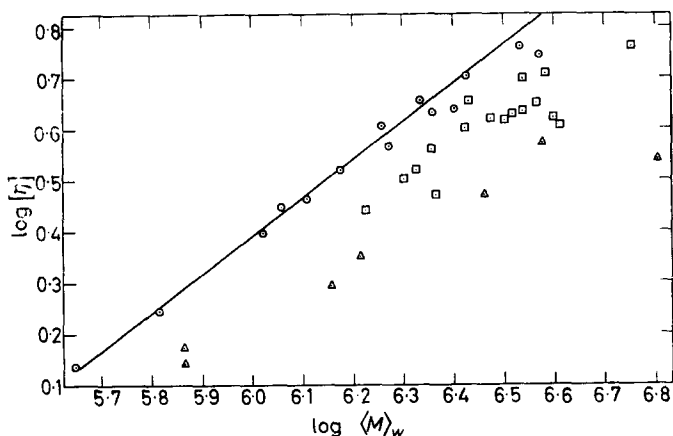


Figure 3—Intrinsic viscosity in benzene versus molecular weight:  $\square$  comb-shaped polymer, series 6;  $\triangle$  randomly branched polymer, series 4;  $\circ$  linear polymer, series 5

#### The second virial coefficient

Figure 4 gives  $A_2$ , the second virial coefficient, as a function of  $\langle M \rangle_w$  for the linear and comb-shaped branched polymers. The data for the linear fractions are fitted by the expression  $A_2 = k_A \langle M \rangle_w^{-\gamma}$  where  $\gamma$  and  $k_A$  are

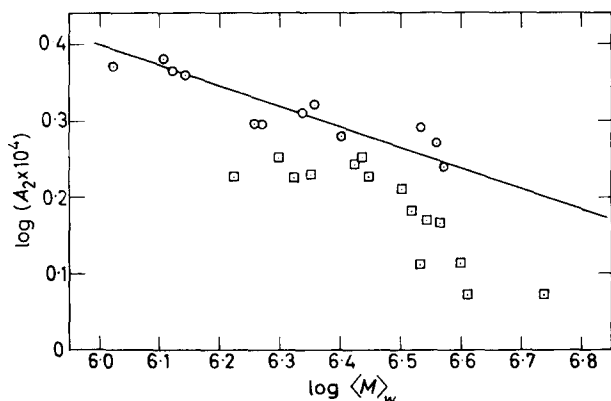


Figure 4—Second virial coefficient versus molecular weight in trichlorobenzene:  $\square$  comb-shaped polymer, series 6;  $\circ$  linear polymer, series 5

0.230 and 0.00594, respectively, for trichlorobenzene. The values of  $(A_2)_b$  for the branched polymer are less than the corresponding values,  $(A_2)_l$  for a

linear polymer of the same molecular weight in every case. The ratio  $(A_2)_b/(A_2)_l$  is given in *Table 4* for the comb-shaped polymers. The  $(A_2)_b/(A_2)_l$  have been computed as  $(A_2)_b/k_A \langle M \rangle_w^{-\gamma}$ , where  $(A_2)_b$  and  $\langle M \rangle_w$  are the parameters for the branched polymer and  $k_A$  and  $\gamma$  are the constants given above. The error in the ratio  $(A_2)_b/(A_2)_l$  is due to experimental errors in both  $(A_2)_b$  and  $\langle M \rangle_w$ , and is estimated to approximately ten to fifteen per cent.

*Table 4.* Parameters for the randomly branched polymer (series 4) and the comb-shaped polymer (series 6)

Fraction	Calc'd $r$	$[\eta_b]/[\eta_l]$	$\langle (S_b^2) \rangle_z / \langle (S_l^2) \rangle_z$	$(A_2)_b / (A_2)_l$	$(S_i/S_a)_b / (S_i/S_a)_l$
4-1-1	0.32	0.345	0.580	—	—
4-2-3	0.36	0.395	0.648	—	—
4-3-2	0.54	0.615	0.678	—	—
4-4-1	0.50	0.590	0.681	—	—
4-4-2	0.58	0.658	0.858	—	—
4-5-1	0.55	0.625	0.870	—	—
4-4-3	0.62	0.705	0.891	—	—
6-20-1	0.616	0.842	—	0.836	—
6-20-M	0.821	0.821	0.966	0.858	0.880
6-30-1	0.556	0.659	—	0.614	—
6-30-M	0.766	0.773	—	0.769	0.734
6-40-1	0.750	0.786	0.949	0.844	0.876
6-41-1	0.670	0.936	0.986	0.804	0.686
6-41-M	0.718	0.804	0.890	0.807	0.978
6-50-1	0.744	0.897	1.01	0.908	0.980
6-51-1	0.524	0.738	0.896	0.799	0.902
6-51-M	0.641	0.738	0.823	0.860	0.734
6-60-1	0.671	0.703	0.924	—	—
6-60-1	0.690	0.703	—	0.709	0.794
6-70-1	0.777	0.804	0.969	0.884	0.886
6-71-1	0.630	0.737	0.853	0.694	0.883
6-80-1	0.693	0.748	0.904	0.809	—
6-81-1	0.553	0.666	0.834	0.701	0.878
6-90-1	0.736	0.848	0.898	0.797	1.02
6-91-1	0.641	0.671	0.902	0.714	0.896

## DISCUSSION

### *Mean square radius of gyration*

It is of interest to compare the ratio of the radii of gyration of branched and linear polymers of a given molecular weight in a good solvent to the corresponding ratio calculated for theta-solvent conditions. It will be seen that the dimensions of the branched polymers increase at a faster rate than those of a linear polymer of corresponding molecular weight as the thermodynamic goodness of the solvent increases. First, however, we must determine the relative dimensions in a theta solvent for a basis of comparison. The latter may be computed if one assumes that random flight statistics are obeyed. This calculation has been given by Zimm and Stockmayer<sup>10</sup> for a randomly branched polymer. The ratio may be obtained for the comb-shaped branched polymers, by use of the Kramers theorem<sup>11</sup>, which

gives for a chain of  $n$  equivalent segments

$$g = (6/n^3) \sum i(n-i) \quad (3)$$

where  $g$  is the ratio of the mean square radii for branched and linear polymers in a theta solvent. The sum is taken over all possible separations of the branched chain into two parts, containing  $i$  and  $(n-i)$  segments respectively. For purposes of this calculation, the branched polymer containing  $n_b$  segments is assumed to have  $k$  branches, each with  $(n_b - n_i)/k$  segments, placed equidistantly on a backbone of  $n_i$  segments. This idealization has negligible effect on the results for the kind of branched polymers of interest here. Thus, the sum of equation (3) for the comb-shaped polymer yields the result<sup>12</sup>

$$g(k, x) = (1 + kx)^{-3} \left\{ (3k - 2) kx^3 + (k + 2) kx^2 + \frac{2k + 1}{k + 1} kx + 1 \right\} \quad (4)$$

where  $x$  is the ratio of the branch length to the backbone length,  $(n_b - n_i)/kn_i$ . For all of the comb-shaped polymers considered here ( $x \leq 0.03$ ), this expression is closely approximated by

$$g \simeq 1/(1 + kx) = n_i/n_b \quad (5)$$

Orofino<sup>13</sup> has used a different technique to obtain an expression for  $g$  for comb-shaped polymers with a random distribution of branch sites on the backbone, which reduces to equation (5) for the kind of branched polymers of interest here. It should be noted that the presence of a few branches attached to other branches rather than to the backbone, as discussed in Part II, will not affect the ratio  $n_i/n_b$ , and thus presumably have little effect on  $g$ , although it would require a separate calculation to prove this.

Values of  $g$  can now be computed for each of the comb-shaped branched polymers of series 6 by use of equation (5) and the data reported in a previous paper<sup>2</sup>. These values are given in Table 4. The  $g$  values are as reliable as the values of  $\langle M \rangle_w$  for the comb-shaped polymer, and the backbone polymer. Thus, a primary source of uncertainty in  $g$  is the molecular weight of the backbone polymer. The molecular weight of the polymer used as the backbone material is, of course, as well known as that of the final graft polymer. There remains, however, the possibility of a difference between the molecular weight of the initial and final backbone material due to selective loss of material in some of the necessary fractionations. We assume here in the calculation of  $g$ , that the average molecular weight of the backbone material is given by that of the initial polymer. (See ref. 2 for a further discussion of this point.) Any error in the backbone molecular weight will be carried over directly to the estimate of  $g$ . The effect of molecular weight polydispersity on  $g$  is here neglected. The experimentally determined ratio of the radii is of course nearest to a  $z$ -average, while  $g$  has been determined using weight average molecular weights. Orofino<sup>13</sup> has given a form for  $\langle g \rangle_z$  for a comb-shaped molecule which is useful in estimating the error made in computing  $\langle g \rangle_z$  from equation (5) with weight average molecular weights, although not strictly applicable to these samples. The error will be negligible for all cases of interest here.

It is evident from *Table 4* that the values observed for  $\langle(\overline{S}_b^2)\rangle_z/\langle(\overline{S}_l^2)\rangle_z$  for the comb-shaped polymers, series 6, in the good solvent are greater than the calculated  $g$ , that is, the dimensions of the branched polymers have increased more than those of the linear molecules in passing from theta solvent to good solvent conditions. It is important to remember that the comb-shaped polymers should have about the same degree of polydispersity as the linear chains<sup>2</sup>, so that this difference should not be due to greater polydispersity in the branched polymer. A similar result is seen for the randomly branched polymers of series 4, but here the values of  $g$  must be estimated from viscosity data by a method discussed later, and the polydispersity of the branched chains might be greater than the linear polymers. An attempted empirical correlation of  $\langle(\overline{S}_b^2)\rangle_z/\langle(\overline{S}_l^2)\rangle_z$  with  $g$  is shown in *Figure 5*. The solid line drawn through the data is based on a theory to be described below. The lower dashed line shows where the data should lie if the ratio of the radii were equal in good and theta solvents.

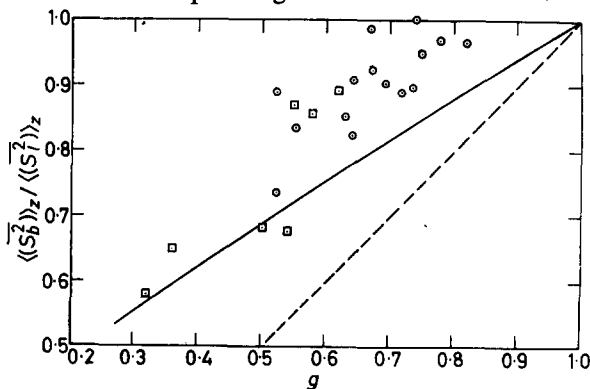


*Figure 5*—Ratio of the mean square radii of gyration for branched and linear polymers in a good solvent versus  $g$ , the same ratio calculated for a theta solvent:  $\circ$  comb-shaped polymers, series 6, in trichlorobenzene;  $\square$  randomly branched polymers, series 4, in butanone. Broken curve is for the ratio in a good solvent equal to that in a theta solvent; the full curve is calculated from equation (11) with  $C_b=C_l$

In order to facilitate discussion of the expansion effect observed here, it is convenient to introduce expansion factors,  $\alpha$ , defined as  $\alpha^2 = (\overline{S}^2)/(\overline{S}^2)_0$ , where  $(\overline{S}^2)$  and  $(\overline{S}^2)_0$  are the mean square radii in thermodynamically non-ideal and ideal (i.e. theta) solvents, respectively. The ratio  $(\alpha_b/\alpha_l)^2$  is then equal to  $(\overline{S}_b^2)/g(\overline{S}_l^2)$ , where the subscripts  $b$  and  $l$  refer to branched and linear polymers, respectively. Unfortunately, there are as yet no rigorous theories which allow prediction of  $\alpha_b/\alpha_l$  for polymers in very good solvents. The first-order perturbation theory of Fixman<sup>14</sup> may be used to obtain an expression for  $\alpha_b/\alpha_l$  for both comb and star-shaped molecules, but the results are limited to solutions which are nearly ideal (to be published). The ratio  $\alpha_b/\alpha_l$  is predicted to be greater than unity for molecules of these shapes in the limit as  $\alpha$  approaches unity (in contradiction to Fixman's result for a four branched star, which is apparently in error).

Ptitsyn<sup>15</sup> has proposed an approximate derivation to account for the effect of branching on  $\alpha$ . The derivation, which closely follows Fixman's<sup>14</sup> suggestion of a generalization of Flory's theory<sup>16</sup> for linear chains, may be given as follows. It is assumed that the number of molecular configurations with radius of gyration  $S$  in  $dS$  is given by

$$F(S) = W(S) 4\pi S^2 \exp[-E(S)/kT] \quad (6)$$

where  $W(S)$  is the probability distribution of  $S$  in the absence of volume effects, and  $E(S)$  is the energy associated with  $\rho(r)$ , the segment density of the polymer chain at a distance  $r$  from the centre of gravity. For a spherically symmetric  $\rho(r)$ ,  $E(S)$  is given by

$$E(S) = n^2 \beta kTC/S^3 \quad (7)$$

where  $\beta$  is the excluded volume integral for a pair of segments, and  $C$  is a constant given by

$$C = \frac{S^3}{2n^2} \int 4\pi r^2 \rho^2(r) dr \quad (8)$$

The expansion coefficient may then be obtained<sup>17</sup> by multiplying  $F(S)$  by  $S^2$  and integrating over all  $S$ . (The integration is not rigorous, but approximations are made according to techniques discussed in ref. 17). The result is

$$\alpha^5 - \alpha^3 = n^2 \beta C / (S^2)^{3/2} \quad (9)$$

where  $C$  is to be determined from equation (8). The familiar result of Flory<sup>16</sup> obtains if a gaussian distribution is assumed for  $\rho(r)$ . If we assume that branched and linear chains are characterized by the same  $W(S)$ , but different  $\rho(r)$ , then

$$\frac{\alpha_b^5 - \alpha_b^3}{\alpha_l^5 - \alpha_l^3} = \frac{C_b}{C_l} \frac{1}{g^{3/2}} \quad (10)$$

where  $C_b$  and  $C_l$  are the numerical constants computed from equation (8). Krigbaum and Trementozzi<sup>18</sup> have pointed out that equation (10), with  $C_b = C_l$ , will be obtained directly from Flory's expression for  $\alpha^5 - \alpha^3$  for a linear polymer if this result is assumed to hold for branched chains with no change in certain parameters.

Unfortunately, the constants  $C_b$  and  $C_l$  are not readily obtained since the correct segment density distribution of the chain with excluded volume is not known. Ptitsyn assumes the same  $\rho(r)$  for both types of chains, giving  $C_b = C_l$ . The ratio  $C_b/C_l$  could be treated as a parameter to be determined by forcing agreement of equation (10) with the first-order perturbation theory of Fixman for a branched molecule. This procedure gives  $C_b/C_l$  equal to 0.519 for a star molecule of four equal branches. Alternatively, the calculation can be altered by using more exact segment density distributions for the branched and linear chains. Thus, it is known that the sum of  $n$  gaussian functions can correctly describe the segment density distribution of a random flight chain, though it is still in error for a chain with excluded volume<sup>14,19</sup>, Casassa and Orofino<sup>20</sup> have obtained  $C_l$  using this approximation for  $\rho(r)$ , and it is possible to do the same calculation for a star-



shaped polymer using the  $\rho_0(r)$  given by Fixman and Stockmayer<sup>19</sup>. As for the linear chain, it is assumed that the  $\rho(r)$  needed in equation (7) for the segment distribution in a good solvent is approximated by the  $\rho_0(r)$  for a theta solvent with the modification that  $\rho(r)$  is normalized to give the radius in a good solvent rather than in a theta solvent. We have done this calculation in the Appendix, and find the ratio  $C_b/C_l$  is given by 1.09, 1.20 and 1.61 when the number of legs in the star-shaped molecule is equal to three, four and eight, respectively.

The reason for the difference between the ratio  $C_b/C_l$  evaluated in these two ways is not clear. It may reflect inadequacies in the approximations made to obtain equation (10), or it may be that one simply cannot expect the constant obtained from the first order perturbation theory to be adequate for  $\alpha$  much larger than unity. It may be noted that values of  $\alpha_b/\alpha_l$  determined from equation (10) differ only negligibly for low  $\alpha$  for these two choices of  $C_b/C_l$ . We point out that equation (10) predicts that for a given  $g$ , the deviation of  $\alpha_b/\alpha_l$  from unity will be strongly dependent on the deviation of  $\alpha_l$  from unity. Thus a highly branched molecule in a solvent such that  $\alpha_l$  is near unity should exhibit an  $\alpha_b/\alpha_l$  ratio only slightly larger than unity.

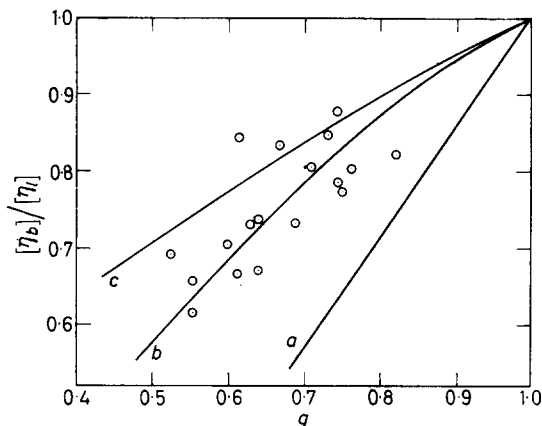
In view of the discrepancies between these two treatments, and the lack of an estimate for the segment density distribution for comb-shaped or randomly branched polymers, we will tentatively compare equation (10) with  $C_b/C_l$  equal to unity to the data of this study. Thus, the line drawn in *Figure 5* has been obtained by setting  $C_b=C_l$  in equation (10), and using the values of  $\alpha_l$  appropriate to the molecular weight of the polymers being studied. It appears that this function provides a reasonable fit to the data, although considerable scatter is evident and the data do not cover a sufficient range to adequately test the theory. Qualitatively, however, the data for the comb-shaped polymer suggest that  $C_b/C_l$  might be somewhat greater than unity. The data can also be fitted within experimental error by the expression  $(\overline{S}_b^2)/(\overline{S}_l^2) \simeq g^{0.4}$ , which is the limit of equation (10) with  $C_b=C_l$  as  $\alpha$  becomes large. (Ratios of  $\alpha_b/\alpha_l$  computed from equation (10) and from the limit of equation (10) for large  $\alpha$  agree within about four per cent when  $g$  and  $\alpha$  are 0.6 and 1.9 respectively, so the limit is rapidly approached.) It should be noted, however, that in general one expects the deviation of  $(\overline{S}_b^2)/(\overline{S}_l^2)$  from  $g$  to depend on the solvent power, i.e. on some parameter such as  $\alpha_l$ . The observation that the branched polymers might be more extended in good solvents than linear polymers of the same molecular weight has been suggested by some previous studies<sup>21-24</sup>, but the uncertainties in polymer structure and the degree of polydispersity of the branched fractions complicated interpretation of the data. The data for the comb-shaped polymers provide evidence for the greater extension of the branched chains, at least for this type of structure. These data are supported by those on the randomly branched polymers, although here the specification of the structure and the degree of polydispersity is less certain. The values of  $g$  (and hence of  $\alpha_b/\alpha_l$ ) assigned to the branched polymers are obtained from a calculation based on their inferred structure rather than by direct measurements of the radii under theta solvent conditions. Thus, although the radii of the branched polymers are definitely

larger than one would expect if the branched and linear molecules were equally expanded, the correct functional dependence of this effect is less certain. It should also be mentioned that these data could also be affected if some unknown impurity, such as hydroxyl groups, were present in the polymer although available evidence indicates the lack of such impurities<sup>2</sup>.

### The intrinsic viscosity

It has been suggested that the ratio  $[\eta_b]_0/[\eta_l]_0$ , where  $[\eta_b]_0$  and  $[\eta_l]_0$  are the intrinsic viscosities of branched and linear polymers of the same molecular weight in a theta solvent, is a function only of the parameter  $g$ , written here as  $f_0(g)$ <sup>19,24</sup>. One may reasonably expect this ratio in a good solvent to depend on  $\alpha$  as well, that is  $f(\alpha, g)$ . It was originally suggested<sup>21</sup> that  $f_0(g)$  could be approximated by  $g^{3/2}$  due to the dependence of the intrinsic viscosity on the volume of the polymer molecule. Fixman and Stockmayer<sup>19</sup> and Zimm and Kilb<sup>25</sup> have obtained theoretical estimates of  $f_0(g)$ , which attempt to account for hydrodynamic effects the above estimate ignores. Both of these derivations are based on star-shaped molecules. In particular, Fixman and Stockmayer have determined the effect of branching on the translational friction constant. It is then assumed that the ratio of the intrinsic viscosity of branched and linear polymers will be proportional to  $h^3$ , the corresponding ratio of the cube of the effective hydrodynamic radii, and that the form of the result will not be too dependent on the particular model chosen for the branched polymer. Thus, the result gives  $f_0(g) = h^3$  where  $h$  is a function of  $g$  (see *Figure 6*). Zimm and Kilb have given a

*Figure 6*—Ratio of the intrinsic viscosities of comb-shaped branched and linear polymers versus  $g$ , the ratio of the radii of gyration calculated for a theta solvent. Curves *a*, *b* and *c* give  $[\eta_b]/[\eta_l]$  equal to  $g^{3/2}$ ,  $h^3$  and  $g^{1/2}$ , respectively



direct calculation of the intrinsic viscosity of a star-shaped molecule in a theta solvent taking approximate account of hydrodynamic interactions. Their results give  $f_0(g) \approx g^{1/2}$  if hydrodynamic interactions are included, and  $f_0(g) = g$  if they are ignored. It is again assumed that the result is good for all types of branched polymers. It is to be emphasized that these results are limited to the behaviour of polymers in an ideal solvent. These functions are given in *Figure 6* along with the experimental values of  $[\eta_b]/[\eta_l]$  observed for the comb-shaped polymers in a good solvent as a function of  $g$ . The

data are in general agreement with the theoretical functions  $f_0(g)$  equal to  $h^3$  or  $g^{1/2}$ . A similar result (not shown in *Figure 6*) is obtained with some data of Melville *et al.*<sup>26</sup> on comb-shaped polymers, if equation (5) is used to compute  $g$ , and if the  $[\eta]/\langle M \rangle_w$  relationship given above is used in place of that given by Melville. (The expression given by them leads to ratios of  $[\eta_b]/[\eta_l]$  greater than unity for some of their data.) This correlation of the ratio  $[\eta_b]/[\eta_l]$  determined in a good solvent with  $f_0(g)$  is unexpected in view of the dependence of  $[\eta]$  on the radius of gyration, and of the differences observed in the expansion factors for branched and linear polymers. Thus, the intrinsic viscosities of a linear polymer in a good solvent may be represented by the relationship

$$[\eta_l] = 6^{3/2} \Phi q_i \alpha_i^{m_i} \langle (S^2)_0 \rangle_z^{3/2} / \langle M \rangle_w \quad (11)$$

where the subscript zero refers to parameters in an ideal solvent,  $q$  is the polydispersity factor<sup>6</sup> (taken to be identical for the linear and comb-shaped branched polymers), and  $\Phi$  is a constant equal to  $2.87 \times 10^{21}$

$$[\eta_b] = 6^{3/2} \Phi q_b \alpha_b^{m_b} \langle (\overline{S^2})_0 \rangle_z^{3/2} f_0(g) / g^{3/2} \langle M \rangle_w \quad (12)$$

( $[\eta]$  in units of deciliters per gramme,  $(S^2)$  in  $\text{cm}^2$ ). We assume an analogous form for  $[\eta_b]$ , given by equation (12). Equation (11) has been derived on the basis of statistical calculations rigorously limited to polymer chains in very poor solvents<sup>27-29</sup>. The quantity  $m_b$  in equation (12) is defined by the relationship  $\alpha_b^{m_b} = [\eta_b]/[\eta_b]_0$ . Combination of equations (11) and (12) leads to the result (the branched and linear chains are assumed to have the same degree of polydispersity)

$$([\eta_b]/[\eta_l]) / ([\eta_b]_0/[\eta_l]_0) = \alpha_b^{m_b} / \alpha_l^{m_l} \quad (13)$$

The value of  $m_l$  is predicted to be about 2.5 for relatively good fractions of a linear polymer<sup>30</sup>. This predicted deviation of  $m_l$  from the value of 3 given in the Flory-Fox expression<sup>31</sup> has been observed experimentally<sup>30, 32-34</sup>. Since the statistical calculations leading to equation (11) are limited to poor solvents however, one can only treat  $m_l$  as a parameter to be determined empirically in good solvents, its value probably being in the range 2.4 to 3. If  $m_b = m_l = m$ , then equation (13) indicates that  $[\eta_b]/[\eta_l]$  is greater than  $[\eta_b]_0/[\eta_l]_0$  to the extent that  $(\alpha_b/\alpha_l)^m$  exceeds unity. Some values of  $[\eta_b]_0$  and  $[\eta_l]_0$  were measured in 2-octanone at 29.8°C, which is reported to be a theta solvent for linear polyvinyl acetates<sup>35</sup>, to allow this prediction to be checked. The data, which are given in *Table 5*, are seen

Table 5

Fraction	$[\eta_b]/[\eta_l]$ Observed in benzene	$[\eta_b]_0/[\eta_l]_0$ Observed in 2-octanone (theta solvent)	$[\eta_b]/[\eta_l]$ Calculated from eq. (13) with $m_b = m_l = 2.5$
6-60-1	0.703	0.506	0.741
6-70-1	0.804	0.745	0.983
6-71-1	0.737	0.428	0.625
6-80-1	0.748	0.498	0.699

to show the trend expected from equation (13) with  $m_b = m_l = 2.5$ , although the agreement is not perfect. The discrepancy is probably caused by the error in determining the radii by light scattering, which would be sufficient to cause the scatter observed. Alternatively, it could be due to differences in the theta conditions for the branched and linear chains, to the assumption that  $m_l = m_b$  or to errors in estimating  $g$ . The data of Thurmond and Zimm<sup>21</sup> on the intrinsic viscosities of randomly branched polystyrene fractions in butanone and a theta solvent are of interest here since these data showed no appreciable deviation of  $[\eta_b]/[\eta_l]$  from  $[\eta_b]_0/[\eta_l]_0$ . This is not unexpected, however, in view of the lower values of  $\alpha_l$  for linear polymers of molecular weight corresponding to that of the branched polymer. Thus, if we use the estimated  $(\alpha_b/\alpha_l)$  from equation (10) with  $C_b/C_l$  equal to unity, then  $[\eta_b]/[\eta_l]$  is found to exceed  $[\eta_b]_0/[\eta_l]_0$  by only ten per cent for the branched polymer of highest molecular weight, becoming essentially unity for the lower fractions in their study.

It is also observed, however, as pointed out above, that the experimentally observed values of  $[\eta_b]/[\eta_l]$  are in essential agreement with the theoretical function of  $f_0(g)$  calculated from hydrodynamic theories, whereas the experimental values of  $[\eta_b]_0/[\eta_l]_0$  are smaller than these theories would indicate. While it is true that the theoretical calculation of  $f_0(g)$  is based on the assumption of a star-shaped molecule, this large  $\alpha$  deviation of the experimental  $f_0(g)$  from the value estimated from the theory is surprising. We do not know if the discrepancy indicates that results based on the star-shaped model are inapplicable for the kinds of branched structure studied here, or if in fact there is a systematic error in the estimate of  $g$  for the comb-shaped polymers.

In view of the agreement between the experimental data for  $[\eta_b]/[\eta_l]$  and the theoretical function of Stockmayer and Fixman for  $f_0(g)$  in those cases where  $g$  could be determined from equation (5) and the known structural parameters, it was decided to use this function to obtain  $g$  for the randomly branched polymers. The values of  $g$  listed in *Table 4* for these polymers were obtained in this manner.

#### *The second virial coefficient*

Rigorous expressions for  $A_2$  in terms of molecular parameters have been developed for linear polymers<sup>3,6</sup>, but they are limited to solutions that are nearly ideal. The problem is, of course, less advanced for branched structures, but a rigorous calculation based on a cruciform molecule indicates that the ratio  $(A_2)_b/(A_2)_l$  should be less than unity in very poor solvents<sup>19</sup>. Fixman and Stockmayer<sup>19</sup> have suggested that the results of some approximate theories, which utilize an average potential obtained by an averaging over all configurations of two molecules separated by a given distance, may be useful in discussing the behaviour of branched polymers. The suggestion is based on their observation that the segment density distribution used in the averaging process is not too different for branched and linear polymers. The approximate theories give  $A_2$  as a function of the parameter  $\beta n^2/(\bar{S}^2)^{3/2}$ , where the function decreases monotonically from unity as the argument increases from zero. Since the parameter  $\beta$  is presumed to be independent of structural variations in a given polymer,

differences in  $A_2$  may be assigned to differences in the radius of gyration for branched and linear polymers. Thus, to the extent that  $(\bar{S}_b^2)$  is less than  $(\bar{S}_l^2)$  at a given molecular weight,  $(A_2)_b$  will be less than  $(A_2)_l$ . In particular, Casassa and Markovitz<sup>37</sup> have given a function of this form which is useful here. It is of interest to note that values of  $(A_2)_l$  calculated from this theory using our values for the radii in a good solvent and those of Schultz<sup>7</sup> in a theta solvent are within twenty per cent of the observed values, but that the calculated values of  $(A_2)_l$  are not quite as dependent on  $\langle M \rangle_w$  as the observed values. This function approaches an asymptotic limit proportional to  $(\bar{S}^2)^{3/2}/\beta n^2$  for values of the argument exceeding 3 or 4. This expression may be incorrect even in the limit of very good solvents since this calculation, like all such treatments to date, does not treat terms due to multiple interaction contacts in a rigorous manner. It may be, however, that the ratio of the asymptotic expressions for  $A_2$  for branched and linear polymers will not be too bad. To this approximation

$$(A_2)_b/(A_2)_l = g^{3/2} (\alpha_b/\alpha_l)^3 \quad (14)$$

If the limit of equation (14) for large  $\alpha$  is substituted into equation (15), then the ratio  $(A_2)_b/(A_2)_l$  is approximated by  $g^{1/2}$ . A similar result has been noted by Krigbaum and Tremontozzi<sup>18</sup>. Thus, the ratio  $(A_2)_b/(A_2)_l$  should approximate the ratio  $[\eta_b]/[\eta_l]$  since we find this to be near  $g^{1/2}$ . This is, in fact, close to the observed behaviour for the ratio, as seen in *Table 4*, indicating some degree of internal consistency to the data observed for the intrinsic viscosity, the virial coefficient and the radii of the branched polymer.

The values of  $A_2$  for the linear polymers have been examined in terms of the dimensionless group  $A_2 \langle M \rangle_w / [\eta]$  which should increase with  $M$  in the usual solvents and become constant for sufficiently good solvents. *Table 2* gives this group as a function  $\langle M \rangle_w$  for some linear fractions. The average value of  $A_2 \langle M \rangle_w / [\eta]$  is found to be 146 in trichlorobenzene and 134 in butanone, in good agreement to the values of 142 found by Chinai *et al.*<sup>38</sup> in acetone, and 139 by Schultz<sup>7</sup> in butanone. A slight trend with  $\langle M \rangle_w$  is evident, however, indicating that the assumptions required for strict constancy of the group are not fulfilled.

#### Reciprocal particle scattering curve

In principle at least, the presence of branching can be detected from the shape of the reciprocal scattering curve if the size of the macromolecule is such that both the initial and asymptotic slopes of the curve are experimentally observable. It has been estimated that  $(\bar{S}^2)$  should be in the range  $10^5$  to  $15 \times 10^5 A^2$  for this condition to be fulfilled<sup>38</sup>. Calling  $S_i$  and  $S_a$  the initial and asymptotic slopes of the  $P^{-1}(\theta)$  curve, respectively, then for a branched polymer<sup>12, 40</sup>,

$$(S_i/S_a)_b = (2/3) [\langle (\bar{S}_b^2) \rangle_z / \langle (\bar{S}_l^2) \rangle_z] [\langle M \rangle_z / \langle M \rangle_w] \mu \Gamma(\mu) \quad (15)$$

where  $(S_l^2)$  is the radius of a linear polymer of the same molecular weight as the branched polymer for which the  $P^{-1}(\theta)$  curve is obtained,  $\mu$  is a constant for a given polymer-solvent system, and  $\Gamma$  is the gamma function. A similar expression written for the linear molecule has the term involving

the ratio of the radii equal to unity. It was shown previously that the branched polymers prepared by the grafting procedure have about the same degree of polydispersity as the linear polymer used as the backbone molecule<sup>2</sup>. It is of interest, then, to compare the ratio of  $(S_i/S_a)_b$  for these polymers to  $(S_i/S_a)_l$  measured for the linear polymer used as the backbone. This ratio should be given by  $\langle(S_b^2)\rangle_z/\langle(S_l^2)\rangle_z$ . These data are given in Table 4. An appreciable scatter is evident, which is to be expected due to the uncertainty in determining the asymptotic slope of the  $P^{-1}(\theta)$  curve, but a general agreement can be observed between the ratio  $(S_i/S_a)_b/(S_i/S_a)_l$  and the ratio of the radii.

#### The Flory constant

The value of  $\Phi^*$  in the expression  $[\eta]=6^{3/2}\Phi^*S^3/M$  has frequently been used as an indication of the presence of branching.  $\Phi^*$  is expected to be about  $2.1 \times 10^{21}$  for linear polymers in the usual good solvents<sup>30, 31</sup>. It has been pointed out by Kurata *et al.*<sup>28</sup> that this is the value one expects from equation (11) if  $\alpha_i$  and  $m_i$  are about 1.4 and 2.5 respectively, and if one assumes the polymer is a reasonably good fraction. The best value of  $\Phi^*$  for the data in trichlorobenzene is about  $2.2 \times 10^{21}$ , in good agreement with the expected value. Combination of equations (11) and (12) for polymers of the same molecular weight yields the result

$$\frac{\Phi_b^*}{\Phi_l^*} = \frac{q_b}{q_l} \frac{f(\alpha, g)}{g^{3/2}} \left(\frac{\alpha_l}{\alpha_b}\right)^3 \quad (16)$$

where  $f(\alpha, g)$  is defined as  $[\eta_b]/[\eta_l]$ . If  $(\alpha_l/\alpha_b)^3$  is approximated by the limit of equation (14) for large  $\alpha$ , and  $f(\alpha, g)$  taken as  $g^{1/2}$ , then  $\Phi_b^*/\Phi_l^* = q_b/q_l$ . Thus, the ratio is dependent on the degrees of polydispersity of the branched and linear polymers if measurements are made in good solvents, rather than on the presence of branching. We note that the values of  $\Phi_b^*$  observed here were in general only slightly lower than the average for  $\Phi^*$ . In view of the deviation of  $\alpha_b/\alpha_l$  from unity, it seems that the observation that  $\Phi_b^*$  exceeds the normal value of  $\Phi^*$  must in itself be regarded as an unreliable indication of the presence of branching.

#### CONCLUSION

We have presented data on two types of high molecular weight branched polymers, one of these polymers being synthesized in such a way that its characteristics are, in principle at least, well known. There are, of course, many factors which may cause difficulty in a study of this type, chemical impurities, slight gel content, polydispersity, to mention a few of the more serious complications. We have endeavoured to eliminate or account for these factors as effectively as possible. The data have been examined in terms of existing theories which are summarized in such detail as seemed necessary for the analysis. We may expect further studies on model branched polymers prepared by anionic methods, which offer some hope of eliminating or reducing the complications encountered here. It will be

of interest, then, to examine data for polymers of different chemical constitution and of high enough molecular weight to give pronounced excluded volume effects to ascertain the universality of the effects found here.

*We wish to thank the Goodyear Tire and Rubber Co. for their contribution to the Michigan Memorial Phoenix Project and the Allied Chemical and Dye Corporation for the financial assistance to one of us (G.C.B.) which made this work possible. We also wish to thank Professor L. H. Cragg of the University of Alberta, and Dr J. A. Manson for their helpful suggestion, and Dr C. H. Lu and Mr M. M. Gurvitch for their aid with portions of the experimental work.*

*Michigan Memorial Phoenix Project  
and Chemical Engineering Department,  
University of Michigan,  
Ann Arbor, Michigan*

*(Received December 1962)*

#### REFERENCES

- <sup>1</sup> HOBBS, L. M. and LONG, V. C. *Polymer, Lond.* 1963, **4**, 479
- <sup>2</sup> BERRY, G. C. and CRAIG, R. A. *Polymer, Lond.* 1964, **5**, 19
- <sup>3</sup> HOBBS, L. M., KOTHARI, S. C., LONG, V. C. and SUTARIA, G. C. *J. Polym. Sci.* 1956, **22**, 123
- <sup>4</sup> MANSON, J. A. and CRAGG, L. H. *J. Polym. Sci.* 1958, **33**, 193
- <sup>5</sup> ZIMM, B. H. *J. chem. Phys.* 1958, **18**, 1616
- <sup>6</sup> CARR, C. L. and ZIMM, B. H. *J. chem. Phys.* 1958, **18**, 1616
- <sup>7</sup> SHULTZ, A. R. *J. Amer. chem. Soc.* 1954, **76**, 3422
- <sup>8</sup> GRAESSLEY, W. W. Private communication
- <sup>9</sup> BILLMEYER, F. W. Private communication
- <sup>10</sup> ZIMM, B. H. and STOCKMAYER, W. H. *J. chem. Phys.* 1949, **17**, 1302
- <sup>11</sup> KRAMERS, H. A. *J. chem. Phys.* 1946, **14**, 415
- <sup>12</sup> BERRY, G. C. *Ph.D. Thesis*, University of Michigan, Ann Arbor, Michigan, 1960
- <sup>13</sup> OROFINO, T. *Polymer, Lond.* 1961, **2**, 295 and 305
- <sup>14</sup> FIXMAN, M. *J. chem. Phys.* 1955, **23**, 1656
- <sup>15</sup> PTITSYN, O. B. and ÉIZNER, Y. E. *Zh. fiz. Khim., Mosk.* 1958, **32**, 2464
- <sup>16</sup> FLORY, P. J. *J. chem. Phys.* 1949, **17**, 303
- <sup>17</sup> GRIMLEY, T. B. *Trans. Faraday Soc.* 1954, **55**, 681
- <sup>18</sup> KRIGBAUM, W. R. and TREMENTOZZI, A. S. *J. Polym. Sci.* 1958, **28**, 295
- <sup>19</sup> FIXMAN, M. and STOCKMAYER, W. H. *Ann. N.Y. Acad. Sci.* 1953, **57**, 334
- <sup>20</sup> CASASSA, E. F. and OROFINO, T. A. *J. Polym. Sci.* 1959, **35**, 553
- <sup>21</sup> THURMOND, C. D. and ZIMM, B. H. *J. Polym. Sci.* 1952, **8**, 477
- <sup>22</sup> FLORY, P. J. and SCHAEFGEN, J. R. *J. Amer. chem. Soc.* 1948, **70**, 2709
- <sup>23</sup> WALES, M., MARSHALL, P. A. and WEISSBERG, S. G. *J. Polym. Sci.* 1953, **10**, 229
- <sup>24</sup> TREMENTOZZI, A. S. *J. Polym. Sci.* 1959, **36**, 113
- <sup>25</sup> ZIMM, B. H. and KILB, R. W. *J. Polym. Sci.* 1959, **37**, 19
- <sup>26</sup> MELVILLE, H. W., PEAKER, F. W. and VALE, R. L. *J. Polym. Sci.* 1958, **30**, 29 and *Makromol. Chem.* 1958, **27**, 140
- <sup>27</sup> KURATA, M. and YAMAKAWA, H. *J. chem. Phys.* 1958, **29**, 311
- <sup>28</sup> KURATA, M., YAMAKAWA, H. and TERAMOTO, E. *J. chem. Phys.* 1958, **28**, 785
- <sup>29</sup> STOCKMAYER, W. H. and ALBRECHT, A. C. *J. Polym. Sci.* 1958, **32**, 215
- <sup>30</sup> KURATA, M., YAMAKAWA, H. and UTIYAMA, H. *Makromol. Chem.* 1959, **34**, 139
- <sup>31</sup> FLORY, P. J. and FOX, T. G. *J. Amer. chem. Soc.* 1951, **73**, 1904 and *J. Polym. Sci.* 1950, **5**, 745
- <sup>32</sup> SCHULZ, G. V. and KIRSTE, R. Symposium über Makromoleküle (Wiesbaden 1959)

<sup>33</sup> ZIMM, B. H., OUTER, C. I. and CARR, P. *J. chem. Phys.* 1950, **18**, 830

<sup>34</sup> KRIGBAUM, W. R. and CARPENTER, D. K. *J. phys. Chem.* 1955, **59**, 1166

<sup>35</sup> FOX, T. G. Private communication

<sup>36</sup> ZIMM, B. H. *J. chem. Phys.* 1946, **14**, 164

<sup>37</sup> CASSASSA, E. F. and MARKOVITZ, H. *J. chem. Phys.* 1958, **29**, 493

<sup>38</sup> CHINAI, S. N., SCHERER, P. C. and LEIR, D. W. *J. Polym. Sci.* 1957, **17**, 117

<sup>39</sup> BENOIT, H., HOLTZER, S. U. and DOTY, P. M. *J. phys. Chem.* 1954, **58**, 635

<sup>40</sup> BENOIT, H. *J. Chim. phys.* 1958, **55**, 540

## APPENDIX

We have to compute

$$C = \frac{4\pi}{2N^2} \left[ \frac{a^2 N}{6} \left( \frac{3f-2}{f^2} \right) \right]^{3/2} \int_0^\infty r^2 \rho^2(r) dr$$

where

$$\rho(r) = f\pi^{-3/2} \sum_{n=0}^{N/t} C_n^3 \exp\{-C_n^2 r^2\}$$

with

$$C_n^2 = \frac{2Na^2}{9f^2} \left[ 1 + 3(f-2) \frac{fn}{N} + 3 \left( \frac{fn}{N} \right)^2 \right]$$

Thus

$$\begin{aligned} 4\pi \int_0^\infty r^2 \rho^2(r) dr &= 4\pi \int_0^\infty r^2 \sum_{j=0}^{N/t} \sum_{i=0}^{N/t} f^2 \pi^{-3} C_j^3 C_k^3 \exp\{-r^2(C_j^2 + C_k^2)\} dr \\ &= f^2 \pi^{-3/2} \sum_{j=0}^{N/t} \sum_{i=0}^{N/t} \frac{C_j^3 C_k^3}{(C_j^2 + C_k^2)^{3/2}} \end{aligned}$$

Passing to the integral and transforming to reduced variables

$$4\pi \int_0^\infty r^2 \rho^2 r dr = \left( \frac{\pi 2a^2 N}{9f^2} \right)^{-3/2} N^2 \int_0^1 \int_0^1 [1 + 3(f-2)(x+y) + 3(x^2 + y^2)] dx dy$$

The first integral is readily accomplished, and the second reduces to two standard integrals after the transformation

$$y = \frac{Kw}{(1-w^2)^{1/2}} - \frac{f-2}{2}$$

where

$$K^2 = (-1/12)(3f^2 - 24f + 16)$$

There results for  $1 \leq f \leq 3$

$$f=1,2, \quad C = \frac{1}{2} \left( \frac{3}{4\pi} \right)^{3/2} \frac{4\sqrt{2}}{3} \tan^{-1} \left( \frac{3}{4} \right) = \frac{1}{2} \left( \frac{3}{4\pi} \right)^{3/2} \times 1.213$$

$$f=3 \quad C = \frac{1}{2} \left( \frac{3}{4\pi} \right)^{3/2} \times 1.327$$



and for  $f \geq 4$

$$C = \frac{1}{2} \left[ \frac{3(3f-2)}{4\pi} \right]^{3/2} \frac{1}{3\sqrt{2}u} \ln \left\{ \left( \frac{3f(f-2) + 2\sqrt{2}\sqrt{(3f-1)u}}{3f(f-2) - 2\sqrt{2}\sqrt{(3f-1)u}} \right)^2 \right. \\ \left. \left( \frac{3f^2 - 4\sqrt{(3f-2)u}}{3f^2 + 4\sqrt{(3f-2)u}} \right) \times \left( \frac{3(f-2)^2 - 4u}{3(f-2)^2 + 4u} \right) \right\}$$

where

$$u = \sqrt{3(f-2)^2 - 4}$$

Thus

$$f=4; \quad C = \frac{1}{2} \left( \frac{3}{4\pi} \right)^{3/2} \times 1.413$$

$$f=8; \quad C = \frac{1}{2} \left( \frac{3}{4\pi} \right)^{3/2} \times 1.594$$

$$\lim_{f \rightarrow \infty} C = \frac{1}{2} \left( \frac{3}{4\pi} \right)^{3/2} 8 \left( 1 - \frac{1}{\sqrt{2}} \right)$$

# Book Reviews

---

## *Phthalocyanine Compounds* *A.C.S. Monograph 157*

F. H. MOSER and A. L. THOMAS

Reinhold: New York; Chapman and Hall: London, 1963. (xiii+365 pp., illus., 6 in. by 9½ in.), 144s or \$18.00

THIS monograph is a welcome addition to library shelves in that it is the first attempt to publish a comprehensive survey on the chemistry, reactions and applications of the phthalocyanines although previous reviews, more specifically on aspects of dyestuffs and pigment chemistry, have appeared in LUB's *The Chemistry of Synthetic Dyes and Pigments* and VENKATERAMAN's treatise.

In the thirty years since the disclosure of the structure of phthalocyanine by LINSTEAD a wealth of data has accumulated, of which a large proportion is documented in this monograph which is adequately supplied with references both to publications in the scientific journals and to the many patent specifications relating to this chromophore. The book surveys the history of the phthalocyanines, physical and chemical properties and their applications to a wide variety of end uses. As might be expected the largest portion is devoted to phthalocyanine dyes and pigments and it is here that perhaps the severest censure can be made. Thus, while the many and varied aspects of phthalocyanine dyes are covered and some attempt made to divide a long chapter into sections, the result is a rather indigestible mass of fact in the form of a non-critical catalogue of, in many cases, detailed verbatim abstracts from patents. It is felt that a little more selective editing in this portion of the book would vastly improve the readability without detracting from the value of the information presented. Also, constructive comment on the application of the various dye structures to different textile materials would have been useful.

A notable point of confusion in the chapter on dyes is in the positioning of the class of increasingly important fibre-reactive dyes here divided into the so-called 's-Triazinyl Dyes' which are well separated from the other fibre-reactive systems included under 'Sulphonic Acid Dyes'. Some overlap, without cross referencing, occurs in the sections on 'Sulphur Dyes' and 'Ternary and Quaternary Dyes', involving tetramethyl isothiuronium types such as C.I.74240 which is not usually found among the generally accepted class of Sulphur Colours. The connection between precursor dyes and the so-called 'leuco dyes' is also not placed in a clear perspective.

There follows a section on Commercial Applications of Phthalocyanines together with an appendix of Colour Index Numbers and manufacturers with trade names of the dyes. The latter contains some notable omissions, particularly the commercially important Alcian Blue 8GX(C.I.74240) and Phthalogen Blue (C.I.74160).

Earlier in the monograph useful chapters on the preparation and manufacture of phthalocyanines are given, the former covering the methods of formation and properties of phthalocyanines of some 44 different metals together with extracts of preparative details, whilst the latter, which draws extensively on BIOS and FIAT information, concentrates on copper phthalocyanine, halogenated phthalocyanines and metal free phthalocyanine together with detailed descriptions of the various methods for converting the product into technically valuable physical forms. A short, but useful account of other substituted phthalocyanines and related macrocyclic structures is given near the end of the book followed by a brief review of the more recently discovered polymeric forms of metal phthalocyanines.

The monograph is, with the above reservations, well set out with many formulae, useful diagrams and tables and appears adequately indexed. In several cases patent equivalents in different countries are given in the tables of references together with dates of publication which are useful to those searching the patent literature. Nomenclature, on the whole, appears to be beyond reproach with the exception of occasional lapses, for example, 1:3-diimino-isoindoline is termed 'diimino phthalimide', and phthalocyanine is stated to be, 'the condensation product of four isoindole groups', which are formulated structurally as iminoisoindole.

Summarizing, this book provides a comprehensive survey of the academic and industrial literature on phthalocyanines which will be generally useful to both specialists and students and the authors are to be congratulated for its compilation.

No doubt future editions will rectify omissions and reorganization of various facets of the contents will extend its value.

N. S. CORBY

*Reactions of Co-ordinated Ligands and Homogeneous Catalysis*  
*Advances in Chemistry Series 37*

American Chemical Society, 1963. (vii+255 pp., 6 in. by 9 in.), \$7.00

A DISCUSSION on co-ordination compounds usually implies a collection of papers on the influence of ligands on the physical and chemical properties of metals or metal ions. By publishing the papers presented at their symposium held in Washington in 1962, the American Chemical Society issues a strong reminder that there is another aspect of this field. In the preface to this volume, BAILAR quite rightly points out that variations in the properties of the groups comprising the ligands are just as important as the way in which the properties of the metal may be affected by co-ordination.

The eighteen papers of which this book is comprised can be divided into two groups. Changes in the properties of molecules when co-ordinated to a metal and the modifications of these ligands, while still co-ordinated, are the main points discussed in the first group of papers. The modifications in question are largely the introduction of substituent groups into ligands of various types. A few papers deal with the preparation and properties of some of the lesser known co-ordination compounds. In addition to offering new material these papers provide a good review of the present state of knowledge in this field, and demonstrate the relevance of this branch of co-ordination chemistry to a variety of studies. Individual authors deal with topics ranging from the importance of the formation of metal ion complexes in a number of biologically important enzymic and non-enzymic processes to rather speculative organometallic chemistry, including a discussion of the way in which the formation of chelates may promote specific reactions.

Catalysis of a number of reactions by metal ions is discussed in the later papers. The systems investigated include solvolysis, hydrogenation, oxidation and amine exchange reactions. Most of these reactions are discussed in terms of catalysis by metal complexes of the formation of complex intermediates.

The resulting volume is a useful addition to the literature on co-ordination chemistry with its emphasis on ligand reactions. Useful lists of references are presented at the end of most papers and some papers give detailed recipes for the preparation of new co-ordination compounds either directly or by modification of preformed chelates. It is unfortunate that no index has been compiled since this book contains a wealth of information which can only be found by a careful study of the individual contributions.

G. C. EASTMOND

The monograph is, with the above reservations, well set out with many formulae, useful diagrams and tables and appears adequately indexed. In several cases patent equivalents in different countries are given in the tables of references together with dates of publication which are useful to those searching the patent literature. Nomenclature, on the whole, appears to be beyond reproach with the exception of occasional lapses, for example, 1:3-diimino-isoindoline is termed 'diimino phthalimide', and phthalocyanine is stated to be, 'the condensation product of four isoindole groups', which are formulated structurally as iminoisoindole.

Summarizing, this book provides a comprehensive survey of the academic and industrial literature on phthalocyanines which will be generally useful to both specialists and students and the authors are to be congratulated for its compilation.

No doubt future editions will rectify omissions and reorganization of various facets of the contents will extend its value.

N. S. CORBY

*Reactions of Co-ordinated Ligands and Homogeneous Catalysis*  
*Advances in Chemistry Series 37*

American Chemical Society, 1963. (vii+255 pp., 6 in. by 9 in.), \$7.00

A DISCUSSION on co-ordination compounds usually implies a collection of papers on the influence of ligands on the physical and chemical properties of metals or metal ions. By publishing the papers presented at their symposium held in Washington in 1962, the American Chemical Society issues a strong reminder that there is another aspect of this field. In the preface to this volume, BAILAR quite rightly points out that variations in the properties of the groups comprising the ligands are just as important as the way in which the properties of the metal may be affected by co-ordination.

The eighteen papers of which this book is comprised can be divided into two groups. Changes in the properties of molecules when co-ordinated to a metal and the modifications of these ligands, while still co-ordinated, are the main points discussed in the first group of papers. The modifications in question are largely the introduction of substituent groups into ligands of various types. A few papers deal with the preparation and properties of some of the lesser known co-ordination compounds. In addition to offering new material these papers provide a good review of the present state of knowledge in this field, and demonstrate the relevance of this branch of co-ordination chemistry to a variety of studies. Individual authors deal with topics ranging from the importance of the formation of metal ion complexes in a number of biologically important enzymic and non-enzymic processes to rather speculative organometallic chemistry, including a discussion of the way in which the formation of chelates may promote specific reactions.

Catalysis of a number of reactions by metal ions is discussed in the later papers. The systems investigated include solvolysis, hydrogenation, oxidation and amine exchange reactions. Most of these reactions are discussed in terms of catalysis by metal complexes of the formation of complex intermediates.

The resulting volume is a useful addition to the literature on co-ordination chemistry with its emphasis on ligand reactions. Useful lists of references are presented at the end of most papers and some papers give detailed recipes for the preparation of new co-ordination compounds either directly or by modification of preformed chelates. It is unfortunate that no index has been compiled since this book contains a wealth of information which can only be found by a careful study of the individual contributions.

G. C. EASTMOND

*Modern Chemical Engineering*

Edited by A. ACRIVOS. Reinhold: New York; Chapman and Hall: London, 1963.  
(ix+604 pp., illus., 6 in. by 9 in.), 156s.

THE subject of Chemical Engineering is still expanding: it has already engulfed much of Surface Chemistry and Colloid Science, and seems now to be bidding for part of Polymer Science. In this book, which is in the nature of an 'Advances' volume, there are two excellent chapters in which polymer scientists will be particularly interested: E. W. MERRILL's Chapter 4 on the non-Newtonian flow of thin liquids, and Chapter 5 by A. G. FREDRICKSON on viscoelastic phenomena in thick liquids.

However, while there is in Chapter 5 considerable discussion of the Weissenberg stresses, effects, and his 'rheogonimeter', the reviewer would have welcomed more discussion on Weissenberg's original theory, and the inclusion of references to his papers. Certainly his name should have appeared in the author index at the end of the volume.

Though the book is written by no fewer than 16 authors, editor ACRIVOS has produced a volume with remarkably little overlapping of material. It is also as up to date as possible, some references being to work published in 1962. To achieve this rapid publication, time has evidently been saved on the printing, which is rather poor for a book of this price.

As a reference work on recent progress in both the fundamentals and applications of the flow properties of polymer solutions, this book can be confidently recommended.

J. T. DAVIES

## ANNOUNCEMENT

### SOCIETY OF CHEMICAL INDUSTRY PLASTICS AND POLYMER GROUP

A symposium on 'The Chemistry of Polymerization Processes' will be held at the Institution of Electrical Engineers, London, W.C.1, on 29 and 30 April 1965. Papers are invited on any aspect of the chemistry of polymerization. Intending contributors should send summaries of their proposed contributions before 1 July 1964, to Dr W. R. MOORE, Department of Chemical Technology, Bradford Institute of Technology, Bradford, Yorkshire.

The full contribution, if the summary is accepted by the Symposium Committee, will be required by not later than 1 December 1964. Further details of the Symposium will be circulated later.

## Note

### *The Absolute Rate Constants of Anionic Propagation by Free Ions and Ion-pairs of Living Polystyrene*

IN OUR first paper<sup>1</sup> on the kinetics of anionic polymerization of styrene in tetrahydrofuran we reported an increase in the apparent rate constant of propagation,  $k_p$ , with decreasing concentration of living ends, (LE). The living ends are ion-pairs, e.g.  $\sim\text{S}^- \text{Na}^+$ , and should be in equilibrium with the respective free ions  $\sim\text{S}^-$  and  $\text{Na}^+$ . For a fraction  $x$  of total living polystyrene dissociated into ions the observed  $k_p$  is given by the sum  $x \cdot k_p' + (1-x) \cdot k_p''$  where  $k_p'$  and  $k_p''$  denote the rate constants of propagation of the free ions and ion-pairs respectively. Since  $x$ , which is given by the equation  $K_{\text{Dis}} = x^2 [\text{LE}] / (1-x)$ , increases with dilution, so should  $k_p$  if  $k_p' > k_p''$ .

The original study of the kinetics covered a relatively narrow range of living end concentrations from  $10^{-3}$  M to  $10^{-2}$  M, and the extrapolation to  $[\text{LE}] = 0$  based on these data yielded a value for  $k_{p,0} = k_p' = 650$  l./mole sec, now considered to be much too low. This value combined with results of conductivity studies by Worsfold and Bywater<sup>2</sup>, led to the erroneous conclusion that the changes in  $k_p$  cannot be accounted for by the dissociation of ion-pairs into ions. This view was supported by the observation<sup>1</sup> that the

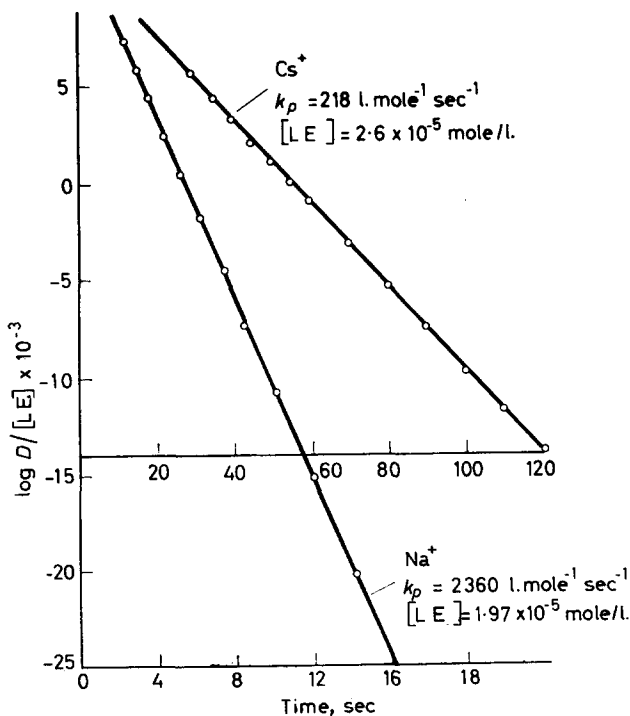
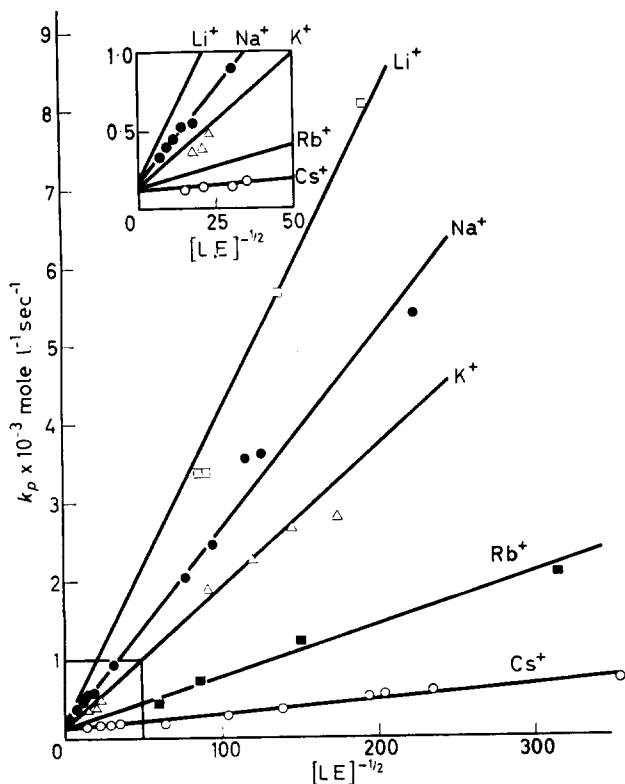


Figure 1

rate of polymerization was not affected by the addition of an excess of  $\text{NaClO}_4$  to the solution of living polystyrene.

Recently, our kinetic studies were extended down to  $[\text{LE}] = 10^{-5}$  M. The rate of polymerization was followed by monitoring the optical density at  $291.4 \text{ m}\mu$  (a characteristic peak of styrene), while the absorption at  $340 \text{ m}\mu$ , determining the concentration of living ends, was frequently checked. Typical plots of  $\log [S]_0/[S]_t/[LE]$  versus  $t$  are shown in *Figure 1*, their slopes giving  $k_p$  for different  $[\text{LE}]$ . In *Figure 2* the  $k_p$  values are plotted versus  $1/[\text{LE}]^{1/2}$  and, as expected for systems in which the degree of dissociation is low (less than 0.05), the experimental points formed straight lines\*. Their slopes give  $k'_p (K_{\text{Dis}})^{1/2}$  and the intercepts determine  $k'_p$  for the respective ion-pairs. All these results were obtained in THF at  $25^\circ\text{C}$ .



*Figure 2*—Effect of counter-ion on absolute rate constant of styrene anionic homopolymerization in THF at  $25^\circ\text{C}$

We have demonstrated therefore that the dissociation of ion-pairs into free ions is responsible for the variations in  $k_p$ , and the slopes of the lines

\*The results obtained for the Li salts are slightly puzzling since it appears that  $x$  exceeds 0.1 at lower concentrations of  $[\text{LE}]$  and nevertheless the points appear not to deviate from the straight line. It was implicitly assumed that the  $\epsilon$  of the free ion is the same as that of an ion-pair. This assumption may not be correct and this could lead to too high values of  $k_p$  at low concentrations.

NOTE

shown in *Figure 2* lead to the following gradation of the respective dissociation constants:

$$K_{\text{Dis, Li}^+} : K_{\text{Dis, Na}^+} : K_{\text{Dis, K}^+} : K_{\text{Dis, Rb}^+} : K_{\text{Dis, Cs}^+} = 440 (?) : 177 : 87 : 11 : 1$$

This sequence is not uncommon and was observed for the negative ions of aromatic hydrocarbons by Hoijtink<sup>3</sup>. The appreciable solvation of Li<sup>+</sup> of Na<sup>+</sup> ions leads to higher dissociation of these salts than those of Cs<sup>+</sup> which presumably gives an unsolvated or poorly solvated Cs<sup>+</sup> ion. Accepting the literature value<sup>2</sup> of  $1.5 \times 10^{-7}$  moles/l. for  $K_{\text{Dis, Na}^+}$  we calculate  $k'_p$  to be 65 000 l./mole sec in THF at 25°C.

From the intercepts the following approximate values of  $k_p$  were calculated: 114 l./mole sec for  $\sim\text{S}^-$ , Cs<sup>+</sup>, 120 l./mole sec for  $\sim\text{S}^-$ , K<sup>+</sup>, 135 l./mole sec for  $\sim\text{S}^-$ , Na<sup>+</sup>, and about 200 l./mole sec for  $\sim\text{S}^-$ , Li<sup>+</sup>. The extremely high reactivity of the free ion  $\sim\text{S}^-$  is therefore remarkable.

The conductivities of various ion-pairs in THF were also investigated. The results for  $\sim\text{S}^-$ , Cs<sup>+</sup> showed a much lower conductivity than those for  $\sim\text{S}^-$ , Na<sup>+</sup>, thus confirming our kinetic results. In the concentration range of  $10^{-3}$  to  $10^{-2}$  M the conductivity of NaClO<sub>4</sub> was found to be 1.5 to 2 times lower than that of  $\sim\text{S}^-$ , Na<sup>+</sup>, and hence our previous results<sup>1</sup> showing the lack of common-ion effect are at least partially justified. The conductivity of Na<sup>+</sup>, BPh<sub>4</sub><sup>-</sup> was found to be  $\sim 70$  times as high as that of  $\sim\text{S}^-$ , Na<sup>+</sup> and therefore a common-ion effect should be observed on addition of this salt. In fact, addition of a twofold excess of Na<sup>+</sup>, BPh<sub>4</sub><sup>-</sup> to  $1.7 \times 10^{-4}$  solution of  $\sim\text{S}^-$ , Na<sup>+</sup> depressed the observed  $k_p$  value of  $\sim 2$  100 l./mole sec to 140 l./mole sec.

Finally, the preliminary experiments showed that the conductivities increase at lower temperatures. Hence, the abnormally low apparent activation energy of anionic polymerization<sup>1,4</sup> is caused by the increasing dissociation at lower temperature of ion-pairs into free ions.

*The financial support of this study by the National Science Foundation Grant G-14393, and by the Quartermaster Corps, Grant DA19-129-AMC-51(N), is gratefully acknowledged.*

D. N. BHATTACHARYYA  
C. L. LEE  
J. SMID  
M. SZWARC

*Chemistry Department,  
N.Y. State University College of Forestry,  
Syracuse, New York*

(Received November 1963)

REFERENCES

- <sup>1</sup> GEACINTOV, C., SMID, J. and SZWARC, M. *J. Amer. chem. Soc.* 1962, **84**, 2508
- <sup>2</sup> WORSFOLD, D. J. and BYWATER, S. *J. chem. Soc.* 1960, 5234
- <sup>3</sup> Private communication; see also DIELEMAN, J. *Thesis*, Free University, Amsterdam, 1962
- <sup>4</sup> DANTON, F. S., WILES, D. M. and WRIGHT, A. N. *J. Polym. Sci.* 1960, **45**, 111



# Contributions to Polymer

Papers accepted for future issues of  
POLYMER include the following:

- The Temperature Dependence of Extensional Creep in Polyethylene Terephthalate*—I. M. WARD
- The Radiation Chemistry of Polymethacrylic Acid, Polyacrylic Acid and Their Esters; An Electron Spin Resonance Study*—M. G. ORMEROD and A. CHARLESBY
- Crystallinity and Disorder Parameters in Nylon 6 and Nylon 7*—W. RULAND
- Rate Dependence of the Strain Birefringence and Ductility of Polyethylene*  
—S. STRELLA and S. NEWMAN
- A Thermodynamic Description of the Defect Solid State of Linear High Polymers*—B. WUNDERLICH
- Graft Copolymerization Initiated by Poly-p-lithiostyrene*—M. B. HUGLIN
- Structure and Properties of Crazes in Polycarbonate and Other Glassy Polymers*—R. P. KAMBOUR
- The Crystallization of Polymethylene Copolymers: Morphology*—J. B. JACKSON and P. J. FLORY
- The Crystallization of Polyethylene II*—W. BANKS, J. N. HAY, A. SHARPLES and G. THOMSON
- Description and Calibration of an Elasto-osmometer*—H. J. M. A. MIERAS and W. PRINS
- Resonance-induced Polymerizations*—R. J. ORR
- Polypropylene Oxide I—An Intrinsic Viscosity/Molecular Weight Relationship*—G. ALLEN, C. BOOTH and M. N. JONES
- Viscosity/Temperature Dependence for Polyisobutene Systems: The Effect of Molecular Weight Distribution*—R. S. PORTER and J. F. JOHNSON
- The Photolytic Decomposition of Poly-(n-butyl)methacrylate*—J. R. MACCALLUM
- Catalysts for the Low Temperature Polymerization of Ethylene*—K. J. TAYLOR
- The Effect of Tension and Annealing on the X-ray Diffraction Pattern of Drawn 6.6 Nylon*—D. R. BERESFORD and H. BEVAN
- Orientation in Crystalline Polymers related to Deformation*—Z. W. WILCHINSKY
- Morphology of Polymer Crystals: Screw Dislocations in Polyethylene, Polymethyleneoxide and Polyethyleneoxide*—W. J. BARNES and F. P. PRICE
- Nuclear Spin-Lattice Relaxation in Polyacetaldehyde*—T. M. CONNOR
- The Morphology of Poly(4-methyl-pentene-1) Crystals*—A. E. WOODWARD
- Proton Spin-Lattice Relaxation Measurements on Some High Polymers of Differing Structure and Morphology [Polyethylene, poly(4-methyl-pentene-1), poly(L-leucine), poly(phenyl-L-aniline), polystyrene and poly( $\alpha$ -methyl-styrene)]*—B. I. HUNT, J. G. POWLES and A. E. WOODWARD

- Infra-red Spectra of Poly(p-ethylene oxybenzoate)*—MATAHUMI ISHIBASHI  
*Sequence Length Distribution and Entropy of Stereoregularity in Homopolymers of Finite Molecular Weight*—A. M. NORTH and D. RICHARDSON  
*The Copolymerization of Methylmethacrylate and Maleic Anhydride*—A. M. NORTH and D. POSTLETHWAITE  
*Polypropylene Oxide II—Dilute Solution Properties and Tacticity*—G. ALLEN, C. BOOTH and M. N. JONES  
*Studies in the Thermodynamics of Polymer-Liquid Systems I—Natural Rubber and Polar Liquids*—C. BOOTH, G. GEE, G. HOLDEN and G. R. WILLIAMSON  
*Studies in the Thermodynamics of Polymer-Liquid Systems II—A Re-assessment of Published Data*—C. BOOTH, G. GEE, M. N. JONES and W. D. TAYLOR  
*Studies in the Thermodynamics of Polymer-Liquid Systems III—Polypropylene + Various Ketones*—W. B. BROWN, G. GEE and W. D. TAYLOR  
*Studies in the Thermodynamics of Polymer-Liquid Systems IV—Effect of Incipient Crystallinity on the Swelling of Polypropylene in Diethylketone*—G. ALLEN, C. BOOTH, G. GEE and M. N. JONES  
*Some Experimental Studies on Enthalpy and Entropy Effects in Equilibrium Swelling on Polyoxypolyene Elastomers*—B. E. CONWAY and J. P. NICHOLSON  
*Copolymerization of Trioxan with Dioxolan*—M. KUČERA and J. PICHLER  
*Thermal Degradation of an Aromatic Polypyromellitimide in Air and Vacuum—Rates and Activation Energies*—S. D. BRUCK  
*The Polymerization of Butadiene with Chromium Acetylacetonate and Aluminium Triethyl*—C. E. H. BAWN, A. M. NORTH and J. S. WALKER  
*The Free Radical Polymerization of N,N-Dimethylacrylamide*—A. M. NORTH and A. M. SCANLAN  
*On the Chemistry of Polymer Chain Folds*—D. C. BASSETT  
*The Polymerization of Propylene Oxide Catalysed by Zinc Diethyl and Water*—C. BOOTH, W. C. E. HIGGINSON and E. POWELL  
*The Anionic Polymerization of Some Alkyl Vinyl Ketones*—P. R. THOMAS, G. J. TYLER, T. E. EDWARDS, A. T. RADCLIFFE and R. C. P. CUBBON

CONTRIBUTIONS should be addressed to the Editors, *Polymer*, 4-5 Bell Yard, London, W.C.2.

Authors are solely responsible for the factual accuracy of their papers. All papers will be read by one or more referees, whose names will not normally be disclosed to authors. On acceptance for publication papers are subject to editorial amendment.

If any tables or illustrations have been published elsewhere, the editors must be informed so that they can obtain the necessary permission from the original publishers.

All communications should be expressed in clear and direct English using the minimum number of words consistent with clarity. Papers in other languages can only be accepted in very exceptional circumstances.

A leaflet of instructions to contributors is available on application to the editorial office.

# The Temperature Dependence of Extensional Creep in Polyethylene Terephthalate

I. M. WARD\*

*Measurements of extensional creep behaviour of unoriented crystalline polyethylene terephthalate have been made over the temperature range of the glass/rubber transition. Time/temperature superposition was found applicable and the shift factors could be fitted to the Williams-Landel-Ferry relationship with a glass/rubber transition temperature parameter of 85°C. Previous dielectric loss measurements within this temperature range are also shown to be consistent with this representation.*

THERE have been many detailed studies of the temperature dependence of viscoelastic behaviour for amorphous polymers (see for example Ferry<sup>1</sup>) and it is now generally established that in the so-called glass/rubber transition range of temperature, the viscoelastic functions at different temperatures can be simply related by an empirical relationship. Such behaviour has been termed thermorheologically simple<sup>2</sup>. For all amorphous polymers the relationship relating the change in behaviour with temperature takes the same mathematical form, although it does not now seem that a universal relationship can be assumed to hold exactly.

The equation relating the frequency shift factor  $a_T$  required to superimpose viscoelastic results at a temperature  $T$  with those at an arbitrary standard temperature  $T_0$  is

$$\log a_T = \{-C_1^0 (T - T_0)\} / \{C_2^0 + T - T_0\}$$

where  $C_1^0$  and  $C_2^0$  are constants. By suitable choice of  $T_0$ , this equation is found to have approximately the same numerical parameters  $C_1^0$  and  $C_2^0$  for many amorphous polymers and it is in this form that it is sometimes quoted<sup>3</sup>. This general equation has become known as the Williams-Landel-Ferry (WLF) equation.

In crystalline polymers, the applicability of such reduction procedures has not been established, although several attempts to obtain empirical shift parameters have been made<sup>4,5</sup>. With polyethylene, there are several conflicting conclusions. Williams and Howard<sup>6</sup>, on the basis of experimental creep data obtained by Hideshima, have concluded that the WLF equation can be applied. Faucher<sup>5</sup>, on the other hand, applied a simple horizontal shift to his stress-relaxation data, and obtained an exponential change of  $a_T$  with temperature. It was suggested by Takemura, however, that the stress-relaxation curves cannot be fitted together by a horizontal shift in time only, but that there must also be a vertical shift to take into account the changes in crystallinity with temperature which will affect the absolute value of the modulus<sup>7</sup>. In a very detailed study of creep and dynamic mechanical measurements Nakayasu, Markovitz and Plazek<sup>8</sup> concluded that quite apart from the difficulty of justifying any vertical shift (either due

\*Present address: Research Dept., I.C.I. Ltd., Fibres Division, Harrogate, Yorkshire.

to the factor  $\rho T / \rho_0 T_0$  or a crystallinity correction) such a shift would still not give superposition of the data to a common curve. They suggest that this is because there are several different viscoelastic processes which contribute to the viscoelastic behaviour in this temperature region and on the basis of rather elaborate separation procedures effected some degree of satisfactory superposition for these individual processes.

It is well known from other dynamic mechanical data that the viscoelastic behaviour of polyethylene is extremely complicated in this temperature range and it appears from this and n.m.r. data that several competing molecular processes occur<sup>9</sup>. In addition there is the change in crystallinity with temperature. It therefore seems worthwhile to consider a crystalline polymer where a somewhat simpler situation exists. In crystalline samples of polyethylene terephthalate it has been shown by i.r., n.m.r. and X-ray studies<sup>10</sup> that the viscoelastic behaviour associated with the glass/rubber transition at about 100°C can be attributed to the onset of main chain motions of the molecules in the non-crystalline regions of the polymer, there being no effects due to side-chain branches since this polymer is linear. Furthermore, X-ray measurements<sup>11</sup> have shown that the crystallinity as determined by X-ray diffraction is constant up to 180°C. It therefore seemed appropriate to study the temperature dependence of extensional creep in crystalline unoriented polyethylene terephthalate and this investigation is described here.

## EXPERIMENTAL

### *Preparation of samples*

The sample used in these measurements was an unoriented heavy monofilament of polyethylene terephthalate (thickness  $\sim 0.100$  in.) which was heat-crystallized by heating at 180°C for one hour.

### *Measurements of deformation*

The extensional creep was measured with the apparatus shown in *Figure 1*. The monofilament sample is suspended from a micrometer head inside a copper tube which is surrounded by an oil-bath, the temperature of which is thermostatically controlled to better than  $\pm 0.1^\circ\text{C}$ . The monofilament is attached to long clamps ( $\sim 12$  in.) at its extremities so that its entire length is well within the controlled temperature volume. The clamp at the lower end of the monofilament is attached via the slug of a differential transformer to the load  $W$ . The total weight of slug and clamp is about 20g, and at each temperature at least 20 h is allowed for the sample to creep under this small load. The subsequent creep under this residual load is thus small compared with that due to the larger applied load. The creep is measured by continuously adjusting the micrometer so as to position the slug in the centre of the differential transformer. This gives a minimum output voltage from the transformer (which is observed on the oscilloscope). The input to the transformer comes from a 2 kc/s oscillator via suitable matching impedances. The monofilament was 12.41 in. in length and the micrometer could be read to  $\pm 0.0005$  in.

## CREEP IN POLYETHYLENE TEREPHTHALATE

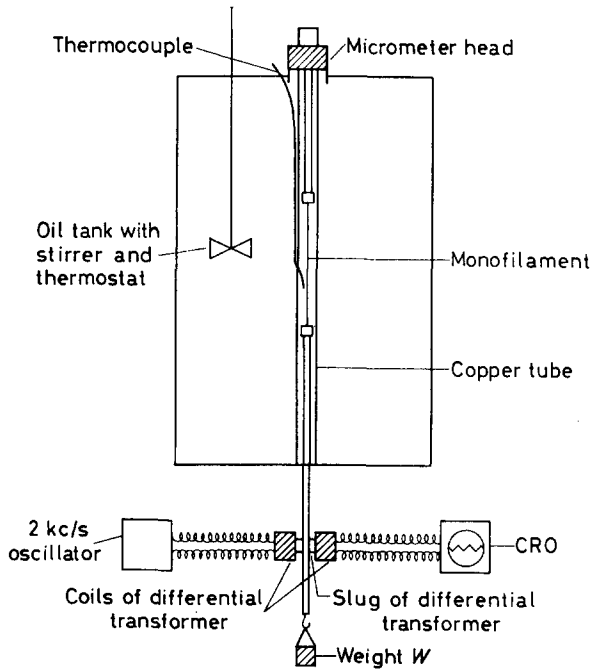


Figure 1—High temperature creep apparatus

### RESULTS

#### *Tests of linearity*

Preliminary measurements were made at 95°C with three levels of applied load (567.3g, 267.8g, 117.3g) to estimate the approximate range of linearity and give some indication of the magnitude of extensional creep. The loads were applied for 2 h 35 min (9 300 sec) during which detailed measurements of creep were obtained. (These results are shown in

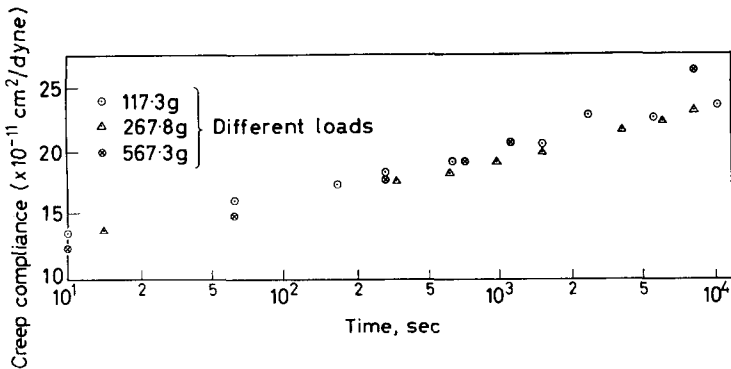


Figure 2—Creep compliance of unoriented PET at 95°C

Figure 2.) The remainder of 24 h was allowed for recovery, and it was noted that the sample had returned to its original length to a very good approximation after this time.

*Detailed creep measurements*

Using the preliminary measurements as a guide, creep data were obtained at temperatures between 115.5°C and 65.0°C. These are shown in Figure 3, where the creep compliance in arbitrary units is plotted against

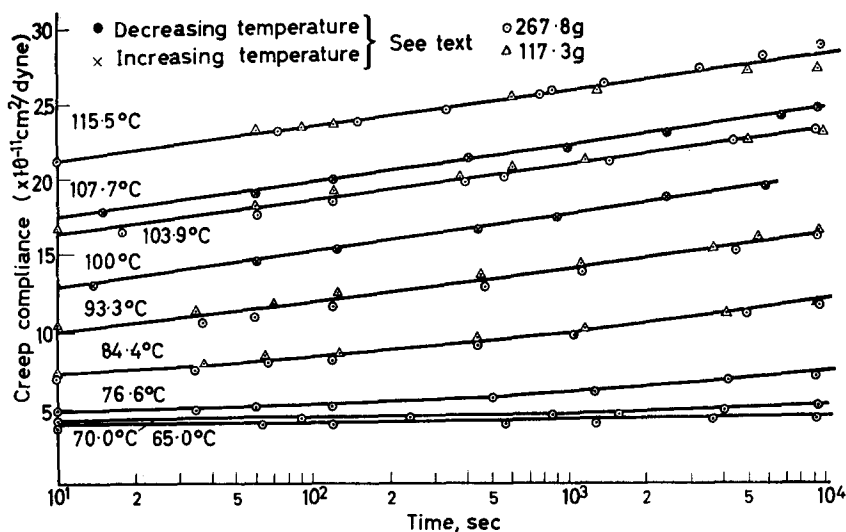


Figure 3—Creep of unoriented PET over range 65° to 115.5°C

time in seconds. The results shown as dots were obtained from results where the temperature was decreased between successive creep measurements, those with crosses were further results obtained on again raising the temperature. In most of the early measurements results were obtained at two levels of load, 267.8g and 117.3g. These are differentiated by circles

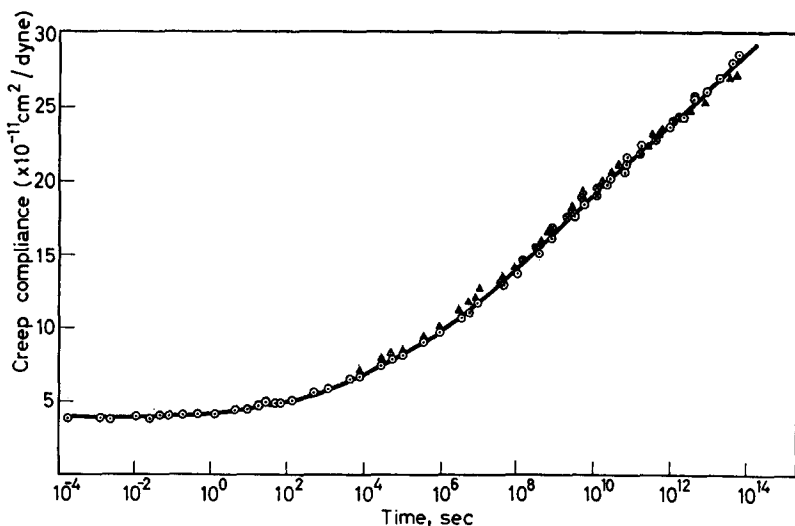


Figure 4—Master creep compliance curve for PET (reduced to 76.6°C)

and triangles respectively. As very good agreement was obtained for the creep compliance for these two levels of load, the curve has been drawn

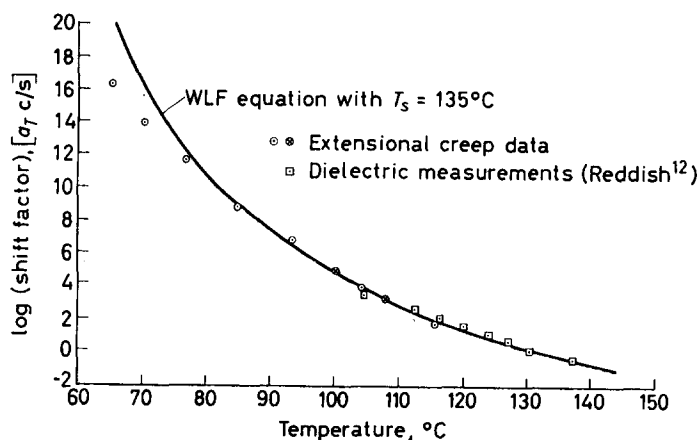


Figure 5—Log (shift factor,  $a_T$ ) as a function of temperature for unoriented PET

through the mean of all the points. In Figure 4, a master curve has been constructed by a horizontal shift procedure as outlined in the introduction; no vertical shift factor was used. Figure 5 shows the shift factor plotted against temperature as for a WLF type equation. Figure 6 shows the shift factor plotted against reciprocal temperature.

#### DISCUSSION

##### Linearity and reproducibility of creep behaviour

It was apparent from preliminary measurements at  $95^\circ\text{C}$  (Figure 2) that there was no significant difference between the creep compliance curves at

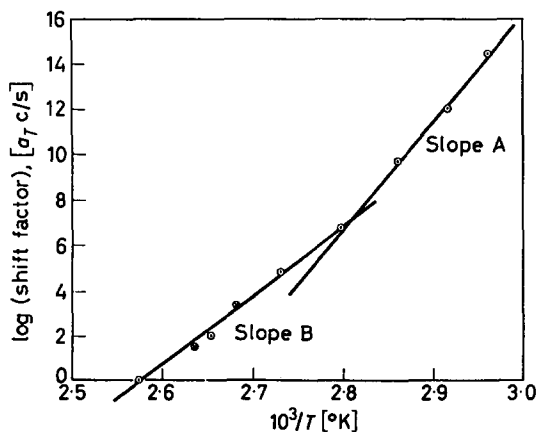


Figure 6—Log (shift factor,  $a_T$ ) versus reciprocal temperature for unoriented PET

the two lower load levels. These two load levels were therefore used repeatedly in the detailed measurements over the range of temperatures

studied. It was also apparent that the creep compliance decreased by a small but significant extent during the first few creep and recovery cycles, possibly due to slight increase in crystallinity under these conditions. When it became apparent, however, that no further decrease in compliance was occurring the complete set of measurements was undertaken. As has been described the procedure was first to lower the temperature between successive runs and then to obtain a series of results with temperature increasing. It will be seen from the diagrams (*Figures 3 and 4*) that these later results are very consistent with the earlier ones, confirming that any further decrease in compliance during the measurements was negligible. It was found that no permanent flow occurred within the range of conditions chosen, i.e. only delayed elasticity was observed.

#### *Temperature dependence of creep behaviour*

The temperature dependence of the creep behaviour has been considered from the two viewpoints of the applicability of the WLF equation and the alternative approach assuming a constant activation energy.

In the region of temperatures 75° to 115°C the creep compliance changes markedly with temperature. It is therefore considered satisfactory to omit the factor  $\rho T / \rho_0 T_0$ , because this is small.

It can be seen from *Figure 4* that a master creep curve can be very satisfactorily constructed using a horizontal shift factor only. The fit is particularly convincing at the higher temperatures where the creep curves are very nearly linear on the logarithmic time scale. In *Figure 5* the log (shift factor,  $a_T$ ) has been plotted against temperature and the points fitted to the WLF equation in its universal form

$$\log a_T = \{ -8.86 (T - T_s) \} / \{ 101.6 + T - T_s \}$$

where  $T_s$  is the arbitrary temperature parameter chosen to give the best fit.

The WLF equation is sometimes equivalently stated as

$$\log a_T = \{ -17.74 (T - T_0) \} / \{ 51.6 + T - T_0 \}$$

where  $T_0 = T_s - 50$ .

In this representation the temperature parameter  $T_0$  is often called the glass/rubber transition temperature. This definition of  $T_0$  is very different from the more usual one in dynamic mechanical measurements where  $T_0$  is defined in terms of the temperature of maximum work loss or maximum change in modulus with temperature. This latter definition of  $T_0$  includes specification of the frequency of measurement whereas the definition in terms of the WLF equation implies a parameter which is independent of frequency.

A reasonably good fit was obtained for the results at the high temperature end with  $T_s = 135^\circ\text{C}$  (or  $T_0 = 85^\circ\text{C}$ , in the alternative representation). As expected for the WLF equation, the results at temperatures below 85°C the 'glass/rubber transition temperature' do not lie on the predicted line.

Secondly a plot was made of  $\log a_T$  against the reciprocal of absolute temperature which is shown in *Figure 6*.



Figure 6 shows that the results cannot be fitted easily to a straight line of constant activation energy. In fact, this representation gives an activation energy which decreases with increasing temperature, as predicted by the WLF equation. However, by fitting the low temperature and high temperature results to a constant activation energy in a somewhat arbitrary fashion, values have been obtained for comparison with dielectric measurements. These values are 172 (Slope A) and 138 kcal/mole (Slope B) for the low and high temperatures respectively.

#### *Comparison with dielectric measurements*

The only other relevant investigation covering a comparable range of temperature and frequency is that of Reddish<sup>12</sup> on the dielectric behaviour of PET. Reddish found two dielectric loss processes, one of which, the high temperature high-frequency loss process, is undoubtedly associated with the glass/rubber transition (see also Ward<sup>10</sup>). Reddish found that his results for the variation of the frequency of maximum dielectric loss  $f_m$  with absolute temperature  $T$  were adequately described by the Arrhenius equation  $f_m = A e^{-E/RT}$ . It has previously been remarked by Payne<sup>13</sup>, however, that the data can be represented equally well by the WLF equation. We have used Reddish's published results (Figure 10 in his paper) and replotted these as  $\log f_m$  against temperature, fitting the points so obtained to the WLF equation in its universal form. It will be seen from Figure 5 that a reasonably good fit can be obtained, again assuming  $T_s = 135^\circ\text{C}$  (or  $T_g = 85^\circ\text{C}$ ).

Reddish, using the Arrhenius equation, obtained an activation energy of 90 kcal/mole. This value is lower than those obtained by treating the extensional creep data in a similar fashion, as expected since all the data are more accurately represented by the WLF equation, and the dielectric loss measurements are equivalent to short-time creep measurements at high temperatures.

#### *Dilatometric measurements*

It is also interesting to compare the value of  $T_g$  which gives a suitable fit to the WLF equation with that obtained from dilatometric measurements. The results of Kolb and Izard<sup>14</sup> on crystalline unoriented PET suggest a value of about  $82^\circ\text{C}$  for the dilatometric  $T_g$  which is in fairly good agreement with the present data.

### CONCLUSIONS

It is concluded that the WLF equation even in its simplified universal form is adequate to describe the variation of extensional creep of crystalline PET with temperature. The value of the glass/rubber transition temperature parameter  $T_g$  obtained in this way is  $85^\circ\text{C}$ .

It is also noted that the dielectric loss data of Reddish are consistent with this representation, and that the dilatometric measurements of Kolb and Izard gave a value of about  $82^\circ\text{C}$  for  $T_g$ .

*This work was undertaken by the author during a period of secondment from I.C.I. Ltd, Fibres Division to the Division of Applied Mathematics, Brown University, Rhode Island, U.S.A.*

*The author is greatly indebted to Professor H. Kolsky for much advice and encouragement and to Mr L. C. Daubeny for constructing the apparatus.*

*With regard to purchase of equipment to undertake these studies, the author wishes to acknowledge the support of the Advanced Research Projects Agency, Department of Defense under ARPA Contract Sd-86 with Brown University.*

*Division of Applied Mathematics,  
Brown University, U.S.A.*

*(Received January 1963)*

#### REFERENCES

- <sup>1</sup> FERRY, J. D. *Viscoelastic Properties of Polymers*. Wiley: New York, 1961
- <sup>2</sup> SCHWARZL, F. and STAVERMAN, A. J. *J. appl. Phys.* 1952, **23**, 838
- <sup>3</sup> WILLIAMS, M. L. *J. phys. Chem.* 1955, **59**, 95
- <sup>4</sup> NAGAMATSU, K. *Kolloidzshr.* 1961, **172**, 141
- <sup>5</sup> FAUCHER, J. A. *Trans. Soc. Rheol.* 1959, **3**, 81
- <sup>6</sup> WILLIAMS, M. L. and HOWARD, W. H. *S.P.E. Trans.* [Society of Plastics Engineers], January 1962, p 74
- <sup>7</sup> TAKEMURA, T. *J. Polym. Sci.* 1959, **38**, 471
- <sup>8</sup> NAKAYASU, H., MARKOVITZ, H. and PLAZEK, D. J. *Trans. Soc. Rheol.* 1961, **5**, 261
- <sup>9</sup> SAUER, J. and WOODWARD, A. E. *Rev. mod. Phys.* 1960, **32**, 88
- <sup>10</sup> WARD, I. M. *Text. Res. (J.)*, 1961, **31**, 650
- <sup>11</sup> FARROW, G. and WARD, I. M. *Brit. J. appl. Phys.* 1960, **11**, 543
- <sup>12</sup> REDDISH, W. *Trans. Faraday Soc.* 1950, **46**, 459
- <sup>13</sup> PAYNE, A. R. In *Rheology of Elastomers*, edited by P. MASON, p 86. Pergamon: London, 1958
- <sup>14</sup> KOLB, H. J. and IZARD, E. F. *J. appl. Phys.* 1949, **20**, 564

# *The Radiation Chemistry of Polymethacrylic Acid, Polyacrylic Acid and Their Esters: An Electron Spin Resonance Study*

M. G. ORMEROD and A. CHARLESBY

*The radiation-induced reactions in polymethacrylic and polyacrylic acids and their methyl, ethyl and n-butyl esters have been studied using electron spin resonance (e.s.r.). The polymers were irradiated at 77°K and their e.s.r. spectra recorded at that temperature. Subsequently they were warmed to room temperature and the free radical decays and reactions followed. Work with certain additives led to the conclusion that trapped electrons rather than free radicals were responsible for the unpaired spins initially observed at 77°K. The e.s.r. results have been correlated with the radiation chemistry of the polymers and compared with those observed in other polymers, in which the ionic species are believed to be less stable.*

THE radiation chemistry of polymers has been extensively studied by different physicochemical methods. Although these methods have evaluated the end products, they give little information as to the nature of the radiation-induced intermediates. To study these intermediates it is necessary to resort either to the use of additives with particular properties—such as electron acceptors or radical scavengers—or to electron spin resonance spectroscopy (e.s.r.).

E.s.r. has been successfully used to study the nature of the free radicals involved in radiation-induced reactions, and in general these results have fitted well with previous physicochemical studies. However, polymethylmethacrylate is a notable exception. E.s.r. studies have not correlated well with the known radiation chemistry. We have therefore reconsidered the problem and have extended the range of measurement in three ways. We have compared a variety of polyacrylates and methacrylates, including samples of polymethylmethacrylates of different tacticities; the studies have been made both at 77°K where radical reactions are inhibited, and at room temperature; and finally we investigated the effect on the e.s.r. spectrum of some additives, in particular some electron acceptors.

## EXPERIMENTAL

The e.s.r. spectra were obtained using a conventional high frequency (400 kc/s) magnetic field modulation X-band spectrometer with phase-sensitive detection. All spectra were recorded as the first derivative of the absorption intensity against variation in magnetic field, and are shown as such in the figures of this paper.

A fuller description of the spectrometer has been given elsewhere (Charlesby, Libby and Ormerod<sup>31</sup>).

The intensities of spectra were obtained by double integration. The free radical concentration could then be found by comparison with a signal from a coal substandard which had been calibrated against  $\alpha,\alpha$ -diphenyl  $\beta$ -picryl hydrazyl.

The following samples were studied:

(1) Atactic polymethylmethacrylate (PMMA) which contained the minimum amount of impurity, e.g. anti-oxidant and u.v. stabilizers. Viscosity average molecular weight =  $1.5 \times 10^6$ . (Specially prepared by I.C.I. Ltd.)

(2) Oriented atactic PMMA (given to us by H. Fischer of the Deutsches Kunststoff Institut, Darmstadt) which had been stretched at 130°C to 400 per cent elongation.

(3) Isotactic PMMA (supplied by Rohm and Haas Co. Ltd) which had a viscosity average molecular weight =  $6 \times 10^5$ .

(4) Syndiotactic PMMA (supplied by Rohm and Haas Co. Ltd) which had a viscosity average molecular weight =  $10^5$ .

- |  |   |  |
|--|---|--|
| (5) Polymethacrylic acid (PMA acid)          | } | (supplied by Polymer Consultant Ltd.)                          |
| (6) Polyethylmethacrylate (PEMA)             |   |  |
| (7) Poly- <i>n</i> -butylmethacrylate (PBMA) |   |  |
| (8) Polyacrylic acid (PA acid)               |   |  |
| (9) Polymethylacrylate (PMA)                 | } | (given by Dr W. Cooper of Dunlop Research Centre, Birmingham.) |
| (10) Polyethylacrylate (PEA)                 |   |  |
| (11) Poly- <i>n</i> -butylacrylate (PBA)     |   |  |

Those samples which were obtained commercially were purified by dissolving them in ethanol or methylenedichloride and then precipitating in excess water, filtering and drying *in vacuo* at 80°C. The mixtures of 95 per cent PMA acid and 5 per cent additive were prepared by dissolving the compounds in ethanol and driving off the solvent using a water pump. All samples were irradiated *in vacuo* at 77°K with  $\gamma$ -rays from a <sup>60</sup>Co source (dose rate = 0.6 Mrad h<sup>-1</sup>). Doses varying from 0.3 to 24 Mrad were used. The samples were studied at 77°K, and then warmed to room temperature so that the free radical reactions could be followed.

## RESULTS

### *Spectra obtained at 77°K*

It was found that irradiation at 77°K gave spectra which in some cases were unstable at 77°K. Because of this, the samples were irradiated to a dose of 1 Mrad—which took nearly two hours—their e.s.r. spectra recorded immediately after irradiation and then recorded again after two weeks storage at 77°K. *Figure 1* shows such spectra taken from polymethacrylic acid and its ethyl and butyl esters. Immediately after irradiation, all these compounds gave a spectrum containing a single line.

The ethyl ester spectrum also had some other weaker lines in the wings, and on keeping at 77°K these outer lines grew at the expense of the inner,

so that a five line spectrum, with additional fine structure, similar to that reported by Ovenall<sup>1</sup> was finally obtained. From the observed decay it would appear that change in spectrum is accompanied by an increase of about two in the concentration of unpaired spins. Similar changes were not observed in the spectra of the acid and its butyl ester on standing at this temperature.

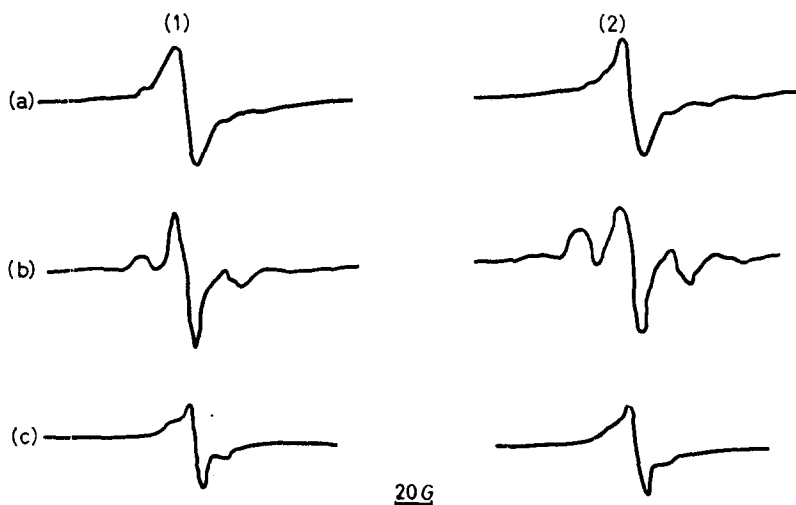


Figure 1—E.s.r. spectra of some compounds irradiated and studied at 77°K: (a) polymethacrylic acid, (b) polyethylmethacrylate, (c) poly-*n*-butylmethacrylate. (1) Immediately after irradiation, (2) two weeks later

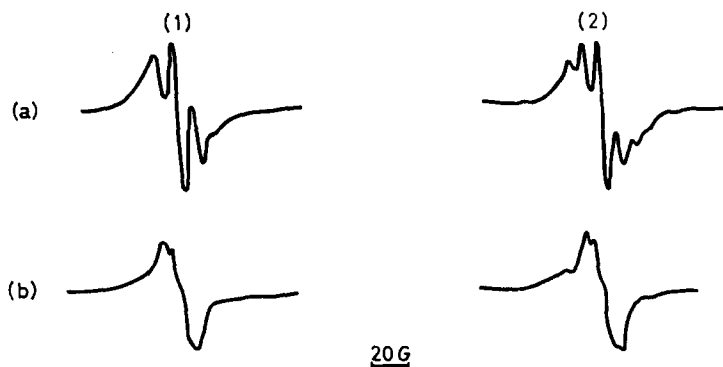


Figure 2—E.s.r. spectra of atactic PMMA (1) irradiated and observed at 77°K: (a) as supplied by the manufacturer, (b) the same material purified. (1) Immediately after irradiation, (2) two weeks later



Figure 3—E.s.r. spectra of isotactic PMMA (3) irradiated and observed at 77°K: (a) as supplied by the manufacturer, (b) the same material purified. (1) Immediately after irradiation, (2) two weeks later

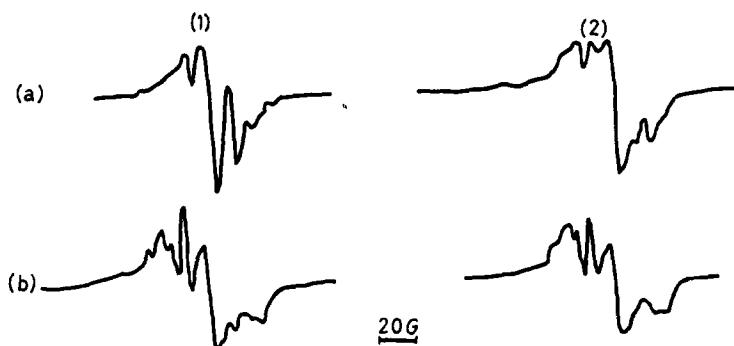


Figure 4—E.s.r. spectra of syndiotactic PMMA (4) irradiated and observed at 77°K: (a) as supplied by the manufacturer, (b) the same material purified. (1) Immediately after irradiation, (2) two weeks later

Each sample of PMMA that was studied gave a different e.s.r. spectrum. The spectrum also depended strongly on the type of impurity that was present in the polymer. This can be seen in *Figures 2, 3 and 4* where some spectra recorded from atactic, isotactic and syndiotactic PMMA in different states of purity are shown. In some cases the spectra changed slightly on keeping the samples at 77°K. This was not accompanied by any detectable change in the unpaired spin concentration. Abraham *et al.*<sup>2</sup> and Ovenall<sup>1</sup> have reported the presence of a 'weak quintet' in low temperature irradiated PMMA. At no time did we observe a spectrum that could be described in this way.

The *G* values for unpaired spins in PMA acid and its esters are shown in *Table 1*. These values were calculated for low doses of radiation in an attempt to minimize changes due to a slow reaction of the unpaired spins during the radiation.

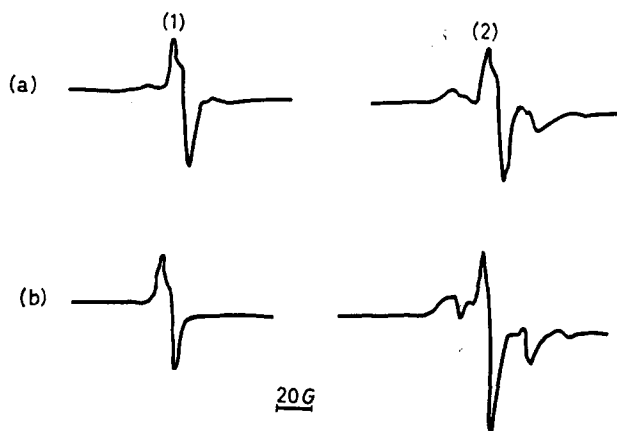
## THE RADIATION CHEMISTRY OF SOME POLYSILOXANES

 Table 1. *G* values for unpaired spins in polymethacrylates and polyacrylates irradiated and studied at 77°K

R	COOR	COOR
	$\begin{array}{c} \text{COOR} \\   \\ -\text{CH}_2-\text{C}- \\   \\ \text{CH}_3 \end{array}$	$\begin{array}{c} \text{COOR} \\   \\ -\text{CH}_2-\text{C}- \\   \\ \text{H} \end{array}$
—H	1.5 ± 0.5	3.0 ± 1.5
—CH <sub>3</sub>	1.6 ± 0.5	3.4 ± 1.1
—C <sub>2</sub> H <sub>5</sub>	1.9 ± 0.6	2.6 ± 0.9
— <i>n</i> .C <sub>4</sub> H <sub>9</sub>	1.3 ± 0.4	2.7 ± 0.9

In order to help identify the unpaired spins observed in PMMA, an oriented specimen was studied. This technique has been used successfully in several polymers (e.g. Kiselev *et al.*<sup>3</sup>, Libby and Ormerod<sup>4</sup>). The spectra are shown in *Figure 5*. They are isotropic and no additional information can be gained from them.

A study has also been made of the effect of additives on the spectra from irradiated PMA at 77°K<sup>5</sup>. The chosen additives were ferrous ammonium sulphate, monomer, tetracyanoethylene (TCNE) and pyromellitic dianhydride (PMDA) in the concentration of 5 per cent additive to 95 per cent polymer.



*Figure 5*—E.s.r. spectra of oriented PMMA (2) irradiated and observed at 77°K: direction of elongation (a) parallel to the magnetic field, and (b) perpendicular to it. (1) Immediately after irradiation, (2) two weeks later

Ferrous ammonium sulphate had little effect but the other additives radically altered the radiation-induced e.s.r. spectrum. Added monomer gave the spectrum previously reported by Ovenall<sup>1</sup>. It consisted of seven lines of hyperfine splitting 23 gauss with another even lined spectrum superimposed [see *Figure 6(a)*]. PMDA gave a single line [*Figure 6(b)*]

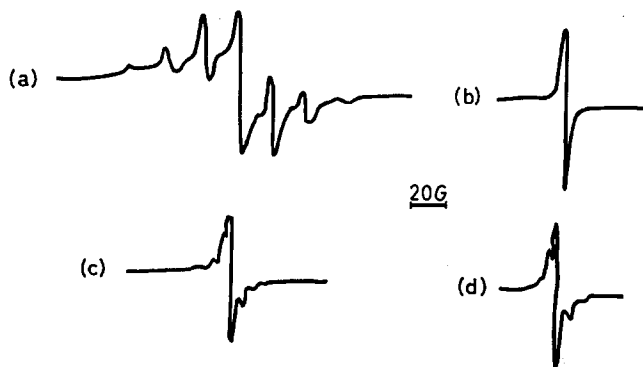


Figure 6—E.s.r. spectra recorded at 77°K: (a) PMA acid plus 5 per cent monomer irradiated at 77°K, (b) PMA acid plus 5 per cent PMDA irradiated at 77°K, (c) PMA acid plus 5 per cent TCNE irradiated at 77°K, (d) the TCNE radical anion

which was much narrower than that obtained from pure PMA acid (Figure 1). The sample was also coloured red by the radiation as opposed to the brown coloration observed in the pure polymer. The same result was obtained with a sample containing only one per cent PMDA. Added TCNE gave a yellow colour and a narrow spectrum with some evidence of hyperfine structure [Figure 6(c)].

For purposes of comparison, we prepared the TCNE radical anion by reduction with sodium iodide in tetrahydrofuran solution. At room temperature, this gave the known nine line spectrum<sup>6</sup>. When cooled to 77°K the resultant solid solution gave the spectrum of Figure 6(d), which is identical with that obtained from the irradiated mixture of PMA acid and TCNE. Furthermore both samples had the same yellow colour.

A spectrum similar to that in Figure 6(b), was obtained when atactic PMMA plus 5 per cent PMDA was irradiated at 77°K, showing that the phenomena described above are not limited to PMA acid alone.

#### Room temperature spectra

The spectra obtained from all the polymethacrylates, except isotactic PMMA, immediately on warming to room temperature are the same as that observed by Schneider *et al.*<sup>7,8</sup>, Uebersfeld<sup>9</sup>, Abraham *et al.*<sup>2</sup> and other workers in irradiated PMMA. This common spectrum has two sets of lines; set A consisting of five lines at 0,  $\pm 23$  and  $\pm 46$  gauss with relative intensities 1:4:6:4:1 and of line width about 5.5 gauss; set B consisting of four lines at  $\pm 11$  and  $\pm 33$  gauss with relative intensities 1:5:5:1 and line width 8 gauss. Although an intensity ratio of 1:3:3:1 is to be expected for a set of four lines<sup>10</sup> the ratio given above gave a better fit with the experimental derivative curve constructed using the above data and assuming a gaussian line shape. The poorness in fit in some parts of the spectrum is probably due to deviation from a gaussian line shape owing to broadening effects such as anisotropy.

When irradiated atactic PMMA was kept *in vacuo* at room temperature,



the spectrum slowly changed shape until after about  $10^3$  hours decay the B set of lines predominated (*Figure 7*). A similar change has been observed by Piette<sup>11</sup>.

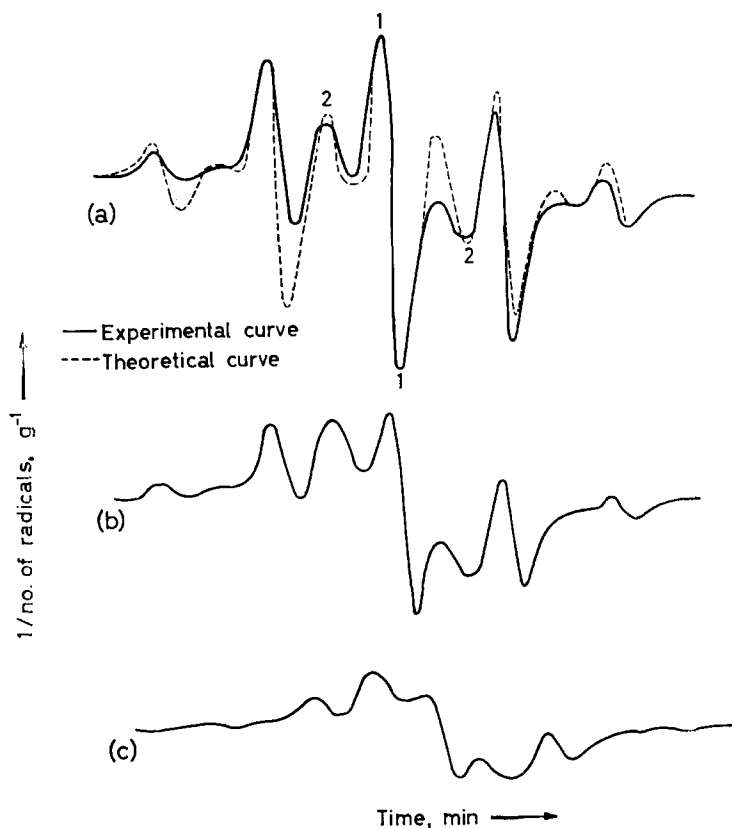


*Figure 7*—E.s.r. spectra of atactic PMMA irradiated at 77°K and viewed at room temperature: (a) 5 minutes after warming to room temperature, (b) after  $2 \times 10^1$  minutes, (c) after  $5 \times 10^4$  minutes

The individual decays of spectra A and B have been studied separately by the following method. From the figures used to synthesize the curve shown in *Figure 7*, the separate contributions of spectra A and B to the size of the peaks marked 11 and 22 were calculated. Hence, knowing the relative intensities of the lines within each spectrum, the separate intensities of the two spectra were computed.

At room temperature the radical concentration in PMA acid remained constant to within experimental error ( $\pm 20$  per cent) over a period of  $6 \times 10^4$  minutes. The decays in the other samples are shown in *Figures 8* to *13*. Radical concentrations have been given as  $G_{\text{radicals}}$ .

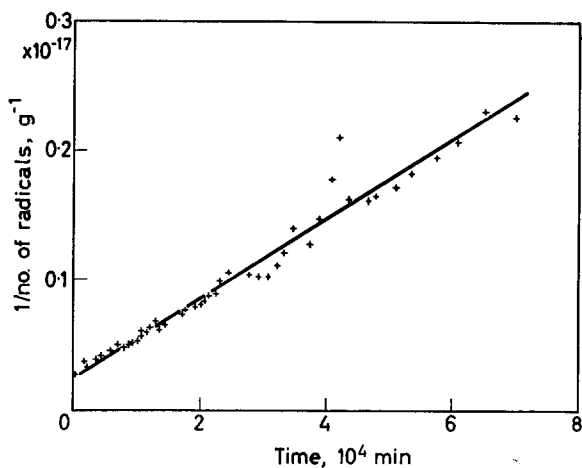


Figure 8—Decay of type A radicals at room temperature in atactic PMMA irradiated at 77°K

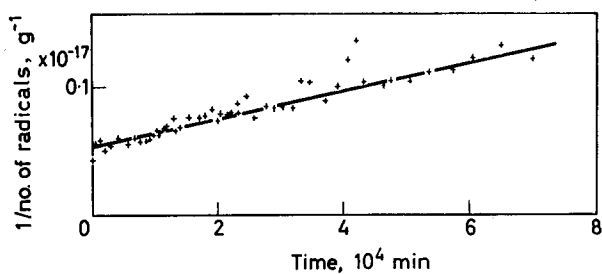


Figure 9—Decay of type B radicals at room temperature in atactic PMMA irradiated at 77°K

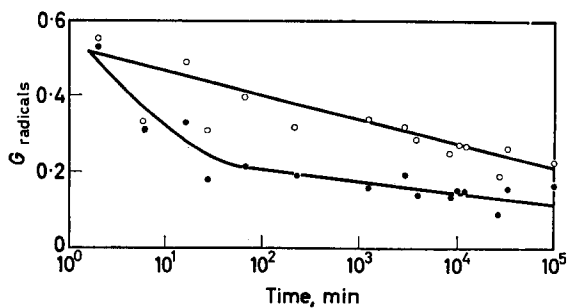


Figure 10—Decay of free radicals in syndiotactic PMMA irradiated at 77°K and studied at room temperature: ○—type A radicals; ●—type B radicals

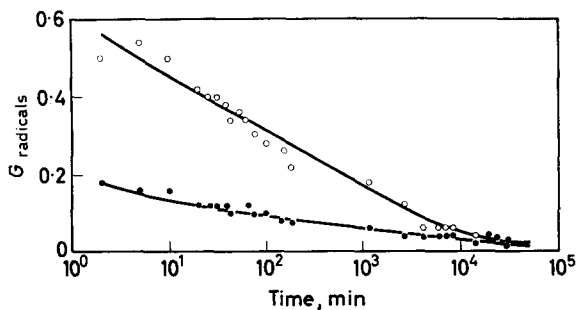


Figure 11—Decay of free radicals in polyethylmethacrylate irradiated at 77°K and studied at room temperature: ○—type A radicals; ●—type B radicals

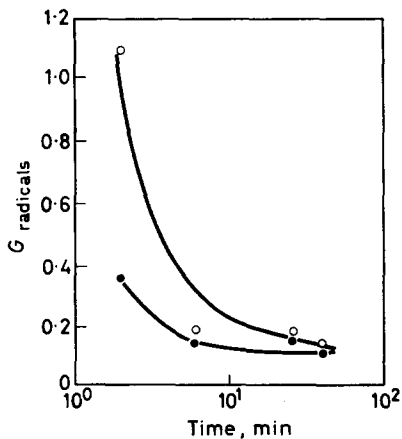


Figure 12—Decay of free radicals in poly-*n*-butylmethacrylate irradiated at 77°K and studied at room temperature: ○—type A radicals; ●—type B radicals

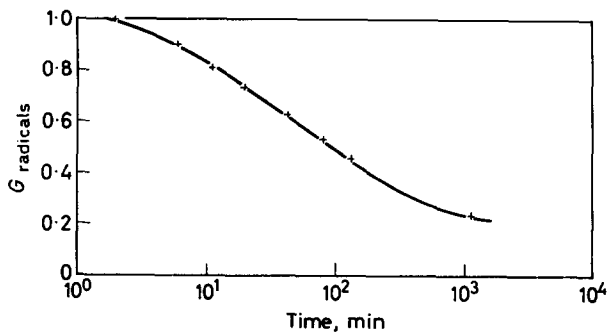


Figure 13—Decay of free radicals in isotactic PMMA irradiated at 77°K and studied at room temperature

In atactic PMMA, both the radicals type A and type B follow a second order decay, i.e.  $d[R\cdot]/dt = k[R\cdot]^2$  and  $1/[R\cdot]_t - 1/[R\cdot]_0 = kt$ , where  $[R\cdot]_t$  is the radical concentration at time  $t$  and  $k$  is a constant. For A,  $k_A = 3.0 \times 10^{-4}$  litre mol<sup>-1</sup> sec<sup>-1</sup>, and for B,  $k_B = 1.3 \times 10^{-4}$  litre mol<sup>-1</sup> sec<sup>-1</sup> (Figures 8 and 9).

In syndiotactic PMMA, atactic PEMA and PBMA the decay is neither second nor first order (Figures 10, 11, 12). The results have been plotted in the form  $G_{\text{radicals}}$  versus  $\log t$  for convenience. For the atactic polymers the radical stability is greater the smaller the ester group. This agrees with the variation in second order transition point; the larger esters are rubber-like at room temperature.

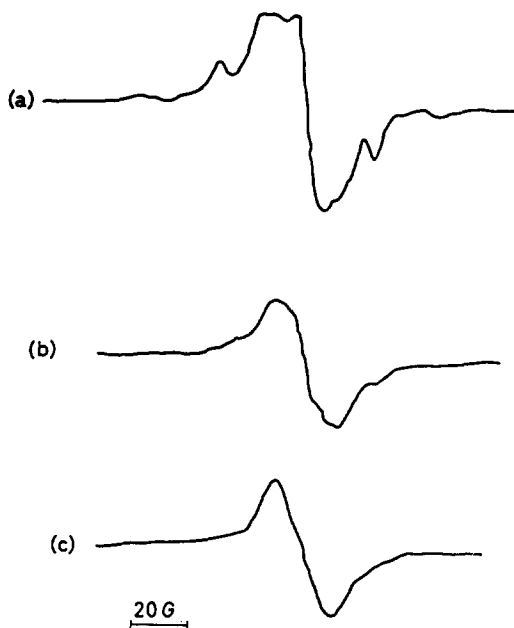


Figure 14—E.s.r. spectra of isotactic PMMA irradiated at 77°K and viewed at room temperature: (a) immediately on warming to room temperature, (b) 10<sup>2</sup> minutes later, (c) 10<sup>3</sup> minutes later

The isotactic PMMA sample gave a room temperature spectrum which was superficially different from the other PMMAs (see Figure 14). Closer examination reveals that the same lines are present but that the set B lines are relatively in far higher concentration. Both radicals decay very quickly (Figure 13). Thus in PMMA, radical stability is greatest in the syndiotactic sample and least in the isotactic.

When ferrous ammonium sulphate or monomer is added to PMA acid the room temperature spectrum is not affected. When the additive is PMDA, on warming a low temperature sample to room temperature the single line observed at 77°K slowly decays and the normal room temperature spectrum appears (Figure 15). In the presence of TCNE the low temperature spectrum decays to give a single stable line (Figure 15).

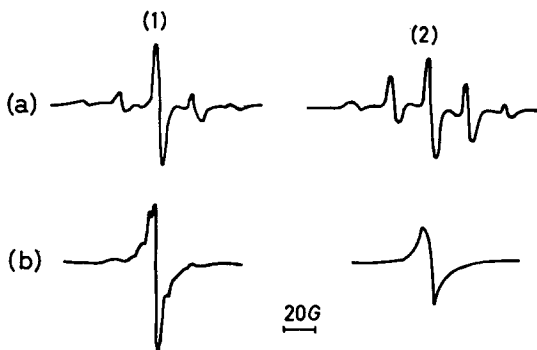


Figure 15—E.s.r. spectra at room temperature of (a) PMA acid plus 5 per cent PDMA, (b) PMA acid plus 5 per cent TCNE. (1) Immediately on warming to room temperature, (2) 24 hours later

POLYACRYLATES

*Low temperature spectra*

Irradiation at 77°K of PAA and its methyl, ethyl and *n*-butyl esters gave at 77°K the spectra shown in Figure 16. The spectra were all basically similar and consisted of a single line with some poorly resolved constituents.

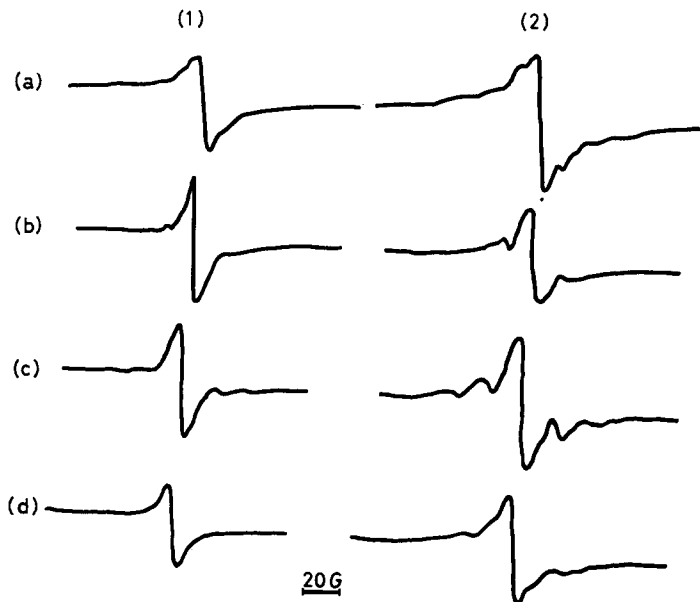


Figure 16—E.s.r. spectra of some polyacrylates irradiated and studied at 77°K: (a) polyacrylic acid, (b) polymethylacrylate, (c) polyethylacrylate, (d) poly-*n*-butylacrylate. (1) Immediately after irradiation, (2) two weeks later

On keeping the samples at 77°K, the single lines decayed slightly and the lines in the wings built up (*Figure 16*). The *G* values for unpaired spins are shown in *Table 1*.

#### Room temperature spectra

On warming to room temperature, the radicals in PBA and PEA decayed too rapidly to be observed. In PAA, a five line spectrum was obtained. The middle three lines were stable, but the outer two decayed. At the same time two more lines appeared near the central line (*Figure 17*). This final spectrum was similar to that reported by Abraham *et al.*<sup>2</sup>.



*Figure 17*—E.s.r. spectra of PA acid irradiated at 77°K and viewed at room temperature: (a) immediately on warming to room temperature, (b) 10<sup>3</sup> minutes later, (c) 10<sup>5</sup> minutes later



*Figure 18*—E.s.r. spectra of PMA irradiated at 77°K and viewed at room temperature: (a) immediately on warming to room temperature, (b) 10<sup>3</sup> minutes later

20G  
└───┘

In PMA, a three line spectrum was obtained which decays fairly rapidly; the central line decayed more slowly than the rest of the spectrum (*Figure 18*).

#### RADIATION CHEMISTRY

The most important feature of the radiation chemistry of the compounds

studied is that while the same gases are evolved from both polyacrylates and polymethacrylates on irradiation, the former compounds crosslink while the latter degrade. In this difference lies the interest in a comparison of the two types of polymer.

### *Polymethacrylates*

The most extensively studied polymethacrylate is PMMA. The major effects are the evolution of gas and main chain degradation. (For a detailed review of the radiation chemistry of PMMA see Charlesby<sup>12</sup> or Chapiro<sup>13</sup>.) The amount of degradation can best be measured by the decrease in intrinsic viscosity with radiation dose (e.g. Alexander *et al.*<sup>14</sup>). Light-scattering measurements have shown that no crosslinks are formed (Shultz *et al.*<sup>15</sup>).  $G_{\text{scissions}}$  given by different authors varies from 1.2 to 2.2 with a most probable value of  $1.9 \pm 0.3$ <sup>13</sup>. However, Parkinson *et al.*<sup>16</sup> found that  $G_{\text{scissions}}$  as estimated by intrinsic viscosity measurements was a function of the length of time the PMMA had been kept after irradiation. Gardner and Epstein<sup>17</sup> have made a similar observation.

The gases evolved consist of the breakdown products of  $\cdot\text{COOCH}_3$  groups plus one hydrogen atom for each  $\cdot\text{COOCH}_3$ <sup>14, 18, 19</sup>. One carboxylic ester group is evolved for every main chain scission.

Although no crosslinking can be detected in PMMA, in polymethacrylates with larger alkyl groups on the ester, degradation and crosslinking occur simultaneously<sup>20, 21</sup>. When the alkyl group is six or more carbon atoms long, the polymer can be gelled by radiation but the amount of crosslinking depends on the isomerism of the alkyl group, suggesting that crosslinking occurs through these groups.

No gas evolution measurements have been made on polymethacrylates other than PMMA.

### *Polyacrylates*

Todd<sup>19</sup> has studied gas evolution from PMA which she found became insoluble after irradiation. The gases evolved were similar qualitatively and quantitatively to those evolved from PMMA, i.e. consisted of the breakdown products of  $\cdot\text{COOCH}_3$  and  $\cdot\text{H}$ . Other reported work is by Shultz and Bovey<sup>22</sup> who carried out all their irradiations in air. They found a small amount of degradation— $0.15 < G_{\text{scissions}} < 0.2$ —but that the predominant effect was crosslinking. As in the polymethacrylates, the number of crosslinks formed depended on the isomerism of the alkyl group.

## DISCUSSION

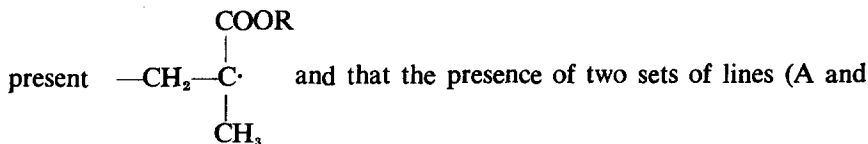
### *Radical identification*

The spectra observed at 77°K are unlike the spectra previously found in other irradiated polymers. Studies on an oriented specimen only yielded negative information. Since these facts are incompatible with the idea that only free radicals were present, we investigated the effects of additives which might be expected to affect ionic reactions.

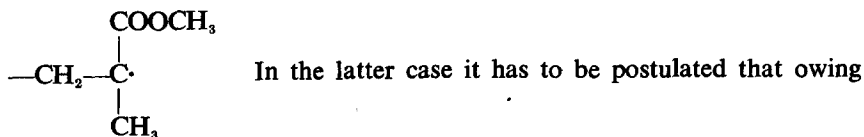
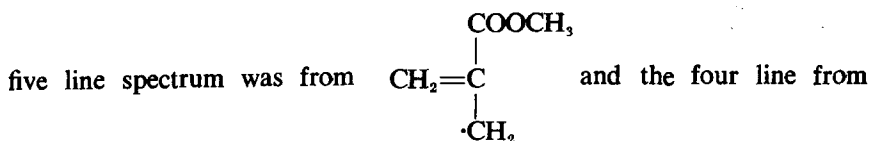
An electron donor—ferrous ammonium sulphate—had no effect, but electron traps—TCNE and PMDA—completely altered the low tempera-

ture PMA acid spectrum. By a comparison of the TCNE-PMA acid spectrum with that from the TCNE anion (*Figure 6*) it can be seen that in the mixture the TCNE anion is also being observed. As the concentration of TCNE was too low to allow the observation of the direct effect of radiation on the additive with a  $G$  value of 1.5, this anion must be formed by the radiation ejecting from the PMA acid an electron which was then trapped by the TCNE. In the PMDA-PMA acid mixture the PMDA anion was probably being observed although this could not be confirmed. Likewise the different colours induced by the radiation in the presence of different additives were probably due to the electrons trapped in different environments, i.e. on impurities such as monomer or catalyst residues. This leads us to the conclusion that in low temperature irradiated PMA acid we were observing an e.s.r. spectrum arising from trapped electrons. In those cases in the other polymers studied where the low temperature e.s.r. spectrum is a single line, we interpret the spectra as being due to electrons similarly trapped on trace impurities. It is the differences in these impurities that gives the wide variation in spectra from one sample of PMMA to another. The spectra observed in purified isotactic and syndiotactic PMMA which consist of several lines are due to free radicals which have arisen from the reactions of the ions before the spectrum could be recorded.

Identification of the room temperature spectra is more difficult. In the polymethacrylates, it has been suggested that there is only one radical



B) can be accounted for by hindered rotation of methyl or methylene groups<sup>2, 23, 24</sup>. The changes in intensity of the two sets of lines during their decay makes it seem most probable that there are separate radicals present. After e.s.r. experiments on polymerizing methyl methacrylate Hotta and Anderson<sup>25</sup> reached this same conclusion. They suggested that the



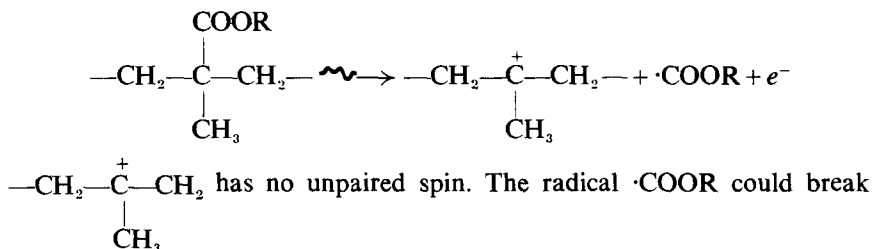
to the position of the methylene hydrogen atoms only the methyl hydrogen atoms react with the unpaired spin<sup>26</sup>. This is rather unlikely, and although this interpretation fits the known facts it is by no means conclusive.



No obvious interpretation of the room temperature polyacrylate spectra presents itself, and at this stage we are unable to offer any explanation for them.

#### *Positive ion formation*

The evidence from our experiments with additives favours the idea that trapped electrons are being observed in polyacrylates and methacrylates at 77°K. In these spectra there was no evidence of the presence of the positive ions which also must be formed. The spectrum from irradiated PMMA plus TCNE is exactly the same as that from the TCNE anion. The failure to observe a positive ion can be explained by one of two assumptions. Either the ion does not have an unpaired spin associated with it or its e.s.r. spectrum is so broad that it cannot be observed. Considering the first assumption, a reaction such as the following could be occurring:



down and its products diffuse through the polymer and combine with other similar gaseous radicals. The drawback to this scheme is that the evolved gases from PMMA are known to be composed of the reaction products of equal numbers of  $\cdot\text{COOCH}_3$  and H $\cdot$  groups<sup>14, 18, 19</sup>. If any of the breakdown products from  $\cdot\text{COOR}$  abstracted a hydrogen atom, an observable free radical would result. In fact there is no evidence of any additional radical in PMA and TCNE as compared with the chemically prepared TCNE anion. The second possibility is that the positive ion, although it contains an unpaired spin, is not being observed. The intensity of an e.s.r. line of given shape is proportional to the signal height and the square of the line width. If a signal of given intensity has its line width increased by a factor of ten, the signal height will be decreased by one hundred. Hence it can be seen that while both negative and positive ions may be present in equal concentrations, if the e.s.r. spectrum of the positive ion has a sufficiently greater line width, its spectrum will not be observed. For the rest of this discussion we will assume that this applies in the poly-methacrylates and -acrylates.

#### *Primary radiation processes*

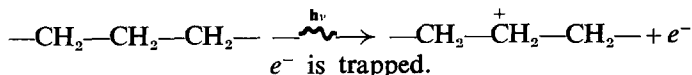
Primary radiation processes can be divided into three overlapping stages—physical, physicochemical and chemical. The physical stage lasts about  $10^{-13}$  second and is the time during which ionization or excitation occurs. (This, and similar data, have been taken from Hart and Platzman<sup>27</sup>.)

During the physicochemical stage ion dissociation, ion-molecule reactions, charge transfer (taking from  $10^{-13}$  to  $10^{-10}$  second) and finally charge recombination with the resultant radical formation occur. The free radicals react during the chemical stage. In solids this can take from less than a second to several months.

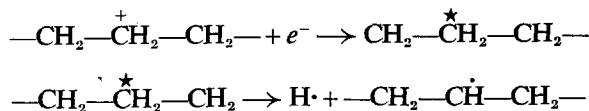
In inorganic solids, ejected electrons are known to be trapped giving rise to colour centres (e.g. Seitz<sup>28</sup>). Formerly in organic polymers irradiated at 77°K, the resultant unpaired spins, which are stable at 77°K, have always been identified as neutral free radicals (Kiselev *et al.*<sup>3</sup>, Libby and Ormerod<sup>4</sup>, Fischer and Hellwege<sup>29</sup>, Graves and Ormerod<sup>30</sup>). Following ionization, charge recombination has occurred comparatively rapidly in these polymers (polyethylene, polypropylene, polytetrafluorethylene and polyamide). In polymeth- and poly-acrylates charge recombination occurs sufficiently slowly for the ions to be observed by e.s.r. Why is this so and what are the steps between ionization and radical formation that allow these differences to occur?

Our e.s.r. spectra obtained at 77°K from the acrylates show marked variations due to the ejected electrons being trapped on different impurities. Other polymers do not show these variations, but presumably impurities trap electrons in the same fashion. The difference between the acrylates and the other polymers is in the —COOR groups, which do not seem to be involved in trapping the electrons since, owing to their much higher concentration, they ought to trap electrons in preference to additives. It is likely that these effects are due to the behaviour of the positive ions, and that either the positive ion mobility or its stability vary. The different behaviours of an ion such as —CH<sub>2</sub><sup>+</sup>— and —COOR<sup>+</sup> can be put down to the polar properties of the —COOR groups.

Let us consider the primary processes in polyethylene in which the free radical —CH<sub>2</sub>— $\dot{\text{C}}\text{H}$ —CH<sub>2</sub> is observed at 77°K (Charlesby *et al.*<sup>31</sup>). It is also known that the charge carriers, which give polyethylene its radiation-induced conductivity, are positive (McCubbin<sup>32</sup>, Wintle and Charlesby<sup>33</sup>). The following set of reactions can be envisaged:



—CH<sub>2</sub>—CH<sub>2</sub><sup>+</sup>—CH<sub>2</sub>— is mobile, i.e. the hole can move along the polymer chain until it reaches the vicinity of a trapped electron.

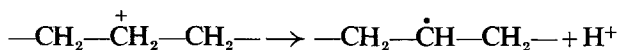
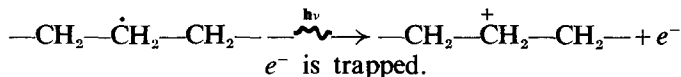


\* represents an excited state. The recombination of a hole and an electron will give sufficient energy to break a bond.

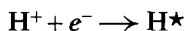
If this reaction scheme is correct, our results with the acrylates can be explained by postulating that the positive charge, —COOR<sup>+</sup>, is compara-

tively immobile at 77°K and only becomes mobile on warming to room temperature.

A slightly different, but equally probable, scheme is the following:



$\text{H}^+$  is mobile and can react with the trapped electron



In this case, one has to postulate that in the polymethacrylates the positive ion  $-\overset{+}{\text{C}}\text{OOR}$  is formed but is stable at 77°K and breaks down at room temperature to give a charged gaseous species which combines with an electron.

Our e.s.r. measurements initially show only the presence of ions, but approximately half the energy from  $\gamma$ -radiation is absorbed by excitation processes<sup>34</sup>. Shultz<sup>35</sup> and Charlesby and Thomas<sup>36</sup> have found that u.v. radiation of wavelength 2537Å (which will not cause ionization) damages PMMA in the same way as <sup>60</sup>Co  $\gamma$ -rays, but u.v. in terms of damage caused by absorbed energy unit, is only one tenth as effective as  $\gamma$ -radiation. We found the same e.s.r. spectrum in room temperature irradiated PMMA for both u.v. and  $\gamma$ -irradiation, but the radicals were formed ten times more effectively with  $\gamma$ -rays. This suggests that excitation is only about five per cent as effective as ionization in producing damage and hence radicals. This small number of free radicals produced by excitation would not be detected by e.s.r. in the presence of the more intense signal from trapped electrons produced by ionization.

Ion-molecule reactions of the type  $\text{CH}_4^+ + \text{CH}_4 \rightarrow \text{CH}_5^+ + \text{CH}_3$  have been shown to occur in irradiated methane gas<sup>37</sup>. It has been proposed that ion-molecule reactions occur in polymers, and in particular in polyethylene<sup>38,39</sup>. If reactions similar to the above were occurring in the acrylate polymers at 77°K, there would be a build-up of free radicals without a corresponding decrease in concentration of ions. This is not observed. This suggests that the radiation-induced ions in these polymers do not react with the polymer but the evidence is by no means conclusive.

Another difference between the polymethacrylates and other polymers is the ability of the polymethacrylates to store charge when irradiated with electrons<sup>40</sup>. The resultant discharges give the well known attractive 'trees'. Other polymers do not show this effect to anything like the same extent, if at all.

### Radical reactions

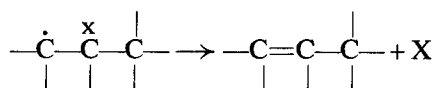
The ions observed at 77°K in the acrylate and methacrylate polymers reacted at room temperature to give the usual observed stable radicals. In PEMA there were other radical species, which were seen at 77°K, intermediate in this change (*Figure 1*). Also the complex arrangement of

lines in the low temperature spectra of irradiated isotactic and syndiotactic PMMA suggest the presence of similar intermediates (Figures 3 and 4). It is probable that such intermediates were involved in reactions of the other compounds studied, but that they were too unstable for a high enough concentration to be built up to allow them to be observed. In PMMA and PMA it is known that the evolved gases result from the removal of a  $-\text{COOCH}_3$  group and a hydrogen atom (Todd<sup>19</sup>). It is therefore expected that the radical intermediates will be  $-\text{CH}_2-\overset{\cdot}{\text{C}}(\text{CH}_3)-\text{CH}_2-$  in the polymeth-

acrylates and  $-\text{CH}_2-\overset{\cdot}{\text{C}}(\text{H})-\text{CH}_2-$  in the polyacrylates and another radical

resulting from the removal of a hydrogen atom. These radicals then react further to give the more stable species that are seen at room temperature.

The slow decay of the room temperature species (radicals type A and B) in the methacrylates leads us to ask by what mechanism they decay. If two radicals on different polymer chains combine, a crosslink is formed. While there is no objection to this as a decay process in the acrylates. Shultz and Bovey<sup>22</sup> have shown that no crosslinks are formed in irradiated PMMA. It is possible that the radicals decay by a rearrangement to give a double bond and a gaseous radical which may or may not combine with another polymer radical, i.e.

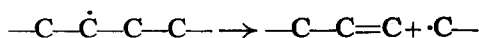


The long term change in optical absorption with time in irradiated PMMA<sup>41,42</sup> is probably due to the slow decay of these stable radicals.

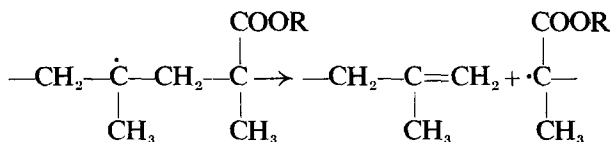
When irradiated PMMA is dissolved, many of the radicals probably combine with one another and thereby raise the molecular weight to a value nearer the original. Parkinson *et al.*<sup>16</sup> observed that the viscosity of irradiated PMMA was lower the longer the PMMA was kept before making the solution. This was because the free radicals in the PMMA had decayed and there were fewer of them left to combine with one another and raise the viscosity. Quoted values of  $G_{\text{scissions}}$  in the literature must be viewed with caution since they probably contain errors of this nature.

#### *The mechanism of main chain degradation*

The main chain scission of the polymethacrylates is either caused by a primary reaction (e.g. ionic) or by a secondary radical reaction. Todd<sup>19</sup> has shown that the addition of a *p*-benzoquinone and  $\alpha,\alpha$ -diphenylpicrylhydrazyl to PMMA gives a considerable reduction in the number of radiation-induced scissions. This indicates that the scissions are formed by a radical reaction. Todd<sup>19</sup> suggests that the reaction involved is a rearrangement of a main chain radical, i.e.



With the additive present the radical reacts and can no longer rearrange. A similar rearrangement has been suggested in polyisobutylene<sup>43</sup> and in polyamides<sup>31</sup>. Since about one acrylate group is destroyed for every main chain scission<sup>14,18,19</sup> we suggest that the removal of a —COOR group leaves a radical which then rearranges to give a scission, i.e.



$\text{---CH}_2\text{---}\dot{\text{C}}\text{---CH}_2\text{---}$  could be one of the radical intermediates observed in



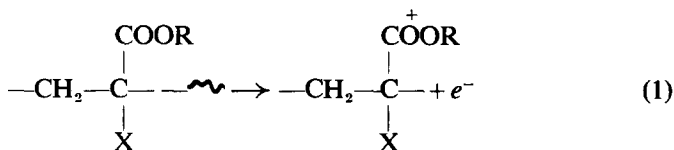
PEMA. It might be expected to give an eight line e.s.r. spectrum as does a similar radical in polypropylene<sup>29</sup> but if the —CH<sub>3</sub> group is unable to rotate freely at 77°K (as in alanine<sup>44</sup>) a different spectrum would result.

The corresponding radical in the polyacrylates,  $\text{---CH}_2\text{---}\dot{\text{C}}\text{---CH}_2\text{---}$  might be less prone to rearrange (because of smaller steric hindrance) which would account for the small number of scissions ( $G=0.2$ ).

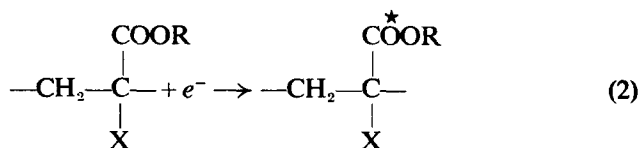
No fate has been suggested for the radical intermediates resulting from a hydrogen atom abstraction. In the polyacrylates and in polymethacrylates with sufficiently long alkyl groups on the ester these radicals are presumably in the alkyl groups and eventually react to give crosslinks. In PMA and PMMA they must react in some other fashion. The evidence we have at present does not give any guide as to what this reaction is.

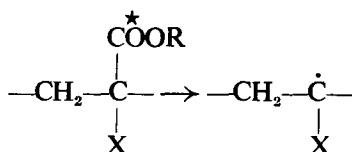
#### *Radiation-induced reactions: the overall picture*

As a summary of the previous discussion, our postulates are given in the following scheme for the radiation-induced reactions in methacrylate and acrylate polymers at room temperature and above, where X represents —H in polyacrylates, —CH<sub>3</sub> in polymethacrylates, and R represents (CH)<sub>n</sub>H.



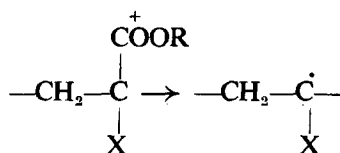
If the positive ion is mobile, it will eventually recombine with the trapped electron to give an excited species.



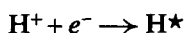


+ gaseous molecules and radicals from  $-\text{COOR}$ . (3)

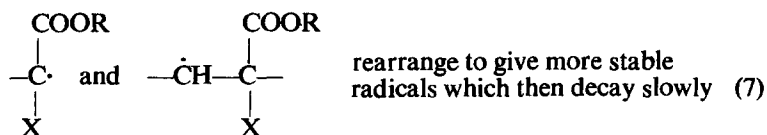
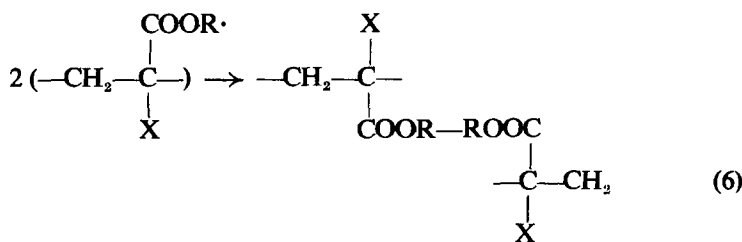
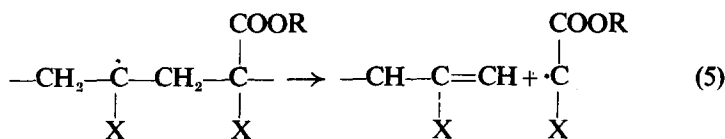
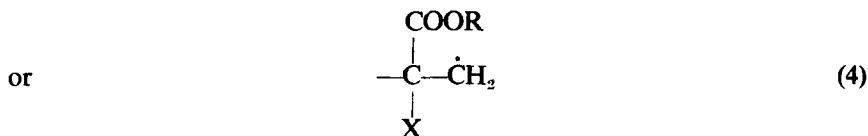
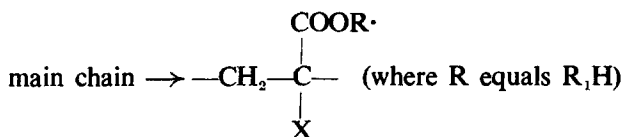
On the other hand, if the positive ion is immobile but unstable, it will decompose as follows:



+ gaseous molecules and radicals from  $-\text{COOR} + \text{H}^+$  (2a)



Radical products abstract H atoms in the longer side chain esters or in the



The differences between the acrylates and methacrylates lie in reactions (5) and (6). The polymethacrylates undergo reaction (5) more readily than the polyacrylates, probably because of steric hindrances due to the methyl group on the main chain. The crosslinking reaction (6) does not occur in PMA acid and PMMA.

*Physics Branch,  
Royal Military College of Science,  
Shrivenham, Swindon, Wilts.*

(Received February 1963)

REFERENCES

- <sup>1</sup> OVENALL, D. W. *J. Polym. Sci.* 1959, **41**, 199
- <sup>2</sup> ABRAHAM, R. J., MELVILLE, H. W., OVENALL, D. W. and WHIFFEN, D. H. *Trans. Faraday Soc.* 1958, **54**, 1133
- <sup>3</sup> KISELEV, A. G., MAKU'SKII, M. A. and LAZURKIN, YU. S. *Vysokomol. Soedineniya*, 1960, **2**, 1678
- <sup>4</sup> LIBBY, D. and ORMEROD, M. G. *J. Phys. Chem. Solids*, 1961, **18**, 316
- <sup>5</sup> ORMEROD, M. G. and STOODLEY, L. G. *Nature, Lond.* 1962, **195**, 262
- <sup>6</sup> PHILIPS, W. D., POWELL, L. C. and WEISSMAN, S. I. *J. chem. Phys.* 1960, **33**, 626
- <sup>7</sup> SCHNEIDER, E. E., DAY, M. J. and STEIN, G. *Nature, Lond.* 1951, **168**, 645
- <sup>8</sup> SCHNEIDER, E. E. *Disc. Faraday Soc.* 1955, **19**, 158
- <sup>9</sup> UEBERSFELD, J. *Ann. Phys., Paris*, 1956, **1**, 395
- <sup>10</sup> INGRAM, D. J. E. *Free Radicals as Studied by Electron Spin Resonance*. Butterworths: London, 1958
- <sup>11</sup> PIETTE, L. H. *NMR and ESR Spectroscopy*, p 218. Pergamon Press: Oxford, 1960
- <sup>12</sup> CHARLESBY, A. *Atomic Radiation and Polymers*, Chapter 19. Pergamon Press: Oxford, 1960
- <sup>13</sup> CHAPIRO, A. *The Radiation Chemistry of Polymeric Systems*. Interscience: New York, 1962
- <sup>14</sup> ALEXANDER, P., CHARLESBY, A. and ROSS, M. *Proc. Roy. Soc. A*, 1954, **223**, 392
- <sup>15</sup> SHULTZ, A. R., ROTH, P. I. and ROTHMAN, G. B. *J. Polym. Sci.* 1956, **22**, 495
- <sup>16</sup> PARKINSON, W. W., BINDER, D. and KIRKLAND, W. K. *O.R.N.L. Rep. No. 2829*, 1959, 177
- <sup>17</sup> GARDNER, D. G. and EPSTEIN, L. M. *J. chem. Phys.* 1961, **34**, 1653
- <sup>18</sup> WALL, L. A. and BROWN, D. W. *J. phys. Chem.* 1957, **61**, 129
- <sup>19</sup> TODD, A. *J. Polym. Sci.* 1960, **42**, 223
- <sup>20</sup> SHULTZ, A. R. *J. Polym. Sci.* 1959, **35**, 369
- <sup>21</sup> GRAHAM, R. K. *J. Polym. Sci.* 1959, **38**, 509
- <sup>22</sup> SHULTZ, A. R. and BOVEY, F. A. *J. Polym. Sci.* 1956, **22**, 485
- <sup>23</sup> INGRAM, D. J. E., SYMONS, M. C. R. and TOWNSEND, M. G. *Trans. Faraday Soc.* 1958, **54**, 409
- <sup>24</sup> SYMONS, M. C. R. *J. chem. Soc.* 1959, 277
- <sup>25</sup> HOTTA, K. and ANDERSON, R. S. *Fourth International Symposium on Free Radical Stabilization*, Appendix p 13. National Bureau of Standards: Washington, 1959
- <sup>26</sup> BAMFORD, C. H. and WARD, J. C. *Trans. Faraday Soc.* 1962, **58**, 971
- <sup>27</sup> HART, E. J. and PLATZMAN, R. L. *Mechanisms in Radiobiology*, Vol. I, Ch. 2. Academic Press: New York, 1961
- <sup>28</sup> SEITZ, F. *Rev. mod. Phys.* 1954, **26**, 7
- <sup>29</sup> FISCHER, H. and HELLWEGE, K. H. *J. Polym. Sci.* 1962, **56**, 33
- <sup>30</sup> GRAVES, C. T. and ORMEROD, M. G. *Polymer, Lond.* 1963, **4**, 81
- <sup>31</sup> CHARLESBY, A., LIBBY, D. and ORMEROD, M. G. *Proc. Roy. Soc. A*, 1961, **262**, 207
- <sup>32</sup> MCCUBBIN, W. L. *Ph.D. Thesis*. University of Durham, 1961
- <sup>33</sup> WINTLE, H. J. and CHARLESBY, A. *J. Photochem. Photobiol.* 1962, **1**, 231
- <sup>34</sup> BETHE, H. *Hand- u. Jb. chem. Phys.* 1933, **24(1)**, 273
- <sup>35</sup> SHULTZ, A. R. *J. phys. Chem.* 1961, **65**, 967
- <sup>36</sup> CHARLESBY, A. and THOMAS, D. K. *Proc. Roy. Soc.* 1962, **269**, 104

- <sup>37</sup> MEISELS, C. G., HAMILL, W. H. and WILLIAMS, R. R. *J. phys. Chem.* 1957, **61**, 1456
- <sup>38</sup> WEISS, J. *J. Polym. Sci.* 1958, **29**, 425
- <sup>39</sup> COLLYNS, B. G., FOWLER, J. F. and WEISS, J. *Chem. & Ind.* **1957**, No. 3, 74
- <sup>40</sup> GROSS, B. *J. Polym. Sci.* 1958, **27**, 135
- <sup>41</sup> CHAPIRO, A. *J. chem. Phys.* 1956, **24**, 295
- <sup>42</sup> BOAG, J. W., DOLPHIN, G. W. and ROTBLAT. *J. Radiation Res.* 1958, **9**, 589
- <sup>43</sup> SLOVOKHOTOVA, N. A. and KARPOV, V. L. *Sb. Rabot Radiatsionnoi Khim.* p 196. Akademia Nauk S.S.S.R.: Moscow: 1955
- <sup>44</sup> MIYAGAWA, I. and ITOH, K. *J. chem. Phys.* 1962, **36**, 2157



# Crystallinity and Disorder Parameters in Nylon 6 and Nylon 7

W. RULAND

*The X-ray method of crystallinity determination developed recently by the author has been applied to a series of samples of Nylon 6 and Nylon 7. The results show variations of degree of crystallinity and disorder parameter as functions of sample and preparation which can be explained by the steric possibilities for interchain hydrogen bonds. Theoretical considerations of the contribution of paracrystalline disorder to the disorder parameter  $k$  have led to a general expression which yields  $k$  as a sum of variances due to thermal motions and lattice imperfections of the first kind on the one hand and paracrystalline disorder on the other. The meaning of the degree of crystallinity in a homogeneous distribution of disorder is discussed. The scattering at wide angles is interpreted in terms of an average chain conformation.*

IN A recent paper<sup>1</sup> the author presented a method of crystallinity determination which allows one to determine a quantitative and a qualitative parameter, the degree of crystallinity and the 'disorder function'. When applying this method to a series of isotactic polypropylene samples it was found that the disorder function was not affected by quenching or annealing whereas the degree of crystallinity changed markedly. This led to the conclusion that the disorder function (which should in principle include the effect of thermal motion as well as of lattice imperfections of any kind) is predominantly determined by thermal motions in isotactic polypropylene. It was argued that such a phenomenon could be expected for linear polymers in which the interchain attraction is due to van der Waals forces only.

The present work is concerned with the crystallinity and disorder parameters in polycaprolactam (Nylon 6) and poly- $\omega$ -heptanolactam (Nylon 7). These polymers were chosen as representative examples of interchain linking by hydrogen bonds for which the above arguments do not hold.

Although considerable X-ray work had already been carried out on Nylon 6 in particular, only one paper dealt so far with the determination of crystallinity (Hendus *et al.*<sup>2</sup>), which had been carried out in the usual way of peak-to-background ratio determination. Other X-ray work dealt with structure determination<sup>3-9</sup> and qualitative aspects of disorder phenomena<sup>2,10,11</sup>. The results of these investigations can be summarized as follows.

In the crystalline forms of Nylon 6 and Nylon 7 the chains are linked together by a regular array of hydrogen bonds which build up a two-dimensional network. These planes are stacked parallel to each other in a way that causes the assembly of hydrogen bonds to lie in planes which are

perpendicular to the chain axis in the case of Nylon 6 and are tilted in Nylon 7. This difference is due to the fact that adjacent chains in Nylon 6 have opposite directions of CO—NH sequences, whereas in Nylon 7 these sequences are in the same direction.

Apart from the crystalline form there seem to exist two distinct mesomorphic forms of Nylon 6, which differ by the correlation between adjacent chain positions. The more ordered form, called smectic,  $\beta$  or  $\gamma$  form, is supposed to have hydrogen bonds distributed in planes perpendicular to the chain axis, but only a rather imperfect pseudo-hexagonal packing of the chains. This disorder is supposed to be produced by a random twisting of the chains between the planes defined by the hydrogen bond distribution. The less ordered form, called nematic,  $\gamma$  or  $\delta$  form is supposed to contain large amounts of unbonded CO—NH groups and a very imperfect parallel arrangement of the chains.

#### THEORETICAL

The basic approach to the problem has already been presented in an earlier paper by the author<sup>1</sup>. Experience gained in the course of the present work has led to further considerations which will be outlined below, using symbols and notations already defined in the earlier paper.

An essential part of the method is the disorder function  $D$  which is defined by the equation

$$x_{cr} = \frac{\int s^2 I_{cr} ds}{\int s^2 I ds} \cdot \frac{\int s^2 f^2 ds}{\int s^2 f^2 D ds} = \text{const.} \quad (1)$$

By this definition,  $D$  represents the overall disorder in the crystalline part of the substance and takes into account all kinds of disorder, averaged over all directions in space.

The disorder can be due to thermal motion or to lattice imperfections; the latter can be divided generally into those which do not affect the line profiles (first kind) and those which do (second kind). A reasonable approximation for  $D$  in the case of thermal motion and lattice imperfections of the first kind will be a spherical gaussian distribution,  $\exp(-ks^2)$ , and it has in fact been found experimentally that such a distribution yields satisfactory results even when thermal motion can be expected to be far from isotropic. In the course of this work calculations have been made taking

$$D = 2e^{-as^2} / (1 + e^{-as^2})$$

which can be regarded as a general expression for the average loss of intensity in diffraction peaks due to paracrystalline disorder (Hosemann<sup>12</sup>), which will be taken as representative for lattice imperfections of the second kind.

Calculating

$$K = \int s^2 f^2 ds / \int s^2 f^2 D ds$$

as a function of  $s_p$ , the upper limit of integration, one finds an array of

nearly straight lines in a  $K/s_p^2$  plot similar to those calculated on the assumption

$$D = e^{-ks^2}$$

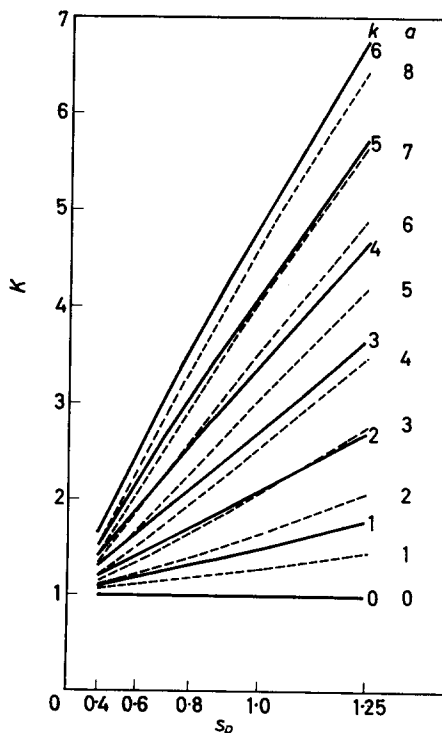


Figure 1— $K/s_p^2$  plot for  $D_1 = e^{-ks^2}$  and  $D_2 = 2e^{-as^2}/(1 + e^{-as^2})$ , valid for Nylon 6 and Nylon 7

An example is shown in *Figure 1*. This proves that it is a valid approximation in the case of paracrystalline disorder as well to represent  $D$  by a gaussian distribution, as had been postulated in the earlier paper. It shows further that lines for a given value of 'a' correspond approximately to those for  $k = 0.7a$ . This relationship will be valid for all substances with similar  $\bar{f}^2$  functions, i.e. all polymers with a C/H ratio of about 0.5 and not too many 'foreign' atoms; in fact,  $K$  versus  $s_p^2$  plots for polypropylene and Nylons turned out to be nearly identical.

One can thus write the following approximation

$$k \simeq 0.5B + 0.7a \quad (2)$$

where  $B$  is a spherically averaged temperature factor taking into account lattice imperfections of the first kind as well, and 'a' a factor determined by the lattice imperfections of the second kind.

Taking 
$$B = 8\pi^2\bar{u}^2$$

where  $\bar{u}^2$  is the average of the mean square deviation of the atoms in any

direction relative to their ideal positions, and

$$a = 2\pi^2 \overline{\Delta^2}$$

where  $\overline{\Delta^2}$  is the average of the mean square deviation of all first neighbour distributions in a paracrystal, one finds

$$k \simeq 4\pi^2 (\overline{u^2} + 0.35\overline{\Delta^2}) \quad (3)$$

On the other hand,  $\overline{\Delta^2}$  contributes to the broadening of the diffraction peaks and can be determined from a study of line width as a function of  $s$  (Hosemann and Bacchi<sup>13</sup>) which should in principle enable one to determine  $\overline{u^2}$  from  $k$ .

The increasing line width will, however, produce a considerable overlap of peaks in the spherical average of  $I(\mathbf{s})$  at higher values of  $s$ , which will lead to an underestimation of peak intensities and thus an overestimation of the contribution of  $\overline{\Delta^2}$  to  $k$ . The application of equation (3) should thus be limited to those cases where the overlap is either negligibly small or can be determined by a detailed study of line profiles.

With respect to the meaning of the degree of crystallinity of  $x_{cr}$  defined by equation (1) it has been shown in the earlier paper that this depends largely on the construction of the line separating the diffraction peaks from the diffuse scattering. Since only crystallite size of more than 30 to 50 Å average diameter and paracrystalline disorder not exceeding a value of about ten per cent for the integral width of the first neighbour distribution relative to the average first neighbour distance produce reasonably sharp diffraction peaks (half-peak width in  $s$  of about 0.02 to 0.03 Å<sup>-2</sup>), these values have been considered as the lower limits of crystallite sizes and upper limits of paracrystalline disorder for structures contributing to  $x_{cr}$ , which is defined as a weight fraction. This definition implies, of course, the existence of distinct domains of ordered and disordered structure, a concept which has often been subject to criticism. An attempt is made in what follows to produce a general model of a disordered structure which does not contain distinct domains of order and disorder, but can produce diffraction peaks sharp enough to be considered as crystalline reflections. A representative model for such a structure is a paracrystal in which the first neighbour distribution can be split into a narrow and a wide distribution. This corresponds to a structure in which the orientation and position of a structural element (a molecule or a molecular segment) with respect to its next neighbour is either well defined or at random, independent of the orientation and position of all other neighbours.

Taking a one-dimensional case for simplicity, one can define a paracrystalline disorder according to Hermans<sup>14</sup> and Hosemann<sup>12</sup> by

$$z(r) = \sum_{n=-\infty}^{\infty} h_n(r)$$

where  $z(r)$  denotes the total distance distribution of unit cell centres,  $h_n(r)$  is the probability distribution for the centre of the  $n$ th neighbour from any given centre,  $\int h_n(r) dr = 1$ ,  $h_0(r) = \delta(r)$  Dirac delta distribution,  $h_{-n}(r) = h_n(-r)$  and  $h_n(r) = h_1^{*n}(r)$ .  $*n$  denotes  $n$  times convoluted.

If  $h_1(r)$  is centred on  $r=a$  and symmetrical about this value, the Fourier transform of  $z(r)$  is given by the well-known expression

$$Z(s) = \frac{1 - H_1^2}{1 + H_1^2 - 2H_1 \cos 2\pi as} \quad (4)$$

where  $H_1$  is the modulus and  $2\pi a$  the argument of the Fourier transform of  $h_1$ .  $Z(s)$  is the paracrystalline lattice factor which shows a series of maxima and minima, the heights of which are given by:

$$Z_{\max.} = (1 + H_1)/(1 - H_1) \qquad Z_{\min.} = (1 - H_1)/(1 + H_1)$$

Defining a peak of order  $n$  by

$$P_n(s) = Z(s) - Z_{\min.}(s); \quad n - \frac{1}{2} < as < n + \frac{1}{2}$$

one finds for the integral width

$$\frac{\int P_n(s) ds}{P_{n \max.}} \simeq \frac{1}{2a} (1 - H_1 n/a)$$

and for the average intensity concentrated in the peaks

$$\langle P \rangle = 2H_1/(1 + H_1)$$

This last equation means that whenever the first order peaks are sharp enough to be considered as crystalline peaks and equation (1) is applied to the total intensity distribution,  $D$  is equal to  $\langle P \rangle$  and  $x_{cr}$  has unit value. Thus, a 'homogeneous' paracrystalline disorder will not be confounded with a heterogeneous disorder due to the existence of crystalline and non-crystalline domains.

If one assumes now that the first neighbour distribution  $h_1$  can be decomposed into a narrow ( $h_{11}$ ) and a broad distribution ( $h_{12}$ )

$$h_1 = x_1 h_{11} + (1 - x_1) h_{12}$$

which for simplicity are considered to be both centred on  $r=a$  and symmetrical about this value, one finds:

$$\begin{aligned} \sum_{n=1}^{\infty} h_n(r) &= \sum_{n=1}^{\infty} [x_1 h_{11} + (1 - x_1) h_{12}]^{*n} \\ &= \sum_{n=1}^{\infty} x_1^n h_{11}^{*n} + \sum_{n=1}^{\infty} n x_1^{n-1} (1 - x_1) h_{11}^{*(n-1)*} h_{12} + \dots \end{aligned}$$

The paracrystalline lattice factor will thus become

$$Z(s) = 1 + 2 \left[ \sum_{n=1}^{\infty} (x_1 H_{11})^n \cos 2\pi nas + \sum_{n=1}^{\infty} n (x_1 H_{11})^{n-1} (1 - x_1) H_{12} \cos 2\pi nas + \dots \right]$$

where  $H_{11}$  is the modulus of the Fourier transform of  $h_{11}$  and  $H_{12}$  that of  $h_{12}$ .

Since  $h_{11}$  is considered to be a narrow distribution and  $h_{12}$  a broad one,  $H_{11}$  is a broad distribution and  $H_{12}$  a narrow one. All terms containing  $H_{12}$  are thus heavily damped and their contribution to  $Z(s)$  is restricted to small values of  $s$ . To a first approximation one can thus neglect these terms

and consider only the first and second terms, which yield

$$Z(s \neq 0) \simeq \frac{1 - (x_1 H_{11})^2}{1 - 2x_1 H_{11} \cos 2\pi as + (x_1 H_{11})^2}$$

This function shows a series of peaks at approximately  $s = n/a$ , similar to those produced by equation (4); the width of the peaks is, however, determined by  $x_1$  as well as by  $H_{11}$ .

$$\frac{\int P ds}{P_{\max.}} \simeq \frac{1}{2a} (1 - x_1 H_{11}) \quad (5)$$

and the average intensity concentrated into the peaks is given by

$$\langle P \rangle = \frac{2x_1 H_{11}}{1 + x_1 H_{11}}$$

which can be decomposed formally into a constant term and a 'disorder function'

$$\frac{2x_1 H_{11}}{1 + x_1 H_{11}} = \frac{2x_1}{1 + x_1} D(s)$$

An evaluation of the scattering in the sense of equation (1) will thus yield

$$x_{cr} = 2x_1 / (1 + x_1)$$

but since only peak widths smaller than  $\approx 0.03 \text{ \AA}^{-1}$  are considered for  $I_{cr}$ ,  $x_1$  must be greater than 0.7 (taking  $a \approx 5 \text{ \AA}$ ), so that  $x_{cr}$  is greater than 0.8, if a homogeneously disordered structure like the one treated here is to be evaluated as being composed of a crystalline and a non-crystalline part. This means on the other hand that  $x_{cr}$  values lower than about 0.8 can only be found when a certain correlation between the ordered and disordered structural elements occurs, i.e. a segregation into ordered and disordered domains.

The model treated above can be considered as a limiting case insofar as the paracrystalline disorder is an extreme case of lattice imperfection, since only first neighbour interactions are taken into account.

#### EXPERIMENTAL

Ten samples of Nylon 6 and three samples of Nylon 7 were chosen for the investigations. The starting material for Nylon 6 was made available by courtesy of Professor P. H. Hermans, that for Nylon 7 was obtained from Dr C. Horn, Union Carbide Chemicals Company, Division of Union Carbide Corporation. The samples are classified as follows.

##### Nylon 6

- Sample 1: Bulk material,  $2 \times 3 \times 0.37 \text{ cm}$
- Sample 2: The same, heated in nitrogen at  $160^\circ\text{C}$  for 18 h
- Sample 3: The same, heated in nitrogen at  $195^\circ\text{C}$  for 10 min
- Sample 4: The same, heated in boiling water for 6 h
- Sample 5: Ground powder

- Sample 6: The same, heated in nitrogen at 195°C for 10 min  
Sample 7: The same, heated in boiling water for 6 h  
Sample 8: The same, heated in boiling water for 6 h, then heated in nitrogen at 200°C for 15 min  
Sample 9: Precipitate from a solution in formic acid, washed with boiling water  
Sample 10: The same, heated in nitrogen at 200°C for 20 min.

#### *Nylon 7*

- Sample 1: Bulk material, disc of 2.75 cm diameter, thickness 0.5 cm, heated to the melting point, quenched and annealed in nitrogen at 200°C for 1 h  
Sample 2: Precipitate from a solution in formic acid, washed with boiling water  
Sample 3: The same, heated in nitrogen at 210°C for 1 h  
Sample 4: The same as sample 1, heated to the melting point and slowly cooled.

The X-ray scattering of these samples was measured at room temperature (20° to 25°C) with a Philips (Eindhoven) diffractometer using a xenon-filled proportional counter, pulse-height discriminator, and copper radiation. Thick samples were used in order to minimize the absorption correction.

In order to check the isotropy of the samples the scattering was studied in transmission as well. A slight anisotropy was found in some cases, for which the correct intensity was calculated from a weighted average of transmission and reflection measurements.

The comparison of transmission and reflection measurements of sample 4 revealed that the crystallinity produced by the treatment in boiling water is not distributed homogeneously over the sample volume. Only a thin layer on the surface is attacked, the core of the sample stays unchanged.

Different possibilities for monochromatization have been tested specially with respect to the elimination of Compton scattering. (A detailed report on this work will be published separately.) The results indicate that it is very difficult to obtain a complete elimination of Compton scattering by crystal monochromators. With a flat lithium fluoride crystal, for example, and an angular dispersion less than a quarter of a degree the scattering of polyethylene measured with copper radiation still contains appreciable amounts of Compton scattering at values of  $s$  ( $2 \sin \theta / \lambda$ ) of about  $0.6 \text{ \AA}^{-1}$ , and is only negligible for values of  $s$  greater than  $1.0 \text{ \AA}^{-1}$ . This is due to the fact that the width of the Compton line is very large for copper radiation (about  $0.04 \text{ \AA}$  at  $s=1.0$  for polyethylene) and the wavelength distribution of Compton scattering overlaps that of the coherent scattering over a large region of scattering angles. At very wide angles ( $s > 1.1$ ) a small but detectable portion of the wavelength distribution of Compton scattering passes even the cobalt  $K$  edge. In view of these results it seems to be more appropriate to measure Compton and coherent scattering together and eliminate the Compton scattering by calculation. This was done with a filter set the thicknesses of which were chosen such that the difference of the transmitted intensity relative to the unfiltered one was practically constant between the two absorption edges. This definition of optimum filter

thicknesses has been discussed<sup>1</sup> and seems to be more appropriate for this type of measurement than the one given by Soules, Gordon and Shaw<sup>15</sup>. The transmission of the filters has been measured using a topaz single crystal as analyser and a continuous wavelength distribution emitted by a Mo-tube below the excitation voltage for MoK. The filters were produced from oxides embedded in polyethylene, a technique which has been described previously (Ruland<sup>16</sup>) and which proved to be very useful for the production of any kind of Ross filters.

## RESULTS

The scattering curves of all samples showed characteristic long-range oscillations at wide angles, some examples of which are shown in *Figure 2* on an  $sI_{coh}/\bar{f}^2$  plot. It has already been shown<sup>1</sup> that the diffuse coherent scattering at wide angles can be interpreted as an interference effect due to the most rigid interatomic vector set of the structure, i.e. the interatomic distances, which are the least affected by thermal motions and disorder phenomena. Insofar as the contribution of the crystalline part to this

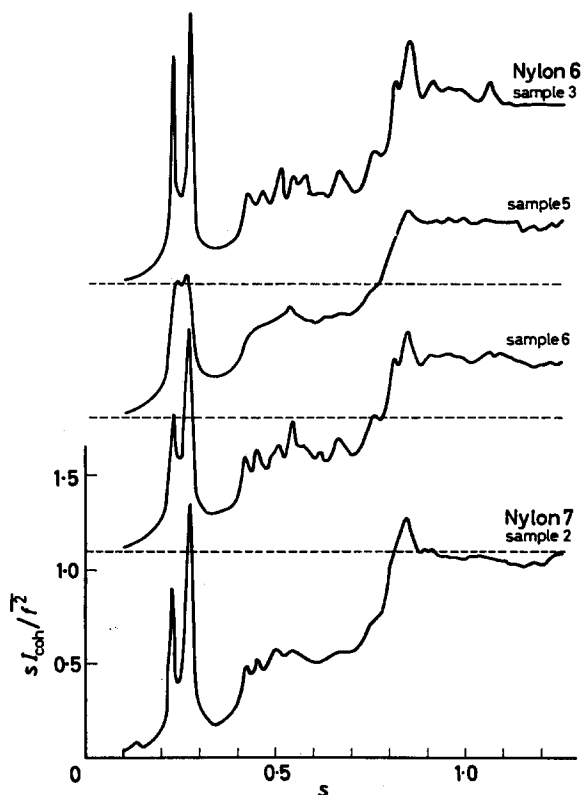


Figure 2— $sI_{coh}/\bar{f}^2$  plot for some Nylon 6 and Nylon 7 samples



scattering is concerned, this interpretation corresponds to that proposed by Amorós, Canut and de Acha<sup>17</sup> for the thermal diffuse scattering of molecular crystals. For the non-crystalline part it is equivalent to the statement of Debye<sup>18</sup> that the wide-angle scattering of liquids is predominantly determined by the molecular scattering functions.

A study of the coherent wide-angle scattering thus yields information on the average conformation of the molecules, where the average is taken over all possible conformations in time (thermal motions) and space (statistical disorder). In polypropylene (Ruland<sup>1</sup>) at room temperature the average conformation of the chains is such that the interference functions for the wide-angle scattering are predominantly determined by the first and second neighbour atoms only. This is not so for the samples studied in this work. It was found that the best model for the average conformation of the molecules in all the samples of Nylon 6 and Nylon 7 regardless of their history is a fairly straight chain with rotational disorder around the axis.

Neglecting hydrogen atoms, the wide-angle scattering due to such a structural model can be calculated as follows.

Considering a chain as a one-dimensional crystal, one finds

$$I(\mathbf{s}) = (1/N) |F^2| \cdot Z(\mathbf{s})$$

where  $I(\mathbf{s})$  denotes the coherent scattering intensity as a function of the reciprocal space vector  $\mathbf{s}$  ( $s = 2 \sin \theta / \lambda$ ) in electron units per atom,  $F$  is the structure factor as a function of  $s$ ,  $N$  is the number of atoms per unit cell, and  $Z(\mathbf{s})$  is the lattice factor.

For a perfect one-dimensional crystal  $Z(\mathbf{s})$  is non-zero only on layers normal to the unique crystal axis with interlayer distances reciprocal to the unit cell dimension along this axis. We introduce a rectangular coordinate system defined by the unit vectors  $\mathbf{e}_1$ ,  $\mathbf{e}_2$  and  $\mathbf{e}_3$ , where  $\mathbf{e}_3$  is in the direction of the chain axis and  $\mathbf{e}_3$  and  $\mathbf{e}_2$  are in the plane of the backbone of the molecule;  $s_1$ ,  $s_2$  and  $s_3$  are the components of  $\mathbf{s}$  in this coordinate system. We can then write  $Z(\mathbf{s})$  as a product of a series of equally spaced one-dimensional Dirac delta distributions along  $s_3$  with a two-dimensional distribution 'constant' on the plane defined by  $s_1$  and  $s_2$

$$Z(\mathbf{s}) = [b] (s_{1,2}) \cdot \sum_{n=-\infty}^{\infty} \delta(s_3 - nb)$$

where  $b$  is the reciprocal unit cell dimension in the direction  $\mathbf{e}_3$ ,  $n$  is the layer index, and  $s_{1,2} = s_1 + s_2$ .

The absolute square of the structure factor for a straight paraffin chain considering carbon atoms only is given by

$$|F^2|(\mathbf{s}) = 2f_c^2 (1 + \cos 2\pi \mathbf{l} \mathbf{s})$$

where  $\mathbf{l}$  is the interatomic vector and  $l$  the aliphatic C—C bond length. Multiplication by  $|F^2|$  causes modulations of the surface density of the layers in  $Z(\mathbf{s})$  which are given by

$$1 + \cos 2\pi(l_2 s_2 + n b l_3) = 1 + (-1)^n \cos 2\pi l_2 s_2$$

where  $l_2$  and  $l_3$  are the lengths of the projection of  $\mathbf{l}$  on to  $\mathbf{e}_2$  or  $\mathbf{e}_3$  and

$l_3 = 1/2b$ . Averaging around the chain axis, these fluctuations become

$$1 + (-1)^n J_0(2\pi l_2 s_{12})$$

with  $J_0$  a Bessel function of the first kind of zero order. Thus

$$I(s_{12}, s_3) = f_c^2 b \sum_{-\infty}^{\infty} [1 + (-1)^n J_0(2\pi l_2 s_{12})] \cdot \delta(s_3 - nb)$$

and finally

$$I(s) = \frac{f_c^2}{2s} b \left\{ 1 + J_0(2\pi l_2 s) + 2 \sum_{n=1}^{\infty} [1 + (-1)^n J_0(2\pi l_2 \{s^2 - n^2 b^2\}^{\frac{1}{2}})] \right\}_{s > nb} \quad (6)$$

The function in braces is shown in *Figure 3* as curve A; the contribution of  $Z(s)$  to this function (curve B) is a series of step functions of equal step heights.

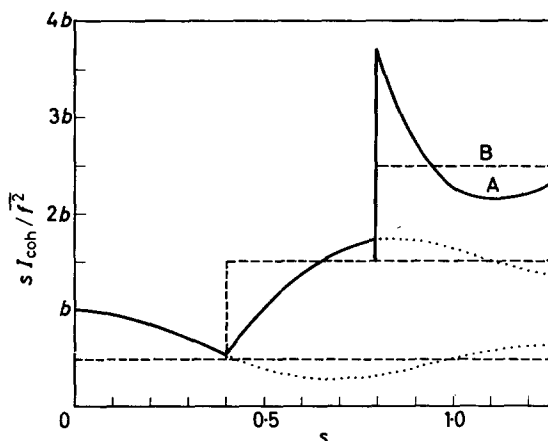


*Figure 3*— $s I_{coh}/\bar{f}^2$  plot for straight paraffin chains (carbon atoms only). Curve A (solid line): complete scattering function. Curve B (dashed line): 'Lattice' factor only. The dotted curves indicate the contribution of the separate layers to curve A

A disorder introduction by random twisting of the chain around its axis will apply a damping factor to the cosine term in  $|F^2|$  due to variations in the direction of  $\mathbf{l}$ , whereas  $Z(s)$  will not be affected much since the repeating distances along the chain axis are not varying markedly. The dominant feature at higher values of  $s$  will thus be the step functions produced by  $Z$ .

The  $s I_{coh}/\bar{f}^2$  plots of all samples studied in this work show steps at  $s \approx 0.4$  and  $0.8 \text{ \AA}^{-1}$ , the latter being more pronounced, as would be expected according to the above calculations. From this one obtains  $b = 0.4 \text{ \AA}^{-1}$  and  $2.5 \text{ \AA}$  for the repeating distance along the chain which is in good agreement with an expected value of  $2.515 \text{ \AA}$ . The absolute value of the step heights corresponds to about  $0.4$  to  $0.5 \text{ \AA}^{-1}$  ( $I_{coh}$  is normalized to electron units per atom) and is independent of crystallinity and disorder. Since the errors in the  $s I_{coh}/\bar{f}^2$  scale are much greater than those in the  $s$  scale one can assume this value to be equal to  $b = 0.4 \text{ \AA}^{-1}$ , which is the expected value according to equation (6). The average chain conformation is thus similar in all samples and corresponds to a fairly straight chain with some random twisting around the axis.

## CRYSTALLINITY AND DISORDER PARAMETERS IN NYLON 6 AND 7

The crystallinity and the overall disorder in the crystalline part were determined using equation (1). The procedure was similar to that previously described<sup>1</sup>; a refinement was introduced by a least-squares test for the determination of the best value of  $k$ . The results are shown in *Table 1*.

Table 1

Nylon 6									
Interval		Sample 3		Sample 4		Sample 6		Sample 7	
$s_o$	$s_p$	$k=0$	$k=3.0$	$k=0$	$k=4.2$	$k=0$	$k=3.0$	$k=0$	$k=5.6$
0.10	0.40	0.260	0.338	0.169	0.242	0.216	0.281	0.214	0.340
0.10	0.65	0.175	0.306	0.102	0.216	0.139	0.242	0.119	0.308
0.10	0.95	0.129	0.326	0.072	0.238	0.105	0.265	0.076	0.322
0.10	1.25	0.091	0.330	0.050	0.245	0.075	0.273	0.054	0.341
$\bar{x}_{cr}$		0.33		0.24		0.27		0.33	
Nylon 7									
Interval		Sample 8		Sample 9		Sample 10			
$s_o$	$s_p$	$k=0$	$k=3.9$	$k=0$	$k=4.4$	$k=0$	$k=3.7$		
0.10	0.40	0.232	0.324	0.253	0.367	0.241	0.331		
0.10	0.65	0.143	0.289	0.143	0.312	0.154	0.302		
0.10	0.95	0.101	0.314	0.101	0.346	0.106	0.317		
0.10	1.25	0.070	0.318	0.072	0.367	0.076	0.329		
$\bar{x}_{cr}$		0.31		0.35		0.32			
Nylon 7									
Interval		Sample 2		Sample 3		Sample 4			
$s_o$	$s_p$	$k=0$	$k=7.1$	$k=0$	$k=7.7$	$k=0$	$k=3.6$		
0.10	0.40	0.331	0.594	0.233	0.440	0.169	0.231		
0.10	0.65	0.172	0.541	0.108	0.366	0.111	0.214		
0.10	0.95	0.108	0.577	0.071	0.409	0.073	0.211		
0.10	1.25	0.075	0.598	0.050	0.433	0.055	0.234		
$\bar{x}_{cr}$		0.58		0.41		0.22			

Samples 1, 2 and 5 of Nylon 6 and sample 1 of Nylon 7 were considered as essentially non-crystalline. The scattering of sample 1, Nylon 6, at small values of  $s$  corresponds to that of the so-called smectic state (see introduction), whereas the rest of the non-crystalline samples show evidence for the preformation of crystalline lattices.

It should be mentioned that the scattering of the original quenched sample of Nylon 7 as well as of one heated in boiling water was essentially the same as that of sample 1, Nylon 7. Although the sample 2 of Nylon 6 and sample 1 of Nylon 7 show some peaks of low intensity within the first interval of integration, a determination of  $x_{cr}$  after equation (1) cannot be justified, since no peaks appear at higher angles. The values for sample 4, Nylon 6, refer to the structure of the surface, the structure of the core corresponds to that of sample 1.

## DISCUSSION

Inspection of *Table 1* shows that different treatments of Nylon 6 and Nylon 7 change not only the crystallinity but also the overall disorder in the crystalline part. Since all the samples have been measured at room temperature and no different crystalline forms occur, the contribution of thermal vibrations to  $k$  should be the same for all samples and the variation of  $k$  should thus be due to lattice imperfections. Designating the thermal

component of  $k$  by  $k_r$  and the component due to lattice imperfections by  $k_D$ , one can assume that  $k_r$  is equal to or smaller than the minimum value found for  $k$  which is 3. Consequently, the minimum values for  $k_D$  are  $k-3$ , which yields values ranging from 0 to 2.6 for Nylon 6 and 0.6 to 5.7 for Nylon 7. This indicates that, for a number of samples, the disorder introduced by lattice imperfections is at least as great as that due to thermal vibrations at room temperature. No attempt was made to carry out line-profile analysis in order to determine  $\overline{\Delta^2}$  values for paracrystalline disorder since this would have largely exceeded the scope of this work. If one assumes, however, that the width of the first diffraction peaks, which are separated best, is entirely due to paracrystalline disorder, one finds  $\overline{\Delta^2}$  values of the order of  $0.2 \text{ \AA}^2$  which would yield a maximum contribution of about 3 to  $k$  following equation (3). This is of the right order of magnitude for the samples of Nylon 6, but is much too low for samples 2 and 3 of Nylon 7. It may thus be possible that the high  $k$  values of these samples of Nylon 7 indicate a considerable contribution from lattice imperfections of the first kind.

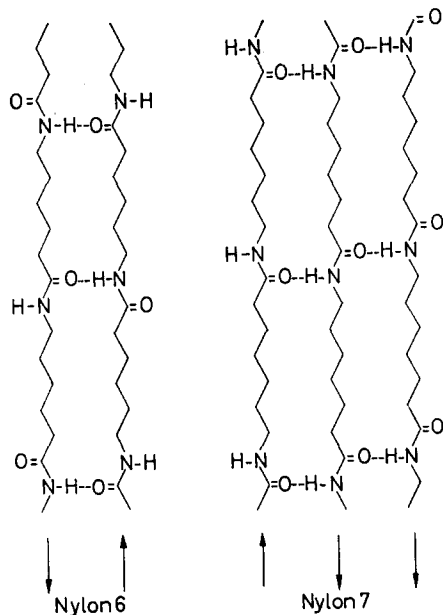
The effects of different treatments on crystallinity and disorder in Nylon 6 and Nylon 7 can be summarized as follows.

The maximum crystallinity of Nylon 6 obtainable by quenching and annealing, heating in boiling water or precipitation out of solution is roughly the same ( $\approx 33$  per cent). Quenching and annealing yields the highest order of the crystalline part, whereas boiling water and precipitation produce crystalline domains with considerable lattice imperfections. A further heat treatment can remove part of these imperfections, but the remaining disorder is still higher than that of the quenched and annealed sample.

Nylon 7 does not develop crystallinity when quenched and annealed or heated in boiling water. Precipitation from solution produces crystallinity the degree of which is somewhat higher but where the disorder is far greater than in the corresponding Nylon 6 samples. Further heat treatment of the precipitate does not increase the order; on the contrary, the crystallinity decreases considerably, whereas the disorder increases slightly. Cooling slowly from the melting point yields far lower crystallinity but a disorder parameter which is only slightly higher than that of the corresponding Nylon 6 sample.

An explanation for the different behaviour of Nylon 6 and Nylon 7 with respect to the treatments cited above can be found in the steric conditions for complete hydrogen bonding between adjacent chains. In Nylon 6 complete hydrogen bonding without chain distortion is possible only when adjacent chains have  $-\text{CO}-\text{NH}-$  sequences in opposite directions whereas for Nylon 7 these sequences can also be in the same direction (see *Figure 4*). A complete hydrogen bonding in a non-crystalline state such as a quenched melt, for example, is thus possible without much strain in the case of Nylon 7, whereas in the case of Nylon 6, considerable twisting of the chains is involved. Accordingly, the scattering of a quenched melt of Nylon 6 shows a diffraction pattern attributed to the smectic form (see introduction), whereas the scattering of the corresponding sample of Nylon 7 indicates a

Figure 4—Possibilities for ordered hydrogen bonding between straight chains of Nylon 6 and Nylon 7



preformation of the crystalline form (diffuse maxima in angular regions corresponding to main crystalline peaks). The higher strain in disordered Nylon 6 may thus be the driving force for the crystallization by annealing, whereas the energy difference between the non-crystalline and the crystalline state of Nylon 7 is too small compared with the activation energy needed for the ordered rearrangement of hydrogen bonds so that the transition from the non-crystalline to the crystalline state does not take place under the same conditions as for Nylon 6.

It is thus understandable that Nylon 7 develops crystallinity only under conditions where a hydrogen bond rearrangement does not require much activation energy, but even then, the crystalline order can be rather imperfect. The excess in imperfections may be explained by some random alternation of linkages between chains of equal and opposite directions of CO—NH sequences, an imperfection which can be regarded as predominantly of the first kind.

Since the above interpretation holds for even- and odd-numbered nylons in general, its validity is being tested by further studies. Preliminary results so far obtained with Nylon 11 and Nylon 12 are favourable.

The information obtained from the wide-angle diffuse scattering allows some conclusions to be drawn on the structure of the non-crystalline part. The appearance of step functions in an  $s I_{coh}/f^2$  plot reveals the existence of rather straight but twisted chains, and the absolute value of the step height indicates that this is the predominant average conformation of the chains in all the samples regardless of crystallinity. This means that the structure of the non-crystalline part should be at least nematic, i.e. bundles of chains without positional correlations other than the parallel arrangement of their axes. Further taking into account that in general the crystalline part

is rather imperfect, one can expect that the boundaries between crystalline and non-crystalline domains are not well defined. This does not mean, however, that separate domains do not exist. As has been pointed out in the theoretical part of this paper, a completely 'homogeneous' disorder can be present only if rather high crystallinity values are found by the method used in this work, whereas low crystallinity values always indicate a segregation of order.

*I am indebted to Drs H. Tompa, R. Hosemann and B. Hargitay for stimulating discussions during the course of this work.*

*The samples of Nylon 6 were made available by courtesy of Professor P. H. Hermans to whom I am grateful.*

*My thanks are also due to Mr J. P. Pauwels for carrying out numerous calculations.*

*Union Carbide Research Associates s.a.,  
Brussels 18, Belgium*

*(Received February 1963)*

#### REFERENCES

- <sup>1</sup> RULAND, W. *Acta cryst. Camb.* 1961, **14**, 1180
- <sup>2</sup> HENDUS, H., SCHMIEDER, K., SCHELL, G. and WOLF, K. A. *Festschrift Carl Wurster*, p 293-319. B.A.S.F.: Ludwigshafen, 1960
- <sup>3</sup> BRILL, R. *Z. phys. Chem. B*, 1943, **53**, 61
- <sup>4</sup> BUNN, W. and GARNER, E. V. *Proc. Roy. Soc. A*, 1947, **189**, 39
- <sup>5</sup> HOLMES, D. R., BUNN, W. and SMITH, D. J. *J. Polym. Sci.* 1955, **17**, 159
- <sup>6</sup> CORRADINI, P. *R.C. Ist. lombardo*, 1957, **91**, 884
- <sup>7</sup> KINOSHITA, Y. *Makromol. Chem.* 1959, **33**, 1
- <sup>8</sup> SLICHTER, W. P. *J. Polym. Sci.* 1959, **26**, 256
- <sup>9</sup> RUSCHER, CH. and VERSÄUMER, H. *Faserforschung u. Textiltechnik*, 1959, **10**, 245
- <sup>10</sup> ZIABICKI, A. *Kolloidzshr.* 1959, **167**, 132
- <sup>11</sup> RUSCHER, CH., GRÖBE, V. and VERSÄUMER, H. *Faserforschung u. Textiltechnik*, 1961, **12**, 214
- <sup>12</sup> HOSEMAN, R. *Z. Phys.* 1950, **128**, 1, 465
- <sup>13</sup> HOSEMAN, R. and BACCHI, S. N. *Direct Analysis of Diffraction by Matter*, p 325. North Holland Publishing Company: Amsterdam, 1962
- <sup>14</sup> HERMANS, J. J. *Rec. Trav. chim. Pays-Bas*, 1944, **63**, 5
- <sup>15</sup> SOULES, J. A., GORDON, W. L. and SHAW, C. H. *Rev. sci. Instrum.* 1956, **27**, 12
- <sup>16</sup> RULAND, W. *Acta cryst., Camb.* 1959, **12**, 679
- <sup>17</sup> AMORÓS, J. L., CANUT, M. L. and DE ACHA, A. *Z. Kristallogr.* 1960, **114**, 39
- <sup>18</sup> DEBYE, P. *Phys. Z.* 1930, **31**, 348

## Note

### *Polyether-Ester Copolymer Prepared from *p*- $\gamma$ -Hydroxypropoxy Benzoate and bis- $\beta$ -Hydroxyethyl Terephthalate*

IT HAS previously been published by Griehl and Lückert<sup>1</sup> that a copolymer was prepared from *p*- $\beta$ -hydroxyethoxy methyl benzoate and bis- $\beta$ -hydroxyethyl terephthalate. In this copolymer the achievable amount of crystallinity is much lower than that of the individual homopolymers, and the crystallization therefore could not be observed in the middle range of copolymer composition.

We have investigated the possibility of the formation of mixed crystals in copolymers prepared from other *p*-hydroxyalkoxy benzoates and bis- $\beta$ -hydroxyethyl terephthalate and have observed the formation of a crystallizable copolymer from *p*- $\gamma$ -hydroxypropoxy methyl benzoate and bis- $\beta$ -hydroxyethyl terephthalate over the entire range of copolymer composition. The X-ray diffraction pattern of the copolymer prepared from 50 mole per cent of *p*- $\gamma$ -hydroxypropoxy methyl benzoate and 50 mole per cent of bis- $\beta$ -hydroxyethyl terephthalate is shown in *Figure 1* as an example. This

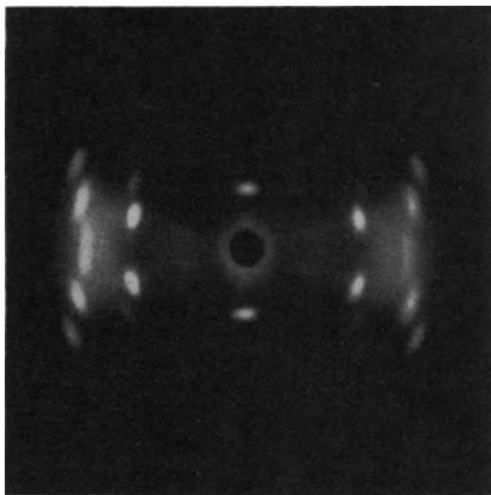


*Figure 1*—X-ray diffraction pattern of copolymer prepared from 50 mole per cent *p*- $\gamma$ -hydroxypropoxy methyl benzoate and 50 mole per cent bis- $\beta$ -hydroxyethyl terephthalate. Drawn 4.3 $\times$  at 25°C. The sample was annealed at 140°C for 1 h. Fibre axis vertical

## NOTE

---

X-ray pattern is not that of either polyethylene terephthalate or poly-*p*-1,3-propylene oxybenzoate.

This result shows that a mixed crystal is formed of the *p*- $\gamma$ -propoxy benzoate unit and the ethylene terephthalate unit, because the values of the repeating period calculated from the molecular configuration of the *p*- $\gamma$ -propoxy benzoate unit (11.07 Å) and of the ethylene terephthalate unit<sup>2</sup> (10.9 Å) are almost the same.

The detailed structures of the copolymer are being studied and a complete paper is in preparation.

M. ISHIBASHI

*Research Institute,  
Nippon Rayon Co. Ltd,  
Uji, Kyoto, Japan*

(Received November 1963)

## REFERENCES

- <sup>1</sup> GRIEHL, W. and LÜCKERT, H. *U.S. Patent No. 3 056 761* (2 October 1962)
- <sup>2</sup> DAUBENY, R. DE P., BUNN, C. W. and BROWN, C. J. *Proc. Roy. Soc. A*, 1954, **226**, 531



# Contributions to Polymer

Papers accepted for future issues of  
*POLYMER* include the following:

- Rate Dependence of the Strain Birefringence and Ductility of Polyethylene*—S. STRELLA and S. NEWMAN
- A Thermodynamic Description of the Defect Solid State of Linear High Polymers*—B. WUNDERLICH
- Graft Copolymerization Initiated by Poly-p-lithiostyrene*—M. B. HUGLIN
- Structure and Properties of Crazes in Polycarbonate and Other Glassy Polymers*—R. P. KAMBOUR
- The Crystallization of Polymethylene Copolymers: Morphology*—J. B. JACKSON and P. J. FLORY
- The Crystallization of Polyethylene II*—W. BANKS, J. N. HAY, A. SHARPLES and G. THOMSON
- Description and Calibration of an Elasto-osmometer*—H. J. M. A. MIERAS and W. PRINS
- Resonance-induced Polymerizations*—R. J. ORR
- Polypropylene Oxide I—An Intrinsic Viscosity/Molecular Weight Relationship*—G. ALLEN, C. BOOTH and M. N. JONES
- Viscosity/Temperature Dependence for Polyisobutene Systems: The Effect of Molecular Weight Distribution*—R. S. PORTER and J. F. JOHNSON
- The Photolytic Decomposition of Poly-(n-butyl) methacrylate*—J. R. MACCALLUM
- Catalysts for Low Temperature Polymerization of Ethylene*—K. J. TAYLOR
- The Effect of Tension and Annealing on the X-ray Diffraction Pattern of Drawn 6.6 Nylon*—D. R. BERESFORD and H. BEVAN
- Orientation in Crystalline Polymers related to Deformation*—Z. W. WILCHINSKY
- Morphology of Polymer Crystals: Screw Dislocations in Polyethylene, Polymethyleneoxide and Polyethyleneoxide*—W. J. BARNES and F. P. PRICE
- Nuclear Spin-Lattice Relaxation in Polyacetaldehyde*—T. M. CONNOR
- The Morphology of Poly(4-methyl-pentene-1) Crystals*—A. E. WOODWARD
- Proton Spin-Lattice Relaxation Measurements on Some High Polymers of Differing Structure and Morphology [Polyethylene, poly(4-methyl-pentene-1), poly(L-leucine), poly(phenyl-L-aniline), polystyrene and poly( $\alpha$ -methyl-styrene)]*—B. I. HUNT, J. G. POWLES and A. E. WOODWARD
- Infra-red Spectra of Poly(p-ethylene oxybenzoate)*—MATAHUMI ISHIBASHI
- Sequence Length Distribution and Entropy of Stereoregularity in Homopolymers of Finite Molecular Weight*—A. M. NORTH and D. RICHARDSON
- The Copolymerization of Methylmethacrylate and Maleic Anhydride*—A. M. NORTH and D. POSTLETHWAITE
- Polypropylene Oxide II—Dilute Solution Properties and Tacticity*—G. ALLEN, C. BOOTH and M. N. JONES

- Studies in the Thermodynamics of Polymer-Liquid Systems I—Natural Rubber and Polar Liquids*—C. BOOTH, G. GEE, G. HOLDEN and G. R. WILLIAMSON
- Studies in the Thermodynamics of Polymer-Liquid Systems II—A Re-assessment of Published Data*—C. BOOTH, G. GEE, M. N. JONES and W. D. TAYLOR
- Studies in the Thermodynamics of Polymer-Liquid Systems III—Polypropylene + Various Ketones*—W. B. BROWN, G. GEE and W. D. TAYLOR
- Studies in the Thermodynamics of Polymer-Liquid Systems IV—Effect of Incipient Crystallinity on the Swelling of Polypropylene in Diethylketone*—G. ALLEN, C. BOOTH, G. GEE and M. N. JONES
- Some Experimental Studies on Enthalpy and Entropy Effects in Equilibrium Swelling on Polyoxypropylene Elastomers*—B. E. CONWAY and J. P. NICHOLSON
- Copolymerization of Trioxan with Dioxolan*—M. KUČERA and J. PICHLER
- Thermal Degradation of an Aromatic Polypyromellitimide in Air and Vacuum—Rates and Activation Energies*—S. D. BRUCK
- The Polymerization of Propylene Oxide Catalysed by Zinc Diethyl and Aluminium Triethyl*—C. E. H. BAWN, A. M. NORTH and J. S. WALKER
- The Free Radical Polymerization of N,N-Dimethylacrylamide*—A. M. NORTH and A. M. SCALLAN
- On the Chemistry of Polymer Chain Folds*—D. C. BASSETT
- The Measurement of Dynamic Bulk Modulus using an Ultrasonic Interferometer*—W. J. PULLEN, J. ROBERTS and T. E. WHALL
- The Polymerization of Propylene Oxide Catalysed by Zinc Diethyl and Water*—C. BOOTH, W. C. E. HIGGINSON and E. POWELL
- Proton Spin-Lattice Relaxation and Mechanical Loss in a Series of Acrylic Polymers*—J. G. POWLES, B. I. HUNT and D. J. H. SANDIFORD
- Solution and Bulk Properties of Branched Polyvinyl Acetates IV—Melt Viscosity*—V. C. LONG, G. C. BERRY and L. M. HOBBS
- The Anionic Polymerization of Some Alkyl Vinyl Ketones*—P. R. THOMAS, G. T. TYLER, T. E. EDWARDS, A. T. RADCLIFFE and R. C. P. CUBBON
- Polpropylene Oxide III—Crystallizability, Fusion and Glass Formation*—G. ALLEN, C. BOOTH, M. N. JONES, D. J. MARKS and W. D. TAYLOR
- Polypropylene Oxide IV—Preparation and Properties of Polyether Networks*—G. ALLEN and H. G. CROSSLEY

CONTRIBUTIONS should be addressed to the Editors, *Polymer*, 4-5 Bell Yard, London, W.C.2.

Authors are solely responsible for the factual accuracy of their papers. All papers will be read by one or more referees, whose names will not normally be disclosed to authors. On acceptance for publication papers are subject to editorial amendment.

If any tables or illustrations have been published elsewhere, the editors must be informed so that they can obtain the necessary permission from the original publishers.

All communications should be expressed in clear and direct English, using the minimum number of words consistent with clarity. Papers in other languages can only be accepted in very exceptional circumstances.

# *Rate Dependence of the Strain Birefringence and Ductility of Polyethylene*

S. STRELLA and S. NEWMAN

*A study of the ductile–brittle transition in the tensile behaviour of linear polyethylene is presented. Equipment for the simultaneous measurement of stress, strain and optical birefringence over a broad range of deformation rates and loading times is described. Low strain birefringence measurements showed that the total molecular orientation increased with decreasing test speed. High pressure polyethylene, which is not ‘brittle’ over the range of investigated test speeds, shows no time-dependent birefringence. Further, X-ray measurements show the same sequences of polymer chain orientation for both cold-drawn and brittle-fractured material. A detailed theory is advanced for explaining the low strain behaviour, the cold-drawing process and the mechanism of the ductile–brittle transition.*

IT HAS long been known that a variety of materials undergo a rate dependent transition in their tensile behaviour. For example, linear polyethylene cold-draws when stretched at low deformation speeds. However, at impact rates of straining, continuous cold-drawing ceases and the behaviour becomes relatively ‘brittle’; that is the polymer ruptures with little or no apparent cold-drawing. The term ‘brittle’ here denotes that the material’s ability to deform or elongate has been greatly reduced, and does not necessarily signify glasslike behaviour.

At the time of the study reported here, there existed only a poor understanding of the mechanisms involved in the ductile–brittle transition of linear polyethylene. Little was known as to the mechanisms involved in the cold drawing of polyethylene, and as to its initial stress/strain behaviour. Thus, any fundamental study of the ductile–brittle transition would also involve a study of the deformation processes occurring over the complete range of the tensile stress/strain response.

In view of the above, several tools were chosen for this investigation. The high speed tension tester provided the basic evidence of the ductile–brittle transition. A second tool, developed particularly for this study, was a birefringence apparatus that would simultaneously measure, along with stress and strain, the strain–optical birefringence coefficient. Since this apparatus indicates the amount of crystal and amorphous orientation that occurs with deformation, it was felt that it would provide clues as to the deformation mechanisms involved in the low strain/time behaviour of polyethylene. The third tool to be used was X-ray spectroscopy needed to determine the morphological changes effected during the cold drawing and brittle fracturing processes. The results of these studies, and the molecular pictures, based on these findings, of the low strain deformation process,

the cold drawing mechanism, and the ductile-brittle transition are given in this paper.

#### EXPERIMENTAL PROCEDURE

The equipment described below was designed to provide a record of the birefringence change accompanying a stress-strain measurement over a broad range of strain rates. Modifications have also been developed to permit the measurement of birefringence as a function of time at a constant strain applied rapidly. With the appropriate recording apparatus, any combination of stress,  $\sigma$ , strain,  $\epsilon$ , birefringence,  $\Delta$ , or time,  $t$ , may be obtained.

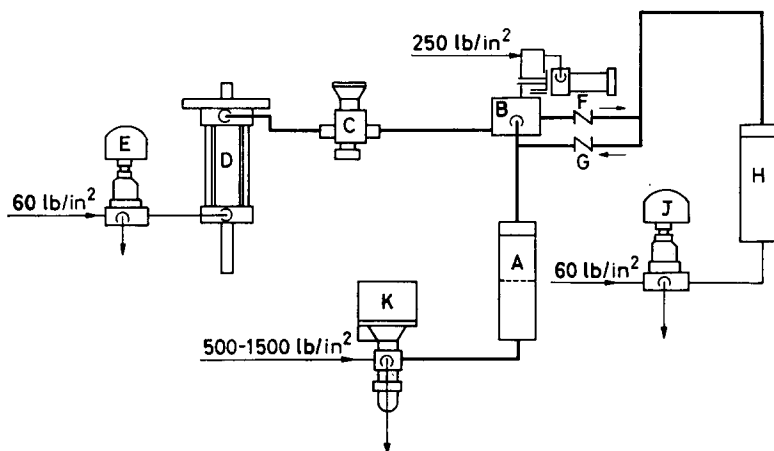


Figure 1—Flow diagram of an hydraulically operated high speed tension tester: A—drive accumulator; B—high speed valve; C—flow control valve; D—hydraulic cylinder; E, J, K—three-way air valves; F, G—check valves; H—storage accumulator

#### High rate tester

Figure 1 shows a flow diagram of the machine. Hydraulic fluid in an accumulator is pressurized by nitrogen. A mechanical valve, operated by a solenoid controlled air cylinder, allows the rapid release of the fluid into a double ended hydraulic cylinder; a needle valve controls the rate of flow into the cylinder. Air pressure is used to return the piston to test position after firing, the fluid in the cylinder being dumped into a second accumulator. The process is repeated until the drive accumulator is empty (over twenty tests are performed before this happens). The drive accumulator is then refilled with the fluid from the storage accumulator. The machine operation is electrically controlled. All components are commercial. A linear potentiometer\* is used to measure the displacement and SR-4 type cells having high resonant frequencies ( $> 10\,000$  c/s) are used to measure the

\*H.E. Sostman Company.

load\*. Available test speeds vary from less than 2 to more than 6 000 in./min. To obtain a rapidly applied constant strain, the piston was displaced by the desired amount from the end position of the piston stroke.

### *Birefringence apparatus*

*The optical arrangement*—The optical system consists principally of a conventional arrangement of a light source and crossed polaroids whose planes of polarization are symmetrically disposed about the stress direction

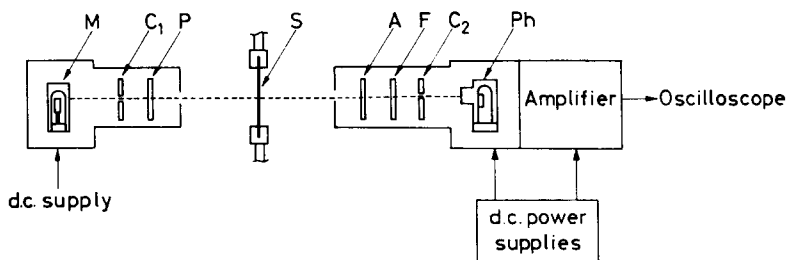


Figure 2—Schematic diagram of optical arrangement: M—mercury light source;  $C_1$ ,  $C_2$ —slits; P, A—polarizer and analyser; S—sample; F—quarter-wave plate; Ph—photocell

of the sample. A schematic arrangement of the system is shown in Figure 2. In the adaptation of this technique to the high rate tensile tester, several requirements have to be met:

(a) The absolute intensity of light must be recorded accurately over a time scale from  $10^{-4}$  sec to minutes.

(b) The intensity must be calibrated in terms of a known amount of birefringence.

(c) Residual birefringence at the start of an experiment must be eliminated or accounted for.

The use of a photomultiplier tube (IP 21) with proper circuitry and light source has permitted the achievement of requirement (a). To provide a light source free of 60 c/s signal noise, an A-H4 mercury lamp was powered by a d.c. voltage supply. In this arrangement the lamp was started with a Tesla coil.

The photomultiplier tube serves as the sensing element for determining the intensity of light restored by any double refraction of the sample located between the crossed polaroids. A bank of dry cell batteries was used to develop the necessary plate voltage free of 60 c/s noise.

Since the output signal of the IP 21 is taken off the anode-ground dropping resistor, the capacitance of a cable connecting the IP 21 tube to a distant recording oscilloscope could potentially function as an effective high frequency shunt to ground. The signal output is the product of tube current and the anode impedance; hence, for a given light intensity of

\*Dynamic Instruments Company.

varying frequency, the output voltage is inversely proportional to frequency when the capacitive reactance becomes less than that of the dropping resistor. To circumvent this shortcoming, a low gain preamplifier was mounted next to the IP 21, thus reducing the connecting capacitance to a negligible value. A good deal of tube noise was introduced into the output signal with this broad band response. This latter effect made high sensitivity determinations somewhat inaccurate. However, because polyethylene has a high strain-optical coefficient the noise effect was not bothersome.

Collimating slits, condensing lenses and quarterwave plate may be included in the optical path as required. Collimating slits were included to limit the area of the sample viewed to 1 mm<sup>2</sup>. An interference filter was used to isolate the 5 461 Å line.

*Frequency response*—As a check on the frequency response of the system, an experiment was performed in which a birefringent quartz wedge was attached to the moving jaw of the high rate tester and driven through the optical path. The intensity follows a cosine function [see equation (1)] of time since the constant velocity of the wedge introduces a linear time increase of the optical phase difference into the optical path. The response of the system may then be gauged by comparing intensity variations from zero to maximum at different rates of wedge speed. Over a range of jaw displacement rates of 8 in./min to 3 000 in./min, it was found that the recorded intensity decreased by only about 2 per cent in a time scale corresponding to about 2 msec. Similar results were obtained on following the intensity of light passed by a motor driven rotating plate containing a rectangular slit. This error is negligible when compared with more serious sources of difficulty discussed below.

*Calibration and accuracy check*—For perfect polarizers, the intensity,  $I$ , of light transmitted on insertion of a birefringent sample between the polarizer and analyser is given by the following equations<sup>1</sup>.

$$I = (I_0/2)K [1 - \cos \delta] \quad (1)$$

$$\delta = (2\pi d\Delta)/\lambda \quad (2)$$

$$\Delta = n_{\parallel} - n_{\perp} \quad (3)$$

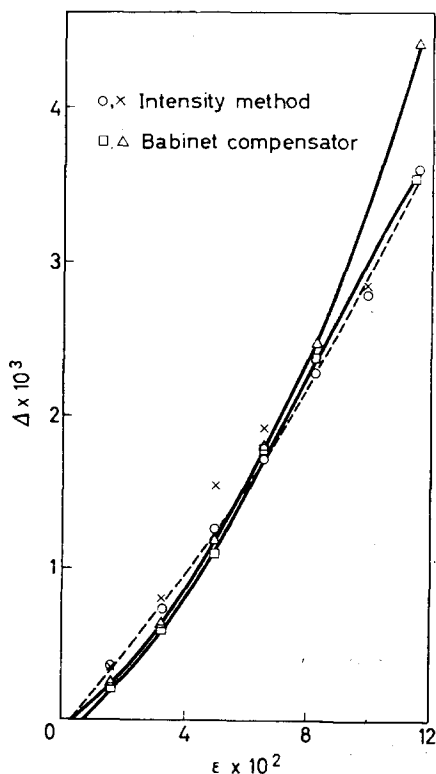
where  $I_0$  is the intensity of incident light and  $\delta$  is the phase difference which is dependent on the thickness,  $d$ , the birefringence,  $\Delta$ , and the wavelength of light  $\lambda$ . The birefringence is defined as the difference in refractive index parallel and perpendicular to the direction of vibration. The factor  $K$  is the transmittance and accounts for loss of light by reflection, absorption, scattering and depolarization encountered in the intensity calibration. The determination of  $I_0$  and  $K$  was as follows: using the polaroids, without the sample in the beam, the intensity may be varied through the equivalent of  $\lambda/2$  retardation by rotation of the analyser through 90° from the position of extinction. This permits a correlation of intensity values for 0 and  $\lambda/2$  retardation. The  $K$  value of the sample is then estimated by removing the analyser and noting the oscilloscope readings before and after insertion of the sample in the optical path. This sample position is then kept fixed through the course of the test. The experiment is completed by returning the analyser and completing the measurement.

## STRAIN BIREFRINGENCE AND DUCTILITY OF POLYETHYLENE

The variation of  $K$  with strain was found to be small, generally less than ten per cent and it was considered justifiable to take the initial value of  $K$  as constant throughout a strain-birefringence measurement.

As a check of the intensity method, absolute measurements of the birefringence of polyethylene as a function of strain were obtained using a

Figure 3—Birefringence,  $\Delta$ , versus static strain,  $\epsilon$ , for high density polyethylene by two methods



precise stretching jig and a Babinet compensator. These results were compared using the intensity method and are shown in Figure 3.

The agreement between the methods is seen to be good. Some deviation is noted at 11–12 per cent strain possibly because of non-uniform strain throughout the sample. This non-homogeneous strain factor clearly represents a major source of error particularly as the yield point of the sample is reached; in fact, since it is difficult to account for, it represents the most important source of variation and necessitates replicate measurements to assure one of representative results.

*Sample preparation*—Films of high density polyethylene (HDPE) ( $\rho=0.95$ ) and of low density polyethylene (Monsanto LDPE 406,  $\rho=0.916$ ) were obtained by compression moulding of finely ground polymer at 350°F. The films were annealed by being allowed to cool slowly under pressure over several hours in a laboratory press. Dumb-bell shaped samples, having a 0.5 in. by 1 in. gauge section, and a 0.003–0.005 in. thickness, were stamped out of the films.

## EXPERIMENTAL RESULTS

*Tensile behaviour of polyolefins*

Table 1 shows tensile data on linear polyethylene (Marlex 50—type 40), low density polyethylene (Monsanto 406), and crystalline polypropylene (Profax). It is observed, from Table 1, that both the linear polyethylene

Table 1. Tensile properties of polyolefins at various strain rates ( $T=23^{\circ}\text{C}$ )

Material	Speed (in./min)	Modulus, $E$ (lb/in <sup>2</sup> )	Yield stress (lb/in <sup>2</sup> )	Ult. elonga- tion, per cent
Marlex 50*	2 000	174 000	4 500	14.0
	200	157 000	4 180	14.3
	20	136 000	3 820	17.3
	2	122 000	3 560	200
	0.2	91 000	3 200	200
Monsanto LDPE: PE 406, annealed*	2 000	69 600	1 640	200
	200	48 600	1 630	200
	20	33 000	1 360	200
	2	26 300	1 250	200
	0.2	20 000	1 075	200
Profax, annealed†	2 000	218 000	5 590	15.8
	200	206 000	5 120	12.9
	20	171 000	4 570	14.7
	2	141 000	4 640	200
	0.2	128 000	4 340	200

\*5 in.  $\times$  5 in.  $\times$  0.1 in. sheet slow cooled from moulding temperature.

†5 in.  $\times$  5 in.  $\times$  0.1 in. sheet annealed at  $135^{\circ}\text{C}$  for three hours in a vacuum oven.

Note: All tests run in duplicate or triplicate.

and crystalline polypropylene cold-draw at deformation speeds below 2 in./min. At speeds above 20 in./min these two materials no longer macroscopically cold-draw. These materials thus undergo a ductile-brittle transition.

The low density polyethylene, on the other hand, remains ductile, even at the fastest speeds employed here. Only at loading times of about  $10^{-5}$  second does high pressure polyethylene show signs of brittle behaviour<sup>2</sup>.

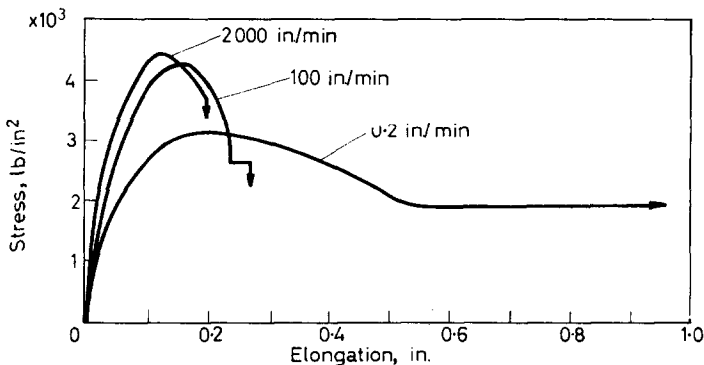


Figure 4—Stress versus elongation for high density polyethylene at different rates of elongation



## STRAIN BIREFRINGENCE AND DUCTILITY OF POLYETHYLENE

Figure 4 shows stress/elongation curves for high density polyethylene. Here again it is observed that the low pressure polyethylene undergoes a ductile-brittle transition in the range of 2 in./min to 100 in./min.

### Birefringence observations

Figure 5 shows the birefringence,  $\Delta$ , versus nominal strain,  $\epsilon$ , behaviour of HDPE over a range of deformation rates from static ( $\sim 0.1$  in./min) to 3000 in./min. As is seen, the initial strain optical coefficient,  $\Delta/\epsilon$ ,

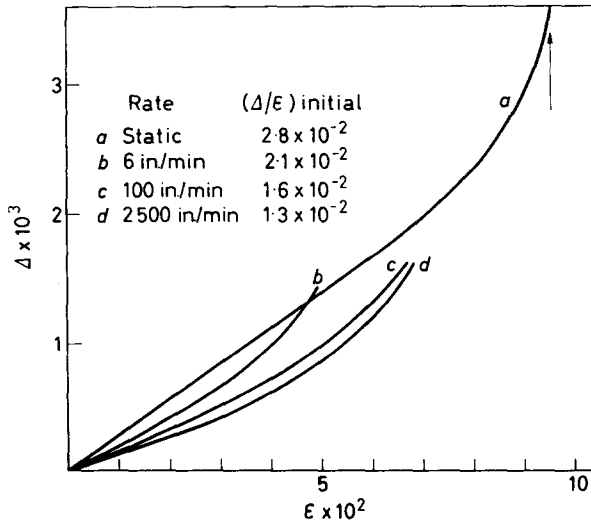


Figure 5—Birefringence versus strain at various strain rates for high density polyethylene

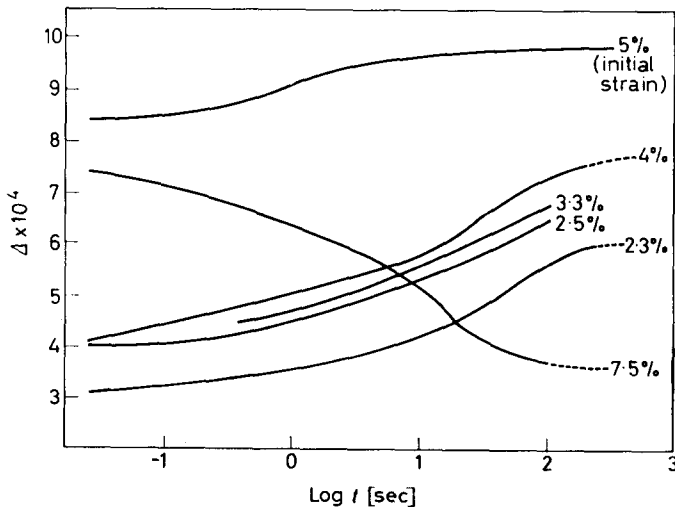


Figure 6—Birefringence versus log time at constant strain for high density polyethylene

increases by a factor of two from the fastest to the slowest test speed. The  $\Delta$  versus  $\varepsilon$  curves also are reasonably linear up to the 3-4 per cent strain level.

Figure 6 shows the birefringence against time,  $t$ , at different strain levels, these strains having been applied in about 1-2 msec and then held constant. Up to the four per cent strain level, the  $\Delta$  versus  $t$  curves have similar shapes. The values of  $\Delta$  about double from short to long times. These data are in agreement with the data obtained from the constant rate of deformation tests. Beyond the four per cent strain level the curves become different in shape. At the 7.5 per cent strain level the birefringence actually decreases with time. This drop off was shown to be a result of localized strain relief with time: measurements of both load and birefringence versus time for large constant strains indicated that the initial load exceeded the longer time yield loads and consequently that the load decreased with time to the drawing load. Thus localized yield was shown to take place resulting in strain relief in other portions of the sample and in a decrease of the observed birefringence.

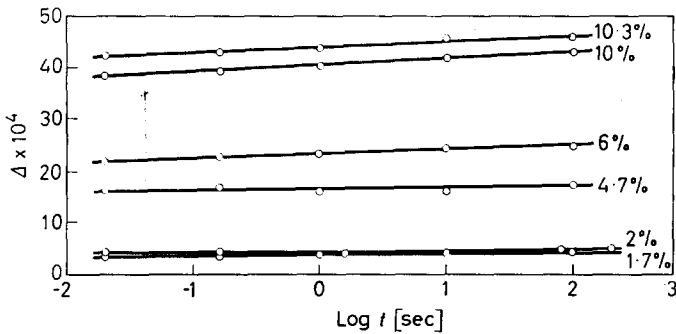
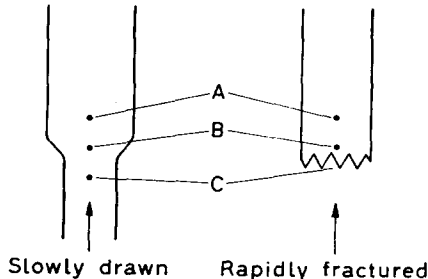


Figure 7—Birefringence versus log time at constant strain for low density polyethylene

Figure 7 shows the  $\Delta$  versus  $t$  behaviour of LDPE for rapidly applied constant strains up to about the ten per cent strain level. Here it is observed that there is little dependence of  $\Delta$  on time, as contrasted with that observed for the HDPE resin.

#### X-ray observations

Using a Norelco microcamera with a  $100 \mu$  collimator and 15 mm sample-to-film distance, photographs were taken in the various zones of HDPE test samples as depicted below.



While the disposition of the  $c$  axis or chain backbone cannot be assessed directly, examination of the alignment of two crystallographic planes does provide a statistical indication of chain orientation. A summary of the results obtained is noted below:

*Position A: undrawn zone*—This shows the typical pattern of randomly oriented polyethylene. The (110) and (200) crystalline rings and the inner diffuse halo from disordered regions are evident. No crystalline orientation is observable.

*Position B: shoulder*—Partial orientation has been produced. The (200) plane shows only a splitting into two arcs about the equator whereas the inner, more intense (110) reflection exhibits four maxima at azimuthal angles corresponding to disposition of the (110) planes at an angle of  $27^\circ$  to  $37^\circ$  to the stretching direction. This suggests orientation of the  $a$  axis perpendicular to the stretch direction and an alignment of the backbone tilted at an angle of roughly  $35^\circ$  to  $40^\circ$  to the stretch direction.

It should also be noted that near the fracture or cold-drawn zone, the diffuse halo is also drawn into arcs in a manner similar to that of the (110) plane indicating that the less ordered regions also orient appreciably on stretching.

*Position C: drawn or fractured region*—For the cold-drawn polymer, the (200) and (110) reflections are found to indicate a high degree of orientation and alignment parallel to the stretch direction. The same observation applies to the fractured edges of the samples broken at displacement rates of 100 and 2 000 in./min.

The X-ray patterns of cold-drawn polyethylene as a function of elongation have been examined in detail by others, Brown<sup>3</sup>, Keller<sup>4</sup>, Horsley and Nancarrow<sup>5</sup>. The main points noted above—of (a) an initial orientation of the  $c$  axis of the crystals about an average angle of roughly  $35^\circ$  to  $40^\circ$  with the stretching direction, and (b) a decrease of this angle to  $0^\circ$  at high elongations—have been noted previously.

For the present report, the essential point is that in the fast fracture tests involving rupture in periods as short as  $10^{-2}$  sec a complete alignment of the polymer chain is achieved in much the same sequence as occurs in the slowly drawn samples over longer time scales. However, it should be noted that the regions of complete  $c$  axis orientation were difficult to find in the high speed 'brittle' fractured samples.

## DISCUSSION

### *Low strain behaviour—birefringence—time studies*

For a completely amorphous, isotropic material, e.g. an elastomer, the observed birefringence due to stretching is a function of the optical anisotropy caused by increasing the molecular end-to-end distance in the direction of increasing strain<sup>6</sup>. In a partially crystalline material above its glass temperature, the situation is complicated by the additional orientation of optically anisotropic crystals. Thus the observed birefringence (neglecting form birefringence) is a function of both amorphous and crystal orientation, i.e.

$$\Delta = \Delta_a + \Delta_c \quad (4)$$

where  $\Delta$  is the observed birefringence,  $\Delta_a$  is the birefringence from the amorphous orientation and  $\Delta_c$  is that from crystal orientation.

From dynamic birefringence studies of polyethylenes, LeGrand<sup>7</sup> showed a marked dependence of the birefringence strain-optical coefficient (SOC) with frequency, even for low density materials. In an attempt to rationalize his observations, LeGrand took the view that the crystals could be represented as discrete particles embedded in an amorphous, viscous matrix. At high frequencies, the crystals could not orient or follow the field because of viscous 'drag' effects.

Stein<sup>8</sup> also measured the dynamic strain-optical coefficient for several different density polyethylenes. He observed a small time-dependence for the low density materials and a relatively large dependence for higher density samples. His SOC/frequency values are in agreement with the SOC/time values presented here. Applying linear viscoelasticity theory, Stein fitted a Maxwell model to the observed frequency dependence, associating  $\Delta_a$  with the strain on the springs and  $\Delta_c$  with that on the dashpots. In doing so he assumed that the amorphous chains responded instantaneously and that the initially unresponsive crystals slowly deformed or rotated.

In the light of present views on the crystal morphology of polyethylene neither of these models can be deemed realistic. The primary structural element of high density polyethylene is held<sup>9</sup> to be lamellae of chains with folded conformation. A considerable portion of the chains emerging from the crystal surface leave it entirely and enter other crystals while the remainder return to the same crystal or terminate in intercrystal regions. The degree of folding regularity of those returning chains is a matter of present day conjecture<sup>10</sup>. The interconnecting chains may be considered the primary elements holding the crystals together in the bulk polymer. Were it not for these chains the mechanical properties of polyethylene would be similar to those of low molecular weight paraffins. These chains transmit applied stresses to the crystals.

An elastomer containing a large amount of rigid filler, the filler being well bonded to the matrix, represents an oversimplified model of polyethylene. For such a material it is quite evident that there will be no time lag (except for negligible inertia effects) in the position change of the filler particles as a bulk sample is stretched and consequently no time-dependent birefringence.

This model cannot be improved by invoking the possibility of a time-dependent crystallographic slip occurring at *low* strains. From *Figure 6* it is seen that the shape of the birefringence/time curves for high density polyethylene does not change up to about the four per cent strain level. It has already been shown that the time dependence of the coefficient is a linear phenomenon, 'linear' being used in the same sense as in viscoelastic theory. Since slip processes are not 'linear' phenomena, one must conclude that such processes do not occur at low strain levels.

It thus seems reasonable that if *all* amorphous chains respond, then any amorphous chain deformation should result in an immediate elastic crystal deformation or rotation. It remains to explain the origin of the time dependence.

## STRAIN BIREFRINGENCE AND DUCTILITY OF POLYETHYLENE

A crude calculation of the number of carbon atoms involved in interconnecting chains can be made if one assumes the crystallites are rectangular parallelepipeds in an amorphous matrix. Such a calculation yields an average value of about ten carbon atoms for high density ( $0.96 \text{ g/cm}^3$ ) polyethylene, about twenty for low density ( $0.91 \text{ g/cm}^3$ ) polyethylene. Flory<sup>10</sup> has also shown that there should be a distribution in the lengths of the interconnecting chains.

It is well known that, for a crosslinked system, as the molecular weight between crosslinks decreases, the mechanical relaxation times of the whole system increase.

It may thus be that in some regions the tie chains are sufficiently short so that the relaxation times of these regions fall within the time scale of the birefringence measurements reported here. That is, at short times the spring constant or 'modulus' of the regions is considerably higher than that at long times.

Since it is known<sup>11</sup> that chemical impurities concentrate in the neighbourhood of growth fronts, it is believed that spherulite perfection is greater toward the centre. This implies that the spherulite density diminishes with distance from the centre. One may then presume that the length of the tie chains decreases, and thus the regional relaxation times increase, as the centre is approached. This possibility will permit a time-dependent strain distribution within the spherulite leading to a time-dependent strain optical birefringence coefficient.

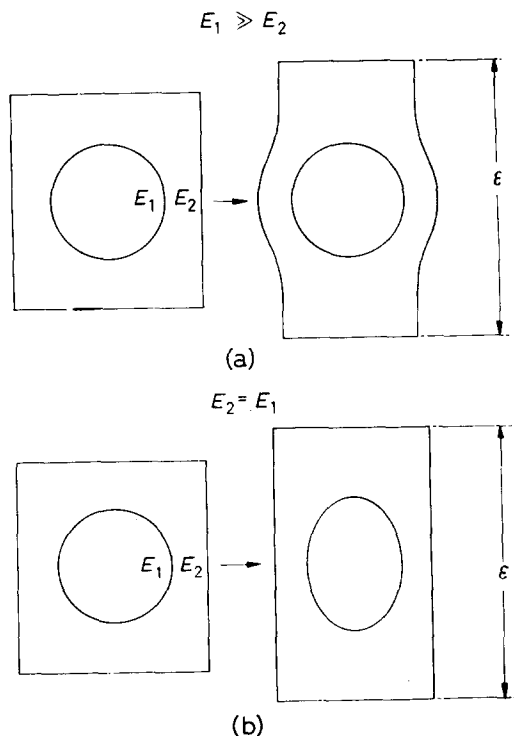


Figure 8—Model for deformation of spherulite

Recognizing that the spherulite possesses a modulus dependent on radius, we may nevertheless approach the matter of time-dependent strain distribution in the following simplified manner. The strain distribution may be arrived at if the spherulite is considered as consisting of a sphere of modulus  $E_1$  within a matrix of modulus  $E_2$ . For a given total deformation, if at short times  $E_1 \gg E_2$ , then only the matrix will be strained, with little deformation of the sphere occurring. However, as time increases, the modulus of the sphere  $E_1$  decreases and consequently the sphere will become more and more deformed. Based on the fact that the  $c$  axis of the crystals has tangential symmetry within the spherulite, it can be shown that, for a given total deformation of the system, if the strain of the sphere is small compared to that of the matrix, then the observed total  $c$  axis orientation is less than if the strain of the sphere is that of the matrix (see *Figure 8*). It is thus postulated that because of a variation in the length of the interlamellar tie chains within the spherulite, the spherulite deformation changes with time and that this change accounts for the observed time-dependent birefringence at low strains.

Further, for LDPE, since  $M_c$ , that is the interlamellar tie chain length, is considerably larger than that for HDPE, then the response times of an interconnecting network should be much smaller than for HDPE. Also, chain folding should be much less regular than for the high density material. Thus for the time scale of the experiments reported here, little time dependence of the strain birefringence of LDPE should be observed. This, as is seen from *Figure 7*, is so.

#### *Large strain behaviour: cold drawing and brittle fracture*

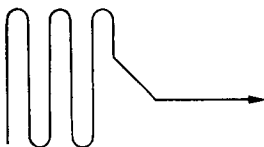
Above four per cent strain, there is a marked deviation from linearity in the dependence of stress and of birefringence on strain (see *Figures 5* and *6*). Principally, one notes a yield point which is suggestive of cold drawing. This observation applies over the entire range of deformation rates investigated. X-ray diffraction studies discussed previously showed that some cold drawing occurs even at the fastest speeds employed here. The ductile-brittle transition is therefore believed to be the condition where brittle fracture has outweighed but not completely supplanted cold drawing. In order to explain this transition it becomes necessary to consider the possible mechanisms involved in deformation. These mechanisms are discussed below.

*Cold drawing\* as a melting process*—A thermodynamic melting, stretching and recrystallization may account for the cold-drawing process. For this mechanism, one might conjecture that fracture would occur if the test speed were such that insufficient time were allowed for recrystallization. Since a melting under adiabatic conditions would demand that the energy input be at least equal to the heat of fusion, let us consider the maximum possible temperature rise. If all the work performed is converted into heat, then from a knowledge of the load/deformation relation, and the heat

\*Necking in itself is probably a macroscopic phenomenon only since crystalline and non-crystalline polymer can be cold-drawn; we are therefore not concerned here with the phenomenon itself but rather with the specific molecular processes involved in the conversion of a random to an oriented structure in polyethylene.

capacity, an average temperature rise of  $\sim 60^\circ\text{C}$  is estimated (see Appendix I). This rise is clearly insufficient to melt any but the lowest melting crystals. The mechanism does not, therefore, appear tenable. Furthermore, Horsley<sup>7</sup> points out that, at  $96^\circ\text{C}$ , the stage of elongation characterized by the splitting of the (110) ring into four distinct maxima does not take place for low density polyethylene. This lack of (110) splitting was not observed in our studies of high density polyethylene. While this is not unequivocal, it does suggest that whatever heating occurs in the sample due to stretching is not sufficient to alter the stretching process.

*Cold drawing as a crystal-stripping process*—It has been postulated<sup>12</sup>, at least for a single lamella, that crystal destruction can occur by a stripping of chains out of the lattice as shown below :



Such a process would involve a local heating immediate to the stripping point. Thus, at faster deformation rates, the stripping process should occur more readily since the heating would be greater as the process becomes more adiabatic. In fact, however, the yield strength and steady state drawing stress increase with drawing rate for high density polyethylene.

It therefore appears that a melting or a stripping away of chains as discussed above cannot occur exclusively; that it may occur in conjunction with or as a modifying influence on other mechanisms cannot be discounted.

*Cold drawing as a slip process*—A comparison of the birefringence/strain relation between high and low density polyethylene discloses considerable differences. As first shown by Kolsky<sup>13</sup> and as indicated in Figure 7, the birefringence of low density polyethylene is essentially a linear function of the strain with very little dependence on time. On slow deformation a low density sample undergoes homogeneous strain and concordantly a gradual rearrangement of crystallites so as to orient the  $c$  axis parallel to the stretching direction. As discussed in more detail previously, this process probably involves gradual deformation of a spherulite into an ellipsoid having ellipsoidal symmetry. Up to about 25 per cent strain, the birefringence and strain are largely recoverable and the integrity of the spherulite is maintained. Here, the internal rearrangement of the spherulite probably takes place by a movement of lamellae with associated tie chains with relatively little disruption or irreversible slippage of portions of lamellae.

On the other hand, for high density polyethylene, necking and the associated localized complete  $c$  axis orientation cannot be avoided even under extremely slow or nearly isothermal conditions<sup>14</sup>. Necking involves annihilation of spherulites, and a drawing out into a fibrous structure. It seems reasonable to assume in this case an intra-lamella crystallographic slip process. The occurrence of slip in crystalline polymers has already been advanced by others<sup>16, 17</sup>.

Adopting the current view that the bulk solid contains lamellae of folded chains, it would be expected that slip may leave the original fold length intact. Some evidence for folding in drawn material does exist<sup>9</sup> but it is not unequivocal. Additionally, stress measurements during crystallization of an oriented melt give evidence of folding<sup>17</sup>.

A regularly folded lamellar structure would be expected to slip parallel to the  $c$  axis and to the fold planes; that is along the (110) planes. Since it is unlikely that each folded chain lies within the same plane, it seems inevitable that some covalent bonds would necessarily be broken and reformed in a slip process. It appears possible to construct dislocations such as a Frank-Read source<sup>18</sup> which will permit easy gliding along the (110) planes, for instance. Such a dislocation is shown in *Figure 9*, where it is seen that the dislocation boundaries lie in and normal to the (110) planes. Also, for a non-folded structure slip can occur at any crystallographic plane parallel to the  $c$  axis.

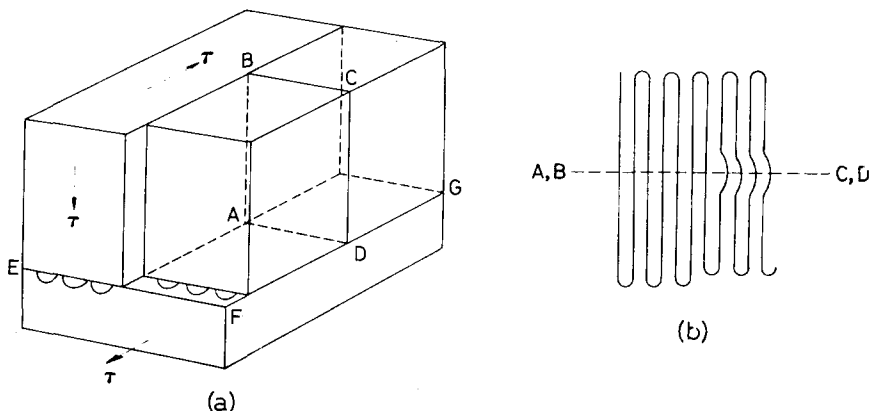


*Figure 9*—Figure representing an example of slip that produces a bent dislocation. This Frank-Read mechanism<sup>18</sup> permits a very large amount of slip on a single slip plane. Plane EFG corresponds to the (110)

Now it has been shown<sup>21</sup> that crystal slip can occur at velocities up to about a tenth of that of the Rayleigh wave velocity,  $C$ . Assuming a modulus of  $\geq 10^{10}$  dyne/cm<sup>2</sup> for the polyethylene crystal, then  $C$  is  $\geq 10^5$  cm/s. This is well above the velocities at which the ductile-brittle transition occurs. However, it has been shown<sup>19, 20</sup>, both theoretically and experimentally (at least for inorganic and metallic crystals), that the stress required to produce slip decreases with decreasing slip velocity. Conversely as the deformation rate and with it the dislocation rate is increased, the system will necessarily experience an increasing stress. In other words, the shear-slip yield stress increases with increasing deformation rate. It is presumed that the tensile strength will only moderately depend on deformation speed. Thus, it is postulated that in the weaker (tensile) parts of the spherulite, the shear yield strength exceeds twice the tensile strength and these parts suffer a tensile fracture whereas the stronger parts still undergo shear yielding.



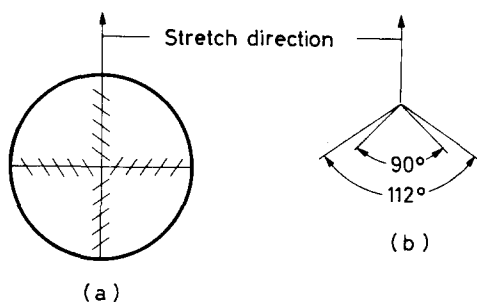
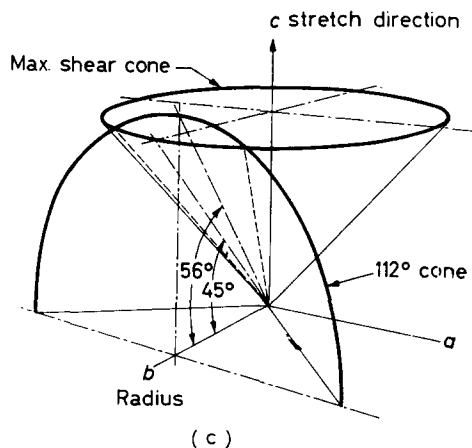


Figure 10—(a) Disposition of (110) planes in a spherulite; (b) Intersection of maximum shear cone and cone tangent to (110) plane. Spherulite radius normal to stretch direction; (c) Spherulite radius parallel to stretch direction



A possible mechanism of the drawing process may be advanced; considering first the spatial orientation of the (110) planes. Since the  $b$  axis of the crystals is known to be parallel to the spherulite radius then the (110) plane lies at about a  $55^\circ$  angle to the  $a$  radius. Further, the  $a$  axis rotates around the radius; thus the (110) planes will be tangential to a  $110^\circ$  cone. For the diameter normal to the stretch direction this cone will intersect the  $45^\circ$  cone of maximum shear. Thus some (110) planes will experience maximum shear. For the diameter parallel to the stretch direction the two cones will not intersect (see Figure 10), and no (110) planes will be at maximum shear. Therefore, the initial shear slip along (110) will occur on the diameter normal to the stretch direction. This appears consistent with the observation from environmental stress cracking that spherulite fracture is always on the diameter normal to the stretch<sup>21</sup>. As slip proceeds, neighbouring radii will be bent normal to the stretch direction, and the ribbon radii will tend to untwist. A persistence of a  $35^\circ$  (110) tilt would be observed in the drawing process. This is indicated from the X-ray evidence that some crystals are at  $35^\circ$  to the stretch direction during the drawing process. The process will continue until the spherulite is destroyed and complete  $c$  axis orientation is obtained.

Now it may be that the requisite stress or force per chain to cause high speed slip is greater than can be withstood by poorly interconnected crystals. These chains will fracture as the strain is increased. However, those

crystals that have sufficient interconnecting chains will still slip, even at the fastest speeds used in this work. Therefore, beyond a critical speed one begins to observe a combination of brittle fracture and ductile drawing and, thereafter, the faster the deformation speed the more brittle the fracture. The combination, of course, results in an apparent brittle fracture.

#### APPENDIX I

For HDPE the draw ratio (at 0.2 in./min crosshead speed) is 10:1, and the drawing stress is  $1.6 \times 10^8$  dyne/cm<sup>2</sup> based on the initial cross section area.

Consider an initial cube of 1 cm side completely drawn down (from  $1 \times 1 \times 1$  cm<sup>3</sup> to  $0.31 \times 0.31 \times 10$  cm<sup>3</sup>). The work,  $W$ , done in the drawing process is

$$\begin{aligned} W &= \int F ds \\ &= 1.60 \times 10^8 \text{ dyne} \times 9 \text{ cm} \\ &= 34 \text{ g cal} \end{aligned}$$

Taking as an average a  $C_p$  of  $0.55 \text{ cal } ^\circ\text{C}^{-1} \text{ g}^{-1}$  and the density as about  $1 \text{ g/cm}^3$  then, the temperature rise,  $\Delta T$ , is

$$\Delta T = W/C_p = 62^\circ\text{C}$$

*We would like to thank Mr Q. A. Tremontozzi for his support of this work.*

*We are indebted also to Dr F. D. Stockton for his proof of the statement that observed birefringence is dependent on the strain distribution within a spherulite, for his many helpful discussions and his careful reading of this manuscript. We wish also to acknowledge the work of Mr A. A. Bibeau and Dr J. Woodbrey for carrying out the X-ray diffraction measurements and for their assistance in interpretation of the results. Lastly we wish to note that Mr Bibeau assisted in some of the birefringence measurements.*

*Monsanto Chemical Company Plastics Division,  
Springfield, Mass., U.S.A.*

*(Received March 1963)*

#### REFERENCES

- <sup>1</sup> JENKINS, F. A. and WHITE, H. E. *Fundamentals of Optics*. McGraw-Hill: New York, 1950
- <sup>2</sup> KAUFER, H. and MARTIN, G. *Kolloidzshr.* 1958, **157**, 124
- <sup>3</sup> BROWN, A. J. *appl. Phys.* 1949, **20**, 552
- <sup>4</sup> KELLER, A. J. *Polym. Sci.* 1955, **15**, 31
- <sup>5</sup> HORSLEY, R. A. and NANCARROW, H. A. *Brit. J. appl. Phys.* 1951, **2**, 345
- <sup>6</sup> TRELOAR, L. R. G. *The Physics of Rubber Elasticity*. Oxford University Press: London, 1949
- <sup>7</sup> LEGRAND, D. G. and ERHARDT, P. F. Paper presented at the American Rheological Society meeting, November 1961
- <sup>8</sup> STEIN, R. S., ONOGI, S. and KEEDY, D. A. *J. Polym. Sci.* 1962, **57**, 801
- <sup>9</sup> STUART, H. A. *Ann. N.Y. Acad. Sci.* 1959, **83**, 3

## RATE DEPENDENCE OF POLYETHYLENE

---

- <sup>10</sup> FLORY, P. J. *J. Amer. chem. Soc.* 1962, **84**, 2857
- <sup>11</sup> KEITH, H. D. Paper on 'Mechanisms of spherulite crystallization' presented at American Chemical Society meeting, Atlantic City, September 1962
- <sup>12</sup> HIRAI, M., KISO, H. and YASUI, T. *J. Polym. Sci.* 1962, **61**, S1
- <sup>13</sup> KOLSKY, H. and SHEARMAN, A. C. *Proc. phys. Soc., Lond.* 1943, **55**, 383
- <sup>14</sup> NEWMAN, S. *J. appl. Polym. Sci.* 1959, **2**, 252
- <sup>15</sup> FRANK, F. C., KELLER, A. and O'CONNOR, A. *Phil. Mag.* 1958, **3**, 64
- <sup>16</sup> ZAUKELIES, D. A. *J. appl. Phys.* 1962, **33**, 2797
- <sup>17</sup> GENT, A. N. and MORRIS, M. C. Paper presented at American Chemical Society meeting, Atlantic City, September 1962
- <sup>18</sup> READ, W. T., Jr. *Dislocations in Crystals*. McGraw-Hill: New York, 1953
- <sup>19</sup> COTTRELL, A. H. *Dislocations and Plastic Flow in Crystals*. Clarendon: Oxford, 1953
- <sup>20</sup> GILMAN, J. J. *Properties of Crystalline Solids*, p 69. ASTM Special Technical Publication No. 283, 1961
- <sup>21</sup> ISAKSEN, R. A., NEWMAN, S. and CLARK, R. J. *J. appl. Polym. Sci.* 1963, **7**, 515

# *A Thermodynamic Description of the Defect Solid State of Linear High Polymers\**

B. WUNDERLICH†

*It is attempted to describe the solid state of linear crystalline polymers using the defect concept. This metastable solid state which is normally found in polymers is described thermodynamically. Changes in state are traced as a function of heating rate. The limiting experimental maximum melting point on fast heating,  $T_m'$ , is described by the equation*

$$\ln X_A = \Delta H_u / R (T_m'^{-1} - T_m^{-1})$$

*which contains as parameters the activity of crystallizable units in the melt,  $X_A$ , the heat of fusion at  $T_m$ ,  $\Delta H_u$ , and the experimental maximum melting point on fast heating of large defect free lamellae into a melt  $X_A = 1$ :  $T_m'$ . For linear polyethylene experimental evidence is cited which supports the theoretical description.*

## THE DEFECTS IN THE CRYSTALLINE SOLID STATE OF LINEAR HIGH POLYMERS

THE crystal structure of solids is usually represented by a regular coherent arrangement of molecules, atoms or ions in space. This 'ideal' crystal structure is demonstrated by the common ball and stick model of crystal lattices. No 'real' crystal, however, conforms exactly to this picture. Even at the absolute zero of temperature zero point vibrational motion remains, disturbing the ideal crystal arrangement. At higher temperatures this thermal motion increases. Other imperfections may result from errors in the arrangement and inclusion of foreign building blocks.

In this article only molecular crystals will be considered. Particular attention will be paid to the prototype of the one dimensional macromolecules: polyethylene.

Molecular crystals in general can be subdivided into the four categories shown in *Table 1*. The one dimensional type crystal occupies a special position among these four types of molecular crystals.

Its atoms are held together strongly in one direction only, forming covalently bonded linear chains. These chains in turn are held together in the three dimensional array by very much weaker secondary forces. In polyethylene the force constant for the  $-\text{CH}_2-\text{CH}_2-$  stretching in the chain is about  $4.0 \times 10^5$  dyne/cm, while the force constant for the separation of the nearest neighbour  $\text{CH}_2$  groups of different chains is estimated to be  $0.16 \times 10^5$  dyne/cm. This leads to the result that during melting for most linear polymers the chain remains intact, no covalent bonds are broken.

\*This paper was presented in part at the 142nd Meeting of the American Chemical Society, Atlantic City, 1962.

†Present address: Department of Chemistry, Rensselaer Polytechnic Institute, Troy, New York.

B. WUNDERLICH

Table 1. Types of molecular crystals

Type	Examples	Configurations formed by the strong covalent forces	Description
0	CO <sub>2</sub> , CH <sub>4</sub>	Isolated complexes	Island crystals, low melting
1	(CH <sub>2</sub> ) <sub>x</sub> , Se <sub>x</sub>	Chains	Linear polymers, intermediate melting
2	Graphite, BN	Two dimensional layers	Plate crystals, high melting
3	SiO <sub>2</sub> , diamond	Three dimensional network	Usually hard, high melting

The melting point  $T_m$  is thermodynamically expressed by

$$T_m = \Delta H_f / \Delta S_f \quad (1)$$

where  $\Delta H_f$  and  $\Delta S_f$  are the enthalpy and entropy of fusion. One has to heat higher to melt the still one dimensionally ordered chains (depolymerization). This second, 'melting' temperature (ceiling temperature,  $T_c$ ) is described thermodynamically<sup>1</sup> by the equation

$$T_c = \Delta H_p / \Delta S_p \quad (2)$$

where  $\Delta H_p$  and  $\Delta S_p$  are the enthalpy and entropy of depolymerization. Data for polyethylene are summarized in Table 2. For polyethylene under normal conditions this depolymerization is an irreversible process leading not to the monomer ethylene, but to various decomposition products. An example for an easily observable ceiling temperature (132°C) is that of a methyl methacrylate solution ( $\sim 0.04 \text{ g cm}^{-3}$ ) in *o*-dichlorobenzene<sup>2</sup>.

Table 2. Equilibrium parameters for polyethylene

	$\Delta H$ (cal/mole CH <sub>2</sub> )	$\Delta S$ (cal/deg mole CH <sub>2</sub> )	$T$ (°K)
Crystalline melting	928 <sup>3</sup>	2.23	415 <sup>4</sup>
Depolymerization	22 350 <sup>5</sup>	34.0 <sup>5</sup>	657

Crystallizing a melt of linear high polymers poses the problem of arranging already one dimensional ordered chains which are randomly entangled into a three dimensional crystalline array. This complicated process leads to a large number of imperfections. This is borne out by the fact that the most perfectly crystallized polyethylene experimentally obtainable still has about five to ten per cent non-ordered material.

Generally there are seven types of defects distinguished in crystalline solids<sup>6,7</sup>, namely (1) phonons, (2) electrons and holes, (3) excitons, (4) vacant lattice sites and interstitial atoms, (5) foreign atoms on interstitial and substitutional positions, (6) dislocations, and (7) two dimensional or surface imperfections. Because of the special nature of linear high polymers, defects which cannot be included in the above categories are also found, namely (8) chain disorder and (9) amorphous defects.

*Phonons*—These are the imperfections connected with the vibration of the lattice. For polyethylene a complete description is given in refs. 8 and 9.

*Electrons, electron holes and excitons*—These are defects mainly of interest in radiation and photochemistry, because of the high electronic

energies involved in most molecular crystals. These imperfections will not be treated in detail here.

*Vacant lattice sites and interstitial atoms*—These can be classified as point defects, and behave differently in linear polymer crystals and in monomeric crystals. The vacancies will mainly arise in connection with other defects such as the ends of chains, which must be classified as foreign atoms because of their different chemical nature. Single interstitial atoms are only possible as monomeric impurities (foreign atoms). Side chains of the proper character may also be called interstitial, but show the characteristic of being immobile and usually an interstitial element in a polymer crystal gives rise to chain disorder and (or) an amorphous defect as has been shown for  $-\text{CH}_3$  side chains off the polyethylene chain<sup>10</sup>.

*Dislocations*—Dislocations which are one dimensional or line imperfections are found analogously to the monomeric crystals. An example is the screw dislocation allowing thickening of the platelet-like growth of polyethylene<sup>11</sup>. Edge dislocations also have been discussed for polyethylene, although experimental proof is still uncertain<sup>12</sup>.

*Two dimensional imperfections*—These include grain boundaries, twin boundaries, phase boundaries and stacking faults as well as the crystal surface. All of these can be found in polymeric crystals. The surface of particular interest is the (001) surface which consists of aligned folds<sup>11</sup>. A one dimensional defect found only in linear high polymers is the fold domain boundary<sup>13</sup>. On the top and bottom of a domain boundary the direction of folding of the chains changes. The twin boundary found most frequently in polyethylene is the (110) plane<sup>14</sup>.

*Chain disorder*—This includes defects like folds, in which the chain turns more or less sharply back on itself. In single crystals grown from dilute solution the fold defects are approximately aligned on the (001) surface of the crystal, forming a two dimensional imperfection. Similar defects not aligned in a surface must be assumed also possible inside the crystal. A chain defect, which has been postulated to explain the thickening of single crystals grown from solution involves an additional  $\text{CH}_2$ — accommodated within a chain by twisting the chain out of and back into the all-*trans* conformation over a range of five  $\text{CH}_2$ — groups<sup>15</sup>. The imperfect alignment, another chain disorder, has its cause in the strong forces along the chain. Any defect requiring more than the available volume will cause a strain in the lattice which is propagated much farther along the chain than at right angles<sup>16</sup>. Chain disorder defects can be classified also as point dislocations along with vacant lattice sites and interstitial atoms.

*Amorphous defect*—This is caused by somewhat larger disturbance of the lattice like a side group which cannot crystallize within the lattice or a major chain disorder<sup>10</sup>. Its characteristic is a decrease of the crystallinity by an amount larger than its own weight. This indicates that an amorphous defect causes several otherwise crystallizable chain units to remain amorphous. For example inclusion of one  $-\text{CH}(\text{CH}_3)-$  in polyethylene was shown to decrease the crystallinity by four to five additional  $-\text{CH}_2-$ <sup>10</sup>. The exact structure of such a defect is not known and it is not expected that there will be a sharp dividing line between amorphous defects and chain disorder as well as vacant lattice sites and interstitial atoms. If the amor-

phous defect gets larger, it may be called a three dimensional imperfection.

This summary of possible imperfections gives a framework for a more exact description of the crystalline solid state of linear high polymers than has been customary. It has to be pointed out, however, that the usual description which pictured the polymer sample as being made up of amorphous and crystalline 'regions'\* is usually still the only possible description because little detailed knowledge has been accumulated about defects as yet. Before full use of the defect model can be made, more experimental work has to be performed. A series of somewhat novel experimental approaches developed in this laboratory are described below.

DESCRIPTION OF  
THE DEFECT SOLID STATE USING  
THERMODYNAMIC TERMS

If we take the solid state of a crystalline linear high polymer as an agglomerate of defect-laden crystalline regions, it is clear that we are not dealing with a substance in an equilibrium state. Far enough removed from the melting temperature this state is metastable in the sense that no detectable changes occur in reasonable time spans.

That this description is valid came first to our attention on crystallizing copolymers of ethylene terephthalate and ethylene sebacate from the glassy state (cold crystallization)<sup>17</sup>. In the 80/20 mole per cent copolymer only 15 per cent by weight of crystalline material was obtained on crystallization at 58°C<sup>18</sup>. The crystalline content was calculated on the basis of heats of fusion and crystallization. The glass transition temperature of this material is 23°C and the melting point of defect-free crystals is above 242°C<sup>18</sup>. Between the crystallization temperature and 150°C the crystalline polymer was stable in the sense that no further crystallization could be detected over the course of days although the mobility of these chains at these temperatures is high enough that if any extended 'amorphous defects' would have been present crystallization should have occurred. On heating further at a rate of about 5°C per hour the heat of crystallization was absorbed to  $\pm 5$  per cent at 210°C, so that a supercooled melt was obtained, which subsequently recrystallized<sup>19</sup>. Further heating showed the melting point† of 242°C for more perfect crystals. The experimental detail could be described by assuming random crystallization (cold crystallization) to a network of interlocking crystallites with roughly speaking 85 per cent of the material concentrated in defects<sup>20</sup>.

To describe the state of a crystallized polymer thermodynamically, the total system is divided into sub-systems, for example coinciding with single crystalline or dendrite boundaries. Such a description is valid when the volume elements are so large that variations due to the molecular structure are unimportant, but on the other hand so small, that the sub-systems are homogeneous<sup>21</sup>.

\*Using the above terminology, all non perfect material is placed into the ill defined three dimensional 'amorphous defect'.

†Throughout this paper the term melting is used for the transition from the crystalline to the amorphous state at any temperature.

The free energy of the crystalline sub-system,  $F_i$ , as well as its volume, energy and mass ( $V_i$ ,  $E_i$ ,  $M_i$ ) is represented in three parts:

$$F_i = m_i^0 \mu_{\text{cryst.}}^0 + \sum_d m_i^d \mu_d + \sum_s m_i^s \mu_s \quad (3)$$

$\mu_{\text{cryst.}}^0$  is the bulk chemical potential of the perfect crystal ( $\partial F_i / \partial m_i^0$ )<sub>T,P</sub>, the  $\mu_{d,s}$  are the terms for the different internal defects  $d$  and surfaces  $s$ , where in general  $d$  refers to point and line defects and  $s$  to two dimensional imperfections.  $m$  represents the effective mass.

The chemical potential of each of the internal defects can be treated like that of a solution<sup>6</sup>

$$\mu_d = (\mu_d)_0 + RT \ln x_i^d \quad (4)$$

where  $x_i^d$  is the activity of the defect. To insert into expression (3) one must sum (4) over all types of defects present.

The surface contributions are best described as

$$\mu_s = \mu_{\text{cryst.}}^0 + \sigma_s \quad (5)$$

where  $\sigma_s$  is the surface free energy per unit weight.  $\mu_s$  is different for each crystallographically and morphologically different surface.

The free energy of the whole polymer in question is given by

$$F = \sum_i F_i \quad (6)$$

The ultimate goal of a thermodynamic description would thus be to obtain a free energy distribution curve. *Figure 1* shows an attempt towards this

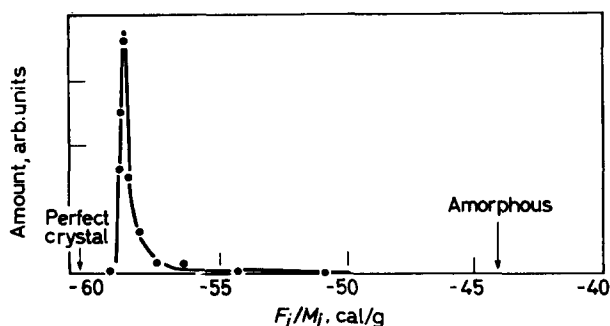


*Figure 1*—Sub-system distribution as indicated by the free energy at 300°K. Sample: Annealed linear polyethylene. Data: refs 3 and 8

goal. Using data of the specific heat of carefully crystallized polyethylene<sup>3</sup> to obtain free energies and extrapolating the free energy of metastable sub-systems to room temperature leads to the curve shown. Values for the completely amorphous and crystalline polymer are marked.

*Figure 2* shows schematically the dependence of the free energy of a single sub-system on temperature. The shaded area indicates the practical limit of the metastable state. The only change of  $F_i$  with temperature up to  $T_B$  is represented almost exclusively by the change in the  $\mu$  and  $\sigma$  of equations 3–5.



The mass of defects remains constant. The change of  $\mu$  and  $\sigma$  has been eliminated in drawing *Figure 2*, so that a line parallel to the abscissa results for the change of  $F_i$  with temperature.

Beyond the shaded area the constancy of the  $m$  no longer holds. Recrystallization and reorganization of the defects occur. This is a kinetic process and as a result  $F_i$  depends upon the heating rate.

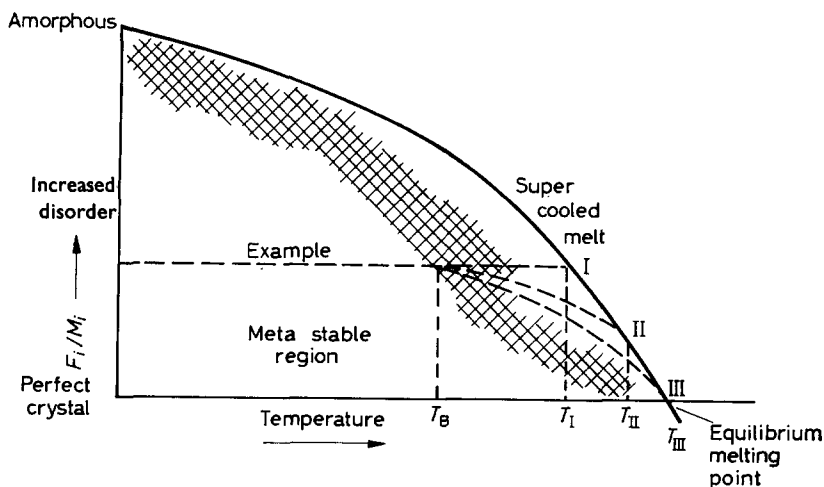


*Figure 2*—Change of the sub-system free energy  $F_i$  on increasing the temperature.  $T_B$ —practical upper limit of the metastable region. I—fast heating rate limit; II—intermediate heating rate; III—slow heating rate

At any point within the area bound by the free energy curve of the supercooled melt and the free energy of the perfect crystal it is impossible to have a spontaneous movement upward because of the positive  $\Delta F$  which would be involved in such a change. A spontaneous movement downward is possible ( $\Delta F < 0$ ), but kinetically hindered by a positive free energy of activation for rearrangement,  $\Delta F^\ddagger > 0$ . This activation energy decreases towards zero in the immediate vicinity of the curve of the supercooled melt. No superheating of linear polymer crystals has ever been observed<sup>22</sup> in normal heating experiments. To the left of the shaded area  $\Delta F^\ddagger$  is so large that the downward move is negligible, to the right the amount of downward curvature depends upon the heating rate. This leads to different cases for the heating of a sub-system, indicated by the broken lines in *Figure 2*.

Case I represents the limit of very fast heating and shows a continuation of the curve of constant  $m$  to yield supercooled melt at  $T_I$  with no intermediate reorganization. A limit which in many polymer systems can be realized experimentally.

Case II shows some reorganization and the temperature where the supercooled melt is reached,  $T_{II}$ , is higher. It represents the intermediate heating rate and leads experimentally to inconclusive results, since it is usually impossible to observe the exact path.

Case III is representative of very slow heating. In the limit of infinitely

slow heating, the melting point of a perfect crystal is expected in such an experiment. The rates needed are extremely slow, for polymethylene<sup>23</sup> rates of 1°/24h still fall far short of fixing the maximum melting point. The discrepancy between the accepted value today and that observed in this experiment was about 5°C<sup>24</sup>.

APPLICATION TO THE EXPERIMENT

The application of the thermodynamic description outlined above is hampered by the fact that the free energy of the supercooled liquid is usually not known and the path is usually neither case I nor case III. If this difficulty can be overcome a measurement of the heat of fusion absorbed in a fast heating experiment can be used to calculate the  $F_i$  distribution as was approximated in *Figure 1*.

Calculations of the equilibrium path on heating have been carried out for random copolymers with no defects except crystallite surfaces which were crystallized under equilibrium conditions<sup>25</sup>. No defects implies that all non-crystallizing copolymer repeating units (B units) are not entering the lattice and determine in the equilibrium state at low temperature the crystallite size. If such a crystallite (sub-system) distribution is heated slowly without losing equilibrium, the heat of fusion/temperature curve can be calculated from the equilibrium path<sup>19, 26</sup>.

Another case which has been solved exactly is that of the cold crystallized material<sup>20</sup>, for which the distribution of crystallites is known. Again special assumptions had to be made for the defects. In this calculation all defects were treated as surfaces. A heating path was assumed which allowed no recrystallization (case I). Although the mathematics turned out to be formidable, reasonable solutions were obtained.

For many sub-system distributions it is, however, possible to determine the melting point tail on fast heating, the experimental maximum melting point  $T_m$ . The experiment involves the quick heating of a slowly cooled sample so that no recrystallization takes place. The most perfect sub-system will then give the experimental maximum melting point. Most conveniently DTA can be used for this experiment<sup>6</sup>.

Data on the crystallization of polymers from the melt and from solution indicate that a folded structure with constant thickness results on isothermal crystallization<sup>11, 27</sup>. This fold length  $f$  is the crystal thickness in the crystallographic  $c$  direction. The fold length gives a lower limit to the surface free energy for each sub-system. For the most perfect sub-system we may neglect all but the (001) surfaces because of small values of  $m_i^s$  and also small  $\sigma_s$  for all but the folded surfaces. The last term of equation (3) then goes over into

$$\sum_s m_i^s \mu_s = m_i^f (\mu_{\text{cryst.}}^0 + \sigma^f) \tag{7}$$

with  $\sigma^f$  the surface free energy per unit weight of folded surface.  $m_i^f \sigma^f$  is equal to  $A_i^f \sigma'^f$ , where  $A_i^f$  is the surface area corresponding to  $m_i^f$  and  $\sigma'^f$  is the appropriate surface free energy per cm<sup>2</sup>.

Assuming furthermore that  $m_i^d$  for the most perfect crystal in the distribution is small, leads to the free energy of this sub-system for which  $i = m$

$$F_m = M_m \mu_{\text{cryst.}}^0 + m'_m \sigma' \quad (8)$$

$M_m$  represents the total weight of the sub-system  $m$ . Since when the last sub-system melts, the melt has reached the composition of the overall concentration, its chemical potential can be written if the non-crystallizable units occur randomly

$$\mu_{\text{melt}} = \mu_{\text{melt}}^0 + RT \ln X_A \quad (9)$$

where  $X_A$  is the activity of crystallizable repeating units (A) in the melt. The point where on fast heating the sub-system goes over into the super-cooled melt is determined by (see *Figure 2*)

$$\mu_{\text{melt}} = F_m / M_m \quad (10)$$

This leads after substitution of (9) and (8) into (10) to

$$\Delta F_u = (m'_m / M_m) \sigma' - RT_m \ln X_A \quad (11)$$

where  $\Delta F_u = \mu_{\text{melt}}^0 - \mu_{\text{cryst.}}^0$ , the bulk free energy of melting at the experimental maximum melting point,  $T_m$ , of a perfectly folded crystal of thickness  $f$  into a melt of activity  $X_A$ .

For  $\Delta F_u$  equation (12) can be substituted if one neglects the change of  $\Delta S_u$  with temperature in this range.

$$\Delta F_u = \Delta H_u - T \Delta S_u = \Delta H_u (1 - T/T_m^0) \quad (12)$$

$\Delta H_u$  and  $\Delta S_u$  are the enthalpy and entropy of fusion.  $T_m^0 = \Delta H_u / \Delta S_u$  is the melting point of infinitely thick lamellae in contact with pure A-melt. Rearrangement of equation (11) leads to

$$\ln X_A = - \frac{\Delta H_u}{RT_m} + \frac{\Delta H_u}{RT_m^0} + \frac{m'_m \sigma'}{M_m RT_m} \quad (13)$$

$T_m^0$  is not experimentally available. It is thus useful to replace  $T_m^0$  by  $T'_m$  the melting point for perfect lamellae of the thickness  $f$  in contact with pure A-melt. At  $T'_m$  for  $X_A = 1$  equation (13) goes over into

$$0 = - \frac{\Delta H_u}{RT'_m} + \frac{\Delta H_u}{RT_m^0} + \frac{m'_m \sigma'}{M_m RT'_m} \quad (14)$$

Substituting equation (14) back into (13), neglecting the small term

$$(m'_m / M_m) (\sigma' / R) (1/T_m - 1/T'_m)$$

yields an equation amenable to experimental use

$$\ln X_A = - \frac{\Delta H_u}{RT_m} + \frac{\Delta H_u}{RT'_m} \quad (15)$$

This equation is identical in form to the equilibrium expression derived by Flory<sup>28</sup> for the melting of copolymers except for  $T'_m$  replacing  $T_m^0$ .

This similarity explains the discrepancy found in previous years in discussing copolymer melting using similarly crystallized polymers with different copolymer content<sup>19</sup> and the melting points obtained on extremely slow heating<sup>29</sup>.

## EXPERIMENTS

(1) Linear polyethylene of the Marlex 50 type crystallized by cooling from above the melting point at a rate between 1° and 6°C/hour has a remarkably constant experimental maximum melting point of 134.4°C<sup>3,10,30</sup> for an experimental heating rate of at least ten times the cooling rate. This is taken as evidence that for all these cooling rates the thickest lamellae have practically the same fold length  $f$  and that during heating no large amount of recrystallization has occurred. Case I of *Figure 2* has been realized practically in these experiments. That only little or no recrystallization occurred was also checked by calorimetry<sup>3</sup>. Since for these polymer samples  $X_A$  can be estimated to be 0.995<sup>31</sup>,  $T'_m$  can be calculated using equation (15). The result 136.2°C checks with experimental  $T'_m$  determinations on polymethylene crystallized similarly<sup>23</sup>. Polymethylene has such a high molecular weight and no branches, so that  $X_A=1.000$ .

(2)  $X_A$  as a function of concentration of foreign units can be calculated from equation (15) using experimental maximum melting points of copolymers crystallized identical to the homopolymer. Experimental maximum melting points determined by DTA<sup>10</sup> showed that including 13 C=O groups per 100 backbone chain CH<sub>2</sub> groups does not vary  $X_A$ . From this it can be concluded that CO is not a non-crystallizable unit, but behaves like a foreign atom on a substitutional position (5). Inclusion of —CHCH<sub>3</sub>— in the polyethylene chain behaves, however, quite differently. Every —CHCH<sub>3</sub>— reduces  $X_A$  proportionately<sup>10</sup>.

(3) If the sample under investigation cannot be cooled slowly through the temperature range to be analysed by heating experiments, very much faster heating rates have to be employed to realize case I. Single crystals grown from solution for example are known to thicken and thus change their surface area on heating<sup>32</sup>. Heating experiments on large (0.1 mm) single crystals as a function of rate showed that for polyethylene crystallized from toluene solution at about 90°C the melting point changed smoothly from 128°C for 0.5°C/min to a constant 121.2°C for rates between 10° and 25°C/min<sup>33</sup>. Experiments of this kind can be used to determine the surface free energy<sup>33</sup> if knowledge of the effect of the defects is known.

*Financial support for this work from the Advanced Research Projects Agency is gratefully acknowledged.*

*Department of Chemistry,  
Cornell University,  
Ithaca, New York*

*(Received February 1963)*

## REFERENCES

- <sup>1</sup> See, for example, DAINTON, F. S. and IVIN, K. J. *Quart. Rev. chem. Soc., Lond.* 1958, **12**, 61
- <sup>2</sup> BYWATER, S. *Trans. Faraday. Soc.* 1955, **51**, 1257

## B. WUNDERLICH

---

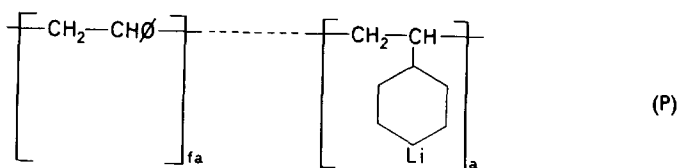
- <sup>3</sup> WUNDERLICH, B. and DOLE, M. *J. Polym. Sci.* 1957, **24**, 201
- <sup>1</sup> CHIANG, R. and FLORY, P. J. *J. Amer. chem. Soc.* 1961, **83**, 2857
- <sup>5</sup> JESSUP, R. S. *J. chem. Phys.* 1948, **16**, 661
- <sup>6</sup> KROGER, F. A. and VINK, H. J. *Solid State Physics*, Vol. III, p 307. Ed. SEITZ, F. and TURNBULL, D. Academic Press: New York, 1956
- <sup>7</sup> VAN BUEREN, H. G. *Imperfections in Crystals*. North Holland Publishing Co.: Amsterdam, 1960
- <sup>8</sup> WUNDERLICH, B. *J. chem. Phys.* 1962, **37**, 1203, 1207
- <sup>9</sup> WUNDERLICH, B. *J. chem. Phys.* 1962, **37**, 2429
- <sup>10</sup> WUNDERLICH, B. and POLAND, D. *J. Polym. Sci.* 1963, **A1**, 357
- <sup>11</sup> See, for example, KELLER, A. *Makromol. Chem.* 1959, **34**, 1
- <sup>12</sup> RENEKER, D. H. 142nd meeting of the American Chemical Society, Atlantic City, 1962
- <sup>13a</sup> GEIL, P. H. and RENEKER, D. H. *J. Polym. Sci.* 1961, **51**, 569
- <sup>13b</sup> BURBANK, R. D. *Bell Syst. tech. J.* 1960, **39**, 1627
- <sup>14</sup> KHOURY, F. and PADDEEN, F. J., Jr. *J. Polym. Sci.* 1960, **47**, 455
- <sup>15</sup> RENEKER, D. H. *J. Polym. Sci.* 1962, **59**, 39S
- <sup>16</sup> FISCHER, E. W. *Ann. N.Y. Acad. Sci.* 1961, **89**, 620
- <sup>17</sup> DOLE, M. *Kolloidzshr.* 1959, **165**, 40
- <sup>18</sup> WUNDERLICH, B. *Thesis*, Northwestern University, 1957
- <sup>19</sup> DOLE, M. and WUNDERLICH, B. *Makromol. Chem.* 1959, **34**, 29
- <sup>20</sup> WUNDERLICH, B. *J. chem. Phys.* 1958, **29**, 1395
- <sup>21</sup> MEIXNER, J. and REIK, H. G. *Handbuch der Physik*, Vol. III/2, p 413. Springer: Berlin, 1959
- <sup>22</sup> UBBELOHDE, A. R. *Quart. Rev. chem. Soc., Lond.* 1950, **4**, 356
- <sup>23</sup> MANDELKERN, L., HELLMANN, M., BROWN, D. W., ROBERTS, D. E. and QUINN, F. A., Jr. *J. Amer. chem. Soc.* 1953, **75**, 4093
- <sup>24</sup> BROADHURST, M. G. *J. chem. Phys.* 1962, **36**, 2578
- <sup>25</sup> FLORY, P. J. *Trans. Faraday Soc.* 1955, **51**, 848
- <sup>26</sup> DOLE, M. *Advanc. Polym. Sci.* 1960, **2**, 221
- <sup>27</sup> GEIL, P. H. 142nd meeting of the American Chemical Society, Atlantic City, 1962
- <sup>28</sup> FLORY, P. J. *Principles of Polymer Chemistry*, p 566. Cornell University Press: Ithaca, N.Y., 1953
- <sup>29</sup> QUINN, F. A., Jr and MANDELKERN, L. *J. Amer. chem. Soc.* 1958, **80**, 3178
- <sup>30</sup> WUNDERLICH, B. and KASHDAN, W. H. *J. Polym. Sci.* 1961, **50**, 71
- <sup>31</sup> BRYANT, W. M. D. *J. Polym. Sci.* 1959, **34**, 569
- <sup>32</sup> STATTON, W. O. and GEIL, P. H. *J. appl. Polym. Sci.* 1960, **3**, 357
- <sup>33</sup> WUNDERLICH, B., SULLIVAN, P., ARAKAWA, T., DICYAN, A. B. and FLOOD, J. F. *J. Polym. Sci.* 1963, **A1**, 3581

# Graft Copolymerization Initiated by Poly-*p*-lithiostyrene

M. B. HUGLIN\*

*Addition of acrylonitrile at  $-15^{\circ}\text{C}$  to poly-*p*-lithiostyrene in the presence of butyl lithium yields a mixture of polystyrene, polyacrylonitrile and graft copolymer. Graft polystyrene co-(*p*-polyacrylonitrile) is separated by solvent extraction and characterized by osmometry, infra-red and elemental analysis. Polymers containing 6 to 145 branches per molecule and having molecular weights of 9 000 to 74 000 are obtained.*

ANIONIC polymerization as a means of preparing of copolymers has been studied via the use of terminal carbanions to initiate the growth of a second vinyl monomer<sup>1,2</sup>, and also via ionic chain transfer reactions between a polymeric carbonium chain and a neutral polymer<sup>3,4</sup>. Equally intriguing, perhaps, is the possibility of grafting a second monomer anionically to specific points of a polymeric chain such as poly-*p*-lithiostyrene (P).



This compound, which is formally a copolymer of styrene and *p*-lithiostyrene, has been prepared by Braun<sup>5</sup>, by the slow addition of previously *p*-iodinated polystyrene to an excess of butyl lithium. In P the ratio *f* of non-substituted to *p*-substituted styrene segments is dependent on the extent of iodination; the subsequent metalation being practically quantitative. Leavitt and Matternas<sup>6</sup> have described a somewhat different route to similar compounds containing lithium in the *o*-, *m*- and *p*- positions and indicated that the *o*-lithio polymer might be particularly useful as it can be prepared from stoichiometric quantities of reactants (see below). Polymers of type P are unstable to heat, air and moisture but, under controlled conditions, undergo many reactions typical of organometallic compounds. Both sets of workers have alluded to the possibility that P itself might behave as a macromolecular analogue of phenyl lithium and initiate anionic polymerization from its *p*-positions.

Some of the difficulties encountered in isolating and using P as a catalyst will first be discussed followed by a description of the characterization of graft copolymers formed by the polymerization of acrylonitrile from *p*-positions of polystyrene.

\*Present address: Department of Chemistry, Royal College of Advanced Technology, Salford, 5.

## ISOLATION OF CATALYST FROM REACTION MIXTURE

When P is prepared by the method of Braun, most of the butyl lithium (a large excess of which is essential to prevent Wurtz-Fittig type cross-linking) remains unused and addition of a suitable monomer leads to a mixture of graft copolymer and homopolymer of the added monomer. Although this direct procedure was finally adopted, some mention will be made of attempts to isolate the catalyst by removing the unused butyl lithium.

*Physical removal*

A solution of P in toluene under nitrogen was prepared at room temperature and the lithio polymer then precipitated at  $-35^{\circ}\text{C}$  with dry petroleum ether. After removal of all butyl lithium by repeated washings of the precipitate, the polymer was pumped dry. It was then, however, insoluble in toluene, ether and tetrahydrofuran and even when left dispersed in liquid monomers *in vacuo*, it neither dissolved nor initiated polymerization at temperatures between  $-35^{\circ}$  and  $+35^{\circ}\text{C}$ . An unsatisfactory elemental analysis of the buff powder was obtained possibly because of hydrolysis during the analysis, although titration of a suspension in benzene against hydrochloric acid yielded a lithium content within two per cent of that corresponding to complete metalation of the poly-*p*-iodostyrene used. It is unlikely that crosslinking occurred as the reaction mixture was homogeneous and an aliquot hydrolysed with methanol to polystyrene could be redissolved in toluene. Using stoichiometric quantities of butyl lithium and a copolymer of styrene and *o*-bromostyrene ( $f=11.5$ ) kindly donated by Dr F. C. Leavitt, the isolated dried poly-*o*-lithiostyrene likewise failed to initiate polymerization although it was soluble in toluene.

*Removal by coupling*

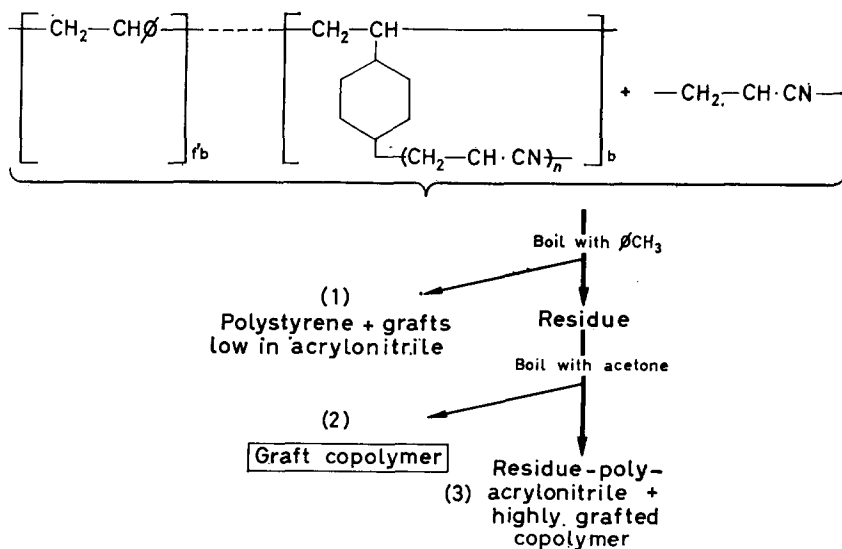
Butyl lithium<sup>7</sup> couples instantaneously with benzyl chloride in dry ether, whereas phenyl lithium<sup>8</sup> is reported to couple slowly or not at all. Using the behaviour of phenyl lithium as an indication of that which would obtain with P, tests were made on the effect of benzyl chloride and acrylonitrile on equal aliquots of phenyl lithium in ether.

In the absence and presence of benzyl chloride, acrylonitrile polymerized immediately at  $-10^{\circ}\text{C}$ . The concentrations of hydrolysed phenyl lithium in the absence and presence of benzyl chloride were 1.68 N and 1.26 N respectively. This latter concentration was also found on hydrolysis one hour after the addition of benzyl chloride. Wittig<sup>9</sup> has found lithium chloride, hydrocarbons and unconsumed reactants when this reaction between equimolar components is allowed to heat up.

Addition of an excess of benzyl chloride in ether to P and butyl lithium in toluene (sufficient to maintain solubility) at  $-10^{\circ}\text{C}$ , followed by that of acrylonitrile, led to removal of butyl lithium by coupling and formation of a graft copolymer as evidenced by its infra-red spectrum and elemental analysis. Ungrafted polystyrene containing 0.8 per cent iodine was also produced. Certainly in the black experiment the 25 per cent reduction in normality can be attributed to the formation of hydrocarbons and this







The reaction conditions are summarized below in *Table 1*.

*Table 1.* Metalation at room temperature and polymerization at  $-15^\circ\text{C}$

<i>Iodinated polystyrene</i> (g atom I)	9.05	6.95	4.67	9.00	6.05	446
<i>Butyl lithium</i> (mole $\times 10^4$ )	223	130	208	335	439	4620
<i>Acrylonitrile</i> (mole $\times 10^4$ )	600	378	565	1210	545	2270
<i>% Conversion of acrylonitrile*</i>	74	75	70	69	73	78
<i>Product yield (g)</i>	4.94	5.60	4.84	6.97	5.47	15.5
<i>Acetone-soluble copolymer (g)</i>	0.69	0.29	0.33	0.73	0.34	0.92
<i>Designation of copolymer</i>	3A	5A	6A	7A	8A	9A

\*Estimated from [product yield—polystyrene content of poly-*p*-iodostyrene]/[acrylonitrile added].

Note: All the graft copolymers 3A—9A were soluble in acetone and dimethyl formamide and insoluble in methanol and water.

#### CHARACTERIZATION OF GRAFT COPOLYMERS

The constituents of the graft copolymers are:

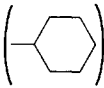
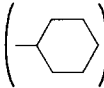
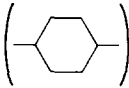
- (1) Styrene + *p*-iodostyrene (< 0.9 per cent) [non-branching segments]
- (2) *p*-substituted styrene [branching loci]
- (3) Acrylonitrile [branches].

If lithiation is complete, as it almost is, then the branching frequency  $1/(1+f)$  has the same values in P and the poly-*p*-iodostyrene. However, as Waack and Doran<sup>10</sup> have verified for a series of alkyl and aryl lithiums, the catalyst efficiency in anionic polymerization is generally low and hence

in this case all the initial 'a' *p*-lithiostyrene segments cannot be assumed to initiate. Those which are utilized, then, are differentiated as 'b' in the reaction scheme on p 137 and must be determined by analysis, as must the branching frequency  $1/(1+f)$  in the graft copolymers.

### Analysis

Acrylonitrile and residual iodine contents were obtained from a Kjeldahl nitrogen determination and elemental analysis. Using polystyrene as standard, the styrene content was estimated from the infra-red absorption at  $14.3 \mu$  of two per cent solutions in dimethyl formamide, which was purified by the method of Grodzinsky *et al.*<sup>11</sup>.

	Infra-red absorption maxima ( $\mu$ )		
Polystyrene		13.2 	14.3 
Poly- <i>p</i> -iodostyrene	12.2 	13.2	14.3
Graft copolymer	4.45 (-CN)	13.2	14.3

In poly-*p*-iodostyrene 1:4 disubstituted benzene absorption occurs at  $12.2 \mu$  with an accompanying decrease in phenyl absorption ( $13.2$  and  $14.3 \mu$ ), dependent on the extent of iodination. Cyanide absorption at  $4.45 \mu$  and phenyl absorption are present in the graft copolymer but the extinction coefficient is too small to utilize the absorption at  $12.2 \mu$  as a means of determining the concentration of branching loci. Consequently the latter can only be estimated in the graft copolymers by difference, viz: Per cent by weight of *p*-substituted styrene =  $100 - (\text{per cent styrene} + \text{per cent } p\text{-iodostyrene} + \text{per cent acrylonitrile})$ . As a check, the per cent styrene by this method was found to be 19.4 for a poly-*p*-iodostyrene containing 44.73 per cent iodine (i.e. 19.0 per cent styrene). The value found, while representing good accuracy does, nonetheless, introduce considerable error into the percentage *p*-substituted styrene, the value of which is affected by the inherent errors of three different analyses.

### Molecular weights

The composition on a per cent by weight basis having been established, characterization in terms of lengths of main and side chains can be calculated from the number-average molecular weight  $\bar{M}_n$  as measured by osmometry.

Osmotic pressures of solutions in dimethyl formamide were measured at  $30^\circ\text{C} \pm 0.02^\circ$  for four concentrations within the range 0.05 to 0.25 g/dl. 'Allerfeinst' membranes (Membran filter—Gesellschaft Sartorius-Werke A.G., Göttingen) were used in two modified<sup>12</sup> stainless steel Zimm-Meyerson osmometers kindly loaned by Dr P. J. T. Tait. Pressure heads,

steady for 24 hours were attained in 48 hours and, after subtraction of residual asymmetry pressures of the order of 0.1 cm for the pure solvent, plots of reduced pressure  $\pi/c$  versus  $c$  were found to exhibit curvature.  $\overline{M}_n$  was obtained from linear plots of  $(\pi/c)^{\dagger}$  versus  $c$ , which could be extrapolated with more certainty.

## Results

Table 2. Characterization of copolymers

Copolymer	3A	5A	6A	7A	8A	9A	Original polystyrene
% acrylonitrile	14.4	47.5	59.9	65.7	82.4	64.7	0
% <i>p</i> -iodostyrene*	0	1.32	1.57	1.71	1.51	0	0
% styrene	84.7	22.7	26.0	10.5	5.42	22.0	100
% <i>p</i> -substituted styrene	0.90	28.4	13.5	22.1	10.6	13.4	0
$1/(1+f')^{\dagger}$	0.011	0.555	0.519	0.678	0.662	0.378	
$10^{-3}\overline{M}_n$	74.1	45.7	34.7	8.8	12.4	42.2	
DP chain	610	231	133	29	21	143	
DP each branch	31	3	8	6	16	9	
No. branches/mol	6	126	45	19	13	145	0
$[\eta]$ dl/g‡	0.368	0.173	0.118	0.083	0.077	0.092	0.385

\*=(230/127) per cent iodine.

† $1/(1+f)=0.0364$  for (3A) and 0.690 for (5A, 6A, 7A, 8A, 9A).

‡Measured at 30°C in dimethyl formamide.

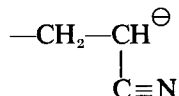
It is clear from Table 2 that acetone effects a fractionation based on acrylonitrile content and on polystyrene chain-length. The apparent efficiency of initiation,  $1/(1+f')$ , is high but once initiated the chains are evidently rapidly terminated for reasons discussed later. This high efficiency is apparent only, for the acetone-soluble fraction alone is being considered. The composition of the non-extracted portion remains unknown and, although it has been described as a mixture of polyacrylonitrile and highly grafted copolymer, the latter may in fact contain only a few branches each of high DP. Moreover the toluene extracts consisted almost entirely of polystyrene, for no —CN infra-red absorption could be detected and the elemental analysis of one sample (expt 3) accorded exactly as polystyrene. Yields of these fractions were of the same order as or generally greater than those of 3A to 9A and hence the overall branching frequency based on initial P is probably less than half the values of  $1/(1+f')$  quoted.

The estimated uncertainty in the values of  $DP_{\text{chain}}$ ,  $DP_{\text{branch}}$  and no. branches/mol. is  $\pm 20$  per cent.

## DISCUSSION

Reasonable yields of block copolymer from 'living' polystyrene and acrylonitrile might, according to Smets<sup>1</sup>, be expected because the growing chain, otherwise insoluble in toluene, is partly kept in solution by the polystyrene to which it is attached. Similar considerations may apply here but the low DPs actually obtained are a likely consequence of first, the com-

petition reaction between P (or growing P) and butyl lithium for the monomer and secondly, possible transfer of the carbanionic charge to nitrogen, leading to cessation of propagation from



and to conjugation and the observed coloration. Chain transfer to monomer is considered unlikely<sup>1,13</sup> but the simultaneous homopolymerization precludes any verification of this.

The ideal  $[\eta]$  for mixtures of the two comonomers cannot be computed from the magnitudes of DP as  $K$  and  $\alpha$  in the relationship  $[\eta]=KM^\alpha$  are not known for polystyrene in dimethyl formamide. Reference to *Table 2* shows that 3A, having the highest  $DP_{\text{chain}}$  and the lowest branching, exhibits the largest  $[\eta]$  as expected. On account of its large degree of branching 9A exhibits a smaller  $[\eta]$  than does 6A and only a slightly greater one than 7A and 8A, although it has the highest molecular weight of these four species. The interactions of numerous branches (all of approximately comparable size), then, reduce  $[\eta]$  to a greater degree than their extension tends to increase it in a good solvent, dimethyl formamide. It is somewhat surprising that a block copolymer containing 80 per cent acrylonitrile should be insoluble in acetone as reported by Frankel *et al.*<sup>2</sup>, whereas a graft copolymer 8A in which the 82.4 per cent acrylonitrile is distributed as numerous small branches is soluble. This anomaly could well be explained by a significant difference in the molecular weight of the polystyrene of the block copolymer for, as already noted, a fractionation based on  $DP_{\text{chain}}$  and per cent acrylonitrile is effected by acetone.

*Department of Inorganic, Physical and Industrial Chemistry,  
The University,  
Liverpool*

*(Received March 1963)*

#### REFERENCES

- <sup>1</sup> CLAES, P. and SMETS, G. *Makromol. Chem.* 1961, **44**, 212
- <sup>2</sup> FRANKEL, M., OTTOLENGHI, A., ALBECK, M. and ZILKHA, A. *J. chem. Soc.* **1959**, 3858
- <sup>3</sup> HAAS, H. C., KAMATH, P. M. and SCHULER, N. W. *J. Polym. Sci.* 1957, **24**, 85
- <sup>4</sup> KAMATH, P. M. and HAAS, H. C. *J. Polym. Sci.* 1957, **24**, 143
- <sup>5</sup> BRAUN, D. *Makromol. Chem.* 1959, **30**, 85
- <sup>6</sup> LEAVITT, F. C. and MATTERNAS, L. U. *J. Polym. Sci.* 1960, **45**, 249
- <sup>7</sup> GILMAN, H. and MORTON, J. W. *Organic Reactions*, Vol. 8, Ch. 6. Wiley: London, 1954
- <sup>8</sup> COATES, G. E. *Organometallic Compounds*, p 8. Methuen: London, 1960
- <sup>9</sup> WITTIG, G. and WITT, H. *Ber. dtsh. chem. Ges. B*, 1941, **74**, 1474
- <sup>10</sup> WAACK, R. and DORAN, M. A. *Polymer, Lond.* 1961, **2**, 365
- <sup>11</sup> GRODZINSKY, J., KATCHALSKY, A. and VOFSI, D. *Makromol. Chem.* 1961, **44-46**, 591
- <sup>12</sup> NORTH, A. M. *Ph.D. Thesis*, Aberdeen, 1957
- <sup>13</sup> GRAHAM, R. K., PANCHACK, J. R. and KAMPF, M. J. *J. Polym. Sci.* 1960, **44**, 411

# Structure and Properties of Crazes in Polycarbonate and Other Glassy Polymers\*

R. P. KAMBOUR

*Crazes in glassy polymers are now known not to be true cracks at all but rather regions containing polymer interconnecting the craze walls, which regions have lower refractive indices than the bulk polymer. Refractive indices of suitable crazes may be determined from the critical angle for total reflection at the craze/bulk polymer interface. From the indices craze compositions may be calculated. Such calculations show polycarbonate crazes to be roughly 50 per cent polymer: 50 per cent void. From electron micrographs of silver-doped crazes the void content appears to be distributed in the form of holes most of which have dimensions in the range 20–200Å. Crazing is seen in essence to be a process of polymer rarefaction involving the conversion of strain energy to surface free energy.*

AS A result of developments<sup>1,2</sup> culminated by microscopic investigations of polystyrene, polymethyl methacrylate, and polycarbonate by Spurr and Niegisch<sup>3</sup>, it is now known that many of the apparent cracks in glassy polymers are not true cracks at all but rather are thin, abruptly bounded regions containing polymeric material and having different optical properties from the surrounding bulk polymer. The included polymeric material is connected to the walls of the pseudocrack (henceforth termed a craze) so that a craze is capable of bearing a tensile load in contrast to the true crack. Polystyrene specimens, the cross sections of which are completely crossed by crazes, still retain 50 per cent of their tensile strengths<sup>4</sup>. Crazes produced here in Lexan® polycarbonate specimens by bending stress under liquid ethanol followed by thorough drying, have tensile strengths greater than the polycarbonate yield stress of  $\sim 8\,000$  lb/in<sup>2</sup>. Crazes are much more capable of 'healing' under heat than are cracks; the polymer material appears to be in an elongated state in the craze and heal allows retraction and disorientation to occur to about the same extent as occurs in a cold-drawn polymer specimen upon heating (i.e. about 90 per cent in polycarbonate crazes).

## OPTICAL PROPERTIES OF CRAZE MARKS

The fact that craze marks reflect light strongly means simply that they have lower refractive indices than the surrounding bulk polymer. Early attempts here to measure craze index involved interferometric studies of polished rectangular slabs cut from crazed specimens such that sections of craze ran completely through each slab. Resultant craze indices were too little different from that of the bulk polymer to account for craze reflectivities. In the light of results discussed below it became apparent that

\*Presented in part at the 142nd meeting of the American Chemical Society, Atlantic City, N.J., September 1962.

sectioning and polishing allow, or cause, gross changes in craze indices due to retraction, solvent evaporation, etc. Crazes are changeable things which must be studied in the natural state.

We have reported earlier<sup>5</sup> that correct refractive indices of crazes and cracks in transparent materials may be quickly and conveniently measured in a non-destructive way by making use of the phenomenon of total internal reflection. The complete requirements for such measurements are listed below.

(1) Samples of known bulk refractive index containing single or well-spaced planar crazes which have thicknesses greater than the wavelength of light.

(2) A parallel, reasonably intense light beam (e.g. a 300 W concentrated arc) was used here as a source.

(3) A means of measuring incident angle of the light beam on the specimen surface to  $\sim \frac{1}{2}^\circ$ .

(4) Two polished transparent triangular wedges or prisms which can be stuck to the specimen surface adjacent to the craze with a suitable transparent substance such as stopcock grease. When craze or crack indices are substantially lower than that of the bulk polymer and the angle between the craze plane and the specimen surface is  $\sim 90^\circ$  (the usual case), the critical angle on the craze plane cannot be attained regardless of incident angle on the specimen surface. The function of the wedges is to reduce the craze plane/specimen surface angle enough to permit attainment of such small angles of incidence on the craze plane.

(5) A translucent screen (e.g. a piece of filter paper) placed against the back side of the specimen makes for convenient observation of the critical angle. At angles above the critical value a shadow of the craze is cast on the screen; at the critical angle the shadow disappears.

The set-up is illustrated in *Figure 1*.

#### *Index results for polycarbonate*

The material studied so far has been Lexan<sup>®</sup> polycarbonate (index  $n=1.58$ ) because large, thick, well-spaced planar crazes can be grown easily in bars of the material by judicious bending in weakly plasticizing liquids such as ethanol (used here) or heptane. In addition planar cracks can be propagated by careful bending in the presence of carbon tetrachloride. Cracks when still full of carbon tetrachloride yield  $n=1.44$ , the index of the liquid, but when dried out  $n=1.00$ . These results are a check on the method.

For a fresh craze produced in ethanol  $n=1.46$ , whereas  $n_{\text{ethanol}}=1.36$ . Removal of the bending stress results in an apparent slow relaxation and recovery process, the craze index rising logarithmically with time toward that of the bulk polymer (*Figure 2*). This rise is usually homogeneous throughout the craze. On the other hand, keeping the bar stressed upon removal from the alcohol results in an initially rapid index drop with a final approach to a value of about 1.27. The kinetics of this process will be discussed below.

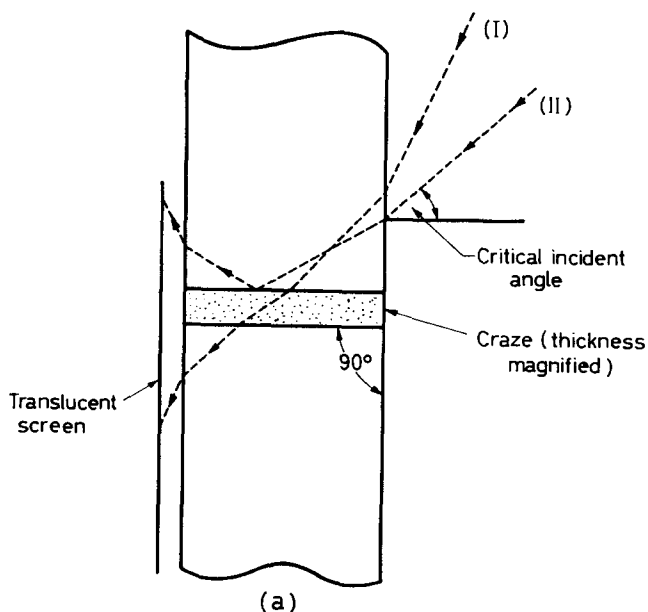
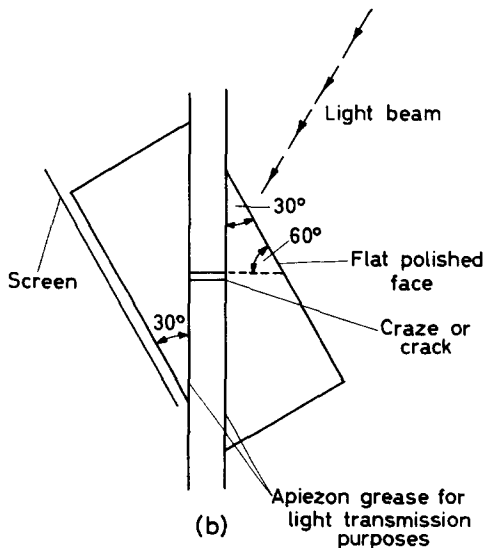


Figure 1—(a) Cross-sectional diagram of set-up for measuring critical angle for total reflection at craze interface. Incident angle of beam I is large enough for beam to pass through craze and register on screen. Beam II is at critical angle and shadow appears on screen. (b) Modified set-up for measuring low craze/crack indices



*Interference effects and frustration of internal reflection*

Under a set-up wherein a thin layer of transparent material of low refractive index is sandwiched in a medium of high refractive index, as

with the craze, there can arise both interference effects from reflections at both craze interfaces and frustration of total reflection due to the enclosed layer having a thickness of the order of magnitude of or smaller than the wavelength of light used. With crazes interference effects can be observed<sup>1</sup> in the reflected beam particularly when a polarizer and analyser are used. In addition many crazes are thin enough to frustrate reflection, judging from electron microscopic evidence discussed later. Appropriate equations for the ratio of reflected to incident light intensities exist for light polarized in either plane which take account of both interference and frustrated reflection effects<sup>6</sup>. That for light polarized perpendicularly to the incident plane is given below.

$$\frac{I_t}{I_i} = \frac{4 \cos^2 \phi [\sin^2 \phi - (n_2/n_1)^2]}{[1 - (n_2/n_1)^2]^2 \sinh^2 u + 4 \cos^2 \phi [\sin^2 \phi - (n_2/n_1)^2]}$$

where  $I_t$  is the intensity of the transmitted beam,  $I_i$  is the intensity of the incident beam,

$$u = \frac{2\pi d}{\lambda (n_2/n_1)} [\sin^2 \phi - (n_2/n_1)^2]^{\frac{1}{2}}$$

$d$  is the thickness of the rare medium,  $n_1$  is the refractive index of the optically dense surrounding medium,  $n_2$  that of the optically rare, thin medium,  $\lambda$  is the wavelength of light in the rare medium ( $=\lambda_{\text{vacuum}}/n_2$ ), and  $\phi$  is the incident angle on the interface.

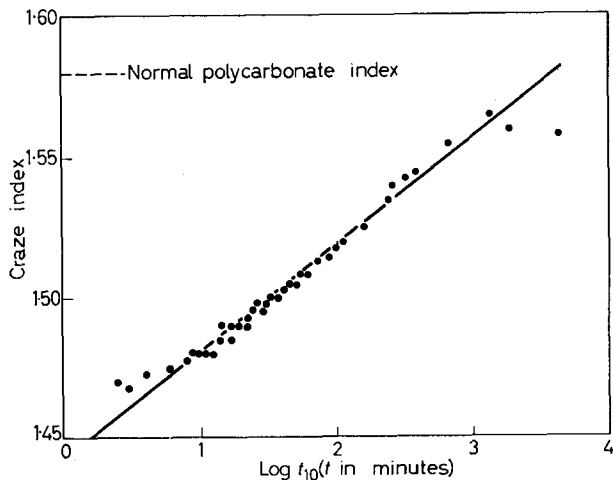


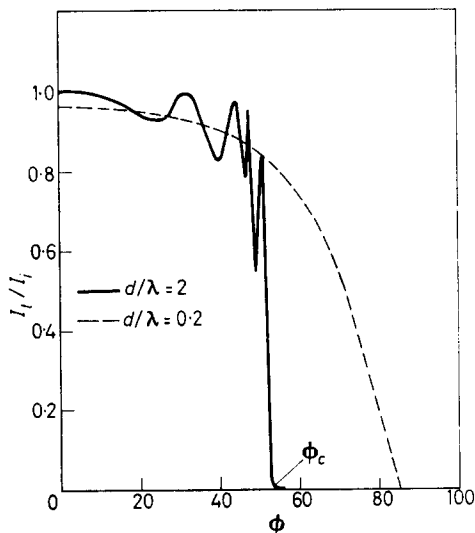
Figure 2—Recovery of craze index when specimen is removed from ethanol and bending jig simultaneously

$I_t/I_i$  versus  $\phi$  is shown in Figure 3 for  $n_2/n_1=0.803$  (e.g. the dried polycarbonate craze) and two values of  $d/\lambda$ . The critical angle  $\phi_c$  for total reflection when  $d/\lambda \gg 1$  is  $53^\circ 40'$ . When  $d/\lambda=2$  (e.g.  $\lambda_{\text{vac.}}=6200 \text{ \AA}$ ,  $d=10000 \text{ \AA}$ ), strong interference effects are predicted but only for  $\phi < \phi_c$ .  $I_t/I_i$  drops abruptly as  $\phi_c$  is approached so that the critical angle can be determined within a degree or so. By contrast interference effects at  $\phi < \phi_c$



and  $d/\lambda=0.2$  (e.g.  $d=1\,000\text{ \AA}$ ) are subdued and  $I_t/I_i$  does not drop abruptly at  $\phi_c$  but rather falls much more gradually. At high values of  $\phi$  light will still be strongly reflected and consequently the eye may not casually differentiate between thin and thick crazes. A more complete picture of the precision of  $\phi_c$  determination as a function of  $d/\lambda$  is afforded by Figure 4 wherein  $I_t/I_i$  versus  $d/\lambda$  is displayed for  $\phi=\phi_c-40'$  and  $\phi_c+40'$  in order to indicate the value of  $I_t/I_i$  at  $\phi_c$  and also how rapidly it is changing at this point. Again it is clear that only crazes over  $5\,000\text{--}10\,000\text{ \AA}$  in thickness will yield reasonably precise values of  $\phi_c$ .

Figure 3—Transmission of light versus incident angle when  $n_2/n_1=0.803$  for two values of craze thickness to wavelength ratio



Large well-spaced crazes are generally thicker and the ones studied optically here are in the thickness range up to  $0.1\text{ mm}$ . Marked interference effects are seen in the reflected beam and the transition from reflection to transmission is reasonably abrupt. The existent uncertainty in critical angle value (about  $1^\circ$  usually) is attributable to a lack of strict planarity of the craze interface and to insufficient collimation of incident beam.

#### Craze composition

From the Lorentz-Lorenz equation as applied to mixtures

$$p_{12} = \frac{n_{12}^2 - 1}{n_{12}^2 + 2} \times \frac{1}{d_{12}} \approx p_1 w_1 + p_2 w_2$$

where  $p$  is the specific polarizability,  $n$  the refractive index,  $d$  the density, and  $w$  the weight fraction of component; the indices and densities are for the pure components. The composition of the craze can be calculated for the two cases: (a) fresh craze, which is assumed to consist of polymer and alcohol; and (b) the dried craze which is assumed to consist of polymer and air which has replaced the alcohol.

Initially volume additivity and weight fraction polarization additivity were assumed in both cases; also birefringent effects in the polymer fraction

were neglected. On these assumptions the alcohol-filled craze was calculated to be 60 per cent copolymer: 40 per cent alcohol by volume, the dried craze 50 per cent polymer: 50 per cent air. These results are in reasonable agreement.

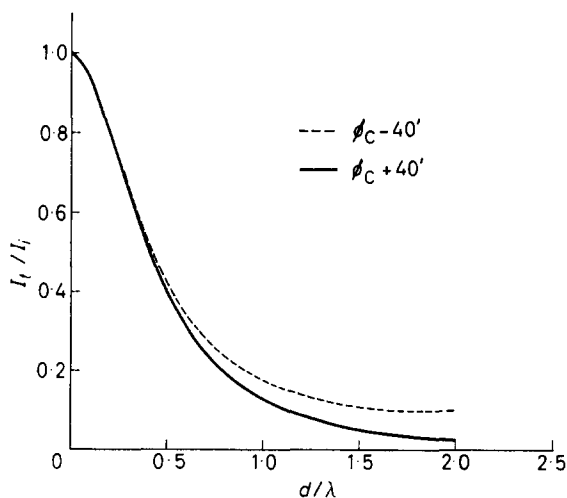


Figure 4—Transmission of light versus craze thickness to wavelength ratio near critical angle  $\phi_c$

A second approximation was subsequently made for the alcohol-filled craze by considering the polarizability of the mixture to be additive in weight fraction polarization of saturated bulk polymer and excess alcohol. The saturation concentration of ethanol in polycarbonate was determined to be 7.3 per cent by weight and volume additivity to hold within experimental error. The index of alcohol-saturated film was determined by immersion in a suitable silicone oil in a Zeiss interference microscope and measurement of fringe displacement. The measurement was effected in a short enough time compared to the known sorption rate of alcohol in polycarbonate to prevent appreciable alcohol concentration changes. In contrast to volume additivity, polarization of the saturated film is not ideal; if  $n=1.580$  for the dry polymer the index is 1.575 instead of the ideally expected value of 1.560 for the saturated film. As a result the ethanol-filled craze composition is recalculated to be 55 per cent polymer: 45 per cent alcohol. Since the uncertainty in craze index by this method is about  $\pm 0.01$ , the uncertainty in composition is a minimum of  $\pm 5$  per cent. Therefore the final conclusion is that polycarbonate crazes are 50–55 per cent polymer by volume.

The substantial polymer density reduction apparent upon crazing may be shown in another way. Figure 5 is a photomicrograph of the surface of a polycarbonate tensile bar in which an ethanol craze was produced under a bending stress. This particular craze is 3 mm wide and extends into the bar about the same distance. Its thickness at this surface is 0.045 mm. Illumination here is bright field reflection using an interference contrast objective. The diagonal lines are scratches imposed on the bar surface

before crazing to act as bench marks to allow determination of the amount of elongation occurring in the process of craze formation. This photograph was taken six hours after removal of the test bar from the bending jig and the alcohol environment. By comparison with other photographs taken at the time of stress removal it is known that some retraction has already taken place by this time. Nevertheless, it is evident from the displacement of the scratches that a relatively permanent, large elongation still exists. Measured from the early photographs the elongation upon crazing is calculated to be about 60 per cent. The surface of the craze here is V-shaped, the depth of the V being 0.005 mm as determined by interferometry. In normal cold drawing and in development of thick crazes in thin film as discussed above, polymer elongation is compensated for by lateral contraction. In craze marks like this one which run deep into the specimen from the surface, the amount of lateral contraction volume wise (i.e. the volume of the V-shaped surface groove) is negligible compared to the amount of volume increase in the stress direction (in this case less than one per cent of it). Consequently the elongation would seem to result in a decrease in polymer density in the craze interior by 0.60/1.60 or about 40 per cent, which is in reasonable agreement with the results of the index calculation\*.

#### *Alcohol mobility in the craze*

In contrast to the apparent healing process of the unstressed craze wherein refractive index changes more or less uniformly throughout the craze, the alcohol evaporation process from the stressed craze produces a non-uniform index change. Specifically the index begins to drop immediately at the bar edge but only after a time lag in the depth of the craze. In fact it is possible to set the light beam angle such that light is not transmitted by any section of the craze having an index less than some value close to that of the fresh craze and to follow the progression of the boundary between the non-transmitting and transmitting sections down to the tip of the craze using a travelling telescope. *Figure 6* shows the progression of such a boundary for  $n=1.42$  down to the craze tip. (The use of  $n=1.42$  rather than 1.46 was necessitated by some incidental physical restrictions on the location of the telescope in relation to the crazed bar and light source and is undoubtedly responsible for the data not extrapolating to the origin.) When the boundary reached the craze tip the stressed bar was immediately re-immersed in ethanol for a day. The craze regained an index of 1.46 and the evaporation boundary was followed again as shown.

That both boundary progressions are linear in  $t^{1/2}$  suggests a diffusion controlled process. Applying the equation  $D \sim x^2/t$  for estimation<sup>7,8</sup> of diffusion coefficients where  $D$  is the diffusion coefficient,  $x$  is the distance

\*Studies of a number of crazes in this way give void contents of 25 to 40 per cent. A number of factors may generate this spread and extant lack of close agreement with the index results. First there is some uncertainty in what to take as craze boundaries. Further, the crazing process may be perturbed locally by the surface. Finally index-based calculations comment only on the rarest layer in the craze; it is not inconceivable that polymer density is somewhat higher at the craze interfaces than in the craze centre plane.

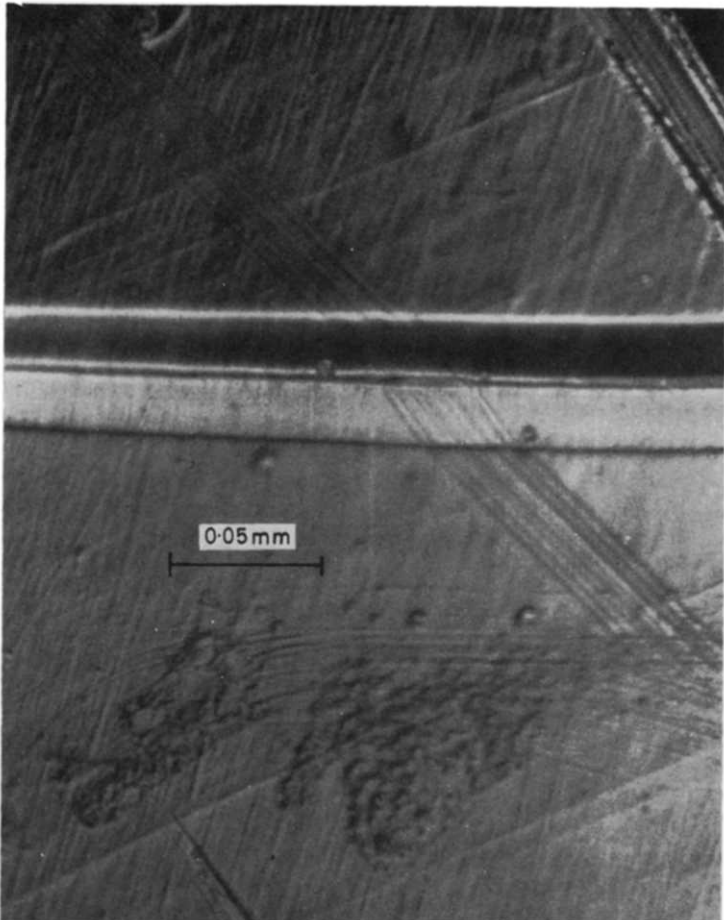


Figure 5—Interference contrast photograph of surface of crazed polycarbonate bar. The craze is the horizontal band. Diagonal lines are scratches imposed before crazing to serve as bench marks

moved of a diffusion boundary in time  $t$  we obtain

$$D \sim 1 \times 10^{-5} \text{ cm}^2/\text{sec}$$

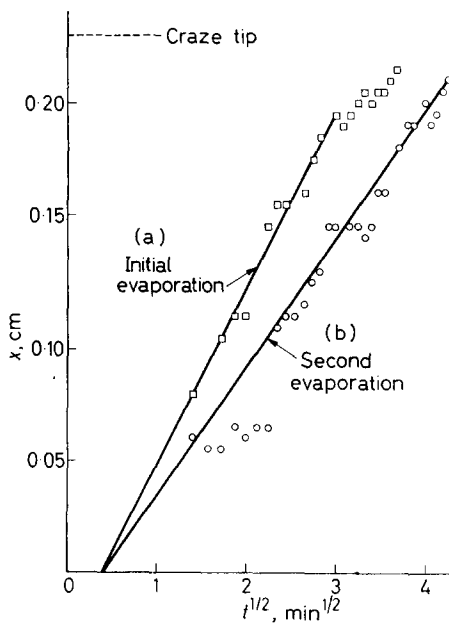
as an estimate of the alcohol diffusivity in the craze. In this case  $x^2/t$  has been taken as the line slope in *Figure 6*. Measurements here of the sorption kinetics of ethanol in thin polycarbonate films of the same molecular weight have given a diffusion coefficient of

$$D \sim 1 \times 10^{-12} \text{ cm}^2/\text{sec}$$

The ratio of alcohol diffusivities in the craze and in the saturated bulk polymer is thus  $10^7$ . Furthermore,  $D = 1 \times 10^{-5} \text{ cm}^2/\text{sec}$  for self-diffusion in liquid ethanol<sup>9,10</sup>. The similarity of this value to that for the excess alcohol in the craze suggests that long-range mobility in the latter is similar

to that in the liquid. In view of all of the other craze properties two alternative interpretations of these mobilities are conceivable: (a) the polymer chains in the craze have very greatly enhanced segmental motion so that the whole craze has a liquid-like mobility; (b) the excess alcohol is concentrated in interconnected holes so that the first stages of evaporation can essentially occur by motion of alcohol out through polymer-free paths. The substantial tensile strengths of crazes even when wet favour the latter alternative.

Figure 6 — Progression of shadow boundary into polycarbonate craze. After initial run still-strained bar was re-immersed in ethanol overnight for solvent recovery. Run (b) is on resoaked, still-strained craze



### Void sizes

It is of interest to know how the space not occupied by polymer is distributed in the craze. That valid indices of refraction for the craze can be measured indicates that the craze is homogeneous over distances of the order of the wavelength of light. If the void content is distributed in the form of discrete holes, these are thus expected to be mostly smaller than  $10^3 \text{ \AA}$ . Simple investigation by electron microscopy of microtomed sections of crazes has so far yielded no information in this regard, partly due to the difficulties in assessing the effects of the cutting process.

In order to make the void content visible the best hope would seem to lie in taking advantage of the open structure to infuse an electron-dense substance into the craze in high concentration, which material can then be hardened *in situ* by reaction, precipitation or freezing. The only other requirement is that contact of the stressed craze with such material should not produce any substantial changes in craze structure (e.g. the material should not be a solvent or a stress corrosion agent). To date saturated aqueous silver nitrate has appeared most suited for such an attempt.

The actual procedure used in this regard has involved removing a crazed bar from the liquid ethanol and immediately restressing it in the dark in saturated silver nitrate solution. After a suitable length of time the bar is removed and left to dry out on the bench top for a period of time. (No study of minimum time requirements has yet been made but four to ten day periods for each part for 2–3 mm deep crazes have appeared adequate.) Sections 500 Å thick are then cut with a Porter-Blum ultramicrotome. They slide off the knife on to a water surface, are picked up on a grid, carbon-backed for strength, and then inspected in an electron microscope.

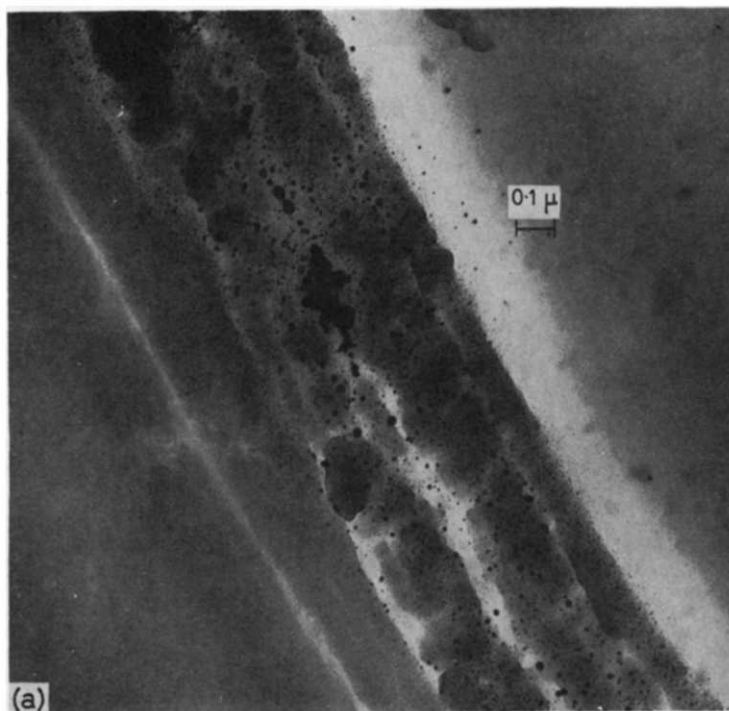


Figure 7—Electron micrographs of ultramicrotomed sections of silver-doped polycarbonate crazes showing in (a) a somewhat coarser structure and (b) a finer one. Sections were cut perpendicular to direction of craze propagation and to craze plane

In contrast to crazes not treated with silver nitrate, the silver-doped crazes show a myriad of spheroidal electron-dense particles (*Figures 7 and 8*). Selected area electron diffraction of the largest of these shows them to be free silver rather than silver nitrate, photoreduction presumably having occurred during the long light exposure prior to sectioning. Furthermore, stereomicrographs show that these particles are distributed throughout the section thickness rather than being concentrated on the surfaces. The particle size distribution is wide, a few irregularly shaped aggregates being  $\sim 10^3$  Å, more being  $\sim 10^2$  Å and a great many being

below 100 Å. In fact inspection of the original micrographs indicates that the lower limit in size is below the resolving power of  $\sim 20$  Å. The peak in the distribution curve, if a peak exists, appears to lie close to, or below, such resolving limits.

If one assumes that the doping process worked ideally, i.e. that saturated silver nitrate replaced the alcohol in the voids completely, that the voids are spheroidal, that all the silver nitrate was crystallized and reduced *in situ* on a submicro scale, and that these processes did not distort the microstructure of the craze, then it is possible to calculate back to the size of the void from the size of the silver particle. (Saturated silver nitrate

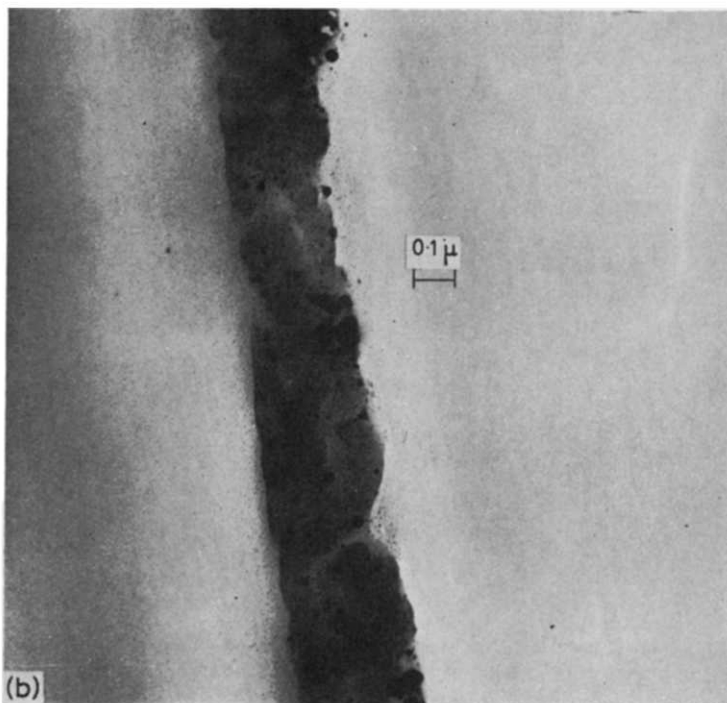


Figure 7(b)— see page 152

contains 69.6 g/100 ml at 23°C and has a density of 2.47 g/cm<sup>3</sup>.) The conclusion is that each particle has a diameter 47 per cent of that of the solution-filled void. There are various uncertainties in such a calculation, however, the largest perhaps being that no silver migration takes place between holes during the precipitation-reduction process. Free energy considerations dictate that such a migration should result in enlargement of the large particles at the expense of the small ones so that the 'grain' of the craze is, if anything, finer than indicated by the silver.

These micrographs, particularly Figure 8 which is of a microtomed section cut perpendicular to the craze plane but parallel to its direction of propagation, also shed some light on an old question, 'How small is the smallest craze mark; does it exist if it is not yet visible to the naked eye?'

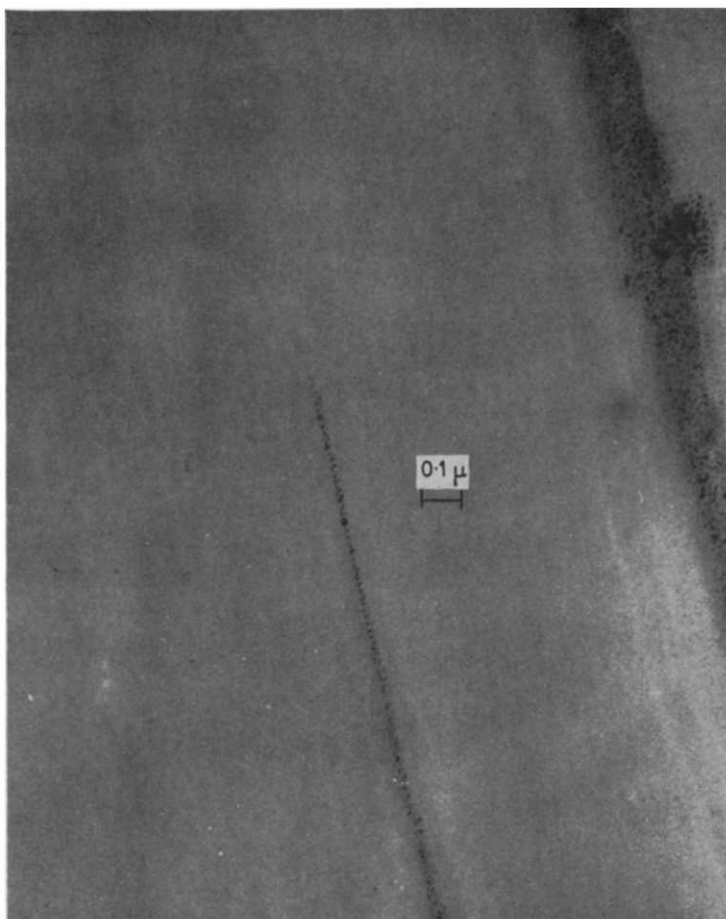


Figure 8—Electron micrograph of polycarbonate section containing silver-doped craze. Section was cut perpendicular to craze plane but parallel to craze propagation direction

Judging from the dimensions of the silver-laden area here, which presumably is a craze tip, crazes 200–400 Å thick exist. As shown earlier such crazes, even when lateral dimensions are large compared to the wavelength of light, will reflect light appreciably only at high incident angles. If such thin crazes exist which also have rather small lateral dimensions (e.g. during craze initiation), they will be invisible to the naked eye.

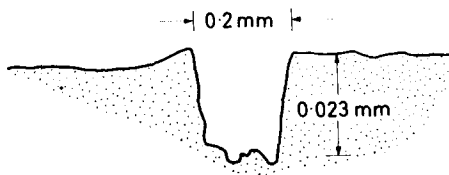
#### *Thick crazes*

In polycarbonate film it is possible to initiate solvent crazes which can grow in thickness up to fractions of, or even whole, millimetres. While still thin, such crazes reflect light in the usual way but such reflectance disappears when craze thickness approaches or exceeds one of the lateral dimensions (i.e. approaches the film thickness). In such cases lateral con-



traction of the film at the craze mark (e.g. see *Figure 9*) becomes great enough to compensate for craze elongation so that substantial void content no longer results. Indeed a smooth transition from craze propagation to cold drawing is possible.

*Figure 9*—Talysurf trace of surface profile of 0.1 mm thick polycarbonate film showing indentation accompanying craze formation. Vertical magnification is ten times horizontal magnification



From the above evidence it becomes apparent that the essential process of craze propagation—polymer rarefaction by elongation without lateral contraction—requires the existence of triaxial stresses. Growth of craze material occurs mainly but not solely at the craze tip. Thickening of the craze occurs behind the craze tip although usually at a rate which appears roughly to be inversely related to the distance from the craze tip. Therefore as at the tip of the true crack in an elastic material, hydrostatic tension is at a maximum at the craze tip; unlike the abrupt disappearance of such stress immediately behind the tip of the true crack, that behind the craze tip falls smoothly with distance. The crazing process then involves the dissipation of strain energy largely through viscous heating and production of surface free energy through hole formation. The presence of a plasticizing agent will both lower the bulk viscosity and the interfacial free energy so that a given strain energy will produce more extensive crazing faster. Something of a balance of properties is required, however, in that too high a concentration of dissolved plasticizer will not permit the maintenance of the hydrostatic tension necessary for the process of rarefaction.

*The author is grateful to Mr R. H. Savage for the photomicrograph shown in Figure 5, to Mr R. S. Owens for the Talysurf trace shown in Figure 9 and to Dr R. E. Robertson for his interest in and discussion of this work.*

G.E. Research Laboratory,  
Schenectady, N.Y.

(Received March 1963)

#### REFERENCES

- <sup>1</sup> BESSONOV, M. I. and KUVSHINSKII, E. V. *Plasticheskie Massy*, 1961, **5**, 57
- <sup>2</sup> LEBEDEV, G. A. and KUVSHINSKII, E. V. *Soviet Physics Solid State*, 1962, **3**, 1957
- <sup>3</sup> SPURR, O. K. and NIEGISH, W. D. *J. appl. Polym. Sci.* 1962, **6**, 585
- <sup>4</sup> SAUER, J. A. and HSAIO, C. C. *Trans. Amer. Soc. mech. Engrs.* 1953, **75**, 895
- <sup>5</sup> KAMBOUR, R. P. *Nature, Lond.* 1962, **195**, 1299
- <sup>6</sup> HALL, E. E. *Phys. Rev.* 1902, **15**, 73
- <sup>7</sup> HARTLEY, G. S. *Trans. Faraday Soc.* 1949, **45**, 820
- <sup>8</sup> FATT, I. J. *phys. Chem.* 1962, **66**, 760
- <sup>9</sup> PARTINGTON, J. R., HUDSON, R. F. and BAGNALL, K. W. *Nature, Lond.* 1952, **169**, 583
- <sup>10</sup> GRAUPNER, K. and WINTER, E. R. S. *J. chem. Soc.* 1952, **201**, 1145

# Contributions to Polymer

*Papers accepted for future issues of  
POLYMER include the following:*

- The Crystallization of Polymethylene Copolymers: Morphology*—J. B. JACKSON and P. J. FLORY
- The Crystallization of Polyethylene II*—W. BANKS, J. N. HAY, A. SHARPLES and G. THOMSON
- Description and Calibration of an Elasto-osmometer*—H. J. M. A. MIERAS and W. PRINS
- Resonance-induced Polymerizations*—R. J. ORR
- Polypropylene Oxide I—An Intrinsic Viscosity/Molecular Weight Relationship*—G. ALLEN, C. BOOTH and M. N. JONES
- Viscosity/Temperature Dependence for Polyisobutene Systems: The Effect of Molecular Weight Distribution*—R. S. PORTER and J. F. JOHNSON
- The Photolytic Decomposition of Poly-(n-butyl)methacrylate*—J. R. MACCALLUM
- Catalysts for Low Temperature Polymerization of Ethylene*—K. J. TAYLOR
- The Effect of Tension and Annealing on the X-ray Diffraction Pattern of Drawn 6.6 Nylon*—D. R. BERESFORD and H. BEVAN
- Orientation in Crystalline Polymers related to Deformation*—Z. W. WILCHINSKY
- Morphology of Polymer Crystals: Screw Dislocations in Polyethylene, Polymethyleneoxide and Polyethyleneoxide*—W. J. BARNES and F. P. PRICE
- Nuclear Spin-Lattice Relaxation in Polyacetaldehyde*—T. M. CONNOR
- The Morphology of Poly(4-methyl-pentene-1) Crystals*—A. E. WOODWARD
- Proton Spin-Lattice Relaxation Measurements on Some High Polymers of Differing Structure and Morphology [Polyethylene, poly(4-methyl-pentene-1), poly(L-leucine), poly(phenyl-L-aniline), polystyrene and poly( $\alpha$ -methyl-styrene)]*—B. I. HUNT, J. G. POWLES and A. E. WOODWARD
- Infra-red Spectra of Poly(p-ethylene oxybenzoate)*—MATAHUMI ISHIBASHI
- Sequence Length Distribution and Entropy of Stereoregularity in Homopolymers of Finite Molecular Weight*—A. M. NORTH and D. RICHARDSON
- The Copolymerization of Methylmethacrylate and Maleic Anhydride*—A. M. NORTH and D. POSTLETHWAITE
- Polypropylene Oxide II—Dilute Solution Properties and Tacticity*—G. ALLEN, C. BOOTH and M. N. JONES
- Studies in the Thermodynamics of Polymer-Liquid Systems I—Natural Rubber and Polar Liquids*—C. BOOTH, G. GEE, G. HOLDEN and G. R. WILLIAMSON
- Studies in the Thermodynamics of Polymer-Liquid Systems II—A Re-assessment of Published Data*—C. BOOTH, G. GEE, M. N. JONES and W. D. TAYLOR

- Studies in the Thermodynamics of Polymer-Liquid Systems III—Polypropylene + Various Ketones*—W. B. BROWN, G. GEE and W. D. TAYLOR
- Studies in the Thermodynamics of Polymer-Liquid Systems IV—Effect of Incipient Crystallinity on the Swelling of Polypropylene in Diethylketone*—G. ALLEN, C. BOOTH, G. GEE and M. N. JONES
- Some Experimental Studies on Enthalpy and Entropy Effects in Equilibrium Swelling on Polyoxypropylene Elastomers*—B. E. CONWAY and J. P. NICHOLSON
- Copolymerization of Trioxan with Dioxolan*—M. KUČERA and J. PICHLER
- Thermal Degradation of an Aromatic Polypyromellitimide in Air and Vacuum—Rates and Activation Energies*—S. D. BRUCK
- The Polymerization of Propylene Oxide Catalysed by Zinc Diethyl and Aluminium Triethyl*—C. E. H. BAWN, A. M. NORTH and J. S. WALKER
- The Free Radical Polymerization of N,N-Dimethylacrylamide*—A. M. NORTH and A. M. SCALLAN
- On the Chemistry of Polymer Chain Folds*—D. C. BASSETT
- Stress/Strain and Swelling Properties of a Peroxide Cured Methylvinyl Silicone*—D. K. THOMAS
- The Measurement of Dynamic Bulk Modulus using an Ultrasonic Interferometer*—W. J. PULLEN, J. ROBERTS and T. E. WHALL
- The Polymerization of Propylene Oxide Catalysed by Zinc Diethyl and Water*—C. BOOTH, W. C. E. HIGGINSON and E. POWELL
- Proton Spin-Lattice Relaxation and Mechanical Loss in a Series of Acrylic Polymers*—J. G. POWLES, B. I. HUNT and D. J. H. SANDIFORD
- Solution and Bulk Properties of Branched Polyvinyl Acetates IV—Melt Viscosity*—V. C. LONG, G. C. BERRY and L. M. HOBBS
- The Anionic Polymerization of Some Alkyl Vinyl Ketones*—P. R. THOMAS, G. T. TYLER, T. E. EDWARDS, A. T. RADCLIFFE and R. C. P. CUBBON
- A Theoretical Treatment of the Modulus of Semi-crystalline Polymers*—W. R. KRIGBAUM, R.-J. ROE and K. J. SMITH, Jr
- Polpropylene Oxide III—Crystallizability, Fusion and Glass Formation*—G. ALLEN, C. BOOTH, M. N. JONES, D. J. MARKS and W. D. TAYLOR
- Polypropylene Oxide IV—Preparation and Properties of Polyether Networks*—G. ALLEN and H. G. CROSSLEY

CONTRIBUTIONS should be addressed to the Editors, *Polymer*, 4-5 Bell Yard, London, W.C.2.

Authors are solely responsible for the factual accuracy of their papers. All papers will be read by one or more referees, whose names will not normally be disclosed to authors. On acceptance for publication papers are subject to editorial amendment.

If any tables or illustrations have been published elsewhere, the editors must be informed so that they can obtain the necessary permission from the original publishers.

All communications should be expressed in clear and direct English, using the minimum number of words consistent with clarity. Papers in other languages can only be accepted in very exceptional circumstances.

A leaflet of instructions to contributors is available on application to the editorial office.

# The Crystallization of Polymethylene Copolymers; Morphology

J. B. JACKSON and P. J. FLORY

*The morphology of a series of melt-crystallized, random copolymers of  $-\text{CH}_2-$  units with small mole percentages of  $-\text{CHR}-$  co-units, where  $\text{R} = n\text{-C}_3\text{H}_7$  or  $\text{CH}_3$ , has been investigated. At concentrations greater than two per cent  $n\text{-C}_3\text{H}_7$  and 5.9 per cent  $\text{CH}_3$  co-unit, spherulites characteristic of the homopolymer are not evident even at  $450\times$  magnification under the polarizing microscope. The absence of spherulites is attributed to the growth of crystallites in which a given copolymer chain may participate only once, leading to a suppression of lamellar crystal growth.*

WE HAVE investigated the development of crystallinity from the melt in a series of polymethylene copolymers using the polarizing microscope as the means of observation. The copolymers comprised  $-\text{CH}_2-$  units with from 1.2 to 6.4 mole per cent of  $-\text{CHR}-$  co-units where R is *n*-propyl or methyl. The samples were available from a previous study<sup>1</sup>; their preparation has been described and the distribution of co-units has been shown to be essentially random. Copolymer compositions are given in the second column of *Table 1*. Also included are the melting points and ultimate percentages of crystallinity attained at the crystallization temperature  $T_c$ ; these data were available from the earlier investigation.

The procedure followed in cooling from the melt is of foremost importance in determining the growth and morphology of the crystalline phase. In order to provide conditions favouring development of crystalline regions of the highest order consistent with the chemical constitution of the sample, cooling from the melt was conducted over an extended period of time. A thin film of the sample was melted on the hot stage of a polarizing microscope, then cooled in  $2^\circ$  steps, each successive temperature being maintained for one hour, until a temperature  $T_c$  was reached at which substantial crystallization would take place according to the results of the previous study<sup>1</sup>. The sample was maintained at  $T_c$  for one day and thereafter the temperature was decreased in steps of  $5^\circ\text{C}$  each half day. Occurrence of crystallization at the temperature  $T_c$  was apparent from the brightening of the previously dark field with polarizer and analyser crossed. For those samples designated as non-spherulitic in *Table 1*, this enhanced transmission of illumination appeared uniform up to a magnification of  $450\times$ . Other samples displayed characteristic spherulitic patterns. Only copolymers of low co-unit content gave evidence of crystallization prior to reaching  $T_c$  in the cooling cycle described above. The morphology in these instances was spherulitic, and comparatively insensitive to acceleration of the cooling schedule.

As summarized in the last column of *Table 1*, spherulites were not observed in the propyl-substituted copolymer except at the lowest co-unit concentration. All of the methyl-substituted copolymers with the exception of the most highly substituted sample were spherulitic. Spherulites in copolymer 9

ranged up to  $20\mu$  in size. Those for copolymers 11 and 2 were smaller (*ca.*  $10\mu$ ); spherulites in the latter sample were poorly defined\*. Attempts to produce spherulites in 'non-spherulitic' samples, or to increase their size in others, by heating to high temperatures (*ca.*  $300^\circ\text{C}$ ) for short periods before crystallizing as described by Banks *et al.*<sup>3</sup> were unsuccessful.

Table 1. Crystallization of polymethylene copolymers

Copolymer No.	Copolymer composition CHR/100 chain C atoms		$T_m$ ( $^\circ\text{C}$ )	$T_c$ ( $^\circ\text{C}$ )	Calculated % crystallinity at $T_c$	Observed growth
2	Propyl	2.0	112	100	18	spherulitic (poorly defined)
4	Propyl	4.6	89	75	8	non-spherulitic
5	Propyl	6.4	75	55	4	non-spherulitic
9	Methyl	1.2	132	120	38	spherulitic
11	Methyl	3.7	111	100	18	spherulitic (small)
13	Methyl	5.9	91	75	5	spherulitic (poor, $2\mu$ )
14	Methyl	6.1	84	70	5	non-spherulitic

According to the earlier studies<sup>1</sup> on the crystallization of copolymers of these types, the co-unit with R as propyl is effectively rejected completely from the crystal lattice at equilibrium. At low levels of crystallinity, such as may be reached in copolymers 4 and 5 at the respective crystallization temperatures  $T_c$ , exceptionally long sequences of the main unit, uninterrupted by co-units are believed to be preferentially engaged in crystallite formation. Assuming one such sequence from a given molecule to have been incorporated in the lattice, it is improbable that the sequence immediately following it in the same chain will likewise be of exceptional length and thus capable of meeting the requirements set by the length dimension of the crystallite. A molecule of the copolymer will, for this reason, be incapable of traversing the same crystallite repetitively, as has been pointed out previously<sup>4</sup>. A crystallite formed at low supercooling must therefore involve approximately as many molecules as there are sequences of units in the direction of the chain axes in the crystallite. An assemblage of macromolecules cannot in general be arranged in lamellae without dissipating the otherwise excessive concentration of amorphous chains adjoining the faces of the lamella<sup>4</sup>. This can be accomplished only if a substantial fraction of the chains emerging from the crystal execute loops, or folds, which enable them to return to the crystallite. For the reason stated above, however, re-entry of the chain will usually be forbidden in a copolymer containing a sufficiency of non-crystallizing co-unit. We conclude that crystallites in copolymers must be severely restricted in their lateral crystal dimensions<sup>4</sup>. If lamellae are a concomitant of spherulitic growth, then the absence of spherulites in the first series of copolymers beyond a co-unit concentration of two per cent finds immediate explanation.

The methyl-substituted co-unit, on the other hand, enters the crystal

\*The observations of Bunn and Alcock<sup>3</sup> on non-linear (high pressure) polyethylene are in accord with our results. They reported growth of small spherulites. A melting point in the range  $120^\circ$  to  $162^\circ\text{C}$  indicates the presence of co-units equivalent to about one per cent *n*-propyl substituent in polymethylene copolymers.

lattice to a limited extent<sup>5</sup>, although it is preferentially relegated to the amorphous phase<sup>1</sup>. The requirement of an uninterrupted sequence of —CH<sub>2</sub>— units for its assignment to the crystal lattice is therefore relaxed to some extent for the second series of copolymers. Persistence of spherulitic growth to somewhat higher co-unit concentrations may thus be comprehended.

A further contrast between the crystallization of copolymers and homopolymers deserves foremost consideration in this connection. Crystallization of homopolymers generally involves nucleated growth of spherulitic regions which approach the ultimate degree of crystallinity (often 50 per cent or more), these being surrounded during their growth by a supercooled melt which remains unchanged until enveloped by spherulites. The levels of crystallinity attainable at  $T_c$  in the crystallization of copolymers are fairly low, especially for higher proportions of the co-units, owing to the limited availability of sequences surpassing the length required for stable crystallites at this temperature. Propagation of growth through the melt should be much more difficult when the concentration of the crystalline phase must remain low. The entire mechanism of crystal growth may be altered drastically in copolymers on this account, quite apart from the consequences of the difference in morphological characteristics of the crystalline regions as discussed above.

In conclusion, crystallization of a copolymer in which the co-unit is largely rejected from the crystal lattice may depart markedly from homopolymer crystallization, both in mechanism and in the morphology of the resulting crystalline phase. Underlying both differences is the essential requirement of sequences comprising units acceptable to the crystal lattice and sufficiently long to generate a stable crystal phase. The suppression of spherulitic growth by the presence of co-units structurally dissimilar to the main unit confirms these generalizations.

*Support of the United States Air Force under grant AFOSR-62-131 is gratefully acknowledged.*

*Department of Chemistry,  
Stanford University,  
Stanford, California*

*(Received March 1963)*

#### REFERENCES

- <sup>1</sup> RICHARDSON, M. J., FLORY, P. J. and JACKSON, J. B. *Polymer, Lond.* 1963, **4**, 221
- <sup>2</sup> BUNN, C. W. and ALCOCK, T. C. *Trans. Faraday Soc.* 1945, **41**, 317
- <sup>3</sup> BANKS, W., HAY, J. N., SHARPLES, A. and THOMPSON, G. *Nature, Lond.* 1962, **194**, 542
- <sup>4</sup> FLORY, P. J. *J. Amer. chem. Soc.* 1962, **84**, 2857
- <sup>5</sup> SWAN, P. R. *J. Polym. Sci.* 1962, **56**, 409

# The Crystallization of Polyethylene II

W. BANKS, J. N. HAY\*, A. SHARPLES and G. THOMSON

*A microscopic study has been made of the crystallization of polyethylene, with the object of throwing light on the anomalous fractional values of the Avrami exponent,  $n$ , observed in previous dilatometric experiments. In the bulk, the polymer crystallizes to give an unresolvable birefringent structure, and it is only after special treatments that thin films of the material are capable of yielding spherulites of measurable dimensions. These treatments are considered to result in a state which is not representative of the bulk crystallized material, so that quantitative comparisons of microscopically and dilatometrically observed rate constants are not justifiable. Studies of the component nucleation and growth processes, however, are considered in relation to possible explanations for the anomalous dilatometric behaviour and it is suggested that a decrease in the density of the spherulites during growth, arising from their dendritic nature, is a complicating factor which reduces the Avrami exponent,  $n$ , from its expected value. As a result,  $n$  cannot be used to make predictions concerning crystallization mechanism.*

AN AVRAMI equation of the form<sup>1,2</sup>

$$W_t/W_0 = \exp(-zt^n) \quad (1)$$

where  $W_t/W_0$  is the weight fraction of liquid material remaining after time  $t$ , has been used by several groups of workers to derive information on mechanism from studies of polymer crystallization. The temperature dependence of the rate constant,  $z$ , is informative, but more important is the value of the exponent,  $n$ . This has been taken in the past as an indication of the nature of the nucleation process, i.e. whether it is instantaneous or sporadic, and also of the number of dimensions in which growth occurs. Thus for the 'standard' case of sporadic nucleation (where the number of nuclei is proportional to the first power of the time) and three-dimensional spherulitic growth,  $n=4$ . Various other possibilities lead to integral values of 1, 2 and 3.

In fact the Avrami equation is dependent on several additional factors and the complete list is as follows:

- (1) the time dependence of the nucleation process;
- (2) the time dependence of the growth process;
- (3) the spacing of the nuclei;
- (4) the number of dimensions in which growth takes place;
- (5) the time dependence of the density of the growing bodies.

With some experimental justification it has previously been assumed that the linear dimensions of the growing bodies are proportional to the first power of the time, that their density is constant and that the nuclei are, in general, randomly spaced. In addition the time dependence of the nucleation

---

\*Present address: Chemistry Department, University, Aberdeen.

process has been taken to be either zero or first order. These assumptions lead to the situation noted above, where the experimentally determined value of  $n$  is used to derive information on factors (1) and (4). It is also an incidental requirement that  $n$  be integral.

In the first part of this study<sup>3</sup> it was found in fact that, for polyethylene,  $n$  is often fractional. Values between 2.0 and 4.0 are possible, depending on molecular weight and temperature of crystallization, and the continuous nature of the variation suggests that the occasional appearance of integral values has no special significance. Fractional values between 2.3 and 4.0 have also been found for other polymers<sup>4,5</sup> and values as low as 1.25 have been obtained for polyethylene crystallized in the presence of unmelted seeds<sup>6</sup>. These observations are obviously inconsistent with previous ideas, and suggest that one, at least, of the above assumptions is incorrect.

Experimental determinations of  $W_1/W_0$  in equation (1) are based on methods which only give a value for the overall amount of crystallized material present. Separate measurements of nucleation and growth can sometimes be made by direct microscopic observation, and hence can be used to check some of the assumptions listed above. This present paper is primarily concerned with such a study for the crystallization of polyethylene, although as current work indicates that many of the phenomena reported here are of general application, occasional reference is also made to results obtained for other polymeric materials.

## EXPERIMENTAL

### *Materials*

A wide range of polyethylene samples, including all those examined in Part I<sup>3</sup>, was studied. This included two separate sets of fractions from Phillips type high-density polyethylenes, with molecular weights ranging from  $3 \times 10^3$  to  $5 \times 10^5$ , unfractionated homopolymers and copolymers with butene and propylene, Ziegler type high density samples, low density samples with a range of melt indices and a high molecular weight ( $7.3 \times 10^5$ ) polymethylene. The various treatments used for preparing the samples are described in the next section.

### *Apparatus*

Samples were melted on a hot plate at known temperatures and then transferred to a specially designed hot-stage, capable of being thermostatically controlled to  $\pm 0.03^\circ\text{C}$ . A check on the absolute accuracy of the temperature of the system was made by determining the melting point of benzoic acid contained between glass cover slips. In general a 16 mm objective was used in conjunction with a  $10\times$  screw micrometer eyepiece, although most of the photographs were taken using the objective only.

## RESULTS

The overall rate constant,  $z$ , (equation 1), is predicted by theory<sup>1,2</sup> to be related to the component nucleation and growth rates,  $N$  and  $G$ . For



example, in the standard case where nucleation is sporadic and growth takes place uniformly in three dimensions to give spherulites,  $n=4$  and

$$z = \pi\rho_c NG^3 / 3\rho_l\chi \quad (2)$$

where  $\rho_c$  and  $\rho_l$  are the densities of the crystalline and liquid phases, and  $\chi$  is taken to be the weight fraction of crystalline material within the growing spherulites. Checks on the dilatometrically determined values of  $z$  thus require accurate and reproducible values for  $N$  and  $G$ , and to achieve this it is considered that the spherulites under observation should have final dimensions of at least  $20\mu$ .

In fact it was found that, of the wide range of polyethylene samples studied, none produced resolvable spherulites of any size; the limit of resolution was about  $2\mu$ . From this it is evident that a quantitative comparison of dilatometrically and microscopically determined rate constants through equation (2) is not possible. Spherulitic samples of polyethylene have, of course, frequently been reported in the literature, but it is considered that in such cases special treatments were probably used involving growth conditions not typical of normal bulk crystallization<sup>7</sup>. However, as it is possible that the nucleation and growth characteristics of these specially prepared samples may throw light on the assumptions on which the Avrami equation is based, quantitative values are reported and discussed later. In addition, it is likely that the factors which lead to the atypical appearance of resolvable spherulites in polyethylene are also relevant to other polymers, and hence may introduce an element of uncertainty into previous studies which have attempted to correlate results from microscopy and dilatometry. For this reason these factors are discussed in detail in the next section.

### *Qualitative observations*

Polyethylene samples crystallized in the bulk, for example, in evacuated and sealed glass tubes of *ca.* 5 mm diameter, and subsequently sectioned, were invariably found to give unresolvable granular birefringent structures, regardless of whether the crystallization was carried out quickly or slowly<sup>7</sup>. Previous workers have reported similar structures, for example, in poly(ethylene terephthalate)<sup>8</sup>. Similar unresolvable structures were also obtained, in general, when the samples were crystallized in thin ( $< 10\mu$ ) or thick ( $> 10\mu$ ) films between glass cover slips, unless special treatments were used. This was so even if melting temperatures as high as  $300^\circ\text{C}$  were used, before crystallization.

Two exceptions were observed. In some samples, particularly in the low molecular weight range (3 to  $30 \times 10^3$ ), spherulites could occasionally be resolved in localized regions of thin films, often, although not invariably, near the edge of the sample. A typical example is given in *Figure 1*, which is a photograph taken of fraction 3 crystallized at  $128.0^\circ\text{C}$  for six hours, after melting at  $200^\circ\text{C}$  for 20 minutes. The usual unresolvable structure can be seen, together with a transition to a region of lower nucleation density, containing readily resolvable spherulites. The fact that the transition is gradual suggests that spherulites are also present in the granular region, but that the nucleation density is so great that they cannot be resolved.



*Figure 1*—Fraction 3 heated for 20 min at 200°C in form of film ca. 5 $\mu$  thick, between glass cover slips. Crystallized at 128.0°C for six hours

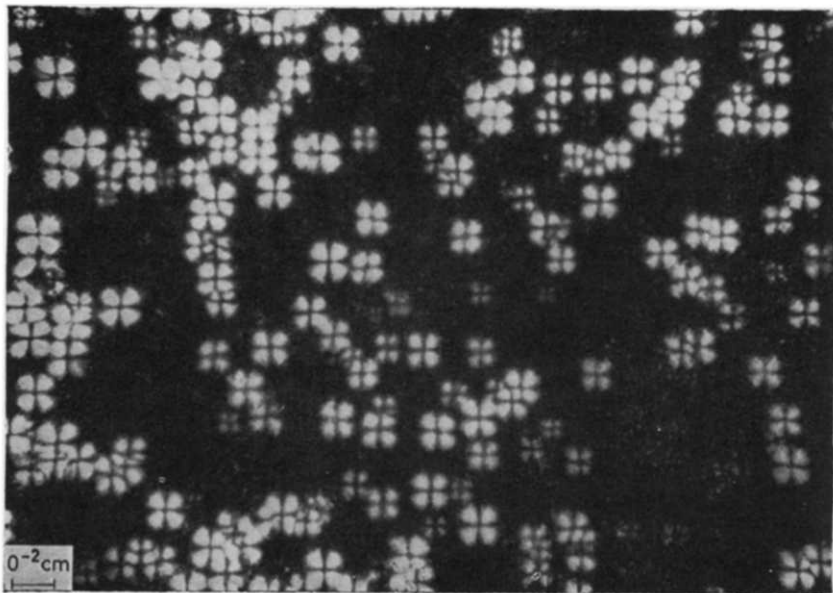


*Figure 2*—Marlex (melt index=5) heated for 10 min at 250°C in the form of film ca. 10 $\mu$  thick, between glass cover slips. Crystallized rapidly by cooling at room temperature

This occasional appearance of regions containing large spherulites in some samples, enabled measurements to be made of nucleation and growth rates, but it is quite obvious that no significance can be attached to the absolute values for the nucleation density, except to say that they represent lower limits.

The second exception is exemplified by *Figure 2*. This shows a sample of Marlex (melt index = 5) with spherulites embedded in a granular background; the crystallization is complete. Observations made during slow growth showed that the spherulites developed by increasing in intensity, but not in diameter, so that they did not exceed the limited size indicated in *Figure 2*. The essential point, however, is that samples showing this type of behaviour are also not amenable to quantitative study.

The possibility that lack of resolution might result from the superposition of spherulites in depth was checked in two ways. First, very thin films were formed by pressing out samples between optically flat glass surfaces under high pressures. The resulting films were estimated to be  $1-2\mu$  thick, but spherulites could still not be resolved. Secondly, observations were made during the course of crystallization in an attempt to resolve the spherulites long before touching occurred. In fact separate entities were never seen, except for the occasional samples mentioned above. From these experiments it was deduced that if spherulites are present in the unresolvable regions, their size must be less than  $2\mu$ .

Spherulites well above this size (e.g.  $100\mu$ ) have, of course, been reported frequently in the literature and in fact one of the first references to spherulitic structure in polymers used polyethylene as the substrate<sup>9</sup>. However, it seems reasonable to deduce from the results described above, that they are not characteristic of the bulk crystallization process. The factors which seem to be most important in promoting the formation of large spherulites are heat and solvents acting on the material in the form of a thin film constrained between two surfaces, and previous microscopic studies on polyethylene and other polymers have often used special treatments involving these conditions during specimen preparation<sup>10,11</sup>. Two typical treatments found to be effective in the present study are as follows. A cover slip with about 10 mg polymer was placed on a hot stage at  $380^{\circ}\text{C}$  for 10 seconds. A second cover slip was then pressed on to the sample and both were removed and cooled in air. Subsequent melting (at up to  $300^{\circ}\text{C}$ ) and crystallization gave an appearance of the type shown in *Figure 3*, with spherulites of up to  $100\mu$  in diameter. Alternatively, a one per cent solution of the sample in toluene was heated to  $100^{\circ}\text{C}$ , and dripped on to a tilted glass slide heated to ca.  $60^{\circ}\text{C}$ . A variety of similar methods is capable of yielding films with resolvable spherulites, although the results are always highly irreproducible in that a wide range of spherulite sizes is obtained on repetitions of a given treatment. Once a thin film between cover slips is obtained in spherulitic form, however, subsequent melting (up to  $300^{\circ}\text{C}$ ) and crystallization gives reproducible nucleation and growth rates.

Several explanations may at first appear capable of accounting for the above observations. First, in many cases degradation is likely to have occurred. That this is not the sole requirement, however, is apparent from

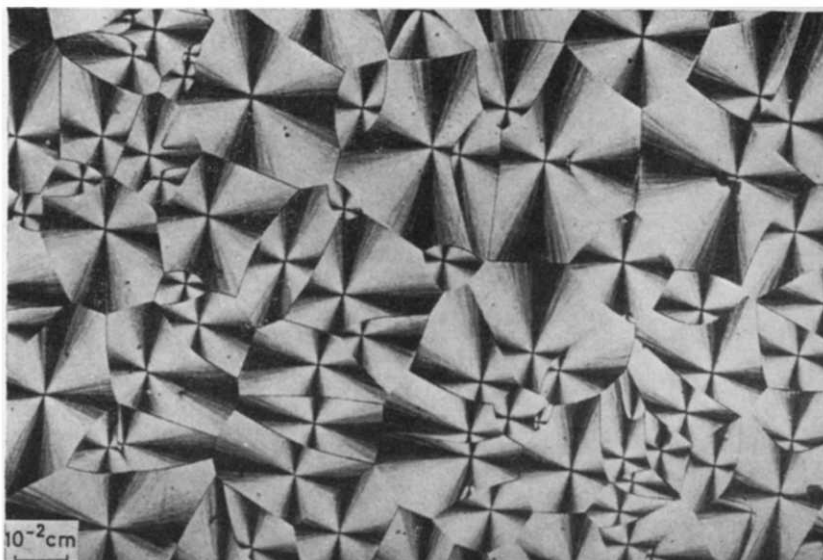


Figure 3—Ziegler type Hostalen heated on open cover slips for *ca.* 10 sec at 380°C, pressed with second cover slip to form film *ca.* 5 $\mu$  thick, and crystallized rapidly by cooling at room temperature

experiments carried out on samples degraded in various ways, and to varying extents, in bulk. None of these products yielded spherulites on subsequent melting and crystallization, either in the bulk or in thin films, provided that the melting temperature did not exceed 300°C. Also, several spherulitic samples were obtained by these special treatments with optical melting points identical to those for the untreated material. Melting point, of course, is not a sensitive test for degradation, and the possibility cannot be excluded in such cases that slight oxidative modification, including a decrease in chain length, was present. Extensive degradation, however, is excluded as a possible explanation. Secondly, there is the possibility that the glass surface is responsible for producing a high nucleation density, and that the treatments in some way modify this surface. Samples crystallized between mica and also between gold-plated glass slides, however, excluded this possibility. Thirdly, filterable heterogeneities can be excluded as a possibility, as it was found that filtration through a number 5 porosity sintered glass filter had no effect on the results.

Finally, the persistence of nuclei in the molten polymer has been suggested on several occasions<sup>8, 12</sup>, unless high temperatures are used to destroy them. With polyethylene, it was in fact found that identical results for the crystallization process could be obtained both microscopically and dilatometrically<sup>6</sup>, for superheatings of as little as 0.1°C and as large as 70°C. As is mentioned above, microscopically observed nucleation and growth rates remain unchanged for temperatures of melting as high as 300°C. (Melting points for polyethylene vary between 105° and 138°C depending

on the sample.) Thus, persistence of nuclei above the melting point does not occur in polyethylene.

Much of the evidence given above suggests that the appearance of resolvable spherulites in polyethylene is determined primarily by physical factors, rather than by extensive chemical modification of the material. This is confirmed by the following observations. If a sample is treated to produce a spherulitic film enclosed between two glass cover slips, and if one of the cover slips is removed, progressive melting and crystallization tends to cause the sample to revert to the unresolvable form. If the initially spherulitic sample is removed completely from the cover slips, either by dissolving or, more simply, by mechanical scraping, the product after melting (at up to 300°C) and crystallizing now gives a completely unresolvable structure, similar to that for the untreated material.

Some recent work by Palmer and his associates<sup>13</sup> has suggested that the explanation for these phenomena is as follows. Adhesion of the molten polymer to the glass (or mica or gold) surface, followed by differential shrinkage of the two materials, is capable of inducing large strains in the film, provided that it is sufficiently thin, and provided also that the temperature range over which shrinkage occurs is sufficiently great. Slight oxidation of the material at high temperatures may also be necessary to enhance adhesion. The strain thus caused is then assumed to be capable of modifying the normal nucleation density, usually to result in a decrease. This extremely plausible suggestion would appear to account for all the observations made in the present study. However, whether or not this explanation is correct, there would seem to be no doubt that the formation of resolvable spherulites in thin films is a phenomenon which is not representative of the crystallization behaviour in bulk polyethylene samples, and so a quantitative comparison of microscopically and dilatometrically determined rate constants is not justifiable. Studies in these laboratories on other polymers, including poly-(decamethylene terephthalate)<sup>5</sup>, nylon 6.6, poly-(trichlorofluoromethane), poly-(ethylene oxide), poly-(propylene), and poly-(oxymethylene), suggest that this effect is a widespread one but not necessarily universal. For this reason it is considered that any microscopic observations made on polymers in thin film form require to be treated with considerable caution.

### *Quantitative data*

Results for nucleation and growth were obtained for a number of specially prepared spherulitic samples and were found always to follow the same general pattern. The data given in this section are thus typical, and were obtained for a sample of fraction 3 which yielded regions of low nucleation density without special treatment. The absence of any special treatment other than the use of the sample in thin film form makes it reasonable to assume that degradation had not occurred. It must be stressed, however, that measurements could only be made on specially selected areas where the nucleation density was sufficiently low to yield resolvable spherulites of adequate size. It does not follow that the ensuing quantitative data for these arbitrarily chosen regions are necessarily relevant to the bulk material.

(a) *Nucleation*—It has previously been suggested<sup>14</sup> that nuclei in high polymers generally stem from heterogeneities; the indications are that this is certainly so for polyethylene. In *Figure 4* typical nucleation plots show

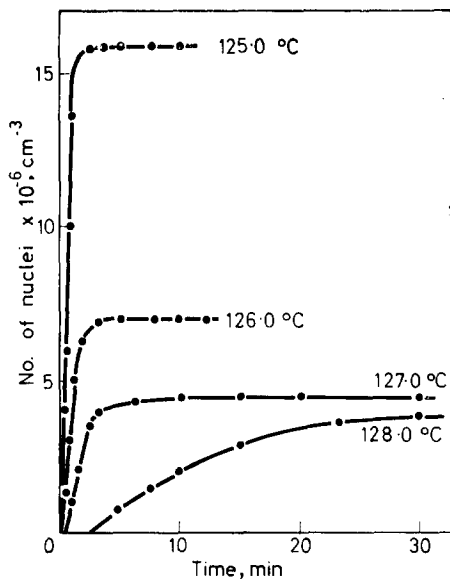


*Figure 4*—Nucleation plots for fraction 3 in thin film form, after melting at 200°C for 20 minutes

that for a given temperature of crystallization, a limit is reached to the number of nuclei formed. (The apparent induction period is considered to be due to the fact that a nucleus is required to reach a given size before it becomes visible.) The shape of the curves is not inconsistent with a first order equation of the form

$$dX/dt = N(X_{\infty} - X)/X_{\infty} \quad (3)$$

where  $X$  is the number of nuclei at time  $t$ , and  $N$  is the nucleation rate constant, but accurate verification of this point is not possible owing to the arbitrary nature of the induction period. If equation (3) is applicable, however, it approximates to the case of sporadic nucleation

$$X = Nt \quad (4)$$

where  $X$  is small compared with the limiting value,  $X_{\infty}$ . It is thus likely that sporadic and predetermined nucleation<sup>2</sup> are in fact limiting cases of the more general situation typified by equation (3) and *Figure 4*, arising when the half-life of the overall crystallization process is small or large, respectively, compared with the time taken to reach the limit,  $X_{\infty}$ .

The existence of a limit to the number of nuclei formed at a given temperature in itself suggests that heterogeneities are involved, and confirmation of this point was obtained by recording the positions of the nuclei photographically, when it was found that they appeared in identical positions in successive experiments.

The important question to be answered is whether the form of the

nucleation plots (*Figure 4*) can explain the fractional values of  $n$  obtained from dilatometry. In general, an equation of the form

$$X = Nt^m \quad (5)$$

where  $m$  is a constant between 0 and 1, would lead to a fractional and constant value for the Avrami exponent, and such a relation might be approximated to by equation (3) over a very limited part of the plot. However, in view of the fact that fractional and constant values of  $n$  can be obtained dilatometrically for a wide range of crystallization conditions and in some cases<sup>5</sup> for at least 95 per cent of the process, this explanation would not seem to be a likely one.

Whether the nucleation in the bulk sample approximates to the sporadic or to the predetermined case cannot unfortunately be decided directly, owing to the arbitrary nature of the observed nucleation plots. However, the maximum value of  $n$  observed for polyethylene in Part I<sup>3</sup> was found to be 4.0, and deviations from this value occurred without discontinuity with changing molecular weight and temperature of crystallization. This suggests that sporadic nucleation and spherulitic growth are in general operative, and that some complicating factor intervenes progressively to decrease  $n$  from its expected value of 4. One fraction, 5908, of low molecular weight was exceptional in that it did in fact show a decrease in  $n$  of approximately one unit during the course of crystallization, indicating that the change from sporadic to predetermined nucleation occurred during the course of the bulk crystallization. The dilatometrically determined results are given in *Figure 5* as a plot of  $n$  versus extent of crystallization.

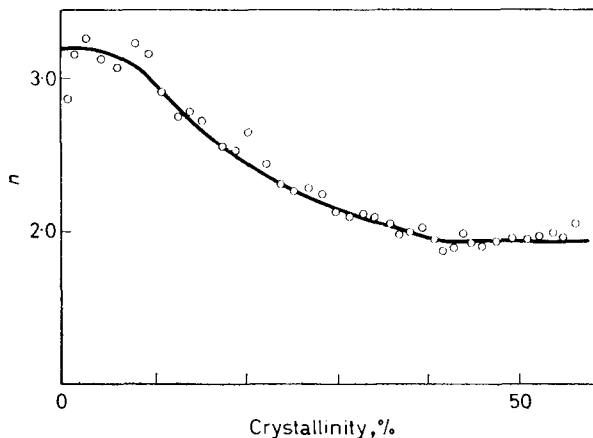
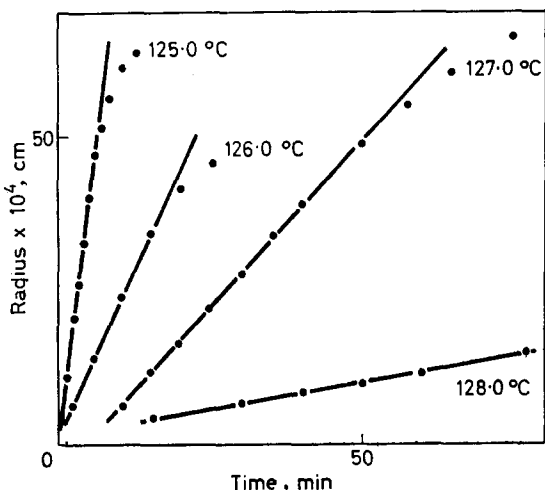


*Figure 5*—Dilatometrically determined values of the Avrami exponent,  $n$ , obtained for the crystallization of fraction 5908 at 125.77°C

(b) *Growth*—Radial growth plots of spherulites for fraction 3 are given in *Figure 6*. In the introduction it was noted that an implicit assumption in the Avrami equation as previously applied, is that the radius of the growing

spherulite should be directly proportional to the time. Previous observations have tended to confirm this point<sup>15</sup>. The results in *Figure 6* conform to a linear relation for the major part of the growth, but significant deviations are apparent just before the spherulites touch. Price *et al.*<sup>16</sup> have noticed

*Figure 6*—Radial growth plots for spherulites from fraction 3 prepared in thin film form, after melting at 200°C for 20 minutes. Growth is followed until the spherulites touch, except for the results at 128.0°C



a similar phenomenon in polyethylene oxide, and have ascribed the decrease in rate to a rise in temperature resulting from the crystallization process. It is most unlikely, however, that this effect would account for the anomalous dilatometry results, as in the latter case deviations from integral values of  $n$  occur at the start of the crystallization and are present throughout. The

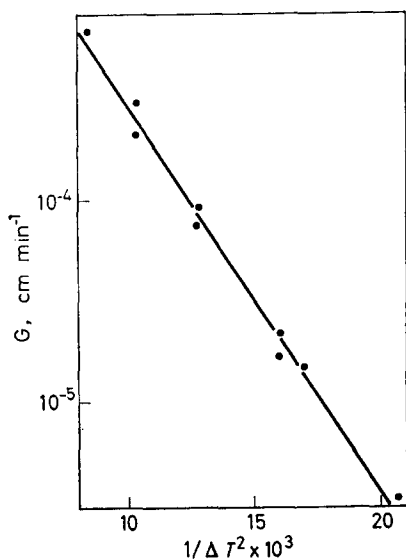


*Figure 7*—Temperature dependence of the growth rate for fraction 3



spherulites growth plots on the other hand are of the required linear form for the major part of the process.

The growth rates derived from *Figure 6* and from similar experiments are plotted in *Figure 7* according to the expected temperature dependence equation<sup>2,3</sup>

$$\log G = A_2 - B_2/\Delta T^2$$

where  $A_2$  and  $B_2$  are effectively constant over the temperature range considered, and  $\Delta T$  is the difference between the melting point (135.9°C in this case<sup>3</sup>) and the crystallization temperature. The slope of the plot,  $B_2$ , is 190, in reasonable agreement with the value of 200 found dilatometrically.

#### DISCUSSION

The deviations which have been observed above in the nucleation and growth plots for polyethylene, are potentially capable of affecting the dilatometrically observed behaviour. Unfortunately, owing to the spuriously low nucleation densities necessarily present in those samples which could be observed microscopically, it is impossible to predict the extent to which these deviations might be present in the bulk crystallization process. It does seem unlikely, however, for the reasons given above, that they are able to account for the anomalous fractional values of the Avrami exponent,  $n$ , observed in Part I<sup>3</sup>.

Two possibilities remain. The first is that the growth of spherulites is not directly related to the formation of crystallinity, in which case microscopic observations are irrelevant to any anomalies in the dilatometrically observed crystallization behaviour. This has previously been suggested by several authors<sup>12, 17, 18</sup>, but has been discounted for polyethylene terephthalate as a result of microbeam X-ray measurements on partly spherulitic samples<sup>19</sup>. An alternative approach is to compare dilatometric and microscopic rate constants, but this is of course excluded for polyethylene owing to the arbitrary nature of the values for nucleation density. Polymers which do produce spherulites readily in the bulk [e.g. polypropylene and poly-(ethylene oxide)] have been studied from this point of view<sup>20</sup>, but in these cases another difficulty arises. With poly-(ethylene oxide), for example, well-defined spherulites can readily be observed in the bulk, grown from instantaneously formed nuclei. The expected value of  $n$  from dilatometric observations is thus 3.0, but the experimentally determined value<sup>21</sup> is in fact 2.0. As some unknown factor must be operative in causing  $n$  to deviate from its expected value, theoretical equations similar to equation (2) cannot be used to compare microscopy and dilatometry data. What can be done is to compare the time scales over which crystallinity and spherulitic structure develop, and with poly-(ethylene oxide) and polypropylene it has been established<sup>20</sup> that the half-lives for the two processes are very similar. For example<sup>20</sup>, for a polypropylene sample crystallizing at 135.9°C, the dilatometric half-life was 62 minutes and that for spherulite growth was 56 minutes. Thus although the coincident development of crystallinity and spherulitic structure in these cases is not incontrovertibly established, the weight of evidence makes it seem very likely. Additional support arises for polyethylene, in

that when spherulitic growth is observed, the temperature coefficient of the process is the same as that for the bulk crystallization (see previous section).

The only possibility remaining is that the density of the growing spherulites is not constant with time. The form of the spherulites during growth is often very fragmented, and in extreme cases may take on the dendritic appearance shown in *Figure 8*. Growth by branching of radiating

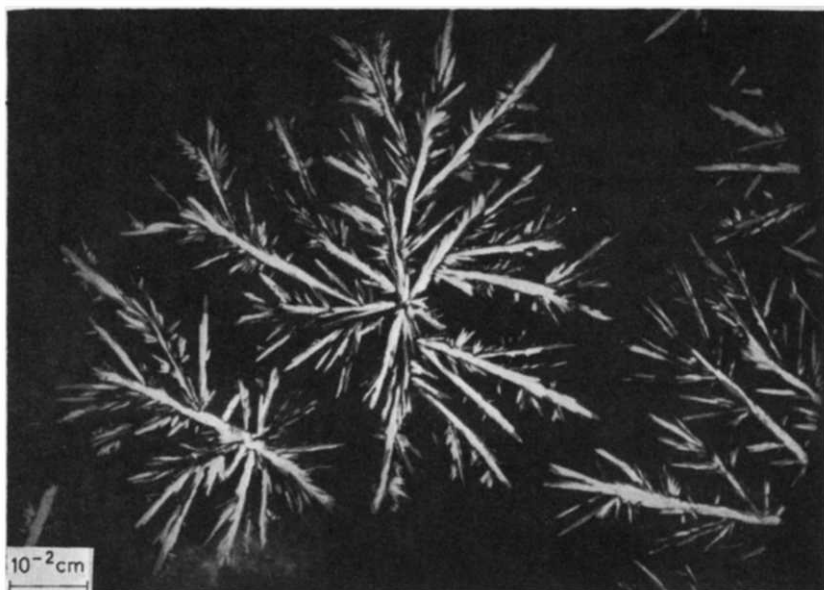


*Figure 8*—Fraction 5908 heated *in vacuo* for two hours at 300°C, in thin film form. Crystallized at 119°C for 18 hours

fibrils is a process which would account for spherulitic development in general, and if this is so it is reasonable to expect that the nature of the packing of these branches would vary at different points along the radius. Variation in spherulite density with time of growth is thus likely to occur, and has been previously suggested for a polyurethane<sup>4</sup>. What is difficult to understand, however, is why this variation should take such a form as to decrease the Avrami exponent from its expected value, and also to maintain it *constant* throughout the course of the crystallization. The density/time relation required to achieve such an effect is extremely complicated and has no obvious relation to any picture of branched spherulitic structure.

The important point, however, is that some additional factor frequently arises in polymer crystallization to complicate the kinetics and so as a result it is not justifiable to use the derived Avrami exponent, *n*, diagnostically in order to make predictions about crystallization mechanism.

*The authors gratefully acknowledge the support of the British Petroleum Company Ltd for part of this work.*

Arthur D. Little Research Institute,  
Inveresk, Musselburgh, Midlothian

(Received March 1963)

## THE CRYSTALLIZATION OF POLYETHYLENE II

---

### REFERENCES

- <sup>1</sup> MORGAN, L. B. *Phil. Trans.* 1954, **247**, 13
- <sup>2</sup> MANDELKERN, L. *Growth and Perfection of Crystals*. Chapman and Hall, London, 1958
- <sup>3</sup> BANKS, W., GORDON, M., ROE, R.-J. and SHARPLES, A. *Polymer, Lond.* 1963, **4**, 61
- <sup>4</sup> ROHLEDER, J. and STUART, H. A. *Makromol. Chem.* 1961, **41**, 110
- <sup>5</sup> SHARPLES, A. and SWINTON, F. L. *Polymer, Lond.* 1963, **4**, 119
- <sup>6</sup> BANKS, W., GORDON, M. and SHARPLES, A. *Polymer, Lond.* 1963, **4**, 289
- <sup>7</sup> BANKS, W., HAY, J. N., SHARPLES, A. and THOMPSON, G. *Nature, Lond.* 1962, **194**, 542
- <sup>8</sup> HARTLEY, F. D., LORD, F. W. and MORGAN, L. B. *Phil. Trans.* 1954, **247**, 23
- <sup>9</sup> BUNN, C. W. and ALCOCK, T. C. *Trans. Faraday Soc.* 1945, **41**, 317
- <sup>10</sup> PRICE, F. P. *J. Polym. Sci.* 1959, **37**, 71
- <sup>11</sup> OHLBERG, S. M., ROTH, J. and RAFF, R. A. V. *J. appl. Polym. Sci.* 1959, **1**, 114
- <sup>12</sup> PRICE, F. P. *J. Amer. chem. Soc.* 1952, **74**, 311
- <sup>13</sup> PALMER, R. P. Private communication
- <sup>14</sup> SHARPLES, A. *Polymer, Lond.* 1962, **3**, 250
- <sup>15</sup> KENYON, A. S., GROSS, R. C. and WURSTNER, A. L. *J. Polym. Sci.* 1959, **40**, 159
- <sup>16</sup> BARNES, W. J., LUETZEL, W. G. and PRICE, F. P. *J. phys. Chem.* 1961, **65**, 1742
- <sup>17</sup> BRENSCHEDE, W. *Kolloidzshr.* 1949, **114**, 35
- <sup>18</sup> RICHARDS, R. B. and HAWKINS, S. W. *J. Polym. Sci.* 1949, **4**, 515
- <sup>19</sup> KELLER, A. *J. Polym. Sci.* 1955, **17**, 291
- <sup>20</sup> BANKS, W. and SHARPLES, A. Unpublished results
- <sup>21</sup> BANKS, W. and SHARPLES, A. *Makromol. Chem.* 1963, **59**, 233

# *Description and Calibration of an Elasto-osmometer*

H. J. M. A. MIERAS and W. PRINS

*An elasto-osmometer is described in which a stretched and swollen strip of crosslinked silicone rubber serves as indicator. The change in retractive force which occurs when the solvent around the strip is replaced by a solution containing a polymeric solute, which does not penetrate into the strip, is inversely proportional to the number average molecular weight of the solute. The instrument can be operated at elevated ( $\sim 90^\circ\text{C}$ ) as well as at room temperature and can yield two or three molecular weights in a working day. Although calibration by means of a sample of known molecular weight is the best operating procedure, it is also possible to put elasto-osmometry on an absolute basis. To this end the network parameters of the swollen silicone strip have to be determined. Examples of both procedures are given for a number of samples of polystyrene and polyethylene, ranging from 2 000 to 14 000 in molecular weight. The theory indicates that with isotropic silicone rubber strips molecular weights up to at least 40 000 should be attainable. The instrument yields erroneous results at molecular weights below 5 000 because of penetration of solute into the swollen strip.*

THE determination of number average molecular weights ( $\bar{M}_n$ ) below roughly 30 000 poses a problem for regular osmometry because of leakage of the solute through the membrane. In the search for suitable alternatives, techniques like cryometry, ebulliometry and vapour pressure lowering have been considerably refined and are in widespread use. Recently<sup>1</sup> it has been demonstrated that one can turn also to a new technique, called 'elasto-osmometry'. This method makes use of the observation that the elastic properties of a gel in equilibrium swelling with a diluent, change when one introduces in the surrounding diluent phase a solute which does not penetrate into the gel phase. From thermodynamics it follows that the lowering of the diluent activity outside the gel will cause a de-swelling of the gel. The de-swelling effect can be measured in several ways, of which the increase in retractive force,  $f - f_0$ , of an elastically deformed gel, strip or filament is preferable from an experimental point of view. It is shown easily<sup>1</sup> that here the quantity  $(f - f_0)/c$  ( $c$  = concentration of polymer in g/ml) at infinite dilution is proportional to  $1/\bar{M}_n$ .

Because the de-swelling is relatively fast (of the order of 10 minutes in our present instrument) and, moreover, constitutes an outward flow of diluent from the gel into the surrounding phase, penetration of low molecular weight solute into the gel occurs to a far less extent than in regular membrane osmometry. Previously published preliminary results<sup>1</sup> have indicated that number average molecular weights in the range of 5 000 to 20 000 can be obtained.

The aim of the present work has been to construct an instrument which could be operated at elevated temperatures (say  $90^\circ\text{C}$  for polyethylene determinations) as well as at room temperature, and which would be fast

and convenient in daily use. With this instrument a series of seven polystyrene samples and one low molecular weight fraction of polyethylene were measured. The polystyrenes were prepared by the Szwarc technique of anionic polymerization<sup>2</sup> and varied in molecular weight from 3 000 to 15 000, as estimated on the basis of existing intrinsic viscosity relations<sup>3</sup>. Calibration was performed by determining the molecular weights of five of the polystyrene samples independently in a thermoelectric vapour phase osmometer<sup>4</sup>. In daily practice it is convenient to use one standard sample as reference throughout.

In principle, elasto-osmometry can also be put on an absolute basis if the activity of the diluent in the gel strip is known. To this end modulus and equilibrium swelling of the strip have to be determined experimentally and existing theories for swollen polymer networks have to be utilized. We will demonstrate the feasibility of this procedure, although it should be said at once that it does not constitute a very practical and accurate way of conducting elasto-osmometry. An advantage is that on the basis of such considerations it is possible to indicate in which way the range of the instrument can be extended to higher molecular weights.

#### THE ELASTO-OSMOMETER

*Figure 1* shows a diagram of the essential components of the elasto-osmometer. The centre glass vessel holds a strip of gel, which in our case consisted of a swollen polydimethylsiloxane strip of 2 to 4 cm length,

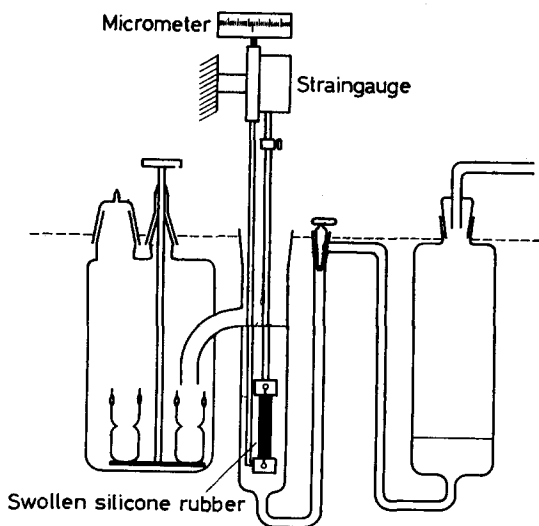


*Figure 1*—Diagram of the elasto-osmometer

0.5 cm width and 0.05 cm thickness. The strip was crosslinked by electron beam irradiation<sup>1</sup>. In toluene the degree of swelling,  $q_1$  (ratio of swollen to dry volume), was about seven. The lower clamp is stationary, the upper one is attached to a strain gauge (model G1-1.5-350, Statham Instruments, 12 401 Olympic Blvd., Los Angeles 64, California), which in turn is

## DESCRIPTION AND CALIBRATION OF AN ELASTO-OSMOMETER

mounted on a micrometer. By means of the micrometer the strip is elongated to a known degree. The theory<sup>1</sup> indicates that the degree of elongation should be kept as low as possible (see also below); we used

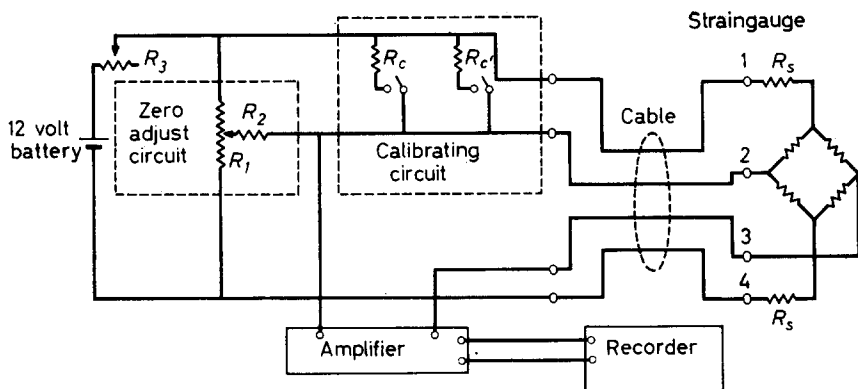


Figure 2—Wiring diagram for the strain gauge.  $R_1=20\text{ k}\Omega$  helipot,  $R_2=33\text{ k}\Omega$ ,  $R_c=100\text{ k}\Omega$ ,  $R_c'=1\text{ M}\Omega$ . The  $100\Omega$  variable resistor  $R_3$  reduces the  $12\text{ V}$  from the battery to the required  $9\text{ V}$  across the input terminals of the strain gauge bridge circuit (1 and 4)

elongations of about 5 to 8 per cent. The output of the strain gauge is measured as indicated in Figure 2, by means of a d.c. amplifier (model 150A, Keithley Instruments, Cleveland 6, Ohio) connected to a  $10\text{ mV}$  recorder (model G-10, Varian Associates, Palo Alto, California). The changes in force,  $f-f_0$ , to be registered are of the order of  $30\text{ mg}$ , which corresponds with about  $20\text{ }\mu\text{V}$  output from the strain gauge. Because of this low force level, the temperature of the strain gauge should not fluctuate by more than  $1^\circ$  or  $2^\circ\text{C}$ . Also, the instrument should be well isolated from mechanical vibrations of the surroundings. In our laboratory this was achieved by placing the instrument on a separately founded pillar in the basement of the building.

Polymer solutions, made up by mixing in the right hand vessel, are pushed into the centre vessel by an excess pressure of nitrogen. A slight excess pressure is maintained throughout the measurement so that the solution is dripping slowly in the left hand vessel. This ensures a constant level of immersion of the clamps holding the strip, which is necessary in order to avoid changes in buoyancy. The change in density of the solution can be neglected. After recording the change in force as a result of the de-swelling, further pressure is applied and a portion of the solution is collected in one of the weighing bottles in the left hand vessel for a precise concentration determination. Four of these weighing bottles are mounted on a revolving glass turret, so that four runs at different concentrations can be done without disturbing the instrument.

All the glass components are completely submerged in a thermostat to avoid precipitation of polymer during manipulation. This is, of course, only required for high temperature runs as for example with polyethylene. For measurements at room temperature it is easier to mount the instrument

outside the thermostat and to provide the measuring cell with a water circulation jacket only.

In a set-up as described above, one can easily carry out two complete concentration-dependent runs plus the required calibration run in one working day.

#### ABSOLUTE ELASTO-OSMOMETRY

The proportionality constant between the measured effect,  $(f-f_0)/c$ , and  $1/\overline{M}_n$  is best established by calibration with one or more samples of known  $\overline{M}_n$ . If, however, one applies current theories for amorphous, swollen, polymer networks, one obtains an equation which can be used for absolute elasto-osmometrical determinations<sup>1</sup>

$$(\partial f/\partial c)_{c \rightarrow 0} = BRT/\overline{M}_n \quad (1)$$

where  $B = \sigma_0 (L_0/L)^2 (q/q_0)^2 [1 + p_e (1 - 2\chi) q^{-1} + p_e (q^{-2} + q^{-3} + \dots)]^{-1}$ . Here  $\sigma_0 = V_0/L_0$  is the cross section in the so-called reference state of the network of volume  $V_0$  and length  $L_0$ , where the degree of swelling,  $q_0$ , is such that the chains are not restrained, i.e. have the same end to end distances as they would have in solution. Besides the degree of swelling under stretch  $q$ , and the length  $L$ , evaluation of  $B$  requires a knowledge of all three network parameters, viz.  $q_0$ ,  $p_e$  and  $\chi$ ;  $q_0$  we have already defined;  $p_e$  is the effective chain length between crosslinks, as measured in number of solvent sites;  $\chi$  is the Huggins polymer-solvent interaction parameter.

These parameters can be determined experimentally as follows. We obtain  $p_e$  by measuring the modulus of the dry strip of crosslinked silicone rubber. Since the crosslinking has been performed in the dry state at the same temperature, the chains are presumably in the unstrained reference state prior to the stretching experiment. Under these conditions we have from rubber elasticity theory:

$$f = \nu_e (RT/L_d) (L/L_d - L_d^2/L^2); \quad (\partial f/\partial L)_{L \rightarrow L_d} = 3\nu_e RT/L_d^2 \quad (2)$$

where  $L_d$  denotes dry unstretched length, and  $\nu_e$  is the number of moles of effective chains in the strip. Therefore  $p_e = V_d/\nu_e \bar{v}$  with  $V_d$  as dry volume and  $\bar{v}$ , the molar volume of the solvent (to be employed later). Subsequently we swell the strip in toluene and measure the change in dimensions so that we obtain the unstretched degree of swelling,  $q_1$ . For a swollen network rubber elasticity theory yields the following force-elongation relation<sup>5</sup>

$$f = \nu_e (RT/L_1) (q_1/q_0)^{\dagger} \{ (L/L_1) - (qL_1^2/q_1 L^2) \} \quad (3)$$

where  $L_1$  is the unstretched, swollen length.

To observe the changes in swelling upon stretching requires more refined experimental techniques than were used in the present work. According to theory, the relation  $q = q_1 (L/L_1)^{\dagger}$  should hold at sufficiently high degrees

of swelling<sup>5</sup>. Inserting this we have from equation (3)

$$(\partial f / \partial L)_{L \rightarrow L_1} = 2.5 \nu_e RT (q_1 / q_0)^3 / L_1^2 \quad (4)$$

so that we obtain  $q_0$  (in toluene) since  $\nu_e$  is already known. With  $p_e$  and  $q_0$  known,  $\chi$  follows from the condition of equality of thermodynamic potential of the solvent inside and outside the strip. Writing this down for the unstretched strip, we have<sup>5</sup>

$$0 = \ln(1 - q_1^{-1}) + q_1^{-1} + \chi q_1^{-2} + (1/p_e)(q_0^{-3} q_1^{-1} - q_1^{-1}) \quad (5)$$

The dimensions  $\sigma_0$  and  $L_0$  in the reference state can be calculated from the dry dimensions  $\sigma_a$  and  $L_a$  by multiplication with  $q_0^\dagger$  and  $q_0^\ddagger$  respectively. This assumes that the unstrained network is isotropic.

In this way the constant  $B$  can be completely determined. In the next section we will compare  $\overline{M}_n$  values obtained through this absolute procedure with  $\overline{M}_n$  values obtained through the regular calibration procedure.

#### RESULTS

Figure 3 shows the change in force  $f - f_0$  as a function of concentration for two of the polystyrene samples (PS-31 and PS-39, see Table I) in toluene. The changes in force take about ten minutes to reach their final values,

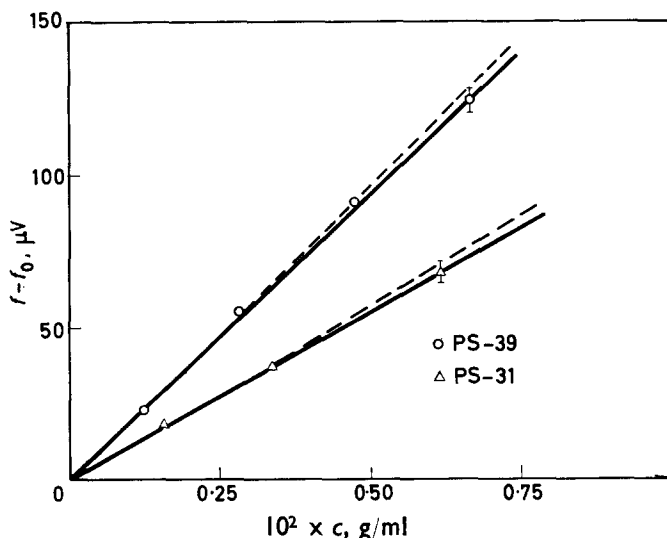
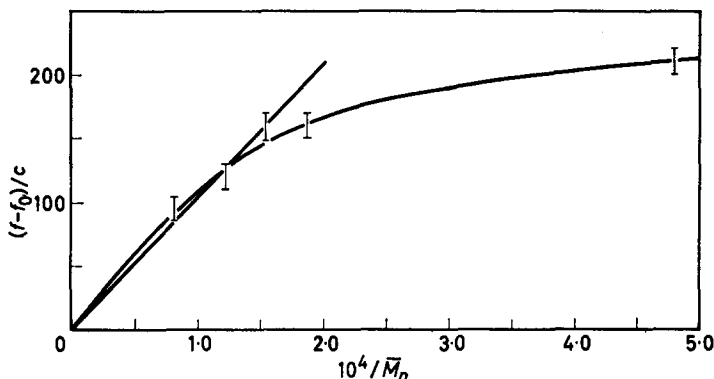


Figure 3—The change in force,  $f - f_0$  (measured in  $\mu\text{V}$ ), as a result of de-swelling the silicone rubber strip with increasing concentrations of polystyrene in toluene

which then remain constant during the time of observation (about an hour). In none of our experiments did any deviation from linear concentration dependence show up. This should not be construed to mean that the second virial coefficient is zero, but simply that it is too small to be observed by this method. The dashed lines in Figure 3 show the effect the second virial



coefficients would have for the PS-31 and PS-39 samples in toluene as calculated from the literature<sup>6</sup>. *Figure 4* shows the  $(f-f_0)/c$  effects for five polystyrene samples plotted versus  $1/\bar{M}_n$  as determined independently. The independent method involved measuring lowering of the vapour pressure of polystyrene solutions in a so-called thermoelectric vapour phase osmometer. In this instrument one places a drop of solution on one junction of a thermocouple and a drop of solvent on the other junction. Exposed to the saturated vapour of the pure solvent, condensation of solvent will occur on the solution drop because of its lower vapour pressure. As a result this junction will warm up slightly compared with the solvent junction. The resulting e.m.f. is measured on a sensitive galvanometer. Osmometers of this type are commercially available or can be constructed in the laboratory. In the latter case they are quite inexpensive and function well up to  $\bar{M}_n$  30 000 in organic solvents. They are, however, a little hard to operate reliably at elevated temperatures ( $\sim 90^\circ\text{C}$ ). A full description of our instrument can be found in the literature<sup>4</sup>.



*Figure 4*—The reduced force change,  $(f-f_0)/c$ , for a series of polystyrene samples in toluene, measured in the elasto-osmometer, plotted versus  $1/\bar{M}_n$ , obtained independently by means of thermoelectric vapour phase osmometry

*Figure 4* demonstrates the feasibility of elasto-osmometry for molecular weights above 5 000. At lower molecular weights the proportionality between  $(f-f_0)/c$  and  $1/\bar{M}_n$  breaks down. Since all points in *Figure 4* have been determined several times, the error limits on the points are quite certain. The breakdown of the proportionality must therefore indicate that penetration of the solute into the gel strip occurs. This penetration must occur while the toluene is being gradually displaced by the polymer solution and ten minutes thereafter, because no further change is observed in the force reading over a period of about one hour. Because the extent of penetration will in general depend on the polydispersity of a sample, the elasto-osmometer will yield uncertain results for samples of unknown  $\bar{M}_n$  even if a complete calibration graph such as that given in *Figure 4* is available. Moreover, the calibration graph depends on the particular strip used, on the temperature and on the degree of elongation (see equation 1),

## DESCRIPTION AND CALIBRATION OF AN ELASTO-OSMOMETER

Since the strip sometimes has to be replaced, or slips out of the clamps and cannot be refastened in a reproducible way, a more convenient procedure is to measure one calibration sample at the start and finish of each series of unknown samples every day and to make use of the proportionality between  $(f-f_0)/c$  and  $1/\bar{M}_n$ . This procedure was followed for the combined data in *Table 1* with sample PS-2 ( $\bar{M}_n=6\,480$ ) as reference. Because of the penetration effect this procedure will of course yield  $\bar{M}_n$  values which are too high for samples of molecular weight lower than 5 000.

*Table 1.* Elasto-osmometry by calibration with respect to sample PS-2

Sample*	26°C		86°C		$\bar{M}_n$ ( $\pm$ standard deviations) by thermoelectric vapour phase osmometry
	$(f-f_0)/c$ arb. units	$\bar{M}_n$	$(f-f_0)/c$ arb. units	$\bar{M}_n$	
PS-43	210 $\pm$ 10	(4 900)	160 $\pm$ 10	5 250	2 080 $\pm$ 0.8%
PS-1	190	(5 500)	—	—	—
PS-39	160	6 500	—	—	5 300 $\pm$ 1.4%
PS-34	160	6 500	120	7 000	—
PS-40	120	8 650	95	8 900	8 170 $\pm$ 1.4%
PS-31	95	11 000	75	11 200	14 000 $\pm$ 7.2%
PE-1	—	—	205	(4 100)	—
PS-2	160	—	130	—	6 480 $\pm$ 1.5%

\*PS denotes polystyrene, PE polyethylene.

*Table 2.* Absolute elasto-osmometry

Character	Strip I at 26°C	Strip II at 86°C
Dry length, $L_d$ (cm)	0.98 $\pm$ 0.02	1.85 $\pm$ 0.02
Dry modulus $(\partial f/\partial L)_{L \rightarrow L_d}$ (dynes/cm)	13 160 $\pm$ 250	9 280 $\pm$ 100
Chain length between crosslinks, $p_c$ (equation 2)	430 $\pm$ 80	265 $\pm$ 50
Unstretched swollen length, $L_1$ (cm)	2.17 $\pm$ 0.02	3.99 $\pm$ 0.02
Stretched swollen length, $L$ (cm)	2.33 $\pm$ 0.02	4.18 $\pm$ 0.02
Degree of swelling, $q$ ( $\approx q_1$ )	7.1 $\pm$ 0.5	7.5 $\pm$ 0.5
'Swollen' modulus $(\partial f/\partial L)_{L \rightarrow L_1}$ (dynes/cm)	7 185 $\pm$ 150	6 220 $\pm$ 100
Degree of swelling at reference state $q_0$ (equation 4)	1.2 $\pm$ 0.2	1.36 $\pm$ 0.2
Huggins interaction parameter $\chi$ (equation 5)	0.455	0.425
Dry cross section $\sigma_d$ (cm <sup>2</sup> )	0.0081 $\pm$ 0.012	0.0066 $\pm$ 0.012
Measured effect $(\partial f/\partial c)_{c \rightarrow 0}$ (dynes ml/g)	14 500 $\pm$ 1 000	20 000 $\pm$ 2 000
$\bar{M}_n$ —calculated	5 000 $\pm$ 2 000	6 000 $\pm$ 2 000
$\bar{M}_n$ —by calibration	6 480 $\pm$ 100	6 480 $\pm$ 100

Sample PS-2 was also used for a test of the feasibility of absolute elasto-osmometry. In *Table 2* we have collected the data on two different gel strips of silicone rubber at two temperatures. From these data the constant  $B$  of equation (1) can in each case be calculated. In the table we have directly listed the  $\bar{M}_n$  values calculated with the help of these data.

Although the possible experimental errors are large, quite reasonable values for  $\overline{M}_n$  are obtained. If necessary the accuracy of the network characterization could be increased by the use of more refined techniques of, for example, measuring the degrees of swelling  $q$  and  $q_1$ . In view of the work involved in characterizing the gel strip, however, and an always remaining uncertainty as to the applicability of network theory, the calibration method seems to be preferable in general.

#### CONCLUSIONS

The instrument described and the measurements performed with it at 26°C and 86°C provide conclusive evidence that elasto-osmometry can be an interesting alternative to other osmometric techniques. Its main advantages are ease of operation even at high temperatures and the relative rapidity with which determinations can be carried out. A drawback is that molecular weights below 5 000 cannot be reliably obtained, although an estimate can be made through the use of a calibration graph (*Figure 4*). The theory used for the evaluation of  $\overline{M}_n$  values without calibration (*Table 2*) can also be used to estimate how the range of the instrument can be extended to higher  $\overline{M}_n$  values. Equation (1) indicates that the measured effect,  $\partial f/\partial c$  or  $(f-f_0)/c$ , will be smaller the higher the degree of elongation. Thus it is profitable to work at the lowest degree of elongation experimentally feasible. This will usually be a few per cent, i.e. sufficient to overcome any slack that may occur. The sensitivity of the elasto-osmometer will be increased if we use a gel strip of low  $q_0$  but large  $q$ , and much more markedly, if the cross section ( $\sim \sigma_0$ ) of the strip is increased. If the de-swelling is a diffusion controlled process, a twofold increase of the cross section will increase the time for the establishment of the new swelling equilibrium by a factor of four. In order to circumvent this cumbersome increase in equilibration time, one could also effectively increase the observed  $f-f_0$  by mounting two or more thin strips parallel to each other. It seems safe to state that in this way the range of the instrument can be boosted from about 20 000 with 10 per cent accuracy to at least 40 000 with 10 per cent accuracy. Further work to substantiate these claims is under way. Also to be investigated is the effect which the use of highly oriented and/or partially crystalline gel strips has on the  $\overline{M}_n$  range which can be covered.

*The authors express their gratitude to Mr Y. Y. Tan of the Kunststoffeninstituut T.N.O., Delft, The Netherlands, who prepared most of the low molecular weight polystyrene samples; to the Central Laboratory of the State Mines, at Geleen, Netherlands, which provided the polyethylene sample, and to Mr J. van Dam, who performed the  $\overline{M}_n$  calibration by means of thermoelectric vapour phase osmometry.*

Laboratory of Physical Chemistry,  
Technische Hogeschool,  
Delft, The Netherlands

(Received March 1963)

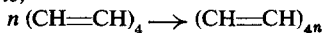
REFERENCES

- <sup>1</sup> YAMADA, S., PRINS, W. and HERMANS, J. J. *J. Polym. Sci.* 1963, **A1**, 2335  
HERMANS, J. J. in *New Methods in Polymer Chemistry*, Interscience: New York, 1963
- <sup>2</sup> SZWARC, M. *Nature, Lond.* 1956, **178**, 168
- <sup>3</sup> MISRA, G. S., RASTOGI, R. C. and GUPTA, V. P. *Makromol. Chem.* 1961, **50**, 72  
BAMFORD, C. H. and DEWAR, M. J. S. *Proc. Roy. Soc. A*, 1948, **192**, 329  
PEPPER, D. C. *J. Polym. Sci.* 1951, **7**, 347
- <sup>4</sup> For a description see:  
VAN DAM, J. and PRINS, W. in *Methods of Carbohydrate Chemistry*. Ed. M. L. WOLFROM, and R. L. WHISTLER, Vol. V. Academic Press: New York, 1964; to appear; or  
VAN DAM, J. *Rec. Trav. chim. Pays-Bas*, 1964, in press
- <sup>5</sup> HERMANS, J. J. *Trans. Faraday Soc.* 1947, **43**, 591 *J. Polym. Sci.* 1962, **59**, 204
- <sup>6</sup> BAWN, C., FREEMAN, R. and KAMALIDDIN, A. *Trans. Faraday Soc* 1950, **46**, 862  
SCHULZ, G. V. and MARZOLPH, M. Z. *Elektrochem.* 1954, **58**, 217

# Resonance-induced Polymerizations

R. J. ORR

The degree of resonance stabilization of a monomer or a polymer may affect the free energy change during polymerization. In some instances, resonance may be entirely responsible for the free energy change in polymerization. Such polymerizations can be considered to be resonance-induced polymerizations. Examples are to be found in some polymerizations of ring compounds by rupture of the ring. For example, calculations on the hypothetical polymerization of cyclo-octatetraene,



show  $-\Delta H_{00}^\circ$  and  $-\Delta S_{00}^\circ$  to be 40 kcal and 24 e.u./mole respectively at 25°C. Resonance factors are responsible for polymerization of partially conjugated systems, such as cyclo-octatriene, and of inorganic compounds, such as phosphonitrilic chlorides.

IN THOSE addition polymerizations where there is an entropy decrease during reaction\*, there must also be an enthalpy decrease, i.e. the reaction must be exothermic. Two origins of the necessary enthalpy change have been recognized: (a) breaking a multiple bond<sup>1</sup>, and (b) opening a ring under strain<sup>2-4</sup>.

This paper will describe another origin for the required enthalpy change—resonance energy. Resonance in either the monomer or the polymer can be responsible for the decrease in enthalpy. Under such conditions, the reaction may be termed a resonance-induced polymerization. By examination of this principle, at least two goals may be attained.

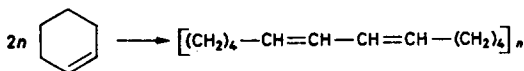
(1) A number of hypothetical reactions may be analysed to determine if they are, or are not, thermodynamically possible. Such a procedure identifies those reactions where a search for a catalyst may be fruitful and exposes those situations where such a search will definitely fail. However, the fact of thermodynamic possibility does not guarantee a catalyst can be found.

(2) Greater insight is gained into certain high temperature decompositions where the polymer decomposes into ring compounds. A better definition of the factors limiting the high temperature performance of such polymers may result.

## THEORETICAL

### *A simple example of resonance-induced polymerization*

An understanding of the principle involved should result by consideration of the hypothetical head-to-head addition of cyclohexane, according to the equation



\*Not all addition polymerizations show such an entropy decrease. Polymerization of sulphur does not.

The replacement of the isolated double bond by the conjugated system results in resonance in the polymer which was not present in the monomer. If the resonance energy of this system is similar to butadiene—3.5 kcal/[CH=CH—CH=CH] unit<sup>5</sup>—then  $-\Delta H_{oo}^0$  of the polymerization would be 1.8 kcal/mole of cyclohexane. While the ceiling temperature of such a polymerization will be low, there should be some temperature below which the polymerization would be thermodynamically possible.

#### *Polymerization of monomers with triple bonds*

Resonance phenomena can be involved in polymerization of compounds with triple bonds in two ways: (1) by making the opening of the multiple bond energetically favourable when it would not otherwise be so, and (2) by augmenting an already favourable enthalpy change.

#### *Polymerization of acetylene*

The enthalpy change in polymerization of acetylene can be considered to result from two factors: (a) replacement of the  $n(\text{C}\equiv\text{C})$  bond system by the more stable  $(\text{C}=\text{C})_n$  system, and (b) the resonance energy stabilizing the conjugated  $(\text{C}=\text{C})_n$  configuration.

By determination of the standard heat of formation/[CH=CH] unit in non-conjugated structures, and comparison of this value with the heat of formation of acetylene<sup>5</sup>, it is possible to estimate what the enthalpy change in polymerization of acetylene would be if there were no resonance<sup>1</sup>.  $-\Delta H_{oo}^0$  for the polymerization of acetylene is 36 kcal/mole in the absence of resonance. To obtain  $-\Delta H_{oo}^0$  when the polymer is stabilized by resonance, it is necessary to consider that the resonance energy per CH=CH unit in a linear chain is a function of the number of units that are conjugated. In Table 1 are the resonance energies of compounds of various lengths as calculated by Brown<sup>6</sup>. Resonance energies are expressed in terms of  $\beta$ , the resonance integral, which has a value of 18 kcal.

Table 1. Dependence of resonance energy on chain length

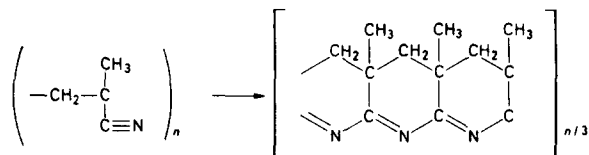
Compound	Resonance energy	Resonance energy/ CH=CH unit
Butadiene	0.47 $\beta$	0.24 $\beta$
Hexatriene	0.99 $\beta$	0.33 $\beta$
Octatetraene	1.52 $\beta$	0.38 $\beta$
Benzene	2.00 $\beta$	0.67 $\beta$

Brown has also shown that in a linear chain the resonance energy/CH=CH unit increases with chain length continuously until it reaches a limiting value of 0.55  $\beta$ , or 10 kcal/CH=CH unit. Thus  $-\Delta H_{oo}^0$  for polymerization of acetylene to a resonance-stabilized chain would be 46 kcal/mole. So, the exothermicity of the reaction depends on the polymer structure which may vary with polymerization conditions. Natta<sup>7</sup> found that, on the basis of optical evidence, polyacetylenes, obtained when metal-organic catalysts are used, are initially in the non-resonating form. Heating of the polymer was necessary to convert to structures in which resonance

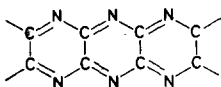
occurred. Presumably the chain, as originally produced, is in a non-planar configuration in which resonance cannot occur<sup>8</sup>. Heating imparts sufficient mobility to the polymer that planarity can be achieved and resonance can occur. The resonance energy therefore exceeds the increase in free energy associated with the less entropy of the molecule in the planar configuration. The change of entropy in polymerization of acetylene may be evaluated by the usual semi-empirical methods<sup>1</sup> from existing thermochemical data<sup>9</sup>, as  $-\Delta S_{gg}^0 = 34.5$  e.u./mole.

#### Polymerization of nitriles

The possibility of polymerizing nitriles can be ascribed entirely to the resonance energy of the resultant polymer. The bond energies of the  $C\equiv N$ ,  $C=N$ , and  $C-N$  groups are simple multiples of each other (in the ratio<sup>9</sup> 3:2:1) so that the opening of these multiple bonds in an addition polymerization will not result in a lower enthalpy and hence addition polymerization will not occur. Only if the resultant polymer is resonance-stabilized will there be an enthalpy change. Resonance can occur in the hetero-atomic systems  $(C=N)_x$  to the same extent as in carbon-containing systems. Calculations<sup>10</sup> have been made indicating *s*-triazine is resonance-stabilized to the same extent as benzene. Thus, in the hypothetical polymerization  $nR-C\equiv N \rightarrow (R-C=N)_n$ ,  $-\Delta H_{gg}^0$  should be 10 kcal/mole. An example of the polymerization of the nitrile group is in the formation of ladder-type structures by the heat treatment of polymethacrylonitrile<sup>11</sup>, according to the following equation



Resonance factors in the polymer must also be responsible for the stability of the polymeric form of paracyanogen.



#### Polymerizability of conjugated ring systems

(a) *Non-aromatic conjugated rings*—Conjugated ring systems may, or may not, be stabilized by resonance energy. Examples are benzene, which is so stabilized, and cyclo-octatetraene, which is not<sup>12</sup>. Any cyclic conjugated compound which is not resonance-stabilized will be polymerizable to polymers which are. Most interesting of these is cyclo-octatetraene. While the type of polymerization envisaged here has not been completely accomplished in practice, cyclo-octatetraene is known to undergo self-condensation to cage-like structures<sup>13</sup> such as

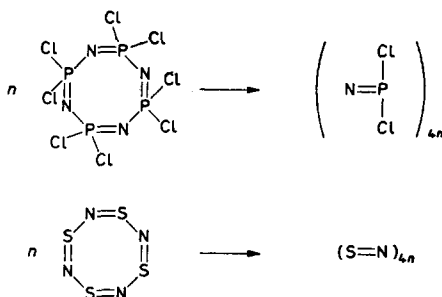


Such structures obviously possess considerable strain energy so that further transformation must be possible, and the above may, therefore, be the first stage in the process.



$-\Delta H_{00}^{\circ}$  for such a reaction would be 40 kcal/mole.  $-\Delta S_{00}^{\circ}$  for the above reaction was found to be 24 e.u./mole at 25°C by the usual semi-empirical methods<sup>1</sup>.

(b) *Inorganic cyclic systems* (i) *Conjugated inorganic rings*—Both the cyclic phosphonitrilic chlorides and sulphur nitrides polymerize to high molecular weight forms<sup>14, 15</sup> according to the reactions :



In both instances the cyclic forms have a hybridized bond structure (i.e. there is only one type of bond in each molecule) and are believed to be resonance-stabilized<sup>15</sup>. While the cyclic phosphonitrilic chloride shown above is in the tetrameric form, other cyclic forms, such as the six-membered trimer, are known and these also polymerize. The fact that polyphosphonitrilic chloride can be decomposed (when pure) into low molecular weight cyclic forms at high temperature<sup>16</sup> indicates that the addition polymerization has a ceiling temperature, and therefore must be exothermic and exo-entropic<sup>1</sup>. This point seems worth emphasizing, since this fact precludes any similarity between these reactions and the polymerization of sulphur, a reaction which has a floor temperature, and must therefore be endothermic and endo-entropic. Paddock<sup>17</sup> reports the phosphonitrilic chloride polymerization is exothermic due to an increase in the P—N bond strength in the polymer\*. Since this must be a result of increased resonance-stabilization of the polymeric form, the reaction may therefore be characterized as resonance-

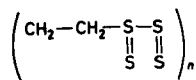
\*A statement by Dewar<sup>19</sup> that the  $\Delta H_f^{\circ}/[\text{NPCl}_2]$  group should be a constant, independent of ring size, does not seem compatible with the fact that phosphonitrilic halides do polymerize, in a reaction which apparently has a ceiling temperature.



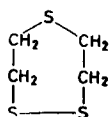
induced. The polymerization of sulphur nitride probably occurs for similar reasons.

Reactions in such inorganic ring systems differ from that of cyclo-octatetraene principally in the extent to which planarity is a pre-requisite for bond hybridization. In organic systems, planarity is essential, while in inorganic systems, where *d* and *f* orbitals may participate, it is not to the same extent. This is demonstrated clearly by the bond hybridization which occurs in the tetrameric form of cyclic phosphonitrilic chloride; even though the ring is non-planar<sup>15</sup>. A conclusion that deviation from planarity does not diminish the degree of resonance-stabilization does not seem warranted. The six-membered trimeric form of phosphonitrilic chloride is known to have a planar form in which the PNP bond angle is 12° less than that in the tetrameric form<sup>17</sup>. This implies that the six-membered ring is under some strain. The molecule could not be expected to tolerate strain, unless there is compensation in the form of resonance-stabilization. In other words, the additional resonance energy made possible by planarity exceeds the amount of strain energy involved. Thus planarity is beneficial to resonance in the nitrogen-phosphorus system, although not as essential as in organic systems.

(ii) *Saturated inorganic rings*—Exothermic addition reactions involving an increase in bond energy on ring opening may also apply to some saturated rings. An example of this is to be noted in the behaviour of Thiokol types of rubber having the formula

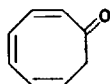


When heated, they tend to decompose<sup>19</sup> into ring compounds of the type

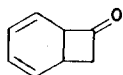


Such material will repolymerize. There is no reason to believe that such rings are under strain. Since they occur when the ceiling temperature of the polymer apparently is exceeded, the polymerization in which they participate may be expected to be exothermic and exo-entropic. The necessary increase in bond energy on ring-opening may probably be attributed to resonance-stabilization of some type in the linear polymer. Analogous behaviour is shown by silicone rubbers<sup>20</sup> which are decomposed by heat into siloxanes.

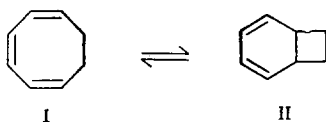
(c) *Partially conjugated rings*—The rapid polymerization of cyclo-octatriene-1,3,5-oxo-7



has been noted<sup>21</sup>. This may proceed through the intermediate



since cyclo-octatriene is in a tautomeric equilibrium<sup>22</sup>.



The presence of appreciable amounts of material under strain (such as II) must result from the resonance of II which is not possible with I. Reactions such as these are therefore resonance-induced.

*The author thanks Polymer Corporation for permission to publish this manuscript. This work was presented in part at the 11th Canadian High Polymer Forum, Windsor, Ontario, Canada, 5-7 September, 1962.*

*Polymer Corporation Limited,  
Research and Development Division,  
Sarnia, Ontario, Canada*

*(Received April 1963)*

#### REFERENCES

- <sup>1</sup> DAINTON, F. S. and IVIN, K. J. *Quart. Rev. chem. Soc., Lond.* 1958, **12**, 16
- <sup>2</sup> DAINTON, F. S., DEVLIN, T. R. E. and SMALL, P. A. *Trans. Faraday Soc.* 1955, **51**, 1710
- <sup>3</sup> SMALL, P. A. *Trans. Faraday Soc.* 1955, **51**, 1717
- <sup>4</sup> DAINTON, F. S., IVIN, K. J. and WALMSLEY, D. A. G. *Trans. Faraday Soc.* 1960, **56**, 1784
- <sup>5</sup> A.P.I. *Project 44*. Tables of thermodynamic data'
- <sup>6</sup> BROWN, R. D. *Austral. J. sci. Res. A*, 1950, **3**, 428. cf. PARTINGTON, J. R. *Advanced Treatise on Physical Chemistry*, Vol. V, p 277. Longmans, Green: London, 1954
- <sup>7</sup> NATTA, G., MAZZANTI, F., PREGAGLIA, G. and PERALDO, M. *Gazz. chim. ital.* 1959, **89**, 465
- <sup>8</sup> WHELAND, G. W. *The Theory of Resonance*. Wiley; New York, 1947
- <sup>9</sup> COTTRELL, T. L. *The Strengths of Chemical Bonds*, p 274. Butterworth: London, 1958
- <sup>10</sup> DAVIES, D. W. *Trans. Faraday Soc.* 1955, **51**, 449
- <sup>11</sup> GRASSIE, N. and HAY, J. N. 'Thermal degradation of polymers', *S.C.I. Monograph No. 13*, p 184
- <sup>12</sup> GINSBURG, D. *Non-Benzenoid Aromatic Compounds*. Interscience: New York, 1959
- <sup>13</sup> JONES, W. O. *J. chem. Soc.* 1953, 2036
- <sup>14</sup> GOEHRING, M. *Quart. Rev. chem. Soc., Lond.* 1956, **10**, 437
- <sup>15</sup> VAN WAZER, J. R. *Phosphorus and Its Compounds*, pp 309 ff. Interscience; New York, 1958
- <sup>16</sup> SHAW, R. A., FITZSIMMONS, B. W. and SMITH, B. C. *Chem. Rev.* 1962, **62**, 247 (see pp 270-271)
- <sup>17</sup> PADDOCK, N. L. *Structure and Reactions in Phosphorus Chemistry*, Royal Institute of Chemistry Lecture Series No. 2, 1962, pp 27-28

## RESONANCE-INDUCED POLYMERIZATIONS

---

- <sup>18</sup> DEWAR, M. J. S., LUCKEN, E. A. C. and WHITEHEAD, M. A. *J. chem. Soc.* **1960**, 2423
- <sup>19</sup> FETTES, E. M. and JORCZAK, J. S. *Industr. Engng Chem. (Industr.)*, 1950, **42**, 2217
- <sup>20</sup> LEWIS, F. M. *Rubb. Chem. Technol.* 1962, **35**, 1222
- <sup>21</sup> VOGEL, E. and HASSE, K. *Liebigs Ann.* 1958, **615**, 22
- <sup>22</sup> COPE, A. C., HAVEN, A. C., RAMP, F. L. and TRUMBULL, E. R. *J. Amer. chem. Soc.* 1952, **74**, 4867

# *Polypropylene Oxide I: An Intrinsic Viscosity/Molecular Weight Relationship*

G. ALLEN, C. BOOTH and M. N. JONES

*The relationship between intrinsic viscosity and weight-average molecular weight determined by light-scattering measurements in hexane solutions has been obtained for a number of fractions and whole polymers of varying degrees of crystallizability. The corresponding relationships for benzene and toluene solutions have been deduced from it. Measurements of the refractive index increments in a number of solvents and the temperature dependence of the intrinsic viscosity in hexane solution are also reported.*

## EXPERIMENTAL

AS A consequence of the programme of research on the polymerization of polyethers which is being carried out in this department a considerable amount of data has accumulated concerning the physical properties of propylene oxide and its solutions. These results will be published in a short series of papers. All the polymers used in the present work were obtained from a zinc diethyl-water catalyst but the results are probably applicable to polymers prepared by other methods.

### *Materials*

Propylene oxide was polymerized using a zinc diethyl-water catalyst in dioxan solution<sup>1</sup> at room temperature. The reaction mixture was dissolved in benzene to which had been added a little methanol and the catalyst residues were removed by centrifugation. The polymer was finally extracted by freeze drying. Hexane, the principal solvent used, was standard hexane dried and distilled from calcium hydride. The fraction boiling between 68° and 70°C at atmospheric pressure was collected. Other solvents were purified by the usual methods.

### *Fractionation*

Two solvent-non-solvent systems were used to fractionate the polymers :

(a) methanol-water at 25°C (fractions denoted M)

(b) isopropanol-water at 74°C (fractions denoted IPA)

The melting point of polypropylene oxide is < 73°C.

Additional fractions (denoted I) were obtained by liquid-liquid phase separation from iso-octane<sup>2</sup>. The remaining samples were whole polymers or fractions obtained by a single-stage separation in methanol at 0°C; fractions soluble and insoluble in methanol at 0°C are denoted respectively by s and i.

### *Viscometry*

Ubbelohde dilution viscometers (shear stress  $\approx 15 \text{ g cm}^{-1} \text{ sec}$ ) were used for the hexane solutions and Desreux-Bischoff viscometers (shear stress  $\approx 0.3 \text{ g}$

cm<sup>-1</sup> sec) for work in benzene and toluene. Kinetic energy corrections were negligible for both viscometers.

#### *Light scattering*

A Brice-Phoenix light-scattering photometer was modified to enable measurements to be made in the range 25° to 60°C. Heating wires were incorporated in the light-scattering compartment behind false walls and the heater voltage was adjusted to bring the temperature to approximately 2°C below that required for the experiment. A small intermittent heater mounted in the cell table supplied the extra energy necessary to achieve the working temperature and to maintain it constant to ±1°C. The cell table was modified to accommodate a dummy cell identical to, and located immediately behind, the light-scattering cell. The intermittent heater was controlled by a contact thermometer mounted in the dummy cell.

Light-scattering measurements for a given polymer sample were made on a stock solution which was centrifuged at 15 000 *g* for three hours and transferred directly to the light-scattering cell. Dilutions were made *in situ* using solvent which had been filtered through VC.100 mμ 'Millipore' filters\*. These filters gave a clarity comparable with results obtained by centrifugation. Solution concentrations were determined at each dilution by removing and evaporating aliquots. Usually four concentrations were studied and measurements of light intensities were made at two wavelengths (4 360 and 5 460 Å) and eleven angles between 30° and 135°. No depolarization of the scattered light was detected. The photometer was calibrated using data supplied by the Phoenix Precision Instrument Company and checked against the polystyrene standard 'Styron 1960'. Three independent measurements at 4 360 Å gave an excess turbidity at 90°  $(3.06 \pm 0.05) \times 10^{-3}$  cm<sup>-1</sup> for a 0.5 per cent (w/v) solution in toluene at room temperature. The accepted value is  $3.16 \times 10^{-3}$  cm<sup>-1</sup>.

#### *Refractive index increments*

A Brice-Phoenix differential refractometer was calibrated with sucrose solutions and checked with potassium chloride solutions. A lagged case was built round the standard water jacket to obtain better temperature control at high temperatures.

## RESULTS AND DISCUSSION

#### *Refractive index increments*

Table 1 records the results of measurements of  $(dn/dc)$  for solutions in a number of solvents at temperatures in the range 25° to 60°C. There was no detectable dependence on molecular weight or concentration and the data are reasonably well represented by the Gladstone-Dale equation

$$(dn/dc) = (n_p - n_s)/\rho$$

where  $n_s$  and  $n_p$  are, respectively, the refractive index of solvent and polymer and  $\rho$  is the density of the polymer.

\*Millipore Filter Corporation, Bedford, Mass., U.S.A.

POLYPROPYLENE OXIDE I

Table 1. Refractive index increments

Solvent	Temperature (°C)	(dn/dc) ml g <sup>-1</sup>	
		4 360 Å	5 460 Å
Hexane	25	0.0775	0.0775 <sup>c</sup>
Hexane	46	0.0887	0.0887 <sup>a</sup>
Hexane	46	0.0895	0.0895 <sup>b</sup>
Hexane	57	0.101	0.101 <sup>a</sup>
Hexane	57	0.104	0.104 <sup>b</sup>
Heptane	40	0.0460	0.0460
Iso-octane	35	0.0655	0.0655
Isceon 113*	25	0.118	0.115
Benzene	25	-0.0530	-0.0448
Chlorobenzene	25	-0.0658	-0.0638
Methanol	25	0.118	0.118 <sup>c</sup>
Methanol	25	0.115	0.115 <sup>d</sup>

<sup>a</sup>  $\bar{M}_v = 0.96 \times 10^6$ ; <sup>b</sup>  $\bar{M}_v = 0.20 \times 10^6$ ; <sup>c</sup>  $\bar{M}_v = 1.22 \times 10^6$ ; <sup>d</sup>  $\bar{M}_v = 1.25 \times 10^6$   
 \*(C<sub>2</sub>F<sub>4</sub> · CCl<sub>2</sub>F<sub>2</sub>). Manufactured by the Imperial Smelting Corporation Ltd.

Light-scattering results

The second virial coefficients,  $A_2$ , weight-average molecular weight,  $\bar{M}_w$ , and Z-average root-mean-square radii of gyration,  $(\bar{S}_z^2)^{\frac{1}{2}}$ , for solutions in hexane at 46°C were computed from plots of:  $(Kc/R_\theta)_{\theta=0}$  versus  $c$ , and  $(Kc/R_\theta)_{c=0}$  versus  $\sin^2(\theta/2)$ , where the symbols have their usual meaning<sup>3</sup>, using the equation

$$(Kc/R_\theta)_{\substack{c \rightarrow 0 \\ \theta \rightarrow 0}} = (1/\bar{M}_w) [1 + \frac{1}{3}\mu^2(\bar{S}_z^2)^{\frac{1}{2}}] + 2A_2c$$

The concentration  $c$  is expressed as g ml<sup>-1</sup> and  $\mu = (4\pi/\lambda) \sin \theta/2$ . Results for the two polymers of lowest molecular weight were obtained at  $\lambda = 5\,460 \text{ \AA}$ ; the other data recorded in Table 2 are mean values of measurements made at two wavelengths.

Table 2. Light-scattering data

Polymer	$\bar{M}_w \times 10^{-5}$	$A_2 \times 10^4$ (cm <sup>3</sup> g <sup>-2</sup> mole)	$(\bar{S}_z^2)^{\frac{1}{2}}$ (Å)	$[\eta]$ (dl/g)
1	36.7	1.84	1120	5.95
2	44.1	0.523	930	5.50
3sM1	39.7	3.37	1000	3.74
4	22.4	0.0	880	2.85
3	13.8	1.72	670	2.65
5i	17.5	1.31	740	2.63
3i	18.2	1.25	750	2.58
6(I)1	13.7	3.55	560	2.50
3sM2	11.9	3.00	550	2.47
3s	15.1	1.83	1040	2.42
2i	10.1	1.26	590	2.24
7i	7.28	1.64	520	1.88
8	8.82	0.937	670	1.69
6(I)2	1.86	2.34	—	0.690
3s(IPA)	1.16	4.02	950	0.520
6(I)3	0.342	3.16	—	0.210

*Intrinsic viscosity/molecular weight relationships*

Figure 1 shows  $\log [\eta]$  versus  $\log \bar{M}_w$  for solutions in hexane at 46°C, from which the equation

$$[\eta] = 1.97 \times 10^{-4} (\bar{M}_w)^{0.67}$$

is obtained. Samples differing in their ability to crystallize from methanol solutions at 0°C (i.e. probably differing in tacticity) and whole polymers are

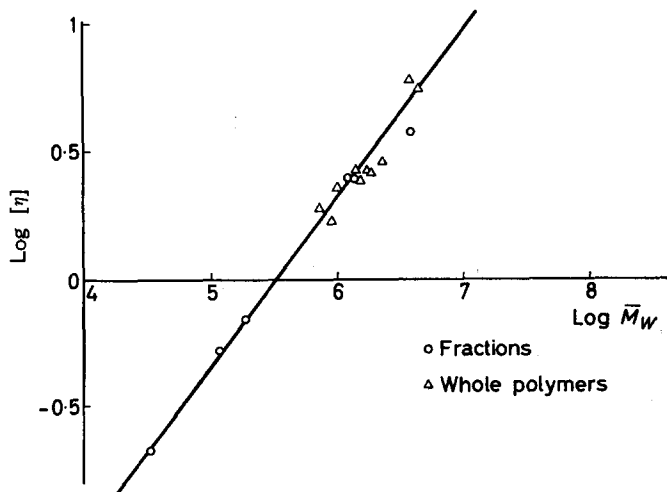


Figure 1—Intrinsic viscosity/molecular weight relationship for polypropylene oxide solutions in hexane at 46°C

Table 3. Intrinsic viscosities of polypropylene oxide solutions

Fraction	$[\eta]$ dl/g		
	(Hexane 46°C)	(Benzene 25°C)	(Toluene 25°C)
3s (IPA) 1	1.41	2.75	2.53
3s (IPA) 2	0.52	0.95	0.91
3s (IPA) 3	0.11	0.16	0.15

represented by the same equation. These results are consistent with numerous investigations on polymers of different tacticity<sup>4</sup>.

This equation, together with intrinsic viscosity measurements made on three fractions in benzene and toluene at 25°C and hexane at 46°C, was used to establish intrinsic viscosity/molecular weight equations for benzene and toluene solutions. The results are recorded in Table 3 and give the equations:

$$\text{Benzene at 25°C: } [\eta] = 1.12 \times 10^{-4} (\bar{M}_w)^{0.77}$$

$$\text{Toluene at 25°C: } [\eta] = 1.29 \times 10^{-4} (\bar{M}_w)^{0.75}$$

Price and Ebert<sup>5</sup> quote for benzene solutions at 25°C

$$[\eta] = 1.4 \times 10^{-4} (\bar{M})^{0.8}$$

but no experimental details are given and so it is not possible to ascertain the origin of this discrepancy.

#### Temperature dependence of the intrinsic viscosity

Figure 2 shows the temperature variation of intrinsic viscosity for three whole polymers and one fraction in hexane solution. The three whole polymers were partially crystalline and precipitation of some crystalline material occurred in the vicinity of 37°C. We conclude that the intrinsic viscosity/molecular weight equation will probably hold over the range 45° to 55°C.

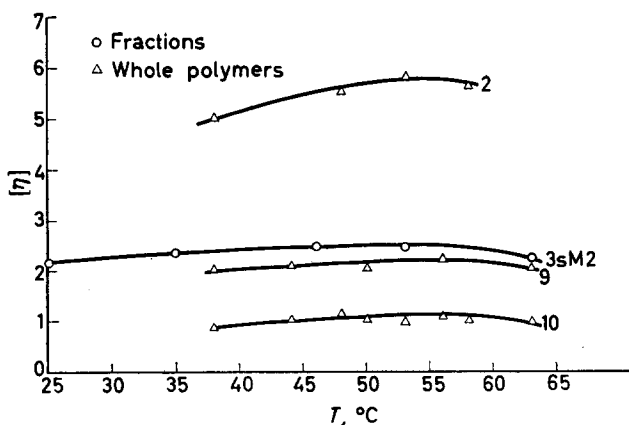


Figure 2—Temperature dependence of the intrinsic viscosity of polypropylene oxide solutions in hexane at 46°C

We thank Dr E. Powell for preparing the polymer samples and C. S. Clemson for experimental assistance.

Chemistry Department,  
University of Manchester

(Received April 1963)

#### REFERENCES

- 1 FURUKAWA, J., TSURUTA, T., SAKATA, R. and SAEGUSA, T. *Makromol. Chem.* 1959, **32**, 90; 1960, **40**, 64
- 2 BOOTH, C., JONES, M. N. and POWELL, E. *Nature, Lond.* 1962, **196**, 772
- 3 ALLEN, P. W. *The Characterization of High Polymers*, Ch. 5. Butterworths: London, 1959
- 4 See for example KRIGBAUM, W. R., KURTZ, J. E. and SMITH, P. *J. phys. Chem.* 1961, **65**, 1984
- 5 EBERT, P. E. and PRICE, C. C. *J. Polym. Sci.* 1959, **34**, 157



# *Viscosity/Temperature Dependence for Polyisobutene Systems*

## *The Effect of Molecular Weight Distribution\**

ROGER S. PORTER and JULIAN F. JOHNSON

*This paper represents a study of the effect of molecular weight distribution on polymer rheology. Results on solutions of polyisobutene of narrow molecular weight,  $M_w/M_n=1.03$ , are compared with previously published viscosity data on similar solutions but with broad and defined distributions,  $M_w/M_n \leq 3.1$ . Complete molecular weight distributions and the narrow fractions were obtained by large-scale polymer column fractionation. Viscosity has been measured as a function of shear on cetane solutions of these polyisobutenes at concentrations from 10 to 100 weight per cent and at seven temperatures from 20° to 135°C. Data are evaluated in terms of flow activation energy, a commonly used viscosity/temperature coefficient. At low shear, flow activation energy for concentrated high polymer systems is generally insensitive to molecular weight and distribution. At low molecular weight, the flow activation increases with molecular weight and homogeneity. Flow activation energies calculated at constant stress are independent of shear over all measurable values, which includes data well into the non-Newtonian range. This conclusion holds for any one polyisobutene system, irrespective of molecular weight, distribution and concentration. Flow activation energies at constant stress are in contrast to activation energies calculated at constant shear rate. The latter decreases markedly with shear as polyisobutene solutions become non-Newtonian. These flow activation energies, as well as viscosities, change more rapidly and over narrower shear rate ranges for narrow compared to broad distribution polymers. This result is probably a reflection of the effect of molecular weight distribution on shear relaxation spectrum.*

THIS paper represents a study of the effect of molecular weight distribution on polymer rheology. Results on solutions of polyisobutene of limiting narrow molecular weight distribution are compared with previously published viscosity data on similar solutions but with broad and now defined polyisobutene distributions. Results on defined distribution polyisobutenes provide an evaluation of the extensive rheological investigations of this polymer reported in the literature. Viscosity measurements have probably been more widely published on butene polymers than on any other systems. Most commonly tested are the highest molecular weight commercial polymers which are pure polyisobutene. These polymers are commonly defined by a single molecular weight or at best by two moments of molecular weight such as weight and number average. The complete molecular weight distribution is required for definitive polymer studies. The distributions for polymers used in this work are given in *Figure 1*.

The narrow polyisobutene fractions were obtained by a recently reported technique of large-scale polymer column fractionation<sup>1</sup>. A kilogramme of

\*Part XI of a series on 'Flow Properties of Polymeric Systems'. Presented in part before the Organic Coatings and Plastics Division at the 145th National Meeting of the American Chemical Society, New York, September 1963.

polyisobutene, Vistanex MS, Enjay Company, Inc., has been chromatographically fractionated. Fifty-gramme polymer batches were eluted through six parallel glass-bead columns under the influence of a solvent and temperature gradient. The molecular weight distributions of fractions were determined by analytical refractionation which is the only accurate dispersion measure for narrow fractions. The fractions have weight-to-number average molecular weight ratios which differ from 1 to 3 per cent, indicating that these are as narrow in distribution as any polymers previously used in rheological studies.

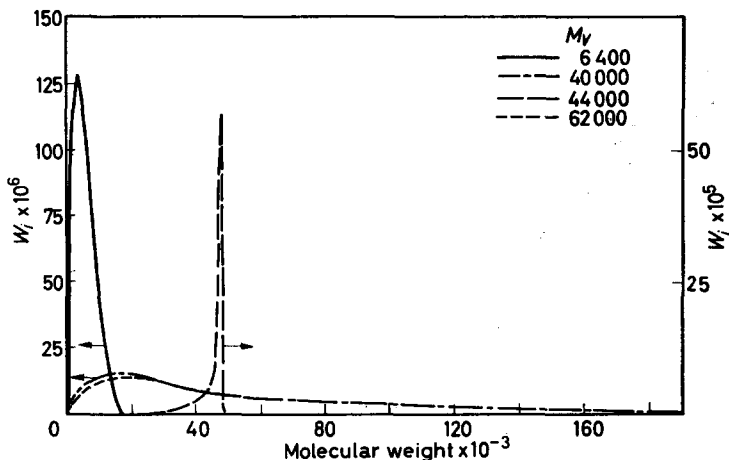


Figure 1—Molecular weight distributions for polyisobutenes

Low and high shear viscosities have been measured on cetane solutions of polyisobutene at concentrations from 10 to 100 weight per cent and at seven temperatures from 20° to 135°C. Low shear measurements were made with crossarm capillary viscometers<sup>2</sup>. Data were evaluated in terms of flow activation energy,  $\Delta E^*$ , sometimes called flow activation heat, which is the most commonly used viscosity/temperature coefficient. It is equal to 2.3 times the product of the gas constant and the slope of the log viscosity versus  $1/T$  [°K] correlation. These correlations are generally slightly curved, giving higher activation energies at lower temperatures. Plots of log viscosity versus  $1/T^2$  are generally more linear, but this interpretation has no theoretical basis.

The low-shear flow activation energies calculated at 125°C for polyisobutene solutions are shown in Figure 2. New data on a narrow distribution fraction,  $M_v = 44\,000$  and  $M_w/M_n = 1.03$ , are compared in this work with previously published solution data on three broader distribution polyisobutenes with  $M_v$  and  $M_w/M_n$  values of 6400 and 2.3; 40000 and 3.1; 62000 and  $\sim 2.9^4$ . Molecular weights were defined by the intrinsic viscosity equation of Fox and Flory<sup>3</sup>. No point of inflection is apparent in Figure 2 as has been previously postulated for the broad distribution polyisobutene,  $M_v = 62\,000^4$ . This indicates that by the theory of Hirai, the heat of polyisobutene entanglement, if present, is small,  $< 0.5$  kcal/mole<sup>5</sup>. The  $\Delta E^*$  for

solutions of various molecular weights and distributions of polyisobutene increase similarly with concentration, with no significant break in values usable for entanglement heat calculations<sup>5</sup>.

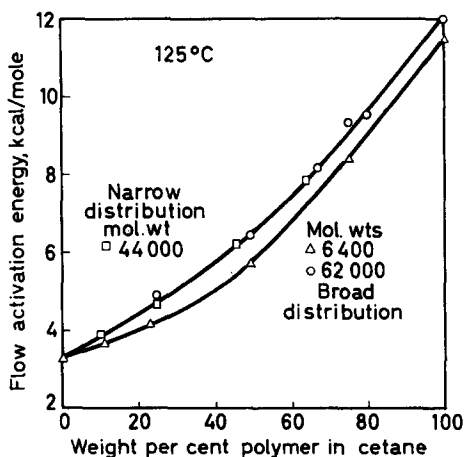


Figure 2—Flow activation energies for polyisobutenes in cetane

Figure 2 indicates that  $\Delta E^*$  and its concentration dependence do not increase greatly with polyisobutene molecular weight. Only the low molecular weight polyisobutene,  $M_v$  6 400, differs significantly from the common curve for the broad distribution polymer,  $M_v$  62 000, and the narrow distribution,  $M_v$  44 000. The common curve for the latter two shows that for equal  $M_v$ , a broader molecular weight distribution leads to a lower  $\Delta E^*$ . Low shear values for  $\Delta E^*$  have been previously established to be independent of molecular weight and, therefore, also independent of molecular weight distribution for bulk polyisobutenes of  $M_v > 100\ 000^8$ .

The concentration dependence of low shear viscosity for these broad and narrow distribution polyisobutenes in cetane is also virtually equivalent<sup>7</sup>. In general, the effect of molecular weight distribution on polyisobutene rheology is not manifested in low shear Newtonian flow. In shear dependence, however, polymer rheology is distinctly influenced by molecular weight distribution.

Solution viscosities of narrow and broad molecular weight distribution polyisobutenes have been measured as a function of shear with a thin-film, double-thermostatted, rotational, concentric cylinder viscometer<sup>8</sup>. For narrow and for broad distribution polyisobutenes, significant non-Newtonian flow is found only at products of polymer molecular weight and volume concentrations which exceed the entanglement transition near 17 000 for polyisobutene<sup>9</sup>. Figure 3 shows viscosity/temperature relationships for a polyisobutene solution at a series of shear rates from low-shear Newtonian flow up to  $2.4 \times 10^5 \text{ sec}^{-1}$ . These are measurements on a 49 weight per cent solution in cetane of limiting narrow distribution polyisobutene,  $M_v$  44 000. All apparent viscosity losses in Figure 3 are entirely reversible, with indications of neither thermal hysteresis nor polymer degradation. Solutions of broad distribution polyisobutenes of the same average molecular weight

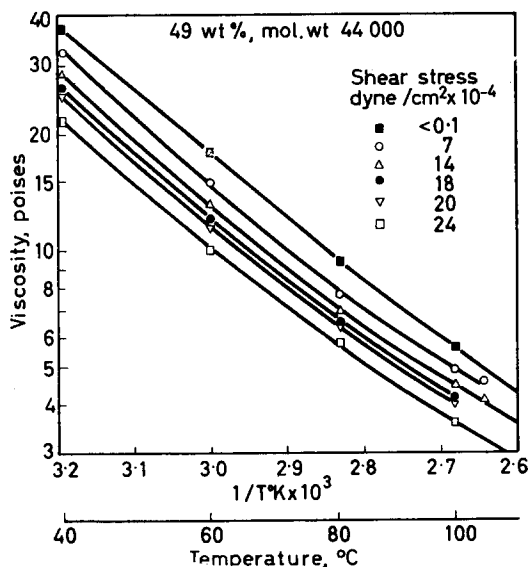


Figure 3—Viscosity/temperature relation for polyisobutene in cetane

show much larger viscosity changes with shear. This is because broad distribution polymers exhibit reversible viscosity losses at lower shear rates and stresses. The difference between shear dependence of viscosity for broad and narrow distribution polymer of similar average molecular weight is illustrated in *Table 1*. The broad distribution exhibits over twice the

Table 1. Shear viscosities, 80°C, 49 weight per cent polyisobutene in cetane

$M_w$	$M_w/M_n$	Viscosity (poises)		Viscosity loss with shear (%)
		Newtonian	$2.4 \times 10^5$ dyne/cm <sup>2</sup>	
50 000	3.1	17.5	2.2	88
44 000	1.03	9.4	5.7	39

percentage change in yielding viscosities from well above to well below the narrow distribution polymer.

Significantly for all polyisobutenes, irrespective of distribution and concentration, the relative viscosity change with shear stress is found to be the same at all test temperatures, see, for example, *Figure 3*. This conclusion holds for broad distributions of other polymer types and has also been confirmed recently for narrow distribution fractions of bulk polystyrene<sup>10</sup>. This feature leads to the conclusion (see *Figure 4*) that flow activation energies at constant stress,  $\Delta E_s^*$ , are entirely independent of stress up to extreme values, which include data well into the non-Newtonian range. The displacement of activation energies at the two temperatures in *Figure 4* is due to the curvature inherent in *Figure 3*.

The fact that flow activation energies at constant stress are independent of molecular weight distribution and stress may represent a general test for the reliability of non-Newtonian polymer viscosities at different tempera-

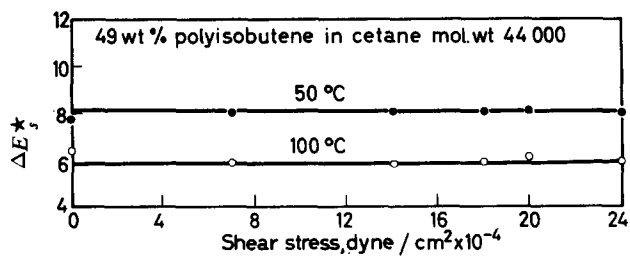


Figure 4—Flow activation energy at constant stress,  $\Delta E_s^*$

tures. Only data on one polymer system stand apart, those given by Philippoff<sup>11</sup>, see discussion by Schott<sup>12</sup>. Bestul and Belcher have theoretically derived from rate theory that activation energies at constant stress should be equal to or greater than those at constant shear rate and that the former should deviate from low shear values only at stresses in excess of those used here<sup>13</sup>.

Flow activation energies, calculated at constant stress, are generally quite different, however, from  $\Delta E^*$  evaluated at constant shear rate. Flow activation energies at constant shear rate,  $\Delta E_r^*$ , decrease with shear as polyisobutene solutions become non-Newtonian. This is illustrated in Figure 5 with broad and narrow distribution polyisobutenes at two concentrations in cetane. Solutions of both broad and narrow distribution polymers

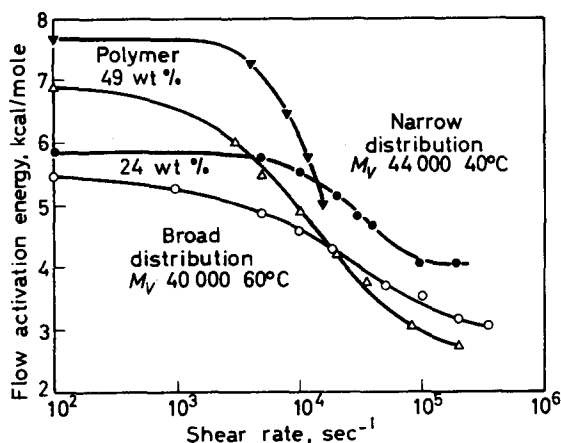


Figure 5—Changes in flow activation energy with shear, polyisobutene in cetane

go through a point of inflection and approach a limiting  $\Delta E_r^*$  at both high and low rates of shear. At the two concentrations in Figure 5, the broad polyisobutene,  $M_w/M_n$  of 3.1, exhibits changes over some four shear decades; whereas, the narrow polymer  $M_w/M_n$  of 1.03 varies over less than half this shear rate range. The viscosity and the  $\Delta E_r^*$  for narrow distribution polymers change more rapidly and over narrower shear rate ranges for broad distribution polymers. This is probably a direct reflection of the effect of molecular weight distribution on the shear relaxation spectra

for polymer systems. The one available expression for relating  $\Delta E_r^*$  and shear involves the Eyring rate theory<sup>13</sup>. It is found here that single hyperbolic functions of this form adequately predict neither the magnitude nor dependence of  $\Delta E_r^*$  changes with shear.

*The authors express appreciation to Mr A. R. Bruzzone for help with the experimental work.*

California Research Corporation,  
Richmond, California

(Received May 1963)

#### REFERENCES

- <sup>1</sup> CANTOW, M. J. R., PORTER, R. S. and JOHNSON, J. F. *Nature, Lond.* 1962, **192**, 752; *J. Polym. Sci.* 1963, **C1**, 187, 195
- <sup>2</sup> JOHNSON, J. F., LETOURNEAU, R. L. and MATTESON, R. *Analyt. Chem.* 1952, **24**, 1505
- <sup>3</sup> FOX, T. G, Jr, and FLORY, P. J. *J. phys. Chem.* 1951, **55**, 221; 1949, **53**, 197
- <sup>4</sup> PORTER, R. S. and JOHNSON, J. F. *Polymer, Lond.* 1962, **3**, 11
- <sup>5</sup> HIRAI, N. *J. Polym. Sci.* 1959, **40**, 255
- <sup>6</sup> JOHNSON, M. F., EVANS, W. W., JORDAN, I. and FERRY, J. D. *J. Colloid Sci.* 1952, **7**, 498
- <sup>7</sup> PORTER, R. S. and JOHNSON, J. F. *Trans. Soc. Rheol.* 1963, **7**, 241
- <sup>8</sup> BARBER, E. M., MUENGER, J. R. and VILLFORTH, F. J., Jr. *Analyt. Chem.* 1955, **27**, 425
- <sup>9</sup> PORTER, R. S. and JOHNSON, J. F. *J. appl. Phys.* 1961, **32**, 2326; *S.P.E. Trans.* 1963, **3**, 18
- <sup>10</sup> RUDD, R. *J. Polym. Sci.* 1960, **44**, 459
- <sup>11</sup> PHILIPPOFF, W. and GASKINS, F. H. *J. Polym. Sci.* 1956, **21**, 205
- <sup>12</sup> SCHOTT, H. and KAGHAN, W. S. *J. appl. Polym. Sci.* 1961, **5**, 175
- <sup>13</sup> BESTUL, A. B. and BELCHER, H. V. *J. appl. Phys.* 1953, **24**, 696

#### ANNOUNCEMENTS

##### OPEN DAYS AT THE LABORATORY OF THE GOVERNMENT CHEMIST

The Laboratory of the Government Chemist is to hold its first Open Days in the new Cornwall House premises on 22 to 23 April 1964. Tickets to visit the Laboratory can be obtained in advance from The Government Chemist, Cornwall House, Stamford Street, London S.E.1. Applicants should state on which day they would like to attend, and whether morning, afternoon, or all day.

##### THE CHEMISTRY OF POLYMERIZATION PROCESSES

The Symposium on the above subject will now be held in London on 22 and 23 April 1965, not 29 and 30 April as announced on page 53 of our January issue. Dr W. R. MOORE, of the Department of Chemical Technology, Bradford Institute of Technology, Bradford 7, will supply details of the meeting on request. Intending contributors are asked to send summaries of their contributions to Dr MOORE before 1 July.

for polymer systems. The one available expression for relating  $\Delta E_r^*$  and shear involves the Eyring rate theory<sup>13</sup>. It is found here that single hyperbolic functions of this form adequately predict neither the magnitude nor dependence of  $\Delta E_r^*$  changes with shear.

*The authors express appreciation to Mr A. R. Bruzzone for help with the experimental work.*

California Research Corporation,  
Richmond, California

(Received May 1963)

#### REFERENCES

- <sup>1</sup> CANTOW, M. J. R., PORTER, R. S. and JOHNSON, J. F. *Nature, Lond.* 1962, **192**, 752; *J. Polym. Sci.* 1963, **C1**, 187, 195
- <sup>2</sup> JOHNSON, J. F., LETOURNEAU, R. L. and MATTESON, R. *Analyt. Chem.* 1952, **24**, 1505
- <sup>3</sup> FOX, T. G, Jr, and FLORY, P. J. *J. phys. Chem.* 1951, **55**, 221; 1949, **53**, 197
- <sup>4</sup> PORTER, R. S. and JOHNSON, J. F. *Polymer, Lond.* 1962, **3**, 11
- <sup>5</sup> HIRAI, N. *J. Polym. Sci.* 1959, **40**, 255
- <sup>6</sup> JOHNSON, M. F., EVANS, W. W., JORDAN, I. and FERRY, J. D. *J. Colloid Sci.* 1952, **7**, 498
- <sup>7</sup> PORTER, R. S. and JOHNSON, J. F. *Trans. Soc. Rheol.* 1963, **7**, 241
- <sup>8</sup> BARBER, E. M., MUENGER, J. R. and VILLFORTH, F. J., Jr. *Analyt. Chem.* 1955, **27**, 425
- <sup>9</sup> PORTER, R. S. and JOHNSON, J. F. *J. appl. Phys.* 1961, **32**, 2326; *S.P.E. Trans.* 1963, **3**, 18
- <sup>10</sup> RUDD, R. *J. Polym. Sci.* 1960, **44**, 459
- <sup>11</sup> PHILIPPOFF, W. and GASKINS, F. H. *J. Polym. Sci.* 1956, **21**, 205
- <sup>12</sup> SCHOTT, H. and KAGHAN, W. S. *J. appl. Polym. Sci.* 1961, **5**, 175
- <sup>13</sup> BESTUL, A. B. and BELCHER, H. V. *J. appl. Phys.* 1953, **24**, 696

#### ANNOUNCEMENTS

##### OPEN DAYS AT THE LABORATORY OF THE GOVERNMENT CHEMIST

The Laboratory of the Government Chemist is to hold its first Open Days in the new Cornwall House premises on 22 to 23 April 1964. Tickets to visit the Laboratory can be obtained in advance from The Government Chemist, Cornwall House, Stamford Street, London S.E.1. Applicants should state on which day they would like to attend, and whether morning, afternoon, or all day.

##### THE CHEMISTRY OF POLYMERIZATION PROCESSES

The Symposium on the above subject will now be held in London on 22 and 23 April 1965, not 29 and 30 April as announced on page 53 of our January issue. Dr W. R. MOORE, of the Department of Chemical Technology, Bradford Institute of Technology, Bradford 7, will supply details of the meeting on request. Intending contributors are asked to send summaries of their contributions to Dr MOORE before 1 July.

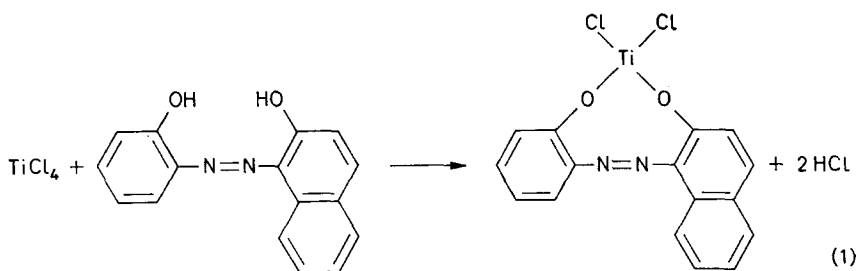
# Catalysts for the Low Temperature Polymerization of Ethylene

K. J. TAYLOR\*

*A new series of catalysts for the polymerization of ethylene is reported. Experimental details are briefly examined in relation to yield.*

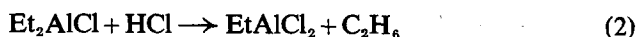
CATALYSTS for the polymerization of ethylene at ambient temperatures and pressures, which are believed to be soluble in the reaction medium, have been reported by Breslow and Newburg<sup>1</sup>, Natta *et al.*<sup>2</sup> and Carrick *et al.*<sup>3</sup>. A new series, including both soluble and insoluble catalysts, is now reported.

In all cases the chelates were prepared *in situ*. In a typical experiment 0.3643 g of *o*-hydroxybenzeneazo- $\beta$ -naphthol was dissolved in 200 ml of dry toluene contained in a 500 ml three-necked round-bottomed flask to yield a bright, orange-red solution. The system was flushed with dry nitrogen before being transferred to a nitrogen glove box. 3 ml of a 5 per cent solution of titanium tetrachloride was added by pipette and a dark, opaque solution (green-black as a thin film) was obtained instantly.



A trace of black precipitate could be seen but a parallel experiment in which this was filtered off gave identical results.

The solution was stirred for 15 minutes before 0.86 ml of diethyl aluminium chloride was added. In addition to removing hydrogen chloride by the reaction



this compound functions as a necessary co-catalyst.

Some chelating agents were insoluble in the toluene and in those cases the mixture was refluxed for one hour before the introduction of the alkyl. This has been indicated where appropriate.

It is known that for catalyst systems of this type the co-catalyst/catalyst ratio should be between three and five and consequently the quantity of alkyl added in each experiment was calculated on the assumption that three molecules of  $\text{Et}_2\text{AlCl}$  were required for each titanium atom present plus one molecule for each molecule of  $\text{HCl}$  liberated in the chelation reaction.

\*Present address: B.I.P. Chemicals Ltd, The Laboratories, Tat Bank Road, Oldbury, Birmingham.



This simple calculation ignores the fact that the  $\text{EtAlCl}_2$  formed may also function as co-catalyst and base. In the former capacity it is so inferior to  $\text{Et}_2\text{AlCl}$  that it may be ignored. However, the possibility that  $\text{EtAlCl}_2$  may compete effectively with  $\text{Et}_2\text{AlCl}$  for  $\text{HCl}$ , thus leaving a higher concentration of co-catalyst than planned, must be considered. In the unlikely event that the  $\text{HCl}$  is neutralized by the  $\text{EtAlCl}_2$  preferentially, the worst error is an increase in the co-catalyst/catalyst from three to five. In practice the discrepancy is likely to be considerably less and the error involved much smaller than that occasioned by the alternative procedure of attempting to remove the hydrogen chloride before the addition of the alkyl. However, for this reason the polymer yields are better considered on a comparative rather than an absolute basis.

Early attempts to isolate and purify the product from equation (1) viz.  $\text{TiCl}_2\text{R}$  (where  $\text{R} = -\text{OC}_6\text{H}_4\text{N}_2\text{C}_{10}\text{H}_6\text{O}-$ ) gave at each stage very good specimens of the dichelate  $\text{TiR}_2$ .

Presumably the equilibrium



was continually displaced to the right as the titanium tetrachloride was destroyed in the air.

However, when the solvent was removed at room temperature by pumping, large shiny black crystals remained, which were stable in air. Elemental analysis showed them to be substantially  $\text{TiCl}_2\text{R}$ ; when redissolved in toluene they gave the expected dark green-black solution, which, in the presence of co-catalyst, would polymerize ethylene. In contrast the very small, lustrous, black crystals of  $\text{TiR}_2$  were almost completely insoluble in toluene and no effective catalyst solution could be prepared from them.

It seems probable, therefore, that  $\text{TiCl}_2\text{R}$  forms one part of an effective catalyst system. However, there is an alternative explanation, i.e. that the more usual Ziegler catalyst  $\text{Et}_2\text{AlCl}-\text{TiCl}_4$  is the active species and that it is formed through the existence of the equilibrium (3) which is continuously displaced to the right as the  $\text{TiCl}_4$  forms the catalyst until all the  $\text{TiCl}_2\text{R}$  has decomposed.

Two pieces of evidence refute this. First, the conventional Ziegler catalyst is insoluble in toluene and may be filtered off, whereas the present catalyst system passes unchanged through a number 2 glass sinter. Secondly, a catalyst for the polymerization of propylene may be prepared by reducing  $\text{TiCl}_4$  to  $\text{TiCl}_3$  followed by the addition of a suitable co-catalyst. If equilibrium (3) is capable of yielding  $\text{TiCl}_4$  to react with  $\text{AlEt}_2\text{Cl}$  for the production of a Ziegler catalyst it should be equally available for the reduction to  $\text{TiCl}_3$ , which is carried out using  $\text{AlEt}_3$  at elevated temperatures. However, no such reduction could be achieved.

The evidence, therefore, leads to the conclusion that  $\text{TiCl}_2\text{R}$  is the active species. The results listed below support the belief in so far as they show that catalytic activity varies with the organic substrate R.

Polymerization reactions were carried out at  $60^\circ\text{C}$  using a flow system; after two hours the polymer was filtered off, washed with acetone, dried and weighed.

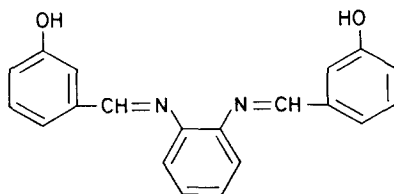
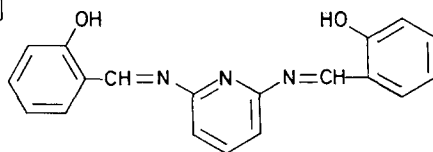
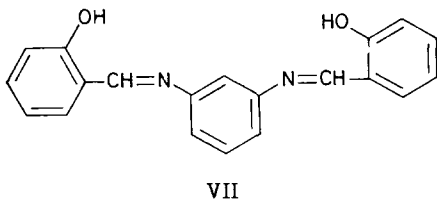
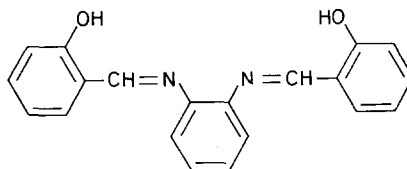
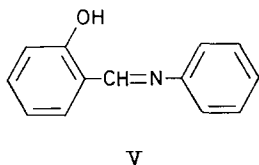
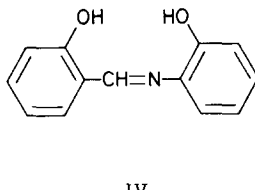
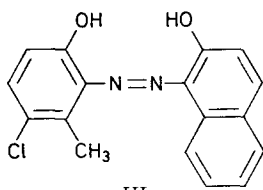
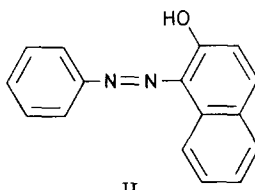
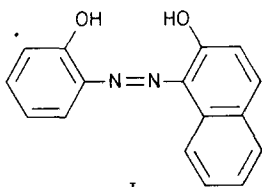
Results with related catalysts for the polymerization of propylene

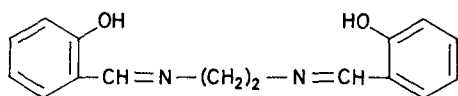
## CATALYSTS FOR LOW TEMPERATURE POLYMERIZATION OF ETHYLENE

indicated that polymer yield varied with each batch of solvent. Determinations of water by the Karl Fischer method on the sodium-dried toluene showed that polymer yield could not be simply related to water content and consequently the results listed below for polyethylene were obtained by using a single solvent batch. As a result a given yield could usually be reproduced to within about 0.2 g, although the heterogeneous systems sometimes showed more scatter.

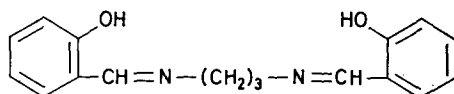
### RESULTS

Chelating agents used :





X



XI

200 ml of toluene and 3.0 ml of a 5 per cent solution of  $\text{TiCl}_4$  in toluene were used in each experiment.

Chelate No.	Molar ratio of chelate to Ti	Yield of polyethylene g	Chelate No.	Molar ratio of chelate to Ti	Yield of polyethylene g
IV	0.5	3.1	V	0.25	11.65
	1.0	3.0		0.5	2.53
	1.0	0.6*		0.5	trace
	1.5	2.9		0.5	9.0
	2.0	3.1		1.0	2.8
	2.0	trace*		1.0	0.5
				2.0	2.2
VI	0.5	0.5		3.0	2.1
	1.0	0.1		4.0	0.3
	2.0	trace		4.0	1.3
VIII	0.5	5.7*		VII	0.25
	1.0	3.7*	0.5		3.2
	2.0	1.4*	1.0		2.4
			1.5		0.5
			2.0		0.2
X	0.5	1.0	IX	0.5	8.1*
	1.0	0.2		1.0	8.9
	2.0	0.4		1.0	8.5*
				2.0	7.7
XI	0.5	1.0	XI	0.5	1.6
	1.0	0.2		1.0	trace
	2.0	0.4		2.0	trace
No added chelate	—	6.2			
	—	6.4			
	—	11.8			
	—	7.0			

\*Refluxed for one hour during preparation of chelate.

At low chelate/Ti ratios some conventional Ziegler catalyst must still be present but at ratios greater than one (in some cases 0.5) the contribution from this source may be neglected.

Hence chelates from VI, X and XI may be considered as inactive, whereas those from VII and IX (which are isomeric with VI) yield catalyst systems. The higher yields obtained when VIII was employed instead of VII are interesting.

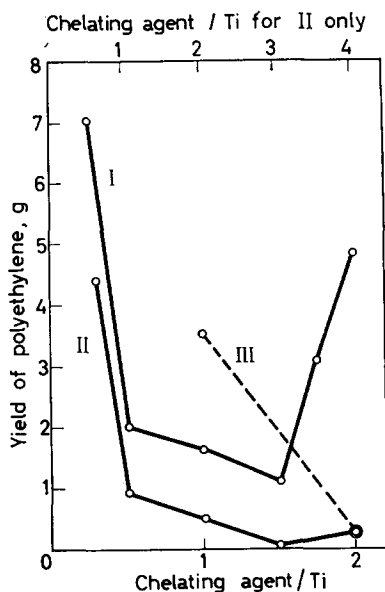


Figure 1

However, the most outstanding feature is the sudden rise in yield at high chelate/Ti ratios when reagent I is used. The contrast with the very similar reagent III is striking, although the latter was selected in the hope of finding differences, since the methyl group interferes sterically with the hydrogen atom at position eight in the naphthalene ring, forcing the two ring systems out of coplanarity.

*This work was performed at the Research Laboratory, Courtaulds Limited, Maidenhead, Berks. My thanks are due to Mr J. Price and Mr J. Watson for practical assistance and to Mr J. S. Ward for helpful discussions and samples of some chelating agents.*

*Courtaulds Ltd,  
Maidenhead, Berks*

*(Received May 1963)*

#### REFERENCES

- <sup>1</sup> BRESLOW, D. and NEWBURG, N. *J. Amer. chem. Soc.* 1959, **81**, 81
- <sup>2</sup> NATTA, G., PINO, P., MAZZANTI, G., GIARRINI, U., MANTICA, E. and PERALDO, M. *J. Polym. Sci.* 1957, **26**, 120
- <sup>3</sup> CARRICK, W., KLUIBER, R., BONNER, E., WARTMAN, I., RUGG, F. and SMITH, J. *J. Amer. chem. Soc.* 1960, **82**, 3883

# *The Photolytic Decomposition of Poly-n-butyl Methacrylate*

J. R. MACCALLUM\*

*The measurement of the absolute rate of photolytic degradation of poly(n-butyl methacrylate) using ultra-violet irradiation on molten polymer films, has been found to be complicated by some physical process becoming rate controlling. It is suggested that because of the high rates of degradation involved, thermal gradients are set up, and the rate becomes a function of the conduction of heat within the sample. The technique used for measuring the rate of depolymerization limits the measurements to films of the order of 0.01 mm thick. The mechanism of degradation is similar to that of poly(methyl methacrylate) in solution, in that initiation takes place at random in the polymer molecule as well as at chain-ends.*

IN RECENT years there has been an increasing interest in the photolytic degradation of high polymers. Elucidation of the mechanism of breakdown is a necessary step in the problem of tackling the prevention of deterioration of physical properties accompanying photochemical degradation. The general progress made in this field has been reviewed by Grassie<sup>1</sup>.

Basically the problem is greatly simplified by exclusion of oxygen and this can be achieved by carrying out degradations either in solution or under high vacuum. The first investigation made under the latter conditions was that of Cowley and Melville<sup>2</sup> who studied the degradation of poly(methyl methacrylate) using ultra-violet radiation of wavelength 2537 Å and in the temperature range 160° to 200°C. These authors found the reaction to be very similar in mechanism to that of the thermally initiated reaction, in that it yielded pure monomer by a depolymerization process, initiated at the unsaturated terminal groups formed in the disproportionation-termination step during polymerization. A rather unusual feature of their investigation was the proposal that the termination reaction was occurring in conditions of viscosity control. A value of 20 kcal/mole was obtained for the activation energy of the termination step which is a metathetical reaction between two radicals and would be expected to have an activation energy of close to zero. Grassie and Melville<sup>3</sup> found no such effect in their thermal degradation studies, presumably because the increase in temperature (about 50°C) lowered the viscosity sufficiently to allow termination to proceed normally.

Several papers have been published reporting the effects of high energy radiation, including ultra-violet, on solutions of poly(methyl methacrylate) and on the polymer at room temperature, when it is a glassy substance. Both Monig<sup>4</sup> and Schultz<sup>5</sup> using light of wavelength 2537 Å found the molecular weight to decrease drastically in the manner of a polymer undergoing a randomly occurring scission reaction. Monig used chloroform, dioxan and benzene as solvents, whereas Schultz degraded the polymer in the form of films. More recently Charlesby and Thomas<sup>6</sup> have shown

\*Present address: Chemistry Department, St Salvador's College, University of St Andrews, St Andrews.

that the solvent played very little part in the reaction as the rate was almost independent of concentration in benzene solutions. The amount of monomer formed was small and these experiments may be complicated by the occurrence of a repolymerization reaction, an event which was improbable under the conditions of Cowley and Melville. However, the outstanding difference between the reaction in a viscous bulk polymer, which is end initiated, and that in solutions, which takes place randomly along the polymer molecule, cannot be explained by the participation of monomer.

The present work deals with the photo-initiated degradation of poly(*n*-butyl methacrylate) using similar conditions to those of Cowley and Melville. It has been reported<sup>7</sup> that the *n*-butyl polymer has much lower  $T_g$  (22°C) than the methyl ester (105°C), and thus it is reasonable to expect diffusion of the molecules to be facilitated.

## EXPERIMENTAL

*Monomer*

*n*-Butyl methacrylate (I.C.I. Ltd) was washed four times with dilute sodium hydroxide and four times with distilled water to remove inhibitor. After drying for 24 hours over anhydrous sodium sulphate, it was filtered and then distilled under reduced pressure (b.pt 55° to 58°C at 25 mm of mercury). The monomer was found to be pure as tested by gas liquid chromatography.

*Polymers*

Table 1 shows details of the preparation of the polymers. Polymerizations were carried to low conversions using recrystallized 2,2'-azo-isobutyronitrile. Polymers were precipitated and twice reprecipitated by methanol from acetone solution. The resulting powder was dried at room temperature by prolonged storage in vacuum.

Table 1. Preparation of polymers

Polymer	% Initiator (w/v)	Preparation	Molecular weight ( $\times 10^{-5}$ )	Temperature of polymerization (°C)
N.B.1	0.05	Bulk	11.0	60
N.B.2	0.50	Bulk	4.6	60
N.B.4	0.20	$\frac{\text{monomer}}{\text{benzene}} = \frac{1}{10}$	0.4	80
N.B.6	0.03	$\frac{\text{monomer}}{\text{benzene}} = \frac{1}{2}$	1.1	80

## DEGRADATION APPARATUS

The apparatus was essentially the same as that used by Cowley and Melville<sup>2</sup>, a dynamic molecular still with a silica port. The heating block was controlled by an ether 'transitrol' and a larger tray (3.2 cm diameter)

was used. The Pirani gauge was situated in a sidearm which was thermostatically controlled in an ice-water mixture. Care was taken to exclude any radiation from the gauge.

An Osram 125 W mercury arc lamp with glass envelope removed, fed through a choke and condenser, was the light source. It was always switched on for about 30 min before use to allow it to reach constant output. Ultraviolet absorption spectra of the polymers were measured using a Perkin-Elmer 137 instrument, on films cast from chloroform solution in a silica cell. Under the experimental conditions used, the Osram low pressure lamp gives more than 90 per cent of its energy output at  $2\,536\text{ \AA}^8$  and can thus be considered as essentially a monochromatic source. The quantitative output of the lamp was not measured.

Wire gauze screens, blackened to minimize reflections, were used to vary the light intensity.

#### MOLECULAR WEIGHT MEASUREMENTS

Number average molecular weights were obtained for some of the undegraded polymers using a modified Fuoss-Mead osmometer<sup>9</sup>. The intrinsic viscosities of degraded samples were measured in chloroform solution at  $25^\circ\text{C}$  and converted to molecular weights using the equation<sup>10</sup>

$$[\eta] = 0.437 \times 10^{-4} M^{0.80} \quad (1)$$

The number average value was calculated on the assumption that  $M_v/M_n = 2.0$ .

#### PRODUCTS OF DEGRADATION

The liquid products of degradation were examined by gas-liquid chromatography and found to be pure monomer, with no trace of butene which is found in the thermal degradation<sup>11</sup>. Infra-red spectra of residual polymer were identical with undegraded polymer.

#### RESULTS

Before commencing a kinetic study proper of the photoreaction a few preliminary points required investigation. These were (a) the possibility of a skin effect whereby most of the light is absorbed in the surface layers of the polymer and the reaction confined to this region; (b) the effect of the state of polish of the copper tray on the rate of degradation: it seemed possible that light reflected from the metal, particularly from a highly polished surface such as one can obtain with copper, might significantly affect the rate of degradation and (c) the region of polymer film-thickness in which it was possible to work without any complications caused by rate-controlling diffusion of monomer or non-uniform heating.

(a) *Skin effect*—Using the same method as Cowley and Melville<sup>2</sup> it was found that light of wavelength  $2\,537\text{ \AA}$  initiates the reaction. From the fact that the absorption of light of this wavelength, as measured on the spectrophotometer, is in the region of five per cent, it is possible to calculate that the skin effect for samples of the thickness used in the degradation experiments (0.004 cm) would be negligible.

(b) *Polish of the tray*—Evaluation of the effect on the reaction of different states of polish of the copper surface was carried out by measuring the actual rate of degradation of the same polymer, under identical conditions, except that the surface polish of the copper tray was varied. *Table 2* shows that the condition of the surface of the tray has no bearing on the rate of degradation.

*Table 2.* Rate of degradation for varying states of polish of tray

<i>State of polish of tray</i>	<i>Relative rate of degradation</i>
Very dull	4.90
Dull	4.66
Moderate polish	4.46
Highly polished	4.92

(c) *Film thickness*—To be in the region in which a chemical rate process is being measured rather than a physical rate process, the overall rate of reaction divided by the weight of sample should be constant. This was not so in the present work, the 'specific rate', i.e. the overall rate divided by the weight of sample, increased with decreasing weight. A graph of specific rate against film thickness is shown in *Figures 1* and *2* and it can be seen

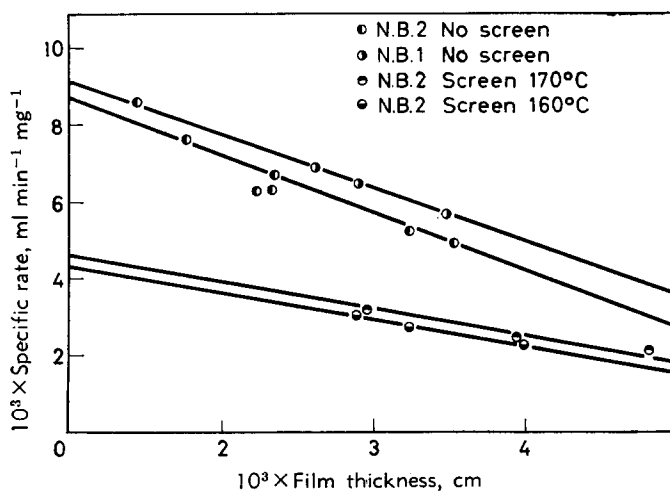


*Figure 1*—Specific rate versus film thickness, initially

that a fairly good linear relationship exists for each polymer sample, within the range of the experiments, both for initial rates and rates after 30 min irradiation. Another interesting linear relationship was found, as shown in *Figures 3* and *4*, in which  $\log$  (measured initial rate) is plotted against weight of sample.

As a further test some degradations were carried out in which the rate was assessed independently of the Pirani gauge. This was achieved by degrading various weights of N.B.4 for 15 min, in which time about nine per cent was volatilized. The rate per minute was calculated by dividing



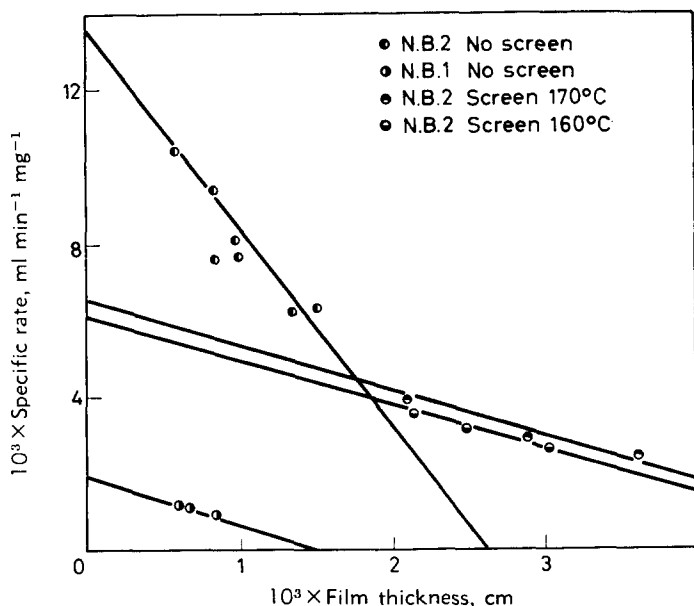


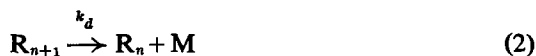
Figure 2—Specific rate versus film thickness, after 30 min irradiation

the total weight of monomer evolved by the time of irradiation. This is a very approximate method of rate measurement, but provided the total degradation is small the error involved will not be excessive. It is apparent from Figures 5 and 6 that this measurement of rate finds the same rate/weight relationships as those made using the Pirani gauge. The error in measuring the rate increases with decreasing sample weight.

A series of experiments was carried out using trays with differing radii. It was possible by this method to study specific rates of degradation with varying surface area/film thickness ratios. The results are plotted in Figures 7 and 8. There is a linear plot for specific rate against film thickness for each tray and yet the log (rate) versus weight plot accommodates all the points on a straight line.

### Mechanism

It seemed necessary at this stage to find out as much as possible about the mechanism of the reaction before attempting to unravel the kinetics. Without making any assumptions about the mode of initiation it is possible to find whether the termination reaction is first or second order. The depropagation process is assumed to be the exact reverse of propagation in polymerization.



The rate of production of monomer  $d[M]/dt = k_d [R]$ , in which  $[M]$  and  $[R]$  are the concentrations of monomer, and polymer radicals respectively, and  $k_d$  the rate constant for the depropagation step. Let the rate of termination be  $k_t' \times [R]$ , for the first order reaction and  $k_t [R]^2$  for second order. If the initiation reaction is stopped by cutting out the radiation then

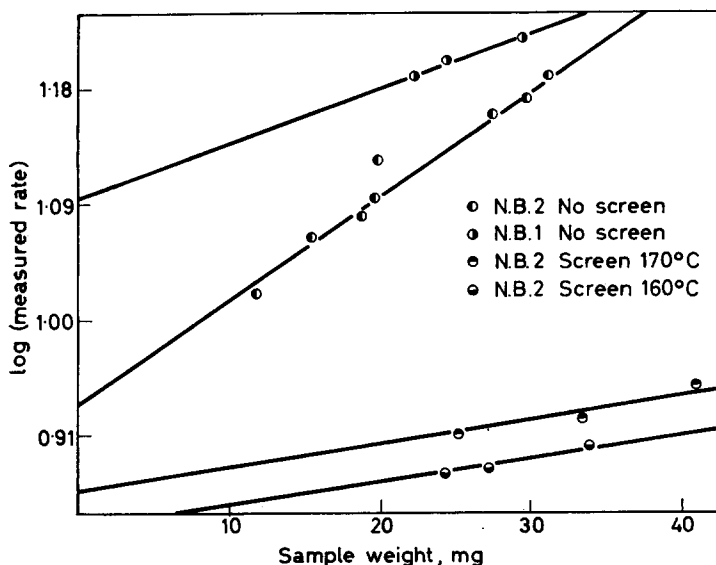


Figure 3—Log (measured rate) versus sample weight, initially

the rate of disappearance of radicals  $-d[R]/dt = k'_t \times [R]$ , or  $k_t [R]^2$ , depending on whether termination is first or second order.

$$\begin{array}{ll}
 \text{First order} & \text{Second order} \\
 -d[R]/dt = k'_t [R] & -d[R]/dt = k_t [R]^2 \quad (3)
 \end{array}$$

On integration

$$\log [R_0] - \log [R] = k'_t t \qquad 1/[R] - 1/[R_0] = k_t t \quad (4)$$

where  $[R_0]$  is the concentration of radicals when the illumination ceased,

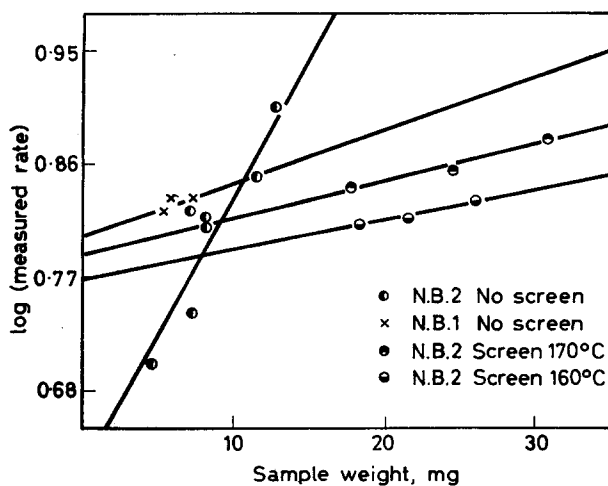
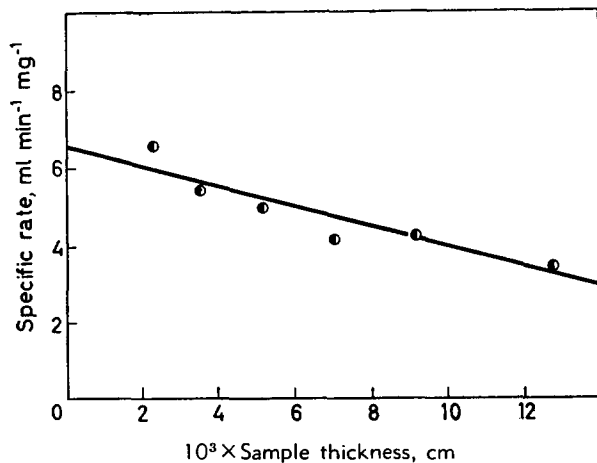


Figure 4 — Log (measured rate) versus sample weight, after 30 min irradiation

Figure 5—Specific rate versus film thickness by non-Pirani measurement, using N.B.4 (no screen)



and  $[R]$  is the concentration at time  $t$ . Since  $d[M]/dt = k_d [R]$  then

$$\begin{aligned} \log r_0 - \log r &= k't \\ 1/r - 1/r_0 &= kt \end{aligned} \tag{5}$$

where  $r_0$  is the rate on stopping irradiation and  $r$  the rate at time  $t$ . Thus a graph of  $\log r$  against  $t$ , or  $1/r$  against  $t$ , will determine whether the termination reaction is first or second order. From Figure 9 it can be seen that for polymer N.B.2 the termination reaction is bimolecular.

Certain speculative conclusions have already been made<sup>11</sup> regarding the mechanism of the photodegradation of poly-*n*-butyl methacrylate in its relation to the thermal reaction. They were based on percentage rate versus percentage degradation curves which have since been found to contain a

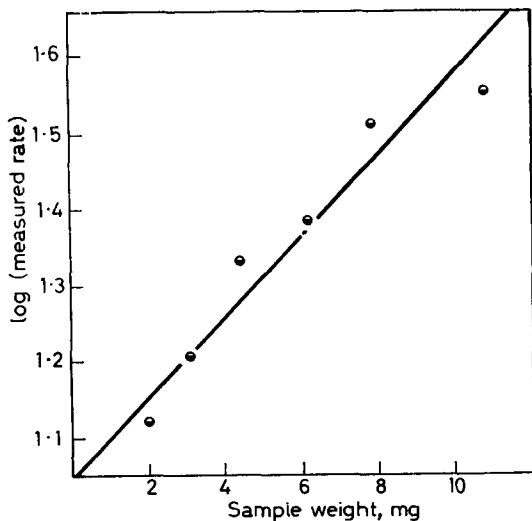


Figure 6—Log (measured rate) versus sample weight. Rates measured independently of Pirani gauge using N.B.4 (no screen)

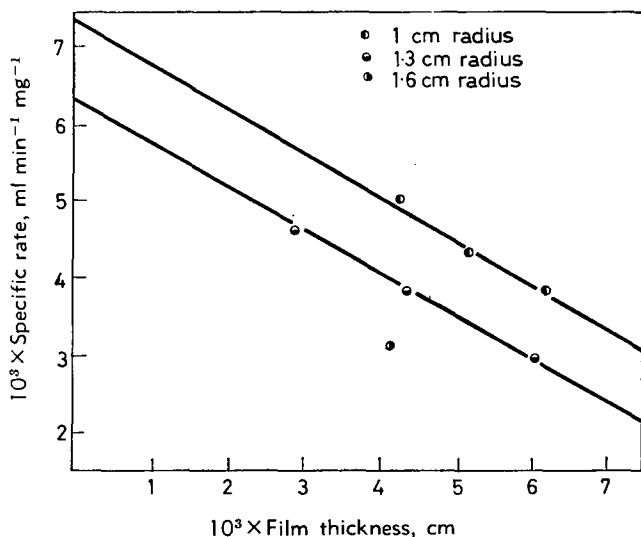


Figure 7—Specific rate versus film thickness using trays of varying sizes

systematic error in the estimation of the percentage degradation. Furthermore this type of evidence can be misleading in that given certain conditions it is impossible to distinguish between a random or chain-end initiated reaction<sup>12</sup>.

The change in molecular weight with progressing degradation can often be useful in elucidating the mechanism of degradation of a polymer. It should be noted that this evidence alone is insufficient to decide finally whether a polymer molecule suffers random or chain-end scission<sup>13</sup>.

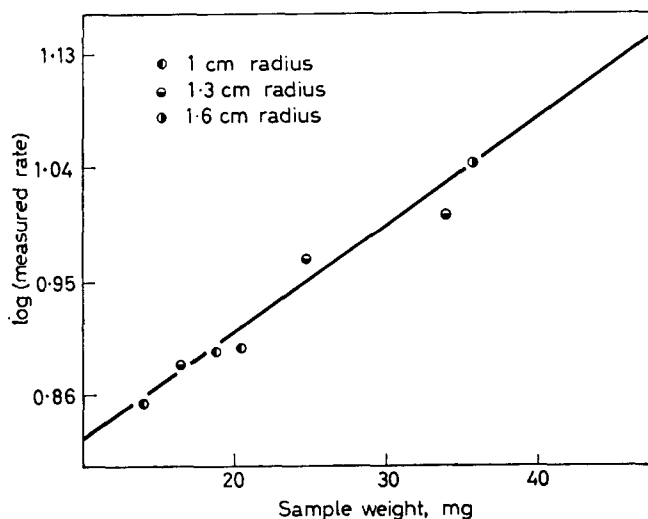


Figure 8—Log (measured rate) versus sample weight

Figure 10 shows how the molecular weights of polymers N.B.2 and N.B.6 change with percentage degradation. The shape of these curves suggests that the reaction is end-initiated and also that for N.B.6 the kinetic chain length is greater than the molecular chain length. No measurements were made to verify whether the termination reaction for N.B.6 was first or second order. Because of the unusual rate/weight relationship it was impossible to make a direct rate comparison with samples of varying molecular weight. However, by measuring the overall percentage degradation under standard conditions it was possible to deduce, at least qualitatively, that the rate of degradation increased slowly with increasing molecular weight. This fact was also apparent from the log (rate) versus weight plots. However, over the fairly wide range of molecular weights used there was but a slight increase in rate.

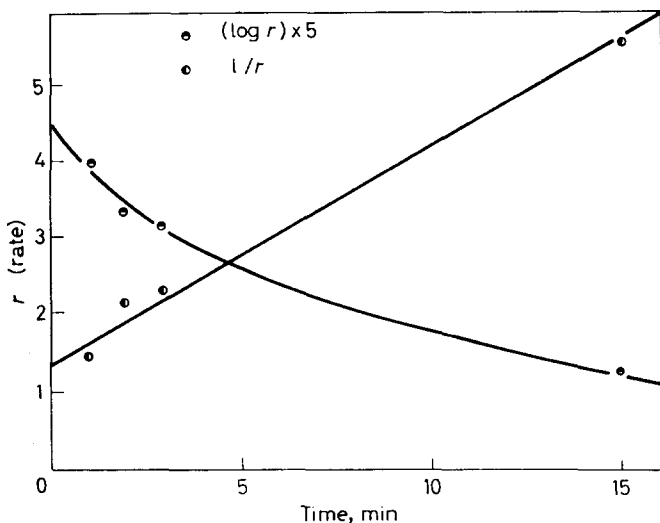


Figure 9—Decay of rate of reaction ( $r$ ) with time, on ceasing irradiation

In order to help clarify the apparent contradiction of the molecular weight/conversion and rate/molecular weight evidence some experiments were attempted whereby the chain-ends at which initiation was likely to occur, i.e. the  $C=C$  units<sup>2</sup>, were modified. A sample of polymer N.B.2 was thermally degraded to completion at 250°C, this was about 29 per cent volatilization. The mechanism of thermal degradation has already been discussed<sup>11</sup>. This thermally degraded polymer was then subjected to ultra-violet radiation and the rate was found to be very much less than that for the untreated polymer. If the photoreaction had been initiated at the same centres as the thermal reaction then the treated polymer should not have degraded at all on irradiation. Chemical modification was tried by bubbling hydrogen through a solution of polymer in chloroform containing a suspension of palladium charcoal catalyst. This treatment had no effect on the intrinsic viscosity of the polymer. It was hoped that some at least of

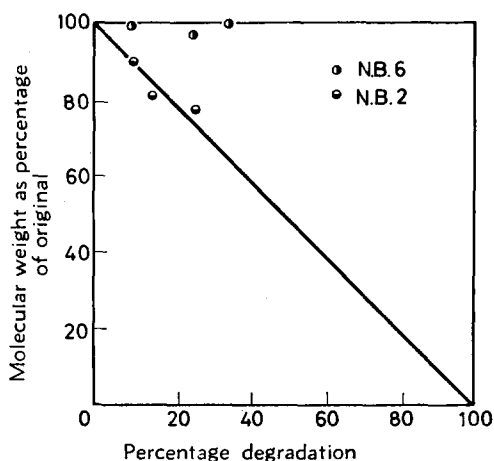


Figure 10—Change of molecular weight with extent of degradation

the unsaturated terminal units would be reduced, as Schultz, Henrici and Olive<sup>14</sup> have shown that this type of hydrogenation is successful. The rate of depolymerization of this sample was exactly the same as for the normal polymer. It was concluded from these experiments that initiation was not taking place solely at the terminal unsaturated units.

As a consequence of this unusual rate/weight relationship the overall percentage degradation increases with decreasing weight, under otherwise identical conditions. A few brief experiments were carried out on samples of poly(methyl methacrylate). They were irradiated under identical conditions as the *n*-butyl ester and the extent of degradation measured. The results are shown in Table 3, from which it is seen that the conversion to monomer after 30 min irradiation increases with decreasing weight, suggesting that under these conditions a similar weight/rate relationship holds for poly(methyl methacrylate) as does for poly(*n*-butyl methacrylate). No actual rate measurements were made on the poly(methyl methacrylate) samples and although these measurements are somewhat scanty, they are, nevertheless, of interest.

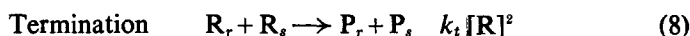
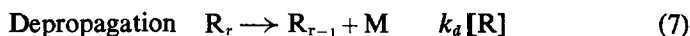
Table 3. Extent of degradation of two samples of polymethyl methacrylate under identical conditions

Sample	Weight of sample (mg)	Percentage degradation
A	51.1	55
	39.2	60
	30.8	61
	20.9	64
B	33.0	57
	26.4	64

#### DISCUSSION

The photodegradation of poly(*n*-butyl methacrylate) is an uncomplicated depolymerization process with no interference from the ester group such as

occurs in the thermal reaction<sup>11</sup>. Assuming there is no transfer the following kinetic scheme can be proposed:



$Q$  is the primary quantum efficiency, and  $I_a$  the rate of light absorption. If concentrations are expressed in mole/cm<sup>3</sup>,  $I_a$  will be given in einstein/cm<sup>2</sup>/sec, and in quanta/cm<sup>2</sup>/sec when concentrations are in molecules/cm<sup>3</sup>.

The rate of production of monomer  $d[M]/dt$  is given by

$$d[M]/dt = (k_d/k_t^{\frac{1}{2}}) (QI_a)^{\frac{1}{2}} \quad (9)$$

The average rate of light absorption over the entire sample is

$$I_a = A(I_0 - I)/V \quad (10)$$

in which  $I_0$  is the incident light per unit area per second,  $I$  the light transmitted per unit area per second,  $A$  the area of sample irradiated and  $V$  the volume of sample. In the present case the whole sample is irradiated and for a given tray  $A$  is constant,  $V$  varies with weight.

According to Beer's law  $\log I_0/I = kcl$ , where  $k$  is the extinction coefficient,  $c$  the concentration of absorbing species, and  $l$  the sample thickness. Therefore

$$1 + \log I_0/I = 1 + kcl \quad (11)$$

and

$$\log(1 + \log I_0/I) = \log(1 + kcl) \quad (12)$$

Experimentally  $I/I_0 = 0.95$  and so  $I_0/I$  is slightly greater than unity, therefore  $\log(I_0/I)$  is numerically small. Making this approximation gives

$$\log I_0/I = \log(1 + kcl) \quad (13)$$

from which it can be deduced that

$$(I_0 - I)I = kcl \quad (14)$$

and assuming that  $I_0 \approx I$  gives

$$I_0 - I = I_0 kcl \quad (15)$$

Substituting in equation (10)

$$I_a = AI_0 kcl / V \quad (16)$$

and since

$$A \times l = V, \quad I_a = I_0 kc \quad (17)$$

Therefore under the experimental conditions used, that is  $I/I_0 \approx 1$ , the average rate of absorption of light is independent of the thickness, and thus of the weight of the sample. Equation (9) now becomes

$$d[M]/dt = (k_d/k_t^{\frac{1}{2}}) (QI_0 kc)^{\frac{1}{2}} \quad (18)$$

Nothing definite is known about  $c$ , the concentration of initiating species, but regardless of its value the initial specific rate of degradation should be independent of weight of sample taken. It seems certain therefore, from *Figures 1 to 8*, that under the present circumstances a physical process is rate controlling.

It is very difficult to assess the role of bulk viscosity of polymer in degradation, particularly in light of recent postulates by Benson and North<sup>15</sup>. However, diffusion control of the termination step can be ruled out as the cause of the present kinetic difficulties, since this would result in a concentration dependent phenomenon, and thus would not be a function of sample weight.

The most likely cause of this abnormal rate/weight relationship would be repolymerization of monomer before it could escape from the film



Qualitatively the results show the correct trend, i.e. faster specific rates for thinner films. However, the results of the experiments carried out with trays of varying geometry do not support this hypothesis. In *Table 4* the overall rates for similar masses in the trays are compared. The films differ quite considerably in thickness, yet the measured rates are comparable. The fact that the rates for the different trays fit the same log (rate) against weight plot supports the evidence that diffusion of monomer out of the film is not rate controlling.

*Table 4*

<i>Weight of sample</i>	<i>Thickness of films (cm × 10<sup>3</sup>)</i>	<i>Measured rate (ml/min × 10<sup>3</sup>)</i>
16.5	2.9	7.1
17.6	5.2	7.6
34.3	6.1	10.1
35.6	4.2	11.0

A similar type of specific rate/sample thickness plot has been observed for the thermal degradation of poly(styrene) and poly(methyl methacrylate)<sup>16</sup>. Here temperatures of 300°C and above were used, and as this is well above the ceiling temperature region of these two polymers repolymerization would be most unlikely to cause the depression in specific rate. It was shown that only for very thin films, of the order of 100–200 Å, could one obtain specific rates which were independent of film thickness.

The likely explanation for the observed results is uneven heating. Although in the photochemical experiments the whole sample will be initially at the reaction temperature, rapid evaporation of monomer will cause thermal gradients, and thus different rates, at varying depths in the sample. The experiments using different sized trays would not test this possibility as heat is transmitted from the sides, as well as from below,

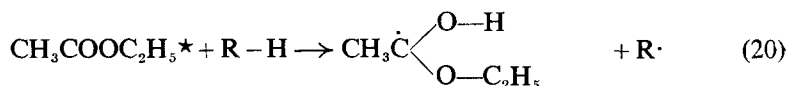


resulting in the total surface area exposed to copper being similar for each tray. It is worth noting that in the present photochemical experiments and in the work of Barlow *et al.*<sup>16</sup> the rates of degradation, and therefore heat-loss, were much higher than those measured by Grassie and Melville<sup>3</sup> who found the rate to be independent of sample size for films up to 0.3 mm thick. It would appear to be coincidental that this thermal effect on the overall rate is a linear function of film thickness, for both photochemical and thermal degradations.

The mechanism of degradation is not the same as that postulated by Cowley and Melville<sup>2</sup> for poly(methyl methacrylate). The experiments carried out on chemically modified polymer show that the unsaturated terminal units are not the only centres of initiation. Furthermore the polymers degraded to very much more than 50 per cent volatilization, the limit expected for an end-initiated mechanism similar to that of poly(methyl methacrylate). This was also true for samples of that polymer degraded under the same conditions as the *n*-butyl ester.

Although the plot of percentage molecular weight against percentage degradation supports an end-initiated reaction Simha, Wall and Bram<sup>13</sup> have shown how, given the appropriate combination of molecular chain length and kinetic chain length, such a curve can be obtained for a randomly initiated reaction. The remaining facts, increasing rate with increasing molecular weight and rates depressed but not stopped by changing the chemical composition of the end groups, suggest a randomly occurring chain scission.

It is proposed that initiation takes place at some site, other than the terminal units, in the polymer molecule, notwithstanding that initiation can concurrently occur at the unsaturated chain-ends. Recently Ausloos and Rebbert<sup>17</sup> have presented evidence of quenching of an excited triplet state, produced during liquid phase photolysis of ethyl acetate, by H atom abstraction from solvent molecules



If a similar reaction took place in the photolysis of poly-*n*-butyl methacrylate in which the H atom was provided by another chain, then R could disproportionate internally giving random scission, and depolymerization. This mechanism is, however, speculative.

One or two factors observed in the present work are in common with Cowley and Melville's results. They found a trend to increased rates with increasing molecular weight. The samples they used could be degraded to over 80 per cent volatilization (see *Figure 5* of reference 2a). However, Cowley and Melville found the specific rate to be independent of sample thickness. There is no apparent explanation for the difference in mechanism of photodegradation of poly(methyl methacrylate) and poly(*n*-butyl methacrylate).

In summary it can be said that the photo-initiated degradation of poly-(*n*-butyl methacrylate) is similar to the photo-initiated reaction of poly(methyl methacrylate) in solution, in that random scission of the polymer molecules occurs. It has been found impossible to measure the

true kinetics of the reaction due to some physical process becoming rate-controlling. Temperature gradients, due to poor heat transfer, are tentatively suggested as the cause of the unusual rate/weight relationship.

*The author wishes to acknowledge the award of an I.C.I. Fellowship by the University of Aberdeen during the tenure of which part of this work was done.*

*Department of Chemistry,  
The University, Aberdeen*

*(Received June 1963)*

#### REFERENCES

- <sup>1</sup> GRASSIE, N. *Chemistry of High Polymer Degradation Processes*. Butterworths: London, 1956
- <sup>2a</sup> COWLEY, P. R. E. and MELVILLE, H. W. *Proc. Roy. Soc. A*, 1951, **210**, 461
- <sup>2b</sup> COWLEY, P. R. E. and MELVILLE, H. W. *Proc. Roy. Soc. A*, 1952, **211**, 320
- <sup>3</sup> GRASSIE, N. and MELVILLE, H. W. *Proc. Roy. Soc. A*, 1949, **199**, 1
- <sup>4</sup> MONIG, H. *Naturwissenschaften*, 1958, **45**, 12
- <sup>5</sup> SCHULTZ, A. R. *J. phys. Chem.* 1961, **65**, 967
- <sup>6</sup> CHARLESBY, A. and THOMAS, D. K. *Proc. Roy. Soc. A*, 1962, **269**, 104
- <sup>7</sup> BUECHE, F. *Physical Properties of Polymers*. Interscience: New York, 1962
- <sup>8</sup> MELVILLE, H. W. *Trans. Faraday Soc.* 1936, **32**, 1525
- <sup>9</sup> MASSON, C. and MELVILLE, H. W. *J. Polym. Sci.* 1949, **4**, 337
- <sup>10</sup> MENCIK, Z. *Chem. Listy*, 1952, **46**, 407
- <sup>11</sup> GRASSIE, N. and MacCALLUM, J. R. *J. Polym. Sci.* In press
- <sup>12</sup> SIMHA, R. *Coll. Czech. chem. Commun.* 1957, **22**, 250
- <sup>13</sup> SIMHA, R., WALL, L. A. and BRAM, J. *J. chem. Phys.* 1958, **29**, 894
- <sup>14</sup> SCHULTZ, G. V., HENRICI, G. and OLIVE, S. Z. *Elektrochem.* 1956, **60**, 296
- <sup>15</sup> BENSON, S. W. and NORTH, A. N. *J. Amer. chem. Soc.* 1959, **81**, 1339
- <sup>16</sup> BARLOW, A., LEHRLE, R. S. and ROBB, J. C. *Makromol. Chem.* 1962, **54**, 230
- <sup>17</sup> AUSLOOS, P. and REBBERT, R. E. *J. phys. Chem.* 1963, **67**, 163

# *Sequence Length Distributions and Entropy of Stereoregularity in Homopolymers of Finite Molecular Weight*

A. M. NORTH and D. RICHARDSON

*Equations are derived for the mean sequence length, the sequence length distribution and the entropy associated with the rearrangement of these sequences in tactic homopolymers or binary copolymers of finite molecular weight. The treatment requires that each addition be described by a single probability factor, and that the degree of polymerization is more than six times the mean sequence length. It is found that the mean sequence length is rather insensitive to molecular weight, but that the number fraction of sequences of length  $m$  and the entropy of sequence rearrangement are appreciably dependent on molecular weight when the polymer contains less than a thousand monomer units. Errors in the limiting [infinite degree of polymerization] equations for these two quantities are particularly important for isotactic polymers. Numerical values of the entropy, designated the entropy of stereoregularity when applied to the case of a tactic homopolymer, are reported over a range of degrees of polymerization, 2 000 to 20.*

WHENEVER a linear polymer molecule is built up from a number of distinguishable units arranged in sequences of varying lengths, the total entropy of the polymer molecule contains an increment due to the possibilities of internal rearrangement of these units. In a copolymer formed from two different monomers, the distinguishable units are derived from each monomeric species. A homopolymer capable of exhibiting stereoregularity (for example the addition polymer formed from  $\text{CH}_2=\text{CXY}$ ) is built up from units which contain an asymmetric carbon atom. The homopolymer can then be considered as a copolymer of the D- and L-derivatives of the same monomer, and must consist of alternate sequences of each isomeric type

... DLLDDDDLDLL ...

For convenience the entropy increment due to the number of possible permutations of these sequences in the molecule will be called 'the entropy of stereoregularity'.

The analogous case of a copolymer

... ABBAAAAABABB ...

has been examined by Orr<sup>1</sup>, who computed the number of ways of arranging the A sequences in the polymer molecule. From this number the corresponding entropy was evaluated as

$$S/k = -P \ln P - (1 - P) \ln (1 - P) \quad (1)$$

where  $P$  was the probability that an A unit in the chain would be followed by another A unit and  $k$  was Boltzmann's constant. Orr has pointed out that this equation is only exact if the permitted number of units in the

longest sequence is infinite. The derivation also contains the basic requirement that the number of sequences in the molecule is very large, so that the degree of polymerization of the molecule under study has to be doubly great. This requirement may cause some difficulty in assessing the exact applicability of equation (1) in practical cases. Furthermore the result is only applicable exactly when  $P_{AA} = P_{BB}$ , a condition which does not apply in many copolymerizations.

The sequence length distributions in homopolymers have been discussed by Coleman<sup>2</sup>, Miyake<sup>3</sup> and Miller and Nielsen<sup>4</sup>. The approach of Coleman and of Miller and Nielsen is based upon the probability of a particular type of addition, whereas that of Miyake is based upon the energy difference between the possible isomers formed. In the present context the former approach is more useful, and will be extended to cover the case of low molecular weight polymer and  $P_{AA} \neq P_{BB}$ . Since many observations of polymer tacticity are based upon measurements of crystallinity of samples of differing molecular weights, it is essential that the usual equations<sup>2,4</sup> for the number fraction of sequence lengths be examined over a range of molecular weights.

Since the entropy of polymerization is often required for polymers of low molecular weight, and since the entropy of stereoregularity is an increment in this term, it is necessary to know the precise sequence length distribution and the entropy relationship of which equation (1) is the limiting form. These variations in the entropy of polymerization might be observable as changes in a phenomenon such as the ceiling temperature of polymerization

$$T_c = \Delta H / \Delta S \quad (2)$$

where  $\Delta H$  and  $\Delta S$  are respectively the enthalpy and entropy changes per mole of monomer as it is converted to polymer.

Since the formation of a polymer molecule takes place step by step, and the way in which a monomer unit adds to a growing polymer chain depends on its configuration with respect to the active terminal unit, this configuration can be traced back until it is considered relative to the initial monomer unit. In the derivation of the sequence length distribution and mean sequence length outlined below, the symbols D and L will be applied to the configuration of a unit with respect to the beginning of the polymer chain, and not to the absolute asymmetry of the unit.

In this paper are described the sequence length distribution, the entropy of stereoregularity, and the ceiling temperature for homopolymers of finite molecular weight. Parts of the treatment are also applicable to normal copolymers in which  $P_{AA} \neq P_{BB}$ .

#### THE SEQUENCE LENGTH DISTRIBUTION

This treatment will make use of two types of quantity. Parameters, subscript  $j$ , will refer to the  $j$ th sequence of D units in a reference molecule which will be an average or typical specimen chosen from a large number of molecules. Quantities, superscript bar, will refer to average values, independent of position in the molecule.

Let  $\rho_{mj}$  be the probability that the  $j$ th D sequence in a reference molecule contains  $m$  monomer units, and let  $P$  be the probability that, in forming the chain, the unit adding to a terminal D unit will take up the same configuration. Then

$$\rho_{mj} = \{(1-P)/P\} P^m + A_j \quad m < x - \sum_{i=1}^{i=j-1} b_i \quad (3)$$

where  $A_j$  is the probability that the  $j$ th D sequence is also the last sequence in the molecule and is curtailed to length  $m$  by this fact,  $b_i$  is the number of D units which in fact exist in the  $i$ th D sequence of this molecule, and  $x$  is the total number of D units in the molecule.

Applying the normalization condition that the probability of forming the  $j$ th sequence is unity if  $x > \sum_{i=1}^{i=j-1} b_i$ , then

$$\{(1-P)/P\} \sum_{m=1}^{m=y_j} P^m = 1 - A_j \quad y_j = x - \sum_{i=1}^{i=j-1} b_i \quad (4)$$

where  $y_j$  is the maximum possible length for the  $j$ th sequence. Now let  $n_D$  and  $n_L$  be the total number of D and L sequences in the molecule. Then

$$A_j = 0 \quad j \neq n_D \quad (5)$$

If the last sequence in the molecule contains D-units

$$\rho_{m, n_D} = P^{m-1}$$

then

$$A_{n_D} = [n_D / (n_D + n_L)] \times P^m \quad (6)$$

Advancing now to quantities descriptive of the 'average' sequence in the molecule, and denoting by  $\bar{a}_m$  the average number of D sequences of length  $m$  in the molecule

$$\bar{a}_m = \sum_{j=1}^{j=n_D} \rho_{mj} = n_D (1-P) P^m / P + \sum_{j=1}^{j=n_D} A_j \quad m < x - \bar{m} (\bar{j} - 1) \quad (7)$$

where  $\bar{m}$  and  $\bar{j}$  are respectively the length and position of the 'average' D sequence in the molecule. Evaluation of the  $A_j$  terms gives

$$\bar{a}_m = n_D P^{m-1} [P / (n_D + n_L) + 1 - P] \quad (8)$$

The average D sequence length is

$$\bar{m} = x / n_D = (1/n_D) \sum_{m=1}^{m=\bar{y}} m \bar{a}_m \quad (9)$$

where  $\bar{y}$  is the largest permissible number of units which may be accommodated in a sequence being formed in the  $j$ th position. Then

$$x = \sum_{m=1}^{m=\bar{y}} m \bar{a}_m = \frac{n_D \left( \frac{P}{n_D + n_L} + 1 - P \right)}{(1-P)^2} \{1 + P^{\bar{y}} (1 + \bar{y} [1 - P])\} \quad (10)$$

From the sum of the first  $n_D$  natural numbers, and the fact that the  $j$ th sequence occurs only once in the molecule,

$$\bar{j} = \frac{1}{2}(n_D + 1) \quad (11)$$

so that

$$\bar{y} = \frac{1}{2}(x + \bar{m}) \quad \bar{m} < \frac{1}{3}x \quad (12)$$

and

$$x = \frac{\left(\frac{n_D}{n_D + n_L} + \frac{x}{\bar{m}}[1 - P]\right)}{(1 - P)^2} \left\{1 - P^{\frac{1}{2}(x + \bar{m})} \left[1 + \frac{1}{2}(1 - P)(x + \bar{m})\right]\right\} \quad (13)$$

Now  $x_D/z = \frac{1}{2}(1 + P_D + P_L)$  where subscripts D, L are applied to quantities relevant to D and L unit sequences respectively, and  $z$  is the degree of polymerization. Then

$$\bar{m}_D^{-1} = \frac{1 - P_D}{F_D} - \frac{2P_D}{z(1 - P_D)(1 + P_D - P_L) \left(1 + \frac{\bar{m}_D(1 + P_L - P_D)}{\bar{m}_L(1 + P_D - P_L)}\right)} \quad \bar{m}_D < \frac{1}{3}x_D \quad (14)$$

$$\bar{m}_L^{-1} = \frac{1 - P_L}{F_L} - \frac{2P_L}{z(1 - P_L)(1 + P_L - P_D) \left(1 + \frac{\bar{m}_L(1 + P_D - P_L)}{\bar{m}_D(1 + P_L - P_D)}\right)} \quad \bar{m}_L < \frac{1}{3}x_L$$

where

$$F_s = 1 - P_s^{\frac{1}{2}(x_s + \bar{m}_s)} \left[1 + \frac{1}{2}(1 - P_s)(x_s + \bar{m}_s)\right] \quad \bar{m}_s < \frac{1}{3}x_s$$

Finally, equation (8) can be rewritten as two equations descriptive of D and L sequences

$$\bar{a}_{m_D} = \frac{P_D^{m_D-1}(1 + P_D - P_L)}{2\bar{m}_D} \left\{z(1 - P_D) + \frac{P_D}{\frac{1 + P_D - P_L}{2\bar{m}_D} + \frac{1 + P_L - P_D}{2\bar{m}_L}}\right\} \quad (15)$$

$$\bar{a}_{m_L} = \frac{P_L^{m_L-1}(1 + P_L - P_D)}{2\bar{m}_L} \left\{z(1 - P_L) + \frac{P_L}{\frac{1 + P_D - P_L}{2\bar{m}_D} + \frac{1 + P_L - P_D}{2\bar{m}_L}}\right\}$$

The simultaneous equations (14) can be solved for  $\bar{m}_D$ ,  $\bar{m}_L$ , using successive approximations, starting from the limiting condition for infinite  $n_s$ ,

$$x_s \text{ Lim. } \bar{m}_s^{-1} \rightarrow 1 - P_s \quad (16)$$

Substitution in equation (15) then yields the two sequence length distributions as functions of  $z$ ,  $P_D$  and  $P_L$  only.

The numerical procedures involved in solving the simultaneous equations (14) are conceptually simple but laborious in practice. However, the solution must be pursued when the system under study is a copolymer for which the two monomer reactivity ratios are unequal.

The case of a homopolymer is rather different, and requires a more precise examination of the meaning of D and L units. Two situations are immediately apparent. These exist when the two ends of the polymer chain are, or are not, distinguishable once the polymerization reaction is completed.

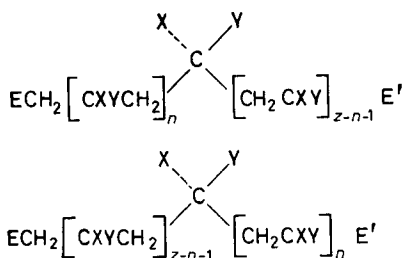


Figure 1—The symmetry of polymer chains

When the polymer chain belongs to space group  $C_s$ , there are two discontinuities in the formation of optical stereosequences, one at the centre and one at the end of the chain. The probabilities  $P_D$ ,  $P_L$  formally undergo an interconversion as the molecule passes the midpoint of its growth. Consequently for the whole chain  $P_D = P_L = \bar{P}$ . Such a situation may exist in poly-substituted methylenes, in certain 1,2 disubstituted olefins, or in certain olefin oxide polymers, and can be visualized from *Figure 1* in which  $E-CH_2-$  is identical with  $E'-$ .

When the polymer chain possesses no plane of symmetry, the only discontinuity in the formation of stereosequences occurs at the chain end. Since most vinyl polymerizations involve a head-to-tail addition of monomer units, they fall into this group [*Figure 1*].

Unless an optically active catalyst causes asymmetric induction during chain growth,  $P_D = P_L = \bar{P}$ , and

$$\bar{m}^{-1} = \frac{1 - \bar{P}}{F} - \frac{\bar{P}}{2x(1 - \bar{P})} \quad \bar{m} < \frac{1}{2}x \quad (17)$$

where

$$F = 1 - \bar{P}^{1+(x+\bar{m})} \left[ 1 + \frac{1}{2}(x + \bar{m})(1 - \bar{P}) \right]$$

$$\bar{a}_m = \bar{P}^{m-1} \left[ \frac{1}{2}\bar{P} + (x/\bar{m})(1 - \bar{P}) \right] \quad (18)$$

The number fraction of D sequences containing  $m$  units is

$$N_{Dm} = \frac{2\bar{a}_m\bar{m}}{z} = \frac{\bar{m}\bar{P}^m}{z} + \bar{P}^{m-1}(1 - \bar{P}) \quad (18a)$$

$\bar{P}^{m-1}(1 - \bar{P})$  is the conventional number fraction derived for polymer of infinite molecular weight, so that the term  $\bar{m}\bar{P}^m/z$  represents the correction for molecular weight effects. The percentage error in the limiting expression is thus  $\bar{P}\bar{m}10^3/z(1 - \bar{P})$ . For  $\bar{P}=0.1, 0.5, 0.9$  [representing

syndiotactic, atactic and isotactic polymer respectively] this error is of magnitude one per cent when the respective degrees of polymerization are 10, 200 and 10 000. Consequently the conventional relationship is a poor approximation for isotactic polymers.

The large increase in  $N_{Dm}$  in low molecular weight polymers is highly significant when interpretations of polymer tacticity are made from extent of crystallinity. These results show quite conclusively that comparison of X-ray diagrams for high and low molecular weight polymers<sup>5</sup> must be interpreted with caution, and cannot be taken as a simple measure of variations in  $\bar{P}$ .

The quantity  $\bar{m}$  turns out to be rather insensitive to variations in  $x$ , and differs from  $(1 - \bar{P})^{-1}$  by more than one per cent only when  $x < 10\bar{m}$ .

#### THE ENTROPY OF SEQUENCE REARRANGEMENT

The number of ways,  $\Omega$ , in which  $n$  sequences, containing the same type of unit but having a distribution of sequence lengths, can be arranged in a polymer molecule is

$$\Omega = n! / \prod_{m=1}^{\bar{m}} \bar{a}_m! \quad (19)$$

The entropy per monomer unit associated with these arrangements is

$$S = \mathbf{k} \left( \frac{\ln n! - \sum_{m=1}^{\bar{m}} \ln \bar{a}_m!}{\sum_{m=1}^{\bar{m}} m \bar{a}_m} \right) \quad (20)$$

An additional term,  $-\mathbf{k} \ln 2/x$ , is required for chains with  $\sigma_h$  symmetry.

Two extreme cases are immediately apparent, perfect isotactic polymer,

$$n=1, \quad \bar{a}_m=0 \text{ when } m \neq z$$

$$\bar{a}_m=1 \text{ when } m = z$$

$$S=0 \quad (21)$$

Stirling's approximation  $(n/e)^n \sim n!$  can be used to evaluate  $\ln n!$  and  $\sum \ln \bar{a}_m!$  with an error of less than one per cent when  $x > 10\bar{m}$ , but for lower degrees of polymerization the factorials must be evaluated directly.

The summations of equation (20) can be evaluated (Appendix):

$$\sum_{m=1}^{\bar{m}} \bar{a}_m = \frac{\xi(1 - \bar{P}^{\bar{m}})}{(1 - \bar{P})} \quad (22)$$

$$\sum_{m=1}^{\bar{m}} m \bar{a}_m = \frac{\xi(1 - \chi \bar{P}^{\bar{m}})}{(1 - \bar{P})^2} \quad (23)$$

$$\sum_{m=1}^{\bar{m}} \bar{a}_m \ln \bar{a}_m = \frac{\xi(1 - \chi \bar{P}^{\bar{m}}) \ln \bar{P}}{(1 - \bar{P})^2} - \frac{\xi(1 - \bar{P}^{\bar{m}}) \ln \bar{P}}{(1 - \bar{P})} + \frac{\xi(1 - \bar{P}^{\bar{m}}) \ln \xi}{(1 - \bar{P})} \quad (24)$$



where

$$\xi = \frac{1}{2}\bar{P} + \bar{n}(1 - \bar{P}), \quad \chi = 1 + \bar{y}(1 - \bar{P}), \quad \bar{n} = z/2\bar{m} \quad (25)$$

The entropy of stereoregularity is given by

$$\begin{aligned} \frac{S}{k} = & \frac{1}{\bar{m}} \ln \frac{x}{\bar{m}} - \frac{1}{\bar{m}} + \frac{\xi \{(1 - \bar{P})(1 - \bar{P}^{\bar{y}}) - (1 - \chi \bar{P}^{\bar{y}})\} \ln \bar{P}}{x(1 - \bar{P})^2} \\ & - \frac{(1 - \bar{P}^{\bar{y}}) \xi \ln \xi}{x(1 - \bar{P})} + \frac{\xi(1 - \bar{P}^{\bar{y}})}{x(1 - \bar{P})} \end{aligned} \quad (26)$$

The substitutions,  $\bar{y} = \frac{1}{2}(x + \bar{m})$ ,  $x = \frac{1}{2}z$ , allow this entropy to be expressed in terms of  $\bar{m}$ ,  $z$  and  $\bar{P}$  only.

Equation (26) can be reduced to equation (1) as  $x + \bar{m}$  tends to infinity. The entropy of stereoregularity can be evaluated by solving equation (17) for  $\bar{m}$  and substituting in (26) or even in (20). Differentiation of equation (26) verifies the intuitive conclusion that the entropy of stereoregularity is

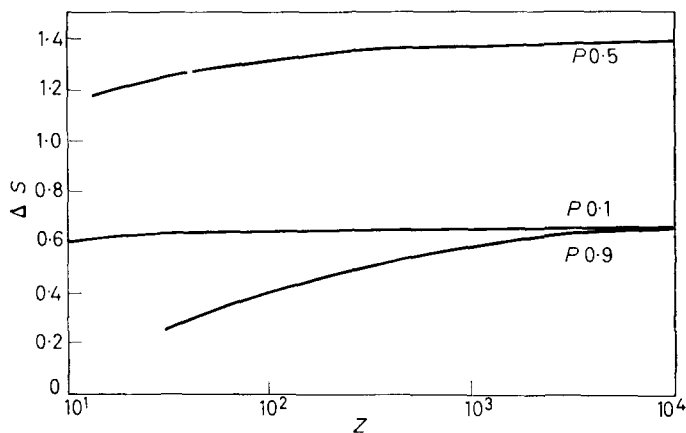


Figure 2—The entropy of stereoregularity

a maximum when  $\bar{P} = \frac{1}{2}$  for high molecular weights, but shifts slightly towards syndiotactic systems as the molecular weight is lowered.

Numerical solutions of the entropy of stereoregularity for polymers with distinguishable chain ends are listed in *Table 1*. Successive approximations for  $\bar{m}$  were continued until the variation was less than one part in a thousand, and Stirling's approximation was used to evaluate factorials when  $x$  was greater than  $20\bar{m}$ . The entropy/degree of polymerization dependence is illustrated graphically for syndiotactic, atactic and isotactic polymers in *Figure 2*, where it can be seen that the entropy is symmetrical about  $P = 0.5$  only at infinite molecular weights.

CEILING TEMPERATURES IN STEREOREGULAR  
POLYMERIZATIONS

The simplest definition of the ceiling temperature is that introduced in equation (2), the ratio of the heat of polymerization to the entropy of polymerization. Both of these quantities are values relevant under a particular set of experimental conditions, and may vary with solvent, monomer state, etc. The entropy of polymerization might also be expected to vary with the molecular weight of the polymer, so that polymer of each molecular weight should have a definite ceiling temperature. In view of this, the general ceiling temperature for a particular polymerization is taken as the limiting value for very high molecular weights<sup>9</sup>. An experimentally observable property, such as rate or degree of polymerization, usually becomes markedly reduced as the ceiling temperature is approached, and the limiting ceiling temperature is obtained by extrapolating a graph of the observed property against temperature<sup>9</sup>, as illustrated in *Figure 3*.

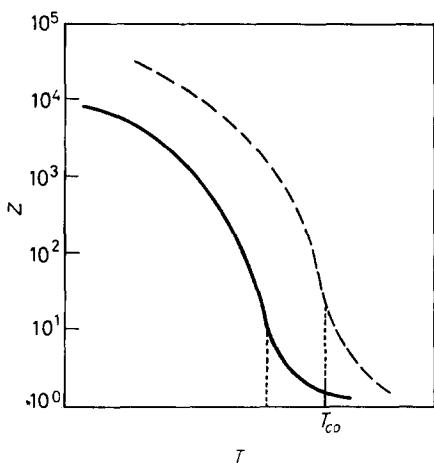


*Figure 3*—Molecular weight of polymer found in a particular reaction as a function of temperature. Solid line, stereoregular polymer; broken line, random polymer

In stereoregular polymerizations the limiting value of the ceiling temperature, involving polymerization to chains containing more than  $10^4$  monomer units, will depend on the entropy of stereoregularity calculated using equation (1). The entropy of polymerization for completely random polymer will thus be less negative than that for perfectly stereospecific polymer by 1.38 cal/degree if all other experimental conditions are maintained constant. The significance of this value can be appreciated by consideration of an example.

A system, for which  $\Delta H$  is  $-7$  kcal/mole (independent of stereo-form) and  $\Delta S$  for completely random polymer is  $-28$  cal/degree, will have limiting ceiling temperatures of  $-23^\circ\text{C}$  and  $-35^\circ\text{C}$  for completely random and perfectly stereospecific polymerizations respectively. These enthalpies and entropies of polymerization are approximately those observed in the polymerization of aldehydes, which polymerizations can yield polymers of varying stereoregularity<sup>6-8</sup>. The dependence of the ceiling temperature on  $\bar{P}$  should be experimentally measurable in such systems.

## ENTROPY OF STEREOREGULARITY

When the heat of polymerization is independent of the stereoregularity

$$\frac{1}{T_c} = \frac{1}{T_{co}} - \frac{1.38}{\Delta H} + \frac{\delta\Delta S}{\Delta H} \quad (27)$$

where  $T_{co}$  is the ceiling temperature for absolutely random polymer and  $\delta\Delta S$  is the entropy of stereoregularity. Measurement of  $T_c$ ,  $T_{co}$  and  $\Delta H$  then allows evaluation of  $\delta\Delta S$ , whereupon two possible values of  $\bar{P}$  can be found and *Table 1* yields the corresponding mean sequence lengths.

*Table 1.* Entropy of stereoregularity

P	Degree of polymerization								
	$\infty$	2 000	1 000	400	200	100	40	20	10
0.1	0.644	0.644	0.643	0.642	0.640	0.637	0.629	0.621	0.603
0.2	0.993	0.990	0.988	0.985	0.980	0.971	0.955	0.938	0.888
0.3	1.215	1.208	1.204	1.200	1.195	1.179	1.150	1.122	1.052
0.4	1.338	1.330	1.326	1.317	1.306	1.288	1.252	1.212	1.137
0.5	1.379	1.367	1.362	1.350	1.334	1.309	1.259	1.223	—
0.6	1.338	1.324	1.319	1.300	1.278	1.244	1.170	1.086	—
0.7	1.215	1.199	1.182	1.162	1.132	1.085	0.972	0.851	—
0.8	0.993	0.970	0.953	0.918	0.872	0.813	0.693	0.570	—
0.9	0.644	0.602	0.572	0.514	0.465	0.400	0.290	0.191	—

It is noticed that measurement of the ceiling temperature cannot differentiate between isotactic and syndiotactic polymer.

The 'tail' in the observed property/temperature plot appears to depend on the monomer, solvent and catalyst compositions<sup>9</sup> so that its exact form is unfortunately not obtainable from a simple general equation. However, the separation of the plots for random and stereoregular polymers can be calculated, when it is apparent that the two 'tails' converge as the molecular weight decreases.

### CONCLUSION

The influence of the chain end has been included in the calculation of the mean sequence length in polymers composed of two distinguishable units. The simultaneous equations for the mean sequence length of either unit are given in equation (14), which is also valid for two-monomer copolymers irrespective of molecular weight or monomer reactivity ratio. The particular case of stereoregular polymers, or of copolymers in which the two monomer reactivity ratios are equal, is extended in equation (17), and the mean sequence length has been used to evaluate the sequence length distribution (18) and the entropy associated with the rearrangement of the sequences (26). Numerical solutions of the entropy of stereoregularity have been recorded.

The usual approximation for the number fraction of sequences, length  $m$ , has been shown to be considerably in error for polymers containing less than a thousand monomer units, the errors being greatest for isotactic polymers.

Knowledge of the heat of polymerization and the ceiling temperatures for completely random and for any given polymer (known to be pre-

dominantly syndiotactic or isotactic) allows evaluation of the probability of forming two like units in succession in the chain, and hence the sequence length distribution.

The treatment reported is only applicable when the mean sequence length is less than one sixth of the degree of polymerization and when each addition is describable by a single probability (penultimate unit effects being negligible).

*Numerical evaluation of the quantities reported above was carried out on the Deuce computer of the University of Liverpool. The authors are indebted to the D.S.I.R. for a maintenance grant to one of them (D.R.).*

Donnan Laboratories,  
University of Liverpool

(Received June 1963)

## APPENDIX

### EVALUATION OF SUMMATIONS USED IN THE TEXT

$$\bar{a}_m = \xi \bar{P}^{m-1}$$

$$\begin{aligned} \text{A. } \sum_{m=1}^{m=\bar{y}} m \bar{a}_m &= \xi \sum_{m=1}^{m=\bar{y}} \frac{d\bar{P}^m}{d\bar{P}} = \xi \frac{d}{d\bar{P}} \left[ \frac{\bar{P}(1-\bar{P}^{\bar{y}})}{1-\bar{P}} \right] \\ &= \frac{\xi \{1-\bar{P}^{\bar{y}}[1+\bar{y}(1-\bar{P})]\}}{(1-\bar{P})^2} \end{aligned}$$

$$\begin{aligned} \text{B. } \sum_{m=1}^{m=\bar{y}} \bar{a}_m \ln \bar{a}_m &= \xi (\ln \bar{P}) \sum_{m=1}^{m=\bar{y}} m \bar{P}^{m-1} - \xi (\ln \bar{P}) \sum_{m=1}^{m=\bar{y}} \bar{P}^{m-1} + \xi (\ln \xi) \sum_{m=1}^{m=\bar{y}} \bar{P}^{m-1} \\ &= \frac{\xi (1-\bar{P}^{\bar{y}}) \ln \bar{P}}{(1-\bar{P})^2} - \frac{\xi (1-\bar{P}^{\bar{y}}) \ln \bar{P}}{(1-\bar{P})} + \frac{\xi (1-\bar{P}^{\bar{y}}) \ln \xi}{(1-\bar{P})} \end{aligned}$$

### REFERENCES

- <sup>1</sup> ORR, R. J. *Polymer, Lond.* 1961, **2**, 74
- <sup>2</sup> COLEMAN, B. D. *J. Polym. Sci.* 1958, **31**, 155
- <sup>3</sup> MIYAKE, A. *J. Polym. Sci.* 1960, **46**, 169
- <sup>4</sup> MILLER, R. L. and NIELSEN, L. E. *J. Polym. Sci.* 1960, **46**, 303
- <sup>5</sup> BURLEIGH, P. H. *J. Amer. chem. Soc.* 1960, **82**, 749
- <sup>6</sup> VOGL, O. *J. Polym. Sci.* 1960, **46**, 261
- <sup>7</sup> NATTA, G., MAZZANTI, G., CORRADINI, P. and BASSI, I. *Makromol. Chem.* 1960, **37**, 156
- <sup>8</sup> FURUKAWA, J., SAEGUSA, T., FUJII, H., KAWASAKI, A., IMAI, H. and FUJII, Y. *Makromol. Chem.* 1960, **37**, 149
- <sup>9</sup> DAINTON, F. S. and IVIN, K. J. *Quart. Rev. chem. Soc., Lond.* 1958, **12**, 61

# The Copolymerization of Methylmethacrylate and Maleic Anhydride

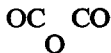
A. M. NORTH and D. POSTLETHWAITE

*A maximum is possible in the rate/composition curve for a copolymerization in which one monomer does not undergo homopolymerization and the termination reaction is diffusion controlled. The maximum can occur without any restriction on the value of the reactivity ratio,  $r_1$ , provided either that the propagation ratio  $k_{pab}/k_{pba}$  satisfies certain conditions, or that the termination reaction is impeded by the introduction of the second monomer into the polymer chain.*

*The copolymerization of methylmethacrylate and maleic anhydride in solution at 30°C (the total monomer concentration being maintained constant) has been shown to involve a diffusion-controlled termination step. The rate of termination decreases with increasing maleic anhydride content, as would be predicted if rearrangement of the conformations of the radical chain is the rate-determining step. The rate constant for addition of methylmethacrylate radicals to maleic anhydride is less than that for addition of maleic anhydride radicals to methylmethacrylate, as would be predicted on steric considerations. Accurate determination of the propagation rate constant, maleic anhydride radical plus methylmethacrylate, and of the hypothetical termination rate constant for a chain of maleic anhydride only, has not been possible in this study.*

KINETIC studies of the free-radical polymerization of methylmethacrylate and maleic anhydride are interesting in that the rate of polymerization appears to pass through a maximum with increasing mole fraction of maleic anhydride<sup>1</sup>, although this monomer is virtually incapable of undergoing homopolymerization. Burnett<sup>2</sup> has shown that such maxima are possible in systems where one monomer does not itself polymerize, but his analysis produced the necessary condition,  $r_1 < 2$ , where  $r_1$  is the monomer reactivity ratio for the compound capable of undergoing homopolymerization. Since all reported values of  $r_1$  for this copolymerization are greater than three<sup>1,3</sup>, the system has remained something of an enigma.

Two aspects of this copolymerization are worthy of further consideration: (a) the density of maleic anhydride is 50 per cent greater than that of methylmethacrylate<sup>1,4</sup>, so that the total monomer molarity in a bulk polymerization increases with maleic anhydride content; (b) the termination reaction may be diffusion-controlled<sup>5</sup>, in which case the conventional rate equation incorporating the cross-termination factor,  $\phi$ , is no longer applicable. Since rotation is possible about the  $H_2C-C(CH_3)(COOCH_3)$  bond, but not about the  $HC-CH$  bond, it is likely that substitution of



maleic anhydride for methylmethacrylate in the polymer chain will markedly affect the diffusive properties of the chain.

The effect of monomer density must depend on the kinetic order of the polymerization rate law. With methylmethacrylate polymerization the rate

varies as monomer to the power 1.1. If it is assumed that the volume of mixing for these two monomers is zero, and that the kinetic order with respect to monomer is independent of composition, the results of Blackley and Melville<sup>1</sup> can be normalized to a monomer density of 0.900. When this is done the maximum is markedly reduced, but is still quite discernible, *Figure 1*.

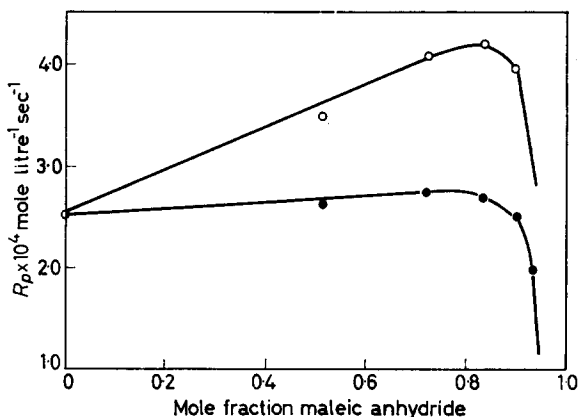


*Figure 1*—Rate of bulk copolymerization at 60°C (Blackley and Melville<sup>1</sup>). O Reported rate of polymerization. ● Rate normalized to a monomer density 0.900

When the termination reaction is diffusion-controlled, the termination rate depends on the composition of the whole polymer chain and not on the chemical nature of the radical end group. Under these conditions the conventional rate expression is not valid, and it is necessary to introduce a termination rate constant  $k_{t(AB)}$  which is a function of the polymer (and hence monomer feed) composition. Under these conditions if the stationary state approximation be applied in the usual way<sup>5</sup>,

$$\frac{R_p}{R_i^\dagger} = \frac{r_1 [A]^2 + 2 [A] [B]}{k_{t(AB)}^\dagger \{ [A] / k_{pab} + [B] / k_{pba} \}} \quad (1)$$

where  $k_{p_{ij}}$  represents the propagation rate constant for addition of radical type  $i$  to monomer type  $j$ , and  $R_p$ ,  $R_i$  are the rates of polymerization and of initiation respectively. Introducing the new variables,  $\epsilon_a = k_{t(AB)}^\dagger / k_{paa}$ ,  $\xi_b = k_{t(AB)}^\dagger / k_{pba}$ ,

$$\frac{R_p}{R_i^\dagger} = \frac{r_1 [A]^2 + 2 [A] [B]}{\epsilon_a r_1 [A] + \xi_b [B]} \quad (2)$$

The conditions for a maximum in the rate/composition curve may be found by differentiating equation (2). Unfortunately explicit conditions can be obtained only if the composition dependence of  $k_{t(AB)}$  is known. The simple extreme exists when  $k_{t(AB)}$  is independent of composition, and the

two components form an ideal mixture. Then setting  $[A] + f[B] = a$ , where  $f$  and  $a$  are constants, equation (2) can be differentiated, and the condition for a maximum yields a quadratic equation in  $[A]_{\max}$ . The equation has real positive roots when

$$fr_1 < 2 \quad (k_{paa}/k_{pba} < 2) \quad (3)$$

$$2 < fr_1 < k_{paa}/k_{pba} \quad (4)$$

Condition (3) is similar to that derived by Burnett and requires (for methylmethacrylate and maleic anhydride polymerized in bulk) that  $r_1$  be less than three. However, condition (4) shows that rate maxima are possible for higher values of  $r_1$ .

If the termination reaction is assumed to exhibit ideal diffusion-controlled behaviour<sup>5</sup>,  $k_{t(A,B)}$  is given by

$$k_{t(A,B)} = k_{taa}x'_a + \zeta_b x'_b \quad (5)$$

Here  $x'_a$  and  $x'_b$  are the mole fractions of each monomer type in the polymer chain,  $k_{taa}$  is the termination rate constant for pure methylmethacrylate, and  $\zeta_b$  is a constant representing the hypothetical rate constant for termination of chains consisting of pure maleic anhydride. The rate equation becomes

$$\frac{R_p}{R_i^{\frac{1}{2}}} = \frac{(r_1 [A]^2 + 2 [A] [B])^{3/2}}{\{k_{taa} ([A] [B] + r_1 [A]^2) + \zeta_b [A] [B]\}^{\frac{1}{2}} \left( \frac{r_1 [A]}{k_{paa}} + \frac{[B]}{k_{pba}} \right)} \quad (6)$$

and the condition for a maximum yields a cubic equation in  $[A]_{\max}$ . The necessary conditions for obtaining positive real roots are then much wider, the most important one being that a maximum is possible when  $k_{paa}/k_{pba} < 2 < fr_1$  so long as  $\zeta_b/k_{taa}$  is less than unity. All the conditions discussed are pertinent only to the achievement of real positive values of  $[A]_{\max}$ , without consideration of the further condition that  $[A]_{\max}$  must be less than or equal to the molar concentration of bulk monomer.

In this work copolymerizations have been carried out in solution so that it has been possible to maintain the total monomer concentration constant at various monomer compositions. The aim of the study was twofold: (a) to discover whether the termination reaction is diffusion-controlled in the copolymerization of mixtures rich in maleic anhydride; and (b) to attempt evaluation of  $r_1$ ,  $k_{pab}/k_{pba}$ , and  $\zeta_b/k_{taa}$  in order to assess the applicability of the conditions for a rate maximum.

## EXPERIMENTAL

### Materials

Methylmethacrylate, B.D.H. purified grade, was freed of inhibitor and distilled under a nitrogen pressure of 20 mm of mercury. The middle fraction was collected, and aliquot portions outgassed on the vacuum line at pressures less than  $5 \times 10^{-5}$  mm of mercury, prepolymerized by ultra-violet (u.v.) irradiation, and residual monomer distilled into the polymerization vessels.

Maleic anhydride was fractionally distilled under a nitrogen pressure of 12 mm of mercury and the middle fraction, b.pt 154°C, collected. Aliquot portions of molten monomer were introduced into the polymerization vessel and outgassed in contact with the solution of  $\alpha,\alpha'$ -azoisobutyronitrile.

AR ethyl acetate was fractionally distilled off calcium hydride. Aliquot portions were outgassed and distilled on the vacuum line.

Sucrose acetate isobutyrate (SAIB) and diisooctyl phthalate (DIOP) were treated with sodium bisulphite and activated charcoal. In order to remove trace impurities which might affect a free-radical polymerization, 1 mg of  $\alpha,\alpha'$ -azoisobutyronitrile was dissolved in aliquot portions of the molten esters, outgassed on the vacuum line, and the azo compound decomposed by u.v. irradiation. Prolonged irradiation over several days caused the formation of coloured polymerization retarders in the esters, so that irradiation was limited to three hours. Esters so treated did not initiate polymerization themselves, indicating that the removal of the azo compound was complete.

$\alpha,\alpha'$ -azoisobutyronitrile was recrystallized three times from ethanol and once from ethyl acetate, stored in the dark at  $-10^\circ\text{C}$ , and used in standard solutions in ethyl acetate.

### *Procedure*

All reaction mixtures were prepared and sealed under an air pressure less than  $5 \times 10^{-5}$  mm of mercury.

Rates of polymerization studied at different monomer feed compositions were observed by gravimetric determination of the polymer yields, samples of each run being analysed after four different times. Each reaction vessel contained four ampoules, capacity 5 ml, into which the polymerization mixture was sealed. The ampoules were opened at 12-hourly intervals, the polymer precipitated in excess methanol at  $-30^\circ\text{C}$ , collected on No. 4 porosity sintered glass crucibles, dried to constant weight at  $100^\circ\text{C}$ , and the yield calculated from the weights of polymer, ampoule plus monomers and ampoule fragments. In no case was the conversion greater than ten per cent. Yields so obtained deviated from a smooth curve by less than one per cent.

Rates of copolymerization of a mixture of monomers (1.20 molar methylmethacrylate and 2.05 molar maleic anhydride) in solvents of varying viscosities were observed using conventional dilatometers. Rates of contraction were converted to rates of polymerization by comparison of dilatometric and gravimetric runs for this monomer composition. All rate determinations were carried out in a water thermostat bath governed to  $30^\circ \pm 0.01^\circ\text{C}$ .

Monomer reactivity ratios were obtained by titration of the maleic anhydride in polymer using the technique of Fritz and Lisicki<sup>6</sup>.

Solution viscosities were determined in an Ubbelohde suspended level viscometer, and were found to be the same at the start and at the finish of each polymerization.



## RESULTS

*Monomer densities and solubilities*

The solubility of maleic anhydride at 30°C was found to be: in ethyl acetate—1.93 mole litre<sup>-1</sup>, in 50/50 v/v ethyl acetate–methylmethacrylate—4.01 mole litre<sup>-1</sup>. In order to obtain reasonable rates of polymerization and measurable polymer yields, it was decided to study polymerizations at a total monomer concentration of 3.25 mole litre<sup>-1</sup>. Because of the low solubility of maleic anhydride, it was found to be impracticable to study monomer compositions beyond 0.63 mole fraction maleic anhydride.

The monomer and solvent densities are required so that polymerizations of different monomer feeds can be made up to the same total volume and total monomer concentration:

Ethyl acetate 0.865 g (cm<sup>3</sup>)<sup>-1</sup>

Methylmethacrylate 0.933 g (cm<sup>3</sup>)<sup>-1</sup>

Maleic anhydride when dissolved in ethyl acetate 1.47 g (cm<sup>3</sup>)<sup>-1</sup>.

The high density observed for maleic anhydride in solution is in agreement with that recorded by Melville and Blackley for bulk monomer.

*Monomer reactivity ratios*

Sixteen samples of polymer were prepared at 30°C using six different monomer feed compositions. In no case was the polymerization continued beyond ten per cent conversion. At these low conversions the dependence of polymer composition on conversion is approximately linear, so that the polymer composition corresponding to zero conversion was obtained by graphical extrapolation. The reactivity ratios were then obtained from the intersections of the lines

$$r_1 = \frac{[B]}{[A]} \left( \frac{d[A]}{d[B]} \right)_0 \left[ 1 - r_2 \frac{[B]}{[A]} \right] - \frac{[B]}{[A]} \quad (7)$$

The monomer and polymer compositions are listed in *Table 1*, and the reactivity ratios obtained from the six 'zero-conversion' lines are

$$r_1 = 4.63 \quad r_2 = -0.18$$

The standard deviations are 1.14 and 0.28 respectively. The ratio,  $r_2$ , of course, can be negative only if a depropagation reaction is taking place in the copolymer. Since there is no experimental evidence for any depropagation equilibrium effects in this system, and since the variance in  $r_2$  covers both positive and negative values, we have assumed a value of 0.00 in all calculations involving  $r_2$ .

Although there is a disappointingly large error in the determination of  $r_1$ , a value less than 3.0 is improbable, and the system cannot obey the  $r_1 < 2$  condition discussed by Burnett.

Table 1. Monomer-polymer compositions at 30°C

[A]/[B] <sub>0</sub>	d [A]/d [B]	% conversion	[A]/[B] <sub>0</sub>	d [A]/d [B]	% conversion
0.587	6.13	1.89	1.56	7.96	8.69
0.587	5.25	3.12	2.56	9.85	4.28
0.587	4.67	6.01	2.56	12.19	5.19
0.906	6.02	7.66	2.56	11.20	7.56
1.40	6.92	4.53	2.56	10.57	9.36
1.40	6.69	8.61	7.19	32.47	5.73
1.56	7.52	3.13	7.19	30.01	8.52
1.56	8.05	6.68	7.19	28.36	9.74

### Viscosity dependence of polymerization rate

All polymerization mixtures consisted of  $1.29 \times 10^{-3}$  M  $\alpha, \alpha'$ -azoisobutyronitrile, 1.20 M methylmethacrylate, 2.05 M maleic anhydride, and variable ratios of ethyl acetate-SAIB or ethyl acetate-DIOP.

The factor converting volume per cent monomer contraction to weight per cent conversion was determined for this monomer composition from comparison of dilatometric and gravimetric observations,

$$R_c = 2.61 \times 10^{-6} \text{ volume per cent second}^{-1},$$

$$R_g = 3.80 \times 10^{-5} \text{ weight per cent second}^{-1},$$

$$R_p = 1.23 \times 10^{-6} \text{ mole litre}^{-1} \text{ second}^{-1},$$

Conversion factor = 14.5.

Because of the high density of maleic anhydride monomer the volume contraction is small at this monomer feed composition.

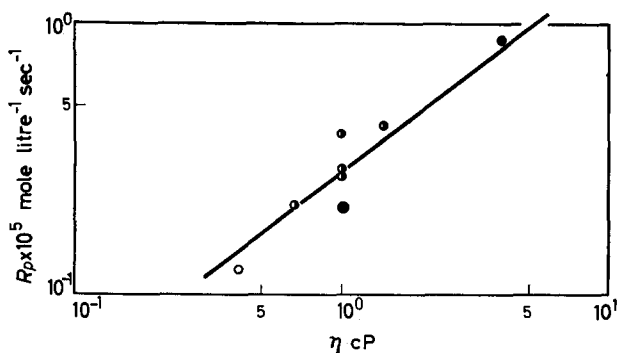


Figure 2—Viscosity dependence of copolymerization rate in solution at 30°C. 1.20 M methylmethacrylate and 2.05 M maleic anhydride. ○ ethyl acetate solvent. ◐ ethyl acetate-SAIB solvent. ● ethyl acetate-DIOP solvent

It was found that the rates of copolymerization depended on the viscosity of the solution over the complete range of viscosities studied, as is illustrated in Figure 2. Since the reaction rate increases with increasing viscosity, the termination reaction must be diffusion-controlled, even at the viscosities

## METHYLMETHACRYLATE AND MALEIC ANHYDRIDE

corresponding to normal solution polymerization. The increase in rate also serves to verify the absence of retarder in the viscous solvent component.

### *Composition dependence of polymerization rates*

All polymerization mixtures consisted of  $1.29 \times 10^{-3}$  M  $\alpha, \alpha'$ -azoisobutyronitrile, 3.25 M total monomer, ethyl acetate as solvent. The variation in copolymerization rate (determined from the initial slope of the yield/time observations) with monomer feed and polymer composition is listed in Table 2.

Table 2. Rates of copolymerization in solution at 30°C

$x_b$ monomer	$x'_b$ polymer	$R_p \times 10^8$ moles litre <sup>-1</sup> second <sup>-1</sup>	$R_p/R_{pA}$
0.000	0.000	1.98	1.00
0.122	0.026	1.91	0.965
0.279	0.066	1.74	0.879
0.391	0.101	1.80	0.909
0.417	0.110	1.74	0.879
0.525	0.151	1.69	0.854
0.631	0.203	1.23	0.622

There is no detectable maximum in the rate/composition curve, although the second derivative of the curve is negative. It is possible that a maximum does exist, but that it occurs at extremely low mole fractions of maleic anhydride, the increase in rate being less than the experimental error.

### DISCUSSION

Since the rate of termination, both in the homopolymerization of methylmethacrylate<sup>5</sup> and in the copolymerization richest in maleic anhydride, is diffusion-controlled, it is reasonable to assume that this diffusion-dependence exists over the whole range of monomer compositions studied.

The experiments in solution at 30°C do not exhibit a rate maximum greater than experimental error. This is not in direct disagreement with the results of Blackley and Melville at 60°C, since the maximum in corrected rate at this temperature is only just larger than the experimental error. Both rate/composition curves are similar in shape, being almost independent of composition until more than 50 mole per cent maleic anhydride.

Under conditions of diffusion-controlled termination and constant monomer concentration, and with the assumption that the efficiency of initiation is independent of composition, equation (1) can be rewritten

$$\frac{R_p}{R_{pA}} = \frac{x_a^2 + 2x_a x_b / r_1}{\left( \frac{k_{t(AB)}}{k_{taa}} \right)^{\frac{1}{2}} \{x_a + k_{pab} x_b / k_{pba}\}} \quad (8)$$

where  $[A] + [B] = a$ ,  $[A]/a = x_a$ .  $R_{pA}$  represents polymerization of A. This

equation contains the unknown variable,  $k_{t(AB)}/k_{taa}$  as well as the unknown constant  $k_{pab}/k_{pba}$ , and so cannot be solved directly for both unknowns. Once the form of the composition-dependence of  $k_{t(AB)}$  is known, however, solution is possible.

In order to attempt preliminary estimation of  $k_{pab}/k_{pba}$  and  $\zeta_b/k_{taa}$  we have assumed that termination is 'ideal' as expressed in equation (5). Equation (8) can then be written as

$$\frac{R_p}{R_{pA}} = \frac{x_a^2 + 2x_a x_b / r_1}{\{x_a + k_{pab} x_b / k_{pba}\} \{x'_a + \zeta_b x'_b / k_{taa}\}^{\frac{1}{2}}} \quad (9)$$

$k_{pab}/k_{pba}$  and  $\zeta_b x'_b / k_{taa}$  should then be obtained from the intersections of the plots  $k_{pab}/k_{pba}$  against  $\zeta_b/k_{taa}$ .

$$\frac{k_{pab}}{k_{pba}} = \frac{(x_a^2 + 2x_a x_b / r_1) (R_{pA} / R_p)}{(x'_a + \zeta_b x'_b / k_{taa})^{\frac{1}{2}} x_b} - \frac{x_a}{x_b} \quad (10)$$

Unfortunately these plots form a band of almost parallel curves, with negative slope, spanning the origin. Since neither of these ratios can be negative, the only possible interpretation is that both ratios differ from zero by a quantity which is less than the experimental error. This error is  $\pm 0.1$  and  $\pm 0.4$  for  $k_{pab}/k_{pba}$  and  $\zeta_b k_{taa}$  respectively.

The conditions  $r_1 \leq 2$  [solution copolymerization],  $r_1 \leq 3$  [bulk copolymerization] and  $k_{paa}/k_{pba} \geq r_1$  are thus not satisfied at 30°C. The certainty with which we can say that these conditions are violated depends on the accuracy with which  $r_1$  has been measured. The values  $r_1 = 3$ ,  $r_1 = 2$ , differ from the mean value by 1.4  $\sigma$  and 2.3  $\sigma$  respectively where  $\sigma$  is the standard deviation in  $r_1$ . Consequently it is possible that  $r_1 \leq 3$ , but highly improbable that  $r_1 \leq 2$ . Although it might be felt that the adjustment in  $r_2$  (-0.18 to zero) implies that a similar reduction should be made in  $r_1$ , examination of the  $r_1$  against  $r_2$  experimental plots shows that a parallel adjustment in  $r_1$  would be an increase of 0.6  $\sigma$ . A maximum in the rate/composition curve can now be explained only if the termination reaction is diffusion-controlled, the rate of termination increasing with maleic anhydride content of the copolymer.

It has been suggested that the rate-determining process in the termination of polymeric free radicals is a segmental rearrangement of the conformations adopted by the polymer chain in solution<sup>7,8</sup>. As a methylmethacrylate unit in the chain is replaced by a maleic anhydride unit, the possibility of rotation about one carbon-carbon bond in the chain is removed. Consequently the number of possible conformations of the chain, and also the rate of rearrangement, would be reduced. Thus a value of  $\zeta_b/k_{taa}$  less than unity, with the consequent possibility of a rate maximum, would be predictable on this basis. A value of  $k_{pab}/k_{pba}$  less than unity might be expected on steric considerations. Unfortunately sufficient information on the reactivity of the maleic anhydride radical is not available for theoretical prediction<sup>9</sup> of this ratio.

*The authors wish to acknowledge the assistance of Mr A. Wright with the determinations of polymer composition and solution viscosity.*

*Donnan Laboratories,  
University of Liverpool*

*(Received June 1963)*

REFERENCES

- <sup>1</sup> BLACKLEY, D. C. and MELVILLE, H. W. *Makromol. Chem.* 1956, **18**, 16
- <sup>2</sup> BURNETT, G. M. *J. Polym. Sci.* 1958, **28**, 642
- <sup>3</sup> DE WILDE, M. C. and SMETS, G. *J. Polym. Sci.* 1950, **5**, 253
- <sup>4</sup> *Chemical Engineer's Handbook*, 3rd ed. New York: McGraw-Hill
- <sup>5</sup> ATHERTON, J. N. and NORTH, A. M. *Trans. Faraday Soc.* 1962, **58**, 2049
- <sup>6</sup> FRITZ, J. S. and LISICKI, N. M. *Analyt. Chem.* 1951, **23**, 589
- <sup>7</sup> BENSON, S. W. and NORTH, A. M. *J. Amer. chem. Soc.* 1962, **84**, 935
- <sup>8</sup> NORTH, A. M. and REED, G. A. *Trans. Faraday Soc.* 1961, **57**, 859
- <sup>9</sup> BAMFORD, C. H. and JENKINS, A. D. *Trans. Faraday Soc.* 1963, **59**, 530

# *The Effect of Tension and Annealing on the X-ray Diffraction Pattern of Drawn 6.6 Nylon*

D. R. BERESFORD and H. BEVAN

*We have studied the effect of extending a filament of drawn 6.6 nylon on the spacing and intensities of the wide and low angle diffraction patterns. Thermal annealing experiments were also performed and the changes in intensities and spacing of the reflections determined. The results show that (a) the long period (from the low angle pattern) and the short period (from the wide angle pattern) extend reversibly; (b) the percentage extension of the long period is greater than that of the fibre; (c) the extension of the short period is only 6 per cent of the fibre extension; (d) for yarns showing a four-point low angle pattern the spots merge on the meridian when the yarn is stressed and (e) thermal annealing increases the intensity of the low angle reflections by a factor of up to 100 as well as increasing the long period. A structural model based on the concept of chain folding is proposed which is consistent with these observations.*

IN THIS paper we have studied the effect of extending a filament of drawn 6.6 nylon on the spacings and intensities of the wide and low angle diffraction patterns. So far only one publication has appeared<sup>1</sup> describing the changes in the low angle diffraction pattern induced by applying tension to a drawn polymer fibre, a polyurethane. However, the effect of tension on the wide angle pattern has been reported for many high molecular weight polymers<sup>2-5</sup> but not for polyamides. The results of this work are relevant to the current discussions of the textural nature of drawn polymers in general<sup>6,7</sup>.

## EXPERIMENTAL AND RESULTS

### *Wide angle diffraction*

The 6.6 nylon was clamped at one end and the yarn which consisted of a number of  $27\mu$  diameter filaments passed over two pulleys mounted in rigid frameworks so that it passed directly in front of the collimated X-ray beam. The free end was fitted with a clamp so that various loads could be applied. The film holder was mounted on a normal fibre camera which was bolted to the same base as the pulley frames and this base was also the mounting for the X-ray tube. This arrangement ensured, as far as possible, that no change could occur in the film-specimen distance during the loading cycle; only a distortion of the base of the frameworks could cause such a change. In view of the small changes expected even distortions of this kind were important, since a change of 1 mm in film-specimen distance would account for the complete shift observed, so a cathetometer was set up and the fibre and the film holder viewed during the loading cycle; no detectable change, i.e.  $< 0.02$  cm, in position was observed. The X-radiation used in the experiment was nickel-filtered  $\text{Cu } K_{\alpha}$  and the ambient conditions were those of the laboratory. The repeating distance along the molecular axis was measured as a function of tension and determined from the spacing

of the (015) reflection, the (015) plane being almost perpendicular to the fibre axis (see *Figure 1*). The X-ray diffraction patterns were recorded for an exposure time of one hour but the yarn was maintained for at least two hours in the stretched state before photography so that the rate of creep was reduced to a level unimportant during this exposure time. As a final check on the stability of the apparatus, three photographs were recorded at each load.

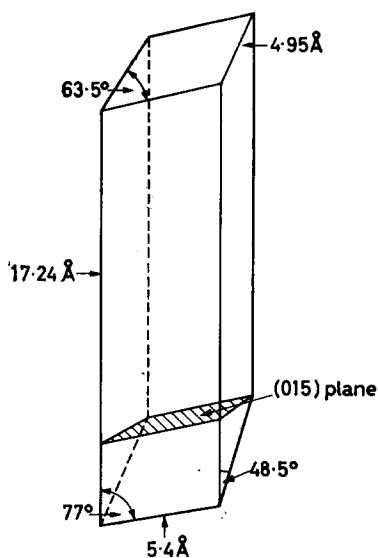


*Figure 1*—Determination of repeat distance

The (015) spacings were measured from Joyce-Loebl microdensitometer traces recorded at a magnification of 2:1. Even with this assistance the measurements were difficult because over the whole cycle the maximum change was  $0.6 \pm 0.1$  per cent. The basic difficulty lies in the breadth of even relatively sharp reflections and the subsequent uncertainty in the position of the peak. The means of the measurements from three different films for each tension are given in *Table 1*. The maximum range at any tension was 0.03 cm.

The load/extension curves were recorded on the Instron extensometer at various constant rates of extension and an extrapolation made to an infinitely slow rate of extension in order to estimate the value of the fibre

*Table 1.* Film-specimen distance = 8.10 cm; (015) separation

Tension g/den.	Mean of 3 films cm	Fibre repeat Å
0.00	16.78	17.25
0.85	16.77	17.26
1.70	16.74	17.27
2.55	16.69	17.31
3.40	16.68	17.30
4.25	16.64	17.33
5.10	16.65	17.34
5.95	16.60	17.38

extension during the X-ray exposures. The X-ray apparatus was not suitable for direct measurement of extension. By this technique an error of less than one per cent was introduced and this was considered satisfactory.

From these results and the extension data from the Instron the following graphs were constructed. *Figure 2* shows a plot of the fibre repeating distance against tension on the fibre and *Figure 3* a plot of the percentage extension of the crystalline lattice versus percentage extension of the yarn.

*Figure 2*—Fibre repeat distance as a function of tension

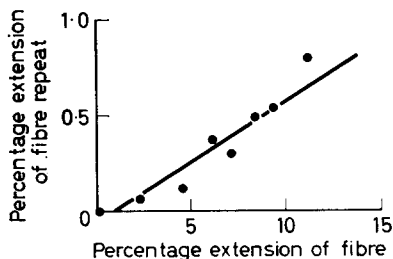
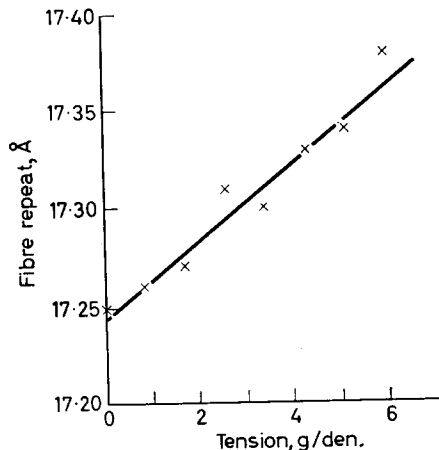


*Figure 3*—Percentage extension of crystalline lattice versus percentage extension of yarn

### *Low angle diffraction*

Photographs were taken with an evacuated Seifert low angle camera at a film-specimen distance of 20 cm using nickel-filtered  $\text{Cu } K_{\alpha}$  radiation. The collimator had an effective aperture of 0.7 mm. Measurements of the long period were made from microdensitometer traces, scanning the film parallel to the meridian, and calculating the long period as a layer line spacing. This gives the long period repeat distance along the direction of the fibre axis.

### *Yarn*

The yarn used in these experiments has a four-point diagram in the unstressed state. A 1 cm length was attached to metal rods by means of bollard clamps. Each rod was passed through a Wilson seal in the side of the Seifert camera, arranged so that the yarn passed horizontally across



the end of the collimator. Stress was applied to the yarn by means of weights attached to the rods by ropes running over pulleys.

Figure 4 shows the low angle patterns for unstressed and stressed yarn. No quantitative measurements were made as we found that an unknown and variable fraction of the tension was lost in the Wilson seals.

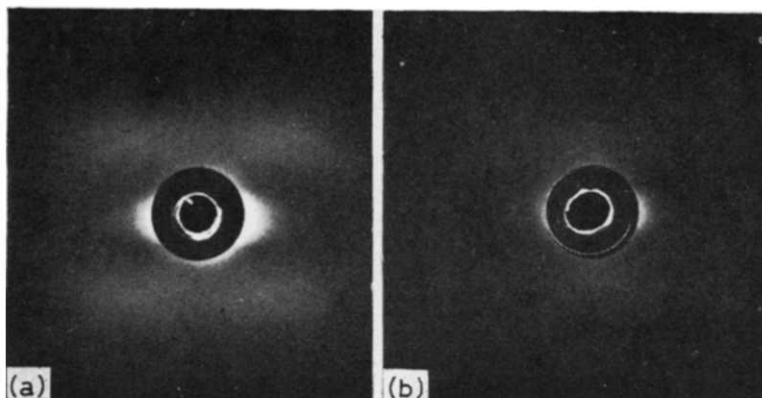


Figure 4—Low angle patterns for (a) unstressed and (b) stressed tyre record

#### Bristle

50 cm lengths of drawn bristle, of 0.024 in. diameter, were extended under constant load for a two hour period. A 2 cm length of the bristle, still under load, was then attached to the sample holder, using 'Araldite' epoxy resin. The load was maintained until the resin was set and then the remainder of the bristle was cut off from the holder. The sample was thus held at constant length. After recording the diffraction pattern one end of the sample was released by cutting and the pattern was again recorded after the sample had relaxed for 24 hours.

The extension of the bristle was measured by making two marks on the bristle about 50 cm apart and measuring their separation with a ruler before and after loading.

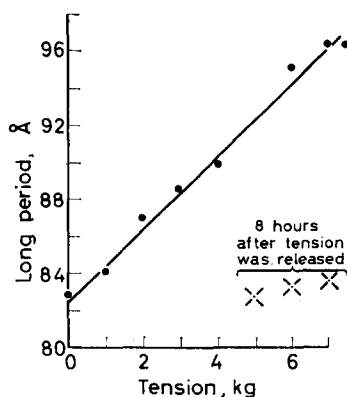


Figure 5—Long period as a function of tension

## THE EFFECT OF TENSION ON 6.6 NYLON

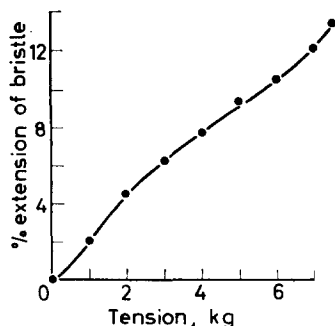


Figure 6—Percentage extension of bristle as a function of tension

Loads up to 7.5 kg (almost the breaking load) were applied to the bristle, a fresh piece being used for each measurement. The reversibility of the bristle extension was checked in a separate experiment. The bristles were stored and stretched under laboratory conditions and although the photographs were taken under vacuum the moisture content of the bulk of the bristle would not change appreciably during the 16 hours needed to record the diffraction pattern. The results are shown in *Figures 5, 6 and 7*. After relaxation from the highest loads the long period shows a small permanent set (*Figure 5*).

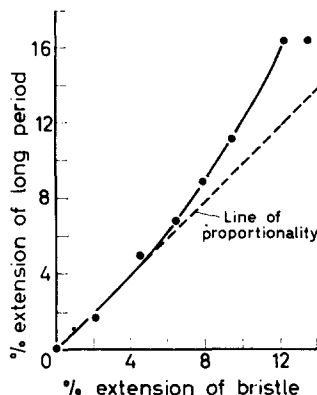


Figure 7—Percentage extension of long period as a function of percentage extension of bristle

### Annealing

Low angle photographs were also recorded for both yarn and bristle fibres which had been thermally annealed. They were heated for half an hour in dry nitrogen and then cooled slowly to room temperature. The long period showed the well known increase with annealing temperature but in addition the intensity of the low angle pattern increased. A factor of about 100 in exposure time was needed to produce low angle photographs of equal integrated intensity from untreated samples and samples annealed at 260°C. The wide angle pattern showed little change in intensity on annealing.

### DISCUSSION

This work shows the following effects when drawn fibres are extended under tension.

(1) The long period (from the low angle pattern) and the short period (from the wide angle pattern) extend reversibly.

(2) The percentage extension of the long period is greater than that of the fibre.

(3) The extension of the short period is only 6 per cent of the fibre extension.

(4) For yarns showing a four-point low angle pattern the spots merge on the meridian when the yarn is stressed.

(5) Thermal annealing increases the intensity of the low angle reflections by a factor of up to 100 as well as increasing the long period.

We will consider the above experimental observations in relation to the current structural models of drawn fibres. These can be divided into two categories, namely those based on the Hess and Kiessig structure<sup>8</sup> and those based on the chain folded structure<sup>6, 7</sup>.

#### *Hess and Kiessig model*

In this model it is assumed that regions of high and low order alternate regularly in the fibre direction and each molecular chain passes through several of these regions. The fibre is built up along its length of units each consisting of an ordered and a disordered region and the long period is equal to the length of one of these units. Several variations of such models have been proposed notably by Hess and Kiessig<sup>8</sup> and Statton<sup>9</sup>. Although the models differ in detail they have in common the two features mentioned above. It is necessary to assume that adjacent regions are staggered to account for the low angle four-point diagram. On stretching a fibre such a model predicts that the fibre extension and the long period extension would be identical because the fibre is entirely made up of units (each equal in length to the long period) laid end to end. We have found that the percentage extension of the low angle spacings and of the fibre are not the same.

#### *Chain folded model*

In this model it is assumed that the material is made up of folded chains forming well defined lamellar regions [*Figure 8(a)*]. Here a molecular chain is confined to a single lamella. This model was originally proposed by Keller<sup>10</sup> for polymers crystallized from dilute solution. Several authors<sup>11-17</sup> have since suggested that a modification of this model also applies to polymers crystallized from the melt. The modified model assumes that the lamellae are poorly defined and linked by molecules. In either form the long period is identified with the lamella thickness and its percentage extension should therefore be the same as that of the fibre for similar reasons as with the Hess and Kiessig model. This does not agree with our observations.

#### *Modifications to the models*

The long period extending by more than the fibre can be explained if we postulate that part of the material does not contribute to the low angle reflections. This part not contributing to the low angle reflections must have a higher elastic modulus than the fibre as a whole and the part giving

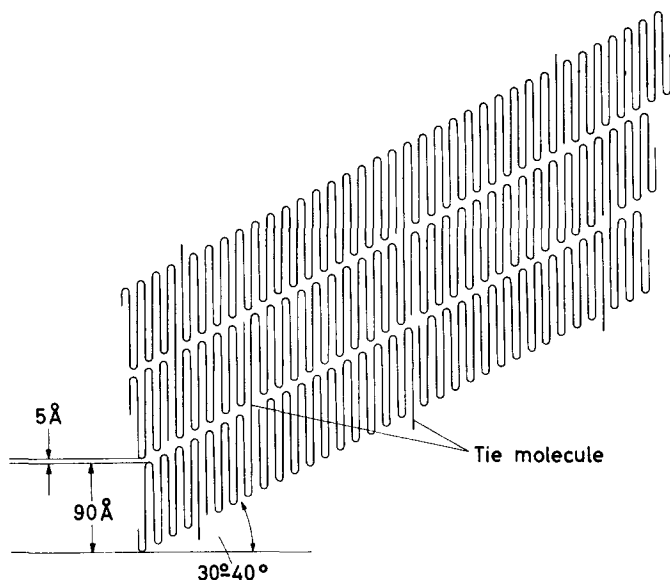


Figure 8(a)—Model comprising folded chains having well defined lamellar regions

rise to the low angle a lower elastic modulus. Thus the material which gives discrete low angle reflections has a higher percentage extension and that which does not contribute has a lower percentage extension.

We now consider the possible nature of the less extensible material and if it can be incorporated in either of the models described above. This material must have the following properties:

- (i) Good short range order (because it gives good wide angle patterns).
- (ii) Poor long range order (because it does not contribute to the low angle reflections).
- (iii) The long range order will increase progressively with thermal annealing, the short range order being unchanged. (Because the intensity of the low angle reflections increases progressively on annealing, while the wide angle intensity is unchanged.)

Let us consider whether the Hess and Kiessig type material can be modified to satisfy the above requirements. Requirement (iii) means that on annealing, this modified material must re-arrange itself into regularly alternating ordered and disordered regions. The initial state must have good short range order and be fairly uniform and since it does not contribute to the low angle pattern there can be no long range order. To attain the annealed state, initially similar parts of the material with the same chain molecules running through them must order and disorder in a regularly alternating sequence. This seems unlikely.

A further difficulty is to explain how, on this model, the long period can increase progressively as the fibre is annealed. This implies that either the ordered or the disordered regions must extend in the fibre direction. The ordered regions cannot change their length appreciably so it must be the

disordered regions which extend. To account for the observed increase in long period of up to 100 per cent on annealing, the disordered regions must extend by at least 100 per cent. In extending they would certainly increase their short range order and therefore contribute more to the wide angle pattern. The changes in the wide angle pattern do not indicate a large increase in the intensity and therefore in the amount of ordered material on annealing, so this is unlikely.

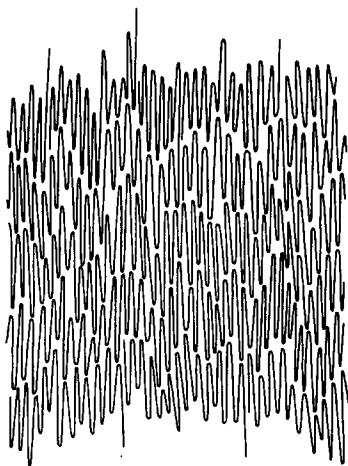
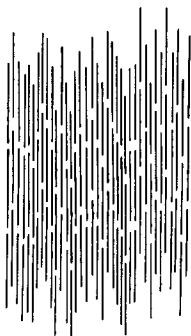


*Figure 8(b)*—This diagram shows two possible ways of arranging folded sheets which do not give low angle reflections. The upper half shows a view perpendicular to the plane containing the folded molecules; the lower half shows a view parallel to this plane, the molecules being considered as regularly folded units. The actual state may well consist of a combination of these effects



We now describe a modification to the chain folded model which enables us to explain our observations. We assume that the chains have a fairly uniform fold length but the folds are not ordered so as to give a periodic variation in the fibre direction. The irregularity can be of several types [see *Figure 8(b)*]. The short range order is preserved but the long range order is lost. The material will have a high elastic modulus. The fact that the intensity of the low angle reflections increases with annealing can be explained by this material progressively increasing its long range order by forming regular lamellae.

Thus the fibre has a range of long range order varying from regular, discrete lamellae joined together by a few tie molecules [*Figure 8(a)*] to regions of irregular lamellae which do not contribute to the low angle reflections [*Figure 8(b)*]. The short range order is fairly uniform throughout the fibre.

When mechanical stress is applied to the fibre the lamellae themselves and the highly interpenetrated regions will stretch elastically by a small percentage of the fibre extension, the moduli of these two regions being similar. In the region of discrete lamellae the tie molecules between lamellae, however, will be subject to much higher stress since between lamellae there are fewer chains per unit area than anywhere else. The stress will extend the tie molecules elastically and may also distort the lamellae in the region of a tie molecule (see *Figure 9*). Thus the gaps between the

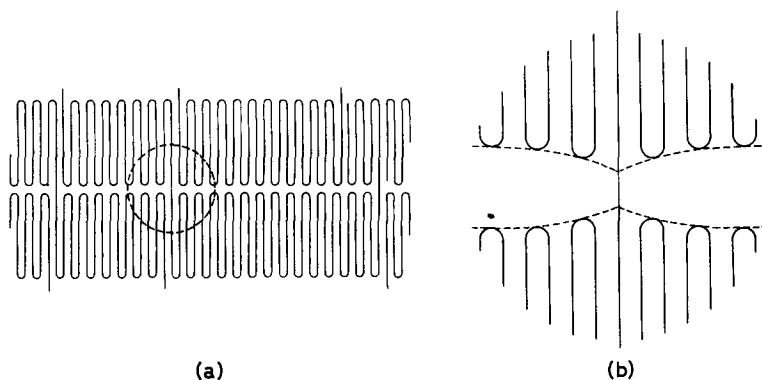


*Figure 9*—(a) Unstressed and (b) stressed region around a tie molecule in the model

lamellae in these highly regular regions will increase with tension by much more than the rest of the material. This will give a percentage increase in the long period greater than that of the fibre.

The authors therefore consider that a plausible model for the structure of drawn polyamide fibres which will account for their observations, consists of chain folded molecules aggregated into states of order which vary between the extremes of discrete lamellar regions with a few tie molecules and regions in which the molecules are so irregularly folded and arranged that individual lamellae are no longer distinguishable.

*Research Department,  
British Nylon Spinners Limited,  
Pontypool, Monmouthshire*

*(Received July 1963)*

REFERENCES

- <sup>1</sup> ZAHN, H. and WINTER. *Kolloidzshr.* 1952, **128**, 142.
- <sup>2</sup> DULMAGE, W. J. and CONTOIS, L. E. *J. Polym. Sci.* 1958, **28**, 275

- <sup>3</sup> MANN, J. and ROLDAN-GONZALES, L. B.R.R.A. publication 'X-ray Measurements of the Elastic Modulus of Cellulose Crystals'
- <sup>4</sup> BAKER, W. O. and FULLER, C. W. *J. Amer. chem. Soc.* 1943, **65**, 1120
- <sup>5</sup> FULLER, C. S., FROSCHE, C. J. and PAPE, N. R. *J. Amer. chem. Soc.* 1942, **64**, 154
- <sup>6</sup> KELLER, A. *Polymer, Lond.* 1962, **3**, 393
- <sup>7</sup> HOSEMANN, R. *Polymer, Lond.* 1962, **3**, 349
- <sup>8</sup> HESS, K. and KIESSIG, H. *Z. phys. Chem. A*, 1944, **193**, 196
- <sup>9</sup> STATTON, W. O. *J. Polym. Sci.* 1959, **41**, 143
- <sup>10</sup> KELLER, A. *Phil. Mag.* 1957, **2**, 1171
- <sup>11</sup> KÄMPF, G. *Kolloidzshr.* 1960, **172(1)**, 50
- <sup>12</sup> FISCHER, E. W. *Disc. Faraday Soc.* 1958, 204
- <sup>13</sup> EPPE, R., FISCHER, E. W. and STUART, H. A. *J. Polym. Sci.* 1959, **34**, 721
- <sup>14</sup> SELLA, C. and TRILLAT, J. J. *C.R. Acad. Sci., Paris*, 1959, **248**, 410
- <sup>15</sup> GEIL, P. H. *J. Polym. Sci.* 1960, **47**, 65
- <sup>16</sup> GEIL, P. H. *J. Polym. Sci.* 1961, **51**, 510
- <sup>17</sup> MAGILL, J. H. and HARRIS, P. H. *Polymer, Lond.* 1962, **3**, 252
- <sup>18</sup> BASSETT, D. C., KELLER, A. and MITSUHASHI, J. *J. Polym. Sci.* 1958, **28**, 365; *Pt. A*, 1963, **1**, 763

# Polypropylene Oxide II\*—Dilute Solution Properties and Tacticity

G. ALLEN, C. BOOTH and M. N. JONES

*Polypropylene oxide has been separated into fractions which differ only in crystallizability. The second virial coefficients of these fractions in hexane at 46°C, measured by light scattering, vary from  $-1.75 \times 10^{-4}$  to  $+4.01 \times 10^{-4}$  cm<sup>3</sup>g<sup>-2</sup> mole<sup>-1</sup>. These results are discussed in terms of the variation of  $\theta$ -point with the structural regularity (degree of tacticity) of the polymer.*

SEVERAL investigations have been made of the influence of the degree of tacticity of a polymer upon its dilute solution properties. The results of these studies have been discussed recently by Krigbaum *et al.*<sup>1</sup> and by Krause and Cohn-Ginsberg<sup>2</sup>. In order to study the effect of the variable of interest, experimental procedures have been used to eliminate or allow for the effects of two other important variables; the average molecular weight and the molecular weight distribution of the sample. We have been able to fractionate polypropylene oxide in such a way as to obtain samples which differ only in degree of isotacticity† and not in average molecular weight or molecular weight distribution, and with these fractions we have investigated the effect of degree of tacticity upon the dilute solution properties of this polymer in a simple and direct manner.

## EXPERIMENTAL AND RESULTS

### Polymer

The sample of polypropylene oxide used was prepared by Dr E. Powell by methods which will be described in detail in a future paper. Briefly, propylene oxide (5.77 mole/l.), zinc diethyl (0.28 mole/l.) and water (0.224 mole/l.) were mixed in dioxan under high vacuum conditions and allowed to polymerize at 25°C for one week. The polymer was isolated in the manner described in Part I, and during this treatment suffered some degradation.

### Fractionation

A solution was made up by dissolving 17.2 g of polypropylene oxide in 3 l. of commercial isooctane at 60°C. The flask containing this solution was then placed in a water bath (controlled to  $\pm 0.01^\circ$ ) and the solution was stirred slowly as the temperature was lowered to 55°C. After standing for one day to allow the polymer to crystallize the supernatant liquid was syphoned off through a glass wool plug. The precipitate was dissolved in benzene and this solution was filtered and freeze-dried. The isooctane solution was cooled further and the process repeated. The whole fractionation was carried out, as far as possible, in the dark. Certain fractions were obtained by allowing the solution to stand for another day or two at the

\*For Part I see: G. ALLEN, C. BOOTH and M. N. JONES, *Polymer, Lond.* 1964, 5, 195.

†X-ray analysis has been used to show that crystalline polypropylene oxide is isotactic.



same temperature (see *Table 1*). It was discovered after this fractionation was complete that liquid-liquid phase separation takes place at 39°C under these conditions and fraction 6 therefore contains some high molecular weight polymer (hence the high  $[\eta]$ ). Fraction 8 was obtained by lowering the temperature to 36°C and then raising it to 40°C, thus taking advantage of the rapid rate of dissolution of the liquid phase to obtain the solid phase. Fraction 9, the bulk of the polymer, was precipitated at 0°C as a mixture of solid and liquid phases. It has been shown<sup>4</sup> that polypropylene oxide of molecular weight higher than about  $10^5$  is insoluble in isooctane at 0°C. The fractionation data, i.e. the temperature at which the fraction was separated, the weight of the fraction as a percentage of the whole polymer and the intrinsic viscosity measured in hexane at 46°C, are given in *Table 1*. Intrinsic viscosities were measured in the manner described in Part I.

*Table 1.* Fractionation data

Fraction No.	$T_m$ (isooctane) °C	Wt%	$[\eta]$ (Hexane at 46°C) (dl/g)
1	55	0.23	—
2	50	0.58	2.39
3	46	2.92	2.52
4	46	0.88	—
5	42	1.75	2.40
6	39	3.79	3.30
7	39	2.33	2.82
8	36 to 40	1.75	2.38
9	0	61.8	2.30
Residue	—	23.9	—

Fractionation by successive precipitation from a single solvent has an advantage over the more usual method used for separating fractions of differing crystallizability, i.e. successive extraction by different solvents, in that equilibrium between the solid and liquid phases is more quickly established and so the process is more easily controlled. We have used solvents other than isooctane, e.g. heptane and cyclohexane, with identical results. Similar fractionations have been reported by Utiyama<sup>5</sup> and Kabayashi<sup>6</sup>.

#### Light scattering

The techniques used in the light scattering measurements have been

*Table 2.* Light scattering data

Fraction No.	$\bar{M}_w \times 10^{-6}$	$A_2 \times 10^4$ $\text{cm}^3 \text{g}^{-2} \text{mole}^{-1}$	$(\bar{S}_z^2)^{\dagger}$	$\bar{M}_z/\bar{M}_w$	$T_m$ (°C)
1	1.34	-1.75	740	—	—
3	1.18	0.31	580	2.0	38
5	1.37	0.45	690	3.0	34
7	1.13	1.43	560	1.7	29
8	0.996	2.31	580	2.5	24
9	1.13	4.01	560	2.1	—

described in Part I. Table 2 records the weight-average molecular weight ( $\overline{M}_w$ ), the second virial coefficient ( $A_2$ ) and the root mean square radii of gyration ( $\overline{S}_z^2$ )<sup>†</sup> measured by light scattering in hexane at 46°C for several of the fractions. Figure 1 shows the plots of  $(Kc/R_\theta)_{\theta=0}$  versus concentration as measured using light of wavelength 4360 Å. Also listed in Table 2 are the highest temperatures at which the fractions precipitated from hexane ( $T_m$ ) and the ratio of the z- to weight-average molecular weight ( $\overline{M}_z/\overline{M}_w$ ) which is a measure of the width of the weight distribution of molecular weights. This ratio was calculated from the equations

$$[\eta] = \Phi 6^{3/2} \frac{(\overline{S}_z^2)^{3/2}}{\overline{M}_z} = \Phi \frac{\overline{M}_w}{\overline{M}_z} 6^{3/2} \frac{(\overline{S}_z^2)^{3/2}}{\overline{M}_w}$$

by use of a value of  $2.1 \times 10^{21}$  for the universal parameter  $\Phi$ . In using the above equations it is assumed that the polymers are random coils in hexane at 46°C. Within the rather large experimental error of this determination, the molecular weight distributions of the fractions are seen to be quite similar.

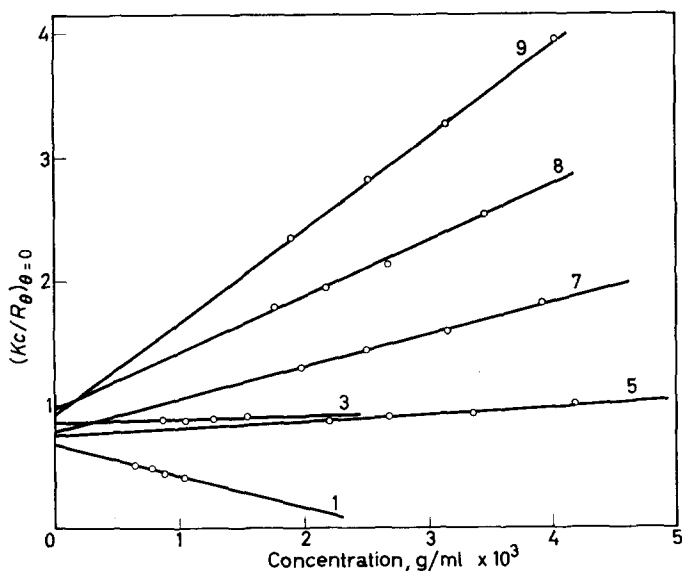


Figure 1— $(Kc/R_\theta)_{\theta=0}$  at 4360 Å versus  $c$  for polypropylene oxide fractions in hexane at 46°C

### Osmometry

Osmotic pressures of solutions of the fractions in toluene at 25°C were measured by Dr M. Senez. Pinner-Stabin osmometers and type 600 gell-cellophane membranes were used. Extrapolations to zero concentration were made by plotting the square root of the reduced osmotic pressure  $(\pi/c)^{1/2}$  against concentration. The number-average molecular weights and the second virial coefficients are given in Table 3 together with the quantity

$\overline{M}_w/\overline{M}_n$  which is a measure of the width of the number distribution of molecular weights. Also included in *Table 3* are similar data obtained for that fraction of the polypropylene oxide which is insoluble in methanol at 0°C (some 18 per cent of the whole polymer). Except for the data for fraction 5 these results, like those obtained from light scattering alone, indicate that the molecular weight distributions of the fractions do not differ greatly, a result which would be predicted from the method used to fractionate the polymer provided only that the degree of tacticity of a polymer is independent of the molecular weight when the molecular weight is high ( $> 10^5$ ).

*Table 3.* Osmometric data

Fraction No.	$\overline{M}_n \times 10^{-5}$	$A_2 \times 10^4$ $\text{cm}^3 \text{g}^{-2} \text{mole}^{-1}$	$\overline{M}_w/\overline{M}_n$
5	2.55	7.4	5.4
7	3.75	7.6	3.0
9	3.70	8.6	3.1
Methanol insoluble	5.50	7.5	3.3

#### *Melting point and crystallization*

The melting points of several of the fractions were measured on the hot stage of a polarizing microscope. Samples were heated to 120°C and then cooled rapidly (in  $< 20$  minutes) to 40°C at which temperature spherulites formed. After growth had apparently finished the temperature was raised at a rate of one degree in five minutes and the temperature at which the last trace of birefringence disappeared was recorded. These temperatures ( $T_m^\circ$ ) are recorded in *Table 4*. The rate of growth of the spherulites was also measured at 40°C by photographing the samples at intervals of time. Plots of the radii of spherulites versus time were linear and radial rates of growth ( $dr/dt$ ) are given in *Table 4*.

*Table 4.* Melting points and rates of crystallization

Fraction No.	$T_m^\circ$ (°C)	$(dr/dt) \times 300$ $\text{mm/min}$
2	71	1.40
3	68	1.31
5	68	0.55
6	64	0.18
7	62	0.13
8	56	—
9	48	—

#### *Spectroscopy*

The high resolution (five parts in  $10^9$  with acetaldehyde) nuclear magnetic resonance spectra of fractions 2, 5 and 7 in both carbon tetrachloride and carbon disulphide were recorded at 35°C and 80°C by use of a Varian A60 spectrometer. The methyl resonance is split into a doublet due to coupling

POLYPROPYLENE OXIDE II

with the methine proton ( $J=6$  c/s) and there is evidence of unresolved finer structure which could arise from long range coupling to the methylene protons. The methylene and methine protons have very similar chemical shifts which result in a complex, poorly resolved, absorption at about  $6.66\tau$  which is presumably the ABC part of an  $ABCX_3$  spectrum. No correlations with crystallizability were observed and there appears to be little hope of determining the relative proportions of iso-, syndio- and hetero-tactic triads in polypropylene oxide by this technique.

The i.r. spectra of evaporated films of several fractions were recorded over the range  $600$  to  $4000\text{ cm}^{-1}$  by use of a Perkin-Elmer (model 21) double beam recording spectrophotometer. The spectra were similar to those reported by Kawasaki *et al.*<sup>7</sup> who attributed the differences between the spectra of amorphous and crystalline polypropylene oxide in the solid state to rotational isomerism. In *Figure 2* are shown the spectra of a sample of crystalline polypropylene oxide ( $A_2=1.85 \times 10^{-4}\text{ cm}^3\text{ g}^{-2}\text{ mole}^{-1}$  in hexane at  $46^\circ$ ,  $\bar{M}_w=1.8 \times 10^6$ ,  $T_m^0=71^\circ\text{C}$ ) recorded at  $23^\circ\text{C}$  and at  $90^\circ\text{C}$ . The disappearance of the band at  $1245\text{ cm}^{-1}$  indicates that it is assignable to a configuration in the crystalline matrix and is not directly attributable to a difference in the tacticity of the polymer. Also in *Figure 2* is a spectrum of fraction 9 recorded at  $23^\circ\text{C}$  which is seen to be similar to that of the molten, more crystalline, polymer.

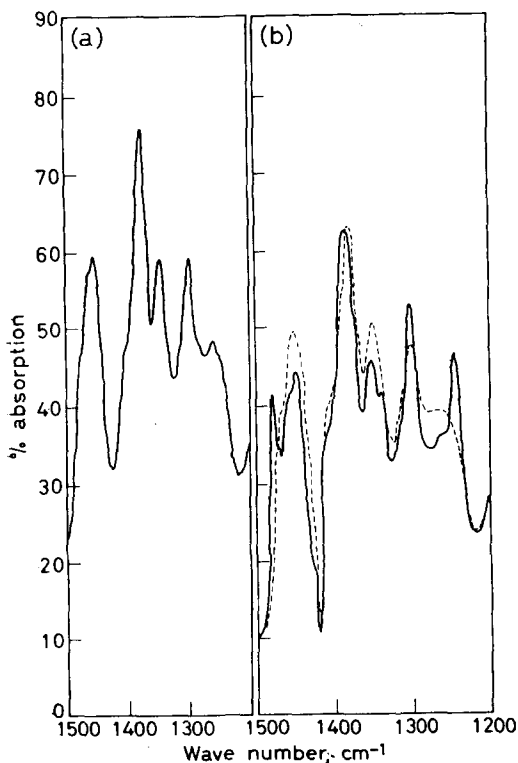


*Figure 2*—Infrared spectrum of fraction 9 at  $23^\circ\text{C}$  (a) and of a more crystalline sample of polypropylene oxide (b) at  $23^\circ\text{C}$  (solid line) and  $90^\circ\text{C}$  (broken line)

## DISCUSSION

From the nature of the fractionation and from the variation of melting points and rates of crystallization from fraction to fraction it can be concluded that the variation of the second virial coefficient in hexane at 46°C is a consequence of differences in degree of structural regularity in the polymers. We assume that the differences are in degree of isotacticity. It may be noted that these variations could not be accounted for by the differences in molecular weight distribution since there is both theoretical<sup>8</sup> and experimental<sup>9</sup> evidence that a polydisperse polymer with a single peaked distribution has the same second virial coefficient as a monodisperse polymer of the same average molecular weight. Differences in branching would not be consistent with the approximately constant values of both  $[\eta]$  and  $\bar{M}_w$ .

The conclusions of the earlier investigators can be summarized as follows:

(a) For a given molecular weight the intrinsic viscosity measured in a good solvent is independent of the tacticity of the polymer. The intrinsic viscosity measured in a poor solvent may vary if the degree of tacticity of the polymer varies<sup>1,2</sup>.

(b) The second virial coefficient is smaller for a more tactic polymer.

(c) The unperturbed dimension is larger for a more tactic polymer although no direct measurements in  $\theta$ -solvents have been made<sup>1,2,10</sup>.

(d) The Flory entropy parameter  $\psi_1$  is larger for a more isotactic polymer<sup>1,11</sup>. The data concerning the heat parameter  $\kappa_1$  are conflicting<sup>1,11</sup>.

The differences in the second virial coefficients between our fractions in the poorer solvent are much larger than those measured between samples of tactic and atactic polymer by other workers. Most probably the method of fractionation used in this work results in fractions with much narrower distributions of degrees of tacticity than have been obtained before and hence a magnification of the effects observed previously. The choice of solvent is also of obvious importance. The constancy of both  $\bar{M}_w$  and  $[\eta]$  was anticipated from the work referred to earlier. We can write the intrinsic viscosity/molecular weight relationship in the form

$$[\eta] = \Phi (\bar{r}_0^2)^3 \alpha^3 / M$$

where  $\alpha$  is the expansion factor ( $\alpha^2 = \bar{r}^2 / \bar{r}_0^2$ ) and  $\bar{r}^2$  and  $\bar{r}_0^2$  are respectively the mean square end-to-end distance and the unperturbed mean square end-to-end distance of the randomly coiled polymer molecule. In order that polymers of differing degree of tacticity should have identical intrinsic viscosity/molecular weight relationships it is necessary that the product  $(\bar{r}_0^2)^3 \alpha$  should be independent of tacticity. As the unperturbed dimensions of the more tactic polymers are presumably the greater it follows that the expansion factor must be correspondingly smaller, as would be expected from the values obtained for the virial coefficients. It is surprising, however, that these two parameters compensate so precisely over the wide range of  $A_2$  values we have measured.

Current theories of dilute polymer solutions enable the problem of the variation of  $A_2$  to be formulated in more precise terms. If it is

assumed that these polymers are random coils in solution (and this may not be a good assumption<sup>12</sup>) the theoretical expression for  $A_2$  for a mono-disperse polymer is

$$A_2 = N_0 \beta n^2 h(z) / 2M^2$$

where  $n$  is the number of chain segments,  $M$  the molecular weight,  $N_0$  Avogadro's number and

$$z = (3/2\pi\bar{r}_0^2)^{3/2} \beta n^2$$

$$\beta = 2V_1\psi_1(1 - \theta/T)$$

$V_1$  is the volume of a solvent molecule and  $\psi_1$  and  $\theta$  the entropy parameter and the  $\theta$ -temperature of Flory's dilute solution theory. The term  $h(z)$  is a series expression in powers of  $z$  which can take many forms depending upon the approximations made in the theory<sup>13</sup>. The existence of so many parameters in this expression necessarily leads to ambiguity in the interpretation of the variation of  $A_2$  with tacticity. From the work of Krigbaum *et al.*<sup>1,10</sup> and of Kinsinger and Wessling<sup>11</sup> it is clear that  $\psi_1$ ,  $\theta$  and  $\bar{r}_0^2$  are all functions of the degree of tacticity of the polymer.

To consider  $\theta$  alone our data show that fraction 1 must have a  $\theta$ -temperature higher than 46°C since  $A_2$  is negative. On the other hand fraction 9 has  $A_2$  equal to  $2.96 \times 10^{-4} \text{ cm}^3 \text{ g}^{-2} \text{ mole}^{-1}$  at 25°C and hence the  $\theta$ -point must be much lower than 25°C for this polymer. It is, of course, impossible to measure the  $\theta$ -points of these polymers in hexane since they crystallize from solution before liquid-liquid phase separation occurs. This large difference in  $\theta$ -points is enough to account for the variation in  $A_2$  observed. Figure 3 shows  $A_2$  as a function of  $\theta$ -point,

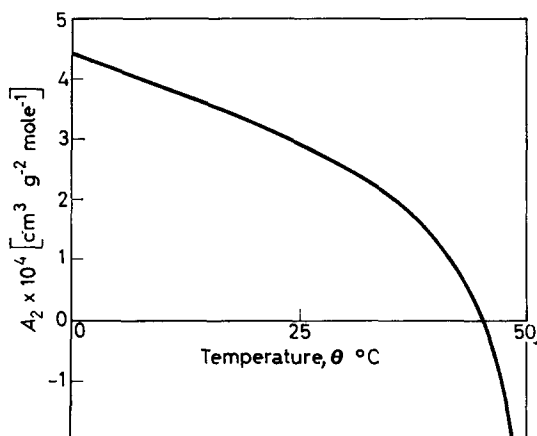


Figure 3—Second virial coefficient at 45°C calculated from Casassa - Markovitz theory as a function of  $\theta$ -temperature

the curve being calculated by use of the Casassa-Markovitz<sup>14</sup> modified expression for  $h(z)$  with the following values of the other parameters:  $M = 10^6$ ,  $\psi_1 = 1$ ,  $V_1 N_0 = 100 \text{ cm}^3$ ,  $n = 10^4$  ( $\bar{r}_0^2$ )<sup>1/2</sup> = 1 000 Å and the temperature

of measurement  $T = 45^\circ\text{C}$ . Measurements of  $A_2$  at temperatures appreciably above the  $\theta$ -point (e.g. toluene at  $25^\circ\text{C}$ ) will be less dependent on the degree of tacticity of the polymer since the dependence of  $A_2$  on  $\theta$  decreases as  $\theta$  decreases.

## CONCLUSIONS

The origin of the dependence of the second virial coefficient (or  $\theta$ ) on tacticity remains obscure. A complete explanation must await more detailed investigations of the properties of tactic polymers in solution since it is probably to be sought in terms of specific interactions when two polymers with a high degree of tacticity (crystallizability) interact in a poor solvent. It would appear, however, that measurements of the second virial coefficient in a poor solvent provide a sensitive qualitative guide to the degree of tacticity of polymers of the type discussed in this paper.

*We wish to express our appreciation to Dr E. Powell for preparing the polypropylene oxide, to Dr M. Senez for the osmotic pressure measurements, to Messrs F. W. Lord and F. D. Hartley of I.C.I. Limited, Blackley, Manchester, for help and advice in determining the rates of crystallization, to Mr D. J. Blears for the n.m.r. spectra, and to Mr C. S. Clemson for experimental assistance.*

Chemistry Department,  
University of Manchester

(Received July 1963)

## REFERENCES

- <sup>1</sup> KRIGBAUM, W. R., KURZ, J. E. and SMITH, P. J. *phys. Chem.* 1961, **65**, 1984
- <sup>2</sup> KRAUSE, S. and COHN-GINSBERG, E. *Polymer, Lond.* 1962, **4**, 565
- <sup>3</sup> See for example STANLEY, E. and LITT, M. J. *Polym. Sci.* 1960, **43**, 453
- <sup>4</sup> BOOTH, C., JONES, M. N. and POWELL, E. *Nature, Lond.* 1962, **196**, 772
- <sup>5</sup> UTIJAMA, H., KOMIYAMA, J., ITANI, H. and TAMURA, M. *Reports on Progress in Polymer Physics in Japan*, 1961, **4**, 127
- <sup>6</sup> KOBAYASHI, T. *Bull. chem. Soc. Japan*, 1962, **35**, 726
- <sup>7</sup> KAWASAKI, A., FURUKAWA, J., TSURUTA, T., SAEGUSA, T., KAKAGAWA, C. and SAKATA, T. *Polymer, Lond.* 1960, **1**, 315
- <sup>8</sup> CASASSA, E. F. *Polymer, Lond.* 1962, **4**, 625
- <sup>9</sup> CASASSA, E. F. and STOCKMAYER, W. H. *Polymer, Lond.* 1962, **3**, 53
- <sup>10</sup> KRIGBAUM, W. R., CARPENTER, D. K. and NEWMAN, S. J. *phys. Chem.* 1958, **62**, 1586
- <sup>11</sup> KINSINGER, J. B. and WESSLING, R. A. *J. Amer. chem. Soc.* 1959, **81**, 2908
- <sup>12</sup> PINO, P., CIARDELLI, F., LORENZI, G. P. and MONTAGNOLI, G. *Makromol. Chem.* 1963, **61**, 207
- <sup>13</sup> STOCKMAYER, W. H. *Makromol. Chem.* 1959, **34**, 139
- <sup>14</sup> CASASSA, E. F. and MARKOVITZ, H. J. *chem. Phys.* 1958, **29**, 493

# Nuclear Spin-Lattice Relaxation in Polyacetaldehyde

T. M. CONNOR

*The spin-lattice relaxation time has been measured in amorphous polyacetaldehyde over the temperature range  $+70^{\circ}\text{C}$  to  $-160^{\circ}\text{C}$ . Two minimum values of  $T_1$  were found, that at low temperatures being associated with rotation of methyl groups and that at high temperatures with the chain backbone motion commencing at the glass transition temperature. A barrier height,  $V_0$ , of  $4.55$  kcal/mole was obtained for the methyl group rotation which does not agree with a classical activation energy  $Q$  of  $2.2$  kcal/mole obtained by another method. The nuclear resonance measurements correlate fairly well with dielectric measurements in the region of the high temperature minimum.*

## EXPERIMENTAL

THE NUCLEAR spin-lattice relaxation time has been measured in an amorphous sample of polyacetaldehyde in the temperature range  $+70^{\circ}\text{C}$  to  $-160^{\circ}\text{C}$ , using pulse techniques<sup>1,2</sup>, a  $\pi$ ,  $\pi/2$  pulse train being employed<sup>3</sup>. The sample was identical to that already used for dielectric studies in this laboratory<sup>4</sup>. It was prepared by the method of Weissermel and Schmieder<sup>5</sup> using silica gel to catalyse the polymerization of pure dry acetaldehyde to give a polymer for which  $M_v = 1.5 \times 10^5$ . The sample was rubbery and almost transparent and was sealed off *in vacuo* and kept at  $0^{\circ}\text{C}$  prior to use. The measurements could not be carried to higher temperatures due to sample decomposition which started to occur at about  $+50^{\circ}\text{C}$ . The induction decay following the  $\pi/2$  pulse always consisted of a single component, which supports the idea that the polymer is truly amorphous over the whole temperature range investigated.

## RESULTS AND DISCUSSION

The experimental results are shown in *Figure 1* where  $\log T_1$  is plotted against reciprocal temperature. The plot shows two minima as expected from the consideration of previous results<sup>6-8</sup> on compounds containing  $\text{CH}_3$  groups in side chains which are capable of rotating around the C—C or C—O bonds joining them to the main polymer chain. In polypropylene<sup>7</sup> and polypropylene oxide<sup>8</sup> this low temperature minimum has been assigned to  $\text{CH}_3$  group motion by deuteration of the  $\text{CH}_3$  group. This is found to reduce the efficiency of the relaxation process by a factor of the order of  $\sim 16$ , as predicted theoretically. The low temperature minimum which occurs at  $-99.5^{\circ}\text{C}$  can thus be associated with rotation of the  $\text{CH}_3$  group in polyacetaldehyde. The high temperature minimum, whose position may be somewhat influenced by sample decomposition, occurs at  $+43.5^{\circ}\text{C}$  and is associated with a less well defined motion of the whole polymer chain. Similar sharp minima are observed in other polymers<sup>3,6-10</sup> and seem to be generally associated with molecular motions which commence at the 'glass transition' temperature. In polyacetaldehyde there is evidence from dielectric



and dilatometric studies<sup>4</sup> that this motion is effectively 'frozen out' at a temperature  $\sim -40^\circ\text{C}$ . No discontinuity is apparent in the  $\log T_1$  curve at this temperature, as is also the case for other polymers. This might be expected if it is assumed that the glass transition is not a true second order process but rather a kinetic phenomenon associated with the unfreezing of a particular mode of the lattice vibrations as the temperature is raised<sup>11</sup>, a view which is not generally held, however<sup>12</sup>.

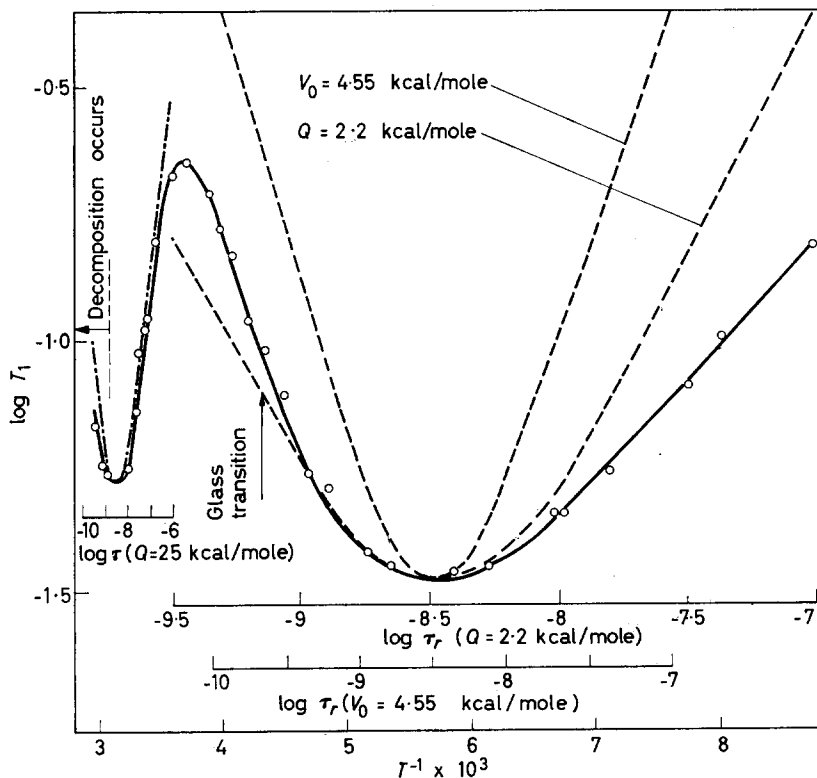


Figure 1—Plots of experimental and theoretical values of  $\log T_1$  for polyacetaldehyde against reciprocal temperature showing correlation time scales derived as described in text

A number of studies of the motions of methyl groups in solids by nuclear resonance techniques have been made, and in particular there have been attempts to relate the reorientation or tunnelling frequency of the  $\text{CH}_3$  groups to the nuclear relaxation times<sup>13-15</sup>. Stejskal and Gutowsky<sup>14</sup> have calculated the temperature dependence of the  $\text{CH}_3$  reorientation frequency assuming sinusoidal barriers to rotation. The reorientational correlation time,  $\tau_r$ , is given by

$$\tau_r = 1/3\pi\nu_r \quad (1)$$

where  $\nu_r$  is the reorientation frequency in cycles per second. By using the theory due to Bloembergen, Purcell and Pound and a Debye spectral

density function<sup>16</sup>, an expression for  $T_1$  was derived which takes into account the rotation of the  $\text{CH}_3$  group and tumbling of the whole molecule. Here, however, it appears that the only other significant motion so far as nuclear relaxation is concerned is that which occurs above the glass transition temperature ( $-40^\circ\text{C}$ ). This motion may be neglected at these low temperatures so that the expression for  $T_1$  can be reduced to the simple form

$$\frac{1}{T_1} = \frac{9\gamma^4 h^2}{40r_0^6} \left[ \frac{\tau_r}{1 + \omega^2 \tau_r^2} + \frac{4\tau_r}{1 + 4\omega^2 \tau_r^2} \right] \quad (2)$$

where  $\omega$  is the resonance frequency (30 Mc/s) and  $r_0$  is the interproton distance in the  $\text{CH}_3$  group. Equation (2) has a minimum value when  $\omega\tau = 0.6157$ , so that the value of  $v_r$  appropriate to the low temperature minimum in  $T_1$  can be found from equation (1). This is  $v_r = 3.25 \times 10^7$  c/s. By interpolating on the diagram given by Stejskal and Gutowsky, this reorientation rate is found to be equivalent to a barrier,  $V_0$ ,  $\sim 1590$  cm<sup>-1</sup> or 4.55 kcal/mole. A classical activation energy for  $\tau_r$  may also be derived from the area under a plot of  $1/T_1$  against reciprocal temperature, using the expression<sup>10</sup>

$$\left\langle \frac{1}{Q} \right\rangle_{\text{av.}} = \frac{2\omega}{3\pi AR} \int_0^{\infty} \left( \frac{1}{T_1} \right) d \left( \frac{1}{T} \right) \quad (3)$$

where  $\langle Q \rangle_{\text{av.}}$  is the mean value of the activation energy at a given temperature (assuming the possibility of a distribution of  $Q$ s). It is assumed that  $\tau_r$  has a simple exponential dependence on temperature over the range under the reciprocal  $T_1$  graph.  $A = 9\gamma^4 h^2 / 40r_0^6$ , which is the value of the constant in equation (2), and is assumed temperature independent. The integral is equivalent to the area mentioned above.  $A$  may be derived from the value of  $T_1$  at the minimum (0.0335 sec) which gives  $A = 3.95 \times 10^9$ . The area is 0.0925 sec<sup>-1</sup> deg<sup>-1</sup> which results in a value  $\langle Q \rangle_{\text{av.}} = 2.2$  kcal/mole. The value of  $A$  may also be obtained directly from the value of  $r_0$  (1.779 Å for a C—H distance of 1.091 Å and a tetrahedral angle) which gives  $A = 4.04 \times 10^9$ , which is close to the experimental value. Activation energies can also be derived from the limiting slopes of the  $\log T_1$  curve. Assuming that there is no distribution of activation energies or frequency factors, then the slope of the curve above the  $T_1$  minimum ( $\omega\tau_r \ll 1$ ) is  $-Q/2.303R$ , and below the minimum ( $\omega\tau_r \gg 1$ ) is  $+Q/2.303R$ . From the experimental curve,  $Q = 3.56$  kcal/mole for  $\omega\tau_r \ll 1$  and  $Q = 1.2$  kcal/mole for  $\omega\tau_r \gg 1$ . These values are consistent with that derived from equation (3), lying on either side of the mean value of 2.2 kcal/mole. This consistency makes it unlikely that there is a wide distribution of activation energies, since equation (3) takes into account the possible presence of such a distribution, whereas values of  $Q$  derived from the slopes do not. The values of the classical activation energy are thus considerably smaller than the barrier height,  $V_0$ . In *Figure 1* two theoretical curves are drawn showing the variation of  $T_1$  with temperature. The first is for the case where  $V_0 = 4.55$  kcal/mole when  $\tau_r$  is derived from the theoretically calculated

values of  $v_r$ , and the second is for  $Q=2.2$  kcal/mole. For both curves  $T_1$  was calculated using equation (2). Over the temperature range considered, the values of  $v_r$  are approaching the classical limit, so that the effect of tunnelling is small and so  $V_0$  can be identified with an activation energy, the  $\tau_r$  scale being slightly non-linear only at its low temperature end. As expected the theoretical  $T_1$  values for  $Q=2.2$  kcal/mole are smaller than the experimental values when  $\omega\tau_r \ll 1$  and larger when  $\omega\tau_r \gg 1$ , although the apparent increase in activation energy as the temperature rises may in part be due to an increase in  $r_0$ , since  $T_1 \propto r_0^6$ . In the region of the  $T_1$  minimum the theoretical curve agrees well with the experimental points. The theoretical curve derived from  $V_0$  does not represent the data satisfactorily. It has been found that in general values of  $Q$  for  $\text{CH}_3$  group rotations derived from  $T_1$  measurements on substituted methanes<sup>17</sup> are slightly lower than the values of  $V_0$  derived from the tunnelling calculations although this is to be expected in the temperature regions where the classical limit is not approached. However, as pointed out, the temperature range is such that there should not be much difference between  $Q$  and  $V_0$ . There seems to be no obvious explanation of the discrepancy.

The high temperature  $T_1$  minimum can be correlated with dielectric measurements<sup>4</sup>. The plot of frequency against temperature of maximum loss is linear in the temperature range  $40^\circ$  to  $5^\circ\text{C}$  and corresponds to an activation energy of 25 kcal/mole. This value was used to construct a correlation time scale which was adjusted so that the minimum temperature of  $+43.5^\circ\text{C}$  corresponded with the value of  $\tau$  given by  $\omega\tau=0.6157$ . The ratio  $\tau_D/\tau$  in this case, where  $\tau_D$  is the dielectric correlation time, is  $\sim 15$  compared with a theoretical value of three expected on the basis of a Debye model<sup>18</sup>. This value may, however, be to some extent influenced by the fact that the sample started to decompose at a temperature just above the minimum. It was found that the dielectric loss curves could be fitted by a Fuoss-Kirkwood distribution of correlation times, with a value for the distribution parameter,  $\beta$ , of 0.53. This value of  $\beta$  was used to calculate  $T_1$  using the expression

$$\frac{1}{T_1} = A \frac{\beta}{\omega} \left[ \frac{(\omega\tau)^\beta}{1 + (\omega\tau)^{2\beta}} + 2 \frac{(2\omega\tau)^\beta}{1 + (2\omega\tau)^{2\beta}} \right] \quad (4)$$

which has been shown<sup>10</sup> to be the modification of Kubo and Tomita's expression<sup>18</sup> for  $T_1$  appropriate when the distribution of correlation times is described by a Fuoss-Kirkwood distribution function.  $A$  was determined as before from the value of  $T_1$  at the minimum. The theoretical values of  $T_1$  obtained are plotted in *Figure 1*, and agree fairly well with the experimental values. It can thus be concluded that the temperature dependences of the dielectric and nuclear correlation times are similar but that the ratio of their magnitudes at a given temperature is larger than might be expected, by a factor of about five.

*This work forms part of the research programme of the Basic Physics Division, and is published by permission of the Director of the National Physical Laboratory. Thanks are due to Dr G. Williams for providing the sample of polyacetaldehyde.*

*Basic Physics Division,  
National Physical Laboratory,  
Teddington, Middlesex*

*(Received August 1963)*

REFERENCES

- <sup>1</sup> HAHN, E. L. *Phys. Rev.* 1950, **80**, 580
- <sup>2</sup> CARR, H. Y. and PURCELL, E. M. *Phys. Rev.* 1954, **94**, 630
- <sup>3</sup> ALLEN, G., CONNOR, T. M. and PURSEY, H. *Trans. Faraday Soc.* 1963, **59**, 1525
- <sup>4</sup> WILLIAMS, G. *Trans. Faraday Soc.* 1963, **59**, 1397
- <sup>5</sup> WEISSERMEL, K. and SCHMIEDER, W. *Makromol. Chem.* 1962, **51**, 39
- <sup>6</sup> KAWAI, T. *J. phys. Soc. Japan*, 1961, **16**, 1220
- <sup>7</sup> POWLES, J. G. and MANSFIELD, P. *Polymer, Lond.* 1962, **3**, 336 and 339
- <sup>8</sup> CONNOR, T. M. Unpublished results on polypropylene oxides
- <sup>9</sup> POWLES, J. G. and LUSZCZYNSKI, K. *Physica, 's Grav.* 1959, **25**, 455
- <sup>10</sup> CONNOR, T. M. *Trans. Faraday Soc.* To be published
- <sup>11</sup> TEMPERLEY, H. N. V. *Changes of State*, p 20. Cleaver-Hume Press: London, 1956
- <sup>12</sup> GIBBS, J. H. and DIMARZIO, E. A. *J. chem. Phys.* 1958, **28**, 373
- <sup>13</sup> POWLES, J. G. and GUTOWSKY, H. S. *J. chem. Phys.* 1955, **23**, 1962
- <sup>14</sup> STEJSKAL, E. O. and GUTOWSKY, H. S. *J. chem. Phys.* 1958, **28**, 388
- <sup>15</sup> DAS, T. P. *J. chem. Phys.* 1956, **25**, 896; 1957, **27**, 763
- <sup>16</sup> BLOEMBERGEN, N., PURCELL, E. M. and POUND, R. V. *Phys. Rev.* 1948, **73**, 679
- <sup>17</sup> STEJSKAL, E. O., WOESSNER, D. E., FARRAR, T. C. and GUTOWSKY, H. S. *J. chem. Phys.* 1959, **31**, 55
- <sup>18</sup> KUBO, R. and TOMITA, K. *J. phys. Soc. Japan*, 1954, **9**, 888

# Orientation in Crystalline Polymers Related to Deformation

Z. W. WILCHINSKY

*A mechanism is proposed to account for the preferred orientation of the crystal  $c$  axis in deformed polymers, the  $c$  axis being parallel to the molecule backbone. It is assumed that tie molecules provide mechanical linkages between the  $c$  axes of neighbouring crystals, so that preferred  $c$  axis orientation takes place in the direction of extension. The orientation is expressed as the weight average  $\langle \cos^2 \phi_\lambda \rangle$  where  $\phi$  is the angle between the  $c$  axis of a crystal and the direction of extension, and  $\lambda$  is the extension ratio. Calculations are presented for the orientation parameter,  $\langle \cos^2 \phi_\lambda \rangle$ , as a function of  $\lambda$  for an idealized fibre and for a sheet whose width remains constant during extension.*

THE MOST commonly observed type of orientation produced by deformation of a polymer is one in which the molecule backbone, or a crystal axis parallel to the molecule backbone, is preferentially oriented in the direction of extension, this orientation being an increasing function of the extension. A mechanism relating the molecular orientation to a uniform deformation of a sample was proposed by Bailey<sup>1</sup> in his studies of polystyrene. The nature of this orientation was described as one that would be experienced by slender rigid rods in a viscous uniformly deformed matrix. Although physically the orienting units cannot be regarded as slender rigid rods, Bailey's approach nevertheless may be quite useful. For example, this type of deformation proposed would transform a spherical region in a polymer into one of ellipsoidal shape. In crystalline polymers containing spherulites, one might expect an initially spherical spherulite to be deformed into an ellipsoidal one. Such deformations have indeed been observed<sup>2,3</sup>. However, if this mechanism is operative in microscopic regions, it would require the crystals to undergo a similar deformation and every crystallographic direction would be unselectively affected. As this does not happen, this mechanism cannot be used for crystalline polymers without further qualifications.

In the present paper, the mechanism considered by Bailey is modified to take into account the presence of undeformed crystals in a crystalline polymer. Relationships between the extension ratio and crystal orientation are then derived for several simple cases.

## MODEL OF THE POLYMER

In order to formulate a relationship between the orientation and the deformation producing it, one needs a physical model providing the appropriate constraints on the movement of the crystals during the deformation of the sample. Also, a chosen model should be consistent with known structural features of polymers. The following model of the polymer was chosen in accordance with the above considerations.

Within a crystal, the molecule backbone is parallel to a principal crystal axis, taken by convention as the  $c$  axis. In this discussion, the term

orientation will refer to the orientation of the  $c$  axis, which, of course, is equivalent to the orientation of the molecule backbone in the crystallized polymer.

It will be assumed that the crystals themselves are not deformed when a sample of polymer is deformed; therefore, there must be mechanical interaction between a crystal and its neighbours. It will be further assumed that crosslinking among molecules is absent and that the interaction is in effect limited to the ends of the crystals, i.e. to the extremities of the crystal  $c$  axes. Such interaction is inherent in the older fringed micelle concept of polymer structure. In the more recent folded chain concept, the interaction can be obtained by postulating the presence of 'tie molecules'<sup>4,5</sup>. The treatment will not be restricted to either of these structural concepts; however, it will be assumed that the interaction is such that the  $c$  axis tends to orient in the direction of the deforming strain.

To complete the picture, the interacting crystallites may constitute a larger structural unit, i.e. the spherulite. However, this is not a necessary requirement for the simple version of the mechanism.

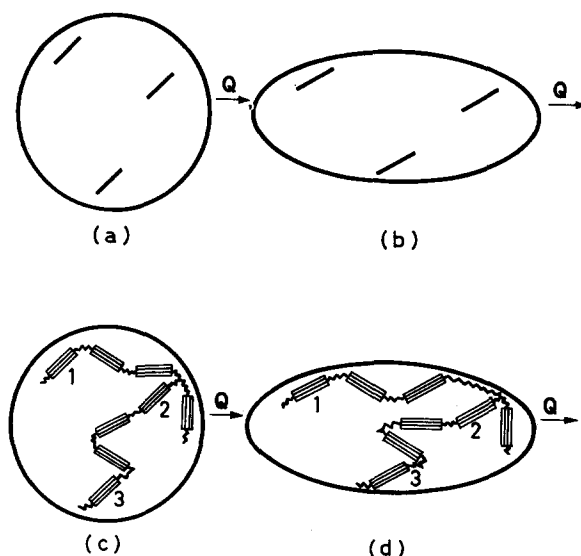


*Figure 1*—Orientation induced by deformation. (a) Spherical region before deformation; three parallel lines in region shown. (b) Orientation of lines in direction  $Q$  is increased after a uniform deformation. (c) Crystals in spherical region, linked by tie molecules. (d) Crystal orientation is increased in direction  $Q$  after orientation

#### DERIVATION OF RELATIONSHIPS BETWEEN ORIENTATION AND EXTENSION RATIO

The nature of the orientation being considered is illustrated schematically in *Figure 1*. A spherical region of a polymer is shown in (a) and an arbitrary direction in the sphere is represented by one of the lines. Other lines parallel

to the first are also shown. Let the polymer be subjected to a deformation such that the deformation ratios in three mutually orthogonal directions do not change from one representative region of the polymer to another. Such a deformation will be referred to as a uniform deformation. After a uniform deformation by an extension in a direction  $\mathbf{Q}$ , the sphere is deformed to an ellipsoid, and the lines have a greater degree of orientation in the  $\mathbf{Q}$  direction. However, as indicated in (b), the orientation of each line has been changed by the same amount. *Figure 1(c)* represents crystallites within a spherical region, the numbered members having the same orientation as the lines in (a). The region after a deformation similar to that of the preceding case is shown in (d). By virtue of the interactions via the tie molecules, the numbered crystallites have the same orientation as the lines in (b). For this simple model, it will be shown later that the final orientation depends only on the initial orientation (with respect to a chosen direction) and the deformation ratios in three orthogonal directions. The final orientation does not depend, for example, on whether a crystal in a spherulite is in a tangential, radial, or any other special position.

Although the deformation on a macroscopic scale may be uniform, it will not be strictly uniform on a microscopic scale, since the crystals are not deformed. This factor will be neglected for the time being, but will be discussed later. Therefore, the change of orientation, according to the foregoing simple concept, will be described in terms of the transformation of a vector in a homogeneous material undergoing a uniform deformation<sup>6</sup>.

Let a unit vector  $\mathbf{R}$  have the direction of the  $c$  axis of a crystallite. In terms of rectilinear coordinates, one may write

$$\begin{aligned}\mathbf{R} &= (x_2 - x_1)\mathbf{i} + (y_2 - y_1)\mathbf{j} + (z_2 - z_1)\mathbf{k} \\ &= X\mathbf{i} + Y\mathbf{j} + Z\mathbf{k}\end{aligned}\quad (1)$$

where  $x_1, y_1, z_1$  and  $x_2, y_2, z_2$  are the coordinates of the ends of the vector and  $X = x_2 - x_1$ , etc.

If a reference direction  $\mathbf{Q}$  is taken along the  $x$  axis, then the direction cosine along this direction may be written

$$\cos \phi = X \quad (2)$$

A measure of the degree of orientation in the direction  $\mathbf{Q}$  can be quantitatively expressed in terms of the parameter<sup>7</sup>  $\langle \cos^2 \phi \rangle$  where the brackets denote a 'weight' average.

In principle, this average can be obtained in the usual way:

$$\langle \cos^2 \phi \rangle = \frac{\sum_i \cos^2 \phi_i \Delta M_i}{\sum_i \Delta M_i} \quad (3)$$

where  $\Delta M_i$  is the weight of material oriented at angle  $\phi_i$ . As a result of a uniform deformation, the orientation of the material  $\Delta M_i$  will have changed from  $\phi_i$  to  $\phi_{i,a}$ , and the orientation parameter after deformation is

$$\langle \cos^2 \phi_a \rangle = \frac{\sum_i \cos^2 \phi_{i,a} \Delta M_i}{\sum_i \Delta M_i} \quad (4)$$

If the summations are replaced by integrals expressed in spherical coordinates, one may rewrite equations (3) and (4), respectively, as

$$\langle \cos^2 \phi \rangle = \frac{\int_0^\pi \int_0^{2\pi} \cos^2 \phi I(\phi, \psi) \sin \phi \, d\psi \, d\phi}{\int_0^\pi \int_0^{2\pi} I(\phi, \psi) \sin \phi \, d\psi \, d\phi} \quad (5)$$

and

$$\langle \cos^2 \phi_d \rangle = \frac{\int_0^\pi \int_0^{2\pi} \cos^2 \phi_d I(\phi, \psi) \, d\psi \, d\phi}{\int_0^\pi \int_0^{2\pi} I(\phi, \psi) \sin \phi \, d\psi \, d\phi} \quad (6)$$

where the axis of the coordinate sphere of unit radius is along the  $x$  axis,  $\psi$  is the angle of longitude and  $I(\phi, \psi)$  is the appropriate distribution function. It may be noted that the orientation after deformation is expressible in terms of the initial distribution.

Let the polymer undergo a deformation characterized by the deformation ratios  $\lambda$ ,  $\mu$  and  $\eta$  along the  $x$ ,  $y$  and  $z$  axes, such that  $\lambda > 1$  and  $\lambda\mu\eta = 1$ . In accordance with the assumed orientation mechanism, the  $c$  axis having an initial orientation in the direction of  $\mathbf{R}$  will have an orientation after deformation in the direction of  $\mathbf{R}_{\lambda, \mu, \eta}$  given by

$$\begin{aligned} \mathbf{R}_{\lambda, \mu, \eta} &= \lambda(x_2 - x_1) \mathbf{i} + \mu(y_2 - y_1) \mathbf{j} + \eta(z_2 - z_1) \mathbf{k} \\ &= \lambda X \mathbf{i} + \mu Y \mathbf{j} + \eta Z \mathbf{k} \end{aligned} \quad (7)$$

Also, after the deformation, the direction cosine of the crystal  $c$  axis along  $x$  is

$$\cos \phi_d = \lambda X / (\lambda^2 X^2 + \mu^2 Y^2 + \eta^2 Z^2)^{1/2} \quad (8)$$

Thus  $\cos \phi_d$  can be expressed in terms of the deformation ratios and the initial direction cosines along the coordinate axes. The orientation parameter after the deformation is then obtained by substituting (8) into the integrand of equation (6). In general, the solution is rather difficult. However, solutions were obtained for two important cases which will be referred to as the ideally stretched fibre and the sheet.

#### *Ideally stretched fibre*

The  $x$  coordinate and the direction of extension will be taken along the fibre axis. For a fibre to maintain a circular cross section during a uniform deformation, the deformation ratios will be  $\lambda$ , and  $\mu = \eta = \lambda^{-1/2}$ . Designating the direction cosine along the fibre axis by  $\cos \phi$  one then obtains by substituting into (8):

$$\cos \phi_d = \cos \phi_\lambda = \lambda X / \{\lambda^2 X^2 + \lambda^{-1} (Y^2 + Z^2)\}^{1/2} \quad (9)$$

In terms of the spherical coordinates  $\phi$  and  $\psi$

$$\cos \phi_\lambda = \cos \phi / (\cos^2 \phi + \lambda^{-3} \sin^2 \phi)^{1/2} \quad (10)$$



since the transformation relationships can be expressed by  $X = \cos \phi$ ,  $Y = \sin \phi \sin \psi$  and  $Z = \sin \phi \cos \psi$ .

The orientation parameter  $\langle \cos^2 \phi_\lambda \rangle$  can be calculated by substituting  $\cos \phi_\lambda$  for  $\cos \phi_a$  in equation (6). If the orientation is initially random, the distribution function  $I(\phi, \psi)$  is a constant, and the integral is readily evaluated to give

$$\langle \cos^2 \phi_\lambda \rangle = \frac{\lambda^3}{\lambda^3 - 1} \left\{ 1 - \frac{\tan^{-1}(\lambda^3 - 1)^{1/2}}{(\lambda^3 - 1)^{1/2}} \right\} \quad (11)$$

Let us now return to the problem arising from non-deformed crystals. Specifically, let us consider these crystals in a spherulite which has been deformed from a spherical to an ellipsoidal shape. In a completely uniform deformation, all regions in the spherulite would be characterized by the same set of deformation ratios. Consider the spherulite divided up initially into laminar regions as indicated in *Figure 2*(a). These shells are not

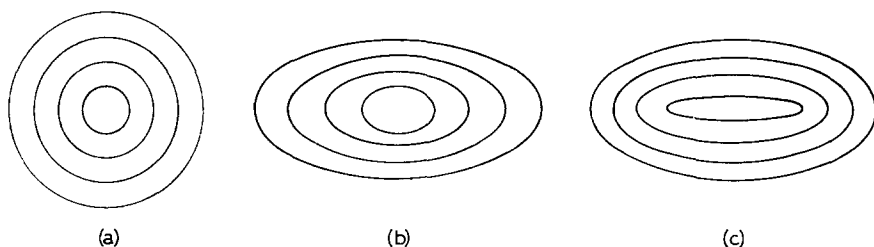


*Figure 2*—Deformation modes within spherulite. (a) Initial spherulite subdivided into spherical shells. (b) Uniform deformation; shapes of all ellipsoidal surfaces are similar. (c) Spherulite deformed to ellipsoidal shape as (b), but thickness of an elemental shell is uniform

intended to imply a laminar growth habit of the spherulite, but serve here only as a 'bookkeeping' device to follow the movement of the crystals within the spherulite. Each region constituting a spherical shell would be deformed to an ellipsoidal shell as indicated in *Figure 2*, (a) and (b). The wall thickness of any ellipsoidal shell is not uniform, but is proportional to the distance from the centre of the shell. To fulfil the geometric requirements of the deformation, the crystals in a spherical shell must be accommodated in the corresponding ellipsoidal shell. This might require a considerable flow of material and a considerable expenditure of energy, accompanied perhaps by disruption of crystals or local recrystallization of the polymer. Furthermore, the situation is aggravated progressively from the inner to the outer shells, since the displacements of crystals become more extreme and the amount of material involved becomes greater. To reduce the severity of this situation, the following mode of deformation was proposed<sup>6</sup>, which in general greatly reduces the displacement of the crystals relative to their neighbours.

Let a spherical shell be deformed into an ellipsoidal shell of approximately uniform thickness as indicated in *Figure 2*(c). The deforming strain

thus tends to be equalized within a shell. Furthermore, in such a deformation carried out with a minimum of rearrangement, the displacements of the crystals relative to each other are smaller in the outer shells, which contain the bulk of the material, and greater in the more highly deformed core, which contains a smaller fraction of the material. The shape of the outermost shell, being the same as that of the spherulite, can be characterized by the extension ratio for the entire specimen. Similarly, the shapes of the inner shells can be characterized by higher extension ratios. It will be assumed that the orientation parameter for any shell is given by equation (11) provided that the effective extension ratio for that shell is used. Then, for the entire deformed spherulite, the orientation parameter  $\langle \cos^2 \phi_\lambda \rangle$ , corrected for the enhanced orientation of the inner shells, can be expressed formally by the following equation

$$\langle \cos^2 \phi_\lambda \rangle = \frac{1}{V} \int_0^V \langle \cos^2 \phi_{\lambda, v} \rangle dV \quad (12)$$

where  $V$  is the volume of the spherulite and  $dV$  is the volume of an elemental shell of uniform thickness having an orientation parameter  $\langle \cos^2 \phi_{\lambda, v} \rangle$ . To evaluate  $\langle \cos^2 \phi_\lambda \rangle$ , the integral was approximated by a summation. Details of the calculations are outlined in the Appendix. The results of the calculations for selected values of  $\lambda$  are also listed there.

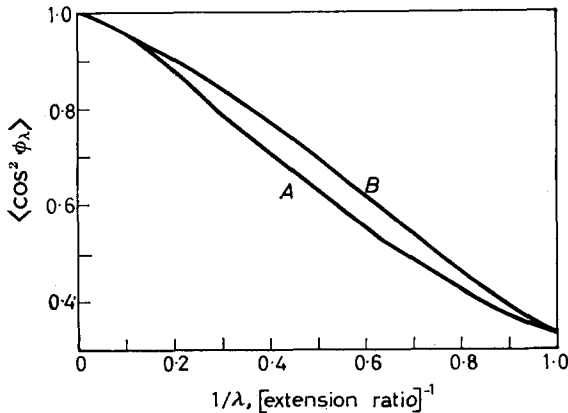


Figure 3—Orientation parameter calculated for an ideally stretched fibre. (A) Uniform deformation. (B) Deformation by mode of Figure 2(c)

Curves for the orientation parameter according to equations (11) and (12) are shown as functions of  $1/\lambda$  in Figure 3. As can be noted, the values differ by approximately ten per cent over a considerable range of  $1/\lambda$ .

*Ideally stretched sheet*

This case is characterized by the deformation ratios  $\lambda, \mu=1$  and  $\eta=1/\lambda$ , i.e. the width remains constant while the thickness changes by the factor  $1/\lambda$ . The expression for  $\cos^2 \phi_\lambda$  is then

$$\cos^2 \phi_\lambda = \lambda^2 \cos^2 \phi / (\sin^2 \phi \cos^2 \psi + \lambda^2 \cos^2 \phi + \lambda^{-2} \sin^2 \phi \sin^2 \psi) \quad (13)$$

Making the substitution of  $\cos^2 \phi_\lambda$  for  $\cos^2 \phi_d$  in equation (6) and integrating with respect to  $\psi$ , one obtains

$$\langle \cos^2 \phi_\lambda \rangle = \frac{1}{2} \int_0^\pi [\lambda^2 \cos^2 \phi \sin \phi / \{(\lambda^2 \cos^2 \phi + \lambda^{-2} \sin^2 \phi) (\lambda^2 \cos^2 \phi + \sin^2 \phi)\}^{1/2}] d\phi \quad (14)$$

A method for integrating the above expression analytically was not found; however, the integral was evaluated numerically by an electronic computer. The values thus obtained are listed in the Appendix.

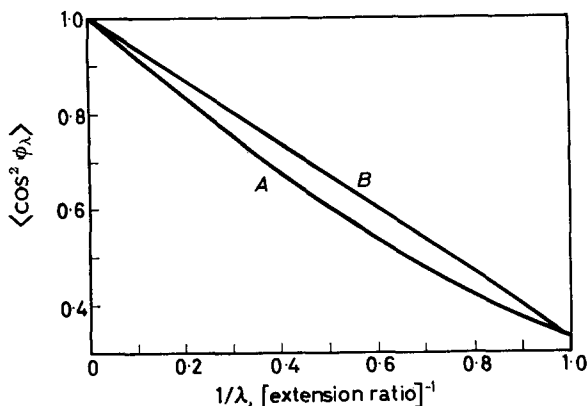


Figure 4—Orientation parameter calculated for a stretched sheet whose width is held constant. (A) Uniform deformation. (B) Deformation by mode of Figure 2(c)

Spherulitic deformation by the mode indicated in Figure 2(c) was also considered for the case of the sheet. Corrections were approximated for the enhanced deformation of the inner laminae of the spherulite by the same general procedure that was used for the fibre case. Further details are given in the Appendix. The orientation parameter, with and without the correction, is shown as a function of  $1/\lambda$  in Figure 4. Approximately the same difference between the two curves was obtained as for the fibre case.

#### DISCUSSION

A test of the derived equations would require accurate measurements of the  $c$  axis orientation for uniformly deformed samples. The orientation measurements can usually be carried out satisfactorily by X-ray diffractometer techniques using pole figure devices<sup>8</sup>. However, preparation of suitable samples may often present a more serious problem due to the tendency of crystalline polymers to neck down during extension. Carefully stretched polyethylene films free of neckdown, and measurements of  $\langle \cos^2 \phi_\lambda \rangle$  for

these films were reported by Stein and Norris<sup>7</sup>. Although the present theoretical development may not be rigorously applicable to those data, it is nevertheless of interest to compare the theoretical and experimental values for  $\langle \cos^2 \phi_\lambda \rangle$ . This is done in *Figure 5*. A rather good agreement is obtained with the curve for an ideally stretched fibre, corrected for the enhanced orientation of the inner regions of the spherulites. Although this is quite encouraging, a more definitive test is desirable.

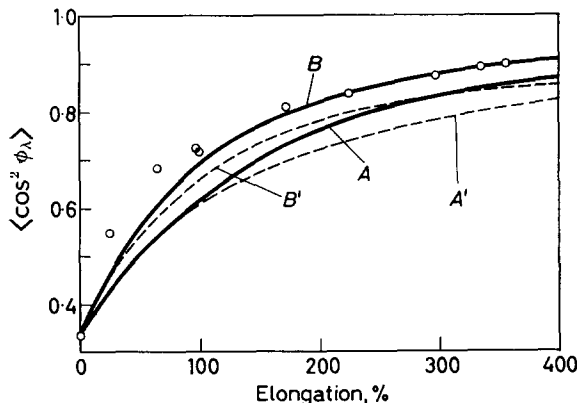


*Figure 5*—Calculated orientation parameters compared with data of Stein and Norris<sup>7</sup> for stretched film. Curve (A): fibre, uniform deformation. (B) Fibre, deformation by mode of *Figure 2(c)*. (A') Sheet, uniform deformation. (B') Sheet, deformation by mode of *Figure 2(c)*

In the evaluation of the orientation parameter, the crystals were considered to be randomly oriented initially. If this condition is not fulfilled, an allowance for the initial orientation can be made provided that the orientation parameter is greater than one third. This orientation parameter would correspond to an extension ratio of say  $\lambda_0$ , had the orientation been random initially. If the actual specimen is extended by a ratio  $\lambda'$ , the resulting orientation parameter would then correspond to an extension ratio of  $\lambda = \lambda_0 \lambda'$  for the polymer with initially random crystal orientation.

A final comment will be made regarding the relationship of the spherulite growth habit to the modes of deformation referred to in *Figure 2*. If the spherulite grows by laminar accretion, then the 'growth rings' can be represented by the concentric laminae in this figure. This type of growth habit has not been observed, to the writer's knowledge. If the spherulite has a radial growth habit, it would be expected to have radial structural regions<sup>9-11</sup>. One such region is represented schematically in *Figure 6(a)*. After deformation, this region is represented by *Figure 6(b)* and (c); the former is by the deformation mode of *Figure 2(b)* and the latter by the mode of *Figure 2(c)*. Further clues regarding spherulite growth habit can sometimes be obtained from a microscopic examination of fractures in polymers. For example, radial cracks in spherulites might be considered

evidence for a radial fibril structure. Radial cracks have been observed<sup>12-15</sup>, but the spherulites in these cases were brittle and were not mechanically deformed. Detailed observations of deformed spherulites might disclose which of the modes of deformation in *Figure 6* is the preferred one.

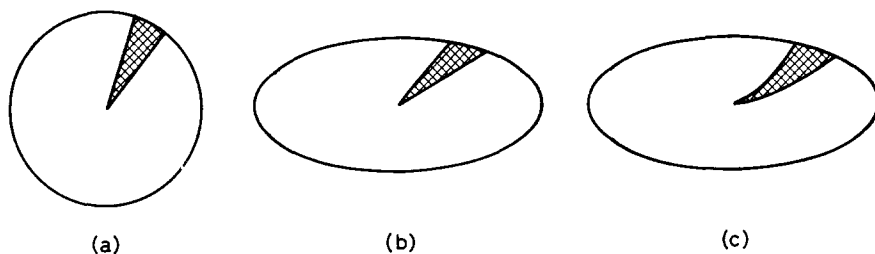


*Figure 6*—Deformation of a radial structure in a spherulite. (a) Before deformation. (b) After uniform deformation. (c) After deformation by mode of *Figure 2(c)*

The author is indebted to Mr Howard Oakley for calculating the values of the integral of equation (14).

*Esso Research and Engineering Company,  
Linden, New Jersey*

(Received July 1963)

## APPENDIX

### CALCULATION OF ORIENTATION PARAMETERS

These calculations are for the fibre and sheet cases discussed for a strictly uniform deformation and also for the modified mode of spherulite deformation illustrated in *Figure 2(c)*.

For a strictly uniform deformation,  $\langle \cos^2 \phi_\lambda \rangle$  for the fibre case was calculated in a straightforward manner by equation (11). For the sheet case, values of  $\langle \cos^2 \phi_\lambda \rangle$  were evaluated by electronic computer for  $\lambda = 1.25, 1.6, 2, 4, 6$  and  $10$ . For  $\lambda = 1$  and  $\infty$ ,  $\langle \cos^2 \phi_\lambda \rangle$  is  $\frac{1}{3}$  and  $1$  respectively. Other values were determined by graphical interpolation from a plot of  $\langle \cos^2 \phi_\lambda \rangle$  versus  $1/\lambda$ . Results of the calculations for the fibre and sheet are listed in columns A of *Table 1*.

The evaluation of  $\langle \cos^2 \phi_\lambda \rangle$  for the modified mode of deformation, which involves an enhanced orientation of the inner region of a spherulite, is expressed formally by equation (12). This equation can be evaluated satisfactorily by the summation

$$\langle \cos^2 \phi_\lambda \rangle = \frac{1}{V_N} \sum_{n=1}^N \langle \cos^2 \phi_{\lambda,n} \rangle (V_n - V_{n-1}) \quad (15)$$

where  $V_n$  is the volume within the  $n$ th ellipsoid starting with  $n=1$  for the

Table 1. Calculated values of  $\langle \cos^2 \phi_\lambda \rangle$ . Columns A are for a uniform deformation within the spherulite. Values in columns B, calculated by equation (15), take into account the enhanced orientation of the inner regions of the spherulite

Fibre			Sheet		
$\lambda$	A	B	$\lambda$	A	B
	1.0000	1.0000		1.0000	1.000
100	0.9984	0.999	20	0.952	0.970
50	0.9956	0.997	10	0.9076	0.932
30	0.9905	0.994	6.6667	0.865	0.898
20	0.9827	0.989	6	0.8516	—
15	0.9735	0.982	5	0.825	0.865
10	0.9523	0.968	4	0.7852	0.833
8	0.9343	0.955	3.333	0.748	0.801
6	0.9017	0.932	2.857	0.709	0.769
5	0.8740	0.911	2.5	0.673	0.737
4	0.8309	0.876	2.222	0.637	0.704
3.5	0.7996	0.852	2	0.6029	0.670
3	0.7580	0.818	1.818	0.569	0.637
2.5	0.7010	0.768	1.667	0.538	0.603
2.25	0.6643	0.732	1.6	0.5223	—
2	0.6205	0.691	1.539	0.507	0.568
1.8	0.5789	0.649	1.429	0.479	0.534
1.6	0.5304	0.596	1.333	0.451	0.499
1.5	0.5034	0.564	1.25	0.4242	0.465
1.4	0.4741	0.529	1.177	0.398	0.431
1.25	0.4281	0.469	1.111	0.374	0.396
1.18	0.4017	0.435	1.052	0.352	0.364
1.11	0.3760	0.398	1	0.3333	0.3333
1.05	0.3530	0.365			
1.01	0.3397	0.342			
1	0.3333	0.3333			

innermost, and  $V_0=0$ ;  $V_N$  is the volume of the spherulite, and  $\langle \cos^2 \phi_{\lambda,n} \rangle$  denotes the orientation parameter for the  $n$ th ellipsoidal shell whose volume is  $V_n - V_{n-1}$ .

The value of  $\langle \cos^2 \phi_{\lambda,n} \rangle$  was taken as the average of the following two calculations considering strictly uniform deformation: (i) the orientation parameter in the direction of extension for an extension ratio  $\frac{1}{2}(\lambda_n + \lambda_{n-1})$ , and (ii) the average of the orientation parameters for  $\lambda_n$  and  $\lambda_{n-1}$ . In this notation  $\lambda_n$  is the effective extension ratio for the  $n$ th ellipsoid. The outermost ellipsoid is the surface of the spherulite, hence for this ellipsoid,  $\lambda_N = \lambda$ , i.e. the extension ratio for sample.

Let  $A_n$ ,  $B_n$  and  $C_n$  be the axes of the  $n$ th ellipsoid,  $A_n$  being the major axis. For the fibre, the following relationships among these axes were used:  $B_n = C_n$ ,  $A_n = \lambda^{3/2} B_n$  and  $A_n - B_n = \alpha$ , where  $\alpha$  is a constant. Then  $A_n$ ,  $B_n$  and  $V_n$  can be expressed in terms of  $\alpha$  and  $\lambda_n$ . The ratio  $V_n/V_N$ , however, is independent of  $\alpha$  and can be written

$$\left(\frac{V_n}{V_N}\right)_{\text{fibre}} = \frac{\lambda_n^{3/2}/(\lambda_n^{3/2} - 1)^3}{\lambda_N^{3/2}/(\lambda_N^{3/2} - 1)^3} \quad (16)$$

For the sheet, the following relationships among the ellipsoid axes were

used:  $A_n = \lambda_n B_n$ ,  $A_n = \lambda_n^2 C_n$ , and  $A_n - C_n = \alpha$ . Then the ratio  $V_n/V_N$  is

$$\left(\frac{V_n}{V_N}\right)_{\text{sheet}} = \frac{\lambda_n^3/(\lambda_n^2 - 1)^3}{\lambda_N^3/(\lambda_N^2 - 1)^3} \quad (17)$$

Results of evaluating equation (15) with the aid of (16) and (17) are listed in columns B of *Table 1*.

## REFERENCES

- <sup>1</sup> BAILEY, J. *India Rubb. World*, 1948, **188**, 225
- <sup>2</sup> HARRIS, P. H. and MAGILL, J. W. *J. Polym. Sci.* 1961, **54**, S47
- <sup>3</sup> STEIN, R. S., RHODES, M. B., WILSON, F. R. and STEDHAM, S. N. *Pure appl. Chem.* 1962, **4**, 219
- <sup>4</sup> GEIL, P. H. Meeting of American Chemical Society, Division of Polymer Chemistry, Preprints of papers presented, 1962, Vol. III, No. 2, p 12
- <sup>5</sup> BASSETT, D. C., KELLER, A. and MITSUHASHI, S. *J. Polym. Sci. A*, 1963, **1**, 763
- <sup>6</sup> WILCHINSKY, Z. W. Meeting of American Chemical Society, Division of Polymer Chemistry, Preprints of papers presented, 1962, Vol. III, No. 2, p 111
- <sup>7</sup> STEIN, R. S. and NORRIS, F. H. *J. Polym. Sci.* 1956, **21**, 381
- <sup>8</sup> WILCHINSKY, Z. W. *J. appl. Phys.* 1960, **31**, 1969
- <sup>9</sup> KELLER, A. *J. Polym. Sci.* 1959, **36**, 361
- <sup>10</sup> KEITH, H. D. and PADDEN, F. J., Jr. *J. Polym. Sci.* 1959, **39**, 123
- <sup>11</sup> KHOURY, F. *J. Polym. Sci.* 1957, **26**, 275
- <sup>12</sup> INOUE, M. *J. Polym. Sci.* 1961, **55**, 443
- <sup>13</sup> REDING, F. P. and WALTER, F. R. *J. Polym. Sci.* 1959, **38**, 141
- <sup>14</sup> REDING, F. P. and BROWN, A. *Industr. Engng Chem. (Industr.)*, 1954, **46**, 1962
- <sup>15</sup> VAN SCHOOTEN, J. *J. appl. Polym. Sci.* 1960, **4**, 122

# *Morphology of Polymer Crystals: Screw Dislocations in Polyethylene, Polymethylene Oxide and Polyethylene Oxide*

W. J. BARNES and F. P. PRICE

*Single crystals of polyethylene, polymethylene oxide and polyethylene oxide have been prepared in suitable solvents at a variety of temperatures. The spacings between successive steps of the terraces and spiral ramps on the crystal surfaces have been measured. It was found that, as predicted by screw dislocation theory, the spacings varied inversely as the supercooling. However, the magnitude of the spacings was almost ten times that predicted by theory. It is proposed that the discrepancy results from the fact that the theory neglects the radius of the strained region around the screw axis. This neglect is tenable when, as in crystals of low molecular weight materials, the step height is of the order of a few Ångström units, but is indefensible when the step height is 100 Å or more as in polymer crystals.*

WHEN the platelike polymer single crystals grown from dilute solution were first observed and described, the most prominent topological features were spiral ramps and sets of terraces<sup>1</sup>. This type of morphology quite obviously resulted from a growth mechanism involving screw dislocations. This growth mechanism was originally proposed by Frank in 1949<sup>2</sup> to account for the growth of crystals of low molecular weight substances at small supercoolings. Actually the terraces and spiral ramps predicted by the theory were not noticed until after 1949. The original theory and its ramifications as later developed<sup>3</sup> were concerned only with growth of crystals of low molecular weight substances. Also the theory was concerned primarily with predictions of the behaviour of dislocations of small (usually unit) Burgers vector. However, experimentally, the heights of the steps of the spirals or terraces frequently were found to be several tens of Ångström units, corresponding to Burgers vectors of ten or more. Thus the assumption was made that the terraces actually observed usually resulted from the piling up of steps of several adjacent screw dislocations, each of unit Burgers vector. In the light of these conclusions it was obviously uninteresting to try to test the detailed predictions of the theory. In particular, no effort was made to see if the spacing between the turns of spirals of single screw dislocations conformed to expectation<sup>3</sup>.

The discovery and investigation of polymer single crystals led to the concept of chain folding<sup>4</sup>. Of particular interest here was the conclusion that the chain folds themselves should be considered as part of the crystal structure<sup>5</sup>, even though the fold length (crystal thickness) changes with crystal preparation temperature. Now the height of the steps of the ramps and terraces on the polymer crystals is the fold length. Thus if the folds are considered a part of the crystal structure, the screw dislocation must by



definition have a unit Burgers vector. Since these step heights are easily observable (100–200 Å), it seemed that observation of these features as functions of preparative conditions might lead both to a verification of the theory and to more detailed insight into the properties of polymer crystals.

It should be noted that the theory is developed on the assumption that the successive layers of the spiral ramps are in actual contact with each other at all times. In reality, at least in polyethylene crystals, it is found that during growth successive layers are splayed out about the screw axis and thus are not in contact<sup>6</sup>. The closely layered structures observed in the electron microscope result from the collapse of the splayed structures when they are sedimented on to the supporting substrate. This discrepancy between theoretical assumption and observation fortunately has no bearing either on the qualitative arguments given above or the quantitative details presented below. This is true because the aspects of the theory with which we will be concerned here result only from the assumption that the rate of step advance is constant, regardless of the mechanism by which new material adds to the step face.

The theory, in its simplest form, predicts that, for spirals uncomplicated by polygonization resulting from non-isotropic growth, the spacing between successive turns of the spiral is

$$y_0 = 4\pi r_c \quad (1)$$

where  $r_c$  is the smallest radius of curvature of the spiral. In the simple theory  $r_c$  was equated to  $\rho_c$ , the radius of curvature of a critical sized growth nucleus. This radius for a cylindrical pillbox type nucleus is given by

$$\rho_c = 2\sigma_s / (\Delta S) (\Delta T) \quad (2)$$

where  $\sigma_s$  is the interfacial energy of the curved surface of the cylinder,  $\Delta S$  is the entropy of fusion and  $\Delta T$  the supercooling. If the assumption that  $r_c = \rho_c$  is valid, then

$$y_0 = 8\pi\sigma_s / (\Delta S) (\Delta T) \quad (3)$$

and since  $\Delta S$  is independently ascertainable, measurement of  $y_0$  as a function of  $\Delta T$  should permit determination of  $\sigma_s$ . The rest of this article is concerned with a description of how well these predictions are borne out.

The polymers used were linear polyethylene (Marlex 50), polyethylene oxide and polymethylene oxide (Delrin). Crystals of each were prepared from suitable solvents at high dilution and examined in the electron microscope. In addition growth spirals on the free surfaces of crystallized bulk polyethylene oxide were also examined.

#### EXPERIMENTAL

The linear polyethylene used was obtained from the Phillips Petroleum Company under the trade name Marlex 50. It was precipitated from 0.01 per cent solution in *p*-xylene at temperatures between 80° and 90°C.

Polymethylene oxide was obtained as the polymer Delrin from E. I. du Pont de Nemours and Company and was used without modification. It was precipitated from 0.01 per cent solution in cyclohexanol at temperatures between 130° and 150°C.

The polyethylene oxide was obtained from the Union Carbide Chemicals Corporation under the trade name Carbowax 6000. This is the same material used in previous investigations<sup>7</sup>. It was precipitated from 0.05 per cent solutions of either pure *p*-xylene or 80 per cent *p*-xylene, 20 per cent cyclohexane solution. Precipitations were carried out in the temperature range of 16° to 30°C. Two solvents were used to investigate the effect of varying solvent power on the spiral spacings. With this polymer it was found that spirals and terraces could be observed on the free surfaces of bulk crystallized samples. Accordingly films of this material were held for several days at fixed temperatures in the range of 48° to 56°C after having been quenched from about 100°C.

The precipitations from dilute solution were carried out by quenching according to the technique of Holland and Lindenmeyer<sup>8</sup>. Here a known small volume of hot solution of ten times the final desired concentration was added with good stirring to nine times that volume of solvent held at the desired precipitation temperature. Immediately after mixing the stirring was stopped. After sufficient time for precipitation had passed, the sample was filtered at temperature and the precipitate redispersed in a non-solvent for further manipulation. This technique eliminates uncertainties about the temperature at which crystals are formed but at the same time results frequently in fractured crystals.

A drop of the suspension of redispersed crystals was placed on a microscope slide and dried. Subsequently the crystals were shadowed with platinum (shadowing angle 30°) and coated with amorphous carbon. The shadowed carbon film containing the crystals was floated off on water and picked up on electron microscope grids. Usually, but not always, the polymer crystals were dissolved from this film by use of suitable solvents. With the polyethylene oxide both from dilute solution and in bulk, the water used to remove the carbon film from the slide also dissolved away the polymer substrate. The shadowed films were then examined in the Siemens Elmiskop I. Photographs of appropriate areas were subsequently measured to give the desired data.

In the single crystals the Archimedes type spirals predicted by the simple screw dislocation theory<sup>3</sup> are not observed. Instead differential growth rates in various crystallographic directions manifested themselves in the well developed polygonization of the ramps and terraces. Accordingly when there was any choice to be made in the direction along which measurements of spiral spacings were taken, that direction was chosen along which the spacings were smallest.

It should be noted that equation (2) predicts that  $\rho_c \Delta T$  should be a constant. Further, equation (3) shows that plots of  $1/y_0$  versus  $T$  should be straight lines of slope  $-\Delta S/(8\pi\sigma_s)$  and intercept  $T_m \Delta S/(8\pi\sigma_s)$ . This fact permits direct experimental determination of the fusion or solution temperature,  $T_m$ .

#### RESULTS AND DISCUSSION

We will first consider the morphology of the screw dislocations in the various types of polymers. The appearance of these structures in polyethylene has been extensively described many times before<sup>9</sup>. All the structures observed by previous investigators were, in fact, found by us.

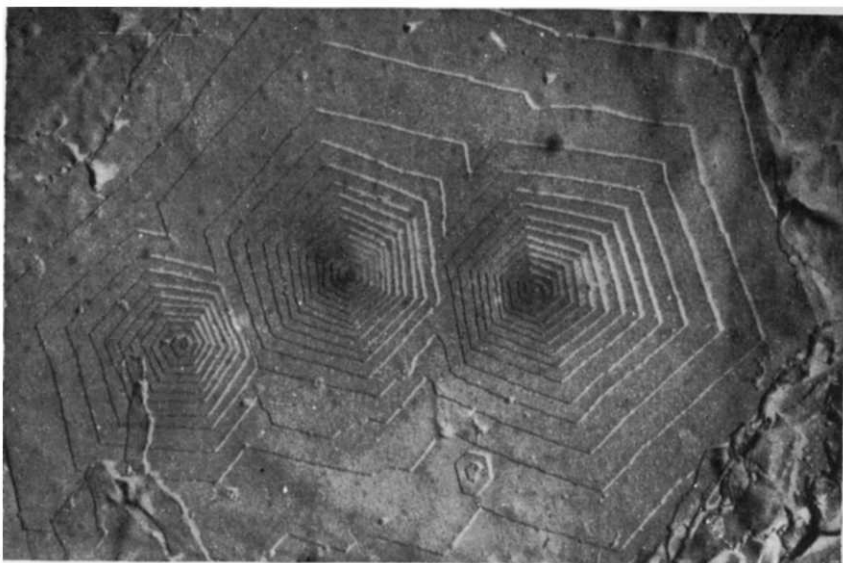
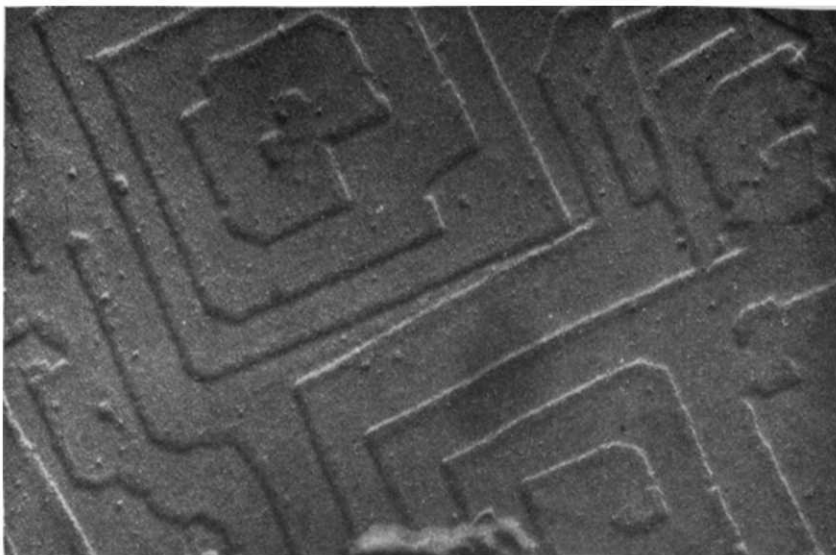


Figure 1—Electron micrograph of shadowed surface replica of single crystal of polymethylene oxide

The typical hexagonal morphology found in single crystals of polymethylene oxide<sup>10</sup> is illustrated by *Figure 1*. This picture shows three sets of ramps resulting from screw dislocations in a single crystal of this polymer. The three spirals did not start at the same time, for the centre one has one more step than one neighbour and three more than the other neighbour. The constancy of step height is remarkable for, where the steps of neighbouring spirals meet, the registry is essentially perfect. It should also be noted that in each spiral the successive layers tend to be twisted with respect to the underlying ones. This results in the edges of successive steps being not quite parallel. Also it is clear that the distances between successive turns of the spirals are not constant but increase as the distance from the screw axis increases. This implies that the rate of advance of the step of the spiral increases as the distance from the screw axis increases. In fact theory shows that the distances between successive turns of the spiral are direct measures of the relative velocities of step advance at various distances from the screw axis. In this polymer the distance between successive turns of the spiral [ $y_0$  of equation (1)] was taken as the average distance for the first eight or less innermost turns. This variation of  $y_0$  with distance from the screw axis is most marked in polymethylene oxide. It is very much less in the other polymers discussed here.

In *Figure 2* are shown typical growth spirals and terraces on a single crystal of polyethylene oxide precipitated from dilute solution. The square morphology of the terraces reflects the underlying crystal structure which favours growth on the 120 crystal faces. The detail in *Figure 2* is interesting in that it shows both a spiral ramp resulting from a single screw dislocation and a set of terraces resulting from the interaction of two nearby screw



*Figure 2*—Electron micrograph of shadowed surface replica of single crystal of polyethylene oxide

dislocations of opposite sense. In this picture also the remarkable constancy in step height is well illustrated.



*Figure 3*—Electron micrograph of shadowed surface replica of bulk crystallized polyethylene oxide crystallized at 50°C

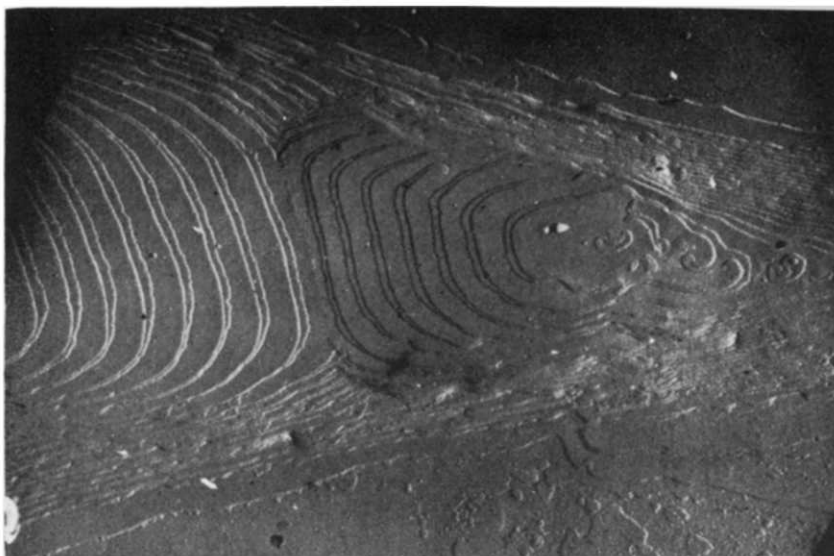


*Figure 4*—Electron micrograph of shadowed surface replica of bulk crystallized polyethylene oxide crystallized at 55°C

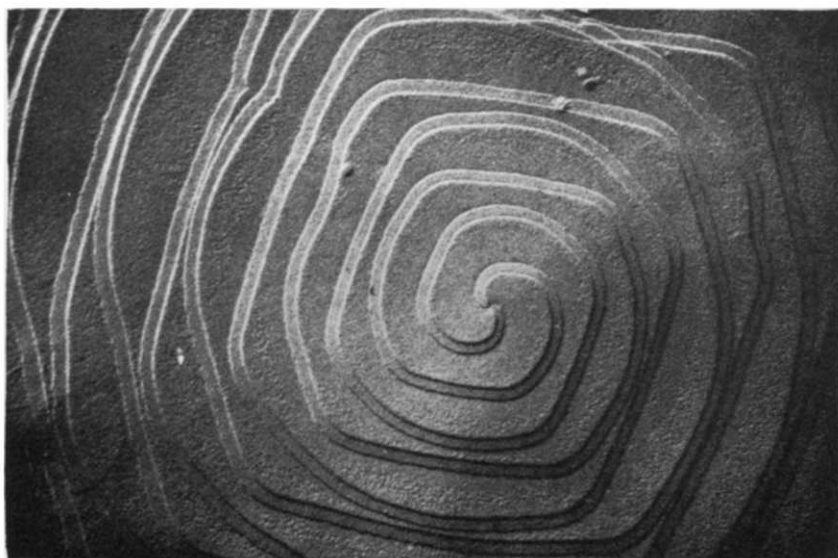


*Figure 5*—Electron micrograph of shadowed surface replica of bulk crystallized polyethylene oxide crystallized at 56°C

*Figures 3, 4 and 5* show replicas of surfaces of bulk polyethylene oxide crystallized at successively higher temperatures. Specimens such as these when examined in the light microscope show well developed spherulite structure. All these pictures show spirals which consist of a double step.

This is immediately apparent in *Figures 4* and *5*, but close inspection of *Figure 3* shows that this spiral also is double, although the definition is quite poor. *Figures 4* and *5* both show that the step is double from its inception. *Figures 3, 4* and *5* also show that as the growth temperature is raised, and hence the growth rate diminished, increasing polygonization results from differences between growth rates in various crystallographic directions.

The doubling of the step is unique to this polymer so far as we know. The phenomenon is most puzzling and is worth some further comment. In the first place, measurement of the step heights from the length of the shadows in the electron micrographs shows each member of the doublet to be about 110 Å in height independent of temperature of preparation. Measurement of small angle X-ray diffraction patterns of samples of this polymer crystallized in bulk in the same temperature range give spacings very close to 200 Å, independent of the crystallization temperature. It seems probable that this 200 Å spacing is connected with the double step observed in the screw dislocations. It may be that some such effect as alternate tilting of the *c* axis with respect to the basal planes makes the actual repeat distance twice the height of the spiral step. Further, since the polymer used has a molecular weight of about  $1.2 \times 10^4$  and since the *c* axis length in the unit cell is 19.4 Å, and since the chain is twisted into a  $7_2$  helix along the *c* direction, only about eight folds of the chain are sufficient to accommodate it into a 100 Å distance. Whether this small number of folds per chain will permit this polymer to follow the same behaviour as other polymers so far as crystallization is concerned is problematical. It is worth noting that Kiessig<sup>11</sup> found a dependence of large angle spacing on molecular weight in bulk crystallized polyethylene oxide of only slightly lower molecular weight than the one employed here.

The results of the study of the effect of growth temperature on spiral spacing are displayed in *Table 1*. Also presented are the values of  $r_c$  calculated from equation (1) and  $r_c \Delta T$  for each temperature.

The data displayed in *Table 1* show that, as expected, the spiral spacing increases with increasing temperature. In the last column are shown values of  $r_c (\Delta T)$ . While the precision of the measurement is not all that might be desired, the values of this quantity are constant for each polymer to within  $\pm 20$  per cent. Thus it appears that, at least within these limits, the predictions of equation (3) are confirmed. However, a cursory inspection of the values of  $r_c$  given in the penultimate column shows them to be significantly larger than expected. In fact if equation (3) is used to calculate  $\sigma_s$ , values of this quantity of 35, 50 and 110 erg/cm<sup>2</sup> are obtained for poly-methylene oxide, polyethylene oxide and polyethylene, respectively. The magnitudes of these quantities are much larger than they should be. In fact for polyethylene previous and probably much more reliable measurements<sup>12</sup> put the magnitude of this quantity as only 10 erg/cm<sup>2</sup>.

Therefore, while it appears that the functional dependence of the spiral spacing on the supercooling is that predicted by equation (3), the magnitude of that dependence is much too large. We will then assume that equation (1) is correct but that  $r_c \neq \rho_c$  and that  $r_c$  is merely the smallest radius of a

Table 1. Effect of growth temperature on spiral spacings in several polymers

Polymer	Temperature °C	Spacing $y_0$ , (Å)	$r_c$ (Å)	$r_c \Delta T$ (Å°C) × 10 <sup>3</sup>
Polymethylene oxide 0.01 % from cyclohexanol(*)	130	720	57	1.6
	135	1 050	84	1.9
	140	1 270	101	1.8
	145	1 960	156	2.0
	150	1 940	154	1.2
				av. 1.7
Polyethylene oxide 0.05 % from 80/20 <i>p</i> -xylene/ cyclohexane(†)	16	850	68	1.6
	20	1 250	99	2.0
	25	1 850	147	2.2
	30	2 450	195	2.0
				av. 1.9
0.05 % from <i>p</i> -xylene(‡)	16	1 450	115	1.8
	20	2 350	187	2.2
	25	3 700	294	2.1
				av. 2.1
Bulk(§)	48	1 150	92	1.4
	50	1 000	80	1.1
	52	1 440	115	1.3
	54	2 610	208	1.9
	55	1 900	151	1.2
				av. 1.4
Polyethylene 0.01 % in <i>p</i> -xylene(¶)	80	1 420	114	4.0
	90	1 470	118	3.0
				av. 3.5

\*  $T_m = 158^\circ$  by extrapolation of  $1/y_0$  versus  $T$  plots.†  $T_m = 40^\circ$  by extrapolation.‡  $T_m = 32^\circ$  by extrapolation.§  $T_m = 63.2^\circ$  by experimental measurement.¶  $T_m = 113^\circ$  from calculations of temperature dependence of crystal thickness (see ref. 13).

pillbox-like crystal protuberance which will grow. As pointed out above, the simple theory of growth by the screw dislocation mechanism assumed a dislocation with a small Burgers vector. In crystals of low molecular weight substances, such a vector has a length of only a few Ångström units. This means that the radius of the strained region around the screw axis is small, probably less than the critical nucleus radius defined by equation (2). Further the volume of this strained region will generally be negligible. In polymer crystals on the other hand, a unit Burgers vector has a length of the order of 100 Å. This means that the radius of the strained region around the screw axis probably is of the order of 100 Å. This length is considerably larger than the critical nucleus radius defined by equation (2). The situation is sketched schematically in Figure 6. Here a step of height  $b$  is advancing across the crystal surface. Up to a distance  $\rho$  from the screw axis addition of new material to the step riser is certainly very

difficult. For the purposes of simplification we will assume that at distances less than  $\rho$  from the screw axis addition is impossible. Further we will assume that  $\rho$  can be defined by  $b = 2\rho \tan \alpha$ . Thus, with low molecular weight substances  $\rho < \rho_c$  where  $\rho_c$  is defined by equation (2). Thus equation

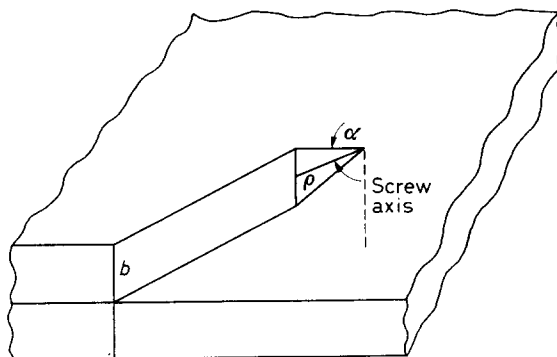


Figure 6—Schematic diagram of step associated with screw dislocation

(2) defines the minimum radius of curvature and the assumption  $r_c = \rho_c$  is justified. With polymers, however, because  $b$  is so large,  $\rho > \rho_c$  and the assumption  $r_c = \rho_c$  is no longer justified. Here the minimum radius must be  $r_c = \rho$  and since  $b$  is defined approximately by  $b = 2\sigma_e / (\Delta S) (\Delta T)$ , where  $\sigma_e$  denotes the fold surface energy,

$$r_c = \sigma_e / (\Delta S) (\Delta T) \tan \alpha \quad (4)$$

For polyethylene assuming  $\sigma_e \approx 100 \text{ erg/cm}^2$ , equation (4) yields  $\alpha = 45^\circ$ , a quite reasonable value.

It appears that, whereas initially it seemed that a study of the details of spiral structure in polymer single crystals might afford both a test of the screw dislocation theory and a measure of interfacial tensions, this is not so. A reasonable explanation for the failure is the neglect in the original theory of the dimensions of the strained region around the screw axis.

*The authors wish to thank Dr J. W. Cahn for several helpful discussions during the course of this investigation.*

General Electric Research Laboratory,  
Schenectady, New York

(Received July 1963)

#### REFERENCES

- <sup>1</sup> KELLER, A. *Growth and Perfection of Crystals*, pp 499 ff. Ed. Doremus, Roberts and Turnbull. Wiley: New York, 1958
- <sup>2</sup> FRANK, F. C. *Disc. Faraday Soc.* 1949, **5**, 48
- <sup>3</sup> BURTON, W. K., CABRERA, N. and FRANK, F. C. *Phil. Trans.* 1951, **A234**, 299
- <sup>4</sup> KELLER, A. *Phil. Mag.* 1957, **2**, 21
- <sup>5</sup> BASSETT, D. C. and KELLER, A. *Phil. Mag.* 1962, **7**, 1553
- <sup>6</sup> MITSUKASHI, S. and KELLER, A. *Polymer, Lond.* 1961, **2**, 109
- <sup>7</sup> BARNES, W. J., LUETZEL, W. G. and PRICE, F. P. *J. phys. Chem.* 1961, **65**, 1742



- <sup>8</sup> HOLLAND, V. F. and LINDENMEYER, P. H. *J. Polym. Sci.* 1962, **57**, 589  
<sup>9</sup> KELLER, A. and BASSETT, D. C. *Roy. microsc. Soc.* 1960, **79**, 243  
<sup>10</sup> RENEKER, D. H. and GEIL, P. H. *J. appl. Phys.* 1960, **31**, 1916  
<sup>11</sup> KIESSIG, VON, H. *Kolloidschr.* 1962, **181**, 1  
<sup>12</sup> TURNBULL, D. and CORMIA, R. L. *J. chem. Phys.* 1961, **34**, 820  
<sup>13</sup> PRICE, F. P. *J. chem. Phys.* 1961, **35**, 1884

# The Morphology of Poly-4-methyl-pentene-1 Crystals

A. E. WOODWARD\*

*Poly-4-methyl-pentene-1 crystals, obtained from 0.06–0.1 per cent xylene solutions by isothermal growth at temperatures from 57° to 92°C as well as under non-isothermal conditions, were investigated by optical and electron microscopy. Crystals grown at temperature in the 57° to 74°C range have square bases and are about 100 Å thick. Some evidence is given which indicates that growth of one lamella upon another can occur by other than a screw dislocation mechanism. Crystals, obtained from a solution cooled slowly from 125°C, show folds across the centre as well as near the corners. These features suggest that the crystals grow as hollow pyramids which collapse upon removal from suspension as found for polyethylene. Those grown at temperatures from 78°C to 92°C showed similar collapse features in addition to a turning-under at the corners.*

It is well known that a number of high polymers can be crystallized from dilute solution giving lamellae of various shapes depending on the polymer, solvent and temperature conditions of growth<sup>1,2</sup>. Furthermore, electron diffraction studies indicate that the polymer chains are perpendicular or near-perpendicular to the crystal face. Due to the fact that the polymer chains are much longer than the lamellar thickness ( $\sim 100$  Å) it is postulated that chain folding occurs. For linear polyethylene there is evidence to indicate<sup>3–5</sup> that the crystals usually grow as hollow pyramids as a consequence of fold staggering. However, the drying procedure necessary for the usual methods of investigation leads to the collapse of these pyramids. To date, the majority of studies on polymer crystals have been confined to linear polyethylene with only one investigation of poly-4-methyl-pentene-1—P4MP1—being described<sup>6</sup>.

In conjunction with a study of molecular motion in polymer crystals by spin-lattice relaxation time measurements, as described in the accompanying paper<sup>7</sup>, an investigation of the morphology of P4MP1 crystals was carried out by use of optical and electron microscopy on preparations grown from dilute xylene solution isothermally at various temperatures as well as under non-isothermal conditions. Evidence was found that is consistent with the interpretation that these crystals grow as hollow pyramids with square or deformed square bases depending on the growth conditions, and that under some conditions growth of new lamellae on top of an existing lamella can be initiated by other than the occurrence of a screw dislocation.

## EXPERIMENTAL

The characteristics of the P4MP1 used are given in the accompanying paper<sup>7</sup>.

Three methods of growing crystals from 0.06–0.1 per cent xylene solutions were used. The first was essentially that employed by Frank,

\*On sabbatical leave from the Physics Department, Pennsylvania State University, 1962–63.

Keller and O'Connor<sup>6</sup> in which a test-tube of 1 in. diameter containing polymer and xylene (analytical reagent grade) was heated to 125°C in a 1-1½ litre oil bath, the heater turned off and the solution allowed to cool to room temperature in the bath.

The second method, involving growth under isothermal conditions, was accomplished by heating the polymer and solvent together in the 1-1½ litre oil bath to 120°-130°C, transferring the solution to a large constant temperature bath ( $\pm 0.5^\circ\text{C}$ ), the solution then being allowed to remain undisturbed for at least 24 hours. Before removal of the sample from the constant temperature bath, slides were prepared for optical microscopy by evaporation of one or two drops of the suspension from a given preparation. Except for the 57°C preparation, which was fast filtered on to paper and the resulting mat dried at room temperature under vacuum, the tubes were then removed from the bath. Electron micrographs were obtained on material from two of these suspensions after prolonged storage at room temperature. Optical microscopy indicated little change in any crystals already present upon removal and storage. However, at least in one case, as mentioned below, further precipitations did take place upon cooling. The preparations at 74°, 78° and 92°C were carried out in 1 in. diameter tubes, those at 66°, 81° and 84°C in ½ in. diameter tubes, and the one at 57°C in a half-filled 500 ml round bottom flask. The times these remained undisturbed in the bath were 25, 90, 41, 24, 92, 45 and 70 hours, respectively. The preparations at 74° and 92°C were left in the bath for an additional 24 and 69 hours, respectively, before cooling to room temperature.

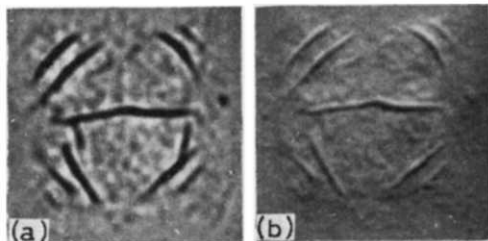


Figure 1—Photomicrographs of a poly-4-methyl-pentene-1 crystal prepared by slowly cooling a 0.080 per cent xylene solution from 125°C: (a) unshadowed, (b) shadowed with aluminium at  $\cot^{-14}$ . Magnification 1260X. Reproduced without reduction

A third method, used for one preparation, involved pouring a concentrated solution at 124°C into about ten times its volume of pure solvent in a one litre flask maintained at 57°C, the contents of the completely filled flask remaining in the bath undisturbed for 125 hours. The precipitated polymer was then recovered by fast filtration followed by drying under vacuum at room temperature.

The photomicrographs, the electron micrographs and the X-ray diffraction photographs were obtained at the Imperial Chemical Industries Ltd, Plastics Division Laboratories. The unshadowed photomicrographs were taken under low numerical aperture illuminating conditions and the shadowed ones under high numerical aperture conditions. A Zeiss photomicroscope and a Phillips Electron Microscope EM 100 (B) were used.

RESULTS AND DISCUSSION

Microscopic examination of material three days or longer after preparation by cooling in the small oil bath (method No. 1—see Experimental) showed it to contain many square based crystals, a number of which exhibited folds across the centre and near the corners. Optical micrographs of what appears to be such a separate crystal are given in *Figure 1*. These and subsequently described collapse features are consistent with the interpretation that the



*Figure 2*—Photomicrograph of a group of poly-4-methyl-pentene-1 crystals prepared as given in *Figure 1*. Aluminium shadowed at  $\cot^{-1}4$ . Magnification 1260X. Reproduced without reduction

P4MP1 lamellae can be grown as hollow square-based pyramids which collapse upon drying, as found for polyethylene<sup>3-5</sup>. Electron micrographs of these crystals were found to be similar to those given earlier<sup>6</sup> and definitely show that they are composed of square lamellae. In addition to the crystals found in this and subsequently described preparations, larger sheets and pieces as well as ribbons were always in evidence. Optical micrographs of other crystals or crystal aggregates obtained in this preparation are given in *Figures 2 and 3*.

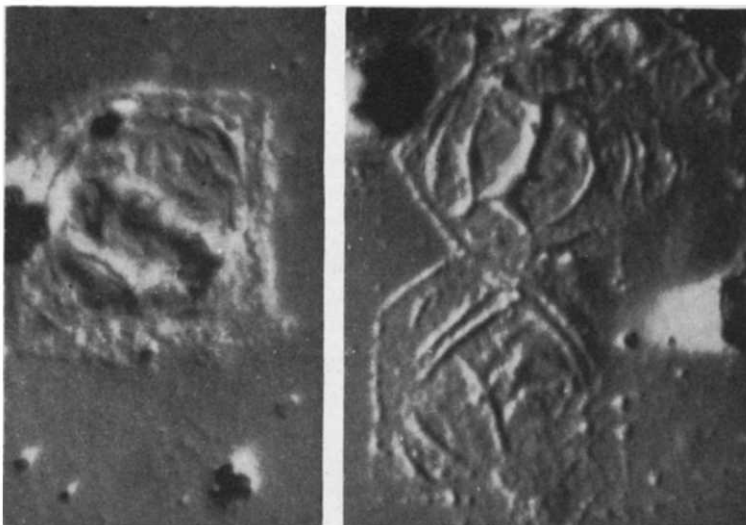


*Figure 3*—Photomicrographs of poly-4-methyl-pentene-1 crystals prepared as given in *Figure 1*. Aluminium shadowed at  $\cot^{-14}$ . Magnification 1 260X. Reproduced without reduction

Isothermal crystallization at 57°C using the second method (see Experimental) was attempted a number of times but in only one such preparation were square crystals obtained (see *Figure 4* of the accompanying paper<sup>7</sup>). The electron micrograph in *Figure 4* of the present paper, taken of the crystal mat of material prepared at 57°C using the third method, also indicates the presence of square crystals which have collapsed flatly, or nearly so, on the filter paper. X-ray diffraction patterns taken with the beam perpendicular and parallel to the mat were similar to those described earlier<sup>6</sup>, indicating the occurrence of considerable chain orientation perpendicular or near-perpendicular to the mat surface. A crystallinity of 65–70 per cent was estimated from the X-ray diagrams, a value which is of the order of that found for annealed melt-formed samples of this same polymer preparation indicating that the crystal aggregates prepared from dilute solution contain about the same amount of disordered regions and/or voids as annealed melt-formed specimens.

## THE MORPHOLOGY OF POLY-4-METHYL-PENTENE-1 CRYSTALS

Isothermal crystallization at 66°C led to the production of many square-based crystals as seen in the photomicrographs in *Figure 5*. Some of these crystals appear to be thickened laterally by screw dislocation growth while for others (right hand side) there are indications that a smaller square-based lamella is lying at the centre of a larger one. This is more evident in the electron micrographs discussed below.

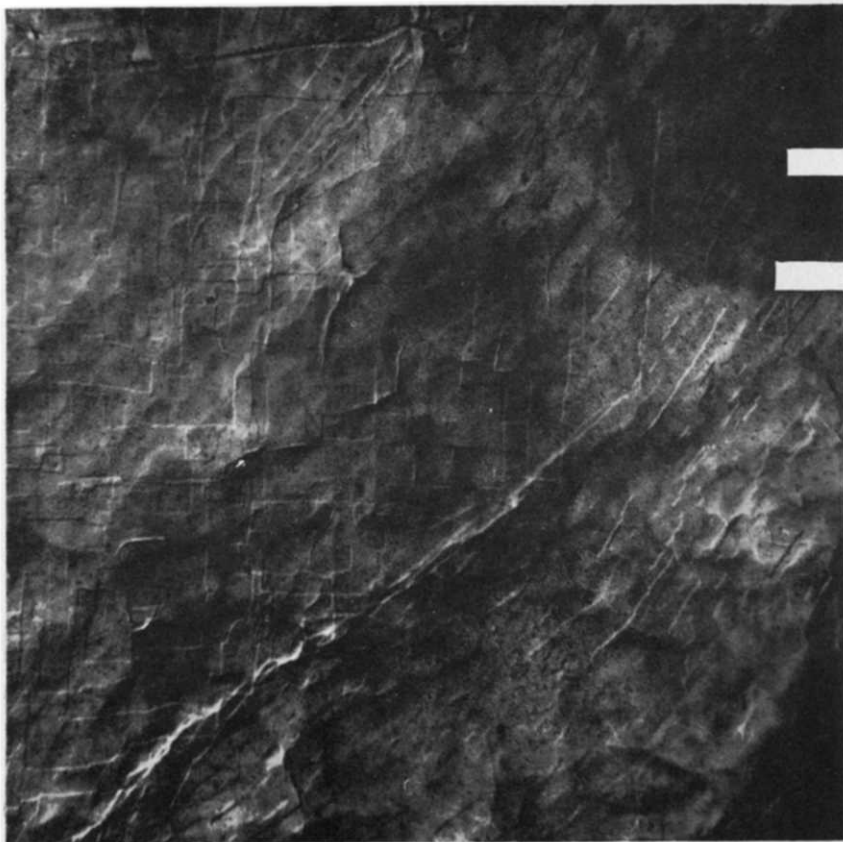


*Figure 4*—Surface replica of a poly-4-methyl-pentene-1 crystal mat. Crystals grown at 57°C from 0.063 per cent xylene solution. Gold-palladium shadowed at  $\cot^{-1} 2$  (Note 1  $\mu$  spacer on RHS)

At a crystallization temperature of 74°C some crystals, up to about 40  $\mu$  square, were obtained from a 0.077 per cent xylene solution. However, the bulk of the polymer in solution came out in layers in which the crystals were embedded, presumably upon evaporation of the solvent from the drops used to prepare the slide. A number of thin rods and needles up to about 10  $\mu$  long were also observed. Microscopic investigation of material obtained after storage of the suspension at room temperature for a prolonged period showed that the layered material was no longer in evidence,

having been replaced by sheets and crystal aggregates. Electron micrographs obtained on three representative crystals (after cooling the suspension prepared at 74°C to room temperature) are given in *Figures 6, 7 and 8*. All of these crystals are found to consist of more than one layer, the largest being of the order of 15–25  $\mu$  square; therefore, due to the high magnification used, only a part of such a layer appears in a micrograph. Some of the smaller layers, such as the one in *Figure 6*, involve growth on a screw

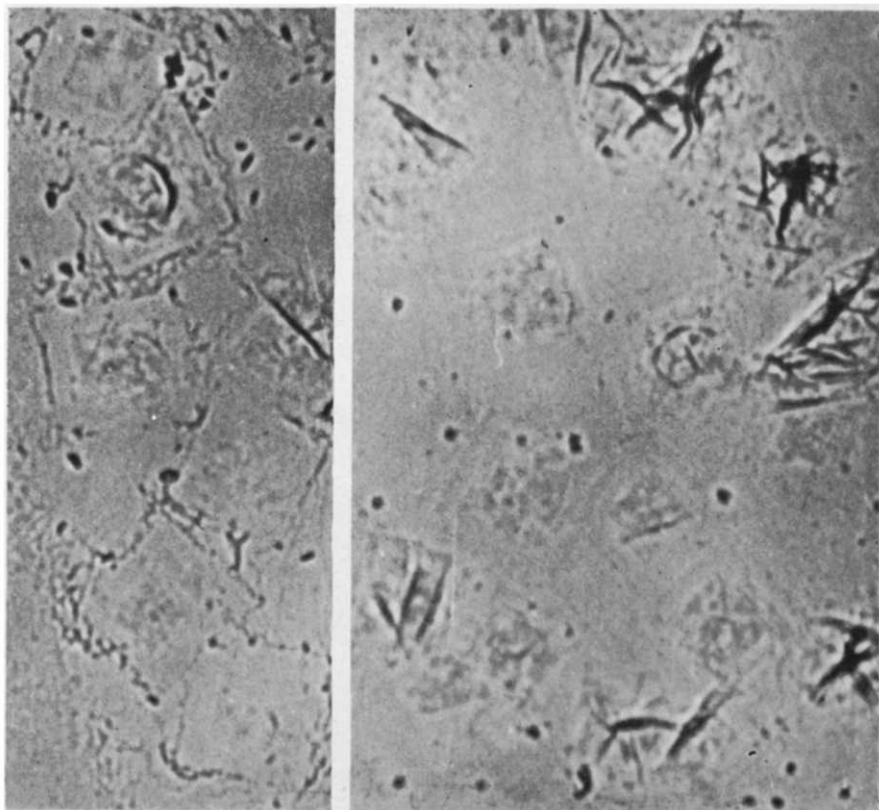


*Figure 5*—Photomicrographs of poly-4-methyl-pentene-1 crystals grown at 66°C from 0.090 per cent xylene solution. Magnification 800X. Reproduced without reduction

dislocation. However, in all three figures lamellae of various sizes which have not grown by a screw dislocation mechanism are found stacked on the larger lamellae. Close inspection of the micrographs reveals lines or ridges, approximately perpendicular to the shadowing direction, which for the smallest lamella are definitely on one of the diagonals, indicating the existence of distinct sectors as found for polyethylene<sup>3,8</sup>. This also appears to be true for the larger squares (15–25  $\mu$ ) as well. Furthermore, the diagonals of a number of the smaller lamellae are on or near to those for the larger associated ones. In *Figure 6* the smallest lamella (on the

right hand side) appears to be at or near the centre of the largest one, and in *Figure 8* the smallest one is centred near or on the midpoint of the next largest one. Furthermore, there are indications that at the centre of the smaller lamella there is a point of attachment to the larger ones, an indication that lateral thickening can occur by other than screw dislocation growth. Finally it has been found from the shadow length at the edge that these lamellae are about 100 Å thick.

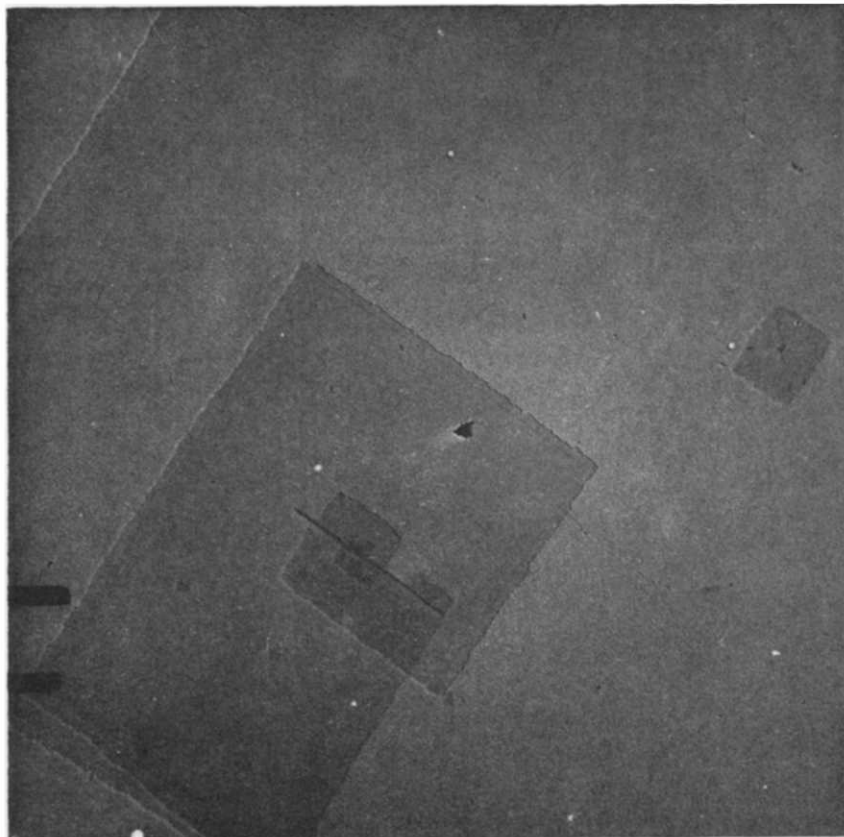


*Figure 6*—Electron micrograph of poly-4-methyl-pentene-1 crystals grown at 74°C from 0.077 per cent xylene solution. Gold-palladium shadowed at  $\cot^{-1} 2.5$  (Note 1 $\mu$  spacer on LHS)

Isothermal crystallization was carried out at four temperatures above 74°C, i.e. 78°, 81°, 84° and 92°C. Individual crystals, appearing as collapsed hemispheres or cups, were observed by optical microscopy on slides prepared from all four suspensions. The optical micrography studies suggested that the crystals grown at 92°C have steeper sides than those grown at 84°C. Some rods and needles were found in the 78° and 81°C preparations while all contained some sheets and pieces.



A closer examination of the crystals grown at  $84^{\circ}\text{C}$  was carried out on material from the room temperature stored suspension using the electron microscope (*Figures 9 and 10*). In addition to showing circumferential and radial collapse features, the electron micrographs suggest that there is also material on the edges of the crystals which has folded under, presumably on drying, an effect previously noted<sup>6</sup>. These crystals therefore appear to

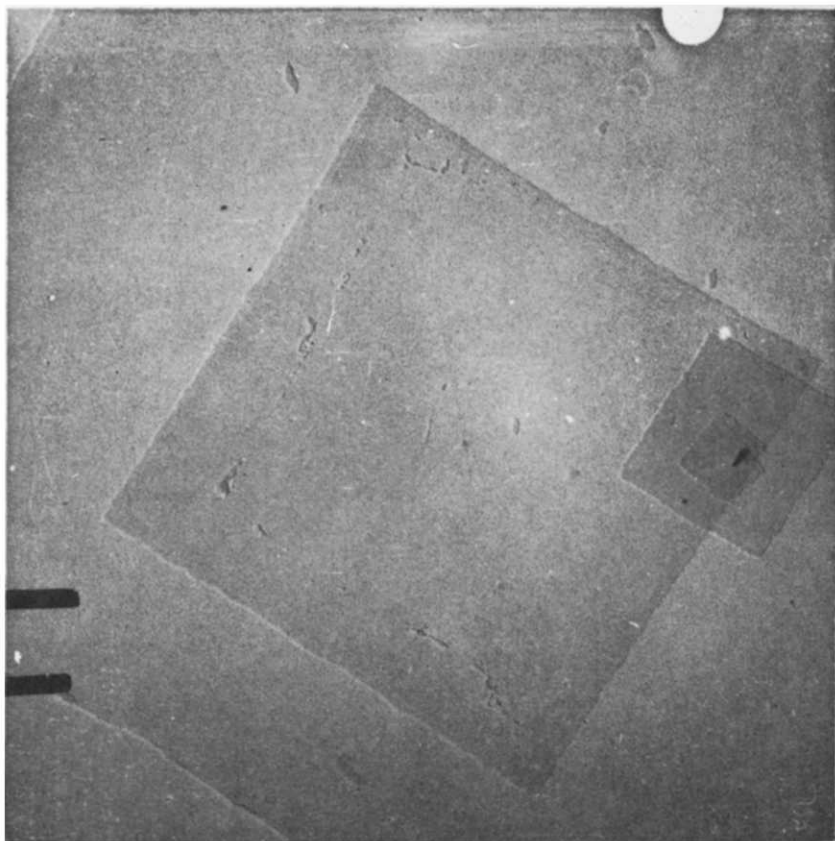


*Figure 7*—Electron micrograph of poly-4-methyl-pentene-1 crystal. Same growth conditions and shadowing as given in *Figure 6*

have square or distorted square bases with the folding-under a collapse feature for a pyramid with steep sides. An increase in the steepness of the pyramidal crystal with increase in growth temperature has also been found for polyethylene<sup>8</sup> and was attributed to a greater staggering of the folds in the polymer chains with respect to one another. Finally, the crystal structure for the  $84^{\circ}\text{C}$  preparation was found to be the normal one (tetragonal), indicating that the apparent difference between these crystals and those obtained at  $74^{\circ}\text{C}$  and below is morphological and not structural.

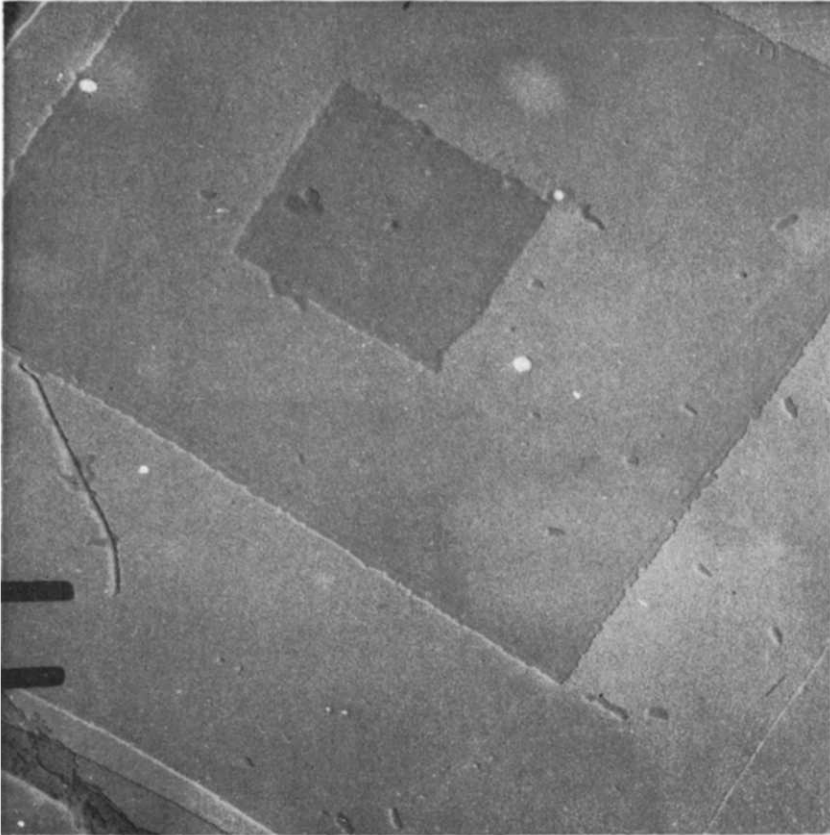


*Figure 8*—Electron micrograph of poly-4-methyl-pentene-1 crystal. Same growth conditions and shadowing as given in *Figure 6*

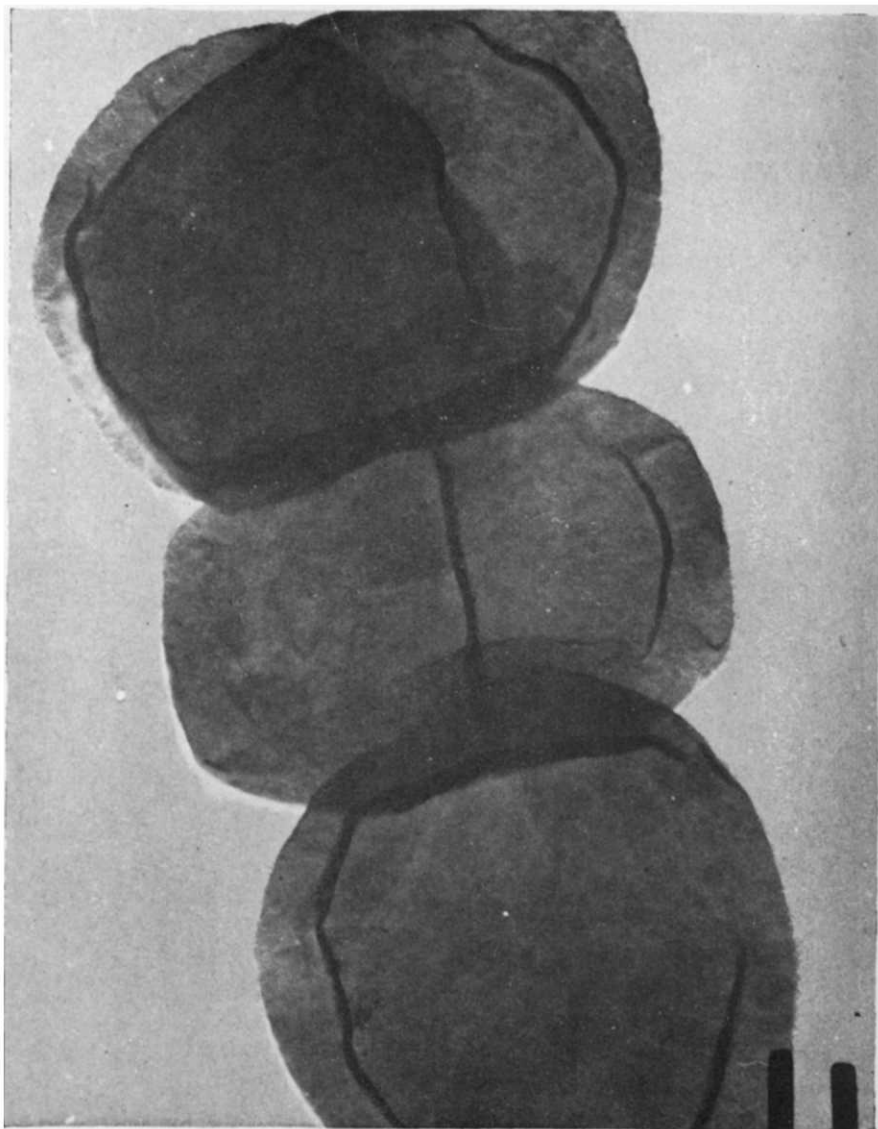


*Figure 9*—Electron micrograph of poly-4-methyl-pentene-1 crystals grown at 84°C from 0.070 per cent xylene solution. Gold-palladium shadowed at  $\cot^{-1} 2$  (Note 1 $\mu$  spacer at bottom)



*Figure 10*—Electron micrograph of part of a poly-4-methyl-pentene-1 crystal grown at 84°C from 0.070 per cent xylene solution shadowed as given in *Figure 9* (Note 1 $\mu$  spacer on LHS)

*The author is greatly indebted to Mr R. P. Palmer, Mr A. J. Cobbold, Miss A. Turner-Jones and other members of I.C.I. Ltd, Plastics Division, for taking the photomicrographs, electron micrographs and X-ray diffraction photographs as well as for various discussions pertaining to this work. Acknowledgement is also made to the John Simon Guggenheim Memorial Foundation for the award of a fellowship.*

*Department of Physics,  
Queen Mary College,  
Mile End Road, London E.1*

*(Received August 1963)*

REFERENCES

- <sup>1</sup> KELLER, A. *Polymer, Lond.* 1962, **3**, 393
- <sup>2</sup> LINDENMEYER, P. H. *J. Polym. Sci. Part C*, 1963, **1**, 5
- <sup>3</sup> RENEKER, D. H. and GEIL, P. H. *J. appl. Phys.* 1960, **31**, 1916
- <sup>4</sup> NIEGISCH, W. D. and SWAN, P. R. *J. appl. Phys.* 1960, **31**, 1906
- <sup>5</sup> BASSETT, D. C. and KELLER, A. *Phil. Mag.* 1961, **6**, 344
- <sup>6</sup> FRANK, F. C., KELLER, A. and O'CONNOR, A. *Phil. Mag.* 1959, **4**, 200
- <sup>7</sup> HUNT, B. I., POWLES, J. G. and WOODWARD, A. E. *Polymer, Lond.* 1964. In press
- <sup>8</sup> BASSETT, D. C., FRANK, F. C. and KELLER, A. *Phil. Mag.* 1963, **8**, 1739, 1763

# Infra-red Spectra of Poly-*p*-ethylene Oxybenzoate

M. ISHIBASHI

Infra-red spectra have been obtained for poly-*p*-ethylene oxybenzoate in the region of 400 to 4 000  $\text{cm}^{-1}$ . Infra-red dichroisms were determined and band assignments were made. Several absorption bands are affected by both annealing and drawing. These crystallization-sensitive bands are not the same as those of polyethylene terephthalate. The results reported here show that

the  $\text{—O}\cdot\overset{\text{O}}{\parallel}\text{C}\cdot\text{C}_6\text{H}_4\text{—}$  portions in the molecule of poly-*p*-ethylene oxybenzoate do not possess a centre of symmetry either in the crystalline or non-crystalline regions, and that the conformation of the  $\text{—O}\cdot\text{CH}_2\cdot\text{CH}_2\cdot\text{O—}$  portions in poly-*p*-ethylene oxybenzoate do not change by crystallization. The results also show that the 'amorphous' bands for polyethylene terephthalate are associated not with the  $\text{CH}_2$  modes but with the relaxation of symmetry of the

$\text{—}\overset{\text{O}}{\parallel}\text{C}\cdot\text{C}_6\text{H}_4\cdot\overset{\text{O}}{\parallel}\text{C}\text{—}$  portions in the non-crystalline region.

POLY-*p*-ETHYLENE OXYBENZOATE is the polyether-ester produced from *p*-hydroxybenzoic acid and ethylene glycol. The repeating unit of poly-*p*-ethylene oxybenzoate is  $\text{—C}_6\text{H}_4\cdot\text{CO}\cdot\text{O}\cdot\text{CH}_2\cdot\text{CH}_2\cdot\text{O—}$  and is similar to that of polyethylene terephthalate, therefore the infra-red (i.r.) spectra of these polymers resemble each other. A great deal of work has been done on the spectral changes by crystallization and on the band assignments for polyethylene terephthalate by many investigators.

In previous papers<sup>1-3</sup>, preliminary i.r. spectra of poly-*p*-ethylene oxybenzoate and the  $\text{CH}_2$  rocking vibrations of its oligomeric series have been described. It has been concluded from these results that the intensity of the absorption bands which correspond to the 'amorphous' bands in polyethylene terephthalate did not exhibit appreciable change on crystallization, and the  $\text{—O}\cdot\text{CH}_2\cdot\text{CH}_2\cdot\text{O—}$  portion in the molecule existed in the *trans* conformation in both non-crystalline and crystalline regions.

The object of the present work is to make clear the spectral changes by crystallization and the band assignments for the spectra of poly-*p*-ethylene oxybenzoate with the aid of these previous data.

## EXPERIMENTAL

### Apparatus

Infra-red spectra were recorded on a Shimadzu Model IR-600 high resolution spectrophotometer with three gratings incorporating a potassium bromide foreprism. The absorption measurements were made in the region of 400 to 4 000  $\text{cm}^{-1}$ . The instrument was carefully calibrated for wave number using hydrogen chloride, ammonia, methane, hydrogen bromide, carbon monoxide and atmospheric carbon dioxide and water vapour. The polarization measurements were taken with silver chloride polarizers.

### Materials

Poly-*p*-ethylene oxybenzoate was prepared according to the method of Cook *et al.*<sup>4</sup> The melting point and the intrinsic viscosity of the polymer were 220°C and 0.72 in a 1:1 tetrachlorethane: phenol mixture at 25°C. As with polyethylene terephthalate, a glassy, non-crystalline specimen of poly-*p*-ethylene oxybenzoate was obtained by quenching from the melt. A fairly crystalline specimen was produced by annealing the non-crystalline specimen at 100°C or higher temperatures for several hours. An oriented, crystalline specimen was produced by drawing the non-crystalline or crystalline specimen at room or higher temperatures. The structural changes of the specimens were verified by X-ray diffraction methods.

### RESULTS

Typical i.r. spectra of the non-crystalline, the unoriented crystalline, and the oriented crystalline specimens of poly-*p*-ethylene oxybenzoate are given in Figure 1. These spectra illustrate that several absorption bands are affected by both annealing and drawing.

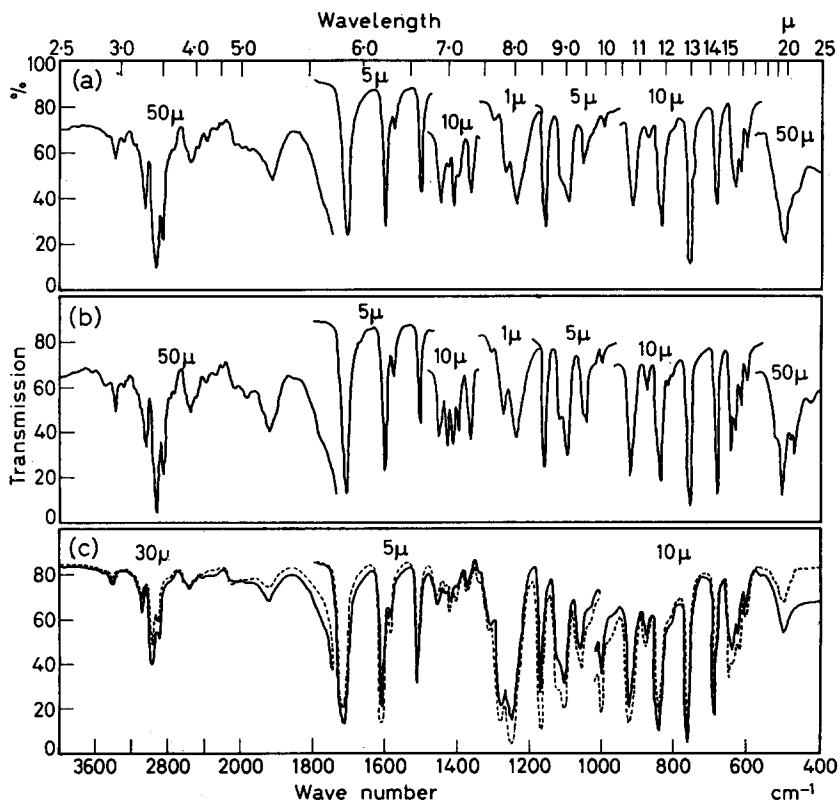


Figure 1—Infra-red spectra of poly-*p*-ethylene oxybenzoate: (a) non-crystalline, (b) unoriented crystalline, (c) oriented crystalline; full line: electric vector perpendicular to stretching direction; broken curve: electric vector parallel to stretching direction. The numerals adjacent to the curves represent specimen thickness in microns

Table 1. Infra-red data for poly-*p*-ethylene oxybenzoate

Non-crystalline		Crystalline		Oriented crystalline			Assignment†
Wave number (cm <sup>-1</sup> )	R.I.*	Wave number (cm <sup>-1</sup> )	R.I.*	Wave number (cm <sup>-1</sup> )	R.I.*	Polarization†	
3 750	VVW						ν(OH) (end groups) 2 × ν(C=O) = 3 424
3 530	VVW	3 510	VVW				
3 410	VW	3 407	VW	3 407	VW	σ	
3 320	VVW	3 320	VVW	3 320	VVW	π	
3 160	VVW	{ 3 180 3 160	{ VVW sh				
3 110	VVW	3 110	VVW	3 110	VVW	?	
3 079	W	3 079	W	3 079	W	σ	12
3 060	sh	{ 3 060 3 052	{ W sh	3 060	sh	π?	5
2 952	W	2 952	W	2 952	W	σ	ν <sub>a</sub> (CH <sub>2</sub> ) ν <sub>s</sub> (CH <sub>2</sub> )
2 880	VW	2 880	VW	2 880	VW	σ	
2 769	VVW	2 769	VVW	2 769	VVW	π	
2 633	sh	2 633	VVW	2 633	sh	π?	
2 570	VW	2 570	VW	2 570	VW	π	
2 500	VVW	2 500	VVW	2 500	VVW	π	
2 410	VW	2 410	VW	2 410	VW	π	
2 100	VVW	2 100	VVW	{ 2 100 2 085	{ VW VVW	π	
1 920	VW	1 928	VW	1 928	VW	σ	
1 712	VS	1 712	VS	1 712	VS	σ	
1 608	S	1 608	S	1 608	S	π	ν(C=O)
1 583	m	1 583	m	{ 1 584 1 582	{ W m	π	16 16'
1 510	S	1 510	S	1 510	S	π	13
1 455	m	1 462	m	1 462	m	π	δ(CH <sub>2</sub> )
1 436	W	1 437	m	1 437	m	σ	
1 421	m	1 421	m	1 421	m	π	
1 408	W	1 408	m	1 408	m	π	
1 372	m	1 372	m	1 372	m	π	1
1 340	VVW	1 340	VVW	1 340	VVW	π	γ <sub>w</sub> (CH <sub>2</sub> )
1 314	VW	1 315	sh	1 315	sh	π	γ <sub>t</sub> (CH <sub>2</sub> )
1 305	sh	1 310	VW	1 310	VW	σ	
1 276	S	1 276	VS	1 276	VS	π	ν(-C-O-)
1 247	VS	1 247	VS	{ 1 250 1 247	{ VS VS	σ	9
						π	ν(-C-O-)
1 169	S	1 169	S	1 169	S	π	17
1 125	sh	1 129	S	1 129	S	π	ν(-C-O-)
1 103	S	1 106	S	1 106	S	π	ν(-O-C-)
1 065	m	{ 1 062 1 056 1 031	{ sh m VW	{ 1 062 1 056 1 031	{ m m VW	σ	14'
1 009	W	1 009	W	1 009	W	π	ν(C-C)
		957	VVW				14
929	m	932	m	932	m	π	6
885	VW	885	W	{ 886 882	{ W W	σ	γ <sub>r</sub> (CH <sub>2</sub> )
848	m	848	m	848	m	σ	
		828	VVW	828	VVW	σ	19'
		813	VVW	{ 813 810	{ VVW VVW	σ	20' + δ(COC)
770	S	770	S	770	S	σ	4
695	m	697	m	697	m	σ	8
		658	W	658	W	π	
645	W	648	W	648	W	σ	
630	VW	630	VW	630	VW	π	18
613	VW	613	VW	613	VW	π	
		538	VVW	538	VVW	π	18'
510	V	515	W	515	W	σ	
		491	VVW				γ <sub>w</sub> (C=O) δ(CCO)
475	VVW	482	VVW	482	VVW	π	
		440	VVW				

\*Relative intensity: VS=Very strong; m=medium; W=Weak; VW=Very weak; VVW=Very very weak; sh=shoulder.

†Polarization: σ=perpendicular; π=parallel.



The wave number, relative intensity, and polarization are shown in *Table 1*. Also shown in the table are preliminary band assignments. The assignments are described in a qualitative manner with the aid of previous data from polyethylene terephthalate<sup>5-13</sup>, poly-*p*-ethylene oxybenzoate<sup>2,3</sup>, benzene<sup>14-18</sup>, and the i.r. dichroisms of absorption bands of poly-*p*-ethylene oxybenzoate because the details of the structure and vibration modes for poly-*p*-ethylene oxybenzoate are not known.

## DISCUSSION

It has been asserted by Ward<sup>6</sup> and Miyake<sup>10</sup> from the i.r. spectrum of polyethylene terephthalate that the absorption bands whose intensity changes with crystallinity are associated with the  $-\text{O}\cdot\text{CH}_2\cdot\text{CH}_2\cdot\text{O}-$  portion in the molecule, and that the spectral change originates from a *trans* conformation of this portion in the crystalline region and a *gauche* conformation in the non-crystalline region. The  $-\text{O}\cdot\text{CH}_2\cdot\text{CH}_2\cdot\text{O}-$  portion is also contained in the molecule of poly-*p*-ethylene oxybenzoate, so that the same crystallization-sensitive bands for polyethylene terephthalate might be expected to appear should they arise from an intramolecular effect associated with the  $-\text{O}\cdot\text{CH}_2\cdot\text{CH}_2\cdot\text{O}-$  portion. The crystallization-sensitive bands of poly-*p*-ethylene oxybenzoate are not the same as those of polyethylene terephthalate. That the bands whose intensity decreases with increase in crystalline content for polyethylene terephthalate do not change appreciably by crystallization is one of the characteristic features of the spectrum for poly-*p*-ethylene oxybenzoate.

It has been suggested by Liang and Krimm<sup>11</sup> that the bands whose intensity decreases with an increase in crystalline content of polyethylene

terephthalate originate from the loss of the symmetry of the  $-\overset{\text{O}}{\parallel}{\text{C}}\cdot\text{C}_6\text{H}_4\cdot\overset{\text{O}}{\parallel}{\text{C}}-$  portion in the non-crystalline region. Recently Boye<sup>19</sup> has shown that almost the same crystal bands are present for both *trans*-poly-1,4-cyclohexylenedimethylene terephthalate and polyethylene terephthalate.

It should be stated from these results that the crystallization-sensitive bands for polyethylene terephthalate and poly-1,4-cyclohexylenedimethylene

terephthalate are associated with the  $-\overset{\text{O}}{\parallel}{\text{C}}\cdot\text{C}_6\text{H}_4\cdot\overset{\text{O}}{\parallel}{\text{C}}-$  portions of these molecules, the 'amorphous' bands whose intensity decreases with increasing crystallinity are associated with the relaxation of the symmetry of the

$-\overset{\text{O}}{\parallel}{\text{C}}\cdot\text{C}_6\text{H}_4\cdot\overset{\text{O}}{\parallel}{\text{C}}-$  portion in the non-crystalline region, and that the absorp-

tion bands which originate from the  $-\text{O}\cdot\overset{\text{O}}{\parallel}{\text{C}}\cdot\text{C}_6\text{H}_4\cdot\overset{\text{O}}{\parallel}{\text{C}}-$  portion in poly-*p*-ethylene oxybenzoate do not exhibit appreciable change, since the

$-\text{O}\cdot\overset{\text{O}}{\parallel}{\text{C}}\cdot\text{C}_6\text{H}_4\cdot\overset{\text{O}}{\parallel}{\text{C}}-$  portion cannot acquire a centre of symmetry by crystallization.

In addition, the bands possibly assigned to the  $-\text{O}\cdot\text{CH}_2\cdot\text{CH}_2\cdot\text{O}-$  portion of poly-*p*-ethylene oxybenzoate do not change appreciably by crystallization with the exception of the  $7\mu$  region associated probably with the  $\text{CH}_2$  bending modes. In this  $7\mu$  region of the spectrum of non-crystalline poly-*p*-ethylene oxybenzoate, two medium and two weak bands are observed and the intensity of these two weak bands increases by crystallization. A similar phenomenon has already been observed in polyamides<sup>20,21</sup>, and it is attributed to coupling in the crystalline region. The two bands in the  $11\mu$  region which have been assigned to a *trans* conformation of the  $-\text{O}\cdot\text{CH}_2\cdot\text{CH}_2\cdot\text{O}-$  portion in poly-*p*-ethylene oxybenzoate<sup>2,3</sup> (possibly the  $\text{CH}_2$  rocking vibrations), do not change appreciably by crystallization. It is suggested from these results that the conformation of the  $-\text{O}\cdot\text{CH}_2\cdot\text{CH}_2\cdot\text{O}-$  portion in the molecule of poly-*p*-ethylene oxybenzoate is essentially the same in both non-crystalline and crystalline regions.

Research Institute,  
Nippon Rayon Co. Ltd,  
Uji, Kyoto, Japan

(Received September 1963)

## REFERENCES

- <sup>1</sup> ISHIBASHI, M. *J. Polym. Sci. Part B*, 1963, **1**, 529
- <sup>2</sup> ISHIBASHI, M. *J. Polym. Sci. Part A*. In press.
- <sup>3</sup> ISHIBASHI, M. *J. Polym. Sci. Part A*. In press
- <sup>4</sup> COOK, J. G., DICKSON, J. T., LOWE, A. R. and WHINFIELD, J. R. *Brit. Pat. No. 604 985* (11 December 1945)
- <sup>5</sup> MILLER, R. G. J. and WILLIS, H. A. *Trans. Faraday Soc.* 1953, **49**, 433
- <sup>6</sup> WARD, I. M. *Industr. Engng Chem. (Industr.)*, 1956, **48**, 905
- <sup>7</sup> TOBIN, M. C. *J. phys. Chem.* 1957, **61**, 1392
- <sup>8</sup> DANIELS, W. W. and KITSON, R. E. *J. Polym. Sci.* 1958, **33**, 161
- <sup>9</sup> GRIME, D. and WARD, I. M. *Trans. Faraday Soc.* 1958, **54**, 959
- <sup>10</sup> MIYAKE, A. *J. Polym. Sci.* 1959, **38**, 479, 497
- <sup>11</sup> LIANG, C. Y. and KRIMM, S. *J. molecular Spectr.* 1959, **3**, 554
- <sup>12</sup> KRIMM, S. *Fortschr. HochpolymerForsch.* 1960, **2**, 51
- <sup>13</sup> TADOKORO, H., TATSUKA, K. and MURAHASHI, S. *J. Polym. Sci.* 1962, **59**, 413
- <sup>14</sup> WHIFFEN, D. H. *Phil. Trans. A*, 1955, **248**, 131
- <sup>15</sup> HERZFELD, N., HOBDEN, J. W., INGOLD, D. K. and POOLE, H. G. *J. chem. Soc.* **1946**, 272
- <sup>16</sup> BAILEY, C. R., CARSON, S. C., GORDON, R. P. and INGOLD, C. K. *J. chem. Soc.* **1946**, 288
- <sup>17</sup> MILLER, F. A. *J. chem. Phys.* 1956, **24**, 996
- <sup>18</sup> WILCOX, W. S., STEPHENSON, C. V. and COBURN, Jr, W. C. 'Far infra-red spectra of substituted aromatic hydrocarbons', pp 5-13 of Report, Wright Air Development Division, Ohio, U.S.A., September 1960
- <sup>19</sup> BOYE, C. A. *J. Polym. Sci.* 1961, **55**, 263
- <sup>20</sup> TOBIN, M. C. and CARRANO, M. J. *J. chem. Phys.* 1956, **25**, 1044
- <sup>21</sup> CANNON, C. G. *Spectrochim. Acta*, 1960, **16**, 302

# Book Reviews

---

## *The Chemistry of Cationic Polymerization*

Edited by P. H. PLESCH

Pergamon Press: Oxford, 1963.

728 pp. 6½ in. by 9½ in. 200s

THIS is the first 'source-book' on cationic polymerizations, and contains chapters by eighteen authors on their special fields.

The book starts with two valuable chapters by Burstall and Treloar on the general properties of carbonium ions and theories of their role in the mechanisms of organic reactions. These are followed by a comparison, by Allen and Plesch, of cationic, anionic and free-radical polymerization reactions. This is a most useful comparison of the features of the different reactions but reveals how the *diversity* of the cationic reactions makes comparison of mechanisms exceedingly complex. This diversity is documented in the remaining chapters, which each review the behaviour of a single monomer or closely related group.

Isobutene polymerization, reviewed by Plesch, is, paradoxically, the most important, industrially speaking, and almost the least understood in detail. It is symptomatic of the experimental difficulties in this field that, almost 25 years after the establishment of a successful industrial process, there is still no detailed understanding of its enormous rate (with  $AlCl_3$ , virtually instantaneous even at  $-200^\circ C$ ).

Styrene and related compounds have been perhaps the most fully investigated monomers. This field is comprehensively and judiciously surveyed in two chapters by Mathieson and Bywater respectively.

Alkenes are reviewed by Fontana: polyenes by Cooper. Eley summarizes the kinetics of polymerization of vinyl ethers.

A great deal of information, not normally known to those who think of polymerization as a reaction of double bonds, is presented in a series of chapters on the polymerization of heterocyclic monomers; epoxides by Eastham; other cyclic oxides by Rose; other oxygen, sulphur and nitrogen heterocycles by Schrage, Lal and G. D. Jones respectively.

The book concludes with chapters on copolymerization by Cundall; the cationic reactions of polymers by Smets and van Beylen; radiation polymerization by Pinner, and a digest of experimental methods by the editor.

The editor asked his contributors to be critical rather than comprehensive. They have largely succeeded in the first aim, though the keenness of the critical eye varies from author to author. But they have managed to be comprehensive as well—the book brings together, for the first time, a very considerable body of information previously available only in the journals and in a number of useful but necessarily over-concise review articles.

The only obvious weakness is the lack of a general summary and conclusion—the 'conspectus' that the editor tells us he had hoped to include but had to go to press without. But to deplore its lack is not to underestimate the difficulty of reaching such a conspectus. As this book reveals most strikingly, the keynote of cationic polymerization is its multifarious character. Not only is the range of monomers and catalysts much wider than in free-radical polymerization, but also co-catalysts and solvents play an important and sometimes dominating role. It is therefore unlikely that there can ever be a general theory as relatively simple and comprehensive as that which describes free-radical polymerizations, and attempts to construct one on the basis of present knowledge could be misleading.

Dr Plesch deserves great credit for this book. He has been no passive editor. Apart from his own chapters, his influence is discernible throughout, in the form of appendices, interjected comments and asides (and occasional disclaimers).

The book is very well produced and illustrated. So it should be—£10 a copy!

D. C. PEPPER

## BOOK REVIEWS

### *The Chemistry and Physics of Rubber-like Substances*

Edited by L. BATEMAN

MacLaren: London; Wiley: New York, 1963.

xiv+784 pp. 168s

THE Natural Rubber Producers' Research Association this year celebrates their silver jubilee and this book, which has been written by past and present members of the Research Association, gives an account of the main scientific studies undertaken by the Association since its inception twenty five years ago. Although the various contributions highlight the N.R.P.R.A. viewpoint, due regard has been paid to relevant work carried out elsewhere and the articles express the development and current state of the physics and chemistry of rubber-like substances. The book, as a whole, is a major contribution to the scientific knowledge of the nature and properties of rubber and elastomers generally. The subjects discussed which vary widely in character and scope cover all aspects of rubber science. These include chemical structure and *cis-trans* isomerism in natural polyisoprenes, structure and properties of latex, theories of rubber solution, rubber-like elasticity, and viscoelastic behaviour and crystallization of natural rubber. On the more applied side there are articles on the strength of rubber, effect of fillers, ozone attack, abrasion and tyre wear. Informative accounts of the mastication and mechano-mechanical reactions of polymers, the chemistry of vulcanization, radiation chemistry and the detailed studies of the oxidation of olefins and sulphides summarize some of the more recent and significant studies carried out at the N.R.P.R.A. The final two chapters of the book deal with network degradation and the correlation of vulcanizate structure and properties.

This is a memorable publication. It is not only a record of the work of an outstanding research institute, but also a remarkable example of the power of the coordinated application of the disciplines of physics, chemistry and biology on a scientific problem and of the value of a fundamental approach to what appeared to be a practical and technological problem. The book is immense value to all workers interested in rubber whether academic or industrial and can be equally recommended to those concerned with the related technologies of plastics, oil and fats and paints. An appendix lists the 452 publications for the N.R.P.R.A. on rubber and related subjects.

C. E. H. BAWN

### *The Stabilization of Polyvinyl Chloride*

F. CHEVASSUS and R. DE BROUTELLES

Translated by EICHORN and SARMIENTO

First English edition, E. Arnold: London, 1963.

385 pp., 6 in. by 9 in., 80s

Two French authors of different experience and style have collaborated to produce a valuable book, the first which attempts to deal comprehensively with degradation and stabilization of PVC in a single volume.

Written in three Parts, the book contains (1) a theoretical study (some 100 pages), (2) a classified account of stabilizers and synergistic mixtures, with a list of U.S. and European manufacturers and their products (this Part amounts to more than 100 pages overall) and (3) a thorough assessment of practical points that arise in the important industrial fields. The latter Part (substantially over 100 pages) appears to be based on direct technical experience whereas the other two represent information collected from available sources.

It is easy to criticize any theoretical account of PVC since sharp differences of scientific interpretation still abound. Indeed, the present book provides the background for some future publication in which pertinent experimental work concerned with polymeric structure, propagation of linear conjugation, ring formation, peroxidation, and the action of different stabilizers under varied conditions of temperature, shear, metal salts, light, oxygen and time might be critically discussed in full mechanistic detail. As it is, the author of this Part deals with these matters as uncontroversially as possible by sketching the main facts and successively quoting from conclusions of many authors almost verbatim. A few passages are not easy

## BOOK REVIEWS

to follow (and perhaps e.g. D. E. Winkler should have been discussed more fully) but over 150 publications are considered or mentioned.

Part II is distinctly informative and will be frequently referred to by those interested in the constitution, source, and essential performance of individual stabilizers and mixtures. Seven principal types of stabilizer are discussed in detail and synergistic combinations are exemplified. Over 350 references—mainly patents—are given.

The third Part contains separate substantial chapters on electrical insulation, the flexible calendered product, rigid PVC, plastisols and organosols, and coatings. These are preceded by a discussion of ageing tests and results, different types of PVC, plasticizers, lubricants, fillers, pigments. The section on types of resin is too brief (9 pages) but information on this important aspect is apparently scarce.

As a whole the book may be warmly recommended. The translation from the French appears to be faithful, even over-faithful. The book is full of figures and tables, with printing up to the high standard expected of Richard Clay. In these circumstances the price is acceptable.

R. R. SMITH, J. A. HORROCKS

### *Modern Petroleum Technology*

E. B. EVANS (Hon. Editor)

The Institute of Petroleum: London, 1962. 3rd ed. viii+873 pp.; 6 in. by 9½ in.  
45s to Members, 50s to Non-members

PREVIOUS editions of this book appeared in 1946 (455 pp) and 1954 (691 pp); in the intervening eight years this subject has changed so greatly that the third edition has been almost completely rewritten even though it sets out to provide only an introduction to the subject. In addition, it is produced in modern format and aesthetically pleasing. The 27 chapters—by different authors—deal successively with the occurrence and production of oil, with the physics and refinery chemistry of petroleum, with fuels and other petroleum products (including oils, greases, waxes and solvents) and finally very fully with the transport of oil. Only the chapter on the production of oil and gas has the same author as its counterpart in the second edition, and even this is somewhat modernized.

The biggest technological revolution since the book was first produced is undoubtedly the replacement by petroleum of all other sources of cheap large-tonnage chemicals, of which the extensive petroleum chemicals industry is the outcome. It is here that the new edition departs widely from the old; the fine chapter on 'chemicals from petroleum' is replaced by the quite differently slanted 'chemistry and physics of petroleum' in which the chemistry is dismissed in a few lines. The economic assessment of the industry has also been omitted. These are clearly deliberate changes which provide more space for discussions of refinery operations and of cracking, reforming and other catalytic processes: however, the range of the book is thereby limited and its interest largely confined to the petroleum technologist, to the exclusion of the chemist.

Within this framework, the book provides a sound introduction and may frequently be consulted by the newcomer with complete satisfaction. It is pleasing that the price is modest in relation to the contents.

H. W. B. REED

### *Industrial Plasticizers*

I. MELLAN

Pergamon: Oxford, 1963.

302 pp.; 6 in. by 9 in., 70s

THIS book is intended as a practical guide to the application of plasticizers and is a sequel to the author's earlier work *The Behaviour of Plasticizers* which described the more theoretical aspects of plasticization.

The first 76 pages describe the plasticization of the most widely used polymers, and the remainder is a catalogue of industrially available plasticizers.

The book gives the impression of carelessly and hurried preparation. The first section is too restricted in scope being merely long abstracts of a few papers, from

## BOOK REVIEWS

### *The Chemistry and Physics of Rubber-like Substances*

Edited by L. BATEMAN

MacLaren: London; Wiley: New York, 1963.

xiv+784 pp. 168s

THE Natural Rubber Producers' Research Association this year celebrates their silver jubilee and this book, which has been written by past and present members of the Research Association, gives an account of the main scientific studies undertaken by the Association since its inception twenty five years ago. Although the various contributions highlight the N.R.P.R.A. viewpoint, due regard has been paid to relevant work carried out elsewhere and the articles express the development and current state of the physics and chemistry of rubber-like substances. The book, as a whole, is a major contribution to the scientific knowledge of the nature and properties of rubber and elastomers generally. The subjects discussed which vary widely in character and scope cover all aspects of rubber science. These include chemical structure and *cis-trans* isomerism in natural polyisoprenes, structure and properties of latex, theories of rubber solution, rubber-like elasticity, and viscoelastic behaviour and crystallization of natural rubber. On the more applied side there are articles on the strength of rubber, effect of fillers, ozone attack, abrasion and tyre wear. Informative accounts of the mastication and mechano-mechanical reactions of polymers, the chemistry of vulcanization, radiation chemistry and the detailed studies of the oxidation of olefins and sulphides summarize some of the more recent and significant studies carried out at the N.R.P.R.A. The final two chapters of the book deal with network degradation and the correlation of vulcanizate structure and properties.

This is a memorable publication. It is not only a record of the work of an outstanding research institute, but also a remarkable example of the power of the coordinated application of the disciplines of physics, chemistry and biology on a scientific problem and of the value of a fundamental approach to what appeared to be a practical and technological problem. The book is immense value to all workers interested in rubber whether academic or industrial and can be equally recommended to those concerned with the related technologies of plastics, oil and fats and paints. An appendix lists the 452 publications for the N.R.P.R.A. on rubber and related subjects.

C. E. H. BAWN

### *The Stabilization of Polyvinyl Chloride*

F. CHEVASSUS and R. DE BROUTELLES

Translated by EICHORN and SARMIENTO

First English edition, E. Arnold: London, 1963.

385 pp., 6 in. by 9 in., 80s

Two French authors of different experience and style have collaborated to produce a valuable book, the first which attempts to deal comprehensively with degradation and stabilization of PVC in a single volume.

Written in three Parts, the book contains (1) a theoretical study (some 100 pages), (2) a classified account of stabilizers and synergistic mixtures, with a list of U.S. and European manufacturers and their products (this Part amounts to more than 100 pages overall) and (3) a thorough assessment of practical points that arise in the important industrial fields. The latter Part (substantially over 100 pages) appears to be based on direct technical experience whereas the other two represent information collected from available sources.

It is easy to criticize any theoretical account of PVC since sharp differences of scientific interpretation still abound. Indeed, the present book provides the background for some future publication in which pertinent experimental work concerned with polymeric structure, propagation of linear conjugation, ring formation, peroxidation, and the action of different stabilizers under varied conditions of temperature, shear, metal salts, light, oxygen and time might be critically discussed in full mechanistic detail. As it is, the author of this Part deals with these matters as uncontroversially as possible by sketching the main facts and successively quoting from conclusions of many authors almost verbatim. A few passages are not easy

## BOOK REVIEWS

to follow (and perhaps e.g. D. E. Winkler should have been discussed more fully) but over 150 publications are considered or mentioned.

Part II is distinctly informative and will be frequently referred to by those interested in the constitution, source, and essential performance of individual stabilizers and mixtures. Seven principal types of stabilizer are discussed in detail and synergistic combinations are exemplified. Over 350 references—mainly patents—are given.

The third Part contains separate substantial chapters on electrical insulation, the flexible calendered product, rigid PVC, plastisols and organosols, and coatings. These are preceded by a discussion of ageing tests and results, different types of PVC, plasticizers, lubricants, fillers, pigments. The section on types of resin is too brief (9 pages) but information on this important aspect is apparently scarce.

As a whole the book may be warmly recommended. The translation from the French appears to be faithful, even over-faithful. The book is full of figures and tables, with printing up to the high standard expected of Richard Clay. In these circumstances the price is acceptable.

R. R. SMITH, J. A. HORROCKS

### *Modern Petroleum Technology*

E. B. EVANS (Hon. Editor)

The Institute of Petroleum: London, 1962. 3rd ed. viii+873 pp.; 6 in. by 9½ in.  
45s to Members, 50s to Non-members

PREVIOUS editions of this book appeared in 1946 (455 pp) and 1954 (691 pp); in the intervening eight years this subject has changed so greatly that the third edition has been almost completely rewritten even though it sets out to provide only an introduction to the subject. In addition, it is produced in modern format and aesthetically pleasing. The 27 chapters—by different authors—deal successively with the occurrence and production of oil, with the physics and refinery chemistry of petroleum, with fuels and other petroleum products (including oils, greases, waxes and solvents) and finally very fully with the transport of oil. Only the chapter on the production of oil and gas has the same author as its counterpart in the second edition, and even this is somewhat modernized.

The biggest technological revolution since the book was first produced is undoubtedly the replacement by petroleum of all other sources of cheap large-tonnage chemicals, of which the extensive petroleum chemicals industry is the outcome. It is here that the new edition departs widely from the old; the fine chapter on 'chemicals from petroleum' is replaced by the quite differently slanted 'chemistry and physics of petroleum' in which the chemistry is dismissed in a few lines. The economic assessment of the industry has also been omitted. These are clearly deliberate changes which provide more space for discussions of refinery operations and of cracking, reforming and other catalytic processes: however, the range of the book is thereby limited and its interest largely confined to the petroleum technologist, to the exclusion of the chemist.

Within this framework, the book provides a sound introduction and may frequently be consulted by the newcomer with complete satisfaction. It is pleasing that the price is modest in relation to the contents.

H. W. B. REED

### *Industrial Plasticizers*

I. MELLAN

Pergamon: Oxford, 1963.

302 pp.; 6 in. by 9 in., 70s

THIS book is intended as a practical guide to the application of plasticizers and is a sequel to the author's earlier work *The Behaviour of Plasticizers* which described the more theoretical aspects of plasticization.

The first 76 pages describe the plasticization of the most widely used polymers, and the remainder is a catalogue of industrially available plasticizers.

The book gives the impression of carelessly and hurried preparation. The first section is too restricted in scope being merely long abstracts of a few papers, from

which tables of data have been taken without modification to ensure uniformity of test methods or of presentation. For example, the data in tables 20 and 20(a) would have been much easier to use if combined. Too often trade names only are given when the chemical name is well known. A full account of the practical methods used for testing plasticizers and the properties required for specific applications should have been given, since this information is essential for satisfactory selection of plasticizers. The space devoted to PVC is disproportionately small in view of its outstanding importance.

The second section consists mainly of data which have been abstracted from manufacturers' literature and similar criticisms apply. Much of the data given is a measure only of the purity of the plasticizer. Since this is only applicable to a particular manufacturer, and might be modified, a section on standard specifications for plasticizers should have been included instead and would have taken less space.

Lack of care is shown by at least three plasticizers, i.e. di-isodecyl adipate, di-isodecyl phthalate and dinonyl phthalate, being included twice with different sets of data.

The book may be of use for reference when data on a particular plasticizer are required but as a guide to the applications of plasticizers it is inadequate.

H. C. MURFITT

*Interaction of Plane-Parallel Double Layers*

DEVEREUX and DE BRUYN

M.I.T. Press: Cambridge, Mass., U.S.A.

361 pp., 7 in. by 10 in., 94s

THE application of the theories of both Derjaguin, and Verwey-Overbeek to problems of sol stability, coagulation etc., requires the evaluation of the interaction energy of charged particle surfaces as they approach one another and of the material, attractive forces (van de Waals) at small separations.

This book is concerned only with the former, treating both like and dissimilar particle surfaces in a common, symmetrical electrolyte solution. After summarizing the essential mathematical treatment and definitions (50 pp approximately), the remainder of the book (300 pages) tabulates the interaction energies, computed on an IBM 7090 machine, for a wide range of experimentally possible, similar and dissimilar, surface potentials and distances of separation giving significant interaction.

The book might well be appreciatively referred to by those regularly concerned with stability and flocculation problems as 'The double layer interaction ready-reckoner', and will no doubt be much used by those lacking stamina and/or computer facilities.

H. W. DOUGLAS

*Physical Properties of Textile Fibres*

W. E. MORTON and J. W. S. HEARLE

Butterworths: London, 1962.

608 pp., 5½ in. by 8½ in., 105s

THE authors set out to write a textbook for textile students proceeding to B.Sc. (Tech.), Dip.Tech. or equivalent in Textile subjects. This book will undoubtedly appeal to a far wider range of readers and should establish itself as a standard work of reference not only in teaching, but in industry. It is very probable that the majority of copies will be sold in industry as the price is rather high for students to spend on a textbook covering only a special aspect of their course.

The authors have covered a very wide range of topics. There are chapters devoted to density, moisture relations, mechanical and electrical properties, optical and thermal properties and friction. Where necessary, the text includes discussion of related forms of materials, e.g. film properties. The authors express the hope in their preface that the text will furnish a background 'which is unlikely to change radically with the passage of time'. They have chosen to start the book with a long section on fibre structure (ten per cent of the total) and it is this section that will probably be altered considerably before the next edition. Experimental facts are



## BOOK REVIEWS

to follow (and perhaps e.g. D. E. Winkler should have been discussed more fully) but over 150 publications are considered or mentioned.

Part II is distinctly informative and will be frequently referred to by those interested in the constitution, source, and essential performance of individual stabilizers and mixtures. Seven principal types of stabilizer are discussed in detail and synergistic combinations are exemplified. Over 350 references—mainly patents—are given.

The third Part contains separate substantial chapters on electrical insulation, the flexible calendered product, rigid PVC, plastisols and organosols, and coatings. These are preceded by a discussion of ageing tests and results, different types of PVC, plasticizers, lubricants, fillers, pigments. The section on types of resin is too brief (9 pages) but information on this important aspect is apparently scarce.

As a whole the book may be warmly recommended. The translation from the French appears to be faithful, even over-faithful. The book is full of figures and tables, with printing up to the high standard expected of Richard Clay. In these circumstances the price is acceptable.

R. R. SMITH, J. A. HORROCKS

### *Modern Petroleum Technology*

E. B. EVANS (Hon. Editor)

The Institute of Petroleum: London, 1962. 3rd ed. viii+873 pp.; 6 in. by 9½ in.  
45s to Members, 50s to Non-members

PREVIOUS editions of this book appeared in 1946 (455 pp) and 1954 (691 pp); in the intervening eight years this subject has changed so greatly that the third edition has been almost completely rewritten even though it sets out to provide only an introduction to the subject. In addition, it is produced in modern format and aesthetically pleasing. The 27 chapters—by different authors—deal successively with the occurrence and production of oil, with the physics and refinery chemistry of petroleum, with fuels and other petroleum products (including oils, greases, waxes and solvents) and finally very fully with the transport of oil. Only the chapter on the production of oil and gas has the same author as its counterpart in the second edition, and even this is somewhat modernized.

The biggest technological revolution since the book was first produced is undoubtedly the replacement by petroleum of all other sources of cheap large-tonnage chemicals, of which the extensive petroleum chemicals industry is the outcome. It is here that the new edition departs widely from the old; the fine chapter on 'chemicals from petroleum' is replaced by the quite differently slanted 'chemistry and physics of petroleum' in which the chemistry is dismissed in a few lines. The economic assessment of the industry has also been omitted. These are clearly deliberate changes which provide more space for discussions of refinery operations and of cracking, reforming and other catalytic processes: however, the range of the book is thereby limited and its interest largely confined to the petroleum technologist, to the exclusion of the chemist.

Within this framework, the book provides a sound introduction and may frequently be consulted by the newcomer with complete satisfaction. It is pleasing that the price is modest in relation to the contents.

H. W. B. REED

### *Industrial Plasticizers*

I. MELLAN

Pergamon: Oxford, 1963.

302 pp.; 6 in. by 9 in., 70s

THIS book is intended as a practical guide to the application of plasticizers and is a sequel to the author's earlier work *The Behaviour of Plasticizers* which described the more theoretical aspects of plasticization.

The first 76 pages describe the plasticization of the most widely used polymers, and the remainder is a catalogue of industrially available plasticizers.

The book gives the impression of carelessly and hurried preparation. The first section is too restricted in scope being merely long abstracts of a few papers, from

which tables of data have been taken without modification to ensure uniformity of test methods or of presentation. For example, the data in tables 20 and 20(a) would have been much easier to use if combined. Too often trade names only are given when the chemical name is well known. A full account of the practical methods used for testing plasticizers and the properties required for specific applications should have been given, since this information is essential for satisfactory selection of plasticizers. The space devoted to PVC is disproportionately small in view of its outstanding importance.

The second section consists mainly of data which have been abstracted from manufacturers' literature and similar criticisms apply. Much of the data given is a measure only of the purity of the plasticizer. Since this is only applicable to a particular manufacturer, and might be modified, a section on standard specifications for plasticizers should have been included instead and would have taken less space.

Lack of care is shown by at least three plasticizers, i.e. di-isodecyl adipate, di-isodecyl phthalate and dinonyl phthalate, being included twice with different sets of data.

The book may be of use for reference when data on a particular plasticizer are required but as a guide to the applications of plasticizers it is inadequate.

H. C. MURFITT

*Interaction of Plane-Parallel Double Layers*

DEVEREUX and DE BRUYN

M.I.T. Press: Cambridge, Mass., U.S.A.

361 pp., 7 in. by 10 in., 94s

THE application of the theories of both Derjaguin, and Verwey-Overbeek to problems of sol stability, coagulation etc., requires the evaluation of the interaction energy of charged particle surfaces as they approach one another and of the material, attractive forces (van de Waals) at small separations.

This book is concerned only with the former, treating both like and dissimilar particle surfaces in a common, symmetrical electrolyte solution. After summarizing the essential mathematical treatment and definitions (50 pp approximately), the remainder of the book (300 pages) tabulates the interaction energies, computed on an IBM 7090 machine, for a wide range of experimentally possible, similar and dissimilar, surface potentials and distances of separation giving significant interaction.

The book might well be appreciatively referred to by those regularly concerned with stability and flocculation problems as 'The double layer interaction ready-reckoner', and will no doubt be much used by those lacking stamina and/or computer facilities.

H. W. DOUGLAS

*Physical Properties of Textile Fibres*

W. E. MORTON and J. W. S. HEARLE

Butterworths: London, 1962.

608 pp., 5½ in. by 8½ in., 105s

THE authors set out to write a textbook for textile students proceeding to B.Sc. (Tech.), Dip.Tech. or equivalent in Textile subjects. This book will undoubtedly appeal to a far wider range of readers and should establish itself as a standard work of reference not only in teaching, but in industry. It is very probable that the majority of copies will be sold in industry as the price is rather high for students to spend on a textbook covering only a special aspect of their course.

The authors have covered a very wide range of topics. There are chapters devoted to density, moisture relations, mechanical and electrical properties, optical and thermal properties and friction. Where necessary, the text includes discussion of related forms of materials, e.g. film properties. The authors express the hope in their preface that the text will furnish a background 'which is unlikely to change radically with the passage of time'. They have chosen to start the book with a long section on fibre structure (ten per cent of the total) and it is this section that will probably be altered considerably before the next edition. Experimental facts are

## BOOK REVIEWS

---

unlikely to be disputed, but fibre structure is largely the interpretation of diffuse spots and haloes on photographs and the recent work of Hosemann and others is already challenging the established theories. In other parts of the book theoretical speculation on measured properties is less obtrusive and the comprehensive cover, together with the juxtaposition of properties of fibres often treated in isolation, makes this book extremely useful to the newcomer to textile technology and science.

There is a very valuable chapter on sampling which puts succinctly the pitfalls that bestrew this subject and this chapter made quite clear to the reviewer the inevitable consequences of different methods of sampling. The remaining chapters in the section on fibre dimensions consider fibre length, diameter and density.

The next section is entitled moisture relations and, in an effort to be really thorough, some very difficult byways of the subject have been explored. The reviewer would dispute, however, whether the BET equation and theories of multi-layer adsorption can really be described as *physical* properties of textile fibres.

The section on mechanical properties is excellent; the complexities of time effects and dynamic testing are introduced after the simpler ideas and the problems of variability have been tackled. It is symptomatic of the unbalance of the research work in this field that only 26 pages could be devoted to deformations other than extensional. This is no fault of the authors. Some of the later chapters on electrical and optical properties are less expansive and, in parts, achieve the breathless quality of a catalogue. In these later chapters it is unusual to find a reference to work published after 1957 which is five years before the date of publication.

The book is produced throughout with excellent line diagrams and many half-tone illustrations. It is a first-class book which will provide a good reference source. If the authors had exercised more discipline over their pens, particularly in the sections on structure and moisture relations, it could have been an excellent one.

K. W. HILLIER

### *Ultrastructure of Protein Fibres*

Edited by RUBIN BORASKY

Academic Press: New York and London, 1963. 72s

THIS book consists of a collection of papers (some of them subsequently expanded) presented to a symposium of the Nineteenth Annual Meeting of the Electron Microscopy Society of America held at Pittsburgh in 1961. The morphology of fibrous proteins and its possible relationship to primary, secondary and tertiary protein structure is discussed by correlating the results of electron microscopy with structural information obtained by chemical and, in particular, X-ray techniques. Modern theories relating biological function, mechanical and physical properties of natural proteinous materials to ultra and molecular structure are presented.

Because of its mode of conception as a series of papers, this book is not a complete exposition on the subject of fibrous protein structure and its biophysical implications. Particularly, it lacks details of the instrumental techniques used to obtain information in this field; this is unfortunate and detracts from the value of the book. Nevertheless as an exposition of modern research work into the ultra structure of fibrous proteins this book is a useful collection of review papers by the experts for the expert or near expert in this field.

H. BLOCK

which tables of data have been taken without modification to ensure uniformity of test methods or of presentation. For example, the data in tables 20 and 20(a) would have been much easier to use if combined. Too often trade names only are given when the chemical name is well known. A full account of the practical methods used for testing plasticizers and the properties required for specific applications should have been given, since this information is essential for satisfactory selection of plasticizers. The space devoted to PVC is disproportionately small in view of its outstanding importance.

The second section consists mainly of data which have been abstracted from manufacturers' literature and similar criticisms apply. Much of the data given is a measure only of the purity of the plasticizer. Since this is only applicable to a particular manufacturer, and might be modified, a section on standard specifications for plasticizers should have been included instead and would have taken less space.

Lack of care is shown by at least three plasticizers, i.e. di-isodecyl adipate, di-isodecyl phthalate and dinonyl phthalate, being included twice with different sets of data.

The book may be of use for reference when data on a particular plasticizer are required but as a guide to the applications of plasticizers it is inadequate.

H. C. MURFITT

*Interaction of Plane-Parallel Double Layers*

DEVEREUX and DE BRUYN

M.I.T. Press: Cambridge, Mass., U.S.A.

361 pp., 7 in. by 10 in., 94s

THE application of the theories of both Derjaguin, and Verwey-Overbeek to problems of sol stability, coagulation etc., requires the evaluation of the interaction energy of charged particle surfaces as they approach one another and of the material, attractive forces (van de Waals) at small separations.

This book is concerned only with the former, treating both like and dissimilar particle surfaces in a common, symmetrical electrolyte solution. After summarizing the essential mathematical treatment and definitions (50 pp approximately), the remainder of the book (300 pages) tabulates the interaction energies, computed on an IBM 7090 machine, for a wide range of experimentally possible, similar and dissimilar, surface potentials and distances of separation giving significant interaction.

The book might well be appreciatively referred to by those regularly concerned with stability and flocculation problems as 'The double layer interaction ready-reckoner', and will no doubt be much used by those lacking stamina and/or computer facilities.

H. W. DOUGLAS

*Physical Properties of Textile Fibres*

W. E. MORTON and J. W. S. HEARLE

Butterworths: London, 1962.

608 pp., 5½ in. by 8½ in., 105s

THE authors set out to write a textbook for textile students proceeding to B.Sc. (Tech.), Dip.Tech. or equivalent in Textile subjects. This book will undoubtedly appeal to a far wider range of readers and should establish itself as a standard work of reference not only in teaching, but in industry. It is very probable that the majority of copies will be sold in industry as the price is rather high for students to spend on a textbook covering only a special aspect of their course.

The authors have covered a very wide range of topics. There are chapters devoted to density, moisture relations, mechanical and electrical properties, optical and thermal properties and friction. Where necessary, the text includes discussion of related forms of materials, e.g. film properties. The authors express the hope in their preface that the text will furnish a background 'which is unlikely to change radically with the passage of time'. They have chosen to start the book with a long section on fibre structure (ten per cent of the total) and it is this section that will probably be altered considerably before the next edition. Experimental facts are

## BOOK REVIEWS

---

unlikely to be disputed, but fibre structure is largely the interpretation of diffuse spots and haloes on photographs and the recent work of Hosemann and others is already challenging the established theories. In other parts of the book theoretical speculation on measured properties is less obtrusive and the comprehensive cover, together with the juxtaposition of properties of fibres often treated in isolation, makes this book extremely useful to the newcomer to textile technology and science.

There is a very valuable chapter on sampling which puts succinctly the pitfalls that bestrew this subject and this chapter made quite clear to the reviewer the inevitable consequences of different methods of sampling. The remaining chapters in the section on fibre dimensions consider fibre length, diameter and density.

The next section is entitled moisture relations and, in an effort to be really thorough, some very difficult byways of the subject have been explored. The reviewer would dispute, however, whether the BET equation and theories of multi-layer adsorption can really be described as *physical* properties of textile fibres.

The section on mechanical properties is excellent; the complexities of time effects and dynamic testing are introduced after the simpler ideas and the problems of variability have been tackled. It is symptomatic of the unbalance of the research work in this field that only 26 pages could be devoted to deformations other than extensional. This is no fault of the authors. Some of the later chapters on electrical and optical properties are less expansive and, in parts, achieve the breathless quality of a catalogue. In these later chapters it is unusual to find a reference to work published after 1957 which is five years before the date of publication.

The book is produced throughout with excellent line diagrams and many half-tone illustrations. It is a first-class book which will provide a good reference source. If the authors had exercised more discipline over their pens, particularly in the sections on structure and moisture relations, it could have been an excellent one.

K. W. HILLIER

### *Ultrastructure of Protein Fibres*

Edited by RUBIN BORASKY

Academic Press: New York and London, 1963. 72s

THIS book consists of a collection of papers (some of them subsequently expanded) presented to a symposium of the Nineteenth Annual Meeting of the Electron Microscopy Society of America held at Pittsburgh in 1961. The morphology of fibrous proteins and its possible relationship to primary, secondary and tertiary protein structure is discussed by correlating the results of electron microscopy with structural information obtained by chemical and, in particular, X-ray techniques. Modern theories relating biological function, mechanical and physical properties of natural proteinous materials to ultra and molecular structure are presented.

Because of its mode of conception as a series of papers, this book is not a complete exposition on the subject of fibrous protein structure and its biophysical implications. Particularly, it lacks details of the instrumental techniques used to obtain information in this field; this is unfortunate and detracts from the value of the book. Nevertheless as an exposition of modern research work into the ultra structure of fibrous proteins this book is a useful collection of review papers by the experts for the expert or near expert in this field.

H. BLOCK

# Notes

---

## *Transitions and Melting of Polytetrafluorethylene (Teflon) under Pressure*

WEIR<sup>1</sup> investigated the pressure/temperature behaviour of the first-order transitions in polytetrafluorethylene (Teflon) up to approximately 10 kilobars and 81°C. A high-pressure transition (near 5 kilobars) and a lower pressure transition (from 20°C at 1 bar to a triple point at 70°C, 4.65 kilobars) were studied. A third equilibrium line was found to proceed from the triple point to higher pressures with increasing temperature, but points were taken only at 75°C and 81°C. Weir<sup>1</sup> found that phase III is approximately two per cent denser than phase II, and that phase I is approximately one per cent less dense than phase II, at the transition lines. Rigby and Bunn<sup>2</sup> showed by means of X-ray studies that Teflon crystals melt at approximately 330°C.

In this Note the phase diagram of crystalline Teflon is extended to higher pressures and temperatures, and the melting curve is measured as a function of pressure.

The apparatus used here is similar to that described by Kennedy and La Mori<sup>3</sup>. A cylinder of Teflon,  $\frac{1}{2}$  in. in diameter and  $1\frac{3}{4}$  in. long, was machined from laboratory stock. Temperatures up to nearly 200°C could be obtained by means of a heavy-duty heating coil wrapped around the outside of the high-pressure cylinder. Temperature was measured by means of a chromel-alumel thermocouple in a well with the hot junction about  $1\frac{3}{4}$  in. from the sample. It was necessary to calibrate these readings separately by means of a second thermocouple in the sample position. The high-pressure transitions were detected simply by measuring the compression curve of Teflon at different temperatures, and taking the average of the onset pressures of the transitions with pressure increasing and pressure decreasing. Piston rotation<sup>3</sup> was not used, but at the low pressure of the transition the double-value of friction, hysteresis, etc. was less than 1.5 kilobars, and the points obtained are probably correct to better than  $\pm 200$  bars. A single run was made at 24°C to check the previous results. The II/III transition was encountered at 5.45 kilobars, which compares very well with Weir's value<sup>1</sup> of 5.41 kilobars, and with Kennedy and La Mori's value<sup>4</sup> of  $5.44 \pm 0.09$  kilobars, but badly with Beecroft and Swenson's value<sup>6</sup> of 6.36 kilobars. No further first-order transitions were encountered at 24°C up to 45 kilobars. There is a slight irregularity near 12 kilobars, which may be the 11 kilobar transition tentatively proposed

NOTES

Table 1. Experimental transition data on Teflon

Transition II to III		I to III		I to melt	
P, kb	t, °C	P, kb	t, °C	P, kb	t, °C
5.45	24	5.17	98	2.8	354
		5.60	120	3.2	357
		6.06	139.5	4.2	363
		7.20	179.5	6.2	376
				8.1	384

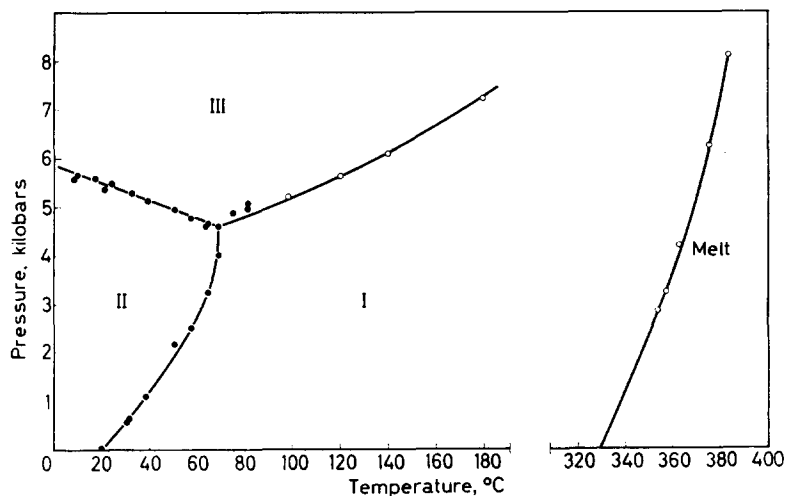


Figure 1. Phase diagram of Teflon

previously<sup>5</sup>, but the evidence is uncertain. All present experimental points are shown in Table 1. The complete phase diagram is shown in Figure 1. It is obvious that the I/III transition line is not straight, but shows distinct curvature. Our I/III transition points agree only poorly with Becroft and Swenson's points<sup>5</sup>, which are determined in almost exactly the same way.

The melting curve was determined by the method of differential thermal analysis (DTA)<sup>6</sup>. Strong DTA signals were obtained at the melting point at lower pressures. No corrections were made for the effect of pressure on the thermocouples. The melting temperatures are probably not correct to better than  $\pm 4^\circ\text{C}$ . No signal was encountered when a point at 10 kilobars was attempted, and when pressure was lowered, no points could then be obtained at lower pressures either. Annealing for a few hours at lower temperatures and pressures did not affect this. When the sample was recovered after the experiments, it could be seen to be much more transparent than it was originally. The reason for such behaviour is not clear.

Weir<sup>1</sup> noted that the extrapolation of the II/III transition line cuts the temperature axis at  $329^\circ\text{C}$ , i.e. very close to the melting point obtained by Rigby and Bunn<sup>2</sup>. From the present experiments it follows definitely, however, that the triple point obtained by Weir<sup>1</sup> is not spurious, and that the II/III transition line does not extend beyond the triple point at  $70^\circ\text{C}$ .

The slope ( $dP/dT$ ) of the melting curve of Teflon I is higher than is usual for organic materials. However, it should be noted that thermodynamic considerations would demand that, when the I/III transition line intersects the melting curve,  $(dP/dT)_{III/liq.}$  must be less than  $(dP/dT)_{I/liq.}$

The author would like to thank Mr L. J. Admiraal for his assistance with much of the experimental work.

C. W. F. T. PISTORIUS

National Physical Research Laboratory,  
South African Council for Scientific and Industrial Research,  
P.O. Box 395, Pretoria, South Africa

(Received March 1964)

#### REFERENCES

- <sup>1</sup> WEIR, C. E. *J. Res. Nat. Bur. Stand.* 1953, **50**, 95
- <sup>2</sup> RIGBY, H. A. and BUNN, C. W. *Nature, Lond.* 1949, **164**, 583
- <sup>3</sup> KENNEDY, G. C. and LA MORI, P. N. in BUNDY, F. P., HIBBARD, W. R. and STRONG, H. M. *Progress in Very High Pressure Research*, p 304. Wiley: New York, 1961
- <sup>4</sup> KENNEDY, G. C. and LA MORI, P. N. *J. geophys. Res.* 1962, **67**, 851
- <sup>5</sup> BEECROFT, R. I. and SWENSON, C. A. *J. appl. Phys.* 1959, **30**, 1793
- <sup>6</sup> NEWTON, R. C., JAYARAMAN, A. and KENNEDY, G. C. *J. geophys. Res.* 1962, **67**, 2559

### Degradation of Vinyl Alcohol–Isopropenyl Alcohol Copolymer by Periodic Acid

IT IS well known that periodic acid selectively attacks and degrades quantitatively 1,2-glycol structures in polymer (I), but it has not been reported that 1-methyl-1,2-glycol structure in polymer (II) was degraded quantitatively by periodic acid. We found that the saponification product of vinyl acetate–isopropenyl acetate copolymer had the 1-methyl-1,2-glycol structure (II), which was degraded by periodic acid.

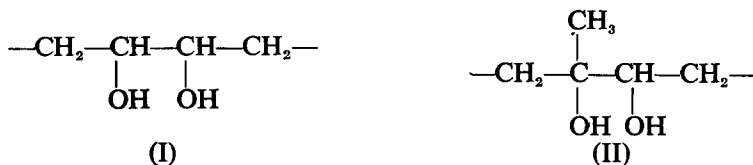


Table 1. Rate of degradation of polymer by periodic acid. 100 mg of polymer dissolved in 20 ml water and 1 ml of 1/200 mol periodic acid solution added

VAc:IPeAc	Initial $\bar{P}$	Final $\bar{P}$	Degradation time (min)
10:0	1320	460	<2
10:0	460	290	<2
10:0	290	205	<2
10:0	205	155	<2
10:0	155	130	<2
10:0	130	110	10
10:0	110	96	5

$$[\eta] = 7.5 \times 10^{-3} \bar{P}^{0.64} \text{ (dl/g)}$$



The slope ( $dP/dT$ ) of the melting curve of Teflon I is higher than is usual for organic materials. However, it should be noted that thermodynamic considerations would demand that, when the I/III transition line intersects the melting curve,  $(dP/dT)_{III/liq.}$  must be less than  $(dP/dT)_{I/liq.}$

The author would like to thank Mr L. J. Admiraal for his assistance with much of the experimental work.

C. W. F. T. PISTORIUS

National Physical Research Laboratory,  
South African Council for Scientific and Industrial Research,  
P.O. Box 395, Pretoria, South Africa

(Received March 1964)

#### REFERENCES

- <sup>1</sup> WEIR, C. E. *J. Res. Nat. Bur. Stand.* 1953, **50**, 95
- <sup>2</sup> RIGBY, H. A. and BUNN, C. W. *Nature, Lond.* 1949, **164**, 583
- <sup>3</sup> KENNEDY, G. C. and LA MORI, P. N. in BUNDY, F. P., HIBBARD, W. R. and STRONG, H. M. *Progress in Very High Pressure Research*, p 304. Wiley: New York, 1961
- <sup>4</sup> KENNEDY, G. C. and LA MORI, P. N. *J. geophys. Res.* 1962, **67**, 851
- <sup>5</sup> BEECROFT, R. I. and SWENSON, C. A. *J. appl. Phys.* 1959, **30**, 1793
- <sup>6</sup> NEWTON, R. C., JAYARAMAN, A. and KENNEDY, G. C. *J. geophys. Res.* 1962, **67**, 2559

### Degradation of Vinyl Alcohol–Isopropenyl Alcohol Copolymer by Periodic Acid

IT IS well known that periodic acid selectively attacks and degrades quantitatively 1,2-glycol structures in polymer (I), but it has not been reported that 1-methyl-1,2-glycol structure in polymer (II) was degraded quantitatively by periodic acid. We found that the saponification product of vinyl acetate–isopropenyl acetate copolymer had the 1-methyl-1,2-glycol structure (II), which was degraded by periodic acid.



Table 1. Rate of degradation of polymer by periodic acid. 100 mg of polymer dissolved in 20 ml water and 1 ml of 1/200 mol periodic acid solution added

VAc:IPeAc	Initial $\bar{P}$	Final $\bar{P}$	Degradation time (min)
10:0	1320	460	<2
10:0	460	290	<2
10:0	290	205	<2
10:0	205	155	<2
10:0	155	130	<2
10:0	130	110	10
10:0	110	96	5

$$[\eta] = 7.5 \times 10^{-3} \bar{P}^{0.64} \text{ (dl/g)}$$

## NOTES

Table 2. Rate of degradation of copolymer by periodic acid. 100 mg of copolymer dissolved in 20 ml water and 1 ml of 1/200 mol periodic acid solution added

<i>VAc:IPeAc</i>	Initial $\bar{P}$	Final $\bar{P}$	Degradation time (min)
9:1	750	395	<2
9:1	395	240	<2
9:1	240	155	5
9:1	155	125	5
9:1	125	98	10
9:1	98	83	15
9:1	83	76	15
8:2	600	270	10
8:2	270	163	15
8:2	163	115	15
8:2	115	92	30
8:2	92	79	30
8:2	79	68	30
8:2	68	66	30

$$[\eta] = 7.5 \times 10^{-3} \bar{P}^{0.84} \text{ (dl/g)}$$

Copolymerization of vinyl acetate-isopropenyl acetate initiated by azobisisobutyronitrile at 70°C was carried out for three hours and the product saponified completely by 8 per cent sodium hydroxide-methanol solution (containing 1 per cent water) at room temperature for 24 hours. The procedure was repeated at 60°C for 1 hour with fresh sodium hydroxide solution. Saponification was over 99.8 per cent complete.

Table 1 shows that the degree of polymerization of polyvinyl alcohol decreased to the theoretical value within two minutes when about 0.2 mol % periodic acid per monomer unit was added to the polymer, of which the concentration was 5g/l. But with vinyl alcohol-isopropenyl alcohol (9:1) or (8:2) copolymer, the time to degrade to constant degree of polymerization by periodic acid increased gradually from 2 to 30 minutes as shown in Table 2.

This fact shows that periodic acid reacts very rapidly with 1,2-glycol structures, and so ring formation with 1,2-glycol, which is the rate-determining step, is very fast under these conditions, but with 1-methyl-1,2-glycol ring formation by periodic acid is slow, so that in (9:1) copolymer the rate of degradation gradually decreases.

If the concentration of periodic acid in these reactions increases up to 10 mol % per monomer unit, the overall rate of degradation of the copolymer is complete within two minutes, and the experimental data are reproducible. We conclude that all 1,2-glycol structures of vinyl alcohol-isopropenyl alcohol copolymers which contain structures (I) and (II) degrade completely in 20 mol % periodic acid (per monomer unit) within ten minutes. We also found that (10:0), (9:1) and (8:2) vinyl acetate-isopropenyl acetate copolymers have 1.3, 1.8 and 2.6 mol % 1,2-glycol bonding respectively; this means that in the copolymerization of vinyl acetate and isopropenyl acetate head to head structures increase with the isopropenyl acetate content.

The author wishes to thank Professor Y. Yamashita, Nagoya University, for his advice throughout the work and Dr S. Iwatsuki for valuable suggestions.

MASARU IBONAI

Industrial Research Institute,  
Aichi Prefecture,  
Chikusa, Nagoya, Japan

(Received October 1963)

### *Anomaly in the Density Dependence of the Diffusion Constant in Polyethylene*

IT HAS been considered for some time an experimental fact that the diffusion constant ( $D$ ) and solubility constant ( $k$ ) governing the flow of small molecules through crystalline polymers decrease with increasing density<sup>1-7</sup>. This result is explained in a straightforward manner by the two-phase model of a crystalline polymer. According to this explanation, the diffusing molecule cannot penetrate the crystal. Therefore, if the crystalline fraction is increased (i.e. the density increased) both  $D$  and  $k$  decrease.

Several insufficiencies of this simple model have been apparent for some time. The most pertinent evidence has been obtained from experiments in which the gas type and crystallinity are both varied. Thus Michaels and Parker<sup>4</sup> observed the permeation coefficient to decrease to a different extent with increasing density of polyethylene for gases of different molecular size. This result is in agreement with the experiments of Jeschke and Stuart<sup>6</sup>. These authors, though in disagreement over detail, agree that the diffusion model of a crystalline polymer must include a factor which accounts for crystal geometry. This conclusion we reached independently several years ago. The experimental evidence for polyethylene is that whilst  $k$  always depends on density,  $D$  does not.  $D$  in fact always *increases* when the density of a specimen is increased by annealing. It turns out that for polyethylene the most significant variable for  $D$  is not density but the original rate of cooling from the melt, i.e. the temperature of crystallization<sup>4</sup>.

Measurements of  $D$  and  $k$  were made with a Sartorius vacuum microbalance following the method described by Ryskin<sup>8,9</sup>. The diffusion of ethane into low pressure polyethylene was observed at 30 cm of mercury pressure at 23.5°C. Under these conditions the diffusion was governed by the laws of Fick and Henry to within the experimental error. The specimens were films of low pressure polyethylene approximately 10 cm × 1 cm × 0.025 cm in size. Before starting the experiment residual gases were pumped from the film until the weight was constant. The ethane was then admitted and the rate of increase of weight due to the absorption of ethane followed with the microbalance and a pen recorder. The resulting curves were then analysed<sup>8-10</sup> to obtain  $D$  and  $k$ .

The specimens were compression moulded films of 'Alathon' 60. Specimens were moulded with densities 0.939 g/cm<sup>3</sup> (quenched into ice-water from the press), 0.953 g/cm<sup>3</sup> (cooled in the press with cooling water) and 0.963 g/cm<sup>3</sup> (cooled in the press without cooling water). Densities were

The author wishes to thank Professor Y. Yamashita, Nagoya University, for his advice throughout the work and Dr S. Iwatsuki for valuable suggestions.

MASARU IBONAI

Industrial Research Institute,  
Aichi Prefecture,  
Chikusa, Nagoya, Japan

(Received October 1963)

### *Anomaly in the Density Dependence of the Diffusion Constant in Polyethylene*

IT HAS been considered for some time an experimental fact that the diffusion constant ( $D$ ) and solubility constant ( $k$ ) governing the flow of small molecules through crystalline polymers decrease with increasing density<sup>1-7</sup>. This result is explained in a straightforward manner by the two-phase model of a crystalline polymer. According to this explanation, the diffusing molecule cannot penetrate the crystal. Therefore, if the crystalline fraction is increased (i.e. the density increased) both  $D$  and  $k$  decrease.

Several insufficiencies of this simple model have been apparent for some time. The most pertinent evidence has been obtained from experiments in which the gas type and crystallinity are both varied. Thus Michaels and Parker<sup>4</sup> observed the permeation coefficient to decrease to a different extent with increasing density of polyethylene for gases of different molecular size. This result is in agreement with the experiments of Jeschke and Stuart<sup>6</sup>. These authors, though in disagreement over detail, agree that the diffusion model of a crystalline polymer must include a factor which accounts for crystal geometry. This conclusion we reached independently several years ago. The experimental evidence for polyethylene is that whilst  $k$  always depends on density,  $D$  does not.  $D$  in fact always *increases* when the density of a specimen is increased by annealing. It turns out that for polyethylene the most significant variable for  $D$  is not density but the original rate of cooling from the melt, i.e. the temperature of crystallization<sup>4</sup>.

Measurements of  $D$  and  $k$  were made with a Sartorius vacuum microbalance following the method described by Ryskin<sup>8,9</sup>. The diffusion of ethane into low pressure polyethylene was observed at 30 cm of mercury pressure at 23.5°C. Under these conditions the diffusion was governed by the laws of Fick and Henry to within the experimental error. The specimens were films of low pressure polyethylene approximately 10 cm × 1 cm × 0.025 cm in size. Before starting the experiment residual gases were pumped from the film until the weight was constant. The ethane was then admitted and the rate of increase of weight due to the absorption of ethane followed with the microbalance and a pen recorder. The resulting curves were then analysed<sup>8-10</sup> to obtain  $D$  and  $k$ .

The specimens were compression moulded films of 'Alathon' 60. Specimens were moulded with densities 0.939 g/cm<sup>3</sup> (quenched into ice-water from the press), 0.953 g/cm<sup>3</sup> (cooled in the press with cooling water) and 0.963 g/cm<sup>3</sup> (cooled in the press without cooling water). Densities were

NOTES

measured by the Archimedes method using ethyl alcohol as the fluid. A portion of each specimen was then annealed at 130°C for 30 hours under nitrogen. The densities of all three specimens after annealing lay between 0.972 and 0.973 g/cm<sup>3</sup>. The spherulite size was measured by taking optical micrographs of thin cross sections using crossed polaroids. The average spherulite size before annealing was 10 microns for the quenched specimen, 50 microns for the water cooled and 90 microns for the slow cooled. The spherulite size did not change during annealing.

*Table 1.* The measured values of density, diffusion coefficient  $D$  and solubility constant  $k$  for the specimens initially crystallized by quenching (Q), by normal cycle with cooling water (NC), by slow cooling without cooling water (SC) and by crystallizing under pressure at 137°C (UP)

<i>Anneal</i>	<i>Density</i> g/cm <sup>3</sup>	$D \times 10^8$ cm <sup>2</sup> /sec	$k$ μg/g · cm Hg	<i>Crystallization</i>
Before	0.939	3.48	9.67	Q
After	0.972	4.05	4.46	Q
Before	0.953	2.01	7.30	NC
After	0.972	3.09	4.06	NC
Before	0.963	1.29	4.95	SC
After	0.973	1.67	5.41	SC
Before	0.975	0.461	4.75	UP

The measurements of  $D$  and  $k$  are given in *Table 1*. If  $k$  is plotted against density the points for all specimens can be fitted to a straight line which passes through the density of the crystal for  $k=0$ . This is the expected result. If  $D$  is plotted against density then the points for the specimens *before* annealing fall on a single curve with a negative slope—again the expected result. However, the increase in  $D$  for each specimen brought about by annealing is quite anomalous.

The dependence of  $D$  on crystallization rate agrees with the hypothesis of Jeschke and Stuart<sup>8</sup> which is that the diffusion takes place at imperfections, grain boundaries and imperfectly ordered regions. Consequently it is necessary to consider the length of path (tortuosity<sup>4</sup>) a diffusing molecule will follow. It is known that the lower the temperature of crystallization: (a) the smaller are the spherulites, (b) the greater is the amount of non-crystallographic branching<sup>11</sup>, (c) the smaller the pitch of the lamellar twist<sup>12</sup> and (d) the smaller the lamellar area<sup>13</sup>. These trends will all lower the tortuosity and so enlarge  $D$ . The increase in  $D$  with increasing rate of cooling from the melt is thus understandable since the faster the rate of cooling the lower the temperature of crystallization.

The increase in  $D$  for a given specimen brought about by annealing can be understood by the opening up of the inter-lamellar boundaries. The annealing causes an increase in lamellar thickness<sup>14</sup> a process which could well enlarge a proportion of the inter-lamellar faults. Another possibility is that annealing produces holes in the lamellae. This is known to occur

when small single crystal lamellae are annealed<sup>14,15</sup>. If annealing produced holes in the lamellae in the bulk polymer the tortuosity would be decreased and  $D$  consequently increased. A third possibility is that whilst the lamella thickness increases during annealing, the lamella area decreases. This hypothesis is quite plausible and would certainly lead to a reduction in tortuosity.

The correlation between  $k$  and density will probably be obvious when a reliable theory for the density of polyethylene emerges from the several now available. It is, however, not possible to explain the observed density dependence of  $D$  and  $k$  by assuming (a) that the inter-lamellar fault is filled with amorphous material, (b) that the density change is caused by the enlargement of the lamellae and a reduction in the width of the inter-lamellar fault and therefore of the amorphous material within it, and (c) that the diffusing molecule can penetrate the amorphous material but not the crystal. This explanation will account for the density dependence of  $k$ . It clearly will not account for the increase in  $D$  which occurs on annealing simultaneously with the increase in density.

There is, however, one hypothesis for the density dependence of  $k$  which, although radical, cannot be avoided. Consider as a model of polyethylene a unit cube made up of thin parallel lamellae with lateral dimensions  $a$  and  $b$  and thickness  $l$  ( $l \ll a \sim b$ ). This is a crude replica of reality. Yet the model is probably good enough for the calculation of the area/volume ratio of lamellar surface of a molecularly homogeneous polymer such as polyethylene. Neglecting the thin edges of the lamellae the surface area/volume is  $2l^{-1}$ . Now the inverse of the average lamellar thickness of polyethylene,  $l^{-1}$ , is found by experiment to depend linearly on density<sup>16</sup>. Therefore the lamellar surface area/volume depends linearly on density. To within the error of our experiments the solubility coefficient defined in terms of volume of absorbing material,  $k_v$  (microgrammes/cm<sup>3</sup> . cm Hg) is also a linear function of density. These correlations lead directly to the hypothesis that absorption in polyethylene occurs on the lamellar surfaces since if this is so it is reasonable to expect  $k_v$  to be proportional to the lamellar surface area/volume ratio. The strength of this hypothesis at the present time is that it is based on two experimental correlations and not on another hypothesis relating density and thermal history.

*The author wishes to thank Dr J. M. Lupton for the specimen UP and Dr R. K. Eby for repeating the experiments to confirm the results. The experiments were performed at the Experimental Station of E.I. du Pont de Nemours and Company.*

N. G. McCrum

*Engineering Laboratory,  
Department of Engineering Science,  
Parks Road, Oxford*

(Received May 1964)

<sup>1</sup> McCALL, D. W. *J. Polym. Sci.* 1957, **26**, 151

<sup>2</sup> KLUTE, C. H. *J. appl. Polym. Sci.* 1959, **1**, 340

## NOTES

---

- <sup>3</sup> ROGERS, C. E., STANNETT, V. and SWZARC, M. *J. phys. Chem.* 1959, **63**, 1406
- <sup>4</sup> MICHAELS, A. S. and PARKER, R. B. *J. Polym. Sci.* 1959, **41**, 53
- <sup>5</sup> MICHAELS, A. S. and BIXLER, H. J. *J. Polym. Sci.* 1961, **50**, 393
- <sup>6</sup> JESCHKE, D. and STUART, H. A. *Z. Naturforsch.* 1961, **16a**, 37
- <sup>7</sup> MICHAELS, A. S. *et al. Industr. Engng Chem., Process Design and Development*, 1962, **1**, 14
- <sup>8</sup> RYSKIN, G. YA. *J. tech. Phys. U.S.S.R.* 1954, **24**, 197
- <sup>9</sup> RYSKIN, G. YA. *Sov. Phys. Solid State Physics*, 1959, **1**, 870
- <sup>10</sup> CRANK, J. *Mathematics of Diffusion*. Oxford University Press, London, 1957
- <sup>11</sup> KEITH, H. D. and PADDEN, F. J. *J. appl. Phys.* 1964, **35**, 1270
- <sup>12</sup> KELLER, A. *Growth and Perfection of Crystals*, edited by R. H. DOREMUS, B. J. ROBERTS and D. TURNBULL. Wiley: New York, 1958
- <sup>13</sup> PALMER, R. P. *Makromol. Chem.* 1964. In press
- <sup>14</sup> STATTON, W. O. and GEIL, P. H. *J. appl. Polym. Sci.* 1960, **3**, 357
- <sup>15</sup> KELLER, A. and BASSETT, D. C. *J. R. microsc. Soc.* 1960, **79**, 243
- <sup>16</sup> BROWN, R. G. and EBY, R. K. *J. appl. Phys.* 1964, **35**, 1156

# Proton Spin-Lattice Relaxation Measurements on Some High Polymers of Differing Structure and Morphology

*Polyethylene, Poly-4-methyl-pentene-1, Poly-L-leucine, Poly-phenyl-L-alanine, Polystyrene and Poly- $\alpha$ -methyl-styrene*

B. I. HUNT, J. G. POWLES and A. E. WOODWARD\*

Proton spin-lattice relaxation times ( $T_1$ ) have been measured at a resonant frequency of 21.5 Mc/s in the temperature range from 77° to 520°K for polyethylene (Rigidex 35) crystals and poly-4-methyl-pentene-1 (P4MPI) crystals grown from dilute solution as well as for melt-formed samples. Exponential decay of magnetization was observed for the polyethylene pellets at all temperatures. On the other hand decay of magnetization describable by two exponentials (two  $T_1$ 's) was found at low temperatures for isothermally grown polyethylene crystals, polyethylene dendrites, P4MPI crystals and melt-formed P4MPI.

All three polyethylene samples showed a  $T_1$  minimum at about 250°K which is believed to be related to the  $\gamma$  mechanical loss maximum found for partially crystalline samples, formerly attributed to motions of three or more  $\text{CH}_2$  units in the amorphous regions. The position of another minimum in the melt was strongly dependent on sample history and is believed to be a consequence of the increased chain mobility in the crystalline areas.

Two  $T_1$  minima were observed for P4MPI, one at about 150°K and another weaker one at 430° to 470°K, the latter being dependent on the sample history. The 150°K minimum is attributed to methyl group reorientation while the higher temperature process is believed to be associated with the glass-rubber transition or possibly a combination of this and a change in the crystalline regions.

Spin-lattice relaxation time measurements have also been made for two synthetic polypeptides, poly-L-leucine (PLL) and poly-phenyl-L-alanine (PPLA). For PLL two  $T_1$  values were found at low temperatures. The shorter  $T_1$  has a minimum value at 174°K similar to the P4MPI crystals which is attributed to methyl group reorientation. A second minimum at about 290°K is attributed to isobutyl or isopropyl group motion. For PPLA a minimum at 200°K and another wide shallow one at 330° to 400°K are found. The first is believed to be due to phenyl motion while the second is believed to be caused by oscillations of the benzyl group with an amplitude which increases with increasing temperature.

We have also studied polystyrene and poly- $\alpha$ -methyl-styrene. The higher temperature  $T_1$  minimum is related to the glass-rubber transition. Polystyrene has a minimum at 260°K and a plateau in the  $T_1$ /temperature curve at 120° to 150°K. Poly- $\alpha$ -methyl-styrene has a broad minimum at 300° to 340°K due, at least partially, to methyl group reorientation. There is also an inflection in the  $T_1$ /temperature curve at 100° to 140°K. The possible relation of these relaxation processes to mechanical loss maxima at low temperatures is discussed.

\*On sabbatical leave from the Physics Department, Pennsylvania State University, 1962-63.



## I. POLYETHYLENE AND POLY-4-METHYL-PENTENE-1

PRIOR to the inception of the present investigation, studies of molecular motion in high polymer crystals obtained by precipitation from dilute solution had been limited to linear polyethylene, mainly using the broad line nuclear magnetic resonance (n.m.r.) technique<sup>1-4</sup> although one dynamic mechanical study<sup>5</sup> and one investigation<sup>3</sup> employing an approximate method of measuring n.m.r. spin-lattice relaxation times ( $T_1$ ) had been made. Following completion of most of the present work, a recent investigation of  $T_1$  as a function of temperature for crystals and for a melt-formed sample of linear polyethylene, in addition to branched polyethylene and a normal paraffin,  $C_{94}H_{190}$ , by McCall and Douglass<sup>6</sup> came to our attention.

In the preparation of polymer crystals from dilute solution the crystal shape obtained depends on a variety of factors, including growth temperature, polymer type, solvent and concentration. Polyethylene gives pyramid-shaped crystal plates under isothermal growth conditions<sup>7</sup> whereas quenching of similar solutions from elevated temperatures leads to dendritic featherlike structures<sup>8</sup>. To date the motional characteristics of polymer crystal samples prepared in different ways have not been systematically studied.

$T_1$  measurements have been carried out on two preparations of polyethylene crystals, one containing lozenge-shaped crystals and the other dendritic growths, as well as on a premelted sample. Some differences between these results and those given previously<sup>3,6</sup> for similar samples have been found.

The preparation of square-shaped crystals of poly-4-methyl-pentene-1 (P4MP1) from dilute solution has been reported<sup>10</sup> but essentially no physical property characterization studies have been carried out. Dynamic mechanical measurements<sup>11,12</sup> and broad-line n.m.r. measurements<sup>13,14</sup> have been reported on melt-formed samples.  $T_1$  measurements are reported here for two P4MP1 samples from dilute solution containing a large proportion of crystals (believed to be collapsed hollow pyramids) and for a sample crystallized by cooling from the melt.

## SAMPLE PREPARATION AND MORPHOLOGY\*

A linear polyethylene, Rigidex 35, was used for the preparation of crystals: m.pt = 135.5°C; density (20°C) = 0.977 g/cm<sup>3</sup> for a sample cooled from the melt at 190°C at a rate of 5° per hour; crystallinity 86 per cent. Two samples of crystals were prepared. The first consisted of crystals grown from a 0.01 per cent (by weight) xylene (AnalaR grade) solution at 84° ± 0.5°C. 100 ml of a polymer solution was heated to 140°C and poured into 2 l. of pure solvent at 84°C. After 24 hours without stirring the precipitate was collected by fast filtration and dried at room temperature under vacuum for three days. This was repeated five times in order to obtain a large enough sample. Optical microscopic examination, using oblique illumination of material deposited by evaporation showed that it contained a number of lozenge-shaped crystals along with some sheetlike

\*This matter is discussed in more detail in the accompanying paper<sup>15</sup>.

material. An optical micrograph taken using a Zeiss photomicroscope with direct illumination of such crystals is given in *Figure 1*. The lozenge clearly visible on the right hand side of this photograph has diagonals  $5\ \mu$  and  $3.5\ \mu$  in length.

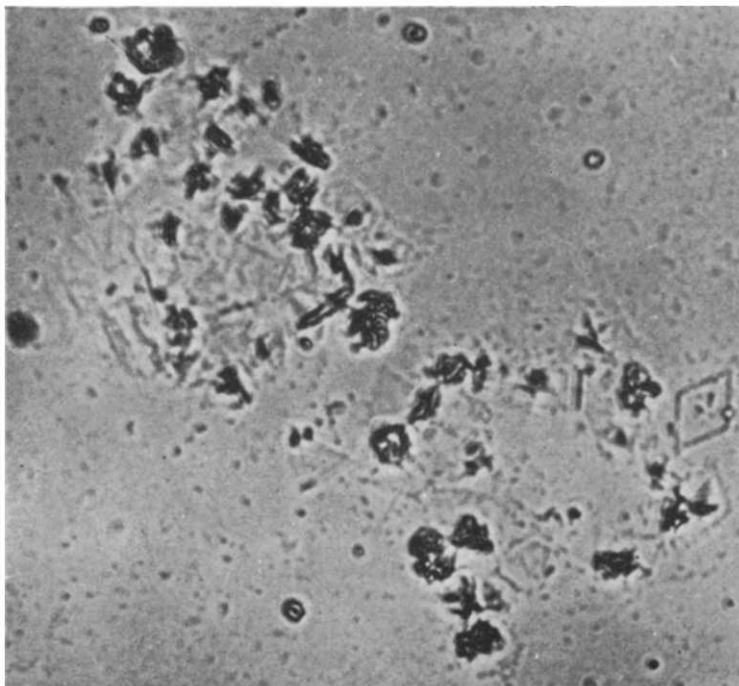


*Figure 1*—Optical micrograph with direct illumination of polyethylene crystals grown from 0.01 per cent xylene solution at  $84^{\circ}\text{C}$  (magnification  $2015\times$ , reproduced without reduction)

The other sample of polyethylene crystals was obtained by cooling a 0.44 per cent xylene solution from  $130^{\circ}\text{C}$  under a room temperature gradient. After two weeks the solution was fast filtered and the precipitate dried for three days under vacuum at room temperature. Optical micrographs taken on portions of a slide prepared by evaporation of a drop of a suspension from a 0.5 per cent solution given in *Figure 2* reveal both split-arm cross types and hedgehog type<sup>8</sup> dendrites.

The P4MP1 was prepared using an aluminium-titanium complex catalyst and had a residual ash content of about 100 p.p.m. Solubility in boiling hexane was less than 5 per cent, attainable crystallinity greater than 65 per cent and the melt flow index  $8.2\ \text{g}/\text{min}$  extruded under 5 kg pressure. One of the P4MP1 specimens was obtained as follows: 0.3 g of polymer was dissolved in 470 ml AnalaR grade xylene at  $120^{\circ}\text{C}$  and the solution allowed to cool under a room temperature gradient. The precipitate was obtained in sheet form after fast filtration on to paper and was dried for

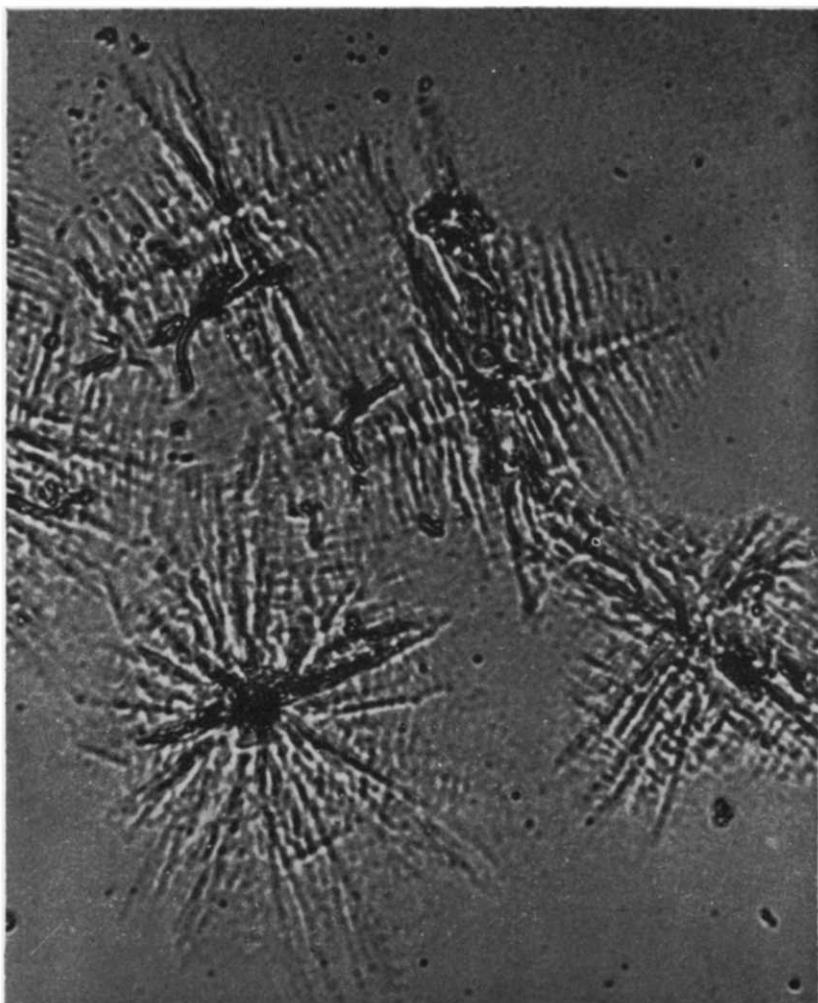


*Figure 2*—Optical micrograph with direct illumination of polyethylene dendrites grown from 0.5 per cent xylene solution cooled from 130°C with room temperature gradient (magnification 800×, reproduced without reduction)

48 hours under vacuum at room temperature. X-ray diffraction measurements indicated a considerable amount of orientation of the polymer chains in a direction perpendicular to the film face and a degree of crystallinity of 70 per cent. The melting point of a piece of this mat was 515°K. *Figure 3* is a photomicrograph of material on a slide prepared from a drop of suspension which contains square crystals or aggregates of such crystals together with other shapes. In other parts of the field sheets and pieces were observed. The wrinkles and folds in the individual crystals are believed to be a consequence of collapse of a hollow pyramidal structure

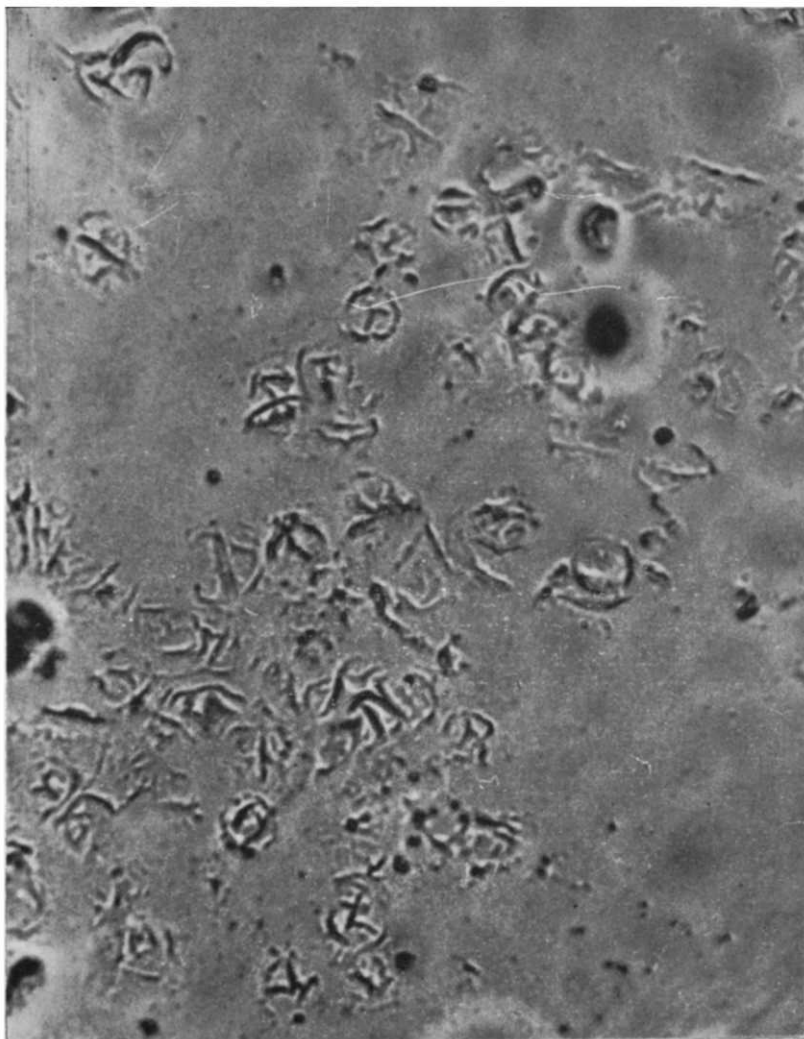


*Figure 3*—Optical micrograph with direct illumination of poly-4-methyl-pentene-1 crystals grown from 0.07 per cent xylene solution cooled from 120°C with room temperature gradient (magnification 800 $\times$ , reproduced without reduction)

upon drying as described in the accompanying paper<sup>15</sup>. The second P4MP1 specimen was grown from dilute solution under isothermal conditions at 57°C using 0.15 g polymer dissolved in 250 ml xylene in a 500 ml round bottom flask at 124°C and subsequently placed in the 57°C bath for 70 hours. A crystal mat was obtained as described for the other P4MP1 sample. The photomicrograph in *Figure 4* of material obtained from a drop of the suspension contains numerous square-based crystals.

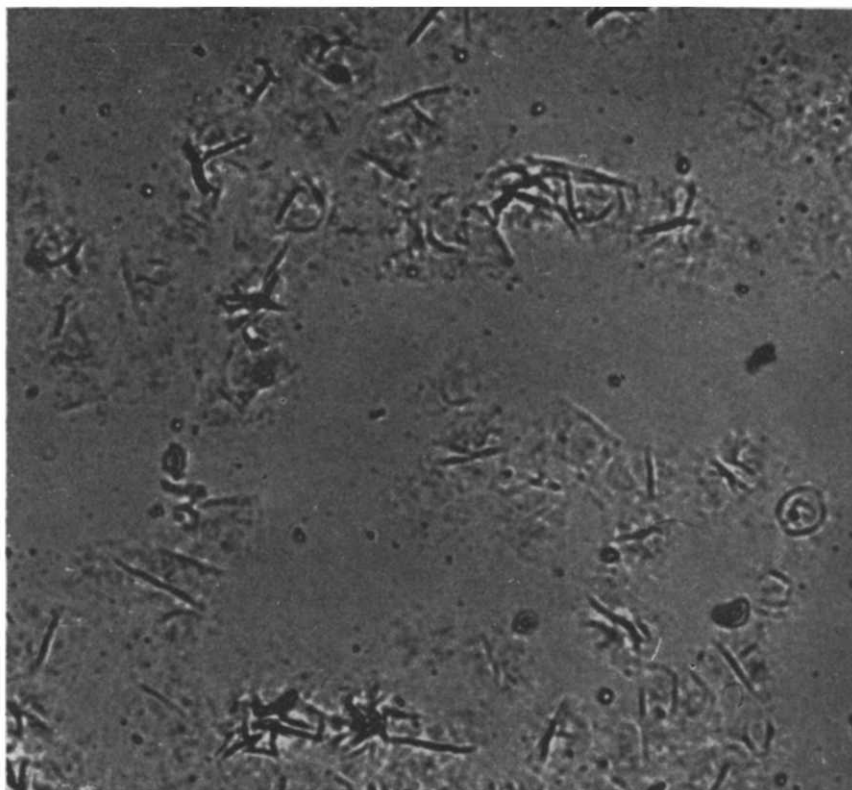


Figure 4—Optical micrograph with direct illumination of poly-4-methyl-pentene-1 crystals grown isothermally at 57°C from 0.07 per cent xylene solution (magnification 800 $\times$ , reproduced without reduction)

## RESULTS

$T_1$  measurements were made with the apparatus of Mansfield and Powles<sup>9</sup> employing a 90°,  $\tau$ , 90° pulse sequence at various time values ( $\tau$ ). This apparatus has been found satisfactory for measurements on glassy as well as partially crystalline polymers<sup>16</sup>. Unlike the previous measurements, some non-exponential decay curves were observed. One example is given in Figure 5 in which the log of the difference in the height of the decay curve after the first 90° pulse ( $h_0$ ) and the height after the second pulse ( $h$ ) is plotted versus time for the polyethylene crystals prepared at 84°C. After the first 15 seconds or so the plot is linear. Subtraction of the contribution from this long  $T_1$  for times less than 15 seconds suggests that there is a second component which also has an exponential decay with a shorter  $T_1$ . The ratio of intensities of the two decay processes is designated  $I_1/I_2$ , which for the curve in Figure 5 is 3/2.

$T_1$  versus temperature plots are given in Figures 6, 7 and 8 for the isothermally grown polyethylene crystals, the dendrites and the as-received

RELAXATION MEASUREMENTS ON SOME HIGH POLYMERS

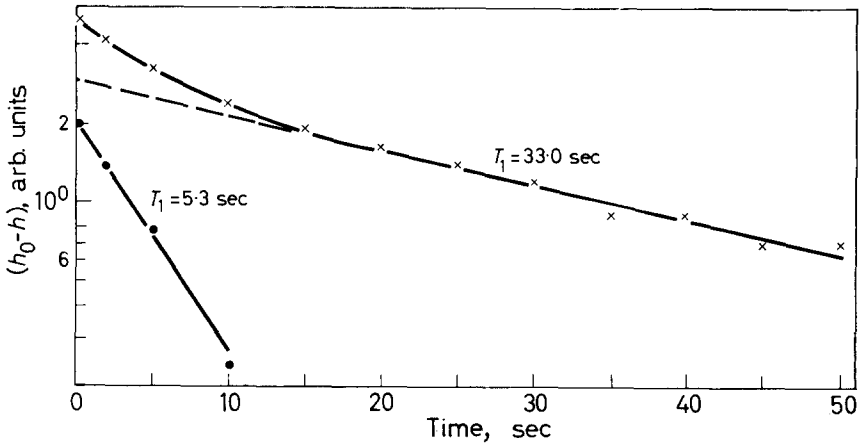


Figure 5—Longitudinal magnetization decay curve at 77°K for isothermally grown polyethylene crystals. × experimental points, --- extrapolation of long  $T_1$  (33 sec) part, ● short  $T_1$  (5.3 sec) part

pellets, respectively. All three samples show a minimum around 250°K; this  $T_1$  minimum occurs at a slightly lower temperature for the heated dendrites and the pellets than for either of the solution-grown crystal samples. At very low temperatures the two crystal preparations exhibited non-exponential decays which can be decomposed into two exponential

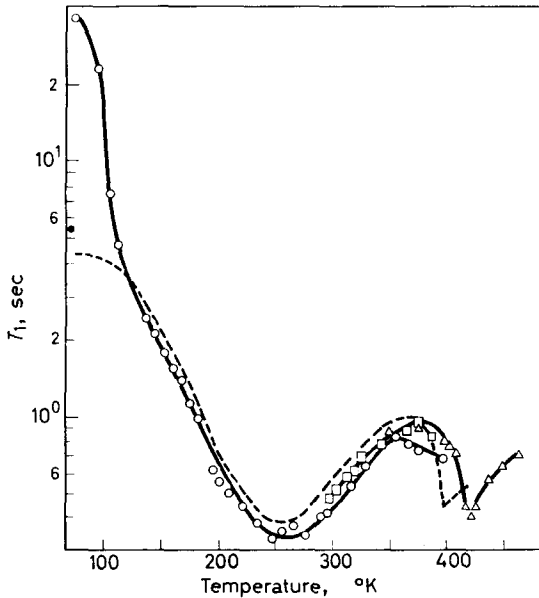
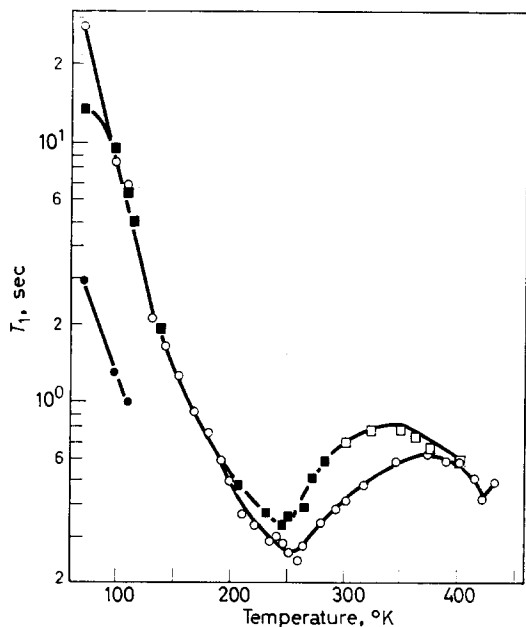
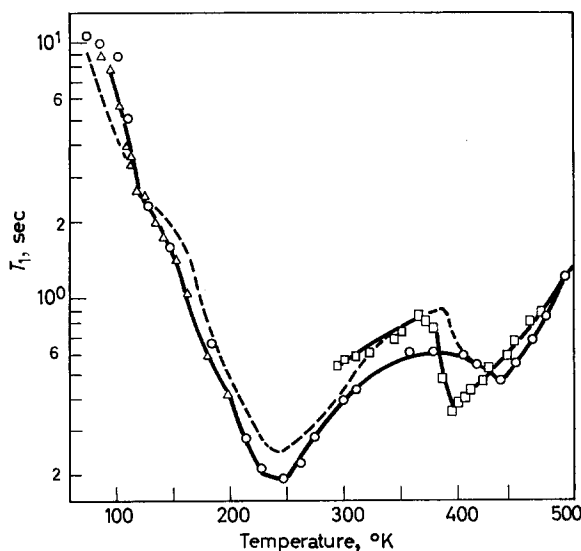


Figure 6—Spin-lattice relaxation time versus temperature for polyethylene crystals obtained from 0.01 per cent xylene solution at 84°C ○, ● heating, □ cooling, △ reheating, --- data of McCall and Douglass<sup>6</sup>

components (see *Figure 5*) and the two  $T_1$  values are given in *Figures 6* and *7*. For the dendrites  $I_1/I_s$  at 77°, 100° and 110°K was 4/3, 4/3 and 3/2, respectively. The heated dendrites and the pellets always showed exponential decays.



*Figure 7*—Spin-lattice relaxation time versus temperature for polyethylene dendrites from 0.44 per cent xylene solution cooled from 130°C with room temperature gradient. ○, ● heating, □ cooling, ■ heating, same sample



*Figure 8*—Spin-lattice relaxation time versus temperature for linear polyethylene pellets, ○ heating, □ cooling, △ new sample, --- data of McCall and Douglass<sup>6</sup>

Another  $T_1$  minimum is observed above the melting point for the isothermally grown crystals, the dendrites and the pellets (see *Figures 6-8*). The heating rate of  $0.6^\circ$  per minute was considered to be slow enough to allow thermal equilibrium to be established in the sample. In addition, for all samples the spin-spin relaxation time,  $T_2$ , became very long at  $409^\circ\text{K}$ , the melting point. Upon cooling, the melted isothermally grown crystals and pellets gave the same  $T_1$ /temperature curve. The  $T_1$  minimum and the large change in  $T_2$  for the pellets occur at temperatures about  $40^\circ$  and  $15^\circ$  respectively lower than in the heating run as shown in *Figure 8*. This is ascribed to supercooling of the sample due to a relatively high cooling rate which in the  $500^\circ$  to  $400^\circ\text{K}$  region was greater than  $1^\circ/\text{min}$ .

The data of McCall and Douglass<sup>6</sup> for Marlex 50 crystals grown at  $80^\circ\text{C}$  from 0.04 per cent xylene solution are indicated in *Figure 6* and for Marlex 50 pellets in *Figure 8*. In both cases there is close agreement in the region of the  $250^\circ\text{K}$   $T_1$  minimum. However, McCall and Douglass report only one  $T_1$  at  $77^\circ\text{K}$  with a value of about 4 sec, whereas we find two  $T_1$ s at  $77^\circ\text{K}$  with values of 5.3 and 36 sec. It is likely that two  $T_1$  values also exist for the crystal sample of McCall and Douglass at  $77^\circ\text{K}$  but due to their approximate method of obtaining  $T_1$  they failed to recognize this fact. Our results indicate that at temperatures above  $93^\circ\text{K}$ , if two  $T_1$ s exist they cannot differ by more than a factor of two. Since a minimum at  $77^\circ\text{K}$  or lower does not appear likely for linear polyethylene, it is our belief that the process leading to the shorter  $T_1$  vanishes in the  $77^\circ$  to  $93^\circ\text{K}$  region and therefore it would be erroneous to connect the short  $T_1$  value at  $77^\circ\text{K}$  with the line through the points at higher temperatures.

Another difference between the previous and the present work for the crystals is the position of the higher temperature  $T_1$  minimum found<sup>6</sup> at about  $400^\circ\text{K}$  for crystals grown at  $80^\circ\text{C}$  and at  $420^\circ\text{K}$  for crystals grown at  $84^\circ\text{C}$  as well as for the sample containing dendrites. This discrepancy may be due to differences in sample morphology but it should be pointed out that for the  $80^\circ\text{C}$  crystals the  $T_1$  minimum is below the melting point while for the  $84^\circ\text{C}$  crystals and the dendrites it is above the melting point. However, the decrease in  $T_1$  with increasing temperature starts at temperatures well below the melting point for all samples indicating that motion of the same type but with lower correlation frequencies does occur below the melting point.

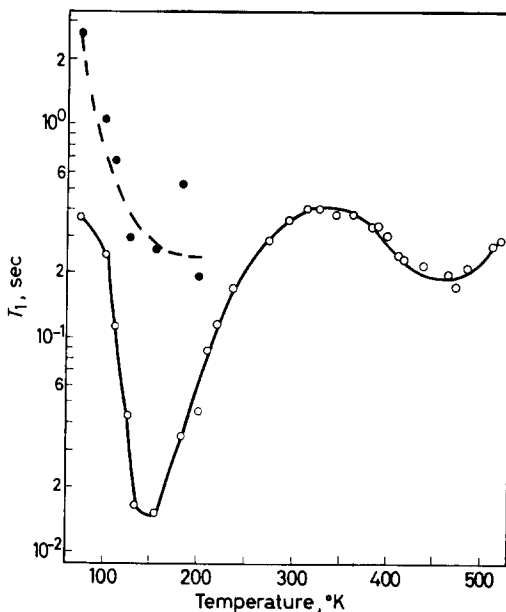
The present results and those of McCall and Douglass<sup>6</sup> differ markedly from those of Slichter<sup>3</sup>, obtained by the saturation method, for crystals of Marlex 50 prepared at  $70^\circ\text{C}$  from 0.1 per cent xylene solution, for the crystals annealed at  $405^\circ\text{K}$  for 24 hours, and for melt-formed material annealed at  $405^\circ\text{K}$  for eight days. Slichter reports a long  $T_1$  of about 200 sec at temperatures from approximately  $210^\circ$  to  $380^\circ\text{K}$  for all samples, in addition to a shorter  $T_1$  that showed a minimum, the characteristics of which were strongly dependent on the specimen. The lowest  $T_{1,\text{min}}$  recorded was about three seconds for the annealed melt-formed sample at approximately  $230^\circ\text{K}$ , a value about ten times higher than any  $T_{1,\text{min}}$  observed in the present work. We have been quite unable to find a long  $T_1$  of the order of 200 sec in any sample. It does not appear likely that these



discrepancies are due only to differences in sample preparation but must arise as a consequence of the different experimental methods employed.

A  $T_1$  minimum at about 410°K for linear polyethylene is reported by Kawai and Hirai (see ref. 17), although no details of sample history are given. Two  $T_1$  minima have been reported<sup>18</sup> for polyoxyethylene  $[\text{CH}_2\text{CH}_2\text{—O}]_n$  at 270°K and 330°K, the latter being coincident with the melting point.

Figure 9—Spin-lattice relaxation time versus temperature for poly-4-methyl-pentene-1 crystal mat obtained from 0.07 per cent xylene solution cooled from 120°C with room temperature gradient



$T_1$  data for P4MP1 are given in Figure 9, for the sample prepared by cooling with a room temperature gradient, in Figure 10 for the sample grown isothermally at 57°C and in Figure 11 for a crystal sample heated for 10 min at 540°K and allowed to cool. Non-exponential decays, decomposable into two exponentials, were apparent at temperatures from 77° to 170°K for the first two samples but only at 77°K for the third one. The intensity ratio,  $I_l/(I_l+I_s)$ , for the room temperature gradient grown sample (Figure 9) was  $(30 \pm 10)$  per cent for temperatures from 77° to 182°K. For the isothermally grown specimen the percentage of long  $T_1$  in the temperature range 77° to 95°K is  $66 \pm 8$  while that from 101° to 178°K is  $36 \pm 5$ . Therefore we assume that here the long  $T_1$  values from 77° to 95°K are connected with the short  $T_1$  values at the higher temperatures, as plotted on Figure 10.  $I_l/I_s$  for the melt-formed sample was 2/3 at 77°K.

Figures 9, 10 and 11 show that in going from the room temperature gradient grown crystals to isothermally grown crystals and then to a sample cooled from the melt the two  $T_1$  curves at low temperatures are shifting closer together until for the melt-formed sample there is presumably over-

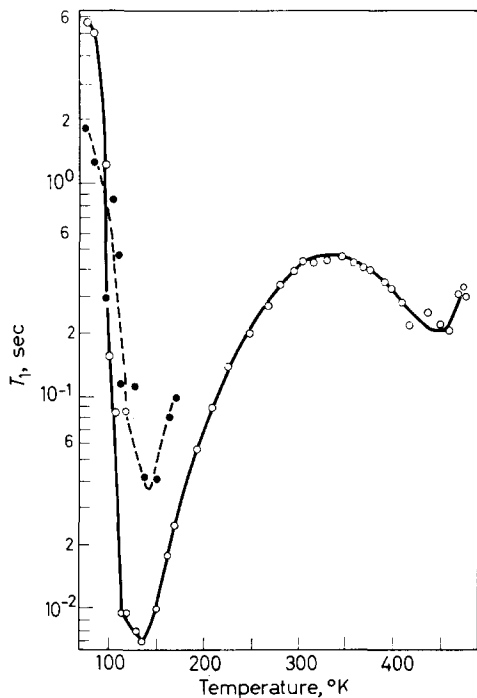
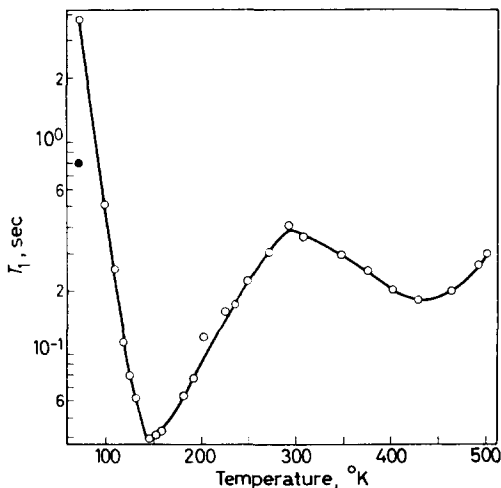


Figure 10—Spin-lattice relaxation time versus temperature for poly-4-methyl-pentene-1 crystals grown at 57°C from 0.07 per cent xylene solution

lap except below 100°K. The  $T_1$  minimum value for the sample cooled from the melt is a factor of three to five higher than for the other two samples. It is also seen that the high temperature minimum around 450°K is much narrower for the isothermally grown crystals. However, due to the small amount of the isothermally grown sample, the signal to noise

Figure 11—Spin-lattice relaxation time versus temperature for poly-4-methyl-pentene-1 cooled from the melt (540°K)



ratio was rather small at the higher temperatures so that the upper minimum is approximate.

Two other P4MP1 runs were made. An as-received sample showed the same general features found for the room temperature gradient grown sample. However, the room temperature gradient grown sample after heating to 513°K gave two  $T_1$ /temperature curves which appeared to cross one another below 200°K as for the isothermally grown sample. The higher temperature minimum was similar in shape, although shallower, to that obtained in the room temperature gradient grown sample.

#### DISCUSSION

We discuss for polyethylene: (1) the occurrence of two  $T_1$  values at low temperatures for solution grown samples but not for melt-formed ones; (2) the existence of a  $T_1$  minimum for all samples in the same temperature region (about 250°K); and (3) the presence of a  $T_1$  minimum above the melting point and its dependence on thermal history.

(1) The presence of two  $T_1$ s at a given temperature indicates that protons with two distinctly different environments which are isolated from each other exist. It is expected for a solid polymer composed principally of  $\text{CH}_2$  units that these different environments are due to morphological differences in the sample. One of the biggest differences in morphology of crystals grown from dilute solution as compared with melt-formed samples is the much larger amount of surface area in the former which might result in a different environment for the  $\text{CH}_2$  units on the surface as compared to those within the body of the material. It would also be expected that differences in proton environment would be found between the amorphous or defect regions and the crystalline parts for all samples. For the polyethylene crystals, however, the intensity ratios,  $I_1/I_2$ , do not appear to be related to the ratio of protons within the crystals to those on the surfaces (about 20/1). There is also the fact that *melt*-formed P4MP1 shows two  $T_1$ s below 100°K, the same as for isothermally grown polyethylene crystals, whereas the morphologies, including the crystal:amorphous ratios, are quite different. Finally, increasing the amorphous content for polyethylene in going from crystals to melt-formed samples seems to lead to a disappearance of two distinct areas of relaxation. Therefore neither of these explanations appears to be satisfactory for both polyethylene and P4MP1 considered together. This difficulty is aggravated if one tries to include the polypeptides (see part II). Poly-L-leucine shows similar low temperature  $T_1$  behaviour to that for P4MP1 crystals but has a different crystal structure and morphology although some chemical similarities exist. On the other hand another polypeptide, poly-phenyl-L-alanine, does not exhibit this  $T_1$  behaviour.

(2) The low temperature  $T_1$  minimum in polyethylene as pointed out by McCall and Douglass<sup>6</sup> occurs in the region in which a mechanical loss maximum has been found. This loss maximum was dependent on the sample history, being at 240°K ( $10^6$  c/s) for as-prepared powder and at 210°K for a moulded sample<sup>19</sup>, a shift in the same direction as the  $T_1$  minimum for crystals and melt-formed samples. The occurrence of the

$T_1$  minima at somewhat higher temperatures than those for the mechanical loss maxima is consistent with the higher effective frequency ( $3.5 \times 10^7$  c/s) of the  $T_1$  measurements. However, this mechanical loss maximum has been reported<sup>5</sup> as greatly reduced, if present at all, in polyethylene crystals and does not appear<sup>20</sup> for normal paraffin samples such as *n*-hexatriacontane ( $C_{36}H_{74}$ ). There is the possibility that the occurrence of a small amount of such motion in portions of the polymer could lead to relaxation of protons throughout the sample due to spin diffusion as suggested earlier<sup>6</sup>, an effect which is not present in mechanical relaxation. The mechanical loss maximum has been interpreted<sup>2</sup> as due to a conformational change involving three or more  $CH_2$  units.

(3) The high temperature  $T_1$  minimum, no doubt, reflects the increased freedom of the polymer chains in the crystalline regions and the ability of a large number of chain units to move by partial rotation about carbon-carbon bonds. This process is probably related to that responsible for the narrowing of the broad n.m.r. line found<sup>4</sup> around 350° to 390°K depending on the sample history in much the same way as does the position of the  $T_1$  minimum. The broad line n.m.r. and  $T_1$  results both indicate that motion at frequencies in the  $10^4$  to  $10^7$  c/s range does occur in the crystalline parts below the melting point. However, the  $T_1$  data show that for movement at frequencies of the order of  $10^7$  c/s to take place, temperatures above the melting point are necessary. A remarkable occurrence in the  $T_1$ /temperature curves is that although the temperature of the minimum is found above the melting point, it is still markedly dependent on sample preparation history indicating that the differences in polymer morphology persist at temperatures above the melting point at least for times shortly following the attainment of such temperatures. However, once the samples are heated well above the melting point these differences become negligible, as noted above.

The minima at about 150°K for P4MP1 are believed to be a consequence of methyl group reorientation at the appropriate frequency ( $3.5 \times 10^7$  c/s), since a line narrowing process attributed to this cause is found for P4MP1 (moulded sample) in the < 77° to 100°K region (effective frequency about  $10^4$  c/s). A similar  $T_1$  minimum, reported<sup>16</sup> for polypropylene, is thought to be due to this type of motion. The existence of two  $T_1$ s in the low temperature region indicates the existence of two separate proton environments as discussed above.

Part if not all of the higher temperature  $T_1$  minimum for P4MP1 is expected to be associated with the glass-rubber transition found by volume-temperature<sup>11</sup>, dynamic mechanical<sup>12</sup> and n.m.r. line width<sup>13</sup> measurements. The latter two methods indicate that this transition occurs at around 330°K ( $10^3$  to  $10^4$  c/s) as compared with 430° to 470°K for the  $T_1$  minimum ( $3.5 \times 10^7$  c/s). There is the possibility that this minimum is related to motional changes in the crystalline regions as well as in the amorphous ones since a change in X-ray lattice spacing at 393°K has been reported<sup>22</sup>. In addition, two mechanical loss peaks have been found<sup>11</sup> at about  $10^2$  c/s, one at about 400°K, the other at about 450°K, well above the glass transition region. However, as indicated below, this  $T_1$  minimum can be described adequately by an equation which assumes one correlation

time or an average correlation time which would indicate the presence of only one process.

Attempts have been made, using a computer, to fit the two minima  $T_1$  versus temperature curves found for polyethylene and P4MP1 employing an equation of the type<sup>23,24</sup>

$$\frac{1}{T_1} = \frac{1}{1.42} \sum_{i=1}^2 \frac{1}{T_{1,\min.,i}} \left[ \frac{\nu_r \nu_{ci}}{1 + (\nu_r/\nu_{ci})^2} + \frac{4\nu_r/\nu_{ci}}{1 + (2\nu_r/\nu_{ci})^2} \right]$$

where  $\nu_r$ , the resonance frequency, is 21.5 Mc/s and  $\nu_{ci}$  is assumed to be of the form

$$\nu_{ci} = \nu_{oi} \exp \left[ (H_i/R) \left( \frac{1}{T_{\min.,i}} - \frac{1}{T} \right) \right]$$

Fixed values of the parameters  $T_{1,\min.,1}$ ,  $T_{1,\min.,2}$  and the corresponding temperatures  $T_{\min.,1}$  and  $T_{\min.,2}$  along with 50 points taken from a smooth curve drawn through the experimental points were fed into the computer which then found the best fit by minimizing the sum of the squares of the deviations of the theoretical  $1/T_1$  from the experimental  $1/T_1$ s. This gives best values for  $H_1$  and  $H_2$ . Some results are given below.

#### *Polyethylene pellets*

$$T_{1,\min.,1} = 0.49 \text{ sec}; \quad \nu_{c1} = 3.5 \times 10^7 \exp \left[ \frac{24.6}{R} \left( 2.27 - \frac{10^3}{T} \right) \right]$$

$$T_{1,\min.,2} = 0.195 \text{ sec}; \quad \nu_{c2} = 3.5 \times 10^7 \exp \left[ \frac{6.74}{R} \left( 4.12 - \frac{10^3}{T} \right) \right]$$

#### *Poly-4-methyl-pentene-1 crystals (room temperature gradient grown)*

$$T_{1,\min.,1} = 0.19 \text{ sec}; \quad \nu_{c1} = 3.5 \times 10^7 \exp \left[ \frac{15.4}{R} \left( 2.2 - \frac{10^3}{T} \right) \right]$$

$$T_{1,\min.,2} = 0.014 \text{ sec}; \quad \nu_{c2} = 3.5 \times 10^7 \exp \left[ \frac{5.1}{R} \left( 6.7 - \frac{10^3}{T} \right) \right]$$

where  $R = 1.98 \text{ cal/mole } ^\circ\text{K}$  and  $T$  is in  $^\circ\text{K}$ .

It is seen from *Figure 12* that a fit can be made more readily with the  $T_1$  temperature data for P4MP1 than with those for polyethylene although in both serious deviations occur. In this treatment the presence of a second  $T_1$  for the P4MP1 crystals below 200 $^\circ\text{K}$  has been ignored.

## II. POLY-L-LEUCINE AND POLY-PHENYL-L-ALANINE

In a recent paper<sup>25</sup> a study of segmental motion in some synthetic polypeptides,  $[\text{NH}-\text{CHR}-\text{CO}]_n$ , by proton magnetic resonance *line width* measurements in the 77 $^\circ$  to 450 $^\circ\text{K}$  range was presented, the polymers investigated including poly-L-leucine,  $[\text{PLL} : \text{R} = -\text{CH}_2-\text{CH}(\text{CH}_3)_2]$  and

poly-phenyl-L-alanine  $[\text{PPLA} : \text{R} = \text{CH}_2-\text{C}_6\text{H}_5]$ .

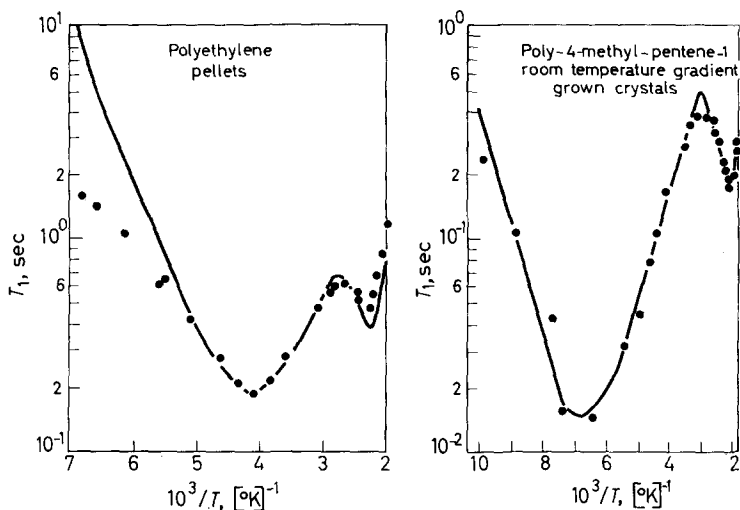


Figure 12—Comparison of theoretical and experimental spin-lattice relaxation time versus reciprocal temperature plots for polyethylene pellets and poly-4-methyl-pentene-1 crystals. — theoretical

To obtain further information concerning the motional processes taking place in these polymers, spin-lattice relaxation time ( $T_1$ ) measurements at 21.5 Mc/s have been made in the temperature range from 77° to 500°K.

## RESULTS

The  $T_1$  measurements were made on samples of PLL and PPLA purchased from Pilot Chemicals Co., prepared as described previously<sup>25</sup>. The PPLA was taken from the same batch as the sample used for the line width studies<sup>25</sup> but the PLL sample was from a new batch. Prior to the measurements at low and at high temperatures both polymers were dried at 100°C overnight under vacuum.

For PLL non-exponential decay curves were found at temperatures from 77° to 174°K. However, the decay curve could again be satisfactorily represented by two exponential terms thereby yielding two  $T_1$  values, one long and one short. The  $I_1/I_s$  ratio was about 4/6. The  $T_1$  data are given in Figure 13. The results are similar to those for room temperature gradient grown poly-4-methyl-pentene-1 crystals (Figure 9), although the lower temperature minimum is about 25° higher and the other minimum is 180° lower than for the P4MP1 crystals.

The decay curves for PPLA were all exponential and the  $T_1$  values derived from them are given in Figure 14. The wide shallow minimum is quite unusual, this type not having been observed previously in polymers in these laboratories.

Figure 13—Spin-lattice relaxation time versus temperature for poly-L-leucine

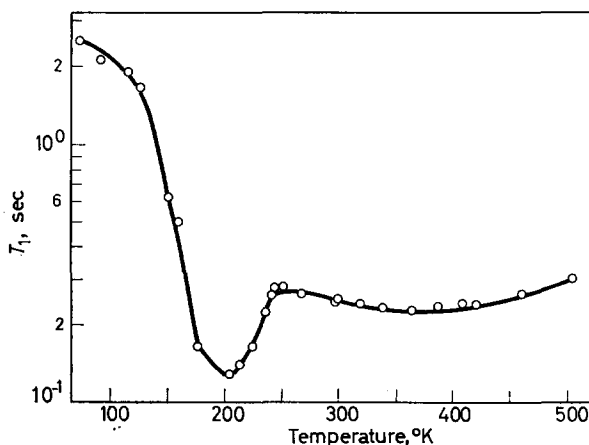
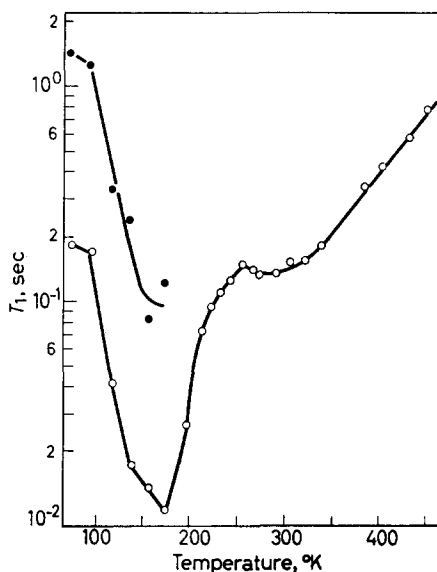


Figure 14—Spin-lattice relaxation time versus temperature for poly-phenyl-L-alanine

#### DISCUSSION

As mentioned in Part I, the existence of two  $T_1$  values, as found in PLL, at a given temperature indicates the existence of two distinctly different proton environments. There is some possibility that this phenomenon might be a consequence of chain folding, but the data for polyethylene (Figures 6 and 7) appear not to support this explanation. The  $T_1$  data show distinct differences between the two polypeptides although they are believed<sup>28</sup> to have the same alpha helix conformation.

The 174°K minimum for PLL is believed to be due to methyl reorientation at a frequency of  $3.5 \times 10^7$  c/s in keeping with the interpretation of the broad line narrowing process at  $< 77^\circ$  to 120°K (about  $10^4$  c/s) and the appearance of a similar  $T_1$  minimum for P4MP1. The 290°K minimum for PLL is probably due to isobutyl or isopropyl group reorientation, since the main chain for this highly hydrogen-bonded system would be expected to be quite rigid at these temperatures. In the broad line n.m.r. measurements<sup>25</sup> the second moment decreases by a factor of 1/3 to 1/2 in the 160° to 300°K region, indicating considerable motion. It is interesting that P4MP1, which has the same side chain, does not appear to show such a process at these temperatures.

The 200°K minimum for PPLA indicated the onset of side-chain motion, possibly involving rotational oscillations of the phenyl group. In the temperature region where the wide shallow  $T_1$  minimum is found the broad line measurements show a steady decrease in second moment with a reduction of about half in going from about 150°K to 400°K. The unusual wideness of the  $T_1$  minimum is indicative either of a single process with a wide distribution of correlation times or a relaxation strength ( $1/T_{1, \text{min.}}$ ) which depends on temperature as a result of the temperature dependent amplitude of oscillation. The latter explanation is preferred by the authors and is consistent with the broad line results<sup>25</sup>.

### III. POLYSTYRENE AND POLY- $\alpha$ -METHYL-STYRENE

THE broad line n.m.r. studies of polystyrene reported to date<sup>27-31</sup> indicate that below the glass transition region little motion, other than low amplitude side-chain oscillation, occurs. However, the discovery of a mechanical loss maximum for this polymer<sup>32, 33</sup> aroused interest in  $T_1$  measurements to see whether  $T_1$  was sensitive to the same motional process.

Poly- $\alpha$ -methyl-styrene, P $\alpha$ MS, has received little attention with respect to n.m.r. or dynamic mechanical measurements with only one broad line n.m.r.<sup>34</sup> and one mechanical properties study<sup>35</sup> being reported.

### RESULTS AND DISCUSSION

The polystyrene sample contained 0.6 to 1 per cent residual monomer. The poly- $\alpha$ -methyl-styrene sample was similar to that used previously for n.m.r. line width studies<sup>34</sup>.

Figure 15 indicates the existence of at least three relaxation processes for each polymer. The process at the highest temperatures is believed to be related to the glass-rubber transformation.

The broad minimum at 300° to 340°K for P $\alpha$ MS is believed to be in part, if not totally, due to  $\alpha$ -methyl group reorientation, since a number of methacrylate ester polymers show similar, but sharper, minima in this region<sup>16, 37</sup>. In addition a line narrowing process, attributed to this type of motion at an effective frequency of about  $10^4$  c/s, is found<sup>34</sup> for P $\alpha$ MS starting around 130°K and ending at about 280°K. The broadness of this  $T_1$  minimum may be some indication of a second process in this temperature



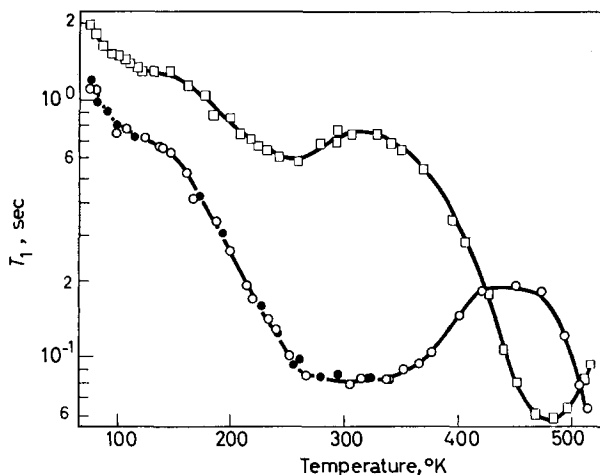


Figure 15—Spin-lattice relaxation time versus temperature for  $\square$  polystyrene and for poly- $\alpha$ -methyl-styrene,  $\circ$  sample No. 1,  $\bullet$  sample No. 2

region. However, it could also be a broad distribution of relaxation times for the methyl reorientation process. A flat dynamic mechanical loss maximum at 120° to 150°K of low strength has been found recently<sup>34</sup> at about  $10^4$  c/s which may or may not be related to the n.m.r. line narrowing centred at about 190°K which was attributed to  $\alpha$ -methyl group reorientation. This may be related to at least part of this  $T_1$  minimum. Since the mechanical loss maximum occurs at least 60° below the temperature at the centre of the line narrowing process, although the motional frequencies are comparable, it is currently believed that the loss maximum and also the  $T_1$  minimum are due at least partially to processes other than methyl group reorientation, possibly involving motion of the phenyl group.

For polystyrene there is little indication from n.m.r. line width measurements of any motional processes in the 77° to 300°K region. However, a small mechanical loss peak<sup>32,33</sup> at low temperatures (about 50°K at  $10^4$  c/s) has been found. P $\alpha$ MS also exhibits<sup>36</sup> a shoulder on the low temperature side (< 50°K) of the 120° to 150°K peak mentioned above. It is possible that this shoulder and the 50°K peak for polystyrene are related to the  $T_1$  relaxation process at about 130°K for both polymers and therefore to one another. However, since two minima and only one loss maximum are found for polystyrene (at temperatures below 300°K and frequencies above  $10^3$  c/s) it is not clear whether the 50°K loss peak is related to either  $T_1$  relaxation process. A  $T_1$  minimum is found at 200°K for another polymer containing a phenyl group, namely PPLA (see Figure 14) which is, however, of greater intensity by a factor of three or more than either the 130°K or 260°K  $T_1$  processes for polystyrene (Figure 15). This process for PPLA has been tentatively attributed to phenyl oscillations, but if a like process occurs for polystyrene, it might be expected at temperatures above 200°K, due to a greater hindrance to such motion

presented by the closer proximity of the main chain. Yet another cause of either the 130°K or 260°K processes could be the reorientational motion of parts of some impurity, such as monomer, leading to proton relaxation in the polymer as a whole by spin diffusion. Therefore, although it is found that a number of phenyl-containing polymers have  $T_1$  relaxation processes in the 77° to 300°K temperature regions the molecular cause of these processes is not yet clear.

It is of interest to point out that poly-cyclohexyl-methacrylate exhibits<sup>37</sup> two shallow minima at about 150°K and 250°K. The one at 250°K has almost the same shape and depth as the 260°K polystyrene minimum and therefore may reflect a similar type of motion.

$T_1$  measurements were also carried out on a polystyrene sample which had been dissolved in toluene, precipitated in a large excess of methanol, the precipitate then being repeatedly washed with methanol and dried under vacuum at room temperature. The  $T_1$  versus temperature curve was almost the same as that in *Figure 15* above 300°K. However, at lower temperatures a deep minimum ( $T_{1,\min.} = 0.04$  sec) at 160°K was found. Upon re-running this specimen after heating to 520°K, the deep minimum was no longer there and the low temperature behaviour was as shown in *Figure 15*. It is thought that the deep  $T_1$  minimum was due to the motion of small amounts of methanol and/or toluene which relaxes the protons of the polystyrene by a spin-diffusion mechanism. To ascertain the amount of methanol and/or toluene in the sample prior to heating, another portion of the precipitated polymer was heated in a vacuum oven at various temperatures in the 54° to 144°C range. The heating times and cumulative percentage weight lost were as follows: 54°C, 32 h, 0.0 per cent; 91°C, 23 h, 0.25 per cent; 106°C, 18 h, 0.25 per cent; 111°C, 29 h, 0.5 per cent; and, 144°C, 42 h, 0.6 per cent. At 144°C there was no change in weight after a 23 h heating period. The loss in weight at 91°C is believed to be a measure of the amount of methanol present and that at 111°C and above of the amount of toluene present. This possibility of getting entirely spurious  $T_1$  minima due to a small proportion of dissolved low molecular weight solvent emphasizes the great care that must be taken in the preparation of polymer samples and is a matter for particular concern with polymer crystal samples.

*We wish to express our gratitude to Mr R. P. Palmer, Mr D. J. H. Sandiford, Dr J. A. E. Kail and other members of I.C.I. Plastics Division for supplying the polyethylene, P4MP1 and polystyrene samples and for undertaking morphological studies on these as described herein. A.E.W. acknowledges the award of a Fellowship by the John Simon Guggenheim Memorial Foundation. B.I.H. was supported by a D.S.I.R. Research Studentship.*

*Department of Physics,  
Queen Mary College,  
Mile End Road, London E.1*

*(Received August 1963)*

## REFERENCES

- <sup>1</sup> HERRING, M. J. and SMITH, J. A. S. *J. chem. Soc.* 1960, 273
- <sup>2a</sup> PETERLIN, A., KRASOVEC, F., PIRKMAJER, E. and LEVSTEK, I. *Makromol. Chem.* 1960, **37**, 231
- <sup>b</sup> PETERLIN, A. and PIRKMAJER, E. *J. Polym. Soc.* 1960, **46**, 185
- <sup>3</sup> SLICHTER, W. P. *J. appl. Phys.* 1961, **32**, 2339
- <sup>4</sup> ODAJIMA, A., SAUER, J. A. and WOODWARD, A. E. *J. phys. Chem.* 1962, **66**, 718
- <sup>5</sup> THURN, H. *Kolloidzshr.* 1960, **173**, 72
- <sup>6</sup> MCCALL, D. W. and DOUGLASS, D. C. *Polymer, Lond.* 1963, **4**, 433
- <sup>7</sup> KELLER, A. *Polymer, Lond.* 1962, **3**, 393
- <sup>8</sup> WUNDERLICH, B. and SULLIVAN, P. J. *Polym. Sci.* 1962, **61**, 195
- <sup>9</sup> MANSFIELD, P. and POWLES, J. G. *J. sci. Instrum.* 1963, **40**, 232
- <sup>10</sup> FRANK, F. C., KELLER, A. and O'CONNOR, A. *Phil. Mag. Ser. VIII*, 1959, **4**, 200
- <sup>11</sup> GRIFFITH, J. H. and RÅNBY, B. G. *J. Polym. Sci.* 1960, **44**, 369
- <sup>12</sup> WOODWARD, A. E., SAUER, J. A. and WALL, R. A. *J. Polym. Sci.* 1961, **50**, 117
- <sup>13</sup> WOODWARD, A. E., ODAJIMA, A. and SAUER, J. A. *J. phys. Chem.* 1961, **65**, 1384
- <sup>14</sup> CHAN, K. S., RÅNBY, B. G., BRUMBERGER, H. and ODAJIMA, A. *J. Polym. Sci.* 1962, **61**, S29
- <sup>15</sup> WOODWARD, A. E. *Polymer, Lond.* 1964, **5**, 293
- <sup>16</sup> POWLES, J. G. and MANSFIELD, P. *Polymer, Lond.* 1962, **3**, 337, 340
- <sup>17</sup> SAITO, N., OKANO, K., IWAYANAGI, S. and HIDESHIMA, T. *Solid State Physics*, Vol. 14, p 344. Ed. SEITZ and TURNBULL. Academic Press: London, 1963
- <sup>18</sup> CONNOR, T. M., READ, B. E. and WILLIAMS, G. *J. appl. Chem., Lond.* 1964, **14**, 74
- <sup>19</sup> WADA, Y., HIROSE, H., UMEBAYASHI, H. and OTOMO, M. *J. phys. Soc. Japan*, 1960, **15**, 2324
- <sup>20</sup> SANDIFORD, D. J. H. Unpublished results
- <sup>21</sup> KLINE, D. E., SAUER, J. A. and WOODWARD, A. E. *J. Polym. Sci.* 1956, **22**, 455
- <sup>22</sup> CHAN, K. S., RÅNBY, B. G. and BRUMBERGER, H. *J. Polym. Sci.* 1962, **58**, 545
- <sup>23</sup> BLOEMBERGEN, N., PURCELL, E. M. and POUND, R. V. *Phys. Rev.* 1948, **73**, 679
- <sup>24</sup> KUBO, R. and TOMITA, K. *Proc. phys. Soc. Japan*, 1954, **9**, 888
- <sup>25</sup> KAIL, J. A. E., SAUER, J. A. and WOODWARD, A. E. *J. phys. Chem.* 1962, **66**, 1292
- <sup>26</sup> BAMFORD, C. H., ELLIOTT, A. and HANBY, W. E. *Synthetic Polypeptides*. Academic Press: New York, 1956
- <sup>27</sup> HOLROYD, L. V., CORDINGTON, R. S., MROWCA, B. A. and GUTH, E. *J. appl. Phys.* 1951, **22**, 696
- <sup>28</sup> ODAJIMA, A., SOHME, J. and KOIKE, M. *J. chem. Phys.* 1955, **16**, 77; *J. phys. Soc. Japan*, 1957, **12**, 272
- <sup>29</sup> SLICHTER, W. P. *S.P.E. II*, 1959, **15**, 303
- <sup>30</sup> KOSFELD, R. *Kolloidzshr.* 1960, **172**, 182
- <sup>31</sup> ODAJIMA, A., SAUER, J. A. and WOODWARD, A. E. *J. Polym. Sci.* 1962, **57**, 107
- <sup>32</sup> SINNOTT, K. M. *S.P.E. Trans.* 1962, **2**, 65
- <sup>33</sup> CRISSMAN, J. M. and McCAMMON, R. D. *J. acoust. Soc. Amer.* 1962, **34**, 1703
- <sup>34</sup> ODAJIMA, A., WOODWARD, A. E. and SAUER, J. A. *J. Polym. Sci.* 1961, **55**, 181
- <sup>35</sup> SAUER, J. A. and KLINE, D. E. *International Congress of Applied Mechanics, Brussels, Belgium, September 1956*, Vol. V, p 368, 1957
- <sup>36</sup> CRISSMAN, J. M., SAUER, J. A. and WOODWARD, A. E. To be published
- <sup>37</sup> POWLES, J. G., HUNT, B. I. and SANDIFORD, D. J. H. *Polymer, Lond.* To be published

# Studies in the Thermodynamics of Polymer-Liquid Systems

## Part I—Natural Rubber and Polar Liquids

C. BOOTH, G. GEE, G. HOLDEN\* and G. R. WILLIAMSON†

*There is a great lack of reliable thermodynamic data on concentrated polymer solutions. This group of papers contributes further measurements, especially on systems consisting of a polar liquid and non-polar polymer, and presents a review of the current situation.*

*This first part records observations on the swelling of natural rubber in several polar liquids, using two different techniques. One of these is the conventional study of vapour pressures; the other is a novel procedure involving measurements of swelling and tension in stretched crosslinked samples. The results are compared with the Flory-Huggins equation, and show that as swelling proceeds and approaches saturation, there is a marked fall in the interaction parameter  $\chi_1$ . At the same time the entropy of dilution falls progressively further below the curves predicted by current theories.*

THE LATTICE theory of Flory and Huggins<sup>1</sup> has been widely used in interpreting the thermodynamic properties of polymer-liquid mixtures. The free energy of dilution  $\Delta\mu_1$  is related to the volume fraction  $\phi_2$  of polymer by the equation

$$\Delta\mu_1/RT = \ln(1 - \phi_2) + \phi_2 + \chi_1\phi_2^2 \quad (1)$$

where  $\chi_1$  is an adjustable parameter. This equation is generally used in theoretical investigations by assuming  $\chi_1$  to be independent of  $\phi_2$  and a linear function of  $1/T$ . With these assumptions the essential qualitative features of polymer-liquid interactions are readily interpreted<sup>1</sup>, but detailed measurements reveal their shortcomings.

Most of the experimental results reported so far are concerned with systems in which both polymer and liquid are relatively non-polar, but in no case has the simple theory been found to fit exactly. The first system to be studied in detail was natural rubber and benzene<sup>2,3</sup>, and here equation (1) held very well over a wide range of  $\phi_2$ , with  $\chi_1 = \text{constant}$ . In general, however, it has been found necessary to add at least one further term  $\chi_2\phi_2^2$ . Measurements of the heat and entropy of dilution have been fewer and less reliable, but the concentration dependence of these quantities has been found to be at variance with prediction.

Some years ago we embarked on a study of the behaviour of systems comprising a non-polar polymer and a polar liquid. Preliminary results<sup>4</sup> suggested that the data deviated from the simple theory in a characteristic manner. We now report more detailed measurements, which confirm our earlier observations.

\*Present address: Shell Chemical Company, Torrance Research Laboratory, P.O. Box 211, Torrance, California, U.S.A.

†Present address: Plastics Laboratory, Shell Chemical Company Ltd, Carrington Works, Urmston, Manchester.

The experimental work to be described falls into two sections. In the first, we report the result of measurements made by conventional vapour pressure techniques; in the second we record the exploration of an alternative possibility, based on a study of the relationship between swelling and elongation in a stretched, crosslinked rubber. This technique enabled us to estimate the entropy of dilution in a highly swollen rubber, but was much more troublesome and showed no advantages in precision.

#### VAPOUR PRESSURE METHOD

The thermodynamic dilution functions were obtained by measuring the vapour pressure of solvent over the polymer solution ( $p_1$ ) relative to that over pure solvent ( $p_1^0$ ) at two temperatures. The vapour pressures were measured by differential manometry except when  $p_1$  approached  $p_1^0$ , when the vapour pressure was measured indirectly by an isothermal distillation technique.

The Gibbs free energy of dilution is given by

$$\Delta\mu_1 = RT \ln (p_1/p_1^0) - B (p_1^0 - p_1) \quad (2)$$

where  $B$  is the second virial coefficient of the solvent vapour and where higher terms are neglected. The entropy ( $\Delta S_1$ ) and heat ( $\Delta h_1$ ) of dilution were obtained as usual from the temperature-dependence of  $\Delta\mu_1$ .

#### EXPERIMENTAL

*Materials*—Deproteinized crepe rubber was purified by precipitation from a dilute solution of benzene by adding methanol, followed by prolonged extraction in a Soxhlet apparatus, under an atmosphere of nitrogen, with the solvent to be used. This rubber was dried and stored under vacuum and in the dark. The densities measured at 0°C, 25°C and 50°C were found to be 0.925, 0.909 and 0.893 g/ml respectively.

'AnalaR' grade acetone and methylethyl ketone were dried with sodium carbonate and distilled. 'AnalaR' grade ethyl acetate was distilled from excess water, dried, and finally distilled after adding 0.5 per cent water. The fractionating column used for the final distillation of all solvents had an efficiency approaching 100 theoretical plates under the conditions of use. Pure solvents were stored under vacuum and in the dark. The densities of the solvents agreed with published values<sup>5</sup>.

*Isothermal distillation*—The apparatus and procedure used have been described by Gee and Orr<sup>3</sup> and by Baker *et al.*<sup>6</sup>. The mole fraction ( $x_2$ ) of the reference solute ( $\alpha$ -Lupene) never exceeded 0.005. It was assumed that deviations from ideality were small at such low concentrations and  $\Delta\mu_1$  was calculated from the equation

$$\Delta\mu_1 = RT \ln (1 - x_2) \quad (3)$$

Only ethyl acetate solutions were used in the isothermal stills.

*Differential manometry*—The apparatus described by Gee and Treloar<sup>2</sup> was used for studying ethyl acetate at 25°C. For all the other measurements we used a simple modification of this apparatus in which the vapour pressure of the pure solvent in the solvent reservoir could be measured at

all times. This vapour pressure was constant throughout an experiment. The procedure followed was similar to that used by Gee and Treloar, except that our manometer was immersed in a constant temperature bath held some 3°C higher than the temperature under study. Measurements were made during adsorption and desorption of the solvent and no significant hysteresis was observed.

*Results*—Values of  $p_1/p_1^0$  at various values of  $\phi_2$  are given in *Table 1*. Values of  $x_2$  (the mole fraction of solute in the reference solution of the isothermal still) at values of  $\phi_2$  near saturation are given in *Table 2*. In all cases  $\phi_2$  was calculated assuming that no volume changes occurred on mixing.

From these we have calculated  $\Delta\mu_1$  from equations (2) and (3) and hence  $\chi_1$ , the parameter of the Flory-Huggins equation (1).

Values of  $\chi_1$  are listed in *Tables 1* and *2*. In order to use equation (2) it was necessary to estimate values of  $B$  for the solvents at the temperatures studied. Since it was clear that the Berthelot equation could not be applied to these polar molecules<sup>7,8</sup> the values obtained for acetone<sup>7</sup> and ethyl acetate<sup>8</sup> at higher temperatures were extrapolated to lower temperatures to give the following approximate values for  $B$ : acetone at 0°C and 25°C,  $B = -2\,600$  and  $-2\,000$  ml mole<sup>-1</sup> respectively; ethyl acetate at 25°C and 50°C,  $B = -2\,300$  and  $-1\,600$  ml mole<sup>-1</sup> respectively. We could find no experimental determinations of  $B$  for methylethyl ketone, so it was assumed that the deviations from the Berthelot equation were similar to those displayed by ethyl acetate: in this way we obtained  $B = -2\,300$  and  $-1\,600$  ml mole<sup>-1</sup> at 25°C and 45°C respectively. The exact value of  $B$  is not important since the correction term is quite small, being at the most some -2 per cent in  $\Delta\mu_1$  and some -6 per cent to -8 per cent in  $\Delta s_1$ .

*Table 1.* Differential manometry—the variation of  $p_1/p_1^0$  and  $\chi_1$  with  $\phi_2$

Acetone			Methylethyl ketone			Ethyl acetate		
$\phi_2$	$p_1/p_1^0$	$\chi_1$	$\phi_2$	$p_1/p_1^0$	$\chi_1$	$\phi_2$	$p_1/p_1^0$	$\chi_1$
	(25°C)			(25°C)			(25°C)	
0.846	0.955	1.370	0.613	0.991	0.871	0.625	0.988	0.879
0.868	0.917	1.423	0.622	0.988	0.877	0.697	0.932	0.882
0.916	0.772	1.557	0.684	0.961	0.918	0.740	0.904	0.927
0.947	0.600	1.652	0.725	0.943	0.966	0.794	0.832	0.957
0.955	0.553	1.714	0.778	0.900	1.030	0.871	0.684	1.059
			0.874	0.723	1.150	0.880	0.647	1.045
			0.924	0.549	1.239	0.949	0.373	1.160
0.927	0.861	1.791	0.959	0.357	1.328	0.983	0.145	1.227
0.936	0.785	1.792	0.967	0.302	1.349	0.999	0.013	1.218
0.958	0.624	1.905				0.999	0.007	1.222
0.985	0.280	2.034		(45°C)			(50°C)	
			0.579	0.990	0.814	0.811	0.780	0.928
			0.626	0.973	0.845	0.898	0.555	0.998
			0.676	0.955	0.887	0.964	0.245	1.040
			0.743	0.903	0.935	0.994	0.043	1.015
			0.800	0.838	0.992			
			0.866	0.709	1.069			
			0.910	0.577	1.155			
			0.954	0.354	1.197			
			0.989	0.095	1.212			

*Entropies and heats of dilution*

Entropies and heats of dilution were calculated as follows. The values of  $\chi_1$  from *Tables 1* and *2* were plotted against the weight fraction  $w_2$  of polymer, and the best smooth curves were drawn through the points.

*Table 2.* Isothermal distillation—the variation of  $x_2$  and  $\chi_1$  with  $\phi_2$  for ethyl acetate

25°C			50°C		
$\phi_2$	$x_2$	$\chi_1$	$\phi_2$	$x_2$	$\chi_1$
0.4196	0.9996	0.705	0.2997	0.9995	0.624
0.4202	0.9997	0.705	0.3433	0.9980	0.638
0.4392	0.9990	0.716	0.3454	0.9983	0.642
0.4393	0.9987	0.715	0.3458	0.9977	0.638
0.4473	0.9985	0.720	0.3893	0.9970	0.669
0.4691	0.9977	0.735	0.4307	0.9957	0.692
0.5007	0.9947	0.750	0.4308	0.9961	0.694

In this way values of  $\chi_1$  at the two temperatures at selected values of  $w_2$  could be read off, and  $\Delta\mu_1$  calculated from equation (1) to derive  $\Delta s_1$  and  $\Delta h_1$  at the mean temperature. Values of  $\Delta s_1$  and  $\Delta h_1$  obtained in this way are given in *Table 3*.

*Table 3.* The entropy (cal deg<sup>-1</sup> mole<sup>-1</sup>) and heat (kcal mole<sup>-1</sup>) of dilution of natural rubber by polar liquids

<i>Acetone</i> (12.5°C)			<i>Methylethyl ketone</i> (35°C)			<i>Ethyl acetate</i> (37.5°C)		
$\phi_2$	$\Delta s_1$	$\Delta h_1$	$\phi_2$	$\Delta s_1$	$\Delta h_1$	$\phi_2$	$\Delta s_1$	$\Delta h_1$
0.943	4.1 <sub>2</sub>	0.96 <sub>3</sub>	0.943	3.5 <sub>5</sub>	0.58 <sub>7</sub>	0.898	2.4 <sub>0</sub>	0.40 <sub>8</sub>
			0.887	2.3 <sub>8</sub>	0.49 <sub>0</sub>	0.796	1.0 <sub>9</sub>	0.22 <sub>0</sub>
			0.778	1.1 <sub>1</sub>	0.26 <sub>7</sub>	0.410	0.08 <sub>3</sub>	0.024 <sub>5</sub>
			0.671	0.57 <sub>3</sub>	0.15 <sub>4</sub>			
<i>Precision</i>			<i>Precision</i>			<i>Precision</i>		
$\Delta s_1/\phi_2^2$ to $\pm 0.36$			$\Delta s_1/\phi_2^2$ to $\pm 0.18$			$\Delta s_1/\phi_2^2$ to $\pm 0.42$		
$\Delta h_1/\phi_2^2$ to $\pm 0.10$			$\Delta h_1/\phi_2^2$ to $\pm 0.06$			$\Delta h_1/\phi_2^2$ to $\pm 0.13$		

Experimental errors are a little hard to evaluate. A measure of the precision of results of this type has been defined in Part II so that sets of data from differing sources could be compared. Such 'precisions' are quoted in *Table 3*. The accuracy (as distinct from the precision) cannot be much better than  $\pm 30$  per cent\*.

#### ENTROPY OF DILUTION FROM SWELLING AND TENSION

Consider a strip of rubber containing  $n_1$  moles of liquid, and held at volume  $V$ , temperature  $T$  and length  $l$  by a hydrostatic pressure  $P$  and a tensile force  $f$ . Then if  $\mu_1$  is the chemical potential of the liquid in the strip,

$$dG = V dP - S dT + f dl + \mu_1 dn_1$$

\*Additional uncertainty is introduced with acetone at 0°C since the natural rubber might be partially crystalline under these conditions\* (see Part IV).

If now the strip is put into contact with liquid, so that  $dn_1$  refers to transfer from liquid to strip, the equation becomes

$$d\Delta G = \Delta V.dP - \Delta S.dT + f dl + \Delta\mu_1.dn_1$$

where  $\Delta G$ ,  $\Delta V$  and  $\Delta S$  now refer to the process of transferring liquid from the free liquid into the strip of rubber and  $\Delta\mu_1 = \mu_1 - \mu_1^0$ ,  $\mu_1^0$  being the chemical potential of the free liquid. By standard methods, we obtain the relationships:

$$\begin{aligned} - \left( \frac{\partial \Delta S}{\partial n_1} \right)_{P, T, l} &= \left( \frac{\partial \Delta\mu_1}{\partial T} \right)_{P, l, n_1} = - \left( \frac{\partial \Delta\mu_1}{\partial n_1} \right)_{P, T, l} \left( \frac{\partial n_1}{\partial T} \right)_{P, l, \Delta\mu_1} \\ \left( \frac{\partial f}{\partial n_1} \right)_{P, T, l} &= \left( \frac{\partial \Delta\mu_1}{\partial l} \right)_{P, T, n_1} = - \left( \frac{\partial \Delta\mu_1}{\partial n_1} \right)_{P, T, l} \left( \frac{\partial n_1}{\partial l} \right)_{P, T, \Delta\mu_1} \end{aligned}$$

whence the entropy of dilution  $\Delta s_1^* = (\partial \Delta S / \partial n_1)_{P, T, l}$  is obtained in terms of three measurable quantities:

$$\Delta s_1^* = - \left( \frac{\partial f}{\partial n_1} \right)_{P, T, l} \frac{(\partial n_1 / \partial T)_{P, l, \Delta\mu_1}}{(\partial n_1 / \partial l)_{P, T, \Delta\mu_1}} \quad (4)$$

The condition  $\Delta\mu_1 = \text{constant}$  is simply ensured by immersing the strip in excess liquid and allowing time for swelling equilibrium, so that  $\Delta\mu_1 = 0$ .

The quantity  $\Delta s_1^*$  obtained in this way requires correction for the decrease in configurational entropy  $-\Delta s_1$  (el) resulting from the deformation of the network by swelling. Assuming additivity, the entropy of dilution  $\Delta s_1$  for uncrosslinked rubber is then obtained from

$$\Delta s_1 = \Delta s_1^* - \Delta s_1 \text{ (el)} \quad (5)$$

The evaluation of  $\Delta s_1$  (el) can be related to that of  $(\partial f / \partial n_1)$ . It will be suggested elsewhere that the best available expression\* for the entropy of deformation  $\Delta S_d$  of a network occupying a unit cube to a block of sides  $\lambda_1, \lambda_2, \lambda_3$  is of the form

$$-T \Delta S_d = C_1 (\lambda_1^2 + \lambda_2^2 + \lambda_3^2 - 3) + C_2 (\lambda_1^{-2} + \lambda_2^{-2} + \lambda_3^{-2} - 3)$$

If a strip of rubber, of dry unstrained cross section  $A_0$ , and length  $l_0$ , is stretched to length  $l$  and swollen to volume fraction  $\phi_2$ , we have

$$\lambda_1 = l / l_0$$

$$\lambda_2^{-2} = \lambda_3^{-2} = l \phi_2 / l_0$$

By differentiation, we then obtain

$$f = -T \left( \frac{\partial \Delta S_d}{\partial l} \right)_{T, \phi_2} = 2A_0 (C_1 \lambda_1 + C_2 \phi_2) (1 - \lambda_1^{-3} \phi_2^{-1}) \quad (6)$$

$$\frac{\partial f}{\partial n_1} = - \frac{2V_1}{l_1} (C_1 \lambda_1^{-2} + C_2 \phi_2^2) \quad (7)$$

\*The use of one of the alternative expressions which have been put forward would not change our estimates of  $\Delta s_1$ (el) sufficiently to affect our final results significantly.



(where  $V_1$  is the molar volume of the liquid) and

$$\Delta s_1(\text{el}) = \left( \frac{\partial \Delta S_d}{\partial n_1} \right) = - \frac{2V_1 \lambda_1}{T} (C_1 \lambda_1^{-2} - C_2 \phi_2^2) \quad (8)$$

To evaluate  $C_1$  and  $C_2$ , we have measured  $f$  as a function of  $\phi_2$  at constant  $\lambda$  and plotted  $f(1 - \lambda^{-3} \phi_2^{-1})^{-1}$  against  $\phi_2$ , obtaining a straight line of slope  $2A_0 C_2$  and intercept  $2A_1 C_1 \lambda_1$ . These values of  $C_1$  and  $C_2$  were then used to calculate  $(\partial f / \partial n_1)$  and  $\Delta s_1(\text{el})$ .

#### EXPERIMENTAL

*Materials*—The vulcanized rubber samples were in the form of rings, all cut with the same die. For the examination of a single liquid a different sample of the rubber was used to determine each differential in equation (4); these three samples were all cut from the same sheet of rubber. Prior to use, the rings were extracted with the appropriate liquid by means of a Soxhlet apparatus operating under an atmosphere of nitrogen. In order to compare the properties of the three rings, they were all swollen at 25°C with the liquid under examination and the equilibrium swelling measured; in no case was any significant difference between the samples observed. The density of the rubber was 0.982 g/ml at 25°C. Acetone, methylethyl ketone, methylpropyl ketone, methyl acetate and ethyl acetate were distilled and dried before use. Methyl acetate was refluxed with acetic anhydride before distillation.

*Determination of  $\partial n_1 / \partial T$* —The rubber ring was stretched on to a glass rod former, immersed in the liquid (which was saturated with nitrogen) and, after sufficient time to reach equilibrium swelling, was removed, blotted dry and weighed. This measurement was carried out at 0°C, 25°C, 35°C and 50°C. The length of the sample was taken as the distance between the two ends of the stretched rubber ring and this increased slightly with rise of temperature. After correction to constant length, the quantity of liquid absorbed was plotted against temperature to give  $(\partial n_1 / \partial T)$  at  $P=1$  atm,  $T=298^\circ\text{K}$ ,  $\Delta \mu_1=0$  and  $l$ =stretched length at  $T=298^\circ\text{K}$ .

*Determination of  $\partial n_1 / \partial l$* —Further series of measurements were made at 25°C, using different formers. The slope of the plot of the quantity of liquid absorbed versus the length of the sample evaluated at the required length, gave  $(\partial n_1 / \partial l)$  under the same conditions as  $(\partial n_1 / \partial T)$ . The equilibrium value of  $\phi_2$  under these same conditions was used in equations (7) and (8) in calculating  $(\partial f / \partial n_1)$  and  $\Delta s_1(\text{el})$ .

*Determination of  $\partial f / \partial n_1$* —The apparatus used and the procedure followed were essentially those of Mullins, Rivlin and Gumbrell<sup>10</sup>. The sample, swollen by addition of liquid, was held at 25°C in a constant temperature enclosure and was elongated by attaching weights to one end, the length being measured as a function of load. The points of difference between our experiments and those of Mullins *et al.* were as follows: our rubber samples were in the form of rings which were looped over two rods, one of which was held rigidly while the other was attached to the Nylon thread leading out of the enclosure to the scale pan; the length of the sample was taken as the distance between the ends of the stretched rubber ring; the samples were allowed only one hour to attain equilibrium after

the addition or removal of liquid; the experiments were carried out in an atmosphere of nitrogen saturated with solvent. The volume fraction of rubber in the sample was subsequently determined by removing the ring, blotting it dry, and weighing it.

Curves of tensile force versus length were plotted for each of the values of  $\phi_2$  examined. These curves were easily interpolated to obtain values of  $f$  for the several values of  $\phi_2$  at constant length. These data can be used to plot  $f/(1 - \alpha^{-3}\phi_2^{-1})$  against  $\phi_2$  provided the length ( $l_0$ ) of the dry, unstretched sample is known. Since we used a ring this value can only be obtained by extrapolation of the curves of  $f$  versus  $l$  to zero tensile force, when the intercept at  $f=0$  is  $l_0\phi_2^{-1}$ . This extrapolation is somewhat uncertain, but we had some ten or more curves for each of five systems to use in determining a value for  $l_0$  and the value obtained,  $l_0=8.37$  cm, is believed to be accurate to  $\pm 0.1$  cm. It might be noted that the individual values of  $C_1$  and  $C_2$ , obtained from the plot of  $f/(1 - \alpha^{-3}\phi_2^{-1})$  against  $\phi_2$ , are fairly sensitive to  $l_0$ : e.g. a +1 per cent change in  $l_0$  produced a +3 per cent change in  $C_1$  and a -10 per cent change in  $C_2$ . However, the resulting change in  $(\partial f/\partial n_1)$  is small (2 per cent) since the changes in  $l_0$ ,  $C_1$  and  $C_2$  compensate in equation (7). The change in  $\Delta s_1$  (el) is rather larger [see equation (8)] but this term is small compared with the other terms in equation (5) and so has less effect upon the value of  $\Delta s_1$ .

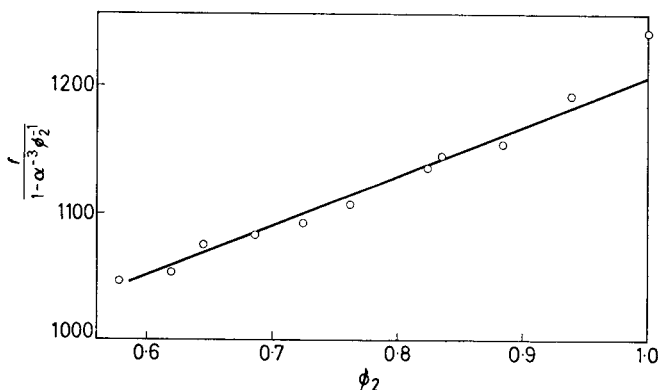


Figure 1—The evaluation of  $\partial f/\partial n_1$  for methylethyl ketone

A plot of  $f/(1 - \alpha^{-3}\phi_2^{-1})$  against  $\phi_2$  for methylethyl ketone is shown in Figure 1. The values of  $C_1$  and  $C_2$  obtained from this plot can be substituted in equation (7) to obtain  $(\partial f/\partial n_1)$  under our standard conditions, and in equation (8) to obtain  $\Delta s_1$  (el).

### Results

Experimental data are summarized in Table 4 and the derived entropies in Table 5. The reliability of the results is very difficult to assess, but we

Table 4. The experimental data for natural rubber at 25°C

Liquid	$\phi_2$	$\gamma_1$ cm <sup>3</sup> mole <sup>-1</sup>	$\lambda_1$	$C_1$ kg cm <sup>-2</sup>	$C_2$ kg cm <sup>-2</sup>	$\partial l / \partial n_1$ kg mole <sup>-1</sup>	$\partial n_1 / \partial l^*$ 10 <sup>4</sup> mole deg <sup>-1</sup>	$\partial n_1 / \partial l^*$ 10 <sup>4</sup> mole cm <sup>-1</sup>
Acetone	0.805	72.0	1.519	2.67	1.90	42.9	0.3 <sub>5</sub>	0.4 <sub>5</sub>
Methyl acetate	0.708	79.8	1.438	2.67	1.49	32.6	0.5 <sub>1</sub>	1.0 <sub>5</sub>
Methylethyl ketone	0.551	89.9	1.454	2.13	1.15	29.5	0.9 <sub>7</sub>	2.5
Ethyl acetate	0.498	98.5	1.525	2.15	1.16	28.2	1.1 <sub>4</sub>	3.4
Methylpropyl ketone	0.437	107.2	1.392	2.57	1.29	40.4	0.9 <sub>3</sub>	6.6

\*Per cm<sup>3</sup> of rubber.

estimate that the three differentials have been measured to about ±15 per cent, so that our final values for the entropy of dilution are subject to an error of at least ±30 per cent. This is comparable with the uncertainty of results from our vapour pressure studies.

Table 5. Derived thermodynamic quantities for natural rubber at 25°C

Liquid	$\phi_2$	$\Delta s_1^*$	$\Delta s_1(\text{el})$	$\Delta s_1$	$\Delta h_1$	$\chi_1$
		cal deg <sup>-1</sup> mole <sup>-1</sup>			cal mole <sup>-1</sup>	
Acetone	0.805	0.78 <sub>4</sub>	0.001	0.78	234	1.28
Methyl acetate	0.708	0.37 <sub>2</sub>	-0.010	0.38	111	1.03
Methylethyl ketone	0.551	0.26 <sub>8</sub>	-0.014	0.28	83	0.80
Ethyl acetate	0.498	0.22 <sub>2</sub>	-0.015	0.24	66	0.74
Methylpropyl ketone	0.437	0.13 <sub>4</sub>	-0.025	0.16	40	0.65

Table 5 also records single values of  $\chi_1$  and  $\Delta h_1$  for each liquid, obtained as follows. The free energy of dilution for the crosslinked elongated rubber is zero at saturation, so that  $\Delta\mu_1$  for the uncrosslinked rubber can be calculated from  $T\Delta s_1(\text{el})$ . Equating this with the Flory-Huggins expression [equation (1)] gives  $\phi_2^2\chi_1 = \Delta s_1(\text{el})/R - \ln(1 - \phi_2) - \phi_2$ .  $\Delta h_1$  is simply given by

$$\Delta h_1 = \Delta\mu_1 + T\Delta s_1 = T\Delta s_1^*$$

COMPARISON OF THEORY AND EXPERIMENT

Figure 2 summarizes the dependence of  $\chi_1$  on  $\phi_2$  at 25°C found by the two techniques. The plots are non-linear and cannot be represented by a power series of positive terms in  $\phi_2$  without using very high powers. This behaviour is qualitatively in accord with that calculated on the basis of the quasi-chemical approximation<sup>11, 12</sup>

$$\chi_1\phi_2^2 = \frac{1}{2}Z [\ln(\beta + 1 - 2\theta) - \ln(\beta + 1) - \ln(1 - \phi_2)] - \phi_2$$

where

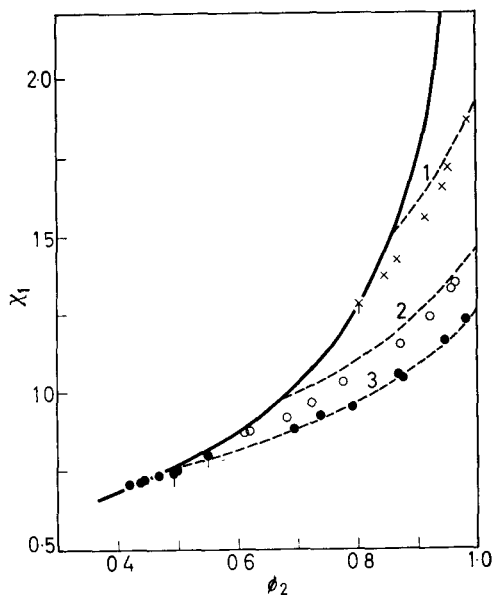
$$\theta = \phi_2(Z - 2)/(Z - 2\phi_2)$$

$$\beta^2 = 1 + 4\theta(1 - \theta)[\exp(2W/ZkT) - 1]$$

Z is the coordination number of the lattice and 2W is the heat absorbed on replacing two like by two unlike contacts. To make a quantitative comparison, we have taken Z = 5 and obtained W from the limiting value of  $\chi_1$  at  $\phi_2 = 1$

$$W/kT = 1 + \chi_1(\phi_2=1) - \frac{1}{2}Z \ln[Z/(Z - 2)]$$

Figure 2— $\chi_1$  versus  $\phi_2$  for natural rubber and acetone ( $\times$ ), methyl-ethyl ketone ( $\circ$ ) and ethyl acetate ( $\bullet$ ). Temperature is 25°C. The tagged points are from elastic measurements. The solid curve is for saturation ( $\Delta\mu_1=0$ ), the broken curves are calculated according to the quasi-chemical theory with  $Z=5$  and  $W/kT$  equal to 1.63 (1), 1.17 (2) and 0.97 (3)



The broken lines in Figure 2 were derived in this way.

A much more critical test of any theory is its ability to reproduce the heat and entropy of dilution. In Figures 3 and 4 some of the data are plotted in a form which facilitates this comparison. Figure 3 shows the concentration dependence of  $\Delta h_1/\phi_2^2$  for two liquids. This quantity is constant in the Flory-Huggins approximation only, but experimentally it is seen to fall much more rapidly with increased uptake of liquid than is predicted by the quasi-chemical treatment.

In Figure 4 experimental values of  $\Delta s_1/\phi_2^2$  are plotted against  $\phi_2$  for comparison with two theoretical curves: (a) Flory-Huggins, (b) the limiting form of the quasi-chemical equation for  $Z=5$ , as  $\Delta h_1$  approaches zero. Curves for different values of  $Z$  are nearly parallel, and only shifted to

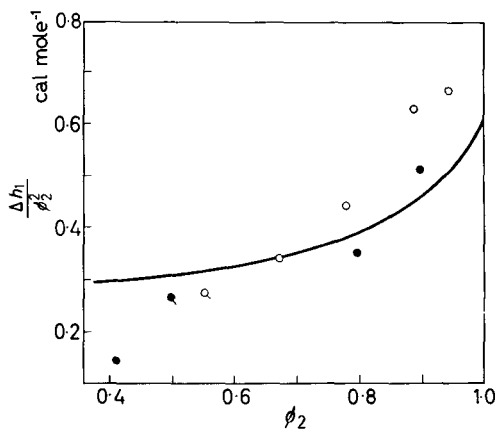


Figure 3— $\Delta h_1/\phi_2^2$  versus  $\phi_2$  for natural rubber and methylethyl ketone ( $\circ$ ) and ethyl acetate ( $\bullet$ ). The curve is calculated according to the quasi-chemical theory with  $Z=5$  and  $W/kT=0.97$

a minor extent by plausible values of  $\Delta h_1$ . It is clear that the concentration dependence is again much greater than predicted while, as  $\phi_1$  approaches zero,  $\Delta s_1$  becomes equal to or greater than the Flory value, and substantially exceeds that calculated for any plausible value of  $Z$ .

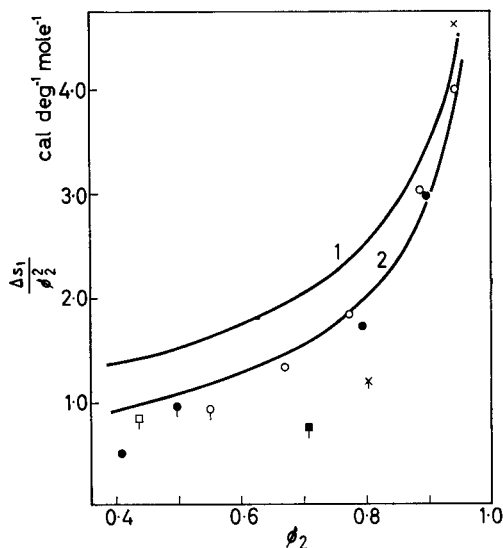


Figure 4— $\Delta s_1/\phi_2^2$  versus  $\phi_2$  for natural rubber and acetone ( $\times$ ), methylethyl ketone ( $\circ$ ), methylpropyl ketone ( $\square$ ), methyl acetate ( $\blacksquare$ ) and ethyl acetate ( $\bullet$ ). The curves are calculated according to Flory's theory (1) and the quasi-chemical theory with  $Z=5$  and  $W/kT=0$  (2)

#### Volume changes on mixing

One possible source of discrepancy between theory and experiment is the occurrence of volume changes. It has been argued that in such cases a fairer comparison requires data at constant volume. These can be obtained approximately by calculating the change in entropy which would be produced by applying a hydrostatic pressure to the mixture to make its volume equal to the sum of the volumes of the unmixed components. Some approximate measurements were made for methylethyl ketone and ethyl acetate using a modification of the apparatus described by Gee and Treloar<sup>2</sup>. The two liquids behaved similarly, showing at  $\phi_2 \sim 0.6$  a maximum contraction of about 2 ml/l. mixture, which was about twice the experimental uncertainty. On this basis we calculate that the entropies of dilution at constant volume might be about ten per cent higher than our measured values at constant pressure. This difference is within our experimental error, and insignificant in relation to the large discrepancies between theory and experiment.

#### CONCLUSIONS

It is difficult to discuss the observed discrepancies without more knowledge of their degree of generality. They confirm completely the approximate data of Gee and co-workers<sup>1,3</sup> and form a systematic group with the natural rubber-benzene data. This very carefully studied system shows (a)  $\chi_1$  constant; (b)  $\Delta s_1$  high when  $\phi_1 \rightarrow 0$ ; (c)  $\Delta s_1$  and  $\Delta h_1$  falling too sharply with increasing  $\phi_1$ . As we go from benzene to increasingly polar liquids

$\chi_1$ ,  $\Delta s_1$  and  $\Delta h_1$  all become increasingly concentration-dependent, while the limit of  $\Delta s_1$  as  $\phi_1$  approaches zero remains high.

The high values of  $\Delta s_1$  in the nearly dry rubber suggest that in the absence of liquid, natural rubber possesses a degree of order (and therefore low entropy) which is ignored in current lattice theories. This point will be further discussed in the following paper.

The sharp fall in both  $\Delta s_1$  and  $\Delta h_1$  as saturation is approached has been held to indicate a state of non-random mixing<sup>3</sup>, and this still seems the simplest explanation. A theoretical treatment of the mixing of a polymer with an associated liquid readily gives curves of the general form illustrated in *Figures 3 and 4*.

*We wish to thank the Natural Rubber Producers' Research Association who supplied the sample of crepe rubber and also the vulcanized rubber rings.*

## *Part II—A Reassessment of Published Data*

C. BOOTH, G. GEE, M. N. JONES and W. D. TAYLOR\*

*Part II contains a complete reassessment of all published data on polymer solutions, using a single method of analysis. Non-polar liquids in non-polar polymers show an entropy of mixing higher than predicted by current theories. The discrepancy is attributed to a degree of order in the solid polymer. Polar liquids in non-polar polymers follow the pattern described in Part I: this behaviour is attributed to non-random mixing at concentrations approaching saturation.*

DESPITE the importance of an accurate knowledge of the thermodynamic properties of polymer solutions, not very many detailed investigations have been described. Examination of the rather scanty data available does not confirm the systematic pattern disclosed in Part I on the basis of our own work, and this has led to a general opinion that specific factors operating in individual systems are large enough to obscure any generalization which goes beyond the most elementary form of the Flory-Huggins equation. In this paper we present a reassessment of all the suitable data we can find, and suggest that further generalization is, in fact, possible.

In the course of our own work, we have been impressed by the difficulty of obtaining reliable estimates of the heat and entropy of dilution from the measurement of vapour pressures at various temperatures. Various authors have used different procedures, and we have in some instances been unable to reproduce their values from their vapour pressure data. We have therefore recalculated the thermodynamic dilution quantities, making use of the method of analysis which we have found most consistently reliable. In this way we were able to evolve criteria for rejecting or accepting data on the basis of the precision of the vapour pressure data alone, with the result that we feel able to make comparisons between different systems studied by different workers with increased confidence.

\*Present address: Walker Laboratory (Biophysics), The Pennsylvania State University, U.S.A.

## METHOD OF ANALYSIS

The experimental data were used to calculate  $\chi_1$ , the parameter of the Flory-Huggins equation<sup>14</sup>,

$$\Delta\mu_1 = RT \ln f_1/f_1^0 = RT [\ln(1-\phi_2) + \phi_2 + \chi_1\phi_2^2]$$

$\chi_1$  is usually a slowly changing function of  $\phi_2$  (indeed for several systems it is independent of concentration) and so is a convenient quantity with which to represent the free energy data. The values of  $\chi_1$  obtained at two temperatures were plotted against  $w_2$ , and smooth curves were drawn through the points. Values of  $\chi_1$  at selected values of  $w_2$  were read off and these values were used to calculate  $\Delta\mu_1$  at the two temperatures studied.  $\Delta s_1$  and  $\Delta h_1$  were then calculated in the usual way. In all calculations we used the densities quoted in the paper from which we took the data. When densities were not quoted for liquids we used the values given by Timmermanns<sup>5</sup>.

Experimental errors were evaluated as follows. We determined a 'standard error' ( $S$ ) of the smooth curve by use of the equation

$$S^2 = \sum_{i=1}^n (\Delta\chi_1)_i / n(n-2)$$

where  $(\Delta\chi_1)_i$  are the deviations of the values of  $\chi_1$  from the smooth curve and  $n$  the number of experimental points. Only experimental points in the range of  $w_2$  for which we quote values of  $\Delta s_1$  and  $\Delta h_1$  were considered. Experimental points having a value of  $\Delta\chi_1$  markedly greater than  $2S$  were rejected. The effect of this error upon the values of  $\Delta s_1$  and  $\Delta h_1$  was computed and is expressed in the tables as a constant error in  $\Delta s_1/\phi_2^2$  and  $\Delta h_1/\phi_2^2$ .

## RESULTS OF THE CALCULATIONS

The following notes and tables summarize the results of our review. A number of investigations were rejected because our method of plotting revealed excessive scatter in the experimental points. In a number of cases our calculations of  $\Delta s_1$  and  $\Delta h_1$  differ markedly from those reported by the original authors.

*Polyisobutylene-benzene*<sup>15</sup>

The data obtained at 25°C and 40°C were analysed. Data obtained at 65°C were very scattered.

Table 1

$w_2$	$\phi_2$	$\Delta s_1$ <i>cal deg<sup>-1</sup> mole<sup>-1</sup></i>	$\Delta h_1$ <i>cal mole<sup>-1</sup></i>
0.8	0.786	1.84	386
0.7	0.682	1.25	280
0.6	0.580	0.79 <sub>5</sub>	213
0.5	0.479	0.43 <sub>5</sub>	125

Precision:  $\Delta s_1/\phi_2^2$  to  $\pm 0.20$  cal deg<sup>-1</sup> mole<sup>-1</sup>.  
 $\Delta h_1/\phi_2^2$  to  $\pm 60$  cal mole<sup>-1</sup>.

These entropies and heats of dilution differ considerably from those quoted by Bawn and Patel. A discrepancy has been noted earlier<sup>16,17</sup>.

*Polyisobutylene-cyclohexane*<sup>15,18</sup>

The data of Bawn and Patel are very scattered and could not be analysed. The paper of Magat and Minnassian contains no experimental data other than smoothed graphs. Values of  $\chi_1$  at various values of  $\phi_2$  could be read off *Figure 3* of their paper. These were analysed, giving results differing slightly from those quoted by Magat and Minnassian.  $\Delta s_1$  was consistently higher than the Flory value, while  $\Delta h_1/\phi_2^2$  was roughly constant at 390 cal mole<sup>-1</sup>.

*Polystyrene-cyclohexane*<sup>16</sup>

The data reported for fraction I at 34°C and 44°C were analysed; the data for the higher molecular weight fraction III were too scattered for our purpose. A small correction (about -3 per cent to  $\Delta s_1$  and  $\Delta h_1$ ) was made to allow for the non-ideality of the vapour.

Table 2

$w_2$	$\phi_2$	$\Delta s_1$ cal deg <sup>-1</sup> mole <sup>-1</sup>	$\Delta h_1$ cal mole <sup>-1</sup>
0.8	0.744	1.49	377
0.7	0.629	0.82 <sub>7</sub>	219
0.6	0.521	0.44 <sub>3</sub>	122
0.5	0.421	0.23 <sub>8</sub>	67. <sub>7</sub>

Precision:  $\Delta s_1/\phi_2^2$  to  $\pm 0.37$  cal deg<sup>-1</sup> mole<sup>-1</sup>.  
 $\Delta h_1/\phi_2^2$  to  $\pm 110$  cal mole<sup>-1</sup>.

These values agree quite well with those obtained by Krigbaum and Geymer who used a different method of analysis. This same system has also been studied by Schmoll and Jenkel<sup>19</sup>, but we were unable to analyse their data by our method.

*Polystyrene-toluene*<sup>20</sup>

These data are very scattered and we could not draw satisfactory curves through the plot of  $\chi_1$  versus  $w_2$ . However, it is clear that  $\Delta s_1$  is a little lower than the Flory value in the concentration range  $\phi_2=0.8$  to 0.4. This is not unreasonable since  $\Delta h_1$  is known to be negative<sup>21-23</sup>.

*Polystyrene-methylethyl ketone*<sup>20</sup>

These data were too scattered to analyse quantitatively or qualitatively.

Table 3

$w_2$	$\phi_2$	$\Delta s_1$ cal deg <sup>-1</sup> mole <sup>-1</sup>	$\Delta h_1$ cal mole <sup>-1</sup>
0.8	0.759	0.84 <sub>0</sub>	78. <sub>5</sub>
0.7	0.647	0.45 <sub>6</sub>	61. <sub>4</sub>
0.6	0.541	0.25 <sub>4</sub>	45. <sub>1</sub>
0.5	0.440	0.14 <sub>2</sub>	31. <sub>6</sub>

Precision:  $\Delta s_1/\phi_2^2$  to  $\pm 0.10$  cal deg<sup>-1</sup> mole<sup>-1</sup>.  
 $\Delta h_1/\phi_2^2$  to  $\pm 30$  cal mole<sup>-1</sup>.



*Polystyrene-propyl acetate*<sup>24</sup>

Data obtained at 25°C and 70°C were analysed.

The results (*Table 3*) agree with those reported by Bawn and Wajid.

*Polystyrene-acetone*<sup>24</sup>

Data obtained at 25°C and 50°C were analysed.

*Table 4*

$w_2$	$\phi_2$	$\Delta s_1$ <i>cal deg<sup>-1</sup> mole<sup>-1</sup></i>	$\Delta h_1$ <i>cal mole<sup>-1</sup></i>
0.9	0.862	0.96 <sub>8</sub>	33. <sub>4</sub>
0.8	0.735	0.32 <sub>2</sub>	17. <sub>2</sub>
0.7	0.618	0.12 <sub>3</sub>	9. <sub>1</sub>
0.6	0.510	0.04 <sub>6</sub>	4. <sub>8</sub>

Precision:  $\Delta s_1/\phi_2^2$  to  $\pm 0.15$  cal deg<sup>-1</sup> mole<sup>-1</sup>.  
 $\Delta h_1/\phi_2^2$  to  $\pm 120$  cal mole<sup>-1</sup>.

Our results do not agree very well with those obtained by Bawn and Wajid.

*Polystyrene-chloroform*<sup>24</sup>

These data are very scattered and we were unable to draw satisfactory curves through the plots of  $\chi_1$  versus  $w_2$ . The precision of  $\Delta s_1/\phi_2^2$  was no better than  $\pm 1$  cal deg<sup>-1</sup> mole<sup>-1</sup>, but one can conclude that  $\Delta s_1$  is lower than the Flory value in the concentration range  $\phi_2=0.8$  to 0.3 while  $\Delta h_1$  is probably negative (see, for comparison, ref. 23).

*Polybutadiene-chloroform*

These data were obtained in our laboratory and are given in the Appendix to this paper. Temperatures of measurement were 0°C and 25°C.

*Table 5*

$w_2$	$\phi_2$	$\Delta s_1$ <i>cal deg<sup>-1</sup> mole<sup>-1</sup></i>	$\Delta h_1$ <i>cal mole<sup>-1</sup></i>
0.8	0.869	1.52	-165
0.7	0.794	0.88 <sub>9</sub>	-142
0.6	0.713	0.53 <sub>3</sub>	-111
0.5	0.623	0.30 <sub>4</sub>	-82. <sub>8</sub>
0.4	0.525	0.15 <sub>5</sub>	-58. <sub>2</sub>

Precision:  $\Delta s_1/\phi_2^2$  to  $\pm 0.13$  cal deg<sup>-1</sup> mole<sup>-1</sup>.  
 $\Delta h_1/\phi_2^2$  to  $\pm 40$  cal mole<sup>-1</sup>.

## REVIEW OF OTHER WORK

*Polydimethylsiloxane-benzene*<sup>25</sup>

Newing has reported heats and entropies of dilution for silicones in benzene. They include the concentration range ( $\phi_2 > 0.3$ ) of interest here, but the original paper gives no free energy data for this range. There is, therefore, no published experimental support for his frequently quoted results, and we have felt obliged to ignore them.

*Polybutadiene-benzene*<sup>2,6</sup>

Jessup has reported values of  $\Delta s_1$  and  $\Delta h_1$  for this system. He measured vapour pressure to determine  $\Delta\mu_1$  and determined  $\Delta h_1$  from calorimetric measurements of the heat of mixing. Both determinations were at 25°C. The precision of these results (included in *Figure 2*) is probably better than that usually obtained by measurement of vapour pressures only.

*Natural rubber-benzene*

Gee and Treloar<sup>2</sup> and Gee and Orr<sup>3</sup> have reported values of  $\Delta s_1$  and  $\Delta h_1$  for this system. Their results were based upon the determination of  $\Delta\mu_1$  at several temperatures by measuring vapour pressures together with a determination of  $\Delta h_1$  for a low molecular weight polyisoprene by calorimetry. Experimental data are presented graphically. The precision of these results (*Figures 1* and *2*) is probably better than that obtained by analysis of vapour pressure data alone.

*Natural rubber-methanol*<sup>1,3</sup>

Ferry, Gee and Treloar have reported values of  $\Delta s_1$  and  $\Delta h_1$  for this system. Vapour pressures were measured at 25°C and 35°C by methods identical to those used by Gee and Treloar<sup>2</sup>. No experimental data are given.

*Polyisobutylene-n-pentane*<sup>6</sup>

Baker *et al.* have reported values of  $\Delta s_1$  and  $\Delta h_1$  for this system derived from measurement of vapour pressure at several temperatures in the range 25°C to 55°C. Mixtures of high molecular weight polyisobutylene with *n*-pentane present the special problem of a mixture near its lower critical solution temperature. The solutions of low molecular weight polyisobutylene (sample II) are comparable with the other systems discussed here. The data are very scattered and were analysed by the authors by a similar method to that used in this paper. Approximate values of  $\Delta s_1$  were obtained in the concentration range  $\phi_2=0.9$  to 0.3 and were similar to Flory values:  $\Delta h_1$  was positive.

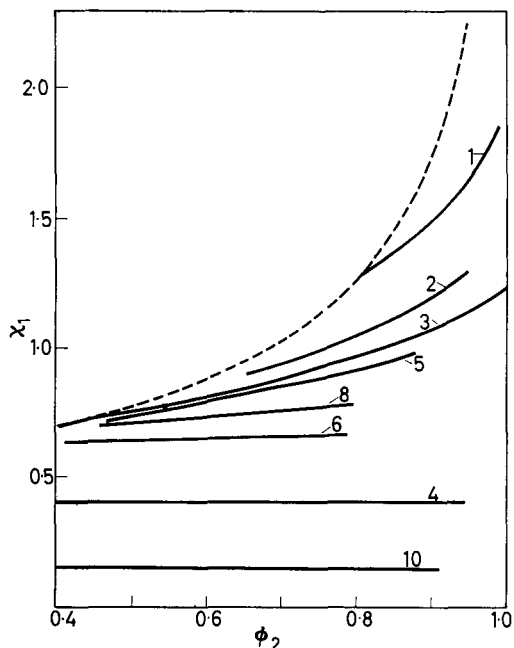
*Other systems*

We have examined in detail only data from which  $\Delta s_1$  and  $\Delta h_1$  could be or had been obtained for concentrated polymer solutions. There are many determinations of  $\Delta\mu_1$  which were confined to a single temperature or which were carried out at several temperatures but with insufficient precision to allow evaluation of  $\Delta s_1$  and  $\Delta h_1$ . Early work has been reviewed by Huggins<sup>27-29</sup>. More recent work includes that of Prager, Bagley and Long<sup>30</sup>, who determined  $\Delta\mu_1$  for a number of polyisobutylene-hydrocarbon mixtures and van der Waals and Hermans<sup>31</sup> who determined  $\Delta\mu_1$  for mixtures of polyethylene and heptane at 109°C. These systems had a constant value of  $\chi_1$  over the concentration ranges studied.

## DISCUSSION

*Figure 1* shows some representative curves of  $\chi_1$  versus  $\phi_2$ . *Figure 2* contains all the entropy data we consider reliable. Reference to our comments

Figure 1— $\chi_1$  versus  $\phi_2$  for the systems natural rubber–acetone (1), –methyl ethyl ketone (2), –ethyl acetate (3), –benzene (4); polystyrene–acetone (5), –*n*-propyl acetate (6); polyisobutylene–benzene (8); and polybutadiene–chloroform (10). The dashed line is the saturation curve  $\Delta\mu_1=0$



on the individual systems will show that only the broad features are to be considered significant. Thus in Figure 2 we bracket curves 4, 7, 8 and 9 as essentially similar, showing  $\Delta s_1$  somewhat higher than the Flory value; the apparent differences among them may well be spurious. One unknown factor is the possible occurrence of volume changes on mixing.

This survey supports the generalization made in the preceding paper that in non-polar systems  $\Delta s_1$  is significantly *higher* than is predicted by

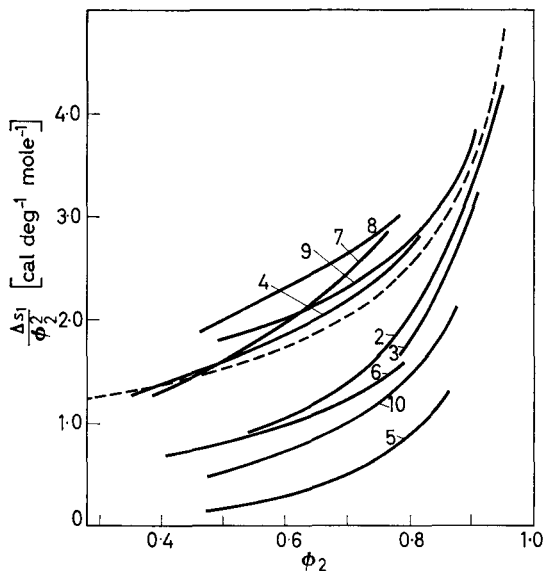


Figure 2— $\Delta s_1 / \phi_2^2$  versus  $\phi_2$  for the systems natural rubber–methyl ethyl ketone (2), –ethyl acetate (3), –benzene (4); polystyrene–acetone (5), –*n*-propyl acetate (6), –cyclohexane (7); polyisobutylene–benzene (8); polybutadiene–benzene (9), –chloroform (10). The dashed line represents the Flory equation

the Flory equation. All mathematical refinements of Flory's analysis of the lattice model lead to equations which contain explicitly the lattice coordination number  $Z$  and the heat of mixing<sup>11,12</sup>. For athermal systems, Flory's value of  $\Delta s_1/\phi_2^2$  is reduced by approximately  $R/Z$ , and a further reduction is associated with positive  $\Delta h_1$ . Krigbaum<sup>32</sup> has criticized these apparently more precise analyses, and has argued that in the athermal case, the true entropy of dilution is intermediate between the two estimates, but considerably closer to Flory's. We can, at any rate, conclude that experimental values of  $\Delta s_1$  in non-polar systems are significantly higher than can be accounted for on the basis of current lattice theories.

The probable origin of this discrepancy can be seen by using the data to evaluate the total entropy of solution. If 1 ml of polymer absorbs  $n_1$  moles of a liquid having a molar volume  $V_1$  ml, the total increase in entropy  $\Delta S$  is given by

$$\Delta S = \frac{1}{V_1} \int_0^{\phi_1} \frac{\Delta s_1}{\phi_2^2} d\phi_1$$

If the Flory equation holds,

$$\Delta s_1^F = -R (\ln \phi_1 + \phi_2) \quad \text{and} \quad \Delta S^F = -\frac{R}{V_1} \frac{\phi_1}{\phi_2} \ln \phi_1$$

This integral is awkward to evaluate graphically, since  $\Delta s_1/\phi_2^2 \rightarrow \infty$  as  $\phi_2 \rightarrow 1$ , and it is therefore convenient to subtract the Flory entropy, giving

$$\Delta S = -\frac{R}{V_1} \frac{\phi_1}{\phi_2} \ln \phi_1 + \frac{1}{V_1} \int_0^{\phi_1} \frac{(\Delta s_1 - \Delta s_1^F)}{\phi_2^2} d\phi_1$$

The data available are not sufficiently precise to permit a very satisfactory evaluation of the integral, but *Figure 2* shows that for  $\phi_2 \rightarrow 0.5$   $(\Delta s_1 - \Delta s_1^F)/\phi_2^2$  lies between 0 and 0.4 for a range of non-polar systems, whence

$$\Delta S \simeq \Delta S^F + \frac{0.2}{V_1} \phi_1$$

If we assume that a moderately dilute solution of a non-polar polymer in a non-polar liquid is a random mixture, the value of  $\Delta S$  at (say)  $\phi_1 = 0.7$  represents  $S_{\text{random mixture}} - S_{\text{dry polymer}} - S_{\text{liquid}}$ . Now in the theoretical derivation of  $\Delta S$ , it is assumed that the dry polymer is completely disordered; if this is not so we shall have

$$\begin{aligned} \Delta S_{\text{expt.}} &= \Delta S_{\text{theor.}} + S_{\text{random polymer}} - S_{\text{actual polymer}} \\ &= \Delta S_{\text{theor.}} + \Delta S_{\text{disorder}} \end{aligned}$$

where the second term measures the increase of entropy arising from disordering the dry polymer.

*Figure 3* gives a comparison of several estimates of  $V_1 \Delta S$ : (1)  $V_1 \Delta S^F$ ; (2) calculated from the quasi-chemical theory with  $Z=5$  and  $W/kT=0.14$ ;

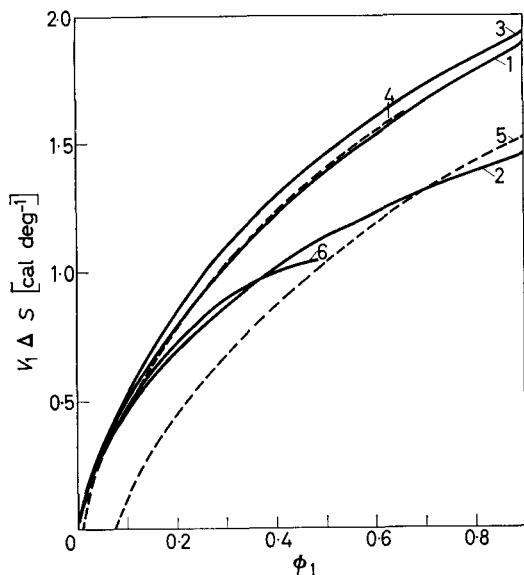


Figure 3— $V_1\Delta S$  versus  $\phi_1$  calculated as described in the text

(3) from the data for natural rubber in benzene. Comparing 1 and 3 gives  $\Delta S_{\text{disorder}} \approx 7 \times 10^{-4}$ ; 2 and 3 gives  $\Delta S_{\text{disorder}} \approx 5 \times 10^{-3} \text{ cal deg}^{-1} \text{ cm}^{-3}$ . Essentially similar results are obtained if this same procedure is applied to curves 7, 8 and 9 of Figure 2, but the displacements required are rather larger. The significance of this quantity may be assessed by comparison with two other estimates of entropy associated with order: (a) experimentally, the total entropy of fusion of natural rubber is  $0.051 \text{ cal deg}^{-1} \text{ cm}^{-3}$ <sup>14</sup>; (b) Flory's lattice theory gives for the increase of entropy in going from complete order to complete disorder approximately

$$(R/V_1) \ln [(Z-1)/e] = 0.0087 \text{ cal deg}^{-1} \text{ cm}^{-3}$$

for  $Z=5^{14}$ . It seems reasonable to suggest that amorphous non-polar polymers possess a degree of order in the solid state, arising from the tendency of adjacent portions of molecules to pack approximately parallel. This is ignored in current lattice theories, though it might be predictable by a more sophisticated analysis which considered in detail the problem of packing without leaving holes. In principle, our method of analysis could be used to compare states of order in different polymers, but this would require much more precise data than are at present available.

Comparison of the concentration dependence of  $S$  with that calculated theoretically provides evidence as to the way in which polymer order disappears with swelling. In Figure 3 curves 4 and 5 are obtained by deducting respectively 0.06 and 0.41  $\text{cal deg}^{-1}$  from the experimental curve 3. If the quasi-chemical calculation is correct, we must conclude that a high degree of polymer order persists in highly swollen rubber. This scarcely seems plausible in the light of our interpretation of its origin, and we consider that this evidence lends support to Krigbaum's criticisms. We therefore take curve 4 to represent the swelling of a disoriented rubber.

Finally in *Figure 3*, curve 6 gives the experimental entropy of swelling, up to saturation, for natural rubber in methylethyl ketone. This falls below curve 3 by  $0.4 \text{ cal deg}^{-1}$  at saturation ( $\phi_1 \simeq 0.5$ ). The interpretation of this difference is that it measures the state of order in the fully swollen system, i.e. if the mixture were random its entropy would be increased by  $4 \times 10^{-3} \text{ cal deg}^{-1} \text{ cm}^{-3}$ . Comparison of the shapes of curves 3 and 6 suggests that this order builds up rapidly as saturation is approached.

## CONCLUSIONS

Two general effects\* contribute to the total entropy of solution of a non-polar polymer, (1) the disorientation of the polymer and (2) the dissolution of the disoriented polymer. With a polar liquid a further effect arises from non-random mixing, especially as saturation is approached. In principle, these effects can be quantitatively interpreted, provided we know the entropy of random mixing of a disoriented polymer. We believe that Flory's equation gives the best estimate available of this quantity. Advances in experimental technique would greatly increase the value of this method of approach.

## APPENDIX

THE VAPOUR PRESSURE OF CHLOROFORM OVER  
POLYBUTADIENE SOLUTIONS

Vapour pressures at  $0^\circ\text{C}$  and  $25^\circ\text{C}$  were measured in the modified manometer described in Part I. Polybutadiene supplied by Polymer Corporation, Sarnia, Canada, was purified by adding acetone to a dilute solution in carbon tetrachloride and drying the precipitated polymer *in vacuo*. The densities were  $0.913$  and  $0.897 \text{ g ml}^{-1}$  at  $0^\circ$  and  $25^\circ\text{C}$  respectively. Chloroform was repeatedly crystallized at  $-70^\circ\text{C}$  before drying with sodium carbonate and distilling in the manner described in Part I. The densities were  $1.521$  and  $1.474 \text{ g ml}^{-1}$  at  $0^\circ$  and  $25^\circ\text{C}$  respectively. The

Table 6. The variation of  $p_1/p_1^0$  and  $\chi_1$  with  $\phi_2$  for the system polybutadiene-chloroform

$\phi_2$	$p_1/p_1^0$	$\chi_1$
25°C	0.406	0.143
	0.493	0.147
	0.556	0.153
	0.657	0.148
	0.717	0.154
	0.821	0.155
	0.966	0.143
0°C	0.536	0.140
	0.632	0.129
	0.780	0.129
	0.836	0.129

\*Any significant volume change occurring on mixing would make a further contribution.

variation of  $p_1/p_1^0$  with the volume fraction of polybutadiene is given in Table 6 together with the Flory-Huggins parameter  $\chi_1$ . The second virial coefficients used in computing  $\chi_1$  were calculated from the Berthelot equation by use of the critical constants selected by Kobe and Lynn<sup>33</sup>.

*We wish to thank Miss C. J. S. Guthrie for assistance with the calculations.*

### Part III—Polypropylene plus Various Ketones

W. B. BROWN\*, G. GEE and W. D. TAYLOR

*Part III presents a study of the swelling of polypropylene in a range of ketones. Vapour pressure measurements were supplemented by simple observations of swelling equilibrium on samples crosslinked by radiation. Although the survey is rather limited in scope, it is in the main consistent with the generalization of Part II. A striking exception is the behaviour at very low liquid levels.*

THIS WORK was planned as a study of the interaction of a non-polar polymer with a range of liquids containing a polar group, with varying lengths of hydrocarbon chain. Polypropylene was selected as the polymer, and vapour pressure studies made on two ketones over a range of temperature. The results at a given temperature can be conveniently expressed, as in Parts I and II, in terms of the concentration dependence of the Flory-Huggins parameter  $\chi_1$ . The temperature coefficient then leads to estimates of the heat and entropy of dilution.

Work of this kind is necessarily rather time-consuming, and it is desirable to supplement it by a simpler, if less powerful, technique. Some limited information concerning the thermodynamics of swelling can be obtained very simply if polymers can be crosslinked to a known extent. Such a polymer has a limited swelling capacity in any liquid, equilibrium being attained when the decrease of free energy on further imbibition of liquid equals the resulting increase in the configurational free energy of the network. To apply the method it is necessary to know how the network free energy depends on swelling, and it has been generally assumed that this is of the form

$$\Delta G_n = 3C(\lambda^2 - 1) \quad (1)$$

where  $\lambda$  is the linear swelling ratio and  $C$  is a temperature-dependent constant. If  $C$  is known,  $\chi_1$  can then be determined at the composition  $\phi_2$  of equilibrium swelling, from the equation

$$-\chi_1\phi_2^2 = \ln(1 - \phi_2) + \phi_2 + 2CV_1\phi_2^{1/3} \quad (2)$$

where  $V_1$  is the molar volume of the liquid. We will present evidence elsewhere that a better (empirical) representation of a large body of data is obtained by replacing (1) by (1')

$$\Delta G_n = 3C_1(\lambda^2 - 1) - 3C_2(1 - \lambda^{-2}) \quad (1')$$

\*Present address: Theoretical Chemistry Institute, University of Wisconsin, U.S.A.

If this is done, equation (2) is modified to (2').

$$-\chi_1\phi_2^2 = \ln(1 - \phi_2) + \phi_2 + 2C_1V_1\phi_2^{1/3}(1 - C_2\phi_2^{4/3}/C_1) \quad (2')$$

We have used this procedure to extend our measurements on polypropylene to a wider range of ketones. Crosslinked specimens were produced, as described below, by electron irradiation, which is assumed to have no effect on the polymer-liquid mixing process. We therefore assume that the values for the swelling of these samples in diethyl and diisopropyl ketones will be equal to those measured on the uncrosslinked polymers. If the same polymer is swollen in both these liquids (2') gives two simultaneous equations from which  $C_1$  and  $C_2$  can be determined. In practice, this is a very imprecise procedure, since the network free energy term is much the smallest term in equation (2'). However, we have verified that our final conclusions\* would not be significantly modified if we replaced these  $C_1$  and  $C_2$  values with averages obtained from the two liquids with the alternative assumptions (a)  $C_2=0$  or (b)  $C_2=C_1$ .

#### EXPERIMENTAL

##### *Polypropylene*

A specimen of essentially amorphous polymer was kindly supplied by I.C.I. Ltd. Before use it was dissolved in toluene at 25°C and cooled to 0°C, when a fraction separated and was removed by filtration. The soluble portion was then precipitated with acetone, redissolved in benzene and freeze dried. The viscosity-average molecular weight of this sample (denoted A) was 20 000 and the density at 25°C was 0.865 g cm<sup>-3</sup>. This density may be compared with those given by Dole<sup>34</sup> for crystalline (0.9050 g cm<sup>-3</sup>) and amorphous (0.8667 g cm<sup>-3</sup>) polypropylene of molecular weights (number-average) 191 200 and 18 900 respectively.

##### *Crosslinking*

Specimens of polymer with four degrees of crosslinking were prepared by irradiating films of polymer with 4 MeV electrons, using doses of 75, 100, 140 and 250 Mrad†. (The films were prepared by compression moulding at 100°C. Strips about 1 cm × 5 cm × 0.15 cm were irradiated in evacuated glass tubes at a rate of 1.0 Mrad/min at ~30°C.) After irradiation the films were extracted twice with hot toluene to remove soluble polymer and dried *in vacuo*. Preliminary experiments showed that further extraction caused no further loss in weight of the dried films.

##### *Swelling liquids*

The eight ketones used were dried over anhydrous magnesium sulphate and distilled. Samples of diethyl and diisopropyl ketones for vapour pressure measurements were further purified by re-drying, passing down

\*It should be noted that attempts to extend the range of liquids to include much better swelling agents failed to give significant results because it is then necessary to have much more precise information about the network free energy.

†We wish to record our thanks to Mr D. Mold and Mr F. Waddington of A.E.I. Ltd for carrying out the irradiations.



an aluminium oxide column to remove peroxides, and distilling through a 3 ft column packed with nickel gauze.

### Measurements

Vapour pressure and isothermal distillation measurements were made as described in Part I. Swelling of the crosslinked samples was determined by weighing. Preliminary experiments in diethyl ketone showed that swelling was complete in 30 hours and was unchanged either by addition of hydroquinone as antioxidant, or by standing for five days. Measurements were carried out at 25°C in test tubes, using 10 ml liquid containing 0.1 per cent hydroquinone and freed from dissolved air by bubbling nitrogen. Samples weighed approximately 0.03 g dry and the weight increase was determined with a reproducibility of about 1 mg.

## RESULTS

Vapour pressure and isothermal distillation measurements on polymer A are given in *Tables 1* and *2*. There is a certain amount of scatter in the concentration dependence of  $\chi_1$ , especially in the region covered by isopiestic

*Table 1.* The variation of  $p_1/p_1^0$  and  $\chi_1$  with  $\phi_2$  for polypropylene (A) in diethyl ketone

25°C			45°C		
$\phi_2$	$p_1/p_1^0$	$\chi_1$	$\phi_2$	$p_1/p_1^0$	$\chi_1$
0.993	0.090	1.58	0.993	0.071	1.37
0.990	0.167	1.86	0.991	0.150	1.83
0.989	0.209	2.00	0.990	0.186	1.97
0.978	0.289	1.65	0.979	0.268	1.66
0.974	0.344	1.68	0.975	0.302	1.61
0.967	0.374	1.57	0.969	0.330	1.48
0.965	0.395	1.56	0.966	0.343	1.46
0.957	0.412	1.42	0.959	0.362	1.32
0.930	0.565	1.34	0.932	0.489	1.21
0.879	0.734	1.20	0.881	0.680	1.12
0.803	0.887	1.09	0.804	0.848	1.02
<i>Isopiestic data</i>					
0.684	0.9946	0.99	0.552	0.9813	0.76
0.563	0.9958	0.82	0.510	0.9880	0.74
0.559	0.9903	0.80	0.470	0.9928	0.71
0.520	0.9988	0.79	0.436	0.9959	0.69
0.482	0.9997	0.76	0.389	0.9989	0.68
0.435	0.9994	0.72	0.361	0.9988	0.66

measurements, which limited the reliability of the entropy calculations (summarized in *Figure 1* by plotting  $\Delta s_1/\phi_2^2$  versus  $\phi_2$ ).

Swelling measurements are given in *Tables 3* and *4*. For each liquid a family of four values of  $\chi_1$  is obtained, covering a small range of  $\phi_2$ . These results are plotted in *Figure 2*, which also includes the vapour pressure

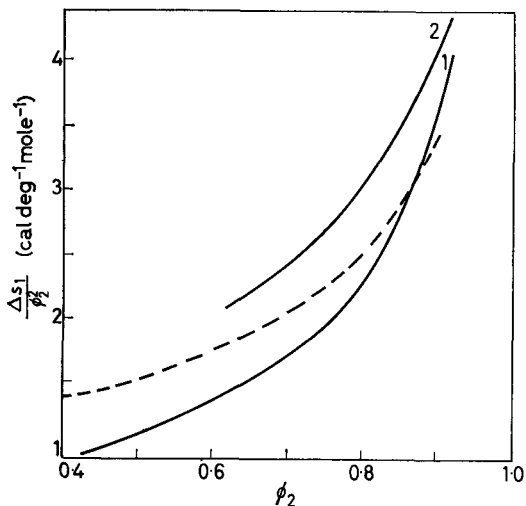
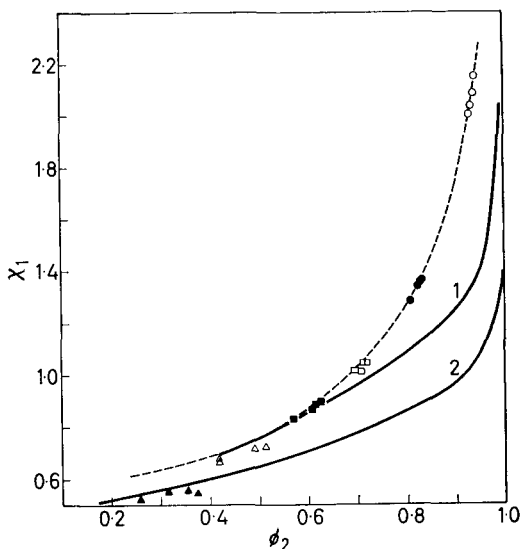


Figure 1— $\Delta s_1/\phi_2^2$  versus  $\phi_2$  for polypropylene and diethyl ketone (1), and diisopropyl ketone (2). The dashed curve is calculated according to Flory's theory

Figure 2— $\chi_1$  versus  $\phi_2$  for polypropylene and acetone (○), methylethyl ketone (●), methyl-*n*-propyl ketone (□), methylisobutyl ketone (■), methyl-*n*-amyl ketone (△) and diisobutyl ketone (▲). The curves are for polypropylene and diethyl ketone (1) and diisopropyl ketone (2). The dashed curve is for saturation ( $\Delta\mu_1=0$ )



data and the saturation curve [the locus of points representing equilibrium swelling of uncrosslinked polymer, obtained by putting  $C_1=C_2=0$  in equation (2')].

#### DISCUSSION

Figure 2 shows a marked increase of  $\chi_1$  with  $\phi_2$ , which becomes very steep as  $\phi_2 \rightarrow 1$ . Over most of the concentration range these curves are very similar to those reported in Part I, but the behaviour at high  $\phi_2$  is quite distinctive, and will be discussed further in Part IV.

The short sections of curves in Figure 2 each represent the lower end of a curve such as those for diethyl and diisopropyl ketones. Although the

Table 2. The variation of  $p_1/p_1^0$  and  $\chi_1$  for polypropylene (A) in diisopropyl ketone

25°C			45°C		
$\phi_2$	$p_1/p_1^0$	$\chi_1$	$\phi_2$	$p_1/p_1^0$	$\chi_1$
0.985	0.134	1.24	0.986	0.115	1.17
0.984	0.149	1.31	0.986	0.095	0.98
0.965	0.236	1.02	0.968	0.194	0.90
0.934	0.421	1.06	0.940	0.372	1.00
0.903	0.521	0.95	0.909	0.461	0.87
0.838	0.699	0.89	0.845	0.648	0.82
0.770	0.812	0.83	0.777	0.757	0.74
0.699	0.876	0.76	0.704	0.850	0.71
0.646	0.923	0.75	0.650	0.894	0.68
<i>Isopiestic data</i>					
0.404	0.9826	0.59	0.367	0.9814	0.53
0.343	0.9895	0.57	0.307	0.9886	0.51
0.327	0.9946	0.60	0.283	0.9940	0.55
0.239	0.9976	0.56	0.231	0.9969	0.54
0.184	0.9977	0.51	0.170	0.9971	0.46
			0.157	0.9998	0.55

Table 3. Derivation of elastic constants from swelling in diethyl (DEK) and diisopropyl (DIK) ketones

Polymer	Radiation dose Mrad	$\phi_2$		$10^4 C_1$	$10^4 C_2$
		DEK	DIK		
P	250	0.625	0.419	1.96	1.24
Q	140	0.608	0.383	1.44	0.81
R	100	0.597	0.334	0.96	0.62
S	75	0.578	0.293	0.55	0.13

Table 4. Swelling in other ketones

Polymer Ketone	P		Q		R		S	
	$\phi_2$	$\chi_1$	$\phi_2$	$\chi_1$	$\phi_2$	$\chi_1$	$\phi_2$	$\chi_1$
Acetone	0.932	2.006	0.934	2.041	0.938	2.087	0.943	2.152
Methylethyl	0.829	1.346	0.830	1.353	0.809	1.285	0.824	1.340
Methyl- n-propyl	0.708	1.016	0.719	1.044	0.715	1.043	0.699	1.016
Methyl-iso- butyl	0.620	0.864	0.631	0.889	0.627	0.894	0.572	0.830
Methyl-n-amyl	0.514	0.725	0.491	0.713	0.419	0.662	0.417	0.675
Diisobutyl	0.374	0.544	0.354	0.551	0.315	0.549	0.258	0.522

concentration range for each liquid is very restricted, there is no doubt that  $\chi_1$  is in every case concentration-dependent, the slope increasing with the value of  $\chi_1$ . All these results therefore support the view developed in Parts I and II that this is normal behaviour for non-polar polymers in polar liquids.

The entropy data shown in *Figure 1* are believed to be comparable in reliability with those surveyed in Part II. For diethyl ketone the entropy of dilution approaches the Flory value at high  $\phi_2$ , in agreement with expectation, and we observe at lower  $\phi_2$  the sharp fall in  $\Delta S_1/\phi_2^2$  characteristic of polar liquids. The data on diisopropyl ketone are unfortunately too scattered for significant values of  $\Delta S_1$  to be calculated below  $\phi_2 \sim 0.7$ . Above  $\phi_2 = 0.7$ ,  $\Delta S_1$  is similar to that for non-polar liquids.

Summarizing, the data reported in this paper increase our confidence in the generalization we sought to make in Part II.

### *Part IV—Effect of Incipient Crystallinity on the Swelling of Polypropylene in Diethyl Ketone*

G. ALLEN, C. BOOTH, G. GEE and M. N. JONES

*Two nominally similar samples of 'amorphous' polypropylene are reported to show differing and very high vapour pressures at diethyl ketone contents less than 5 per cent (v/v). On the basis of a comparison with the system polyethylene oxide and chloroform, this behaviour is attributed to minor but different degrees of crystalline order in the two samples. This is therefore a further factor to be taken into account in the swelling behaviour of polymers of unknown tacticity.*

THE WORK described in Part III showed an unexpectedly sharp rise in  $\chi_1$  as  $\phi_1 \rightarrow 0$ . This region was therefore re-examined, using a fresh sample of polymer. Results were qualitatively similar but with marked quantitative differences which evidently reflect some small difference between the polymers. The purpose of this paper is to report these findings and discuss their significance.

#### EXPERIMENTAL

##### *Polypropylene*

A second sample of amorphous polypropylene (also supplied by I.C.I. Ltd) was treated as described in Part III. The purified polymer (denoted B) had a viscosity-average molecular weight of 25 000 and a density at 25°C of 0.857 g cm<sup>-3</sup>. The following observations led us to doubt that this sample was completely amorphous: (1) on cooling a toluene solution to -30°C a solid precipitated; (2) when viewed under a polarizing microscope a diffuse melting point could be detected at 60° to 70°C (compare the melting point of isotactic polypropylene = 176°C). Subsequent examination of sample A (Part III) revealed similar properties.

##### *Vapour pressures*

Vapour pressure measurements for polypropylene + diethyl ketone were made by the technique already described, special attention being given to very low concentrations of liquid. The results are given in *Table 1*, which also includes the calculated values of  $\chi_1$  (corrected for non-ideality of the solvent vapour). It is evident that the sharp rise in  $\chi_1$  as  $\phi_2 \rightarrow 1$  is even more marked with the new sample (B) than with A (see Part III). The significance of this rise is more clearly indicated in *Figure 1* in which the

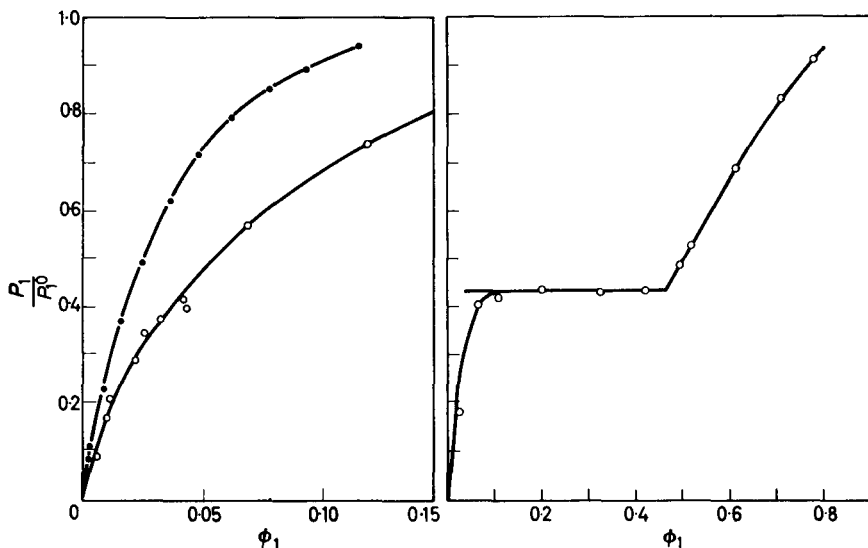


Figure 1— $p_1/p_1^0$  versus  $\phi_1$  for diethyl ketone and polypropylene A (○) and B (●) at 25°C

Figure 2— $p_1/p_1^0$  versus  $\phi_1$  for polyethylene oxide and chloroform at 25°C

reduced vapour pressure is plotted against  $\phi_1$ . As  $\phi_2 \rightarrow 1$ , the Flory-Huggins equation reduces to  $p_1/p_1^0 = \phi_1 \exp(1 + \chi_1)$ , so that the rapidly rising  $\chi_1$  is a reflection of the steep and strongly curved vapour pressure plot.

#### DISCUSSION

It is noteworthy that samples A and B, although supposedly similar, show such striking quantitative differences. We believe that this fact, and the general shape of the vapour pressure curves can be qualitatively understood by taking account of the crystallinity of the polymer.

Experimental studies of the mixing of crystalline polymers with liquids have generally concentrated on the lowering of the melting point of the polymer, but in *Figure 2* we show the results of some hitherto unpublished vapour pressure measurements on mixtures of polyethylene oxide and chloroform\*. These data show very well the features one would expect for such a system: a rapidly rising  $p_1$  up to  $\phi_1 \sim 0.1$  due to dissolution of molecules of lower melting point (low molecular weight molecules and molecules having structural defects) and to swelling of amorphous regions in the bulk polymers; a constant  $p_1$  between  $\phi_1 \sim 0.1$  and  $0.47$  in which the concentration of the polymer in solution is the equilibrium solubility of polyethylene oxide in chloroform at the temperature of the experiment; and a portion of the vapour pressure curve for the molten polymer above  $\phi_1 \sim 0.47$ .

Comparison with *Figure 2* suggests that the steep vapour pressure curves in *Figure 1* are to be attributed to the crystallinity of the polymer. Since polypropylene, in contrast to polyethylene oxide, consists of polymer molecules differing in degree of tacticity and hence in ability to crystallize, it is not surprising that there is no portion of the vapour pressure curve

\*Details of which are in the Appendix to this paper.

Table 1. The variation of  $p_1/p_1^0$  and  $\chi_1$  with  $\phi_2$  for polypropylene (B) in diethyl ketone

25°C			35°C		
$\phi_2$	$p_1/p_1^0$	$\chi_1$	$\phi_2$	$p_1/p_1^0$	$\chi_1$
0.882 <sub>5</sub>	0.932 <sub>5</sub>	1.51	0.881 <sub>6</sub>	0.904 <sub>4</sub>	1.46
0.905 <sub>3</sub>	0.887 <sub>0</sub>	1.61	0.904 <sub>7</sub>	0.860 <sub>6</sub>	1.56
0.921 <sub>0</sub>	0.845 <sub>9</sub>	1.71	0.920 <sub>6</sub>	0.816 <sub>1</sub>	1.64
0.936 <sub>7</sub>	0.788 <sub>2</sub>	1.81	0.936 <sub>5</sub>	0.755 <sub>5</sub>	1.76
0.950 <sub>8</sub>	0.712 <sub>9</sub>	1.91	0.950 <sub>7</sub>	0.679 <sub>8</sub>	1.85
0.963 <sub>0</sub>	0.619 <sub>9</sub>	2.00	0.963 <sub>0</sub>	0.588 <sub>6</sub>	1.95
0.974 <sub>8</sub>	0.492 <sub>2</sub>	2.11	0.974 <sub>8</sub>	0.466 <sub>5</sub>	2.05
0.983 <sub>7</sub>	0.367 <sub>6</sub>	2.21	0.983 <sub>7</sub>	0.342 <sub>3</sub>	2.14
0.991 <sub>2</sub>	0.227 <sub>7</sub>	2.31	0.991 <sub>3</sub>	0.211 <sub>3</sub>	2.25
0.996 <sub>3</sub>	0.111 <sub>9</sub>	2.44	0.996 <sub>3</sub>	0.118 <sub>0</sub>	2.49
0.997 <sub>7</sub>	0.081 <sub>3</sub>	2.59	0.997 <sub>7</sub>	0.072 <sub>6</sub>	2.48

where  $p_1$  is constant. The rapid rise in  $p_1$  is no doubt due to the insolubility of the more stereoregular molecules in the sample. In other words, the first additions of liquid to the polymer are not uniformly dispersed, but are confined to disordered regions of the polymer-liquid mixture in which the liquid concentration, and therefore  $p_1$ , is comparatively high. This explanation suggests the possible use of vapour pressure studies at low liquid levels to study minor degrees of crystalline order.

## APPENDIX

THE VAPOUR PRESSURE OF CHLOROFORM OVER  
POLYETHYLENE OXIDE SOLUTIONS

Vapour pressures at 25°C were measured in the modified manometer described in Part I. Polyethylene oxide was purified by adding cyclohexane to a dilute solution in carbon tetrachloride and drying the precipitated polymer *in vacuo*. The molecular weight, by end group analysis, was 6 000 (measured by the manufacturer Oxirane Ltd, Manchester) and the density was estimated to be 1.248 g/ml at 25°C (by extrapolating the known densities for lower molecular weight polymers<sup>35</sup> to 6 000). The chloroform was the sample described in Part II. The results are given in Table 2.

Table 2. The variation of  $p_1/p_1^0$  with  $\phi_2$  for polyethylene oxide and chloroform

$\phi_2$	$p_1/p_1^0$	$\phi_2$	$p_1/p_1^0$
0.216	0.912	0.576	0.433
0.286	0.833	0.673	0.431
0.382	0.687	0.799	0.437
0.480	0.526	0.894	0.418
0.505	0.486	0.934	0.407
		0.975	0.181

Department of Chemistry,  
University of Manchester

(Received August 1963)

## REFERENCES

- <sup>1</sup> FLORY, P. J. *Principles of Polymer Chemistry*, Ch. 12. Cornell University Press: New York, 1953
- <sup>2</sup> GEE, G. and TRELOAR, L. R. G. *Trans. Faraday Soc.* 1942, **38**, 147
- <sup>3</sup> GEE, G. and ORR, W. J. C. *Trans. Faraday Soc.* 1946, **42**, 507
- <sup>4</sup> BOOTH, C., GEE, G. and WILLIAMSON, G. R. *J. Polym. Sci.* 1957, **23**, 3
- <sup>5</sup> TIMMERMANN, J. *Physicochemical Constants of Pure Organic Compounds*. Elsevier: Amsterdam, 1950
- <sup>6</sup> BAKER, C. H., BROWN, W. B., GEE, G. ROWLINSON, J. S., STUBLEY, D. and YEADON, R. B. *Polymer, Lond.* 1962, **3**, 215
- <sup>7</sup> LAMBERT, J. D., ROBERTS, G. A. H., ROWLINSON, J. S. and WILKINSON, V. J. *Proc. Roy. Soc. A*, 1949, **149**, 113
- <sup>8</sup> LAMBERT, J. D., CLARK, J. S., DUKE, J. F., HICKS, C. L., LAWRENCE, S. D., MORRIS, D. M. and SHONE, M. G. T. *Proc. Roy. Soc. A*, 1959, **249**, 414
- <sup>9</sup> ROBERTS, D. E. and MANDELKERN, L. *J. Amer. chem. Soc.* 1955, **77**, 781
- <sup>10</sup> MULLINS, L., RIVLIN, R. S. and GUMBRELL, S. M. *Trans. Faraday Soc.* 1953, **49**, 1495
- <sup>11</sup> ORR, W. J. C. *Trans. Faraday Soc.* 1944, **40**, 320
- <sup>12</sup> GUGGENHEIM, E. A. *Proc. Roy. Soc. A*, 1944, **183**, 203
- <sup>13</sup> FERRY, J., GEE, G. and TRELOAR, L. R. G. *Trans. Faraday Soc.* 1945, **41**, 340
- <sup>14</sup> FLORY, P. J. *Principles of Polymer Chemistry*, Ch. 12. Cornell University Press: New York, 1953
- <sup>15</sup> BAWN, C. E. H. and PATEL, R. D. *Trans. Faraday Soc.* 1956, **52**, 1664
- <sup>16</sup> KRIGBAUM, W. R. and GEYMER, D. O. *J. Amer. chem. Soc.* 1959, **81**, 1859
- <sup>17</sup> SENEZ, M. and DAOUST, H. *Canad. J. Chem.* 1962, **40**, 734
- <sup>18</sup> MAGAT, H. and DER MINNASSIAN, L. *J. Chim. phys.* 1951, **48**, 574
- <sup>19</sup> SCHMOLL, K. and JENKEL, R. *Z. Elektrochem.* 1956, **60**, 756
- <sup>20</sup> BAWN, C. E. H., FREEMAN, R. J. F. and KAMILIDIN, A. B. *Trans. Faraday Soc.* 1950, **46**, 677
- <sup>21</sup> TOMPA, H. *Polymer Solutions*, Ch. 5. Butterworths: London, 1956
- <sup>22</sup> SCHULZ, G. V. and HORBACH, A. *Z. phys. Chem.* 1959, **22**, 377
- <sup>23</sup> AMAYA, K. and FUJISHIRO, R. *Bull. chem. Soc. Japan*, 1956, **29**, 270
- <sup>24</sup> BAWN, C. E. H. and WAJID, M. J. *Trans. Faraday Soc.* 1956, **52**, 1658
- <sup>25</sup> NEWING, M. J. *Trans. Faraday Soc.* 1950, **46**, 613
- <sup>26</sup> JESSUP, R. S. *J. Res. Nat. Bur. Stand.* 1958, **60**, 47; 1959, **62**, 1
- <sup>27</sup> HUGGINS, M. L. *Industr. Engng Chem. (Industr.)*, 1943, **35**, 216
- <sup>28</sup> LENS, J. *Rec. Trav. chim. Pays-Bas*, 1932, **51**, 971
- <sup>29</sup> BAUGHAN, E. C. *Trans. Faraday Soc.* 1948, **44**, 495
- <sup>30</sup> PRAGER, S., BAGLEY, E. and LONG, F. A. *J. Amer. chem. Soc.* 1953, **75**, 2742
- <sup>31</sup> VAN DER WAALS, J. H. and HERMANS, J. J. *Rec. Trav. chim. Pays-Bas*, 1950, **69**, 971
- <sup>32</sup> KRIGBAUM, W. R. *J. Polym. Sci.* 1956, **19**, 159
- <sup>33</sup> KOBE, K. A. and LYNN, R. E. *Chem. Rev.* 1953, **52**, 117
- <sup>34</sup> WILKINSON, R. W. and DOLE, M. J. *Polym. Sci.* 1962, **58**, 1089
- <sup>35</sup> CURME, G. E. and JOHNSTON, F. *Glycols*, p 183. Reinhold: New York, 1953

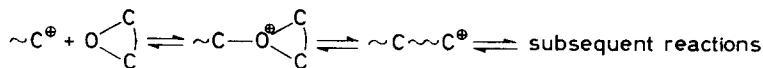
# Copolymerization of Trioxan with Dioxolan

MILOSLAV KUČERA and JIRI PICHLER

The authors have studied the bulk copolymerization of dioxolan with excess trioxan. The  $\sim\text{Si}^{\oplus}\text{HSO}_4^{\ominus}$  complex was used as initiator. The copolymerization scheme is too complicated for an exact analysis; it was therefore simplified by making several assumptions which proved plausible in a subsequent check of theory against experiment. In the authors' opinion copolymerization takes place on active centres ( $\sim\text{trioxan}^+$ ,  $\sim\text{dioxolan}^+$ ) which are of approximately the same activity or, in other words, addition of the monomeric unit of any type does not alter the quality of the active centre. Dioxolan enters the polymer chain during copolymerization more readily than trioxan. A comparison of the rates of polymerization of pure components leads to opposite results. A probable explanation of this is that the actual concentration of dioxolan in the neighbourhood of an active centre is higher than the analytical (overall) concentration. In terms of this view the active centres are preferentially solvated by dioxolan. Similar effects in other pairs of monomers in ionic copolymerization have been described in the literature. Quantitative data about solvation of active centres are not known. Solvation, however, influences the value of monomer reactivity ratios. The authors define the so-called 'modified monomer reactivity ratios' which make it possible to calculate the composition of the copolymer. The calculation has been verified experimentally in the range of low concentrations of dioxolan.

PREPARATION of high molecular weight polyacetal by copolymerizing trioxan with dioxolan seems to be a simple matter. Both components have a similar chemical structure and their physical properties cause no trouble in copolymerization. The reaction has received due interest in various laboratories and some of the results have been published<sup>1,2</sup>. Dioxolan can serve as a model substance for studies in copolymerization of its derivatives with trioxan. We therefore did not content ourselves with available data (which are of preliminary character), but sought more detailed information. Copolymerization of trioxan with dioxolan can serve also as a model for studies in the cationic copolymerization of heterocycles containing two oxygen atoms.

The basic considerations concerning the addition of separate monomer molecules on active centres are based on our previous work dealing with the homopolymerization of trioxan<sup>3-5</sup>. Also the experimental technique of some of the measurement is that of the previous communications. The copolymerization is assumed to proceed as follows:

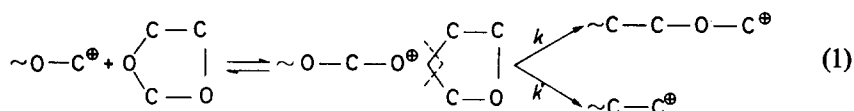


The symbol  $\text{O} \begin{array}{c} \diagup \text{C} \\ \diagdown \text{C} \end{array}$  can stand for either trioxan or dioxolan which



react with an active centre with subsequent formation of a transitional complex whose decomposition either regenerates the original active centre or an active centre linked to a correspondingly longer chain. The rate-determining step in the trioxan polymerization is known<sup>4</sup>. The polymerization of dioxolan has already been studied<sup>6</sup>. Unfortunately, we do not know which is the quicker reaction, the formation of an active centre with dioxolan or its decomposition through a subsequent reaction. The electron density at the oxygen atoms in trioxan differs from that in dioxolan and this could produce differences in rate constants of addition on active centres.

When compared with trioxan, dioxolan is a somewhat different copolymerization component. Its complex with an active centre can decompose in two different ways: either it regenerates an active centre of the original structure or it can decompose to yield a centre having a different structure:



A result of the asymmetric structure of the dioxolan molecule may be a preferential splitting of a certain —O—C— link of the transitional complex.

#### EXPERIMENTAL

##### *Purification and preparation of raw materials*

Trioxan and the initiator were purified as described<sup>3</sup>.

Dioxolan was prepared by condensing ethylene glycol with formaldehyde in the presence of a strong mineral acid as catalyst<sup>10</sup>. Ethylene glycol was a pure commercial product; paraformaldehyde was 75 per cent pure and sulphuric acid 96 per cent. Formaldehyde was used in 15 per cent excess over theory. Sulphuric acid was used in the amount of two per cent based on the glycol. The dioxolan–water azeotrope obtained upon distillation was dehydrated by calcium chloride and dioxolan was dried by a two-stage distillation over sodium. The purity of dioxolan was checked by gas chromatography<sup>12</sup> and the water content by the K. Fischer method. Dioxolan used for further work was chromatographically pure and contained approximately 100 p.p.m. water.

##### *Apparatus*

Copolymerization was carried out in glass vessels of approximately 20 ml content provided with metal caps with rubber gasketing covered by a polyethylene foil. The cap was provided with a bore for the use of a hypodermic needle. Mixing of the reaction mixture was secured by rotating these reactors in a thermostatically controlled bath. The polymerization of trioxan and dioxolan alone was studied in dilatometers as described<sup>11</sup>.

##### *Technique*

The mixture of monomers was measured out from thermostatically controlled burettes into the reactors containing initiator solution which had previously been measured out from a microburette. The reactors were

## COPOLYMERIZATION OF TRIOXAN WITH DIOXOLAN

closed and placed in a thermostatically controlled bath. Polymerization was halted by 1 ml of 25 per cent aqueous ammonia injected into the reactor through the hypodermic needle and by cooling. The contents of the reactors were extracted at room temperature by distilled water and filtered. The content of unreacted monomers was determined chromatographically<sup>11</sup> in the filtrate.

## RESULTS

Results of analysis of the monomer phase in trioxan-dioxolan copolymerization are shown in *Table 1*. Copolymerization took place at 70°C and was initiated by the  $\sim\text{Si}^{\oplus}\text{HSO}_4^{\ominus}$  complex<sup>3</sup>.

For a study of copolymerization it is very useful to compare the rate of copolymerization with the rate of polymerization of pure monomer components in otherwise identical conditions. Conversion curves of the polymerization of trioxan and dioxolan at 70°C are shown in *Figure 1*.

*Table 1.* Composition of monomer feed and of copolymer

Series	Run No.	Conversion %	Monomer		Polymer		n
			$x_T$	$x_D$	$y_T$	$y_D$	
I	—	0	0.96	0.04	—	—	—
	1	3.4	0.967	0.033	0.94	0.06	0.517
	2	4.7	0.965	0.035	0.94	0.06	0.568
	3	18.8	0.966	0.034	0.921	0.079	0.843
	4	24.3	0.97	0.03	0.943	0.057	0.543
	5	38.9	0.98	0.02	0.943	0.057	0.512
II	—	0	0.962	0.038	—	—	—
	1	18.5	0.964	0.036	0.951	0.049	0.739
	2	23.3	0.967	0.033	0.946	0.054	0.646
	3	31.0	0.968	0.032	0.949	0.051	0.679
	4	59.1	0.968	0.032	0.957	0.043	0.817
	5	69.7	0.971	0.029	0.958	0.042	0.812
III	—	0	0.920	0.080	—	—	—
	1	15.2	0.933	0.067	0.865	0.135	0.506
	2	18.6	0.923	0.077	0.907	0.093	0.835
	3	23.0	0.954	0.046	0.808	0.192	0.278
	4	29.2	0.942	0.058	0.867	0.133	0.484
	5	41.2	0.933	0.067	0.902	0.098	0.738
	6	50.2	0.967	0.033	0.874	0.126	0.410
IV	—	0	0.798	0.202	—	—	—
	1	30.4	0.845	0.155	0.691	0.309	0.489
	2	33.7	0.838	0.162	0.721	0.279	0.577
	3	43.0	0.844	0.156	0.739	0.261	0.620
	4	53.7	0.827	0.173	0.774	0.226	0.794
	5	62.0	0.830	0.170	0.779	0.221	0.814

NOTE:  $x_T$  denotes molar ratio of trioxan in monomer feed.  
 $x_D$  denotes molar ratio of dioxolan in monomer feed.  
 $y_T$  denotes molar ratio of trioxan in the copolymer.  
 $y_D$  denotes molar ratio of dioxolan in the copolymer.

Initiator concentration: I:  $3.3 \times 10^{-3}$  mole  $\text{kg}^{-1}$

II:  $2.5 \times 10^{-4}$  mole  $\text{kg}^{-1}$

III:  $8.2 \times 10^{-3}$  mole  $\text{kg}^{-1}$

IV:  $3.3 \times 10^{-3}$  mole  $\text{kg}^{-1}$

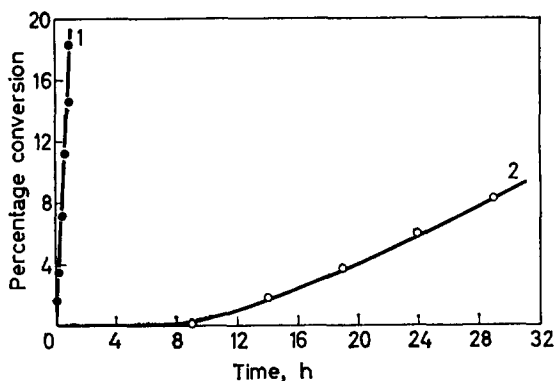
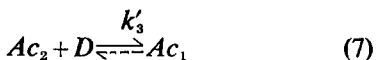
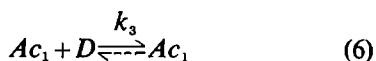
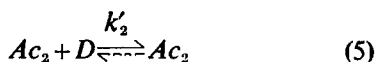
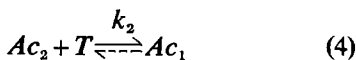
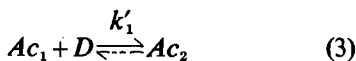
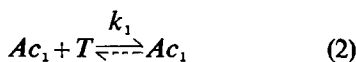


Figure 1—Conversion curve of the copolymerization of trioxan and dioxolan. Temperature 70°C, initiator concentration  $2.1 \times 10^{-3}$  mole  $\text{kg}^{-1}$ . (1) trioxan; (2) dioxolan

### DISCUSSION

Let us designate concentrations as follows: trioxan molecules by  $T$ , dioxolan molecules by  $D$ , the active centre  $\sim \overline{\text{O}}-\text{C}^{\oplus}$  as  $Ac_1$  and the active centre  $\sim \text{C}-\text{C}^{\oplus}$  as  $Ac_2$ . The copolymerization can be described as follows:



where  $k_1, k'_1, k_2, \dots, k_3$  are rate constants of the rate-determining steps of the body of consecutive reactions giving rise to a new active centre linked to a longer chain. This scheme has no exact analytical solution. An approximate solution is possible if the two following assumptions hold:

(1) The reverse reactions do not take place. Since the polymerization of trioxan and its copolymerization with dioxolan (in the range of compositions studied) is accompanied by the precipitation of polymer out of solution, the depolymerization is suppressed. Precipitation can reduce depolymerization of macromolecules to a negligible extent.

(2) One of the rate constants,  $k$  or  $k'$  in equation (2) is negligible when compared with the other or, alternatively, the reactivities of  $Ac_1$  and  $Ac_2$  are the same. Let us consider several possible cases.

#### Case I

If  $k \rightarrow 0$ , then  $k_3 = k'_3 = 0$ .

The remaining four equations form a reaction scheme from which Alfrey and Goldfinger deduced their copolymerization equation<sup>7</sup>. The function obtained upon integrating the copolymerization equation can be written in the following form ( $T_0$  and  $D_0$  stand for the initial concentration of trioxan and dioxolan):

$$\frac{k_2}{k_2 - k_2'} \ln \left( \frac{D_0 T}{D T_0} \right) + \frac{k_1 k_2 - k_1 k_2'}{(k_1 - k_1')(k_2 - k_2')} \ln \left( \frac{D_0 [T k_2 (k_1 - k_1') + D k_1' (k_2 - k_2')]}{D [T_0 k_2 (k_1 - k_1') + D_0 k_1' (k_2 - k_2')]} \right) = \ln \left( \frac{D}{D_0} \right) \quad (8)$$

Case II

If  $k' = 0$ , then  $k_1' = k_2' = 0$ .

The copolymerization scheme degrades in this case to the two reactions (2) and (6). The solution of this simplified scheme yields

$$T/T_0 = (D/D_0)^{k_2/k_1} \quad (9)$$

Case III

Assuming that  $A_{c_1}$  and  $A_{c_2}$  possess the same activity this case is formally identical with case II. If the activity of  $A_{c_1}$  and  $A_{c_2}$  is equal, the relation  $k_1' k_2 = k_1 k_2'$  must hold and the second term on the LHS of equation (8) is zero. Upon rearrangement one obtains

$$T/T_0 = (D/D_0)^{k_2/k_1'} \quad (10)$$

The solution of cases II and III is identical with an equation developed for a different mechanism by Wall<sup>8</sup>.

Evaluation of the results in *Table 1* by means of equation (8) is impossible. Let us assume therefore that in the first approximation reactivities of both active centres are not too different one from the other, or that, in equation (1),  $k \gg k'$ . In such a case we can use an approximate but simple formula

$$T/T_0 = [D/D_0]^n \quad (11)$$

The last column of *Table 1* which gives the values of  $n$  shows that  $n$  is roughly constant. The dependence of experimental values of  $\log T/T_0$  versus  $\log D/D_0$  is shown in *Figure 2*. The scatter in  $n$  is large, especially in high conversions; nevertheless, we may conclude that the assumptions made are roughly fulfilled. It is evident from *Table 1* that dioxolan disappears from the monomer phase at a faster rate than trioxan. A glance at curves 1 and 2 of *Figure 1* will show that the rate of homopolymerization of trioxan is higher than that of dioxolan. The explanation of this contradiction is difficult. It may be assumed as a qualitative explanation that dioxolan is preferentially solvated on active centres; the product of the rate constant and the actual concentration is higher for dioxolan than for trioxan. Similar effects were first observed and described by Rakova and Korotkov<sup>9</sup>.

If an active centre is preferentially solvated by one of the components of the system,  $n$  cannot be identical with the ratio  $k_2/k_2'$  since we substitute analytical (overall) concentrations in equation (10) and the actual concentration in the nearest neighbourhood may be different. But even in these conditions a linear dependence of  $\log T/T_0$  versus  $\log D/D_0$  should hold. This is justified as follows.

Let us designate the actual concentrations of trioxan and dioxolan as  $T$  and  $D$  and the analytical concentrations as  $T_A$  and  $D_A$  respectively. If we now use for expressing the actual concentration in the neighbourhood of

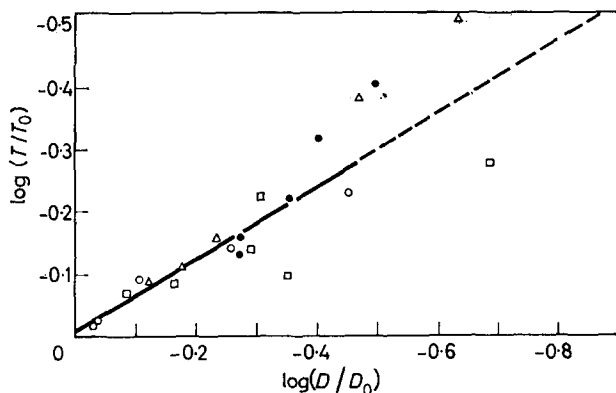


Figure 2—Dependence of  $\log T/T_0$  versus  $\log D/D_0$ . Slope  $n=0.57$

the solvated active centre a relation similar to the Freundlich absorption isotherm, we may write

$$T/T_0 = \alpha (T_A/T_0)^p \quad \text{and} \quad D/D_0 = \beta (D_A/D_0)^q$$

In these expressions  $\alpha$ ,  $\beta$ ,  $p$  and  $q$  are constants. Substituting in (10) and rearranging gives

$$\log T_A/T_0 = \log a + b (k_2/k'_2) \log D_A/D_0 \quad (12)$$

In equation (12)

$$a = (\beta/\alpha)^{1/p} \quad ; \quad q/p = b < 1$$

Equation (12) is the equation of a straight line (see *Figure 2*).

The monomer reactivity ratios  $r_1 = k_1/k'_1$  and  $r_2 = k_2/k'_2$  as defined in the general theory cannot be used to calculate copolymerization diagrams in this type of ionic polymerization with solvated active centres unless the constant  $b$  is known. The value of  $n$  can be established directly by experiment. Let us again use the assumption that  $k_1 k'_2 = k_2 k'_1$ . Then

$$n = b k_2/k'_2 = b k_1/k'_1$$

Let us introduce

$$k_2/b k'_2 = l_1 \quad \text{and} \quad b k_1/k'_1 = l_2$$

where  $l_1$  and  $l_2$  are 'modified monomer reactivity ratios' which can be used in a solvated system.

In our case  $l_1 l_2 = 1$ ; it follows from *Table 1* that  $l_1 = 1.75$  ('modified monomer reactivity ratio' of the faster reacting monomer dioxolan) and therefore for trioxan  $l_2 = 0.57$ . The copolymerization curve for these values of  $l_1$  and  $l_2$  is shown in *Figure 3* which also displays experimental points.

A serious handicap in attempts to verify the right shape of the copolymerization curve lies in the change of properties of the polymerizing system trioxan-dioxolan at higher contents of dioxolan. Polydioxolan and copolymers with a high content of D are soluble in the reaction medium and the experimental technique used by us is no longer suitable. The solubility of the product being formed can invalidate some of the basic assumptions

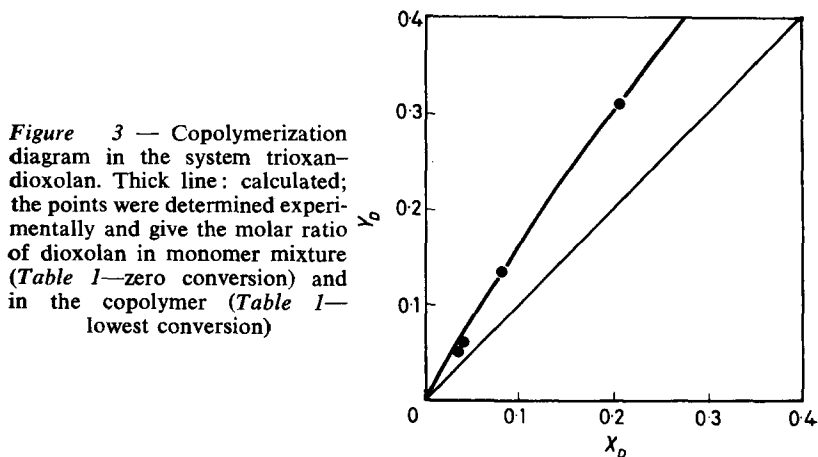


Figure 3 — Copolymerization diagram in the system trioxan-dioxolan. Thick line: calculated; the points were determined experimentally and give the molar ratio of dioxolan in monomer mixture (Table I—zero conversion) and in the copolymer (Table I—lowest conversion)

(e.g. the assumed suppression of the depolymerization by precipitation of the product). That is why systems with a higher dioxolan content have not been studied so far.

#### CONCLUSION

Exact analysis of the copolymerization of trioxan and dioxolan is impossible at present. An approximate solution is possible at the cost of making several assumptions. The acceptability of such assumptions is open to discussion; however, experimental results correspond with good accuracy to relationships derived theoretically. Equations used make it possible (together with values of constants derived in the paper) to calculate the composition of the product of bulk copolymerization of dioxolan in excess trioxan and to attempt a solution of the mechanism of the processes involved.

Research Institute of Macromolecular Chemistry,  
Brno, Czechoslovakia

(Received October 1963)

#### REFERENCES

- <sup>1</sup> U.S. Patent No. 2 989 511
- <sup>2</sup> JAACKS, V. *Dissertation*. University of Mainz, 1959
- <sup>3</sup> KUČERA, M. and SPOUSTA, E. *J. Polym. Sci.* In press
- <sup>4</sup> KUČERA, M. and SPOUSTA, E. *J. Polym. Sci.* In press
- <sup>5</sup> KUČERA, M. and SPOUSTA, E. *J. Polym. Sci.* In press
- <sup>6</sup> OKADA, N. I. *Kogyō Kagaku Zasshi*, 1962, **65**, 691; *Chem. Abstr.* 1962, **57**, 15345
- <sup>7</sup> ALFREY, T. and GOLDFINGER, G. *J. chem. Phys.* 1944, **12**, 205
- <sup>8</sup> WALL, F. T. *J. Amer. chem. Soc.* 1941, **63**, 1862
- <sup>9</sup> RAKOVA, G. V. and KOROTKOV, A. A. *Dokl. Akad. Nauk S.S.S.R.*, 1958, **199**(5), 982
- <sup>10</sup> WALKER, F. J. *Formaldehyde*, 2nd ed., p 234. New York, 1953
- <sup>11</sup> KUČERA, M. and SPOUSTA, E. *Chem. Listy*, 1963, **57**, 842
- <sup>12</sup> OTTO, K. Unpublished results, Research Institute of Macromolecular Chemistry, Brno

# *Polymer Physics Meeting— Shrivenham April 1964*

APPROXIMATELY one hundred and sixty scientists attended a polymer physics meeting held at the Royal Military College of Science on 1 to 3 April. At a short business meeting, it was resolved to continue meetings of this type and also provide for one-day meetings on topics of current interest under the auspices of a British polymer physics discussion group. Initially, at least, the group will not be affiliated to an existing Institute or Society and a provisional committee of eight under the Chairmanship of Professor F. C. FRANK (University of Bristol) has been elected. Dr I. M. WARD, I.C.I. Ltd, Fibres Division, Harrogate, Yorks., is the Secretary.

There follow abstracts of all the papers presented for discussion at this meeting.

## **Session on Crystalline Morphology**

### *Introductory Talk: Recent Results, Trends and Problems in the Research on the Morphology of Crystalline Polymers*

A. KELLER, H. H. Wills Physics Laboratory, University of Bristol,  
Royal Fort, Bristol 8

A general survey on present-day morphological research was presented. This included results and ideas from Bristol University and elsewhere as far as available to the author. The issues around which this survey was centred included: relation between crystallization from solution and from the melt, the problem of regular or irregular folds, deformation processes in terms of the morphology, and the effect of the morphology on physical properties.

## SHORT CONTRIBUTIONS

### *A Single Crystal Model for the Crystallization Rate of Bulk Polymethylene*

M. GORDON and I. H. HILLIER, Chemistry Department,  
Imperial College of Science and Technology, London S.W.7

New dilatometric measurements on the primary bulk crystallization kinetics of polymethylene, in absence of the usual secondary crystallization, are fitted to variants of a single-crystal folded-chain platelet model. Non-coherent secondary nucleation, leading to spherulitic growth, is rejected. Extensive use of computers has made possible improvements in the statistical analysis. There appear to be two kinds of coherent, secondary two-dimensional nucleation acts, one associated with corner sites and another with face-sites on the growing platelets. An equation by Eyring, which generalizes Maxwell's treatment for the relaxation of matter is shown to fit the secondary process (lamellar thickening), which can be kinetically isolated, more exactly than an empirical  $\log(t)$  relationship. Electron microscopy supports the existence of lamellae in polyethylene.

## *The Nucleation Process in Polymer Crystallization*

A. SHARPLES, Arthur D. Little Research Institute, Inveresk,  
Musselburgh, Midlothian, Scotland

A study has been made of the factors which affect the nucleation of spherulites in crystallizing polymer systems. In general, the nuclei are found to arise from heterogeneities, which suggests that control over their concentration should be easier to achieve than would have been expected for a homogeneous process. In fact, strain partial melting below the true melting point and, exceptionally, variation of melt temperature above the melting point, were all found to affect the subsequent nucleation density.

## *Strain-induced Crystallization in Natural Rubber*

E. H. ANDREWS, Queen Mary College, London E.1

The techniques employed in an earlier study of thermal crystallization in natural rubber (*Proc. Roy. Soc. A*, 1962, **270**, 232) have been used to investigate the kinetics and morphology of strain-induced crystallization in this material. Cast films, strained to known extents, were held at various temperatures from  $-28^{\circ}\text{C}$  to  $+20^{\circ}\text{C}$  and examined on the cold-stage of the Elmiskop I electron microscope. As the pre-strain varies from 0 to 200 per cent there is a gradual transition from a spherulitic mode of crystallization to a fibrillar one, the crystalline filaments running *perpendicular* to the direction of extension. These filaments are named  $\alpha$  filaments. In highly strained films ( $>300$  per cent extension) filaments lying *in* the direction of strain ( $\gamma$  filaments) are found. The  $\gamma$  filaments are shown to be composed of  $\alpha$  filament nuclei arranged in chain formation and to arise from the differential effects of strain and temperature on the kinetics of crystallization. The interpretation is confirmed by electron diffraction evidence.

The morphology and molecular orientation of the  $\alpha$  filaments are briefly discussed.

## *The Texture of Melt Crystallized Polyethylene as Revealed by Selective Oxidation*

R. P. PALMER and A. J. COBBOLD, Research Department, I.C.I. Ltd,  
Plastics Division, Welwyn Garden City

It has been discovered that when fuming nitric acid oxidizes bulk samples of polyethylene crystallized from the melt, preferential attack on the links between the lamellar crystals occurs with the consequent release of fragments of these crystals. The reaction is not confined to the surface of samples and lamellar crystals can be separated from relatively massive specimens for further study.

Selected area electron diffraction results show that the molecular chains are oriented approximately perpendicular to the plane of the lamella and that the sheets are substantially single crystals.

The lamellar crystals and reaction products from samples with different thermal histories treated for different times have been examined by a variety of physical methods.

Analysis of the results confirms that the attack occurs preferentially at the amorphous regions which in the linear polymer are almost exclusively located between the lamellar crystals. In branched polymers some amorphous material probably exists as defects within the lamellae. After a treatment sufficient to release the individual lamellae from the bulk the molecular chain length is equal to the lamella thickness and thus at this stage no folds or links remain. At shorter times there is a progressive reduction in molecular weight and increase in crystallinity (and associated changes in other structural parameters). Comparison of the results from quenched samples with those from annealed samples suggests that the reaction may



discriminate between intralamellar folds and interlamellar links. Certainly folds are attacked as was demonstrated by an experiment on single crystals grown from solution. Careful control of the reaction conditions is necessary to obtain reproducible weight loss curves and a preliminary study of these suggests that it may be possible to estimate the amount of interlamellar amorphous material.

### *Some Observations on the Structure of Nylon 6.6 Spherulites Crystallized from the Melt*

P. H. HARRIS, British Nylon Spinners Ltd, Pontypool, Monmouthshire

Thin melt-crystallized films of Nylon 6.6 have been examined by transmission electron microscopy. At low beam intensities little structure is observed but at normal intensities a marked contrast enhancement occurs apparently coincident with the loss of crystallinity. The structure observed after this change can be correlated with that observed previously in the polarizing microscope.

Positively birefringent spherulites exhibit a conventional shearlike morphology but negatively birefringent and non-birefringent spherulites show no evidence of this.

It is considered that the contrast enhancement induced by the electron beam is probably due to thickness variations determined by the initial molecular orientation.

### *The Effect of Polymer Crystallization on Cationic Polymerization of Trioxan in Solution*

L. LEESE and M. W. BAUMBER, BX Plastics Ltd, Manningtree, Essex

The work of Kern and Jaacks on polymerization of trioxan in methylene chloride has been extended by a study in ethylene dichloride. Kinetics have been investigated chemically and by adiabatic calorimetry and results indicate that during an induction period soluble low molecular weight polymer is produced which eventually forms crystal nuclei. These initiate an accelerating reaction whose rate depends on the area of crystal surface available for polymer deposition or formation and equations have been obtained which describe the observed kinetics. The kinetic arguments are supported by photomicrographs of crystals at the various stages of polymerization, which indicate a progressive increase in the size of the original crystals rather than constant formation of fresh nuclei. The evidence strongly suggests that polymerization takes place at the growing crystal surface.

### **Session on Molecular Structure and Radiation Damage**

#### *Introductory Talk: The Determination of Polymer Structure by X-ray Diffraction*

C. W. BUNN, Royal Institution, London W.1

In principle, X-ray diffraction methods can give detailed information on the structure of crystalline polymers—the chain conformation, the stereo positions of side-groups (for instance, whether vinyl polymers are isotactic or syndiotactic), the arrangement of the molecules and the density of crystalline regions. A detailed crystal structure determination is a lengthy task, but sometimes valuable information on some of the aspects mentioned can be obtained readily and quickly.

The chain repeat distance (obtained straightforwardly from fibre photographs), together with basic stereochemical data like bond lengths and angles and the principle of staggered bonds, may point definitely to a particular chain conformation. The general distribution of intensity in the fibre diffraction pattern is also a valuable and powerful indication of the conformation, and may lead, for helical chains, to a knowledge of the number of monomer units and the number of turns of the helix

## *The Nucleation Process in Polymer Crystallization*

A. SHARPLES, Arthur D. Little Research Institute, Inveresk,  
Musselburgh, Midlothian, Scotland

A study has been made of the factors which affect the nucleation of spherulites in crystallizing polymer systems. In general, the nuclei are found to arise from heterogeneities, which suggests that control over their concentration should be easier to achieve than would have been expected for a homogeneous process. In fact, strain partial melting below the true melting point and, exceptionally, variation of melt temperature above the melting point, were all found to affect the subsequent nucleation density.

## *Strain-induced Crystallization in Natural Rubber*

E. H. ANDREWS, Queen Mary College, London E.1

The techniques employed in an earlier study of thermal crystallization in natural rubber (*Proc. Roy. Soc. A*, 1962, **270**, 232) have been used to investigate the kinetics and morphology of strain-induced crystallization in this material. Cast films, strained to known extents, were held at various temperatures from  $-28^{\circ}\text{C}$  to  $+20^{\circ}\text{C}$  and examined on the cold-stage of the Elmiskop I electron microscope. As the pre-strain varies from 0 to 200 per cent there is a gradual transition from a spherulitic mode of crystallization to a fibrillar one, the crystalline filaments running *perpendicular* to the direction of extension. These filaments are named  $\alpha$  filaments. In highly strained films ( $>300$  per cent extension) filaments lying *in* the direction of strain ( $\gamma$  filaments) are found. The  $\gamma$  filaments are shown to be composed of  $\alpha$  filament nuclei arranged in chain formation and to arise from the differential effects of strain and temperature on the kinetics of crystallization. The interpretation is confirmed by electron diffraction evidence.

The morphology and molecular orientation of the  $\alpha$  filaments are briefly discussed.

## *The Texture of Melt Crystallized Polyethylene as Revealed by Selective Oxidation*

R. P. PALMER and A. J. COBBOLD, Research Department, I.C.I. Ltd,  
Plastics Division, Welwyn Garden City

It has been discovered that when fuming nitric acid oxidizes bulk samples of polyethylene crystallized from the melt, preferential attack on the links between the lamellar crystals occurs with the consequent release of fragments of these crystals. The reaction is not confined to the surface of samples and lamellar crystals can be separated from relatively massive specimens for further study.

Selected area electron diffraction results show that the molecular chains are oriented approximately perpendicular to the plane of the lamella and that the sheets are substantially single crystals.

The lamellar crystals and reaction products from samples with different thermal histories treated for different times have been examined by a variety of physical methods.

Analysis of the results confirms that the attack occurs preferentially at the amorphous regions which in the linear polymer are almost exclusively located between the lamellar crystals. In branched polymers some amorphous material probably exists as defects within the lamellae. After a treatment sufficient to release the individual lamellae from the bulk the molecular chain length is equal to the lamella thickness and thus at this stage no folds or links remain. At shorter times there is a progressive reduction in molecular weight and increase in crystallinity (and associated changes in other structural parameters). Comparison of the results from quenched samples with those from annealed samples suggests that the reaction may

discriminate between intralamellar folds and interlamellar links. Certainly folds are attacked as was demonstrated by an experiment on single crystals grown from solution. Careful control of the reaction conditions is necessary to obtain reproducible weight loss curves and a preliminary study of these suggests that it may be possible to estimate the amount of interlamellar amorphous material.

### *Some Observations on the Structure of Nylon 6.6 Spherulites Crystallized from the Melt*

P. H. HARRIS, British Nylon Spinners Ltd, Pontypool, Monmouthshire

Thin melt-crystallized films of Nylon 6.6 have been examined by transmission electron microscopy. At low beam intensities little structure is observed but at normal intensities a marked contrast enhancement occurs apparently coincident with the loss of crystallinity. The structure observed after this change can be correlated with that observed previously in the polarizing microscope.

Positively birefringent spherulites exhibit a conventional shearlike morphology but negatively birefringent and non-birefringent spherulites show no evidence of this.

It is considered that the contrast enhancement induced by the electron beam is probably due to thickness variations determined by the initial molecular orientation.

### *The Effect of Polymer Crystallization on Cationic Polymerization of Trioxan in Solution*

L. LEESE and M. W. BAUMBER, BX Plastics Ltd, Manningtree, Essex

The work of Kern and Jaacks on polymerization of trioxan in methylene chloride has been extended by a study in ethylene dichloride. Kinetics have been investigated chemically and by adiabatic calorimetry and results indicate that during an induction period soluble low molecular weight polymer is produced which eventually forms crystal nuclei. These initiate an accelerating reaction whose rate depends on the area of crystal surface available for polymer deposition or formation and equations have been obtained which describe the observed kinetics. The kinetic arguments are supported by photomicrographs of crystals at the various stages of polymerization, which indicate a progressive increase in the size of the original crystals rather than constant formation of fresh nuclei. The evidence strongly suggests that polymerization takes place at the growing crystal surface.

### **Session on Molecular Structure and Radiation Damage**

#### *Introductory Talk: The Determination of Polymer Structure by X-ray Diffraction*

C. W. BUNN, Royal Institution, London W.1

In principle, X-ray diffraction methods can give detailed information on the structure of crystalline polymers—the chain conformation, the stereo positions of side-groups (for instance, whether vinyl polymers are isotactic or syndiotactic), the arrangement of the molecules and the density of crystalline regions. A detailed crystal structure determination is a lengthy task, but sometimes valuable information on some of the aspects mentioned can be obtained readily and quickly.

The chain repeat distance (obtained straightforwardly from fibre photographs), together with basic stereochemical data like bond lengths and angles and the principle of staggered bonds, may point definitely to a particular chain conformation. The general distribution of intensity in the fibre diffraction pattern is also a valuable and powerful indication of the conformation, and may lead, for helical chains, to a knowledge of the number of monomer units and the number of turns of the helix

in the repeat distance. The principles underlying this interpretation will be illustrated.

Preliminary interpretation on these lines should be followed up as far as possible, by the determination of the unit cell dimensions from the positions of the reflections (the unit cell leads to an accurate value for the density of crystalline regions), and the determination of atomic positions from the intensities of the reflections. The possibilities are limited by the circumstance that these determinations cannot be done directly, but must be attempted by trial and error methods.

## SHORT CONTRIBUTIONS

*Intermolecular Forces in Polymers—Calculation of Electrostatic Lattice Energies in Polyamides and Polypeptides*

C. G. CANNON, Research Department, B.N.S. Ltd, Pontypool

The importance of intermolecular forces in high polymer structures was reviewed with emphasis on structures growing from the melt or high concentration solutions. Calculations of the dipole contribution to the lattice energies of polyamides and polypeptides (R. G. C. ARRIDGE and C. G. CANNON, *Proc. Roy. Soc.* In press) show that electrostatic forces between CONH groups are responsible for about 5 kcal/mole. Approximate analysis of the relative magnitudes of electrostatic forces and hydrogen bonding reveal a balance between these two contributions which must be involved in the  $\alpha$  fold to  $\beta$  extended configurational changes in proteins.

*Conformation-sensitive Bands in the Infra-red Spectra of Polymers*

A. ELLIOTT, King's College, London W.C.2

The spectra of many polymers vary to some extent according to the relative amounts of crystalline and non-crystalline material present, and bands are sometimes referred to as 'crystalline' or 'amorphous'. Some of the latter are due to certain chain conformations and their intensity is a measure of the occurrence of such conformations, rather than of the non-crystalline forms. Estimates of crystalline/amorphous ratios based on such bands may be misleading.

*Introductory Talk: Survey of Recent Developments in Polymer Radiation Research*

A. CHARLESBY, Royal Military College of Science, Shrivenham

Exposure of polymers to high energy radiation produces a number of changes which can be used to study (i) radiation processes in solids, (ii) polymeric systems (when the degree of modification can be readily controlled by the radiation dose and intensity), (iii) radiation effects in macromolecules, with particular reference to intermediate processes which are of considerable importance in radiobiology.

At low doses purely physical effects appear such as radiation-induced conductivity and thermoluminescence. At higher doses small chemical changes result which cause drastic modifications in the physical properties.

The early work on polymerization showed that radiation merely initiates the reaction by the provision of radicals. Subsequent work has shown that ionic reactions can also be initiated by radiation. It would therefore appear that u.v. light, which can only provide excited species, is unable to produce such ionic systems.

It has recently been shown that ionic polymerization induced by radiation can be greatly enhanced by the presence of a variety of apparently inactive solid materials. This would point to unusual effects on the polymer/solid interface.

discriminate between intralamellar folds and interlamellar links. Certainly folds are attacked as was demonstrated by an experiment on single crystals grown from solution. Careful control of the reaction conditions is necessary to obtain reproducible weight loss curves and a preliminary study of these suggests that it may be possible to estimate the amount of interlamellar amorphous material.

### *Some Observations on the Structure of Nylon 6.6 Spherulites Crystallized from the Melt*

P. H. HARRIS, British Nylon Spinners Ltd, Pontypool, Monmouthshire

Thin melt-crystallized films of Nylon 6.6 have been examined by transmission electron microscopy. At low beam intensities little structure is observed but at normal intensities a marked contrast enhancement occurs apparently coincident with the loss of crystallinity. The structure observed after this change can be correlated with that observed previously in the polarizing microscope.

Positively birefringent spherulites exhibit a conventional shearlike morphology but negatively birefringent and non-birefringent spherulites show no evidence of this.

It is considered that the contrast enhancement induced by the electron beam is probably due to thickness variations determined by the initial molecular orientation.

### *The Effect of Polymer Crystallization on Cationic Polymerization of Trioxan in Solution*

L. LEESE and M. W. BAUMBER, BX Plastics Ltd, Manningtree, Essex

The work of Kern and Jaacks on polymerization of trioxan in methylene chloride has been extended by a study in ethylene dichloride. Kinetics have been investigated chemically and by adiabatic calorimetry and results indicate that during an induction period soluble low molecular weight polymer is produced which eventually forms crystal nuclei. These initiate an accelerating reaction whose rate depends on the area of crystal surface available for polymer deposition or formation and equations have been obtained which describe the observed kinetics. The kinetic arguments are supported by photomicrographs of crystals at the various stages of polymerization, which indicate a progressive increase in the size of the original crystals rather than constant formation of fresh nuclei. The evidence strongly suggests that polymerization takes place at the growing crystal surface.

### **Session on Molecular Structure and Radiation Damage**

#### *Introductory Talk: The Determination of Polymer Structure by X-ray Diffraction*

C. W. BUNN, Royal Institution, London W.1

In principle, X-ray diffraction methods can give detailed information on the structure of crystalline polymers—the chain conformation, the stereo positions of side-groups (for instance, whether vinyl polymers are isotactic or syndiotactic), the arrangement of the molecules and the density of crystalline regions. A detailed crystal structure determination is a lengthy task, but sometimes valuable information on some of the aspects mentioned can be obtained readily and quickly.

The chain repeat distance (obtained straightforwardly from fibre photographs), together with basic stereochemical data like bond lengths and angles and the principle of staggered bonds, may point definitely to a particular chain conformation. The general distribution of intensity in the fibre diffraction pattern is also a valuable and powerful indication of the conformation, and may lead, for helical chains, to a knowledge of the number of monomer units and the number of turns of the helix

in the repeat distance. The principles underlying this interpretation will be illustrated.

Preliminary interpretation on these lines should be followed up as far as possible, by the determination of the unit cell dimensions from the positions of the reflections (the unit cell leads to an accurate value for the density of crystalline regions), and the determination of atomic positions from the intensities of the reflections. The possibilities are limited by the circumstance that these determinations cannot be done directly, but must be attempted by trial and error methods.

## SHORT CONTRIBUTIONS

*Intermolecular Forces in Polymers—Calculation of Electrostatic Lattice Energies in Polyamides and Polypeptides*

C. G. CANNON, Research Department, B.N.S. Ltd, Pontypool

The importance of intermolecular forces in high polymer structures was reviewed with emphasis on structures growing from the melt or high concentration solutions. Calculations of the dipole contribution to the lattice energies of polyamides and polypeptides (R. G. C. ARRIDGE and C. G. CANNON, *Proc. Roy. Soc.* In press) show that electrostatic forces between CONH groups are responsible for about 5 kcal/mole. Approximate analysis of the relative magnitudes of electrostatic forces and hydrogen bonding reveal a balance between these two contributions which must be involved in the  $\alpha$  fold to  $\beta$  extended configurational changes in proteins.

*Conformation-sensitive Bands in the Infra-red Spectra of Polymers*

A. ELLIOTT, King's College, London W.C.2

The spectra of many polymers vary to some extent according to the relative amounts of crystalline and non-crystalline material present, and bands are sometimes referred to as 'crystalline' or 'amorphous'. Some of the latter are due to certain chain conformations and their intensity is a measure of the occurrence of such conformations, rather than of the non-crystalline forms. Estimates of crystalline/amorphous ratios based on such bands may be misleading.

*Introductory Talk: Survey of Recent Developments in Polymer Radiation Research*

A. CHARLESBY, Royal Military College of Science, Shrivenham

Exposure of polymers to high energy radiation produces a number of changes which can be used to study (i) radiation processes in solids, (ii) polymeric systems (when the degree of modification can be readily controlled by the radiation dose and intensity), (iii) radiation effects in macromolecules, with particular reference to intermediate processes which are of considerable importance in radiobiology.

At low doses purely physical effects appear such as radiation-induced conductivity and thermoluminescence. At higher doses small chemical changes result which cause drastic modifications in the physical properties.

The early work on polymerization showed that radiation merely initiates the reaction by the provision of radicals. Subsequent work has shown that ionic reactions can also be initiated by radiation. It would therefore appear that u.v. light, which can only provide excited species, is unable to produce such ionic systems.

It has recently been shown that ionic polymerization induced by radiation can be greatly enhanced by the presence of a variety of apparently inactive solid materials. This would point to unusual effects on the polymer/solid interface.

Early work also showed the possibility of either degrading or crosslinking polymers by exposure to radiation. The degradation of polymethyl methacrylate has revealed that while the effects of u.v. and gamma radiation at room temperature are apparently identical they may differ very considerably at higher temperatures, possibly due to selective absorption by u.v. at the ends of the chains.

Some experiments are outlined which attempt to discover the nature of the reinforcement of rubbers by carbon black and of silicones by silica.

A relatively new field of radiation research concerns solid state polymerization. Two divisions may be considered (i) those in which the perfection of crystallinity is important; this generally provides an oriented polymer and (ii) a series of monomers in which imperfections and crystalline defects are important. At low temperatures radiation-induced polymerization in acrylonitrile goes to a maximum of 4.6 per cent and then ceases. On subsequent warming polymerization may go further. It is suggested that this is due to electrons trapped within the crystal, which are released at the transition points.

The crosslinking of polymers in solution is discussed and the importance of molecular configuration on the gelation dose outlined.

#### SHORT CONTRIBUTIONS

### *The Effect of Crystallinity on the Stability of Free Radicals in Irradiated Polyethylene*

M. G. ORMEROD, Royal Military College of Science, Shrivenham

The decay rates of free radicals in irradiated polyethylenes have been measured using electron spin resonance. It has been found that the free radical stability is strongly dependent on crystallinity and crystallite size.

### *Relation Between Radiation Induced Physical Changes and Crystalline Ordering in Polyethylene*

T. KAWAI, A. CHARLESBY, A. KELLER and M. G. ORMEROD,

University of Bristol and Royal Military College of Science, Shrivenham

#### *Part I. Solution grown single crystals*

Radiation-induced insolubility is very much reduced in single crystal preparations as compared with the bulk. Even within single crystals this depends on preparation conditions and it is inferred that it is a function of lamellar packing. Changes in the still fully soluble material—for low doses insufficient to produce gel—have been followed up by viscometry and light scattering in order to obtain information concerning inter- and intra-molecular crosslinking and possible preference of fold sites. Results concerning the effect of annealing of the radiation-induced insolubility and effects of radiation on molecular refolding when single crystals are annealed subsequent to irradiation are described.

#### *Part II. Bulk samples*

Large variations were found in the radiation-induced insolubility even in the melt crystallized specimens dependent on physical treatments such as crystallization conditions, annealing and deformation, for the same chemical changes involved. These variations are attributed to differences in neighbour-to-neighbour coordination of the molecules in general and to packing of lamellae within the bulk in particular. Such variations in the radiation-induced changes are indicative of differences in the materials which are inaccessible by other methods and could thus be used in the characterization of the polymer sample.

in the repeat distance. The principles underlying this interpretation will be illustrated.

Preliminary interpretation on these lines should be followed up as far as possible, by the determination of the unit cell dimensions from the positions of the reflections (the unit cell leads to an accurate value for the density of crystalline regions), and the determination of atomic positions from the intensities of the reflections. The possibilities are limited by the circumstance that these determinations cannot be done directly, but must be attempted by trial and error methods.

## SHORT CONTRIBUTIONS

*Intermolecular Forces in Polymers—Calculation of Electrostatic Lattice Energies in Polyamides and Polypeptides*

C. G. CANNON, Research Department, B.N.S. Ltd, Pontypool

The importance of intermolecular forces in high polymer structures was reviewed with emphasis on structures growing from the melt or high concentration solutions. Calculations of the dipole contribution to the lattice energies of polyamides and polypeptides (R. G. C. ARRIDGE and C. G. CANNON, *Proc. Roy. Soc.* In press) show that electrostatic forces between CONH groups are responsible for about 5 kcal/mole. Approximate analysis of the relative magnitudes of electrostatic forces and hydrogen bonding reveal a balance between these two contributions which must be involved in the  $\alpha$  fold to  $\beta$  extended configurational changes in proteins.

*Conformation-sensitive Bands in the Infra-red Spectra of Polymers*

A. ELLIOTT, King's College, London W.C.2

The spectra of many polymers vary to some extent according to the relative amounts of crystalline and non-crystalline material present, and bands are sometimes referred to as 'crystalline' or 'amorphous'. Some of the latter are due to certain chain conformations and their intensity is a measure of the occurrence of such conformations, rather than of the non-crystalline forms. Estimates of crystalline/amorphous ratios based on such bands may be misleading.

*Introductory Talk: Survey of Recent Developments in Polymer Radiation Research*

A. CHARLESBY, Royal Military College of Science, Shrivenham

Exposure of polymers to high energy radiation produces a number of changes which can be used to study (i) radiation processes in solids, (ii) polymeric systems (when the degree of modification can be readily controlled by the radiation dose and intensity), (iii) radiation effects in macromolecules, with particular reference to intermediate processes which are of considerable importance in radiobiology.

At low doses purely physical effects appear such as radiation-induced conductivity and thermoluminescence. At higher doses small chemical changes result which cause drastic modifications in the physical properties.

The early work on polymerization showed that radiation merely initiates the reaction by the provision of radicals. Subsequent work has shown that ionic reactions can also be initiated by radiation. It would therefore appear that u.v. light, which can only provide excited species, is unable to produce such ionic systems.

It has recently been shown that ionic polymerization induced by radiation can be greatly enhanced by the presence of a variety of apparently inactive solid materials. This would point to unusual effects on the polymer/solid interface.



Early work also showed the possibility of either degrading or crosslinking polymers by exposure to radiation. The degradation of polymethyl methacrylate has revealed that while the effects of u.v. and gamma radiation at room temperature are apparently identical they may differ very considerably at higher temperatures, possibly due to selective absorption by u.v. at the ends of the chains.

Some experiments are outlined which attempt to discover the nature of the reinforcement of rubbers by carbon black and of silicones by silica.

A relatively new field of radiation research concerns solid state polymerization. Two divisions may be considered (i) those in which the perfection of crystallinity is important; this generally provides an oriented polymer and (ii) a series of monomers in which imperfections and crystalline defects are important. At low temperatures radiation-induced polymerization in acrylonitrile goes to a maximum of 4.6 per cent and then ceases. On subsequent warming polymerization may go further. It is suggested that this is due to electrons trapped within the crystal, which are released at the transition points.

The crosslinking of polymers in solution is discussed and the importance of molecular configuration on the gelation dose outlined.

#### SHORT CONTRIBUTIONS

### *The Effect of Crystallinity on the Stability of Free Radicals in Irradiated Polyethylene*

M. G. ORMEROD, Royal Military College of Science, Shrivenham

The decay rates of free radicals in irradiated polyethylenes have been measured using electron spin resonance. It has been found that the free radical stability is strongly dependent on crystallinity and crystallite size.

### *Relation Between Radiation Induced Physical Changes and Crystalline Ordering in Polyethylene*

T. KAWAI, A. CHARLESBY, A. KELLER and M. G. ORMEROD,

University of Bristol and Royal Military College of Science, Shrivenham

#### *Part I. Solution grown single crystals*

Radiation-induced insolubility is very much reduced in single crystal preparations as compared with the bulk. Even within single crystals this depends on preparation conditions and it is inferred that it is a function of lamellar packing. Changes in the still fully soluble material—for low doses insufficient to produce gel—have been followed up by viscometry and light scattering in order to obtain information concerning inter- and intra-molecular crosslinking and possible preference of fold sites. Results concerning the effect of annealing of the radiation-induced insolubility and effects of radiation on molecular refolding when single crystals are annealed subsequent to irradiation are described.

#### *Part II. Bulk samples*

Large variations were found in the radiation-induced insolubility even in the melt crystallized specimens dependent on physical treatments such as crystallization conditions, annealing and deformation, for the same chemical changes involved. These variations are attributed to differences in neighbour-to-neighbour coordination of the molecules in general and to packing of lamellae within the bulk in particular. Such variations in the radiation-induced changes are indicative of differences in the materials which are inaccessible by other methods and could thus be used in the characterization of the polymer sample.

*The Thermoluminescence of Polyethylene and Other Polymers*

R. H. PARTRIDGE, Royal Military College of Science, Shrivenham

Many polymers irradiated with ionizing radiation at  $-196^{\circ}\text{C}$  exhibit thermoluminescence on subsequent warming. The thermoluminescence glow curves of polyethylenes and paraffins exhibit distinctive glow peaks due to their crystalline and amorphous regions. Kinetic studies of the glow peaks have shown that they are very sensitive to the molecular motion in the polymer, as also applies for u.v.-induced phosphorescence. Oxygen has a considerable effect on these glow curves.

This technique may be of value as an analytical tool in studying molecular configuration, and has been used to assess crystallinity in single crystals of polyethylene.

**Session on Visco-elasticity and Properties of Solid Polymers***Introductory Talks**(i) Rheology of Concentrated Polymer Solutions*

L. R. G. TRELOAR, College of Science and Technology, Manchester

Molecular theories of the rheological properties of polymers and polymer solutions are of two kinds. The first considers any given polymer molecule to be subjected to viscous forces arising from the flowing liquid in which it is immersed; the second treats the assembly of polymer molecules as a strained network which is continuously relaxing. This second type of theory, developed by Lodge, is an extension of the statistical theory of rubber elasticity; it gives a quantitative explanation of the normal stresses in shear flow (Weissenberg effects) and predicts a simple relation between mechanical and optical properties in any state of flow.

The basis of Lodge's theory was discussed, and methods designed to test its conclusions considered.

*(ii) Viscoelastic Relaxation in Polymer Liquids*

J. LAMB, University of Glasgow

Non-Newtonian behaviour of liquids is associated with a decrease in the effective viscosity with increasing frequency of an applied cyclic shearing stress and is accompanied by evidence of solid-like behaviour in the observed increase in the shear modulus of rigidity. Alternating stress measurements are amplitude independent under normal experimental conditions and it is now possible to work with shear waves varying from audio frequencies to thousands of megacycles per second.

A description is given of the results of an extensive series of measurements on a range of polydimethyl siloxane liquids of viscosity grades ranging from 100 cS to 100000 cS. Using reduced variables the components of the shear modulus and the dynamic viscosity have been determined as a function of frequency, normalized to a temperature of  $30^{\circ}\text{C}$ .

The theory of Rouse, originally devised to account for the viscoelastic behaviour of monodisperse polymers in dilute solution, has been developed by Ferry and others to explain the behaviour of undiluted polydisperse liquid polymers. It is shown that this theory adequately described the viscoelastic relaxation of low molecular weight siloxane liquids in which entanglement coupling is absent. The theory has been further developed in order to account for the viscoelastic behaviour of the higher molecular weight siloxanes in which entanglement contributions to the steady flow viscosity predominate.

It has proved possible to predict successfully the viscoelastic behaviour over some seven decades of frequency from a knowledge only of the molecular weight distribution and of the dependence of the steady flow viscosity on molecular weight.

## SHORT CONTRIBUTIONS

*On the Relationship of the Viscoelastic Functions of Polymeric Solids at Different Temperatures*

N. G. McCrum and E. L. Morris, Engineering Laboratory, Oxford

A theory is proposed to explain the agreement obtained by KÈ between the activation energies for creep ( $\Delta H_c$ ), stress relaxation ( $\Delta H_{sr}$ ) and internal friction ( $\Delta H_{if}$ ). The theory is used to rectify the existing discrepancy between  $\Delta H_c$  and  $\Delta H_{sr}$  for the  $\beta$ -relaxation in polymethyl methacrylate and  $\Delta H_{if}$ . The discrepancy is shown to be due to the assumption that the limiting moduli do not vary with temperature. The discrepancy is eliminated by assuming that both limiting compliances have the same temperature dependence. A comparable discrepancy between  $\Delta H_c$  and  $\Delta H_{if}$  for the low temperature relaxation in polytetrafluorethylene is shown to be eliminated by the same assumption. In the light of these results criticism is made of many of the determinations of  $\Delta H_c$  and  $\Delta H_{sr}$  for relaxations other than the glass/rubber relaxation.

*Dielectric, Nuclear Resonance and Mechanical Relaxation in Polypropylene Oxide Polymers*

G. WILLIAMS, T. M. CONNOR and B. E. READ, National Physical Laboratory, Teddington

Various high molecular weight polypropylene oxides have been studied using dielectric, nuclear resonance and mechanical relaxation techniques to study the molecular motions in the polymer.

Dielectric loss measurements were made on an amorphous high molecular weight ( $M_w = 1.2 \times 10^6$ ) polypropylene oxide at 1 atm pressure over the frequency range  $10^{-4}$  to  $10^5$  c/s and over the temperature range  $-80^\circ\text{C}$  to  $+20^\circ\text{C}$ . One relaxation region was observed corresponding to the chain backbone motion. Over the frequency range  $10^2$  c/s to  $10^5$  c/s ( $-10^\circ\text{C}$  to  $-40^\circ\text{C}$ ) the pressure was varied from 1 to 3000 atm with considerable effect on the relaxation process. The temperature and pressure dependence of the relaxation process are discussed in terms of current models. Activation volumes and energies at constant volume are calculated.

The nuclear spin-lattice relaxation time,  $T_1$ , has been measured as a function of temperature at 30 Mc/s for a similar sample. In this case, two minima are found in the  $T_1$  values, the high temperature one ( $\sim 0^\circ\text{C}$ ) corresponding to the process observed by dielectric studies. The low temperature minimum ( $\sim -125^\circ\text{C}$ ) results from relaxation through rotation of the methyl groups attached to the chain backbone. This assignment was substantiated by investigation of samples where the side chain groups had been deuterated. These showed the expected decrease in efficiency of the relaxation process by a factor of  $\sim 16$  around the low temperature minimum. Samples of varying crystallinity (a function of the stereoregularity of the polymer) have been studied and it appears that the low temperature minimum moves to higher temperatures as the degree of crystallinity is increased. The data are also used to derive activation energies for the processes concerned.

Mechanical measurements at 0.3 c/s on amorphous and crystalline samples show a loss peak at  $-65^\circ\text{C}$ , also apparently corresponding to the chain backbone motion. There is a good correlation between the frequency of molecular motion derived from these measurements and the frequencies derived from the nuclear resonance and dielectric measurements.

*Mechanical Anisotropy in Oriented Polymers*

D. W. HADLEY, P. R. PINNOCK and I. M. WARD, I.C.I. Ltd, Fibres Division, Harrogate

To a first approximation, an oriented synthetic fibre or uniaxially oriented polymer film can be considered as a transversely isotropic elastic solid, whose mechanical

behaviour at low strains is specified by five independent elastic constants. Measurements of four of these constants have been undertaken in a number of fibres and films, including polyethylene terephthalate, polyethylene, Nylon and polypropylene.

In fibres, two of the elastic constants, corresponding to the extensional and torsional modulus, can be determined by comparatively straightforward methods. Two others, corresponding to a transverse modulus and a Poisson's ratio, have been determined using microscope techniques, and these are described. Usually, measurements of birefringence have also been undertaken, to give an indication of optical anisotropy.

The overall pattern of mechanical and optical anisotropy in different polymers is discussed, drawing from some previously published data. An attempt to explain the optical and mechanical anisotropy in terms of a simple model has met with limited success. This assumed that a partially oriented system consists of units whose properties remain unchanged by the orientation process.

### *The Dependence of the Ultimate Properties of Polymethyl methacrylate on Molecular Weight*

J. P. BERRY, Rubber and Plastics Research Association, Shawbury

The classical (flaw) theories of brittle fracture and tensile strength can be applied to the behaviour of polymers in the glassy state. It can be shown that the tensile strength is determined by (a) the energy required for the formation of new surface in the material (the fracture surface energy), (b) the size of the inherent flaw and (c) the Young's modulus. The influence of molecular weight on these parameters for polymethyl methacrylate has been established. In common with other mechanical properties, the dependence of the fracture surface energy on molecular weight can be represented by  $\gamma = A - B/M$  where  $M$  is the molecular weight, and  $A$  and  $B$  are arbitrary constants. By extrapolation, the upper limiting value is  $1.55 \times 10^5$  erg/cm<sup>2</sup> while the surface energy, and hence the tensile strength, should become zero for a polymer of molecular weight 25000. This value is in good agreement with that found directly from brittle strength measurements.

### **Session on Solution Properties**

#### *Introductory Talks*

##### *(i) Techniques of Measurement*

H. G. JERRARD, University of Southampton

Many physical techniques may be used for the study of large molecules in solution. In the majority of these techniques the motion or orientation of the molecules as a group or the effects of the molecules on some incident form of energy is observed. The methods include sedimentation using high speed ultracentrifuges, viscometry, light scattering electrophoresis, dielectric dispersion studies, and those involving the measurement of birefringence induced by hydrodynamic flow or by the application of an electric or acoustic field. In this paper these techniques and their requirements in the way of purity, concentration of solution and apparatus are reviewed. The information which is obtained about the molecules is discussed.

##### *(ii) The Ultracentrifuge*

G. T. GREENWOOD, University of Edinburgh

A general review is given of the application of the ultracentrifuge to the study of the physical properties of polymer solutions.

Recent advances in instrumentation and cell design are outlined. The relative merits of absorption, schlieren and interference optics are discussed. The use

## SHORT CONTRIBUTIONS

*On the Relationship of the Viscoelastic Functions of Polymeric Solids at Different Temperatures*

N. G. McCrum and E. L. Morris, Engineering Laboratory, Oxford

A theory is proposed to explain the agreement obtained by KÈ between the activation energies for creep ( $\Delta H_c$ ), stress relaxation ( $\Delta H_{sr}$ ) and internal friction ( $\Delta H_{if}$ ). The theory is used to rectify the existing discrepancy between  $\Delta H_c$  and  $\Delta H_{sr}$  for the  $\beta$ -relaxation in polymethyl methacrylate and  $\Delta H_{if}$ . The discrepancy is shown to be due to the assumption that the limiting moduli do not vary with temperature. The discrepancy is eliminated by assuming that both limiting compliances have the same temperature dependence. A comparable discrepancy between  $\Delta H_c$  and  $\Delta H_{if}$  for the low temperature relaxation in polytetrafluorethylene is shown to be eliminated by the same assumption. In the light of these results criticism is made of many of the determinations of  $\Delta H_c$  and  $\Delta H_{sr}$  for relaxations other than the glass/rubber relaxation.

*Dielectric, Nuclear Resonance and Mechanical Relaxation in Polypropylene Oxide Polymers*

G. WILLIAMS, T. M. CONNOR and B. E. READ, National Physical Laboratory, Teddington

Various high molecular weight polypropylene oxides have been studied using dielectric, nuclear resonance and mechanical relaxation techniques to study the molecular motions in the polymer.

Dielectric loss measurements were made on an amorphous high molecular weight ( $M_w = 1.2 \times 10^6$ ) polypropylene oxide at 1 atm pressure over the frequency range  $10^{-4}$  to  $10^5$  c/s and over the temperature range  $-80^\circ\text{C}$  to  $+20^\circ\text{C}$ . One relaxation region was observed corresponding to the chain backbone motion. Over the frequency range  $10^2$  c/s to  $10^5$  c/s ( $-10^\circ\text{C}$  to  $-40^\circ\text{C}$ ) the pressure was varied from 1 to 3000 atm with considerable effect on the relaxation process. The temperature and pressure dependence of the relaxation process are discussed in terms of current models. Activation volumes and energies at constant volume are calculated.

The nuclear spin-lattice relaxation time,  $T_1$ , has been measured as a function of temperature at 30 Mc/s for a similar sample. In this case, two minima are found in the  $T_1$  values, the high temperature one ( $\sim 0^\circ\text{C}$ ) corresponding to the process observed by dielectric studies. The low temperature minimum ( $\sim -125^\circ\text{C}$ ) results from relaxation through rotation of the methyl groups attached to the chain backbone. This assignment was substantiated by investigation of samples where the side chain groups had been deuterated. These showed the expected decrease in efficiency of the relaxation process by a factor of  $\sim 16$  around the low temperature minimum. Samples of varying crystallinity (a function of the stereoregularity of the polymer) have been studied and it appears that the low temperature minimum moves to higher temperatures as the degree of crystallinity is increased. The data are also used to derive activation energies for the processes concerned.

Mechanical measurements at 0.3 c/s on amorphous and crystalline samples show a loss peak at  $-65^\circ\text{C}$ , also apparently corresponding to the chain backbone motion. There is a good correlation between the frequency of molecular motion derived from these measurements and the frequencies derived from the nuclear resonance and dielectric measurements.

*Mechanical Anisotropy in Oriented Polymers*

D. W. HADLEY, P. R. PINNOCK and I. M. WARD, I.C.I. Ltd, Fibres Division, Harrogate

To a first approximation, an oriented synthetic fibre or uniaxially oriented polymer film can be considered as a transversely isotropic elastic solid, whose mechanical

behaviour at low strains is specified by five independent elastic constants. Measurements of four of these constants have been undertaken in a number of fibres and films, including polyethylene terephthalate, polyethylene, Nylon and polypropylene.

In fibres, two of the elastic constants, corresponding to the extensional and torsional modulus, can be determined by comparatively straightforward methods. Two others, corresponding to a transverse modulus and a Poisson's ratio, have been determined using microscope techniques, and these are described. Usually, measurements of birefringence have also been undertaken, to give an indication of optical anisotropy.

The overall pattern of mechanical and optical anisotropy in different polymers is discussed, drawing from some previously published data. An attempt to explain the optical and mechanical anisotropy in terms of a simple model has met with limited success. This assumed that a partially oriented system consists of units whose properties remain unchanged by the orientation process.

### *The Dependence of the Ultimate Properties of Polymethyl methacrylate on Molecular Weight*

J. P. BERRY, Rubber and Plastics Research Association, Shawbury

The classical (flaw) theories of brittle fracture and tensile strength can be applied to the behaviour of polymers in the glassy state. It can be shown that the tensile strength is determined by (a) the energy required for the formation of new surface in the material (the fracture surface energy), (b) the size of the inherent flaw and (c) the Young's modulus. The influence of molecular weight on these parameters for polymethyl methacrylate has been established. In common with other mechanical properties, the dependence of the fracture surface energy on molecular weight can be represented by  $\gamma = A - B/M$  where  $M$  is the molecular weight, and  $A$  and  $B$  are arbitrary constants. By extrapolation, the upper limiting value is  $1.55 \times 10^5$  erg/cm<sup>2</sup> while the surface energy, and hence the tensile strength, should become zero for a polymer of molecular weight 25000. This value is in good agreement with that found directly from brittle strength measurements.

### **Session on Solution Properties**

#### *Introductory Talks*

##### *(i) Techniques of Measurement*

H. G. JERRARD, University of Southampton

Many physical techniques may be used for the study of large molecules in solution. In the majority of these techniques the motion or orientation of the molecules as a group or the effects of the molecules on some incident form of energy is observed. The methods include sedimentation using high speed ultracentrifuges, viscometry, light scattering electrophoresis, dielectric dispersion studies, and those involving the measurement of birefringence induced by hydrodynamic flow or by the application of an electric or acoustic field. In this paper these techniques and their requirements in the way of purity, concentration of solution and apparatus are reviewed. The information which is obtained about the molecules is discussed.

##### *(ii) The Ultracentrifuge*

G. T. GREENWOOD, University of Edinburgh

A general review is given of the application of the ultracentrifuge to the study of the physical properties of polymer solutions.

Recent advances in instrumentation and cell design are outlined. The relative merits of absorption, schlieren and interference optics are discussed. The use

of sedimentation velocity measurements to give information regarding polymer homogeneity, molecular weight and molecular weight distribution is illustrated by examples. Difficulties due to the concentration dependence of the sedimentation coefficient and also to diffusion are stressed. Mention is made of the potentialities of sedimentation measurements in a density gradient. Sedimentation equilibrium measurements are covered very briefly.

## SHORT CONTRIBUTIONS

*Investigation of High Polymers by Light Scattering*

B. R. JENNINGS, University of Southampton

In addition to the measurement of molecular anisotropy and weight, light scattering can be used to indicate hydrodynamic properties of molecules in dilute solution. A brief description of the apparatus used is given. Some typical results are presented from an investigation of a synthetic high polymer (poly-*N*-tertiary butyl acrylamide) in methanol. These show that the molecules are stiff, and are unable to assume random coiling as a result of the bulky substituents. The application of the Flory universal constant to such a system is discussed. Possible extensions of the technique, such as the information obtained when an electric field is applied to the solution, are mentioned.

*The Viscoelastic Properties of Dilute Solutions of Polystyrene in Different Solvents*

J. LAMB, University of Glasgow

The viscoelastic properties of dilute solutions of polystyrene in toluene have been measured under alternating shear stress at frequencies of 38 and 73 kc/s and at temperatures from +50°C to -70°C. Seven narrow molecular weight fractions were employed ranging in molecular weight from  $4.8 \times 10^4$  to  $1.2 \times 10^6$ . Measurements have also been made for solutions of the same polymer samples in less good solvents, methylethyl ketone and cyclohexane. In this way, it has been possible to investigate the relaxational behaviour of the polystyrenes as a function of molecular weight, concentration and solvent. A general picture emerges from this work and, under certain conditions, agreement is found with the theory of Zimm whilst, under other conditions, the Rouse theory appears to hold.

A description is given of the interpretation of these results.

*The Fractionation of Some Poly-(Ethers) by Crystallization from Dilute Solution*

C. PRICE, G. ALLEN and C. BOOTH, University of Manchester

Three partially tactic poly-(ethers), poly-(propylene oxide), poly-(*t*-butylethylene oxide), poly-(styrene oxide), were fractionated by crystallization from dilute solution. The first two polymers fractionated with respect to structure rather than molecular weight, whilst the third fractionated with respect to molecular weight. An attempt has been made to explain these data by taking into account the relative magnitudes by which the molecular weight and various structural factors can depress the melting point of crystalline polymers. Supplementary experimental evidence required in this description was obtained by fractionating poly-(ethylene oxide).

---

Professor F. C. FRANK summarized the proceedings in a closing address.

behaviour at low strains is specified by five independent elastic constants. Measurements of four of these constants have been undertaken in a number of fibres and films, including polyethylene terephthalate, polyethylene, Nylon and polypropylene.

In fibres, two of the elastic constants, corresponding to the extensional and torsional modulus, can be determined by comparatively straightforward methods. Two others, corresponding to a transverse modulus and a Poisson's ratio, have been determined using microscope techniques, and these are described. Usually, measurements of birefringence have also been undertaken, to give an indication of optical anisotropy.

The overall pattern of mechanical and optical anisotropy in different polymers is discussed, drawing from some previously published data. An attempt to explain the optical and mechanical anisotropy in terms of a simple model has met with limited success. This assumed that a partially oriented system consists of units whose properties remain unchanged by the orientation process.

### *The Dependence of the Ultimate Properties of Polymethyl methacrylate on Molecular Weight*

J. P. BERRY, Rubber and Plastics Research Association, Shawbury

The classical (flaw) theories of brittle fracture and tensile strength can be applied to the behaviour of polymers in the glassy state. It can be shown that the tensile strength is determined by (a) the energy required for the formation of new surface in the material (the fracture surface energy), (b) the size of the inherent flaw and (c) the Young's modulus. The influence of molecular weight on these parameters for polymethyl methacrylate has been established. In common with other mechanical properties, the dependence of the fracture surface energy on molecular weight can be represented by  $\gamma = A - B/M$  where  $M$  is the molecular weight, and  $A$  and  $B$  are arbitrary constants. By extrapolation, the upper limiting value is  $1.55 \times 10^5$  erg/cm<sup>2</sup> while the surface energy, and hence the tensile strength, should become zero for a polymer of molecular weight 25000. This value is in good agreement with that found directly from brittle strength measurements.

### **Session on Solution Properties**

#### *Introductory Talks*

##### *(i) Techniques of Measurement*

H. G. JERRARD, University of Southampton

Many physical techniques may be used for the study of large molecules in solution. In the majority of these techniques the motion or orientation of the molecules as a group or the effects of the molecules on some incident form of energy is observed. The methods include sedimentation using high speed ultracentrifuges, viscometry, light scattering electrophoresis, dielectric dispersion studies, and those involving the measurement of birefringence induced by hydrodynamic flow or by the application of an electric or acoustic field. In this paper these techniques and their requirements in the way of purity, concentration of solution and apparatus are reviewed. The information which is obtained about the molecules is discussed.

##### *(ii) The Ultracentrifuge*

G. T. GREENWOOD, University of Edinburgh

A general review is given of the application of the ultracentrifuge to the study of the physical properties of polymer solutions.

Recent advances in instrumentation and cell design are outlined. The relative merits of absorption, schlieren and interference optics are discussed. The use



of sedimentation velocity measurements to give information regarding polymer homogeneity, molecular weight and molecular weight distribution is illustrated by examples. Difficulties due to the concentration dependence of the sedimentation coefficient and also to diffusion are stressed. Mention is made of the potentialities of sedimentation measurements in a density gradient. Sedimentation equilibrium measurements are covered very briefly.

## SHORT CONTRIBUTIONS

*Investigation of High Polymers by Light Scattering*

B. R. JENNINGS, University of Southampton

In addition to the measurement of molecular anisotropy and weight, light scattering can be used to indicate hydrodynamic properties of molecules in dilute solution. A brief description of the apparatus used is given. Some typical results are presented from an investigation of a synthetic high polymer (poly-*N*-tertiary butyl acrylamide) in methanol. These show that the molecules are stiff, and are unable to assume random coiling as a result of the bulky substituents. The application of the Flory universal constant to such a system is discussed. Possible extensions of the technique, such as the information obtained when an electric field is applied to the solution, are mentioned.

*The Viscoelastic Properties of Dilute Solutions of Polystyrene in Different Solvents*

J. LAMB, University of Glasgow

The viscoelastic properties of dilute solutions of polystyrene in toluene have been measured under alternating shear stress at frequencies of 38 and 73 kc/s and at temperatures from +50°C to -70°C. Seven narrow molecular weight fractions were employed ranging in molecular weight from  $4.8 \times 10^4$  to  $1.2 \times 10^6$ . Measurements have also been made for solutions of the same polymer samples in less good solvents, methylethyl ketone and cyclohexane. In this way, it has been possible to investigate the relaxational behaviour of the polystyrenes as a function of molecular weight, concentration and solvent. A general picture emerges from this work and, under certain conditions, agreement is found with the theory of Zimm whilst, under other conditions, the Rouse theory appears to hold.

A description is given of the interpretation of these results.

*The Fractionation of Some Poly-(Ethers) by Crystallization from Dilute Solution*

C. PRICE, G. ALLEN and C. BOOTH, University of Manchester

Three partially tactic poly-(ethers), poly-(propylene oxide), poly-(*t*-butylethylene oxide), poly-(styrene oxide), were fractionated by crystallization from dilute solution. The first two polymers fractionated with respect to structure rather than molecular weight, whilst the third fractionated with respect to molecular weight. An attempt has been made to explain these data by taking into account the relative magnitudes by which the molecular weight and various structural factors can depress the melting point of crystalline polymers. Supplementary experimental evidence required in this description was obtained by fractionating poly-(ethylene oxide).

---

Professor F. C. FRANK summarized the proceedings in a closing address.

# Some Experimental Studies on Enthalpy and Entropy Effects in Equilibrium Swelling of Polyoxypropylene Elastomers

B. E. CONWAY and J. P. NICHOLSON

*Measurements on the equilibrium swelling of some polyoxypropylene elastomers by a series of solvents are reported with the purpose of distinguishing entropy and enthalpy effects in the thermodynamics of the swelling process. Values of the  $\chi$  parameter have been obtained, and from direct measurements of the heat of swelling in a Tian-Calvet microcalorimeter, the  $\chi_H$ , or enthalpy interaction parameter, has been obtained. The values of  $\chi_S$ , the corresponding entropy parameter, are then deduced and it is shown that there is a linear relation (or 'compensation effect') between the  $\chi_H$  and  $\chi_S$  terms. In no solvent can the  $\chi_S$  term be neglected.*

*Diffusion calculations have been made in which it is shown that heats of mixing of liquids in thin layers can be accurately measured in the microcalorimeter without use of stirring and its consequent difficulties.*

IN PREVIOUS work on equilibrium swelling of elastomers by various solvents, the swelling behaviour has usually been characterized by the interaction parameter  $\chi$ . However, the relative importance of entropy and enthalpy effects in determining  $\chi$ , and hence the equilibrium swelling, has received little attention. In the present work, we have therefore examined the role of entropy and enthalpy effects in the equilibrium swelling of some *polar* elastomers by several solvents, using a direct calorimetric method for the determination of the enthalpy change associated with the swelling.

In a previous paper, Conway and Tong<sup>1</sup> have reported measurements on the equilibrium swelling of polyurethane elastomers by methanol, benzene and 1,4-dioxan. In order to study in more detail the effect of size and structure of the solvent molecules on the polymer-solvent interaction the swelling of these elastomers by ten aliphatic alcohols, cyclohexane, *n*-hexane and carbon tetrachloride has been investigated. As would be expected for mixtures of polar solvents with a polar polymer, the systems show large deviations from the regular Flory lattice model of a polymer solution.

## EXPERIMENTAL

### *Heats of swelling and heats of solution*

The heats of swelling and solution were measured in a Tian-Calvet microcalorimeter. The construction and general theory of this instrument has been fully described by Calvet<sup>2</sup>. The model used in these measurements had four experimental cells each surrounded by a thermopile consisting of 144 thermocouples. The thermopiles were connected to a Liston-Becker

d.c. amplifier and the amplifier output was fed to a recorder. The area under the curve drawn by the recorder pen is directly proportional to any heat change in the experimental cell and heats of swelling and solution can be measured directly using electrical calibration for exothermic processes. Compensatory electrical heat can conveniently be added during endothermic processes. In practice, Joule electrical calibrations were carried out after each measurement.

A block of the elastomer was frozen in liquid nitrogen and drilled to produce shavings of polymer. After drying *in vacuo*, these thin films of polymer swelled to equilibrium solvent uptake in less than one hour with all solvents studied. The heat of swelling measurements were carried out in copper-plated glass cells, 18 mm by 90 mm external dimensions. The fragment of polymer was enclosed in a small perforated glass tube at the end of a control rod and submerged in several millilitres of mercury at the bottom of the experimental cell. The solvent was pipetted into the cell on top of the mercury. When temperature equilibrium was reached the control rod was raised 3–4 cm so that the polymer was lifted into the solvent and swelling rapidly occurred. Cells were always made up in duplicate with the exception that polymer was omitted from the second 'blank' cell which was placed in the reference socket of the calorimeter. The control rods were always raised simultaneously so that any adventitious heat effects (such as a heat of wetting) on moving the glass tube out of the mercury into the alcohol would cancel out. Separate experiments showed

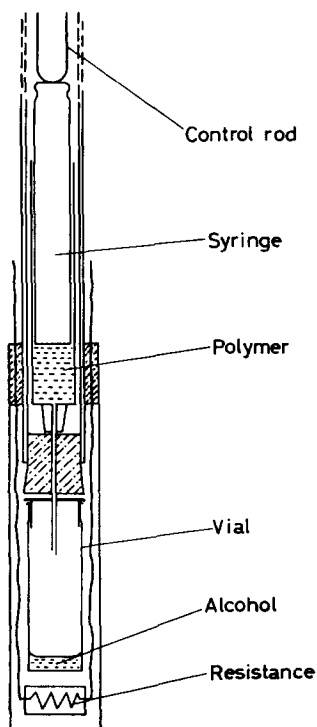


Figure 1—Heat of solution cell (not to scale)

that these heat changes were only 1–2 per cent of the measured heat of swelling so that with compensation in the reference cell these effects were negligible. The weights of polymer used in the experiments were *ca* 0.01 g and were weighed precisely, and the heat changes measured were in the range 0.02–0.2 calorie. Measurements were reproducible to within one per cent.

A modified experimental cell (*Figure 1*) was used to measure the heat of solution of a corresponding linear polypropylene oxide polymer (molecular weight 4 000) in ethanol and *n*-butanol. The needle of a 1 ml hypodermic syringe pierced a cork which was plugged firmly into one end of the glass tube used to support the mixing cell in the calorimeter socket. A small glass vial was fixed to the syringe with a vapour-tight seal by thrusting the needle through the rigid polyethylene stopper of the vial. The vial was surrounded by a copper cylinder which fitted the calorimeter socket smoothly to provide good thermal contact. 0.05–0.02 g of polymer was weighed into the syringe and 0.05–0.5 g of alcohol into the vial before the cell was assembled and placed in the calorimeter. When thermal equilibrium was reached, the glass control rod bearing on the upper end of the syringe piston was depressed so that the polymer dropped into the alcohol at the bottom of the vial. By weighing both syringe and vial after the experiment, a double check on the composition of the mixture could be made. A small 500 ohm heating resistance was fitted inside the cell at the base of the glass vial so that the heat absorbed on mixing could be measured by the method of electrical compensation.

Three main sources of error are possible in heats of mixing measured with this type of cell. The mechanical work done in forcing the viscous polymer through the syringe needle produces a small heating effect. This was measured in separate experiments and was found to be 0.02–0.03 calorie, depending on the quantity of polymer in the syringe. As this heat of injection is about ten per cent of the measured heat of mixing, and is itself reproducible to within five per cent, the overall uncertainty introduced is less than one per cent. The free vapour space over the solution is about 2 ml and the change in vapour pressure on mixing is accompanied by a small heat effect. Calculation shows this to be negligible with the dilute solutions used and in the worst possible case, with ethanol over concentrated polymer solutions, the error would be about two per cent. Finally, the polymer is denser than the alcohol and after injection into the vial the components tend to form two separate layers after which mixing is by diffusion only. The runs were continued for several hours until the recorder pen had returned to the experimental zero and the absorption of heat appeared to be complete. Diffusion calculations show (see Appendix) that with the quantities of material used (0.2–0.5 g) the worst possible error due to incomplete mixing is unlikely to exceed two per cent under the experimental conditions used. Experimentally, the overall error in the heats of mixing is  $\pm 5$  per cent.

#### *Volume changes on mixing*

The volume changes on mixing the liquid polyoxypropylene polymer (molecular weight 4 000) with ethanol and *n*-butanol were measured. A

volumetric tube<sup>4</sup> (300 mm by 6 mm internal dimensions) fitted with a ground glass stopper was prepared from precision bore glass tubing. A small nail sealed in glass was placed in the tube to act as a magnetic stirrer. The appropriate amount of polymer was transferred to the tube by means of a long syringe needle. The alcohol was carefully run in to form a separate layer above the polymer and the tube was closed and immersed in a thermostat at 25°C. The lengths of the two liquid layers were measured by means of the cathetometer and the position of the alcohol/air meniscus relative to a reference mark on the tube was carefully determined. The two liquid layers were thoroughly mixed by raising and lowering the internal stirrer many times with the magnet. The position of the meniscus relative to the mark was again determined. The smallest relative volume change detectable with this apparatus was  $\pm 0.02$  per cent.

### Swelling measurements

Small strips of the elastomers, each weighing approximately 0.2 g, were suspended in tubes of solvent. At appropriate intervals the polymer strips were removed from the solvent and quickly wiped dry between sheets of absorbent paper. The swollen polymer was then transferred to a stoppered weighing bottle so that the weight of polymer plus imbibed solvent could be determined\*. For the thermodynamic calculations, it was necessary to obtain the true equilibrium solvent uptake as exactly as possible. With the higher molecular weight alcohols, perceptible increases in weight of the polymer samples still continued after ten to twelve days immersion in the solvent. No exact mathematical expression could be utilized to make the extrapolation which would yield the weight of solvent imbibed after an infinite time of swelling but this could be estimated with sufficient accuracy by plotting the weight of the swollen polymer against the reciprocal of the square of the swelling time ( $t$ ) in days. The shallow curve which resulted was then extrapolated to  $1/t^2=0$  to give the equilibrium weight, as shown in *Figure 2*. All determinations were made in duplicate.

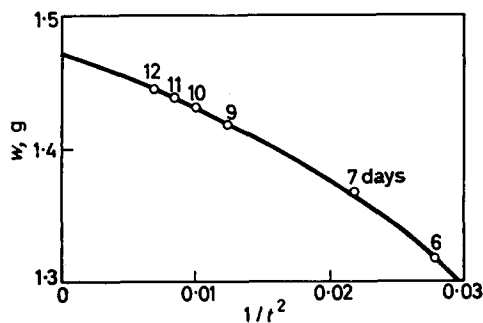


Figure 2—Weight of *n*-amyl alcohol ( $w$ ) imbibed by polymer sample plotted against  $1/t^2$ , where  $t$  = time of swelling, in days

\*In the previous work of Conway and Tong<sup>1</sup>, it was shown that the equilibrium weight change method gave results in satisfactory agreement with those obtained from observations of dimensional changes of immersed polymer samples.

## EQUILIBRIUM SWELLING OF POLYOXYPROPYLENE ELASTOMERS

### *Materials*

The compositions of the three polyoxypropylene elastomers crosslinked by toluene diisocyanate, have been reported in a previous paper<sup>1</sup>. The alcohols used as the swelling solvents were dried over anhydrous magnesium sulphate and fractionally distilled. Middle fractions boiling within half a degree of the literature boiling points were taken. The butanol isomers were fractionated several times until vapour phase chromatograms showed that contamination of the samples by the other isomers was negligible. The *n*-hexane, cyclohexane and carbon tetrachloride were Fisher certified reagents which were used without further purification. The linear polymer used as a model for the crosslinked elastomers in the measurements on the volume change on mixing, was a polypropylene oxide sample with approximate molecular weight 4 000 which was separated from a batch of Union Carbide polypropylene oxide and characterized in previous work<sup>5</sup>. The density of the polymer was measured by weighing a degassed sample in a density bottle against the same volume of distilled water and was found to be 0.998 at 25°C.

### RESULTS

The equilibrium mean volume fractions  $\phi_2$  of the three polymers in the swollen gel are given for the various solvents at 25°C in *Table 1*. The

*Table 1.* Equilibrium volume fractions and heats of swelling at 25°C

<i>Solvent</i>	<i>Polymer*</i>	$\phi_2$	$\Delta H$ cal/g
Methanol	1	0.278	1.67
	2	0.205	1.61
	3	0.110	1.51
Ethanol	1	0.251	3.19
	2	0.174	3.14
	3	0.092	3.25
<i>n</i> -Propanol	1	0.189	3.76
	2	0.127	3.94
	3	0.067	4.03
<i>i</i> -Propanol	1	0.230	4.57
	2	0.162	—
	3	0.081	—
<i>n</i> -Butanol	1	0.184	3.98
	2	0.129	4.15
	3	0.064	4.51
<i>i</i> -Butanol	1	0.204	4.62
	2	0.136	—
	3	0.062	—

*continued overleaf*

Table 1—continued

Solvent	Polymer*	$\phi_2$	$\Delta H$ cal/g
<i>sec</i> -Butanol	1	0.214	5.48
	2	0.151	—
	3	0.072	—
<i>t</i> -Butanol	1	0.244	4.86
	2	0.164	—
	3	0.083	—
<i>n</i> -Amylol	1	0.198	3.94
	2	0.130	3.11
	3	0.063	4.12
<i>i</i> -Amylol	1	0.195	3.88
	2	0.134	—
	3	0.063	—
<i>n</i> -Hexane	1	0.608	1.69
	2	0.561	1.69
	3	0.526	1.71
Cyclohexane	1	0.429	2.72
	2	0.359	3.02
	3	0.293	3.30
Carbon tetrachloride	1	0.179	-1.07
	2	0.114	-1.12
	3	0.061	-1.01

\*Note: The designation of the elastomer samples as polymers 1, 2 and 3 corresponds with that used in our previous paper<sup>1</sup>. For convenience the compositions are reproduced below:

Polymer 1	PPG (2 025)	1.5 moles
	Triol	1.0 "
	TDI	3.0 "
Polymer 2	PPG (2 025)	3.0 "
	Triol	1.0 "
	TDI	4.5 "
Polymer 3	PPG (2 025)	6.0 "
	Triol	1.0 "
	TDI	7.5 "

PPG denotes polyoxypropylene glycol (number average mol. wt 2 025)  
 Triol denotes 1,2,6-*tris*-(hydroxypolyoxypropylene) hexane, mol. wt 1 500  
 TDI denotes 2,4-Toluene diisocyanate.

heats of swelling also tabulated are expressed as calories per gramme of polymer and the amounts of solvent in the mixtures have been defined by their equilibrium concentrations in the swollen gels.

The volume changes on mixing the linear polymer of molecular weight 4 000 with ethanol and *n*-butanol are shown in *Figure 3* as the observed contraction, expressed as a percentage of the total volume, plotted against the composition of the mixture.

The heats of mixing,  $\Delta H$ , for the linear polymer 4 000-alcohol mixtures in the composition range  $\phi_2=0$  to 0.5 have been represented in *Figure 4* by plotting  $\chi_H$  against  $\phi_2$ , where  $\chi_H$  is defined by

$$\chi_H = \Delta H / RTn_1\phi_2 \quad (1)$$

$\Delta H$  is the heat change when  $n_1$  moles of solvent are mixed with the

polymer to give a solution or gel in which the volume fraction of the polymer is  $\phi_2$ .

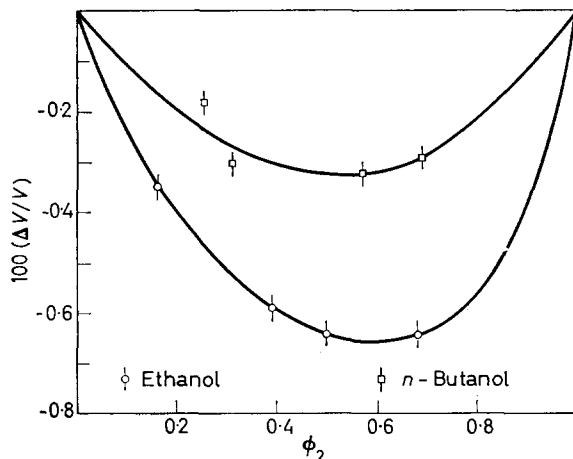


Figure 3—Volume change on mixing polypropylene oxide (mol. wt 4 000) with ethanol and *n*-butanol

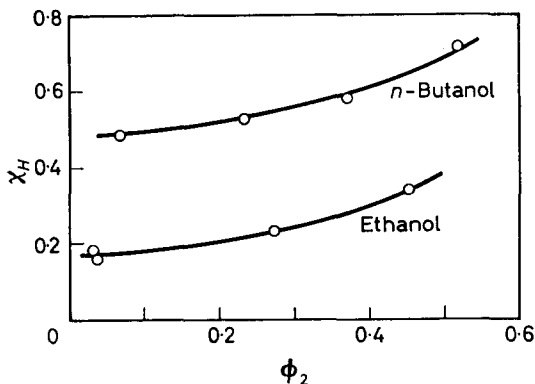


Figure 4— $\chi_H$  for polypropylene oxide (mol. wt 4 000) with ethanol and *n*-butanol

## DISCUSSION

### *Deduction of interaction parameters*

The swelling of amorphous, isotropic polymers can be discussed in terms of the Flory equation for the Gibbs free energy of mixing in polymer-solvent systems and the statistical theory of elastic networks.

At equilibrium swelling, it may be shown<sup>6</sup> that for a network in which the chain ends are linked trifunctionally

$$\chi\phi_2^2 = -\ln(1-\phi_2) - \phi_2 - (\rho_2 V_1 / M_c) (\phi_2^{1/3} - 2\phi_2/3) \quad (2)$$

where  $\phi_2$  is the volume fraction of the polymer in the swollen network,



$M_c$  the mean molecular weight per crosslinked unit,  $\rho_2$  the density of the dry polymer,  $V_1$  the molar volume of the solvent and  $\chi$  the Flory-Huggins interaction parameter.

It follows from the theory of ideal rubbers<sup>7</sup> that the retractile force  $\tau$  at an extension ratio  $\alpha_e$  is given by

$$\tau = RT (v_e/V) (\alpha_e - 1/\alpha_e^2) \quad (3)$$

where  $v_e$  is the number of elastic elements (in moles) in the volume  $V$  of dry polymer. Since  $\rho_2/M_c = v_e/V$ , equations (2) and (3) can be combined, with the elimination of  $(v_e/V)$ , to give

$$\tau = \frac{-RT (\alpha_e - 1/\alpha_e^2) [\ln (1 - \phi_2) + \phi + \chi \phi_2^2]}{V_1 (\phi_2^{1/3} - \frac{2}{3}\phi_2)} \quad (4)$$

As the values of  $\tau$  at given equilibrium extension ratios ( $\alpha_e$ ) have been measured for the three polymer samples, as previously reported<sup>8</sup>, equation (4) can be used with the equilibrium swelling data to calculate  $\chi$  values for the different liquids. Conway and Tong<sup>1</sup> showed that the elastic properties of the polypropylene oxide rubbers sufficiently resemble those of ideal rubbers to be represented by an equation of the form (3) over the range of extension ratios encountered in the swelling experiments. Since the statistical theory of rubber elasticity is used in the derivation of both equations (2) and (3) it might be expected that any failure of the model to represent the elastic behaviour of the elastomers used would, to a first approximation, be rendered less serious by a mutual cancellation of errors.

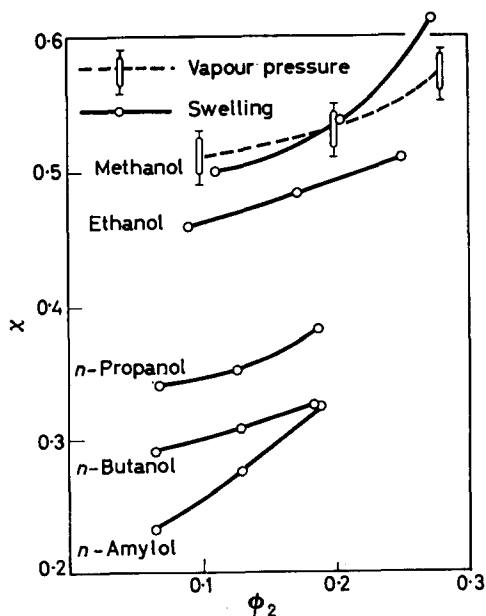


Figure 5—Values of the interaction parameter  $\chi$  for five *n*-alcohols

## EQUILIBRIUM SWELLING OF POLYOXYPROPYLENE ELASTOMERS

The lattice theory assumes mixing at constant volume and, since it is difficult to measure the volume change when an elastomer is swollen by a solvent, the linear polypropylene oxide was taken as a model for the elastomer. The maximum volume changes observed on mixing this liquid polymer with ethanol and *n*-butanol were, respectively, contractions of 0.3 per cent and 0.6 per cent of the total volume of the mixture. These are not sufficiently large to invalidate a comparison of the  $\chi$  values for ethanol and *n*-butanol, and probably also for the other solvents studied.

Using equation (4),  $\chi$  values at 25°C were calculated for the solvents studied at the different extents of swelling observed with the three polymer specimens. The results for the *n*-alcohols are shown in Figure 5 where  $\chi$  values are plotted against the volume fraction of polymer in the swollen network. Results for the alcohol isomers and the three non-polar solvents (*n*-hexane, cyclohexane and carbon tetrachloride) are summarized in Tables 2 and 3.

Table 2. Approximate  $\chi$  values at  $\phi_2=0.15$  (calculated on the assumption that  $\chi_H$  is not very dependent on concentration)

Alcohol	$\chi$	$\chi_H$	$\chi_S$
<i>n</i> -Propanol	0.36	0.73	-0.37
<i>i</i> -Propanol	0.42	0.95	-0.57
<i>n</i> -Butanol	0.33	0.94	-0.61
<i>i</i> -Butanol	0.34	1.19	-0.85
<i>sec</i> -Butanol	0.38	1.43	-1.05
<i>t</i> -Butanol	0.40	1.35	-0.95
<i>n</i> -Amylol	0.29	1.11	-0.82
<i>i</i> -Amylol	0.30	1.17	-0.87

Table 3.  $\chi$  values for *n*-hexane, cyclohexane and carbon tetrachloride (at various values of  $\phi_2$ )

Solvent	$\phi_2$	$\chi$	$\chi_H$	$\chi_S$
<i>n</i> -Hexane	0.53	0.79	1.06	-0.27
Cyclohexane	0.29	0.61	1.13	-0.52
Carbon tetrachloride	0.06	0.24	-0.21	0.45

An independent check on this method of calculating the interaction parameter is desirable. Conway and Lakhnawal<sup>9</sup> measured the vapour pressure of methanol over solutions of polypropylene oxide polymers of different molecular weights and calculated the variation of  $\chi$  with molecular weight and concentration. Their results can be extrapolated to give an approximate  $\chi$  value for a polymer of infinite molecular weight at different concentrations. These  $\chi$  values for  $\phi_2=0.1, 0.2$  and  $0.3$  are plotted in Figure 5 and although they are only accurate to  $\pm 0.02$  the agreement between the values obtained by the two methods is to be considered quite satisfactory.

The calculated interaction parameters are noticeably concentration

dependent as might be expected considering both the polar interactions in the system and the fact that  $\chi$  values increasing with concentration are common in non-polar polymer-solvent mixtures. The solvent power of the five *n*-alcohols increases (and hence  $\chi$  decreases) with increasing chain length. The straight chain alcohols are better solvents than their branched isomers. Thus *i*-, *sec*- and *t*-butanol have higher  $\chi$  values than *n*-butanol, and *i*-propanol higher than *n*-propanol. The measurements on *n*-hexane and cyclohexane show that the two hydrocarbons are poorer solvents than the alcohols (see Table 3). Carbon tetrachloride has high swelling power, comparable with that of *n*-amyl alcohol, an effect which evidently arises on account of its unexpected exothermic heat of mixing with the polymer.

*Relation between the enthalpy and entropy parameters,  $\chi_H$  and  $\chi_S$*

The parameter  $\chi$  was originally introduced in the Flory-Huggins equation as an enthalpy term but in practice the method of its evaluation leads to the deduction of a 'free energy of interaction' parameter. At a given temperature the interaction parameter can be written as the sum of a heat and an entropy term

$$\chi = \chi_H + \chi_S$$

$\chi_H$  values for the solvents were calculated from measured heats of swelling using equation (1). Results for the five *n*-alcohols are shown in Figure 6

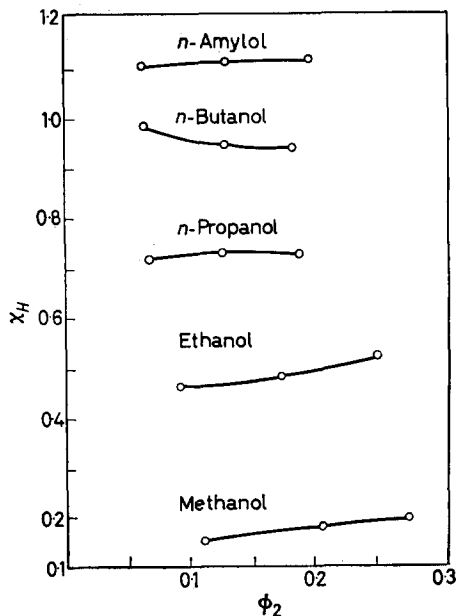
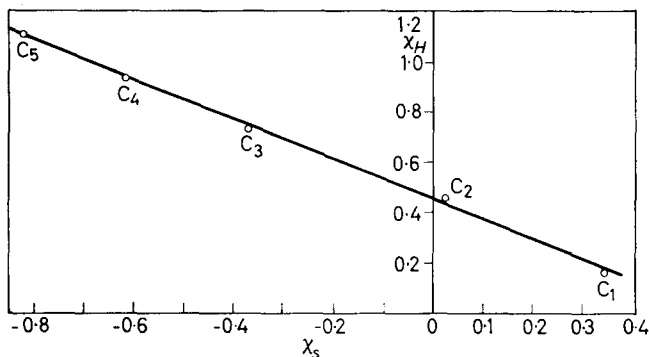


Figure 6—Values of the heat of interaction parameter  $\chi_H$  for the five *n*-alcohols

and for the other solvents in Tables 2 and 3.  $\chi_H$  values for the alcohols are all positive, corresponding to endothermic mixing, and are less concentration dependent than the overall  $\chi$  values.  $\chi_H$  increases with chain length as would be expected since the interaction of the hydroxyl groups

with the ether oxygen atoms of the polymer chain is probably favourable to exothermic mixing.  $\chi_H$  values for mixing of ethanol and *n*-butanol with the linear polymer (mol. wt 4 000) are less than those measured with the elastomers, but the decrease from butanol to ethanol is approximately the same (see *Table 4*).

To determine whether the different swelling powers of the alcohols and their isomers toward the polymer were due mainly to differences in heats of mixing, or whether they arose significantly from the entropies, the appropriate  $\chi_s$  values were obtained as the differences between  $\chi$  and  $\chi_H$ . The values of  $\chi$  decrease while those of  $\chi_H$  increase or, in other words, the swelling power of the alcohol increases while the heat of swelling is becoming increasingly positive and would therefore be expected to reduce the extent of swelling.  $\chi_H$  is plotted against  $\chi_s$  in *Figure 7* for the five *n*-alcohols (at a constant value of  $\phi_2=0.15$ ) and there is a linear inverse variation of  $\chi_H$  with  $\chi_s$ .



*Figure 7*— $\chi_H$  and  $\chi_s$  for the five *n*-alcohols

The relationship between  $\chi_H$  and  $\chi_s$  shown in *Figure 7* is a further example of a compensation effect often found between enthalpy and entropy terms, e.g. in regard to heats and entropies of solution, of vaporization (Barclay and Butler rule<sup>11</sup>), of ionization and of activation in kinetic processes (e.g. in catalysis<sup>12</sup>). The origin of this kind of effect was first examined in general statistical mechanical terms by Longuet-Higgins<sup>13</sup> and Ruetschi<sup>14</sup>, and by Laidler<sup>15</sup> for ionization processes. In the present case, a greater degree of interaction implied by lower  $\chi_H$  values corresponds to a more ordered system with deeper local potential wells for librations or oscillations of elements of the polymer-solvent lattice, resulting in a diminished entropy or a more negative excess entropy. In more detailed molecular terms, we may suggest the following effects in the solutions as leading to the observed behaviour. The zeroth order lattice theory calculates entropy of mixing on the basis of two structureless pure components forming a random mixture. A positive  $\chi_s$  denotes a negative excess entropy, where the excess entropies are calculated relative to the 'ideal' value given by the lattice theory<sup>3</sup>. The results shown in *Figure 7* indicate that methanol has a negative excess entropy of mixing, ethanol an almost ideal entropy, while

*n*-propanol, *n*-butanol and *n*-amyl alcohol swell the polymer with a progressively greater entropy of mixing than the lattice theory predicts.

These excess entropies, together with the inverse coupling of the heat and entropy of swelling, are explicable if the structure of the alcohol in the pure solvent and in the swollen gel is considered. When the alcohol swells the polymer the hydrogen bonded structure of the pure solvent is broken down and is partially replaced by H-bonds between the alcohol hydroxyl groups and the ether oxygen atoms in the polymer backbone. A positive heat of mixing and a positive excess entropy of mixing is the expected consequence of a breakdown in hydrogen bonding in the gel relative to the pure solvent. If a locally ordered H-bonded arrangement of alcohol molecules around the polymer chains is more easily formed with small alcohol molecules than with large ones then the progressively larger excess entropies of swelling in passing from methanol to *n*-amyl alcohol are understandable.

The methyl side groups of the polypropylene oxide chains will sterically hinder the approach of the alcohol hydroxyl groups to the ether oxygen atoms of the chain. Additional steric hindrance due to the branched chain structure in the isomers of *n*-propanol and *n*-butanol may further reduce H-bonding giving a greater positive heat of mixing and positive excess entropy (positive  $\chi_H$  and negative  $\chi_S$ ) relative to the straight chain alcohols. The data in *Table 2* support this hypothesis. The small difference in  $\chi$  values between *n*-amyl and *i*-amyl alcohol is possibly because in *i*-amyl alcohol the branch in the hydrocarbon chain is remote from the hydroxyl group and does not greatly influence hydrogen bonding behaviour.

The  $\chi$  values shown in *Table 3* for the three non-polar solvents cannot be compared in detail with those for the alcohols, since they are at different concentrations and both  $\chi$  and  $\chi_S$  are strongly concentration-dependent. The results show, however, that even for non-polar solvents,  $\chi_S$  is rather sensitive to the size and shape of the molecule.

It is clear that variations in the swelling behaviour of different solvents towards polymers should not too readily be assumed to be due only to differences in the heats of mixing. Investigators have sometimes calculated an overall  $\chi$  value from the experimental results involving measurements which refer to the free energy of the system and have written

$$\chi = \chi_H + \text{constant}$$

assuming that the constant term is the same through an homologous series. Variations in  $\chi$  have then been discussed in terms of variation of the heat of swelling, without this quantity being measured experimentally. The experimental results on the polar solutions studied here, where the relationship between heat and entropy effects is more complex, show in an extreme form the weakness of this approach.

## APPENDIX

### RATE OF HEAT ABSORPTION IN THE CALORIMETER CELL WHEN MIXING IS CONTROLLED BY DIFFUSION

Although Calvet<sup>16</sup> claims that stirring is unnecessary in the Tian-Calvet calorimeter, other investigators<sup>17</sup> have used stirring during measurements of

heats of reaction and solution. As the heats of swelling and solution observed in the present experiments were of the order 0.05–0.5 calorie, no stirring was used in order to minimize errors, and the thermal change was assumed to be complete when the pen of the temperature/time recorder had returned to the baseline established at the beginning of the experiment.

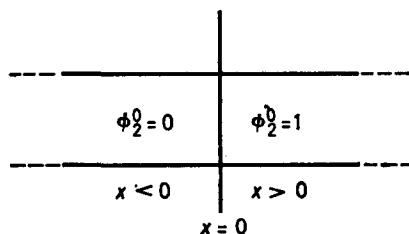
It may be argued that the experiments were terminated before mixing was really complete, because the final stages of the thermal change might take place very slowly over a long period of time causing an imperceptible deflection of the pen from the experimental zero on the recorder. To investigate the case in which mixing is controlled entirely by diffusion, the rates of mixing for two different arrangements of polymer and solvent were calculated.

Diffusion coefficients for binary mixtures of low molecular weight liquids are of the order  $10^{-5}$  cm<sup>2</sup> sec<sup>-1</sup> at room temperature and about  $10^{-7}$  cm<sup>2</sup> sec<sup>-1</sup> for solutions of high polymers (molecular weight  $> 10^5$ ) in simple organic solvents. We assume, as an approximation, a diffusion coefficient of  $10^{-6}$  cm<sup>2</sup> sec<sup>-1</sup> for the polymer of molecular weight 4 000 in ethanol and *n*-butanol.

*Diffusion through a plane boundary bisecting a cylinder of infinite length*

The model used for the calculation is shown in Figure 8.

Figure 8—Initial conditions for diffusion across a boundary in an infinite cylinder



If the plane through  $x=0$  initially separates pure polymer and pure alcohol, then after diffusion for time  $t$ , the volume fraction of polymer,  $\phi_2^t$ , at a distance  $x$  from the boundary is given by

$$\phi_2^t = \frac{\phi_2^0}{2} \left( 1 - \frac{2}{\pi^{1/2}} \int_0^y e^{-y^2} dy \right) \quad (6)$$

where

$$y = x/2 (Dt)^{1/2} \quad (7)$$

$D$  is the diffusion coefficient, and  $\phi_2^0$  is the volume fraction of polymer at zero time. After infinite time, equilibrium is reached and since  $\phi_2^0$  equals either 0 or 1 depending on the sign of  $x$ ,  $\phi_2^{t(\infty)} = \frac{1}{2}$  throughout the cylinder at  $t = \infty$ .

Since the quantity in parentheses in equation (6) is tabulated<sup>18</sup> as a function of  $y$ ,  $\phi_2^t$  can be evaluated. The rate of approach to equilibrium was calcu-

lated for the region 2 mm thick which is bounded by the planes  $x = +1.0$  mm and  $x = -1.0$  mm. The calorimeter cell is a cylinder of approximately 1 cm<sup>2</sup> cross-sectional area and thus if 0.1 g of polymer is added to 0.1 g of alcohol without stirring, then two layers of material each about 1 mm thick will be left to mix by diffusion.

Assuming that the heat of mixing is given by equation (1) then

$$\Delta H = (\chi_H / V_1) RTV \phi_1 \phi_2 \quad (8)$$

where  $\chi_H$  is assumed to be independent of concentration. When equal volumes of polymer and alcohol mix, then

$$\phi_2^{t(\infty)} = \phi_1^{t(\infty)} = 0.5 \quad (9)$$

and

$$\Delta H^{t(\infty)} = K \phi_1^{t(\infty)} \phi_2^{t(\infty)} \quad (10)$$

where  $\Delta H^{t(\infty)}$  is the total enthalpy change after infinite time, i.e. at equilibrium, and  $K$  is a combination of the constants in equation (8). After time,  $t$ , the amount of heat change is given by

$$\Delta H^t = K \phi_1^t \phi_2^t \quad (11)$$

or writing  $\Delta H^t$  as a fraction of the complete enthalpy change, we have

$$\frac{\Delta H^t}{\Delta H^{t(\infty)}} = \frac{\phi_1^t \phi_2^t}{\phi_1^{t(\infty)} \phi_2^{t(\infty)}} \quad (12)$$

Thus, the fraction of the final heat change which has occurred at any instant can be determined by calculating from equation (6) the variation with time of the composition of the system. In *Figure 9*,  $\Delta H^t / \Delta H^{t(\infty)}$  is plotted against  $t^{\dagger}$  for the 2 mm segment of the infinite cylinder considered above, and after five hours it is seen that over 95 per cent of the heat change will have taken place.

#### *Diffusion from a layer at one end of a cylinder of finite length*

Kawalki has tabulated<sup>19</sup> (see also ref. 18) the distribution of material in a finite cylinder where the diffusing substance is initially concentrated at one end of the cylinder in a layer occupying one quarter of the volume. By calculating volume fractions for a system in which the polymer and alcohol, in layers of thickness 1 mm and 3 mm respectively, are mixing by diffusion, the fraction of the total heat of mixing realized after a given interval can be plotted against  $t^{\dagger}$ , as in *Figure 9*. In this case, 98 per cent of the heat change is complete after six hours.

In order to measure the rate of heat absorption in mixing experiments, where mechanical stirring had been reduced to a minimum, the experimental cell was half filled with mercury to partially immerse the syringe needle so that when the polymer was injected it floated up through the mercury and formed a layer beneath the alcohol. Two experiments were carried out under these conditions in which 0.217 g polymer was allowed to mix with 0.159 g *n*-butanol and 0.057 g polymer with 0.622 g alcohol. The fraction of the total heat of mixing which had registered on the recorder

## EQUILIBRIUM SWELLING OF POLYOXYPROPYLENE ELASTOMERS

after a given time was obtained by summing successive areas under the temperature/time curve. The results are plotted in *Figure 9*, and in both cases over 98 per cent of the thermal change was observed to be complete after six hours.

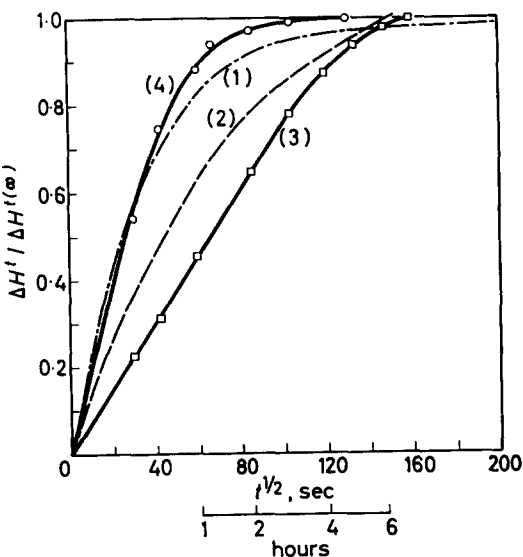


*Figure 9*—Experimental and theoretical curves for fraction of total heat change complete after a given time when mixing is diffusion controlled (1) 2 mm section of infinite cylinder; (2) 4 mm finite cylinder; (3) 0.217 g polymer plus 0.159 g alcohol (experimental); (4) 0.0572 g polymer plus 0.622 g alcohol (experimental)

The results show that adequate mixing by diffusion can be obtained in the experimental cell provided that the total volume of solution produced is less than about 0.5 ml, that care is taken to keep the area of initial contact between the two components as large as possible, and that distances through which they must diffuse are kept down to one or two millimetres. With diffusion coefficients around  $10^{-5} \text{ cm}^2 \text{ sec}^{-1}$ , as in simple liquid mixtures, the situation is even more favourable. With the high sensitivity and long-term stability of the Tian-Calvet microcalorimeter, it is as accurate, and less troublesome, to work with small quantities of material and eliminate mechanical stirring as it is to use larger volumes of materials which would give greater total heats but also require mechanical stirring to give complete mixing.

*Grateful acknowledgement is made to the Defence Research Board, Department of National Defence, Canada, for support of this work on Grant No. 9530-15.*

*The technical assistance of Mr M. B. I. Janjua is also acknowledged.*

*Department of Chemistry,  
University of Ottawa,  
Ottawa, Canada*

*(Received September 1963)*



REFERENCES

- <sup>1</sup> CONWAY, B. E. and TONG, S. C. *J. Polym. Sci.* 1960, **46**, 113
- <sup>2</sup> CALVET, E. and PRAT, H. *Microcalorimetrie, Applications Physicochimiques et Biologiques*. Masson: Paris, 1956
- <sup>3</sup> CONWAY, B. E. and LAKHANPAL, M. L. *J. Polym. Sci.* 1960, **46**, 75
- <sup>4</sup> ALLEN, G., GEE, G. and NICHOLSON, J. P. *Polymer, Lond.* 1961, **2**, 56
- <sup>5</sup> CONWAY, B. E. and BIDINOSTI, D. R. In course of publication
- <sup>6</sup> FLORY, P. J. and REHNER, J. *J. chem. Phys.* 1943, **11**, 521
- <sup>7</sup> FLORY, P. J. *Principles of Polymer Chemistry*. Cornell University Press: Ithaca, New York, 1953
- <sup>8</sup> CONWAY, B. E. *J. Polym. Sci.* 1960, **46**, 129
- <sup>9</sup> CONWAY, B. E. and LAKHANPAL, M. L. *J. Polym. Sci.* 1960, **46**, 93
- <sup>10</sup> ZACHARIASEN, W. H. *J. chem. Phys.* 1935, **3**, 158; *Phys. Rev.* 1932, **39**, 185
- <sup>11</sup> BARCLAY, I. M. and BUTLER, J. A. V. *Trans. Faraday Soc.* 1938, **34**, 1445
- <sup>12</sup> CREMER, E. *Advances in Catalysis*, Vol. VII, p 75. Academic Press: New York, 1955
- <sup>13</sup> LONGUET-HIGGINS, H. C. *Proc. Roy. Soc. A*, 1951, **205**, 247
- <sup>14</sup> RUETSCHI, P. *Z. phys. Chem.* 1958, **14**, 277
- <sup>15</sup> LAIDLER, K. J. *Trans. Faraday Soc.* 1959, **55**, 1725
- <sup>16</sup> CALVET, E. and PRAT, H. *Progrès Récent en Microcalorimetrie*, p 8. Dunod: Paris, 1958
- <sup>17</sup> LOVERING, E. J. and LAIDLER, K. J. *Canad. J. Chem.* 1962, **40**, 26
- <sup>18</sup> JOST, W. *Diffusion in Solids, Liquids and Gases*. Academic Press: New York, 1952
- <sup>19</sup> KAWALKI, W. *Ann. Phys., Lpz. [Wied. Ann.]* 1894, **52**, 166

# Radiation Effects in Polyvinyl Acetate

L. D. MAXIM\*, R. H. MARCHESSAULT, V. STANNETT† and C. H. KUIST\*

*The radiation behaviour of polyvinyl acetate was investigated. A specially prepared polyvinyl acetate (pure, high molecular weight, essentially linear) was subjected to high energy gamma radiation. After 10 Mrad (the gelation dose) an insoluble network was formed and the soluble fraction decreased with increasing dose. The variation of molecular weight up to the gel point was followed by osmometry and viscosity measurements. After gelation, the course of the reaction was studied by analysis of soluble fractions, and swelling behaviour in acetone and methyl ethyl ketone. A new apparatus for making equilibrium vapour sorption measurements is described and analysed theoretically.*

*Application of current radiation theory fairly well describes experimental results. The polymer undergoes simultaneous crosslinking and chain scission. The ratio of scission to crosslinking is 0.04/1.0. The G value for crosslinking is 0.1 crosslinks/100 eV, as determined by molecular weight, and soluble fraction data. The G value as determined from swelling measurements is somewhat higher.*

*Acetic acid is evolved, the amount is proportional to the total dose. This relation is given by the equation:*

$$\text{Per cent acetic acid} = 1.36 \times 10^{-2} (r)^{0.7}$$

HIGH energy radiation produces profound changes in the structure of high polymeric materials. Most polymers when subjected to high energy radiation fall into two categories, those which primarily degrade, and those which primarily crosslink.

Although much has been published on radiation effects in many polymers, relatively little has been published on polyvinyl acetate. This is rather unexpected as polyvinyl acetate is a material of considerable industrial importance.

Miller *et al.*<sup>1</sup> suggested a simple rule for the radiation behaviour of vinyl type polymers. Polymers with two side chains attached to a single carbon (e.g.  $-\text{CH}_2\text{CR}_1\text{R}_2-$ ) degrade; polymers with a single side chain (e.g.  $-\text{CH}_2\text{CHR}_1-$ ) crosslink. Here hydrogen is not considered a side chain, while other substituents (e.g. chlorine, fluorine, etc.) are taken as such. The explanation offered is that the removal of an  $\alpha$  hydrogen atom from a group  $-\text{CH}_2-\text{CHR}_1-$  leaves a radical molecule which is resonance stabilized with the side group. Hydrogen abstraction from a neighbouring molecule leaves another stable free radical. These two radicals can then react to form a crosslink. Abstraction of a hydrogen atom from molecules with a tertiary carbon does not produce any such resonance stabilization. Here the molecule would degrade first. This appears to be a useful general rule although it does not explain the crosslinking of polyethylene, in which no

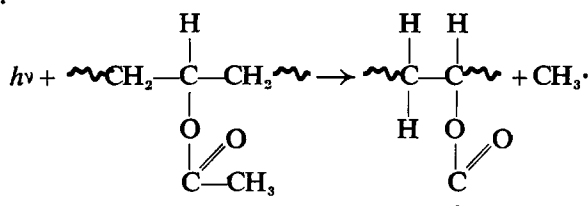
\*Present address: National Starch & Chemical Corporation, Plainfield, N.J.

†Present address: Camille Dreyfus Laboratory, Research Triangle Institute, Durham, N.C.

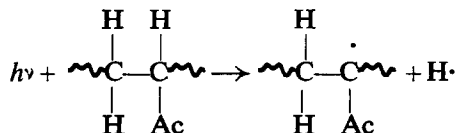
resonance effects of this type are possible. On the basis of this rule one would expect polyvinyl acetate, being a polymer of the type ( $-\text{CH}_2-\text{CHR}_1-$ ), to undergo primarily a crosslinking reaction.

Charlesby and Pinner<sup>2</sup> reported polyvinyl acetate as both crosslinking and degrading when subjected to high energy radiation (0–300 Mrad) in the presence of air. Experimental  $G$  values ranged from 0.26–0.31. These were derived from solubility studies on the crosslinked material. Crosslinking was believed to occur at least partly through the acetate side chains. This conclusion was prompted by the known difficulty of crosslinking dry polyvinyl alcohol.

Todd<sup>3</sup> reported polyvinyl acetate as degrading when subjected to *ca.* 50 Mrad *in vacuo*. By mass spectrographic analysis, methane and hydrogen in the ratio of 0.7/1.0 were identified as the major products. Rupture of the  $\alpha$  carbon would liberate methyl radicals and account for the formation of methane.

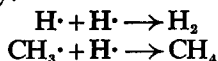


Irradiation might also remove a hydrogen atom



(although here the hydrogen was shown removed from the  $\alpha$  carbon, any other hydrogen might be removed).

This could be followed by:

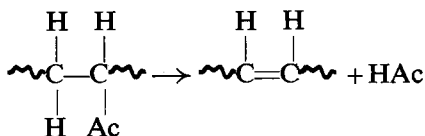


These reactions would account for the production of hydrogen and methane. Todd's data did not, however, include any molecular weight studies, nor did it give any reference to the absolute quantities of volatiles released.

Work undertaken at General Electric, however, reported that polyvinyl acetate crosslinked upon irradiation<sup>4</sup>. In a patent for a process of producing crosslinked polyvinyl alcohol, polyvinyl acetate was first crosslinked by irradiation, and subsequently deacetylated to produce the polyvinyl alcohol. The fact that this process produced substantially quantitative yields shows that crosslinking occurred on the polyvinyl alcohol moiety of the original polymer. This would correlate with Miller's theory of resonance stabilization.

Abraham *et al.*<sup>5</sup> studied the electron spin resonance of irradiated polyvinyl acetate. They observed a single line in the spectrum of relatively low intensity. An approximate  $G$  value (number of radicals produced per 100 eV incident radiation) was calculated to be about 0.3.

The mechanism of thermal degradation of polyvinyl acetate has been investigated by Grassie and others<sup>6</sup>. Here acetic acid splits out, leaving a double bond in the main chain, which subsequently enters into crosslinking reactions:



One might expect an analogous mechanism to occur with irradiation degradation; however, Todd<sup>3</sup> reported no acetic acid evolved.

Thus a literature search did not conclusively indicate exactly what happened to polyvinyl acetate upon irradiation. Depending upon the author quoted, one can assert that polyvinyl acetate crosslinks, degrades, or both crosslinks and degrades.

The purpose of this study was to determine the radiation behaviour of polyvinyl acetate. Previous investigators have examined only discrete parts of the picture.

Current radiation theory offers several experimental methods for arriving at theoretical conclusions. By following the variation in molecular weight, soluble fraction, network swelling, and using also more conventional methods of analysis (infra-red, gas chromatography), insight can be gained into the 'kinetics' and mechanism of radiation reactions.

#### THEORY

For polymers which crosslink primarily, the average molecular weight will increase up to the gel point. At the gel point the material will first become insoluble. The soluble fraction will decrease with increasing dose beyond the gel point, finally reaching a limiting value dependent on the ratio of scission to crosslinking. Formally, the reaction can be divided into two areas: the pre-gel reaction and the post-gel reaction.

##### *The pre-gel reaction*

The complete mathematical picture of the variation of molecular weight with dose has been developed by Charlesby<sup>7</sup>. For a polymer with an initially random molecular weight distribution the following relation applies

$$(1/u_1') = (1/u_1) + (p_0 - \frac{1}{2}q_0) r \quad (1)$$

where  $u_1$  denotes initial number average degree of polymerization,  $u_1'$  is the number average degree of polymerization after dose  $r$ ,  $p_0$  is the fraction of main chain units scissioned by unit dose,  $q_0$  is the fraction of main chain units crosslinked by unit dose, and  $r$  is the radiation dose (Mrad). The quantities  $p_0$  and  $q_0$  are of fundamental importance for the material in question. These quantities represent the susceptibility of a material to scission or crosslinking. Another quantity of fundamental significance is the  $G$  value. The  $G$  value is the number of 'events' (i.e. scissions, crosslinks, molecules of gas evolved, etc.) per 100 eV radiation. The  $G$  value for scission is given by equation (2).

$$G_s = 0.96 \times 10^6 p_0/w \quad (2)$$

where

$$w = \text{mer weight}$$

The  $G$  value for crosslinking is given by the relation

$$G_c = 0.48 \times 10^6 q_0/w \quad (3)$$

The proportionality constant between  $G_c$  and  $q_0$  is one half that between  $G_s$  and  $p_0$  as a crosslink involves the linking together of two chains.

#### *The post-gel reaction*

Charlesby<sup>8</sup> has shown that a material becomes insoluble when there is, on the average, one crosslink per weight average molecule.

The  $G$  value for crosslinking can be calculated by the formula

$$G = 0.48 \times 10^6 / r_{\text{gel}} \bar{M}_w \quad (4)$$

where  $\bar{M}_w$  is the initial weight average  $\bar{M}_w$  and  $r_{\text{gel}}$  denotes dose for incipient gelation. If the initial molecular weight distribution is random then  $\bar{M}_w/\bar{M}_n = 2$  and equation (4) becomes

$$G = 0.24 \times 10^6 / r_{\text{gel}} \bar{M}_n \quad (5)$$

After the gelation dose  $r_{\text{gel}}$  the material rapidly becomes insoluble reaching a limiting value dependent on the ratio of scission to crosslinking.

Charlesby and Pinner<sup>2</sup> have derived an expression for the variation of soluble fraction with dose for a material with an initially random molecular weight distribution.

$$s + s^{\dagger} = p_0/q_0 + 1/q_0 u_1 r \quad (6)$$

A plot of  $s + s^{\dagger}$  versus  $1/r$  will have an intercept of  $p_0/q_0$  and a slope of  $1/q_0 u_1$ . For other distributions, plots of  $s + s^{\dagger}$  against  $1/r$  will only be linear at doses sufficiently high for the distribution to become random.

#### SWELLING THEORY

Most amorphous polymers, if not crosslinked, dissolve in a number of organic solvents. These same polymers, when crosslinked, will only swell to an equilibrium value, which depends on the polymer, solvent, crosslink density, etc.

Thermodynamically speaking, this equilibrium swelling will be reached when the free energy involved in mixing the polymer with the solvent  $\Delta F_m$  is balanced by the elastic free energy  $\Delta F_{el}$  of the network which is due to the swelling restraints imposed by the crosslinks.

Hermans<sup>9</sup> has derived an expression relating the solvent activity, polymer solvent interaction, volume swelling ratio, and molecular weight between crosslinks etc. shown below

$$\ln a = \left(1 - \frac{1}{Q}\right) + \frac{1}{Q} + \mu \left(\frac{1}{Q^2}\right) + \frac{\rho V}{M_c} \left[ \left(Q_0^{-2/3}\right) \left(\frac{1}{Q}\right)^{1/3} - \frac{1}{Q} \right] \quad (7)$$

where  $a$  is solvent activity,  $Q$  is swelling ratio,  $\rho$  is polymer density,  $V$  is molar volume of solvent,  $\mu$  is Flory-Huggins polymer solvent interaction

parameter,  $M_c$  is molecular weight between crosslinks, and  $Q_0$  denotes reference degree of swelling in which state the polymer chains have their unrestrained or freely dispersed end to end distance. If the solvent activity is equal to unity, equation (7) can be rearranged to calculate the molecular weight between crosslinks.

$$M_c = \frac{\rho V [(Q_0)^{-2/3} (1/Q)^{1/3} - 1/Q]}{-[\ln(1 - 1/Q) + 1/Q + \mu (1/Q)^2]} \quad (8)$$

The  $G$  value for crosslinking is related to the molecular weight between crosslinks<sup>8</sup> as follows

$$G = 0.48 \times 10^6 / r M_c \quad (9)$$

#### EXPERIMENTAL

Solvents were purified in a 60 cm temperature compensating column packed with glass beads operated at atmospheric pressure. Throughput at a reflux ratio of 9/1 was approximately 1.5 ml/min. Solvent purity was determined by gas chromatography.

The same system was used for vinyl acetate purification. However, the column was operated at 600 mm of mercury to minimize the possibility of thermal polymerization.

Purified vinyl acetate monomer was polymerized in bulk at 50°C, using 0.1 per cent azobis-isobutyronitrile as an initiator. Conversions were limited to about 10 per cent to ensure relatively linear polymer<sup>10</sup>. The number average molecular weight of the polymer was 270 000. Polymer purification was accomplished by precipitation in hexane to remove monomer and leach out very low molecular weight fractions. The precipitated polymer was redissolved in methanol and precipitated with distilled water twice. The purified polymer was isolated by a technique similar to the frozen benzene method described by Goldberg<sup>11</sup> and Lewis and Mayo<sup>12</sup>. A conventional freeze drying apparatus was employed for this purpose.

Thus isolated, the polymer was dissolved in distilled ethyl acetate, and films were cast from this solution.

#### Irradiation

Polymer samples in the form of 0.5 mm thick films *ca.* 500 mg, were placed in Pyrex ampoules for irradiation in the <sup>60</sup>Co source at Brookhaven National Laboratories. The ampoules were equipped with ground glass standard taper joints so that they could be joined to a vacuum line (mercury diffusion pump, backed by a commercial Hi Vac pump). Samples were evacuated to 10<sup>-5</sup> mm of mercury and maintained at this pressure for about 16 hours to remove traces of solvent, adsorbed volatiles, etc.

The ampoules were then sealed under vacuum. Exposure doses were varied from 1–250 Mrad. The dose rate used was 1.21 × 10<sup>6</sup> rad/h. Since there was some question as to whether  $G$  values increased above the second order transition temperature of the polymer, irradiation was performed at a temperature above the  $T_g$  for polyvinyl acetate. The most convenient temperature (due to equipment limitations) was 50°C. Dose rates were checked and calibrated by the ferrous oxidation method, which is standard for this operation<sup>13,14</sup>. The irradiation was performed at Brookhaven National Laboratories through the courtesy of Dr Donald Metz.

## MOLECULAR WEIGHT DETERMINATIONS

Intrinsic viscosities were run in acetone using a one point viscosity measurement method. Intrinsic viscosities were calculated using the Sakurada equation<sup>15,16</sup> and these were converted to number average molecular weights by the equation<sup>17</sup>

$$[\eta] = 1.76 \times 10^{-4} (M_n)^{0.68} \quad (10)$$

Direct measurement of number average molecular weight was made using Zimm-Meyerson osmometers in acetone. A period of 24 hours was required to reach equilibrium and readings were taken on the second filling. Molecular weights were calculated from the formula

$$\bar{M}_n = \frac{RT}{\rho_{sol} (\Delta h/C)_{C=0}} \quad (11)$$

## SWELLING MEASUREMENTS

Swelling studies were run in an apparatus designed by C. H. Kuist of National Starch and Chemical Corpn. *Figure 1* represents the experimental apparatus.

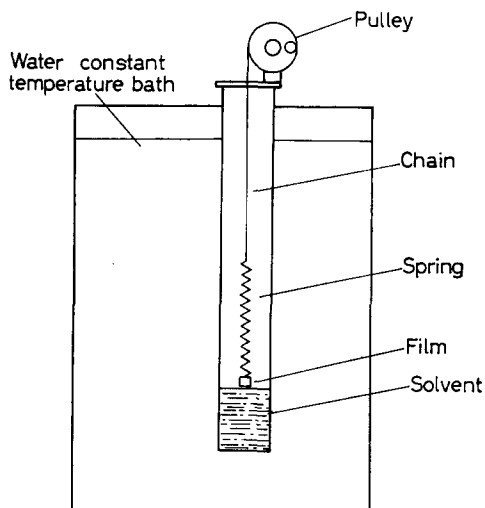


*Figure 1*—Kuist column schematic

This consists of a glass tube about 40 cm long immersed in a constant temperature bath. Approximately 100 ml of the solvent to be used is placed in the tube. A small fused quartz helix (spring) is supported in the tube from a chain attached to a pulley. The polymer sample is cut into a small square (film) and placed on a Nichrome hook attached to the spring. The film is lowered into the solvent for about two hours and then raised above the solvent level. Approximately eight hours (depending on film thickness,  $M_c$ , etc.) is required to reach a constant weight, measured by the spring extension. If  $W_t$  denotes total weight (determined by spring extension),  $W_h$  is weight of Nichrome hook,  $W_i$  is initial film weight,  $F$  is fraction of insolubles,  $W_{pc}$  is corrected weight of polymer, and  $W_s$  is the weight of absorbed solvent, then:

$$W_t = W_h = W_{pc} + W_s$$

$$W_{1(F)} = W_{pc}$$

$$W_{pc} + W_s = W_{pc} = W_s \quad (12)$$

and

$$Q = \frac{(\rho_p)(W_s) + 1}{\rho_s W_{pc}} \quad (13)$$

where  $\rho_p$  is the polymer density and  $\rho_s$  the solvent density. The  $Q$  value determined will, of course, vary with the height of the film above the solvent. If the activity gradient in the column is linear then extrapolation to unit activity gives the desired  $Q$  from which  $M_c$  can be calculated.

From a theoretical point of view it can be shown that the activity gradient should be linear. If the activity of the solvent is defined as

$$a = p/p_0 \quad (14)$$

where  $p$  is actual pressure and  $p_0$  the saturation pressure, and if the solvent vapour behaves as an ideal gas then

$$p = nRT/v \quad (15)$$

where

$$n/v = C \text{ mole/litre}$$

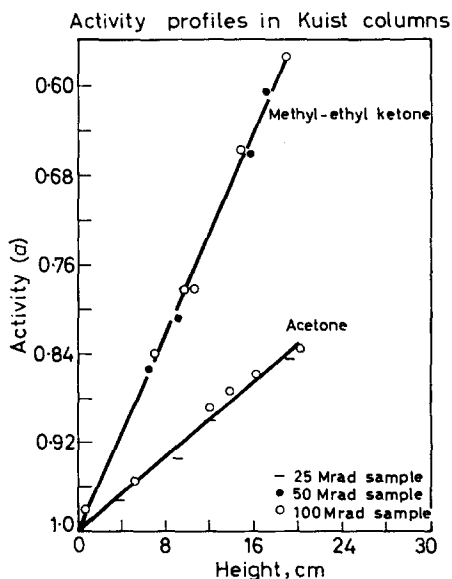
Substituting

$$a = CRT/p_0 \quad (16)$$

If the diffusivity is independent of concentration, then Fick's law applies. (The column is isothermal.) From Fick's law

$$\frac{\partial c}{\partial t} = -D\nabla^2 C \quad (17)$$

Figure 2—Activity profiles in Kuist columns





At the steady state

$$\frac{\partial c}{\partial t} = 0 \quad (18)$$

For the unidirectional case:

$$\frac{\partial c}{\partial x} = 0, \quad \frac{\partial c}{\partial z} = 0 \quad \text{and therefore } C = C_1 + C_2 y \quad (19)$$

Thus a linear activity profile would be expected throughout the column. This was checked by calculating the activity for a series of films with known  $M_c$  as a function of column height. The films were calibrated by measuring their swelling at unit activity in a swelling balance apparatus similar to that described by Rijke and Prins<sup>18</sup>.

As expected, activity profiles are linear, but contrary to expectation the activity gradient depends on solvent as shown in *Figure 2*. This is probably due to certain limitations of the experimental set up, principally that of preventing convection currents over the columns. Humidity in the atmosphere sometimes presented a problem if the samples absorbed water, thereby giving high values for the swelling measurement and perhaps affecting the activity profile itself. Although empirical equations could have been derived to account for these effects, no attempt was made in this direction as any equation would not have been of general validity. Should any variable in the design of the column be changed (e.g. size of chain hole, column length, etc.) the activity gradient will change. However, as long as isothermal conditions are maintained this gradient will be linear.

#### RESULTS AND DISCUSSION

Polyvinyl acetate was found to undergo both crosslinking and degradation when subjected to high energy radiation. At doses above 10 Mrad the

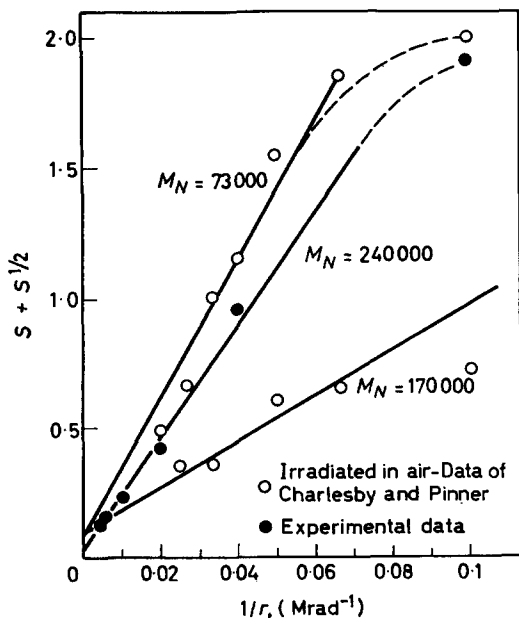


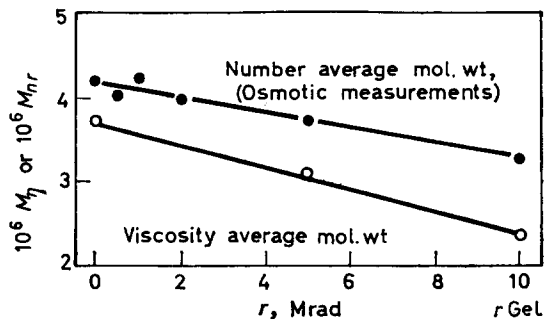
Figure 3—Reciprocal dose against  $s + s^{1/2}$  for polyvinyl acetate

material became insoluble. Values of  $s+s^1$  versus  $1/r$  are plotted in Figure 3. The data of Charlesby and Pinner<sup>2</sup> for air irradiated polyvinyl acetate are included for reference. Except for the first point, a linear plot is obtained. The deviation of the first point is due primarily to the fact that a completely random molecular weight distribution, as assumed in the derivation of equation (6), probably does not exist initially. Since radiation is a random process, the actual curve should approach the theoretical linear curve for a random initial distribution. In fact, this is so. The intercept from Figure 3 corresponding to the ratio of  $p_0/q_0$  is equal to about 0.040. This indicates that crosslinking occurs predominantly. As can be seen the ratio of degradation to crosslinking is higher in the presence of oxygen. The effect of oxygen during the irradiation of polymers is not completely understood. For some polymers the presence of oxygen tends to accelerate degradation, for others little or no effect is observed, frequently results are erratic in this respect. With polyisobutylene the rate of chain cleavage was found to be independent of environment (air, nitrogen, or *in vacuo*); however<sup>19</sup>, the products of degradation were affected. Literature results differ with respect to polymethyl methacrylate, one study showing no oxygen effect<sup>20</sup>, the other indicating oxygen as an inhibitor for the degradation reaction<sup>21</sup>. Polyethylene has been found to react with oxygen during irradiation<sup>22</sup>, to require greater doses for gelation<sup>23</sup>, or to undergo degradation<sup>24</sup> in the presence of oxygen. Alexander and Toms<sup>23</sup> found that the ratio  $p_0/q_0$  increased in the presence of oxygen, not because of a decrease in  $q_0$  but rather because of an increase in  $p_0$ . With polystyrene which crosslinks *in vacuo*, no gel can be produced in the presence of oxygen regardless of the magnitude of the dose<sup>23,25</sup>. In the light of the results of Alexander and Toms this would indicate that  $p_0$  is increased in oxygen to the point where  $p_0$  is greater than  $2q_0$  [cf. equation (1)]. In the case of polyvinyl acetate the ratio of  $p_0/q_0$  is lower *in vacuo* than in air. In addition the  $G$  value for crosslinking is lower *in vacuo* than in air. This would indicate that the effect of oxygen is to increase both  $p_0$  and  $q_0$ , the former at a faster rate.

#### Molecular weight changes up to the gel point

The change of molecular weight with dose was followed by two methods, osmometry and viscosity. Osmometry was used because it gave direct information on the number average molecular weight, which is used in all

Figure 4—Variation of molecular weight with dose for irradiated polyvinyl acetate



theoretical equations. Viscosity relations were also used as a number of authors (particularly Black and Lyons<sup>26</sup>) reported that direct measurement of the number average molecular weight was not as informative in cases such as radiation-induced chain fracture where the bonds are broken at random, as the value is unduly weighted by breaks occurring at the ends of the molecular chains. Equation (1) indicates that a plot of  $1/\mu'_1$  versus  $r$  should be linear with a slope of  $(p_0 - q_0/2)$ . Figure 4 shows the data plotted in this manner. Assuming that the ratio of degradation to crosslinking is known from solubility measurements as 0.040, simultaneous solution of equation (3) with the limiting degradation crosslinking ratio yields a  $G$  value. The  $G$  value obtained from these data was 0.098, i.e. about 0.1 crosslinks/100 eV. For an initially random distribution, with crosslinking the only reaction, the ratio of the number average molecular weight at the gel point to the initial number average molecular weight can be calculated to be  $M'_n = 1.33 M_n$ . Since degradation also occurs, the actual value of this ratio should be lower. The value obtained from osmometry is 1.28, and is, therefore, quite reasonable.

Number-average molecular weights derived from viscosity measurements are also plotted in Figure 4. The calculated  $G$  value is 0.143, somewhat higher than that calculated by osmometry. The ratio ( $M'_n/M_n$ ) at the gel point is equal to 1.57, a value not to be expected in the case of crosslinking and degradation of an initially random polymer. This tends to indicate that the viscosity expression is not as reliable as that obtained from osmometry and that disturbing effects due to end scission are not important. Further, the viscosity expressions presuppose a linear polymer. After any radiation the polymer is extensively branched, so that number average molecular weight approximations by viscosity techniques are subject to error. An approximate expression for the viscosity of branched polymers has been derived by Stockmayer *et al.*<sup>27</sup>. However, this expression does not adequately describe experimental results at high degrees of branching<sup>28</sup>. Whenever possible, then, it is desirable to have osmotic measurements to determine changes in molecular weights (this is particularly true in polymers which crosslink primarily).

#### *Analysis of soluble fractions*

As can be seen from equation (6) it is possible to calculate a  $G$  value from the variation in solubility with dose, as well as the limiting ratio of degradation to crosslinking. From the slope of the line in Figure 3 a  $G$  value of 0.093 (0.1) has been calculated.

If the initial distribution of molecular weights is random then it is possible to calculate a  $G$  value from the dose necessary to produce incipient gelation. Using equation (5) a  $G$  value of 0.104 was calculated.

#### SWELLING STUDIES

From an analysis of the variation of molecular weight between crosslinks, it is possible to calculate  $G$  values for crosslinking. Using equation (8),  $M_c$  for any given degree of swelling at unit activity can be calculated. Substitution into equation (9) yields a  $G$  value.  $G$  values calculated from swelling measurements show considerable variation. Tabulated results are shown

## RADIATION EFFECTS IN POLYVINYL ACETATE

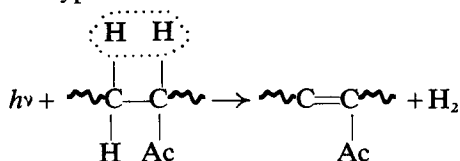
in Table 1. The large variations observed are probably due to the fact that measurements are fundamentally of low accuracy. Chain entanglements appear as crosslinks, yielding a higher number of crosslinks than actually occur. Further a comparatively small error in the determination of the ratio of the swollen volume to the dry volume leads to a rather large error in the calculation of the molecular weight between crosslinks. This small error results in considerably less error in the determination of the solvent activity.

Table 1. *G* values from swelling studies

Dose (Mrad)	<i>q</i>	<i>G</i> value
25	29.8	0.10
50	8.00	0.80
100	5.36	0.90
150	4.84	1.0
250	4.50	0.7

### MECHANISM OF CROSSLINKING REACTION

Infra-red analysis indicated two important facts. At low doses (1–5 Mrad) unsaturation appears. This is evidenced by the appearance of a band at  $6.1 \mu$ , see Figure 5. This could be explained by either (a) molecular hydrogen abstraction of the type



or (b) a free radical mechanism such as

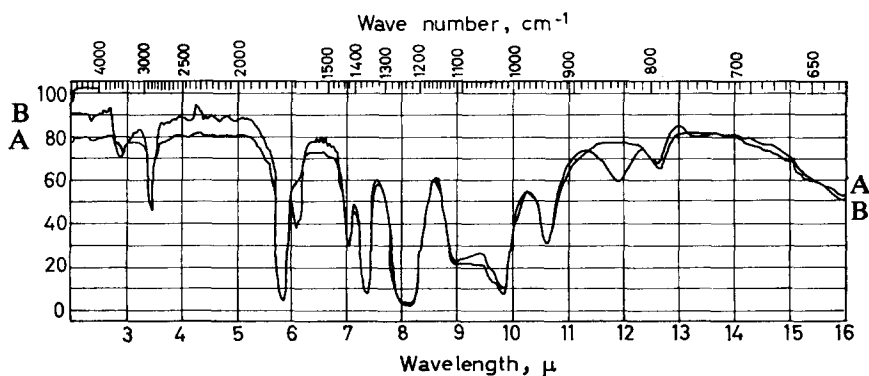
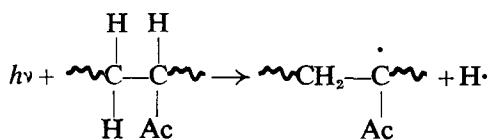


Figure 5—Infra-red spectra of irradiated polyvinyl acetate: A—control; B—1.5 Mrad

and subsequent hydrogen abstraction

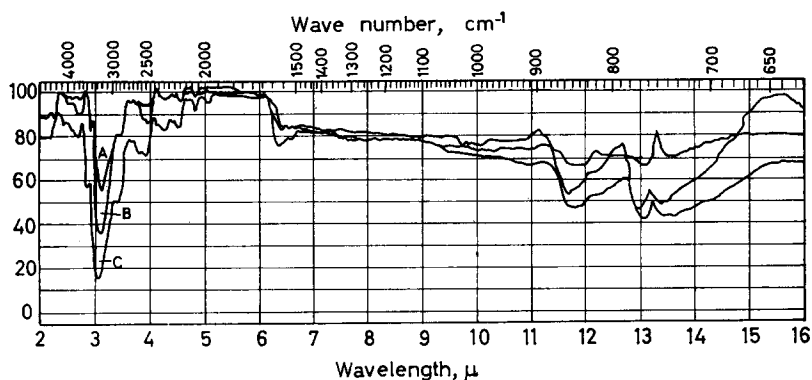
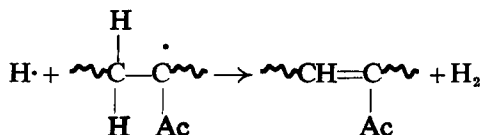


Figure 6—Differential infra-red spectra of irradiated polyvinyl acetate: curve A—5 Mrad; curve B—100 Mrad; curve C—250 Mrad

At higher doses, differential spectra indicated strong bands at 3.1 and 11.8 microns (see Figure 6). This would correspond to a hydroxyl group. The hydroxyl in acetic acid would account for this, but a spectra of acetic acid (Figure 7) showed a much broader 3.3 micron band and no band at

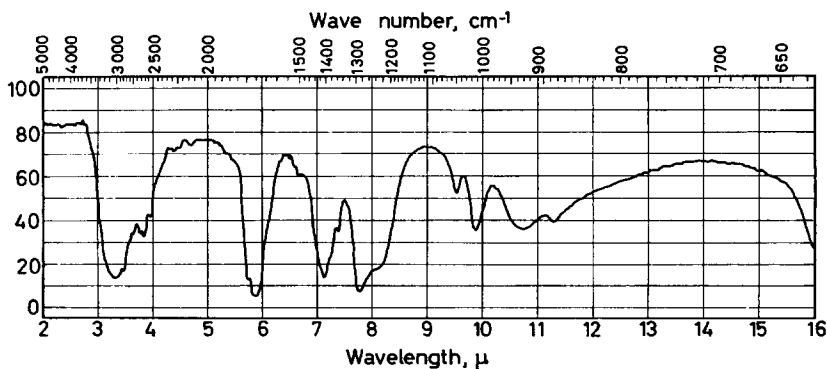


Figure 7—Infra-red spectrum of acetic acid

11.8 microns. The possibility that these bands might shift position and shape was investigated by exposing un-irradiated films to acetic acid vapour, and running these films against a control. Results of these runs are shown on Figure 8, and correspond exactly to Figure 6, indicating that this was the case and that acetic acid was evolved. In order to quantitate these results, samples were opened under water and titrated with 0.1002 N sodium

## RADIATION EFFECTS IN POLYVINYL ACETATE

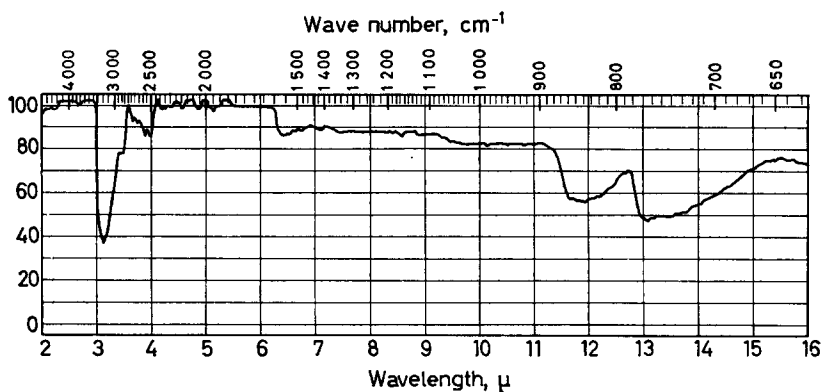


Figure 8—Differential infra-red spectrum of polyvinyl acetate swollen with acetic acid versus polyvinyl acetate

hydroxide. Choosing the 250 Mrad value for acetic acid by titration, infra-red values were normalized. The amount of acetic acid evolved versus dose is plotted in Figure 9. Over the range 50–250 Mrad the empirical equation relating the percentage acetic acid to dose (Mrad) is

$$\text{acetic acid (per cent)} = 1.36 \times 10^{-2} (r)^{0.7} \quad (20)$$

The amount of acetic acid is proportional to the dose to the 0.7 power. If a strictly random process were to take place the amount of acetic acid

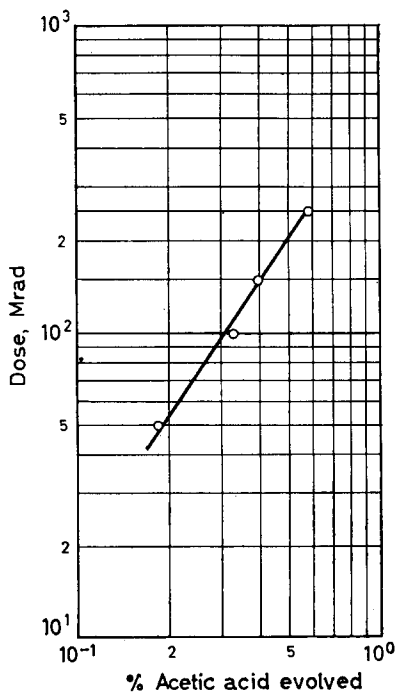


Figure 9—Relation between amount of acetic acid given off and dose (Mrad) for irradiated polyvinyl acetate

evolved would be proportional to the dose to the 1.0 power. The  $G$  value for gas evolution will, of course, vary. This effect has been noted previously for the disappearance of vinyl unsaturation and appearance of vinylene unsaturation in polyethylene<sup>28</sup>. A similar behaviour was observed in the radiolysis of *n*-hexane and other paraffins<sup>29</sup>. In these cases the amount of unsaturation increased linearly at first and then tapered off. One other possibility presents itself—it is possible that the reaction is diffusion controlled. If radiation is a random process and the dose rate is kept constant, then the rate of reaction will also be a constant. If it is further assumed, however, that a reversible reaction takes place, the net rate of reaction is:

$$\begin{aligned} \text{Net rate} &= \text{Rate at which product forms} - \text{rate at which product recombines} \\ \text{Rate at which product forms} &= K \text{ (for given dose rate)} \\ \text{Rate at which product recombines} &= k(c)^n \\ \text{Net rate (observed)} &= K - k(c)^n \end{aligned} \quad (21)$$

The concentration of product ( $c$ ) in equation (21) will be a function of the diffusivity, type of diffusion, etc. Thus it is very possible that an apparent complex dependence of product on dose may result. This effect has been observed in thermal degradation studies.

*The authors are grateful to Dr D. Metz of Brookhaven National Laboratories for performing the irradiation. One of us (L.D.M.) received financial assistance from the National Starch & Chemical Corporation while this work was being performed.*

*Department of Chemistry,  
State University College of Forestry,  
Syracuse University, Syracuse 10, N.Y.*

*(Received November 1963)*

#### REFERENCES

- <sup>1</sup> MILLER, A. A., LAWTON, E. J. and BALWIT, J. S. *J. Polym. Sci.* 1954, **14**, 503
- <sup>2</sup> CHARLESBY, A. and PINNER, S. H. *Proc. Roy. Soc. A*, 1959, **249**, 367
- <sup>3</sup> TODD, A. *J. Polym. Sci.* 1960, **47**, 223
- <sup>4</sup> *Brit. Pat. No. 798 146* 'Crosslinked polyvinyl alcohol', General Electric Co., 1958, 16 July
- <sup>5</sup> ABRAHAM, R. J. and WHIFFEN, D. H. *Trans. Faraday Soc.* 1958, **54**, 1133
- <sup>6</sup> GRASSIE, N. *Trans. Faraday Soc.* 1952, **48**, 372
- <sup>7</sup> CHARLESBY, A. *Proc. Roy. Soc. A*, 1954, **222**, 542
- <sup>8</sup> CHARLESBY, A. *Atomic Radiation and Polymers*, p 140. Pergamon: New York, 1960
- <sup>9</sup> HERMANS, J. J. *Trans. Faraday Soc.* 1947, **43**, 591
- <sup>10</sup> MATSUMOTO, M. and OHYANAGI, Y. *J. Polym. Sci.* 1960, **46**, 520
- <sup>11</sup> GOLDBERG, A. I. *Industr. Engng Chem. (Industr.)*, 1947, **39**, 1570
- <sup>12</sup> LEWIS, F. M. and MAYO, F. R. *Industr. Engng Chem. (Anal.)*, 1945, **17**, 134
- <sup>13</sup> WEISS, J. *Nucleonics*, 1952, **10** (7), 28
- <sup>14</sup> *ASTM: D1671-59T*
- <sup>15</sup> SAKURADA, I. *Chem. High Polymers (Tokyo)*, 1945, **2**, 253
- <sup>16</sup> VARAHDIAH, V. V. and RAO, M. R. *J. Polym. Sci.* 1956, **19**, 379
- <sup>17</sup> PETERLIN, A. in 'Die Physik der Hochpolymeren, Band II: 'Das Makromolekul in Lösungen', Ed. H. A. STUART, p 305. Springer: Berlin
- <sup>18</sup> RIJKE, A. M. and PRINS, W. *J. Polym. Sci.* 1962, **59**, 171
- <sup>19</sup> ALEXANDER, P., BLACK, R. M. and CHARLESBY, A. *Proc. Roy. Soc. A*, 1955, **232**, 31
- <sup>20</sup> ALEXANDER, P., CHARLESBY, A. and ROSS, M. *Proc. Roy. Soc. A*, 1954, **223**, 392
- <sup>21</sup> WALL, L. A. and BROWN, D. W. *J. Res. nat. Bur. Stand.* 1956, **57**, 131

## RADIATION EFFECTS IN POLYVINYL ACETATE

---

- <sup>22</sup> CHARLESBY, A. *Proc. Roy. Soc. A*, 1952, **215**, 187
- <sup>23</sup> ALEXANDER, P. and TOMS, D. *J. Polym. Sci.* 1956, **22**, 343
- <sup>24</sup> CHAPIRO, J. *J. Chim. phys.* 1955, **52**, 246
- <sup>25</sup> FENG, P. Y. and KENNEDY, J. W. *J. Amer. chem. Soc.* 1955, **77**, 847
- <sup>26</sup> BLACK, R. M. and LYONS, B. J. *Proc. Roy. Soc. A*, 1959, **253**, 322
- <sup>27</sup> STOCKMAYER, W. H. and FIXMAN, M. *Ann. N.Y. Acad. Sci.* 1953, **57**, 334
- <sup>28</sup> CHARLESBY, A. *Atomic Radiation and Polymers*, p 289. Pergamon: New York, 1960
- <sup>29</sup> DOLE, M., MILNER, D. C. and WILLIAMS, T. F. *J. Amer. chem. Soc.* 1958, **80**, 1580
- <sup>30</sup> MILLER, A. A., LAWTON, E. J. and BALWIT, J. S. *J. phys. Chem.* 1956, **60**, 599



# The Polymerization of Butadiene with Chromium Acetylacetonate and Aluminium Triethyl

C. E. H. BAWN, A. M. NORTH and J. S. WALKER\*

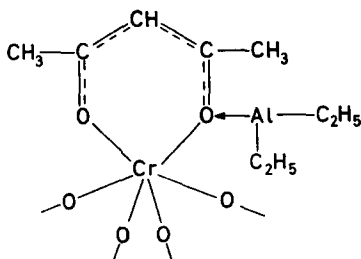
*Butadiene may be polymerized to predominantly 1,2-polybutadiene by a homogeneous complex formed in situ from chromium acetylacetonate and triethyl aluminium. The complex contains two to six growing polymeric chains per chromium atom, and the propagation reaction exhibits the kinetic features of a simple bimolecular addition of monomer to an active centre. The growing chains can transfer to excess aluminium alkyl in the system, which reaction predominates in controlling the polymer molecular weight. The excess aluminium alkyl also retards the polymerization, presumably by complexing with and deactivating the catalytic species.*

ALTHOUGH most catalysts in Ziegler-type polymerizations are heterogeneous in nature, several soluble catalysts (which are considered to function by a Ziegler-type mechanism) have been reported<sup>1-9</sup>.

Soluble catalytic systems have several advantages over insoluble catalysts for kinetic studies. Although they are generally less active than heterogeneous catalysts, mechanistic studies are facilitated since all the transition metal compound used should be available for polymerization, and the catalyst should not be deactivated by adsorption of polymer on the surface.

The initiator adopted for this study was the catalyst formed by the reaction of chromium acetylacetonate with triethyl aluminium. Natta *et al.*<sup>8</sup> showed that the soluble product of this reaction polymerized butadiene, giving polymers containing a high percentage of 1,2 linkages. They proved that, depending on the ratio of the components used and the time of ageing of the catalyst system prior to monomer addition, syndiotactic 1,2-polybutadiene, isotactic 1,2-polybutadiene, or mixtures of both could be obtained.

The structure of the complex formed by the reaction of chromium acetylacetonate with triethyl aluminium has been investigated by Sartori and Costa<sup>10</sup>. From an X-ray and infra-red (i.r.) analysis of the solid product, and from the composition of the gases evolved, the complex has been assigned the structure



\*Present address: Dunlop Research Centre, Fort Dunlop, Birmingham.

One ethyl group is removed from each of the three aluminium alkyl molecules reacting with the original chromium acetylacetonate, the electron transfer reducing the valence state of the chromium. The final valency of the chromium is then considered to be formally zero (as in dibenzene chromium), and the structure of the acetylacetonate rings is maintained in the complex.

The present work was undertaken to ascertain: (a) whether such a catalyst is in fact soluble, or is a dispersion of colloid-size particles; (b) the importance of transfer reactions to aluminium alkyl in governing the molecular weight of the polymer formed and (c) the significant kinetic parameters of the growth reaction. Information on these points has been gathered from kinetic studies of the rate of polymerization, and from radio-tracer studies in which polarized metal-carbon bonds have been decomposed with tritiated methanol,  $\text{CH}_3\text{OT}$ .

#### EXPERIMENTAL

##### *Materials*

*Benzene (analytical reagent grade)*—was treated with concentrated sulphuric acid, 2N sodium bicarbonate solution, and distilled water. After drying over calcium hydride for two days, the solvent was refluxed over freshly crushed calcium hydride for 24 hours. The benzene was finally fractionally distilled off fresh calcium hydride using a column 50 cm long and 4 cm diameter, packed with Fenske helices, the reflux ratio being 5 : 1. The middle fraction, b.pt  $79^\circ\text{--}80^\circ\text{C}$ , was collected and stored over freshly crushed calcium hydride until required.

*Toluene (analytical reagent grade)*—was purified in the same way as benzene, b.pt  $110^\circ\text{--}111^\circ\text{C}$ .

*Triethyl aluminium (17.3 per cent w/w in methyl cyclohexane)*—was obtained from I.C.I. Ltd, and was used without further purification. The triethyl aluminium was analysed by hydrolysis and measurement of the solid and gaseous products. The samples for analysis were handled using the same procedure as those samples taken for polymerization studies. The alkyl, after handling in the dry box, contained:

Al-Et	:	89.9 per cent of all Al-X bonds
Al-H	:	8.1 per cent

Gas-liquid chromatography showed that hydrogen and ethane were the only gases evolved on hydrolysis.

The nitrogen [B.O.C. white spot grade] used to purge the dry box was purified by passage over a 4 ft column containing lumps of sodium metal; a 3 ft column containing copper powder heated to  $200^\circ\text{C}$ ; a trap surrounded by liquid nitrogen; two 4 ft columns containing magnesium perchlorate; a 4 ft column of phosphorus pentoxide; and a 4 ft column containing sodium sputtered on glass wool.

*Chromium acetylacetonate*—was prepared by the method of Cooperstein<sup>11</sup>. The precipitated product was repeatedly recrystallized from

## BUTADIENE POLYMERIZATION

benzene-petroleum ether, air dried, and stored as benzene solutions over calcium hydride. No reaction or decomposition of the chromium acetylacetonate solution was observed, m.pt 215°C.

*Butadiene* gas [British Hydrocarbon Chemical Ltd]—was dried by passing through columns of silica gel, anhydrous magnesium perchlorate and Linde molecular sieves, type 4A. The butadiene was condensed on to a solid sample of the polymerization catalyst, outgassed, and stored at 8°C for several hours. Residual butadiene was distilled from this catalyst, monomer, polymer mixture as required.

*Tritiated methanol* ( $\text{CH}_3\text{OT}$ )—was prepared by adding tritiated water (1m curie) dropwise to freshly prepared sodium methoxide. The solution was refluxed for 30 min, and the mixture of methanol and tritiated methanol (b.pt 68°–72°C) distilled off. The active methanol was diluted with dry analytical reagent grade methanol, and stored over Linde molecular sieves, type 4A.

### PROCEDURE

All experiments were prepared using a conventional high vacuum system maintained at an air pressure less than  $5 \times 10^{-5}$  mm mercury.

#### *Handling triethyl aluminium and chromium acetylacetonate solutions*

It was found that reproducible rates of polymerization were obtained when an ampoule technique was used for introducing catalyst components into a reaction mixture.

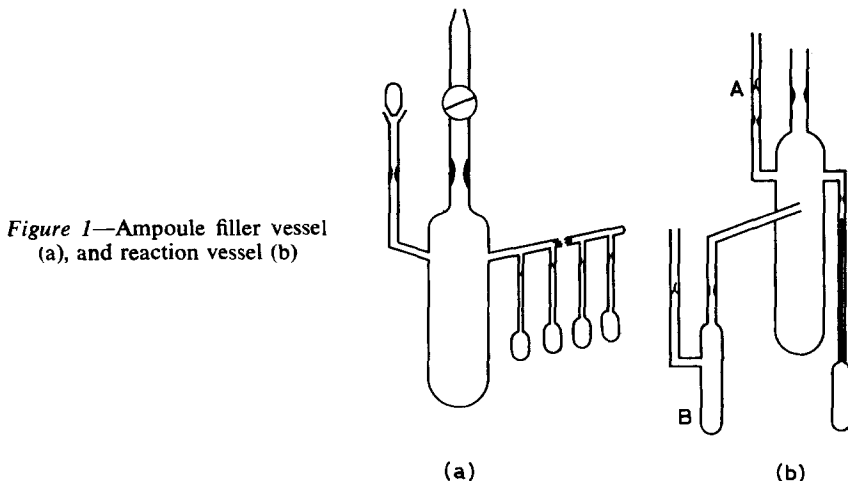


Figure 1—Ampoule filler vessel (a), and reaction vessel (b)

An ampoule-filler vessel [Figure 1(a)] was flamed for 15 min on the vacuum line, and filled with dry nitrogen. The vessel was filled with stock solution of triethyl aluminium in the dry box. The solution was then outgassed on the vacuum line, sealed off, and stored until required. In this way it was possible to prepare a large number of polymerization runs in which the aluminium alkyl had the same history of exposure in the dry box.

The solutions of chromium acetylacetonate were handled in the same way.

*Preparation of a polymerization run*—One ampoule of each catalyst component was placed in the reaction vessel [Figure 1(b)]. The whole was then evacuated and gently flamed for 15 min. Butadiene and benzene were distilled in, and the reaction vessel sealed off. When the reaction components had reached thermal equilibrium at  $-2^{\circ}\text{C}$  the vessel was shaken to break the ampoules and mix the reagents. It was found that at temperatures above  $-2^{\circ}\text{C}$ , losses of butadiene occurred due to evaporation during transference to a dilatometer or other observation appendage. Below  $-2^{\circ}\text{C}$  precipitation of solid benzene occurred.

Rates of polymerization were measured by observing the contraction in conventional Pyrex glass dilatometers, using a cathetometer reading to 0.001 cm. The density of liquid butadiene at its saturated vapour pressure<sup>12</sup>, and the density of 1,2-polybutadiene determined by Natta, Porri, Zanini and Fiore<sup>13</sup> were used to convert rates of contraction to rates of conversion. Conversions so calculated agreed ( $\pm 4$  per cent) with those measured gravimetrically. Monomer and solvent were distilled into the reaction vessel from graduated containers maintained at the freezing points, and the total volumes and reagent concentrations at each temperature were calculated using literature values for the coefficients of cubical expansion<sup>13,14</sup>.

Measurements at  $-2^{\circ}\text{C}$  were made in a Townson and Mercer 'Minus Seventy' thermostat, the temperature fluctuation during any experiment being  $\pm 0.01^{\circ}\text{C}$ . Measurements at higher temperatures were conducted in a water bath fitted with a mercury-toluene regulator and a Sunvic control. The temperature fluctuation using this system was also  $\pm 0.01^{\circ}\text{C}$ .

*Isolation of polymer*—In order to avoid oxidative crosslinking of the 1,2-polybutadiene, the reaction mixture was quenched by freezing in liquid nitrogen, and reattached to the vacuum line by the break seal A [Figure 1(b)]; 2 ml of degassed methanol were distilled in to terminate the reaction, and then solvent, methanol and monomer were pumped off using a freeze drying technique. Fresh toluene was distilled on to the mixture of polymer and catalyst residues. The solution was again subjected to freeze drying to remove last traces of methanol, and redissolved in toluene. Catalyst residues were removed by filtration through a number 4 porosity sinter crucible.

When polymer samples were to be obtained at different times during a polymerization run, additional appendages, B [Figure 1(b)], were attached to the dilatometer filling vessel.

#### *Radiotracer counting of the polymer solutions*

The radioactivity of tritium-containing solutions was measured using an Ekco type N 664A scintillation counter. The phosphor was diphenyl oxazole<sup>15</sup>, and the sample count per second was measured at five or ten minute intervals over several hours using an Ekco Automatic Scaler, type N 530F. The background was measured using dry oxygen-free solutions of the phosphor in toluene. All solutions were stored at least two hours in the absence of light before counting. All the toluene solutions were prepared on the vacuum line using dried, deoxygenated materials.

## BUTADIENE POLYMERIZATION

*Intrinsic viscosities*—Intrinsic viscosities of toluene solutions of polybutadiene were determined in an Ubbelohde suspended level viscometer at 30°C, and converted to molecular weights using the relationship<sup>16</sup>

$$[\eta] = 1.10 \times 10^{-3} \bar{M}_v^{0.62}$$

*Infra-red analysis of the polymers*—The percentages of the various stereo-isomers present were calculated from the bands at 10.3  $\mu$  (*trans* 1,4-), 11.0  $\mu$  (1,2-) and 15.8  $\mu$  (*cis* 1,4-) using the extinction coefficients quoted by Hampton<sup>17</sup>. These wavelengths were chosen since predominantly 1,2-polybutadienes show absorptions at 13.7  $\mu$  and 14.4  $\mu$ <sup>18</sup> which interfere with other methods of computing the percentage of *cis*-1,4-polybutadiene.

### RESULTS

*Structure of the polybutadienes*—The polybutadienes, obtained from polymerizations in which an 11.6 to 1 mole ratio triethyl aluminium to chromium acetylacetonate was mixed in the presence of monomer at 30°C, were analysed by i.r. spectroscopy and found to consist of 12 per cent *cis*-1,4-polybutadiene, 18 per cent *trans*-1,4-polybutadiene and 70 per cent 1,2-polybutadiene.

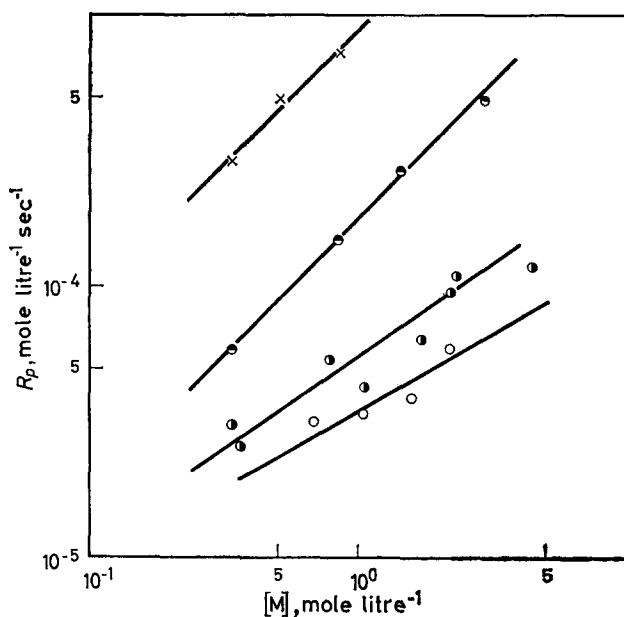


Figure 2—Dependence of polymerization rate on monomer concentration

- × 45°C,  $[\text{Cr}(\text{acac})_3] = 6.2 \times 10^{-3}$  mole litre<sup>-1</sup>,  $[\text{Al}]/[\text{Cr}] = 11.6$
- 30°C,  $[\text{Cr}(\text{acac})_3] = 8.8 \times 10^{-3}$  mole litre<sup>-1</sup>,  $[\text{Al}]/[\text{Cr}] = 11.6$
- 20°C,  $[\text{Cr}(\text{acac})_3] = 4.3 \times 10^{-3}$  mole litre<sup>-1</sup>,  $[\text{Al}]/[\text{Cr}] = 11.6$
- 2°C,  $[\text{Cr}(\text{acac})_3] = 6.3 \times 10^{-3}$  mole litre<sup>-1</sup>,  $[\text{Al}]/[\text{Cr}] = 11.6$

*The dependence of polymerization rate on monomer concentration*

The dependence of the initial rate of polymerization upon the concentration of monomer for a series of runs containing a mole ratio triethyl aluminium to chromium acetylacetonate of 11.6 are illustrated in *Figure 2*.

A least square analysis of these logarithmic plots suggests that the observed monomer kinetic order is unity at 45°C and 30°C, but is less than unity at 20°C and -2°C. In view of the scatter in the results at the two lower temperatures it is doubtful whether the lower kinetic order is significant.

In order further to examine the kinetic order with regard to monomer, and to ascertain whether or not any auto-acceleration or auto-retardation was occurring during the reaction, the rate of polymerization in individual runs was examined as a function of time. When the monomer kinetic order is unity, and the number of active sites is invariant,

$$\ln(R_p/R_{p0}) = -k_p [C^*] t = \ln([M]/[M]_0) \quad (1)$$

where  $[C^*]$  is the constant concentration of active polymerization sites. Graphs of  $\ln(R_p/R_{p0})$  against time for runs carried out at -2°C, 20°C and 45°C are illustrated in *Figure 3*. In every case the graph is a straight

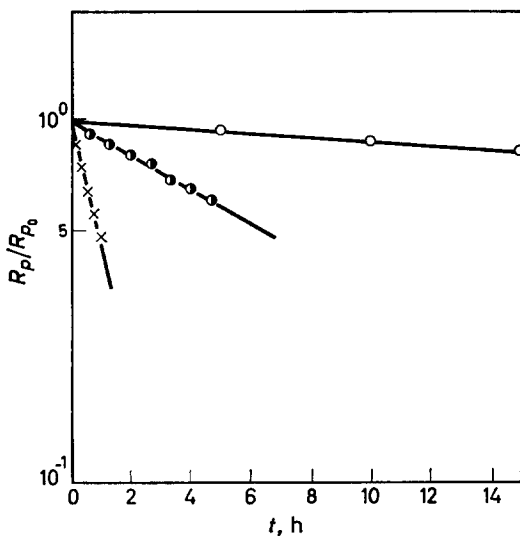


*Figure 3*—Logarithm of relative polymerization rate against time  
 × 45°C   ● 20°C   ○ -2°C

line, indicating that monomer disappears by a first order mechanism and that the concentration of propagating centres is constant. A coincidental balancing of a non-unity monomer order and a time-dependent concentration of active centres in all the runs studied is sufficiently improbable to be discounted.

*The dependence of initial polymerization rate on catalyst concentration*

Unless stated to the contrary, all 'catalyst concentrations' refer to the molar concentration of chromium acetylacetonate in the system prior to reaction, the aluminium to chromium ratio being 11.6. All rates and con-

## BUTADIENE POLYMERIZATION

centrations are values at zero time, the subscript 0 being omitted for convenience. Logarithmic plots of polymerization rate against catalyst concentration are illustrated in *Figure 4*. From the slopes of these graphs it is

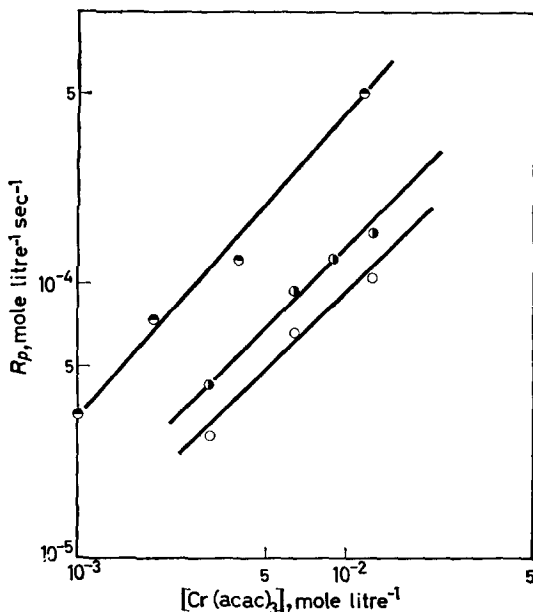


*Figure 4*—Dependence of polymerization rate on  $[\text{Cr}(\text{acac})_3]$

- 30°C,  $[M]=1.75$  mole litre<sup>-1</sup>,  $[\text{Al}]/[\text{Cr}]=11.6$
- 20°C,  $[M]=2.24$  mole litre<sup>-1</sup>,  $[\text{Al}]/[\text{Cr}]=11.6$
- -2°C,  $[M]=2.27$  mole litre<sup>-1</sup>,  $[\text{Al}]/[\text{Cr}]=11.6$

clear that the rate of polymerization is directly proportional to the initial molar concentration of chromium acetylacetonate at constant aluminium to chromium mole ratio and constant monomer concentration.

The rate of polymerization can be written as

$$R_p = k' [M] [\text{Cr}(\text{acac})_3] \quad (2)$$

where  $k'$  is some constant which may be a single reaction rate constant or a complex ratio of rate constants. The aluminium to chromium ratio is constant.  $k'$  can be evaluated from the data of *Figures 2* and *4*. Values so obtained are listed in *Table 1*. The temperature dependence of these

*Table 1*. Values of  $k' = R_p/[M] [\text{Cr}(\text{acac})_3]$  at  $[\text{Al}] : [\text{Cr}]$  mole ratio of 11.6 : 1

Temperature °C	$k'$ from monomer dependence litre mole <sup>-1</sup> sec <sup>-1</sup>	$k'$ from catalyst dependence litre mole <sup>-1</sup> sec <sup>-1</sup>
45	$1.3 \times 10^{-1}$	$1.3 \times 10^{-1}$
30	$2.0 \times 10^{-2}$	$2.3 \times 10^{-2}$
20	$7.5 \times 10^{-3}$	$6.2 \times 10^{-3}$
-2	$3.4 \times 10^{-4}$	$4.5 \times 10^{-4}$

constants can be expressed as an Arrhenius activation energy, which is 20 kcal/mole.

*Variation of initial polymerization rate with triethyl aluminium to chromium acetylacetonate mole ratio*

The rates of polymerization obtained for a series of experiments at 30°C in which the monomer concentration (1.86 mole litre<sup>-1</sup>) and the chromium acetylacetonate concentration (6.6 × 10<sup>-3</sup> mole litre<sup>-1</sup>) were constant, but in which the aluminium triethyl concentration was varied, are illustrated in Figure 5. The rate of polymerization is an inverse function of the aluminium triethyl concentration.

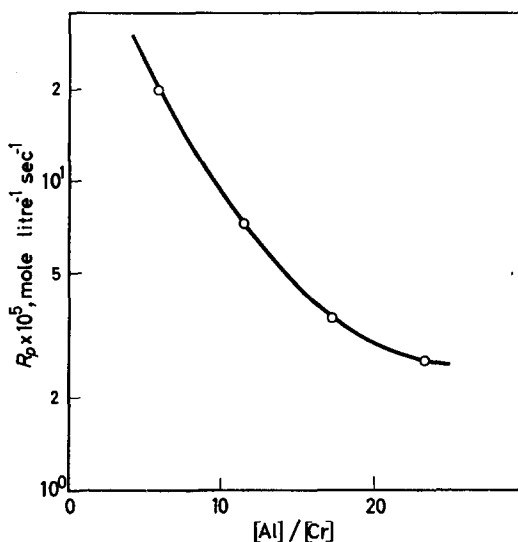


Figure 5—Polymerization rate against aluminium to chromium ratio, 20°C.  $[M]=1.86$ ,  $[\text{Cr}(\text{acac})_3]=6.6 \times 10^{-3}$

*Radiotracer determination of the concentration of active centres*

Feldman and Perry<sup>19</sup> have shown that the total concentration of polymeric anionic centres  $[N_t]$  at any time  $t$  during the polymerization can be determined from the radioactivity of the polymers when the reaction is terminated with tritiated methanol, CH<sub>3</sub>OT. There is the possibility that growing coordinated anionic polymer chains may transfer from the active site of polymerization to excess aluminium alkyl, so the total number of anionic centres is given by

$$[N_t] = [N_0] + [N_f] \quad (3)$$

where  $[N_0]$  is the initial concentration of active centres,  $[N_f]$  the concentration of polymeric alkyl groups attached to free aluminium alkyl, and the concentration of actively propagating sites remains constant throughout the reaction.

Equation (3) can be written as

$$[N]_t = [N_0] + k_f (r-3) [N_0] [\text{Cr}(\text{acac})_3] t \quad (4)$$



## BUTADIENE POLYMERIZATION

where  $k_t$  is the rate constant for the transfer reaction,  $r$  is the mole ratio aluminium ethyl to chromium acetylacetonate at time  $t$ , and the active catalyst is assumed to be formed from three molecules of triethyl aluminium and one of chromium acetylacetonate<sup>10</sup>.

Thus radiotracer analysis of the concentration of anionic polymeric species during a polymerization should yield  $[N_0]$  and  $k_t$ .

Counts of the activity of different samples of the same polymer were found to be reproducible to within  $\pm 6$  per cent, and counts of the original tritiated methanol were reproducible to within 1 per cent. The kinetic isotope effect in the quench reaction was assumed to be  $3.7^{19}$ .

The numbers of anionic centres so estimated are plotted against the time of reaction for a series of temperatures in *Figure 6*.

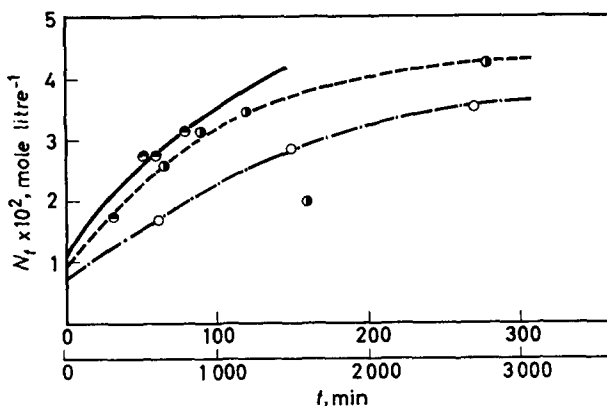


*Figure 6*—Number of anionic polymer chains versus time

- 30°C,  $R_p = 7.32 \times 10^{-5}$  mole litre<sup>-1</sup> sec<sup>-1</sup>,  $[M] = 1.75$  mole litre<sup>-1</sup>; upper time scale
- 20°C,  $R_p = 2.9 \times 10^{-5}$  mole litre<sup>-1</sup> sec<sup>-1</sup>,  $[M] = 1.75$  mole litre<sup>-1</sup>; upper time scale
- -2°C,  $R_p = 3.0 \times 10^{-6}$  mole litre<sup>-1</sup> sec<sup>-1</sup>,  $[M] = 1.75$  mole litre<sup>-1</sup>; lower time scale

The points show considerable scatter. Since no auto-acceleration was observed in these polymerizations, it is probable that the number of active propagating centres is constant throughout the reaction. Under these circumstances it is probable (though not certain) that this number is a function of the catalyst concentration and not of temperature. Also low values for the number of anionic centres are more likely to be in error than high values (due to incomplete hydrolysis of polymeric aluminium alkyls<sup>20</sup>). Consequently, the curves of *Figure 6* have been drawn with the significance of high values weighted relative to low values, and with the possibility of a temperature-independent intercept introduced as an additional restriction.

We note that equation (4) does not predict a straight line graph of  $N_t$  against time, since  $r-3$  is time dependent. It must be emphasized that the experimental points of *Figure 6* allow a wide choice of intercept. That value chosen, however, is one obtained by varying the parameters of equation

(4) so that all three calculated curves fitted the experimental points *and* the condition that they have a common intercept. The initial concentration of active sites, and hence the number of propagating centres per chromium atom, obtained in this way are listed in *Table 2*.

The problem cannot be solved by choosing an initial  $[Al]/[Cr]$  ratio of 3.0, since a different catalytic complex is formed under these conditions.

Values of the transfer rate constant  $k_t$ , calculated from the initial slopes of these curves, and of the propagation rate constant, defined as

$$k_p = R_p/[M][N]_0 \quad (5)$$

are also listed in *Table 2*.

*Table 2.* Number of propagating sites; transfer and propagation rate constants

Temperature °C	$R_p \times 10^5$ mole litre <sup>-1</sup> sec <sup>-1</sup>	$[N_0] \times 10^2$ mole litre <sup>-1</sup>	$\frac{[N_0]}{[Cr(acac)_3]}$	$k_t \times 10^3$ litre mole <sup>-1</sup> sec <sup>-1</sup>	$k_p \times 10^4$ litre mole <sup>-1</sup> sec <sup>-1</sup>
30	7.3	1.0	6	9.2	42.0
20	2.9	0.8	4	5.1	20.5
-2	0.30	0.7	4	0.48	2.45

The two rate constants can be expressed in the Arrhenius form, and are (for an aluminium to chromium mole ratio of 11.6):

$$k_p = 2.5 \times 10^8 \exp(-15\,000/RT)$$

$$k_t = 1.6 \times 10^9 \exp(-15\,500/RT)$$

#### *The molecular weights of the polymers*

The variation in the average molecular weights with chromium acetylacetonate concentration, monomer concentration, and aluminium to chromium ratio is set forth in *Table 3*.

*Table 3.* Molecular weights (by viscometry) of polybutadienes

Temperature °C	$[Cr(acac)_3] \times 10^3$ mole litre <sup>-1</sup>	$[M]$ mole litre <sup>-1</sup>	$\bar{M}_v \times 10^{-3}$	$\frac{[Al]}{[Cr]}$
30	0.64	1.75	0.22	11.6
30	0.97	1.75	0.18	11.6
30	1.9	1.75	0.22	11.6
30	3.9	1.75	0.14	11.6
45	5.9	2.3	0.27	12.0
45	5.9	2.3	2.14	6.0
45	5.9	4.5	3.54	6.0
45	5.9	2.3	3.22	3.0

The results indicate that the molecular weights of the polymers increase with monomer concentration, are inversely proportional to the concentration of excess aluminium alkyl, and are independent of the concentration of chromium acetylacetonate. If it is assumed that the concentration of propagating centres is constant during the reaction, and that transfer to

aluminium alkyl is the predominant reaction governing polymer molecular weight, the temperature dependence of the molecular weight is given by

$$M_p = (M_m A_p / A_t) \exp \{ -(E_p - E_t) / RT \} [M] / [AlEt_3 \text{ excess}] \quad (6)$$

where  $M_m$  is the molecular weight of monomer, and  $A_p$ ,  $A_t$ ,  $E_p$ ,  $E_t$  are the Arrhenius coefficients of the propagation and transfer reactions.  $E_p - E_t$  is thus evaluated as +1.0 kcal/mole.

#### DISCUSSION

One of the most noticeable features of these experiments is the difficulty in obtaining reproducible results. This difficulty can be directly attributed to the oxygen and water sensitivity of the dilute aluminium alkyl and catalyst solutions. Thus it was found that solutions stored in ground glass vessels in the dry box, or prepared using a burette procedure, gave consistently lower polymerization rates than solutions stored and handled in ampoules.

It is unfortunate that both the radiotracer determination of the number of anionic centres in the system, and the viscometric determination of low molecular weights, introduce additional errors of considerable magnitude. Consequently it is necessary to assess critically the kinetic results before using them in a mechanistic interpretation of the reaction.

The dilatometric method of following the course of the polymerization is relatively accurate, so that the study of the rate of change of polymerization velocity is probably the most sensitive determination reported. This study shows definitely that the monomer disappears by a first order mechanism, and that there is no auto-acceleration or auto-retardation during the reaction. This latter fact is important, since it can be used as an additional restriction in the plotting and interpretation of less reliable data.

The rates of polymerization, reported in the section on the effect of monomer and catalyst concentrations, are the highest reproducible self-consistent rates obtained with newly supplied triethyl aluminium after investigating a variety of experimental procedures. Every experimental error encountered led to reduced rates of polymerization, and no rates significantly higher than the reported results were ever encountered. Consequently, it is felt that magnitudes of the rates are correct within an estimated variance of 12 per cent. Both the monomer kinetic order at low temperatures (calculated from the dependence of initial rate on initial monomer concentration) and the catalyst kinetic order at higher concentrations can be interpreted as less than unity. In both cases, however, the divergence is less than the experimental error, and the former possibility is not in accord with the rate/time studies. Consequently these variations cannot be treated as significant within the limitations of these experiments.

The greatest experimental error obviously arises in the determination of the number of polymeric anionic groups in the system. On top of the obvious difficulties in isolating and counting the weakly emitting tritiated samples, the following sources of inaccuracy must be recorded.

(1) The hydrolysis of alkyl aluminium with large or polymeric alkyl groups does not always proceed with 100 per cent efficiency<sup>20</sup>.

(2) The kinetic isotope effect,  $I = k_m / k_T$  was assumed<sup>19</sup> to be 3.7.

Recently Kohn *et al.*<sup>21</sup> have shown that the kinetic isotope effect in the polymerization of propylene with titanium tetrachloride and aluminium diethyl chloride is 1.30. Bier, Hoffman, Lehmann and Seydel (*see ref. 22*) have suggested that there is no measurable kinetic isotope effect when propylene is polymerized with titanium tetrachloride and aluminium alkyls and quenched with tritiated methanol. The high value 3.7 was used for the kinetic isotope effect in this work since any error so introduced would tend to cancel an error due to incomplete hydrolysis. In the light of these uncertainties, and because of the difficulties of drawing meaningful curves in *Figure 6*, the number of growing chains per chromium atom and the rate constants for the transfer reaction would encompass a systematic error as great as a factor of two. The number of growing chains per chromium atom can thus range from two to six.

The molecular weight/intensity relationship was determined for polymers, molecular weight  $10^5$  to  $10^6$ , and its applicability to the present system is doubtful. In any case, the viscometric determination of such low molecular weights is extremely inaccurate, so that the results reported here show relative trends rather than exact absolute magnitudes.

In view of the errors in the radiotracer experiments, and in the viscometric determination of low molecular weight, the agreement between the values of  $E_p - E_t$  calculated by each method  $-0.5$  and  $+1.0$  kcal/mole respectively must be regarded as satisfactory.

It is possible to discuss several facets of this polymerization reaction in the light of the kinetic results.

In the first place the catalyst complex formed from triethyl aluminium and chromium acetylacetonate must be a soluble one. The large ratio of propagating chains to chromium atoms would not be possible in a system of colloidal aggregates. By comparison the fraction of transition metal atoms active in a heterogeneous polymerization<sup>19,21</sup> varies from  $10^{-3}$  to  $10^{-1}$ .

The propagation process is first order in monomer, and appears to involve an ordinary bimolecular addition of monomer to the growth site. The formation of a prior  $\pi$ -bond charge transfer complex is unlikely, since this would lead to low values for the observed Arrhenius pre-exponential factor  $A_p$ , and probably for the activation energy  $E_p$ .<sup>22</sup> It is extremely unlikely that a charge transfer complex could be formed with a positive entropy of formation. Furthermore such a complex might be expected to involve the *cis* configuration of butadiene, and the polymer obtained is predominantly 1,2, which further makes prior complexing unlikely. It is mere speculation to discuss the steric requirements imposed on the approaching monomer molecule by the various groups of the complex, but the low entropy of activation for propagation suggests that these are not too restrictive.

The concentration of active sites remains constant throughout the course of the polymerization, and initiation is virtually instantaneous. There is no termination reaction, the principal reaction governing the molecular weight of the polymer being one whereby the polymer chain transfers from the active catalyst site to a molecule of free alkyl aluminium. The activation energy for this process is very similar to that for propagation, so that

molecular weights are rather insensitive to temperature.

It is not yet entirely clear why the presence of excess aluminium alkyl reduces the rate of polymerization. A simple hypothesis can be propounded, based upon the suggestion by Sartori and Costa that at high aluminium to chromium ratios a complex containing six molecules of aluminium alkyl per molecule of chromium acetylacetonate can be formed. If this complex, containing all the oxygens of the acetylacetonate groups bonded to aluminium, is inactive, the concentration of  $\text{Cr}(\text{acac})_3(\text{AlEt}_3)_6$  depends on the dissociation constant,  $K$  of the  $\text{Cr}(\text{acac})_3(\text{AlEt}_3)_6$ , and the rate of polymerization is

$$R_p = \frac{k_p [M] [\text{Cr}(\text{acac})_3]_0}{1 + K [\text{AlEt}_3 \text{ excess}]^6} \quad (7)$$

where  $K < 1$  and  $[\text{Cr}(\text{acac})_3]_0$  is the total concentration of chromium acetylacetonate in the system. Such a rate expression can be fitted to the experimental results of *Figure 5*, but there is no further evidence for such a scheme. It seems probable that the real situation involves complexing of chromium acetylacetonate with 1, 2, 3, 4, 5 or 6 molecules of triethyl aluminium, and the mechanism whereby the propagation sites become de-activated remains obscure.

Donnan Laboratories,  
University of Liverpool,  
Liverpool 7

(Received November 1963)

#### REFERENCES

- <sup>1</sup> BAWN, C. E. H. and SYMCOX, R. *J. Polym. Sci.* 1959, **34**, 139
- <sup>2</sup> BRESLOW, D. S. and LONG, W. P. *J. Amer. chem. Soc.* 1960, **82**, 1953
- <sup>3</sup> ZGONNIK, V. H., DOLGOPLOSK, B. A., KROPOCHER, V. A. and NIKOLAEV, N. I. *Dokl. Akad. Nauk, SSSR*, 1962, **145**, 1285
- <sup>4</sup> NATTA, G., PINO, P., MAZZANTI, G., GIANINNI, U., MANTICA, E. and PERALDO, M. *Chim. e Industr.* 1957, **26**, 120
- <sup>5</sup> BRESLOW, D. S. and NEWBURG, N. R. *J. Amer. chem. Soc.* 1959, **79**, 5072
- <sup>6</sup> CHIEN, J. C. W. *J. Amer. chem. Soc.* 1960, **81**, 86
- <sup>7</sup> CARRICK, W. L., SMITH, J. J., KLUBER, R. W., WARTMAN, L. H., RUGG, R. H. and BONNER, F. M. *J. Amer. chem. Soc.* 1960, **82**, 3883
- <sup>8</sup> NATTA, G., PORRI, L., ZANINI, G. and FIORE, L. *Chim. e Industr.* 1959, **41**, 526, 1163
- <sup>9</sup> HENDERSON, J. F. *International Symposium on Macromolecular Chemistry, Paris 1963*. Edited by M. MAGAT. Interscience: New York, 1963
- <sup>10</sup> SARTORI, G. and COSTA, G. *Z. Elektrochem.* 1959, **63**, 108
- <sup>11</sup> COOPERSTEIN, M. *Ph.D. Thesis*. Pennsylvania State College, 1952
- <sup>12</sup> BLOUT, E. R., HOHENSTEIN, W. P. and MARK, H. 'Butadiene'. *Monomers*, p 28. Interscience: New York, 1951
- <sup>13</sup> NATTA, G., PORRI, L., ZANDI, G. and FIORE, L. *Chim. e Industr.* 1959, **41**, 1163
- <sup>14</sup> *Handbook of Chemistry and Physics*, 41st ed., p 2067. Chemical Rubber Publishing Company: Cleveland, 1959
- <sup>15</sup> HAYES, F. N., OTT, D. G. and KERR, V. N. *Nucleonics*, 1962, **14**, 42
- <sup>16</sup> SCOTT, R. L., CARTER, W. C. and MAGAT, M. *J. Amer. chem. Soc.* 1949, **71**, 220
- <sup>17</sup> HAMPTON, R. R. *Analyt. Chem.* 1949, **21**, 923
- <sup>18</sup> BINDER, J. L. *J. Polym. Sci.* 1963, **A1**, 47
- <sup>19</sup> FELDMAN, C. F. and PERRY, E. *J. Polym. Sci.* 1960, **46**, 217
- <sup>20</sup> PINO, P., BRESLOW, D. L. Private communications
- <sup>21</sup> KOHN, E., SCHUURMANS, J. L., CAVENDER, J. V. and MENDELSON, R. A. *J. Polym. Sci.* 1962, **58**, 681
- <sup>22</sup> LEE, C. L., SMID, J. and SZWARC, M. *Trans. Faraday Soc.* 1963, **59**, 1192

## Note

---

### *Copolymerization of Ethylene with tert-Butyl Acrylate in the Presence of n-Butyl Lithium and Titanium Tetrachloride*

ZIEGLER-TYPE catalysts made with *n*-butyl lithium and titanium tetrachloride polymerize ethylene<sup>1</sup> and *tert*-butyl acrylate<sup>2</sup>, separately, to crystalline polymer. It was, therefore, of interest to attempt the copolymerization of ethylene and *tert*-butyl acrylate with this same system. Catalysts for the study were prepared and polymerizations were conducted by the general methods used to polymerize *tert*-butyl acrylate<sup>2</sup>. Flow of ethylene was maintained throughout the course of the polymerization. Unless otherwise stated, introduction of ethylene and *tert*-butyl acrylate was begun simultaneously. At the end of three hours, polymerization was stopped and the polymer precipitated by addition of a 50/50 (v/v) mixture of methanol and water. The polymer was washed with the methanol-water mixture, dried under vacuum at 55°C and weighed. The dried polymer was extracted with boiling acetone to remove amorphous poly(*tert*-butyl acrylate) and with boiling chloroform to remove crystalline poly(*tert*-butyl acrylate). Each extraction was repeated until no further polymer dissolved. The polymer which was dissolved by acetone and by chloroform consisted entirely of poly(*tert*-butyl acrylate) while the polymer which remained undissolved contained both ethylene and *tert*-butyl acrylate. In the early stages of the work the undissolved polymer was also extracted with solvents for polyethylene, i.e. boiling monochlorobenzene, hot tetrahydronaphthalene and hot *cis*-decahydronaphthalene. These extractions did not remove any polymer and were discontinued. The composition of the polymer was determined by the method of thermogravimetric analysis<sup>3</sup> (heating rate 10°/min in nitrogen). This method of analysis gave 98–99 per cent *tert*-butyl acrylate when applied to homopolymer and gave values which were reproducible to ±5 percentage units on copolymers containing 35 per cent *tert*-butyl acrylate and ±0.2 percentage unit on polymers containing 1.5 per cent. The reproducibility of polymerizations carried out under identical conditions was ±2 percentage units in the weight of insoluble polymer and in the mole percentage of *tert*-butyl acrylate in the insoluble polymer.

Experiments were carried out to investigate the effect of the following variables on the incorporation of *tert*-butyl acrylate in polyethylene: method of adding monomer, preparation, concentration and composition of catalyst, and temperature of polymerization. The rate of addition of *tert*-butyl acrylate was varied from dropwise addition of dilute monomer to immediate introduction of the entire sample. Ethylene flow and addition of *tert*-butyl acrylate were either started simultaneously or the ethylene was allowed to polymerize for a fixed interval of time before *tert*-butyl acrylate

## NOTE

was added. Ethylene was not introduced after the *tert*-butyl acrylate because, in the absence of ethylene, *tert*-butyl acrylate polymerized almost instantaneously. Variation in the rate of addition of *tert*-butyl acrylate had no effect on the total yield of chloroform insoluble polymer or on the amount of *tert*-butyl acrylate incorporated in the chloroform insoluble polymer. Introduction of ethylene before adding *tert*-butyl acrylate did not influence the total amount of monomeric *tert*-butyl acrylate that was copolymerized with ethylene but did increase the amount of insoluble polymer and the mole ratio of ethylene to *tert*-butyl acrylate in the insoluble polymer.

Table 1. Results of copolymerizations at 25°C in the presence of catalysts made with *n*-butyl lithium and titanium tetrachloride (Total time ethylene was introduced 10 min.)

Concentration of TiCl <sub>4</sub> moles/l. × 10 <sup>2</sup>	Mole ratio Li/Ti	Ageing time of catalyst at 20°–25°C, min	Time elapsed between start of addition of ethylene and addition of <i>tert</i> -butyl acrylate, min	Wt % of insoluble polymer	Mole % <i>tert</i> -butyl acrylate in insoluble polymer
2.20	3/1	0	10	15.2	2.0
2.20	3/1	10	10	22	3.5
2.20	3/1	5	5	9.2	3.6
2.20	3/1	10	5	8.3	1.3
2.20	3/1	10	0	11	8.0
2.20	4/1	10	0	10	22
2.20	5/1	10	0	9	18
2.20	6/1	10	0	6	8
1.60	4/1	10	0	10	10
1.28	5/1	10	0	28	46

Experiments in which the time the catalyst was aged (20° to 25°C) varied from 0 to 10 min and the time the ethylene was allowed to flow before introducing *tert*-butyl acrylate varied from 0 to 10 min are summarized in Table 1, lines 1 to 5. These experiments show that the maximum amount of *tert*-butyl acrylate was incorporated in the polymer when the ethylene and *tert*-butyl acrylate were introduced, simultaneously, into a catalyst mixture that had aged for 10 min.

Another series of experiments, summarized in Table 1, lines 5 to 10, showed that when the concentration of titanium tetrachloride was kept at  $2.2 \times 10^{-2}$  moles/l., the maximum amount of *tert*-butyl acrylate was incorporated in the copolymer when the lithium to titanium ratio was 4/1. However, when the concentration of *n*-butyl lithium was held constant at  $6.4 \times 10^{-2}$  moles/l. the maximum amount of *tert*-butyl acrylate was incorporated in the polymer when the lithium to titanium ratio was 5/1. Copolymerizations were run at -15°C, 0°C, 10° to 13°C, ambient room temperature (~ 25°C) and 60° to 65°C using catalysts prepared and aged

## NOTE

at 20° to 25°C. The maximum mole percentage of *tert*-butyl acrylate in the copolymer (46 per cent) occurred when polymerizations were carried out at ambient room temperature. At -15°C little polymer formed and at 60° to 65° the insoluble polymer contained mostly polyethylene.

These experiments show that when polymerization conditions are properly chosen, *tert*-butyl acrylate and ethylene can be copolymerized in the presence of a catalyst made with *n*-butyl lithium and titanium tetrachloride. The copolymers formed are, probably, block copolymers resulting from the addition of monomeric *tert*-butyl acrylate to a growing molecule of polyethylene. This conclusion is supported by the observations that homopolymer of polyethylene is not found in the polymerizate and that some of the copolymers show lines in their X-ray diffraction patterns that are characteristic of crystalline polyethylene and also lines that are characteristic of crystalline poly(*tert*-butyl acrylate). Growing polyethylene chains initiated by Ziegler catalysts have been shown to have long lives in systems in which conversions are high<sup>4-6</sup>. It is suggested that monomeric *tert*-butyl acrylate can add to growing chains of polyethylene but that ethylene cannot add to growing chains of poly(*tert*-butyl acrylate).

*The authors wish to thank Mr John Skogman for preparing the monomeric tert-butyl acrylate and Miss E. C. Eberlin and Mr E. A. Battistelli for carrying out the thermogravimetric analyses.*

E. A. H. HOPKINS\*  
M. L. MILLER

*Exploratory Research Department,  
Central Research Division,  
American Cyanamid Company,  
Stamford, Conn., U.S.A.*

(Received November 1963)

## REFERENCES

- <sup>1</sup> ZIEGLER, K., HOLZKAMP, E., BREIL, E. and MARTIN, H. *Angew. Chem.* 1955, **67**, 541
- <sup>2</sup> HOPKINS, E. A. H. and MILLER, M. L. *Polymer, Lond.* 1963, **4**, 75
- <sup>3</sup> DUVAL, C. *Inorganic Thermogravimetric Analyses*. Elsevier: Amsterdam, 1953
- <sup>4</sup> NATTA, G. J. *Polym. Sci.* 1959, **34**, 21
- <sup>5</sup> FELDMAN, C. F. and PERRY, E. J. *Polym. Sci.* 1960, **46**, 217
- <sup>6</sup> BIER, G., GUMBOLDT, A. and LEHMANN, G. *Trans. Plast. Inst., Lond.* 1960, **28**, 98

\*Present address: Department of Chemistry, Yale University, New Haven, Conn., U.S.A.



# *Thermal Degradation of an Aromatic Polypyromellitimide in Air and Vacuum*

## *I—Rates and Activation Energies*

S. D. BRUCK

*The thermal degradation of a polypyromellitimide (condensation product of pyromellitic anhydride and an aromatic diamine, designated as 'H-film' by E. I. du Pont de Nemours and Company, Inc.) was studied in air and vacuum in the range of 400° to 700°C by thermogravimetry using a recording electro-balance. Although this organic polymer is remarkably stable in air up to approximately 420°C, at temperatures in excess of this it begins to volatilize. At 485°C practically total volatilization takes place within approximately five hours. In a vacuum ( $\sim 10^{-3}$  mm of mercury) the polymer shows even greater heat stability with no appreciable weight loss even after prolonged exposure to temperatures up to approximately 500°C. Above this temperature it begins to volatilize leaving a brittle, carbonized residue which appears to reach a limiting weight corresponding to approximately 45 per cent of the original sample and showing no infra-red absorption bands. From the thermal degradation profiles the rates of volatilization were calculated, from which the Arrhenius relationship gave an activation energy of 33 kcal/mole and 74 kcal/mole for the degradation in air and vacuum, respectively. The general shapes of the rate curves of this polymer as the result of thermal degradation in vacuum resemble those of polytrivinylbenzene as investigated by other workers.*

SYNTHETIC polymers that are stable at high temperatures are of great importance in a variety of applications such as protective coatings, nose cones for missiles, ablative heat shields for satellites and for numerous other aero-space uses in which electrical insulating materials are expected to function at extreme environmental conditions. These recent technological demands have resulted in vigorous research and development efforts in the U.S.A. and elsewhere aimed at the synthesis and characterization of high polymeric materials capable of reliably performing under the above conditions.

Such important technical challenges, however, can only be met successfully in the long run if enough appropriate fundamental information is available for guiding the synthesis and subsequent optimum utilization of new as well as existing materials. While much kinetic and thermodynamic information is available on simple compounds, reliable data are relatively meagre on high molecular weight polymeric materials. Although certain engineering tests such as those performed in electric arcs are quite common on composite materials, the individual degradation processes are often non-analysable due to the contributions of extraneous materials also present in the sample. Such extraneous agents may include asbestos, glass, adhesives, pigments, and also various contaminants from the heat source. Experiments such as these, while sometimes valuable for some applications, cannot provide the fundamental information essential for the thorough and reliable evaluation of polymeric materials.

A more fundamental approach to the thermal degradation of polymers has been followed by several workers, in the U.S.A. and elsewhere, including Jellinek<sup>1,2</sup>, Grassie and Kerr<sup>3,4</sup>, Madorsky and Straus<sup>5-10</sup> and Wall<sup>11-14</sup>. These and other studies led to the quantitative determination of rates and activation energies for many fractionated and unfractionated polymers by both the pressure and loss-of-weight methods and also yielded important theoretical predictions concerning polymer degradation processes<sup>15</sup>.

The object of this part of the present investigation was to: (a) study the thermal stability of an unfractionated sample of a new experimental polypyromellitimide (du Pont's H-film) both in air and in vacuum, (b) determine the rates of degradation by thermogravimetry, (c) calculate the respective activation energies, and (d) compare these with data for previously studied materials by other investigators.

#### EXPERIMENTAL DETAILS

##### *Instrumentation*

The thermogravimetric studies were carried out with a Cahn RG electro-balance the operation of which is based on the null-balance principle. The capacity of this instrument (sample plus container) is 0 to 1 000 mg (on loop A) with an ultimate precision of  $2 \times 10^{-7}$  g. In all the present experiments the weight of the samples was kept between 4 and 7 mg.

As the weight of the sample changes the balance beam tends to deflect momentarily, thereby changing the amount of light reaching the phototube. The current of the phototube is amplified, then applied to a coil on the beam which is held in a magnetic field. This action exerts a force which restores the beam to its original position. The time constant of the balance is 0.05 sec. Because of this, the relative position of the sample with respect to a thermocouple that may be positioned immediately below it changes only momentarily and can be considered, for all practical purposes, to be constant. Good temperature control is thereby made possible. This feature of the balance is desirable to the present work, and distinguishes it from the operation of many other types of instruments.

The output of the electro-balance is fed to a 1 mV recorder. One of the channels (1 mV) was connected to the balance output terminals and the other channel was so calibrated that the temperature of the thermocouple located under the sample could be directly translated into °C from the millivolt recording trace. An electronic cold-junction compensator was employed between the thermocouple and recorder.

The balance mechanism was sealed into a special Pyrex vacuum housing rigidly mounted by means of custom designed supports, and equipped with O-ring joints for the connection of hangdown tubes. This vacuum bottle was directly sealed to a Pyrex vacuum manifold, McLeod pressure gauge, traps, an oil diffusion pump and to mechanical pumps. For the experiments that were carried out below 500°C the specially designed and fabricated hangdown tube was made of Pyrex glass, whereas for higher temperatures Vycor or quartz was used. A thermocouple (iron-constantan to 500°C, and chromel-alumel above this temperature) was inserted through a joint into the hangdown tube so that its tip was immediately below the sample.

To prevent overheating of the O-ring, the joint was cooled by circulating water through a thin copper coil.

The furnace, capable of operating up to 1 000°C, was vertically mounted on a specially designed jack assembly which automatically positioned it horizontally and vertically with respect to the sample hangdown tube. Localized control of the furnace temperature was possible by means of ten binding posts on the front shunt panel. By the use of resistance wires the temperature of any particular portion of the furnace could be varied, if needed. Uniform temperature along the furnace axis could thus be achieved. For the control of the furnace temperature a chromel-alumel thermocouple was used in conjunction with an indicating temperature controller. Temperature fluctuation as sensed by the thermocouple under the sample was considerably less than  $\pm 1^\circ\text{C}$ .

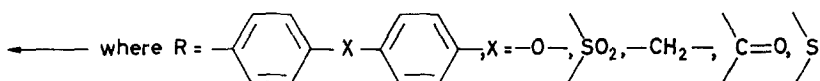
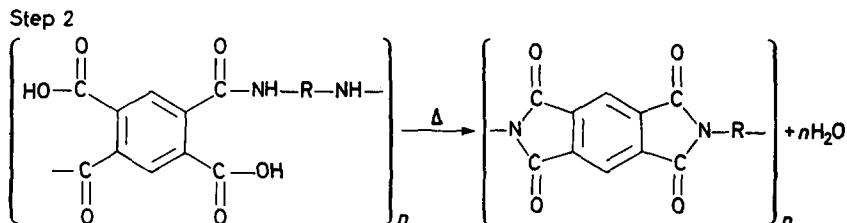
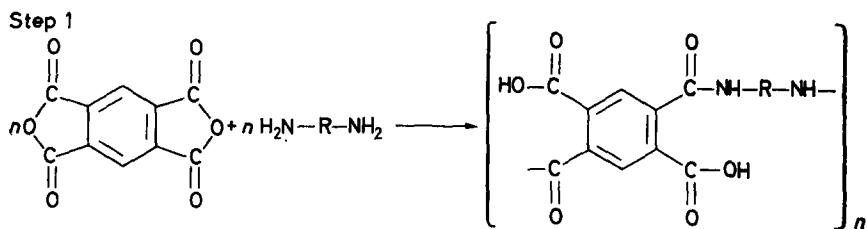
The vacuum experiments were carried out in the pressure range of  $10^{-3}$  mm of mercury. In a typical experiment the sample was first evacuated to this pressure and then the pre-heated furnace was rapidly raised into position. In the case of those experiments that were conducted under atmospheric conditions (air), thermal equilibrium was usually reached within 15 minutes from the start of the heating. During this period very little volatilization (less than one per cent) of the sample took place at the experimental temperatures chosen. In vacuum, thermal equilibrium was usually reached within 25–30 minutes. Because of the nature of the degradation process in vacuum, some volatilization of the sample was unavoidable during the heating-up period. However, temperature ranges were so selected that this volatilization was kept below eight per cent of the total weight of the sample.

### Materials

One mil (0.001 in.) thickness samples of H-film was used. The term 'H-film' arises from the material's ability to exceed class H (180°C) insulation requirements.

## RESULTS

Polypyromellitimides have been reported to have exciting possibilities as insulating materials due to their unique mechanical and electrical properties in the temperature range of approximately  $-40^\circ\text{C}$  to  $+300^\circ\text{C}$ <sup>16</sup>. The preparation of these polymers reportedly involves a two-step process<sup>16-18</sup>. In the first step, pyromellitic anhydride is reacted in a solution of dimethylformamide or dimethylacetamide with an aromatic diamine to form poly-pyromellitimic acid (polyamide acid). This is followed by a second step in which films are cast from solution and heat is applied to bring about an intramolecular cyclodehydration with the formation of an insoluble and infusible polyimide. The general scheme may be summarized in steps 1 and 2 (overleaf). Elemental microanalyses and the infra-red (i.r.) spectrum (see below) of H-film used in the present investigation indicate that this polyimide is, most likely, the condensation product of pyromellitic dianhydride and 4,4'-diaminodiphenylether ( $\text{X}=\text{—O—}$  in the reaction below).



or other groups.

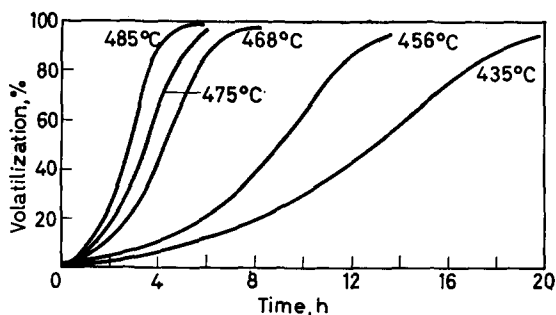


Figure 1—Thermal degradation of H-film in air

The first series of thermogravimetric experiments was carried out under atmospheric conditions in the presence of air. *Figure 1* illustrates the volatilization of the polymer as a function of time at various temperatures. As indicated, practically complete volatilization takes place in the temperature range of 468°–485°C after 5 to 8 hours of heating. At 435°C the volatilization is much slower and below 400°C the polymer shows practically no weight loss. In general, to obtain reliable data on rates from thermogravimetric experiments, it is necessary to choose conditions under which the rates of degradation are neither impractically slow nor so fast that the polymer suffers excessive degradation during the heating-up period prior to the attainment of thermal equilibrium. As already noted this was usually reached within 15 min and during this period less than one per cent weight loss was observed.

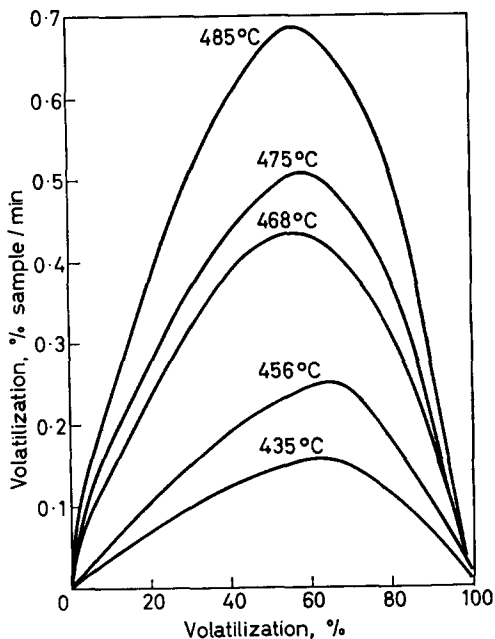


Figure 2—Rates of thermal degradation of H-film at various temperatures in air

In *Figure 2* the rates of volatilization are plotted against percentage volatilization. These rates were calculated from the volatilization/time curves with the aid of an electronic computer. The data in *Figure 2* indicate that distinct maxima were reached between approximately 55 and 65 per cent volatilization at the higher experimental temperatures.

Usually, the activation energies for the degradation of polymers can be obtained from either extrapolated initial rates or from maximum rates<sup>19</sup>, unless the degradation follows simple kinetics from which the order and rate constants of the reaction can be obtained. Tetrafluorethylene, for example, follows a simple first order reaction<sup>7</sup>, but many other polymers exhibit very complex rate patterns.

In view of the shapes of the curves in *Figure 2* (lack of apparent straight line portions that can be extrapolated to zero per cent volatilization), the activation energy was calculated from maximum rates. According to the well-known Arrhenius equation,  $k = Se^{-(E/RT)}$ , where  $k$  is the rate constant,  $S$  is a frequency factor,  $E$  is activation energy,  $R$  the gas constant, and  $T$  denotes absolute temperature. By plotting the logarithm of maximum rates (here expressed in per cent of sample volatilized per minute) versus the inverse of the absolute temperatures, a straight line relationship was obtained as illustrated in *Figure 3*. The slope of this line gave an activation energy of 33 kcal/mole for the thermal degradation of H-film in air under atmospheric conditions.

The second series of experiments was conducted in vacuum ( $\sim 10^{-3}$  mm of mercury). *Figure 4* shows the per cent volatilization as a function of time at various temperatures. Thermal equilibrium was reached usually within 25 to 30 min from the time the pre-heated furnace was raised. Zero

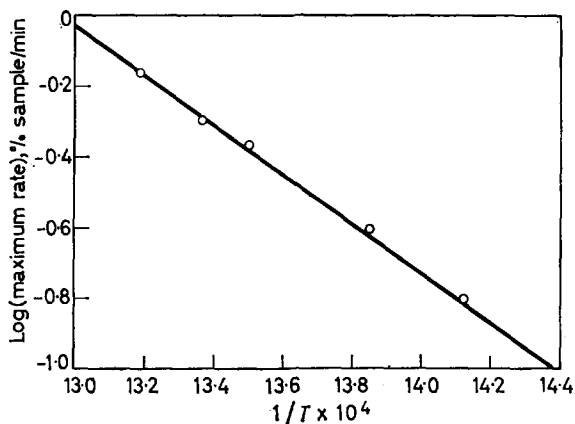


Figure 3—Arrhenius plot for thermal degradation of H-film in air

time again signifies the time at which this thermal equilibrium had been attained. Due to the nature of the degradation process some weight loss was unavoidable during the heating-up period at the higher temperature but this was kept below eight per cent.

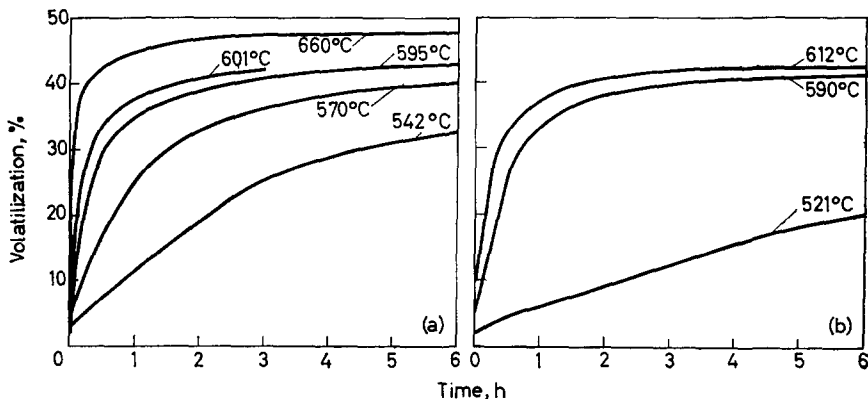


Figure 4—Thermal degradation of H-film in vacuum

Figure 5 illustrates the rate curves for experiments carried out at 570°, 590°, 595° and 601°C, respectively. The data indicate early maxima in the rates of degradation, followed by a rapid decrease in rate in each case; beyond approximately 40 per cent volatilization the rates are very slow and little further loss of weight takes place. This is in contrast to the thermal degradation in air where practically 100 per cent volatilization was observed. Thermal degradation in vacuum leaves a brittle, dark-grey, carbonized residue which retains the general shape of the original sample. The i.r. absorption spectrum of the original H-film and that of the carbon-

# THERMAL DEGRADATION OF AN AROMATIC POLYPYROMELLITIMIDE

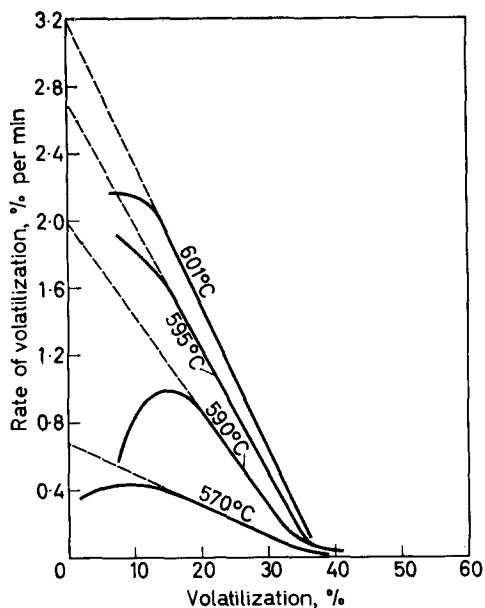


Figure 5—Rates of thermal degradation of H-film in vacuum at various temperatures

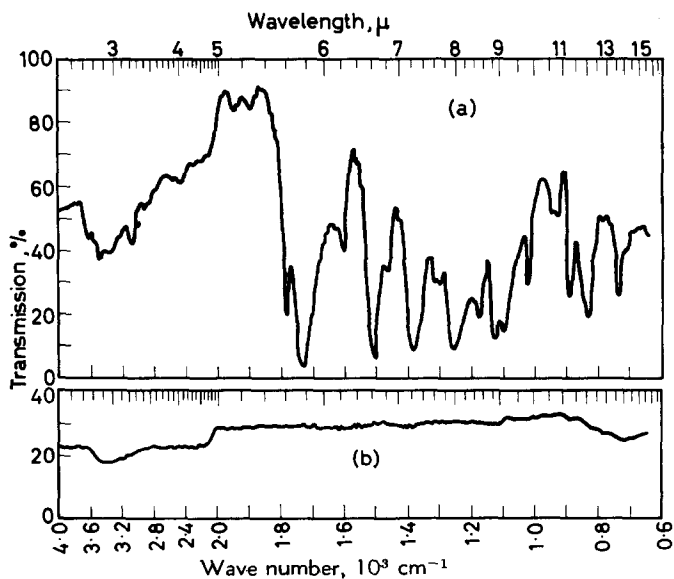
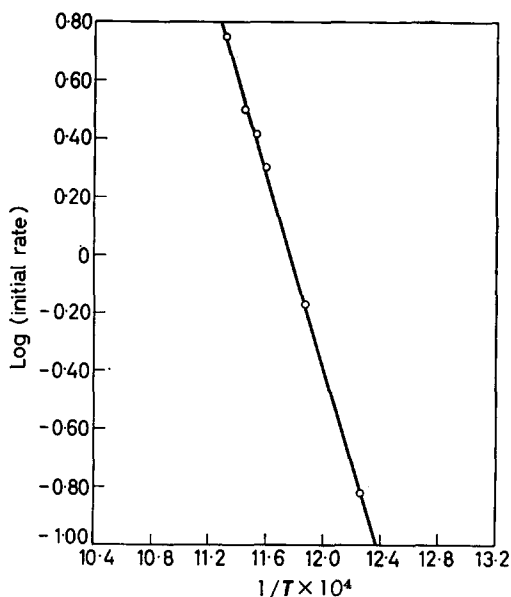


Figure 6—Infra-red spectra of undegraded H-film (a) and carbonized residue (b)

ized residue remaining after vacuum pyrolysis at 639°C for 20 hours are illustrated in *Figure 6* (both spectra were obtained with potassium bromide pellets of the materials for reasons of comparison, although the undegraded yellow H-film may be used directly for absorption measurements). The i.r. spectrum of the carbonized residue (b) indicates practically no absorption bands as compared to the undegraded sample (a) and confirms the carbonization process<sup>20</sup>.



*Figure 7*—Arrhenius plot for thermal degradation of H-film in vacuum

*Table 1.* Rates and activation energies for the thermal degradation of H-film in air and vacuum

Thermal degradation	Temp. °C	Total time hours	Total volatilization %	Rates per cent sample/min		Activation energy kcal/mole
				Extrapolated initial	Maximum	
Air	485	5.5	98.4	—	0.685	33
Air	475	5.5	93.3	—	0.510	
Air	468	9.0	98.9	—	0.435	
Air	456	13.5	94.6	—	0.252	
Air	435	20.0	95.6	—	0.157	
Vacuum	660	20.0	49.0	*	—	74
Vacuum	612	20.0	45.2	5.620	—	
Vacuum	601	3.0	42.3	3.180	—	
Vacuum	595	10.0	43.3	2.700	—	
Vacuum	590	16.0	43.4	1.990	—	
Vacuum	570	18.0	41.9	0.680	—	
Vacuum	542	18.0	38.6	0.150	—	
Vacuum	521	18.0	32.1	†	—	

\*Rates too fast for reliable measurement and extrapolation.

†Degradation complicated by side reactions at this low temperature.



In order to calculate the activation energy, an Arrhenius type curve was constructed by plotting the logarithm of the 'apparent initial rates' versus the inverse of the absolute temperatures at which the degradations were carried out (*Figure 7*). The 'apparent initial rates' were obtained by extrapolating the straight line parts of the rate curves to zero per cent volatilization. These 'apparent initial rates' relate to the actual initial rates and indicate what the latter would have been without the interference of complicating side reactions. *Table I* summarizes the data on the maximum and initial rates together with the calculated activation energy for the thermal degradations in air and vacuum, respectively.

#### DISCUSSION

The practically total volatilization of the polymer during thermal degradation in air in contrast to its behaviour in vacuum is most likely due to oxidative cleavage occurring at the imide bonds. The low activation energy calculated for degradation in air indicates such a process. The thermal degradation of H-film in vacuum is somewhat similar to that of polytrivinylbenzene studied by Madorsky and Straus<sup>9</sup> and by Winslow and associates<sup>21, 22</sup>. The rate versus volatilization curves (*Figure 5*) strongly resemble those of polytrivinylbenzene in the early appearance of maxima, followed by straight line (first-order) portions and in the formation of carbonized residues amounting to approximately 45 to 50 per cent of the original sample. It is important to note, however, that polytrivinylbenzene is highly crosslinked (unlike polypyromellitimide) since the monomer is trifunctional. In general, highly crosslinked polymers are converted upon heating to carbonized structures, whereas polymers in which the backbone undergoes primarily scission reactions tend to vaporize completely without leaving any appreciable quantity of residue.

The structure of the present polypyromellitimide sample indicates stiff benzene rings which hinder chain mobility and rotation and hence exert a stabilizing influence similar to crosslinks. As a result, a carbonized residue forms upon vacuum pyrolysis where oxidative processes are minimized or eliminated. The fact that H-film has no melting point and no glass transition temperature below 500°C substantiates this argument.

The exact mechanism of the degradation process in vacuum appears to be complicated by side reactions. Due to the insolubility of this material in any known solvent, fractionation and further purification were not carried out. Consequently one cannot make a conclusive statement as to whether the process follows a random free-radical initiated breakdown. For a purely random breakdown Simha and Wall predicted on theoretical grounds the appearance of maxima in the rate versus volatilization curves at approximately 26 per cent of vaporization<sup>15</sup>. This has subsequently been found to apply for many but not all polymers. The thermal degradation of H-film in vacuum is apparently complicated by non-random processes that seem to have been characteristic also of polytrivinylbenzene<sup>9</sup>, polystyrene<sup>3-5</sup> and others. The high activation energy of 74 kcal/mole for thermal degradation in vacuum definitely suggests carbon-carbon or carbon-nitrogen scission. A comparison of activation energies for vacuum pyrolysis of

Table 2. Activation energies for the thermal degradation of selected polymers in vacuum

<i>Polymer</i>	<i>Activation energy kcal/mole</i>	<i>Reference</i>
Polypyromellitimide (H-film)	74	Present study
Polytrivinylbenzene	73	9
Polymethylene (linear)	72	19
Poly( $\alpha$ -methylstyrene)	65	14
Polypropylene (linear)	58	19
Polystyrene (Mol. wt = 230 000)	55	19
Polybenzyl	50	19
Polyisobutylene	49	19
Poly(methylmethacrylate)	30-52*	19
Polycaprolactam (Nylon-6)	24-43†	13

\*Varies apparently with mechanism of initiation and molecular weight.

†Depending on moisture content.

selected polymers may be obtained from Table 2 which indicates this material has the highest activation energy among hydrogen polymers. The high thermal stability, lack of a melting point and unique mechanical and electrical properties of this material undoubtedly offer an important challenge for further investigations.

In concluding this discussion, a few words on the difficulties inherent in thermogravimetry may be appropriate. Some of these have been summarized<sup>19</sup> as: (a) spattering, (b) delay in vaporization of volatile products due to diffusion, (c) temperature control and measurement, and (d) problems arising from fast degradations during the heating-up period. In the present investigation the use of a Cahn RG electro-balance readily permitted the degradation of small samples (4-7 mg) and this situation plus the fact that the film was only 0.001 in. thick minimized points (a), (b), and, to a considerable extent, (c). Uniformity of temperature in the vicinity of the sample and thermocouple was assured by the use of a furnace with uniform temperature along its vertical axis (see Experimental section). As has already been discussed, the judicious choice of degradation temperatures minimized or eliminated point (d).

Another problem that has been reported only recently by several investigators<sup>22-26</sup> may arise from thermo-molecular flow. This phenomenon was the subject of a mathematical treatment by Thomas and Poulis<sup>27</sup> making use of the classical Knudsen theory. In brief, the problem manifests itself in mass changes that occur at low pressures owing to the temperature inhomogeneity of the sample and temperature gradient along the hangdown wire (the balance beam and the wire being at different temperatures). In the present investigation the effect of thermo-molecular flow was indeed observed as evidenced by an apparent rapid weight loss when the temperature inside the sample tube started to climb. However, this initial depression in weight was soon reversed as the heating-up period proceeded towards equilibrium conditions. The recorder trace indicating the weight changes of the sample was usually reversed and its position nearly re-established (save for the loss of material that volatilized during this heating-up period) by the time the thermocouple reached equilibrium. A typical recorder trace is reproduced in Figure 8. It is estimated that the

## THERMAL DEGRADATION OF AN AROMATIC POLYPYROMELLITIMIDE

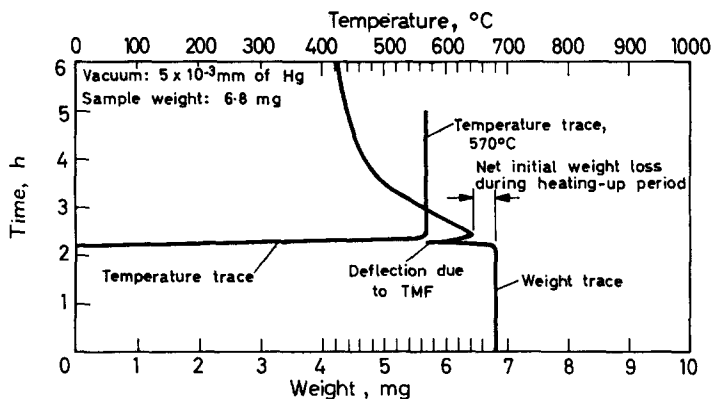


Figure 8—Typical disturbance due to thermo-molecular flow (TMF) with the Cahn RG electro-balance

mass changes due to thermo-molecular flow alone were quite low, probably in the low microgramme ranges, which did not influence the results to any significant extent. The reason for this relatively minor disturbance as compared with some of the more serious ones reported by others may be due to the small size and thickness of the samples, the use of a very thin (0.025 mm in diameter) hangdown wire, and fairly uniform temperature along the vertical axis of the furnace.

*This work is supported by the Bureau of Naval Weapons, Department of the U.S. Navy, under Contract N0w62-0604-c.*

*The author thanks Mr J. E. Young and Mr R. E. Ruckman for the infra-red spectra, and Mr Stanley Favin for the computer programming of the kinetic data. Special thanks are due to Dr W. G. Berl for his encouragement and efforts in obtaining the necessary support for this work. The samples of H-film were obtained through the courtesy of Dr L. E. Amborski of E. I. du Pont de Nemours and Company, Incorporated.*

*This paper was presented at the Symposium of Ring-containing Polymers, Division of Polymer Chemistry, 147th National Meeting, American Chemical Society, Philadelphia, Pennsylvania, 5 to 10 April 1964.*

*Applied Physics Laboratory,  
The Johns Hopkins University,  
8 621 Georgia Avenue,  
Silver Spring, Maryland, U.S.A.*

(Received October 1963)

### REFERENCES

- <sup>1</sup> JELLINEK, H. H. G. *J. Polym. Sci.* 1948, **3**, 850
- <sup>2</sup> JELLINEK, H. H. G. *J. Polym. Sci.* 1949, **4**, 13
- <sup>3</sup> GRASSIE, N. and KERR, W. W. *Trans. Faraday Soc.* 1957, **53**, 234

- <sup>4</sup> GRASSIE, N. and KERR, W. W. *Trans. Faraday Soc.* 1959, **55**, 1050
- <sup>5</sup> STRAUS, S. and MADORSKY, S. L. *J. Res. nat. Bur. Stand.* 1961, **65A**, 243
- <sup>6</sup> STRAUS, S. and MADORSKY, S. L. *J. Res. nat. Bur. Stand.* 1962, **66A**, 401
- <sup>7</sup> MADORSKY, S. L., HART, V. E., STRAUS, S. and SEDLAK, V. A. *J. Res. nat. Bur. Stand.* 1953, **51**, 327
- <sup>8</sup> MADORSKY, S. L., MCINTYRE, D., O'MARA, J. H. and STRAUS, S. *J. Res. nat. Bur. Stand.* 1962, **66A**, 307
- <sup>9</sup> MADORSKY, S. L. and STRAUS, S. *J. Res. nat. Bur. Stand.* 1959, **63A**, 261
- <sup>10</sup> MADORSKY, S. L. and STRAUS, S., *J. Res. nat. Bur. Stand.* 1954, **53**, 361
- <sup>11</sup> WALL, L. A. and STRAUS, S. *J. Polym. Sci.* 1960, **44**, 313
- <sup>12</sup> STRAUS, S. and WALL, L. A. *J. Res. nat. Bur. Stand.* 1958, **60A**, 39
- <sup>13</sup> STRAUS, S. and WALL, L. A. *J. Res. nat. Bur. Stand.* 1959, **63A**, 269
- <sup>14</sup> BROWN, D. W. and WALL, L. A. *J. phys. Chem.* 1958, **62**, 848
- <sup>15</sup> SIMHA, R. and WALL, L. A. *J. phys. Chem.* 1952, **56**, 707
- <sup>16</sup> AMBORSKI, L. E. Paper presented at the 144th National Meeting, American Chemical Society, Los Angeles, California, 31 March-5 April 1963
- <sup>17</sup> VANDEBERG, E. J. and OVERBERGER, C. G. (quoting Jones, J. I.) *Science*, 1963, **141**, 176
- <sup>18</sup> FROST, L. W. and BOWER, G. M. Paper presented at the 144th National Meeting, American Chemical Society, Los Angeles, California, 31 March-5 April 1963
- <sup>19</sup> MADORSKY, S. L. *J. Res. nat. Bur. Stand.* 1959, **62**, 219
- <sup>20</sup> PLYLER, E. K. and BALL, J. J. *J. opt. Soc. Amer.* 1948, **38**, 988
- <sup>21</sup> WINSLOW, F. H., BAKER, W. O., PAPE, N. R. and MATREYEK, W. *J. Polym. Sci.* 1955, **16**, 101
- <sup>22</sup> WINSLOW, F. H. and MATREYEK, W. *J. Polym. Sci.* 1956, **23**, 315
- <sup>23</sup> KATZ, O. M. and GULBRANSEN, E. A. in *Vacuum Microbalance Techniques*, Vol. I, p 111. Plenum Press: New York, 1961
- <sup>24</sup> CZANDERNA, A. W. in *Vacuum Microbalance Techniques*, Vol. I, p 129. Plenum Press: New York, 1961
- <sup>25</sup> WOLSKY, S. P. in *Vacuum Microbalance Techniques*, Vol. I, p 143. Plenum Press: New York, 1961
- <sup>26</sup> CZANDERNA, A. W. and HONIG, J. M. *J. phys. Chem.* 1959, **63**, 620
- <sup>27</sup> THOMAS, J. M. and POULIS, J. A. in *Vacuum Microbalance Techniques*, Vol. III, p 15. Plenum Press: New York, 1963

# The Free Radical Polymerization of *N,N*-Dimethylacrylamide

A. M. NORTH and A. M. SCALLAN

*The free radical homopolymerization and copolymerization of N,N-dimethylacrylamide has been investigated at 50°C. Individual rate constants have been obtained for all the relevant propagation, transfer, and termination processes. The high propagation rate constant is due to the abnormal reactivity of the free radical rather than the monomer.*

ALTHOUGH detailed studies<sup>1,2</sup> of the solution polymerization of acrylamide have been made, no values have yet been reported for the rate constants of the polymerization of *N,N*-dialkylacrylamides. In this publication are reported conventional studies of the free radical homopolymerization and copolymerization of *N,N*-dimethylacrylamide.

## EXPERIMENTAL

### Materials

*N,N*-dimethylacrylamide was kindly supplied by British Nylon Spinners.

The monomer was dried over freshly ground calcium hydride, and fractionally distilled on the vacuum line at 30°C. Traces of inhibitor which co-distilled with the monomer were removed by prepolymerizing to 20 per cent conversion, the residual monomer being distilled directly into the reaction vessel.

*Methylmethacrylate*, B.D.H. purified grade, was freed of inhibitor and distilled under a nitrogen pressure of 20 mm of mercury. The middle fraction was collected, and aliquot portions outgassed on the vacuum line at pressures less than  $5 \times 10^{-5}$  mm of mercury, prepolymerized by ultraviolet irradiation, and residual monomer distilled into the polymerization vessels.

*Styrene* was treated in the same way as methylmethacrylate.

*Toluene*, analytical reagent grade, was dried by refluxing over sodium. In one series of experiments sulphur compounds were removed by refluxing with mercuric acetate solution. However, kinetic experiments using toluene so treated were identical with those carried out using untreated toluene, and the procedure was dispensed with in later experiments.

$\alpha,\alpha'$ -Azobutyronitrile (AZBN) was recrystallized three times from ethanol and stored in the dark at  $-10^\circ\text{C}$ .

### Procedure

Rates of polymerization were observed using conventional dilatometers, immersed in a water thermostat bath governed to  $50^\circ \pm 0.01^\circ\text{C}$ . The meniscus movement was observed using a cathetometer reading to  $\pm 0.001$  cm.

Molecular weights were determined from intrinsic viscosities (measured in an Ubbelohde suspended level viscometer) using the relationship of

Trossarelli and Meirone<sup>3</sup>. Instantaneous number average molecular weights were calculated from weight average values measured on whole polymer samples (polymerization being carried to a finite monomer-polymer conversion) using the equation derived by Schultz<sup>4</sup>.

The rotating sector was constructed from brass with two apertures capable of variation from 0° to 90° segmental angle. The sector was driven by a Jones and Stevens [Type R.Z.G.] induction motor with a continuously variable gear box. The sector was arranged so as to chop the light beam at its focal point.

All measurements of polymerization rate were carried out below five per cent conversion monomer to polymer.

Copolymer compositions were determined by microanalysis of the nitrogen content.

## RESULTS

### *The contraction-conversion factor*

Seventeen polymerizations were carried out in which the resulting polymer was weighed, and the fractional conversion so obtained compared with the contraction observed. The average value of the percentage volume contraction corresponding to 100 per cent conversion was obtained as 16.9 (standard deviation 1.3).

### *Rates of homopolymerization*

The dependences of the rate of polymerization upon the concentrations of monomer and of initiator (AZBN) are illustrated in *Figures 1* and *2*. The polymerization rate is proportional to the first power of the monomer concentration and the square root of the initiator concentration only at high monomer and low initiator concentrations.

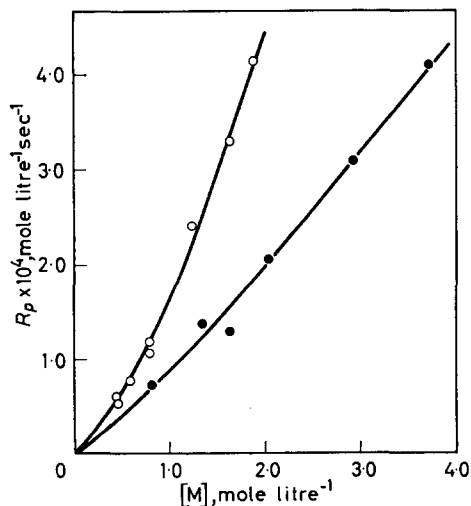


*Figure 1*—Rate of polymerization against monomer concentration. ○ [Init.]  $1.32 \times 10^{-2}$  mole litre<sup>-1</sup>; ● [Init.]  $2.17 \times 10^{-3}$  mole litre<sup>-1</sup>

Figure 2—Rate of polymerization against square root  $\alpha, \alpha'$ -azoisobutyronitrile concentration;  $[M]$   $0.81 \text{ mole litre}^{-1}$ .  $\circ$  Experimental points. Unbroken line represents curve calculated assuming primary radical combination

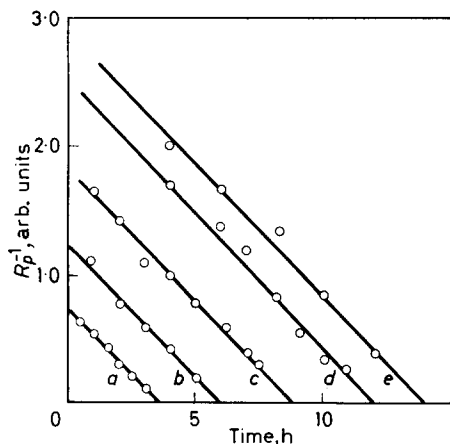
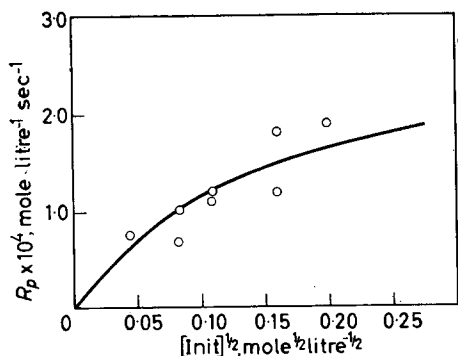


Figure 3—Determination of inhibition periods.  $[\text{Init.}]$ ,  $4.0 \times 10^{-2} \text{ mole litre}^{-1}$ . Benzoquinone concentrations: a,  $1.3 \times 10^{-3}$ ; b,  $3.5 \times 10^{-3}$ ; c,  $1.6 \times 10^{-3}$ ; d,  $2.4 \times 10^{-3}$ ; e,  $3.5 \times 10^{-3}$  (all mole litre $^{-1}$ ). Monomer concentrations: a,  $8.1 \times 10^{-1}$ ; b,  $4.1 \times 10^{-1}$ ; c,  $8.1 \times 10^{-1}$ ; d,  $4.1 \times 10^{-1}$ ; e,  $8.1 \times 10^{-1}$  (all mole litre $^{-1}$ )

Rates of initiation were calculated from inhibition times using the kinetic analysis of Burnett and Cowley<sup>5</sup>. Benzoquinone was used as inhibitor, and plots of reciprocal rate of polymerization against time are illustrated in Figure 3. Comparison of the rates of initiation so obtained with literature values for the rate of decomposition of AZBN<sup>6</sup> yields an initiator efficiency in this system of 0.38.

When the rate of initiation is compared with the rate of polymerization at high monomer and low catalyst concentrations it is possible to obtain the ratio

$$k_p / (2k_{tc} + 2k_{td})^{\frac{1}{2}} = R_p / [M] R_i^{\frac{1}{2}} \quad (1)$$

where  $k_p$ ,  $k_{tc}$ ,  $k_{td}$  are the rate constants for propagation, termination by combination and termination by disproportionation respectively. At  $50^\circ\text{C}$  the ratio had the value,

$$k_p / (2k_{tc} + 2k_{td})^{\frac{1}{2}} = 1.78 \text{ litre}^{\frac{1}{2}} \text{ mole}^{-\frac{1}{2}} \text{ sec}^{-\frac{1}{2}}$$

*Degrees of polymerization*

It was found that the measured degrees of polymerization were less than one twentieth of the kinetic chain lengths,  $\nu = R_p/R_t$ . This implies that chain transfer reactions are very important in determining the molecular weights of the polymers. Under these circumstances the polymer size distribution is such that the instantaneous number average molecular weight is half the weight average molecular weight.

The inverse degree of polymerization can be related to the rate of polymerization and to the rate coefficients for the various transfer processes by the equation

$$\bar{P}_n^{-1} = \frac{k_{JM}}{k_p} + \frac{k_{JS} [S]}{k_p [M]} + \frac{(k_{tc} + 2k_{td})}{k_p^2 [M]^2} \cdot R_p \quad (2)$$

where  $k_{JM}$ ,  $k_{JS}$  are the rate constants for transfer to monomer (M) and polymer (S) respectively. The term,  $R_p (k_{tc} + 2k_{td})/k_p^2 [M]^2$  is less than four per cent of the other terms, so that equation (2) can be approximated by

$$\bar{P}_n^{-1} = \frac{k_{JM}}{k_p} + \frac{k_J [S]}{k_p [M]} \quad (3)$$

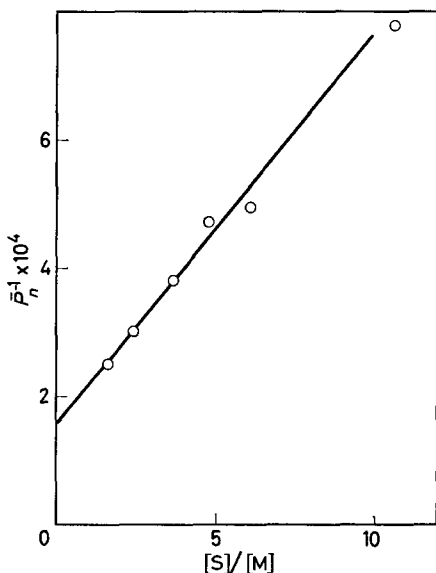


Figure 4—Inverse degree of polymerization against toluene to monomer mole ratio

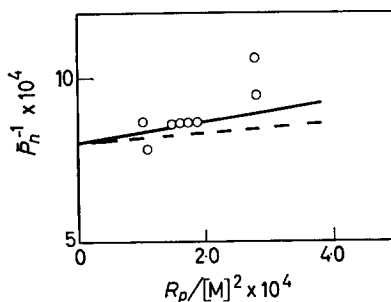
A plot of the inverse degree of polymerization against the ratio  $[S]/[M]$  for polymers prepared at 50°C is illustrated in Figure 4, from which

$$k_{JM}/k_p = 1.5 \times 10^{-4}, \quad k_{JS}/k_p = 0.61 \times 10^{-4}$$

Plots of  $\bar{P}_n^{-1}$  against  $R_p/[M]^2$  at constant values of  $[S]/[M]$  should yield the ratio  $(k_{tc} + 2k_{td})/k_p^2$  thus determining whether termination occurs by combination or disproportionation. Such a plot is illustrated in Figure 5, on which are entered the lines for termination by disproportionation and



Figure 5—Inverse degree of polymerization against quotient of rate of polymerization by square of monomer concentration. ○ Experimental points. Full line, calculated assuming termination by disproportionation; broken line, calculated assuming termination by combination



termination by combination calculated from the ratio  $(2k_{tc} + 2k_{td})/k_p^2$ . While the experimental error does not allow an unambiguous decision to be reached, the results do suggest that disproportionation is the predominant termination process.

The free radical lifetime in a photopolymerization (rate of photopolymerization  $3.05 \times 10^{-5}$  mole litre $^{-1}$  sec $^{-1}$  at 50°C) was found, by the use of intermittent illumination, to be nine seconds.

The value of  $(2k_{tc} + 2k_{td})/k_p$  so obtained was  $3.1 \times 10^{-4}$  at 50°C.

Knowledge of all the ratios  $(2k_{tc} + 2k_{td})/k_p$ ,  $(2k_{tc} + 2k_{td})/k_p^2$ ,  $k_{fM}/k_p$ , and  $k_{fs}/k_p$  allows calculation of the individual rate constants. Values for 50°C are listed in Table 1.

Table 1. Rate constants in the homopolymerization of *N,N*-dimethylacrylamide at 50°C

Rate constant	Magnitude, litre mole $^{-1}$ sec $^{-1}$
$k_p$	11 000
$2(k_{tc} + k_{td})$	$3.8 \times 10^7$
$k_{fM}$	1.65
$k_{fs}$	0.67

#### Copolymerization with methylmethacrylate and styrene: copolymer composition

The compositions of a series of copolymers prepared at different monomer feeds were determined by microanalysis, and are illustrated in

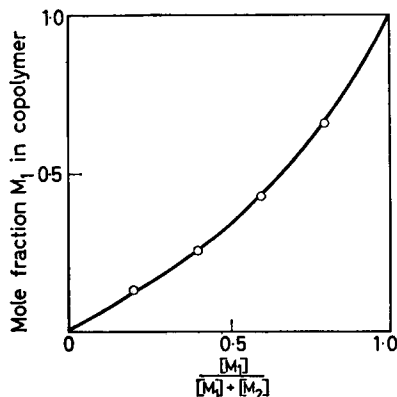
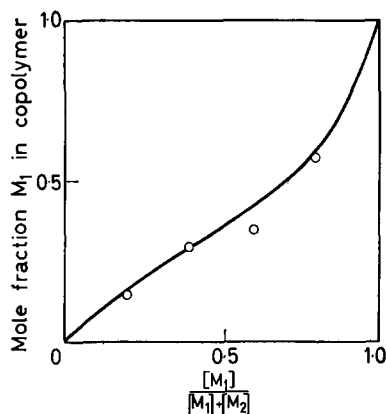


Figure 6—Copolymer compositions,  $M_1$ , *N,N*-dimethylacrylamide,  $M_2$ , methylmethacrylate. ○ Experimental points. Line calculated for  $r_1=0.45$ ,  $r_2=1.8$

Figure 7—Copolymer compositions.  $M_1$ , *N,N*-dimethylacrylamide,  $M_2$ , styrene. ○ Experimental points. Line calculated for  $r_1=0.23$ ,  $r_2=1.23$



Figures 6 and 7. The reactivity ratios were obtained from the intercepts of plots

$$r_1 = \frac{[B]}{[A]} \left( \frac{d[A]}{d[B]} \right) \left[ 1 - r_2 \frac{[B]}{[A]} \right] - \frac{[B]}{[A]} \quad (4)$$

and are listed in Table 2.

Also listed in Table 2 are the Alfrey-Price  $Q$ ,  $e$  values for the relevant copolymerizations.

Table 2. Copolymerization parameters at 50°C.  $M_1$ : *N,N*-dimethylacrylamide

$M_2$	$r_1$	$r_2$	$Q_1$	$Q_2$
Methyl-methacrylate	$0.45 \pm 0.08$	$1.80 \pm 0.18$	0.34	0.74
Styrene	$0.23 \pm 0.13$	$1.23 \pm 0.43$	0.33 mean value 0.33	1.0

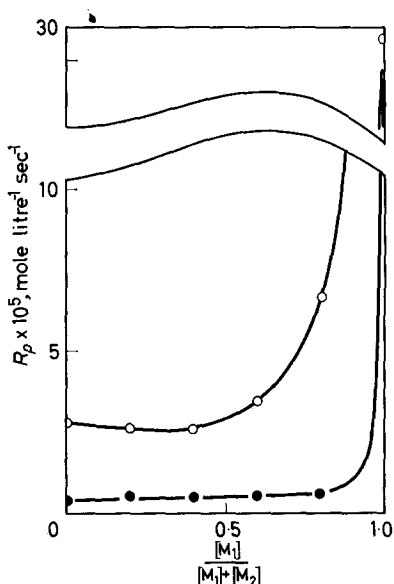
  

$M_2$	$e_1$	$e_2$	$k_{p12}$ mole litre <sup>-1</sup> sec <sup>-1</sup>	$k_{p21}$ mole litre <sup>-1</sup> sec <sup>-1</sup>
Methyl-methacrylate	+0.05	+0.40	24 000	380
Styrene	+0.34 mean value +0.20	-0.8	48 000	110

#### Copolymerization rates

The rates of copolymerization at 50°C in which the total molarity of both monomers was maintained constant (2.92 mole litre<sup>-1</sup> in toluene), and the concentration of initiator was also constant [ $2.17 \times 10^{-3}$  mole litre<sup>-1</sup>] are illustrated in Figure 8. Rates of polymerization were calculated from rates of contraction using the equation of Melville, Noble and Watson<sup>7</sup>.

Figure 8—Copolymerization rate against monomer composition  $[M_1] + [M_2] = 2.92$  mole litre<sup>-1</sup>,  $[Init.] = 2.17 \times 10^{-3}$  mole litre<sup>-1</sup>. ○  $M_2$  methylmethacrylate; ●  $M_2$  styrene



#### DISCUSSION

##### *The homopolymerization*

The greatest source of error in this work lies in the determination of the rates of initiation. The standard deviation in the measurements was about ten per cent, but considerable doubt is attached to the assumption that each benzoquinone molecule is responsible for stopping one radical chain. Although the assumption seems valid for methylmethacrylate<sup>8</sup>, and in the inhibition of vinyl acetate by duroquinone<sup>9</sup>, it has been reported that benzoquinone may terminate two radical chains in styrene polymerization<sup>9</sup>.

If each benzoquinone molecule is responsible for the termination of two radical chains, the initiator efficiency would be 0.76 and the ratio  $k_p / (2k_{tc} + 2k_{td})^{\frac{1}{2}}$  should be 1.25. By comparison with the methacrylate systems, however, and since there is evidence for primary radical recombination in these experiments, the low initiator efficiency seems more reasonable, and we have reported all rate constants on the assumption that one inhibitor molecule terminates one radical chain.

The existence of primary radical termination reactions is inferred from the fact that the monomer kinetic order is 1.4 at high initiator and low monomer concentrations, and that the initiator kinetic order is much less than 0.5 under the same conditions.

A comparison of the propagation rate constant with values for some other common monomers, Table 3, shows that propagation is much more rapid with *N,N*-dimethylacrylamide than for most common monomers, but is less than the unsubstituted acrylamide.

The rate of the propagation reaction is a measure of the reactivity of a radical for its own monomer. However, an assessment of the radical reactivity can be deduced from the velocity of transfer to the same substrate, here toluene.

Table 3. Some propagation rate constants

Monomer	$k_p$ (reference) litre mole <sup>-1</sup> sec <sup>-1</sup>	Temperature °C	$k_{fs}$ (reference) litre mole <sup>-1</sup> sec <sup>-1</sup>
Styrene	176 <sup>10</sup>	60	0.002 <sup>11</sup>
Methylmethacrylate	734 <sup>10</sup>	60	0.015 <sup>12</sup>
Methylacrylate	2 090 <sup>10</sup>	60	0.564 <sup>13</sup>
<i>N,N</i> -Dimethylacrylamide	11 000	50	0.67
Acrylamide	18 000 <sup>11</sup>	25	—

These constants are also listed in Table 3, and show that the reactivity in this reaction appears to run parallel to the propagation rate constant, but further information on the separate reactivities of monomer and free radical can be more easily deduced from the copolymerization studies.

#### The copolymerization

It follows from the  $Q$  values and the individual rate constants reported in Table 2 that the monomer *N,N*-dimethylacrylamide is less reactive than either styrene or methylmethacrylate, but that the radical is very much more reactive.

The rates of copolymerization are interesting in that when analysed by the conventional rate equation

$$R_p = \frac{R_i^\dagger (r_1 [M_1]^2 + 2 [M_1] [M_2] + r_2 [M_2]^2)}{(r_1^2 \delta_1^2 [M_1]^2 + 2\phi r_1 r_2 \delta_1 \delta_2 [M_1] [M_2] + r_2^2 \delta_2^2 [M_2]^2)^{\frac{1}{2}}} \quad (5)$$

values of the constant  $\phi$  are obtained which are negative and dependent on the monomer feed composition, Table 4. In equation (4),  $\phi$  is defined as

$$\frac{k_{t12}}{2(k_{t11}k_{t22})^{\frac{1}{2}}}$$

$k_{t11}$ ,  $k_{t22}$  and  $k_{t12}$  represent termination reactions between radicals containing the electrons of unpaired spins on two groups of monomer 1, two groups of monomer 2, and one of each respectively. The constants,  $\delta_1$ ,  $\delta_2$  represent the rate constant ratios  $(2k_{t11})^{\frac{1}{2}}/k_{p11}$ ,  $(2k_{t22})^{\frac{1}{2}}/k_{p22}$  respectively.

Table 4. Copolymerization termination parameters

Comonomer	Mole fraction <i>N,N</i> -dimethyl- acrylamide in monomer feed	$\phi$	$k_{t(12)} \times 10^{-7}$ litre mole <sup>-1</sup> sec <sup>-1</sup>
Methylmethacrylate	1.0	—	3.8
	0.8	-6	0.9
	0.6	-11	1.9
	0.4	-16	2.3
	0.2	-58	1.9
	0.0	—	3.3
Styrene	1.0	—	3.8
	0.8	-2	6.0
	0.6	-62	4.4
	0.4	-120	4.9
	0.2	-320	3.3
	0.0	—	6.5

## THE FREE RADICAL POLYMERIZATION OF *N,N*-DIMETHYLACRYLAMIDE

Quite obviously negative values of  $\phi$  are impossible if such a kinetic equation is correct. It has been suggested<sup>14,15</sup> that the concept of the  $\phi$  factor in copolymerization requires re-examination when the termination processes are diffusion-controlled. Under these circumstances the relevant rate equation<sup>14</sup> is

$$R_p = \frac{R_i^\dagger (r_1 [M_1]^2 + 2 [M_1] [M_2] + r_2 [M_2]^2)}{k_{t(12)}^\dagger (r_1 [M_1]/k_{p11} + r_2 [M_2]/k_{p22})} \quad (6)$$

where  $k_{t(12)}$  is a rate constant which depends not on the end group of the terminating radical, but upon its whole composition.  $k_{t(12)}$  thus depends also on the monomer feed composition.

Values of  $k_{t(12)}$  calculated using equation (6) are also entered in *Table 4*, and appear quite reasonable. With methylmethacrylate the rate constant passes through a minimum at intermediate copolymer chain compositions.

In conclusion it may be stated that the free radical polymerization of *N,N*-dimethylacrylamide occurs less rapidly than that of acrylamide, but more rapidly than that of most common monomers. The unusually reactive entity appears to be the free radical rather than the monomer.

*The authors wish to express their indebtedness to Professor C. E. H. Bawn, who suggested these, and related, studies.*

*Department of Inorganic, Physical and Industrial Chemistry,  
Donnan Laboratories,  
University of Liverpool*

*(Received November 1963)*

### REFERENCES

- <sup>1</sup> DAINTON, F. S. and TORDOFF, M. *Trans. Faraday Soc.* 1957, **53**, 499
- <sup>2</sup> DAINTON, F. S. and SISLEY, W. D. *Trans. Faraday Soc.* 1963, **59**, 1369, 1377, 1385
- <sup>3</sup> TROSSARELLI, L. and MEIRONE, M. *J. Polym. Sci.* 1962, **57**, 445
- <sup>4</sup> SCHULTZ, G. V. *Z. phys. Chem. N.F.*, 1956, **8**, 290
- <sup>5</sup> BURNETT, G. M. and COWLEY, P. R. E. *J. Trans. Faraday Soc.* 1953, **49**, 1490
- <sup>6</sup> BAWN, C. E. H. and MELLISH, S. F. *Trans. Faraday Soc.* 1951, **47**, 1216
- <sup>7</sup> MELVILLE, H. W., NOBLE, B. and WATSON, W. F. *J. Polym. Sci.* 1947, **2**, 229
- <sup>8</sup> BEVINGTON, J. C. and GHANEM, R. A. *Trans. Faraday Soc.* 1955, **51**, 946
- <sup>9</sup> COHEN, S. G. *J. Amer. chem. Soc.* 1945, **67**, 17; 1947, **69**, 1057
- <sup>10</sup> MATHESON, M. S., AUER, E. E., BEVLACQUA, E. B. and HART, E. J. *J. Amer. chem. Soc.* 1949, **71**, 497, 2610; 1951, **73**, 1700, 5395
- <sup>11</sup> GREGG, R. A. and MAYO, F. R. *Disc. Faraday Soc.* 1947, **2**, 328
- <sup>12</sup> BASU, S., SEN, J. N. and PALIT, S. R. *Proc. Roy. Soc. A*, 1952, **214**, 247
- <sup>13</sup> DAS, S. K., CHATTERJEE, S. R. and PALIT, S. R. *Proc. Roy. Soc. A*, 1955, **227**, 252
- <sup>14</sup> ATHERTON, J. N. and NORTH, A. M. *Trans. Faraday Soc.* 1962, **58**, 2049
- <sup>15</sup> NORTH, A. M. *Polymer, Lond.* 1963, **4**, 134

# On the Chemistry of Polymer Chain Folds

D. C. BASSETT\*

*The X-ray pattern of aggregated isotactic poly-4-methyl-pentene-1 crystals has been studied at various stages of oxidation and chlorination. While the wide angle pattern remains unaltered during reaction the low angle maxima corresponding to layer thickness are much intensified, often by a factor of 20 or more. This is interpreted as showing that both oxygen and chlorine react with polymer preferentially at chain folds. It is suggested that oxidation, which involves chain scission, selects folds as reaction site because their strained backbone configurations may reduce the activation energy of reaction. Chlorination, on the other hand, is supposed to occur preferentially in the side groups which are removed from their normal crystalline packing where the chain folds.*

THE demonstration that solution-grown polymer crystals contain the molecules in chainfolded configurations<sup>1</sup> leads naturally to the question of whether the chain folds may provide specific sites for chemical reaction. Several experiments have now been interpreted in this way. (1) It has been suggested<sup>2,3</sup> that the radiation crosslinking of polyethylene crystal aggregates occurs preferentially between chain folds and more recent work<sup>4</sup> is in agreement with this. (2) Fuming nitric acid is reported to attack the folds of polyethylene crystals<sup>5</sup>. Also, (3) the progressive hydrolysis of chainfolded amylose crystals proceeds through a stage of constant low molecular weight which may indicate that molecular cleavage has occurred at chain folds<sup>6</sup>. On the other hand, direct electron-microscopic and X-ray examination has given no indication that the halogenation of polyethylene crystals occurs preferentially at surface layers<sup>7</sup>. Now, we report low-angle X-ray diffraction data which show that oxidation and chlorination of poly-4-methyl-pentene-1 crystals occur predominantly at the fold surfaces.

Isotactic poly-4-methyl-pentene-1 (P4MP) crystallizes from supersaturated dilute xylene solution ( $\sim 0.1$  per cent concentration) as tabular platelets within which the molecules are folded<sup>8,10</sup>. Oriented films with fibre symmetry may be prepared by filtration, the fibre axis lying essentially normal to all crystal platelets. Such films diffract X-rays incident in their plane to give maxima in the low angle region at intervals related to the layer thickness ( $\sim 100$  Å). Whereas polyethylene<sup>9</sup> and polyoxymethylene<sup>10</sup> crystal aggregates show four to five orders of maxima, P4MP exhibits only one (two at most) which is, nevertheless, sharply defined<sup>8</sup>.

The intensity of low-angle X-ray scattering from aggregates of thin tabular crystals is proportional, *inter alia*, to the square of the integrated difference of electron density encountered in passing from one layer to the next. If the surface atoms of one layer intermesh suitably with those of its neighbour, then this electron-density-difference and the related X-ray structure factor may be small. In this case, the corresponding low-angle X-ray diffraction maxima will be weak and only the strongest may readily

\*Present address: J. J. Thomson Physical Laboratory, Whiteknights Park, Reading, Berks.

be detected. Thus the apparent decrease in the number of orders of low-angle X-ray diffraction caused by a small structure factor may mask variations in intensity usually attributed to fluctuations in layer thickness<sup>11</sup> and irregular stacking<sup>12,4</sup> of the component crystals. However, if sufficient electron-dense atoms can be introduced at the layer interfaces, the resulting increase in X-ray scattering should reveal the presence of higher order diffraction maxima. This is the principle of our experiments.

Crystals of inhibitor-free, isotactic P4MP were grown isothermally from 0.1 per cent xylene solution between 30° and 70°C and collected as thin oriented films by filtering<sup>10</sup>. (If crystallization was incomplete the filtration was carried out at the crystallization temperature<sup>13</sup>.) Four strips were cut from such a film of which three were heated to 170°C for 30 min in sealed thin-walled glass tubes under respectively one atmosphere of air, one atmosphere of nitrogen and diffusion pump vacuum. Afterwards, the tubes were opened and all four samples examined by X-ray diffraction in a camera capable of recording both the low-angle pattern and the first two wide angle arcs. For equal exposures, the intensities of these wide angle arcs were identical for all four specimens (*Figure 1*). In the low-angle region, however, the air-sealed sample was distinguished from the others

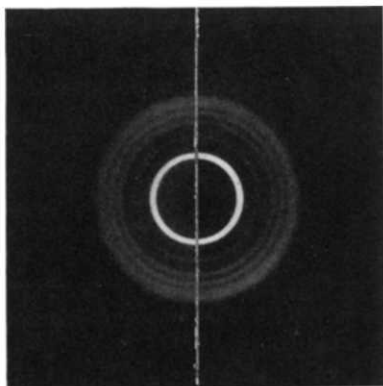


*Figure 1*—A comparison of the stronger wide angle X-ray reflections of a P4MP crystal film after annealing at 170°C for 30 min in air (LHS) and in nitrogen

by having a much stronger pattern showing three to four orders of X-ray reflection instead of one or two (*Figure 2*). The increase in scattered intensity in *Figure 2* has been judged to be  $\sim 20$  by noting that the reflection was attenuated approximately to the strength given by the control at the fourth X-ray film of a sequence in which the film transmission factor was 2.7. Infra-red examination of the control and the air-sealed sample showed that only the latter had high carbonyl absorption between 1700 and 1750  $\text{cm}^{-1}$ , i.e. it contained chemically bound oxygen, while the control was almost oxygen free. A direct determination on another sample oxidized for 30 min at 170°C showed an oxygen content of  $1.1 \pm 0.1$  per cent; the total weight change was not greater than this amount.

Following the earlier discussion, one can say immediately that the oxidized sample has a greater electron-density-difference at the fold surfaces than the others. However, since the wide-angle X-ray pattern is unchanged

after oxidation (*Figure 1*), one deduces that the lamellar interiors are largely unaffected and, therefore, that the electron-density-difference is positive and a consequence of oxygen atoms attached to folds. The alternative, in which oxygen adds randomly to the polymer and thereby increases a density difference of either sign at fold surfaces, would require an uptake of oxygen two orders of magnitude higher for the same electron-density-difference. This possibility is thus also excluded by the quantity of gas absorbed, since,

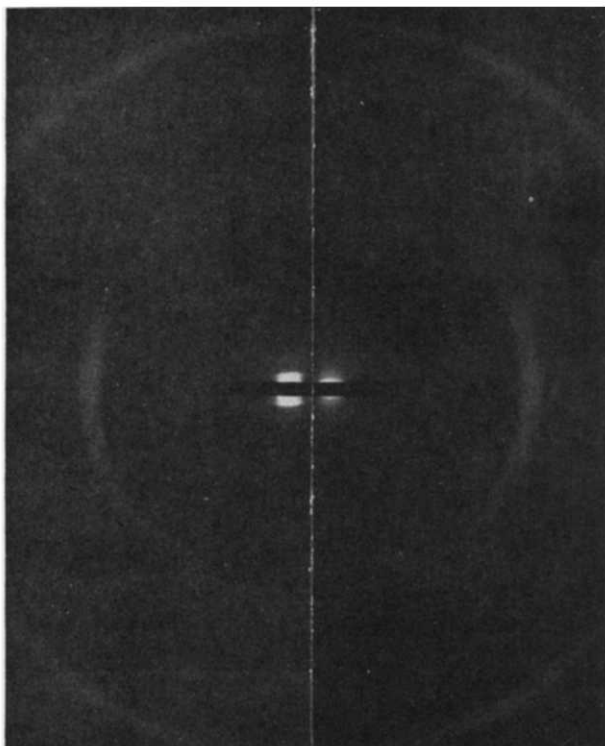


*Figure 2*—The same samples as in *Figure 1*, showing the low angle patterns and the first two wide angle reflections. The higher order maxima in the low angle pattern have been lost in printing

if this were distributed at random throughout the lamellae, it would increase the electron-density-difference by only one per cent and the scattered X-ray intensity by two per cent. The evidence shows, therefore, that the oxygen adds preferentially to chain folds as compared to atoms within the lamellae.

If the initial net electron-deficit at fold surfaces is small negative as opposed to small positive, then, in the early stages of oxygen addition to folds it must be cancelled out before an electron-excess can be established. Accordingly, the system should pass through a state of approximately zero structure factor. Indications of just such a decrease have been found for



oxidation times of half an hour at 100°C which provide further confirmation of our conclusion.

So far these selective sites for oxidation have only been shown to exist in solution-grown isotactic P4MP crystals; whether they are also found in the bulk polymer is, however, an important question. At present we are unable to decide this from a similar qualitative examination of the X-ray low-angle scattering since we do not have a bulk sample with the required degree of long period regularity. However, since (i) the comparative oxidation kinetics show a close similarity between bulk- and solution-crystallized P4MP<sup>14</sup> and (ii) oxidation proceeds with no change in the wide-angle X-ray pattern (Figure 3) one may argue in favour of the bulk sample also being oxidized preferentially at folds.

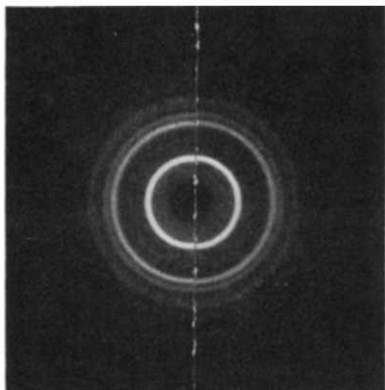


Figure 3—The wide angle X-ray pattern of a 0.010 in. moulded film before (LHS) and after oxidizing to tackiness at 170°C

Similar experiments have also been performed on the chlorination of P4MP crystal films. Specimens were exposed to chlorine gas at 60°C for intervals between  $\frac{1}{2}$  and 20 hours. After  $\frac{1}{2}$  hour (five per cent weight gain), a marked increase in the intensity of the low-angle X-ray maxima was observed and after 20 hours (15 per cent weight gain) these were very strong while the wide angle pattern was still unchanged from the control. Once again this indicates selective chemical action at folds, though here P4MP crystals behave quite differently from those of polyethylene where halogenation is not primarily a surface phenomenon<sup>7</sup>.

Chemical reactions may take place preferentially at folds for two different reasons. On the one hand, a reaction may be physically confined to fold regions as, for example, with a reactant which has only penetrated between polymer lamellae<sup>15</sup>. On the other hand, some specific property of the folds themselves may result in their selection as reaction sites. This could involve (a) steric factors, e.g. allowing reactants a closer approach to the polymer molecule; (b) distorted bond configurations in the fold and (c) changes in the environment of the side groups. We suggest that (b) and (c) are involved in the present examples.

The carbon backbone in a polyolefin fold is likely to consist, as a first approximation, of *trans*-gauche bond sequences (or diamond-lattice paths) with superimposed rotations about single bonds which are required for

steric reasons<sup>16</sup>. As a consequence, the fold surface free energy is high, being  $\sim 100$  erg  $\text{cm}^{-2}$  for polyethylene. In a reaction involving backbone cleavage, this strain energy could reduce the activation energy, i.e. promote preferential reaction at folds as compared to sites in the lamellar interiors. Polymer oxidation generally involves chain scission and there is evidence for this occurring in P4MP. Solution recrystallization of the oxidized polymer yields crystals which were observed to melt on the hot stage of a phase-contrast optical microscope at  $206^\circ\text{C}$ ,  $25^\circ\text{C}$  lower than identically grown crystals of the original polymer. Furthermore, if oxidation is prolonged much beyond 30 min at  $170^\circ\text{C}$ , the specimen films begin to melt and, as has also been found<sup>14</sup> at  $100^\circ\text{C}$ , the final product of oxidation is a liquid. Another indication is the morphology of the melt-crystallized oxidized polymer which displays a coarseness of texture attributable to the presence of mobile low molecular weight species<sup>17</sup>.

A corollary of this interpretation is that, in a chain folded system, reactions which do not involve chain cleavage should show much less energetic preference for occurrence at folds. This appears to apply for the halogenation of polyethylene<sup>7</sup>. Yet in P4MP, where chlorination is also confined mainly to substitution for hydrogen, the reaction occurs preferentially at folds. We suggest the following explanation for this. Every second main chain carbon atom in P4MP carries an isobutyl side group and, in the process of folding, these are presumably taken out of the regular crystalline packing of the subcell. This 'disordered' array of side groups may, therefore, very reasonably provide a particularly favourable reaction site at which chlorination would occur more readily than elsewhere in the lamellae.

In conclusion, the advantage offered by P4MP over other polymers in experiments of this type (in which low-angle X-ray intensities are examined for an indication of reaction sites) is that it affords a sensitive means of detection due to a fortuitous intermeshing of folds and a correspondingly small X-ray structure factor. For this reason, it serves as a model polyolefin in which specific chemical reactions at the folds can be investigated very simply. Preliminary results of further application of the method show that carbon tetrachloride swells the polymer by penetrating between lamellae preferentially and that halogen residues may be grafted on the polymer at chain folds by irradiation<sup>15</sup>, in agreement with other recent work<sup>2,4</sup>.

*I am most grateful to Dr F. H. Winslow and Mr W. Matreyek for supplying the original polymer and for the use of their chlorination apparatus. I am also indebted to Dr H. D. Keith for criticism of this manuscript, to Mr J. P. Luongo for performing the infra-red examination and to Dr R. Salovey for assistance on several occasions.*

*Bell Telephone Laboratories Inc.,*

*Murray Hill, N.J., U.S.A.*

*(Received November 1963)*

#### REFERENCES

<sup>1</sup> KELLER, A. *Phil. Mag.* 1957, **2**, 1171

<sup>2</sup> SALOVEY, R. and KELLER, A. *Bell Syst. tech. J.* 1961, **40**, 1397 and 1409

- <sup>3</sup> SALOVEY, R. *J. Polym. Sci.* 1962, **61**, 463
- <sup>4</sup> SALOVEY, R. and BASSETT, D. C. *J. appl. Phys.* In press
- <sup>5</sup> PALMER, R. P. and COBBOLD, A. J. *Makromol. Chem.* 1964, **74**, 174
- <sup>6</sup> MANLEY, R. S. Private communication
- <sup>7</sup> KELLER, A., MATREYEK, W. and WINSLOW, F. H. *J. Polym. Sci.* 1962, **62**, 291
- <sup>8</sup> FRANK, F. C., KELLER, A. and O'CONNOR, A. *Phil. Mag.* 1959, **4**, 200
- <sup>9</sup> KELLER, A. and O'CONNOR, A. *Nature, Lond.* 1957, **180**, 1289
- <sup>10</sup> BASSETT, D. C., DAMMONT, F. R. and SALOVEY, R. *Polymer, Lond.* In press
- <sup>11</sup> HOSEMANN, R. and BAGCHI, S. N. *Direct Analysis of Diffraction by Matter.* North-Holland: Amsterdam, 1962
- <sup>12</sup> MITSUHASHI, S. and KELLER, A. *Polymer, Lond.* 1961, **2**, 109
- <sup>13</sup> BASSETT, D. C. and KELLER, A. *Phil. Mag.* 1962, **7**, 1553
- <sup>14</sup> WINSLOW, F. H. and MATREYEK, W. Private communication
- <sup>15</sup> BASSETT, D. C. and SALOVEY, R. *J. Polym. Sci.* 1964, **132**, 503
- <sup>16</sup> FRANK, F. C. Unpublished work
- <sup>17</sup> KEITH, H. D. and PADDEN, F. J. *J. appl. Phys.* 1963, **34**, 2409

# *Stress/Strain and Swelling Properties of a Peroxide-cured Methylvinyl Silicone*

D. K. THOMAS

*The stress/strain behaviour of peroxide-cured methylvinyl silicones in simple extension is found to be completely described by the Rivlin equation up to moderate elongations. Analysis of the values obtained for the elastic constant  $C_1$  shows the efficiency of dichlorobenzoyl peroxide as a crosslinking agent to be very dependent upon concentration. Values ranging from 136 to 42 per cent have been obtained, and the results are discussed in the light of possible mechanisms for crosslinking. Combining the results of stress/strain measurements with those of equilibrium swelling in benzene leads to a value of  $\mu$  (the interaction constant for polymer and benzene) which is independent of crosslink density and is in close agreement with the value of 0.52 obtained by Bueche for polydimethylsilicone and benzene.*

A PHYSICAL determination of the density of crosslinking in a rubber vulcanizate can be made from equilibrium stress/strain measurements or equilibrium swelling measurements. Use of the latter method requires knowledge of the interaction parameter ( $\mu$ ) relevant to the polymer and solvent being used and this can be obtained by combining the results of stress/strain and swelling measurements<sup>1</sup>. Once a value for  $\mu$  has been established over the practical range of cure the very simple swelling method can be used for further estimates of crosslink density.

Application of these methods is valid only if assumptions inherent in the statistical theory of rubberlike elasticity are close to the truth and this is most readily verified by a study of the relationship between stress, strain and temperature in simple extension.

In the present work the stress/strain behaviour at constant temperature of a methylvinyl silicone crosslinked with dichlorobenzoyl peroxide has been studied and the results used to evaluate the crosslinking efficiency of the peroxide. The interaction parameter  $\mu$  for silicone and benzene has been calculated from stress/strain and swelling measurements and its dependence upon crosslink density observed.

## EXPERIMENTAL

### *Materials*

The polymer used in this work was a methylvinyl silicone containing 0.2 mole per cent of vinyl groups: the crosslinking agent was bis-1,4-dichlorobenzoyl peroxide.

### *Compounding and vulcanization*

The polymer and crosslinking agent were mixed on a laboratory roll mill; no fillers were incorporated. Vulcanization was carried out by heating

in a press at 1 500 lb/in<sup>2</sup> for 10 min at 120°C followed by 24 h at 250°C in an air circulating oven.

### Stress/strain measurements

All stress/strain measurements were made in simple extension at 28°C on unfilled rubbers. Owing to the fragile nature of the vulcanizates no attempt was made to condition the specimens by the application of high loads prior to making the stress/strain measurements. The applied force was increased in stepwise fashion and the strain measured at a fixed time interval after application of the load, this time interval was normally three minutes but in one instance was increased to 30 min.

### Swelling measurements

About 0.2g of rubber was immersed in a large excess of benzene for 72 h at constant temperature (28°C). It had been established previously that this was time enough to reach the equilibrium swollen condition. The swollen rubber was then withdrawn, surface dried, and weighed; finally the solvent was removed by evaporation and the dry rubber weighed. Knowing the densities of rubber and solvent at 28°C the volume fraction of rubber ( $V_r$ ) in the swollen material can be calculated. The soluble fraction is obtained from the initial and final dry weight of the rubber.

Table 1. Results of stress/strain measurements on peroxide-cured silicones at various g peroxide per 100 g of rubber

0.5		1.0		1.5		2.0		2.0	
Stress $\times 10^{-4}$ dyne/ cm <sup>2</sup>	Exten- sion ratio (after 3 min)	Stress $\times 10^{-4}$ dyne/ cm <sup>2</sup>	Exten- sion ratio (after 3 min)	Stress $\times 10^{-4}$ dyne/ cm <sup>2</sup>	Exten- sion ratio (after 3 min)	Stress $\times 10^{-4}$ dyne/ cm <sup>2</sup>	Exten- sion ratio (after 3 min)	Stress $\times 10^{-4}$ dyne/ cm <sup>2</sup>	Exten- sion ratio (after 30 min)
0.230	1.067	0.464	1.098	0.404	1.074	0.380	1.067	0.248	1.045
0.304	1.093	0.614	1.136	0.534	1.105	0.448	1.094	0.408	1.080
0.378	1.115	0.764	1.179	0.664	1.140	0.456	1.119	0.606	1.126
0.562	1.182	1.136	1.300	0.988	1.231	0.828	1.199	0.766	1.167
0.636	1.211	1.436	1.420	1.118	1.272	1.044	1.264	0.924	1.217
0.710	1.243	1.734	1.562	1.248	1.318	1.372	1.384	1.084	1.264
0.784	1.273	2.034	1.726	1.378	1.362	1.588	1.472	1.244	1.315
0.858	1.310	2.332	1.914	1.508	1.417	1.806	1.575	1.404	1.373
0.932	1.344	2.632	2.082	1.638	1.468	1.916	1.629	1.562	1.442
1.006	1.385	2.930	2.334	1.768	1.525	2.132	1.747	1.722	1.511
1.080	1.426			1.898	1.590	2.350	1.876		
1.154	1.470			2.028	1.654	2.460	1.948		
1.228	1.514			2.158	1.726	2.676	2.094		
1.302	1.565			2.288	1.797	2.894	2.243		
1.376	1.617								
1.450	1.673								
1.524	1.736								
1.598	1.800								

## RESULTS AND DISCUSSION

### Stress/strain behaviour

The statistical theory of rubberlike elasticity predicts that the modulus of a crosslinked rubber should be a function of network chain concentration and temperature only. This relationship between force ( $f$ ) and extension ( $\lambda$ ) for a vulcanizate of initial cross sectional area  $A_0$  is

$$f = 2A_0C(\lambda - \lambda^{-2}) \quad (1)$$

STRESS/STRAIN OF A PEROXIDE-CURED METHYLVINYL SILICONE

where  $C$  is the elastic constant. The relationship between  $C$  and network structure is

$$C = \frac{1}{2} \nu k T \tag{2}$$

where  $\nu$  is the density of network chains per unit volume,  $k$  is the Boltzmann constant, and  $T$  the absolute temperature.

In practice the stress/strain behaviour of rubbers in simple extension is better described by the Rivlin<sup>2</sup> equation which contains an additional term dependent upon extension

$$f = 2A_0 (C_1 + \lambda^{-1}C_2) (\lambda - \lambda^{-2}) \tag{3}$$

The experimental data for methylvinyl silicones shown in *Table 1* have been analysed according to equations (1) and (3) and the results are shown in *Figures 1* and 2. If equation (1) is applicable  $\frac{1}{2} f A_0^{-1} (\lambda - \lambda^{-2})^{-1}$  should be independent of  $\lambda$ . *Figure 1* shows that this not so; for all the vulcanizates studied a negative slope is obtained varying from 0.07 for the lightest cure to 0.2 for the most highly cured sample. *Figure 2* shows that the experi-

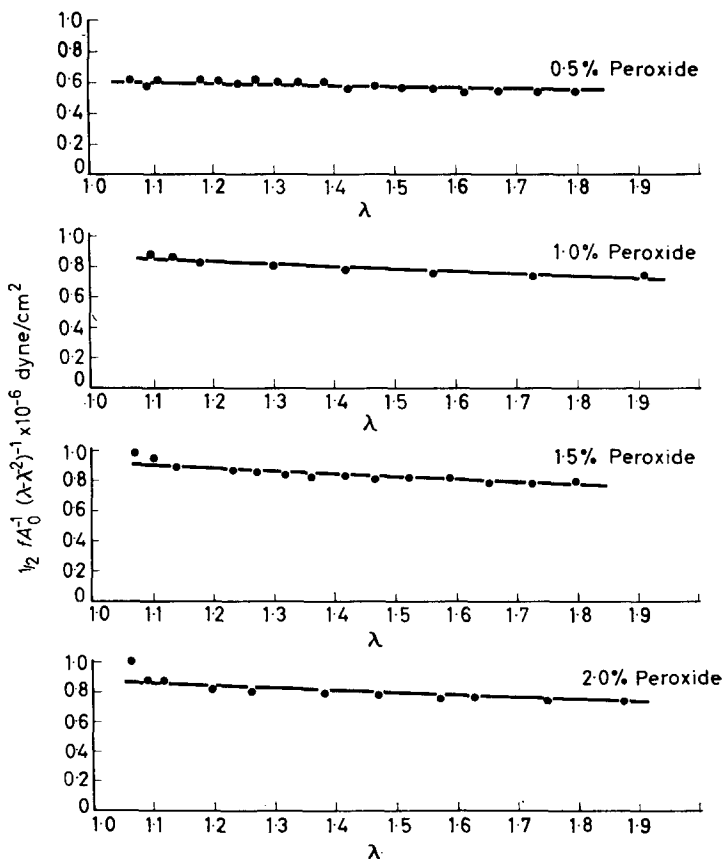


Figure 1—Simple elasticity theory applied to silicone vulcanizates

mental data are completely described by the Rivlin equation and the values obtained for  $C_1$  and  $C_2$  are shown in *Table 2*.

*Table 2.* Values of  $C_1$  and  $C_2$  from the Rivlin equation

g of peroxide per 100 g of polymer	$C_1 \times 10^{-6}$ dyne/cm <sup>2</sup>	$C_2 \times 10^{-6}$ dyne/cm <sup>2</sup>
0.5	0.438	0.19
1.0	0.532	0.35
1.5	0.571	0.38
2.0	0.555	0.40

The quantity  $C_1$  in equation (3) is identified with  $C$  in equation (1)<sup>3,4</sup> and is related in the same way to the network structure.  $C_2$  is regarded as a measure of departures from simple elasticity theory but its relationship to the assumptions involved in that theory is still not clear. The values of  $C_2$  given in *Table 2* show it to be a variable quantity and it is instructive at this stage to consider whether these variations are significant when viewed in the light of experimental errors. The greatest uncertainty in calculating

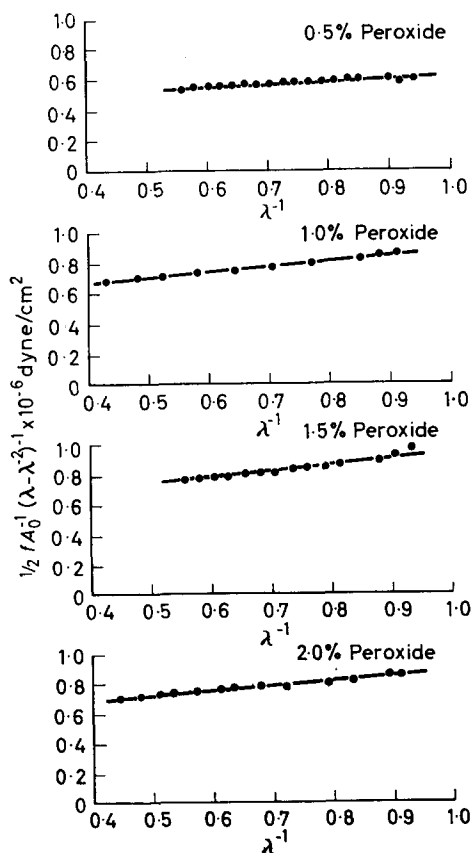


*Figure 2*—Modified stress/strain equation applied to silicone vulcanizates

$C_2$  from stress/strain measurements in simple extension arises from the method of determining the unstretched length ( $l_0$ ) of the rubber specimen. This is normally done by extrapolating the load/extension curve to zero load and for this purpose readings have to be taken at very low loads where errors of measurement are relatively great. Taking the case where  $C_2 = 0.35 \times 10^6$  dyne/cm<sup>2</sup> and placing the maximum possible variation of  $\pm 1$  per cent on  $l_0$  one gets limiting values of 0.29 and  $0.42 \times 10^6$  dyne/cm<sup>2</sup> for  $C_2$ . For the same variation in  $l_0$ ,  $C_1$  varied by a much smaller amount ( $\pm 4$  per cent).

On this basis the  $C_2$  value for the lightest cure is significantly different from the other three which in themselves do not differ significantly. The view has been expressed that  $C_2$  is a time dependent quantity<sup>5</sup>, i.e. the existence of  $C_2$  is due to a failure to attain true equilibrium in the stress/strain measurements. Undoubtedly true equilibrium conditions were not realized in the present work but it is probable that a large fraction of the total creep occurred during the time lapse between application of load and measurement of strain. To verify this the 2.0 per cent peroxide vulcanizate was subjected to a stress/strain experiment in which 30 minutes were allowed to elapse between loading and measurement of strain. The values of  $C_1$  and  $C_2$  obtained were 0.57 and  $0.35 \times 10^6$  dyne/cm<sup>2</sup> respectively. Hence although  $C_2$  has decreased by about 12 per cent the errors inherent in these experiments are too great to view this as significant. It is important to note that  $C_1$  is almost unaffected by changing the time lapse from 3 to 30 minutes.

#### *The evaluation of crosslink density and crosslinking efficiency*

Identifying  $C_1$  of the Rivlin equation with  $C$  of equation (1) allows the number average molecular weight between crosslinks ( $M_c$ ) to be calculated.

$$C_1 = \frac{1}{2} \nu kT = \rho RT / 2M_c$$

where  $\rho$  is the density of the vulcanizate and  $R$  the gas constant. In these calculations a correction for network defects in the form of loose chain ends is usually applied and the value of  $M_c$  obtained from equation (4)

$$C_1 = (\rho RT / 2M_c) (1 - 2M_c / M) \quad (4)$$

where  $M$  is the initial molecular weight of polymer =  $6 \times 10^5$  and  $\rho = 1.08$ .

The crosslink density ( $1/2M_c$ ) and crosslinking efficiency expressed as (moles of crosslinks per gramme)/(moles of peroxide decomposed per gramme) are shown in *Table 3*.

Little is known about the nature of the crosslinks introduced into methylvinyl silicones by peroxides; the introduction of a small concentration of vinyl groups makes for a more efficient use of the crosslinking agent because these groups are far more reactive towards free radicals than are the methyl groups on the polymer. The very high crosslinking efficiency shown in *Table 3* for low peroxide concentration is puzzling; a polymerization reaction involving vinyl groups is unlikely in view of the low vinyl content of the polymer. The sharp fall in crosslinking efficiency as peroxide concentration is raised is striking and it appears that here, as with



Table 3. Crosslink density and crosslinking efficiency in peroxide-cured methylvinyl silicone

<i>g of peroxide for 100 g of silicone</i>	<i>Crosslink density (1/2M<sub>c</sub>) × 10<sup>5</sup></i>	<i>% crosslinking efficiency</i>
0.5	1.787	136
1.0	2.135	81
1.5	2.279	58
2.0	2.220	42

polydimethyl silicones cured with benzoyl peroxide<sup>6</sup>, it is not possible to develop a high degree of cure. This belief is supported by the volume swelling data of *Figure 3* which show that  $V_r$  reaches a constant value at a concentration of peroxide of about 1.3 per cent.

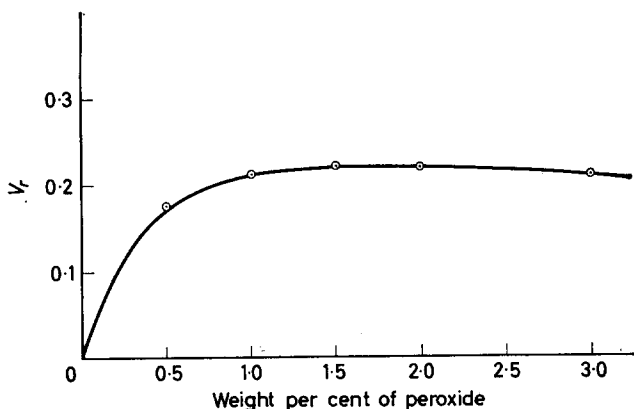
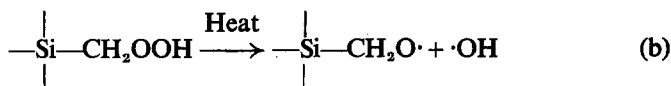
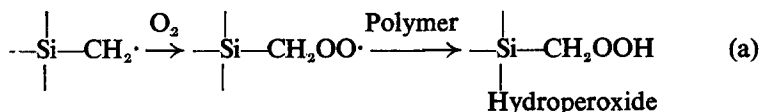


Figure 3—Equilibrium swelling of peroxide-cured silicone in benzene at 28°C

The free radicals produced by thermal decomposition of peroxide either add to vinyl double bonds or abstract hydrogen atoms from methyl groups in the polymer. In either case free radicals are formed on the polymer which dimerize to give crosslinks. With a low concentration of peroxide the number of radicals produced on the polymer will likewise be small and this will reduce the rate of dimerization, i.e. a polymer radical will, on the average, live longer in systems containing low concentrations of curing agent. Under these conditions oxygen present in the system will be more likely to react with polymer-free radicals, and, assuming oxidation to proceed in the manner accepted for hydrocarbons, this leads, via the production of thermally unstable hydroperoxides, to a net increase in the number of free radicals in the system.



The polymer radicals produced in stage (b) may dimerize to form peroxide-type crosslinks and results of continuous stress-relaxation measurements<sup>7</sup> on these vulcanizates suggest the presence of a fraction of thermally unstable crosslinks.

The rapid fall in crosslinking efficiency as the concentration of dichlorobenzoyl peroxide increases must be due to one or more side reactions which are wasteful of free radicals. A likely process is one in which free radicals from the crosslinking agent combine with those produced on the polymer. In this way benzoate groups become attached to the vulcanizate and the crosslinking efficiency is adversely affected. A reaction of this kind would become more likely as the density of crosslinks in the material increases since this would tend to reduce the mobility of polymer free radicals in the rubber matrix.

#### Calculation of $\mu$ for benzene and silicone

The swelling of crosslinked polymers has been considered by Flory and Rehner<sup>8</sup> who derived a relationship between the free energy of mixing of polymer and solvent and the retractive forces opposing swelling [equation (5)]. They later produced a slightly modified form<sup>9</sup> of this equation [equation (6)].

$$-\ln(1 - V_r) - V_r - \mu V_r^2 = 2C_1 V_0 R^{-1} T^{-1} V_r^{\frac{1}{2}} \quad (5)$$

$$-\ln(1 - V_r) - V_r - \mu V_r^2 = 2C_1 V_0 R^{-1} T^{-1} [V_r^{\frac{1}{2}} - (\frac{1}{2} V_r)] \quad (6)$$

In both equations  $V_r$  is the volume fraction of rubber in the swollen vulcanizate at equilibrium,  $C_1$  the elastic constant,  $V_0$  the molar volume of the swelling liquid,  $R$  the gas constant and  $T$  the absolute temperature.

The values of  $C_1$  used in equations (5) and (6) should be those for the swollen vulcanizates, but in view of the extremely brittle nature of these materials such measurements were not possible. The errors introduced by using  $C_1$  (dry) are probably small in view of the low values found for  $C_2$ .

The value of  $\mu$  has been calculated from equations (5) and (6) and the results are shown in Table 4. The value found is, within the limits of

Table 4. Interaction constant  $\mu$  for methylvinyl silicone and benzene at 28°C

g peroxide for 100 g of polymer	$\mu$ from equation (5)	$\mu$ from equation (6)
0.5	0.51	0.52
1.0	0.53	0.54
1.5	0.54	0.55
2.0	0.51	0.52

experimental error, a constant over the range of crosslink density studied, the mean from equations (5) and (6) being 0.52<sub>5</sub> and 0.53<sub>3</sub>, respectively. These results are in close agreement with that of 0.52 obtained by Bueche<sup>10</sup> for a polydimethyl silicone and benzene at 25°C.

*The author is indebted to Mr R. Sinnott for preparing the vulcanizates and to Mr P. H. Milward for his assistance in performing some of the stress/strain measurements.*

*The Royal Aircraft Establishment,  
Farnborough, Hants.*

*(Received November 1963)*

REFERENCES

- <sup>1</sup> MULLINS, L. J. *Polym. Sci.* 1956, **29**, 225
- <sup>2</sup> RIVLIN, R. S. *Phil. Trans. A*, 1948, **240**, 459
- <sup>3</sup> MULLINS, L. J. *Polym. Sci.* 1956, **19**, 225
- <sup>4</sup> MULLINS, L. J. *appl. Polym. Sci.* 1959, **2**, 1
- <sup>5</sup> CIFERRI, A. *J. Polym. Sci.* 1961, **54**, 149
- <sup>6</sup> BUECHE, A. M. *J. Polym. Sci.* 1955, **40**, 105
- <sup>7</sup> THOMAS, D. K. Unpublished results
- <sup>8</sup> FLORY, P. and REHNER, J. *J. chem. Phys.* 1943, **11**, 521
- <sup>9</sup> FLORY, P. *J. chem. Phys.* 1950, **18**, 108
- <sup>10</sup> BUECHE, A. M. *J. Polym. Sci.* 1955, **40**, 97

# *The Measurement of Dynamic Bulk Modulus using an Ultrasonic Interferometer*

W. J. PULLEN, J. ROBERTS and T. E. WHALL

*The dynamic bulk modulus of polymethylmethacrylate (PMMA) is measured at a frequency of 1 Mc/s using an ultrasonic interferometer. The polymer tested is in the form of a thin disc specimen or a powder.*

ONE EXPERIMENTAL approach to the investigation of the relationship between mechanical properties of a polymer and its molecular structure is to study the frequency dependence of its viscoelastic behaviour. If the loading cycle is applied for a time which is much smaller than the relaxation time of the polymer then viscous effects can be more or less eliminated and an elastic modulus measured. This investigation is concerned with the measurement of this high frequency modulus so that later work on the frequency dependence of mechanical properties can be based on it.

The techniques described are also required for another purpose, namely the comparison of the mechanical properties of a series of polymers in which a basic chain structure has been progressively modified with certain additional chemical groups. Many of the polymers prepared in such an investigation are, in the first instance, available only in powder form and in small quantities which are not easily processed.

An ultrasonic interferometer of the form described by Hubbard and Loomis<sup>1</sup> seems to be particularly suited to present requirements. It is a compact system capable of being developed for the testing of small quantities of material at ultrasonic frequencies. It is used here at a frequency of approximately 1 Mc/s which seems to be a suitable loading cycle for PMMA. Sound velocities are measured in the liquids silicone oil and dimethyl phthalate and in suspensions of PMMA powder in these liquids. From these velocities the required elastic modulus, i.e. adiabatic bulk modulus or its reciprocal, the compressibility, of the polymer is calculated. Alternatively the acoustic path length in disc specimens is measured and used to calculate the modulus.

Values of bulk modulus or compressibility at comparable frequencies can be calculated from results given in the literature concerned with the propagation of stress wave pulses or ultrasonic waves in blocks, plates or rods of PMMA. The physical dimensions of such specimens are rather larger than the powder particles and thin discs tested here but it will be useful to calculate a few values taking the density<sup>2</sup> of PMMA to be 1.19 g/cm<sup>3</sup>. Taking a Poisson's ratio<sup>3</sup> of 0.35 Kolsky's<sup>4</sup> pressure bar experiments gave a compressibility of  $K_2 = 1.3 \times 10^{-11}$  cm<sup>2</sup>/dyne. The duration of the propagated pulse was approximately 20  $\mu$ sec. Similar experiments by Davies and Hunter<sup>5</sup> gave  $K_2 = 1.5 \times 10^{-11}$  cm<sup>2</sup>/dyne. Rinehart and

McClain's<sup>5, 6</sup> stress wave experiments where the duration of the propagated pulse is approximately 2  $\mu$ sec give  $K_2 = 1.4 \times 10^{-11}$  cm<sup>2</sup>/dyne. Wada's results<sup>7</sup> for the velocity of longitudinal and transverse waves at 1.08 Mc/s give  $K_2 = 1.7 \times 10^{-11}$  cm<sup>2</sup>/dyne.

The above is a summary of the required theory. For suspensions of small particles Urick's<sup>8</sup> theory is applied. For the plate, theory given by Klein and Hershberger<sup>9</sup> is utilized.

#### THEORETICAL

##### *Polymer in powder form*

For present purposes it is assumed that the particles in suspension are much smaller than the wavelength of the sound. In this case, the suspension is considered to be an ideal mixture of the two materials<sup>8</sup>. The densities and compressibilities are then additive properties of their proportions in the composite medium.

Thus, following Urick<sup>8</sup>,

$$\rho_0 = \rho_2\beta + \rho_1(1 - \beta) \quad (1)$$

and

$$K_0 = K_2\beta + K_1(1 - \beta) \quad (2)$$

where  $\rho_0$  is the density of the suspension and  $K_0$  its adiabatic compressibility.

Subscripts 1 and 2 refer to the corresponding properties for the liquid and suspended particles respectively, with  $\beta$  denoting the volume percentage of particles. The velocity of sound in the suspension is given by:

$$V_0 = \frac{1}{(\rho_0 K_0)^{\frac{1}{2}}} = \left\{ \frac{1}{[\rho_2\beta + \rho_1(1 - \beta)][K_2\beta + K_1(1 - \beta)]} \right\}^{\frac{1}{2}} \quad (3)$$

in which  $K_1 = 1/\rho_1 V_1^2$ ,  $V_1$  being velocity of sound in the suspending liquid. From equation (2)

$$K_2 = \{K_0 - K_1(1 - \beta)\} / \beta \quad (4)$$

For the given errors in  $K_0$ ,  $K_1$  and  $\beta$ , the expected maximum error  $\delta K_2$  in the calculated value of  $K_2$  can be deduced from equation (4). Thus

$$\delta K_2 = \frac{\delta K_0}{\beta} - \frac{\delta K_1}{\beta}(1 - \beta) + (K_1 - K_0) \frac{\delta \beta}{\beta^2} \quad (5)$$

for  $\beta = 0.12$ ,  $K_0 = 5.82 \times 10^{-11}$  cm<sup>2</sup>/dyne,  $K_1 = 6.17 \times 10^{-11}$  cm<sup>2</sup>/dyne,  $K_2 \sim 2 \times 10^{-11}$  cm<sup>2</sup>/dyne and errors of one per cent in  $K_0$ ,  $K_1$  and  $\beta$  gives  $\delta K_2/K_2 \sim 13$  per cent. If an error in  $\beta$  alone is considered, i.e.  $\delta K_0 = \delta K_1 = 0$ , then  $\delta K_2/K_2 \sim 12$  per cent. On the other hand an error in  $K_0$  alone gives  $\delta K_2/K_2 \sim 4$  per cent. Similarly an error in  $K_1$  alone yields  $\delta K_2/K_2 \sim 4$  per cent. Thus, for the example above, a greater error may be tolerated in  $K_1$  and  $K_0$  than in  $\beta$ . It should be noted that in this system the compressibility  $K_2$  is obtained independently of the other elastic constants, e.g. Poisson's ratio of the solid.

##### *Polymer in moulded form*

Following Klein and Hershberger<sup>9</sup>, consider a standing wave system in a liquid column, produced by an ultrasonic source. If, with temperature

and frequency unchanged, a plane parallel slab of the solid is immersed in the liquid with its major axis parallel to the plane wavefront, the antinodal planes are displaced and this displacement  $\Delta S$  can be measured.

The velocity of sound in the solid is calculated using the relationship<sup>9</sup>

$$\Delta S = d(\mu - 1)/\mu \quad (6)$$

where  $\mu$  is given by:

$$\mu = \frac{V_s}{V_l} = \frac{\text{Velocity of sound in solid}}{\text{Velocity of sound in liquid}} \quad (7)$$

and  $d$  is the thickness of the slab. The velocity of sound in the liquid  $V_l$  is found from half-wavelength and frequency measurements. The required compressibility of the solid  $K_2$  is calculated from the velocity of sound in the solid using the equation<sup>10</sup>

$$V_s^2 = 3(1 - \nu)/\rho K_2(1 + \nu) \quad (8)$$

where  $\nu$  is Poisson's ratio for the solid. Equation (8), which is derived for solid media in bulk, applies here as the disc specimen is surrounded by the liquid medium. Taking<sup>9</sup>  $\nu = 0.35$  gives

$$K_2 = 1.44/\rho V_s^2 \quad (9)$$

The method is satisfactory for solids having an acoustic impedance (i.e.  $V_s\rho$ ) similar to that of the liquid. If the acoustic impedances are very dissimilar a significant proportion of the incident sound wave is reflected at the liquid/solid interface and this simple method fails.

#### EXPERIMENTAL

##### *The ultrasonic interferometer*

The general features of the interferometer are mainly as given by Hubbard and Loomis<sup>1</sup>. A piezoelectric crystal is mounted at the base of a vertical steel chamber which contains the liquid. At the top of the chamber is a reflecting steel plate which is moved parallel to the direction of propagation of the sound beam by a micrometer screw. The crystal is energized by a constant frequency source, which is indirectly coupled to it. Loose coupling is provided to eliminate the effects of a variable load on the frequency of the source. A frequency meter is used to measure the frequency of the exciting e.m.f.

*Figure 1* is a schematic diagram of the interferometer. Ultrasonic waves are produced in the liquid column by the crystal. The presence of the reflector plate produces a standing wave system. As the micrometer screw moves the reflector plate, a valve voltmeter indicates voltage maxima at regular half-wave intervals, due to the reaction of the standing wave system on the crystal. The movement of the micrometer screw is calibrated and gives the half-wavelength directly. Hence, on measuring the frequency with a frequency meter the velocity of sound may be calculated.

The work described in this paper is a preliminary investigation and therefore the apparatus used may be greatly improved with respect to accuracy.

For the major part of the study no temperature control is used, the liquid column being at room temperature. Where necessary, a heated oil bath with stirring facilities provides a means of controlling the temperature. The movement of the plate is measured with a dial gauge, calibrated to the nearest 0.01 mm. An operating frequency of approximately 1 Mc/s is used and checked by a crystal frequency meter. Facilities for measuring wavelength and controlling temperature are to be improved at a later stage.

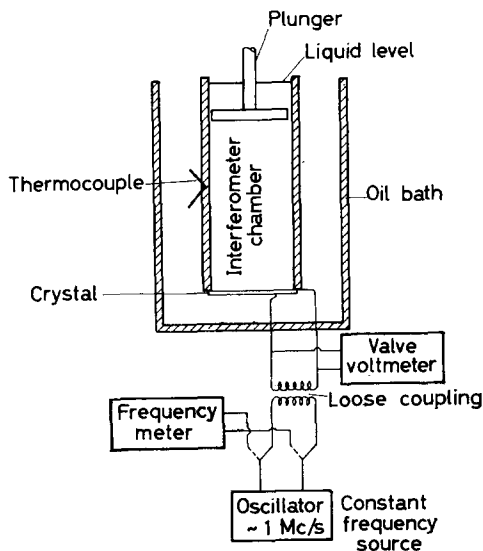


Figure 1—The ultrasonic interferometer

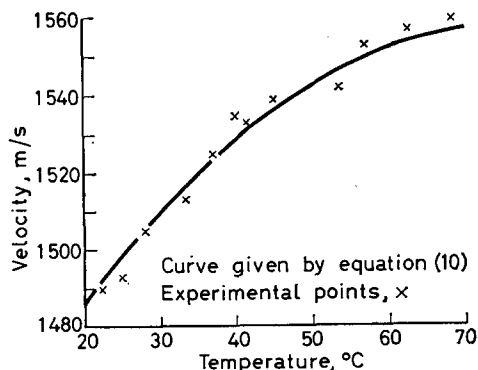


Figure 2—The velocity of sound in water as a function of temperature

Figure 2 shows the variation in the velocity of sound in water with temperature. The curve corresponds to the equation<sup>11</sup>

$$C = 1\,557 - 0.0245(74 - t)^2 \text{ m/sec} \quad (10)$$

where  $t$  is the temperature in °C.

The points around the curve are those obtained with the interferometer and these data are used to establish the approximate magnitude of the

maximum error to be expected in the measurement of velocity. The suggested value is  $\pm 0.4$  per cent.

#### *Application to powders*

The interferometer chamber used for the study of powders contains a liquid column of approximate length 6 cm and diameter 3 cm. Hubbard and Loomis<sup>1</sup> have shown that when the wavelength in the liquid is short in comparison to the diameter of the tube, the effects of the walls of the vessel may be neglected entirely. Klein and Hershberger<sup>9</sup> state that to be reliable, measurements should be taken at a considerable number of wavelengths from the source. In the present powder experiments the reflector plate is kept at distances between 3 cm and 4 cm from the source. Wavelengths of the order of 1 mm are measured and therefore these conditions are satisfied.

Examination under a microscope shows that the PMMA particles used are spherical in shape. The powder is commercially produced and the particles of random size. Measurements of the sizes of one hundred of these particles are made as a justification for employing equations (1) and (2). The results are given later in *Table 1*.

Three liquids are investigated for use as suspending media. They are dimethyl phthalate, silicone oil M.S. 550 and a water-sodium chloride-Teepol system.

All of these systems have densities within the range required to produce a stable suspension. The water-sodium chloride-Teepol system is found to be unsatisfactory as the particles do not deflocculate. Dimethyl phthalate and silicone oil are found to be satisfactory suspending media. The former is most suitable for use with PMMA, its density being closer and occluded air being more easily removed. Silicone oil is thought to be more useful for general purposes. Its greater viscosity produces a more stable suspension than dimethyl phthalate and it contains only infinitesimally small proportions of plasticizing agent whereas dimethyl phthalate is in itself a plasticizing agent. Silicone oil is also capable of being employed over a wide temperature range.

Occluded air is removed from the suspension by placing it in a vacuum until no further air is seen to escape. The compressibility of the powder is determined by measuring the densities of powder and liquid, and velocity of sound in liquid and suspension. Knowing the concentration of particles, application of equations (1) to (4) gives the required adiabatic compressibility.

#### *Application to moulded specimens*

In this case, a liquid column of height 2 cm and diameter 3 cm is employed.

The positions of nodal plains are measured relative to a fixed reference point. It is desirable for this reference point to be less than 1 cm from the source, since no means of temperature control is used in the preliminary experiments. If the temperature varies then the wavelength of sound in the fluid will change. As a result, the nodal planes alter their positions with



respect to the reference point. The displacement of any nodal plane, relative to the reference point, is proportional to the number of half-wavelengths separating the former from the source. Therefore, for nodal planes far from the source, a small variation in wavelength can produce a large change in position. Since we wish to know the displacement of nodal planes caused by the introduction of the specimen, temperature variations produce an error which must be reduced. Thus, only those nodal planes near to the source are considered and the ultrasonic chamber is modified to allow the reflector plate to come within 0.25 cm of the crystal. This has the disadvantage that measurements made near the source are not as reliable as those taken farther away<sup>9</sup>. A better solution is improved temperature control but the precaution employed is thought sufficient for present purposes.

The specimen, in the form of a thin disc, is placed at the base of the chamber, a thin layer of the liquid separating it from the optically flat surface of the latter.

Before a measurement is taken, a plot of galvanometer deflection against reflector displacement ensures that the standing wave system has not been affected by maladjustment of the apparatus.

## EXPERIMENTAL RESULTS

*Polymer powders*

Table 1 gives the results obtained for polymer powders.

Table 1. Polymer powder results: 1.018 Mc/s  
(a) *Suspensions of PMMA in dimethyl phthalate*

Volume concentration of particles $\beta$	Adiabatic compressibilities		
	Liquid $K_1$ $\text{cm}^2/\text{dyne}$	Suspension $K_0$ $\text{cm}^2/\text{dyne}$	Solid $K_2$ $\text{cm}^2/\text{dyne}$
0.129	$3.94 \times 10^{-11}$	$3.71 \times 10^{-11}$	$2.1 \times 10^{-11}$
0.128	3.91	3.67	2.0
0.128	3.93	3.72	2.3
0.128	3.94	3.71	2.1
0.128	3.94	3.71	2.1

Mean value of  $K_2 = 2.1 \times 10^{-11}$

(b) *Suspensions of PMMA in silicone oil M.S.550*

0.128	$6.12 \times 10^{-11}$	$5.66 \times 10^{-11}$	$2.5 \times 10^{-11}$
0.128	6.12	5.71	2.9
0.128	6.18	5.64	1.9
0.128	6.20	5.71	2.4
0.128	6.25	5.68	1.8

Mean value of  $K_2 = 2.3 \times 10^{-11}$

Measurements of specific gravity at a temperature of 25°C give the density of dimethyl phthalate as 1.189 g/cm<sup>3</sup>. Similarly, for silicone oil M.S. 550 a density of 1.062 g/cm<sup>3</sup> is found.

## MEASUREMENT OF DYNAMIC BULK MODULUS

The mean room temperature during these experiments is 25°C. A variation of as much as 1.5°C may occur between determinations of velocity in liquid and suspension, when using the present facilities. However, the sensitivity of the apparatus is such that the resulting change in velocity may be neglected. This is seen on investigation of the way in which  $K_1$  and  $K_0$  vary over this temperature range. The variations in  $K_1$  and  $K_0$  are attributed to errors in the determination of wavelength and particle concentration, which can be reduced with improved apparatus.

The values of  $K_2$  given in *Table 1* are calculated on the assumption that equations (1) and (2) are valid. Size measurements of one hundred particles show a rough approximation to a normal distribution having a mean value of  $84 \times 10^{-4}$  cm, 95 per cent of the particle diameters being within the range  $13 \times 10^{-4}$  cm to  $155 \times 10^{-4}$  cm. At a frequency of 1 Mc/s wavelengths are of the order of 1 mm. Thus the ratio of wavelength to mean particle diameter is approximately ten.

### *Moulded specimens*

A plate of 0.82 mm thickness was chosen for the investigation. Measurements of compressibility by the powder method indicate that this thickness produces a nodal plane displacement of less than half a wavelength.

*Table 2* shows the results of observations made using water and silicone oil as liquid media. Displacements of three nodal planes are measured and an average value of  $\mu$  calculated. As before, experiments are conducted at a frequency of 1.018 Mc/s. Average room temperatures of 25°C and 24°C. are noted for studies employing water and silicone oil respectively. Once again, a variation of up to 1.5°C is tolerated during the course of the experiment.

*Table 2. Results for moulded specimens*  
(a) *Specimen in water*

<i>Mean of three nodal displacements <math>\Delta S</math> mm</i>	$\mu = d / (d - \Delta S) = V_2 / V_1$	<i>Adiabatic compressibility of PMMA <math>K_2</math> cm<sup>2</sup>/dyne</i>
0.29	1.55	$2.3 \times 10^{-11}$
0.27	1.49	2.5
0.28	1.52	2.4
0.25	1.44	2.6
0.26	1.47	2.5

*Mean value of compressibility =  $2.5 \times 10^{-11}$  cm<sup>2</sup>/dyne*

(b) *Specimen in silicone oil*

0.30	1.58	$3.2 \times 10^{-11}$
0.33	1.67	2.9
0.33	1.67	2.9
0.32	1.64	3.0
0.32	1.64	3.0

*Mean value of compressibility =  $3.0 \times 10^{-11}$  cm<sup>2</sup>/dyne*

The velocity of sound in water is taken as  $1.50 \times 10^3$  m/sec from *Figure 2*. The density of the polymer is found to be  $1.18$  g/cm<sup>3</sup>. Using values obtained in the powder measurements, the estimated velocity of sound in silicone oil M.S. 550 at 24°C is  $1.23 \times 10^3$  m/sec.

#### CONCLUSIONS

Comparison of the literature results given in the introduction with present data suggests that the system is better used with powders than with moulded specimens. Thus the apparatus certainly facilitates the comparison of measured physical properties of new polymers, which are only available in powder form and may not be immediately suitable for moulding into test specimens. It should be added that the technique may also be applied to materials other than polymers.

With moulded specimens the mean values of compressibility in each set of experiments are in fair agreement, considering the scatter of results within a given set, so that it does seem worth giving the system further consideration as a means of measuring the dynamic bulk modulus of polymers in moulded form.

*Ministry of Aviation,  
Explosives Research and Development Establishment,  
Waltham Abbey, Essex*

*(Received November 1963)*

#### REFERENCES

- <sup>1</sup> HUBBARD, J. C. and LOOMIS, A. L. *Phil. Mag.* 1928, **5**, 1177
- <sup>2</sup> PENN, W. S. *High Polymeric Chemistry*, p 171. Chapman and Hall: London, 1949
- <sup>3</sup> DAVIES, E. D. H. and HUNTER, S. C. Unpublished War Office Report, 1960
- <sup>4</sup> KOLSKY, H. *Proc. phys. Soc. B*, 1949, **62**, 676
- <sup>5</sup> RINEHART, J. S. and McCLAIN, W. C. *J. appl. Phys.* 1960, **31**, 1809
- <sup>6</sup> RINEHART, J. S. *Nature, Lond.* 1962, **194**, 369
- <sup>7</sup> WADA, Y. *J. phys. Soc. Japan*, 1958, **13**, 1390
- <sup>8</sup> URICK, R. J. *J. appl. Phys.* 1947, **18**, 983
- <sup>9</sup> KLEIN, E. and HERSHBERGER, W. D. *Phys. Rev.* 1931, **37**, 760
- <sup>10</sup> HUETER, T. F. and BOLT, R. H. *Sonics*, p 27. Wiley: London, 1954
- <sup>11</sup> VIGOUREUX, P. *Ultrasonics*, p 101. Chapman and Hall: London, 1952

# The Polymerization of Propylene Oxide Catalysed by Zinc Diethyl and Water

C. BOOTH, W. C. E. HIGGINSON and E. POWELL

*Propylene oxide has been polymerized by use of the zinc diethyl and water catalysts. Kinetic studies of the effects of varying the monomer, zinc diethyl and water concentrations in dioxan solutions have been made. The products of these polymerization reactions have been characterized both with regard to molecular weight and to crystallizability. The results are discussed in terms of the cationic mechanism proposed by Colclough for similar polymerization systems.*

ZINC DIETHYL with water as co-catalyst is one of the more effective catalysts for the polymerization of propylene oxide. High conversions to partially crystalline polymers of very high molecular weight can be attained at room temperature in one day. Early industrial interest in zinc dialkyl catalysts<sup>1</sup> was followed by investigations of polymerization reactions catalysed by zinc diethyl with water and other co-catalysts carried out by Furukawa *et al.*<sup>2</sup>, Chu and Price<sup>3</sup>, and Gluhov<sup>4</sup> while zinc dibutyl with several co-catalysts has been studied by Bailey and France<sup>5</sup> and by Garty *et al.*<sup>6</sup>. All these investigations were exploratory in nature encompassing a range of catalysts, co-catalysts, monomers and solvents. In this work we have studied in detail a single system; zinc diethyl and water in dioxan solvent with propylene oxide as monomer.

For convenience of describing the experimental work, the paper is divided into two sections: the investigation of the polymerization reaction is described in section I, while the characterization of the polymeric products of the reaction is described in section II.

## I—KINETICS OF THE POLYMERIZATION REACTION

### EXPERIMENTAL

#### *Materials*

The methods used to purify the propylene oxide and methylene dichloride have been described in another paper<sup>7</sup>. Dioxan was purified by the method of Vogel<sup>8</sup> or by the method of Morantz and Warhurst<sup>9</sup>. Hexane and diethyl ether were dried over sodium before fractionating. All these liquids were stored over calcium hydride in the absence of air. Zinc diethyl was prepared by the method of Noller<sup>10</sup>. Since the vapour attacked stopcock grease the storage vessel was isolated from the vacuum line by use of a Springham valve.

#### *Procedure*

A vacuum line technique, similar to that described in the earlier paper<sup>7</sup> was used for filling all reaction vessels. Measured volumes of solvent,

monomer and zinc diethyl were distilled into the reaction vessel while water was transferred using an Agla micrometer syringe via self-sealing serum caps\*. The reactants were mixed at room temperature for a few minutes in order that the gas, a large proportion of which is evolved almost instantaneously<sup>11</sup>, might be pumped off before sealing the reactor.

In order to isolate the polymer produced the reaction products were dissolved in benzene to which methanol had been added in sufficient quantity (about one per cent) to precipitate the catalyst. Catalyst residues were removed by centrifuging for one hour at 13 000 g and the polymer was finally recovered by freeze drying.

Dilatometers consisted of 20 ml bulbs sealed to 20 cm lengths of 3 mm bore Veridia tubing. The dilatometric method was known to be valid for the polymerization of epoxides using other catalysts<sup>12</sup>. Its applicability to this reaction was confirmed by opening several dilatometers at differing extents of reaction and determining the weight of polymer produced.

## RESULTS

### *Solubility of the catalyst*

Before this work was started it was known from Gluhov's results that at high water concentrations the immediate products of the reaction were a gas (assumed to be ethane) and a colourless solution from which a white solid could be obtained by evaporation. Some time later a yellow solution was formed (Furukawa isolated a yellow solid) and later still a white precipitate. At lower water concentrations the precipitate was not formed and at very low water concentrations the solution remained colourless. Since it seemed desirable to work with soluble catalysts, some time was devoted to defining the conditions under which precipitation occurred. Following Gluhov, dioxan was used as solvent because of its miscibility with water. No polymerization of dioxan, or copolymerization with propylene oxide, was observed in experiments designed to investigate this possibility. Reproducible results were obtained by adding the zinc diethyl after the water had been mixed with the monomer solution. It was found that the concentration of monomer and zinc diethyl, as well as the concentration of water, were important variables in determining the colour of the solution and the apparent solubility of the catalyst. For example, at 25°C a solution with  $[M]_0 \dagger = 1.44$  M,  $[C]_0 = 0.078$  M and  $[W]_0 = 0.055$  M was clear to the eye but reducing  $[M]_0$  to 0.721 M or raising  $[W]_0$  to 0.078 M both resulted in the formation of a precipitate. In the dilatometric work reported in this paper, in which solutions with  $[M]_0 = 1.44$  M were polymerized at 61°C, clear (though not colourless) solutions were obtained provided  $[W]_0/[C]_0 < 1.0$  and  $[M]_0/[C]_0 > 15$ . In the results which follow special mention will be made whenever precipitation was visible during a run.

Furukawa<sup>2</sup> has pointed out that some of the products of the reaction of zinc diethyl and water form colloidal solutions in benzene. We measured the intensity of the light scattered at 90° from solutions of zinc diethyl,

\*Very small quantities of water were measured as vapour in bulbs of known volume before distilling into the dilatometer.

† $[M]$ ,  $[C]$  and  $[W]$  are respectively the propylene oxide monomer, the zinc diethyl catalyst and the water co-catalyst concentrations. Subscript 0 refers to the initial concentration.

water and propylene oxide in dioxan. The Rayleigh ratio increased as the concentration of water was increased in mixtures in which no precipitate was observed. This observation leads us to doubt that much advantage is to be gained by working in apparently clear solutions.

#### Evolution of gas

The gas evolved during the reaction was found by both mass spectrometry and vapour phase chromatography to be mainly ethane (95 per cent) and ethylene (5 per cent). The amount of gas evolved was measured by connecting a reaction vessel of known volume to a mercury manometer and measuring the pressure developed. Corrections were made for the vapour pressure of propylene oxide and dioxan and for the solubility of ethane in the solution<sup>13</sup>. With  $[M]_0 = 5.77$  M,  $[C]_0 = 0.28$  M and  $[W]_0/[C]_0 = 0.50$ , the molar ratio of gas evolved (assuming it all to be ethane) to zinc diethyl added reached 0.5 in less than ten minutes and then rose slowly to 1.0 over the next four hours, when evolution of gas ceased. Burgess and Colclough<sup>14</sup> have reported that a further mole of 'ethane' per mole of zinc ethyl was evolved when an excess of water was added to a reaction mixture after polymerization was completed. With  $[W]_0/[C]_0 = 1.0$  similar results were obtained; the molar ratio of ethane evolved to catalyst added rose rapidly to 1.0 and then slowly over the next four hours to 1.6; at this point the reaction mixture was completely hydrolysed by adding water and the remaining 'ethane' was evolved. Bruce and Hitchen<sup>15</sup> have studied the reactions between zinc diethyl and water in dioxan and have found that with  $[W]_0/[C]_0 = 1.0$  gas evolution did not cease until 24 hours had elapsed, when 1.99 mole of 'ethane' had been evolved for each mole of catalyst added.

#### Kinetic data— $[W]_0/[C]_0 = 0.40$

Our early experiments confirmed the findings of others<sup>2,4,6</sup> that the molar ratio of water to zinc diethyl is an important variable in the polymerization reaction. No polymerization could be detected when water was absent.

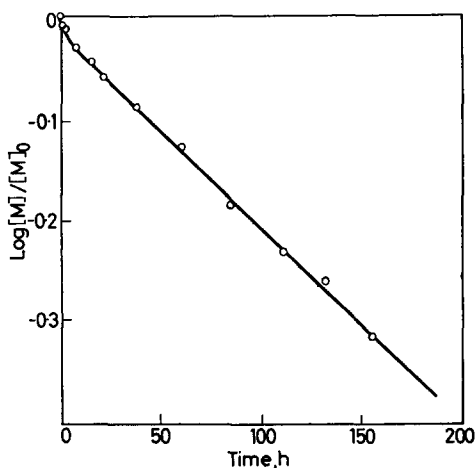


Figure 1—Log  $([M]/[M]_0)$  versus time for the polymerization of propylene oxide at 61°C with  $[M]_0 = 0.721$  M,  $[C]_0 = 0.0786$  M and  $[W]_0/[C]_0 = 0.40$

Increasing  $[W]_0$  increased the amount of polymer produced in a given time up to a sharp maximum at  $[W]_0/[C]_0=1.0$ , followed by a decrease to zero at  $[W]_0/[C]_0=2.0$ . We have examined in detail only the catalyst system  $[W]_0/[C]_0=0.40$  at  $61^\circ\text{C}$ . These conditions were chosen for experimental convenience at an early stage in the investigation.

A typical first order plot for the polymerization at  $61^\circ\text{C}$  with  $[W]_0/[C]_0=0.40$  is shown in *Figure 1*. After a period of faster rate in the first 5 to 10 per cent conversion, the polymerization follows a first order rate law for the disappearance of monomer. The initial fast reaction has not been studied in detail but it appears that the reaction slows down considerably before 10 per cent of the monomer has been consumed. In some experiments it was possible to estimate the initial rate of the reaction by drawing a tangent to the conversion versus time curve at zero time. The amount of monomer consumed during the period when the fast reaction is predominant ( $M_T$ ) was estimated by extrapolating the linear portion of the first order plot back to zero time.

The first order dependence of the rate of the secondary reaction on monomer concentration was confirmed, and the first order dependence on monomer concentration of the initial rate of the first reaction was established, by a series of experiments in which  $[M]_0$  was varied. The first order rate constants ( $k_1 = -d \ln [M]/dt$ ) obtained from the linear portions of the first order plots, and the initial rates ( $R_i$ ) divided by  $[M]_0$  are given in *Table 1* together with estimates of  $M_T$ . The results of a series of experiments in which the concentration of zinc diethyl and water was varied are given in *Table 2* in which a second order rate constant of the secondary reaction (defined as  $k_2 = k_1/[C]_0$ ) and the corresponding value of  $R_i/[M]_0^{-1}[C]_0^{-1}$  are recorded. A first order dependence on  $[C]_0$  of both

*Table 1.* The effect of varying monomer concentration:  $[C]_0=0.0786\text{ M}$ ;  $[W]_0/[C]_0=0.40$ ,  $T=61^\circ\text{C}$

$[M]_0, \text{M}$	$10^3 k_1, h^{-1}$	$10^3 R_i/[M]_0^{-1}, h^{-1}$	$M_T, \%$
0.721	2.83	14.0	6
1.100	3.19	13.5	—
1.442	3.04	13.7	4
1.799	3.42	13.9	3

*Table 2.* The effect of varying catalyst concentration:  $[M]_0=1.442\text{M}$ ;  $[W]_0/[C]_0=0.40$ ;  $T=61^\circ\text{C}$

$[C]_0$ M	$10^2 k_2$ l. mole $^{-1}$ h $^{-1}$	$10^2 R_i/[M]_0^{-1}[C]_0^{-1}$ l. mole $^{-1}$ h $^{-1}$	$M_T$ %
0.0786	3.7*	18*	4
0.103	4.0	14	6
0.118	3.6	14	—
0.142	3.6*	20*	—
0.220	2.9	14	14

\*Average of several results (see, for example, *Table 1*) at different values of  $[M]_0$ .

the rate of the secondary reaction and initial rate of the fast reaction is indicated. Garty *et al.*, who used zinc dibutyl with an equimolar concentration of water, have found that the first order dependence on  $[C]_0$  falls off at high  $[C]_0$ ; our data are consistent with this finding.

The second order rate constants ( $k_2$ ) for the secondary reaction with  $[W]_0/[C]_0=0.40$  at 25°C, 46°C and 61°C were 0.0053, 0.0164 and 0.038 l. mole<sup>-1</sup> h<sup>-1</sup> respectively. The data at 25°C and 46°C were obtained on a single polymerization during which the temperature was raised. The reaction at 25°C exhibited a short induction period followed by a polymerization curve similar to that at 61°C (*Figure 1*) but no useful estimate of the temperature dependence of the initial rate of the fast reaction could be obtained from these data. The results give a good Arrhenius plot from which an activation energy of 10 kcal mole<sup>-1</sup> is obtained.

*Table 3.* The variation of the rate of polymerization with solvent:  $[M]_0=1.442$  M;  $[C]_0=0.0786$  M;  $[W]_0/[C]_0=0.40$ ;  $T=61^\circ\text{C}$

<i>Solvent</i>	$10^3 k_1$ h <sup>-1</sup>	$10^3 R_t[M]_0^{-1}$ h <sup>-1</sup>
Dioxan	3.0	14
Diethyl ether	8.0	—
Methylene chloride	4.5	38
Hexane	13.6	56

Diethyl ether, methylene chloride and hexane were also used as solvents in the dilatometers. In all solvents a fast reaction was followed by a slower first order reaction. The values of  $k_1$  and  $R_t[M]_0^{-1}$  obtained are given in *Table 3*. Precipitation could be seen in the hexane solution.

*Other observations*— $[W]_0/[C]_0=0.40$

The kinetic data indicate that the secondary reaction is not terminated to any measurable extent. This finding was confirmed by adding monomer (*in vacuo* via a break seal) to reaction vessels in which the initial charge of monomer had been completely polymerized. In all cases the second charge of monomer polymerized.

Additional information on the nature of the catalyst was obtained as follows. Zinc diethyl (0.0786 M) and water ( $[W]_0/[C]_0=0.4$ ) in dioxan were heated in a dilatometer for two days at 61°C before monomer (1.442 M) was added *in vacuo* via a break seal. Neither the shape of the conversion versus time curve nor the rate of the secondary reaction ( $k_2=0.04$  l. mole<sup>-1</sup> h<sup>-1</sup>) were changed by this procedure although precipitation occurred in the catalyst solution (which did not dissolve when monomer was added). In a second experiment 10 per cent of the monomer was added initially and the remainder after heating as before. In this experiment no fast reaction was observed. The rate of the secondary reaction was almost unchanged ( $k_2=0.045$  l. mole<sup>-1</sup> h<sup>-1</sup>) although, as before, precipitation occurred.



*The effect of water concentration*

The effect of the value of  $[W]_0/[C]_0$  upon the overall rate of reaction has been investigated by others<sup>2,4,6</sup> and our own results, obtained by measuring the extent of polymerization in 16 hours at 25°C, show the same features (see earlier). In order to obtain quantitative data several dilatometric runs were made in which  $[W]_0/[C]_0$  was varied. In the absence of water no contraction in volume was observed over a period of several weeks at 61°C. Typical polymerization curves for  $[W]_0/[C]_0$  in the range 0.20 to 0.60 are shown in *Figure 2*. Above  $[W]_0/[C]_0=0.5$  the rate of reaction was difficult to measure by our technique both because of the speed of the reaction and because of the high viscosity of the resulting solution. With  $[W]_0/[C]_0=0.50$  the initial fast reaction was observed; with  $[W]_0/[C]_0=0.70$  the data fitted a first order plot from the start (data at  $[W]_0/[C]_0=0.60$  were indeterminate in this respect). It can be seen from

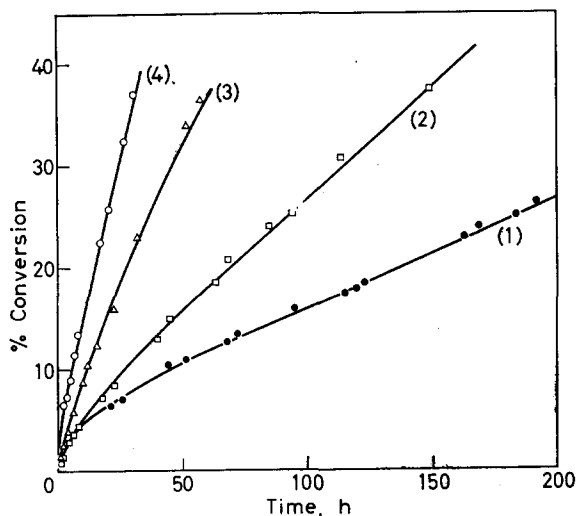


*Figure 2*—Percentage conversion versus time for the polymerization of propylene oxide at 61°C with  $[M]_0=1.442$  M,  $[C]_0=0.786$  M and  $[W]_0/[C]_0=0.20$  (1), 0.40 (2), 0.50 (3) and 0.60 (4)

*Figure 2* that the absence of a period of faster rate cannot be taken to prove the absence of a fast reaction since the rate of the secondary reaction increases more rapidly with increasing  $[W]_0/[C]_0$  than the rate of the initial reaction, and the two polymerization curves could merge. The first order rate constants of the second reaction which were determined in these experiments are listed in *Table 4*. With  $[W]_0/[C]_0 > 0.5$  the reaction was not carried to a high enough conversion to enable one to decide whether the reaction was truly first order. We have found no simple dependence of  $k_1$  on  $[W]_0$ .

Kinetic measurements have been made at a high water concentration,  $[W]_0/[C]_0=1.50$ . This system exhibited an initial slow period followed by

## POLYMERIZATION OF PROPYLENE OXIDE

Table 4. The effect of water concentration upon  $k_1$ :  $[C]_0=0.0786$  M;  $T=61^\circ\text{C}$

$[W]_0/[C]_0$	$[M]_0$ M	$10^3 k_1$ $h^{-1}$
0.20	1.442	1.4
0.40	1.442	3.0
0.50	1.442	7.8
0.60	1.442	13.2
0.70	0.721	18.1

a fast reaction, a result which illustrates the difficulty of interpreting the data obtained by single point measurements of the overall rate. In addition the difference between the reactions at  $[W]_0/[C]_0$  say 0.5 and 1.5 emphasizes the danger of generalizing from our study of the catalyst system  $[W]_0/[C]_0=0.40$ .

## II—CHARACTERIZATION OF THE POLYMERS

### EXPERIMENTAL

Polymers were isolated in the manner described earlier but were protected from oxidative degradation by the addition of 0.1 to 0.5 per cent by weight of an antioxidant (Stavox, Binox M and Nonox W.S.L. were all used). Polymers required for examination by infra-red spectroscopy or cryoscopy were not so protected.

The techniques used in fractionating the polymers from dilute solutions in iso-octane and in determining intrinsic viscosities have been described earlier<sup>16,17</sup>. Viscosity-average molecular weights ( $\bar{M}_v$ ) were calculated from the intrinsic viscosity measured in benzene at  $25^\circ\text{C}$  by use of the equation<sup>16</sup>

$$[\eta] = 1.12 \times 10^{-4} \bar{M}_v^{0.77}$$

Number-average molecular weights were determined in recrystallized benzene in a simple laboratory cryoscope.

### RESULTS

#### *Fractionation*

Two polymers were fractionated from iso-octane solution (polymer concentration  $0.2$  g dl<sup>-1</sup>). The results are given in Table 5: these are the temperature of separation  $T_m$ , the weight  $w_i$  (as a percentage of the weight of polymer fractionated) and the intrinsic viscosity  $[\eta]_i$  of each fraction. Both polymers were prepared in dioxan solution at  $25^\circ\text{C}$  with  $[M]_0=5.77$  M,  $[C]_0=0.280$  M and  $[W]_0/[C]_0=0.20$  (polymer 70,  $[\eta]=5.56$  dl g<sup>-1</sup>, conversion 70 per cent) or 0.50 (polymer 62,  $[\eta]=7.74$  dl g<sup>-1</sup>, conversion 81 per cent).

The first fractions precipitated were opaque solids (though somewhat swollen with solvent) and all had the same intrinsic viscosity. Fractions separated at lower temperature were transparent liquid gels and, as expected for liquid-liquid phase separation, differed in intrinsic viscosity. In each case intermediate fractions were translucent gels, i.e. a visible mixture of solid and liquid phases. Such fractions are labelled with an asterisk in Table 5.

Table 5. The fractionation data

Fraction	Polymer 70			Polymer 62		
	$T_m$ °C	$w_t$	$[\eta]_t$ $dl\ g^{-1}$	$T_m$ °C	$w_t$	$[\eta]_t$ $dl\ g^{-1}$
1	50	3.5	8.0	50	4.5	8.6
2	46	5.2	8.1	41	14.1	8.6
3	42	2.1	7.6	34*	13.3*	12.2*
4	39*	4.8*	10.6*	31	11.8	11.7
5	33→40	4.5	7.8	25	16.3	8.6
6	33*	8.2*	12.1*	22	7.0	5.2
7	30	10.9	11.5	16	7.8	3.22
8	26	11.9	9.3	0	5.9	1.18
9	22	10.2	5.1	—	21.1	0.02
10	17	5.7	2.37			
11	0	4.4	0.82			
12	—	34.8	0.42			
$\Sigma w_t$	—	106.2	—	—	101.8	—
$\Sigma w_t[\eta]_t$	—	—	5.57	—	—	6.57
$\Sigma w_t$	—	—	—	—	—	—

\*These fractions contain solid polymer.

Our interpretation of the initial part of the fractionation ( $> 40^\circ\text{C}$ ) is in other papers<sup>17, 18</sup> where additional fractionation data are presented. The fractionation occurs only on the basis of ability to crystallize since the molecular weight distributions, as well as the average molecular weights, of the fractions are identical. The differences in solubility are assumed to be due to differences in the degree of isotacticity of the fractions, and the whole polymer is thought to consist of species having a marked variation in the degree of isotacticity (which is independent of the molecular weight provided it is not very low).

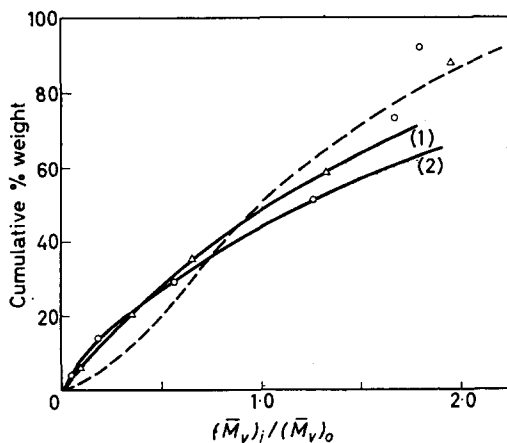


Figure 3—Reduced molecular weight distributions for polypropylene oxides 62 (1) and 70 (2). The dashed curve is the most probable distribution

The part of the polymer which separates below 40°C fractionates mainly on the basis of molecular weight. In both samples there was a large fraction soluble in iso-octane at 0°C which had a very low molecular weight. The molecular weight distribution of the high molecular weight polymer was obtained by analysing the data for the fractions separating between 0° and 39°C. In *Figure 3* the cumulative weight per cent<sup>19</sup> is plotted against the reduced viscosity-average molecular weight  $(\bar{M}_v)_i/(\bar{M}_v)_0$  {where  $(\bar{M}_v)_0$  is calculated from the weight-average  $[\eta]$  of the fractions}. Both distributions are similar (the solid lines have been drawn without considering the fractions marked with an asterisk in *Table 5* which contain solid polymer) and both are wider than the most probable distribution<sup>20</sup> which is also shown in *Figure 3*. The ratio  $\bar{M}_w/\bar{M}_n$  calculated from the curves of *Figure 3* is about 3; with the low molecular weight fraction included in the assessment the ratio is about 1 000. It might be noted that the effect of a distribution of the degree of isotacticity upon the liquid-liquid phase separation would be to narrow the determined molecular weight distribution.

The molecular weight distribution of the crystalline fractions is the same as those shown in *Figure 3*, i.e. all the high molecular weight polymer has the same molecular weight distribution. The evidence for this is indirect for the two fractionations reported here {for example  $(\bar{M}_v)_0$  is the same as  $(\bar{M}_v)_i$  for the first fraction in both cases}, but direct evidence has been obtained<sup>17</sup>. For example, a sample of polypropylene oxide discussed elsewhere<sup>17</sup> was precipitated from methanol at 0°C (a solid-liquid phase separation) and  $\bar{M}_w/\bar{M}_n$  of the insoluble fraction was 3.3<sup>17</sup>. The soluble portion was fractionated and  $\bar{M}_w/\bar{M}_n$  of the high molecular weight polymer was 3. We have not discussed these data here since the polymer was a degraded sample<sup>17</sup>, but the molecular weight distribution of the high molecular weight polymer as prepared must have been wider than  $\bar{M}_w/\bar{M}_n=3$  since random scission would narrow the molecular weight distribution. This sample was prepared with  $[W]_0/[C]_0=1.0$ .

#### *The low molecular weight fraction*

In order to isolate the low molecular weight fraction from a number of polymers a simple separation in iso-octane at 0°C was adopted. Samples were dissolved in iso-octane at 60°C at a concentration of about 1 g l.<sup>-1</sup> and then cooled to 0°C for one day. The supernatant liquid was decanted and evaporated. The low molecular weight fraction so obtained was an inhomogeneous mixture of a small amount of solid (presumably crystalline) polymer and an oil. Further fractionation from iso-octane at lower temperatures gave a partial separation of the solid and liquid polymers, e.g. at -30°C the soluble polymer was a clear oil. As a rough guide we estimate that linear polypropylene oxide of molecular weight less than 10<sup>5</sup> is soluble in iso-octane at 0°C.

The number-average molecular weights of two low molecular weight fractions (i.e. soluble in iso-octane at 0°C) are given in *Table 6*. In both cases the number average degree of polymerization is 5. Since it is known that the dimers and trimers of propylene oxide are volatile under the

Table 6. The molecular weights of the low molecular weight fraction

$[W]_0/[C]_0$	Temperature of polymerization °C	Conversion %	$[\eta]$ dl g <sup>-1</sup>	Low molecular weight fraction			
				Wt fraction	$[\eta]$ dl g <sup>-1</sup>	$\bar{M}_v \times 10^{-4}$	$\bar{M}_n$
0.4	61	83	8.0	0.18	0.39	3.9	320
0.7	25	98	9.65	0.10	0.20	1.6	300

conditions of drying used<sup>22</sup> we collected the benzene distillate from several samples: small amounts of polymer (< 1 weight-per cent of the whole) were volatile but the number-average degree of polymerization of this polymer was found to be 4. Examination of the volatile components of the reaction mixture by gas chromatography confirmed the absence of any appreciable quantity of volatile polymers. We conclude that the low molecular weight fraction consists of a tetramer plus the low molecular weight tail of the high polymer. The relative amounts of tetramer and high polymer can be estimated. It seems reasonable to assume that  $\bar{M}_v$  of the soluble high polymer is at least  $5 \times 10^4$  (the whole of one low molecular weight fraction has  $\bar{M}_v \approx 4 \times 10^4$ ) and that the corresponding  $\bar{M}_n$  is not very low (say  $> 5000$ ). Using these values one would obtain values of the average molecular weights of the whole fraction of  $\bar{M}_v \approx 10000$  and  $\bar{M}_n \approx 300$  if the tetramer comprised about 80 weight-per cent of the low molecular weight fraction. One would expect the amount of high polymer in the low molecular weight fraction to fall as the molecular weight of the whole polymer increased.

Infra-red spectra of the dry low molecular weight fractions showed no absorption due to unsaturation and no absorption due to hydroxyl provided the reaction was terminated by adding methanol: if water was added to terminate the reaction a hydroxyl absorption was detected. The number of hydroxyl end groups per molecule of a fraction of a low conversion sample was determined by phthaloylation according to the method used by Price and St Pierre<sup>21</sup>. The polymer was prepared at 25°C with  $[M]_0 = 5.77$  M,  $[C]_0 = 0.280$  M and  $[W]_0/[C]_0 = 0.70$  and was terminated by adding water at 9.6 per cent conversion. Seventy five weight-per cent of the polymer was soluble in iso-octane at 0°C and this fraction had  $\bar{M}_n = 230$ . The number of —OH groups per molecule was 0.6. The n.m.r. spectra of low molecular weight fractions derived from polymers terminated by adding methanol showed a peak attributable to —OMe groups. The fraction soluble at —30° showed a lower proportion of —OMe protons than the whole sample, indicating that the —OMe groups (and the —OH groups) are associated with the high molecular weight linear polymer: the tetramer apparently has no detectable end groups and we think a cyclic molecule more plausible than a linear tetramer with hydrocarbon end groups.

#### The crystalline fraction

Other solvents can be used to separate those fractions which crystallize most easily (e.g. heptane and cyclohexane have been used). At an early stage in this work methanol at 0°C was chosen as the solvent in which

POLYMERIZATION OF PROPYLENE OXIDE

to make a simple separation into insoluble and soluble fractions, in order that some comparison might be made between the crystallizability of polymers produced in different ways without fractionating them more completely. Polymers were dissolved in methanol at 30° to 40°C at a concentration of about 1 g l.<sup>-1</sup> and the methanol was cooled to 0°C for two days. The precipitate was separated by filtering the suspension as quickly as possible. Both the soluble and insoluble fractions were isolated by evaporating the methanol and then freeze drying from benzene. The

Table 7. Separation in methanol at 0°C

Polymer	$[\eta]$ dl g <sup>-1</sup>	Wt fraction insoluble	$[\eta]$ (dl g <sup>-1</sup> ) of insoluble polymer
70	5.56	0.10	7.80
62	7.74	0.17	9.14

results obtained with the polymers we fractionated serve to illustrate the usefulness of this separation (Table 7). It can be seen that a greater percentage of polymer 62 is insoluble (as would be predicted from the fractionation data since a greater percentage of polymer 62 separates as solid fractions from iso-octane). The intrinsic viscosities of the insoluble fractions are higher than those of the soluble fractions. This would be expected since the low molecular weight fraction will not crystallize (either because it is cyclic or because of end group effects). Moreover, any undetected liquid-liquid phase separation will raise  $[\eta]$  of the insoluble fraction; the high  $[\eta]$  for the insoluble fraction of polymer 62 compared with the early fractions in Table 5 suggests that some liquid-liquid phase separation took place with this polymer in methanol at 0°C.

In what follows we have used the weight-per cent of a sample which is insoluble in methanol at 0°C as an arbitrary measure of the crystallinity of the sample. For convenience in writing we refer to it as the crystalline fraction.

The effect of conversion— $[W]_0/[C]_0 = 0.40$

The variation of the polymer characteristics with conversion were studied by preparing a master batch of the reactants in solution and pouring this

Table 8. The effect of conversion on the polymer:  $[M]_0 = 1.442$  M;  $[C]_0 = 0.103$  M;  $[W]_0/[C]_0 = 0.40$ ;  $T = 61^\circ\text{C}$

Conversion %	$[\eta]$ dl g <sup>-1</sup>	Crystalline fraction			Low molecular weight fraction		
		Wt fraction	Wt fraction (corrected)	$[\eta]$ dl g <sup>-1</sup>	Wt fraction	Wt fraction (monomer)	$[\eta]$ dl g <sup>-1</sup>
4.0	0.26	0.03	—	—	0.72	0.03	0.10
11.4	0.70	0.05	0.23	2.40	0.75	0.09	0.10
40.5	2.72	0.18	0.26	3.73	0.30	0.12	0.09
55.0	4.20	0.23	0.30	4.80	0.27	0.14	0.08
80.9	5.50	0.25	0.30	6.42	0.20	0.16	—

solution into several reaction vessels which were frozen down together and sealed off independently. The results of such an experiment are given in *Table 8*. For this polymer ( $[W]_0/[C]_0=0.40$ ) there is linear increase in  $\bar{M}_v$  at high conversion (*Figure 4*) and it seems possible to conclude that a large quantity of low molecular weight polymer (presumably the tetramer) is produced early in the reaction, i.e. during the period of fast rate. [A similar, though less marked, deviation from linearity was observed

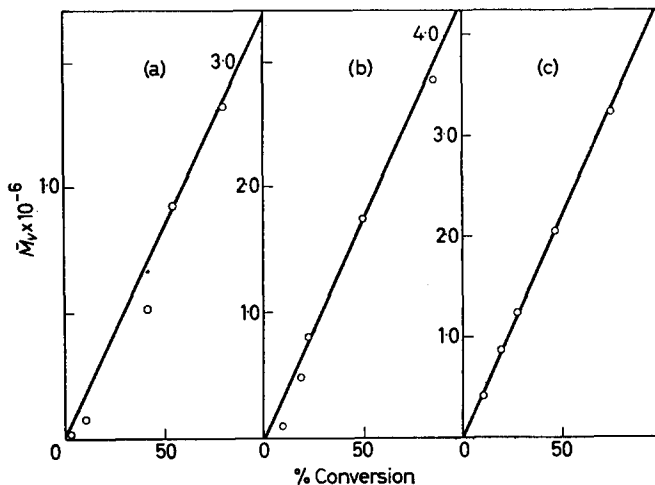


*Figure 4*— $\bar{M}_v$  versus per cent conversion for polypropylene oxide prepared at 61°C with  $[M]_0=1.442$  M,  $[C]_0=0.103$  M and  $[W]_0/[C]_0=0.40$  (a), and prepared at 25°C with  $[M]_0=5.77$  M,  $[C]_0=0.280$  M and  $[W]_0/[C]_0=0.80$  (b) or 1.00 (c)

with  $[W]_0/[C]_0=0.80$  but with  $[W]_0/[C]_0=1.00$  the plot of  $\bar{M}_v$  versus conversion is linear and goes through the origin (*Figure 4*.)

The crystalline fraction increases rapidly with conversion. However, if it is assumed that the low molecular weight fraction does not crystallize from methanol at 0°C, then the crystalline fraction of the high molecular weight polymer (corrected weight-fraction in *Table 8*) varies very little with conversion and is constant when  $\bar{M}_v$  is high. The low molecular weight fraction decreases with increasing conversion but the actual amount of polymer in the low molecular weight fraction (i.e. the weight fraction based on monomer in *Table 8*) increases with increasing conversion. Since we have already argued that the bulk of a low molecular weight fraction of this type (note that  $\bar{M}_v \approx 10\,000$ ;  $\bar{M}_n$  is unmeasured but is presumably around 300) when taken at high conversion is tetramer we conclude that tetramer is produced throughout the reaction.

#### *The effect of catalyst concentration— $[W]_0/[C]_0=0.40$*

Several polymerization reactions in which the catalyst concentration was varied were allowed to proceed to completion. The results are given in

POLYMERIZATION OF PROPYLENE OXIDE

Table 9. The variation of  $\bar{M}_v$  with  $[C]_0$ :  $[M]_0=1.442$  M;  $[W]_0/[C]_0=0.40$ ;  $T=61^\circ\text{C}$

$[C]_0$ M	$\bar{M}_v \times 10^{-6}$	$\bar{M}_v[C]_0 \times 10^{-5}$
0.0786	2.5	2.0
0.118	1.8	2.1
0.142	1.44	2.0
0.180	0.96	1.7

Table 9, and show that  $\bar{M}_v$  is directly proportional to  $[C]_0^{-1}$ . No systematic data were obtained concerning possible changes in the crystalline or low molecular weight fractions with  $[C]_0$ .

The effect of temperature— $[W]_0/[C]_0=0.45$

Samples from the same master batch were polymerized at  $25^\circ$ ,  $45^\circ$ , and  $60^\circ\text{C}$  for 17 days. The resulting polymers were characterized with the results given in Table 10; the crystalline fraction increases as the temperature of polymerization decreases.

Table 10. The effect of temperature:  $[M]_0=5.4$  M;  $[C]_0=0.54$  M;  $[W]_0/[C]_0=0.45$

Polymerization temperature, $^\circ\text{C}$	$[\eta]$ $dl\ g^{-1}$	Crystalline fraction	Low molecular weight fraction
25	5.61	27	0.35
45	5.60	23	0.35
60	5.62	16	0.36

Other observations— $[W]_0/[C]_0=0.40$

The effect upon the polymer of adding additional monomer to a reaction which had already gone to completion was investigated. A master batch was prepared with  $[M]_0=1.442$  M,  $[C]_0=0.142$  M and  $[W]_0/[C]_0=0.40$ , and was divided into three portions and polymerized at  $61^\circ\text{C}$ . Additional monomer was added to two of the vessels and this was polymerized at  $61^\circ\text{C}$ . The results are given in Table 11. The viscosity-

Table 11. The effect of adding monomer to the polymer

Monomer	Conversion %	$\bar{M}_v \times 10^{-6}$	Low molecular weight fraction
1st charge	100	1.6	0.23
+2nd charge	90	3.5	0.12
+2nd charge	90	3.2	0.15

average molecular weight of the polymer increases roughly in proportion to the increase in amount of polymerized monomer, while the amount of low molecular weight polymer increases very little. Taken together with our earlier data on the increase in  $\bar{M}_v$  with conversion and the kinetic data, these results indicate that the weight distribution of molecular weights of



the high polymer does not change appreciably with increasing conversion and that there is no transfer reaction.

Since the high polymer is formed by a reaction which has many characteristics of a 'living' polymerization, e.g. no termination or transfer reactions, it is a puzzling fact that the molecular weight distribution is very wide. It has been suggested that this apparent anomaly might be the result of a scission reaction and the following experiment was performed to investigate this possibility. A solution of reactants was prepared ( $[M]_0 = 1.442 \text{ M}$ ,  $[C]_0 = 0.142 \text{ M}$  and  $[W]_0/[C]_0 = 0.40$ ) and divided into two portions. Both portions were completely polymerized at  $61^\circ\text{C}$  when an extra charge of zinc diethyl and water was added (via a break seal in high vacuum) to one of the vessels. Both were then stored in the dark at room temperature for three weeks. The results are given in *Table 12*

*Table 12.* The effect of adding catalyst to the polymer

Polymer	Stored with catalyst		Stored without catalyst	
	$[\eta]$ dl g <sup>-1</sup>	Low molecular weight fraction	$[\eta]$ dl g <sup>-1</sup>	Low molecular weight fraction
A	3.5	0.21	5.3	0.18
B	3.5	0.13	8.8	0.02

(polymer A) and it can be seen that the polymer is degraded by zinc diethyl and water, and that the mode of degradation is, apparently, random scission of the chains; the increase in the low molecular weight fraction (assuming linear polymer of molecular weight less than  $10^5$  is soluble in iso-octane at  $0^\circ\text{C}$ ) is approximately that expected for random scission of a polymer with a molecular weight distribution similar to those shown in *Figure 3* from  $[\eta] = 5.3$  to  $3.5 \text{ dl g}^{-1}$ . In another experiment dry polymer ( $[\eta] = 9.5 \text{ dl g}^{-1}$ ) which had been extracted in iso-octane at  $0^\circ\text{C}$ , was then dissolved in dioxan *in vacuo* and a part of it treated with zinc diethyl and water ( $[W]_0/[C]_0 = 0.5$ ) at  $25^\circ$  for three weeks. The results of this experiment (polymer B in *Table 12*) confirm the above findings.

It was also found that polymer could be degraded slightly by leaving the polymer sealed in the polymerization vessel after completion of the polymerization reaction. Some of the scatter in our observations of  $\bar{M}_v$  at high conversion might be explained by this finding.

No data were obtained concerning possible changes in the crystallinity of the polymer caused by scission reaction.

#### *Effect of water concentration*

The effect of water concentration upon the variation of  $\bar{M}_v$  with conversion has already been discussed. In *Table 13* are given the results of the characterization of polymers prepared at  $25^\circ$  with differing values of  $[W]_0/[C]_0$ . Similar, though less complete, data were obtained at  $61^\circ\text{C}$ , with lower monomer and catalyst concentrations.  $\bar{M}_v$  in *Table 13* is corrected to 100 per cent conversion by assuming that it increases linearly

POLYMERIZATION OF PROPYLENE OXIDE

Table 13. The effect of water concentration on the polymer:  $[M]_0=5.77$  M;  $[C]_0=0.28$  M;  $T=25^\circ\text{C}$

$[W]_0/[C]_0$	Conversion %	$[\eta]$ dl g <sup>-1</sup>	$\overline{M}_v(\text{corrected}) \times 10^{-6}$	Crystalline fraction	Low molecular weight fraction
0.20	70	5.56	2.2	0.10 (0.13)	0.22
0.25	—	—	—	0.10	—
0.40	—	—	—	0.11	—
0.50	81	7.74	2.9	0.17 (0.20)	0.17
0.60	85	8.50	3.0	—	—
0.70	—	—	—	0.19 (0.21)	0.10
0.80	99	11.0	3.6	0.20	—
0.90	—	—	—	0.23	—
1.00	98	15.5	5.5	0.24 (0.25)	0.04
1.10	99	22.0	7.7	0.35	0.11

Note: Figures in parentheses give values corrected for the non-crystallizing fraction.

with conversion. The effect on  $\overline{M}_v$  of changing  $[W]_0/[C]_0$  is marked, especially when  $[W]_0/[C]_0 \rightarrow 1$ . This increase is due to an increase in the molecular weight of the high polymer and cannot be attributed to a drop in the amount of tetramer produced, although when correction is made for the low molecular weight fraction  $\overline{M}_v$  changes very little at low  $[W]_0/[C]_0$ . With  $[W]_0/[C]_0 > 1$ ,  $\overline{M}_v$  eventually decreases; a polymerization carried out at  $60^\circ\text{C}$  with  $[M]_0=1.34$  M,  $[C]_0=0.111$  M and  $[W]_0/[C]_0=1.50$  gave a polymer with  $[\eta]=0.09$  dl g<sup>-1</sup> ( $\overline{M}_v \approx 10^4$ ) and  $\overline{M}_n=1700$ .

The low molecular weight fraction decreases with increasing water concentration. At  $[W]_0/[C]_0=1.0$  the amount of tetramer produced must be negligible since a part of the low molecular weight fraction must be low molecular weight linear polymer. This observation is confirmed by the linear variation of  $\overline{M}_v$  with conversion noted earlier for  $[W]_0/[C]_0=1.0$ . The crystalline fraction increases with increasing  $[W]_0/[C]_0$ . The increase is not due to the decreasing amount of low molecular weight polymer; values corrected for this non-crystallizing fraction are given in parentheses in Table 13. It is possible that the increase may be due to increasing amounts of liquid-liquid phase separation as the molecular weight increases but we have no information on this point.

DISCUSSION

It is obvious from the results we have presented that the polymerization of propylene oxide by zinc diethyl and water is an extremely complicated process. We can only discuss in detail the polymerization carried out with a mole ratio of water to zinc diethyl of 0.4 (there are insufficient data at other ratios). So far as we can tell, both from the experiments in which precipitate was present during polymerization (see p 488) and from the overall reproducibility of the work, the polymerization reactions involve soluble species only. We have to explain:

(1) a polymerization reaction which has neither a transfer nor a termination reaction. The rate of reaction is directly proportional to  $[M]$  and to  $[C]_0$  (at least up to  $[C]_0=0.18$  M) and the activation energy is about

10 kcal mole<sup>-1</sup> (though the data of *Table 10* qualify this value). The product of this reaction is a linear high polymer with a wide molecular weight distribution ( $\bar{M}_w/\bar{M}_n \approx 3$ ) and a distribution of degrees of isotacticity. The viscosity-average molecular weight of the polymer increases linearly with increasing conversion and also with decreasing catalyst concentration ( $\bar{M}_v \propto [C]_0^{-1}$ ). At least one end group is —OMe when the polymerization is terminated with methanol.

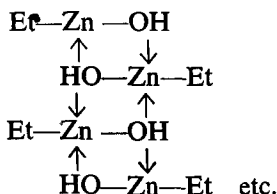
(2) a faster polymerization reaction at the beginning of the polymerization. This reaction rapidly slows down and cannot be detected after ten per cent conversion. The initial rate is directly proportional to both  $[M]_0$  and  $[C]_0$ . The estimates of the amount of monomer consumed during the period of fast rate suggest that this quantity is dependent on the catalyst concentration but not on the monomer concentration. The product of the reaction is a tetramer (probably cyclic), though production of tetramer continues after ten per cent conversion.

(3) a reaction which results in random scission of the polymer. Account must also be taken of the various effects of increasing  $[W]_0/[C]_0$ : i.e. the decreasing amount of tetramer, falling to about zero at  $[W]_0/[C]_0=1.0$ ; the increasing rates of both the slow reaction (up to  $[W]_0/[C]_0=1.0$ ) and the fast reaction (up to  $[W]_0/[C]_0=0.5$ ); and the increasing  $\bar{M}_v$  of the high polymer.

The number of zinc atoms involved in catalysing these reactions must be fewer than the number present in the system since a proportion are precipitated. Some idea of the number directly attached to the high polymer molecules (assuming the —OMe groups arise from scission of  $\geq C-O-Zn$  bonds) can be obtained by calculating the number of molecules of high polymer produced. From *Table 4* by assuming  $\bar{M}_w/\bar{M}_n \approx 5$  we have  $\bar{M}_n [C]_0 \approx 4 \times 10^4$  when  $[M]_0$  is 1.44 M, from which one can calculate that one molecule of high polymer is produced for each 500 zinc atoms present. If the wide molecular weight distribution is due to a scission reaction then this ratio may be more like 5 000 to 1. If the tetramer is included in this analysis ( $\bar{M}_n$  of the whole polymer is around 2 000 when  $[C]_0 \approx 0.1$  M) one finds that more than half the zinc atoms in the system might be involved directly in polymerization. However, the tetramer has no —OMe end groups and may be formed by a cyclization reaction which leaves the catalyst active (see later) and so it is probable that fewer zinc atoms are involved in catalysing the fast reaction than this estimate.

It appears that there are two distinct catalyst species one of which is present in fairly high concentration and the other in very low concentration. The expected products of a reaction between zinc diethyl and water are  $EtZnOH$  and  $Zn(OH)_2$  which are formed rapidly<sup>11, 15</sup>, and  $EtZnOZnEt$ ,  $EtZnOZnOH$ ,  $EtZnOZnOZnEt$  etc. formed more slowly. Since the catalysts survived a preheating period in the presence of an excess of ethyl groups it seems reasonable to assume that species containing —OH groups are not important catalysts. It also seems reasonable to suppose that species containing a large number of zinc atoms will be largely insoluble. On the other hand  $EtZnOZnEt$  will be a soluble species present in fairly high

concentration. It is less likely to associate than  $\text{EtZnOH}$ ,  $\text{EtZnOZnOH}$  or species such as  $\text{EtZnOR}$  (where R is a short polyether chain) which may be formed from the hydroxyl-containing molecules when monomer is present during the reaction: these species probably associate to give large complexes, e.g.



We assume that  $\text{EtZnOZnEt}$  is the important catalyst species for the initial reaction.

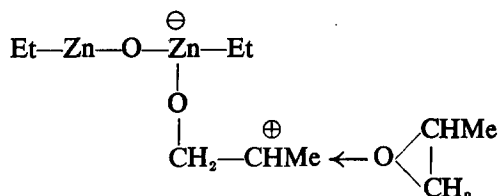
We cannot identify a catalyst species for the secondary reaction. However, we suggest that this species is essentially monomeric (or perhaps, a stable dimer) but only because of its very low concentration. Justification for this view is found in the fall-off in the dependence of rate on  $[\text{C}]_0$  noted at high  $[\text{C}]_0$  which is presumably due to association of the species. Moreover, at a given  $[\text{C}]_0$  the concentration of this species would have to increase as  $[\text{W}]_0$  increases in order to explain the increase in rate. It is therefore interesting to compare our results at  $[\text{W}]_0/[\text{C}]_0=0.40$  with those of Garty *et al.*<sup>6</sup> who worked at  $[\text{W}]_0/[\text{C}]_0=1.0$  (where incidentally the reaction appears to be more straightforward and where, therefore, their method of measuring the total polymerization is probably reliable). Garty *et al.*<sup>6</sup> report a fractional dependence of rate on  $[\text{C}]_0$  at  $[\text{C}]_0 > 0.02 \text{ M}$  compared with  $[\text{C}]_0 > 0.2 \text{ M}$  in our system (*Table 2*). Since the increase in rate of the secondary reaction with increasing water concentration is accompanied by an increase in the crystalline fraction it seems possible that the production of isotactic polymer is favoured when the catalyst is more highly associated: however, as mentioned earlier, we have not investigated systematically the effect of  $[\text{C}]_0$  upon the crystalline fraction (but compare data in *Table 10* with those in *Table 13*).

There are many points of similarity between our results and the results reported for the polymerization of propylene oxide by ferric chloride and water<sup>7</sup> and by aluminium trimethyl and water<sup>23</sup>. It is of interest, therefore, to compare the reaction scheme involving cationic active centres proposed by Colclough and Wilkinson<sup>23</sup> for these systems with our results\*.  $\text{EtZnOZnEt}$  is analogous to the species chosen by Colclough as the catalyst for the initial reaction. The reaction is envisaged as proceeding through a cationic active centre†

\*We do not, of course, have any direct evidence which would lead us to prefer the cationic mechanism to, say, the coordinate anionic mechanism proposed by Price and Osgan<sup>24</sup>. However, only Colclough has attempted a complete and consistent explanation of all the reactions involved in these polymerization systems.

†It is convenient\*\* to represent the site of polymerization as a solvated carbonium ion rather than as an

oxonium ion: viz.  $-\text{CHMe}-\overset{\oplus}{\text{O}} \begin{array}{l} \text{CHMe} \\ | \\ \text{CH}_2 \end{array}$



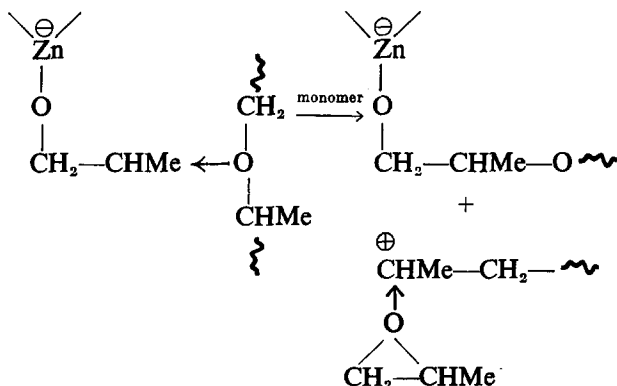
Several reaction paths are possible:

- (1) Solvation of the cation with monomer (shown above);
- (2) Solvation with an oxygen in the polymer chain (which must occur preferentially at a point removed from the cation by four monomer units) leading to cyclization;
- (3) Reaction with an oxygen in the counter ion which gives the species



(where  $n$  denotes a small polymer chain). This species will probably associate into large complexes and be relatively inactive. This reaction then is the cause of the rapid decrease in rate of the initial reaction;

- (4) Solvation with an oxygen in a second polymer chain leading to a scission reaction:



The species  $\text{EtZnO(CHMeCH}_2\text{O)}_n\text{ZnEt}$  is analogous to that favoured by Colclough as the catalyst for the secondary reaction. Only the small fraction which is unassociated (or semi-bridged complexes containing zinc atoms which are not fully coordinated) is considered to be active. However, the association would have to be irreversible in order to ensure a first order dependence of rate upon  $[\text{C}]_0$  and also the formation of so few high polymer molecules. It seems more likely that the soluble  $\text{EtZnO(CHMeCH}_2\text{O)}_n\text{ZnEt}$  continues to produce cyclic polymer (and to increase  $n$ ) throughout the reaction while the high polymer is produced by another unidentified species present in the system in very low concentration. The cationic initiation, propagation and termination mechanism to give an overall non-terminated polymerization<sup>23</sup> seems readily applicable to such a species, as do Colclough's suggestions concerning the production of the stereoregular polymer at associated catalyst sites.

We have assumed that the faster rates of reaction as  $[\text{W}]_0/[\text{C}]_0$  is

increased are due to increased concentrations of the unidentified catalyst species. The scission reaction (see earlier) will be catalysed by soluble  $\text{EtZnO}(\text{CH}_2\text{CHMeO})_n\text{ZnEt}$  etc., as well as the unidentified catalyst itself. As  $[W]_0/[C]_0$  is increased above 0.5, the concentration of active centres, other than the unidentified catalyst species, will decrease and hence the increase in  $\bar{M}_v$  as the rate of reaction increases, in the region  $0.5 < [W]_0/[C]_0 < 1.0$ , can be understood.

*We wish to thank Dr R. O. Colclough for many helpful discussions concerning the interpretation of our data, Dr M. N. Jones for contributing to our understanding of the composition of the polymers and Professor G. Gee, who initiated this investigation, for his continued help and advice.*

University of Manchester  
Manchester 13

(Received November 1963)

- <sup>1</sup> See, for example, BORROWS, E. T. and STEWART, D. G. *British Pats. Nos. 785 053 and 793 065*
- <sup>2</sup> FURUKAWA, J., TSURUTA, T., SAKATA, R., SAEGUSA, T. and KAWASAKI, A. *Makromol. Chem.* 1959, **32**, 90  
SAKATA, R., TSURUTA, T., SAEGUSA, T. and FURUKAWA, J. *Makromol. Chem.* 1960, **40**, 64
- <sup>3</sup> CHU, N. S. and PRICE, C. C. *J. Polym. Sci.* 1963, **1(A)**, 1105
- <sup>4</sup> GLUHOV, N. A. Private communication
- <sup>5</sup> BAILEY, F. E. and FRANCE, H. G. *J. Polym. Sci.* 1960, **45**, 243
- <sup>6</sup> GARTY, K. T., GIBB, T. B., Jr and CLENDINNING, R. A. *J. Polym. Sci.* 1963, **1(A)**, 85
- <sup>7</sup> GEE, G., HIGGINSON, W. C. E. and JACKSON, J. B. *Polymer, Lond.*, 1962, **3**, 231
- <sup>8</sup> VOGEL, A. I. *A Textbook of Practical Organic Chemistry*, p 175. Longmans, Green: London, 1954
- <sup>9</sup> MORANTZ, D. and WARHURST, E. *Trans. Faraday Soc.* 1955, **51**, 1375
- <sup>10</sup> NOLLER, C. R. *Organic Syntheses*, Collective Vol. 2, Ed. A. H. BLATT, p184. Wiley: New York, 1947
- <sup>11</sup> See, for example, HEROLD, R. J., AGGARWAL, S. L. and NEFF, V. *Canad. J. Chem.* 1963, **41**, 1368
- <sup>12</sup> GEE, G., HIGGINSON, W. C. E. and MERRALL, G. T. *J. chem. Soc.* 1959, 1345
- <sup>13</sup> PRAUSNITZ, J. M. and SHAIR, F. H. *J. Amer. Inst. chem. Engrs*, 1961, **1**, 682
- <sup>14</sup> BURGESS, A. and COLCLOUGH, R. O. Private communication
- <sup>15</sup> BRUCE, J. M. and HITCHEN, G. Private communication
- <sup>16</sup> ALLEN, G., BOOTH, C. and JONES, M. N. *Polymer, Lond.* 1964, **5**, 195
- <sup>17</sup> ALLEN, G., BOOTH, C. and JONES, M. N. *Polymer, Lond.* 1964, **5**, 257
- <sup>18</sup> ALLEN, G., BOOTH, C., JONES, M. N., MARKS, D. J. and TAYLOR, W. D. *Polymer, Lond.* In press
- <sup>19</sup> SCHULZ, G. V. and DINGLINGER, A. *Z. phys. Chem.* 1939, **B43**, 47
- <sup>20</sup> See, for example, FLORY, P. J. *Principles of Polymer Chemistry*, p 318. Cornell University Press: New York, 1953
- <sup>21</sup> PRICE, C. C. and ST PIERRE, L. E. *J. Amer. chem. Soc.* 1956, **79**, 897
- <sup>22</sup> COLCLOUGH, R. O. Private communication
- <sup>23</sup> COLCLOUGH, R. O. and WILKINSON, K. *J. Polym. Sci.* 1964, **4(C)**, 311
- <sup>24</sup> PRICE, C. C. and OSGAN, M. J. *J. Amer. chem. Soc.* 1956, **78**, 4787

## ANNOUNCEMENTS

### THERMAL ANALYSIS

(Thermogravimetric and Differential Thermal Analysis)

On 13 and 14 April 1965, the Northern Polytechnic is to hold a two day Symposium on the above subject. Main lectures will be given by Professor P. D. Garn (U.S.A.), Dr G. Guiochon and Dr M. Harmelin (France), and Professor W. W. Wendlandt (U.S.A.). Short contributed papers (approximately 20 minutes) are also invited on aspects of the technique and application of thermal analysis, including applications to polymers. In conjunction with this Symposium there will be an apparatus exhibition displaying a wide range of commercially available equipment.

Those wishing to be kept informed of arrangements for the Symposium are asked to contact Dr B. R. Currell, Northern Polytechnic, Holloway Road, London, N.7.

### CHEMISTRY OF POLYMERIZATION PROCESSES

A Symposium on 'The Chemistry of Polymerization Processes', organized by the Plastics and Polymer Group of the Society of Chemical Industry, will be held at the Institution of Electrical Engineers, London on 22 and 23 April 1965. Over 20 papers, dealing with aspects of radical, stereospecific, ionic and other aspects of polymerization, will be presented and discussed. Programmes and registration forms can be obtained from the Assistant Secretary, Society of Chemical Industry, Belgrave Square, London, S.W.1.

# *Molecular Weight Distributions of the Side Chains of Radiation Initiated Graft Copolymers*

J. D. WELLONS, A. SCHINDLER and V. STANNETT

*The grafted side chains of cellulose acetate-polystyrene grafts have been separated from the cellulosic backbone by acid hydrolysis. The molecular weight distributions of the polystyrene resulting from a mutual and a pre-irradiation graft polymerization have been determined using a column elution technique. Both samples had unusually broad molecular weight distributions; however, whereas the mutual product had a broad single distribution, the pre-irradiation sample had a two-peak distribution and had a large amount of polymer of very narrow and very high molecular weight. Some reasons for the differences are presented.*

IT HAS been repeatedly shown that both heterogeneous mutual radiation and pre-irradiation grafting processes are diffusion controlled, even under conditions where there is considerable swelling of the substrate. It might be anticipated, therefore, that unusually broad molecular weight distributions of the grafted side chains will be found. Unfortunately, no information on this subject is available owing to the difficulties of separation of the pure graft copolymer and the removal of the polymer backbone. The cellulose acetate-styrene grafting system is convenient in that it enables one to separate the pure grafts and to acid hydrolyse away the cellulosic backbone. Two preparations have been made, therefore, one mutual and one pre-irradiation, the graft copolymers separated and hydrolysed and the resulting polystyrene fractionated. The results of the study will be reported in this paper.

## EXPERIMENTAL

### *Preparation of graft copolymers*

Both samples were prepared by irradiation of 4.0 g of cellulose acetate (D.S. 1.84, viscosity average molecular weight, about 55 000) in the form of thin (1.0 mil) films to a total dose of 10.0 Mrad at 300 000 rad/h. The 'mutual' sample was irradiated at 25°C in an 80-20 styrene-pyridine mixture after degassing by three freeze-thaw cycles under high vacuum.

The pre-irradiation sample was irradiated, after degassing under high vacuum, at -78°C. After irradiation the film was kept at -78°C while an excess of degassed 80-20 styrene-pyridine mixture was admitted through a break seal. The mixture was then allowed to melt and left to polymerize at room temperature for 72 h.

The thin grafted films were freed from both homopolymers by repeated alternate extractions with benzene and a 70-30 acetone-water mixture;



7.16 g of 'mutual' graft copolymer containing 56.7 per cent of combined polystyrene and 4.67 g of 'pre-irradiation' graft containing 56.8 per cent of combined polystyrene were obtained.

The graft copolymers were hydrolysed by swelling in a 75–20–5 acetone–dimethyl formamide–water mixture, adding an excess of 75 per cent sulphuric acid and leaving for two hours. Water was then added to form a 6 per cent acid solution and the mixture refluxed for 24 h. The polystyrene residue was isolated by filtration and washing, dissolving in benzene and reprecipitating in methanol. Infra-red analysis showed no contamination with cellulose or cellulose acetate.

### Fractionation

Both the polystyrene samples were fractionated by the column elution method which was originally developed by Baker and Williams<sup>1</sup>, and has recently been shown by different authors<sup>2,3</sup> to yield very accurate results. The experimental technique, in its essential details, corresponded to the one described by Breitenbach, Burger and Schindler<sup>2</sup>.

The glass column inside the aluminium mantle was of 25 mm diameter and of 350 mm length, and was heated to 60°C at the top and kept at 15°C at the bottom. A coarse grade of Celite was used as a filling material. The elution was performed with a benzene–ethanol mixture, its concentration gradient being obtained by a constant volume mixer of 200 ml capacity. The flow rate was adjusted with a micro needle valve to 5 ml/h. The fractions were collected automatically at constant eluate volumes of about 15 ml.

The fractions were isolated by evaporation of the eluant and drying of the residue in a vacuum at elevated temperature. The fractions were characterized by single point measurements of the specific viscosities,  $\eta_s$ , in toluene at 30°C and the intrinsic viscosities were obtained by<sup>4</sup>

$$[\eta] = \eta_s / c (1 + 0.28\eta_s)$$

The molecular weights were calculated by the relationship given by Fox and Flory<sup>5</sup>

$$[\eta] = 9.77 \times 10^{-5} M_v^{0.73}$$

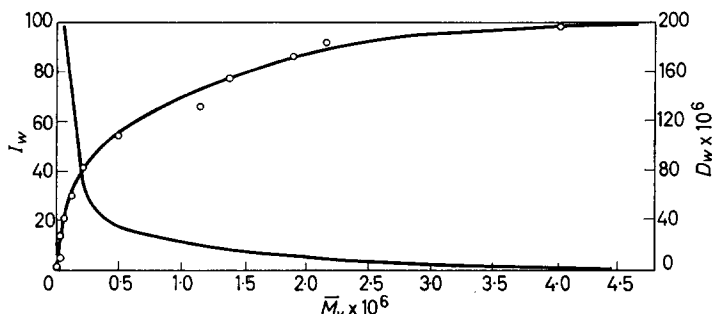


Figure 1—Cumulative and differential molecular weight distribution for polystyrene from mutual radiation graft copolymer

## RADIATION INITIATED GRAFT COPOLYMERS

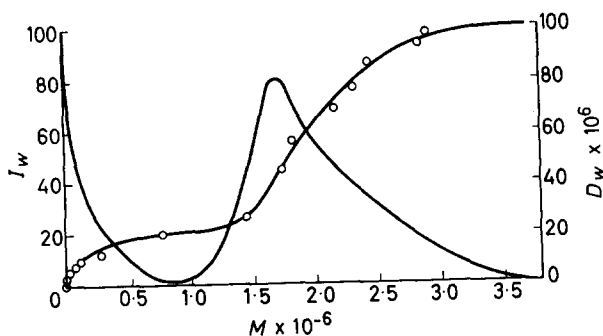


Figure 2—Cumulative and differential molecular weight distribution for polystyrene from pre-irradiation graft copolymer

The results of the fractionations are summarized in *Tables 1* and *2*, and the integral and differential molecular weight distribution curves of both samples are shown in *Figures 1* and *2*. Weight-average and number-average molecular weights of the samples were obtained graphically<sup>6</sup>, the  $M_w$  being equal to the area between the ordinate and the integral distribution curve, and  $1/M_n$  being accessible by integration of the plot of cumulative weight percentages versus the reciprocal molecular weights of the fractions.

Table 1. Fractionation of mutual heterogeneous polystyrene

Fraction number	$W$ $Wt$ (mg)	$W_t$ $Wt$ %	$I_{(w)}$	$[\eta]$	$\bar{M}_v$
1-9	4.2	2.65	1.325	0.0903	11 600
10-11	2.8	1.77	3.535	0.173	28 000
12*	10.9	6.87	7.855		
13	8.5	5.36	13.970	0.250	46 600
14	13.3	8.39	20.845	0.340	71 000
15	17.5	11.03	30.555	0.538	133 000
16	17.9	11.29	41.715	0.745	208 000
17	19.9	12.55	53.635	1.40	493 000
18	19.4	12.23	66.025	2.61	1 160 000
19	17.7	11.16	77.72	3.00	1 400 000
20	8.4	5.30	85.95	3.76	1 910 000
21	11.2	7.06	92.13	4.13	2 170 000
22	6.9	4.35	97.835	6.51	4 060 000
	158.6	100.01			

\*Sample destroyed before analysis completed.

From the graphic representations of the results it is obvious that the preparation method has a pronounced influence on the form of the molecular weight distribution of the grafted side chains. The distribution of the sample prepared by the mutual irradiation technique is very broad with the emphasis on the low molecular weight side. The calculated average

Table 2. Fractionation of pre-irradiated heterogeneous polystyrene

Fraction number	$W$ $Wt (mg)$	$W_i$ $Wt \%$	$I_{(w)}$	$[\eta]$	$\bar{M}_v$
1-8	2.3	0.87	0.435	0.017	1 210
9-10	3.9	1.48	1.610	0.036	3 270
11-12	1.7	0.64	2.670	0.053	5 560
13-15	3.0	1.14	3.560	0.072	8 400
16	2.5	0.95	4.605	0.128	18 600
17	2.3	0.87	5.515	0.171	27 700
18	3.0	1.14	6.520	0.257	48 400
19	3.8	1.44	7.810	0.355	75 300
20	4.3	1.63	9.345	0.482	115 000
21	10.3	3.90	12.110	0.933	282 000
22	31.0	11.75	19.935	1.96	783 000
23	4.0	1.52	26.570	3.06	1 440 000
24	41.0	15.54	35.100	3.11	1 470 000
25	12.2	4.62	45.180	3.51	1 740 000
26	44.1	16.71	55.845	3.62	1 810 000
27	5.6	2.12	65.260	3.63	1 820 000
28	17.4	6.59	69.615	4.24	2 250 000
29	21.0	7.96	76.890	4.30	2 300 000
30	29.0	10.99	86.365	4.48	2 430 000
31	7.7	2.92	93.320	5.01	2 830 000
32	13.6	5.15	97.355	5.10	2 900 000
	263.7	99.94			

values of the molecular weight were  $M_w = 8.3 \times 10^5$  and  $M_n = 9.0 \times 10^4$  yielding a ratio as high as  $M_w/M_n = 9.2$ .

The differential form of the molecular weight distribution of the sample prepared by pre-irradiation technique shows distinctly that the overall distribution can be described by the superposition of two distributions. The one distribution, including the low molecular weight part, is again very broad with  $M_w/M_n = 15.0$  ( $M_w = 1.98 \times 10^5$  and  $M_n = 1.32 \times 10^4$ ). The second distribution, which comprises about 80 per cent of the total weight, is rather narrow with  $M_w/M_n = 1.09$  ( $M_w = 1.99 \times 10^6$  and  $M_n = 1.83 \times 10^6$ ). The total sample had a  $M_w = 1.63 \times 10^6$ ,  $M_n = 5.7 \times 10^4$  and  $M_w/M_n = 28.6$ .

#### DISCUSSION

The broad single-peak distribution found with the mutual sample is not unexpected. It is known that with the film thickness and monomer-solvent mixture used the graft polymerization is diffusion controlled. The average chain length reached will be dependent on the distance of the growth site from the film surfaces resulting in the broad spectrum of chain lengths actually found.

The two-peak molecular weight distribution of the polystyrene side chains produced by the pre-irradiation process is quite different from the mutual product. The 20 per cent of polymer contained in the low molecular weight portion has a very broad distribution and is presumably formed from the growth and mutual termination of radical chains present in the more mobile, more accessible regions of the polymer. More than 97 per cent

of the radicals are present in this state. The 80 per cent of very high molecular weight polymer must be due to the slow growth of a very small proportion of radicals, trapped probably in crystalline regions of the film. It is possible that these continue to grow until the sample tubes are opened and the chains terminated due to the addition of solvent. Since the trapped radicals are all present at the beginning and probably start growing at similar times, this mechanism would account for both the very high molecular weight and the comparatively narrow distribution. It is interesting to note that very similar differences were recently reported<sup>7</sup> for polyacrylamide produced by the mutual and pre-irradiation polymerization of acrylamide crystals.

Since we have a good measure of the number average molecular weights of the side chains it is possible to calculate the  $G$  value for grafted chains with both methods of preparation. The data yield values of  $G_{(\text{chains})}$  per 100eV as 1.04 for the mutual technique and 1.12 for the pre-irradiation. The closeness of the two values and the slightly larger value for the pre-irradiation are somewhat surprising. It is known<sup>8</sup> that the monomer, when present during the irradiation, exerts a strong protective effect on the cellulose acetate. This, plus the fact that a considerable number of radicals probably terminate in the swollen film without adding monomer, to any extent, would account for the lower efficiency of the mutual process under the conditions used.

The pre-irradiation was carried out at  $-78^{\circ}\text{C}$  and the monomer-solvent mixture was also admitted at this low temperature; these conditions apparently lead to the efficient use of the trapped radicals and help bring the  $G$  values for the two processes closer together. It is of interest, also, that the pre-irradiation preparation only produced 0.15 g (5.2 per cent of total) of homopolystyrene. This indicates that at  $-78^{\circ}\text{C}$  the trapped radicals were almost entirely macroradicals.

*The authors gratefully acknowledge the financial support of this investigation by the Celanese Corporation of America and the U.S. Army Research Office (Durham). We would also like to thank Mrs Jane Graper for her help with the experimental work.*

Camille Dreyfus Laboratory,  
Research Triangle Institute,  
Durham, North Carolina, U.S.A.

(Received November 1963)

#### REFERENCES

- <sup>1</sup> BAKER, C. A. and WILLIAMS, R. J. P. *J. chem. Soc.* **1956**, 2352
- <sup>2</sup> BREITENBACH, J. W., BURGER, H. G. and SCHINDLER, A. *Mh. Chem.* **1962**, **93**, 160
- <sup>3</sup> SCHULZ, G. V., SCHOLZ, A. and FIGINI, R. V. *Makromol. Chem.* **1962**, **57**, 220
- <sup>4</sup> SCHULZ, G. V. and SING, G. *J. prakt. Chem.* **1942**, **161**, 161
- <sup>5</sup> FOX, T. G. and FLORY, P. J. *J. Amer. chem. Soc.* **1951**, **73**, 1915
- <sup>6</sup> MUSSA, C. *J. Polym. Sci.* **1958**, **28**, 596
- <sup>7</sup> BAYSAL, B., ADLER, G., BALLANTINE, D. and GLINES, H. *Polymer Letters*, **1963**, **1**, 257
- <sup>8</sup> STANNETT, V. *U.S. A.E.C. Publication, TID 7643*, p 259-267. November 1962

# Proton Spin Lattice Relaxation and Mechanical Loss in a Series of Acrylic Polymers

J. G. POWLES, B. I. HUNT and D. J. H. SANDIFORD

*Measurements are reported of the proton spin lattice relaxation time,  $T_1$  (effective frequency 35 Mc/s), and for the dynamic mechanical loss (at about 200 c/s) for a series of acrylic polymers with a variety of  $\alpha$  main chain and of side chain substituents. The highest temperature  $T_1$  minimum can always be associated with the main (softening) mechanical loss peak. Lower temperature  $T_1$  minima can usually be associated with the presence of particular groups, e.g. if a methyl side group is present there is a  $T_1$  minimum (for our frequency) at about 260° K. An  $\alpha$ -methyl group gives a  $T_1$  minimum below 90° K. In neither case is there an associated mechanical loss. Bulkier groups, e.g. ethyl give  $T_1$  minima at a slightly higher temperature together with a mechanical loss process. A phenyl side group gives no obvious effect whereas a flexible cyclohexyl group gives interesting effects in both  $T_1$  and  $\tan \delta$ .*

WE HAVE measured the proton spin lattice relaxation time,  $T_1$ , as a function of temperature for a series of acrylic polymers with a variety of  $\alpha$  main chain and side chain substituents. The lower temperature limit was 77° K and the upper temperature limit was only determined by thermal decomposition of the material. The apparatus has been described elsewhere<sup>1</sup>. The measurements were made at a resonance frequency,  $\nu_r$ , of 21.5 Mc/s by the 90°, 90° pulse method. The recovery of longitudinal magnetization was always exponential. We have also measured the dynamic mechanical losses in the frequency region of about 200 c/s by the vibrating reed method<sup>2</sup>. For some of the mechanical measurements the samples were filled with 66 per cent 'Tufknit'<sup>3</sup>. This reduces the losses and allows the main absorption peak to be exactly determined. It can be shown to have negligible effect on the positions of  $\tan \delta$  maxima<sup>3,4</sup>. For lower temperatures, below the main loss region, mechanical measurements were made on the *same* material as used for the n.m.r. work. Some of the mechanical results at temperatures between 100° and 400° K are those of Hoff *et al.*<sup>5</sup>. The preparation of the polymethylmethacrylate samples is described elsewhere<sup>6</sup>. The other samples were prepared as described in reference 5.

The spin lattice relaxation time is expected to depend on the rate of molecular motion,  $\nu_c = 1/2\pi\tau_c$ , where  $\tau_c$  is the correlation time for the motion through the formula<sup>7,8</sup>

$$\frac{1}{T_1} = \frac{1}{1.42 T_{1\text{min}}} \left[ \frac{\nu_r/\nu_c}{1 + (\nu_r/\nu_c)^2} + \frac{4\nu_r/\nu_c}{1 + (2\nu_r/\nu_c)^2} \right] \quad (1)$$

provided there is no distribution of correlation times. There is a minimum of  $T_1$  when  $\nu_c = 1.62\nu_r$ , which is 35 Mc/s in this case. If there are several distinct molecular motions, several more or less distinct  $T_1$  minima should be observed (see figures) and the right hand side of equation (1) can be

replaced by a sum of such terms. It is safe to get a  $\nu_c(T)$  value from a  $T_1$  minimum value but the deduction of  $\nu_c(T)$  from other values of  $T_1$  is more subtle. In our measurements we always found that *all* the protons relaxed at the same rate even though, as seen below, we have often associated a  $T_1$  minimum with the motion of a particular group of protons.

For the mechanical measurements a peak of the mechanical loss ( $\tan \delta$ ) curve means that  $\nu_c$  is practically equal to the frequency of measurement at that temperature.

The  $T_1$  and mechanical results for a commercial polymethylmethacrylate (PMMA) in *Figure 1* have been given elsewhere<sup>9</sup> but are included for

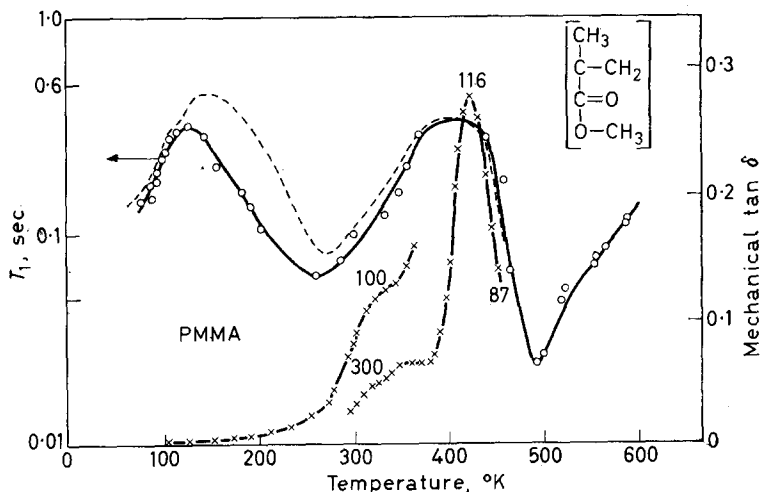


*Figure 1*—Proton spin lattice relaxation time,  $T_1$ , at 21.5 Mc/s and mechanical loss,  $\tan \delta$ , at the frequencies indicated on the curves as a function of absolute temperature for a sample of commercial polymethylmethacrylate. The mechanical loss curve which includes the principal loss maximum is for material diluted with 66 per cent Tufknit<sup>9</sup>. The lower temperature curve is for the pure polymer. The dashed curve is Kawai's  $T_1$  result<sup>10</sup>

comparison. *Figures 2 to 11* show the  $T_1$  and  $\tan \delta$  results for a series of similar polymers in which the  $\alpha$  group may be H,  $\text{CH}_3$ ,  $\text{C}_2\text{H}_5$  or Cl and the terminal group of the side chain may be  $\text{CH}_3$ ,  $\text{C}_2\text{H}_5$ ,  $n\text{-C}_4\text{H}_9$ , phenyl or cyclohexyl. Earlier measurements by Kawai<sup>10</sup> on PMA (polymethylacrylate), PMMA, PEA (polyethylacrylate), PEMA (polyethylmethacrylate) and Pn-BMA (poly-*n*-butylmethacrylate) are included on the figures for comparison. Generally our results and Kawai's agree quite well although his  $T_1$  values at low temperatures tend to be rather larger. We feel that our results are rather more accurate than Kawai's owing to our improved apparatus, for instance we think we always see *all* the protons since our pulse length and recovery time are very short<sup>1</sup>. Moreover we feel it is very valuable to compare n.m.r.  $T_1$  measurements and mechanical measurements for the *same* sample. The extension of the measurements to other sub-

## PROTON SPIN LATTICE RELAXATION

stituents including C1, phenyl and cyclohexyl has introduced several new features which we discuss below.

In all cases, except the cyclohexyl derivatives (*Figures 10 and 11*), the highest temperature minimum of  $T_1$  and the main peak in  $\tan \delta$  are readily associated with the softening or  $\alpha$  process, presumed to be connected with large scale motions of the main chain. The interpretation of similar

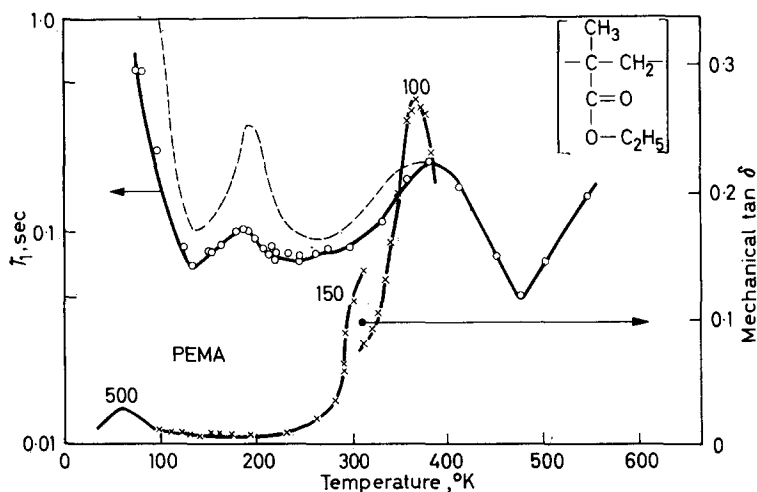


Figure 2—As Figure 1 but for polyethylmethacrylate

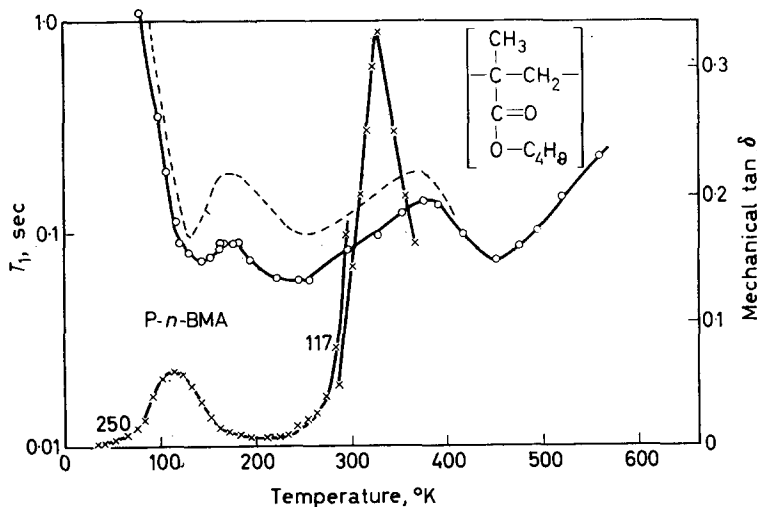


Figure 3—As Figure 1 but for poly-*n*-butylmethacrylate

mechanical data for these compounds has been discussed by Hoff, Robinson and Willbourn<sup>5</sup>. The difference in temperature for the  $T_1$  minimum where  $\nu_c \approx 3.5 \times 10^7$  c/s and the  $\tan \delta$  maximum (where  $\nu_c \approx 10^2$  c/s) varies from

about 66° for PMMA and PMCIA (polymethyl  $\alpha$ -chloroacrylate), about 80° for PMA and PEA to about 105° for PEMA and PECIA (polyethyl  $\alpha$ -chloroacrylate). The corresponding  $T_1$  minimum in PPhMA (polyphenylmethacrylate) was not observed owing to decomposition. In PchMA (polycyclohexylmethacrylate) and PchCIA (polycyclohexyl  $\alpha$ -chloroacrylate) this

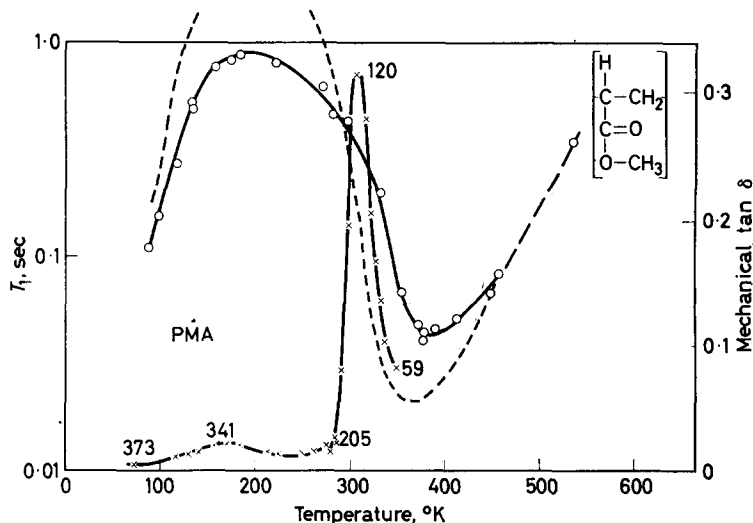


Figure 4—As Figure 1 but for polymethylacrylate

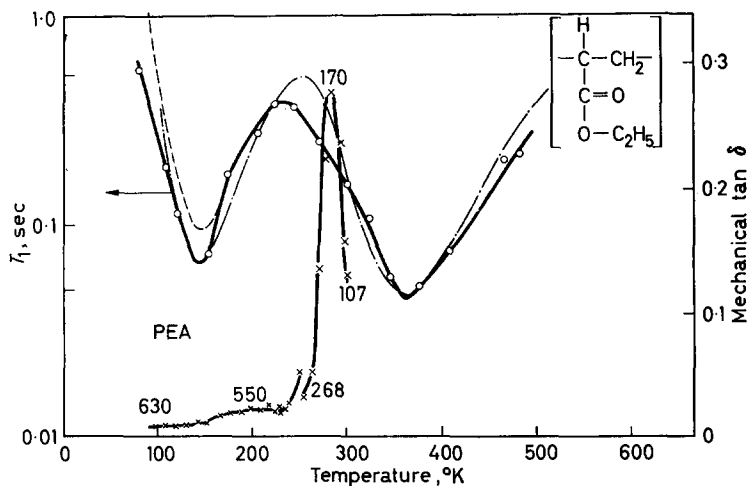


Figure 5—As Figure 1 but for polyethylacrylate, the chain-dotted curve is a theoretical one discussed on page 512

$T_1$  minimum is obscured by overlap of another process as discussed below. If one assumes that

$$\nu_c = \nu_0 \exp -\Delta E/RT \quad (2)$$



the temperature shifts mentioned above correspond to plausible  $\Delta E$  values.  $T_{1\text{min}}$  values in the range 0.02 to 0.07 sec are typical of values encountered for reorientation for these proton groups. We have not attempted to correlate with n.m.r. line narrowing data, which at least fixes the temperature at which  $\nu_c \approx 10^4$  c/s, and other mechanical and dielectric data because the measurements are available for only a few of these polymers (for such an analysis of PMMA see reference 9).

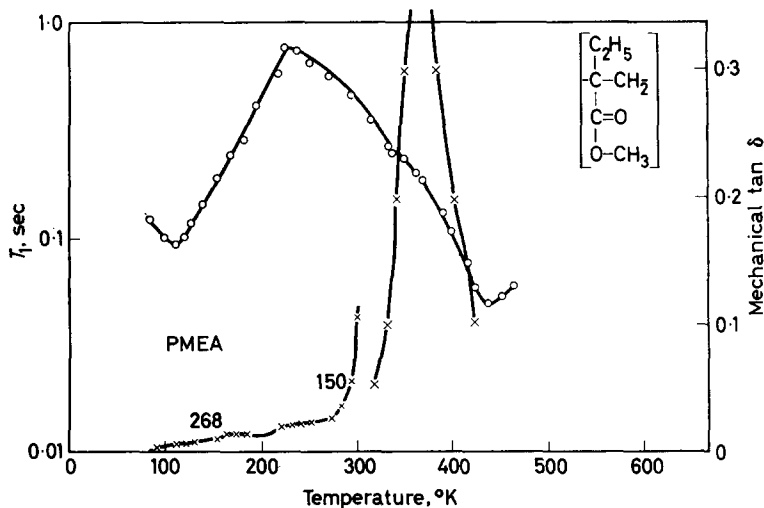


Figure 6—As Figure 1 but for polymethylethacrylate

The lower temperature  $T_1$  minima are readily associated with the presence of a particular side group, as suggested by Kawai<sup>10</sup>.

A  $T_1$  minimum near 260°K is associated with  $\alpha$ -methyl group reorientation probably mainly about the  $C_3$  axis of symmetry, which can occur without main chain motion. This minimum is present in PMMA, PEMA, *Pn*-BMA, PPhMA and PchMA but is notably absent when the  $\alpha$ -methyl group is replaced by H or  $C_2H_5$  or Cl as in PMA, PEA, PMEa, PMClA, PEClA and PchClA. The temperature at which this minimum occurs is more constant than for that associated with main chain motion and the barrier to reorientation may therefore be largely controlled by forces internal to the molecule. Substitution of the larger ethyl group on the main chain as in PMEa (polymethylethacrylate) (Figure 6) may be expected to increase the hindrance to reorientation of this group. If the increase is moderate the temperature at which the  $T_1$  minimum occurs should increase but it should be of comparable intensity. For this latter reason the indication of a weak relaxation process at about 320°K in PMEa is unlikely to be due directly to the ethyl group. The rather rounded upper minimum in this substance, as compared with that in PMMA or PEMA suggests that the  $\alpha$ -ethyl group is so restricted that it can only move when the main chain does, so that the upper minimum really includes both processes. Alternative explanations are given below.

When the side chain is terminated by a methyl group a  $T_1$  minimum usually occurs below  $77^\circ\text{K}$  as seen in PMMA, PMA and PMCIA and is therefore associated with reorientation of this group, probably again about the  $C_3$  axis. An exception to this rule is PMEA. We can associate the minimum at  $110^\circ\text{K}$  with the side chain methyl, but at a higher temperature than usual because of increased hindrance to its reorientation occasioned by the bulky  $\alpha$ -ethyl group. On the other hand the terminal methyl of the ethyl group may well have freedom of reorientation comparable to that of an ester methyl group and so give a  $T_1$  minimum at low temperatures. The  $T_1$  minimum at  $110^\circ\text{K}$  would then be at least partially attributed to the  $\alpha$  ethyl group. The rest of it, or possibly an even lower temperature  $T_1$  minimum, would then be due to the ester methyl group (see below) and this would make PMEA consistent with PMMA etc. More simply one might suggest that an ethyl group gives a  $T_1$  minimum at  $110^\circ\text{K}$  whether it is on the side or the main chain. This makes PMEA consistent with PEMA and PEA.

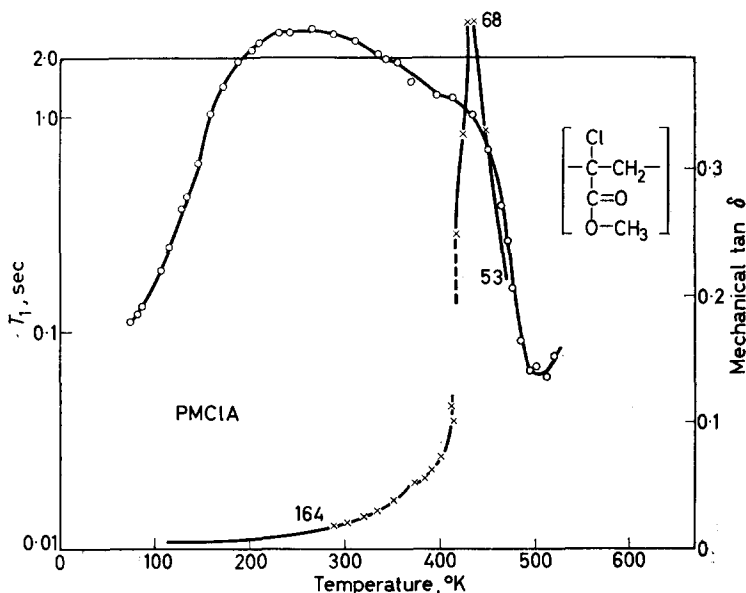


Figure 7—As Figure 1 but for polymethyl  $\alpha$ -chloroacrylate

With the more bulky ethyl group terminating the side chain the corresponding minimum moves up to about  $135^\circ\text{K}$  as in PEMA, PEA and PECIA and is presumed to be due to motion of all or part of the ethyl group. The even more bulky *n*-butyl group moves the minimum up only slightly to about  $145^\circ\text{K}$  as in *Pn*-BMA. The decreasing effectiveness of bulk in increasing the temperature of the  $T_1$  minimum no doubt reflects the increasing internal mobility of the group so that again it may be only part of the group reorienting, probably the methyl group. Even longer flexible substituents are therefore not expected to raise the temperature of this minimum appreciably.

PROTON SPIN LATTICE RELAXATION

The polymer containing a phenyl group (*Figure 9*) shows neither a characteristic  $T_1$  minimum nor a clearly defined mechanical loss process at low temperatures to be associated with the phenyl. Presumably the bulky rigid phenyl group is not able to reorient by large angles unless the main chain moves. The ' $\alpha$ -methyl'  $T_1$  minimum is broader than in the other compounds.

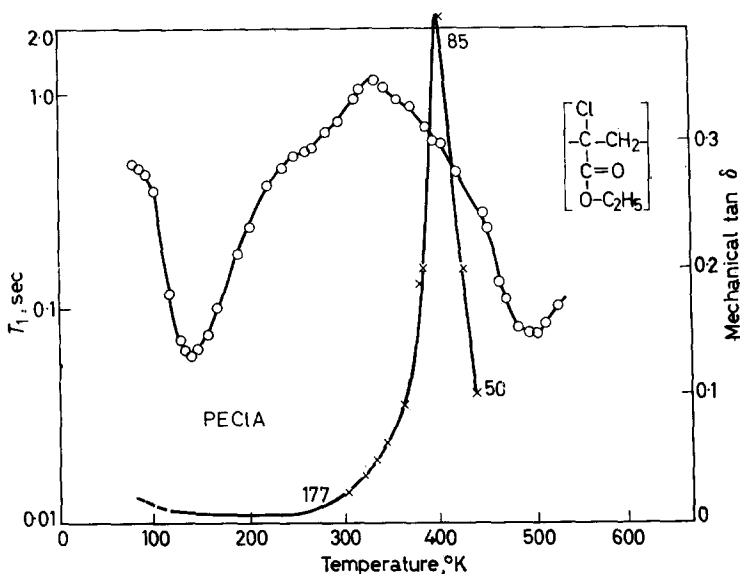


Figure 8—As Figure 1 but for polyethyl  $\alpha$ -chloroacrylate

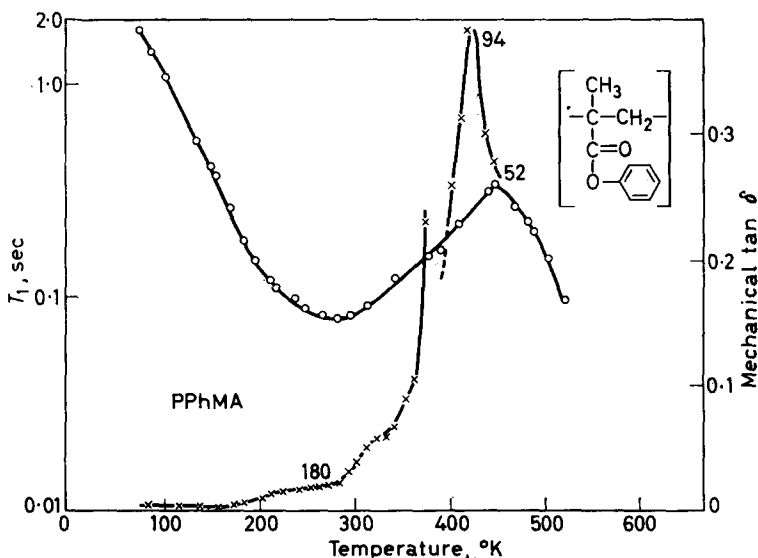


Figure 9—As Figure 1 but for polyphenylmethacrylate

In the cyclohexyl containing compounds PchMA and PchCIA the well known<sup>5,11</sup> mechanical loss maximum at 250°K and 230°K for about 100 c/s is seen in *Figures 10* and *11*. The apparent activation energy for this process, presumed to be associated with the internal flexibility of the cyclohexyl group, is 11 kcal mole<sup>-1</sup>. Consequently a  $T_1$  minimum (corresponding to  $\nu_c \approx 3.5 \times 10^7$  c/s) is expected at about 440°K which is up near the softening point of the material. We take it therefore that the unusual broad flat high temperature minimum in PchMA is due to two close processes, the cyclohexyl internal motion and the main chain motion which are still to some extent distinguishable at the highest temperatures at which the material exists. The same interpretation is probably valid for PchCIA at the higher temperatures where again one seems to have the beginning of a rather broad minimum. We had a similar but less certain case of this effect in PMEA, discussed above.

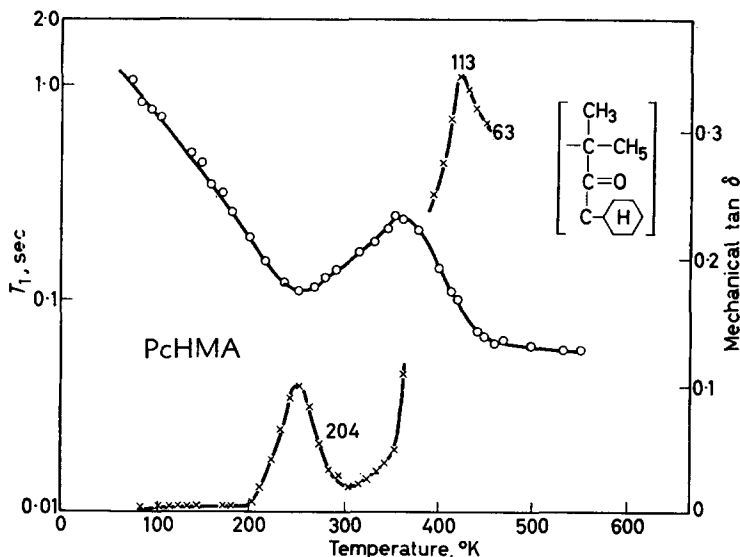


Figure 10—As Figure 1 but for polycyclohexylmethacrylate

Generally speaking it is possible to fit the experimental curves to equation (1) suitably generalized to a sum of such terms. The fit is by no means perfect and an example of a best fit assuming an Arrhenius type temperature dependence for the  $\nu_c$ s as in equation (2) is shown in *Figure 5*. This was obtained by assuming the  $T_{1\text{min}}$  values and temperatures and getting the best fit for equations (1) and (2) by minimizing the sum of squares of the discrepancies in  $T_1^{-1}$  for fifty points, using a computer. For PEA this gave  $\Delta E$  values of 15.8 and 3.88 kcal mole<sup>-1</sup> for the upper and lower minima respectively. These  $\Delta E$  values cannot be interpreted immediately as true activation energies because of the possible effect of distributions of correlation times<sup>9,12</sup>. Equations (1) and (2) together correspond to almost

symmetrical  $T_1$  curves at high temperatures on the figures. Up near the softening point one might expect  $\nu_c$  to increase more rapidly than exponentially with increasing temperature. The high temperature side of the upper  $T_1$  minima should therefore curve noticeably upwards. In fact it curves markedly downwards in PMMA and is almost linear in PEMA, Pn-BMA and PEA. This is unlikely to be explained by a distribution of correlation times<sup>12</sup>. It might be associated with well known peculiarities in behaviour of liquid polymers<sup>13</sup>. Fuller investigation of this by going to higher temperatures is frustrated by decomposition of the material.

In PECIA (Figure 8) a curving over of the  $T_1$ /temperature curve occurs at the low temperatures although no further  $T_1$  minimum below 77°K is anticipated in view of the chemical structure unless it is due to reorientation of the terminal methyl of the ethyl group which, however, is not indicated in PEMA or PEA.

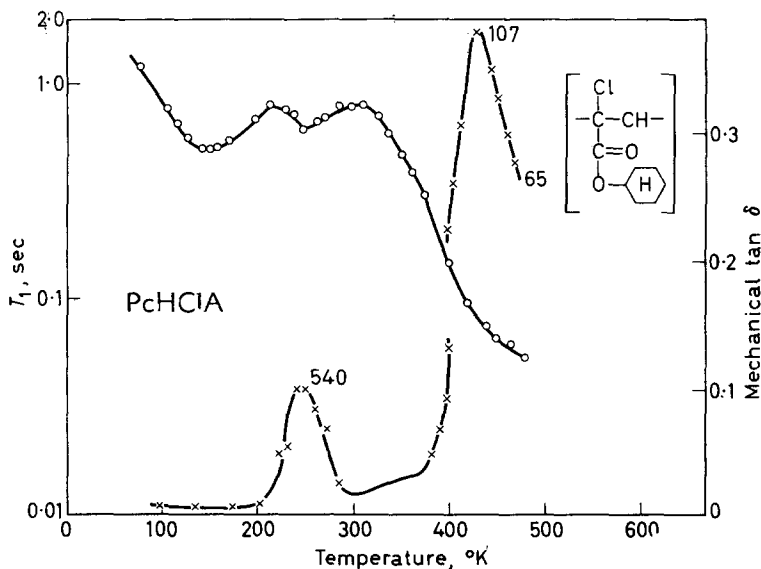


Figure 11—As Figure 1 but for polycyclohexyl  $\alpha$ -chloroacrylate

As discussed elsewhere<sup>9</sup> for PMMA it is not possible to correlate the lower temperature  $T_1$  minima with even lower temperature mechanical loss data in a satisfactory manner. For PEMA the mechanical peak at 60°K might be associated with the ethyl  $T_1$  minimum at 136°K. However, the pronounced  $\tan \delta$  peak in Pn-BMA at 115°K can hardly be connected with the  $T_1$  minimum at 143°K due to the butyl group, owing to the combination of small change in temperature and large frequency ratio. It is possible both in PEMA and Pn-BMA that  $T_1$  is most sensitive to motion of part of the group, say the methyl group, whereas the mechanical measurements are sensitive to different motions. This would then be consistent with PMMA where no mechanical loss peak is observed and is not expected for methyl  $C_3$  reorientation. It is not possible to correlate these

fairly strong low temperature mechanical processes in PEMA and *Pn*-BMA with  $\alpha$  methyl group motion since the  $T_1$   $\alpha$ -methyl group minimum is at the same temperature in both PEMA and *Pn*-BMA whereas the mechanical maxima are at considerably different temperatures. In PMA and PEA there are mechanical subsidiary maxima at 166° and 200°K respectively with activation energy  $\sim 7$  kcal mole<sup>-1</sup>. They should therefore be at about 450°K for  $3.5 \times 10^7$  c/s and so in  $T_1$  will be confounded with the softening minimum and not observed. The suspected mechanical process in PECIA below 100°K may possibly be associated with the weak and uncertain process in proton  $T_1$  at 280°K. If that is so, the analogous 60°K mechanical process in PEMA may also have a corresponding  $T_1$  process but it is obscured by the strong relaxation of the  $\alpha$ -methyl group.

An interesting feature of the replacement of the  $\alpha$ -methyl group by a chlorine atom which is of comparable size is seen by comparing PchMA and PchCIA (*Figures 10 and 11*). In the absence of the strong relaxation due to the methyl group ( $1/T_{1,\text{min.}} \simeq 9 \text{ sec}^{-1}$ ) in PchMA two weaker relaxation processes appear ( $1/T_{1,\text{min.}} \simeq 2 \text{ sec}^{-1}$ ) in PchCIA. These possibly could be due to a further manifestation of the flexibility of the cyclohexyl group besides that giving the strong mechanical loss at 230°K. In PchMA both processes would be obscured by the  $\alpha$ -methyl minimum. This interpretation, rather than that it is associated with a small amplitude movement of the C—Cl bond which might relax the protons, is reinforced by the absence of a clear  $T_1$  process in that temperature range in PMCIA (*Figure 7*). On the other hand there is a possible  $T_1$  relaxation process at a similar temperature, 260°K, in PECIA.

We have discussed the motion of individual groups of protons although in fact all the protons relax. This is to be expected because firstly the protons are so close in these substances that the protons in one moving group produce sufficiently strong magnetic fields at all the others to relax them also. Secondly the inactive protons would in any case be relaxed by the active protons by spin diffusion.

Clearly the interpretation of both  $T_1$  and  $\tan \delta$  is satisfactory in general for this series of polymers. On the other hand there are several important matters of detail, some of which we have enumerated, which remain to be explained. There is little doubt that deuteration of selected groups of protons would help in the interpretation of  $T_1$ , as was found to be the case in polypropylene<sup>14</sup>.

*Particular thanks are due to Miss D. A. Thomas for careful preparation and measurement of specimens used in the mechanical investigations.*

*Physics Department,  
Queen Mary College (University of London),  
Mile End Road, London E.1.*

*Research Department,  
I.C.I. Plastics Division,  
Welwyn Garden City, Herts.*

*(Received November 1963)*

## PROTON SPIN LATTICE RELAXATION

---

### REFERENCES

- <sup>1</sup> MANSFIELD, P. and POWLES, J. G. *J. sci. Instrum.* 1963, **40**, 232
- <sup>2</sup> ROBINSON, D. W. *J. sci. Instrum.* 1955, **32**, 2
- <sup>3</sup> SANDIFORD, D. J. H. and THOMAS, D. A. *Kolloidschr.* 1962, **181**, 4
- <sup>4</sup> TAKAYANAGI, M. *Mem. Fac. Engng Kyushu*, 1963, **23**, 1
- <sup>5</sup> HOFF, E. A. W., ROBINSON, D. W. and WILLBOURN, A. H. *J. Polym. Sci.* 1955, **18**, 161
- <sup>6</sup> POWLES, J. G., STRANGE, J. H. and SANDIFORD, D. J. H. *Polymer, Lond.* 1963, **4**, 401
- <sup>7</sup> BLOEMBERGEN, N., PURCELL, E. M. and POUND, R. V. *Phys. Rev.* 1948, **73**, 679
- <sup>8</sup> KUBO, R. and TOMITA, K. *J. phys. Soc. Japan*, 1954, **9**, 888
- <sup>9</sup> POWLES, J. G. and MANSFIELD, P. *Polymer, Lond.* 1962, **3**, 337
- <sup>10</sup> KAWAI, T. *J. phys. Soc. Japan*, 1961, **16**, 1220
- <sup>11</sup> HEIJBOER, I. J. *Kolloidschr.* 1960, **171**, 7
- <sup>12</sup> POWLES, J. G. IUPAC Symposium Report, Wiesbaden, October 1959
- <sup>13</sup> POWLES, J. G., HARTLAND, A. and KAIL, J. A. E. *J. Polym. Sci.* 1961, **55**, 361
- <sup>14</sup> POWLES, J. G. and MANSFIELD, P. *Polymer, Lond.* 1962, **3**, 340

# *Solution and Bulk Properties of Branched Polyvinyl Acetates IV—Melt Viscosity*

V. C. LONG\*, G. C. BERRY† and L. M. HOBBS‡

*The melt viscosities of some randomly branched and some comb shaped branched polyvinyl acetate fractions were compared to the viscosities of linear polymer over a range of molecular weights. The melt viscosity of the branched polymer was usually higher than that of linear polymer of the same weight average molecular weight. The extent of this increase was related to the molecular weight of the branches but no correlation could be found which included the number of branches per molecule. This unusual behaviour is believed to be due to the fact that the length of the branches in the polymers of this study was above the critical chain length for polyvinyl acetate which made it possible for the branches to be engaged in intermolecular chain entanglements.*

THE flow behaviour of molten polymers is a subject of considerable interest, both from theoretical and practical viewpoints. Fair success has been achieved in correlating the rheology and molecular parameters for linear polymers. However, the treatment of the branching parameter has not been as successful, and it was the intention of this study to extend the present knowledge in this area.

The melt viscosities of two series of branched polyvinyl acetate fractions have been compared to the viscosity of linear material over a molecular weight range of  $4 \times 10^5$  to  $5 \times 10^6$ . The branched structures investigated were of two types, random (series 4) and comb shaped (series 6). Fractions of linear material (series 5) were studied to provide a basis of comparison for the branched polymers. The polymers used have been fully characterized in earlier publications<sup>1-3</sup> and the reader is referred to these articles for descriptions of the samples.

## EXPERIMENTAL

### (1) *Melt viscosity measurement*

The polymers used in the melt viscosity measurements were isolated from filtered benzene solutions by the freeze-drying technique. Care was taken to remove all traces of residual solvent. Cylindrical test specimens, 0.57 in. in diameter, were then moulded at 155°C in a plunger type mould.

The melt viscosities were measured with a Williams parallel plate plastometer<sup>4</sup> which had an upper plate weighing 5.0 kg. Aluminium foil was used as a parting agent. Viscosities in the range  $10^6$  to  $10^9$  poise may be measured with an error of about five per cent in the middle of the span, the error increasing toward either limit.

\*Present address: E. I. du Pont de Nemours & Co., Wilmington, Delaware.

†Present address: Mellon Institute, Pittsburgh, Pennsylvania.

‡Present address: Bennettsville, South Carolina.



The measurements were made at two temperatures. The viscosities of selected fractions of series 4 and 5 (randomly branched and linear) were measured at  $155^\circ \pm 0.5^\circ\text{C}$  in a circulating air oven<sup>5</sup>. The viscosity of grafted branched fractions of series 6 and the linear fractions of series 5 were measured at  $183^\circ\text{C}$  because of the high viscosities of the grafted polymers<sup>6</sup>. These measurements were carried out in a nitrogen atmosphere as a precaution against degradation. In addition, the samples were placed under nitrogen after evacuation prior to use to eliminate absorption of oxygen. Thermal stability was no problem at  $155^\circ\text{C}$  as evidenced by no reduction in either melt viscosity repeated on the same sample or intrinsic viscosity as measured before and after the melt viscosity measurements. At  $183^\circ\text{C}$  the linear fractions were stable within experimental error but the branched material exhibited some signs of degradation as may be seen in *Table 2*. This degradation, however, should not affect the qualitative nature of the results.

## (2) Treatment of data

The melt viscosity in poises was calculated<sup>4</sup> by

$$\eta = 8.21 \times 10^6 W / mV^2 \quad (1)$$

where  $W$  is the load on the sample in kg and  $V$  is the sample volume in  $\text{cm}^3$ . In this equation,  $m$  is the slope in  $\text{cm}^{-4} \text{sec}^{-1}$  of the linear portion of the curve obtained when the reciprocal of the plate separation to the fourth power is plotted versus time. Equation (1) has been obtained under the assumptions that the flow is essentially Newtonian for the low shear rates encountered, that there is zero radial flow at the plates, that the axial flow is negligible compared to the radial flow, that steady-state flow conditions are realized, and that the diameter to height ratio exceeds about ten. The average shear rate  $\bar{s}$  may be estimated<sup>7</sup> from

$$\bar{s} = 1.158 \times 10^6 (L^{5/2}W) (V^{3/2}\eta)^{-1} \quad (2)$$

where  $L$  cm is the plate separation. The low shear rates calculated from equation (2) ( $\bar{s}$  less than  $0.01 \text{ sec}^{-1}$ , the maximum  $\bar{s}$  occurring for samples of lowest  $\eta$ ), together with the absence of any dependence of  $\eta$  on the height to diameter ratio and experimental realization of a linear portion in the plot of  $(1/L)^4$  versus time provide support for the use of equation (1) to compute  $\eta$ . In addition, data obtained here for the linear fractions at  $155^\circ\text{C}$  fit very well with  $\eta/Mw$  data obtained by Fox and Nakayasu<sup>8</sup> at the same temperature on lower molecular weight fractions using capillary viscometers.

There still remains the possibility, however, that steady-flow conditions were not realized for some samples and that the value of  $m$  measured was in fact too high. This would be most likely to occur for the higher viscosity samples. In this case, the value of  $\eta$  reported would be too low, and would not change the character of the results, namely, increased  $\eta$  due to branching. We do not believe this latter source of error to be very important for this study.

A more serious source of error could be the presence of an impurity, hydroxyl groups for example, in the branched polymer which can cause

anomalous behaviour in some systems (see for example ref. 7). We have examined the possible presence of hydroxyl groups, the most likely contaminant, and have concluded that they can only be present in very small amounts, if at all<sup>2</sup>.

Thus, we assert that equation (1) is the correct relation for analysis of our data, and that effects to be noted are due to the structural character of the polymer chains, i.e. the type of branching present.

The melt viscosity of the linear fractions may be represented by the relation  $\eta_l = K_T \langle M \rangle_w^a$  where  $a = 3.65$  and  $\log K_T$  is  $14.47_5$  at  $155^\circ\text{C}$  and  $14.99_1$  at  $183^\circ\text{C}$ . The ratios  $\eta_{br}/\eta_l$  at constant molecular weight were determined graphically. The subscripts *br* and *l* refer to branched and linear chains respectively.

#### RESULTS AND DISCUSSION

A complete description of the molecular flow process that results in the macroscopic property of the melt viscosity of a polymeric system does not exist although progress has been made for linear polymers. It has been generally assumed that a branched polymer should exhibit a lower melt viscosity  $\eta$  than a linear chain if comparisons are made at the same molecular weight and temperature<sup>9, 10, 11, 15</sup>. The results of this study show that this is not necessarily correct, and that the ratio  $\eta_{br}/\eta_l$  can exceed unity for some types of branched structure. All ratios of  $\eta_{br}/\eta_l$  considered here are at constant temperature and molecular weight. It should be noted that Tung<sup>12</sup> has observed differences in the activation energies for the melt flow of branched and linear polyethylene that would indicate  $\eta_{br}/\eta_l > 1$  for these chains at high temperatures, as he has pointed out. This may not be a general situation, however, and Tung's results may be intimately connected with the presence of many very short chain (2 to 4C atoms) branches in polyethylene. Ratios of  $\eta_{br}/\eta_l > 1$  have also been reported for

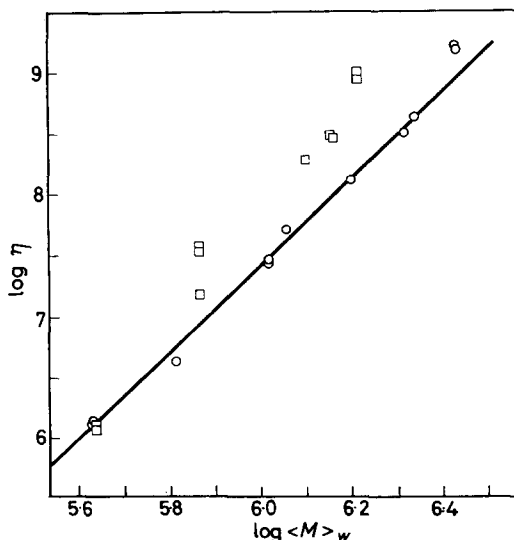


Figure 1—Melt viscosity at  $155^\circ\text{C}$  versus molecular weight:  $\square$  randomly branched polymers, series 4;  $\circ$  linear polymer, series 5

some polymers branched by irradiation, but these data are difficult to analyse since many parameters are being varied simultaneously<sup>18</sup>.

The melt viscosity data obtained here are given as a function of molecular weight in *Figures 1* and *2* and *Tables 1* and *2*. It is immediately evident that many of the branched polymers have viscosities greater than those of linear chains of the same molecular weight, and further that the effect is quite large ( $\eta_{br}/\eta_l$  ca. 10) in some cases. We will show below that existing theories

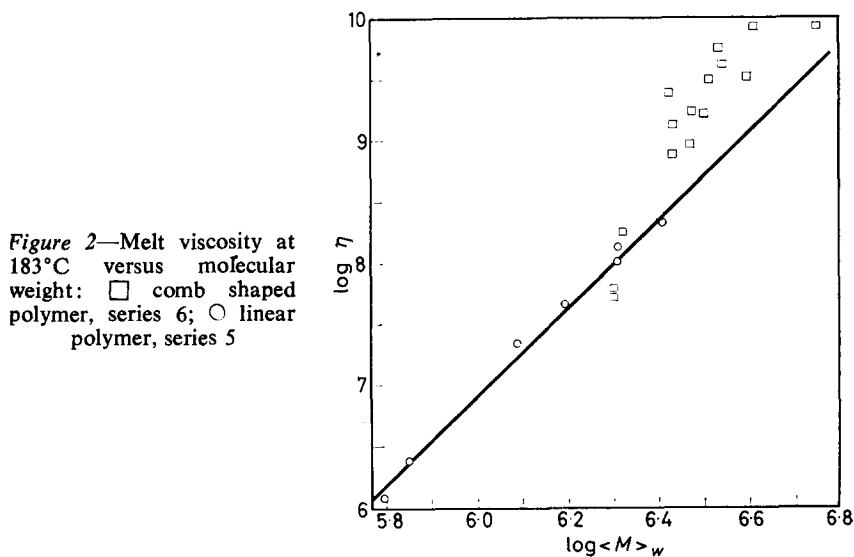


Figure 2—Melt viscosity at 183°C versus molecular weight: □ comb shaped polymer, series 6; ○ linear polymer, series 5

Table 1. Data for the linear polymer (series 5)

Fraction	$T$ (°C)	$\langle M \rangle_w \times 10^{-6}$	$\eta \times 10^{-8}$ (poise)
5-3-2	155	2.66	15.5
5-3-2	155	2.66	(15.7)†
5-2-3	183	2.53	20.5
5-3-3	155	2.17	4.41
5-3-3	183	2.17	1.37
5-3-3	183	2.17	(1.03)
Mixture*	155	2.07	3.33
5-5-3	155	1.57	1.30
5-T†	183	1.57	0.651
5-T	183	1.57	(0.610)
5-6-2	155	1.14	0.542
5-6-2	183	1.14	0.223
5-6-3	155	1.05	0.313
5-6-3	155	1.05	(0.315)
5-7-1	183	0.71	0.0249
5-7-2	155	0.65	0.0442
5-7-2	183	0.65	0.0120
5-7-4	155	0.43	0.0129
5-7-4	155	0.43	(0.0138)

\*Fractions 5-3-2 and 5-6-3 combined.

†Unfractionated polymer 5.

‡( ) denotes second measurement on a single sample.

## PROPERTIES OF BRANCHED POLYVINYL ACETATES IV

Table 2. Data for the randomly branched polymer (series 4) and the comb shaped polymer (series 6)

Fraction	$T$ ( $^{\circ}C$ )	$\langle M_{br} \rangle_w \times 10^{-6}$	$\langle M_g \rangle_w \times 10^{-3}$	$g$	$\eta \times 10^{-8}$ (poise)	$\eta_{br}/\eta_l$
4-4-2	155	1.64	78	0.58	8.92	5.65
4-4-2	155	1.64	78	0.58	(10.3)†	(6.53)
4-5-1	155	1.43	62	0.55	3.10	3.00
4-5-1	155	1.43	62	0.55	(3.13)	(3.03)
Mixture*	155	1.25	—	—	1.97	—
4-5-2	155	0.730	56	0.66	0.383	4.49
4-5-2	155	0.730	56	0.66	(0.353)	(4.14)
4-4-3	155	0.731	42	0.62	0.152	1.85
4-5-3	155	0.432	46	0.69	0.0127	1.06
4-5-3	155	0.432	46	0.69	(0.0117)	(0.98)
6-20-M	152	2.80	118	0.821	66.8	5.2
6-20-M	183	2.80	118	0.821	(9.51)	(2.9)
6-40-1	183	2.00	37.0	0.750	0.506	0.53
6-40-1	183	2.24	37.0	0.751	(0.624)	(0.66)
6-41-M	183	2.09	36.0	0.718	1.88	1.63
6-50-1	180	2.71	47.4	0.744	7.87	2.53
6-50-1	183	2.71	47.4	0.744	(7.08)	(2.35)
6-51-M	183	3.21	48.8	0.641	16.4	2.26
6-70-1	183	2.65	149.6	0.777	24.7	10.8
6-71-1	183	3.43	134	0.630	55.9	7.70
6-80-1	183	3.29	122	0.693	31.4	5.29
6-81-1	183	4.11	127	0.553	84.4	6.32
6-90-1	183	3.45	94	0.736	40.7	5.76
6-91-1	183	3.96	87.4	0.641	40.2	3.47

\*Fractions 4-4-2 and 4-4-3 combined.

†( ) denotes second measurement on a single sample.

for the melt viscosity of linear chains may not be extended in a straightforward way to explain this behaviour, as has been previously supposed<sup>14,15</sup>, and will suggest some reasons for the deficiency.

The effect of branching on the isothermal melt viscosity for systems where interchain entanglements may be ignored has been treated theoretically by Ham<sup>16</sup> in a normal coordinate calculation of the relaxation times for melt flow. This calculation yields

$$\eta'_{br}/\eta'_l = g \quad (3)$$

where the primes denote viscosities under conditions of no interchain entanglements and  $g$  is the ratio of the mean square radii of branched and linear chains under theta-conditions. The parameter  $g$  is always less than or equal to unity. The same result may be extracted from the work of Bueche<sup>17</sup> or of Zimm and Kilb<sup>18</sup>. The effects of chain entanglement may be formally introduced by defining a function  $\phi$  such that

$$\eta = \eta' \phi \quad (4)$$

In general,  $\phi$  may be a complicated function of chain length, structure, etc., but  $\phi \geq 1$ . Thus, the ratio  $\eta_{br}/\eta_l$  becomes

$$\eta_{br}/\eta_l = g\phi_{br}/\phi_l \quad (5)$$

Equation (5) anticipates that chain entanglements may be accounted for

by determining the proper dependence of the chain mobility factor on molecular weight and chain structure, as has been suggested by others<sup>16, 19, 20</sup>.

As a first approximation, one might try to carry over Bueche's method of calculating  $\phi_l$  to obtain an expression for  $\phi_{br}$  since there is nothing in that calculation explicitly requiring linearity in the chain. In so doing, one must ignore all details of the chain geometry and consider instead only conformation averaged segment density functions. Necessarily then, the only remaining parameter related to branching will be some function of averaged dimensions, such as  $g$ . In fact, Bueche<sup>15</sup> has given the result  $\eta_{br} = g^{3.5}\eta_l$ , or  $\phi_{br} = g^{2.5}\phi_l$  without providing details of the calculation. This result is in good accord with empirical results obtained by Fox and Allen<sup>14</sup> on star shaped polymers although other details do not agree. It is clear that this expression cannot fit our data, however, since  $g \leq 1$  and we find  $\eta_{br} > \eta_l$  in some cases. Moreover, examination of the data in *Table 2* reveals that samples with the same value for  $g$  may have different values for  $\eta_{br}/\eta_l$ . This indicates that any model that ignores the details of the chain geometry (e.g. number and length of branches, etc.), using instead smoothed segment density functions, cannot provide an adequate general prescription for  $\phi_{br}/\phi_l$ .

Thus, we are led to conclude that the details of the structure of the chain must have a strong effect on the flow properties, no doubt through an effect on the probability for entanglement of various segments of the chain. Simple equivalence of  $g$ , that is of average chain dimensions, does not ensure equivalence of flow properties. Other variables, such as distribution and length of branches in the structure, appear to be required for a complete description of  $\eta_{br}$ . This suggests that  $\phi_{br}/\phi_l$  could depend on some

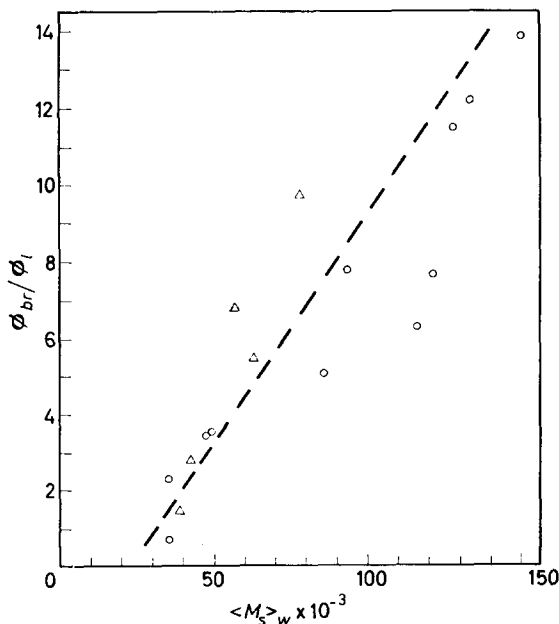


Figure 3—Ratio  $\phi_{br}/\phi_l$  calculated on  $\eta_{br}/g\eta_l$  versus the molecular weight of branches in a branched polymer:  $\triangle$  randomly branched polymer, series 4;  $\circ$  comb shaped polymer, series 6

detail of the chain geometry, such as the branch length or frequency in a comb shaped polymer, if only this parameter were varied while the main features of the chain geometry were held constant. In particular, one can vary the length of the branches in a comb shaped polymer containing a relatively few branches of length short compared to the backbone. This is the approach taken here, and *Figure 3* shows the correlation between  $\phi_{br}/\phi_l$ , calculated as  $\eta_{br}/g\eta_l$ , and the molecular weight of the branches  $\langle M_s \rangle_w$  in a comb shaped polymer. The values of  $\langle M_s \rangle_w$  are taken from Part II<sup>2</sup>. In addition, data for the randomly branched series 4 have been included in *Figure 3* since the chain geometry is not very different from that of the comb shaped polymers. Here  $\langle M_s \rangle_w = \langle M_{br} \rangle_w / (2k + 1)$  where  $k$  is the number of branches in a chain of molecular weight<sup>3</sup>  $\langle M_{br} \rangle_w$ . It is clear that a strong dependence of  $\phi_{br}/\phi_l$  on  $\langle M_s \rangle_w$  does exist, and that it yields  $\phi_{br}/\phi_l = 1$  for  $\langle M_s \rangle_w \approx 28\,000$ . The fact that this value of  $\langle M_s \rangle_w$  is in good agreement with the critical chain length of linear polyvinyl acetate determined by Fox and Nakayasu<sup>8</sup> is significant and will be commented on below. Various other correlations were attempted, e.g.  $\phi_{br}/\phi_l$  versus  $g$ ,  $k$ , etc., but these uniformly showed considerable scatter. The absence of a clear dependence of  $\phi_{br}/\phi_l$  on  $k$  at a given value for  $\langle M_s \rangle_w$  for the comb shaped polymers is surprising, but probably the data are not extensive enough or the span in  $k$  is not large enough to reveal such a dependence.

The dependence of  $\phi_{br}/\phi_l$  on the length of a branch exhibited above is evidence that the presence of branches can alter the effect of the cooperative motion of segments necessary for flow provided the branches are long enough. It has been suggested several times that the cooperative motion of segments should be enhanced in a branched structure due to the chain geometry, thus leading to a decreased viscosity<sup>9,11</sup>. This is probably correct in the absence of chain entanglements, but the very fact that the segments must experience an enhanced cooperative mode of flow can make the existence of chain entanglements more important in branched polymers. That is, the branched polymer may be more effectively trapped by its entanglements because its various arms do not allow a simple snaking motion through the entanglements. The observation that  $\phi_{br}/\phi_l$  decreases to unity as the branch length decreases to the critical chain length supports this view since this should represent the minimum chain length upon which effects due to interchain entanglements of the branches should appear. Opposing this effect, the probability for interchain entanglement must decrease with branching due to the more compact nature of the chain structure.

We suggest, then, that branching can cause an increase in the melt viscosity provided that:

- (1) the branches are long enough to become engaged in interchain entanglements, e.g. at least longer than the critical chain length, and
- (2) the chain structure is such that the chain elements have a high probability for *interchain* entanglement.

A comb polymer with very short branches is an example for which condition 1 is not fulfilled, and a star polymer with all the branches emanating from a single node provides an example for which condition 2 is not obeyed, unless the branches are very much longer than the critical chain length. It

is clear that the single parameter  $g$  will not in itself be sufficient to characterize  $\eta_{br}/\eta_l$  under these circumstances.

Obviously it would be desirable to have these ideas expressed quantitatively and to be able to give  $\phi_{br}/\phi_l$  in terms of the chain configuration, chain length, etc. Unfortunately, this problem does not appear near a general solution. The failure of the attempted modification of Bueche's results for a linear chain suggests that a considerable amount of detail about the chain configuration must be included in the calculation, and in particular that the use of conformation averaged segment density functions will not be sufficient. This will require a more precise statement about the nature of interchain entanglements.

*This paper is based on a portion of theses submitted by V. C. Long in 1958 and G. C. Berry in 1960 in partial fulfillment of the requirements of the degree of Doctor of Philosophy: a portion of this paper was presented to the International Symposium on Macromolecular Chemistry, Montreal, Canada, 31 July 1961.*

*This work was supported by the Michigan Memorial-Phoenix Project through contributions by the Goodyear Tire and Rubber Company and by the Allied Chemical and Dye Corporation through a fellowship grant to one of us (G.C.B.). We express appreciation to Dr L. H. Cragg of the University of Alberta, to Dr J. A. Manson of the Air Reduction Company and to Dr T. G. Fox of the Mellon Institute for helpful suggestions and stimulating discussions.*

Chemical Engineering Department,  
University of Michigan,  
Ann Arbor, Michigan.

(Received December 1963)

#### REFERENCES

- <sup>1</sup> HOBBS, L. M. and LONG, V. C. *Polymer, Lond.* 1963, **4**, 479
- <sup>2</sup> BERRY, G. C. and CRAIG, R. G. *Polymer, Lond.* 1964, **5**, 19
- <sup>3</sup> BERRY, G. C., HOBBS, L. M. and LONG, V. C. *Polymer, Lond.* 1964, **5**, 31
- <sup>4</sup> DIENES, G. F. and KLEMM, H. F. *J. appl. Phys.* 1946, **7**, 458
- <sup>5</sup> LONG, V. C. *Ph.D. Thesis*, University of Michigan, Ann Arbor, Michigan, 1958
- <sup>6</sup> BERRY, G. C. *Ph.D. Thesis*, University of Michigan, Ann Arbor, Michigan, 1960
- <sup>7</sup> LONGWORTH, R. and MORAWETZ, H. *J. Polym. Sci.* 1958, **29**, 307
- <sup>8</sup> FOX, T. G. and NAKAYASU, H. Abstracts of Papers, 137th Meeting of the American Chemical Society, III, April 1960
- <sup>9</sup> WEIL, L. L. *Thesis*, Columbia University, New York, N.Y., 1945
- <sup>10</sup> FOX, T. G. and LOSHACK, S. *J. appl. Phys.* 1955, **26**, 1680
- <sup>11</sup> MOORE, L. D. *J. Polym. Sci.* 1959, **36**, 155
- <sup>12</sup> TUNG, L. H. *J. Polym. Sci.* 1960, **46**, 409
- <sup>13</sup> CHARLESBY, A. and THOMAS, D. *Symposium über Makromolekullen*, 1959. I-C-8
- <sup>14</sup> FOX, T. G. and ALLEN, V. R. Preprints, Division of Polymer Chemistry, American Chemical Society, V3, No. 1, 6 (1962)
- <sup>15</sup> BUECHE, F. *J. Polym. Sci.* 1959, **42**, 551
- <sup>16</sup> HAM, J. S. *J. chem. Phys.* 1957, **26**, 625
- <sup>17</sup> BUECHE, F. *J. chem. Phys.* 1952, **20**, 1959; 1956, **25**, 599
- <sup>18</sup> ZIMM, B. H. and KILB, R. W. *J. Polym. Sci.* 1959, **37**, 19
- <sup>19</sup> FERRY, J. D. *Viscoelastic Properties of Polymers*. Wiley: New York, 1961
- <sup>20</sup> PETICOLAS, W. L. *J. Polym. Sci.* 1962, **58**, 1405

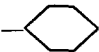
# The Anionic Polymerization of Some Alkyl Vinyl Ketones

P. R. THOMAS, G. J. TYLER, T. E. EDWARDS, A. T. RADCLIFFE  
and R. C. P. CUBBON

Five alkyl vinyl ketones branched  $\beta$  and  $\gamma$  to the vinyl group have been prepared and polymerized by free radical and anionic initiators. The anionic initiators gave rise to crystalline high melting polymers. The lithium initiated polymerization of isopropyl vinyl ketone under some conditions yielded two types of crystalline polymer. Thermal depolymerization of the crystalline poly isopropyl vinyl ketones obtained from anionic initiators indicated that the polymers contained some linkages in the chains other than those expected from 1,2 addition polymerization.

SINCE the stereospecific polymerization of  $\alpha$ -olefins<sup>1</sup> to give highly crystalline polymers, many new stereoregular polymers have been prepared not only from olefins but also from monomers containing polar groups, such as the carbonyl group. These include acrylic esters<sup>2</sup>, vinyl esters<sup>3</sup> and aldehydes<sup>4</sup>. Previous work in these laboratories led to the synthesis of crystalline polymers from *N,N*-disubstituted acrylamides<sup>5</sup>. A continuation of this study of the polymerization of carbonyl containing monomers which are branched  $\beta$  or  $\gamma$  to the vinyl group led to a study of some alkyl vinyl ketones. Five monomers were prepared and subjected to free radical and anionic polymerization. These monomers are shown in *Table 1*.

Table 1. Alkyl vinyl ketones,  $\text{CH}_2=\text{CHCOR}$

R	Boiling point °C/mm Hg	$n_D^{20}$
$-\text{CH}(\text{CH}_3)_2$	50/70	1.4188
$-\text{CH}_2\text{CH}(\text{CH}_3)_2$	62/52	1.4241
$-\text{C}(\text{CH}_3)_3$	64/100	1.4225
$-\text{CH}_2\text{C}(\text{CH}_3)_3$	58/60	1.4411
	89/20	1.4731

With the exception of *t*-butyl vinyl ketone which has been prepared previously<sup>6</sup>, the ketones were obtained by treating the appropriate acyl chloride in methylene chloride solution with ethylene and aluminium chloride. The chloroethyl ketone so obtained was subsequently dehydrochlorinated with triethylamine in dry ether solution.

The monomers were characterized by reduction to the saturated ketones and conversion of these to their semi-carbazones. When highly purified, the vinyl ketones polymerized spontaneously.



## EXPERIMENTAL

*Preparation of alkyl vinyl ketones (general procedure)*

Freshly powdered aluminium chloride (1.1 mole) was suspended in dry methylene chloride (250 ml) contained in a 5-necked reaction flask fitted with a stirrer, thermometer, gas bubbler and gas exit tube. The mixture was cooled to  $-50^{\circ}\text{C}$  and freshly distilled acyl chloride (1 mole) dissolved in dry methylene chloride (250 ml) was added slowly. The ethylene was then passed through the mixture at such a rate that the temperature did not rise above  $-25^{\circ}\text{C}$  until absorption ceased. The reaction mixture was then poured on to a mixture of crushed ice and dilute hydrochloric acid. The methylene chloride layer was separated, washed with water, dried and distilled to remove solvent. The product was then distilled under reduced pressure. During this distillation some dehydrochlorination took place.

The distillate was dissolved in 500 ml of dry ether and triethylamine (1 mole) was added. The mixture was boiled under reflux for 72 hours after which the precipitated triethylamine hydrochloride was filtered off. The ethereal solution was distilled and the product finally distilled under reduced pressure. The resulting alkyl vinyl ketone was stored over an inhibitor.

*Characterization of the monomers*

The new monomers, isopropyl—, isobutyl—, neopentyl— and cyclohexyl vinyl ketones, were characterized by palladium/charcoal reduction to the corresponding saturated ketones. The properties of the saturated ketones and their derivatives are listed in *Table 2*.

*Table 2.* Characterization of the novel alkyl vinyl ketones

Alkyl vinyl ketone $\text{CH}_2=\text{CH.CO.R}$	Properties of saturated ketone				Derivatives of saturated ketone, M.pt $^{\circ}\text{C}$		
	Found		Literature		2,4-DNP*	Oxime	Semi-carbazone
	B.pt $^{\circ}\text{C}$	$n_D^{20}$	B.pt $^{\circ}\text{C}$	$n_D^{20}$			
$-\text{CH}(\text{CH}_3)_2$	114	1.4188	114	—	111–112	—	191
$-\text{CH}_2\text{CH}(\text{CH}_3)_2$	134	1.4040	135	1.4070	—	—	138
$-\text{CH}_2\text{C}(\text{CH}_3)_3$	94/ 150 mm	1.4105	92/ 150 mm	1.4160	135	—	154–156
$-\text{C}_6\text{H}_{11}$	198	—	—	—	—	68	150

2,4-DNP is 2,4-dinitrophenylhydrazone.

*Anionic polymerization*

Toluene, free from sulphur compounds, was dried over sodium wire. The toluene was distilled off the sodium in an atmosphere of nitrogen as required. Isopropyl vinyl ketone, which was shown to be pure by gas chromatographic analysis, was dried over anhydrous sodium sulphate. The monomer was distilled under reduced pressure of nitrogen prior to use.

In a typical experiment, the required amounts of solvent and monomer were introduced into a nitrogen swept flask with hypodermic syringes. The monomer solution was stirred by a mercury sealed stirrer unit and brought to the required polymerization temperature. The initiator was introduced through a serum cap using a hypodermic syringe. The polymer was recovered by precipitation in methanol.

## RESULTS AND DISCUSSION

*Free radical polymerization*

Free radical initiation of these monomers gave, in general, polymers which melted below 100°C. Their X-ray spectra showed them to be either amorphous or very poorly crystalline. *t*-Butyl vinyl ketone, a monomer which is the most highly branched near to the carbonyl, gave the highest melting polymer. Potassium persulphate-sodium metabisulphite initiator in aqueous solution gave poly(*t*-butyl vinyl ketone) in 67 per cent yield. This product possessed an inherent viscosity measured in dichloroacetic acid of 2.0 and softened at about 90°C. It showed slight crystallinity.

*Anionic polymerization*

Anionic polymerization of these vinyl ketones in, for example, toluene solution, using lithium alkyls as initiators, gave polymers having higher softening points and improved crystallinity. Samples of poly(*t*-butyl vinyl ketone) and poly(cyclohexyl vinyl ketone) having softening points above 240°C were prepared using lithium methyl as a heterogeneous initiator. The most interesting results were, however, obtained with isopropyl vinyl ketone which gave highly crystalline polymers quite readily, even in homogeneous systems. A comparison of the X-ray spectra of poly(isopropyl vinyl ketone) obtained by free radical and anionic initiation is shown in *Figure 1*.

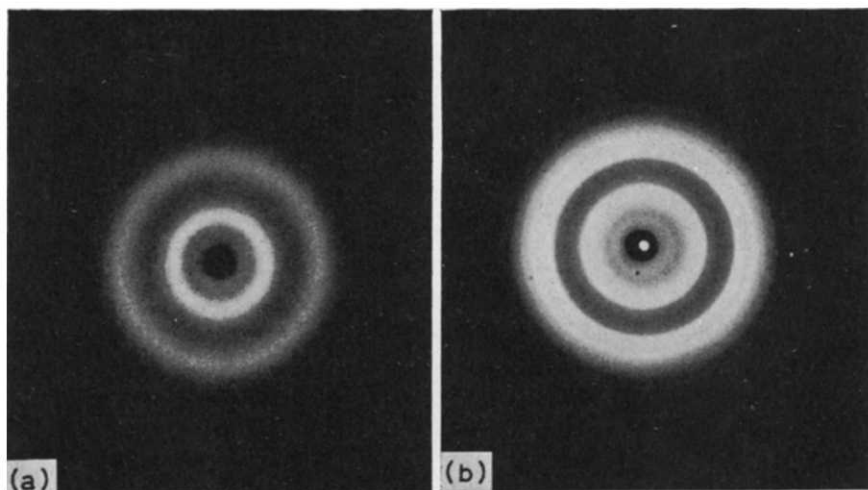


*Figure 1*—X-ray photographs of poly isopropyl vinyl ketone (a) free radical and (b) sodium hydride initiated polymer

Among initiators which gave highly crystalline polymers were lithium dust, sodium hydride, lithium borohydride, lithium methyl, lithium butyl and ethyl magnesium bromide.

The most highly crystalline samples of poly(isopropyl vinyl ketone) melted at about 220°C to a colourless liquid. The polymer depolymerized during this thermal treatment. *Figure 2* shows how the inherent viscosity

of the polymer falls with time of heating at a temperature as low as 98°C. This product was obtained by initiation with sodium hydride.

While amorphous polymer obtained by spontaneous polymerization is unchanged by this heat treatment, the crystalline polymer depolymerizes until the solution viscosity reaches a steady value. We interpret this result as meaning that while the amorphous polymer is entirely a 1,2 structure, the crystalline polymer contains a 'foreign' link in addition to the predominant 1,2 structure. The 'foreign' link is thermally unstable and is responsible for the thermal depolymerization. There was no significant difference in the infra-red spectrum between amorphous and crystalline poly(isopropyl vinyl ketone).

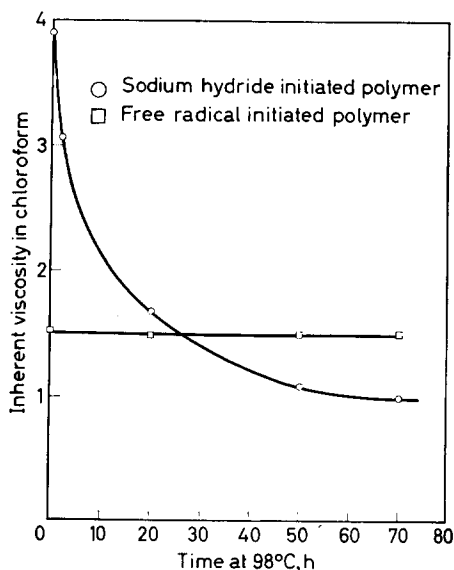


Figure 2—Depolymerization of poly isopropyl vinyl ketone at 98°C (boiling *n*-heptane)

The possibility that more than one type of propagation step can take place in the anionic polymerization was confirmed by a careful examination of the polymer obtained by polymerization of the ketone in toluene with lithium dust at -25°C. In some experiments, it was possible to separate, by ether extraction, a crystalline fraction from the bulk of the polymer which possessed a different X-ray spectrum from normal crystalline poly(isopropyl vinyl ketone). These spectra are shown in Figure 3.

The crystalline ether soluble polymer was very unstable and depolymerized rapidly at 90°C. The X-ray spectrum of this material was surprisingly similar to that of polyethylene. Only very small quantities could be obtained. Elemental analysis showed a higher carbon content than would be expected from normal poly(isopropyl vinyl ketone) and there were some differences in the infra-red spectrum, but these were difficult to interpret since the ether soluble fraction was inevitably contaminated with atactic poly(isopropyl vinyl ketone). Although this thermally unstable crystalline polymer was not isolated from the products of other heterogeneous initiators, it is probable that the thermally labile link is present in

small concentration in the main chain of most of the crystalline poly(isopropyl vinyl ketones) prepared by anionic initiation.

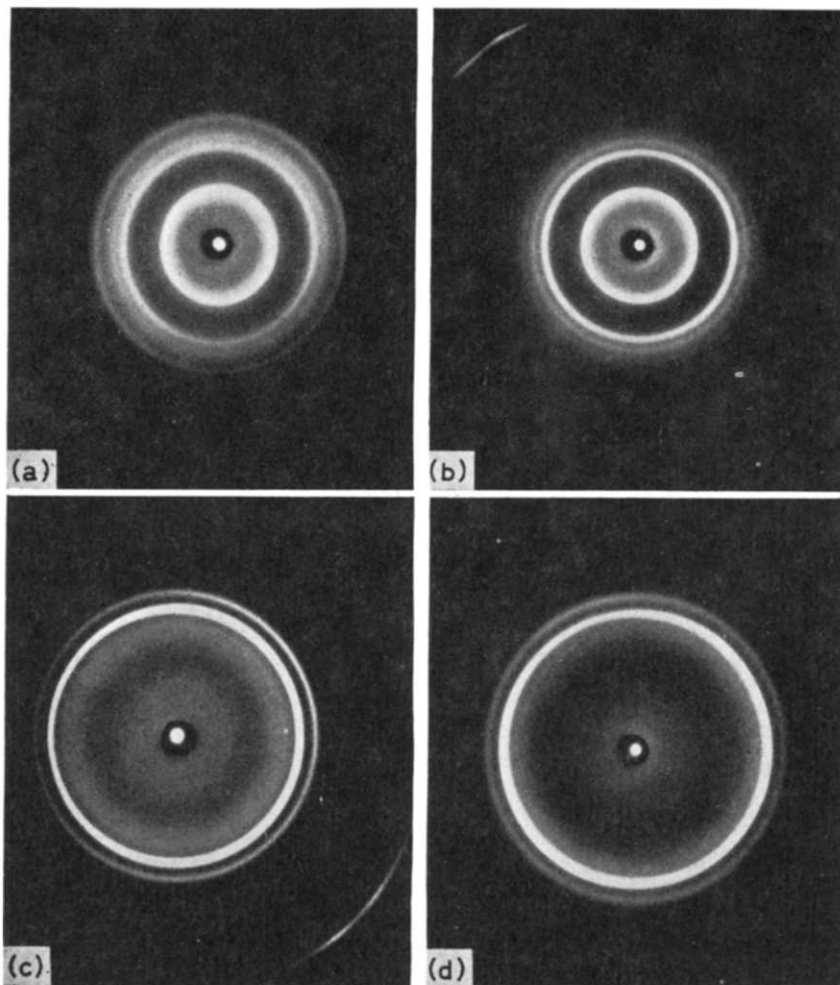
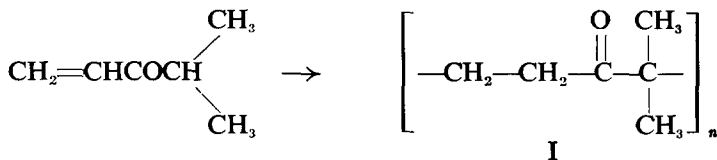
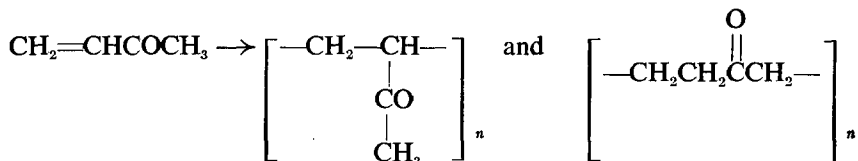


Figure 3—X-ray photographs of poly isopropyl vinyl ketone: (a) polymer obtained by initiation with lithium in toluene at  $-25^{\circ}\text{C}$ , (b) ether insoluble fraction, (c) ether soluble and (d) X-ray spectrum of polyethylene

There appear to be two mechanisms which could give rise to poly addition processes different from 1,2 addition. First, 1,4 addition could give a linear polymer containing a gem dimethyl group.

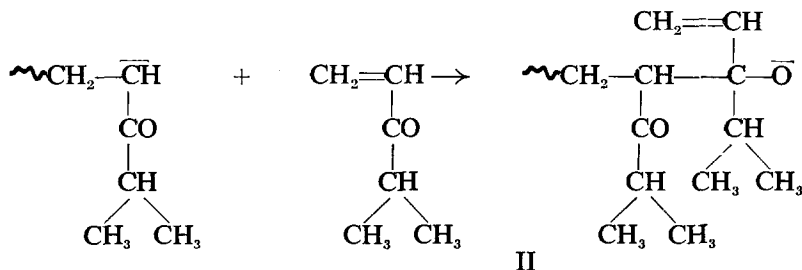


This polymer is the product one would expect if the monomer polymerizes in its conjugated enolic form by 1,4 addition. This type of polymerization has been observed in the polymerizations of acrylamide and methacrylamide initiated by sodium or sodium alkoxides<sup>7</sup>. More recently it has been shown that polymerization of methyl vinyl ketone by sodium *tert*-butoxide in toluene yields a polymer which contains some 1,4 links<sup>8</sup>:



The poly(methyl vinyl ketone) was subjected to the Schmidt reaction. Hydrolysis of the resultant amide groups yielded  $\gamma$  amino butyric acid, showing that some non-vinyl polymerization had taken place. This type of 1,4 polymerization could not take place in *tert*-butyl vinyl ketone, and, in fact, poly(*tert*-butyl vinyl ketones) prepared using anionic initiators were found to be thermally stable.

The second possibility is the addition of the growing anion to the carbonyl group of a monomer molecule to give an alkoxide anion at the end of the polymer chain and a vinyl side chain.



Initiation by alkoxide ion would continue chain growth but, in this case, a thermally unstable  $\beta$  ether link would be formed. This reaction could also take place at a carbonyl group attached to a polymer chain, thereby giving chain branching. Such an addition, however, would be more sterically hindered than addition of the carbanion to a monomer molecule. While the thermal stability of the proposed structure I is not established, it seems unlikely that it would be unstable at 98°C. Structure II contains a  $\beta$  ether link and would be expected to break down at the ether oxygen at elevated temperatures. This, therefore, seems to be a more likely 'foreign' group in the polymer chain, although, at present, there is no experimental evidence to support this conclusion.

*The authors wish to thank British Nylon Spinners Limited for permission to publish this work.*

Research Department,  
British Nylon Spinners Limited,  
Pontypool, Mon.

(Received October 1963)

REFERENCES

- <sup>1</sup> NATTA, G., PINO, P., CORRADINI, P., DANUSSO, F., MANTICA, E., MAZZANTI, G. and MORAGLIO, G. *J. Amer. chem. Soc.* 1955, **77**, 1708  
NATTA, G., PINO, P. and MAZZANTI, G. *Gazz. chim. ital.* 1957, **87**, 528
- <sup>2</sup> MILLER, M. L. and RAUHUT, C. E. *J. Amer. chem. Soc.* 1958, **80**, 4115  
GARRETT, B. S. *et al. J. Amer. chem. Soc.* 1958, **81**, 1007
- <sup>3</sup> HAAS, H. C., EMERSON, E. S. and SCHULER, N. W. *J. Polym. Sci.* 1956, **22**, 291  
FORDHAM, J. W. L. and MCCAIN, G. H. Abstracts of Papers to 133rd Meeting of American Chemical Society 1958, p 18R
- <sup>4</sup> FURUKAWA, J., SAEGUSA, T., FUJII, H., KAWAKASI, A., IMAI, H. and FUJII, Y. *Makromol. Chem.* 1960, **37**, 149
- <sup>5</sup> BUTLER, K., THOMAS, P. R. and TYLER, G. J. *J. Polym. Sci.* 1960, **48**, 357
- <sup>6</sup> OVERBERGER, C. G. and SCHILLER, A. M. *J. Polym. Sci.* 1961, **54**, S30
- <sup>7</sup> BRESLOW, D. S., HULSE, G. E. and MATLACK, A. S. *J. Amer. chem. Soc.* 1957, **79**, 3760
- <sup>8</sup> IWATSUKII, S., YAMASHITA, Y. and ISHII, Y. *J. Polym. Sci.* 1963, **B1**, 545

# A Theoretical Treatment of the Modulus of Semi-crystalline Polymers

W. R. KRIGBAUM, R.-J. ROE\* and K. J. SMITH, Jr†

*Previous treatments of the modulus of semi-crystalline polymers were based on the assumption that the amorphous chains are disposed in a manner resembling an elastomeric network. While the crystallites may perform the same function as crosslinks, we believe that the formation of crystallites leaves the remaining amorphous chains under considerable tension. The large modulus increase observed on crystallization is thus due to the fact that the network chains are near full extension, even in the absence of an external force.*

*Theoretical treatment along these lines yields an expression for the initial Young's modulus  $E_0$  in terms of the degree of crystallinity  $\omega$ . This relation contains one adjustable parameter, and the same parameter appeared in our treatment of the variation of crystallinity with temperature. Comparison with data for polyethylene shows that the theoretical modulus values are of the correct order of magnitude. Furthermore, the temperature dependence of both  $E_0$  and  $\omega$  for a given sample can be represented by the two theoretical relationships using the same value for the adjustable parameter. Thus, these equations can be combined to yield an expression for the modulus which has no adjustable parameter. At temperatures sufficiently below the melting point a linear dependence of  $E_0$  upon  $1/(1-\omega)$  is predicted, and the experimental data appear to obey this behaviour.*

STATISTICAL theory<sup>1-3</sup> has been remarkably successful in treating the characteristic long-range elastic behaviour of rubberlike materials through consideration of the entropy loss of the individual network chains upon deformation. It would seem that the same general approach might be applicable to the treatment of semi-crystalline bulk polymers. Typical values for the modulus of a vulcanized rubber, a semi-crystalline polymer, and the polymer crystallite itself, are of the order of  $10^7$ ,  $10^9$ , and  $10^{12}$  dyne/cm<sup>2</sup>, respectively. In a crystalline polymer one finds the ordered, crystalline regions surrounded by, or interspersed with, less well ordered amorphous regions. Since the crystalline portions are much more rigid<sup>4</sup>, most of the strain accompanying deformation of a bulk sample must occur in the amorphous regions. Furthermore, the polymer molecules will generally pass through both crystalline and amorphous regions, hence the crystallites should act in the same manner as crosslinks to prevent the slippage of one molecule past another. Thus, it is not difficult to find parallel features in the structural organization of semi-crystalline and elastomeric network polymers. It might therefore appear that the results of the network treatments could be directly applied if only the number of effective network chains in the semi-crystalline polymer could be estimated. An *a priori* calculation of this number for crystalline homo-

\*Electrochemicals Department, E. I. du Pont de Nemours and Co., Niagara Falls, N.Y.

†Chemstrand Research Center, Inc., Durham, N.C.

polymers does not appear to be possible at the present time. If, however, co-monomer units which cannot crystallize are interspersed randomly along the chain, these will serve to subdivide the molecule into sequences of units which are capable of crystallization, and the necessary information concerning this sequence distribution can be computed statistically. This is essentially the approach taken by Nielsen and Stockton<sup>5</sup>, and by Jackson, Flory, Chiang and Richardson<sup>6</sup>. The former authors have further modified the gaussian network treatment through introduction of an approximate correction for the filler action of the crystallites.

These treatments are obviously less general than that for elastic networks, since homopolymers must be excluded from consideration. A more serious shortcoming is the fact that the calculated moduli are considerably smaller than the experimental values. This result comes as no surprise since, as Treloar<sup>7</sup> has pointed out, the magnitude of the modulus observed for crystallized natural rubber can only be approximated by gaussian network theory if one adopts the untenable position that the remaining amorphous chains are comprised of a single isoprene unit. This impasse suggests that the foregoing treatments have overlooked a fundamental difference in the status of the amorphous chains in a crystalline polymer and those in an elastomeric network.

In an earlier paper<sup>8</sup> we have shown that the variation of the degree of crystallinity of an unstrained polymer with temperature can be predicted from statistical considerations. If one makes the plausible assumption that the chains are in their unperturbed random flight conformations when the crystal nuclei are introduced, then it can be shown that the remaining amorphous chain sections will be brought under increasing tension as crystallization progresses. Eventually the entropy decrease associated with this increasing deformation will counterbalance the driving force for further crystallization, and the process will cease. We conclude, therefore, that the amorphous chains in a bulk polycrystalline sample are in a highly strained state, even in the absence of an external macroscopic stress. The distribution of conformations in such a system of chains near their fully extended lengths can no longer be described adequately by gaussian statistics, so that the calculation has to be made in terms of inverse Langevin statistics, which gain importance in rubber networks only at high relative elongations. We anticipate that the deformation of such a network composed of highly extended chains will require much larger forces than would be needed for a rubber network having an equal number of chains, but with unperturbed displacement distributions.

This paper will present an estimate of the modulus, and its variation with crystallinity, of a semi-crystalline bulk polymer. The theoretical predictions will be compared with experimental data for several samples of polyethylene.

#### THEORY

We consider a cube of unit volume of a semi-crystalline polymer sample. Let the small crystallites imbedded in the sample be interconnected by  $\nu$  amorphous chains, each of which consists of  $t$  statistical links. We want to calculate the change in free energy,  $\Delta F$ , of the sample which occurs



when it is stretched uniaxially in the  $z$  direction by a factor  $\alpha$ . Then the force  $f$  necessary to maintain this length, and the initial Young's modulus  $E_0$ , can be obtained from the relations:

$$f = (\partial \Delta F / \partial \alpha)_{p, T} \quad (1)$$

$$E_0 = \lim_{\alpha \rightarrow 1} \left( \frac{\partial f}{\partial \alpha} \right)_{p, T} = \lim_{\alpha \rightarrow 1} \left( \frac{\partial^2 \Delta F}{\partial \alpha^2} \right)_{p, T} \quad (2)$$

We will first consider a single amorphous chain. If the ends of the chain which are attached to crystallites are separated by a distance  $r_c$ , the entropy  $S_0$  of the chain is

$$S_0 = -kt \left[ \frac{r_c}{tb} \beta_c + \ln \frac{\beta_c}{\sinh \beta_c} \right] \quad (3)$$

where  $k$  is Boltzmann's constant,  $b$  is the length of a statistical link, and

$$\beta_c = \mathcal{L}^{-1}(r_c/tb) \quad (4)$$

$\mathcal{L}^{-1}$  denoting the inverse Langevin function. If the end-to-end distance changes upon deformation of the bulk sample to  $r'_c = \gamma r_c$ , the entropy now becomes

$$S_\gamma = -kt \left[ \frac{\gamma r_c}{tb} \beta'_c + \ln \frac{\beta'_c}{\sinh \beta'_c} \right] \quad (5)$$

where

$$\beta'_c = \mathcal{L}^{-1}(\gamma r_c/tb) \quad (6)$$

The change in enthalpy on stretching an amorphous chain is generally small and, for simplicity, it will be neglected, so that the free energy change for a single chain is represented by  $-T(S_\gamma - S_0)$ .

The extent of deformation  $\gamma$  of the individual chains will depend upon the angle  $\theta$  which the initial end-to-end vector  $r_c$  of the amorphous chain makes with the stretching direction. Since the bulk sample is initially isotropic, the number of chains having their end-to-end vectors in the direction between  $\theta$  and  $\theta + d\theta$  is equal to  $v \sin \theta d\theta$  ( $0 \leq \theta \leq \pi/2$ ). The total free energy change on stretching,  $\Delta F$ , is obtained by summing the contributions of the individual chains

$$\Delta F = -T \int_0^{\pi/2} (S_\gamma - S_0) v \sin \theta d\theta \quad (7)$$

By substituting equations (3) and (5) into (7), and differentiating with respect to  $\alpha$ , we obtain

$$\begin{aligned} E_0 &= \lim_{\alpha \rightarrow 1} \left( \frac{\partial^2 \Delta F}{\partial \alpha^2} \right)_{p, T} \\ &= \lim_{\alpha \rightarrow 1} v k T \frac{r_c}{b} \int_0^{\pi/2} \left[ \frac{\partial \beta'_c}{\partial \gamma} \left( \frac{\partial \gamma}{\partial \alpha} \right)^2 + \beta'_c \left( \frac{\partial^2 \gamma}{\partial \alpha^2} \right) \right] \sin \theta d\theta \end{aligned} \quad (8)$$

Since  $\gamma \rightarrow 1$  when  $\alpha \rightarrow 1$ , we have

$$\lim_{\alpha \rightarrow 1} \beta'_c = \beta_c$$

and

$$\lim_{\alpha \rightarrow 1} \frac{\partial \beta'_c}{\partial \gamma} = \frac{r_c}{tb} \frac{\beta_c^2 \sinh^2 \beta_c}{\sinh^2 \beta_c - \beta_c^2} \quad (9)$$

and equation (8) becomes

$$E_0 = \nu kT \left[ \frac{r_c^2}{tb^2} \frac{\beta_c^2 \sinh^2 \beta_c}{\sinh^2 \beta_c - \beta_c^2} \int_0^{\frac{\pi}{2}} \left( \frac{\partial \gamma}{\partial \alpha} \right)_{\alpha \rightarrow 1}^2 \sin \theta \, d\theta + \frac{r_c \beta_c}{b} \int_0^{\frac{\pi}{2}} \left( \frac{\partial^2 \gamma}{\partial \alpha^2} \right)_{\alpha \rightarrow 1} \sin \theta \, d\theta \right] \quad (10)$$

We now require an explicit expression relating  $\gamma$  to  $\alpha$ ,  $\theta$ , and the crystallinity  $\omega$ . When the bulk sample is stretched by a factor  $\alpha$ , a unit linear dimension along the direction making an angle  $\theta$  with the draw axis is deformed to a relative length  $\lambda$  given by

$$\lambda = [\alpha^2 \cos^2 \theta + (1/\alpha) \sin^2 \theta]^{1/2} \quad (11)$$

However, since the crystallites are much more rigid than the amorphous chains, the deformation  $\lambda$  is borne almost entirely by the amorphous region. Thus the actual deformation suffered by an amorphous chain is larger than  $\lambda$ , and depends upon the relative proportions of crystalline and amorphous material. Consider a line segment of length  $l$  drawn through the sample. The line will pass through alternate crystalline and amorphous regions many times and, on the average, a fraction  $\omega$  of its total length will be in the crystalline regions and a fraction  $(1-\omega)$  in the amorphous regions. When the length of the line segment is changed to  $\lambda l$  due to deformation of the bulk sample by a factor  $\alpha$ , we will assume that the increase in length from  $l$  to  $\lambda l$  has actually resulted from an increase in the length of the line in the amorphous portions from  $(1-\omega)l$  to  $(\lambda-\omega)l$ . Hence, the average deformation of the amorphous part may be set equal to

$$\gamma_a = (\lambda - \omega) / (1 - \omega) \quad (12)$$

We equate the deformation  $\gamma$  of the end-to-end vector  $\mathbf{r}_c$  to the average amorphous deformation  $\gamma_a$ , thus

$$\gamma = \gamma_a = [(\alpha^2 \cos^2 \theta + \{1/\alpha\} \sin^2 \theta)^{1/2} - \omega] / (1 - \omega) \quad (13)$$

Equation (13) will not be correct if an extensive orientation and alignment of the crystallites occurs on stretching the sample. It should be valid, however, when the deformation is small (especially in the limit  $\alpha=1$  which is of interest here), and also when the time scale of the modulus measurement is shorter than the relaxation time for crystallite orientation.

For the limiting values of the derivatives of  $\gamma$  required in equation (10) we obtain

$$\left(\frac{\partial\gamma}{\partial\alpha}\right)_{\alpha\rightarrow 1} = \frac{3\cos^2\theta - 1}{2(1-\omega)} \quad (14)$$

and

$$\left(\frac{\partial^2\gamma}{\partial\alpha^2}\right)_{\alpha\rightarrow 1} = \frac{1}{2(1-\omega)} \left\{ 2 - \frac{(3\cos^2\theta - 1)^2}{2} \right\} \quad (15)$$

Integration of equation (10), after substitution of (14) and (15), leads to

$$E_0 = \nu kT \frac{r_c}{b} \left[ \frac{r_c}{tb} \frac{\beta_c^2 \sinh^2 \beta_c}{\sinh^2 \beta_c - \beta_c^2} \times \frac{1}{5(1-\omega)^2} + \beta_c \frac{4}{5(1-\omega)} \right] \quad (16)$$

The end-to-end vector distance  $r_c$  (and therefore  $\beta_c$ ) depends upon the mode and the extent of crystallization. In the paper cited<sup>8</sup>, it was shown that for folded chain morphology the equilibrium degree of crystallinity can be represented quite satisfactorily by a relation based on the assumption

$$r_c \simeq N^{1/2} b \quad (17)$$

where  $N$  is the number of statistical segments present in an amorphous chain when its two ends have just deposited themselves on the surface of the growing crystallites. Employing the relations

$$t = (1-\omega) N \quad (18)$$

and

$$\nu = \rho / M_0 N \quad (19)$$

where  $M_0$  is the molecular weight of a statistical segment and  $\rho$  is the density of the sample, we obtain

$$E_0 = \frac{\rho RT}{M_0} \left[ \frac{1}{5} \frac{1}{N(1-\omega)^3} \times \frac{\beta_c^2 \sinh^2 \beta_c}{\sinh^2 \beta_c - \beta_c^2} + \frac{4}{5} \frac{\beta_c}{N^{1/2}(1-\omega)} \right] \quad (20)$$

with

$$\beta_c = \mathcal{L}^{-1} \{ 1 / [N^{1/2}(1-\omega)] \} \quad (21)$$

Equation (20), which relates the Young's modulus to the degree of crystallinity, contains only one adjustable parameter,  $N$ . However, the value of  $N$  is not arbitrary, and it can be determined from an analysis of experimental data concerning the temperature dependence of the degree of crystallinity  $\omega$ . For example, in homopolymers forming folded chain crystallites  $\omega$  is related to  $T$  through the theoretical expression<sup>8</sup>

$$\frac{1}{T} = \frac{1}{T_M^0} + \frac{R}{\Delta H_f} \ln (\sinh \beta_c / \beta_c) \quad (22)$$

where  $\Delta H_f$  is the heat of fusion per mole of statistical segments and  $T_M^0$  the melting point of the polymer. Since  $\beta_c$  is a function of  $\omega$  and  $N$ , the latter is adjusted until the best agreement is obtained between the observed degree of crystallinity at a temperature well below the melting point and the corresponding value of  $\omega$  calculated from equation (22).

DISCUSSION AND COMPARISON WITH DATA  
FOR POLYETHYLENE

In Figure 1 the values of  $E_0$  calculated according to equations (20) and (22)

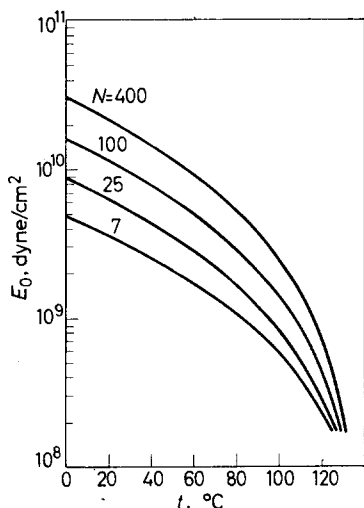


Figure 1—Initial Young's modulus  $E_0$  calculated for polyethylene according to equations (20) and (22)

are plotted against  $T$  for several different values of  $N$ . To the various physical constants appearing in these equations the values pertaining to polyethylene were assigned, i.e.  $\rho = 0.94 \text{ g/cm}^3$  (about the average of crystalline and amorphous densities),  $t_M^0 = 137^\circ\text{C}$ ,  $M_0 = 140$ , and  $\Delta H_f = 9.4 \text{ kcal/mole}$  (on the assumption that a statistical segment consists of ten  $\text{CH}_2$  units<sup>9</sup>). The plots in Figure 1 can be used as master curves and, by overlaying the observed modulus data, the value of the parameter  $N$  can be determined. A stringent test of the theory is afforded by the requirement that the temperature dependence of  $\omega$  must be fitted with the same value of  $N$ .

Figures 2, 3 and 4 represent such a test. The experimental data refer to

Figure 2—Theoretical modulus values calculated with  $N=80$  (smooth curve) compared with experimental values obtained for Marlex 50 by Kawai<sup>10</sup> (● measured after 50 sec, ○ extrapolated to 1 sec)

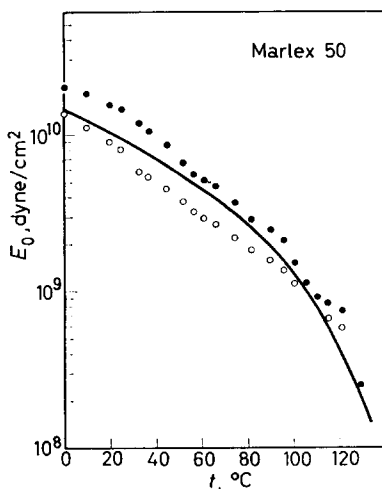
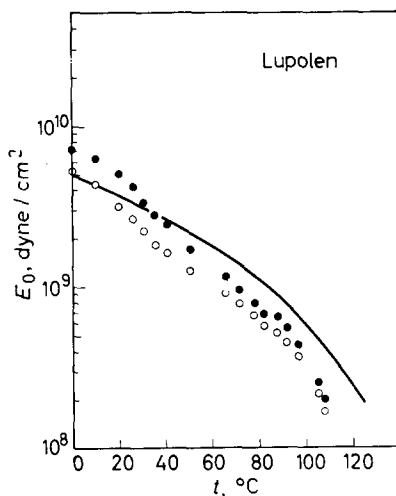


Figure 3—Modulus calculated with  $N=7$  compared with experimental data of Kawai<sup>10</sup> for Lupolen (symbols as in Figure 2)



two samples of polyethylene. One polymer is Marlex 50 of intrinsic viscosity 1.43 (xylene solution at 75°C), which was crystallized for an hour at 125°C and cooled slowly to room temperature, while the second polymer is a Lupolen of melt index 1.0 containing 1.6 branch units per 100 carbon atoms as measured by infra-red techniques, and which was crystallized at 100°C for an hour and cooled slowly to room temperature. Both samples were then annealed again for two hours at 125° and 105°C, respectively. Each polymer sample thus treated was divided into two portions for density and modulus measurement. We are indebted to Dr I. Uematsu of this laboratory for the preparation of these samples and for the crystallinity data referred to below. Values of the Young's modulus represented by open circles in Figures 2 and 3 were obtained by Kawai<sup>10</sup> from measurement of the force 50 seconds after elongation. The derivation of equation (20) involved the assumption that the crystallites do not orient or rearrange. Stein<sup>11</sup> has concluded from measurement of the dynamic birefringence at various frequencies that it requires approximately one second for the crystallites to change orientation. Kawai<sup>10</sup> has also measured modulus

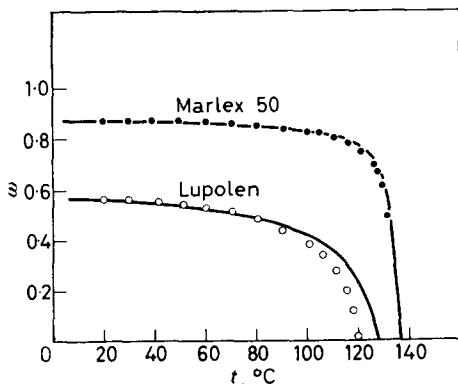


Figure 4—The degree of crystallinity  $\omega$  calculated for Marlex 50 and Lupolen using the same  $N$  values employed in the respective modulus calculations

values at times of 100, 500 and 1 000 sec after elongation. These indicate some decay of force with time. The values represented by filled circles in *Figures 2* and *3* were obtained through linear extrapolation of  $\log E_0$  versus  $\log \text{time}$  (see Nagamatsu<sup>12</sup>) to a time of one second. This interval should be ample for complete rearrangement of the amorphous segments, while still being short enough to exclude most of the effects of crystallite alignment. The fitted values of  $N$  were then used to compute the degree of crystallinity according to equation (22). These predicted values are represented by the full curves in *Figure 4*, while the circles designate experimental data.

As is evident from the figures,  $N$  values of 80 for Marlex 50 and 7 for Lupolen offer a very good representation of the data for both the modulus and degree of crystallinity. The extrapolated one second moduli fall somewhat above the theoretical curve, but the agreement is still entirely satisfactory. The deviations observed just below the melting point for Lupolen arise from the fact that in the foregoing equations no attempt has been made to take into account the depression of the melting point due to branching. A more thorough analysis of the variation of crystallinity near the melting point will be given in a subsequent paper.

Since equations (20) and (22) were able to predict the absolute values of the modulus and degree of crystallinity, and also their variations with temperature, through the assignment of one value for the adjustable parameter  $N$ , this suggests that  $N$  can be eliminated by solving the system of simultaneous equations (20) and (22) for  $E_0$  as a function of  $T$  and  $\omega$ . By adopting the notation

$$Z \equiv \frac{1}{N^{1/2}(1-\omega)} = \mathcal{L}^{\beta}\{\beta_c\} \quad (23)$$

equation (20) may be rewritten as

$$E_0 = \frac{\rho RT}{M_0} \left[ \frac{1}{5} \frac{Z^2 \beta_c^2 \sinh^2 \beta_c}{\sinh^2 \beta_c - \beta_c^2} \left( \frac{1}{1-\omega} \right) + \frac{4}{5} \beta_c Z \right] \quad (20a)$$

Equation (21) contains only  $\beta_c$  and  $\omega$  as explicit variables, hence  $\beta_c$  can, in principle, be solved in terms of  $\omega$ , and substitution of this solution into equation (20a) would lead to the desired relation. We will adopt a simpler approach by noting that at temperatures far below the melting point the first term in equation (20a) predominates, and therefore under these conditions a good approximation is furnished by

$$E_0 \simeq \frac{\rho RT}{M_0} \frac{1}{5} Z^2 \beta_c^2 / (1-\omega) \quad (24)$$

Examination of equations (22) and (23) reveals that  $\beta_c$  and  $Z$  are constants at a given temperature, thus equation (24) immediately suggests that  $E_0$  is directly proportional to  $1/(1-\omega)$  at a fixed temperature lying sufficiently below the melting point. The proportionality constant for polyethylene at 20°C may be computed as  $1.258 \times 10^9$  dyne/cm<sup>2</sup>, and the straight line drawn in *Figure 5* represents the predicted linear relationship with a slope equal to the value mentioned. The three points were computed from

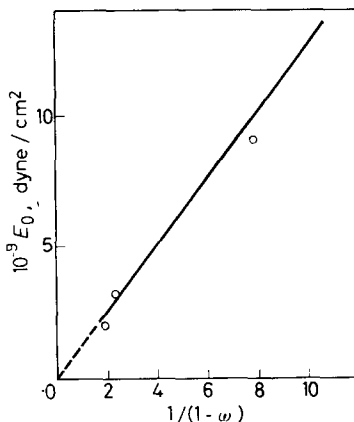


Figure 5—A test of the linear relation between modulus  $E_0$  and  $1/(1-\omega)$  predicted theoretically for temperatures well below the melting point

the observed values of  $E_0$  and  $\omega$  at  $20^\circ\text{C}$  for Marlex, Lupolen and Yukalon (lowest modulus). The latter polymer contains 2.0 branch units per 100 carbon atoms, and was heat treated in a similar manner to that described above for the modulus measurements. Equation (22) is strictly valid only for homopolymers, but evidently the linear relationship (24) is obeyed even for moderately branched polymers, indicating that at these low temperatures the main factor limiting the degree of crystallinity is the strain imposed on the intervening amorphous chains, rather than the slight difference in the chemical potential of the amorphous phase arising from the presence of branched units. More experimental data will be required to confirm the predicted linear dependence of  $E_0$  with  $1/(1-\omega)$ . Figure 5 nevertheless demonstrates that the present theory succeeds in predicting the absolute values of the modulus without recourse to any adjustable parameters.

Finally, we turn to a comparison with earlier treatments<sup>5, 6</sup> of the modulus of crystalline polymers. Both of these bear some resemblance to the present one in that the crystallites are assumed to act as crosslinks, and the theoretical approach parallels that employed in the treatment of rubber elasticity. Values of the modulus calculated according to the previous treatments were, however, smaller than the experimental values by at least an order of magnitude. This arises from the fact that the strain imposed upon the amorphous chains by crystallization has been neglected. The gaussian approximation, normally employed for calculation of the elastic force of an amorphous rubber at small strains, is no longer adequate in representing the entropy of chains which have been deformed almost to their full extension at high degrees of crystallization. If we expand the inverse Langevin function (21), retaining only the first term, i.e.

$$\beta_c \approx 3/[N^{1/2}(1-\omega)] \quad (25)$$

and substitute this into equation (20), an expression is obtained for  $E_0$  corresponding to the gaussian approximation

$$E_0 \approx \frac{\rho RT}{M_0 N} \left[ \frac{3}{5} \frac{1}{(1-\omega)^3} + \frac{12}{5} \frac{1}{(1-\omega)^2} \right] \quad (26)$$

For Marlex 50, shown in *Figure 2*, the modulus value at 20°C calculated according to equation (26) with  $N = 80$  is  $8.8 \times 10^8$  dyne/cm<sup>2</sup>. This is lower, by more than a factor of ten, than the observed value or the value calculated according to the more exact equation (20). Thus, the gaussian approximation is inadequate at high degrees of supercooling. On the other hand, equation (26) may furnish a useful estimate of the variation of the initial modulus with temperature in the region just below the melting point. Expansion of equation (22) yields

$$\frac{1}{1-\omega} \approx \left[ \frac{2N_u \Delta H_u}{3R} \left( \frac{1}{T} - \frac{1}{T_M^0} \right) \right] \quad (27)$$

where  $N_u$  is the number of repeating units in the amorphous chain between crystal nuclei and  $\Delta H_u$  is the heat of fusion per mole of repeating units. Substitution of this relation into equation (26) yields the desired result

$$E_0 = \frac{2\rho T \Delta H_u}{5M_u} \left( \frac{1}{T} - \frac{1}{T_M^0} \right) \left[ 4 + \left( \frac{2N_u \Delta H_u}{3R} \right)^{1/2} \left( \frac{1}{T} - \frac{1}{T_M^0} \right)^{1/2} \right] \quad (28)$$

We believe this work demonstrates convincingly that the strain imposed on the remaining amorphous chains is one of the most important factors in determining both the degree of crystallinity and the modulus of semi-crystalline polymers.

*Support of the U.S. Army Research Office (Durham) under grant 31-124-G202 is gratefully acknowledged.*

*Department of Chemistry,  
Duke University, Durham, N.C.*

*(Received December 1963)*

#### REFERENCES

- <sup>1</sup> WALL, F. T. *J. chem. Phys.* 1942, **10**, 485
- <sup>2</sup> JAMES, H. M. and GUTH, E. *J. chem. Phys.* 1943, **11**, 455
- <sup>3</sup> FLORY, P. J. *Chem. Rev.* 1944, **35**, 51  
FLORY, P. J. *J. chem. Phys.* 1950, **18**, 108
- <sup>4</sup> SUKURADA, I., NUKUSHIMA, Y. and ITO, T. *J. Polym. Sci.* 1962, **57**, 651
- <sup>5</sup> NIELSEN, L. E. and STOCKTON, F. D. *J. Polym. Sci.* 1963, **1A**, 1995
- <sup>6</sup> JACKSON, J. B., FLORY, P. J., CHIANG, R. and RICHARDSON, M. J. *Polymer, Lond.* 1963, **4**, 237
- <sup>7</sup> TRELOAR, L. R. G. *The Physics of Rubber Elasticity*, Second edition, p 273. Oxford University Press: London, 1958
- <sup>8</sup> ROE, R.-J., SMITH, K. J., Jr and KRIGBAUM, W. R. *J. chem. Phys.* 1961, **35**, 1306
- <sup>9</sup> VOL'KENSTEIN, M. V. *Configurational Statistics of Polymeric Chains* (Translated by S. N. and M. J. TIMASHEFF), p 429. Interscience: New York, 1963
- <sup>10</sup> KAWAI, H. Private communication
- <sup>11</sup> STEIN, R. S. Paper presented at the American Physical Society Meeting, Baltimore, Md, 1962
- <sup>12</sup> NAGAMATSU, K. *Kolloidzshr.* 1960, **172**, 141



# Book Review

## *The Friction and Lubrication of Solids*

### Part II

F. P. BOWDEN and D. TABOR. (The International Series of Monographs on Physics). Clarendon Press: Oxford, 1964. xx + 544 pp. 6 in. by 9½ in., 84s

FRICITION between solid bodies plays a very important part in our civilization. Nevertheless, it is not one of the fashionable and glamorous research subjects, and physics textbooks usually do not say much more about it than that friction is an irreversible process and that heat is generated when one solid body is made to rub against another. A monograph on this subject is therefore to be welcomed. The one under review 'is a sequel to the first volume published in 1950 (revised 1954) . . .'. Twenty three of its twenty four chapters again deal almost exclusively with the work of the authors and their research students, whereas the concluding chapter on 'Some early work on sliding and rolling friction' (13 pp) gives at least some indication of the long history of the subject. It also makes reference to what appears to be a much more complete and up-to-date review (it is printed in Russian) by I. V. Kragelskii and V. S. Shchedrov entitled *Development of the Science of Friction* and published in 1956 by the Soviet Academy of Sciences.

The first volume described mainly the frictional behaviour of metals in terms of the formation and shearing of 'interfacial junctions'. In the second volume an adhesion mechanism of friction for metals is outlined and an attempt is made to show how far these concepts, with some modification, may be applied to the frictional behaviour of non-metals.

This is a thought-provoking book. It is not easy to glean from it how the frequently referred to 'interfacial junctions' are thought to be formed. The claim is made that with the application of a tangential stress 'combined stresses at the regions of contact produce junction growth', and that this model 'does explain one of the most puzzling features of metallic friction: that for rigorously cleaned surfaces the coefficient of friction tends to infinity, whereas in the presence of only small amounts of surface contamination the coefficient of friction falls to values of the order of unity'. Surely, this is a bold statement. The coefficient of friction is defined as the ratio of the force of friction to the normal load. The force of friction is called forth by a tangential shearing stress. Do the authors suggest that by rigorous cleaning of a frictional contact a material able to withstand an infinite shearing stress can be produced? They quote a little later on friction experiments on the cleavage face of rocksalt and with clean steel on rocksalt where the coefficient of friction has been about 0.7 to 0.8.

Skiing and ice-skating depend on the melting of the surface layers of the snow and ice by frictional heating, and it is a well-established practice to 'wax' the wooden runners of skis in order to prevent the formation of very thin adhesive layers by the combined blotting actions of the porous snow and the porous wood.

In a chapter on 'The friction and deformation of polymeric materials', the comparatively low friction of polytetrafluorethylene has been singled out for discussion.

Electrostatic effects (p 235) are only just mentioned, and 'stick-slip motion' (p 78) has received a similarly sketchy treatment.

This book has been very well produced and contains a large number of beautiful and interesting photographs, which enhance its value. It should form a useful basis for arousing the curiosity of physicists and engineers in the fascinating subjects of friction and wear and in stimulating discussions and some clear thinking on their mechanisms.

R. SCHNURMANN

# Note

## *Gamma Radiolysis of Poly-2-vinylpyridine*

ALTHOUGH the effects of ionizing radiation on aromatic hydrocarbons has been investigated in many laboratories, little information concerning heterocyclic analogues has been reported.

The study of these should, however, offer the possibility of investigating some fundamental processes in radiation chemistry. As a matter of fact, the reactivity of heterocyclic compounds towards free radicals is very similar to that of aromatic hydrocarbons but the former are much more reactive in ionic processes. Moreover  $n-\pi$  excited state reactions are possible.

In this paper gel point determinations and crosslinking-degradation ratios are reported for poly-2-vinylpyridine. The results are discussed and compared with those published for polystyrene.

### EXPERIMENTAL

#### (a) *Polymer synthesis and sample preparation*

Polymerization was carried out in a sealed bulb at 60°C using thoroughly outgassed monomer and azobis-isobutyronitrile as initiator. The polymer was precipitated in heptane from benzene solution and dried. The molecular weight was determined by light-scattering in benzene solution with a SOFICA apparatus. Films 0.01 mm thick were cast from a benzene solution on a mercury surface and dried at 80°C under  $10^{-5}$  mm of mercury pressure to constant weight.

#### (b) *Irradiation*

Irradiation was performed in sealed bulbs under vacuum at ordinary temperature with a  $^{60}\text{Co}$  source at a dose rate of 0.25 Mr/h. A ferrous sulphate dosimeter was used.

#### (c) *Solubility experiments*

The soluble fraction of the irradiated samples was extracted in a Soxhlet apparatus and determined by ultra-violet absorption spectroscopy ( $\lambda_{\text{max.}} = 263 \text{ m}\mu$ ,  $\epsilon = 3 \text{ } 100$ ). The results were shown to be independent of solvent and support used for casting the film.

### RESULTS AND DISCUSSION

The gelling dose  $r_{\text{gel}}$ , extrapolated from *Figure 1*, is 2.5 Mr. The weight average molecular weight  $M_w$  of the sample being 742 000, a  $G$  value of 0.26 crosslinks per 100 eV can be calculated<sup>1</sup> from

$$r_{\text{gel}}M_w = 0.48 \times 10^6 / G$$

In *Figure 2*, the results are plotted according to the relation<sup>1</sup>

$$S + \sqrt{S} = p_0/q_0 + 2r'_{\text{gel}}/r$$

where  $S$  is the soluble fraction at dose  $r$ ,  $r'_{\text{gel}}$  is the gelling dose that would

NOTE

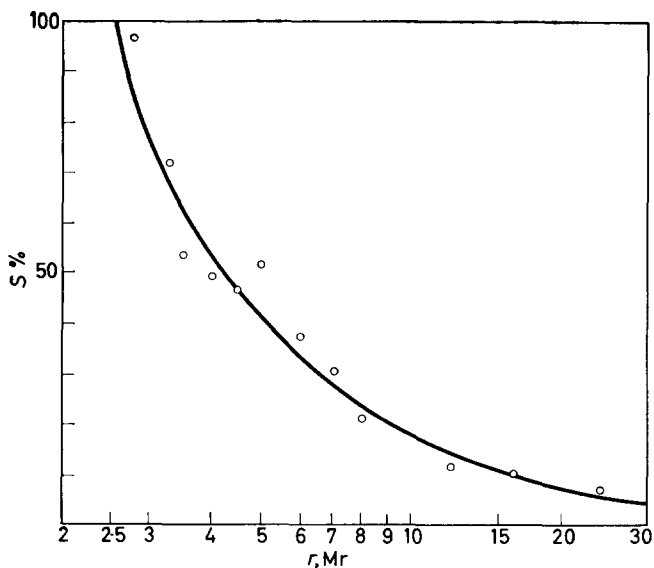


Figure 1—Soluble fraction of poly-2-vinylpyridine as a function of dose  $r$  in Mr

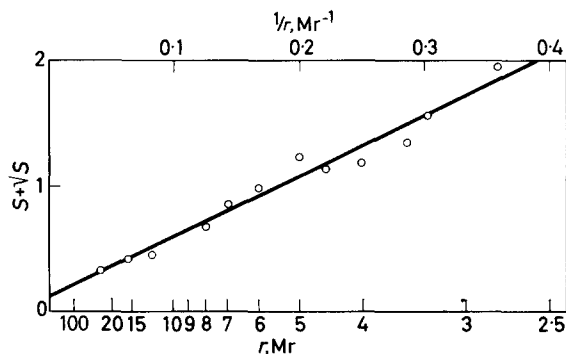


Figure 2—Plot of  $S + \sqrt{S}$  (where  $S$  denotes soluble fraction) versus dose  $r$  in Mr

be observed in the absence of main chain fracture,  $p_0$  is the density of main chain fracture per unit dose, and  $q_0$  is the proportion of units cross-linked per unit dose.  $p_0/q_0$  is found to be 0.1. The non-zero value of  $p_0/q_0$  shows that crosslinking is accompanied by a small amount of chain fracture. A true  $G'$  value for crosslinking of 0.27, which would be observed in the absence of main chain fracture, is calculated from the relation

$$G/G' = r'_{gel}/r_{gel}$$

$G$  values for crosslinking and  $p_0/q_0$  values reported in the literature<sup>2</sup> for polystyrene vary respectively between the limits 0.03 to 0.05 crosslinks per 100 eV and 0 to 0.35. Poly-2-vinylpyridine is therefore five to nine times less stable towards ionizing radiation than polystyrene.

The difference between poly-2-vinylpyridine and polystyrene cannot be attributed entirely to the enhanced reactivity towards free radicals since pyridine is not more than three times as reactive as benzene in such reactions<sup>3</sup>. First ionization potentials are also similar<sup>4</sup>. Other properties of the molecules thus have to be taken into account in order to justify the experimental results. One of these is the basicity of the nitrogen atom; the latter can abstract a proton from a positive ion intermediate and thus prevent a fast recombination with the expelled electron, as has been shown recently for amines<sup>5</sup>. The resulting free radicals could then combine to give crosslinks between the polymer chains. Differences in electron affinity of the rings (twice as large for pyridine as for benzene in the gaseous phase<sup>6</sup>) could also be important in other ionic processes. Reaction of a  $n-\pi$  excited state could afford another explanation: in heterocycles  $\pi-\pi$  excited states are easily deactivated by internal conversion to  $n-\pi$  excited states<sup>7</sup> which could promote hydrogen abstraction from the main polymer chain and radical formation. Such a mechanism has been proposed to explain the crosslinking of polyethylene under ultra-violet irradiation in the presence of benzophenone<sup>8</sup>.

A detailed study of gamma radiolysis of vinylpyridine polymers and low molecular weight heterocyclic analogues is in progress.

*We are very grateful to Professor L. de Brouckère for her interest in this work.*

*We also wish to thank Dr R. Van Leemput for help in the light-scattering experiments.*

*Finally, we are much indebted to the Belgian Nuclear Centre in Mol for irradiation facilities.*

C. DAVID  
A. VERHASSELT  
G. GEUSKENS

*Service de Chimie Générale II,  
Faculté des Sciences,  
Université Libre de Bruxelles,  
Belgium*

*(Received July 1964)*

#### REFERENCES

- <sup>1</sup> CHARLESBY, A. *Atomic Radiation and Polymers*. Pergamon: Oxford, 1960
- <sup>2</sup> CHAPIRO, A. *Radiation Chemistry of Polymeric Systems*. *High Polymers*, Vol. XV. Interscience: New York, 1962
- <sup>3</sup> WALLING, C. *Free Radicals in Solution*. Wiley: New York, 1957
- <sup>4</sup> MOSTAFA, F., EL SAYED, M. and KASHA, M. *J. chem. Phys.* 1961, **34**, 334
- <sup>5</sup> BUSLER, W. R., MARTIN, D. H. and WILLIAMS, F. *Disc. Faraday Soc.* 1963, **36**, 102
- <sup>6</sup> LOVELOCK, J. E. *Nature, Lond.* 1961, **189**, 729
- <sup>7</sup> MATAGA, N. and TSUNO, S. *Bull. chem. Soc. Japan*, 1957, **30**, 368
- <sup>8</sup> BURTON, M., KIRBY-SMITH, J. S. and MAGEE, J. L. *Comparative Effects of Radiation*. Wiley: New York, 1960

# *Polypropylene Oxide III—Crystallizability, Fusion and Glass Formation*

G. ALLEN, C. BOOTH, M. N. JONES, D. J. MARKS and W. D. TAYLOR

*Specimens of poly(propylene oxide) have been prepared from four catalysts and in one instance fractions differing in crystallizability have been obtained. Dilatometric studies show that the glass transition is unaffected by crystallizability whereas the melting point increases as the fractions become more crystalline. The upper limits for  $T_g$  and  $T_m$  are, respectively,  $-74^\circ$  and  $+75^\circ\text{C}$ .*

THE difficulties encountered in measuring transition temperatures in polymers are well known and arise principally from differences in thermal history and in the interpretation of static and dynamic measurements<sup>1,2</sup>. Many of the difficulties are minimized by the use of dilatometric and allied techniques employing low rates of heating. In our studies of the physical properties of polyethers we have sought further simplification by defining  $T_m$  as the temperature at which last traces of crystallinity disappear<sup>1</sup> and  $T_g$  as the temperature at which the coefficient of expansion of the polymer changes<sup>2</sup> from a value characteristic of a liquid ( $\sim 8 \times 10^{-4} \text{ deg}^{-1}$ ) to that of a solid ( $\sim 2 \times 10^{-4} \text{ deg}^{-1}$ ).

## EXPERIMENTAL

In addition to dilatometric methods, measurements of the coefficient of linear thermal expansion were also used to determine glass transitions in some cases where less than 0.5 g of polymer was available.

### *Dilatometry*

Transition temperatures above  $-30^\circ\text{C}$  were determined in conventional glass dilatometers using mercury as the containing fluid. In poly(propylene oxide), however,  $T_g$  lies below the freezing point of mercury and furthermore the polymers of low molecular weight were swollen by all liquids with suitably low freezing points. This problem was finally resolved by melting the specimen, under a vacuum, into a thin copper bellows (Drayton Regulator Co. type AS 18511) and sealing the container with soft solder. The bellows assembly was then sealed into a glass dilatometer, and methanol was used as the dilatometric fluid. A minor disadvantage of this technique is that the bellows subjects the sample to a slight anisotropic strain during the measurement of  $T_g$  but comparison with other methods suggests that this has no detectable effect on the transition temperature. For the specimens of high molecular weight it was possible to revert to a conventional dilatometric procedure using methyl cyclohexane or iso-octane as the dilatometric fluid.

### *Measurement of linear expansion*

When the quantity of polymer was too small for accurate dilatometry, the specimen was moulded into a small disc approximately 1 mm thick and placed on a brass cooling-block mounted on insulated supports inside an airtight Perspex box. A Philips displacement pickup (GM 5537) was mounted on the brass block with its probe resting on a glass microscope cover slide placed on the surface of the specimen, the leads from the pickup being connected to a direct-reading measuring bridge (GM 5536/01) via an airtight seal. When the apparatus was completely assembled the Perspex box was evacuated and the brass block was cooled below the transition temperature of the polymer. The change in thickness of the polymer disc was then measured at one degree intervals as the block warmed up. A plot of transducer reading against temperature had two linear branches which intersected at the transition temperature and gave results within  $\pm 0.5^{\circ}\text{C}$  of the dilatometric value where comparison was possible. Although this method was very convenient for measuring  $T_g$ , it failed to give reliable coefficients of linear expansion because of the difficulties of assessing accurately the contribution from the expansion of the supports and the body of the pickup to the overall movement of the probe.

### *Rates of heating*

Prior to the determination of  $T_m$ , the polymer specimen was maintained at the temperature at which its rate of crystallization was a maximum (about  $30^{\circ}\text{C}$ ) until no further contraction in volume ensued. Dilatometric readings were then made at intervals of  $2^{\circ}$  to  $3^{\circ}\text{C}$  as the sample warmed up, the sample being thermostatically controlled at each temperature until an equilibrium reading was obtained. On average, approximately two hours was required for each point.

Rates of heating employed in the estimation of  $T_g$  by dilatometric and linear expansivity studies varied from one to five degrees per hour. The polymer was first quenched below its glass transition temperature and the necessary readings were made as the temperature rose. Under these conditions  $T_g$  for a given sample was reproducible to  $\pm 1.0^{\circ}\text{C}$  and no significant effect of the rate of heating was evident.

### *Materials*

Most of the polymers used in this work were made in our laboratories using the catalysts listed in *Table 1*. A crude fractionation on the basis of solubility in methanol or acetone at  $0^{\circ}\text{C}$  was used to separate 'amorphous' and 'crystallizable' specimens in this phase of the work. The whole polymer, from which were obtained several fractions of different degrees of crystallinity whose properties are reported in *Table 2*, was made using a zinc diethyl-water catalyst in dioxan solution. The fractionation process from iso-octane solutions has already been described<sup>3</sup>. Fractions 1a, 3a, 5a, were obtained by solid-liquid phase separation and were similar to fractions 1 to 8 discussed earlier<sup>4</sup>. Fractions 2a, 4a, 6a, etc. were too small for examination and the origin and some properties of fraction 9 have already been described<sup>4</sup>. In all cases the polymers were carefully heated and dried under

POLYPROPYLENE OXIDE III

a vacuum to remove last traces of monomer and solvent before being used.

Since most of the polymers were produced with hydroxyl end groups, those with molecular weights below 5 000 were etherified by reacting their sodium salts with methyl iodide in order to avoid the effect of hydrogen bonding on physical properties. Low molecular weights were determined from cryoscopic measurements in benzene. Molecular weights in excess of  $10^4$  were estimated from measurements of intrinsic viscosities,  $[\eta]$ , in benzene solution at 25°C using the relation<sup>4</sup>

$$[\eta] = 1.12 \times 10^{-4} (\bar{M}_v)^{0.77}$$

or were measured by light scattering (cf. Table 2).

Degrees of crystallinity of polypropylene oxide samples were obtained from density measurements since a universally accepted method for measuring crystallinity is not available. For this purpose a linear relation between 'weight per cent crystallinity' ( $x$ ) and volume was assumed and the densities of the crystalline and amorphous regions were assumed to be  $\rho_c = 1.157 \text{ g cm}^{-3}$  (X-ray crystal density<sup>6</sup>) and  $\rho_a = 1.002 \text{ g cm}^{-3}$  respectively.

$$x = 100 (1 - \rho_a / \rho) [\rho_c / (\rho_c - \rho_a)]$$

Densities of high molecular weight specimens were measured by flotation in copper sulphate solutions. A simple pycnometer technique was used for the low molecular weight specimens.

Results and discussion

Table 1 contains results for low molecular weight oils and for polymers of high molecular weight separated into 'amorphous' and 'crystalline' fractions on the basis of solubility in methanol at 0°C. Subsequent work showed that this procedure was unsatisfactory because the crystalline separation was inefficient and the amorphous fraction, in particular, had a very broad molecular weight distribution. Nevertheless the results are of

Table 1—Some physical properties of poly(propylene oxide)

Catalyst	End group	$\bar{M}_n$	$\bar{M}_v$	Density* g cm <sup>-3</sup>	T <sub>m</sub> °C	T <sub>g</sub> °C	10 <sup>4</sup> α † deg <sup>-1</sup>	Crystal- linity ‡ %
NaOCH <sub>3</sub>	OCH <sub>3</sub>	1 500	—	1.002	—	-92	—	—
	OCH <sub>3</sub>	2 000	—	1.002	-72	-86	7.8	—
	—	—	—	—	—	—	±0.2	—
	OCOCH <sub>3</sub>	2 000	—	—	-67	—	—	—
KOH	OH	2 000	—	—	-63	—	—	—
	OCH <sub>3</sub>	3 200	—	1.002	—	-81	—	—
SrCO <sub>3</sub>	OH	—	10 <sup>4</sup>	1.059§	+66.5	-75	—	41
	OH	—	10 <sup>5</sup>	1.056§	+66.5	-75	—	39
Zn(C <sub>2</sub> H <sub>5</sub> ) <sub>2</sub> -H <sub>2</sub> O	OH	—	10 <sup>6</sup>	1.002	—	-75	7.3 ±0.2	— 7
	OH	—	10 <sup>6</sup>	1.010	+68	-75		
	OH	—	10 <sup>6</sup>	1.057§	+69	-75		

\*Measured at 20°C.

†In the melt.

‡Estimated from densities.

§Fraction insoluble in methanol at 0°C.

some interest because other workers use similar methods of fractionation for poly(propylene oxide). As one would expect,  $T_m$  and  $T_g$  become independent of molecular weight. In addition  $T_m$  is independent of the nature of the catalyst and close to the values reported by Price and co-workers<sup>7</sup> for polymer produced with a  $\text{FeCl}_3$  catalyst. Thus all the crystallizable material is probably of the same stereospecific form, namely the isotactic configuration identified by Natta and Corradini<sup>8</sup>.

In the low molecular weight oils the melting point varies with the nature of the end group. For example, methylation decreases  $T_m$  by  $10^\circ\text{C}$  for one sample; simultaneously its apparent molecular weight determined cryoscopically in benzene is halved and so is the viscosity of the oil. These effects are due to the elimination of hydrogen bonding. Acetylation produces an intermediate result, and though easier to perform it is not preferable to methylation.

#### *Vitrification and crystallizability*

The glass transitions of the various specimens of poly(propylene oxide) show no trend with crystallinity,  $T_g = -(74 \pm 2)^\circ\text{C}$  for all fractions and is, presumably, independent of stereoregularity. Dynamic mechanical loss spectra obtained over a range 0.01 to 1000 c/s support this conclusion since the position of the loss peak at a given frequency is also independent of crystallinity<sup>10</sup>.

#### *Crystallizability and melting points*

The highest melting point observed in the first phase of the work was  $69^\circ\text{C}$ , somewhat lower than the upper limit reported by Price and co-workers<sup>7</sup> ( $72^\circ$  to  $76^\circ\text{C}$ ). Some discrepancy might arise from the different methods used to estimate  $T_m$  but insufficient detail is available for a comparison to be made of the melting point techniques. On the other hand the melting points of Price and Chu<sup>7</sup> were all obtained by the same method and therefore the order of increasing melting point is likely to be significant. The other possibility is that  $\text{FeCl}_3$  produces a more crystalline polymer and this is supported by the fact that the first poly(propylene oxide) fraction obtained from iso-octane has a melting point of  $73^\circ\text{C}$ , four degrees higher than that of the parent polymer obtained from a zinc diethyl-water catalyst.

Since the fractions obtained from iso-octane solutions differ in crystallizability rather than molecular weight we were able to examine the effect of crystallizability and (by implication) stereoregularity on some physical

Table 2. Some properties of poly(propylene oxide) fractions\*

Fraction No.	$10^{-6} \bar{M}_w$	$10^4 A_2 \dagger$ $\text{cm}^3 \text{g}^{-2}$ mole	Density ‡ $\text{g cm}^{-3}$	$T_m$ $^\circ\text{C}$	$T_g$ $^\circ\text{C}$	$10^{4\alpha} \S$ $\text{deg}^{-1}$	Crystallinity    %	$p$
1a	1	0.0	1.090	73	-75	8.0	61	0.98
3a	1.8	1.8	1.043	71	-74	7.7	30	0.97
5a	1.3	3.6	1.021	66	-75	7.6	14	0.93
9	1.1	4.0	1.015	58	-72	7.4	10	0.86

\*Precipitated from iso-octane solution.

† $n$ -Hexane solution at  $46^\circ\text{C}$ .

‡Measured at  $20^\circ\text{C}$ .

§In the melt.

|| Estimated from densities.



properties of poly(propylene oxide). The results are summarized in *Table 2*.  $T_m$  decreases with crystallizability and follows the trend observed<sup>4</sup> in the second virial coefficient of solutions in *n*-hexane at 46°C. Such a decrease in  $T_m$  has been predicted and in the case of polypropylene already demonstrated<sup>8</sup>. The melting point data can be used to estimate the fraction of monomer units in, say, isotactic placements ( $p$ ) by means of the equation

$$(1/T_m^0 - 1/T_m) = R/\Delta H_f \cdot \ln p \quad (1)$$

The values of  $p$  given in *Table 2* have been calculated in this way assuming  $T_m^0 = 75^\circ\text{C}$  and  $\Delta H_f = 2\,000$  cal (mole repeat unit)<sup>-1</sup>. In spite of the rapid decline in crystallizability only a relatively small change in  $p$  is obtained. For polypropylene<sup>8,9</sup> on the other hand  $p$  decreases to a value close to 0.5 (characteristic of an atactic polymer).

In any discussion of these results, it is worth bearing in mind that the use of equation (1) is of quite unknown reliability in this context. The equation was derived<sup>11</sup> from a highly idealized lattice model to account for melting point variations with composition in random copolymers. Its usefulness in estimating degrees of tacticity has not been tested on polymer fractions for which independent values of  $p$  are available. Thus it is possible that the values of  $p$  calculated for poly(propylene oxide) are not significant. However, taking the information at its face value, the difference between the results for the two polymers is most probably due to the difference in fractionation methods. Fraction 9 of poly(propylene oxide) comprised almost 75 wt % of the high molecular weight polymer and the value of  $T_m$  obtained dilatometrically will be approximately that of the most highly crystalline polymer molecules in the fraction. If further fractions can be obtained by use of a better solvent at lower temperatures it seems possible that  $p$  might fall to 0.5. An attempt to use toluene as a solvent for this purpose was unsuccessful.

Alternatively the values assumed for  $T_m^0$  and  $\Delta H_f$  may be in error for poly(propylene oxide) since the highest melting point was measured on a fraction only 60 per cent crystalline and there is no experimental value for  $\Delta H_f$  as for poly(propylene). However, this uncertainty may not have an important bearing on the results because if  $T_m^0 = 80^\circ\text{C}$  or  $\Delta H_f = 3\,000$  cal mole<sup>-1</sup> the lowest value of  $p$  is still  $> 0.80$ .

*Department of Chemistry,  
University of Manchester*

*(Received December 1963)*

#### REFERENCES

- <sup>1</sup> MANDELKERN, L. *Chem. Rev.* 1956, **56**, 903
- <sup>2</sup> GEE, G., HARTLEY, P. N., HERBERT, J. M. B. and LANCELEY, H. A. *Polymer, Lond.* 1960, **1**, 365
- <sup>3</sup> BOOTH, C., JONES, M. N. and POWELL, E. *Nature, Lond.* 1962, **196**, 772
- <sup>4</sup> ALLEN, G., BOOTH, C. and JONES, M. N. *Polymer, Lond.* 1964, **5**, 195
- <sup>5</sup> ALLEN, G., BOOTH, C. and JONES, M. N. *Polymer, Lond.* 1964, **5**, 257
- <sup>6</sup> NATTA, G., CORRADINI, P. and DALL'ASTA, G. *Atti. Accad. Lincei (Classe sci. fis. mat. e. nat.)*, 1956, **20**, 408

- <sup>7</sup> CHU, N. S. and PRICE, C. C. *J. Polym. Sci. A*, 1963, **1**, 1105  
PRICE, C. C. and OSGAN, M. J. *Amer. chem. Soc.* 1956, **78**, 4787
- <sup>8</sup> NEWMAN, S. J. *J. Polym. Sci.* 1960, **47**, 111
- <sup>9</sup> MILLER, R. L. *J. Polym. Sci.* 1962, **57**, 975
- <sup>10</sup> WETTON, R. E. *Ph.D. Thesis*, University of Manchester, 1962
- <sup>11</sup> FLORY, P. J. *Trans. Faraday Soc.* 1955, **51**, 848

# Polypropylene Oxide IV—Preparation and Properties of Polyether Networks

G. ALLEN\* and H. G. CROSSLEY†

*Stable vulcanizates of copolymers of propylene oxide and butadiene monoxide have been prepared and some physical properties studied. The cohesive energy density of a copolymer containing 84 per cent polypropylene oxide is determined from swelling measurements to be  $83 \text{ cal cm}^{-3}$ . The dynamic properties of the copolymer are similar to those of natural rubber. From a thermodynamic point of view the copolymer is more ideal in its rubbery behaviour than natural rubber.*

ATTEMPTS to crosslink poly(propylene oxide) by conventional free radical, photochemical or  $\gamma$ -irradiation methods usually lead to degradation instead of network formation. Fairly stable networks suitable for physical investigations are formed when copolymers containing butadiene monoxide are crosslinked through the substituent vinyl groups. In a previous study of the swelling and thermoelastic properties of polypropylene oxide Conway and Tong<sup>1,2</sup> used polyurethane networks. Unfortunately their thermoelastic data were analysed by a method<sup>3</sup> which has subsequently been shown<sup>4</sup> to be inadequate for the investigation of the thermodynamics of rubber elasticity and the results show inconsistencies when re-examined by a more refined procedure. We have, therefore, obtained thermoelastic data for the propylene oxide-butadiene monoxide copolymer and, in addition, examined the dynamic properties of this elastomer.

## EXPERIMENTAL

### *Preparation of elastomers*

Polypropylene oxide, polybutadiene monoxide and copolymers containing five to twenty per cent butadiene monoxide were prepared in dioxan solution at room temperature using a zinc diethyl-water catalyst<sup>5a</sup>. Iodine values and infra-red analysis of the polymers containing butadiene monoxide showed that the vinyl groups were intact and the composition of the unreacted monomer mixture was consistent with random copolymer structures. Molecular weights were  $\sim 10^6$  in every case. Most of the crystallizable material was removed prior to crosslinking by a crude fractionation of the raw polymer (cf. page 555) from methanol solution at 0°C.

Mechanically weak networks were obtained by irradiating with u.v. light, polypropylene oxide sensitized with two per cent acetone or benzophenone and sealed under vacuum in 'Hysil' tubes. These specimens were unsuitable for further study. Polybutadiene oxide crosslinked rapidly without a sensitizer under otherwise identical conditions. Degradation always occurred when the polymers were irradiated in air. The best networks were obtained

\*Department of Chemistry, The University, Manchester, 13

†John Dalton Technical College, Newton Heath, Manchester.

from polybutadiene monoxide and also from the copolymer using a conventional sulphur recipe :

100 parts polymer, 1.5 parts sulphur, 1.0 part z.d.c.

curing for  $7\frac{1}{2}$  minutes at  $155^{\circ}\text{C}$ . Extraction of the network using a 25 per cent solution of acetone in benzene removed about 30 per cent by weight of low molecular weight material. This extract did not contain carbonyl groups normally found in degraded polyethers and the low molecular weight species originated, presumably, in the polymerization mechanism.

#### *Swelling measurements*

Analytical reagent grade solvents were dried prior to use. The amount of swelling was determined by removal of the specimen from the solvent, the surface was quickly dried with filter paper and the swollen specimen was then transferred to a tared weighing bottle and re-weighed. This procedure was carried out in a thermostatically controlled room at  $22^{\circ} \pm 1^{\circ}\text{C}$ , and was repeated for each specimen until equilibrium swelling was attained.

#### *Stress measurements*

Stress/strain curves were determined by hanging known loads on a strip of elastomer and measuring the resulting extension ratio.

Thermoelastic measurements were made at constant length by suspending the rubber strip from one arm of a balance and adjusting the weights in the other pan to counterbalance the tension. All the measurements were made with the sample suspended in an atmosphere of 'white spot' nitrogen and thermostatically controlled to  $\pm 0.1$  degree.

In all measurements of stress the time scale was chosen so that stress relaxation effects did not contribute detectably to the results. Errors from this source were further reduced by relaxing the specimen at the highest temperature and extension ratio before the series of experiments was begun.

## RESULTS

#### *Cohesive energy density*

For the 5:1 propylene oxide-butadiene monoxide copolymer and also for polybutadiene monoxide swelling measurements in a range of solvents (including *n*-alkanes, aliphatic ketones, benzene and toluene) showed a sharp maximum for diethyl- and methyl-isopropylketones. This corresponds to a solubility parameter of  $9.1 \text{ cal}^{\frac{1}{2}} \text{ cm}^{-3/2}$  and cohesive energy density of  $83 \text{ cal cm}^{-3}$ . From the degree of swelling in benzene, assuming  $\chi = 0.20^1$ , the average molecular weight between crosslinks was estimated to be  $10^4$  for the polybutadiene monoxide vulcanizate and  $3 \times 10^4$  for the copolymer.

#### *Rubber elasticity*

The investigation was confined to the copolymer vulcanizate because the polybutadiene monoxide tended to crosslink further at the temperatures used in the thermoelastic measurements. Strips of elastomer cut from the first set of vulcanizates showed a discontinuity at  $55^{\circ}\text{C}$  in the temperature dependence of the length of a strip subjected to a small constant load. Since

polypropylene oxide melts in the range 50° to 70°C, this behaviour was attributed to the presence of crystalline material and subsequently all raw copolymers were fractionated several times before vulcanization. Results presented in *Figure 1* show that the length/temperature dependence was then of the form characteristic of a rubber. Stress/temperature measurements made at atmospheric pressure are summarized in *Figure 2* for extension ratios  $\lambda=1.2$  to 2.3. From these data the coefficient  $[\partial \ln(f/T)/\partial T]_{P,L}$  was computed and the energetic contribution ( $f_e$ ) to the

*Figure 1*—Length/temperature relationships: (a) before; (b) after removal of crystallizable polymer

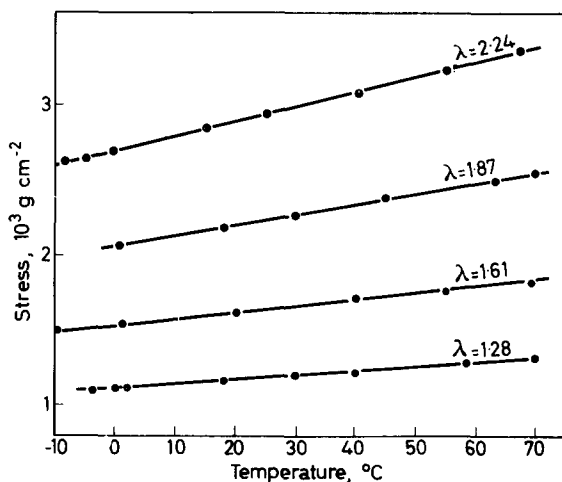
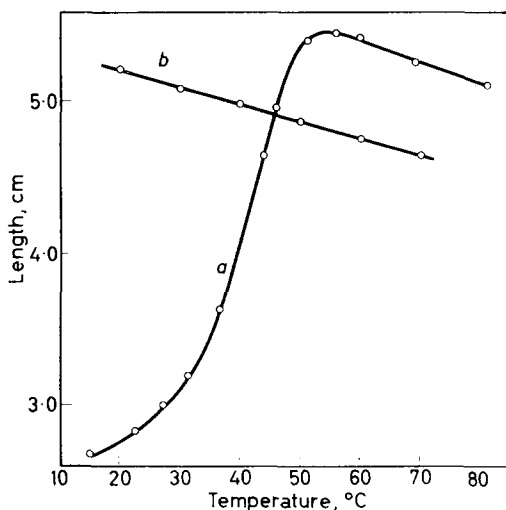


*Figure 2*—Stress/temperature relationships at various  $\lambda$

total elastic force ( $f$ ) was estimated from Flory's equation<sup>4</sup>

$$f_e/f = -T [\partial \ln (f/T) / \partial T]_{P,L} - \alpha T / (\lambda^3 - 1) \quad (1)$$

where  $\alpha = V^{-1} (\partial V / \partial T)_{P,L}$ .

Table 1. Thermoelastic data for a 5:1 propylene oxide-butadiene monoxide copolymer at 300°K

$\lambda$	$-T [\partial \ln (f/T) / \partial T]_{P,L}$	$\alpha T / (\lambda^3 - 1)^*$	$f_e/f$	$\frac{\partial \ln \langle r_0^2 \rangle}{\partial T}$ deg <sup>-1</sup>
1.28	0.25	0.18	0.06 ± 0.05	2 × 10 <sup>-4</sup>
1.61	0.21	0.06	0.15 ± 0.05	5 × 10 <sup>-4</sup>
1.87	0.04	0.04	0.00 ± 0.02	0.0
2.24	0.01	0.02	-0.01 ± 0.02	~0.0

\* $\alpha$  measured in a subsidiary experiment was 6.6 × 10<sup>-4</sup> deg.<sup>-1</sup>

### Dynamic properties

The glass transitions<sup>5b</sup> of polybutadiene monoxide and polypropylene oxide -75° ± 2°C, lie close to the value for natural rubber. Dr B. E. Read kindly measured the mechanical loss curve for the 5:1 copolymer vulcanizate at approximately 1 c/s using a torsion pendulum. Again the results were similar to those obtained<sup>6</sup> for a natural rubber vulcanizate of approximately the same degree of crosslinking (cf. Figure 3).

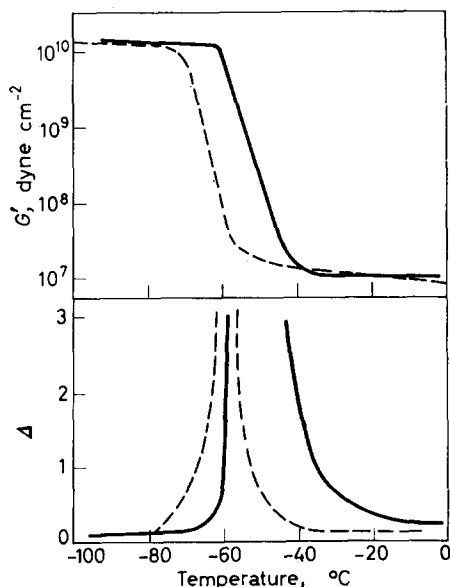


Figure 3—Comparison of dynamic properties of polymer with natural rubber.  
— natural rubber  
- - - polyether

### DISCUSSION

Since the physical properties of the two homopolymers are very similar we may expect the properties of the copolymer vulcanizate containing 84 per cent propylene oxide to be close to those of the corresponding propylene oxide vulcanizate. It is not surprising, therefore, that the cohesive

energy density of the copolymer is about ten per cent smaller than the internal pressure of polypropylene oxide<sup>7</sup>  $P_i=90 \text{ cal cm}^{-3}$ , since in the cases where data are available it is known that the ratio of  $P_i/\text{c.e.d.}$  lies in the range 1.1 to 1.2 for polymers.

Comparison of the properties of the copolymer and natural rubber shows that although their glass transitions and dynamic properties are similar, the polyether is a more ideal rubber from the thermodynamic point of view. Roe and Krigbaum<sup>8</sup> found for natural rubber

$$f_e/f \simeq 0.20 \quad (2)$$

using the method which we have employed for the polyether and the validity of their conclusion has been confirmed recently for natural rubber by a more rigorous procedure. For the polyether the elastic force is almost entirely entropic\* in origin and  $f_e/f$  probably does not exceed 0.1.

Equation (1) is derived<sup>4</sup> from a polymer chain model incorporating restricted internal rotation about main-chain bonds and  $f_e/f > 0$  when the unperturbed dimensions of the chain are temperature dependent, since

$$f_e/f = T (\partial \ln \langle r_0^2 \rangle / \partial T) \quad (3)$$

Thus our thermodynamic data imply that the temperature coefficient for polypropylene oxide is very small and probably positive.

*The authors thank Mr S. J. Hurst for the preparation and analysis of the copolymers. One of us (H.C.) is grateful to the Governors of Newton Heath Technical College for permission to undertake the work.*

Department of Chemistry,  
University of Manchester

(Received December 1963)

#### REFERENCES

- <sup>1</sup> CONWAY, B. E. and TONG, S. C. *J. Polym. Sci.* 1960, **46**, 113
- <sup>2</sup> CONWAY, B. E. *J. Polym. Sci.* 1960, **46**, 129
- <sup>3</sup> See for example GEE, G. *Trans. Faraday Soc.* 1946, **42**, 585
- <sup>4</sup> FLORY, P. J. *Trans. Faraday Soc.* 1961, **57**, 829
- <sup>5a</sup> POWELL, E. *Ph. D. Thesis*, University of Manchester, 1962
- <sup>5b</sup> MARKS, D. J. *Ph. D. Thesis*, University of Manchester, 1961
- <sup>6</sup> SCHMIEDER, K. and WOLF, K. *Kolloidzshr.* 1953, **143**, 149
- <sup>7</sup> ALLEN, G., GEE, G., MANGARAJ, D., SIMS, D. and WILSON, J. G. *Polymer, Lond.* 1960, **1**, 467
- <sup>8</sup> ROE, R.-J. and KRIGBAUM, W. R. *J. Polym. Sci.* 1962, **61**, 167

\*Conway's evidence<sup>2</sup> is not relevant since the thermoelastic analysis used leads to the conclusion that natural rubber is also an ideal elastomer.

# The Polymerization of Vinylcarbazole by Electron Acceptors I

L. P. ELLINGER

*The polymerization of vinylcarbazole has been initiated by organic electron acceptors of widely different electron affinity, including chloranil, sym. trinitrobenzene, tetranitromethane, maleic anhydride, tetrachlorethylene, acrylonitrile, and methyl methacrylate. In many cases, polymerization is accompanied by the development of characteristic colours. Characteristic features of these polymerizations have been studied in bulk and in toluene solution. The stronger acceptors initiate polymerization in aqueous dispersion. The conjugation of the lone pair electrons of vinylcarbazole with the vinyl group, which is manifested in the ultra-violet spectrum, is enhanced by these acceptors.*

*Methyl methacrylate and acrylonitrile, which copolymerize with vinylcarbazole in free radical initiated polymerization, yield essentially pure polyvinylcarbazole. In methanol solution and in the presence of chloranil, 9-(1'-methoxyethyl)-carbazole, and on illumination with visible light 1,2-trans-dicarbazylcyclobutane, are formed.*

*Carbon tetrachloride does not initiate polymerization in absence of light, but polymerization occurs after lengthy exposure to daylight, or in the dark in the presence of methyl methacrylate. The mechanism and special features of the polymerization are discussed. It is concluded that in the absence of solvent and in non-ionizing solvents there is only partial transfer of one electron. Activation is thought to be due, simultaneously, to partial charge transfer and to increased polarization of the N—CH=CH<sub>2</sub> group.*

N-VINYLCARBAZOLE can be polymerized by heating<sup>1, 2, 8</sup>, free radical forming catalysts<sup>3, 4, 5, 8, 14</sup>, inorganic and organic cationic catalysts<sup>6, 7, 8, 14, 37, 38</sup>, Ziegler catalysts<sup>9, 10, 11</sup>, and by high energy radiation<sup>12, 13</sup>. Of these free radical, ionic and radiation initiated polymerizations comply essentially with the pattern to be expected as regards choice and concentration of initiator, conditions, effects of impurities and of inhibitors, and the effect of oxygen. High molecular weight polymers are obtained only under carefully defined conditions and by use of very pure materials.

Oxidizing agents other than typical free radical initiators can initiate the polymerization<sup>8, 14, 15</sup>. Thus under the conditions of the Bozel-Moletra oxidation of olefins by hot aqueous alkaline sodium dichromate, vinylcarbazole is polymerized in high yield to a product of fairly high molecular weight which is free from oxidation products<sup>8, 15</sup>.

If alkaline sodium dichromate produces a small concentration of a partial oxidation product (vinylcarbazole from whose vinyl group a hydrogen atom has been removed, or to whose double bond OH has been added), this should be oxidized further more readily than the parent monomer. It is surprising that under the rather vigorous conditions of the chromate treatment oxidation products are not formed from either monomer or polymer. It was therefore considered that the effect of sodium dichromate on the monomer, though sufficient to effect polymerization, does not involve the complete abstraction of a hydrogen, addition of —OH, or complete transfer of either a proton or of an electron.



Thus the lone pair of electrons on the vinylcarbazole nitrogen might make the molecule sufficiently electron-donating to facilitate partial electron transfer to an electron acceptor, the  $\text{N}-\text{CH}=\text{CH}_2$  group becoming simultaneously sufficiently polarized for polymerization of the monomer to occur.

Preliminary attempts at polymerization of vinylcarbazole by organic electrophilic compounds were immediately successful<sup>16</sup>. The acceptors were chosen as representing various classes of compounds known to give characteristically coloured electron-transfer complexes, in the presence or absence of solvent, with nucleophilic molecules. These compounds include chloranil, maleic anhydride, 1,3,5-trinitrobenzene, chloro-2,4-dinitrobenzene, tetracyanoethylene and tetranitromethane, and all of these proved initiators either at ambient temperature or at temperatures below  $80^\circ\text{C}$ <sup>16, 35</sup>.

Some features of polymerizations by these electron acceptors are now described. Their range has been extended also to representatives of several classes of quite weak electron acceptors<sup>36</sup>. These include ethyl cyanoacetate, cyclopentadiene, and in particular acrylonitrile and methyl methacrylate, which are known to form copolymers with vinylcarbazole in free radical polymerizations<sup>31-33</sup>.

Polymerization of vinylcarbazole by halogens<sup>3</sup> may proceed by an initiation mechanism involving electron transfer<sup>17</sup>. The work here described is limited to polymerization by organic electron acceptors.

Evidence for resonance in the  $\text{N}-\text{C}_{(1,3)}$  bond of vinylcarbazole has been sought in the ultra-violet and infra-red absorption spectra of this monomer<sup>16</sup>.

The polymerization of vinylcarbazole by carbon tetrachloride in the dark at ambient temperature with colour development<sup>13</sup>, which has been confirmed in the presence of methyl methacrylate<sup>18</sup>, and denied for pure carbon tetrachloride<sup>16, 29</sup>, is now shown not to occur. Polymerization occurs in the presence of methyl methacrylate, but is due to the latter and not to the carbon tetrachloride.

Very recently Scott, Miller and Labes have stated that vinylcarbazole polymerization can be initiated by chlorine, by chloranil and related quinonoid compounds, by tetracyanoethylene and related compounds, and by Wurster salts, but that it does not occur in methanol, and that it is slowed down by water<sup>17</sup>. These workers postulate that initiation is by an oxidative reaction between monomer and initiator resulting in a vinylcarbazole Wurster free radical cation.

#### MATERIALS

Vinylcarbazole (BASF Chemicals Ltd) once recrystallized grade, recrystallized from methanol before use, m.pt  $64.7^\circ\text{C}$ .

Chloranil (L. Light & Co. Ltd) recrystallized from benzene.

1,3,5-Trinitrobenzene (B.D.H. Ltd, Lab. grade).

Chloro-2,4-dinitrobenzene (Hopkins & Williams Ltd, Lab. grade).

Tetranitromethane (L. Light & Co. Ltd) was steam distilled, washed with alkali, water, and dried over magnesium sulphate.

Maleic anhydride (Griffin & George Ltd) was recrystallized from benzene.

Tetrachlorethylene (Griffin & George Ltd) was washed repeatedly with concentrated aqueous caustic soda and water, dried over magnesium sulphate, and fractionated, a cut b.pt 121° to 122° being used.

Acrylonitrile (B.D.H. Ltd) was distilled through a Vigreux column, the fraction b.pt 76° to 79° being used.

Methyl methacrylate (I.C.I. Ltd) was fractionated *in vacuo* for removal of stabilizer; in several experiments the stabilized monomer was used.

Carbon tetrachloride (Griffin & George Ltd) was washed with dilute aqueous sodium carbonate, with water, dried over magnesium sulphate, and the fraction b.pt 78°C was isolated.

Ethyl cyanoacetate (B.D.H. Ltd) was redistilled, b.pt 52°–56°/1.25 mm.

Cyclopentadiene was prepared by pyrolysis of dicyclopentadiene and redistilled immediately before use.

Dichloromethane (Griffin & George Ltd, redistilled grade) was used as spectroscopic solvent without further purification.

N-Allylcarbazole was prepared<sup>19</sup>, and recrystallized twice from methanol m.pt 56° to 57°.

N-Acetylcarbazole was prepared by heating carbazole (6 g) and acetic anhydride (5 g) in presence of a drop of sulphuric acid at 100° for 5 minutes. The product was recrystallized twice from ethanol<sup>20</sup>, m.pt 76°.

'Nonex 64', polyethylene glycol 1 000 mono-oleate (Union Carbide Ltd).

#### EXPERIMENTAL

Well cleaned glass equipment was used, but no attempt was made to remove moisture films and other trace impurities. The work was carried out in air and in diffuse day or artificial light unless otherwise stated.

Following polymerization in the absence of solvent, the polymer was dissolved in approximately 5 ml boiling benzene per g of vinylcarbazole (weight before polymerization), and the polymer was precipitated from this solution by the addition of about 2 ml of methanol per ml benzene.

Following polymerization in toluene solution a similar proportion of methanol was added to precipitate the polymer. The precipitated polymer was freed from residual monomer by four extractions with boiling methanol (10 ml methanol per g monomer in each extraction). The high molecular weight polymers obtained with methyl methacrylate required thorough trituration at this stage. This procedure was modified when polymer of very low molecular weight was obtained from polymerizations in aqueous dispersion. The polymers were extracted with approximately 3.5 ml of boiling methanol per g of vinylcarbazole. The polymers were dried at ambient temperature *in vacuo*.

For polymerization in aqueous dispersion, monomer (200 g) was dispersed in water (700 ml) containing 10 ml of a three per cent aqueous solution of polyethyleneglycol 1 000 mono-oleate ('Nonex 64') by stirring with a wing stirrer at 700 rev/min, and heating in a water bath. At a selected temperature the electron acceptor was added, and heating was continued for 5 to 30 minutes, the bath temperature increasing by 1° to 10°C.

Relative viscosities were determined using one per cent benzene solutions of the polymers in an Ostwald viscometer type A.

To determine chlorine, samples were burned in oxygen in the presence of ammonium carbonate. After reaction with silver nitrate, the silver chloride was determined spectrophotometrically. To determine the nitrile group, samples were digested with concentrated hydrochloric acid, alkali was added, and the ammonia liberated was determined. The procedure was checked against blanks prepared from styrene-acrylonitrile copolymers, the limit being 0.003 to 0.2 per cent of CN.

In the polymers prepared with ethyl cyanoacetate, i.r. absorption spectrophotometry was used to detect the nitrile group; the limit of detection was 0.25 per cent (see *Table 5*).

#### RESULTS

##### (a) *Ultra-violet absorption spectra of N-vinylcarbazole and of related compounds*

The ultra-violet spectra of *N*-vinylcarbazole and of *N*-acetylcarbazole, in which conjugation in the N—C<sub>(1,3)</sub> bond is possible, and of related *N*-alkylcarbazoles in which such conjugation cannot occur (*N*-methyl-, *N*-ethyl-, *N*-allyl- and poly-*N*-vinyl-carbazole) have been determined; they are shown in *Figure 1* and *Figure 5*.

##### (b) *Infra-red absorption spectrum of N-vinylcarbazole*

This was determined on a nine per cent solution of the monomer in methylene dichloride using 0.05 mm thickness. The following peaks due to the vinyl group were noted:

cm <sup>-1</sup>	Assignment
1 640, 1 625 doublet	C=C bond stretching
963	Hydrogen deformation mode of —CH=C—
866	Out of plane deformation of the hydrogens of =CH <sub>2</sub>

##### (c) *Ultra-violet and infra-red absorption spectra of some vinylcarbazole-acceptor solutions*

The u.v. absorption spectra of a  $2 \times 10^{-5}$  M vinylcarbazole solution in dichloromethane (determined against the solvent), and the absorption spectra containing a similar concentration of vinylcarbazole and several concentrations of tetranitromethane or tetrachlorethylene (determined against the same acceptor concentration in solvent) are shown in *Figure 2*. It is noticeable that while the position of the absorption bands has not changed markedly, they have become less sharp and in every case the absorption has increased, the increase being dependent on the electron affinity and the concentration of the acceptor. The effect of chloranil is, both qualitatively and quantitatively, almost identical with that of tetranitromethane.

The i.r. absorption spectrum of vinylcarbazole in tetrachlorethylene was found to be identical with that obtained in carbon tetrachloride. The i.r. spectrum of the monomer in carbon tetrachloride or carbon bisulphide was not affected significantly in the presence of tetranitromethane, nor was any interaction with acrylonitrile or methyl methacrylate observed.

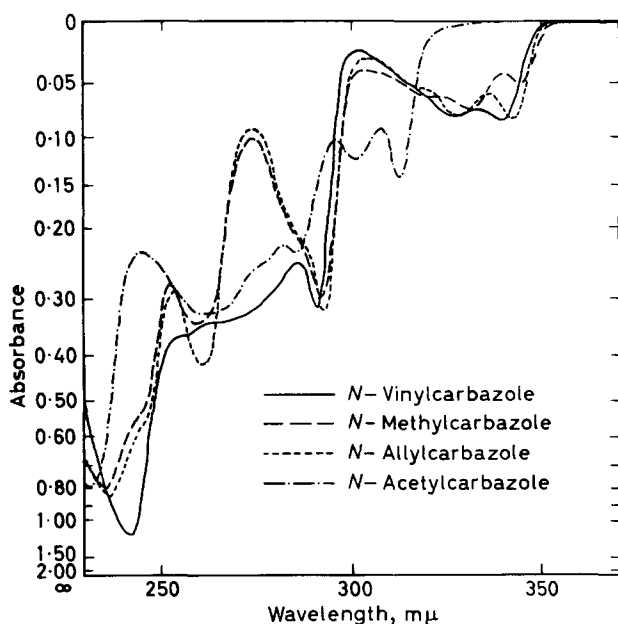


Figure 1—Ultra-violet absorption spectra of *N*-vinylcarbazole, *N*-methylcarbazole, *N*-allylcarbazole and *N*-acetylcarbazole.  $2 \times 10^{-3}$  M solutions in dichloromethane

#### (d) Polymerization of vinylcarbazole by electron acceptors

Organic compounds representative of several classes of electron acceptors varying widely in their electron affinity were shown to initiate polymerization of vinylcarbazole (Table I). With the stronger electron acceptors a characteristic colour developed quite rapidly, more slowly with the weaker acceptors, while with the weakest acceptors the mixture remained colourless, or slowly developed a very pale yellow tinge. The polymers were colourless or almost colourless after isolation.

Control experiments have been carried out for these and for the other polymerizations to ensure that the thermal polymerization rate is insignificant over the period of the experiment.

Since it was noted that (at least with chloranil as initiator) the polymerization rate is speeded up somewhat by daylight, the polymerizations here described have been carried out with the partial or complete exclusion of light except where stated otherwise.

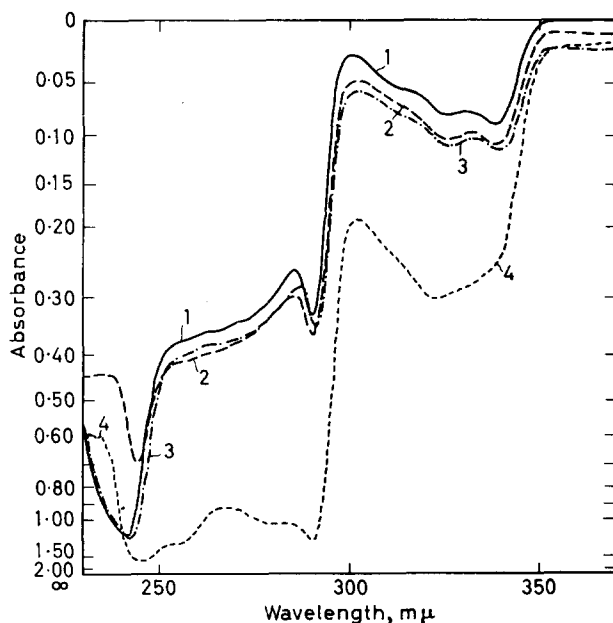


Figure 2—Ultra-violet absorption spectra of vinylcarbazole alone and in the presence of tetranitromethane or tetrachlorethylene. 1,  $2 \times 10^{-5}$  M vinylcarbazole; 2,  $2 \times 10^{-5}$  M vinylcarbazole and  $2 \times 10^{-3}$  M tetrachlorethylene against  $2 \times 10^{-5}$  M tetrachlorethylene; 3,  $2 \times 10^{-5}$  M vinylcarbazole and  $2 \times 10^{-5}$  M tetranitromethane against  $2 \times 10^{-5}$  M tetranitromethane; 4,  $2 \times 10^{-5}$  M vinylcarbazole and  $2 \times 10^{-3}$  M tetranitromethane, against  $2 \times 10^{-3}$  M tetranitromethane, all in dichloromethane.

Table 1. Bulk polymerization of vinylcarbazole by electron acceptors

Compound	Wt, % on monomer	Polymerization			Product	
		Temp., °C	Time, h	Colour	Yield, %	Relative viscosity
Chloranil	0.5	70	24	mauve	71.2	1.199
1,3,5-Tri-nitrobenzene	2	80	48	red	64.4	1.124
Chloro-2,4-dinitrobenzene	2	80	48	orange	52.2	1.129
Maleic anhydride	5	80	1	light yellow	76.6	1.184
Trichlorethylene	25	80	20	colourless	high	—
Tetrachlorethylene	1	80	72	orange	77	1.173
Acrylonitrile	5	70	24	colourless	50.7	1.204
Methyl methacrylate	5	80	24	colourless	39.6	8.040
Ethyl cyanoacetate	2.8	60	72	light yellow	31.6	1.253
Cyclopentadiene	29.3	55	72	very light yellow	6.2	—

POLYMERIZATION OF VINYL CARBAZOLE BY ELECTRON ACCEPTORS I

Solution polymerizations were carried out in toluene, since it dissolves the monomer, polymer and the acceptors studied, has a low dielectric constant, and can be used over a wide temperature range.

Table 2. Polymerization of vinylcarbazole by electron acceptors in toluene solution. Vinylcarbazole, 10 g

Compound	g	Polymerization				Polymer	
		Toluene, ml	Temp., °C	Time, h	Colour	Yield, %	Relative viscosity
Chloranil	0.1	100	80	24	mauve	65.2	1.123
Tetracyan-ethylene	0.1	35	80	2.2	pink	93.5	1.105
Maleic anhydride	0.1	35	80	24	yellow	30.4	1.143
Methyl methacrylate	1.0	20	100-10	94	colourless	69.9	1.829

Chloranil and tetranitromethane effect rapid polymerization in aqueous dispersion in high yield at 60° to 70°, yielding polymer of much lower molecular weight than polymerization in bulk or toluene solution. These polymerizations are accompanied by some hydrolysis of the monomer to acetaldehyde. With picric acid and 2,4-dinitroresorcinol in aqueous dispersion polymerization is accompanied by more severe hydrolysis.

The polymerizations were also studied under oxygen or nitrogen atmospheres, since the free radical polymerization of vinylcarbazole in aqueous dispersion is subject to a well marked oxygen effect<sup>39</sup>.

Table 3. Polymerization of vinylcarbazole by electron acceptors in aqueous dispersion. For other quantities see 'Experimental'

Compound	g	Polymerization		Polymer	
		Temp. of addn, °C	Atmosphere	Yield, %	Relative viscosity
Chloranil	2	70	Oxygen	93.7	1.031
Chloranil	2	70	Nitrogen	98.3	1.027
Tetranitromethane	0.2	60	Air	56.8	1.043
Tetranitromethane	1	70	Air	13.5	1.035
				47	1.075
Tetranitromethane	2	60	Air	96.9	1.046
Tetranitromethane	2	60	Nitrogen	96.9	1.043
Tetranitromethane	2	60	Oxygen	95.9	1.046
2,4-Dinitroresorcinol	0.25	65	Air	83.7	1.027

Polymerizations with tetranitromethane and dinitroresorcinol were complete within three minutes of the initiator addition, and were accompanied by a sharp temperature rise; with chloranil there was little polymerization while the monomer was dispersed, but it occurred rapidly soon after stirring had ceased. While these polymerizations were performed in daylight, the

duration of these experiments was too brief for any appreciable photochemical effect.

The effect of the concentration of selected initiators on the molecular weight of the polyvinylcarbazole has been examined, and the polymers have been, where possible, analysed for incorporation of initiator.

Table 4. Bulk polymerization of vinylcarbazole by chloranil, tetrachlorethylene and maleic anhydride

Compound	Polymerization				Polymer		
	on monomer, %	Temp., °C	Time, h	Yield, %	Relative viscosity	Chlorine %	Carboxyl, %
Chloranil	0.5	70	22	71.2	1.199	0.02	—
Chloranil	1.0	70	22	73.8	1.239	0.03	—
Chloranil	2.0	70	22	74.9	1.194	0.02	—
Chloranil	5.0	70	22	63.5	1.176	0.11	—
Chloranil	63.7	70	0.2	87.4	1.140	1.38	—
Maleic anhydride	1.0	80	3.5	58	1.489	—	<0.013
Maleic anhydride	1.0	80	24	79	1.138	—	<0.1
Maleic anhydride	5	80	1.0	76.6	1.184	—	<0.013
Maleic anhydride	25.4	80	0.6	83.5	1.140	—	<0.013
Tetrachlorethylene	1.0	90	25	43.2	1.15	0.02	—
Tetrachlorethylene	1.0	80	72	77	1.173	0.02	—
Tetrachlorethylene	1.0	80	72	69.9	1.175	0.05	—
Tetrachlorethylene	10.0	80	72	{ 76.6 2.2	{ 1.165 1.27	{ 0.01 —	{ — —
Tetrachlorethylene	43.0	80	72	{ 57.9 20.6	{ 1.176 1.250	{ <0.01 <0.01	{ — —
Tetrachlorethylene	86.0	80	72	42.5	1.140	0.03	—

While the typical mauve and yellow colouration developed quite rapidly with chloranil and maleic anhydride respectively, especially with the higher concentrations of these initiators, initiation by tetrachlorethylene resulted in slow development through yellow and orange to a bright red, the depth and intensity of the colouration increasing with the proportion of tetrachlorethylene. This colour was discharged completely when the mixture was dissolved in benzene, and the purified polymer was dead white.

Only a faint yellow tinge was developed in the polymerizations with acrylonitrile. Infra-red examination of the polymer has shown this to be identical with other polyvinylcarbazole samples, and there is no trace of absorption due to the nitrile group. From polymerizations in the presence of the higher acrylonitrile concentrations, the polyvinylcarbazole separated as an opaque gel.

Methyl methacrylate stabilized against free radical polymerization was used for the first three polymerizations shown in Table 5, but a sample freed from stabilizer by fractionation was the initiator in the other examples. No colour was developed in the polymerizations with methyl methacrylate. The products were, before isolation of the polyvinylcarbazole, somewhat opaque and apparently inhomogeneous. Some polymerization of the methyl methacrylate may have occurred. The high relative viscosity of polyvinyl-

POLYMERIZATION OF VINYL CARBAZOLE BY ELECTRON ACCEPTORS I

Table 5. Bulk polymerization of vinylcarbazole by acrylonitrile, methyl methacrylate, ethyl cyanoacetate and cyclopentadiene

Compound	Polymerization			Polymer			
	on monomer, %	Temp., °C	Time, h	Yield, %	Relative viscosity	Nitrile, %	Hydrolysable carboxyl %
Acrylonitrile	5	70	72	50.7	1.204	<0.003	—
				2.1 (benzene-insoluble)		7.5	—
Acrylonitrile	13.7	70	72	88.15	1.236	0.005	—
				7.05 (benzene-insoluble)		10	—
Acrylonitrile	27.5	70	72	93.6	1.216	0.016	—
Methyl methacrylate	1.0	80	27.5	23.3	2.071	—	<0.013
Methyl methacrylate	2.0	80	25.3	23.2	5.299	—	<0.013
Methyl methacrylate	5.0	80	24	39.6	8.040	—	<0.013
Methyl methacrylate	5.0	80	24	69.7	4.25	—	<0.1
Methyl methacrylate	38.2	80	48	77.4	2.49	—	<0.1
Ethyl cyanoacetate	2.9	60	72	31.6	1.253	<0.25	—
Ethyl cyanoacetate	29.5	60	72	83.9	1.251	<0.25	—
Ethyl cyanoacetate	58.6	60	72	87.5	1.133	<0.25	—
Cyclopentadiene	0.35	55	72	0	—	—	—
Cyclopentadiene	1.8	55	72	Traces	—	—	—
Cyclopentadiene	17.1	55	72	2.7	—	—	—
Cyclopentadiene	34.2	55	72	6.2	—	—	—

carbazole prepared in the presence of methyl methacrylate has been confirmed. Products of relative viscosities up to 29 have been obtained with 5 to 7 per cent methyl methacrylate in numerous polymerizations over the temperature range 70° to 110°C, the relative viscosities of the polymers being essentially independent of the polymerization temperatures over this range.

Even the polymer samples of the highest relative viscosity prepared with methyl methacrylate have been completely soluble in benzene giving clear solutions. Polyvinylcarbazole prepared with methyl methacrylate in bulk polymerization consists of fairly fibrous, somewhat brittle, opaque, white flakes, distinct from the white powder obtained from polymerizations with the other acceptors.

No attempt has yet been made to isolate any Diels–Alder adduct from the reaction product with cyclopentadiene. The quantity of polymer was too small for viscosity determinations, but its solubility and behaviour on heating were characteristic.

(e) Kinetic experiments

Kinetic experiments have been carried out in toluene solution using chloranil as initiator. The effect of varying the concentration of chloranil on the rate of polymerization has been determined at 80° (Figure 3). In selected cases the relative viscosities of the polymers have been determined



(Table 6). Following conversions of more than 30 per cent, rather viscous solutions were obtained.

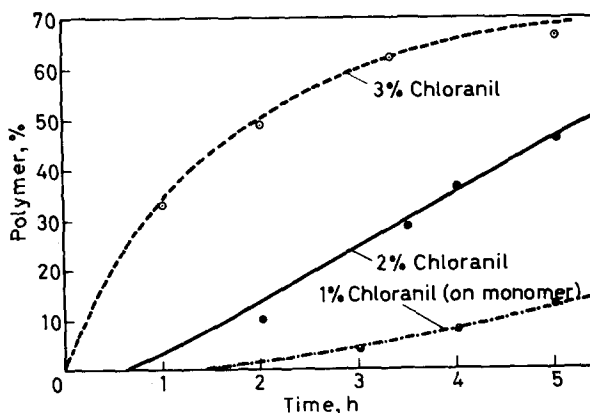


Figure 3—Vinylcarbazole polymerization by chloranil in toluene solution. 10% w/w vinylcarbazole in toluene; temperature, 80°C

Table 6. Solution polymerization of vinylcarbazole by chloranil. Vinylcarbazole, 25 g.Toluene, 250 ml. Temperature, 80°

Chloranil on monomer, %	Time, h	Polymer	
		Yield, %	Relative viscosity
1	24	65.2	1.123
2	7	66.5	1.09
3	3.3	51.2	1.05
4	3.3	62.1	1.017

The effect of monomer concentration on the rate of polymerization was studied at ambient temperature in presence of two per cent (on monomer) of chloranil (Figure 4).

(f) *Carbon tetrachloride*

In initial experiments<sup>18</sup> it was found that there is no spontaneous development of an orange colour accompanied by polymerization when vinylcarbazole is allowed to stand with 30 per cent of carbon tetrachloride, nor if it is dissolved in carbon tetrachloride and allowed to stand in the dark or in daylight, at ambient temperature, or at temperatures up to the boiling point, over a period of several hours.

The matter was studied, however, more closely both in light and dark, and in presence and absence of methyl methacrylate<sup>18</sup>.

The mixtures kept in the light remained colourless for over two days, although during the latter part of this period the crystal-liquid mixture

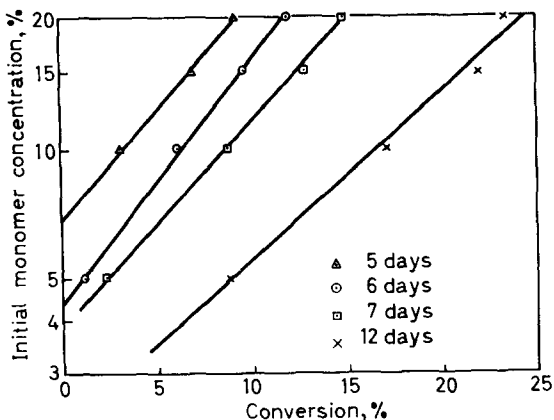


Figure 4 — Vinylcarbazole polymerization by chloranil in toluene solution. Temperature,  $\sim 20^\circ$

Table 7. Polymerization in mixtures of vinylcarbazole-carbon tetrachloride with and without methyl methacrylate. Vinylcarbazole, 1.85 g and carbon tetrachloride, 0.8 g were used in all experiments. Temperature:  $\sim 20^\circ\text{C}$

Methyl methacrylate, g	Light conditions	Time, h	Polymer		
			Yield, %	Relative viscosity	Chlorine %
Nil	Light	120	73	1.138	0.13
0.7	Light	120	62.7	1.2	0.11
Nil	Dark	336	Nil	—	—
0.7	Dark	336	3.3	—	—

became homogeneous and syrupy. After five days the mixture had set solid, and had assumed an intense red (carbon tetrachloride alone), or orange (carbon tetrachloride and methyl methacrylate) colouration. The mixtures kept in the dark were perfectly colourless after nine days.

(g) Effect of electron acceptors on vinylcarbazole in methanol

Only chloranil has been examined in any detail, and tetranitromethane in a few experiments. The solutions, which contained (usually) 1.33% w/v vinylcarbazole and 0.0133% w/v chloranil, were a characteristic brown-mauve colour. On standing in the dark for 25 days at ambient temperature, 9-(1'-methoxyethyl)-carbazole which, following recrystallization from methanol, melts at  $89^\circ$  to  $90^\circ$ , was isolated by precipitation by water in 71 per cent yield. Found C, 79.9; H, 6.7; N, 6.3 per cent; mol. wt, 231 (in benzene).  $\text{C}_{15}\text{H}_{15}\text{ON}$  requires C, 80.0; H, 6.7; N, 6.2 per cent; mol. wt, 225. This compound was solvolysed on warming with methanolic hydrogen chloride to carbazole (yield, 68.2 per cent; m.pt  $242^\circ$  to  $244^\circ$ ) and dimethyl acetal. The latter was readily hydrolysed to acetaldehyde, identified as the 2,4-dinitrophenylhydrazone.

In the light, solutions of vinylcarbazole and chloranil or tetranitromethane deposited 1,2-trans-dicarbazylcyclobutane<sup>21</sup>. 9-(1'-Methoxyethyl)-

carbazole was formed simultaneously, but remained in solution. Small concentrations of carbazole were obtained occasionally.

## DISCUSSION

The u.v. absorption spectra (Figures 1 and 5) of *N*-substituted carbazoles, which are not subject to conjugation in the bond between the substituent carbon and nitrogen atoms, are seen to show a strong narrow absorption band in the range 257 to 264  $m\mu$ . The broadening of this band in the spectrum of *N*-acetylcarbazole is regarded as indicating conjugation in this band, despite steric hindrance in the conjugated planar resonance hybrid.

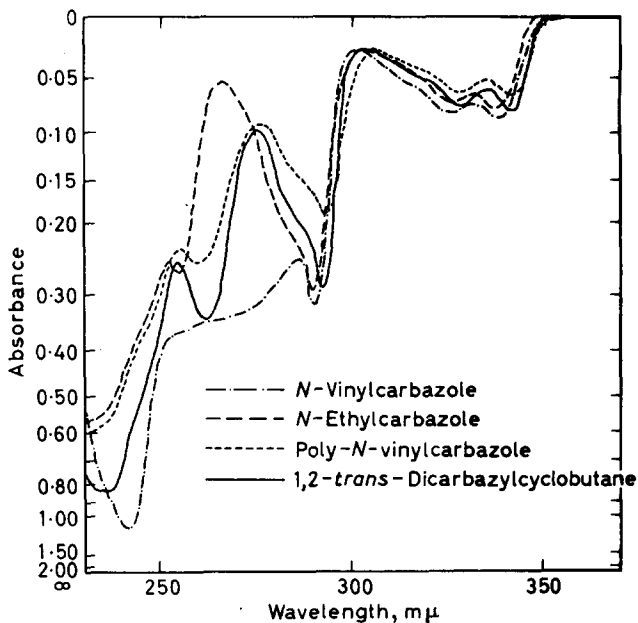


Figure 5—Ultra-violet absorption spectra of *N*-vinylcarbazole, *N*-ethylcarbazole, poly-*N*-vinylcarbazole, 1,2-(*trans*)-dicarbazylcyclobutane.  $2 \times 10^{-5}$  M solutions in dichloromethane

In the i.r. spectrum the band maxima at 963 and 866  $cm^{-1}$  show some shift from the range of reported maxima for vinyl groups attached<sup>23-25</sup> to carbon at 995-985; 915-905  $cm^{-1}$ . This is also ascribed to the effect of conjugation of the vinyl group with the lone pair of electrons on the nitrogen.

An interesting feature of the i.r. spectrum of vinylcarbazole is the doublet at 1 640, 1 625  $cm^{-1}$  in the C=C bond stretching region. Multiplicity of this band has also been observed in vinyl ethers, where it has been ascribed either to Fermi resonance of the C=C fundamental with an overtone, or to the presence of more than one rotationally isomeric species<sup>22</sup>. In the symmetrical vinylcarbazole molecule, rotationally isomeric species are not possible; Fermi resonance is the most likely explanation for this doublet.

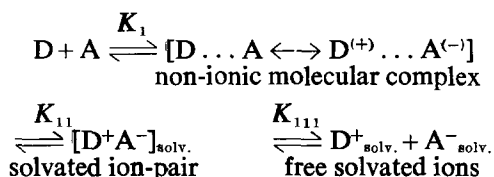
Since the lone pair electrons of the nitrogen of vinylcarbazole are

involved both in conjunction with the attached vinyl group, and in the formation of complexes with electron accepting molecules, some spectroscopic evidence linking these two functions may be expected. The main features of the u.v. absorption spectrum are found to be enhanced (*Figure 2*), but not altered appreciably in the presence of such electron acceptors. This enhancement increases with the electron accepting power of the acceptor and with its concentration. The retention of the main features of the absorption in the presence of these acceptors indicates that the absorption spectra of these acceptors are not themselves altered greatly in the region studied, unless compensating changes occur in the two components of the complex.

Electron acceptors of widely ranging electron affinity have been shown to be polymerization initiators. The concept of electron acceptor in this context is drawn widely, beyond the limitation imposed by the term ' $\pi$ -electron acceptor'. Of these the typical  $\pi$ -acceptors were found to give more or less intense colours with vinylcarbazole, due to wide band absorption, while many of the weaker acceptors (acrylonitrile, methyl methacrylate, ethyl cyanoacetate and cyclopentadiene) develop little or no colour, or develop colour very slowly [tetrachlorethylene, which is reported to be an electron donor in the presence of iodine (see ref. 26 p 78, refs. 135, 140)].

These polymerizations are shown to have several characteristic features, including the wide range of electron accepting power of the effective initiators; a characteristic dependence of the molecular weight of the polymers prepared in bulk on the identity, but not usually on the concentration of the initiator; the preparation of essentially pure homopolymer following initiation by acrylonitrile and methyl methacrylate, which are known to copolymerize with vinylcarbazole 'on free radical initiation'<sup>31-33</sup>; and the absence of certain characteristic features of free radical and ionic polymerization.

The addition of a free radical or the removal or addition of an electron or proton is normally a sufficient step to initiate and maintain the growth of an ethylenic or vinyl polymer molecule until termination occurs. In interactions in which both donor and acceptor are organic molecules, electron transfer is only partial except under the most favourable conditions. Of the following equilibria (charges in brackets are partial),



it is known that  $K_{11}$  and  $K_{111}$  are very small compared with  $K_1$ , except with strong acceptors (e.g. halogenated quinones, tetracyanoethylene or tetracyanoquinodimethane) and highly nucleophilic donors (e.g. tetramethyl-*p*-phenylenediamine) in polar solvents<sup>27</sup>. Even these donors and acceptors yield un-ionized complexes in solvents of low or moderate dielectric constant, and it is only on the addition of solvents of high electric constant that conversion to ion-radicals is observed by, for instance, the appearance

of e.s.r. absorption. In the absence of solvent, evidence of the complete transfer of one electron is limited to pairs comprising the strongest organic acceptors and donors, and even here the incidence of transfer becomes appreciable only under favourable conditions. These are much more stringent than those applying here<sup>42</sup>.

With vinylcarbazole in bulk or in toluene solution, and with most of the organic acceptors here described, electron transfer is thus considered to be only partial. This view is supported by the small degree of interaction in the u.v., and the absence of interaction in the i.r., spectra.

The *N*-vinyl group of vinylcarbazole is subject to mesomeric polarization:  $\text{>}^{(+)}\text{N}-\text{CH}=\text{CH}_2^{(-)}$ . Partial transfer of a lone pair electron from the nitrogen to an acceptor not only increases the positive charge on the nitrogen but also enhances this polarization. The extent to which polarization is increased depends not only on the degree of charge transfer, but also on the degree of polarization in the acceptor. With such weak acceptors as methyl methacrylate and acrylonitrile, which are themselves unsymmetrical and subject to marked polarization, dipole interaction with vinylcarbazole will result in increased polarization of the latter, while the degree of electron transfer is likely to be too small to contribute appreciably, if at all.

Charge transfer being electrostatic is regarded as a short range effect, not transmitted through the vinylcarbazole molecules, while polarization should be longer in range, being transmissible from one monomer molecule to another.

Interaction between vinylcarbazole and the weaker acceptors is insufficient to yield readily recognized complexes. Results on the rates of complex formation are as yet lacking, though there is evidence that they may range widely<sup>34</sup>.

It is thought that both monomer molecules involved in the initiation step of polymerization require activation by acceptor molecules, activation of only one of the molecules being inadequate. The observed second order rate dependence in respect of acceptor of the polymerization in toluene solution, as well as the comparatively slow rates of polymerization both in bulk and in toluene solution, are consistent with this view.

*Figure 6* shows a representation of the initiation step of the bulk polymerization by acrylonitrile. Several features will be noted. In their interaction with the vinylcarbazole molecules the acrylonitrile molecules are polarized in the opposite direction to that required for copolymerization. This accounts for the absence of copolymerization when acrylonitrile and methyl methacrylate are used over a wide range of relative concentrations as initiators. The dipolar interaction should provide some steric control at least over the initiation reaction, favouring the syndiotactic configuration. Any resultant stereospecificity in the polyvinylcarbazole may, however, not be easily recognized because of the large size of the carbazyl group<sup>10</sup>.

*Figure 6* indicates also that the formation of a bond between the two vinylcarbazole molecules involves not only the loss of a double bond but also necessitates a 1,3-hydrogen shift. Such a hydrogen shift is often regarded as involving a carbonium ion intermediate, but, at least with

the weaker acceptors, electron transfer is clearly insufficient to support the formation of such an intermediate. The occurrence of hydrogen shift under these conditions is a characteristic feature, not only of the initiation step, but of the subsequent propagation stages also. *Figure 6* also indicates that with the loss of one double bond in the initiation step, one of the two acceptor molecules involved in the initiation is eliminated, becoming available for complex formation with another monomer molecule. Qualitative comparison shows the acceptor affinity of saturated *N*-alkylcarbazoles to be much smaller than that of vinylcarbazole, and the complexing power of the growing polymer chain is thought to be very largely associated with its terminal double bond. The initiation is thus regarded as involving a number of steps.

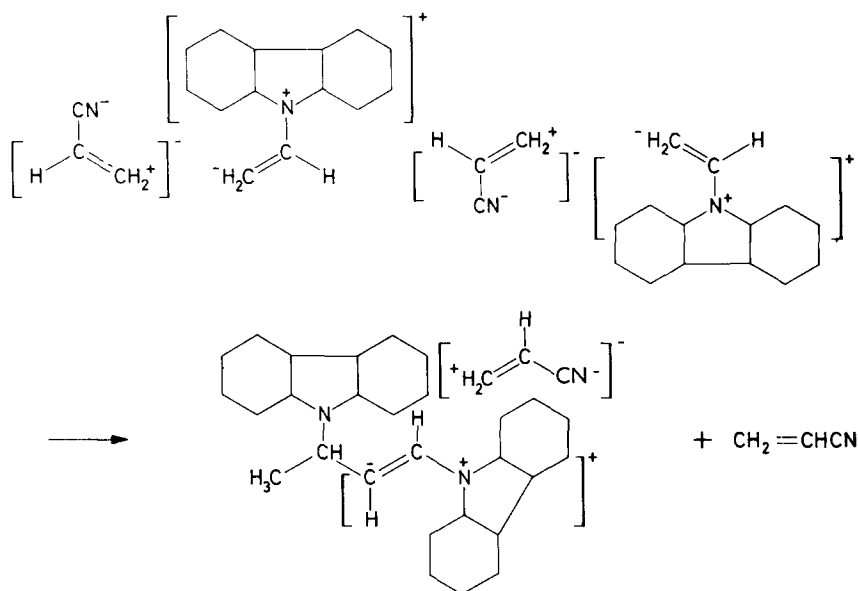


*Figure 6*—Polymerization of vinylcarbazole in the presence of acrylonitrile. All charges shown are partial charges

The rate of initiation depends on the nature of the acceptor and on the conditions. It is slow, and has a moderate positive temperature coefficient in polymerizations in bulk or in toluene. Under these conditions the initiation reaction is appreciably slower than the propagation reaction<sup>39</sup>. The propagation must, as regards the addition of a further monomer molecule, require similar steps as the initiation reaction. Whether it is necessary for adding monomer molecules to be activated by interaction with the acceptor molecules, or whether uncomplexed vinylcarbazole molecules add, activated possibly under the polarizing effect of the growing chain end, cannot be determined from the available evidence, but addition of complexed vinylcarbazole molecules appears more likely by analogy with the initiation reaction. If the initiation has to be formally complete before the first propagation step involving the addition of a complexed monomer

molecule starts, then the rates of initiation and propagation would be expected to be similar. If the propagation step involving a complexed monomer molecule starts before the steps of the previous initiation or propagation stage have been completed and at an energetically favourable point, propagation will be faster than initiation. A further complexed monomer molecule must thus be available at the appropriate moment, and this is the more likely the greater the concentration of monomer.

Chain growth by the addition of oligomer or polymer units rather than monomer molecules (whether complexed or not) can be shown to be subject to such severe steric hindrance, as to be most unlikely.

The growing end of the polymer chain is regarded as carrying the terminal double bond. Proof of its presence in the polymer has not yet been obtained, and there is some indication<sup>39</sup> that under the influence of the complexed acceptor molecule, it adds methanol during the normal isolation procedure. If the double bond can be preserved, it should leave the polymer open to further growth, and possibly even to grafting.

Elimination of the acceptor molecule associated with the terminal double bond of the chain either by dissociation (especially in solution), or by transfer to another monomer or uncomplexed polymer molecule (favoured in bulk), will result in termination of chain growth. Its occurrence will be determined by the relative affinities of the growing polymer chain and of monomer for the acceptor and, in solution, on the dielectric constant and solvent properties of the diluent.

If addition of a (complexed) monomer molecule in the propagation proceeds through several steps, including at least an intermediate one during which the first step of the addition of the subsequent monomer molecule is energetically favourable (see above), then termination will ensue, if the subsequent monomer molecule is not suitably available. The relative importance of this mode of termination cannot yet be assessed.

Finally oxidation or addition of acceptor involving the formation of a covalent bond can contribute to termination, but the results suggest that this is unimportant except in the presence of a high acceptor concentration.

Some kinetic consequences can now be outlined: let  $M$  denote monomer,  $A$  acceptor,  $M_{\text{suffix}}$  uncomplexed polymer molecule, the suffix referring to the number of monomer units in the polymer molecule, e.g.  $n$ ,  $x$ ,  $x$  being the number of monomer units in a polymer molecule at the point of termination.

$MA$  denotes the 1 : 1 monomer-acceptor complex.

$M_{\text{suffix}}A$  is the polymer-acceptor complex containing one molecule of acceptor per polymer molecule.

$k_c$ ,  $k_d$ ,  $k_i$ ,  $k_p$ ,  $k_t$  are respectively the rate constants of complex formation, complex dissociation, initiation, propagation and termination.

$K$  is the equilibrium constant of complex formation, and  $R_p$  and  $R_t$  are the rates of complex propagation and termination.

$\bar{n}_x$  is the degree of polymerization.

The following reactions can then be considered.

*Complex formation*

This is treated as a reversible reaction. For the monomer



and the equilibrium constant of complex formation is

$$K = k_c/k_d = [MA]/[M][A] \quad (2)$$

*Initiation and propagation*

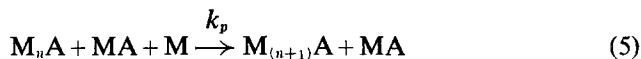
If the initiation step involves the interaction of two complexed monomer molecules, followed by elimination of one of the acceptor molecules, then in solution



If the propagation reaction involves the addition of further complexed monomer molecules, the propagation reaction is written similarly



As explained above, there is evidence<sup>39</sup> that  $k_p$  is larger than  $k_i$ . In the absence of solvent, the eliminated acceptor molecule may transfer to another monomer molecule



The rate of propagation becomes thus

$$R_p = k_p [M_nA] [M] \quad (6)$$

It will be noted that the same expression would apply to bulk polymerization if chain growth proceeds by the addition of uncomplexed monomer molecules.

*Termination*

Termination is thought to occur mainly by dissociation of the polymer complex. In the absence of solvent, the acceptor will transfer directly to another uncomplexed molecule (which is most likely to be monomer), so that



and

$$R_t = k_t [M_xA] [M] \quad (8)$$

In solutions of increasing dilution, dissociation of the polymer-acceptor complex, not followed by immediate complex formation, will become increasingly important. Under these conditions

$$R_t = k_d [MA] \quad (9)$$

This equation may require further elaboration if termination involves not only dissociation of the complex, but also deactivation of the inter-



mediate state, before reaction with a further molecule of (complexed) monomer occurs.

#### *Degree of polymerization*

This is described by the ratio of propagation and termination rates, and in the absence of solvent by the ratio of equation (6) with (8) or (9). For bulk polymerization

$$\bar{n}_x = R_p / R_t = k_p [M_n A] [M] / k_t [M_x A] [M] \quad (10)$$

Since the ratio  $[M_n A] / [M_x A]$  will be constant, the degree of polymerization will under these conditions itself be a constant typical of the monomer and independent of initiator concentration. This is in good agreement with the experimental results. It does not apply to polymerizations in solution for which

$$\bar{n}_x = k_p [M_n A] [M] / k_t [M_x A] \quad (11)$$

Under these conditions the degree of polymerization of the polyvinylcarbazole is proportional to the monomer concentration<sup>39</sup>, and inversely proportional to the initiator concentration (*Table 6* and ref. 39).

Results here described are in good agreement with equation (10) and, as far as they are presented, with equation (11). There is ample additional support<sup>39</sup> for the general picture presented by equation (11), and in due course more detailed examination of this may throw light on the propagation mechanism, and on the deviation observed with methyl methacrylate.

While the rate constants of initiation and termination should be closely related to the equilibrium constant of equation (2), and should thus depend on the nature of the acceptor, it is not yet known whether the rate constant of propagation is solely typical of the monomer or also dependent on the acceptor. In bulk polymerization a high degree of polymerization will be favoured by the smallest possible difference in the acceptor affinities of monomer and of growing polymer. While some patterns are discernible, much further study is required.

In hydroxylic solvents of high dielectric constant such as water and methanol, vinylcarbazole and chloranil or tetranitromethane are thought to yield solvated ion-pair intermediates, which with chloranil have a characteristic intense colouration<sup>26</sup>. Reaction of the vinylcarbazole through a cationic intermediate is presumably limited by its solubility. In solution (e.g. in methanol) protolysis is the preferred reaction. At ambient temperature it is largely limited to the addition of one molecule of solvent, but with rising temperature carbazole and, for instance, dimethyl acetal form an increasing proportion of the product. If the mutual solubility is partial or low (e.g. in water) polymerization occurs as alternative to protolysis, though some of the latter is observed in the formation of acetaldehyde and carbazole. The molecular weight of the polymer is typically low, and the rate of polymerization under these conditions is notably high. The latter is surprising, in view of the reported powerful inhibition of the cationic polymerization of vinylcarbazole by aliphatic nitrocompounds<sup>7</sup>.

The formation of 1,2-*trans*-dicarbazyl cyclobutane which proceeds as competing reaction in daylight is regarded, in view of the structure of the

product<sup>21</sup>, as proceeding through free radical intermediates formed by the photosensitizing effect of the coloured complex.

The view that polymerization of vinylcarbazole by chloranil, tetracyanoethylene, and by related organic acceptor molecules proceeds by an oxidative reaction<sup>17</sup> has been considered, both in respect of single and two electron transfers. Single electron transfer yielding unstable free radical ions proceeds normally only to a small extent between organic molecules of sufficiently similar structure to suggest mesomeric interaction, and then under closely specified conditions of solvent and pH, which do not apply here<sup>34,40,41</sup>. Two-electron transfer oxidation by chloranil has been described, but requires somewhat more vigorous conditions<sup>29,30</sup>.

The reported<sup>13</sup> polymerization of vinylcarbazole by carbon tetrachloride in the dark at ambient temperature is regarded as due to an impurity<sup>28,16</sup>. Polymerization in the presence of carbon tetrachloride and of methyl methacrylate<sup>18</sup> in the dark is thought to be due to the methyl methacrylate. The discolouration and polymerization observed in daylight even with pure carbon tetrachloride is explained by the known photolysis of the latter, yielding chlorine atoms and  $\cdot\text{CCl}_3$  radicals; these unstable species are electron acceptors, and the observed colour may be due to electron transfer.

*The author wishes to thank Mr E. Freeman for experimental assistance, Mr P. A. B. Butler for the infra-red spectra, Professor C. E. H. Bawn and Dr A. Ledwith, Liverpool University, for their encouragement and valuable discussions, Dr S. A. Miller for his interest, the Ministry of Aviation for their support of this work, and the British Oxygen Company Limited for permission to publish this paper.*

*The British Oxygen Company Limited,  
Scientific Centre,  
Deer Park Road, London, S.W.19*

*(Received January 1964)*

#### REFERENCES

- <sup>1</sup> ISHII, T. and HAYASHI, M. *J. Soc. org. Synth., Japan*, 1949, **7**, 41
- <sup>2</sup> British Oxygen Co. Ltd. *Brit. Pat. No. 718 912* (1953)
- <sup>3</sup> Badische Anilin- u. Soda-Fabrik. *German Pat. No. 931 731; Brit. Pat. No. 739 438* (1955)
- <sup>4</sup> DAVIDGE, H. *J. appl. Chem.* 1959, **9**, 553
- <sup>5</sup> British Oxygen Co. Ltd. *Brit. Pat. No. 831 913* (1960)
- <sup>6</sup> SCHILDKNECHT, C. E., ZOISS, A. O. and GROSSER, F. *Industr. Engng Chem. (Industr.)*, 1949, **41**, 2891
- <sup>7</sup> SOLOMON, O. F., DIMONIE, M. and TOMESCU, M. *Makromol. Chem.* 1962, **56**, 1
- <sup>8</sup> REPPE, W. 'Acetylene chemistry', U.S. Dept of Commerce O.T.S., *B.D. Rep.*, 18, 852-S, 1949  
REPPE, W. *Neue Entwicklungen auf dem Gebiet der Chemie des Acetylens und Kohlenoxyds*, p 18. Springer: Berlin, 1949
- <sup>9</sup> SOLOMON, O. F., DIMONIE, M. and AMBROZH, K. *Rev. Chim. (Bucharest)*, 1960, **11**, 520  
SOLOMON, O. F., DIMONIE, M., AMBROZH, K. and TOMESCU, M. *J. Polym. Sci.* 1961, **52**, 205

- <sup>10</sup> HELLER, J., TIESZEN, D. O. and PARKINSON, D. B. *J. Polym. Sci. Pt A*, 1963, **1**, 125
- <sup>11</sup> Montecatini Societa, *Brit. Pat. No. 914 418* (1963)
- <sup>12</sup> RESTAINO, A. J., MESROBIAN, R. B., MORAWETZ, H., BALLANTINE, D. S., DIENES, C. D. and METZ, D. J. *J. Amer. chem. Soc.* 1956, **78**, 2939
- <sup>13</sup> CHAPIRO, A. and HARDY, G. *J. chim. Phys.* 1962, **59**, 993
- <sup>14</sup> I.G. Farben-Industrie, A.G. *German Pat. No. 664 231* (1938)
- <sup>15</sup> COPENHAVER, J. W. and BIGELOW, M. H. *Acetylene and Carbon Monoxide Chemistry*, p 63. Reinhold: New York, 1949, P.B. 33272
- <sup>16</sup> ELLINGER, L. P. *Chem. & Ind.* **1963**, 1982
- <sup>17</sup> SCOTT, H., MILLER, G. A. and LABES, M. M. *Tetrahedron Letters*, 1963, No. 17, 1073
- <sup>18</sup> BREITENBACH, J. W. and SNRA, C. *Polymer Letters*, 1963, **1**, 263
- <sup>19</sup> LEVY, B. *Mh. Chem.* 1912, **33**, 17; *Chem. Abstr.* 1912, **6**, 1435
- <sup>20</sup> BOESEKEN, J. *Rec. Trav. chim. Pays-Bas*, 1912, **31**, 364
- <sup>21</sup> ELLINGER, L. P., FEFNEY, J. and LEDWITH, A. In preparation
- <sup>22</sup> OWEN, N. L. and SHEPPARD, N. *Proc. chem. Soc., Lond.*, Sept. 1963, 264
- <sup>23</sup> MURRAY, H. L. and THORNTON, V. *Analyt. Chem.* 1952, **24**, 318
- <sup>24</sup> SHEPPARD, N. and SUTHERLAND, G. B. B. M. *Proc. Roy. Soc. A*, 1949, **196**, 195
- <sup>25</sup> SHEPPARD, N. and SIMPSON, D. M. *Quart. Rev. chem. Soc., Lond.* 1952, **6**, 1
- <sup>26</sup> BRIEGLEB, G. *Elektronen-Donator-Acceptor-Komplexe*. Springer: Berlin, 1961
- <sup>27</sup> LIPTAY, W., BRIEGLEB, G. and SCHINDLER, K. *Ber. Bunsenges. phys. Chem.* 1962, **66**, 331
- <sup>28</sup> SCOTT, H. and LABES, M. M. *Polymer Letters*, 1963, Part B, I, No. 8, 413
- <sup>29</sup> DOST, N. and VAN NES, K. *Rec. Trav. chim. Pays-Bas*, 1951, **70**, 403
- <sup>30</sup> BRAUDE, E. A., JACKMAN, L. M. and LINSTEAD, R. *J. chem. Soc.* **1954**, 3548, 3564
- <sup>31</sup> CHANEY, D. W. to American Viscose Corp. *U.S. Pat. No. 2 537 031* (1950)
- <sup>32</sup> SAKURAI, R., TANABE, T. and NAGAO, H. *U.S. Pat. No. 2 902 335* (1959)
- <sup>33</sup> ALFREY, T., Jr and KAPUR, S. L. *J. Polym. Sci.* 1949, **4**, 215
- <sup>34</sup> WHELAND, G. W. *Advanced Organic Chemistry*, 3rd ed. Wiley: New York, 1960
- <sup>35</sup> ELLINGER, L. P. to British Oxygen Co. Ltd. *Brit. Pat. Appl. No. 33 625/63*
- <sup>36</sup> ELLINGER, L. P. to British Oxygen Co. Ltd. *Brit. Pat. Appl. No. 43 933/63*
- <sup>37</sup> REPPE, W., KEYSSNER, E. and DORRER, E. *U.S. Pat. No. 2 072 465* (1937)
- <sup>38</sup> SARGENT, D. E. *U.S. Pat. No. 2 560 251* (1951)
- <sup>39</sup> ELLINGER, L. P. Unpublished results
- <sup>40</sup> MICHAELIS, L., SCHUBERT, M. P. and GRANICK, S. *J. Amer. chem. Soc.* 1939, **61**, 1981
- <sup>41</sup> FOSTER, R. and THOMPSON, T. J. *Trans. Faraday Soc.* 1962, **58**, 860
- <sup>42</sup> OTTENBERG, A., HOFFMAN, C. J. and OSIECKI, J. *J. chem. Phys.* 1963, **38**, 1898

# On the Morphology of Polymer Crystals

D. C. BASSETT\*, F. R. DAMMONT and R. SALOVEY

*Crystals of isotactic poly-4-methylpentene-1 and of polyoxymethylene have been grown from dilute solution. The X-ray long period has been measured as a function of crystallization temperature for poly-4-methylpentene-1 in xylene and for polyoxymethylene in furfuryl alcohol. Polyoxymethylene crystals are flat-based hexagonal hollow pyramids in which the molecules are parallel to the pyramidal axis. On the other hand, poly-4-methylpentene-1 forms square, nearly planar, lamellae in which the molecules are normal to the layers. The slight departure from planarity suggested by morphological detail is related to a slight distortion of the subcell due to chain-folding.*

VIRTUALLY all our knowledge of molecular chain-folding in high polymers has come from examination of solution-grown polyethylene crystals. This paper is concerned with the investigation of chain-folded crystals in two further high polymers, namely, poly-4-methylpentene-1 (P4MP) and polyoxymethylene (POM).

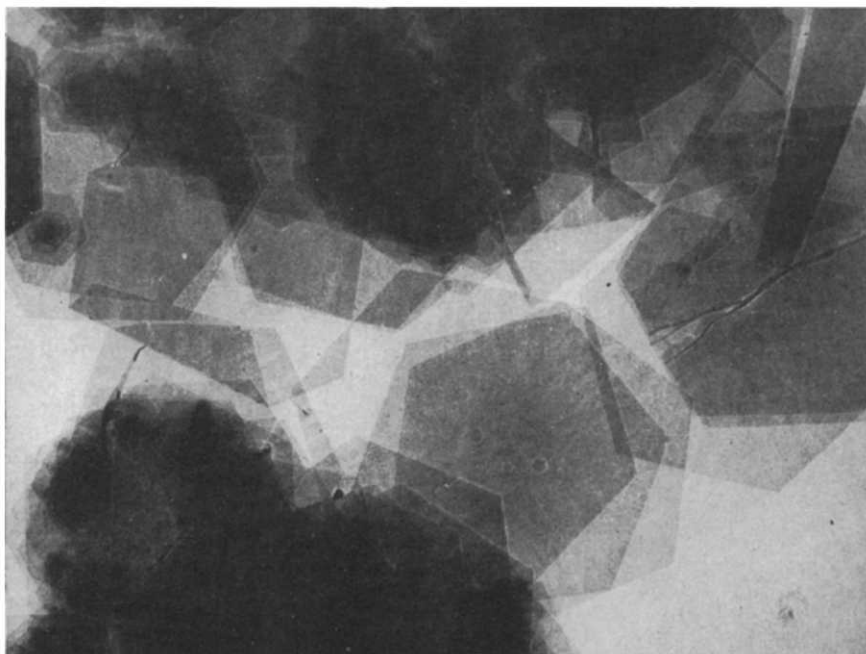


Figure 1—POM crystals formed from bromobenzene solution at  $\sim 130^{\circ}\text{C}$ .  
Magnification:  $\times 4\,000$ ; reduced  $\frac{1}{4}$  on reproduction

\*Present address: J. J. Thomson Physical Laboratory, Whiteknights Park, Reading, Berkshire.



*Figure 2*—An electron diffraction pattern from a POM crystal

#### POLYOXYMETHYLENE CRYSTALS

Du Pont 500 NC 10 Delrin polyoxymethylene resin has been crystallized from bromobenzene and from furfuryl alcohol. The former system has been used for all morphological observations reported, but because bromo-

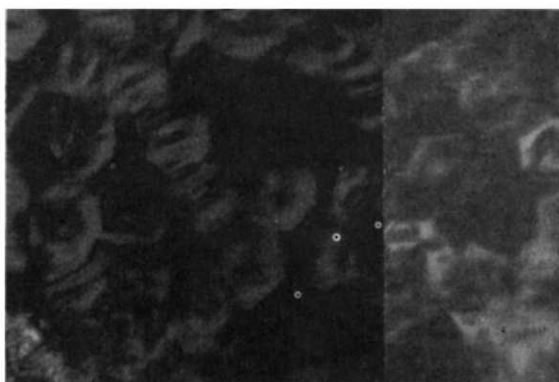


*Figure 3*—Hollow pyramidal POM crystals seen partially collapsed on a glycerin substrate with Reichert interference contrast optics. Magnification:  $\times 800$ ; reproduced without reduction

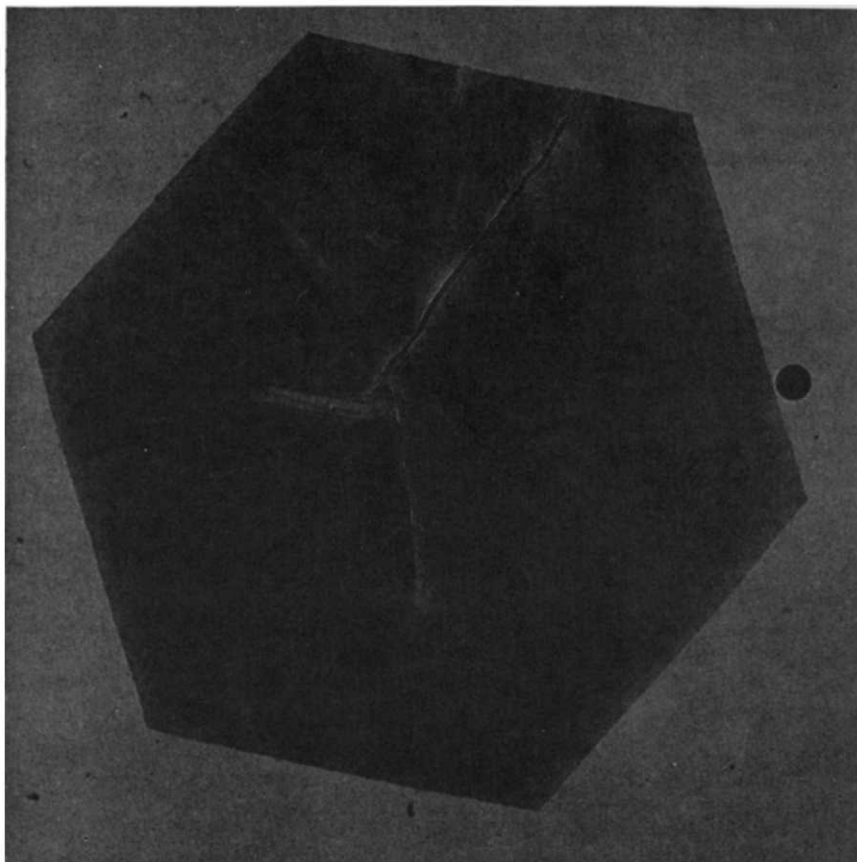


*Figure 4*—A POM monolayer in electron bright field exhibiting almost uniform diffraction contrast. Magnification:  $\times 12\ 000$ ; reproduced without reduction

benzene is a poor solvent, solutions in furfuryl alcohol have been employed in the preparation of larger quantities of material required for other studies.

*Figure 1* shows crystals grown at  $\sim 130^{\circ}\text{C}$  from supersaturated 0.05 per cent solution in bromobenzene. There is a high proportion of monolayers together with crystals which have growth terraces associated with giant screw dislocations. An electron diffraction pattern from such a crystal is shown in *Figure 2* and indicates that the subcell is hexagonal (or trigonal, since the two cannot be distinguished in a Laue photograph showing only  $hk0$  reflections). Similar observations on crystals formed under different conditions have been reported previously<sup>1,2</sup>.

In suspension the crystals are non-planar. This may be deduced from *Figure 3* which shows crystals which have been sedimented on glycerin and viewed with Reichert interference contrast optics. Several of them have a central hexagonal pyramid which is flat-based since it terminates in a planar border. One may deduce accordingly that before sedimentation the whole

crystal was a flat-based, hexagonal pyramid. When sedimented on a solid substrate, these crystals collapse completely, but without change of outline, to hexagonal lamellae (*Figure 1*). This suggests strongly that in the hollow pyramids the molecular  $c_s$  axis is everywhere parallel to the pyramidal axis so that collapse may occur by molecular displacement along  $c_s$ . Confirmatory evidence for this hypothesis is provided by electron microscopic observations which show that molecules are everywhere normal to collapsed lamellae. Thus in bright field (*Figure 4*), Bragg diffraction contrast is uniform except at the edges and along certain characteristic streaks. Again in 10·0 dark field (*Figure 5*) uniform contrast indicates that the same family of  $\{10\cdot0\}_s$  planes is everywhere normal to the lamellae. Notice in *Figure 5*

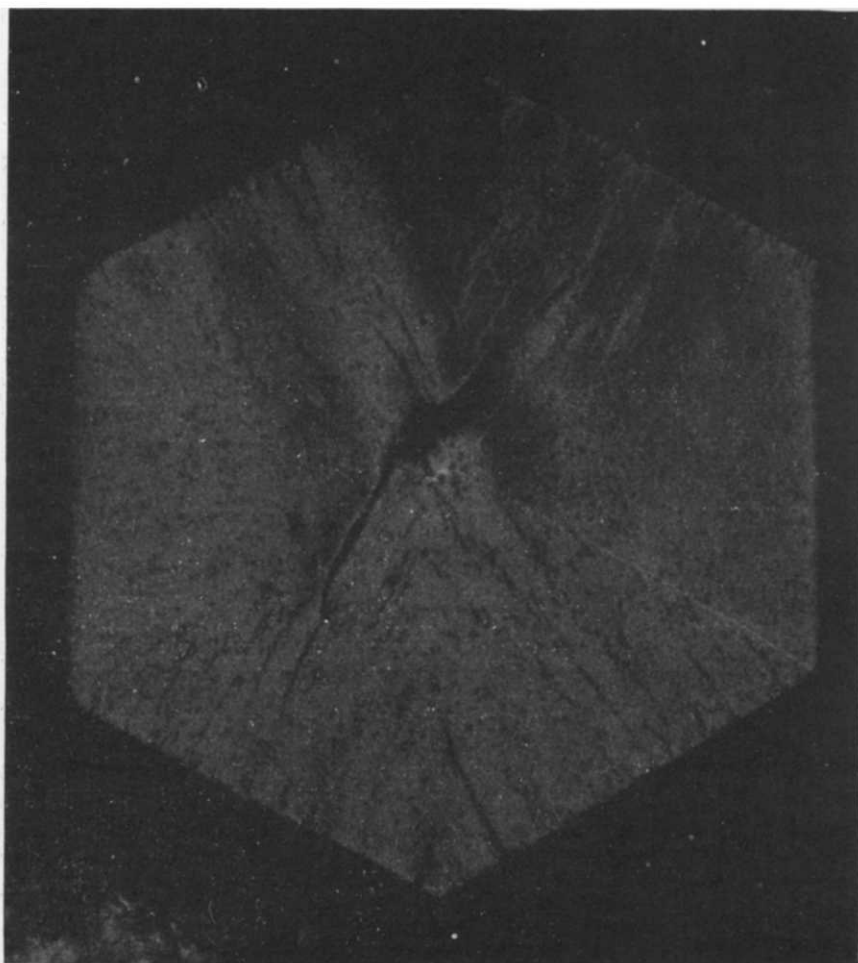
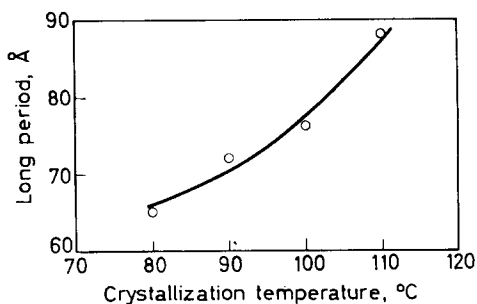


*Figure 5*—A POM monolayer viewed in 10·0 electron dark field corresponding to planes which are vertical on the page. Magnification:  $\times 8\,000$ ; reproduced without reduction

that the characteristic non-diffracting streaks are absent when the diffracting planes are not fold planes. This is important for the discussion.

The variation of lamellar thickness (X-ray long period) with crystallization temperature is displayed in *Figure 6* for crystals formed from 0.04 per cent solution in furfuryl alcohol. A large variation (from 60 to 93 Å) has also been found for polymer crystallized from bromobenzene. Because of the difficulties of temperature control, the only isothermal value we quote in this case is 88 Å at 135°C. It is interesting to note that this same value is obtained at 110°C from furfuryl alcohol. Qualitatively at least, all current theories of chain-folding (cf. review<sup>3</sup>) predict that the same fold length would occur at different temperatures in different solvents since fold length is a function of surface free energy. To our knowledge, however, the effect has not been reported previously.

*Figure 6*—Variation of X-ray long period with crystallization temperature for POM crystals grown from 0.04 per cent furfuryl alcohol solution



#### POLY-4-METHYLPENTENE-1 CRYSTALS

The isotactic polymer used in these experiments was supplied in powder form by the Tennessee Eastman Company. By the commencement of these experiments it had become slightly oxidized since the density at 23.7°C of a freshly moulded 0.07 in. film was 0.838 compared to a value of 0.827 obtained similarly two years earlier\*. Chain-folded crystals have been grown from dilute solution in xylene as in earlier studies<sup>4</sup> and their X-ray long period is shown in *Figure 7* as a function of crystallization temperature.

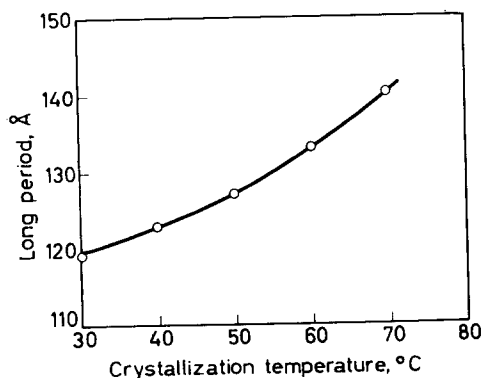


*Figure 7*—Variation of X-ray long period with crystallization temperature for P4MP crystals grown from 0.1 per cent xylene solution

\*W. Matreyck (private communication).



These values (and those of POM reported above) were measured with slit collimation and are therefore subject to a systematic increase of about two per cent; this has not been corrected for, since it is of a similar magnitude to the random errors of measurement.

An unusual feature of the X-ray measurements is that, for increased accuracy, the initially weak low-angle maxima were intensified by either oxidation or chlorination of the sample<sup>5</sup>. A typical procedure for oxidation was to heat the polymer at 170°C in air for thirty minutes. Chlorination was achieved by exposure to the gas at 60°C for an hour or so. Chlorination is somewhat to be preferred since the more strongly scattering chlorine atoms introduced at the fold surfaces give stronger X-ray low angle maxima.

P4MP monolayers are best prepared at the higher crystallization temperatures, especially at 70°C, although in this range a 'hot filtration' technique<sup>6</sup> is essential to avoid an appreciable fraction of soluble polymer crystallizing on cooling and producing thinner borders and overgrowths on lamellae. The concentration of the solution should also be kept low ( $\sim 0.01$  per cent) to prevent the formation of more complex crystals<sup>7</sup>. Observation of such monolayers has revealed no indication of markedly non-planar habits. For example, examination after sedimentation on glycerin, which preserves much of the non-planar morphology of polyethylene<sup>8</sup> and of POM crystals, shows only planar monolayers. Furthermore, apparently planar lamellae have been observed while still floating in suspension with the dark field optical technique (cf. ref. 8). This is quite consistent with the characteristic crumples seen in more complex crystals after sedimentation<sup>4</sup>, since in these, layers appear to splay apart in suspension in similar fashion to multilayer polyethylene crystals<sup>9</sup>.

Electron microscopic examination of individual lamellae shows, further, that they are very perfect. There are no major changes across sector boundaries; on the contrary, regular and extensive moiré patterns (*Figures 8 and 9*) indicate a very uniform molecular orientation throughout the crystal. Electron diffraction indicates that this is normal to the layers<sup>4</sup> (*Figure 10*). In 200 dark field (*Figure 9*), however, some slight streaking exists parallel to the diffracting planes, but only in sectors where these are not fold planes. The overall diffraction contrast in these sectors is also weaker. These features are significant and will be discussed presently.

#### DISCUSSION

The only observations which require further comment are those relating to non-planarity. It has been pointed out that the growth of polymer crystals by folding molecules along the growing faces requires each growth face to bound a sector of crystal which is distinguished from its neighbours by having a different fold plane<sup>10</sup>. It also implies that the crystallographic symmetry of each sector is, in general, lowered by the presence of chain-folds<sup>11</sup>. Consequently, the subcell itself may be distorted so that if sectors are to join along low-index directions, the lamellae must be non-planar<sup>11</sup>. This distortion has been measured by moiré techniques in both POM and P4MP<sup>12</sup>. In addition, there may be the more familiar staggering of chain-folds leading to hollow pyramids in which the fold surfaces have low

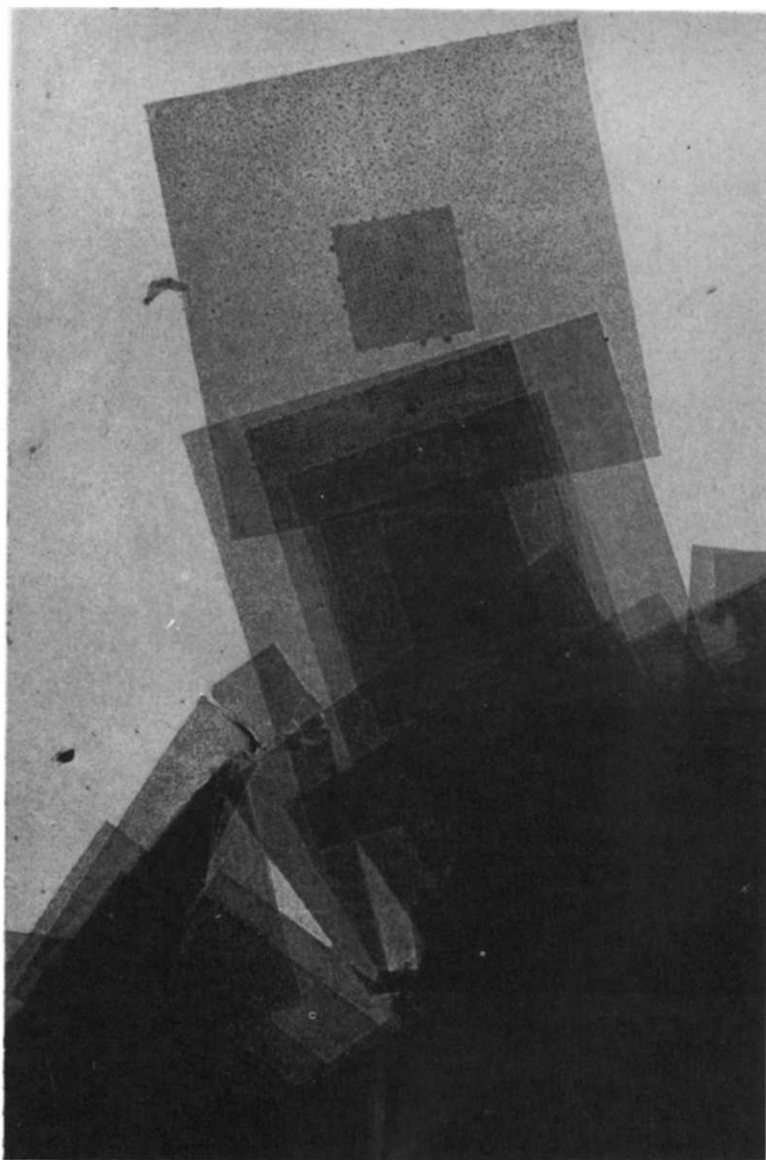


*Figure 8*—P4MP crystals grown at 65°C from 0.01 per cent xylene solution. Magnification:  $\times 4\,500$ ; reproduced without reduction

subcell indices<sup>2, 8, 14</sup>. In general, the two contributions to non-planarity will occur together, although the latter will be dominant.

On sedimentation it is possible, in principle, to remove fold staggering by displacing molecules along their length. If carried out uniformly, this

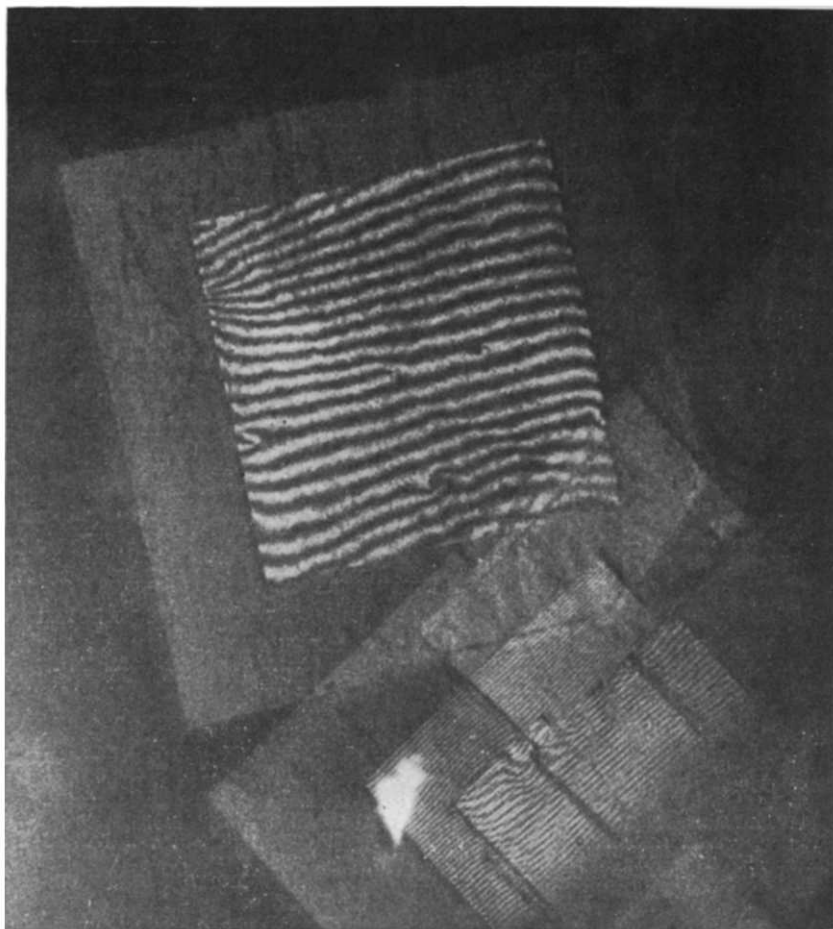


*Figure 9*—P4MP crystals viewed in electron dark field through the 200 reflection corresponding to planes which are nearly vertical on the page. Magnification:  $\times 10\,000$ ; reduced 8/10 on reproduction

process should leave no discontinuities in a crystal. However, any conicalness due to subcell distortion cannot be removed without lateral deformation and it has been suggested elsewhere<sup>12</sup> that this is the origin of the non-diffracting streaks observed in POM and P4MP crystals. Collapse of a very shallow pyramid may be achieved by slight molecular tilting within the fold planes. If this occurred locally, then the tilted regions would be seen as non-diffracting streaks in dark field in just the way observed in both POM and P4MP. If, on the other hand, it occurred uniformly throughout the crystal, then the observed difference in overall diffracted intensities between sectors in P4MP crystals would be accounted for. This may be seen as follows.

The qualitative difference in brightness is explained by a tilt of the lattice about a normal to the growth face in each sector. This would weaken the

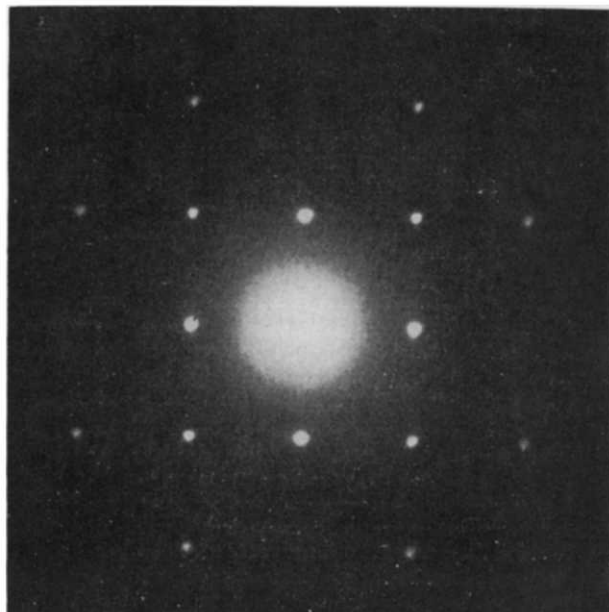


Figure 10—An electron diffraction pattern from a P4MP crystal

diffracted intensities in dark field from sectors where the diffracting planes are not fold planes. Moiré evidence<sup>12</sup> indicates that the  $\{200\}_s$  spacing changes fractionally by  $\sim 10^{-3}$  depending on whether or not the planes are fold planes. In terms of conicalness, the angular deficit from  $360^\circ$  in circumnavigating a monolayer would be  $12'$ . The uniform tilt of chains in the fold planes required to remove this and form a planar layer is  $\sim 2.3^\circ$ . The half width of the 200 reflection is  $\sim 2^\circ$  (cf. ref. 13) so that the observed contrast differences might correspond to  $\sim 0.5^\circ$  uniform tilt of the molecules. Since this is in addition to larger tilts in the streaks discussed above, it appears that in P4MP crystals both phenomena can be accounted for on the basis of removal of a slight conicalness due to a fractional increase of  $\sim 10^{-3}$  in the spacing of  $\{200\}_s$  fold planes.

Turning now to non-planarity caused by oblique fold packing, one may extend the ideas developed for polyethylene<sup>8,14,2</sup> to the present cases. The origin of oblique fold packing is attributed to folds being too bulky to be accommodated comfortably in a plane normal to the stems. Thus, asymmetries in the folds would tend to cause related asymmetries in the shape of the resultant hollow pyramid. Consequently, our observations are explicable if folds in P4MP have a projected area almost equal to that of their stems, which models suggest to be the case. The flat-based hollow pyramid found for POM requires only that the dominant asymmetries of the folds are normal to the growth faces. It is not necessary for the folds to have a

plane of symmetry between the stems, only that any asymmetries in the fold planes are slight.

*We are indebted to Dr H. D. Keith for critical discussion of the manuscript.*

*Bell Telephone Laboratories Inc.,  
Murray Hill, N.J., U.S.A.*

*(Received January 1964)*

#### REFERENCES

- <sup>1</sup> GEIL, P. H., SYMONS, N. K. J. and SCOTT, R. G. *J. appl. Phys.* 1959, **30**, 1516
- <sup>2</sup> RENEKER, D. H. and GEIL, P. H. *J. appl. Phys.* 1960, **31**, 1916
- <sup>3</sup> KELLER, A. *Polymer, Lond.* 1962, **3**, 393
- <sup>4</sup> FRANK, F. C., KELLER, A. and O'CONNOR, A. *Phil. Mag.* 1959, **4**, 200
- <sup>5</sup> BASSETT, D. C. *Polymer, Lond.* 1964, **5**, 457
- <sup>6</sup> BASSETT, D. C. and KELLER, A. *Phil. Mag.* 1962, **7**, 1553
- <sup>7</sup> LEUGERING, H. J. *Kolloidschr.* 1960, **172**, 184
- <sup>8</sup> BASSETT, D. C., FRANK, F. C. and KELLER, A. *Phil. Mag.* 1963, **8**, 1739 and 1763
- <sup>9</sup> MITSUHASHI, S. and KELLER, A. *Polymer, Lond.* 1961, **2**, 109
- <sup>10</sup> KELLER, A. and O'CONNOR, A. *Disc. Faraday Soc.* 1958, **25**, 114
- <sup>11</sup> BASSETT, D. C., FRANK, F. C. and KELLER, A. *Nature, Lond.* 1959, **184**, 810
- <sup>12</sup> BASSETT, D. C. *Phil. Mag. Ser. VIII*, 1964, **10**, 595
- <sup>13</sup> AGAR, A. W., FRANK, F. C. and KELLER, A. *Phil. Mag.* 1959, **4**, 32
- <sup>14</sup> BASSETT, D. C. and KELLER, A. *Phil. Mag.* 1961, **6**, 345

# *Radiolysis of Polyisobutene IV— A Study of the Role of Free Radicals in the Fracture Reaction using Radioactive Additives*

G. AYREY and D. T. TURNER

*The influence of additives on the formation of polymer radicals and macromolecular fractures in polyisobutene by exposure to 4 MeV electrons has been studied using phenyl-<sup>3</sup>H-sec-butyl-<sup>35</sup>S<sub>1</sub>-disulphide, thiophenol-<sup>3</sup>H, thiophenol-<sup>35</sup>S, and nitrobenzene-<sup>14</sup>C.  $G(\text{polymer radicals})$  was found to decrease from a maximum value of 7.3 at a concentration of thiophenol of  $3$  to  $5 \times 10^{-4}$  mole/g to 4.5 to 5.4 at about  $15 \times 10^{-4}$  mole/g and then to remain constant. As this decrease may be due partly to the scavenging of  $\text{H}\cdot$  and  $\text{CH}_3\cdot$  precursors, it is supposed that the primary polymer radicals are formed by processes which are relatively insensitive to the presence of large concentrations of a 'protective agent'.*

*Comparison of the effects of thiophenol on yields of radicals and fractures leads to the conclusion that two types of primary polymer radical are formed. One is due to the fracture of C—H and C—CH<sub>3</sub> bonds,  $4.2 \geq G(\text{---}) \geq 2.7$ , and the other to direct fracture of the main chain of carbon atoms,  $G(\text{---}\cdot) \geq 3.1$ . Nitrobenzene-<sup>14</sup>C, which is only slightly soluble, combines with the polymer,  $G(\text{combined nitrobenzene}) = 1.2$ , and increases the  $G(\text{fractures})$  value by 0.6 after a dose of 5 Mrad. An explanation is suggested for the contrasting effects of thiophenol and nitrobenzene at low concentrations. Thiophenol reduces the yield of fractures by stabilizing the radical  $\text{---}\cdot$  and preventing  $\beta$ -bond scission. Nitrobenzene fails to do this but instead further increases the yield of fractures by preventing the 'fracture-offsetting' combination of the radicals,  $\text{---}\cdot$ , formed by  $\beta$ -bond scission of  $\text{---}\cdot$ .*

IN Part III<sup>1</sup>, effects of various additives on the radiolytic degradation of polyisobutene were studied. The work has now been extended, first to find whether the yield of polymer radicals is depressed by a large concentration of 'protective agent' and hence to learn whether radicals have precursors which can be deactivated by energy transfer, and secondly, to correlate yields of fractures and polymer radicals in the hope of gaining insight into the way in which additives influence polymer degradation.

For the first objective, use of phenyl-<sup>3</sup>H-sec-butyl-<sup>35</sup>S<sub>1</sub>-disulphide as an additive in relatively low concentrations permitted unequivocal determination of the yield of polymer radicals<sup>2</sup>. However, as the disulphide is not readily miscible with the polymer, this type of work has now been extended to higher concentrations using labelled thiophenols. Earlier studies by Mde Sebban-Danon on radiation-induced graft polymerization indicate that styrene depresses the yield of radicals from polyisobutene<sup>3</sup>. Further considerations of whether the polymer yields free radicals by direct fracture of the main chain of carbon atoms or by elimination of  $\text{H}\cdot$  and  $\text{CH}_3\cdot$  led to apparently conflicting conclusions and it may be helpful to seek such detailed information from simpler systems where polymerization of the additive does not occur.

Toward the second objective of the influence of certain additives on the yield of fractures, labelled thiophenol and nitrobenzene were studied as examples of additives which, respectively, decrease and increase the yield of fractures. Henglein and Schneider have previously studied polymer degradation and radical yields on radiolysis of polyisobutene<sup>4</sup>. They used <sup>131</sup>I and diphenylpicrylhydrazyl and interpreted their results in terms of fracture of the main chain of carbon atoms. However, since they worked with polymer solutions, their work is not directly comparable with that reported here.

## EXPERIMENTAL

*Polyisobutene*

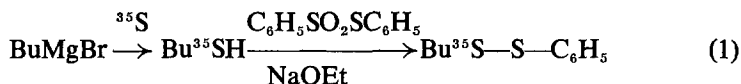
A sample of polyisobutene (Vistanex) was precipitated from analytical reagent grade (AR) petroleum ether (b.pt 30° to 40°C) with methanol twice and dried by outgassing *in vacuo* for several weeks at 40° to 60° ([ $\eta$ ] in toluene at 30° = 1 250 g<sup>-1</sup> cm<sup>-3</sup>).

*Phenyl-sec-butyldisulphide*

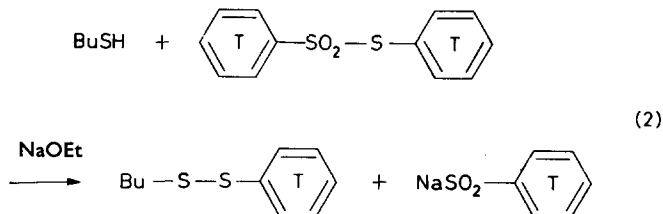
A mixture of thiophenol and *sec*-butanethiol was oxidized with iodine in alkaline solution. The mixed disulphide separated by distillation and fractional distillation through an 18 in. Vigreux column, had b.pt 72° to 75°/0.1 mm, and showed only one peak when analysed by gas-liquid chromatography (GLC) on a 4 ft column of 10 per cent Apiezon L on glass beads at 150° (Found: C, 60.5; H, 7.1; S, 32.2 per cent; C<sub>10</sub>H<sub>14</sub>S<sub>2</sub> requires: C, 60.5; H, 7.1; S, 32.4 per cent). The sample was stored in a refrigerator, but no special precautions were taken and no disproportionation was observed during twelve months.

*Phenyl-<sup>3</sup>H-sec-butyl-<sup>35</sup>S<sub>1</sub>-disulphide*

Two labelled disulphides were prepared separately and mixed for final dilution and purification. Phenyl-*sec*-butyl-<sup>35</sup>S<sub>1</sub>-disulphide was prepared by reaction (1) on a 2 mm scale. The radiochemical yield was 20 per cent. Wilzbach irradiation<sup>5</sup> of phenylbenzenethiolsulphonate yielded a tritium—



labelled product which was purified and used in a similar reaction (2) to



yield phenyl-<sup>3</sup>H-*sec*-butyldisulphide. The two disulphides were mixed to give a ratio of total tritium activity to total sulphur-35 activity of

$^3\text{H}:^{35}\text{S}:5:1$ . This ratio is close to the optimum for liquid scintillation counting of doubly labelled samples<sup>6</sup>. The doubly labelled disulphide was diluted with pure inactive disulphide and redistilled through a small Vigreux column. Comparison of specific activities before and after dilution indicated a radiochemical purity of  $\sim 96$  per cent. GLC analysis indicated a chemical purity of  $> 99.9$  per cent. The final specific activities were  $0.5 \text{ mc/mm}$  for tritium and  $0.1 \text{ mc/mm}$  for sulphur-35.

#### *Thiophenol*

Commercial thiophenol was purified by fractional distillation *in vacuo*, b.pt  $54^\circ/13 \text{ mm}$ .

#### *Thiophenol- $^3\text{H}$*

Thiophenol- $^3\text{H}$  was prepared by exchange with tritiated water and purified by distillation (specific activity:  $3 \mu\text{C/mm}$ ).

#### *Thiophenol- $^{35}\text{S}$*

Thiophenol- $^{35}\text{S}$  (specific activity:  $4 \mu\text{C/mm}$ ), prepared by reaction of phenyl magnesium bromide with sulphur-35, was a gift from Mr E. Percey.

#### *Nitrobenzene*

A commercial product was purified by distillation.

#### *Nitrobenzene- $^{14}\text{C}$*

Labelled nitrobenzene was purchased from the Radiochemical Centre, Amersham. After dilution with pure nitrobenzene the specific activity was  $1 \mu\text{C/mm}$ .

#### *Procedure*

Finely chopped samples of outgassed polymer (0.2 to 1.0 g) were weighed into Pyrex glass ampoules and additive injected from a micrometer syringe. With phenyl-*sec*-butyldisulphide, low b.pt petroleum ether (free from aromatics) was used as a common solvent to speed homogenization and was then largely pumped off ( $< 5$  per cent, on weight of polymer, remaining). The ampoules were frozen, the contents degassed *several* times by freezing, pumping and thawing cycles, which also served to distribute the other additives evenly over the polymer surface. Finally, the ampoules were sealed at  $< 10^{-4}$  mm of mercury and stored for 2 to 10 days.

Samples were irradiated in a 4 MeV beam of electrons from a linear accelerator at a dose rate of 1 Mrad/min at ca.  $20^\circ$  (water cooling)<sup>1</sup>. The irradiated samples were removed from the ampoules 1 to 3 days after irradiation and dissolved in AR toluene. The polymer was separated from uncombined radioactive material, after initial pumping *in vacuo*, by precipitation with methanol followed by centrifuging and disposal of supernatant liquid. This separation was repeated two or three times until the polymer recovered from un-irradiated controls ( $> 95$  per cent recovery), which had contained the maximum amount of radioactive additive (e.g. for thiophenol about  $0.2 \text{ cm}^3/\text{g}$ ), had been reduced to constant activity close to zero.



The polymer was dried at 40° to 60° *in vacuo* for about one week and then dissolved in anhydrous toluene. Aliquot portions were taken for concentration checks, viscometry and assay. Number average molecular weights ( $\bar{M}_n$ ) were estimated using the Fox-Flory relationship<sup>7</sup> with the assumption of a random molecular weight distribution, i.e.  $\bar{M}_v = 1.85 \bar{M}_n$ . Yields of fractures in moles per gramme of polymer  $F$  were calculated from the equation  $F = (\bar{M}_n)^{-1} - (\bar{M}_n)_0^{-1}$ , where  $(\bar{M}_n)_0$  is the number average molecular weight of the polymer prior to irradiation ( $2.2 \times 10^5$ ).

#### Radiochemical assay

Additives and polymer samples were assayed in toluene solution in a liquid scintillation counter (Ekco Type N664A). Internal standards were added to all samples and count-rates were corrected for background, counter efficiency and decay. For singly labelled compounds, the standard error of assay was  $\pm 3$  per cent. Doubly labelled samples were assayed using methods described previously<sup>6</sup> and the standard error was about  $\pm 5$  per cent.

#### Calculation of $G$ values

$G$  values were calculated from equation (3) in which  $n$  is the number of moles of product per gramme of polymer and  $R$  the dose in Mrad.

$$G_{(\text{specified product})} = 9.6nR^{-1} \times 10^5 \quad (3)$$

## RESULTS AND DISCUSSION

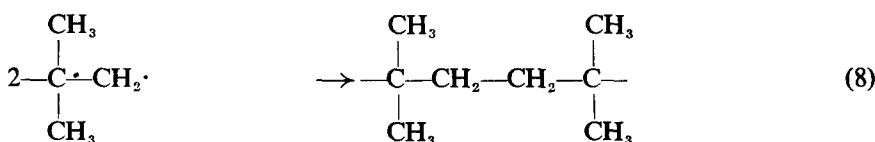
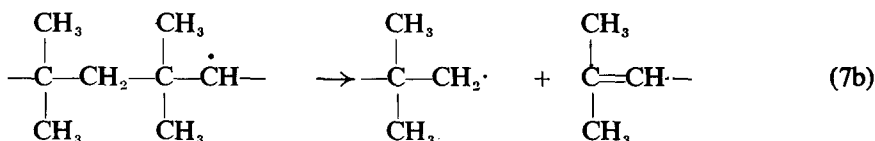
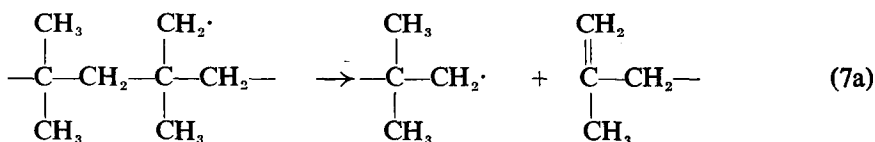
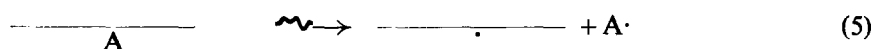
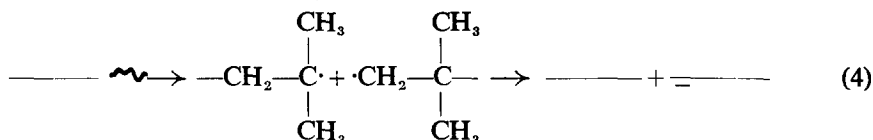
### Fractures<sup>1</sup>

The analysis of viscosity data to provide estimates of yields of fractures by the simple procedure adopted in this work requires justification<sup>8</sup>. The viscosity/molecular weight relationship used was established by Fox and Flory for approximately monodisperse samples of linear polymer obtained by fractionation and, therefore, can only be applied with caution to irradiated polyisobutenes. The direct decision as to whether any crosslinking occurs on irradiation is difficult to settle experimentally although a comparison of light scattering and viscosity data does suggest that there cannot be much, if any, branching in polyisobutene after low doses at 20°. Less directly, in previous work with a sample of polyisobutene chosen for detailed study because of its closeness to a random molecular weight distribution, it was found that analysis of viscosity data after doses  $< 10$  Mrad gave  $G_{(F, \text{fractures})} = 4.1$ . This value was confirmed by direct measurements of number average molecular weights by osmometry after smaller doses  $\leq 1.5$  Mrad for which the most precise measurements could be achieved. It is concluded that viscosity measurements provide a fair estimate of yields of fractures provided the polymer approximates a random molecular weight distribution. This is believed to be true of the polymer used in the present work in view of the closeness of experimental values of  $\bar{M}_v$  in toluene/ $\bar{M}_n = 1.9$  to 2.2 to the theoretical value for such a distribution of 1.85. Possibly, however, departures from an exactly random distribution may be responsible for the slightly higher value of  $G_{(F)} = 4.4$  as shown in *Figures 1*,

3 and 4. The apparent decrease in  $G_{(F)}$  after higher doses is in agreement with a previous report.

It seems safe to assume that the analysis of viscosity data is also valid for results obtained with the additives studied in the present work. The decrease in the yield of fractures with increasing concentration of additive in *Figures 1* and *3* is in agreement with previous results reported for di-*n*-butyl disulphide and thiophenol.

The fracture mechanism is complex and in order to account for accompanying chemical changes it was found necessary previously to postulate both direct fracture of the main chain of carbon atoms [reaction (4)] and, additionally, indirect fracture following the elimination of a lateral substituent H or  $\text{CH}_3$  [both represented by A in the schematic reactions (5) and (6)]. These reactions also result in gas formation  $G_{(A,)} \equiv G_{(\text{H}_2+\text{CH}_4)} = 2 \cdot 1$ .



Evidence will be presented in the next section for formation of the radical  $\text{---} \cdot$  postulated in reaction (4). In the highly viscous medium it seems likely that collisions of the closely spaced pair of radicals will be highly favoured and that reaction by disproportionation is most likely on steric grounds. It should be recalled that radical intermediates in the direct fracture of the polyisobutene molecule have previously been postulated for rather general reasons (cf. Bovey<sup>10</sup>). Moreover, this reaction is the sole mode of polymer radical formation invoked by Henglein and Schneider to explain their results on the radiolysis of polyisobutene in solution.

Hydrogen formation by reactions (5) and (6) is to be expected by analogy with the radiation chemistry of numerous saturated hydrocarbons<sup>11</sup>. An indication that 'thermal' gas radical precursors are involved on irradiation of polyisobutene is provided by the observation that after a dose of about 40 Mrad  $G_{(A_2)}$  decreases to a limiting value of 1.8 and this is accompanied by a decrease in the yield of double bonds; these observations are consistent with the scavenging of  $A\cdot$  by  $C=C$ . It seems reasonable to accept the view that  $A\cdot$  will sometimes be formed [in reaction (5)] with sufficient excess energy to abstract a hydrogen atom [by reaction (6)] in a first collision<sup>12,13</sup>. Reference to a value of  $G(\text{---}) \geq 2.7$ , derived in the following section, suggests that this 'hot' radical reaction is more important than the corresponding 'thermal' one, cf.  $G_{(A_2 \text{ scavenged})} = 0.3$ . As pointed out in relation to the radiation crosslinking of polyethylene, the 'hot' radical mechanism results in the formation of a close-lying pair of polymer radicals<sup>12,13</sup>.

In the virtual absence of crosslinks and internal double bonds in irradiated polyisobutene it would appear that almost all the polymer radicals formed in reactions (5) and (6) suffer  $\beta$ -bond scission [reaction (7)].  $\beta$ -bond scission has previously been considered in detail in relation to the considerable steric strain in the polyisobutene molecule with reference to reaction (7a) by Wall<sup>14</sup>. The only additional point made here is that  $\beta$ -bond scission of the other possible predominant radical of type  $\text{---}$  formed by loss of a hydrogen atom,  $G_{(H_2)} = (0.6 \text{ to } 0.75) A_2$ , would also result in formation of the polymer radical  $-\text{C}(\text{CH}_3)_2-\text{CH}_2\cdot$  [reaction (7b)]. These radicals would also be formed in close-lying pairs and, in contrast to most other polymer radicals formed from polyisobutene, would be expected to combine as in reaction (8). Consistently, a sterically strained  $-\text{CH}_2-\text{CH}_2-$  group has been detected in irradiated polyisobutene by infra-red analysis<sup>15</sup>.

#### *Polymer radical yields and types*

From the results in *Figure 1* it can be shown that about  $2 \times 10^{-4}$  mole/g of the disulphide is required to scavenge about  $10^{-5}$  mole/g of polymer radicals. In other experiments on the irradiation of saturated hydrocarbons of viscosity  $\sim 10^{-2}$  poise the scavenger concentration required is one order of magnitude less. Therefore, it is supposed that in the highly viscous polymer ( $\eta \sim 10^8$  to  $10^9$  poise<sup>7</sup>) the close-lying pairs of polymer radicals, described in the previous section, do react preferentially with each other (cf. refs. 16 and 17).

The role of phenyl-*sec*-butyldisulphide as a radical scavenger has been discussed in a preliminary note<sup>2</sup> in which it was shown that the yield of polymer radicals may be equated to the yield of sulphenyl groups combined with the polymer. The observed value of  $G_{(R\cdot)} = G_{(\text{polymer radicals})}$  of 7.3 after a dose of 1 Mrad (*Figure 1*) seems reliable as it agrees with values for  $G_{(\text{hydrocarbon radicals})}$  reported for low molecular weight hydrocarbons<sup>11</sup>. However, such values are expected to be underestimates because the scavenger is likely to react with the polymer radical precursor  $A\cdot$ . When the scavenger concentration is only  $2 \times 10^{-4}$  mole/g, substantially only the thermal radicals will be scavenged. A precise estimate of the yield of thermal radicals is not available but from an observation that the rate of  $A_2$  evolution decreases

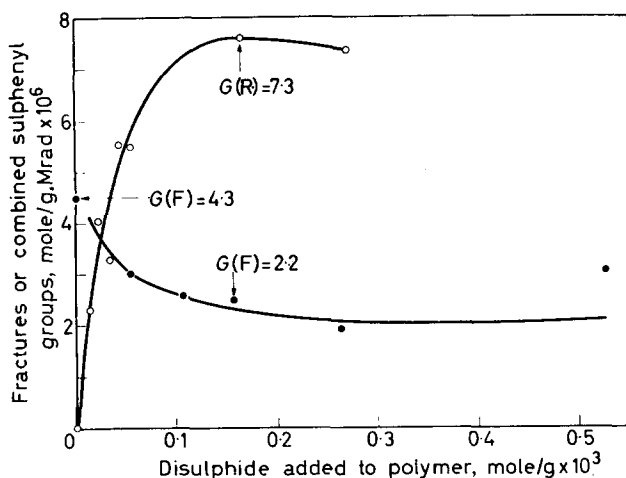


Figure 1—Radical scavenging by phenyl-*sec*-butyl-disulphide and its influence on the yield of fractures. ○ Combined sulphenyl groups using phenyl-<sup>3</sup>H-*sec*-butyl-<sup>35</sup>S<sub>1</sub>-disulphide (fourth precipitation); dose: 1 Mrad; ● Fractures using unlabelled disulphide; dose: 5 Mrad

to a constant value while the overall concentration of double bonds continues to increase (see ref. 1) it seems reasonable to suppose that  $G_{(\text{polymer radicals})}$  may be an underestimate to the extent of  $G_{(\text{A}_2 \text{ scavenged})} = 0.3$ . As this is a relatively small correction it is preferred to use the experimentally determined values of  $G_{(\text{polymer radicals})} = 7.3$ . From other experiments on the depression of the gas yield<sup>1</sup>, it is believed that 'hot' radical gas precursors may also be scavenged to a significant extent by larger concentrations of an additive such as thiophenol (see below).

The influence of high concentrations of a protective agent on the yield of polymer radicals was studied using thiophenol which has the advantage of being readily miscible with polyisobutene and, unlike the disulphide, does not need to be introduced with carrier solvent. Thiophenol-<sup>3</sup>H(C<sub>6</sub>H<sub>5</sub>SH + C<sub>6</sub>H<sub>5</sub>ST) is known to scavenge polymer radicals via reactions (9) and (10).



An alternative, that some radicals are scavenged with formation of RSC<sub>6</sub>H<sub>5</sub>, is rejected on the basis of experiments with thiophenol-<sup>35</sup>S similar to those yielding the results in Figures 2 and 3. Concentrations of 1 and 2 × 10<sup>-3</sup> mole/g C<sub>6</sub>H<sub>5</sub><sup>35</sup>SH after a dose of 15 Mrad affected the yield of fractures in a similar manner to tritiated thiophenol (Figure 3) but, significantly, did not result in any detectable introduction of <sup>35</sup>S-activity into the polymer. Presumably the sulphenyl radicals formed in reactions (9) and (10) eventually combine to form diphenyl disulphide, and neither these radicals nor the disulphide can compete with thiophenol for reaction with the

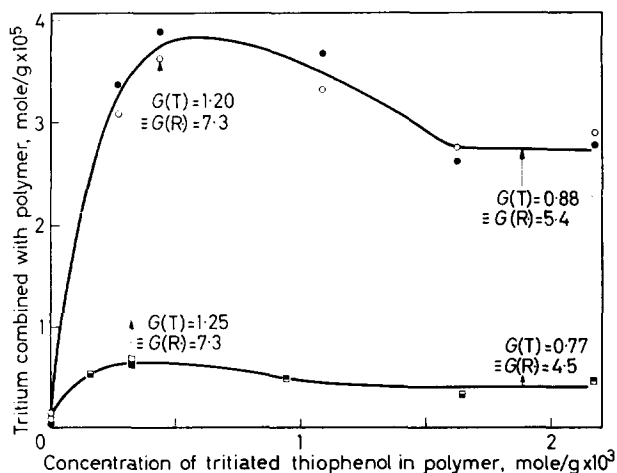


Figure 2—Radical scavenging by tritiated thiophenol. Dose: 30 Mrad. ○ 2nd precipitation, ● 3rd precipitation; Dose: 5 Mrad: □ 2nd precipitation, ■ 3rd precipitation

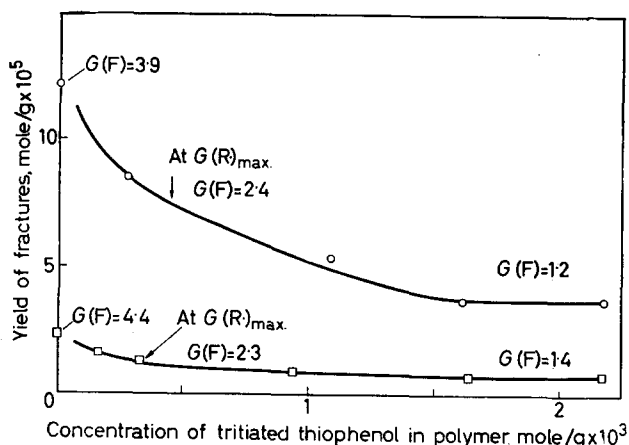


Figure 3—Influence of tritiated thiophenol on yield of fractures. ○ Dose of 30 Mrad, after 3rd precipitation; □ Dose of 5 Mrad, after 3rd precipitation

polymer radicals. Neither, apparently, do thiophenol or sulphenyl radicals add to the double bonds which are formed in polymer molecules during irradiation, a process which could have complicated any subsequent analysis.

With competitive reactions such as (9) and (10), an isotope effect is almost certain to operate. Inspection of Figure 2 yields a value of  $G$  (polymer radicals determined via thiophenol-<sup>3</sup>H) =  $G_{(T)} = 1.2$  and if this value is compared with  $G_{(R)} = 7.3$  (see Figure 1) a value for the isotope effect  $k_H/k_T = 6$  is obtained. This value seems somewhat low when compared

with a value of  $k_H/k_T=9.6$  at  $20^\circ$  which may be calculated<sup>18</sup> from data on the reaction of butanethiol-<sup>2</sup>H with polystyrene radicals at  $60^\circ$  and  $70^\circ$ <sup>19</sup>. However, low values for isotope effects have also been reported on  $\gamma$ -irradiation of deuterated polystyrenes<sup>20</sup> and may be rather general in radiation chemistry where energy deposition and initial chemical changes are so localized that neither reference to the ambient temperature nor the application of homogeneous kinetics may be appropriate.

Accepting the value  $k_H/k_T=6.0$ , the yield of polymer radicals may be derived as a function of the concentration of combined tritium from the relation  $G_{(R\cdot)}=6G_{(T)}$ . Such information is of more direct value in leading to an understanding of the nature of 'protection' against high energy radiation than similar information on the suppression of ultimate molecular products, because in the latter there is the ambiguity that the additive may have the dual role of radical scavenger and energy transfer agent. *Figure 2* shows that, by increasing the concentration of tritiated thiophenol, the yield of polymer radicals is decreased from 7.3 to 4.5 to 5.4 and then is little affected by further increase up to a concentration of  $2 \times 10^{-3}$  mole/g. In view of the high residual yield of polymer radicals it is concluded that these are formed from precursors which are, for the most part, little affected by large concentrations of an additive which from both its structure and known behaviour would generally be classified as a good 'protective agent'. As for the smaller number of polymer radicals which are suppressed by thiophenol,  $G_{(R\cdot)}=1.9$  to 2.8, it remains to be decided experimentally to what extent this is due to the interception of the likely precursors  $H\cdot$  and  $CH_3\cdot$  [cf. reactions (7) and (8)].

Although the initial aim of the present work was only to consider overall yields of polymer radicals it is possible to proceed further and adduce evidence that two general types of radical are formed, i.e.  $\text{---}\cdot$  and  $\text{---}\cdot$ . The former type is associated with gas formation, being formed by the fracture of C—H and C—CH<sub>3</sub> bonds [cf. reactions (5) and (6)]. The maximum yield of this radical may be inferred as  $2G_{(H_2+OH_2)}=4.2$  and, hence, it may be concluded that the total yield must be supplemented by the formation of radicals not associated with gas formation (i.e.  $\text{---}\cdot$ ), to the extent of at least  $7.3-4.2=3.1$ . Direct evidence for formation of radicals of the other type  $\text{---}\cdot$  may be adduced by a comparison of yields of radicals and fractures in *Figures 1, 2* and *3*, the results in the latter two figures being the more strictly comparable as they were obtained from aliquots from single samples. At the concentration of tritiated thiophenol corresponding to  $G_{(R\cdot), \text{max}}$ , the corresponding yield of fractures is too low to account for the experimentally observed yield of radicals even when it is assumed that every fracture corresponds to the formation of two polymer radicals. According to these considerations, summarized in *Table 1*,  $G(\text{---}\cdot) \geq 2.7$  and, therefore, in conjunction with preceding reasoning, this value may be placed between the following limits  $4.2 \geq G(\text{---}\cdot) \geq 2.7$ .

Concerning the rather small decrease in  $G_{(R\cdot)}$  with high concentrations of thiophenol, the data are not sufficiently precise to analyse to what extent each type of polymer radical has been suppressed.

Table 1. Comparison of observed  $G_{(\text{radical})}$  values with maximum values calculated from the yield of fractures

Scavenger	Disulphide		Tritiated thiophenol		
Scavenger concentration	At $G_{(\text{R}\cdot)}$ , max.	At $G_{(\text{R}\cdot)}$ , max.	ca. $2 \times 10^{-3}$ mole/g		
Dose (Mrad)	1	5	30	5	30
(i) $G_{(\text{radicals})}$ observed	7.3	7.3	7.3	4.5	5.4
(ii) $G_{(\text{radicals})}$ calculated as					
$2G_{(\text{fractures})}$	4.4	4.6	4.8	2.8	2.4
(i) - (ii)	2.9	2.7	2.5	1.7	3.0

More direct information on the types of free radical formed by irradiation of a polymer is to be expected from electron spin resonance (e.s.r.) studies. Tsvetkov, Molin and Voyedevodskii<sup>21</sup> have irradiated polyisobutene at  $-196^\circ$  and, after a dose of 40 Mrad, have detected a doublet which was assigned to the radical  $-\text{C}(\text{CH}_3)_2-\dot{\text{C}}\text{H}-$ . On warming to room temperature the signal disappeared completely, which shows that the radicals do not remain trapped at the higher temperature. Similar results were obtained independently by Loy and interpreted in the same way<sup>22</sup>. The absence of radicals of the type  $-\text{C}-\dot{\text{C}}-$  is not surprising, especially as their formation is probably depressed at  $-196^\circ$ . The formation of other radicals of the type  $-\text{C}-\dot{\text{C}}-$  cannot be excluded because of the general problem of achieving adequate trapping conditions plus difficulties in the complete interpretation of e.s.r. signals.

#### Role of scavengers in polymer degradation

Many additives at a concentration of the order  $10^{-3}$  mole/g decrease the yield of fractures formed by irradiation of polyisobutene. At such a concentration there is evidence that both radical scavenging and more general energy transfer effects occur and it would be difficult to assess their relative importance. At lower concentrations,  $\sim 10^{-4}$  mole/g, these additives have diverse effects some decreasing and others increasing the yield of fractures<sup>1</sup>. This discussion is limited to effects observed in this low concentration range in which it is assumed that radical scavenging effects predominate to such an extent that, in a first approach, more general energy transfer effects may be neglected.

It will be seen from *Figure 3* that the present experimental data do not provide information about the influence of very low concentrations of thiophenol on polymer degradation and the interpolation showing a gradual decrease in the yield of fractures is based on previous results. In *Figure 4* the effect of nitrobenzene in increasing the yield of fractures has been confirmed and followed well beyond maximum solubility in the polymer.

A case has been made in the previous section that thiophenol reacts with polymer radicals of type  $-\text{C}-\dot{\text{C}}-$  to form a stable polymeric product. On this basis, it is postulated that protection is due to the prevention of  $\beta$ -bond scission, i.e. reaction (9) replaces reaction (7). It is suggested that nitrobenzene fails to prevent  $\beta$ -bond scission and instead increases the yield of fractures by scavenging polymer radicals which otherwise would combine

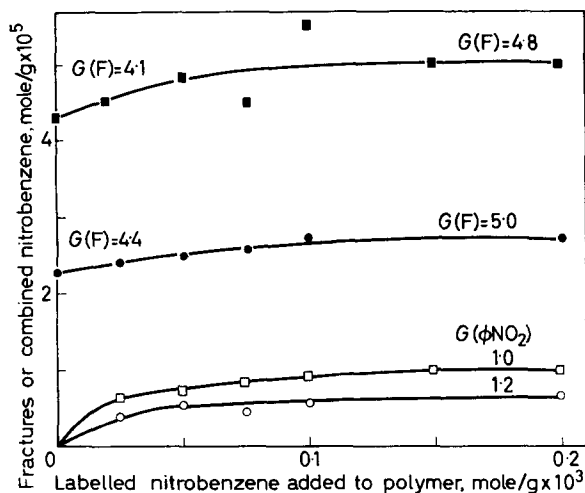


Figure 4—Scavenging by labelled nitrobenzene and its influence on the yield of fractures. Dose: 5 Mrad, ● fractures, ○ combined nitrobenzene; Dose: 10 Mrad, ■ fractures, □ combined nitrobenzene (4th precipitation)

by reaction (8). In the simplest case and using the concept that a low concentration of scavenger would fail to capture the closest-spaced polymer radicals from reaction (4), two molecules of nitrobenzene would be combined with the polymer for each additional fracture [cf. reaction (11)].



The results in Figure 4 show that at its maximum, albeit low, concentration in the polymer, nitrobenzene increases  $G_{(\text{fractures})}$  by 0.6 and 0.7 and  $G_{(\text{nitrobenzene combined with polymer})} = 1.2$  and 1.0 after doses of 5 and 10 Mrad, respectively. Taking into account the likelihood of scavenger depletion at the higher dose, these results agree with the simple analysis suggested above. However, it must be pointed out that although an adduct of the type shown in reaction (11) probably is formed initially, this itself has been shown to scavenge further radicals in other systems<sup>23-26</sup>. If this occurs in the present system then  $G_{(\text{nitrobenzene combined with polymer})}$  would provide an underestimate of the yield of polymer radicals and the agreement with the subject case would be fortuitous.

*This work was presented at the Southeastern Regional American Chemical Society Meeting held 14 to 16 November at Charlotte, N.C.*

*It is gratefully acknowledged that this work originated as part of the programme of research undertaken by the Natural Rubber Producers' Research Association and that samples were irradiated at Wantage Research Laboratories (A.E.R.E.). The University of London is thanked for a grant*



from the Central Research Fund for the purchase of gas chromatography equipment (G.A.).

Isotope Unit, Queen Elizabeth College, (G.A.)  
University of London,  
London, W.8

Camille Dreyfus Laboratory, (D.T.T.)  
Research Triangle Institute,  
Durham, North Carolina

(Received February 1964)

#### REFERENCES

- <sup>1</sup> TURNER, D. T. *J. Polym. Sci.* 1964, **A2**, 1721
- <sup>2</sup> AYREY, G. and TURNER, D. T. *J. Polym. Sci.* 1963, **B1**, 185
- <sup>3</sup> SEBBAN-DANON, J. *J. Chim. phys.* 1960, **57**, 1123ff
- <sup>4</sup> HENGLEIN, A. and SCHNEIDER, C. *Z. phys. Chem.*, N. F. 1959, **19**, 367
- <sup>5</sup> WILZBACH, K. E. *J. Amer. chem. Soc.* 1957, **79**, 1013
- <sup>6</sup> OKITA, G. T., KABARA, J. J., RICHARDSON, F. and LE ROY, G. V. *Nucleonics*, 1957, **15**, 111
- <sup>7</sup> FOX, T. G. and FLORY, P. J. *J. Amer. chem. Soc.* 1948, **70**, 2384
- <sup>8</sup> ALEXANDER, P., BLACK, R. M. and CHARLESBY, A. *Proc. Roy. Soc. A*, 1955, **232**, 31
- <sup>9</sup> TURNER, D. T. To be published
- <sup>10</sup> BOVEY, F. A. *Effects of Ionizing Radiation on Natural and Synthetic High Polymers*, p 118, Wiley: New York, 1958
- <sup>11</sup> CHAPIRO, A. *Radiation Chemistry of Polymeric Systems*. Interscience: New York, 1962
- <sup>12</sup> MILLER, A. A., LAWTON, E. J. and BALWIT, J. S. *J. phys. Chem.* 1956, **60**, 599
- <sup>13</sup> PRAVEDNIKOV, A. N. and MEDVEDEV, S. S. *Trudy I Vsesoyuzn. Soveshchaniya po Radiatsionnoi Khim.* p 269. Academy of Sciences of the U.S.S.R.: Moscow, 1958
- <sup>14</sup> WALL, L. A. *J. Polym. Sci.* 1955, **17**, 141
- <sup>15</sup> HIGGINS, G. M. C. and TURNER, D. T. *J. Polym. Sci.* 1964, **A2**, 1713
- <sup>16</sup> PREVOT-BERNAS, A., CHAPIRO, A., COUSIN, C., LANDLER, Y. and MAGAT, M. *Disc. Faraday Soc.* 1952, **12**, 98
- <sup>17</sup> NOYES, R. M. *J. Amer. chem. Soc.* 1955, **77**, 2042
- <sup>18</sup> SWAIN, C. G., STIVERS, E. C., REUWER, R. F. and SCHAAD, L. J. *J. Amer. chem. Soc.* 1958, **80**, 5885
- <sup>19</sup> WALL, L. A. and BROWN, D. W. *J. Polym. Sci.* 1954, **14**, 513
- <sup>20</sup> WALL, L. A. and BROWN, D. W. *J. phys. Chem.* 1957, **61**, 129
- <sup>21</sup> TSVETKOV, YU. D., MOLIN, YU. N. and VOYEDEVODSKII, V. V. *Vysokomol. Soedineniya*, 1959, **1**, 1805 [*Polymer Science U.S.S.R.* 1961, **2**, 165]
- <sup>22</sup> LOY, B. R. *J. Polym. Sci.* 1963, **A1**, 2251
- <sup>23</sup> INAMOTO, N. and SIMAMURA, O. *J. org. Chem.* 1958, **23**, 408
- <sup>24</sup> BEVINGTON, J. C. and GHANEM, N. A. *J. chem. Soc.* 1959, 2071
- <sup>25</sup> JACKSON, R. A. and WATERS, W. A. *J. chem. Soc.* 1960, 1653
- <sup>26</sup> NORRIS, W. P. *J. Amer. chem. Soc.* 1959, **81**, 4239

# Studies on Amylose and Its Derivatives V\*—The Sedimentation of Amylose Acetate in Dilute Solution

J. M. G. COWIE and P. M. TOPOROWSKI

*Sedimentation and viscosity measurements have been carried out on seven fractions of amylose acetate dissolved in nitromethane at a temperature of 25°C. The effect of pressure on the sedimentation constant has been investigated and the relation between  $S_0^0$  and  $\bar{M}_w$  was found to be  $S_0^0 = 4.14 \times 10^{-15} \bar{M}_w^{0.38}$ . Data obtained previously for the acetate dissolved in nitromethane, and chloroform have been reassessed using a modification of the Flory theory proposed recently by Kurata and Stockmayer, and it has been found that the amylose acetate molecule can be regarded as a flexible coil with negligible draining. The possibility of a helical form in solution is also discussed.*

THE hydrodynamic relations proposed by Flory and Fox have proved adequate in describing the dilute solution behaviour of those polymer-solvent systems in which an essentially gaussian distribution of the polymer coil segments is observed. This theory imposes an upper limit of 0.8 to the value of  $\nu$ , the exponent in the Mark-Houwink equation

$$[\eta] = KM^\nu \quad (1)$$

and cannot be used to analyse systems in which  $\nu$  exceeds this limit. While most flexible synthetic polymers have  $\nu$  well within the range 0.5 to 0.8, many cellulose derivatives and several solvent-polymer systems, which are notably polar in character, possess  $\nu$  values greater than 0.8. To explain this violation of the Flory-Fox upper limit, a molecule having a 'stiff' chain, with correspondingly larger free draining characteristics, has been postulated. However, recent refinements of the Flory treatment of long range interactions, by Kurata, Stockmayer and others<sup>1</sup>, have extended the upper limit for  $\nu$  to 1.0, for non-draining molecules. This now allows any flexible molecule to exhibit large  $\nu$  values when dissolved in very good solvents, without requiring the introduction of large free draining corrections.

This new theory is used to interpret the results obtained from an investigation of the sedimentation velocity behaviour of amylose acetate in nitromethane and also to reassess data obtained previously<sup>2</sup>.

## EXPERIMENTAL

### Samples

The preparation and fractionation of amylose acetate has been described

\*Issued as N.R.C. No. 8183. Part IV. COWIE, J. M. G. *Makromol. Chem.* 1963. 59, 189.

elsewhere<sup>2</sup>. The fractions used in this work are mainly those used before and the remainder were characterized in a similar manner.

### *Solvents*

Nitromethane was fractionally distilled through a Podbielniak Heli-Pak column. The middle fraction (boiling point 101°C) was collected and used in all physical measurements.

Reagent grade chloroform was used without further purification.

### *Viscosity*

Intrinsic viscosities were measured in a Cannon-Ubbelohde semi-micro dilution viscometer or in a shear viscometer of the type described by Cragg and van Oene<sup>3</sup>.

### *Sedimentation velocity*

Sedimentation velocity measurements were made using a Spinco model E ultracentrifuge equipped with phase plate schlieren optics and a rotor temperature control unit. The fractions, dissolved in nitromethane, were spun at 59 780 rev/min using 12 mm aluminium centrepieces, at a temperature of 25°C. Sedimentation constants ( $S$ ) were evaluated from the relation

$$S = (1/\omega^2 r) (dr/dt) \quad (2)$$

where  $r$  is the distance of the boundary in cm from the centre of rotation at time  $t$  (sec), and  $\omega$  is the angular velocity measured in radians/sec.  $S$  can be obtained from the slope of the plot  $\log r$  against  $t$ , which is linear when pressure effects are small. The duration of the runs varied from about 40 min for the large molecular weight fractions to 100 min for the smallest.

### *Partial specific volume*

The densities of several solutions of amylose acetate in nitromethane were determined in a Sprengel-Ostwald pycnometer having a volume of approximately 21 ml. From this the partial specific volume of the polymer could be calculated and was found to be 0.754 cm<sup>3</sup>/g.

## RESULTS

### *Pressure dependence of $S$*

It was originally pointed out by Mosimann and Signer<sup>4</sup> that when polymer molecules are subjected to large force fields, such as are experienced during high speed sedimentation velocity runs in an ultracentrifuge, a considerable pressure difference is produced between the meniscus and the bottom of the cell. This can amount to as much as 200 atmospheres and will induce changes in solvent viscosity and density as well as in the specific volume of the solute, which will result in a change in the sedimentation coefficient of the dissolved polymer.

Several investigators have treated the problem in more detail<sup>5-10</sup>, and it has been shown that unless the effect of pressure is considered, appreciable error in the calculation of  $S^0$  may arise. This is particularly true for organic solvents with high compressibilities.

The dependence of the sedimentation constant on pressure was expressed by Oth and Desreux<sup>5</sup> and by Fujita<sup>7</sup> in the form

$$S = S^0 [1 - \mu P + (0) P^2] \quad (3)$$

where  $S$  is the sedimentation coefficient at pressure  $P$ ,  $S^0$  is the value of  $S$  at  $P=0$ , and  $\mu$  is a parameter containing the dependence of density, partial specific volume, and frictional coefficient on pressure.

The hydrostatic pressure at any point in the cell can be obtained from the relation

$$P = \frac{1}{2} \omega^2 r_0^2 \rho_0 (y - 1) \quad (4)$$

where  $r_0$  and  $r$  denote the radial distances of the meniscus and the boundary from the centre of rotation,  $\rho_0$  is the solvent density, and  $y = (r/r_0)^2$ . This leads to a relation between  $S$  and  $r$

$$S = S^0 [1 - m (y - 1)] \quad (5)$$

where  $m$ , the pressure correction factor, is

$$m = \frac{1}{2} \mu \omega^2 \rho_0 r_0^2 \quad (6)$$

Equation (5) expresses  $S$  as a linear function of  $y$ , an approximation which is valid when  $m(y-1)$  is small compared with unity.

Fujita put the more empirical treatment of Oth and Desreux on a rigorous mathematical basis and arrived at a differential equation of flow, relating the sedimentation coefficient at zero concentration to both the pressure and concentration dependent parameters. The equation has been solved by Wales<sup>9</sup> and by Billick<sup>10</sup> who have demonstrated its applicability to the polystyrene-cyclohexane system. Billick has shown that Fujita's equation can be expressed as a series, which in one form can be written as

$$\ln r = \ln r_0 + S^0 \omega^2 t - B^0 (\omega^2 t)^2 + \dots \quad (7)$$

where  $S^0$  is the sedimentation coefficient corrected for pressure at any given concentration and

$$B^0 / (S^0)^2 = \{m(2\alpha + 1) - \alpha\} / (1 + \alpha) \quad (8)$$

Here  $\alpha$  is the concentration dependent parameter defined by

$$S^0 = S^0 / (1 + \alpha) = S^0 / (1 + K_s c) \quad (9)$$

To assess the importance of the pressure correction for the present system, data for sample ATAF5 were treated according to the various methods available. Oth and Desreux suggested an extrapolation method whereby the polymer is run at various speeds and  $S$  measured at a fixed position in the cell each time.  $S^0$  was then obtained by plotting  $S$  against  $\omega^2$  and extrapolating to  $\omega^2 = 0$ . Fraction ATAF5 was run at 59 780, 50 740 and 42 040 rev/min for each of four concentrations and  $S$  was calculated at a fixed value of 6.5 cm from the centre of rotation.  $S^0$  obtained by this method is shown in *Table I*.

It was also possible to obtain  $S^0$  from equation (7) using a least squares procedure. To obtain a sufficiently large range the sedimentation was allowed to continue until the boundary was almost at the bottom of the

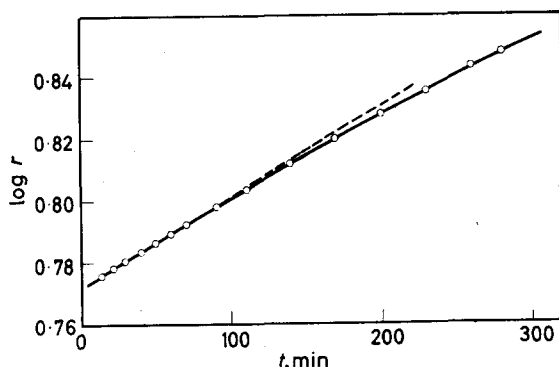


Figure 1—Graph of  $\log r$  against  $t$  for amylose acetate ATA F5 at speed 59 780 rev/min and concentration 0.6 per cent, showing experimentally determined points (solid curve) and the limiting tangent (broken line)

cell. Figure 1 shows a plot of  $\log r$  against  $t$ , which starts off with a short linear portion and then curves gently, indicating the increasing effect of pressure on the boundary movement as it progresses down the cell. Equation (7) was applied over this whole range and the values of  $S^0$  obtained are listed in Table 1. Also shown in this table is  $S^0$  calculated

Table 1.  $S^0$  for ATA F5 in nitromethane calculated by various methods

Conc. %	Speed rev/min	$S^0$ (eqn 2)	$S^0$ (eqn 7)	$S^0$ (eqn 10)	$S^0$ (at 6.5 cm)
0.600	59 780	2.84	2.91	2.91	2.98
	50 740	2.89	2.93	2.92	
0.446	59 780	3.30	3.34	3.36	3.50
	50 740	3.37	3.54	3.46	
	42 040	3.41	3.40	3.40	
0.318	59 780	3.96	3.99	4.00	4.01
	50 740	4.07	4.05	4.10	
	42 040	4.12	4.17	4.12	
0.204	59 780	5.00	5.04	5.10	5.10
	50 740	5.03	5.11	5.10	
	42 040	5.20	5.30	5.28	

from equation (2) (i.e. the linear portion of  $\log r$  against  $t$ ). These were measured from separate runs of short duration, and are comparable to those corrected for pressure effects. Finally  $S^0$  was also obtained<sup>7</sup> from

$$\ln y/2\omega^2t = S^0 [1 - \frac{1}{2}m(y-1)] \quad (10)$$

together with values for  $m$ , which are shown in Table 2.

## STUDIES ON AMYLOSE AND ITS DERIVATIVES V

Table 2. Pressure correction factors for amylose acetate in nitromethane

Conc. %	Speed rev/min	$B^0 \times 10^{26}$	$m$	$\mu \times 10^9$
0.600	59 780	3.94	0.53	0.68
	50 740	2.19	0.23	0.41
0.446	59 780	4.64	0.50	0.64
	50 740	6.82	0.39	0.69
	42 040	1.94	0.22	0.56
0.318	59 780	6.02	0.44	0.57
	50 740	3.03	0.25	0.44
	42 040	3.84	0.14	0.38
0.204	59 780	10.67	0.47	0.60
	50 740	10.92	0.39	0.70
	42 040	17.54	0.36	0.93

Values for  $S^0$  calculated from equations (7) and (10) are very close while the results using equation (2) are about two per cent lower. However, this is within the limits of error for the various  $S^0$  values computed at different speeds, and it appears that calculation of  $S^0$  from the limiting tangent to the  $\log r$  against  $t$  curve is sufficient to yield values comparable in accuracy to those corrected for pressure for this particular system. It has also been found<sup>11</sup> that for the polystyrene-cyclohexane system, the slope of the limiting tangent will give  $S^0$  within three per cent of that corrected for pressure. The sedimentation coefficients at zero concentration and pressure ( $S_0^0$ ) for the other samples (see Table 3) have been calculated

Table 3. Sedimentation and viscosity parameters for amylose acetate in nitromethane at 25°C

Sample	$M_w \times 10^{-6}$ *	$10^{13}S_0^0$	$K_s$	$[\eta]$ †	$K_s/[\eta]$
ATA F1	4.800	13.2	5.88	7.70	0.76
ATA F5	2.450	10.0	4.10	4.40	0.93
ATA F8	1.400	8.3	4.07	2.65	1.54
SA 2	1.020	7.5	2.40	1.87	1.28
SA 4	0.735	6.8	2.10	1.43	1.47
DSA 1	0.165	3.7	0.67	0.40	1.67
DSA 2	0.150	3.4	0.59	0.36	1.64

\*See ref. 2. †Concentration in g/100 ml.

using the initial slope method, from runs of short duration.

The extrapolation method of Oth and Desreux, where  $S^0$  was calculated at 6.5 cm, was not as accurate as the other methods and, as Fujita stresses, equation (10) is more generally applicable.

Values of  $B^0$ ,  $m$  and  $\mu$  are collected in Table 2. These are found to be lower than the corresponding values calculated for polystyrene in cyclohexane<sup>10,11</sup> and in toluene<sup>10</sup>. The pressure parameter  $\mu$  has an average value of  $0.6 \times 10^{-9}$  as compared with  $1.0 \times 10^{-9}$  for polystyrene-toluene<sup>10</sup> and  $1.75 \times 10^{-9}$ ,  $1.66 \times 10^{-9}$  for polystyrene in cyclohexane<sup>10,11</sup>.

As expected  $m$  decreases generally with a lowering of  $\omega$ , and is smaller than the value quoted for polystyrene. Billick<sup>10</sup> has shown that the pressure

correction is more important than the concentration effect and that at high speed the latter effect can probably be ignored even in good solvents. It is certainly a minor factor for amylose acetate in nitromethane as  $m$  is greater than  $B^0/(S^0)^2$  by only 12 to 15 per cent for runs at the top speed.

#### *Sedimentation velocity*

Values of  $S^0$  were plotted as  $1/S^0$  against  $c$  and extrapolated to  $c=0$  to give  $S_0^0$  which is listed in *Table 3* for each fraction. The relation between  $S_0^0$  and  $\overline{M}_w$  was calculated from a log/log plot (*Figure 2*), and is expressed by

$$S_0^0 = 4.14 \times 10^{-15} \overline{M}_w^{0.38} \quad (11)$$

Kurata and Stockmayer<sup>1</sup> have shown that for coiled polymers without draining, the relation

$$\nu_s = (2 - \nu)/3 \quad (12)$$

will be valid, where  $\nu$  is the exponent in equation (1) and  $\nu_s$  that in equation (11). Substituting  $\nu_s = 0.38$  in equation (12) gives  $\nu = 0.86$  as compared with the experimentally determined<sup>2</sup> value of 0.87.

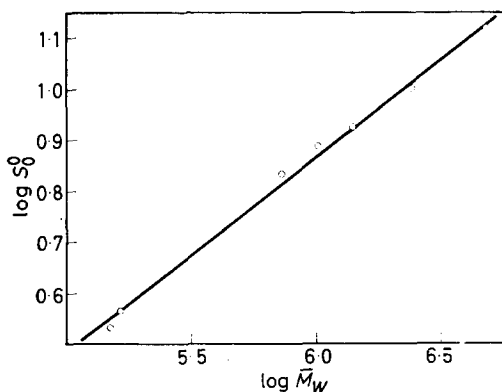


*Figure 2*—Log/log plot showing the variation of sedimentation coefficient ( $S_0^0$ ) with weight average molecular weight ( $\overline{M}_w$ ) for amylose acetate in nitromethane at 25°C

Also tabulated is the concentration dependent parameter  $K_s$ . Van Holde and Wales<sup>12</sup> found that for several polymers in good solvents, the ratio  $K_s/[\eta]$  was approximately constant with a value of 1.6. To obtain this they assumed that the volume of the polymer molecule could be calculated from the Flory equivalent sphere model, and from the results obtained here it may be possible to use this approximation for the lower acetate fractions but certainly not for the higher ones where the ratio is considerably less than 1.6.

#### *Unperturbed dimensions of amylose acetate*

The extension of the Flory-Fox theory now makes it possible to estimate the unperturbed dimensions of polymers in systems with  $\nu > 0.8$ , and

Stockmayer and Fixman<sup>13</sup> have proposed the equation

$$[\eta] = KM^{1/2} + 0.51 B\Phi_0 M \quad (13)$$

relating intrinsic viscosity to molecular weight for flexible polymers with negligible draining effects. [ $B$  should not be confused with  $B^0$  in equation (7).] Thus a plot of  $[\eta] \times M^{-1/2}$  against  $M^{1/2}$  will yield  $K$  as intercept and the unperturbed dimensions can be calculated from

$$K = \Phi_0 [\langle r^2 \rangle_0 / M]^{3/2} \quad (14)$$

where  $\Phi_0 = 2.8 \times 10^{21}$  and  $[\eta]$  is in g/100 ml.

Figure 3—The dependence of  $[\eta] M^{-1/2}$  on  $M^{1/2}$  for amylose acetate in chloroform (●) and nitromethane (○) at 30°C. Data used from ref. 2

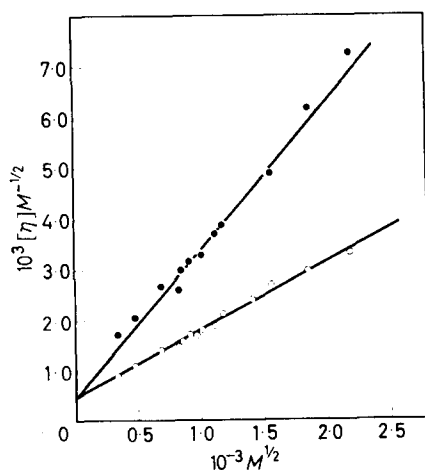


Figure 3 shows this plot for amylose acetate in chloroform and nitromethane at 30° (using data from ref. 2) in which the intercept is  $K = 4.8 \times 10^{-4}$ . Values of  $\langle r^2 \rangle_0^{1/2}$  calculated from  $K$  are shown in Table 4 together with the corresponding  $\alpha_\eta$  for each fraction.

Table 4. Unperturbed dimensions of amylose acetate at 30°C

Sample	$\langle r^2 \rangle_0^{1/2} \text{Å}$	$[\eta]^*$	$[\eta]_0^\dagger$	$\alpha_\eta$
ATA F1	1 207	7.300	1.052	1.91
ATA F5	860	4.200	0.752	1.77
ATA F8	650	2.500	0.568	1.64
SA 2	556	1.820	0.485	1.55
SA 4	474	1.370	0.411	1.49
DSA 1	224	0.396	0.195	1.27
DSA 2	213	0.350	0.186	1.24

\*See ref. 2. †Calculated from  $K$ .

The expansion factors obtained from equation (14) are much larger than those quoted previously<sup>2</sup>, which were calculated from the Orofino-Flory



relation<sup>14</sup>, while the unperturbed dimensions are correspondingly smaller than before. This is not unexpected as the latter relation is valid only for systems with  $\nu \leq 0.8$ . The parameter  $B$  can be related to the Flory interaction parameter  $\chi_1$  by

$$B = \bar{v}_2^2(1 - 2\chi_1)/V_1N_A \quad (15)$$

where  $\bar{v}_2$  is the specific volume of the polymer,  $V_1$  the solvent molar volume and  $N_A$  is Avogadro's number. Table 5 shows  $B$  and  $\chi_1$  for both solvents.

Table 5. Interaction parameters for amylose acetate at 30°C

Solvent	$B \times 10^{28}$	$\chi_1$
Chloroform	21.20	0.386
Nitromethane	9.31	0.473

It is interesting to compare the data in Table 5 with the results quoted by Higginbotham<sup>15</sup> for osmotic pressure measurements on amylose acetate. He reported  $\chi_1 = 0.450$  for the acetate in nitroethane and  $\chi_1 = 0.396$  in chloroform; both are within five per cent of the values obtained here.

#### Flory-Mandelkern equation

It has been shown by Flory and Mandelkern<sup>16</sup> that the molecular weight of a polymer can be estimated from the intrinsic viscosity and sedimentation constant using the relation

$$M = \{S_0^0 [\eta]^{1/3} \eta_0 N_A / \bar{\beta}(1 - \bar{v}_2 \rho)\}^{3/2} \quad (16)$$

where  $\bar{\beta} = (\Phi_0^{1/3} P_0^{-1})$  is a constant for most polymer-solvent systems. The only modification necessary to bring equation (16) to consistency with the other equations is the introduction of the factor  $(\alpha_\eta / \alpha_f)$  in  $\bar{\beta}$ , where  $\alpha_f$  is the corresponding expansion factor in the equation relating the frictional coefficient to the molecular weight<sup>17</sup>. This ratio is unity in a theta solvent and 0.97 in the asymptotic limit of good solvents, which means  $\bar{\beta}$  should only vary between 2.7 and  $2.6 \times 10^6$ , and will be within these limits for all systems having  $\nu \leq 1$ . Table 6 lists  $\bar{\beta}$  for the amylose acetate-nitromethane system for which there is an average value of  $2.36 \times 10^6$ , somewhat lower than the theoretical  $\bar{\beta}$ . However, if a Zimm-Schulz<sup>18</sup> type distribution is assumed,

Table 6. Universal constant  $\bar{\beta}$  for amylose acetate in nitromethane

Sample	$\bar{\beta} \times 10^{-6}$	$\bar{\beta} \times 10^{-6*}$
ATA F1	2.25	2.36
ATA F5	2.43	2.55
ATA F8	2.38	2.49
SA 2	2.36	2.48
SA 4	2.41	2.53
DSA 1	2.32	2.44
DSA 2	2.20	2.31

\*Corrected for heterogeneity.

with a breadth parameter  $y=2$ , as used previously<sup>2</sup>, then a heterogeneity correction may be applied to  $\bar{\beta}$  which is

$$q_p^{1/3} q_p^{-1} = (y+1)^{3/2} [\Gamma(y+1)]^{4/3} [\Gamma(y+\frac{3}{2}-\epsilon)]^{-1} [\Gamma(y+\frac{3}{2}+3\epsilon)]^{-1/3} \quad (17)$$

Here  $\epsilon = \frac{1}{3}(y - \frac{1}{2})$  and  $q_p^{1/3} q_p^{-1}$  is found to be 1.05. This gives an average  $\bar{\beta}$  of  $2.45 \times 10^6$  which is closer to the theoretically expected value; but what is more significant is that  $\bar{\beta}$  is constant over a molecular weight range of  $0.15$  to  $4.8 \times 10^6$ .

#### DISCUSSION

Consideration of the solution properties of amylose acetate in the light of the modified Flory theory suggests that, when dissolved in chloroform or nitromethane, the molecule can be regarded as a flexible coil with little or no draining. However, information is more difficult to derive about the fine structure of the molecule, and other than the observation that a rodlike conformation is unlikely with such a low  $\bar{\beta}$  factor, one can only speculate on the possibility of a helical structure being present in solution.

Dombrow and Beckmann<sup>19</sup>, who investigated the sedimentation behaviour of several amylose acetate samples in methyl acetate, obtained results which indicated the molecules were in an outstretched helical form, as their calculated dimensions were in good agreement with helix dimensions established by X-ray methods. As the polymer exhibits a high steric factor<sup>1</sup>, it would not be unreasonable for it to be composed of helical sections connected by very short random coil portions acting as flexible joints (i.e. an interrupted helix), and it is possible to estimate the length of such a helical segment from the relation (derived in this form in ref. 1 from the original in ref. 20)

$$\langle r^2 \rangle_0 / n = (1 - \xi) l^2 S + \xi b_0^2 x \quad (18)$$

where  $n$  is the degree of polymerization,  $l$  is the bond length,  $S$  is the skeletal factor of the random coil sections,  $b_0$  is the effective monomer length in the helix,  $\xi$  is the fraction of monomer units in a helical sequence, and  $x$  is the weight average length of such a sequence. In the limiting case of almost 100 per cent helical content one can put  $\xi=1$  and obtain<sup>1</sup>

$$\langle r^2 \rangle_0 / n = \{ \langle r^2 \rangle_0 / M \} \cdot M_0 = x b_0^2 \quad (19)$$

and thus  $A^2 = x b_0^2 / M_0$  in which  $M_0$  is the molecular weight of a monomer unit. This relation is probably oversimplified as it does not take into account interaction between adjacent segments and assumes random orientation of each successive segment. If this is ignored and  $b_0$  is taken<sup>2</sup> as 3 Å, then  $x \sim 9$  units and each helical section would be  $\sim 27$  Å which is considerably less than the persistence length  $q$  (47 Å) calculated for amylose acetate<sup>2</sup> using the wormlike chain model of Kratky and Porod<sup>21</sup>. However, as  $q$  was calculated from unperturbed dimensions which are probably too large, according to the modified theory used here,  $q$  also would be overestimated.

This type of interrupted helical structure has been suggested for unsub-

stituted amylose<sup>22-24</sup>, and should be considered as a possible conformation for the acetate. Such a structure would still be able to behave as a flexible random coil while retaining its essentially helical character.

*The authors wish to thank Dr S. Bywater for the interest he has shown in this investigation.*

*Division of Applied Chemistry,  
National Research Council,  
Ottawa, Canada*

*(Received February 1964)*

#### REFERENCES

- <sup>1</sup> KURATA, M. and STOCKMAYER, W. H. *Fortschr. Hochpolymer Forsch.* 1963, **3**, 196, and references therein
- <sup>2</sup> COWIE, J. M. G. *J. Polym. Sci.* 1961, **49**, 455
- <sup>3</sup> CRAGG, L. H. and VAN OENE, H. *Canad. J. Chem.* 1961, **39**, 203
- <sup>4</sup> MOSIMANN, H. and SIGNER, R. *Helv. chim. Acta*, 1944, **27**, 1123
- <sup>5</sup> OTH, J. and DESREUX, V. *Bull. Soc. chim. Belg.* 1954, **63**, 133
- <sup>6</sup> ERIKSSON, A. F. V. *Acta chem. Scand.* 1956, **10**, 360
- <sup>7</sup> FUJITA, H. *J. Amer. chem. Soc.* 1956, **78**, 3598
- <sup>8</sup> ELIAS, H.-G. *Makromol. Chem.* 1959, **29**, 30
- <sup>9</sup> WALES, M. J. *Amer. chem. Soc.* 1959, **81**, 4758
- <sup>10</sup> BILLICK, I. H. *J. phys. Chem.* 1962, **66**, 1941
- <sup>11</sup> BYWATER, S. and COWIE, J. M. G. Unpublished results
- <sup>12</sup> WALES, H. and VAN HOLDE, K. E. *J. Polym. Sci.* 1954, **14**, 81
- <sup>13</sup> STOCKMAYER, W. H. and FIXMAN, M. *J. Polym. Sci.*, Part C, 1963, **1**, 137
- <sup>14</sup> OROFINO, T. A. and FLORY, P. J. *J. chem. Phys.* 1957, **26**, 1067
- <sup>15</sup> HIGGINBOTHAM, R. S. *Shirley Inst. Mem.* 1950, **24**, 221
- <sup>16</sup> FLORY, P. J. and MANDELKERN, L. *J. chem. Phys.* 1952, **20**, 212
- <sup>17</sup> STOCKMAYER, W. H. and ALBRECHT, A. C. *J. Polym. Sci.* 1958, **32**, 215
- <sup>18</sup> SCHULZ, G. V. *Z. phys. Chem. B.* 1939, **43**, 25  
ZIMM, B. H. *J. chem. Phys.* 1948, **16**, 1099
- <sup>19</sup> DOMBROW, B. A. and BECKMANN, C. O. *J. phys. Colloid Chem.* 1947, **51**, 107
- <sup>20</sup> NAGAI, K. *J. chem. Phys.* 1961, **34**, 887
- <sup>21</sup> KRATKY, O. and POROD, G. *Rec. Trav. chim. Pays-Bas*, 1949, **68**, 1106
- <sup>22</sup> HOLLO, J. and SZEJTLI, J. *Periodica Polytechn.* 1958, **2**, 25
- <sup>23</sup> KUGE, T. and SOZABURO, O. *Bull. chem. Soc. Japan*, 1961, **34**, 1264
- <sup>24</sup> RAO, V. S. R. and FOSTER, J. F. *Biopolym.* 1963, **1**, 527

# The Melting of Defect Polymer Crystals

B. WUNDERLICH

*Melting of imperfect crystals is treated, using the methods of irreversible thermodynamics. A reproducible limiting heating path of zero entropy production from the metastable solid to the supercooled molten state is described. Experimental evidence shows that this 'equilibrium' heating path can often be approximated by heating fast enough so that reorganization and recrystallization in the crystalline aggregates are minimized, but not so fast that superheating is experienced. Expressions for the melting of perfect homopolymer lamellae, defect copolymer lamellae, and for the experimental maximum melting point of copolymers are discussed. For polyethylene a self-consistent set of data based on melting experiments carried out under zero entropy production heating is given. By this method the equilibrium maximum melting point for polyethylene homopolymer is found to be 142°C, while the surface free energy of a (001)-surface of polymer lamellae is about 75 erg/cm<sup>2</sup>.*

THE crystallization of flexible linear high polymers is generally carried out by cooling a melt or solution from above its melting or dissolution temperature to temperatures where crystallization can take place. This mode of crystallization introduces a severe restriction on the crystal formation, since linear high polymer melts or solutions can be looked upon as being already crystallized in one dimension, namely along the chain direction. Because of the ability of rotation around backbone chain bonds, a highly entangled starting material must be straightened out to form a crystal. Under such circumstances nucleation is also quite impeded. Measurements<sup>1</sup> showed that polyethylene, for example, exhibits homogeneous nucleation from the melt only at more than 60°C supercooling. Crystal growth occurs thus in general far below the equilibrium temperature and the resulting crystallites are far from equilibrium shape. No macroscopic single crystals have been demonstrated as yet.

The usual region of X-ray crystalline order in a linear high polymer is only of the magnitude of 100 Å in one or more directions. Besides the smallness of crystallites, or crystalline sub-systems, as they will be called below, a large number of interior defects are possible. Most of these are non-equilibrium defects. Overall, we have a very imperfect crystalline aggregate, which is metastable at low temperatures, and has the possibility of undergoing reorganization to more stable states at sufficiently high temperatures. It will melt lower than the equilibrium melting point because of the large surface of the crystals and of its imperfections.

The equilibrium theory of crystallization and melting of linear high polymers has been worked out by Flory<sup>2</sup>. It requires kinetically a rejection of short perfect crystallizable sequences of a molecule over longer ones by the advancing crystal surface and a redistribution of already crystallized sequences, a process which even in careful experiments can only be incomplete<sup>3</sup>. To fit experimental data over the whole melting range to an equilibrium crystalline distribution it was found necessary to fit the maximum crystallinity reached on crystallization by limiting the smallest

possible crystallite size, to fit the most perfect crystallite melting point empirically to a temperature lower than the equilibrium melting point, and to fit the intermediate points by a correlation function<sup>4</sup>. It was also shown that even on slow cooling with rates of the order of 1°C/hour the resulting crystallite distribution is closer to the limit of random or cold crystallization<sup>5</sup> than to the equilibrium crystallization limit<sup>4</sup>.

On *melting a hypothetical equilibrium crystallite distribution*, the same difficulties arise as in crystallization. A redistribution of crystallized perfect crystallizable sequences has to take place on raising the temperature, and the partially molten material must mix to form a homogeneous melt. If one starts with a non-equilibrium distribution and heats slowly, one follows in general a very complicated and often irreproducible path. The crystallite distribution will partially reorganize and recrystallize to a more perfect crystallite distribution before final melting. Accordingly the final melting has no relation to the crystallite distribution present in a metastable state at low temperature.

In this paper an attempt is made to overcome these difficulties by treating the heating of a metastable crystallite distribution using a heating path approximating *zero entropy production*. This description is a general one, not necessarily bound to polymer crystallite distributions. The practical advantage lies in the fact that the crystallite distribution can at low temperature be analysed by X-ray, density and microscopy methods and this information can be used to supplement thermal measurements on heating. Three equations will be derived. An equation for the melting point of perfect lamellae [equation (21)] will be given. This equation was first derived by Tammann<sup>6</sup> for a case where thickening was hindered mechanically by restraining the lamellae between glass plates. A fresh equation for the melting temperature of a defect copolymer lamella will be derived [equation (26)] and tested on previously published data. Finally the copolymer melting equation for the maximum experimental melting point of lamellae<sup>7</sup> of identical thickness will be shown to fit the zero entropy production condition [equation (31)]. A self-consistent set of experimental data on equilibrium melting point, surface energy and activities of copolymer melts of polyethylene will be presented.

#### IRREVERSIBLE MELTING

A thermodynamic description of the state of a polymer is often only possible by division of the whole sample into a sufficient number of sub-systems<sup>8</sup>. The sub-systems are assumed to be homogeneous. The free energy of the different crystalline sub-systems is called  $F_{ci}$ . The volume, enthalpy, entropy and masses are called  $V_{ci}$ ,  $H_{ci}$ ,  $S_{ci}$  and  $M_{ci}$ . The corresponding quantities of amorphous sub-systems are  $F_{aj}$ ,  $V_{aj}$ ,  $H_{aj}$ ,  $S_{aj}$  and  $M_{aj}$ . The agglomerate of all sub-systems is assumed to form a closed system which allows only heat exchange with the surroundings. The sub-systems among themselves form a set of open systems, which may exchange heat as well as matter.

At any one time there may be *amorphous, amorphous and crystalline*, or *crystalline* sub-systems present. For example, far enough above the melting region only amorphous matter is present. Only one sub-system is needed for the description of the whole sample. In the melting region both

types of sub-systems are found. Any of the extensive quantities of the whole sample is represented by an equation of the type

$$X = \sum_i X_{ci} + \sum_j X_{aj} \quad (1)$$

The crystalline state far enough below the melting range may have no separate amorphous sub-systems. Then

$$X = \sum_i X_{ci} \quad (1a)$$

To the assembly of sub-systems the formalism of *irreversible thermodynamics*<sup>9</sup> will be applied to get information on the entropy changes caused by phase changes and by changes of the defect population of crystalline polymers.

For any one sub-system the change in entropy during the time interval  $dt$  is given by

$$dS = dH/T - dF/T \quad (2)$$

The *entropy change* in turn can be separated into a contribution due to the flow of heat and matter across the sub-system boundary  $d_e S$  and a contribution due to entropy production  $d_i S$  within the sub-system caused by irreversible processes<sup>9</sup>. Accordingly

$$dS = d_i S + d_e S \quad (3)$$

The *free energy* of any crystalline sub-system has been separated into three contributions<sup>8</sup>

$$F_{ci} = m_{ci}\mu_{ci}^0 + \sum_d m_{di}\mu_{di} + \sum_s m_{si}\mu_{si} \quad (4)$$

$\mu_{ci}^0$  is the bulk chemical potential of the part of the sub-system which is X-ray perfect,

$$\mu_{ci}^0 = (\partial F_{ci} / \partial m_{ci})_{T,p} \quad (5)$$

The  $\mu_{di}$  represent the chemical potentials of the defects, while the  $\mu_{si}$  give the contribution of the surfaces;  $m$  denotes the corresponding masses, such that

$$m_{ci} + \sum_d m_{di} + \sum_s m_{si} = M_{ci} \quad (6)$$

The description of the *amorphous sub-systems* requires some additional clarification. Customarily the term amorphous is attached to the disordered condensed state of matter. Linear high polymers may exhibit a large variety of different degrees of order and orientation. In this treatment the amorphous sub-system is defined so that it is related to the equilibrium state above the melting region. Its properties below the melting region are identical to a supercooled melt of the same composition, temperature and pressure. Surface effects caused by the presence of crystalline sub-systems are eliminated by adding these to the crystalline sub-system. The free energy of the amorphous sub-system is accordingly best described by

$$F_{aj} = m_{aj}\mu_{aj} + \sum_b m_{bj}\mu_{bj} \quad (7)$$

where  $\mu_{aj}$  is the chemical potential of the crystallizable constituents of the

sub-system and the  $\mu_{bf}$  represent the foreign non-crystallizable defect material.

If surface effects influence the whole non-crystalline regions, this part of the sample is not called an amorphous sub-system, but treated as an amorphous defect<sup>9</sup>. The *amorphous defect* is a three-dimensional defect. One expects, however, no sharp division between point defects and three-dimensional defects. All sizes of defects are possible and to decide from what size on a defect is called three-dimensional is somewhat arbitrary. A disordered region treated as a three-dimensional defect would appear in the expression for  $F_{ci}$  in the sum of defect contributions.

For any *one* sub-system the *flow and production of entropy* can be derived from equations (2), (3) and (4) or (7) if internal temperature and pressure gradients are negligible:

$$d_e S = (d\Phi / dT) - \sum_v (\mu_k d_e m_k) / T \quad (8)$$

$$d_p S = - \sum_k (\mu_k d_i m_k) / T \quad (8a)$$

$d\Phi$  represents the resultant flow of energy during the time interval  $dt$  due to heat and matter transfer<sup>9</sup>. Combining equations (3), (8), (4) and (7) allows the description of the total change in entropy of an amorphous sub-system and a crystalline sub-system during the time interval  $dt$  at constant temperature and pressure

$$T dS = d\Phi_{aj} + d\Phi_{ci} + [\Delta\mu_{ci}^0 d_e m_{ci} + \sum_d \Delta\mu_{di} \Delta_e m_{di} + \sum_s \Delta\mu_{si} \Delta_e m_{si}] - \mu_{ci}^0 d_i m_{ci} - \sum_d \mu_{di} d_i m_{di} - \sum_s \mu_{si} d_i m_{si} \quad (9)$$

The  $\Delta\mu$  terms represent the appropriate changes on transfer of crystalline, defect or surface polymer from the crystalline to the amorphous sub-system. The resultant flow of energy  $d\Phi_{aj} + d\Phi_{ci}$  consists of the external heat flow from the surroundings  $d_e Q_{aj} + d_e Q_{ci}$  and the exchange due to transport of mass and energy across the *aj/ci* boundary. The latter must, due to the conservation laws, be zero, so that

$$d\Phi_{aj} + d\Phi_{ci} = d_e Q_{aj} + d_e Q_{ci} \quad (10)$$

The *entropy flow* across the closed system boundary containing the crystalline and amorphous sub-systems is then

$$d_e S = (d_e Q_{aj} + d_e Q_{ci}) / T \quad (11)$$

and  $d_e S$  is determined solely by the heat flow, a calorimetrically measurable quantity.

The *entropy production*  $d_p S$  consists of two sources: (1) the matter transfer between sub-systems *i* and *j* and (2) the change in amounts of perfectly crystalline matter, different defects and surfaces within the crystalline sub-system *ci*

$$T d_p S = [\Delta\mu_{ci}^0 d_e m_{ci} + \sum_d \Delta\mu_{di} \Delta_e m_{di} + \sum_s \Delta\mu_{si} \Delta_e m_{si}] - [\mu_{ci}^0 d_i m_{ci} + \sum_d \mu_{di} d_i m_{di} + \sum_s \mu_{si} d_i m_{si}] \quad (12)$$

The first bracket represents melting or crystallization, defined as transition

between a crystalline sub-system and an amorphous sub-system, while the second bracket describes changes in the defect and surface population of the crystalline sub-system. No processes which cause an entropy production are assumed to occur in the amorphous sub-system. This is true only well above the glass transition temperature. At or below the glass transition temperature, on the other hand, changes in defect population and melting of crystalline sub-systems which are of interest in this treatment become negligible. In this temperature range close to the glass transition only processes in the amorphous sub-system remain important. A kinetic description of the changes in amorphous polymers in the vicinity of the glass transition has been given in ref. 10.

#### ZERO ENTROPY PRODUCTION MELTING

Despite the simplifying assumption of no temperature and pressure gradients, equation (12) represents a very complex situation. On heating a metastable crystalline polymer through the melting range we expect reorganization, melting and recrystallization. Each of these processes is time dependent and, in general, if all three processes take place, it is difficult if not impossible to separate experimentally the entropy production terms. The characteristic time constants for each process, however, may be distinguishable, so that by a proper choice of heating rates one or more of the processes may be kept to a negligible contribution. This *principle of fast heating* to observe the fastest process only by freezing all others kinetically has first been applied to treat the melting of polymer crystallite distributions<sup>11</sup> obtained by cold crystallization<sup>12</sup>.

If we can exclude all recrystallization and reorganization by fast heating, we reach a limit which allows the direct transformation of metastable crystalline sub-systems into supercooled melt. The second term in the brackets of equation (12) is then zero throughout the heating because  $d_m$  is zero for each defect if there is no reorganization. In addition there are only negative  $d_m$  terms if there is no recrystallization. Melting of the crystalline sub-system  $ci$  can only occur at temperatures where the first bracket of equation (12) is zero or positive because of the second principle of thermodynamics which prohibits a negative  $d_m S$  term. If now superheating of crystalline sub-systems is avoided on melting, the change in free energy on melting is zero. An overall *zero entropy production path* is followed. In other words equilibrium melting of a defect crystalline sub-system is achieved by freezing all irreversible processes.

Before applying this zero entropy production heating mode to actual situations it is of value to analyse the available information on superheating of crystals, since superheating will finally limit the reorganization and recrystallization processes which can be excluded by fast heating.

#### SUPERHEATING OF CRYSTALS

The problem of superheating of crystals is a relatively old one. *Experimentally* it was successfully demonstrated on albite<sup>13,16</sup> and other high viscosity silicates<sup>14</sup>, gallium<sup>15</sup>, tin<sup>17</sup>, *p*-toluidine<sup>18</sup>, quartz<sup>19</sup>, and phosphorus pentoxide<sup>20</sup>. Superheatings obtained ranged from a few to several hundred degrees. In every case superheating was only possible by heating the interior



of a single crystal, leaving at least the edges below the melting point or by heating faster than the melt could progress inward from the edges of the crystal. Superheating on heating of crystals without internal temperature gradient which keeps the whole crystal at the same temperature is thus *not an analogue of supercooling of melts*, a conclusion previously drawn in 1910 by Tammann<sup>21</sup>. A melt can be supercooled without the appearance of crystals, because of hindered nucleation, while crystals will normally have points on their surfaces or edges where melting can start. Superheating will occur when there is no internal temperature gradient only if the melting velocity lags behind the heating rate of the overall crystal. We will at any one time have melt present on the surface of the superheated crystal.

No melt velocity values on polymer crystals are available as yet. *Experiments on fast melting* of single crystal growth spirals of linear polyethylene<sup>22</sup> grown from solution showed that no increase in melting point is observable for heating rates up to 20°C/min. This indicates that for rates up to 20°C/min no superheating takes place. Since the growth spirals had a half-width of at least 0.001 cm, rates of advancement of the crystal/melt interface of 10<sup>-2</sup> cm/min or slower in the crystallographic *a/b* plane should have been detected. ( $\bar{M}_w = 1.25 \times 10^5$ ,  $\bar{M}_n = 1.1 \times 10^4$ , estimated accuracy of melting point detection at highest heating rates  $\pm 2^\circ\text{C}$ .) The theoretical expression derived by Ainslie, Mackenzie and Turnbull<sup>19</sup> would have predicted a slower rate of melting. More rapid rates of measurement, it is hoped, will be available in the future to allow a discussion of this discrepancy. From the experimental evidence it is expected that superheating effects for the above mentioned polymers are not important for heating rates below 20°C/min. Most experiments to be described below have been carried out with either the same linear polyethylene, or with copolymers of comparable or smaller molecular weight with rates equal to or less than 20°C/min.

#### SINGLE CRYSTALLINE SUB-SYSTEM MELTING

##### (a) *Isolated single crystal lamellae, general equations*

For a single crystal heated through the melting range, a two sub-system model, consisting of a single crystalline sub-system and an amorphous sub-system, can be used. At low temperature only the single crystal lamella exists and the amorphous sub-system mass is zero. The free energy of the crystalline sub-system can be simplified to a single term in equation (1a). Further simplifications can be made on equation (4). Polymer single crystal lamellae are often only of the order of 100 Å thick, but large in the other two dimensions. This leads to a preponderance of the lamella surface which is in addition the location of the polymer chain folds or ends [(001)-surface]. Neglecting other surfaces leaves for the surface free energy term in equation (4)

$$\sum m_{sl}\mu_{sl} = m_{(001)}\mu_{(001)} \quad (13)$$

Changing from surface mass unit to surface area, *A*, gives

$$m_{(001)}\mu_{(001)} = m_{(001)}\mu_{el}^0 + A_{(001)}\sigma_{(001)} \quad (14)$$

where  $\sigma_{(001)}$  is the specific surface free energy of the lamella. The area

is equal to

$$A_{(001)l} = 2M_{cl} / \rho_{cl} l \quad (15)$$

where  $M_{cl}$  is the total weight of the lamella sub-system,  $\rho_{cl}$  is its density and  $l$  is the thickness of the lamella.

The contribution of the *defects* is  $\Sigma m_{ai}\mu_{ai}$ , so that equation (4) now becomes

$$F_{cl} = (M_{cl} - \Sigma m_{ai}) \mu_{cl}^0 + \Sigma m_{ai}\mu_{ai} + (2M_{cl} / \rho_{cl} l) \sigma_{(001)l} \quad (16)$$

The free energy of the *amorphous material* after complete melting of the sub-system  $cl$  is described by equation (7).

The *melting condition* for a zero entropy production heating path is that the change in free energy on melting is zero, or that

$$F_{cl} = F_{al} \quad (17)$$

(b) *Defect-free homopolymer lamellae melting*

Usually there is insufficient information on defects available to allow use of equation (17). Reasonable success was achieved in treating relatively perfect polyethylene homopolymer lamellae as free of internal defects<sup>9,22</sup>. The equation for the experimental melting point under zero entropy production conditions is identical to the result of Tammann<sup>6</sup>, who treated the melting equilibrium for *perfect lamellae* kept in the lamella morphology by restraining the material between glass plates, and thus freezing the reorganization. With the polymer the fast heating rate prevents a change in lamella morphology. The melting point lowering can be derived from equations (16), (17) and (7). If there are no defects the  $\Sigma$  term in equation (16) is zero and for a homopolymer  $bj$  terms in equation (7) are zero, so that

$$\mu_{cl}^0 + \left( \frac{2\sigma_{(001)l}}{\rho_{cl} l} \right) = \mu_{al} \text{ (at } T_m) \quad (18)$$

$\mu_{al} - \mu_{cl}^0$  is the free energy of fusion  $\Delta F_u$  per gramme of bulk polymer

$$\Delta F_u = \Delta H_u - T \Delta S_u \quad (19)$$

If we now assume that the entropy of melting  $\Delta S_u$  and the enthalpy of fusion  $\Delta H_u$  are temperature independent, equation (19) can be written

$$\Delta F_u = \Delta H_u (1 - T_m / T_m^0) \quad (20)$$

where  $T_m^0$  represents the equilibrium melting point of a macroscopic crystal. The melting point lowering  $\Delta T = T_m^0 - T_m$  can be expressed in terms of equations (18) and (20) as

$$\Delta T = 2\sigma_{(001)l} T_m^0 / \Delta H_u \rho_{cl} l \quad (21)$$

Polymer samples available for these experiments are not strictly homopolymers in the sense that occasionally chain ends occur. These will act as copolymer units and lower the activity of the polymer melt and influence the crystalline sub-system free energy, so that  $\Delta F_u$  becomes dependent upon the concentration of these copolymer units. The next step is to develop an expression which includes the effect of these copolymer units as well as the effect of defects in the crystalline sub-system.

(c) Copolymer lamellae of crystallinity  $c_w$ 

Since frequently no details about the sum  $\Sigma m_{cd}\mu_{cd}$  of equation (16) are known, they must be estimated. One way is to introduce a single term for the sum, which involves the weight fraction crystallinity. The concept of crystallinity is quite familiar to the polymer chemist. It treats all defects according to their percentage of order. Completely crystalline polymer chain units represent  $c_w = 1.0$  and amorphous units are assigned  $c_w = 0$ . All defects are assigned values according to their order compared with these two limits. Depending upon the measure of order used, some of which are specific volume, enthalpy of fusion, crystalline X-ray scattering, and crystalline infra-red absorption, various  $c_w$  values are obtained. Here then a free energy definition of  $c_w$  is used.

$\Sigma m_{cd}\mu_{cd}$  is divided into two parts. One represents the 'fully crystalline portion'; the other the 'amorphous'. For example in defect polyethylene copolymer, defects consisting of  $\text{CH}_2$  units only will have a chemical potential between the chemical potential of the amorphous and that of crystalline  $\text{CH}_2$  and can be treated formally as being made up of appropriate fractions of these two parts. Defects caused by foreign point defects like OH units, which crystallize in the polyethylene lattice, can be included in the  $\mu_{cl}$  term, which now becomes an average depending upon the concentration of OH. Non-crystallizable defects like  $-\text{CH}_3$  units, which do not fit into the lattice and cause an amorphous defect of 4 or 5 additional  $\text{CH}_2$  even on slow crystallization<sup>7</sup>, are treated as being amorphous and the  $\text{CH}_2$  involved in the same defect can be treated analogously to the  $\text{CH}_2$  defects described above. Equation (16) becomes now

$$F_{cl} = c_w \overline{M_{cl}\mu_{cl}} + (1 - c_w) \overline{M_{cl}\mu_{adl}} + (2M_{cl}/\rho_{cl}l) \sigma_{(001)l} \quad (22)$$

$\overline{\mu_{cl}}$  and  $\overline{\mu_{adl}}$  are the appropriate average chemical potentials of the crystalline and amorphous portions;  $\overline{\mu_{cl}}$  includes contributions from all completely or partially crystallizable repeating units, while  $\overline{\mu_{adl}}$  contains contributions only from defects of crystallinity less than 1.0.

The free energy of the amorphous sub-system of the same composition is analogously written as

$$F_{al} = c_w \overline{M_{cl}\mu_{al}} + (1 - c_w) \overline{M_{cl}\mu_{adl}} \quad (23)$$

Substituting equations (22) and (23) into equation (17) leads to

$$\overline{\mu_{cl}} + 2\sigma_{(001)l}/c_w\rho_{cl}l = \overline{\mu_{al}} \quad (24)$$

$\overline{\mu_{al}}$ , the average chemical potential of all crystallizable units in the molten state, can be written for random copolymers

$$\overline{\mu_{al}} = \overline{\mu_{al}^0} + (RT/M_{al}^0) \ln X_A \quad (25)$$

where  $X_A$  is the activity of the crystallizable units, a quantity which must generally be evaluated experimentally.  $M_{al}^0$  is the average molecular weight. Treating the free energy of fusion  $\overline{\mu_{al}^0} - \overline{\mu_{cl}}$  similarly, as in part (b) above,

leads to the final melting point equation

$$\Delta H_u \left[ \frac{1}{T_m} - \frac{1}{T_m^0} \right] = \frac{2\sigma_{(001)l}}{c_w \rho_{cl} T_m} - \frac{R \ln X_A}{M_{cl}^0} \quad (26)$$

where  $T_m^0$  is the equilibrium melting point of a macroscopic crystal formed by the crystallizable units into a melt of activity  $X_A = 1$ .

#### MELTING OF SUB-SYSTEM DISTRIBUTIONS

##### (a) *Mixing of amorphous sub-systems*

To melt a sub-system distribution so that zero entropy production is approximated requires each crystalline sub-system to melt at such a temperature that the change in free energy in going from the crystalline state to the amorphous is zero. This process introduces the need to know about another time-dependent process, namely, the *mixing in the amorphous sub-systems*.

If we start with a distribution of crystalline sub-systems only and melt so that *no mixing* occurs, the equations developed in the previous sections can be applied to a distribution. In fact from enthalpy or volume determinations conclusions about the sub-system distribution could be drawn.

On crystallization, however, there will be in general a *rejection of certain constituents* of the melt by the advancing crystallization front; and an enrichment in lower molecular weights, in shorter sequences of crystallizable repeating units, and in foreign defects in the lower temperature crystallizing sub-systems will take place. On melting such a crystallite distribution the reverse process will occur. The amorphous sub-systems formed at the start of the melting will have a higher concentration of non-crystallizable units. On progressing melting, the temperature where sub-systems will melt must depend upon the degree of *mixing reached with previously molten sub-systems*. Under these circumstances reproducibility is reached for the case of *complete mixing* in the amorphous phase; that means it is assumed that all molten crystalline sub-systems form *one* amorphous sub-system which is homogeneous throughout the sample.

Another case where information on the complete melting range is obtainable is the cold crystallization<sup>12</sup>. Here random nearest-neighbour crystallization down to limiting sequence length is assumed. This implies that there is no separation of non-crystallizable sequences and accordingly, on remelting, mixing can be assumed to be instantaneous. For this treatment no defects are allowed for the interior of the crystalline sub-systems and the melting point is fixed by the surface defects and the sequence length distribution of amorphous crystallizable sequences<sup>5</sup>.

The case which will be treated here in some detail is the *upper melting end of a copolymer* on zero entropy melting. This melting point of the most perfect crystalline sub-system has been called the experimental maximum melting point. This case is particularly simple since for the last few per cent of sub-systems melting, no noticeable change in amorphous composition is expected and its composition is known from the chemical structure of the copolymer. In addition only the most perfect sub-systems will be left to melt, allowing simplifications in the defect description. The

mixing problem is also minimized since at that temperature a melt unrestricted by crystalline sub-systems is present. Complete mixing will be assumed in part (b).

(b) *Upper melting range of a copolymer*

For the upper melting range of a copolymer we expect again an equation of the type of equation (26) to hold, since we can express the liquid free energy by equation (25). Since for the most perfect sub-systems,  $c_w$  will be close to one, the main problem for experimental evaluation of the melt end or the *maximum experimental melting point* on zero entropy production melting is to have information on lamellar thickness and on surface free energies. For copolymer series of the same host lattice it is possible to eliminate the surface term by crystallizing samples of different copolymer content so that  $l$  is the same for the most perfect sub-systems. In this case we can eliminate the surface term from two different samples:

$$\Delta H_u^I \left[ \frac{1}{T_m^I} - \frac{1}{T_m^0} \right] = \frac{2\sigma_{(001)l}}{c_w \rho_{cl} l T_m^I} - \frac{R \ln X_A^I}{M_{al}^0} \quad (27)$$

$$\Delta H_u^{II} \left[ \frac{1}{T_m^{II}} - \frac{1}{T_m^0} \right] = \frac{2\sigma_{(001)l}}{c_w \rho_{cl} l T_m^{II}} - \frac{R \ln X_A^{II}}{M_{al}^0} \quad (28)$$

The  $T_m^I$  and  $T_m^{II}$  represent the experimental maximum melting points of the two distributions of characteristics  $X_A^I$  and  $X_A^{II}$ . Neglecting the small difference in the surface free energy term arising from non-identical  $T_m$ s and assuming that  $\Delta H_u^I = \Delta H_u^{II}$  yields on subtracting equation (27) from (28)

$$M_{al}^0 \frac{\Delta H_u}{R} \left[ \frac{1}{T_m^{II}} - \frac{1}{T_m^I} \right] = -\ln \frac{X_A^{II}}{X_A^I} \quad (29)$$

If  $X_A$  is the homopolymer with  $X_A^I = 1$

$$M_{al}^0 \frac{\Delta H_u}{R} \left[ \frac{1}{T_m^{II}} - \frac{1}{T_m^I} \right] = -\ln X_A^{II} \quad (30)$$

where  $T_m^I$  is the melting point of the lamellae of thickness  $l$  in contact with a melt  $X_A = 1$ . If the crystals are grown with non-folded morphology, as was recently shown on polyethylene by Wunderlich and Arakawa<sup>23</sup>, equation (30) becomes

$$M_{al}^0 \frac{\Delta H_u}{R} \left[ \frac{1}{T_m} - \frac{1}{T_m^0} \right] = -\ln X_A \quad (31)$$

which is the melting point equation for an infinitely thick lamella under zero entropy production. Since an infinitely thick lamella is the equilibrium shape of a crystal  $T_m^0$  is now maximum melting point in the Flory<sup>2</sup> sense.

SUMMARY OF EXPERIMENTAL DATA ON POLYETHYLENE  
A large volume of data on polyethylene polymer and copolymer melting

under conditions which approach zero entropy production has been collected in our laboratory<sup>7, 22-24, 27</sup>.

In order to treat the melting of a single polymer lamella or the melting end to the degree of approximation of equation (26) eight constants have to be evaluated, namely:  $T_m^0$ , the equilibrium melting point of a macroscopic crystal into pure  $(\text{CH}_2)_\infty$  melt;  $T_m$ , the melting point of the subsystem on hand at low temperature under zero entropy production conditions;  $\sigma_{(001)l}$ , the surface free energy of the lamella;  $X_A$ , the activity of the crystallizable units in the melt;  $\Delta H_u$ , the enthalpy of fusion;  $\rho_{cl}$ ,  $c_w$ , and  $l$ , the density, free energy crystallinity, and thickness of the lamella.  $\Delta H_u$  for polyethylene crystals was assumed to be the value determined by calorimetry as a function of temperature

$$\Delta H_u = 54.6 + 0.1716t - 6.36 \times 10^{-4}t^2 \quad [t \text{ in } ^\circ\text{C}] \quad (32)$$

With a solid solution of copolymers in the polyethylene crystal lattice, a linear interpolation between the  $\Delta H_u$  of polyethylene and the  $\Delta H_u$  of the solute homopolymer was used.

$\rho_{cl}$  was determined by density gradient columns or pycnometry. From  $\rho_{cl}$ ,  $c_w$  was calculated at room temperature wherever possible. Since  $c_w$  on the specific volume and heat of fusion scale are usually in good agreement it is a good approximation to use the same  $c_w$  for the free energy scale since we have made already the assumption that

$$\Delta F_u = \Delta H_u (1 - T/T^0)$$

The lamellar thickness,  $l$ , was determined by interference microscopy on solution-grown lamellae<sup>25</sup> or by low angle X-ray diffraction on bulk samples<sup>26</sup>. To use the low angle X-ray data needs some caution, since the result is an average value, and strictly one should use the maximum value. Thus in using data for  $l$  in equation (26) determined by low angle X-ray diffraction not the experimental maximum melting point  $T_m$  was used, but an average value, which was taken at the peak of the melting specific heat. This temperature is 1.0° to 1.5°C lower than  $T_m$ . It is felt that no more than a  $\pm 0.5^\circ\text{C}$  uncertainty is introduced by this procedure of matching X-ray and heat of fusion averages.

$T_m^0$ ,  $T_m$ ,  $X_A$ , and  $\sigma_{(001)l}$  have been determined using the here developed zero entropy melting equations on five sets of polyethylene, polymethylene and copolymer experiments.

To find  $X_A$  for the standard linear polyethylene used (Marlex 50,  $\overline{M}_w = 1.25 \times 10^5$ ,  $\overline{M}_n = 1.1 \times 10^4$ ), polymethylene of high molecular weight ( $X_A = 1$ ) was crystallized using identical slow crystallization rates as for the polyethylene (1.2°C/hour). Inserting the experimental maximum melting points found by DTA (135°C and 137°C) into equation (30) gives  $X_A = 0.995$ .

To establish the *activity of different copolymer units* of polyethylene, five copolymer series with increasing amounts of  $-\text{[CO]}-$ ,  $-\text{[CH}_2\text{C(OH)H]}-$ ,  $-\text{[CH}_2\text{C(CH}_3\text{)H]}-$ ,  $-\text{[CH}_2\text{C(OCOCH}_3\text{)H]}-$  and  $-\text{[CH}_2\text{C(C}_2\text{H}_5\text{)H]}-$  copolymer repeating units were crystallized and their melting points compared to identically treated polyethylene<sup>7, 27</sup>. Analysis

of melting point data was again made using equation (30). Combining melting points with information on crystallinity and unit cell X-ray scattering shows that C=O and C(OH)H form *point defects* by being accommodated on a CH<sub>2</sub> lattice position; this means they are crystallizable units and  $X_A$  is not influenced by their presence. The three others, however, are not forming a solid solution;  $X_A$  decreases proportionally to their increasing concentration. The crystallinity drops on incorporating these copolymer units, which means additional (CH<sub>2</sub>) units are hindered on crystallization by the presence of the copolymer. Since also the unit cell dimensions change, it must be concluded that these copolymer units form *amorphous defects* inside the polymer lamellae.

The third set of data was obtained to gain information on  $T_m^0$ . It was observed that when linear polyethylene is crystallized under hydrostatic pressure above 4 000 atm, lamellae are developed which are so thick that the surface influence is negligible<sup>23,26</sup>. Thicknesses of these *extended chain lamellae* of up to 3 microns were measured. The surface term in equation (26) becomes negligible for such large  $l$  and with the above value for  $X_A$ ,  $T_m^0$  can be calculated to be 142°C using the measured  $T_m$  of 140°C.

The last two sets of experiments were concerned with determination of  $\sigma_{(001)}$ . Single crystal growth spirals of the standard polyethylene from solution were melted under the microscope<sup>22</sup> after their thickness was determined by interference microscopy. Heating rates had in this case to be higher than 10°C/min, to avoid thickening, and to approach zero entropy production. In addition three melt-crystallized samples of the standard polyethylene were melted using DTA methods<sup>23</sup>. Their thickness was measured by low angle X-ray diffraction<sup>26</sup>. The crystallization temperature was varied by using different hydrostatic pressures. The pressure was kept low enough, however, so that the extended chain crystals which formed in addition to folded lamellae were small enough not to interfere with the folded crystal melting maximum. *Table 1* summarizes all these measurements.

*Table 1.* Surface free energies of polyethylene as calculated using equations (21) and (26)

Sample	Cryst. condition	$\rho_{cl}$ (g/cm <sup>3</sup> )	(Å)	$t_m$ (°C)	$\sigma_{(001)l}$ (erg/cm <sup>2</sup> )	
					Eq. (21)	Eq. (26)
1	Decane solution, 101°C	~0.971	132	117.4	96	79
2	Xylene solution, 90°C	~0.975	149	122.8	83	71
3	Chlorobenzene solution, 89°C	~0.974	144	122.4	83	70
4	Toluene solution, 91°C	~0.976	144	121.2	88	75
5	Tetrachlorethylene sol., 81°C	~0.976	129	118.5	90	77
6	Melt, 1 atm, 130°C	0.980	~400	133.7	82	71
7	Melt, 2 000 atm, 170°C	0.983	~600	135.2	94	82
8	Melt, 2 760 atm, 186°C	0.986	~400	133.2	89	80

$\sigma_{(001)l}$  as calculated by equation (26) has a somewhat higher degree of precision, in particular among the five solution-crystallized samples, for which the most accurate thickness measurements are available. The standard

deviation of a single measurement as calculated by equation (21) is  $\pm 5$  erg/cm<sup>2</sup>, while the values calculated by equation (26) show  $\pm 4$  erg/cm<sup>2</sup>. More experiments with a greater spread in density are necessary to establish the melting point dependence of lamellae on density and crystallinity.

The above described experiments present a self-consistent set of data for polyethylene. There are in addition a few *independent bits of information* which can strengthen the results obtained by zero entropy production melting. The equilibrium maximum melting point of paraffins as a function of chain length has been of longstanding interest. A recent extrapolation<sup>28</sup> gave for an infinite chain length  $141^\circ \pm 2.3^\circ\text{C}$ —in good agreement with the here calculated  $142^\circ\text{C}$ . Surface free energies can be estimated from crystallization kinetics using a kinetic theory of lamellar growth<sup>29</sup>. The value obtained by this technique<sup>30</sup> is 83 to 110 erg/cm<sup>2</sup>, again the same order of magnitude, although lower as well as higher estimates on different theories of crystallization have been postulated. An estimation<sup>31</sup> of branch points, ends and double-bonds of a similar polymer as the standard polymer used in this research resulted in a mole fraction of CH<sub>2</sub> units of 0.995. This value is well within the error limit of the measured value.

*Financial support from the National Science Foundation is gratefully acknowledged. The experimental work cited was supported by the Office of Naval Research and the Advanced Research Projects Agency.*

*Department of Chemistry,  
Rensselaer Polytechnic Institute,  
Troy, N.Y., U.S.A.*

*(Received February 1964)*

## REFERENCES

- <sup>1</sup> CORMIA, R. L., PRICE, F. P. and TURNBULL, D. *J. chem. Phys.* 1962, **37**, 1533
- <sup>2</sup> FLORY, P. J. *Trans. Faraday Soc.* 1955, **51**, 848
- <sup>3</sup> RICHARDSON, M. J., FLORY, P. J. and JACKSON, J. B. *Polymer, Lond.* 1963, **4**, 221
- <sup>4</sup> KILIAN, H. G. *Kolloidzchr.* 1963, **189**, 23
- <sup>5</sup> WUNDERLICH, B. *J. chem. Phys.* 1958, **29**, 1395
- <sup>6</sup> TAMMANN, G. *Z. anorg. Chem.* 1920, **110**, 166
- <sup>7</sup> WUNDERLICH, B. and POLAND, D. *J. Polym. Sci.* 1963, **1A**, 357
- <sup>8</sup> WUNDERLICH, B. *Polymer, Lond.* 1964, **5**, 125
- <sup>9</sup> PRIGOGINE, I. *Thermodynamics of Irreversible Processes*, 2nd ed. Interscience: New York, 1961
- <sup>10</sup> WUNDERLICH, B., BODILY, D. and KAPLAN, M. *J. appl. Phys.* 1964, **35**, 95
- <sup>11</sup> WUNDERLICH, B. *J. chem. Phys.* 1958, **29**, 1395
- <sup>12</sup> DOLE, M. *Kolloidzchr.* 1959, **165**, 40
- <sup>13</sup> DAY, A. L. and ALLEN, E. T. *Carnegie Inst. Wash. Publ. No. 31*, 1905
- <sup>14</sup> DOELTER, C. *Z. Elektrochem.* 1906, **12**, 413
- <sup>15</sup> VOLMER, M. and SCHMIDT, O. *Z. phys. Chem. B*, 1937, **35**, 467
- <sup>16</sup> GREIG, J. W. and BARTH, T. F. W. *Amer. J. Sci. A*, 1938, **35**, 93
- <sup>17</sup> KHAIKIN, S. E. and BENE, N. P., *C.R. Acad. Sci. U.R.S.S.* 1939, **23**, 31
- <sup>18</sup> SEARS, G. W. *J. Phys. Chem. Solids*, 1957, **2**, 37
- <sup>19</sup> AINSLIE, N. G., MACKENZIE, J. D. and TURNBULL, D. *J. phys. Chem.* 1961, **65**, 1718
- <sup>20</sup> CORMIA, R. L., MACKENZIE, J. D. and TURNBULL, D. *J. appl. Phys.* 1963, **34**, 2239
- <sup>21</sup> TAMMANN, G. *Z. phys. Chem.* 1910, **68**, 17



## B. WUNDERLICH

---

- <sup>22</sup> WUNDERLICH, B., SULLIVAN, P., ARAKAWA, T., DICYAN, A. B. and FLOOD, J. F. *J. Polym. Sci.* 1963, **1A**, 3581
- <sup>23</sup> WUNDERLICH, B. and ARAKAWA, TAMIO. *J. Polym. Sci.* 1964, **2A**, 3697
- <sup>24</sup> WUNDERLICH, B. and KASHDAN, W. H. *J. Polym. Sci.* 1961, **50**, 71
- <sup>25</sup> WUNDERLICH, B. and SULLIVAN, P. *J. Polym. Sci.* 1962, **56**, 19
- <sup>26</sup> GEIL, P. H., ANDERSON, F. R., WUNDERLICH, B. and ARAKAWA, T. *J. Polym. Sci.* 1964, **2A**, 3707
- <sup>27</sup> BODILY, D. and WUNDERLICH, B. *J. Polym. Sci.* 1965, in press
- <sup>28</sup> BROADHURST, M. G. *J. chem. Phys.* 1962, **36**, 2578
- <sup>29</sup> FRANK, F. C. and TOSI, M. *Proc. Roy. Soc. A*, 1961, **263**, 323
- <sup>30</sup> WUNDERLICH, B. *J. Polym. Sci.* 1963, **1A**, 1245
- <sup>31</sup> BRYANT, W. M. D. *J. Polymer. Sci.* 1959, **34**, 569

# Thermal Expansion and Viscoelasticity of Rubber in Relation to Crosslinking and Molecular Packing

P. MASON\*

*The effects of crosslinking upon the specific volume, thermal expansion coefficient, glass-transition temperature ( $T_g$ ) and viscoelasticity of rubber have been studied. Materials were prepared by heating purified natural rubber with varying amounts of dicumyl peroxide. This procedure formed networks by intermolecular carbon-carbon bonding, and an approximately 60-fold range of crosslinking density was obtained. The crosslink density could be estimated with reasonable confidence up to about  $10^{20}$ /g. At this level the effects observed were, approximately, a 1 per cent decrease in specific volume; 23 per cent and 6 per cent decreases in the thermal expansion coefficients respectively below and above  $T_g$ ; 5°C increase in  $T_g$ ; and a displacement of the viscoelastic response by +5°C. These changes are accounted for in terms of the reduction in free volume consequent upon crosslinking.*

*There was also a qualitative change in behaviour, the thermal expansion and viscoelastic transitional regions widening as the crosslinking increased. The thermal expansion behaviour is explained in terms of a linear increase in the variance of the monomeric free volume with crosslinking up to  $10^{20}$ /g. At higher densities the crosslinks are so close that their packing effects interact and the nature of the phenomenon changes.*

A NON-CRYSTALLINE polymer above its glass-transition temperature is essentially a liquid. If the chain molecules are now bonded by sufficient crosslinks to form a single network, the possibility of flow is removed and the crosslinked polymer manifests a high elasticity whose dependence on the density and distribution of the crosslinks is still the subject of intensive study<sup>1</sup>. However, it also retains some liquid-like characteristics, such as its expansivity, viscoelasticity and glass-transition behaviour, and the present paper examines the way in which these properties are modified by crosslinking.

Progress in understanding either the elastic or the liquid-like behaviour is largely dependent on the ability to measure the degree of crosslinking attained. For a natural rubber system this problem has been solved on the basis of the study by Moore and Watson<sup>2</sup> of the reaction between natural rubber and di-*tert*-butyl peroxide. This reaction produces a network of rubber molecules crosslinked by carbon-carbon bonds, and quantitative analysis of the reaction products enabled the number of crosslinks to be determined. Mullins<sup>3</sup> then demonstrated that substantially the same values of crosslink density were obtained from measurements of swelling, using the Flory-Huggins equation together with certain semi-empirical corrections.

In the work now reported a similar method of direct crosslinking was used to avoid the complicating effect of 'foreign' atoms in the crosslinks. A wide range of crosslinking density was covered, and the specific volumes

\*Present address: Division of Textile Physics, C.S.I.R.O. Wool Research Laboratories, Ryde, Sydney, Australia.

at 20°C, together with the thermal expansion behaviour on passing through the glass transition, were combined to relate the structural effects of crosslinking to changes in molecular packing around each crosslink.

Dynamic mechanical behaviour was also measured and, in addition to the expected quantitative shift of the response with crosslinking, qualitative changes in the character of the response were found. This phenomenon had previously been observed by Gordon and Grieverson<sup>4</sup> with crosslinked resins, and the present results indicate also the close connection with the volume expansion through the glass-transition region.

#### PREPARATION OF MATERIALS

All specimens were prepared from a single batch of purified natural rubber supplied by the U.S. Rubber Company. After acetone extraction chemical analysis gave an ash content of 0.2 ( $\pm 0.2$ ) per cent, and infra-red and ultra-violet examination confirmed that there was no substantial organic impurity.

Fifteen portions of the batch were then mixed by mastication with recrystallized dicumyl peroxide in proportions ranging from 1 to 50 parts per hundred parts of rubber by weight. Small samples of the mixed materials were taken at this stage for the determination of intrinsic viscosity and thence the molecular weight before crosslinking. Specimens were moulded in the form of sheets for density, swelling and glass-transition measurements and narrow cylinders for dynamic testing in a torsion pendulum. Crosslinking was effected by heating in a conventional rubber press for one hour at 140°C.

After crosslinking the materials were extracted with acetone for 48 hours and then heated *in vacuo* at 50°C to constant weight. From this point up to the time of testing the materials were stored *in vacuo* in the dark.

#### EXPERIMENTAL TECHNIQUES

Specific volumes were measured by weighing 3 to 4 g specimens on a milligramme balance, first in air and then immersed in ethanol. Weighing was carried out at temperatures between 19° and 21°C and the resulting specific volumes were reduced to 20°C using the measured thermal expansion coefficients discussed below. Three specimens of each material were used and the standard error of the mean value for each material was  $10^{-4}$  cm<sup>3</sup>/g. Taking into account such sources of error as incorrect temperature measurement and absorption of water vapour by the alcohol, the relative error for a single material could be as much as  $\pm 5 \times 10^{-4}$  cm<sup>3</sup>/g.

A similar buoyancy technique was used to study the change in specific volume with temperature. Specimens of about 15 g in weight supported on a Nylon thread from the arm of a milligramme balance were quenched by immersion in ethanol in a Dewar flask at about -90°C. Temperature was measured with copper-constantan thermocouples spaced in the liquid around the specimen. The system was stirred continuously and the heat gain from the surroundings produced a rise in temperature of approximately 1°C in 3 min. At intervals of 1°C the stirring was interrupted, the specimen weighed, and the specific volume calculated using the density of ethanol

as given by the formula of Timmermans<sup>5</sup>. For most of the materials the resulting specific volume/temperature curve increased in slope sufficiently abruptly on passing from the glassy to the liquid state for the glass-transition temperature to be estimated to within about 1°C. For the very highly crosslinked materials, however, the transition was more gradual and no well-defined singularity in the thermal expansion could be identified: this behaviour is discussed in further detail below.

The dynamic behaviour of the materials was studied by means of a conventional torsion pendulum<sup>6</sup> in which part of the restoring couple was provided by the torsion of the test specimen in the form of a rubber cylinder approximately 5 cm long and 0.1 cm in diameter. By appropriate selection of torsion wires and the weights providing the inertia of the moving system the period of oscillation was kept in the region of two seconds throughout the working temperature range of -80°C to +80°C. The components of the complex shear modulus were then calculated from observations of the period and damping of the oscillations at suitably spaced temperatures.

Quantitative estimation of the degree of crosslinking was obtained for the more lightly crosslinked materials by measuring the equilibrium swelling in *n*-decane and relating the values directly to the data of Moore and Watson. These results were checked by using the physical method of calculation developed by Mullins<sup>3</sup>, which allows for the initial molecular weight of the individual samples, and good agreement was found. Moore and Watson's observations extended up to crosslink densities of about  $11 \times 10^{19}$ /gramme; for the more highly crosslinked samples beyond this 'calibration' region, Mullins's method was again used to give at least an approximate indication of the magnitude of crosslinking densities that were obtained. Both methods provided values of  $M_c^*$ , the number average molecular weight of chain segments between adjacent crosslinks, and the crosslink densities were calculated as  $N_0/2M_c^*$  crosslinks/gramme,  $N_0$  being Avogadro's number.

*Table 1* shows the range of values obtained for the swelling ratio, molecular weight and degree of crosslinking. Application of Mullins's treatment to the more highly crosslinked materials of Moore and Watson shows that the linear relation between physical and chemical estimates of crosslinking is valid up to about  $7 \times 10^{19}$ /g. Above this level the physical estimate deviates from the chemical by an amount rising to about ten per cent at the highest degree of crosslinking then reported, viz.  $11 \times 10^{19}$ /g. Quantitative treatment of the present series is thus restricted to the first eight levels of crosslinking.

## RESULTS

Qualitatively the results confirmed the expected picture that increasing the degree of crosslinking reduces the specific volume, increases the glass-transition temperature, and displaces the pattern of viscoelastic behaviour towards higher temperatures. The principal relevant measurements are listed in *Table 2*.

Table 1. Determination of crosslink density

Material	Dicumyl peroxide % by wt of rubber	Initial mol. wt $\times 10^5$	Equilibrium swelling in n-decane $v_r$	Segmental mol. wt $M_c^*$	Crosslink density $\times 10^{19}/g$
1	1	2.53	0.220	28 600	1.05
2	2	2.32	0.253	17 200	1.75
3	3	2.31	0.284	11 600	2.60
4	4	2.16	0.307	8 250	3.65
5	5	2.12	0.340	6 480	4.65
6	6.5	2.10	0.385	4 580	6.58
7	8	2.68	0.408	3 870	7.81
8	10	2.15	0.447	2 890	10.4
Estimated values†					
9	13	2.07	0.488	1 800	16.7
10	16	2.07	0.541	1 300	23.2
11	20	1.96	0.587	1 040	29
12	25	1.40	0.635	800	37
13	32	1.47	0.694	590	51
14	40	1.23	0.733	485	62

†These values are outside the range for which quantitative calculation is valid. They are quoted as useful estimates having an accuracy which decreases as the degree of crosslinking increases.

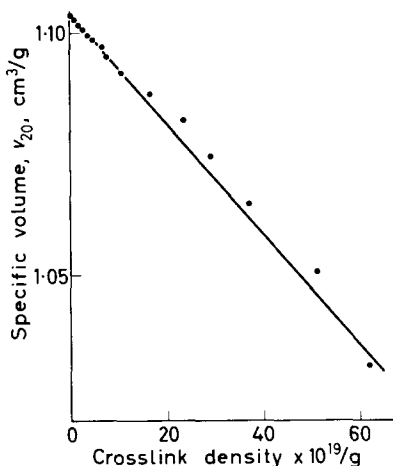
Table 2. Properties of crosslinked materials

Crosslink density $\times 10^{19}/g$	Specific volume at 20°C $cm^3/g$	Glass-transition temperature °C	Temperature of internal viscosity maximum °C	Thermal expansivity $\times 10^{-4}/°C$	
				Glassy	Liquid
0.0	1.103 <sub>8</sub> †	ca. -71.0	—	ca. 1.6	ca. 7.3
1.05	1.102 <sub>8</sub>	-69.8	-65.6	2.2	7.5
1.75	1.101 <sub>8</sub>	-70.4	-64.9	2.2	7.3
2.60	1.100 <sub>8</sub>	-69.5	-65.5	2.0	7.5
3.65	1.099 <sub>5</sub>	-69.3	-64.5	2.1	7.3
4.65	1.098 <sub>8</sub>	-68.8	-64.1	1.9	7.4
6.6	1.097 <sub>1</sub>	-68.1	-63.0	1.9	7.2
7.8	1.095 <sub>1</sub>	-66.9	-62.4	1.9	7.2
10.4	1.092 <sub>0</sub>	-65.9	-61.0	1.6	7.0
-----					
16.7	1.087 <sub>5</sub>	-62.2	-57.2	1.4	6.5
23.2	1.082 <sub>1</sub>	-60.7	-56.3	1.5	6.3
29	1.074 <sub>9</sub>	-54.9	-54.0	—	—
37	1.065 <sub>0</sub>	(-51; -47)	(-49; -32)	—	—
51	1.050 <sub>9</sub>	(-40; -37)	(-47; -28)	—	—
62	1.031 <sub>5</sub>	(-39; -31)	(-46; -13)	—	—

†By extrapolation.

Considering first the densification produced by crosslinking, *Figure 1* shows how the specific volume at 20°C decreases as the degree of crosslinking increases. The extent of the changes may be appreciated in relation to the specific volume of the unit cell, which is approximately 1.0 cm<sup>3</sup>/g, so that at the highest degrees of crosslinking the density is approaching that of a single crystal; thermally induced crystallization, by contrast, would not reduce the specific volume below about 1.07 cm<sup>3</sup>/g. A more detailed plot of these data over the quantitative crosslinking range shows that each crosslink reduces the volume of the polymer by 113 Å<sup>3</sup>. The structural implications of this result have been discussed elsewhere<sup>7</sup>.

*Figure 1*—Specific volume of crosslinked rubber at 20°C



At the lower levels of crosslinking, normal thermal expansion behaviour was observed; the specific volume/temperature relationship was linear in the liquid state and only slightly curved in the glassy state, so that extrapolation of these lines through a transition zone some six or seven degrees wide enabled the glass-transition temperatures to be determined. At the higher degrees of crosslinking, however, the transition zone broadened and merged with the increasing curved line on the glassy side, so that it became impossible to identify a single glass-transition point. Specific volume/temperature plots illustrating this behaviour for three materials spaced through the range are shown in *Figure 2*.

The glass-transition temperatures which could be clearly defined are listed in *Table 2* and the values for materials within the quantitative crosslinking range are plotted in *Figure 3*. There is an approximately linear dependence, the glass-transition temperature increasing by 1°C for an increase in crosslink density of  $2 \times 10^{19}/g$ .

*Table 2* also lists the expansion coefficients  $\alpha_G$  and  $\alpha_L$  for the glassy and liquid states. There is considerable scatter, but the data in the quantitative region are consistent with the relations:

$$\alpha_G = (2.24 - 0.52 \times 10^{-20} X) 10^{-4} / ^\circ C$$

$$\alpha_L = (7.50 - 0.44 \times 10^{-20} X) 10^{-4} / ^\circ C \quad (1)$$

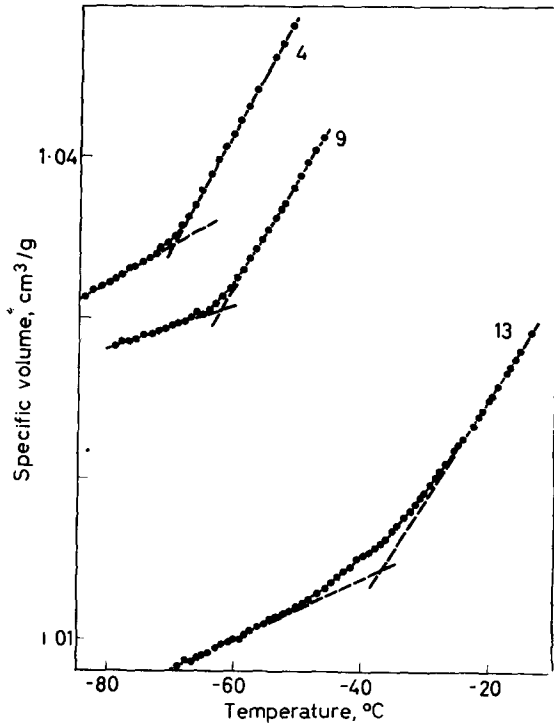


Figure 2—Thermal expansion of crosslinked rubber. Curve 4:  $3.65 \times 10^{19}$  crosslinks/g; Curve 9: ca.  $17 \times 10^{19}$  crosslinks/g; Curve 13: ca.  $51 \times 10^{19}$  crosslinks/g

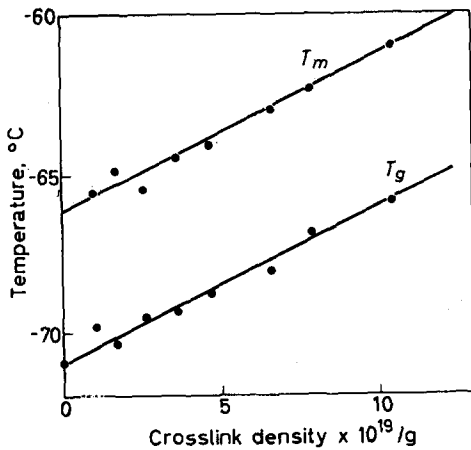


Figure 3—Variation in transition temperatures with degree of crosslinking

Thus the coefficients decrease by 23 per cent and by 6 per cent respectively for crosslinking to the level of  $10^{20}$ /g. It may be observed that at this level approximately  $2\frac{1}{2}$  per cent of the monomers in the system are crosslinked. The product

$$(\alpha_L - \alpha_G) \times T_g = 0.106 + 0.004 \times 10^{-20} X$$

and is thus approximately constant and reasonably close to the value 0.113 found by Simha and Boyer<sup>8</sup> as the average for a wide range of polymers.

The torsion pendulum measurements generated sets of values of the elastic component,  $G'$ , and the viscous component,  $G''$ , of the dynamic shear modulus at a frequency of approximately 0.5 c/s. For the present purposes the results may be summarized quantitatively, as in *Table 2*, by the values of  $T_m$ , the temperature at which  $G''$  passes through its maximum. It is seen from *Figure 3* that, inside the range of quantitative crosslinking,  $T_m$  is approximately 5°C higher than the glass-transition temperature.

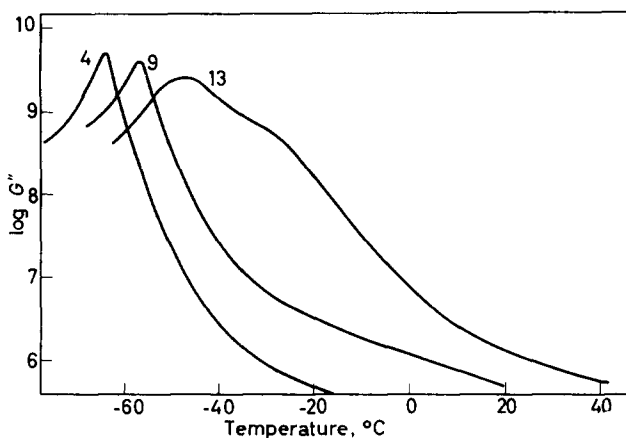


*Figure 4*—Dispersion of imaginary shear modulus with temperature. Curve 4:  $3.65 \times 10^{19}$  crosslinks/g; Curve 9: ca.  $17 \times 10^{19}$  crosslinks/g; Curve 13: ca.  $51 \times 10^{19}$  crosslinks/g

Qualitatively there is a parallel between the changing shape of the dynamic response curves and the changing shape of the thermal expansion curves as the crosslinking density increases. Thus *Figure 4* shows the internal viscosity component  $G''$  for the same three materials whose thermal expansion was illustrated in *Figure 2*. For material 4 a conventional plot is obtained showing an increase of some four or five decades in  $G''$  as the temperature decreases through the rubber-glass transition region, followed by a sharp decrease after the peak at  $T_m$ ; the curve for the more highly crosslinked material 9 is displaced towards higher temperatures and slightly broadened; the response for the very highly crosslinked material 13, however, is both displaced and considerably altered in shape, suggestive of the existence of two peaks differing in temperature by some 20°C.



## DISCUSSION

Within the quantitative crosslinking range there is a reduction in volume (at 20°C) of 113 Å<sup>3</sup> for each crosslink introduced. This may be contrasted with the average volume per monomeric unit, which is approximately 124 Å<sup>3</sup>. In a previous analysis<sup>7</sup> it was shown that approximately 34 Å<sup>3</sup> of the contraction was due to a diminution in free volume, whereas the free volume component of the average monomeric volume was only 10 Å<sup>3</sup>. A treatment in terms of the Fox-Flory representation<sup>9</sup> of free and occupied volumes was adequate to describe both the densification and the change in glass-transition temperature over the range.

Such a treatment, however, does not relate to changes in the *width* of the transition, and to account for these in terms of packing it is necessary to examine the change in the distribution of free volume which is brought about by crosslinking. (A purely formal treatment of this problem in terms of chain lengths between crosslinks has been given by Ueberreiter and Kanig<sup>10</sup>.) It is the *localization* of part of the free volume which distinguishes the network structure from the true liquid state where the free volume is available<sup>11</sup> throughout the system.

In the non-crosslinked rubber there will be an instantaneous distribution of the free volume,  $v_f$ , which may be specified by associating a free volume  $v'_f$  with each monomer. Denoting the specific volume of the rubber at temperature  $T$  by  $v$ , the fractional free volume  $f$  is  $v_f/v$ . The glass-transition temperature  $T_g$  may be associated with a definite value  $f_g$  of this parameter, which may be taken numerically<sup>12</sup> to be 0.025. Corresponding primed quantities, referred to a single monomeric unit rather than to a gramme of rubber, may be obtained by writing the mean volume associated with each monomer as

$$\bar{v}' = \frac{Mv}{nN_0}$$

$M$  being the molecular weight of the rubber,  $n$  the number of monomeric units per molecule and  $N_0$  Avogadro's number. For simplicity the system is taken to be monodisperse.

As the variation in  $v'_f$  about  $\bar{v}'$  is small compared with  $\bar{v}'$  itself, the monomeric free volume,  $v'_f$  and the monomeric fractional free volume,  $f'$  are related by

$$f' = v'_f / \bar{v}' = \frac{nN_0}{Mv} v'_f \quad (2)$$

The geometry of the packing may be defined by the distribution function  $p(f')$  representing the density of monomeric units with fractional free volume  $f'$ . Following the procedure of scaling down the bulk parameters to the molecular level, the effective  $T_g$  for a monomeric unit will be determined by the condition  $f' = f_g$ . Thus in 1 g of rubber at temperature  $T$

$$\text{the number of monomers in the glassy state} = \int_0^{f_g} p \, df'$$

and the number of monomers in the liquid state =  $\int_{f_g}^{\infty} p \, df'$

$$\text{with the normalizing relation } \int_0^{\infty} p \, df' = N_0 n / M \quad (3)$$

Hence, if  $\alpha_G$  and  $\alpha_L$  are the expansivities in the glassy and liquid states respectively,

$$\alpha = \left\{ \int_0^{f_g} p \, df' \times \alpha_G + \int_{f_g}^{\infty} p \, df' \cdot \alpha_L \right\} / \int_0^{\infty} p \, df'$$

whence 
$$\alpha - \alpha_G = \frac{M \Delta \alpha}{N_0 n} \int_{f_g}^{\infty} p \, df' \quad (4)$$

where  $\Delta \alpha = \alpha_L - \alpha_G$ .

The value of the integral representing the number of monomers in the liquid state decreases from  $N_0 n / M$  at temperatures well above  $T_g$ , where  $\alpha = \alpha_L$ , to zero at temperatures well below  $T_g$  where  $\alpha = \alpha_G$ . If all monomers had the same fractional free volume  $f'$ , the transition would take place at a single temperature. The 'smearing out' of the transition may be attributed to the existence of a distribution of values of  $f'$ , and the temperature interval over which  $\alpha$  decreases from  $\alpha_L$  to  $\alpha_G$  gives a measure of the width of this distribution. Thus assuming  $f'$  to be normally distributed at temperatures above  $T_g$ , the mean  $f'$  will necessarily be equal to the macroscopic value  $f$ , so that the distribution may be written

$$p = p(f') = \frac{1}{\sigma \sqrt{2\pi}} \exp \left\{ -(f' - f)^2 / 2\sigma^2 \right\} \quad (5)$$

$\sigma$  being the standard deviation. Hence from equation (3)

$$\alpha - \alpha_G = \frac{M \Delta \alpha}{N_0 n} \frac{1}{\sigma \sqrt{2\pi}} \int_{f_g}^{\infty} \exp \left\{ -(f' - f)^2 / 2\sigma^2 \right\} df' \quad (6)$$

In the vicinity of  $T_g$  the standard deviation  $\sigma$  in the liquid phase may be taken to be sensibly constant so that the temperature enters into the integral in equation (6) solely through its influence on  $f$ . A numerical value for  $\sigma$  may then be obtained from the consideration that 90 per cent of the area under the normal distribution curve lies between limits which are  $1.645 \sigma$  on either side of the mean. Thus  $\alpha - \alpha_G$  will fall from  $0.95 \Delta \alpha$  to  $0.05 \Delta \alpha$  for a change in  $f$  of  $3.29 \sigma$ . It has been pointed out<sup>9,12</sup> that the temperature coefficient of the fractional free volume is  $\Delta \alpha$ , so that the range of temperature  $\Delta T$  over which this fall in  $(\alpha - \alpha_G)$  occurs is given by

$$\Delta \alpha \times \Delta T = 3.29 \sigma \quad (7)$$

Values of  $\Delta T$ , the temperature interval over which the central 90 per cent

of the transition takes place, were obtained from plots of  $\alpha$  against  $T$ , and the variation in  $\Delta T$  with crosslinking is shown in *Figure 5*.

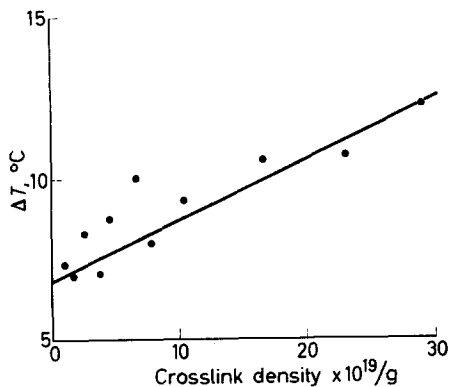


*Figure 5*—Variation in width of transition region with degree of crosslinking

There is an approximately linear relationship up to intermediate levels of crosslinking represented by

$$\Delta T = 6.8 + 1.9 \times 10^{-20} X$$

From equation (1)

$$10^4 \Delta \alpha = 5.26 + 0.08 \times 10^{-20} X$$

so that

$$10^4 \Delta \alpha \Delta T = 35.7 + 10.5 \times 10^{-20} X \quad (8)$$

Combining equations (5) and (6) gives

$$\sigma = (10.7 + 3.2 \times 10^{-20} X) 10^{-4} \quad (9)$$

This equation shows how the breadth of the distribution increases with increase in crosslinking.

For the non-crosslinked rubber, the monomeric volume at  $T_g$  is approximately  $116 \text{ \AA}^3$ , so that the mean monomeric free volume is  $0.025 \times 116 \text{ \AA}^3$ , i.e.  $2.90 \text{ \AA}^3$ ; using equation (9) the standard deviation of this free volume is  $116 \times 10^{-7} \times 10^{-4} \text{ \AA}^3$ , i.e.  $0.124 \text{ \AA}^3$ . At  $X = 10^{20}/g$ , the standard deviation rises to  $0.161 \text{ \AA}^3$ , and at  $3 \times 10^{20}/g$  it is  $0.236 \text{ \AA}^3$ .

The effects of crosslinking are illustrated in *Figure 6* which shows the distribution of monomeric free volume for these three conditions, calculated for  $-50^\circ\text{C}$ , a temperature in the liquid-like régime for all three materials. The curve for the highly crosslinked material is only of qualitative significance, partly because a considerable proportion of the monomers are in the glassy state ( $v' < 2.9 \text{ \AA}^3$ ); partly because the crosslink density is well beyond the 'calibration' range, as discussed above; but primarily because at this degree of crosslinking there is a considerable overlapping between regions surrounding individual crosslinks, so that the distribution of free volume is distorted. At this level of crosslinking the average chain between crosslinks contains only about 14 monomeric units, and the average spatial distance between crosslinks is about  $19 \text{ \AA}$ , allowing for only three or four main chains to be packed between them. There will thus be considerable

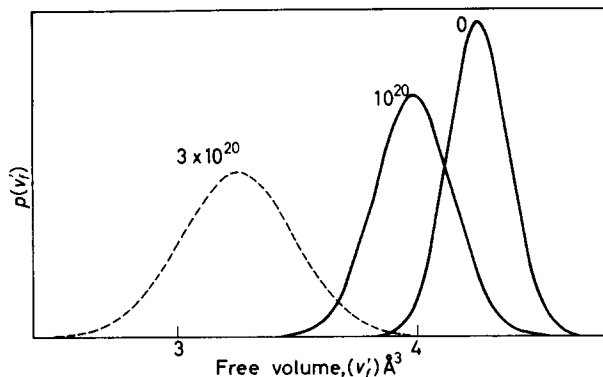


Figure 6—Distribution of monomeric free volume at three different crosslink densities

interaction affecting the packing of neighbouring crosslinks, and it seems that at a slightly higher degree of crosslinking this interaction reaches the level of a super-network throughout the structure, as suggested by the relaxation behaviour (cf., for example, curve for material 13 in Figure 4).

It thus appears that the effects of crosslinking up to a density of  $10^{20}$ /g may be interpreted as a broadening of the distribution of free volume between the monomeric units. Above this level the crosslinks are so close that their packing effects interact and further structural rigidity is developed on a much grosser scale than the liquid-like texture of the original material.

*The experimental work described above was carried out in the laboratories of the Natural Rubber Producers' Research Association in Welwyn Garden City, Hertfordshire, England. The author's thanks are due to his colleagues of that Association for helpful discussions and advice.*

*The Natural Rubber Producers' Research Association,  
Welwyn Garden City, Hertfordshire*

(Received February 1964)

#### REFERENCES

- <sup>1</sup> CIFERRI, A. *J. Polym. Sci.* 1961, **54**, 149
- <sup>2</sup> MOORE, C. G. and WATSON, W. F. *J. Polym. Sci.* 1956, **19**, 237
- <sup>3</sup> MULLINS, L. *J. appl. Polym. Sci.* 1959, **2**, 1
- <sup>4</sup> GORDON, M. and GRIEVESON, B. M. *J. Polym. Sci.* 1958, **29**, 9
- <sup>5</sup> *International Critical Tables*, Vol. III, p 27. McGraw-Hill: New York, 1928
- <sup>6</sup> FLETCHER, W. P., GENT, A. N. and WOOD, R. *Proceedings of the Third Rubber Technology Conference*, p 382. Institute of Rubber Industries London: 1954
- <sup>7</sup> MASON, P. J. *J. chem. Phys.* 1961, **35**, 1523
- <sup>8</sup> SIMHA, R. and BOYER, R. F. *J. chem. Phys.* 1962, **37**, 1003
- <sup>9</sup> FOX, T. G and FLORY, P. J. *J. appl. Phys.* 1950, **21**, 581
- <sup>10</sup> UEBERREITER, K. and KANIG, G. *J. chem. Phys.* 1950, **18**, 399
- <sup>11</sup> HIRSCHFELDER, J., STEVENSON, D. and EYRING, H. *J. chem. Phys.* 1937, **5**, 896
- <sup>12</sup> WILLIAMS, M. L., LANDEL, R. F. and FERRY, J. D. *J. Amer. chem. Soc.* 1955, **77**, 3701

### CORRECTION

The line immediately preceding equation 11 on page 536 of this volume should read:

deformed to a relative length  $\lambda$  given by

It is regretted that although correct in page proof this line was changed inadvertently during final preparation for machining.

# *The Crystallization Kinetics of Polymer-Diluent Mixtures: The Temperature Coefficient of the Process*

L. MANDELKERN

*The overall crystallization kinetics of polyethylene- $\alpha$ -chloronaphthalene mixtures have been studied over a concentration range extending from pure polymer to 0.01 per cent polymer mixture. Major attention has been given in the analyses to the temperature coefficient of the process and to the dependence of the crystallization rate on concentration. It is concluded that even for the very dilute solutions studied crystallization is not a unimolecular process, a plurality of molecules being involved. The temperature coefficient of the crystallization process can be interpreted in terms of nucleation acts which are continuous with decreasing polymer concentration. However, it must be realized that for dilute systems the effective polymer concentration needs to be considered rather than the nominal composition of the mixture.*

THE study and analyses of the crystallization kinetics of pure polymer systems, from the melt, has greatly aided in elucidating the nature of the fundamental mechanisms involved in the crystallization process<sup>1,2</sup>. Of prime importance has been the conclusion that the general mathematical formulation of the kinetics of phase changes is obeyed. Furthermore, from an analysis of the temperature coefficients of the crystallization process the significant role played by nucleation acts in both initiating the new phase in the supercooled melt and in its subsequent development has been deduced. It seems highly desirable, therefore, that this type of experiment and analysis be extended over the complete composition range at which a polymer is capable of crystallizing. Of particular interest is the very dilute range where 'single crystals' are formed and where the polymer chains in the crystals are arranged in some sort of folded array. An analysis of the temperature coefficient of crystallization, as a function of concentration, should help develop an understanding of the nucleation act in dilute polymer systems. Comparisons can then be made to see what changes there are, if any, as the polymer concentration is increased. Direct electron microscopic observations of the growth of 'single crystals' from very dilute solutions have given evidence that the growth process is nucleation controlled<sup>3</sup>.

Consequently we report the results and analysis of the temperature coefficient of the crystallization kinetics of polyethylene- $\alpha$ -chloronaphthalene mixtures over a composition range extending from pure polymer to a 0.01 per cent polymer solution. Since a detailed quantitative analysis of the isotherm shape is quite complex<sup>4,5</sup> we limit our major considerations to an analysis of the temperature coefficient of the process. A preliminary report of these results has been given previously<sup>2,6</sup>.

## EXPERIMENTAL

The polymer sample utilized in this research was an unfractionated linear polyethylene (Marlex-50) which was used in other physicochemical studies previously reported<sup>7,8</sup>. The diluent,  $\alpha$ -chloronaphthalene, was of reagent grade and used as received.

The kinetic studies, over the complete composition range, were made utilizing dilatometric techniques. Mercury was used as the confining fluid throughout. The dilatometers were basically of the conventional U-type design, and those used for the pure polymer and the more concentrated mixtures have already been described in detail. Although of the same basic design, the dilatometers for the dilute solutions possess some novel features both in their construction and operation. The problems encountered in dilute solution dilatometry arise from the large amount of solution required and the relatively high thermal expansion coefficient of the organic solvent. This situation then requires a dilatometer with a rather long expanse of capillary stem and consequently very accurate temperature control, particularly for isothermal experiments, is required. These requirements led to the construction of a dilatometer of 1 mm i.d. calibrated capillary about 35 cm long. The sealed sample chamber was approximately 140 mm long and 35 mm in diameter. The calibrated stem and sample chamber were connected, in U-shape fashion, by means of ordinary capillary tubing having approximately 2 mm i.d. The dilatometer observations were conducted in a silicone-oil thermostat maintained accurate to  $\pm 0.01^\circ\text{C}$ , and the height of the mercury column in the calibrated capillary was read by means of a cathetometer with an accuracy of 0.005 mm. A dilatometer built to these specifications and operated in the manner described allowed for a quantitative study of the crystallization process.

The high fluidity of the dilute solution introduces some complications in the constructing and filling of the dilatometer. The first step in constructing and filling a dilatometer for a dilute solution was to seal a  $2\frac{1}{2}$  in. length of the ordinary capillary tubing to one end of a length of 35 mm tubing. The other end of the tubing was sealed off to give a bulb about 14 cm long. A weighed amount of polymer was then dropped into the bulb through the capillary and the entire assembly was reweighed. The required amount of  $\alpha$ -chloronaphthalene was then introduced into the bulb through a length of finely drawn out tubing which passed through the capillary and extended about  $\frac{1}{2}$  inch into the bulb. The bulb assembly was reweighed and the amount of liquid present was thus determined. The bulb was then partially immersed in a small oil bath at about  $130^\circ\text{C}$  to form an initial solution. Mixing was accomplished by spinning the bulb by the stem, care being taken not to get any solution into the capillary tubing. When the polymer was uniformly dispersed the bulb was cooled to room temperature. This initial dissolution of the polymer was found to be necessary in order to avoid difficulties in the subsequent required dissolution processes within the sealed dilatometer. The bulb and its contents were again reweighed.

The bulb was then placed in a container of dry ice, maintained in a vertical position with the capillary tubing protruding, and the contents frozen. A 35 cm length of 1 mm i.d. Trubore tubing, with a 10/30 female joint at one end, was sealed to the open end of the plain capillary. The

ordinary capillary was then heated and formed into a U-bend, The completed dilatometer was then removed from the dry ice, still in an inverted position, and its contents were allowed to thaw. The dilatometer was then weighed maintaining it in its inverted position.

After weighing the contents, the dilatometer was again frozen and while being kept frozen the assembly was attached, by means of a double swivel arrangement of 10/30 joints, to the conventional vacuum apparatus used for filling dilatometers with mercury. When the system was sufficiently evacuated, the dry ice was quickly removed from around the sample bulb. Mercury was now allowed to trickle slowly into the dilatometer, while the dilatometer itself was rotated about the double swivel. When the dilatometer had been rotated through  $180^\circ$ , and was in an upright position, enough mercury had been admitted to fill the dilatometer. The dilatometer was then removed from the vacuum line, and the mercury level in the capillary stem was adjusted by means of a hypodermic syringe equipped with a No. 22 needle, 12 in. long. The dilatometer was then reweighed to establish the total amount of mercury that had been added. The dilatometer was clamped into a specially constructed holder designed to support the great weight of such a huge dilatometer.

Prior to the study of the crystallization kinetics, at a pre-determined fixed temperature, the dilatometer was heated above the melting temperature to remove all vestiges of crystallinity. The dilatometer was then quickly transferred to the controlled thermostat and the scale height read as a function of time. Approximately 5 to 10 minutes were required for the dilatometer and its contents to reach thermal equilibrium.

#### RESULTS AND DISCUSSION

The crystallization kinetic experiments were performed over a range of temperatures at low undercoolings in the vicinity of the melting temperature. Samples covering the complete composition range, from pure polymer to very dilute solutions, were investigated. The time scale of the crystallization process ranged from minutes to weeks in the temperature and concentration range studied. Typical isotherms, obtained for the crystallization from the dilute solutions, have already been described<sup>2</sup>. When the relative fraction transformed is plotted against the logarithm of time, the isotherms for a given concentration can be superposed one upon another merely by shifting along the horizontal axis. This property is also typical of pure homopolymers crystallizing from the bulk. The shape of the individual isotherms is also very similar to those observed in bulk. In fact, as has been noted previously<sup>2</sup>, the isotherms for dilute solution crystallization adhere more closely to the theoretical isotherms deduced for bulk polymer crystallization than do the pure polymer systems themselves. However, it would be misleading to conclude, prematurely at least, that the same detailed mechanisms were involved in both cases. The above remarks in respect to the shapes of the isotherms hold for polymer concentrations ranging from 0.01 per cent to about 3 per cent. The rate of crystallization from dilute solution is again typified by a strong negative temperature coefficient. For example, for a 0.25 per cent solution the time at which half of the transformation occurs



increases by a factor of  $10^4$  when the temperature is raised from  $97^\circ$  to  $104^\circ\text{C}$ .

At the higher polymer concentrations, isotherm shapes similar to those previously reported for diluent mixtures of polyethylene oxide and of polydecamethylene adipate were obtained<sup>9</sup>. As the pure polymer is diluted the shape of the isotherms changes. The crystallization process becomes more protracted and the apparent autocatalytic character of the process becomes much more diffuse. In this concentration range the isotherms are no longer superposable over the complete transformation range. The isotherms for the whole polymer, crystallized from the melt, over the temperature range  $120^\circ$  to  $131^\circ\text{C}$  have already been reported<sup>2</sup>, and are similar in shape to those for the very dilute systems.

The mathematical theory for the kinetics of phase changes of the solute species from a binary mixture has been summarized by Turnbull<sup>4</sup>. The theory has been shown to be applicable to the precipitation of a variety of monomeric substances<sup>10-12</sup> and has recently been applied to an analysis of the kinetics of the heat precipitation of collagen from dilute solution<sup>13</sup>. We shall utilize this theory as a framework within which to analyse the temperature coefficient of the polyethylene- $\alpha$ -chloronaphthalene mixtures.

The basic assumption is made, in the theoretical development, that the number of centres of the new phase are all formed at time  $t=0$  and grow independent of one another without any mutual impingement. Besides\* accounting for the initiation of the new phase, cognizance must be given to the growth process and mechanism. For a dilute system of growing centres, growth will be governed by processes occurring either at the particle/solution interface or by the diffusion of the solute (crystallizing) species to the interface. A detailed analysis of the mathematical problem with concurrent interfacial and diffusional processes has also been given<sup>4</sup>. These considerations give good qualitative agreement with the experimental isotherms. Since for present purposes we are not concerned with the details of the isotherm shape, but only with the temperature coefficient of the process, we can with no sensible error consider the growth mechanisms independent of one another. The diffusional flux will be greatest when the particles are smallest. Under these circumstances the growth rate should be controlled by interfacial processes. As the growing centres increase in size the decrease in the flux of the material at the surface will increase the influence of the diffusion mechanism. Since in the dilute range the temperature coefficient of the process is independent of the extent of the transformation (deduced from the superposability of the isotherms) we shall limit our considerations to the initial portions of the transformation and interface controlled growth. This limitation can be further justified by the microscopic observation of the growth of single crystals<sup>3</sup>. As will be developed subsequently, there are

\*The assumption that all the growing centres are initiated at time  $t=0$  is made solely for the purpose of mathematical simplification and not for any physically justifiable *a priori* reason. The independence of growth and lack of impingement of centres upon one another is physically reliable for the crystallization from a dilute solution. However, when the concentration of the crystallizing species is increased in the initial supercooled liquid mixture, impingement of growing centres upon one another with the concomitant cessation of growth can be expected. The mathematical methods developed by Avrami now need to be invoked. When the more complicated physical process of mutual impingement is accounted for, the mathematical necessity of limiting the initiation of growing centres to the time  $t=0$  is eliminated. In the more concentrated systems, and for the pure polymer, it is thus possible to allow growing centres to be generated during the entire course of the reaction. Fortunately, the functional relations between the fraction transformed and the time are of very similar form for the two cases.

still more compelling theoretical reasons to restrict the analyses to the range of small amounts of the transformation for the more concentrated polymer-diluent mixtures.

If  $X(t)$  is the relative extent of the transformation at time  $t$ , then in the limit of small amounts transformed<sup>4</sup>

$$\ln(1-X) = -\frac{4}{3} \pi V^2 (C_0 - C_\infty)^2 n_i G^3 t^3 \quad (1)$$

where  $V$  is the molar volume of the solute species,  $C_0$  the initial concentration of crystallizing species,  $C_\infty$  the final concentration in the supernatant fluid at the end of the transformation,  $G$  is the interface reaction constant or growth rate and  $n_i$  is the number of particles formed at  $t=0$ . Equation (1) is derived under the assumption that growth is uniform in three dimensions. If it is assumed that subsequent to initiation, one dimension remains fixed while growth is cylindrically symmetric an expression similar in form to equation (1) is obtained with the exponent of  $t$  being reduced to two. In the dilatometric experiments, of present concern, the volume of the system is measured as a function of time, so that  $X$  is conveniently identified with  $(V_0 - V_t)/(V_0 - V_\infty)$ , where  $V_0$  is the initial volume,  $V_\infty$  the final volume and  $V_t$  is the volume at time  $t$ . Hence the simplified theoretical isotherms are of the form

$$\ln\{(V_\infty - V_t)/(V_\infty - V_0)\} = -kt^n \quad (2)$$

The temperature dependent terms will be embodied in the parameter  $k$ .

The major contributions to this parameter, as far as its temperature coefficient is concerned, are the quantities  $n_i$  and the growth rate constant  $G$ . It has been amply demonstrated that in bulk polymers, in concentrated mixtures and in dilute solutions the growth rate is nucleation controlled<sup>2, 3, 17</sup>. To avoid the adoption of a specific growth process, the details of which are quite complex in terms of the deposition of chain units on a developing crystal face<sup>18</sup>, we shall assume that the critical free energy for growth nucleation is related to that for initiation<sup>2</sup> by a factor  $\bar{a}$ . We have assumed that for a given temperature and concentration a constant number of growing centres are activated at  $t=0$ . For a very special case the number of such centres could be independent of the supersaturation or crystallization temperature. More generally, however, irrespective of whether they are formed homogeneously or heterogeneously, the initial rate at which centres are formed, and consequently their number, will depend directly on the free energy  $\Delta F^*$  of forming a primary nucleus of critical size<sup>19</sup>. A similar set of assumptions was adopted by Turnbull<sup>10</sup> in his study and analysis of the precipitative kinetics of barium sulphate.

By using steady-state nucleation theory for condensed systems<sup>20</sup>, and the assumptions indicated above, over the complete concentration range the relation that

$$k(v_2, T) = k_0 \exp\left\{\frac{-nE_D(v_2)}{RT} - \frac{(1+n\bar{a})\Delta F^*(v_2)}{RT}\right\} \quad (3)$$

is obtained. Our concentrations are now\* expressed in terms of the volume

\*Within the limitations described, equation (3) will be valid over the complete concentration range since an equation of the form of equation (2) is obtained irrespective of polymer concentration. In equation (3)  $n$  is the exponent of  $t$ , and it is assumed that  $\Delta F^*$  for the interfacial controlled process is equal to  $\bar{a}\Delta F^*$  where  $\Delta F^*$  is the free energy required for the formation of a primary nucleus. If we had assumed sporadic nucleation, then in the limit of small  $X$  the exponent of  $t$  would be  $n+1$  for the same growth geometry.

fraction of polymer  $v_2$ , and  $E_D$  represents the activation energy for transport for nucleation. In general  $k_0$  depends on temperature and concentration. However, our experiments are limited to temperatures in the vicinity of the melting temperature so that the contribution of the second term in the argument of the exponential will dominate. Hence we focus attention on the influence of this term.

The limitations imposed in the analysis of the dilute polymer system require that attention be limited to the initial portions of the isotherm. Moreover, it is well known that in the more concentrated systems,  $\Delta F^*$  is a function of the extent of the transformation<sup>5</sup>. A much more complex theoretical isotherm results which, however, can be reduced to equation (2) in the limits of small amounts of the transformations. We limit our considerations to the early stages of the transformation by examining the temperature coefficient of the crystallization at the time  $\tau_{0.9}$ . This quantity is defined as the time when  $1 - X = 0.9$ , so that only ten per cent of the total transformation has occurred. Therefore from equations (2) and (3)

$$\log(1/\tau_{0.9}) = (1/n) [\log k_0(v_2) + \log \log(1/0.9)] - \frac{E_D(v_2)}{2.3 RT} - \left[ \frac{1+n\bar{a}}{n} \right] \frac{\Delta F^*(v_2)}{2.3 RT} \quad (4)$$

Because of the restricted temperature range of our experiments, we can anticipate that the major contribution to the temperature dependence of the rate will be embodied in the last term of equation (4).

For a polymer-diluent mixture, the free energy of forming a three-dimensional nucleus of critical size is given by<sup>9</sup>

$$\Delta F^* = \frac{8\pi\sigma_u^2\sigma_e}{\Delta f_u^2} - \frac{4\pi RT\sigma_u^2 \ln v_2}{\Delta f_u^2} \quad (5)$$

where  $\Delta f_u$  is the free energy of fusion of a polymer unit from the pure crystalline phase to the melt at the specified composition. It can be approximated by  $\Delta f_u = \Delta H_u(T_m - T)/T_m$ . For a cylindrically shaped nucleus containing  $\rho$  crystalline sequences in cross section and  $\gamma$  units in length the critical dimensions are given by

$$\gamma^* = (4\sigma_e - 2RT \ln v_2) / \Delta f_u \quad (6)$$

and

$$\rho^* = 4\pi\sigma_u^2 / \Delta f_u^2 \quad (7)$$

where  $\sigma_e$  is the interfacial free energy per mole of chain units associated with the emergence of the chain from the 001 face of the nucleus and  $\sigma_u$  is the corresponding excess free energy resulting from the interface parallel to the chain axis. Hence  $\Delta F^*$  can be rewritten as

$$\Delta F^* = (8\pi\sigma_u^2\sigma_e / \Delta f_u^2) - RT \ln v_2 \rho^* \quad (8)$$

When  $v_2 = 1$  equations (5) to (8) all reduce to the results previously derived for a pure polymer of infinite molecular weight.

In calculating  $\Delta F^*$  and the dimensions of a critical size nucleus for a polymer-diluent mixture an additional term must be included in the expres-

sion for the free energy of forming a nucleus in addition to that for a pure system. This term,  $\ln v_2$ , is an entropic contribution and represents the probability of selecting the  $\rho$  crystalline sequences from a mixture where the composition is  $v_2$  in the vicinity of the polymer chains. The resulting free energy surface still contains a saddle point whose coordinates are given by equations (5) to (7). For mixtures of monomeric substances and for concentrated polymer-diluent mixtures, where the density of polymer segments is uniform throughout the mixture,  $v_2$  can be identified with the nominal concentration. However, for dilute polymer systems where the segment distribution is non-uniform  $v_2$  must represent the effective polymer concentration within the swollen coil. The probability of selecting the required number of sequences (whether from a single chain or a plurality of chains) must depend on the local concentration. It has been pointed out<sup>21</sup> that for very dilute solutions ( $v_2 \leq 10^{-3}$ )  $\gamma^*$  and  $\Delta F^*$  would be very difficult to satisfy at undercoolings comparable to those observed in bulk crystallization, when the nominal polymer concentration is used in equations (5) and (6). However, this difficulty will not be as great as anticipated since the local concentration of polymer segments in a dilute solution will be many times greater than the nominal concentration. Moreover, since merely by increasing the undercooling and thus lowering the value of  $\rho^*$ ,  $\Delta F^*$  will, according to equation (8), approach the corresponding value for the pure polymer. The amount of undercooling required to accomplish the above  $\rho$  will of course depend on the appropriate value of  $v_2$  that needs to be used. As will be seen below greater undercoolings are indeed required in order for the crystallization of dilute solution to proceed at comparable rates to crystallization in the bulk.

In view of the above discussion and in consideration of equations (4) and (5) we analyse our data by making plots of  $\log(1/\tau_{0.9})$  against  $T_m^2/T(\Delta T)^2$  for the polymer-diluent mixtures which encompass the complete composition range. According to equation (4) straight lines should be obtained (for a temperature region in the vicinity of the melting temperature), whose slopes should depend on polymer concentration according to the relation

$$S = \text{slope} = - \left( \frac{1 + n\bar{a}}{n} \right) \left( \frac{8\pi\sigma_u^2\sigma_e}{2 \cdot 3R\Delta H_u^2} - \frac{4\pi\sigma_u^2 T \ln v_2}{\Delta H_u^2} \right) \quad (9)$$

the foregoing analysis being predicated on the rate-determining nucleation processes being continuous with concentration.

In order to make the plots indicated by theory it is necessary to assign a value to  $T_m$ , the melting temperature of the polymer-diluent mixture. Jackson, Flory and Chiang<sup>22</sup> have pointed out that in such mixtures different melting temperatures are obtained depending on whether initially the polymer is directly crystallized from the mixture or if well annealed bulk crystallized polymer is mixed with diluent at the appropriate concentration. Mixtures prepared by the latter procedure are higher melting and morphological contributions leading to a lowered melting point are avoided. The differences in melting temperature are first observed at a concentration of about fifty per cent polymer and the disparity in melting temperature increases significantly as the polymer concentration is decreased. In very

dilute solutions, depending on the thermodynamic nature of the solvent, differences in melting temperatures of as much as  $14^\circ$  have been reported. For polyethylene- $\alpha$ -chloronaphthalene mixtures of present concern the difference in melting temperature for a 0.01 per cent mixture is found to be  $9^\circ$ . Equilibrium melting temperatures are required for the application of nucleation theory. Hence the melting temperatures used in the calculation of  $\Delta T$  for a given concentration were directly measured<sup>23</sup> utilizing polymer crystallized in the bulk for 40 days at  $130^\circ\text{C}$ . For the dilute polyethylene- $\alpha$ -chloronaphthalene solution this melting temperature is  $117.5^\circ$  to  $118^\circ$ .

In Figure 1,  $\log 1/\tau_{0.9}$  is plotted against the temperature function  $T_m^2/T (\Delta T)^2$  with  $\Delta T$  being computed in the manner indicated above. The data encompass the complete composition range from pure polymer to a 0.01 per cent solution. A family of straight lines results in accordance with theory. The slopes of the straight lines steadily increase as the polymer concentration decreases from that of the pure system to a 1 per cent mixture. On subsequent dilution, however, for the hundredfold change in concentration in going from a 1 per cent to a 0.01 per cent solution, the slope remains essentially invariant with decreasing polymer concentration.

According to equation (13) the slopes from these plots should be a linear function of  $-\log v_2$ . Curve A of Figure 2 is the appropriate plot according to this deduction, with the nominal concentration of each mixture being used. The data adhere to a linear relation up to a polymer concentration corresponding to  $v_2=0.97$ . With further dilutions deviations set in, and a polymer concentration higher than the nominal one would have to be

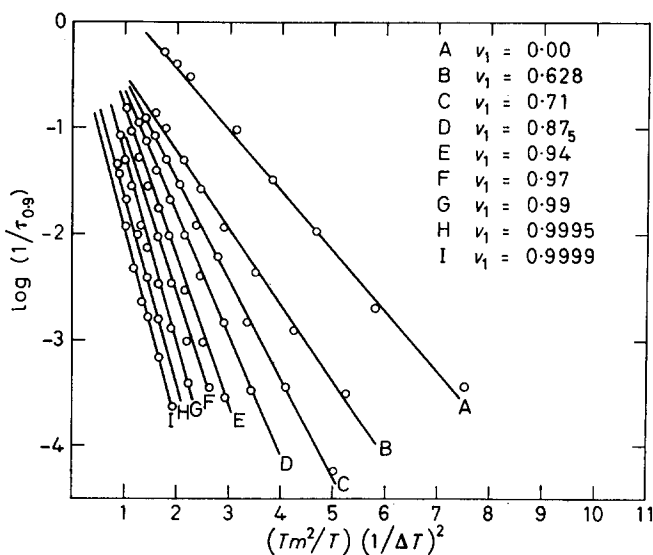


Figure 1—Plot of  $\log (1/\tau_{0.9})$  against temperature variable  $(T_m^2/T) (1/\Delta T)^2$  for polyethylene- $\alpha$ -chloronaphthalene mixture. Volume fraction of diluent in each mixture,  $v_1$ , is indicated. (Reprinted by permission from *The Crystallization of Polymers* by L. Mandelkern. Copyright 1964. McGraw-Hill, New York.)

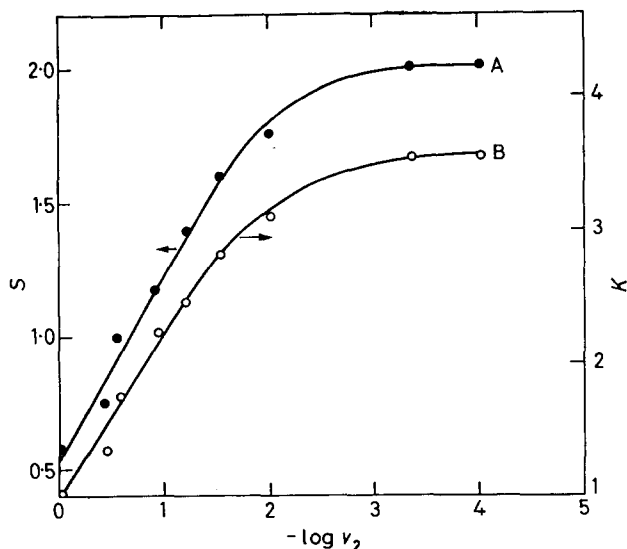


Figure 2—Plot of slope  $S$  and relative slope  $K$  (data from Figure 1) against  $-\log v_2$ . (Reprinted by permission from *The Crystallization of Polymers* by L. Mandelkern. Copyright 1964. McGraw-Hill, New York.)

utilized in order to satisfy the requirement of linearity. For the more dilute system, since the solution is no longer uniform with respect to the concentration of polymer segments, the effective volume fraction of polymer needs to be used. To satisfy the linearity requirements the effective volume fraction  $v_2$  would have to be of the order of two to three per cent. If these values are taken, then the plot in Figure 2 would be linear over the complete concentration range. It does not appear unreasonable that a concentration of this magnitude does indeed represent the concentration of polymer segments within the domain of the swollen polymer coil. It should be noted that the matter in question does not concern the composition of the crystalline phase which is assumed pure. Rather it is concerned with the local concentration of polymer segments in the supercooled liquid.

If the above explanation of curve A of Figure 2 is accepted, then the slope of the linear portion can be interpreted in terms of equation (9). If the factor  $(1 + n\bar{a})/n$  is taken to be of order unity, then from the value of the slope, the quantity  $\sigma_u/\Delta H_u$  is found to be approximately  $1 \times 10^{-2}$  when we take for an average value  $T = 378^\circ\text{K}$ . Turnbull and Cormia<sup>24</sup> have deduced a mean interfacial free energy of about 8 erg/cm<sup>2</sup>, from the temperature coefficient of crystal nucleation in isolated droplets of  $n\text{-C}_{17}\text{H}_{36}$  and  $n\text{-C}_{18}\text{H}_{38}$ . This corresponds to a value of  $\sigma_u$  in the range 50 to 100 cal mole<sup>-1</sup>. Since  $\Delta H_u \approx 10^3$  cal mole<sup>-1</sup>, the ratio of  $\sigma_u/\Delta H_u$  for polyethylene is expected to be approximately 5 to  $10 \times 10^{-2}$ . This is a factor of 5 to 10 times greater than we have deduced from the analysis of curve A in Figure 2. Although exact quantitative agreement is not obtained, the results are not unreasonable when viewed in terms of the simplified theory presented. In particular, we should note the widespread experimental

result that the values of the interfacial energies deduced from studies of overall crystallization kinetics are invariably much lower than those expected on other grounds<sup>2</sup>. However, we can conclude that we are dealing with a nucleation-controlled phase transition, the functional dependence of the nucleation rate on polymer concentration being as predicted.

The latter statement can be examined more closely by examining the ratio of the slope at a concentration  $v_2$  to the slope for the pure polymer. Defining

$$K = (\text{slope for } v_2) / (\text{slope for } v_2 = 1)$$

it is found that for linear polyethylene

$$K = 1 - 0.9 \log v_2 / (\sigma_e / \Delta H_u) \quad (10)$$

Curve B of *Figure 2* is a plot of  $K$  against  $-\log v_2$ . Again a straight line is obtained in the moderately dilute and concentrated range but deviations are observed for polymer concentrations less than  $v_2 = 0.03$ . The basis for this deviation must be the same as in the previous case and the same explanation will hold. From the linear portion we deduce the fact that the ratio of  $\sigma_e / \Delta H_u = 0.75$ . However, several completely independent experiments and analyses<sup>22, 25, 26</sup> have led to the ratio of  $\sigma_e / \Delta H_u$  of approximately 4.5. Hence, from the present experiments, one also deduces a low value for the magnitude of the other interfacial energy involved in nucleus formation.

It should be noted, however, that the low values of  $\sigma_e$  and  $\sigma_u$  deduced from the above analyses are essentially the same values that are deduced from the temperature coefficient of overall crystallization in the bulk. In fact the product  $\sigma_e \sigma_u^2$  deduced from the linear portions of the two curves in *Figure 2* stands in very good quantitative agreement with that deduced from the slope of curve A in *Figure 1*, utilizing the rate constant appropriate to  $v_2 = 1$ . The low values generally deduced for the product  $\sigma_e \sigma_u^2$  from studies of the temperature coefficient of the rate of crystallization in bulk has not received a completely quantitative explanation. A possible explanation is that the nucleation process is catalysed by heterogeneities so that the critical free energy for nucleation is substantially lowered while its temperature dependence is maintained. Irrespective of the reason, it is clear that the same factors causing the low value are operative with dilution since similar values are deduced for  $\sigma_e \sigma_u^2$ . If nucleation catalysts are the cause then their effect is independent of the polymer concentration.

For the pure polymer to about a three per cent solution the admittedly approximate formulation developed adequately describes the experimental results. The change of the slopes in *Figure 1* with concentration can be attributed to the  $\ln v_2$  term in  $\Delta F^*$  where  $v_2$  is identified with the nominal composition. At higher dilution, the value of  $v_2$  required has to be redefined, to conform with physical reality. This corresponds to a concentration of polymer segments within the swollen coil of the order of from two to three per cent. A consistency in the analysis of the temperature coefficient of crystallization is thus achieved over the complete concentration range without the necessity of postulating any changes in the molecular nature of the nucleation process.

Although the temperature coefficient of the crystallization rate becomes independent of the concentration for nominal polymer concentrations less than one per cent, it is clear from the data in *Figure 1* that the time scale of the experiments is not independent of concentration. In other words, the overall rate of crystallization at a fixed undercooling is dependent on the concentration while the temperature dependence of the rate is concentration independent. We observe from the figure that at a fixed value of the temperature function  $(T_m^2/T)(1/\Delta T)^2$  the crystallization rate steadily decreases with decreasing polymer concentration. We examine this phenomenon more closely in *Figure 3*, where the undercooling required for

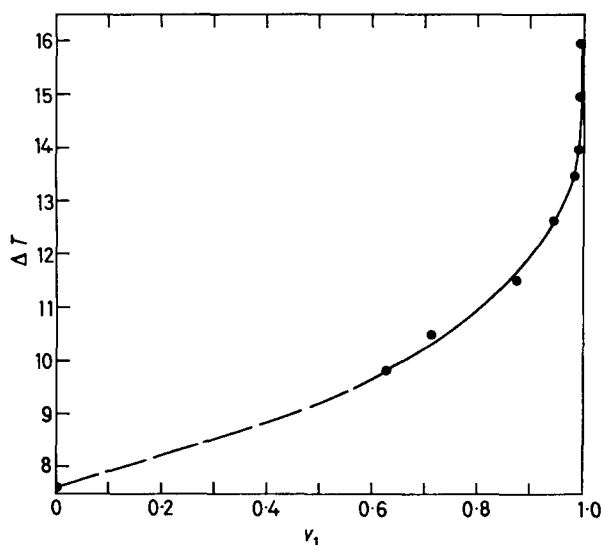


*Figure 3*—Plot of undercooling required for  $\log(1/\tau_{0.9})=3$  against volume fraction of diluent in mixture

$\log(1/\tau_{0.9})=3$  is plotted against the composition variable  $v_1$ . From the pure polymer to the very dilute solution the undercooling needed to achieve the same rate of crystallization has to be steadily increased as the polymer concentration is decreased. The rate of change is much more pronounced in the dilute polymer range and even for the 0.01 per cent solution it is clear that the crystallization rate has not become independent of concentration. This effect cannot be attributed to nucleation catalysts since in *Figure 1* the slopes do not change in the concentration range 1 per cent to 0.01 per cent. Hence we can conclude that the crystallization process has not as yet become unimolecular and must involve the participation of more than single molecules in the rate-determining step. This effect must reflect the additional influence of concentration dependent terms on the crystallization process, as well as the influence of concentration on the critical free energy for nucleus formation. This is seen quite easily from equation (1) (see ref. 4). Undoubtedly, for a polymer of infinite molecular weight in an



infinitely dilute solution a unimolecular crystallization process will be expected. It is clear that this condition is not achieved even for a 0.01 per cent polymer solution. In the present experiments, therefore, the participation of a plurality of molecules in the nucleation process is indicated.

*The author wishes to acknowledge the very skilled experimental assistance of Mr F. A. Quinn, Jr of the National Bureau of Standards.*

*This work was supported by a contract with the Division of Biology and Medicine, U.S. Atomic Energy Commission.*

*Department of Chemistry and  
Institute of Molecular Biophysics,  
Florida State University,  
Tallahassee, Florida*

*(Received February 1964)*

## REFERENCES

- <sup>1</sup> MANDELKERN, L., QUINN Jr, F. A. and FLORY, P. J. *J. appl. Phys.* 1954, **25**, 830
- <sup>2</sup> MANDELKERN, L., in DOREMUS, R. H., ROBERTS, B. W. and TURNBULL, D. (eds.) *Growth and Perfection of Crystals*. Wiley: New York, 1958
- <sup>3</sup> HOLLAND, V. and LINDENMEYER, P. J. *Polym. Sci.* 1962, **57**, 589
- <sup>4</sup> TURNBULL, D. *Solid State Physics*, Vol. III, p 225. Academic Press: New York, 1956
- <sup>5</sup> GORNICK, F. and MANDELKERN, L. *J. appl. Phys.* 1962, **38**, 907
- <sup>6</sup> MANDELKERN, L. and QUINN Jr, F. A. Abstracts of the 134th Meeting of the American Chemical Society, Chicago, Ill., September 1958
- <sup>7</sup> QUINN Jr, F. A. and MANDELKERN, L. *J. Amer. chem. Soc.* 1958, **80**, 3178
- <sup>8</sup> MANDELKERN, L., ROBERTS, D. E., HALPIN, J. C. and PRICE, F. P. *J. Amer. chem. Soc.* 1960, **82**, 46
- <sup>9</sup> MANDELKERN, L. *J. appl. Phys.* 1955, **26**, 443
- <sup>10</sup> TURNBULL, D. *Acta metallurgica*, 1953, **1**, 684
- <sup>11</sup> DOREMUS, R. H. *J. phys. Chem.* 1958, **62**, 1068
- <sup>12</sup> JAYCOCK, M. J. and PARFITT, G. D. *Trans. Faraday Soc.* 1961, **57**, 791
- <sup>13</sup> CASSEL, J. M., MANDELKERN, L. and ROBERTS, D. E. *J. Amer. Leath. Chem. Ass.* 1962, **57**, 556
- <sup>14</sup> FRISCH, H. L. and COLLINS, F. C. *J. chem. Phys.* 1953, **21**, 2158
- <sup>15</sup> WEST, C. and ZENER, C. *J. appl. Phys.* 1950, **21**, 5
- <sup>16</sup> MARKOWITZ, H. *J. appl. Phys.* 1950, **21**, 1198
- <sup>17</sup> FLORY, P. J. and MCINTYRE, A. D. *J. Polym. Sci.* 1955, **18**, 592
- <sup>18</sup> FLORY, P. J. *J. Amer. chem. Soc.* 1962, **84**, 2857
- <sup>19</sup> AVRAMI, M. *J. chem. Phys.* 1939, **7**, 1103; 1940, **8**, 212
- <sup>20</sup> TURNBULL, D. and FISHER, J. C. *J. chem. Phys.* 1949, **17**, 71
- <sup>21</sup> HOFFMAN, J. D. and LAURITZEN, J. I. *J. Res. Nat. Bur. Stand. A*, 1960, **64**, 73
- <sup>22</sup> JACKSON, J. B., FLORY, P. J. and CHIANG, R. *Trans. Faraday Soc.* 1963, **59**, 1906
- <sup>23</sup> MANDELKERN, L., POSNER, A. S., DIORIO, A. F. and ROBERTS, D. E. *J. appl. Phys.* 1961, **32**, 1509
- <sup>24</sup> TURNBULL, D. and CORMIA, R. L. *J. chem. Phys.* 1961, **34**, 820
- <sup>25</sup> CORMIA, R. L., PRICE, F. P. and TURNBULL, D. *J. chem. Phys.* 1962, **37**, 1333
- <sup>26</sup> RICHARDSON, M. J., FLORY, P. J. and JACKSON, J. B. *Polymer, Lond.* 1963, **4**, 221

# Note

## *Mechanism of Copolymerization of Sulphur Dioxide with Olefins, Initiated by Hydroperoxides*

THE copolymerization of olefins with sulphur dioxide, initiated by benzoyl peroxide or ultra-violet light, clearly proceeds by a free radical mechanism. The nature of the hydroperoxide-initiated reaction is less certain since in the styrene-sulphur dioxide system it has been shown that hydroperoxides (and peracids) may simultaneously initiate both the cationic formation of polystyrene and the free radical formation of a styrene polysulphone<sup>1</sup>. The cationic process is suppressed by electron donors and by addition of solvents of lower dielectric constant<sup>1-4</sup>.

While it did not seem likely that hydroperoxides would initiate the cationic formations of *olefin* polysulphones it was thought desirable to check this by measuring the relative reactivity of hexene-1 and cyclopentene using the techniques previously described<sup>5</sup>. The relative rates of addition of the two olefins at  $-54^{\circ}$  and  $20^{\circ}\text{C}$ , using *t*-butyl hydroperoxide as initiator, were found to be 0.30 and 0.28 respectively, compared with values of 0.28 and 0.34 for photochemical initiation (20-fold excess of sulphur dioxide)<sup>5,6</sup>. This confirms that only the free radical intermediates in the reaction between hydroperoxides and sulphur dioxide are effective in initiating polymerization in the olefin-sulphur dioxide systems.

It has been shown<sup>7</sup> that when sulphur dioxide is added to hydroperoxidized polyethylene, the resulting polymer contains no sulphone groups. Any RO-radicals formed in the reaction between ROOH and SO<sub>2</sub> are therefore likely to add olefin before SO<sub>2</sub>. However, one cannot exclude the possibility of a strongly reversible reaction  $\text{RO} + \text{SO}_2 \rightleftharpoons \text{ROSO}_2$ , the product of which might add an olefin.

*E.C.E. is indebted to B.I.P. Chemicals Ltd for making it possible to undertake this work.*

E. C. EATON\*  
K. J. IVIN

*Department of Physical Chemistry,  
University of Leeds*

*(Received September 1964)*

### REFERENCES

- <sup>1</sup> SCHULZ, R. C. and BANIHASCHEMI, A. *Makromol. Chem.* 1963, **64**, 140
- <sup>2</sup> BARB, W. G. *Proc. Roy. Soc. A*, 1952, **212**, 66
- <sup>3</sup> TOKURA, N., MATSUDA, M., SHIRAI, I., SHIINA, K., OGAWA, Y. and KONDO, Y. *Bull. chem. Soc. Japan*, 1962, **35**, 1043
- <sup>4</sup> HERZ, J., HUMMEL, D. and SCHNEIDER, C. *Makromol. Chem.* 1963, **63**, 12; 1963, **64**, 95
- <sup>5</sup> HAZELL, J. E. and IVIN, K. J. *Trans. Faraday Soc.* 1962, **58**, 176
- <sup>6</sup> HAZELL, J. E. and IVIN, K. J. *Trans. Faraday Soc.* 1962, **58**, 342
- <sup>7</sup> EATON, E. C. and IVIN, K. J. *Polymer, Lond.* In press

\*Now at B.I.P. Chemicals Ltd., Oldbury, Birmingham.

## Classified Contents

- Absolute rate constants of anionic propagation by free ions and ion-pairs of living polystyrene, 54
- Activation energies and rates of thermal degradation of an aromatic polypyromellitimide in air and vacuum, 435
- Alkyl vinyl ketones, anionic polymerization of some, 525
- Amylose and its derivatives, studies on, V—  
The sedimentation of amylose acetate in dilute solution, 601
- Anionic polymerization of some alkyl vinyl ketones, 525
- Anomaly in the density dependence of the diffusion constant in polyethylene, 319
- Butadiene, polymerization of, with chromium acetylacetonate and aluminium triethyl, 419
- Calibration of an elasto-osmometer, 177
- Catalysts for the low temperature polymerization of ethylene, 207
- The Chemistry of Cationic Polymerization*, review of, 310
- The Chemistry and Physics of Rubber-like Substances*, review of, 311
- Chemistry of polymer chain folds, 457
- Copolymerization of ethylene with *tert*-butyl acrylate in the presence of *n*-butyl lithium and titanium tetrachloride, 432
- Copolymerization of methylmethacrylate and maleic anhydride, 237
- Copolymerization of trioxan with dioxolan, 371
- Crystalline polymers, melting of, 611  
— morphology of, 283, 293, 579  
— orientation in, related to deformation, 271
- Crystallinity and disorder parameters in Nylon 6 and Nylon 7, 89
- Crystallizability, fusion and glass formation [of polypropylene oxide], 547
- Crystallization kinetics of polymer-diluent mixtures: the temperature coefficient of the process, 637<sub>1</sub>
- Crystallization of polyethylene II, 163
- Crystallization of polymethylene copolymers; morphology, 159
- Defect solid state, thermodynamic description of the, of linear high polymers, 125
- Degradation of vinyl alcohol-isopropenyl alcohol copolymer by periodic acid, 317
- Density dependence of diffusion constant, anomaly in, in polyethylene, 319
- Description and calibration of an elasto-osmometer, 177
- Dilute solution properties and tacticity [of polypropylene oxide], 257
- N,N*-Dimethylacrylamide, free radical polymerization of, 447
- Dynamic birefringence of polymethylacrylate, 1
- Dynamic bulk modulus, measurement of, using an ultrasonic interferometer, 471
- Effect of molecular weight distributions on viscosity/temperature dependence for polyisobutene systems, 201
- Effect of tension and annealing on the X-ray diffraction pattern of drawn 6.6 Nylon, 247
- Enthalpy and entropy effects, some experimental studies on, in equilibrium swelling of polyoxypropylene elastomers, 387
- Entropy of stereoregularity and sequence length distributions in homopolymers of finite molecular weight, 227
- Ethylene, catalysts for the low temperature polymerization of, 207  
— copolymerization of, with *tert*-butyl acrylate in the presence of *n*-butyl lithium and titanium tetrachloride, 432
- Free radical polymerization of *N,N*-dimethylacrylamide, 447
- The Friction and Lubrication of Solids*, Part II, review of, 543
- Gamma radiolysis of poly-2-vinylpyridine, 544
- Graft copolymerization initiated by poly-*p*-lithiostyrene, 135
- Graft copolymers, radiation-initiated, molecular weight distributions of side chains of, 499
- Homopolymers of finite molecular weight, sequence length distributions and entropy of stereoregularity in, 227

- Industrial Plasticizers*, review of, 312
- Infra-red spectra of poly-*p*-ethylene oxybenzoate, 305
- Interaction of Plane-Parallel Double Layers*, review of, 313
- Intrinsic viscosity and light scattering measurements [on branched polyvinyl acetates], 31
- Maleic anhydride, copolymerization of methylmethacrylate and, 237
- Measurement of dynamic bulk modulus using an ultrasonic interferometer, 471
- Mechanism of copolymerization of sulphur dioxide with olefins, initiated by hydroperoxides, 649
- Melt viscosity [of branched polyvinyl acetates], 517
- Melting of defect polymer crystals, 611
- Melting and transitions of polytetrafluorethylene (Teflon) under pressure, 315
- Methylmethacrylate and maleic anhydride, copolymerization of, 237
- Methylvinyl silicone, stress/strain and swelling properties of a peroxide-cured, 463
- Modern Chemical Engineering*, review of, 53
- Modern Petroleum Technology*, review of, 312
- Molecular weight distributions of the side chains of radiation initiated graft copolymers, 499
- Morphology of polymer crystals, 579
- screw dislocations in polyethylene, polyethylene oxide and polyethylene oxide, 283
- Morphology of poly-4-methyl-pentene-1 crystals, 293
- Natural rubber-polar liquid systems, thermodynamics of, 343
- Nuclear spin-lattice relaxation in polyacetaldehyde, 265
- Nylon 6 and Nylon 7, crystallinity and disorder parameters in, 89
- Orientation in crystalline polymers related to deformation, 271
- Photolytic decomposition of poly-*n*-butyl methacrylate, 213
- Phthalocyanine Compounds*, review of, 51
- Physical Properties of Textile Fibres*, review of, 313
- Polyacetaldehyde, nuclear spin-lattice relaxation in, 265
- Polyacrylic acid, radiation chemistry of, an e.s.r. study, 67
- Poly-*n*-butyl methacrylate, photolytic decomposition of, 213
- Polycarbonate, structure and properties of crazes in, and other glassy polymers, 143
- Polyether-ester copolymers prepared from *p*- $\gamma$ -hydroxypropoxy benzoate and bis- $\beta$ -hydroxyethyl terephthalate, 103
- Polyethylene, anomaly in density dependence of diffusion constant in, 319
- crystallization of, II, 163
- proton spin-lattice relaxation measurements on, 323
- rate dependence of strain birefringence and ductility of, 107
- screw dislocations in, 283
- Polyethylene oxide, screw dislocations in, 283
- Poly-*p*-ethylene oxybenzoate, i.r. spectra of, 305
- Polyethylene terephthalate, temperature dependence of extensional creep in, 59
- Polyisobutene, radiolysis of, IV, study of role of free radicals in fracture reaction using radioactive additives, 589
- Polyisobutene systems, viscosity/temperature dependence for, effect of molecular weight distributions, 201
- Poly-L-leucine, proton spin-lattice relaxation measurements on, 336
- Poly-*p*-lithiostyrene, graft copolymerization initiated by, 135
- Polymer Physics Meeting—Shrivenham April 1964, 378
- Polymerization of butadiene with chromium acetylacetonate and aluminium triethyl, 419
- Polymerization of propylene oxide catalysed by zinc diethyl and water, 479
- Polymerization of vinylcarbazole by electron acceptors I, 559
- Polymethacrylic acid, radiation chemistry of, an e.s.r. study, 67
- Poly-4-methyl-pentene-1 crystals, morphology of, 293
- proton spin-lattice relaxation measurements on, 324
- Poly- $\alpha$ -methyl-styrene, proton spin-lattice relaxation measurements on, 339
- Polymethylacrylate, dynamic birefringence of, 1
- Polymethylene copolymers, crystallization of: morphology, 159
- Polymethylene oxide, screw dislocations in, 283
- Polyoxypropylene elastomers, some experimental studies on enthalpy and entropy effects in equilibrium swelling of, 387

- Poly-phenyl-L-alanine, proton spin-lattice relaxation measurements on, 336
- Polypropylene-ketone systems, thermodynamics of, 362, 367
- Polypropylene oxide I—An intrinsic viscosity/molecular weight relationship, 195
- II—Dilute solution properties and tacticity, 257
- III—Crystallizability, fusion and glass formation, 547
- IV—Preparation and properties of polyether networks, 553
- Polystyrene, absolute rate constants of anionic propagation by free ions and ion-pairs of living, 54
- proton spin-lattice relaxation measurements on, 339
- Polytetrafluorethylene (Teflon), transitions and melting of, under pressure, 315
- Polyvinyl acetate, radiation effects in, 403
- Polyvinyl acetates, solution and bulk properties of branched, 19, 31, 517
- Preparation and properties of polyether networks [using polypropylene oxide], 553
- Propylene oxide, polymerization of, catalysed by zinc diethyl and water, 479
- Proton spin-lattice relaxation measurements on some high polymers of differing structure and morphology, 323
- Proton spin-lattice relaxation and mechanical loss in a series of acrylic polymers, 505
- Radiation chemistry of polymethacrylic acid, polyacrylic acid and their esters: an e.s.r. study, 67
- Radiation effects in polyvinyl acetate, 403
- Radiation-initiated graft copolymers, molecular weight distributions of side chains of, 499
- Radiolysis of polyisobutene IV—A study of the role of free radicals in the fracture reaction using radioactive additives, 589
- Rate dependence of the strain birefringence and ductility of polyethylene, 107
- Rates and activation energies of thermal degradation of an aromatic polypyromellitimide in air and vacuum, 435
- Reactions of Co-ordinated Ligands and Homogeneous Catalysis*, review of, 52
- Resonance-induced polymerizations, 187
- Screw dislocations in polyethylene, polymethylene oxide and polyethylene oxide, 283
- Sedimentation of amylose acetate in dilute solution, 601
- Semi-crystalline polymers, theoretical treatment of the modulus of, 533, 636
- Sequence length distributions and entropy of stereoregularity in homopolymers of finite molecular weight, 227
- Solution and bulk properties of branched polyvinyl acetates II—Synthesis of some branched polyvinyl acetates, 19
- III—Intrinsic viscosity and light scattering measurements, 31
- IV—Melt viscosity, 517
- Some experimental studies on enthalpy and entropy effects in equilibrium swelling of polyoxypropylene elastomers, 387
- The Stabilization of Polyvinyl Chloride*, review of, 311
- Stress/strain and swelling properties of a peroxide-cured methylvinyl silicone, 463
- Structure and properties of crazes in polycarbonate and other glassy polymers, 143
- Studies on amylose and its derivatives V—The sedimentation of amylose acetate in dilute solution, 601
- Studies in the thermodynamics of polymer-liquid systems I—Natural rubber and polar liquids, 343
- II—A reassessment of published data, 353
- III—Polypropylene plus various ketones, 362
- IV—Effect of incipient crystallinity on the swelling of polypropylene in diethyl ketone, 367
- Study of the role of free radicals in the fracture reaction using radioactive additives in the radiolysis of polyisobutene, 589
- Synthesis of some branched polyvinyl acetates, 19
- Tacticity and dilute solution properties [of polypropylene oxide], 257
- Temperature coefficient of crystallization [of polymer-diluent mixtures], 637
- Temperature dependence of extensional creep in polyethylene terephthalate, 59
- Theoretical treatment of the modulus of semi-crystalline polymers, 533, 636
- Thermal degradation of an aromatic polypyromellitimide in air and vacuum I—Rates and activation energies, 435
- Thermal expansion and viscoelasticity of rubber in relation to crosslinking and molecular packing, 625
- Thermodynamic description of the defect solid state of linear high polymers, 125

- Transitions and melting of polytetrafluoroethylene (Teflon) under pressure, 315
- Trioxan, copolymerization of, with dioxolan, 371
- Ultrastructure of Protein Fibres*, review of, 314
- Vinyl alcohol-isopropenyl alcohol copolymer, degradation of, by periodic acid, 317
- Vinylcarbazole, polymerization of, by electron acceptors I, 559
- Viscoelasticity and thermal expansion of rubber in relation to crosslinking and molecular packing, 625
- Viscosity/temperature dependence for polyisobutene systems: the effect of molecular weight distribution, 201
- X-ray diffraction pattern of drawn 6.6 Nylon, effect of tension and annealing on, 247

### Author Index

- ALLEN, G., BOOTH, C. and JONES, M. N.: Polypropylene oxide I—An intrinsic viscosity/molecular weight relationship, 195
- — — Polypropylene oxide II—Dilute solution properties and tacticity, 257
- — GEE, G. and JONES, M. N.: Studies in the thermodynamics of polymer-liquid systems IV—Effect of incipient crystallinity on the swelling of polypropylene in diethyl ketone, 367
- — JONES, M. N., MARKS, D. J. and TAYLOR, W. D.: Polypropylene oxide III—Crystallizability, fusion and glass formation, 547
- and CROSSLEY, H. G.: Polypropylene oxide IV—Preparation and properties of polyether networks, 553
- AYREY, G. and TURNER, D. T.: Radiolysis of polyisobutene IV—A study of the role of free radicals in the fracture reaction using radioactive additives, 589
- BANKS, W., HAY, J. N., SHARPLES, A. and THOMSON, G.: The crystallization of polyethylene II, 163
- BARNES, W. J. and PRICE, F. P.: Morphology of polymer crystals: screw dislocations in polyethylene, polymethylene oxide and polyethylene oxide, 283
- BASSETT, D. C.: On the chemistry of polymer chain folds, 457
- DAMMONT, F. R. and SALOVEY, R.: On the morphology of polymer crystals, 579
- BAWN, C. E. H.: review of *The Chemistry and Physics of Rubber-like Substances*, 311
- NORTH, A. M. and WALKER, J. S.: The polymerization of butadiene with chromium acetylacetonate and aluminium triethyl, 419
- BERESFORD, D. R. and BEVAN, H.: The effect of tension and annealing on the X-ray diffraction pattern of drawn 6.6 Nylon, 247
- BERRY, G. C. and CRAIG, R. G.: Solution and bulk properties of branched polyvinyl acetates II—Synthesis of some branched polyvinyl acetates, 19
- HOBBS, L. M. and LONG, V. C.: Solution and bulk properties of branched polyvinyl acetates III—Intrinsic viscosity and light scattering measurements, 31
- See LONG, V. C., BERRY, G. C. and HOBBS, L. M.
- BEVAN, H.: See BERESFORD, D. R. and BEVAN, H.
- BHATTACHARYYA, D. N., LEE, C. L., SMID, J. and SWARC, M.: The absolute rate constants of anionic propagation by free ions and ion-pairs of living polystyrene, 54
- BLOCK, H.: review of *Ultrastructure of Protein Fibres*, 314
- BOOTH, C.: See ALLEN, G., BOOTH, C. and JONES, M. N.
- HIGGINSON, W. C. E. and POWELL, E.: The polymerization of propylene oxide catalysed by zinc diethyl and water, 479
- See ALLEN, G., BOOTH, C., GEE, G. and JONES, M. N.
- GEE, G., HOLDEN, G. and WILLIAMSON, G. R.: Studies in the thermodynamics of polymer-liquid systems I—Natural rubber and polar liquids, 343
- — JONES, M. N. and TAYLOR, W. D.: Studies in the thermodynamics of polymer-liquid systems II—A reassessment of published data, 353
- See ALLEN, G., BOOTH, C., JONES, M. N., MARKS, D. J. and TAYLOR, W. D.

- Transitions and melting of polytetrafluoroethylene (Teflon) under pressure, 315
- Trioxan, copolymerization of, with dioxolan, 371
- Ultrastructure of Protein Fibres*, review of, 314
- Vinyl alcohol-isopropenyl alcohol copolymer, degradation of, by periodic acid, 317
- Vinylcarbazole, polymerization of, by electron acceptors I, 559
- Viscoelasticity and thermal expansion of rubber in relation to crosslinking and molecular packing, 625
- Viscosity/temperature dependence for polyisobutene systems: the effect of molecular weight distribution, 201
- X-ray diffraction pattern of drawn 6.6 Nylon, effect of tension and annealing on, 247

### Author Index

- ALLEN, G., BOOTH, C. and JONES, M. N.: Polypropylene oxide I—An intrinsic viscosity/molecular weight relationship, 195
- — — Polypropylene oxide II—Dilute solution properties and tacticity, 257
- — GEE, G. and JONES, M. N.: Studies in the thermodynamics of polymer-liquid systems IV—Effect of incipient crystallinity on the swelling of polypropylene in diethyl ketone, 367
- — JONES, M. N., MARKS, D. J. and TAYLOR, W. D.: Polypropylene oxide III—Crystallizability, fusion and glass formation, 547
- and CROSSLEY, H. G.: Polypropylene oxide IV—Preparation and properties of polyether networks, 553
- AYREY, G. and TURNER, D. T.: Radiolysis of polyisobutene IV—A study of the role of free radicals in the fracture reaction using radioactive additives, 589
- BANKS, W., HAY, J. N., SHARPLES, A. and THOMSON, G.: The crystallization of polyethylene II, 163
- BARNES, W. J. and PRICE, F. P.: Morphology of polymer crystals: screw dislocations in polyethylene, polymethylene oxide and polyethylene oxide, 283
- BASSETT, D. C.: On the chemistry of polymer chain folds, 457
- DAMMONT, F. R. and SALOVEY, R.: On the morphology of polymer crystals, 579
- BAWN, C. E. H.: review of *The Chemistry and Physics of Rubber-like Substances*, 311
- NORTH, A. M. and WALKER, J. S.: The polymerization of butadiene with chromium acetylacetonate and aluminium triethyl, 419
- BERESFORD, D. R. and BEVAN, H.: The effect of tension and annealing on the X-ray diffraction pattern of drawn 6.6 Nylon, 247
- BERRY, G. C. and CRAIG, R. G.: Solution and bulk properties of branched polyvinyl acetates II—Synthesis of some branched polyvinyl acetates, 19
- HOBBS, L. M. and LONG, V. C.: Solution and bulk properties of branched polyvinyl acetates III—Intrinsic viscosity and light scattering measurements, 31
- See LONG, V. C., BERRY, G. C. and HOBBS, L. M.
- BEVAN, H.: See BERESFORD, D. R. and BEVAN, H.
- BHATTACHARYYA, D. N., LEE, C. L., SMID, J. and SWARC, M.: The absolute rate constants of anionic propagation by free ions and ion-pairs of living polystyrene, 54
- BLOCK, H.: review of *Ultrastructure of Protein Fibres*, 314
- BOOTH, C.: See ALLEN, G., BOOTH, C. and JONES, M. N.
- HIGGINSON, W. C. E. and POWELL, E.: The polymerization of propylene oxide catalysed by zinc diethyl and water, 479
- See ALLEN, G., BOOTH, C., GEE, G. and JONES, M. N.
- GEE, G., HOLDEN, G. and WILLIAMSON, G. R.: Studies in the thermodynamics of polymer-liquid systems I—Natural rubber and polar liquids, 343
- — JONES, M. N. and TAYLOR, W. D.: Studies in the thermodynamics of polymer-liquid systems II—A reassessment of published data, 353
- See ALLEN, G., BOOTH, C., JONES, M. N., MARKS, D. J. and TAYLOR, W. D.

- BROWN, W. B., GEE, G. and TAYLOR, W. D.: Studies in the thermodynamics of polymer-liquid systems III—Polypropylene plus various ketones, 362
- BRUCK, S. D.: Thermal degradation of an aromatic polypyromellitimide in air and vacuum I—Rates and activation energies, 435
- CHARLESBY, A.: See ORMEROD, M. G. and CHARLESBY, A.
- CONNOR, T. M.: Nuclear spin-lattice relaxation in polyacetaldehyde, 265
- CONWAY, B. E. and NICHOLSON, J. P.: Some experimental studies on enthalpy and entropy effects in equilibrium swelling of polyoxypropylene elastomers, 387
- CORBY, N. S.: review of *Phthalocyanine Compounds*, 51
- COWIE, J. M. G. and TOPOROWSKI, P. M.: Studies on amylose and its derivatives V—The sedimentation of amylose acetate in dilute solution, 601
- CRAIG, R. G.: See BERRY, G. C. and CRAIG, R. G.
- CROSSLEY, H. G.: See ALLEN, G. and CROSSLEY, H. G.
- CUBBON, R. C. P.: See THOMAS, P. R., TYLER, G. J., EDWARDS, T. E., RADCLIFFE, A. T. and CUBBON, R. C. P.
- DAMMONT, F. R.: See BASSETT, D. C., DAMMONT, F. R. and SALOVEY, R.
- DAVID, C., VERHASSELT, A. and GEUSKENS, G.: Gamma radiolysis of poly-2-vinylpyridine, 544
- DAVIES, J. T.: review of *Modern Chemical Engineering*, 53
- DOUGLAS, H. W.: review of *Interaction of Plane-Parallel Double Layers*, 313
- EASTMOND, G. C.: review of *Reactions of Co-ordinated Ligands and Homogeneous Catalysis*, 52
- EATON, E. C. and IVIN, K. J.: Mechanism of copolymerization of sulphur dioxide with olefins, initiated by hydroperoxides, 649
- EDWARDS, T. E.: See THOMAS, P. R., TYLER, G. J., EDWARDS, T. E., RADCLIFFE, A. T. and CUBBON, R. C. P.
- ELLINGER, L. P.: The polymerization of vinylcarbazole by electron acceptors I, 559
- FLORY, P. J.: See JACKSON, J. B. and FLORY, P. J.
- GEE, G.: See BROWN, W. B., GEE, G. and TAYLOR, W. D.
- See ALLEN, G., BOOTH, C., GEE, G. and JONES, M. N.
- GEE, G.: See BOOTH, C., GEE, G., HOLDEN, C. and WILLIAMSON, G. R.
- See BOOTH, C., GEE, G., JONES, M. N. and TAYLOR, W. D.
- GEUSKENS, G.: See DAVID, C., VERHASSELT, A. and GEUSKENS, G.
- HAY, J. N.: See BANKS, W., HAY, J. N., SHARPLES, A. and THOMSON, G.
- HIGGINSON, W. C. E.: See BOOTH, C., HIGGINSON, W. C. E. and POWELL, E.
- HILLIER, K. W.: review of *Physical Properties of Textile Fibres*, 313
- HOBBS, L. M.: See BERRY, G. C., HOBBS, L. M. and LONG V. C.
- See LONG, V. C., BERRY, G. C. and HOBBS, L. M.
- HOLDEN, G.: See BOOTH, C., GEE, G., HOLDEN, G. and WILLIAMSON, G. R.
- HOPKINS, E. A. H. and MILLER, M. L.: Copolymerization of ethylene with *t*-butyl acrylate in the presence of *n*-butyl lithium and titanium tetrachloride, 432
- HORROCKS, J. A.: See SMITH, R. R. and HORROCKS, J. A.
- HUGLIN, M. B.: Graft copolymerization initiated by poly-*p*-lithiostyrene, 135
- HUNT, B. I., POWLES, J. G. and WOODWARD, A. E.: Proton spin-lattice relaxation measurements on some high polymers of differing structure and morphology, 323
- See POWLES, J. G., HUNT, B. I. and SANDIFORD, D. J. H.
- IBONAI, M.: Degradation of vinyl alcohol-isopropenyl alcohol copolymer by periodic acid, 317
- ISHIBASHI, M.: Polyether-ester copolymer prepared from *p*- $\gamma$ -hydroxypropoxy benzoate and bis- $\beta$ -hydroxyethyl terephthalate, 103
- Infra-red spectra of poly-*p*-ethylene oxybenzoate, 305
- IVIN, K. J.: See EATON, E. C. and IVIN, K. J.
- JACKSON, J. B. and FLORY, P. J.: The crystallization of polymethylene copolymers: morphology, 159
- JOHNSON, J. F.: See PORTER, R. S. and JOHNSON, J. F.
- JONES, M. N.: See ALLEN, G., BOOTH, C. and JONES, M. N.
- See ALLEN, G., BOOTH, C., GEE, G. and JONES, M. N.
- See BOOTH, C., GEE, G., JONES, M. N. and TAYLOR, W. D.



- See ALLEN, G., BOOTH, C., JONES, M. N., MARKS, D. J. and TAYLOR, W. D.
- KAMBOUR, R. P.: Structure and properties of crazes in polycarbonate and other glassy polymers, 143
- KRIGBAUM, W. R., ROE, R.-J. and SMITH, Jr, K. J.: A theoretical treatment of the modulus of semi-crystalline polymers, 533, 636
- KUČERA, M. and PICHLER, J.: Copolymerization of trioxan with dioxolan, 371
- LEE, C. L.: See BHATTACHARYYA, D. N., LEE, C. L., SMID, J. and SWARC, M.
- LONG, V. C.: See BERRY, G. C., HOBBS, L. M. and LONG, V. C.
- BERRY, G. C. and HOBBS, L. M.: Solution and bulk properties of branched polyvinyl acetates IV—Melt viscosity, 517
- MACCALLUM, J. R.: The photolytic decomposition of poly-*n*-butyl methacrylate, 213
- MCCRUM, N. G.: Anomaly in the density dependence of the diffusion constant in polyethylene, 319
- MANDELKERN, L.: The crystallization kinetics of polymer-diluent mixtures: the temperature coefficient of the process, 637
- MARCHESSAULT, R. H.: See MAXIM, L. D., MARCHESSAULT, R. H., STANNETT, V. and KUIST, C. H.
- MARKS, D. J.: See ALLEN, G., BOOTH, C., JONES, M. N., MARKS, D. J. and TAYLOR, W. D.
- MASON, P.: Thermal expansion and viscoelasticity of rubber in relation to crosslinking and molecular packing, 625
- MAXIM, L. D., MARCHESSAULT, R. H., STANNETT, V. and KUIST, C. H.: Radiation effects in polyvinyl acetate, 403
- MIERAS, H. J. M. A. and PRINS, W.: Description and calibration of an elastometer, 177
- MILLER, M. L.: See HOPKINS, E. A. H. and MILLER, M. L.
- MURFITT, H. C.: review of *Industrial Plasticizers*, I, 312
- NEWMAN, S.: See STRELLA, S. and NEWMAN, S.
- NICHOLSON, J. P.: See CONWAY, B. E. and NICHOLSON, J. P.
- NORTH, A. M.: See BAWN, C. E. H., NORTH, A. M. and WALKER, J. S.
- and POSTLETHWAITE, D.: The copolymerization of methylmethacrylate and maleic anhydride, 237
- NORTH, A. M. and RICHARDSON, D.: Sequence length distributions and entropy of stereoregularity in homopolymers of finite molecular weight, 227
- and SCALLAN, A. M.: The free radical polymerization of *N,N*-dimethylacrylamide, 447
- ORMEROD, M. G. and CHARLESBY, A.: The radiation chemistry of polymethacrylic acid, polyacrylic acid and their esters: an electron spin resonance study, 67
- ORR, R. J.: Resonance-induced polymerizations, 187
- PEPPER, D. C.: review of *The Chemistry of Cationic Polymerization*, 310
- PICHLER, J.: See KUČERA, M. and PICHLER, J.
- PISTORIUS, C. W. F. T.: Transitions and melting of polytetrafluorethylene (Teflon) under pressure, 315
- PORTER, R. S. and JOHNSON, J. F.: Viscosity/temperature dependence for polyisobutene systems: the effect of molecular weight distribution, 201
- POSTLETHWAITE, D.: See NORTH, A. M. and POSTLETHWAITE, D.
- POWELL, E.: See BOOTH, C., HIGGINSON, W. C. E. and POWELL, E.
- POWLES, J. G., HUNT, B. I. and SANDIFORD, D. J. H.: Proton spin lattice relaxation and mechanical loss in a series of acrylic polymers, 505
- See HUNT, B. I., POWLES, J. G. and WOODWARD, A. E.
- PRICE, F. P.: See BARNES, W. J. and PRICE, F. P.
- PRINS, W.: See MIERAS, H. J. M. A. and PRINS, W.
- PULLEN, W. J., ROBERTS, J. and WHALL, T. E.: The measurement of dynamic bulk modulus using an ultrasonic interferometer, 471
- RADCLIFFE, A. T.: See THOMAS, P. R., TYLER, G. J., EDWARDS, T. E., RADCLIFFE, A. T. and CUBBON, R. C. P.
- READ, B. E.: Dynamic birefringence of polymethylacrylate, 1
- REED, H. W. B.: review of *Modern Petroleum Technology*, 312
- RICHARDSON, D.: See NORTH, A. M. and RICHARDSON, D.
- ROBERTS, J.: See PULLEN, W. J., ROBERTS, J. and WHALL, T. E.
- ROE, R.-J.: See KRIGBAUM, W. R., ROE, R.-J. and SMITH, Jr, K. J.
- RULAND, W.: Crystallinity and disorder parameters in Nylon 6 and Nylon 7, 89

- SALOVEY, R.: See BASSETT, D. C., DAMMONT, F. R. and SALOVEY, R.
- SANDIFORD, D. J. H.: See POWLES, J. G., HUNT, B. I. and SANDIFORD, D. J. H.
- SCALLAN, A. M.: See NORTH, A. M. and SCALLAN, A. M.
- SCHINDLER, A.: See WELLONS, J. D., SCHINDLER, A. and STANNETT, V.
- SCHNURMANN, R.: review of *The Friction and Lubrication of Solids*, Part II, 543
- SHARPLES, A.: See BANKS, W., HAY, J. N., SHARPLES, A. and THOMSON, G.
- SMID, J.: See BHATTACHARYYA, D. N., LEE, C. L., SMID, J. and SWARC, M.
- SMITH, Jr, K. J.: See KRIGBAUM, W. R., ROE, R.-J. and SMITH Jr, K. J.
- SMITH, R. R. and HORROCKS, J. A.: review of *The Stabilization of Polyvinyl Chloride*, 311
- STANNETT, V.: See WELLONS, J. D., SCHINDLER, A. and STANNETT, V.  
— See MAXIM, L. D., MARCHESSAULT, R. H., STANNETT, V. and KUIST, C. H.
- STRELLA, S. and NEWMAN, S.: Rate dependence of the strain birefringence and ductility of polyethylene, 107
- SWARC, M.: See BHATTACHARYYA, D. N., LEE, C. L., SMID, J. and SWARC, M.
- TAYLOR, K. J.: Catalysts for the low temperature polymerization of ethylene, 207
- TAYLOR, W. D.: See BROWN, W. B., GEE, G. and TAYLOR, W. D.  
— See BOOTH, C., GEE, G., JONES, M. N. and TAYLOR, W. D.  
— See ALLEN, G., BOOTH, C., JONES, M. N., MARKS, D. J. and TAYLOR, W. D.
- THOMAS, D. K.: Stress/strain and swelling properties of a peroxide-cured methylvinyl silicone, 463
- THOMAS, P. R., TYLER, G. J., EDWARDS, T. E., RADCLIFFE, A. T. and CUBBON, R. C. P.: The anionic polymerization of some alkyl vinyl ketones, 525
- THOMSON, G.: See BANKS, W., HAY, J. N., SHARPLES, A. and THOMSON, G.
- TOPOROWSKI, P. M.: See COWIE, J. M. G. and TOPOROWSKI, P. M.
- TURNER, D. T.: See AYREY, G. and TURNER, D. T.
- TYLER, G. J.: See THOMAS, P. R., TYLER, G. J., EDWARDS, T. E., RADCLIFFE, A. T. and CUBBON, R. C. P.
- VERHASSELT, A.: See DAVID, C., VERHASSELT, A. and GEUSKENS, G.
- WALKER, J. S.: See BAWN, C. E. H., NORTH, A. M. and WALKER, J. S.
- WARD, I. M.: The temperature dependence of extensional creep in polyethylene terephthalate, 59
- WELLONS, J. D., SCHINDLER, A. and STANNETT, V.: Molecular weight distributions of the side chains of radiation initiated graft copolymers, 499
- WHALL, T. E.: See PULLEN, W. J., ROBERTS, J. and WHALL, T. E.
- WILCHINSKY, Z. W.: Orientation in crystalline polymers related to deformation, 271
- WILLIAMSON, G. R.: See BOOTH, C., GEE, G., HOLDEN, G. and WILLIAMSON, G. R.
- WOODWARD, A. E.: The morphology of poly-4-methyl-pentene-1 crystals, 293  
— See HUNT, B. I., POWLES, J. G. and WOODWARD, A. E.
- WUNDERLICH, B.: A thermodynamic description of the defect solid state of linear high polymers, 125  
— The melting of defect polymer crystals, 611

# Contributions to Polymer

*Papers accepted for future issues of*

*POLYMER include the following:*

- Kinetic Measurements on the Cobalt-60 Gamma-initiated Polymerization of Isobutene in the Presence of Zinc Oxide*—F. L. DALTON
- The Effect of Oxidation on Spherulite Size in Polyethylene Films*—H. A. LANCELEY.
- Molecular Weight Dependence of Isothermal Long Period Growth of Polyethylene Single Crystals*—A. PETERLIN
- The Upturn Effect in the Non-Newtonian Viscosity of Polymer Solutions*—Mrs S. P. BUROW, A. PETERLIN and D. T. TURNER
- Thermal Conductivities of Polymers I—Polyvinyl Chloride*—R. P. SHELDON and Sister K. LANE
- Intramolecular Hydride Shift Polymerization by Cationic Mechanism III—Structure Analyses of Deuterated and Non-deuterated Poly-4-methyl-1-pentene*—G. G. WANLESS and J. P. KENNEDY
- Thermal Degradation of an Aromatic Polypyromellitimide in Air and Vacuum II—The Effect of Impurities and the Nature of Degradation Products*—S. D. BRUCK
- On Free Radical Polymerizations with Rapidly Decaying Initiators*—C. H. BAMFORD
- Cationic Transannular Polymerization of Norbornadiene*—J. P. KENNEDY and J. A. HINLICKY
- Multiple Glass Transitions of Block Polymers*—R. J. ANGELO, R. M. IKEDA and M. L. WALLACH
- Radiochemical Studies of Free Radical Vinyl Polymerization III—Bulk Polymerization of Styrene, p-Methoxystyrene and p-Chlorostyrene*—G. AYREY, F. G. LEVITT and R. J. MAZZA
- Cationic Polymerization of 3-Methylbutene-1 IV—Molecular Weight/Intrinsic Viscosity Relationship for Poly-3-methylbutene-1*—I. H. BILLICK and J. P. KENNEDY
- Lower Critical Solution Phenomena in Polymer-Solvent Systems*—G. ALLEN and C. H. BAKER
- The Thermal Degradation of Polypropylene Promoted by Organic Halogen Compounds*—A. R. CAVERHILL and G. W. TAYLOR
- The Bulk Crystallization Kinetics of Polypropylene and Polybutene*—M. GORDON and I. H. HILLIER
- The Use of Frictional Coefficients to Evaluate Unperturbed Dimensions in Dilute Polymer Solutions*—J. M. G. COWIE and S. BYWATER
- The Infra-red Spectrum of Syndiotactic Polypropylene*—I. J. GRANT and I. M. WARD

- Application of Irreversible Thermodynamics to the Kinetics of Polymer Crystallization from Seeded Nuclei*—R.-J. ROE and W. R. KRIGBAUM
- Thermal Conductivities of Polymers II—Polyethylene*—R. P. SHELDON and Sister K. LANE
- Consequences of Chlorine Exchange between Methyl Chloride and Aluminium Chloride in Cationic Polymerization*—J. P. KENNEDY and F. P. BALDWIN
- Intramolecular Hydride Shift Polymerization by Cationic Mechanism V—The Effect of Temperature and Monomer Concentration on the Structure and Molecular Weight of Poly-3-methylbutene-1*—J. P. KENNEDY, W. W. SCHULZ, R. G. SQUIRES and R. M. THOMAS
- The Effect of Crystallization Conditions and Temperature on the Polymorphic Forms of Polyethylene*—J. G. FATOU, C. H. BAKER and L. MANDELKERN
- Cocrystallization in Copolymers of Alpha Olefins I—Copolymers of 4-Methylpentene with Linear Alpha Olefins*—Miss A. TURNER JONES
- Some Grafting Reactions Involving Polyolefin Sulphones*—E. C. EATON and K. J. IVIN
- Light Scattering and Ultra-violet Absorption Studies on Dilute Aqueous Solutions of Poly-4-vinylpyridinium Chloride*—D. O. JORDAN, T. KURUCSEV and R. L. DARSKUS
- Yield Stress Behaviour of Polymethylmethacrylate*—J. A. ROETLING
- Pyrolysis-Hydrogenation—GLC of Poly- $\alpha$ -olefins*—J. VAN SCHOOTEN and J. K. EVENHUIS
- Monomer-Polymer Equilibrium and Ceiling Temperature for Tetrahydrofuran Polymerization*—C. E. H. BAWN, R. M. BELL and A. LEDWITH
- Monomer Reactivity Ratios of a Ternary System*—J. T. KHAMIS
- Entropy of Stereoregularity in Aldehyde Polymerization*—A. M. NORTH and D. RICHARDSON

CONTRIBUTIONS should be addressed to the Editors, *Polymer*, c/o Butterworths, 125 High Holborn, London, W.C.1.

Authors are solely responsible for the factual accuracy of their papers. All papers will be read by one or more referees, whose names will not normally be disclosed to authors. On acceptance for publication papers are subject to editorial amendment.

If any tables or illustrations have been published elsewhere, the editors must be informed so that they can obtain the necessary permission from the original publishers.

All communications should be expressed in clear and direct English, using the minimum number of words consistent with clarity. Papers in other languages can only be accepted in very exceptional circumstances.

A leaflet of instructions to contributors is available on application to the editorial office.